ADVANCEMENT IN POLYMER-BASED MEMBRANES FOR WATER REMEDIATION

Edited by
Sanjay K. Nayak
Kingshuk Dutta
Jaydevsinh M. Gohil

ELSEVIER

ADVANCEMENT IN POLYMER-BASED MEMBRANES FOR WATER REMEDIATION

ADVANCEMENT IN POLYMER-BASED MEMBRANES FOR WATER REMEDIATION

Edited by

SANJAY K. NAYAK
Vice Chancellor, Ravenshaw University, Cuttack, Odisha, India

KINGSHUK DUTTA
Scientist, Advanced Polymer Design and Development Research Laboratory (APDDRL), School for Advanced Research in Petrochemicals (SARP), Central Institute of Petrochemicals Engineering and Technology (CIPET), Devanahalli, Bengaluru, India

JAYDEVSINH M. GOHIL
Scientist, Advanced Polymer Design and Development Research Laboratory (APDDRL), School for Advanced Research in Petrochemicals (SARP), Central Institute of Petrochemicals Engineering and Technology (CIPET), Devanahalli, Bengaluru, India

ELSEVIER

Elsevier
Radarweg 29, PO Box 211, 1000 AE Amsterdam, Netherlands
The Boulevard, Langford Lane, Kidlington, Oxford OX5 1GB, United Kingdom
50 Hampshire Street, 5th Floor, Cambridge, MA 02139, United States

Copyright © 2022 Elsevier Inc. All rights reserved.

No part of this publication may be reproduced or transmitted in any form or by any means, electronic or mechanical, including photocopying, recording, or any information storage and retrieval system, without permission in writing from the publisher. Details on how to seek permission, further information about the Publisher's permissions policies and our arrangements with organizations such as the Copyright Clearance Center and the Copyright Licensing Agency, can be found at our website: www.elsevier.com/permissions.

This book and the individual contributions contained in it are protected under copyright by the Publisher (other than as may be noted herein).

Notices
Knowledge and best practice in this field are constantly changing. As new research and experience broaden our understanding, changes in research methods, professional practices, or medical treatment may become necessary.

Practitioners and researchers must always rely on their own experience and knowledge in evaluating and using any information, methods, compounds, or experiments described herein. In using such information or methods they should be mindful of their own safety and the safety of others, including parties for whom they have a professional responsibility.

To the fullest extent of the law, neither the Publisher nor the authors, contributors, or editors, assume any liability for any injury and/or damage to persons or property as a matter of products liability, negligence or otherwise, or from any use or operation of any methods, products, instructions, or ideas contained in the material herein.

British Library Cataloguing-in-Publication Data
A catalogue record for this book is available from the British Library

Library of Congress Cataloging-in-Publication Data
A catalog record for this book is available from the Library of Congress

ISBN: 978-0-323-88514-0

For Information on all Elsevier publications
visit our website at https://www.elsevier.com/books-and-journals

Publisher: Susan Dennis
Editorial Project Manager: Aera F. Gariguez
Production Project Manager: Joy Christel Neumarin Honest Thangiah
Cover Designer: Miles Hitchen

Typeset by MPS Limited, Chennai, India

Contents

List of contributors xiii
About the editors xvii
Foreword xxi
Preface xxiii
Acknowledgments xxvii

I

Water remediation using polymeric microfiltration and ultrafiltration membrane technologies

1. Microfiltration and ultrafiltration membrane technologies 3

Ananya Bardhan, Aanisha Akhtar and Senthilmurugan Subbiah

1.1 Introduction 3
- 1.1.1 Basics of membrane process 3
- 1.1.2 Historical overview of ultrafiltration and microfiltration membranes 5

1.2 Membrane science and theory 6
- 1.2.1 Solute and solvent transport through microfiltration/ultrafiltration membranes 6
- 1.2.2 Concentration polarization 9
- 1.2.3 Membrane material and geometry 11
- 1.2.4 Mode of operation in the membrane process 12
- 1.2.5 Fouling in microfiltration and ultrafiltration membranes 14

1.3 Membrane characterization methods 18
- 1.3.1 Invasive methods 19
- 1.3.2 Noninvasive methods 22

1.4 Module design and process configuration 25
- 1.4.1 Module design 25
- 1.4.2 Process configuration 27
- 1.4.3 Commercial fabrication techniques employed for polymeric flat sheet and hollow-fiber membranes 30

1.5 Application of polymeric ultrafiltration and microfiltration membranes 33
- 1.5.1 Potable water reuse 33
- 1.5.2 Recovery of dye and pigments 36
- 1.5.3 Treatment of effluent generated by dairy processing industries 36
- 1.5.4 Treatment of oily wastewater 37
- 1.5.5 Recovery of heavy metal from industry effluent 37

1.6 Summary 39
References 39

2. Polymer-based microfiltration/ ultrafiltration membranes 43

Ananya Bardhan and Senthilmurugan Subbiah

2.1 Introduction 43
2.2 Polymers as raw material to synthesize microfiltration/ultrafiltration membranes 44
- 2.2.1 Classification 44
- 2.2.2 Membrane fabrication method microfiltration/ultrafiltration 44
- 2.2.3 Commercial status of membrane fabrication techniques 53

2.3 Effect of polymer-enhanced microfiltration/ ultrafiltration membranes 59
- 2.3.1 Structural property 59
- 2.3.2 Functionalization methods for membrane surface 61
- 2.3.3 Physiochemical properties 66

2.4 Recent advances made in polymeric microfiltration/ultrafiltration membranes for water remediation application 68
- 2.4.1 Polymeric nanocomposite membranes 69
- 2.4.2 Literature review on the recent advances made in the field of polymeric microfiltration/ultrafiltration for water remediation application 71

2.5 Microplastics and polymeric membranes 73

2.6 Prospective 74
References 75

3. Polymer-based nano-enhanced microfiltration/ultrafiltration membranes 81
Amalia Gordano

3.1 Introduction 81
3.2 Nanocomposite membranes 83
3.3 Hollow fiber nano-enhanced membranes 84
3.4 Main aspects in membrane performances 88
3.4.1 Fouling membranes 88
3.4.2 Permeability and selectivity 89
3.4.3 Physical properties 89
3.5 Carbon nanotubes and graphene oxide 89
3.5.1 Fouling 92
3.5.2 Permeability and selectivity 93
3.5.3 Physical properties 94
3.6 Metallic nanoparticles 95
3.6.1 Titanium dioxide 95
3.6.2 Silver 96
3.6.3 Copper 100
3.6.4 Zinc oxide 101
3.6.5 Fouling 102
3.6.6 Permeability and selectivity 104
3.6.7 Physical properties 104
3.7 Stability of nanocomposite membranes 105
3.8 Future research 106
3.9 Challenges and future perspectives 107
3.10 Conclusions 108
References 108
Further reading 118

II
Water remediation using polymeric nanofiltration membrane technologies

4. Nanofiltration membrane technologies 121
Tina Chakrabarty, Arnab Kanti Giri and Supriya Sarkar

4.1 Introduction 121
4.2 Operation principle and transport mechanism 124
4.2.1 Nanofiltration pore model development and progress 124
4.2.2 Diffusion and filtration mechanism 125
4.2.3 Role of membrane charge on NF performance 126
4.3 Types of polymeric membranes and application domain 127
4.3.1 Polymer used in membrane synthesis 128
4.3.2 Other types of NF membranes 129
4.3.3 Application of NF membrane 132
4.4 Polymeric membrane structure and configurations 134
4.5 NF membrane preparation technologies 136
4.5.1 Interfacial polymerization 136
4.5.2 Phase inversion 137
4.5.3 Posttreatment of porous support 138
4.5.4 Layer-by-layer assembly 139
4.5.5 Hollow fiber NF membrane 140
4.6 Commercially available membranes 141
4.7 Limitations and key mitigation strategies 145
4.7.1 Nexus between NF properties: fouling and antifouling 145
4.7.2 Generation of membrane retentate 147
4.8 Summary and future directions 148
References 149

5. Polymer-based nanofiltration membranes 159
Abdulaziz Alammar and Gyorgy Szekely

5.1 Introduction 159
5.2 Polymer-based nanofiltration membranes 161
5.2.1 Natural and bioinspired nanofiltration membranes 164
5.2.2 Mixed-matrix nanofiltration membranes 165
5.2.3 Block-copolymer nanofiltration membrane 166
5.2.4 Intrinsic microporous polymer-based nanofiltration membrane 167
5.3 Preparation of polymer-based nanofiltration membranes 168
5.3.1 Phase inversion 168
5.3.2 Interfacial polymerization 170
5.3.3 Layer-by-layer assembly 171
5.3.4 Posttreatment 172
5.4 Thin-film polymer composite nanofiltration membranes 174

5.5 Effect of polymeric support 175
5.6 Potential of polymer-composite nanofiltration membranes for water desalination 178
5.7 Polymers for solvent-resistant nanofiltration membranes 180
5.8 Commercialization status and commercial viability 181
5.9 Summary and future direction 185
References 187

6. Polymer-based nanoenhanced nanofiltration membranes 197
Shaghayegh Goudarzi, Nahid Azizi, Reza Eslami and Hadis Zarrin

6.1 Introduction 197
6.1.1 Introduction to nanoenhanced nanofiltration membranes 197
6.2 Mixed matrix polymer-based nanoenhanced nanofiltration membranes 203
6.2.1 Introduction 203
6.2.2 Asymmetric mixed matrix nanofiltration membranes prepared by phase inversion 204
6.2.3 Thin-film polymer nanocomposite nanofiltration membranes 208
6.3 Electrospun nanofibrous polymers for nanofiltration applications 217
6.3.1 Introduction to electrospinning 217
6.3.2 Electrospun nanofiber application in nanofiltration 219
6.4 Nanoenhanced hollow-fiber nanofiltration membranes 224
6.5 Commercialization status and commercial viability 225
6.6 Summary and future directions 226
Abbreviations 227
References 227

7. Polymer-based bioinspired, biomimetic, and stimuli-responsive nanofiltration membranes 237
Nahid Azizi, Shaghayegh Goudarzi, Reza Eslami and Hadis Zarrin

7.1 Introduction 237
7.2 Bioinspired membranes and their applications 238
7.2.1 Dopamine-based nanofiltration membrane 238
7.2.2 Tannic acid-based nanofiltration membranes 246
7.2.3 Other bioinspired nanofiltration membranes and their application 249
7.3 Biomimetic membranes 251
7.3.1 Aquaporin-based biomimetic membranes 251
7.3.2 Application of aquaporin-based biomimetic nanofiltration membranes 254
7.3.3 Aquaporin-based biomimetic nanofiltration membranes with hollow fiber configuration 256
7.4 Stimuli-responsive/smart membranes 257
7.4.1 pH-responsive membranes 257
7.4.2 Magnetically responsive membranes 258
7.4.3 Temperature-responsive membrane 260
7.4.4 Photo-responsive membranes 261
7.4.5 CO_2-responsive nanofiltration membranes 263
7.4.6 Stimuli-responsive membranes with hollow fiber configuration 263
7.5 Commercial status and future directions 264
7.6 Summary 266
Nomenclature 266
References 267

III
Water remediation using polymeric reverse and forward osmosis membrane technologies

8. Reverse and forward osmosis membrane technologies 275
Soleyman Sahebi, Mohammad Sheikhi, Mohammad Kahriz, Nasim Fadaie, Zahra Shabani, Sanaz Ghiasi, Norollah Kasiri and Toraj Mohammadi

8.1 Introduction 275
8.2 Classification of osmotic processes and basic concept 276
8.2.1 Transport membrane mechanism 277
8.3 Reverse osmosis and forward osmosis membranes 280

8.4 Concentration polarization in an osmotic-driven membrane 281
8.4.1 External concentration polarization 281
8.4.2 Internal concentration polarization 282
8.5 Reverse osmosis and forward osmosis membrane fabrication methods 283
8.6 Advances in forward osmosis and reverse osmosis membranes' structures and properties 284
8.6.1 Reverse osmosis membrane development 284
8.6.2 Forward osmosis membrane development 285
8.7 Custom designs of flat sheet forward osmosis and reverse osmosis membranes 292
8.7.1 Selective rejection layer 296
8.7.2 Support polymeric layer 297
8.7.3 Support backing fabric 298
8.8 Concluding remarks and recommendations 301
References 301

9. Polymer-based reverse osmosis membranes 311
Jasneet Kaur Pala, Anirban Roy and Asim K. Ghosh

9.1 Introduction 311
9.2 Asymmetric polymer-based reverse osmosis membranes 312
9.3 Thin-film composite membrane 316
9.3.1 Reverse osmosis membranes for boron removal 321
9.3.2 Reverse osmosis membranes for antifouling/chlorine tolerant 321
9.3.3 Hollow fiber reverse osmosis membranes 322
9.4 Potential of different polymer-based reverse osmosis membranes for brackish water desalination 323
9.5 Polymer-based reverse osmosis membranes for seawater desalination 324
9.5.1 Polyelectrolyte membranes 325
9.5.2 Aquaporin biomimetic membranes 326
9.5.3 Supramolecular polymers and water-soluble polymers 327
9.6 Commercialization status and commercial viability 328
9.7 Summary and future direction 329
References 331

10. Polymer-based nano-enhanced reverse osmosis membranes 335
Hiren D. Raval and Mrinmoy Mondal

10.1 Introduction 335
10.2 Preparation strategies of polymer-based nano-enhanced reverse osmosis membranes 337
10.2.1 Conventional nanocomposite or mixed matrix membrane 338
10.2.2 Thin-film composite with nanocomposite substrate 338
10.2.3 Thin-film nanocomposite 338
10.2.4 Nanocomposite located at membrane surface 339
10.3 Polymer nanocomposite reverse osmosis membranes 341
10.3.1 Carbon based 342
10.3.2 Metal and metal oxides based 350
10.3.3 Other nanoparticles 360
10.4 Potential of different polymer-based nanocomposite reverse osmosis membranes for water desalination 363
10.5 Potential other applications of polymer nanocomposite reverse osmosis membranes in water treatment 368
10.6 Commercialization status and viability 369
10.7 Way forward 369
10.8 Conclusion 370
Acknowledgment 370
References 370

11. Reuse and recycling of end-of-life reverse osmosis membranes 381
J. Contreras-Martínez, J.A. Sanmartino, M. Khayet and M.C. García-Payo

11.1 Introduction 381
11.2 Reverse osmosis membrane technology 382
11.3 Reverse osmosis membranes and modules 384
11.4 Fouling in reverse osmosis separation process: problem, prevention, and cleaning protocols 386
11.4.1 Inorganic fouling 387

11.4.2 Colloidal fouling 388
11.4.3 Organic fouling 389
11.4.4 Biofouling 390
11.4.5 Fouling prevention and mitigation 391
11.5 End-of-life reverse osmosis membrane modules: reuse and recycling techniques 394
11.5.1 Cleaning strategies adopted for reverse osmosis fouled membranes and discarded modules 395
11.5.2 Reuse of discarded reverse osmosis membrane modules 399
11.5.3 Recycling discarded reverse osmosis membrane modules 399
11.6 Applications of reverse osmosis recycled membranes in other membrane processes 403
11.6.1 Reverse osmosis recycled membranes in ultrafiltration and microfiltration process 406
11.6.2 Reverse osmosis recycled membranes in membrane distillation, membrane biofilms reactors, and electrodialysis separation processes 407
11.7 Conclusions 408
Acknowledgments 409
References 409

12. Polymer-based forward osmosis membranes 419

Soheila Shokrollahzadeh and Yasamin Bide

12.1 Introduction 419
12.1.1 Important notes in forward osmosis membrane transport 419
12.1.2 Concentration polarization 420
12.2 Polymer-based flat sheet forward osmosis membranes 422
12.2.1 Single-layer membranes 422
12.2.2 Dual-layer membranes 429
12.2.3 Layer-by-layer membranes 438
12.2.4 Double-skinned membranes 446
12.2.5 Impregnated membranes 446
12.2.6 Biomimetic membranes 448
12.3 Polymer-based hollow fiber forward osmosis membranes 449
12.3.1 Single-layer membranes 449
12.3.2 Dual-layer membranes 453
12.3.3 Layer-by-layer membranes 454
12.3.4 Double-skinned membranes 454
12.3.5 Biomimetic membranes 456
12.4 Commercialization status and commercial viability 458
12.5 Summary and future directions 460
Abbreviations 461
Nomenclature 462
References 463

13. Polymer-based nano-enhanced forward osmosis membranes 471

Salam Bakly, Ibrar Ibrar, Haleema Saleem, Sudesh Yadav, Raed Al-Juboori, Osamah Naji, Ali Altaee and Syed Javaid Zaidi

13.1 Introduction 471
13.2 Polymer-based mixed matrix forward osmosis membranes 472
13.2.1 Overview 472
13.2.2 Common membrane preparation and modification approaches 473
13.2.3 Nanomaterials classification 474
13.3 Polymer-based nanocomposite flat sheet forward osmosis membranes 475
13.3.1 Methods for nanocomposite forward osmosis membrane preparation 479
13.3.2 Nanomaterials-incorporated support/substrate layer 479
13.3.3 Nanomaterials-incorporated selective/active layer 483
13.3.4 Nanomaterials-incorporated support/substrate and selective/active layers 486
13.4 Polymer-based nanocomposite hollow fiber forward osmosis membranes 486
13.4.1 Active layer modifications 487
13.5 Nanofibrous-based forward osmosis membranes 490
13.6 Nanomaterials used in surface modification of forward osmosis membranes 491
13.7 Polymer-based stimuli-responsive forward osmosis membranes 491
13.8 Commercialization status of the forward osmosis membranes 495
13.9 Summary and future directions 496
References 498

IV

Water remediation using polymeric membranes in electrodialysis, electrodialysis reversal, capacitive deionization and membrane distillation technologies

14. Electrodialysis, electrodialysis reversal and capacitive deionization technologies 505

Tatiane Benvenuti, Alexandre Giacobbo, Carolina de Moraes da Trindade, Kayo Santana Barros and Tatiana Scarazzato

14.1 Introduction 505
14.2 Structure of ion-exchange membranes 507
14.2.1 Anion-exchange membranes 511
14.2.2 Cation-exchange membranes 511
14.2.3 Bipolar membranes 512
14.3 Electrodialysis, electrodialysis reversal, and selective electrodialysis 513
14.3.1 General description of electrodialysis cells: configuration and operating principles 513
14.3.2 Transport equations and driving forces 515
14.3.3 Achievements in the use of electrodialysis, electrodialysis reversal, and selective electrodialysis as water remediation methods 517
14.4 Capacitive deionization-based technologies 519
14.4.1 General description of capacitive deionization cells: configuration, operating principles, and flow patterns 520
14.4.2 Evaluation of the efficiency and performance of the capacitive deionization-based technologies 522
14.4.3 Achievements in use of capacitive deionization-based technologies as water remediation methods 523
14.5 Limitations and key mitigation strategies 526
14.5.1 Process cost 526
14.5.2 Membrane clogging 528
14.5.3 Membrane selectivity 530
14.6 Summary and future directions 531
Acknowledgments 532
References 532

15. Polymeric membranes in electrodialysis, electrodialysis reversal, and capacitive deionization technologies 541

K. Khoiruddin, Anita K. Wardani, Putu T.P. Aryanti and I.G. Wenten

15.1 Introduction 541
15.2 Ion-exchange membranes and their fabrication processes 543
15.2.1 Ion-exchange membranes' classification 543
15.2.2 Preparation of ion-exchange membranes 543
15.2.3 Recent developments in polymeric ion-exchange membranes 546
15.3 Application and performance of ion-exchange membranes in electrodialysis 546
15.3.1 Desalination with electrodialysis 546
15.3.2 Wastewater treatment 549
15.3.3 Preferential ion separation 550
15.3.4 Other ionic separations 550
15.4 Application and performance of ion-exchange membranes in electrodialysis reversal 551
15.4.1 Principle of electrodialysis reversal 551
15.4.2 Desalination of high-concentration solution 552
15.4.3 Other ion separation processes 555
15.5 Application and performance of ion-exchange membranes in membrane capacitive deionization 556
15.5.1 Role of ion-exchange membrane in membrane capacitive deionization 556
15.5.2 Desalination processes 558
15.5.3 Membrane capacitive deionization applications in other deionization processes 558
15.6 Concluding remarks 559
References 559

16. Polymeric nano-enhanced membranes in electrodialysis, electrodialysis reversal and capacitive deionization technologies 569

Elham Jashni and Sayed Mohsen Hosseini

16.1 Introduction 569
16.2 Preparation of polymer-based nano-enhanced ion-exchange membranes 580
16.2.1 Blending 583
16.2.2 In situ technique 584
16.3 Analysis of different ion-exchange membranes for water treatment 586
16.4 Commercialization status and commercial viability 587
16.5 Summary and future directions 590
References 591

17. Polymer-based membranes for membrane distillation 597

Arun Saravanan, Kanupriya Nayak and Bijay P. Tripathi

Abbreviations 597
Nomenclature 598
17.1 Introduction 598
17.1.1 Dearth of water 598
17.1.2 History of membrane distillation 599
17.1.3 Recent trends in polymer-based membranes in membrane distillation 600
17.2 Principle and different configurations of membrane distillation 600
17.2.1 Membrane distillation principle 600
17.2.2 Direct contact membrane distillation 601
17.2.3 Air gap membrane distillation 601
17.2.4 Sweep gas membrane distillation 602
17.2.5 Vacuum membrane distillation 603
17.3 Fabrication techniques and module designs of MD membrane 603
17.3.1 Phase inversion 604
17.3.2 Stretching 605
17.3.3 Sintering 605
17.3.4 Electrospinning 605
17.3.5 MD membrane modules and designs 608
17.4 Membrane materials for MD 610
17.5 Characteristics of MD membrane 611
17.5.1 Liquid entry pressure 611
17.5.2 Membrane thickness 612
17.5.3 Pore size and pore size distribution 612
17.5.4 Porosity and tortuosity of membrane 613
17.5.5 Mechanical properties 614
17.5.6 Thermal conductivity 614
17.6 Operational parameters in membrane distillation 615
17.6.1 Feed temperature 615
17.6.2 Flow rate 615
17.6.3 Feed concentration 616
17.6.4 Air gap and long operation 616
17.6.5 Membrane type 617
17.7 Fouling and wetting phenomena 617
17.8 Prevention methods of fouling and wetting 619
17.9 Temperature and concentration polarization 623
17.10 Applications of membrane distillation 624
17.11 Economics and energy consumption of membrane distillation 624
17.12 Conclusion and future directions in membrane distillation 626
Acknowledgments 627
References 627

Index 637

Preface

In the ever-increasing quest for environmentally friendly and low energy separation processes, membrane-based technologies are rapidly overtaking the conventional thermal- and chemical-based technologies. Since the inception of Loeb-Sourirajan and composite polymer membranes, membrane-based separation technology has been able to establish a solid foundation. Accordingly, this book focuses on the advanced membrane science and engineering behind the separation processes, within the domain of polymer-based membrane systems.

Chapter 1 is the introductory chapter of Section 1, and it contains fundamental aspects of polymeric microfiltration (MF)/ultrafiltration (UF) flat sheet and hollow fiber membranes, transport phenomena for solute/solvent molecules, and different types of MF/UF membranes used for different applications.

Chapter 2 elaborates on the use of different polymers as raw materials for membrane (flat sheet and hollow fiber) fabrications, including 3D printing technique, along with morphological characteristics. This chapter covers the most recent advancements made regarding the preparation, modification, and performance of polymeric MF and UF membranes for water remediation (including industrial applications).

Chapter 3 particularly focuses on the mixed matrix and nano-powered UF and MF membranes. Detailed discussions on membrane fouling, permselectivity, and physical properties of nano-enhanced hollow fiber and flat sheet membranes have been included.

Chapter 4 is the introductory chapter of Section 2, and it contains fundamental discussion on the nanofiltration process, with emphases on the operating principle and transport mechanism, different types of polymer-based nanofiltration (NF) membranes, structure and configuration, and application domain. In addition, membrane preparation techniques for commercial NF membranes have been discussed, along with their properties. Limitations and key mitigation strategies have also been highlighted.

Chapter 5 deals with the intrinsic properties and separation mechanisms of ultrathin NF membranes for water treatment, desalination, and organic solvent nanofiltration. Potentials of advanced polymers, such as natural polymers, bioinspired polymers, block copolymers, and intrinsic microporous polymers, have been discussed, with focus on scalability prospects and application viability in NF processes.

Chapter 6 covers the advances made in various nano-enhanced NF membranes (flat sheet and hollow fiber), prepared by incorporation of nanoscale materials (like graphene oxide and carbon nanotubes). Applications of mixed matrix, thin-film nanocomposites, thin-film polymer nanocomposites, metal organic framework–integrated thin-film nanocomposites, electrospun nanofibrous polymeric membranes, etc. in water remediation have been included.

Chapter 7 is focused on the preparation and application potential of various NF membranes, based on dopamine, tannic acid, and protein channels (including

aquaporin and lipids). It also includes modifications of pores and surfaces of membranes, as well as incorporation of artificial channels within block copolymers to fabricate biomimetic-based nanofiltration membranes. In addition, application efficiency of various smart membranes that are pH, temperature, CO_2, light and/or magnetic responsive, prepared using various functional and block copolymers, has been discussed.

Chapter 8 is the introductory chapter of Section 3, and it is specially focused on the fundamental aspects of polymeric reverse osmosis (RO) and forward osmosis (FO) membranes, transport phenomena, transport models and equations, and different types of RO and FO membranes used for different applications. Also included are detailed discussions on the concentration polarization in osmotic-driven membrane processes.

Chapter 9 reviews the commercially available RO membranes, along with the recent developments in advanced polymeric RO membranes. In addition, discussion on performance-enhanced chlorine-resistant RO membranes, based on the modification of existing membranes as well as synthesized new polymeric membranes, has been included.

Chapter 10 presents a comprehensive analysis of nano-enhanced RO membranes. Carbon materials, metals and metal oxides, and other nano-sized materials used for the preparation of nano-enhanced RO membrane have been discussed. The effect of nanomaterials on the properties of the resulting membranes, such as permeate flux, selectivity, chlorine resistance, and antifouling characteristics, has been analyzed, along with the comments on desalination application, commercial viability, and future scope of nano-enhanced RO membranes.

Chapter 11 provides an overview on the different procedures adopted and techniques developed to avoid the disposal of discarded RO membrane modules in landfills, and to recycle or reuse them in other applications.

Chapter 12 provides an in-depth analysis of flat sheet and hollow fiber FO membranes, based on polymers. The use of various polymers for fabrication of different types of FO membranes has been reviewed. In addition, effects of support layer, multilayer coating, types of polymers, solvents, monomers, additives, surface modifications, and so on have been included, along with water flux and reverse salt flux for flat sheet and hollow fiber FO membranes. Application potentials of various commercial FO membranes have also been included.

Chapter 13 comprehensively covers fabrication processes of flat sheet and hollow fiber membranes that are modified by incorporation of nanoparticles and discusses on stimuli-responsive membranes, such as pH-responsive, electric field-responsive, and salt-responsive membranes, for water purification. The main challenges associated with the commercialization are also discussed to identify the future research directions.

Chapter 14 is the introductory chapter of Section 4, and it especially deals with membrane technologies based on ion transport, using ion-exchange membranes, under applied electrical potential gradients. Operational principles, transport equations, configurations, applications, and limitations of electromembrane processes (such as electrodialysis, electrodialysis reversal, selective electrodialysis, and capacitive deionization) have been discussed.

Chapter 15 reviews the classifications, preparations, and characterizations of ion-exchange membranes. Applications of electrodialysis, electrodialysis reversal, and

capacitive deionization technologies for desalination, ion removal and recovery, deacidification and demineralization, and preferential ion separation using laboratory-made and commercial polymeric ion-exchange membranes have been discussed, along with comments on separation efficiency, energy consumption, and operational cost.

Chapter 16 focuses on the use of nanoscale materials for the fabrication of polymeric nano-enhanced ion-exchange membranes to get improved electrochemical properties and stability in industrial applications. It particularly includes an overview on the use of polymeric nano-enhanced ion-exchange membranes in electrodialysis, electrodialysis reversal, and capacitive deionization processes related to water treatment and desalination, suggesting possible directions to overcome the existing challenges in future.

Chapter 17 is devoted to the rudimentary concepts, literature reviews on membrane distillation (MD) development, various MD configurations, methods to fabricate MD polymeric membranes, MD modules, operational parameters, and challenges for mitigating the wetting and fouling effects.

Enriched with critically analyzed and expertly opined contributions from several well-known researchers around the world, this book is likely to serve as one of the most comprehensive and authoritative literature that has ever been published in this field and will undoubtedly serve as a potent source of information for those interested in this field. Therefore, as the editors, we believe that this book will enjoy readerships from all concerned sectors of our society, that is, academia, industries, policy makers, and general public. We wish you all an enriching reading experience!

Sanjay K. Nayak[1], Kingshuk Dutta[2] and Jaydevsinh M. Gohil[3]

[1]Director General and Chief Executive Officer, School for Advanced Research in Polymers-LARPM, Central Institute of Plastic Engineering and Technology, Bhubaneswar, Odisha, India [2]Scientist, Advanced Polymer Design and Development Research Laboratory (APDDRL), School for Advanced Research in Polymers (SARP), Central Institute of Plastics Engineering and Technology (CIPET), Devanahalli, Bengaluru, India [3]Scientist, CIPET: SARP – APDDRL, Hi-Tech Defence and Aerospace Park, Devanahalli, Bengaluru, Karnataka, India

Foreword

It is difficult to estimate the number of research papers starting with sentences like "Water is life; it is essential for all human activities" or "The availability of pure water defines the potential for development." It seems that we all agree on this point. To bring it into practice is a different story. The need for water purification remains critical in all parts of the world. The scope may be different from the crave for drinking water in refugee camps, in slum areas, and in crowded villages to the need of water for increased production in industrial zones. However, it is a shared search for water, more water, and more pure water. Eyes are upon the technologies that will make this possible.

Is the thirst of the world ever going to be quenched? It is hardly likely that this will be the case. There is the commendable initiative of aiming at providing water for every person on this planet, as part of the sustainable development goals. Clean water is considered to be a human right. However, "human rights" do not exist, since they are a human invention. They are not enforceable. Categorizing the need of water as a right may deviate the discussion to the question of who is legally obliged to provide this water. This may be a vulnerable starting position in providing water, while it also confirms inequality. The right for water hides an enormous misdistribution of water sources: why would an Australian or a Canadian have access to much more water than a citizen of Niger or Sudan, simply because she or he is born there? Instead, it may be wiser not to give water rights to anyone, but to share what the Earth is offering us. The "water right" then becomes a concern for all of us, and is not a donation from the rich to the poor anymore. It converts into a need for technologies that can optimize what we have. Indeed, when shared equally, the average standards of a person would decrease with growing world population, making clear that technological solutions are in everyone's interest. This is what this book is about: water remediation, in view of sharing the resources we have, with the help of the most universal technologies that can do this: membranes. A choice was made for polymeric membranes, since these would offer the broadest potential for solutions, taking technical aspects into account, but also economic, environmental, and societal factors.

The book is divided into four parts. In the first part, low-pressure technologies (microfiltration and ultrafiltration) are addressed in three chapters. The key question is: what can these technologies offer us to resolve the challenges mentioned above? The authors of these chapters are not sitting back to relax and look at what was done in the past; they have addressed how membranes can be fabricated in various ways, with various polymers, for various applications. This stretches from fundamental principles to fancy novel solutions with mixed-matrix membranes and nano-enhanced membranes.

In the second part, the attention is for water sources requiring the removal of smaller substances, which is typically

necessary for low-grade water sources such as wastewater for recycling or other impaired water sources. Different types, structures, and configurations are discussed, along with the use of new polymers: natural polymers, bioinspired polymers, block copolymers, and intrinsic microporous polymers. This goes as far as membrane modifications and hybrid structures with dopamine, tannic acid, and protein channels, and functional membranes with response to various external factors.

The third part is crucial for the "water-for-all" idea. A viable technology for desalination would solve most of the threat that not enough water is available for everyone, particularly for the next generations to come. Reverse osmosis (RO) is the technology that gives hope to achieve this, with proven performance for large-scale applications but with much room left for improvement in view of developing a cost-effective, high-performance technology that can be applied all over the world. The six chapters in this part take commercial membranes as a starting point, and expand this to nano-enhanced membranes, and other advanced materials such as dopamine-based polymers, rigid star amphiphilic polymers, zeolite-channel, and CNT-induced channel-based bioinspired membranes; biomimetic membranes; and stimuli responsive RO membrane. A similar approach can be used for integrated processes where forward osmosis (FO) may play a role.

The last part of the book addresses non-pressure-driven membrane technologies such as electrodialysis, capacitive deionization, and membrane distillation in view of their use in water remediation. These processes are complementary to pressure-driven membrane processes, and one conclusion is that a complete portfolio of membrane processes is needed for a universal approach toward satisfying the world's thirst. If anything is to be declared a human right, it may have to be the technology to purify water, not the water itself. This book will give you the inspiration on how this can be done—not because we are obliged but because consuming water with respect for our neighbor and giving her or him the same tools for water treatment as we have, defines us as human.

Bart Van der Bruggen
Professor, Process Engineering for Sustainable Systems, Department of Chemical Engineering, KU Leuven, Leuven, Belgium

List of contributors

Aanisha Akhtar Department of Chemical Engineering, Indian Institute of Technology, Guwahati, India

Abdulaziz Alammar Department of Chemical Engineering and Analytical Science, The University of Manchester, Manchester, United Kingdom

Raed Al-Juboori Water and Environmental Engineering Research Group, Department of Built Environment, Aalto University, Aalto, Espoo, Finland

Ali Altaee Centre for Green Technology, School of Civil and Environmental Engineering, University of Technology Sydney, Broadway, NSW, Australia

Putu T.P. Aryanti Department of Chemical Engineering, Universitas Jenderal Achmad Yani, Cimahi, Indonesia

Nahid Azizi Nanoengineering Laboratory for Energy and Environmental Technologies, Department of Chemical Engineering, Ryerson University, Toronto, ON, Canada

Salam Bakly Centre for Green Technology, School of Civil and Environmental Engineering, University of Technology Sydney, Broadway, NSW, Australia

Ananya Bardhan Department of Chemical Engineering, Indian Institute of Technology, Guwahati, India

Tatiane Benvenuti Science, Innovation, and Modeling in Materials Post-Graduation Programm – PROCIMM, Department of Exact and Technologic Sciences, State University of Santa Cruz – UESC, Ilhéus, Brazil

Yasamin Bide Department of Chemical Technologies, Iranian Research Organization for Science and Technology (IROST), Tehran, Iran

Tina Chakrabarty The Environmental Research Group, R&D, Tata Steel, Jamshedpur, India

J. Contreras-Martínez Department of Structure of Matter, Thermal Physics and Electronics, Faculty of Physics, Complutense University of Madrid, Madrid, Spain

Carolina de Moraes da Trindade Federal Institute of Pará -IFPA - Campus Óbidos, Óbidos, Brazil

Reza Eslami Nanoengineering Laboratory for Energy and Environmental Technologies, Department of Chemical Engineering, Ryerson University, Toronto, ON, Canada

Nasim Fadaie Centre of Excellence for Membrane Science and Technology, School of Chemical, Petroleum and Gas Engineering, Iran University of Science and Technology (IUST), Tehran, Iran

M.C. García-Payo Department of Structure of Matter, Thermal Physics and Electronics, Faculty of Physics, Complutense University of Madrid, Madrid, Spain

Sanaz Ghiasi Centre of Excellence for Membrane Science and Technology, School of Chemical, Petroleum and Gas Engineering, Iran University of Science and Technology (IUST), Tehran, Iran

Asim K. Ghosh Desalination and Membrane Technology Division, Bhabha Atomic Research Centre, Mumbai, India

Alexandre Giacobbo Department of Materials Engineering, Federal University of Rio Grande do Sul - UFRGS, Porto Alegre, Brazil

Arnab Kanti Giri Department of Chemistry, Karim City College, Jamshedpur, India

Amalia Gordano Research Institute on Membrane Technology, Rende, Italy

Shaghayegh Goudarzi Nanoengineering Laboratory for Energy and Environmental Technologies, Department of Chemical Engineering, Ryerson University, Toronto, ON, Canada

Sayed Mohsen Hosseini Department of Chemical Engineering, Faculty of Engineering, Arak University, Arak, Iran

Ibrar Ibrar Centre for Green Technology, School of Civil and Environmental Engineering, University of Technology Sydney, Broadway, NSW, Australia

Elham Jashni Department of Chemical Engineering, Faculty of Engineering, Arak University, Arak, Iran

Mohammad Kahriz Centre of Excellence for Membrane Science and Technology, School of Chemical, Petroleum and Gas Engineering, Iran University of Science and Technology (IUST), Tehran, Iran

Norollah Kasiri Centre of Excellence for Membrane Science and Technology, School of Chemical, Petroleum and Gas Engineering, Iran University of Science and Technology (IUST), Tehran, Iran

M. Khayet Department of Structure of Matter, Thermal Physics and Electronics, Faculty of Physics, Complutense University of Madrid, Madrid, Spain; Madrid Institute of Advances Studies of Water (IMDEA Water Institute), Madrid, Spain

K. Khoiruddin Department of Chemical Engineering, Institut Teknologi Bandung, Bandung, Indonesia; Research Center for Nanosciences and Nanotechnology, Institut Teknologi Bandung, Bandung, Indonesia

Toraj Mohammadi Centre of Excellence for Membrane Science and Technology, School of Chemical, Petroleum and Gas Engineering, Iran University of Science and Technology (IUST), Tehran, Iran

Mrinmoy Mondal Membrane Science and Separation Technology Division, CSIR-Central Salt and Marine Chemicals Research Institute, Bhavnagar, India

Osamah Naji Centre for Green Technology, School of Civil and Environmental Engineering, University of Technology Sydney, Broadway, NSW, Australia

Kanupriya Nayak Department of Materials Science and Engineering, Indian Institute of Technology Delhi, New Delhi, India

Jasneet Kaur Pala Water Energy Nexus Laboratory, Department of Chemical Engineering, BITS Pilani-Goa, Zuarinagar, India

Hiren D. Raval Membrane Science and Separation Technology Division, CSIR-Central Salt and Marine Chemicals Research Institute, Bhavnagar, India

Anirban Roy Water Energy Nexus Laboratory, Department of Chemical Engineering, BITS Pilani-Goa, Zuarinagar, India

Soleyman Sahebi Mana Energy and Sorin Refining Company Pty. Ltd., Tehran, Iran; Centre of Excellence for Membrane Science and Technology, School of Chemical, Petroleum and Gas Engineering, Iran University of Science and Technology (IUST), Tehran, Iran

Haleema Saleem Center for Advanced Materials (CAM), Qatar University, Doha, Qatar

J.A. Sanmartino Department of Structure of Matter, Thermal Physics and Electronics, Faculty of Physics, Complutense University of Madrid, Madrid, Spain

Kayo Santana Barros Department of Materials Engineering, Federal University of Rio Grande do Sul - UFRGS, Porto Alegre, Brazil

Arun Saravanan Department of Materials Science and Engineering, Indian Institute of Technology Delhi, New Delhi, India

Supriya Sarkar The Environmental Research Group, R&D, Tata Steel, Jamshedpur, India

Tatiana Scarazzato Department of Materials Engineering, Federal University of Rio Grande do Sul - UFRGS, Porto Alegre, Brazil

Zahra Shabani Centre of Excellence for Membrane Science and Technology, School of Chemical, Petroleum and Gas Engineering, Iran University of Science and Technology (IUST), Tehran, Iran

Mohammad Sheikhi Centre of Excellence for Membrane Science and Technology, School of Chemical, Petroleum and Gas Engineering, Iran University of Science and Technology (IUST), Tehran, Iran

Soheila Shokrollahzadeh Department of Chemical Technologies, Iranian Research Organization for Science and Technology (IROST), Tehran, Iran

Senthilmurugan Subbiah Department of Chemical Engineering, Indian Institute of Technology, Guwahati, India

Gyorgy Szekely Advanced Membranes and Porous Materials Center, King Abdullah University of Science and Technology, Thuwal, Saudi Arabia

Bijay P. Tripathi Department of Materials Science and Engineering, Indian Institute of Technology Delhi, New Delhi, India

Anita K. Wardani Department of Chemical Engineering, Institut Teknologi Bandung, Bandung, Indonesia

I.G. Wenten Department of Chemical Engineering, Institut Teknologi Bandung, Bandung, Indonesia; Research Center for Nanosciences and Nanotechnology, Institut Teknologi Bandung, Bandung, Indonesia

Sudesh Yadav Centre for Green Technology, School of Civil and Environmental Engineering, University of Technology Sydney, Broadway, NSW, Australia

Syed Javaid Zaidi Center for Advanced Materials (CAM), Qatar University, Doha, Qatar

Hadis Zarrin Nanoengineering Laboratory for Energy and Environmental Technologies, Department of Chemical Engineering, Ryerson University, Toronto, ON, Canada

About the editors

Prof. (Dr.) Sanjay K. Nayak is currently the Vice Chancellor of Ravenshaw University, Odisha, India. He was the Former Director General of Central Institute of Petro-chemicals Engineering & Technology (CIPET), a Higher Technical Education Institute under Department of Chemicals & Petrochemicals, Ministry of Chemicals & Fertilizers, Govt. of India. Prof. Nayak has more than 33 years of experience in Teaching, Research, and Technical Consultancy. As a passionate educationist, Prof. Nayak holds dual PhD degree both in Science and Engineering, and also conferred with DSc degree on "Advanced Thermoplastic Composites & Nanocomposites." He has mentored more than 50 scholars for PhD program and 75 students for their MTech/ME theses. He has around 500 publications in peer-reviewed international journals, more than 300 international conference papers and several patents and designs to his credit. In addition, he has been the author/editor of 30 books/book chapters with leading international publishers. Moreover, he has been actively contributing toward indigenous technology development through funded research projects and consultancy services to the industries. He is also the recipient of many awards, like "Distinguished Scientist Award" in appreciation to his contribution to Polymer Science & Technology by Asian Polymer Association (APA), "Commendable Faculty Award" for Research in Material Science & High Citation Index (as per Scopus), National Awards for Technology Innovations in Petrochemicals and Downstream Plastics Processing Industry and Lifetime Achievement Award by FICCI/India Chem in 2018, Department of Chemicals & Petrochemicals, Govt. of India, for Distinguished Contribution to Indian Plastics Industry. He has been awarded "Honoris Causa (Honorary Doctorate)" from Utkal University and Biju Patnaik University of Technology (BPUT), Odisha, India, in 2017 and 2020, respectively. He has also been featured as one of the top 2% of the global scientists in the field of polymers in a study by Prestigious Stanford University, United States.

Dr. Kingshuk Dutta, FICS, is currently employed as a scientist in the Advanced Polymer Design and Development Research Laboratory of the Central Institute of Petrochemicals Engineering and Tech-nology, India. Prior to this appointment, he had worked as an Indo-US postdoctoral Fellow at the Cornell University, United States (2018–19) and as a national postdoctoral fellow at the Indian Institute of Technology – Kharagpur, India

(2016–17), both funded by the Science and Engineering Research Board, Govt. of India. Earlier, as a senior research fellow funded by the Council of Scientific and Industrial Research, Govt. of India., he had carried out his doctoral study at the University of Calcutta, India (2013–16). He possesses degrees in both technology (BTech and MTech) and science (BSc.), all from University of Calcutta. He was also a recipient of the prestigious Graduate Aptitude Test in Engineering (GATE) and National Scholarships, both from the Ministry of Human Resource Development, Govt. of India. His areas of research interest lie in the fields of electrochemical, bioelectrochemical and photoelectrochemical devices, water treatment, and polymers. Until date, he has contributed to 51 experimental and review papers in reputed international platforms, 25 book chapters, and many national and international presentations. In addition, he has edited/coedited two books published by Elsevier. He has also served as a guest associate handling editor for *Frontiers in Chemistry* and a peer-reviewer for over 160 journal articles, conference papers, book chapters, and research project proposals. He is a life member and an elected fellow of the Indian Chemical Society, a life member of the International Exchange Alumni Network (US Department of State), and a member of the Science Advisory Board (United States). Earlier, he held memberships of the International Association for Hydrogen Energy (United States), the International Association of Advanced Materials (Sweden), the Institute for Engineering Research and Publication (India), and the Wiley Advisors Group (United States).

Dr. Jaydevsinh M. Gohil is currently holding a scientist position at the School for Advanced Research in Polymers—Advanced Polymer Design & Development Research Laboratory (SARP: APDDRL) (Bengaluru, India), an R&D wing of the Central Institute of Plastics Engineering & Technology (CIPET). He had received his BSc degree in Applied Chemistry (Sardar Patel University) in 2000, MSc degree in Plastics Technology (Sardar Patel University) in 2002, and PhD degree in Chemistry (Bhavnagar University) in 2008. Prior to his present appointment, he had worked as a postdoctoral fellow at the University of Western Ontario, Canada (2011–14) and at the Indian Institute of Technology (IIT) Bombay, India (2009–11,) funded by the Ontario Centers for Excellence/the Natural Science and Engineering Research Council/the BioGenerator Energy Solution Inc., Canada, and IIT Bombay/DOW Chemicals, respectively. Earlier he was awarded Senior Research Fellowship from the Council of Scientific and Industrial Research (CSIR), New Delhi, India (2006–08), and during that period, he had carried out his doctoral study at the CSIR-Central Salt & Marine Chemicals Research Institute (CSMCRI), India. He had served as an assistant professor in the Department of Material Science at Sardar Patel University from August 2015 to October 2015, and later on joined and worked at Laboratory for Advanced Research in Polymeric Materials (SARP:

LARPM), CIPET, Bhubaneswar, as a pool scientist from October 2015 to November 2016. He has more than 30 peer-reviewed papers/book chapters to his credit published in international journals. His research interest includes development of membranes and membrane processes for environmental applications (water purification and treatment) and energy generation (fuel cells), design and development of novel and smart polymers, bioinspired materials, and hybrid materials for membrane molecular separation and energy generation.

Acknowledgments

To start with, we are thankful to the publisher Elsevier, Dr. Kostas Marinakis and Susan Dennis (both, Senior Acquisition Editor, Elsevier), Aera Gariguez (Editorial Project Manager, Elsevier), and the entire team of Elsevier for bringing out this book.

We are also thankful to the esteemed reviewers of our book proposal for their suggestions, inputs and final approval, as well as to the contributing authors for contributing their excellent informative chapters.

We are also grateful to Dr. Bart Van der Bruggen (Professor, Process Engineering for Sustainable Systems, Department of Chemical Engineering, KU Leuven, Leuven, Belgium; Editor-in-Chief, Separation and Purification Technology, Elsevier; and Executive Editor, *Journal of Chemical Technology and Biotechnology*, Wiley) for writing a "Foreword" for this book.

Finally, we would like to express our love and gratitude toward our family members for their continuous support and unconditional patience.

Sanjay K. Nayak
Kingshuk Dutta
Jaydevsinh M. Gohil

CHAPTER

1

Microfiltration and ultrafiltration membrane technologies

Ananya Bardhan, Aanisha Akhtar and Senthilmurugan Subbiah

Department of Chemical Engineering, Indian Institute of Technology, Guwahati, India

1.1 Introduction

1.1.1 Basics of membrane process

A membrane is a semipermeable barrier that allows selective permeation of one or more constituents in the presence of chemical potential as a driving force due to differences in pressure, temperature, and concentration across the membrane surface. The membrane separation phenomenon can be categorized based on the separation mechanism; for example, the conventional filtration processes such as microfiltration (MF), ultrafiltration (UF) are used to separate immiscible solid particles from the gaseous or liquid stream by applying differential pressure. The separation efficiency of these membranes is the function of pore size and charge of the membrane. The advanced membrane separation processes, such as reverse osmosis (RO) and membrane distillation (MD), separate the dissolved solutes from liquid and selectively allow water to pass through a membrane by diffusion mechanism. Also, few membrane separation processes combine multiple transport phenomena improving the separation efficiency; for example, both nanofiltration (NF) and electrodialysis (ED) are developed by combining the concept of membrane pore-based separation, diffusion, and charge. In the conventional membrane process (Fig. 1.1), the feed stream is divided into permeate/product and retentate/reject streams. The fraction of feed stream that permeates through the membrane is called permeate, whereas the fraction of feed stream rejected by the membrane is termed as retentate/reject.

The performance of membranes is determined based on their flux and selectivity at standard operating conditions. The flux of the membrane is defined as solvent flow rate through the membrane per unit membrane surface area. The selectivity of a membrane

Advancement in Polymer-Based Membranes for Water Remediation
DOI: https://doi.org/10.1016/B978-0-323-88514-0.00001-2

© 2022 Elsevier Inc. All rights reserved.

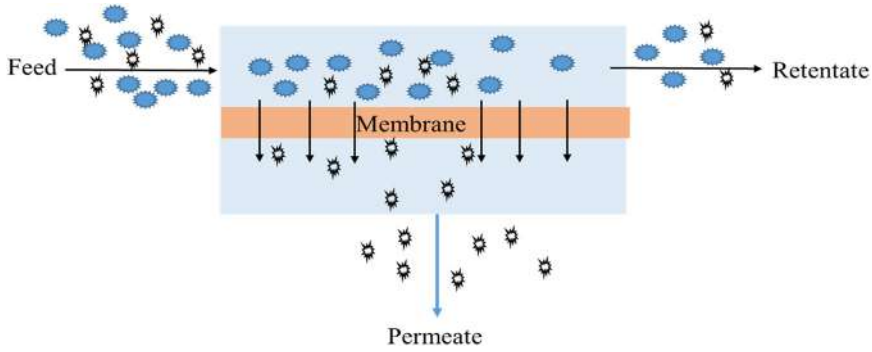

FIGURE 1.1 Schematic representation of a membrane separation process.

can be expressed in terms of retention factor (or rejection). For the liquid phase, the selectivity of a membrane is expressed in terms of retention factor (R):

$$R = 1 - \left(\frac{c_p}{c_f}\right) \tag{1.1}$$

where c_f and c_p are solute concentrations of permeate and feed streams. R is a dimensionless factor, ranging from 0 (complete retention) to 1 (both solvent and solute moves freely).

The permeation rate (or, flux, J) through the membrane is directly proportional to the driving force $\left(\frac{dX}{dx}\right)$, that is, $J\alpha\left(\frac{dX}{dx}\right)$.

Based on the driving force, the membrane processes can be further classified into (Mulder, 1991):

1. Pressure-driven membrane process (such as MF, UF, NF, and RO)
2. Concentration driven membrane process (such as dialysis, pervaporation, membrane extraction, and forward osmosis)
3. Temperature driven membrane process (such as MD and thermos-osmosis)
4. Electric potential driven membrane process (such as ED, electro filtration, and electrochemical ion exchange)

On an industrial scale, the pressure-driven membrane processes are most widely used and implemented. In the pressure-driven membrane process, the pressure gradient between the feed and permeate side acts as a driving force for permeation. In this chapter, we cover only the MF and UF processes.

The application of UF/MF for water purification is increasing due to its removable capacity of bacteria and viruses from the contaminated water sources. However, irreversible fouling is the main drawback of the membrane process compared to conventional sand filtration. The UF process can be used to remove unwanted particles that are bigger than the membrane pore size; namely viruses, color, odor, and some colloidal natural organic matter. Compared with the traditional water treatment process, the UF technology has higher processing efficiency, better treatment effect, and lower energy consumption. In many water treatment applications, to reduce the fouling intensity on the RO/NF membrane, the UF/MF process is used as a pretreatment system (Li, Jiang, & Li, 2018). The

pore size of the UF membrane varies from 1 to 100 nm, where operating pressure is in the range of 2−10 bar. UF can retain the molecules which are more significant than its pore size (i.e., molecular weight, M_w ~1000−80,000 Da) such as various proteins and viruses. Polysulfone (PSU) and polyethersulfone (PES) membranes are most commonly used for UF process.

A porous MF membrane (pore size ranging between 0.1 and 10 μm) is usually used to retain the liquid's fine suspended particles or colloids. These substances are composed of organic compounds such as emulsified oily particles and reportedly MF process can effectively remove 95% of the organic compounds (such as oil and grease) from the oily wastewater (Wang, Chen, Zhang, Yin, & Wang, 2009). In the MF process, the separation occurs by simple sieving (or size exclusion) mechanism at relatively low operating pressure (0.1−2.5 bar). The membrane materials used for the preparation of MF membranes are usually hydrophilic (or partially hydrophilic) polymers [such as cellulose acetate (CA), polycarbonate, polyimide, polyamide (PA)] or hydrophobic polymers [such as polypropylene (PP)]. Materials such as PP and polyvinylidene fluoride (PVDF) are frequently used for MF application.

1.1.2 Historical overview of ultrafiltration and microfiltration membranes

The separation and purification process is one of the critical unit operations in any chemical process to recover the desired products. Compared to conventional separation and purification techniques, the UF and MF processes are most widely used in various industries due to their benefits such as easy to use, high separation efficiency, and low energy consumption.

1.1.2.1 Microfiltration membrane

The MF membrane is used to separate impurities (such as particles, viruses, and bacteria) with a size range of 0.1−10 μm from a solvent or low molecular weight component. In the MF process, the separation mechanism is based on the sieving process. Compared to other filtration processes, the applied pressure in the MF process is relatively low (<2 bars). The first commercial application of the MF membrane was in biological and pharmaceutical manufacturing in the 1960s. MF membranes were mainly used in sterile filtration (microorganisms' removal) in the pharmaceutical industry and final filtration (particle removal) of the rinse water in the semiconductor industry. Not so stringent as in the pharmaceutical industry, MF was also used in the sterilization of beer and wine, and clarification of cider and other juices. In the mid-1980s, MF was introduced to the water treatment industry because of its cost-effectiveness in the prefiltration application. The application of MF (and UF) in water treatment gained massive momentum after the cryptosporidium outbreak in the United States in 1992. From 2000, desalination industry started using both MF and UF as an advanced pretreatment system for seawater desalination to reduce fouling potential in the RO process.

1.1.2.2 Ultrafiltration membrane

In early 1907, the UF membrane was first studied in a laboratory (or small scale) for separation applications. The first commercial UF membrane was introduced in the

mid-1960s by Millipore and Amicon (Ahmed, Balkhair, Albeiruttye, & Shaibaan, 2020). UF membrane has an asymmetric porous structure. Initially, CA was one of the primary membrane materials for preparing the UF membrane. However, due to its poor thermal/chemical stabilities, narrow pH tolerance, and high biodegradability, the other polymeric blends (such as aromatic PAs, PSU, PVDF, PES) were also employed. By the end of the 1980s, due to continuous R&D in hollow fiber and spiral-wound module configuration, the conventional tubular membrane configurations were replaced with hollow fibers and spiral-wound modules. In the early stage of UF module development, one of the prime applications of the UF process was the recovery of electrophoretic paints from rinse water. With tubular CA membranes, a remarkable amount of paints and water can be recovered from rinse water without any additional thermal or chemical stability. The UF process also plays a significant role in the dairy processing industries, ranging from recovery of protein, lactose, lactic acid from whey to concentration of milk (for dietary purposes or cheese production). Due to its wide range of applications, the UF process covers a broad spectrum of the membrane market.

1.2 Membrane science and theory

1.2.1 Solute and solvent transport through microfiltration/ultrafiltration membranes

In the membrane process, the membranes act as a semipermeable barrier that allows passage of specific components called "solvent" while restricting certain molecules in a mixture called "solute". The ability to control the rate of permeation of solvent species selectively in the membrane is one of the essential properties of the membrane.

Based on the membrane cross-sectional structure, they are categorized as symmetric and asymmetric. The symmetric membrane structure provides a uniform pore size across the membrane thickness. The asymmetric membrane has two layers, namely a dense separation layer and the support layer. MF membrane is always symmetric in nature; but to reduce solvent flow resistance in UF membrane, they are fabricated with a thick porous support layer and a thin dense separation layer. In an MF membrane, the solvent flow resistance is generated by a symmetric support layer. In contrast, in UF membranes, the dense top layer provides more resistance to solvent transport than the support layer.

Fig. 1.2 represents the possible pore geometry in a porous membrane. The membrane pores can form either a straight parallel cylindrical channel or an irregular network of channels connected internally from one end of the membrane to another. In another aspect, the membrane is made of a spherical particle, the membrane channel across the membrane thickness. In parallel cylindrical channel geometry, each cylindrical channel's length is equal and almost equal to the membrane thickness. Assuming all pores have a similar radius, the volume flux (J_v) through these pores may be described by the Hagen–Poiseuille equation:

$$J_v = \frac{\varepsilon r^2}{8\eta\tau}\left(\frac{\Delta P}{\Delta x}\right) \tag{1.2}$$

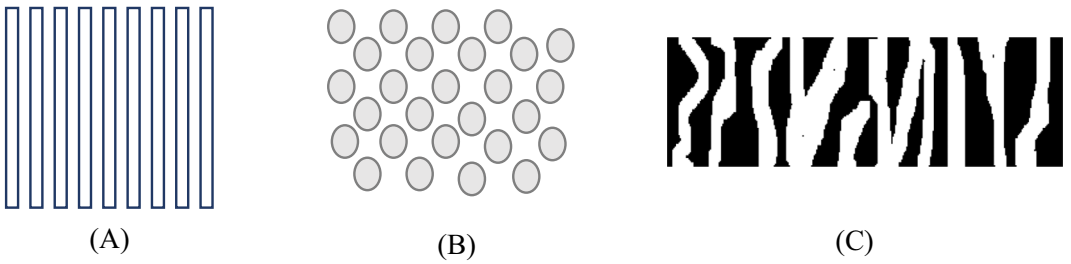

FIGURE 1.2 Characteristic pore geometry in porous membranes.

The solvent flux (J) is proportional to the driving force (pressure difference, ΔP) across a membrane of thickness Δx, and is inversely proportional to the viscosity, η. The surface porosity, ε, can be defined as the ratio of pore area to the membrane area (A_m) multiplied by the number of pores (n_p). For cylindrical pores, the pore tortuosity (τ) is equal to unity. The Hagen–Poiseuille equation provides solvent flux through membranes with parallel cylindrical pores.

Similarly, for a membrane with a system of closely packed spheres, the Kozeny–Carman equation can describe the volume flux:

$$J_v = \frac{\varepsilon^3}{K\eta S^2(1-\varepsilon)^2}\left(\frac{\Delta P}{\Delta x}\right) \tag{1.3}$$

where ε is the volume fraction of the pores; S is the internal surface area; and K is the Kozeny–Carman constant, which depends on the shape of the pores and tortuosity.

In porous membranes such as UF and MF membranes, the permeation mechanism occurs by (1) dissolution of permeating molecules in the membrane, (2) diffusion of dissolved molecules, and (3) desorption of penetrant molecules to the downstream side. The permeation also occurs due to the gradient of pressure. The transport models for the MF and UF membranes are the Knudsen flow (or Knudsen diffusion) and friction models.

Depending on the membrane material, the solvent permeation mechanism varies. The solute particle and membrane pore size determine the component that will be retained or permeated through the membrane (Fig. 1.3).

If an asymmetric membrane (or composite membrane) is used for solvent and solute separation, the solvent and solute molecule diffuses from the high to the low-pressure side. Depending upon the membrane structure, the transport of the molecules through the membrane can be explained through the friction model.

It is another approach used to describe transport through the porous membrane. This model considers porous membranes, and the solvent and solute passage occurs through both viscous flow and diffusion. In the given model, the pore size is assumed to be so small that the solute molecule cannot pass freely through the membrane pores. During transportation of solvent–solute molecule through membrane channels, the friction occurs between (1) solute molecule and pore size; (2) solvent and pore wall, and (3) solute and solvent. The frictional force (F) per mole is directly proportional to the velocity difference (or relative velocity). Here, the proportionality factor is called the frictional coefficient, f.

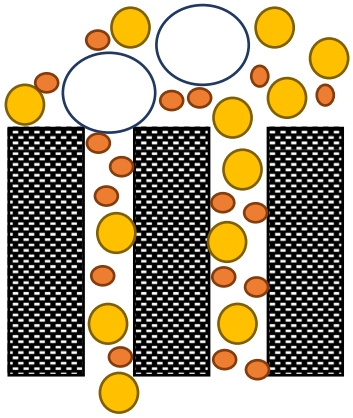

FIGURE 1.3 Permeation of solute molecules through the membrane depending on the size of the molecules.

Considering the permeation of the solvent and solute through a membrane and assuming the membrane as a frame of reference (i.e., $v_m = 0$), the frictional force between solute and pore wall can be expressed as:

$$F_{sm} = -f_{sm}(v_s - v_m) = -f_{sm}v_s \tag{1.4}$$

The frictional force between solvent and pore wall can be expressed as:

$$F_{wm} = -f_{wm}(v_w - v_m) = -f_{wm}v_w \tag{1.5}$$

The frictional force between solute and solvent can be expressed as:

$$F_{sw} = -f_{sw}(v_s - v_w) \tag{1.6}$$

The frictional force between solvent and solute can be expressed as:

$$F_{ws} = -f_{ws}(v_w - v_s) \tag{1.7}$$

The subscripts s, w, and m represent solute, solvent, and membrane, respectively. The terms f_{sm}, f_{wm}, f_{sw}, and f_{ws} represent the interaction between the solute-membrane, solvent-membrane, solute-solvent, and solvent-solute, respectively.

The frictional force per mole of solute is given by:

$$F_{sm} = -f_{sm}v_s = -f_{sm}\left(\frac{J_s}{c_{sm}}\right) \tag{1.8}$$

If we define a parameter b that relates the frictional coefficient between the solute-membrane, f_{sm}, and solute-solvent, f_{sw}, then the term b can be expressed as:

$$b = \left(\frac{f_{sw} + f_{sm}}{f_{sw}}\right) = 1 + \left(\frac{f_{sm}}{f_{sw}}\right) \tag{1.9}$$

The solute flux can be given as:

$$J_s = -\frac{RT}{f_{sw}b}\left(\frac{dc_{sm}}{dx}\right) + \frac{c_{sm}v_s}{b} \tag{1.10}$$

The coefficient for distribution of solute between the bulk and the membrane is given by:

$$K = \frac{c_{sm}}{c} \tag{1.11}$$

The fractional coefficient between the solute and solvent, f_{sw}, can be written as:

$$D_{sw} = \frac{RT}{f_{sw}} \tag{1.12}$$

where D_{sw} is the diffusion coefficient for the solute in dilute solutions.

The friction factor, b, is significant when the friction between the solute and the membrane, f_{sm}, is greater than friction between the solute and the solvent, f_{sw}.

The term solute rejection,

$$R = \frac{c_p - c_f}{c_p} = 1 - \left(\frac{c_f}{c_p}\right) \tag{1.13}$$

The relationship between rejection (R) and flux (J_v) is given as follows:

$$R = 1 - \left(\frac{c_p}{c_f}\right) = 1 - \left(\frac{J_s}{c_f J_v}\right) \tag{1.14}$$

where permeate concentration can be expressed as: $c_p = \frac{J_s}{J_v}$

By substituting $J_s = \overline{c_s}(1-\sigma)J_v + \frac{\omega\Delta\pi}{c_f J_v}$ in Eq. (1.14), we get:

$$R = 1 - \left[\frac{\omega\Delta\pi + (1-\sigma)J_v\bar{c}}{c_f J_v}\right] = 1 - \frac{(1-\sigma)\bar{c}}{c_f} - \frac{\omega\Delta\pi}{c_f J_v} \tag{1.15}$$

1.2.2 Concentration polarization

Both UF and MF membranes are porous, and separation occurs based on the size difference between solute molecule and membrane pore. These pores allow the solvent and the smaller molecules (smaller than the membrane pore size) and retain back the more giant molecules (larger than the membrane pore size). Concentration polarization (CP) is one of the essential phenomena in all membrane processes, and it cannot be nullified. It is defined as the ratio between solute concentration in the membrane surface and solute concentration in bulk solution. It usually varies between 1 and above. To reduce the fouling potential on the membrane surface, the CP should be maintained near to 1 such that deposition of fouling component can be minimized. Due to CP, the true rejection by the membrane is consistently higher than observed rejection from experimental results.

The true rejection (R_{true}) membrane can be calculated by estimating the actual concentration of solute on the membrane surface by using film theory as given below:

$$R_{true} = \left(\frac{C_{fm} - C_p}{C_{fm}}\right) \times 100$$

where C_{fm} is the concentration of solute at the membrane surface.

According to film-theory model, the solute molecules are transported toward membrane surface due to convective solvent flux across the membrane pores. But due to membrane selectivity, the solute molecules are stopped near the membrane surface, and their concentration will be increasing higher than the bulk feed concentration. Due to solute concentration differences in the CP layer, the solute molecule will diffuse from membrane surface to bulk solution. At steady state, solute balance at CP layer is given below:

$$J_s = J_v c_p - D_{AB}\left(\frac{dC}{dx}\right) \tag{1.16}$$

Boundary conditions:

$$x = 0; C = C_f, \text{and } x = L, C = C_{fm}$$

By integrating the above mass balance equation, the concentration of solute at membrane surface can be calculated as given below:

$$\left(\frac{C_{fm} - C_p}{C_f - C_p}\right) = e^{\left(\frac{J_v}{k}\right)} \tag{1.17}$$

The hydraulic/water permeability of the UF and MF membranes can be calculated by using the pure water flux data. The water flux is calculated by using permeate mass versus experimental time data. The hydraulic permeability can be calculated from Hagen–Poliseuille's Eq. (1.2) as given below:

$$J_v = \frac{n\pi r_w^4 \Delta P}{8\mu l} \tag{1.18}$$

$$L_p = \frac{J_w l}{A\Delta P} = \frac{\varepsilon r_w^2}{8\mu} \tag{1.19}$$

where J_w, r_w, n, ΔP, l, μ, A, L_p, and ε are water flux, pore radius, pore surafce density, trans-membrane pressure, membrane thickness, viscosity, area of the membrane, hydraulic permeability constant, and surface porosity, respectively.

The average hydraulic radius (r_w) can be calculated using:

$$r_w = \left(\frac{8\mu}{\varepsilon} L_p\right)^{0.5} = \left(\frac{8\mu}{\varepsilon} L_p'\right)^{0.5} \tag{1.20}$$

For the case of composite membrane, the effective thickness of the membrane is not known. Therefore the water permeability (L_p) can be calculated from the slope of the permeate water flow versus TMP.

The above-presented mass transport model for UF/MF membrane is applicable to liquid phase solvent transportation. However, in the membrane process like MD, the pervaporation solvent is transported across the micropores membrane in vapor form. The membrane transport model for vapor transport through micropores membrane is presented in respective chapters.

1.2.3 Membrane material and geometry

Cellulose acetate is the first membrane material. These cellulose materials are made of two glucose molecules, and each molecule is associated with three hydroxyl groups. The base of the UF membrane can be produced by replacing the hydroxyl group with the acetyl group. In the early days, casting of UF membrane was done by using the CA solution. The CA powder is dissolved in the acetone solution, where a small amount of magnesium perchlorate is added as a swelling agent. There is some limitation of cellulose acetated membrane specifically on resistance to chlorine. Based on the type of membrane materials used for the fabrication of the membrane, they are classified as polymeric or organic membrane and ceramic or inorganic membrane.

The polymeric membrane is reported to have the following advantages while comparing with others: relatively cheap, manufacturing is easy, and availability of a wide range of pore size. Because of these advantages, many industries use polymeric membranes for various applications such as clarification, concentration, and wastewater treatment. Apart from the merits mentioned above, there are some limitations on operating conditions (temperature, pH, chlorine tolerance) of the polymeric membrane that can hinder these membranes' application. The various other materials that are used to fabricate the polymeric membrane are PES, PA, PSU, PP, PVDF, and so on. In the early 1980s, the inorganic membrane or ceramic membrane were commercially used because of their advantages over the polymeric membrane (chemical, thermal stability, high mechanical strength). MF and UF ceramic membranes are well established and available in the market. The ceramic NF/UF membranes are under development for many applications by applying a special dense layer coating on MF membrane as porous support. The inorganic or ceramic MF and UF membrane are fabricated with a combination of inorganic materials such as kaolin, γ-alumina, titanium, α-alumina, and zirconia. Generally, the ceramic membrane thickness is in the range of 2−5 mm; but depending on the specific application of the membrane, it can vary beyond this limit. A thin film of 10−100 μm of ceramic coating is done over the symmetric porous support to fabricate the ceramic UF membranes. Even though the ceramic membranes are expected to have a long life than the polymeric membrane for high fouling causing applications, they are more expensive than the polymeric membrane, and this is observed to be the most significant disadvantage in the application of the ceramic membrane.

Depending on the membrane geometry, the UF and MF membrane configurations can be classified as flat, tubular type, spiral-wound, and hollow-fiber configuration.

The flow channels between the flat sheet membrane are in the range of 0.5−2.5 mm wide, and the diameter of the tube in the tubular membrane range from 6 to 25 mm. Both spiral-wound and hollow-fiber modules are invented to achieve a high membrane surface area per unit volume. The hollow-fiber module is widely used in UF/MF applications because it does not require a dense separation layer. But in the case of RO/NF membrane, a dense separation layer is a must, and due to the nonavailability of low-cost hollow fiber (HF) membrane with a dense layer, spiral-wound module made of flat sheet membranes are widely used in the industry. For example, Toyoba is the only supplier for hollow-fiber cellulose triacetate (CTA) membrane for commercial RO applications. And many players are supplying UF/MF hollow-fiber modules for commercial applications—GE, Dow, Hifulx, etc.

1.2.4 Mode of operation in the membrane process

Different modes of operation are adopted in the membrane separation process to improve hydrodynamics near the membrane surface—namely, dead-end, cross-flow, and hybrid-flow filtration.

In dead-end filtration mode (Fig. 1.4), the feed is tangentially pressurized through the membrane surface and permeate is collected from the other side of the membrane. In the dead-end filtration process, the solute molecules are expected to accumulate on the membrane surface; thus a stable filter cake grows in the membrane surface, resulting in an increase in solvent flow resistance through the membrane and cake layer. The accumulation of solute molecules leads to a decrease in membrane efficiency due to the clogging of the membrane's pores. Generally, the dead-end flow configuration is used in a batch separation process or lab-scale experimental setup. For example, the dead-end filtration process is used for precious metal catalyst filtration in hydrogenation reaction; silicon tetrachloride filtration in polysilicon production; the concentration of lithium fluoride, liquid food, and catalyst in aqueous solution and caprolactam production. The dead-end filtration mode needs cleaning the accumulated solutes on the membrane's surface after achieving critical flux. This mode of filtration is recommended for the solute concentration process. When the feed is less fouling in nature, a dead-end filtration mode is employed in the MF clarification process. In some of the practical applications of membrane filtration, the accumulation of renitent particle is so severe that the dead-end filtration process becomes impractical, and other mode of filtration, that is, cross-flow filtration is applied so that the tangential flow of the cross-flow mode can shear away the accumulated particles from the surface of the membrane.

In the dead-end filtration process, a high concentration of solute particles accumulates adjacent to the membrane surface, resulting in flux reduction with operating time. The dynamic flux of dead-end filtration can be calculated as given below:

$$J = \left(\frac{1}{A_m}\right)\frac{dv}{dt} = \frac{\Delta P}{u(R_m + R_c)} \tag{1.21}$$

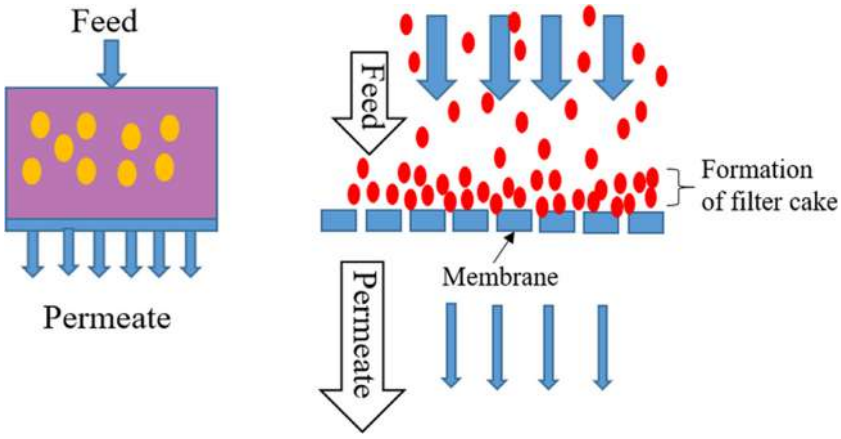

FIGURE 1.4 Dead-end filtration.

where J, A_m, ΔP, u, R_m, and $R_c(=M\alpha)$ represents the flux, membrane area, TMP, membrane resistance, cake resistance, and specific resistance, respectively.

In the dead-end filtration, the mass of the cake grows since

$$M = VC_b t \tag{1.22}$$

where C_b, V, and t represent the feed concentration, permeate volume, and time, respectively.

$$\frac{t}{V} = \left(\frac{R_m u}{\Delta P A_m}\right) + \left(\frac{C_b \alpha u V}{2\Delta P A_m^2}\right) \tag{1.23}$$

The cake resistance is dependent on the specific resistance and the specific resistance is dependent on cake voidage. It is sensitive to the structure of the cake and forces that are dominant during the formation of the cake. In the case of dead-end filtration of colloidal substances, the specific resistance is a function of the concentration of feed, initial filtration velocity, and ionic environment.

$$\alpha = 180\frac{(1-\varepsilon)}{\rho P d_p^2 \varepsilon^3} \tag{1.24}$$

In the cross-flow filtration mode (Fig. 1.5), the feed flows parallel to the membrane surface. That creates turbulence near the surface and enables better mixing of solutes between bulk feed and near the membrane surface layer. This turbulence minimizes the CP and provides optimal solvent flux, and the filtration continues for a long time without membrane regeneration. The cross-flow mode operation is widely used in all industrial membrane separation processes to reduce fouling intensity.

In hybrid-flow filtration (Fig. 1.6), both dead-end and cross-flow filtrations are combined discretely to achieve some of the specialized requirements. For example, some of MF/UF based separation processes are operated in two phases, that is, (1) filtration and (2) regeneration phase. In the filtration phase, membrane is operated either on dead-end or cross-flow mode. In the regeneration phase, membrane is flushed in cross-flow mode or backwashed in dead-end mode.

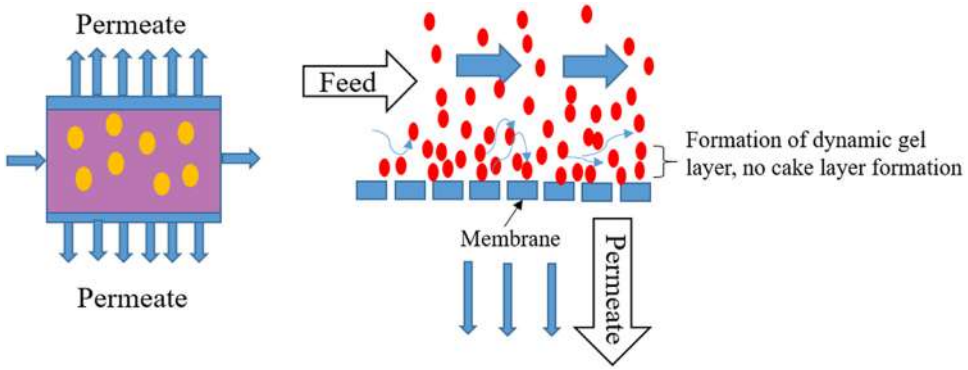

FIGURE 1.5 Cross-flow filtration.

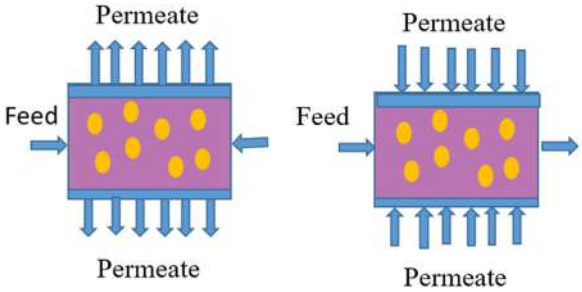

FIGURE 1.6 Hybrid-flow filtration.

1.2.5 Fouling in microfiltration and ultrafiltration membranes

The performance of the UF and MF membrane process is governed by the various models described above. All those models are derived based on the kind of interaction between membrane, solute, and solvent. In the membrane filtration process, the pore blocking leads to increased membrane resistance to filtration and reduces the flux at constant pressure operating conditions. These models are used to interpret the fouling phenomena of the membrane during the filtration operation.

The permeate flux through MF/UF membrane pores can be calculated using Hagen–Poliseuille's equation [Eq. (1.2)].

$$J_v = \frac{\Delta P}{\mu R_m} \tag{1.25}$$

where J_v, ΔP, μ, and R_m represent the permeate flux, TMP, permeate viscosity, and hydraulic resistance of the membrane. From Eq. (1.25), it is seen that resistance is directly proportional to the TMP and inversely proportional to the viscosity. When the particles are larger than the size of the pore and the active membrane area is blocked, then the complete blocking model is considered; in this case, the permeate can be increased by increasing the TMP (driving force) which is dependent on feed velocity.

Similarly, if the particles are smaller that the size of pore. Then also the fouling may occur due to internal pore-blocking. The particle enters into the pores and gets either deposited or adsorbed inside the pore wall. As a result, the pore volume reduces and then the internal pore-blocking model is considered. Here, the membrane resistance is increased due to the pore size reduction. The internal pore blocking is independent of the velocity of the feed. The fouling mechanism can be described by the partial pore-blocking model, where the particle might bridge the pore but not completely block the pore. The effect of partial pore blocking is similar to that of internal pore blocking. Another type of fouling mechanism occurred where the formation of the cake occurred on the surface of the membrane by the particle that does not enter the membrane's pores. In this case, overall resistance is the resistance offered by the membrane plus the cake resistance. The mathematical model for MF/UF process based on the above described pore-blocking mechanism is summarized in Table 1.1.

The fouled UF and MF membrane performance after cleaning can also be calculated by using the flux decay coefficient equations, flux recovery ratio, and resistance removal

TABLE 1.1 Various models of ultrafiltration and microfiltration membranes to predict the flux.

Name of the model	Mathematical model	
Complete pore blocking model	$\ln(J^{-1}) = \ln(J_0^{-1}) + k_b t$	(1.26)
Standard pore blocking model	$J^{-0.5} = J_0^{-0.5} + k_s t$	(1.27)
Internal pore blocking model	$J^{-1} = J_0^{-1} + k_i t$	(1.28)
Cake filtration	$J^{-2} = J^{-2} + K_c t$	(1.29)

J = flux with operating time; J_0 = intitial flux at $t = 0$; t = time; k = constants where subscripts "b," "s," "i," and "c" represent complete, standard, internal pore blocking, and cake filtration, respectively.

equations. Flux recovery ratio (FRR) or resistance removal (RR) can determine membrane cleaning efficiency. Cleaning efficiency can be concluded from the higher repeatability of FRR. It is better to clean the membrane when the flux decay coefficient (m) reaches approximately 90% at different operating conditions. The flux recovery (FR) can be calculated as follows:

$$\mathrm{FR} = \left(\frac{J_c}{J_n}\right) \times 100\% \tag{1.30}$$

where J_c and J_n represent pure water flux permeability of cleaned membrane and pure water permeability of new membrane.

If the value of FR is greater than 100%, it is an indication of membrane damage due to cleaning. For conventional cleaning operation, the value of FR should be lesser than 100%. After every cleaning, it is not sure that the flux can be restored to a new membrane with the current cleaning procedure. The permanent loss in the flux is calculated in terms of flux decline (FD) percentage.

$$\mathrm{FD} = \left(1 - \frac{J_c}{J_0}\right) \times 100\% \tag{1.31}$$

Therefore the addition of FR and FD should be always 100%. The membrane fouling is an unavoidable phenomenon that occurs on membrane surfaces, which leads to the decline of membrane flux. Therefore it is essential in almost all applications that the membrane is cleaned at regular intervals using appropriate advanced process control algorithms (Chew et al., 2018). Typical membrane maintenance activities are (1) physical cleaning, (2) chemical cleaning, and (3) partial or total replacement of membrane module (Lin, Lee, & Huang, 2010).

1.2.5.1 Regeneration by physical cleaning

Physical cleaning methods use mechanical forces to dislodge and remove deposits from the membrane surfaces and pores. Conventional physical methods include forward and reverse flushing, backwashing, air flushing, sponge ball cleaning, and CO_2 back permeation (Ebrahim, 1994). Unconventional methods for physical cleaning include ultrasound (Muthukumaran, Kentish, Stevens, & Ashokkumar, 2006), electrical, and magnetic fields (Tarazaga, Campderros, & Padilla, 2006). The unconventional methods are yet to be

proven in operating water and wastewater treatment plants or in domestic water purification applications.

Hydraulic cleaning is done to remove the foulant with turbulent cross-flow across the surface facing the retentate side. Backwashing is done by using reversed flow pushed from the permeate side to feed of membrane. It loosens up or dislodges the foulant from the membrane pore and losing fouling cakes and are is usually done for a membrane that can withstand reverse permeate flow to remove debris that was blocking the pores and attached sludge cake. Backwashing is more effective than forwarding flashing. The removal of short-term fouling contents like a big flock can only be removed from the membrane surface by backwashing. One of the disadvantages of the backwashing/back-flushing (Fig. 1.7) is that it requires more energy. In the back-flushing process, the deionized water (DI water) can provide better cleaning because the ions present could reduce the removal efficiency of natural organic fouling.

Air backwashing is usually not used in the UF membrane due to the size of the air bubble (100 nm−1 μm), which is double higher than the average pore size of the UF membrane. Air sardine is typically used for UF for cross-flow but not for dead-end filtration. For UF membrane, the air back-flushing is usually not preferred because the size of the air-bubble (100 nm to 1 μm), which is twice the average pore-size of the UF membrane. The disadvantage of this technique is that uniform airflow through the whole membrane is not possible. Compressed air may cause membrane damage at high pressure.

In the UF and MF membrane filtration processes, the solute concentration increases on the membrane surface, resulting in increased energy consumption due to the requirement of high pressure pumping to overcome the resistance of the fouling layer (Hilal, Kochkodan, Al-Khatib, & Levadna, 2004). The fouling of the membrane is caused by the organic molecules, inorganic materials (Na, Mg, Al, Si, P, and K), and microorganisms. The irreversible fouling takes place (compression of the cake layer, pore-blocking, or gel concentration) but it needs more energy and cleaning chemicals to clean. The cleaning efficiency is affected by the composition of the backwashing solution. In the case of UF and MF, the permeate is used as a backwashing liquid. Reportedly, it is always suggested to use DI water because ions present in permeate can reduce natural organic foulant removal efficiency.

The backwashing efficiency also depends on the foulant that it deals with and pressure applied in the permeate side. The more adhere foulant requires much higher force to remove. The backwashing can be done automatically by fixing the set point when TMP reaches a fixed set point. Back-pulsing is another physical cleaning method, widely used for ceramic membranes.

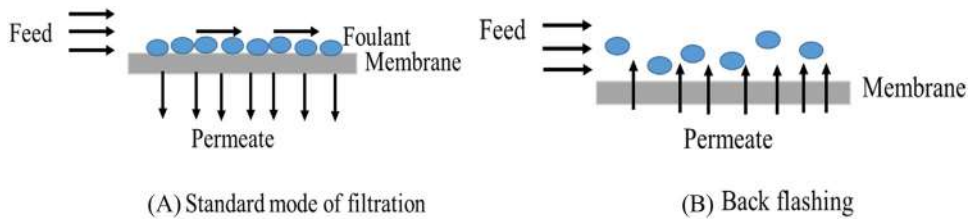

FIGURE 1.7 Schematic diagram of (A) standard mode of filtration and (B) back-flushing.

In these techniques, the TMP is inverted cyclically by pumping the permeate water in the opposite direction of feedwater flow. This phenomenon can lift the fouling layer from the membrane surface. During backwash, the permeate is pumped continuously at constant positive pressure.

Technically, the back-pulsing process is very similar to backwashing. However, the fundamental difference between a back-pulse and a back-flush is the force and time used to lift accumulated deposits off the membrane. (Ning Koh, Wintgens, Melin, & Pronk, 2008). Back pulsing is done by a series of solenoid valves to regulate the flow in the membrane module. Commonly, back-pulses are generated either based on a series of solenoid valves that regulate the flow in the module and the permeate flow from a reservoir, or a piston that moves front and forth and causes flow reversal through the membrane.

The estimation of optimum backwash pressure for MF and UF membranes is a very important aspect of achieving efficient backwash without membrane damage. In both spiral-wound and hollow-fiber modules, due to pressure drop in permeate channel/inside the fiber, the backwash flux is expected to be low at a dead end. This may result in low backwash efficiency in membrane dead end.

The backwash water temperature can be increased to achieve minimum water flux at dead by maintaining optimal back wash pressure to address this issue (Fig. 1.8).

The required water temperature and backwash temperature can be calculated by modeling the backwash process of both the spiral-wound and HF modules. The model of HF backwash is presented in the author's previous work (Sangrola et al., 2020).

1.2.5.2 *Regeneration by chemical cleaning*

Chemical cleaning involves both chemical and physical processes (Porcelli & Judd, 2010). Chemical cleaning of membranes involves three steps, namely (1) mass transfer of the cleaning chemical from the bulk solution to the fouling layer; (2) chemical reaction between the cleaning chemical and the deposits in the membrane fouling layer; and (3) mass transfer of the deposits from the fouling layer to the bulk solution, which is controlled by hydrodynamics. The efficiency of cleaning chemicals strongly depends on the chemical reactivity of the cleaning chemicals since the third step of mass transfer can take place only after the chemical reaction has weakened the deposit-membrane and deposit–deposit bonds. Optimized membrane cleaning processes require the identification of suitable cleaning chemicals, their composition, and flow conditions.

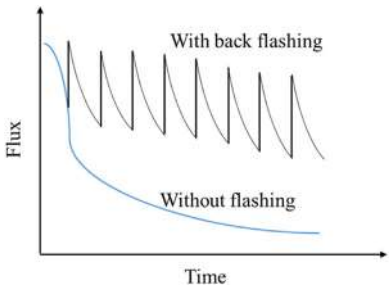

FIGURE 1.8 Effect of back-flushing.

Depending on fouling composition and dominant fouling mechanism, chemical cleaning is used. Three primary types of cleaners are as follows:

1. Acid cleaners (consisting of acid, surfactant, deformers, and inhibitors)
2. Neutral cleaners (consisting of surfactants, deformers, and enzymes)
3. Alkali cleaners (consisting of alkalis, depressing soil agent, surfactant, and oxidizers)

Cleaning agents (such as, NaOH, NaClO, HNO_3, Ultrasil) are commonly used for UF/MF membrane to remove the fouling caused by juice materials and textile effluents. In this process, an elevated temperature is advantageous as foulants are reportedly more readily dissolved at high temperatures. Therefore in addition to the physical/chemical cleaning, an elevated temperature cleaning (i.e., around 80°C) are also suggested for ceramic membranes.

However, excessive use of cleaning chemicals may also cause early degradation of the membranes. Reportedly, excessive exposure of NaClO can potentially result early degradation of PVDF membrane (Hajibabania, Antony, Leslie, & Le-Clech, 2012). If physical or chemical cleaning is unable to restore membrane flux, then partial or total replacement of membrane modules is undertaken (Regula et al., 2014). The partial membrane module replacement is recommended wherein multiple membrane modules are connected in series. The cost of water production and energy consumption increases when membranes foul/scale.

Among the above alternatives for membrane system maintenance, physical techniques are applied more frequently to regenerate the membrane. In domestic water purification applications, chemical cleaning is not a practical solution from an implementation perspective, and frequent replacement of membrane may not be acceptable. Among physical cleaning methods, it has been proven that backwashing with permeate water is robust and easy to implement in domestic water purification applications (Hajibabania, Antony, Leslie, & Le-Clech, 2012). In HF membrane backwash, the water is circulated opposite to the regular water flux direction. Many researchers have reported studies comparing membrane regeneration efficiency of physical cleaning methods. In general, membrane regeneration efficiency is estimated by comparing the membrane flux before and after performing membrane cleaning.

1.3 Membrane characterization methods

Membrane characterization leads to the determination of the membrane transport parameters and structural and morphological properties. For practical application of the membrane, the membrane surface characterization plays an important role. The surface characterization of membranes helps in understanding the properties of membrane surface; it also helps in understanding the relationship between the membrane structure and its properties. The surface characterization can be applied to study the various aspects of membrane surface properties such as chemical composition, morphology, wettability, and in case of certain specific application, (such as biomedical applications) the biocompatibility is also studied.

The membrane can be chosen for a given application based on the parameters derived from characterization methods. These methods can be categorized into two levels based on the process of implementation: (1) invasive and (2) noninvasive (Xu, Huang, & Wan, 2009).

In the invasive procedure, the membrane would not be in regular operation mode, detached from operation for offline analysis. The noninvasive procedure can be applied for both offline and online analysis. The methods used for bulk membrane polymer analysis, membrane surface properties, pore size, and pore size distribution analysis are called invasive methods. The techniques used to estimate membrane transport parameters using solvent–solute flux measurement in the actual application are called noninvasive methods. The invasive procedure is generally used in the laboratory while developing a new membrane for a given application. The noninvasive procedure is used to benchmark and monitor the different membranes for a given application.

1.3.1 Invasive methods

In this section, the characterization techniques for the polymeric membrane surfaces are reviewed on basis of the chemical composition, morphologies, and wettability of the membrane surfaces.

1.3.1.1 Chemical composition of the membrane surface

The chemical composition analysis of the membrane surface provides a brief understanding about the elements present on the membrane; and this analysis can be used to study the severity of the fouling by analyzing the fouled membrane surface such that the kind of foulant adhered on the membrane surface can be identified.

1.3.1.1.1 Attenuated total reflectance Fourier transform infrared spectroscopy

The attenuated total reflectance Fourier transform infrared (ATR-FTIR) spectroscopy is conventionally used to characterize a surface or near surface characterization of membranes. This includes the characterization of both chemical composition and physical structure on membrane surface. However, the ATR-FTIR cannot be considered as a surface-sensitive technique because this analysis is not only performed at the surface but it penetrates inside the membrane up to micron level.

1.3.1.1.2 X-ray photoelectron spectroscopy

For surface chemical analysis compared to FTIR, the X-ray photoelectron spectroscopy (XPS) method is a more surface sensitive analytical method. It provides qualitative and quantitative information on the atomic composition down to a depth of typically 0.5–10 nm depending on the take-off angle. The XPS is a technique based on a photo-electronic effect. Although XPS is surely a powerful technique for surface chemistry analysis, the samples must be stable within the ultrahigh vacuum chamber of the spectrometer. In such case, a very porous material such as a membrane with high porosity may pose problems as well as those having a solvent residue.

1.3.1.1.3 Energy dispersive X-ray spectroscopy

Energy dispersive X-ray spectroscopy (EDS) is a chemical microanalysis technique, which is often applied in combination with a scanning electron microscope (SEM). When a beam of high energy electrons is focused on a specimen, the electrons are absorbed or scattered by the specimen; and secondary electrons, Auger electrons, characteristic X-rays, and backscattered electrons are emitted from the sample during bombardment. In EDS spectra, the X-ray intensity is usually plotted against energy. They consist of several approximately Gaussian-shaped peaks being characteristic of the elements present. Most of the chemical elements used in UF and MF membranes' fabrication can be identified by EDS. The only limitation is whether the particular type of detector window registers soft X-ray of the light elements. The EDS can provide the following analytical information (Xu et al., 2009):

1. Qualitative analysis: Elements with atomic numbers from that of beryllium to uranium can be detected. The minimum detection limits vary from about 0.1 weight percent to a few percent depending on the element and matrix.
2. Quantitative analysis: Quantitative results are readily obtained without standards. The accuracy of standardless quantitative analysis is highly sample dependent. Greater accuracy is obtained using known standards with similar structure and composition as those of the unknown sample.
3. Line profile analysis: The electron beam is scanned along a preselected line aided by an SEM image across the sample while X-rays are detected for discrete positions along the line. Analysis of the X-ray energy spectrum at each position provides plots of the relative elemental concentration for each element versus position along the line. This technique is very useful in analyzing the distribution of elements on the surface or at the cross-section of a membrane.
4. Elemental mapping: Characteristic X-ray intensity is measured relative to lateral position on the sample surface. Variations in X-ray intensity then indicate the relative elemental concentrations across the surface. Maps are recorded using image brightness intensity as a direct function of the local concentration of the elements present. Lateral resolution of about 1 μm is possible.

1.3.1.2 Morphologies of the membrane surface

To study morphology of polymeric membranes, X-ray diffraction, neutron scattering, and microscopy technology are few available techniques. In this section, we will briefly discuss about the basic principles of some of the widely used techniques used for characterization of the surface morphology of the polymeric membranes such as SEM, environmental scanning electron microscopy (ESEM), and atomic force microscopy (AFM).

1.3.1.2.1 Scanning electron microscope

For characterization of membrane surface, SEM is the most widely recognized electron microscope. SEM unit contains an electron gun that supplies the electron beam, a series of condenser lenses to manipulate the electron beam path, some scanning coils for scanning control, a sample chamber to hold the sample, and a set of detectors to collect the signal. The electron beam is generated and accelerated by the electron gun as a divergent beam, reconverged and focused by the condenser lenses, and finally made into a beam scanning

across the sample. Each kind of particle and electromagnetic wave can be a potential signal available to form the image of the focused surface. The SEM is a widely used characterizing technique due to the following advantages:

1. For SEM analysis, the specimen can be directly taken from the sample without further procedure. If the sample is a nonconducting material, the sample needs an additional metal (usually gold) coating. And this is the case for most of the polymeric materials used for membranes unless their surface charge has been modified.
2. Magnification can be modulated to a wide range continuously. Using SEM, even at high magnification, the images with good resolution and enough brightness can still be obtained.
3. High resolving ability: The wavelength limitation of the optical microscope is about 200 nm, but it is not difficult for the SEM to reach a resolution as good as below 10 nm.

The SEM is now a nearly a standard tool for investigating surface properties of membranes, including the surface topography, the change of surface by modification, the adsorption of biomacromolecules, fouling, and so on. The SEM is also applied in the observation of the cross-section of the membranes. Cross-section investigation is extremely useful for characterization of the asymmetric membranes and complicated membranes. By the surface and cross-section investigation of an SEM, basic parameters such as thickness and pore diameters can be decided. Because the imaging area of the SEM is rather tiny, the measurement of pore diameter using a single SEM unit may lead to error in measurement. Therefore it is recommended to use average of multiple SEM images.

To analyze the polymeric membranes with SEM/FESEM, the sample should be first washed with ionized water and dried at vacuum oven at 50°C−60°C. To get cross-sectional morphology, the membranes sample must be raptured in liquid nitrogen. For polymeric membranes, the sample needs to be electroconductive for current, using gold/palladium/platinum metals. Drying of wet membranes requires a freeze-drying treatment. Another choice is to replace the water in the membrane by liquid with low surface tension to avoid the destruction by the capillary force. For the preparation of a cross-section sample, a freeze-fracturing operation is required to prevent the deformation of the porous structure.

1.3.1.2.2 Environmental scanning electron microscopy

In contrast to SEM, the ESEM can operate even at a pressure as high as 50 Torr, or at a temperature as of the specimen environment through a range of vacuum, temperature, and gas compositions. ESEM has low sensitivity to contaminants, that is, a sample with water, volatile materials, or gaseous emissions can also be investigated. It can provide a saturated vapor environment for a hydrated specimen. In ESEM, state of samples need not to be fixed. Thus a dynamic process such as tension and deformation can be recorded as a sustaining course. Unlike SEM in ESEM the samples need not to be charged/ conductor. This elimination of charging the sample (using metal coat) preserves the delicate sample surface. The only limitation of this process is the limited resolution, therefore ESEM is unsuitable for obtaining membrane images with fine structure.

1.3.1.2.3 Atomic force microscopy

For polymeric membranes, an AFM (Fig. 1.9) is a prominent characterization tool capable of revealing the surface structure of membranes with superior spatial resolution. From

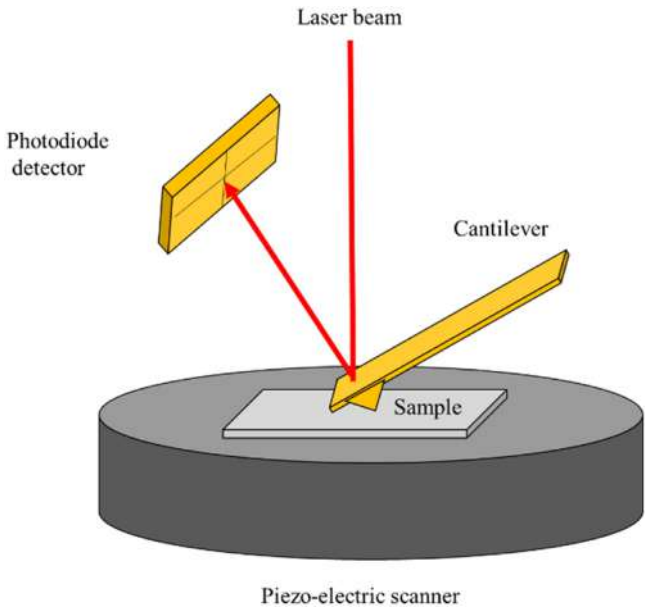

FIGURE 1.9 Schematic representation of an atomic force microscopy (AFM).

the tens of microns to nanometers, an AFM has been developed into a multifunctional technique suitable for characterization of the adhesion, mechanical, topographic, and other similar properties.

An AFM can be operated in various mode developed and adapted to cope with the demand of the field-specific research. Taking consideration of the scope of this chapter, this section presents only some of the most popular modes of AFM operation for polymeric membranes such as contact mode, noncontact mode, and amplitude modulation or dynamic force mode. In contact mode, since the tip of the AFM is in constant contact with the sample surface, a significant frictional force can potentially damage, destroy, or sweep soft samples like polymers or biological macromolecules. Thus, a noncontact mode of widely adapted for polymeric membranes. However, the only disadvantage of this mode is that the image comes with low lateral and z-resolution compared to the contact mode. To overcome this issue, the amplitude modulation or dynamic force mode is advised. In this mode, the tip of the AFM vibrates above the sample surface; and this method also enables the contact with the sample surface for a very short period and that ensures no damage to the sample surface. This mode provides nondestructive nature of the image.

1.3.2 Noninvasive methods

1.3.2.1 Inline method

The inline method (Fig. 1.10) is used to monitor the overall UF/MF membrane plant's performance in real time by measuring the feed temperature, solvent, solute flux, and pressure drop data in an actual plant.

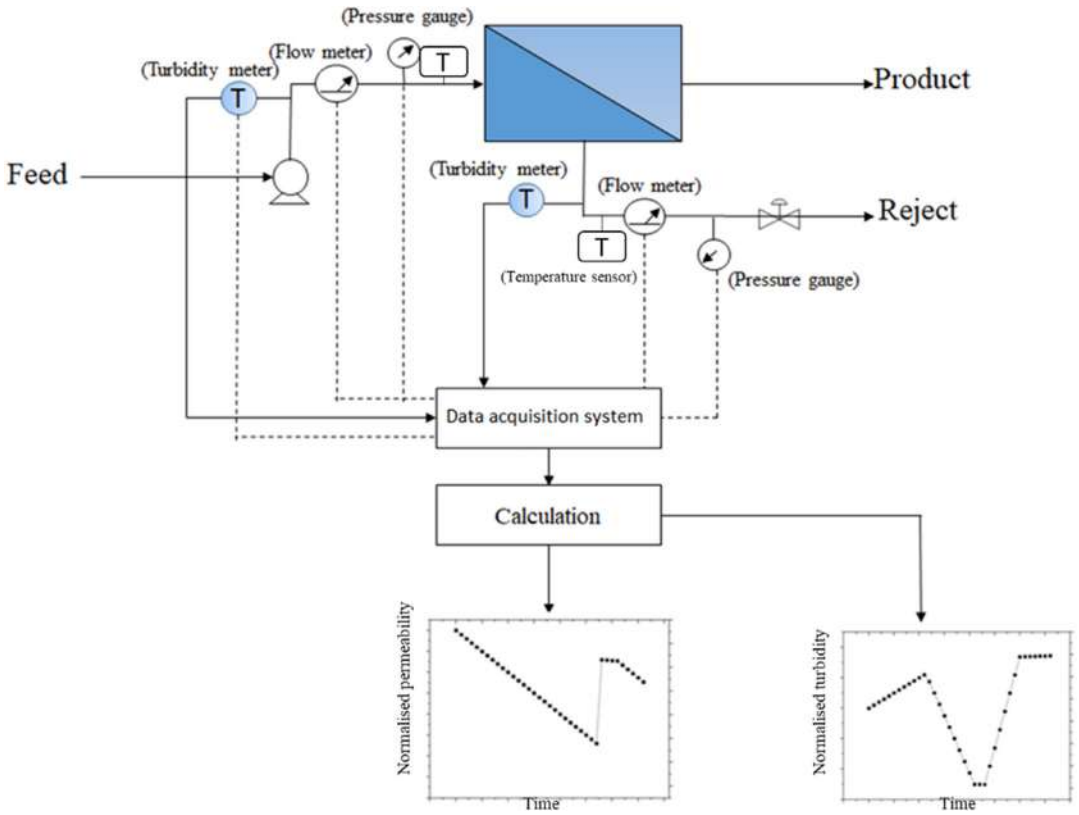

FIGURE 1.10 Schematic representation of an inline method.

The measured data is stored in the data acquisition system, and then they are used to calculate the membrane transport parameter such as normalized membrane permeability and selectivity by using the equation presented in Section 1.1. The calculated membrane transport parameters are displayed to plant operators. Apart from the conventional sensor listed above, the advanced sensor like the ultrasound sensor is used to measure the thickness of the fouling layer at the membrane surface in real time, such that the membrane health can be analyzed in real time to rectify the severe membrane fouling that may lead to permanent damage of the membrane. The use of such a sensor may not be economical for smaller capacity MF/UF plants. Therefore methods like at-line and offline are adopted to monitor the membrane performance in the discrete interval.

1.3.2.2 At-line method

For small-scale membrane application, the at-line method is preferred (Fig. 1.11). In this method, the performance of the membrane is characterized by manual sampling, followed by discontinuous sample preparation, measurement, and evaluation. A small membrane test cell is placed parallel to the actual UF/MF process line in this method. The test cell

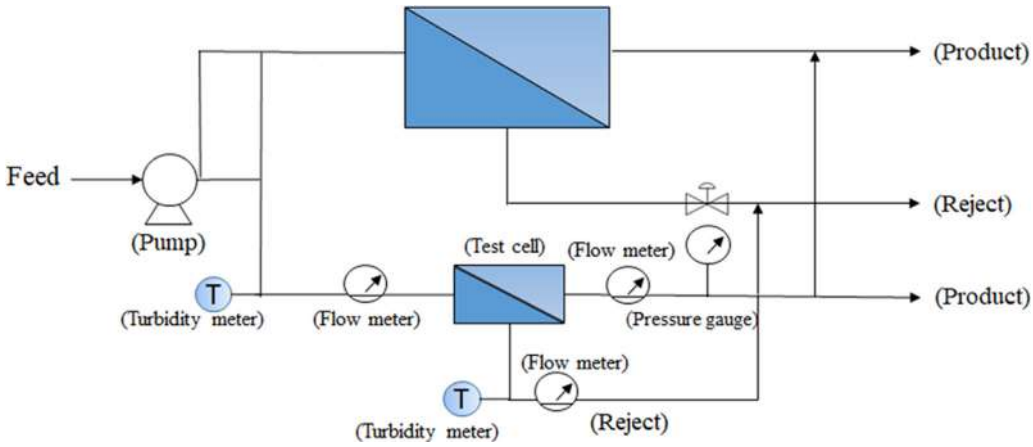

FIGURE 1.11 Schematic representation of at-line method.

operating condition is maintained as similar to the actual plant. Here, the membrane performance is measured in terms of solute/solvent and pressure drop.

The given information is obtained manually using the data obtained from turbidity, flow rate, and pressure gauge. In this method, direct process control is not possible since the material properties can usually change between sampling time and the availability of the results.

1.3.2.3 Offline method

For laboratory test scale setup, the offline method is preferred to characterize the properties of a new membrane. To determine membrane performance, two modes of testing are conventionally preferred, namely dynamic and static. In dynamic experiments, the feed is continuously pumped along the membrane in a cross-flow mode. On a small scale, though the recovery is slight, the solution composition changes insignificantly along the length. This is a well-defined method of estimating fouling (and biofouling) for MF, membrane bioreactor (MBR), and forward osmosis (FO) membrane process on a small (or laboratory) scale. In this method, after the membrane is mounted in a filtration cell, deionized distilled water is passed through the cell till constant flux is obtained. After which, the feed solution with foulants is allowed to flow through the membrane for a certain period. After that again, the feed solution is replaced with deionized distilled water. In between these processes, chemical and mechanical cleaning is also performed. The difference between the membrane permeability and rejection before and after the filtration, washing, and cleaning steps serve as an essential indicator of fouling, its reversibility, and cleaning efficiency. Another prime indicator of fouling is change in permeability. This can be analyzed using the mathematical models to conclude about fouling mechanism (that includes pore blocking, intermediate pore blocking, cake filtration, and pore constriction).

1.4 Module design and process configuration

1.4.1 Module design

The polymeric membranes are fabricated as either flat-sheet or hollow fiber with a single channel. Similarly, the ceramic membranes are fabricated as: (1) single channel (2) multichannel membrane. These membranes are further modularized to achieve a high membrane surface area per unit volume of the membrane module/element. The primary objective of modularizing a membrane is to pack a large area of the active membrane into a relatively small volume (but with high packing density) while maintaining system hydraulics to minimize CP, fouling, and scaling. The four basic membrane module configurations are demonstrated for polymeric membranes: (1) plate-and-frame, (2) spiral-wound, (3) hollow-fiber, and (4) tubular membrane module (Warsinger et al., 2018).

1.4.1.1 Plate-and-frame membrane module

The plate-and-frame membrane module consists of several "plates" placed one after another, maintaining a spacing using a sealing gasket between two adjacent frames. A plate has two parallel perforated membranes supported by a gap between them. A flat membrane is fitted on each perforated support layer, and every plate has an opening near the perimeter, which leads to permeate channel. Here, the feed flows over each membrane and permeates through the membrane leaving through permeate channel. Here the feed and permeate channel is separated by the polymeric spacers. The packing density of such modules is about 100−400 $m^2\ m^{-3}$.

1.4.1.2 Tubular module

In the tubular membrane (Fig. 1.12), the feed solution always flows through the center of the tubes while the permeate flows through the porous supporting tubes into the module housing. The packing density of the tubular membrane ranges between 164 and 328 $m^2\ m^{-3}$ (Hoek, 2013). The tubular modules are expensive due to the module's low surface areas, but the increased surface area can reduce costs.

1.4.1.3 Spiral-wound module

The spiral-wound module design of the membrane module spacers is used and operated under the turbulent flow condition. In the spiral-wound design, the pressure drop is high due

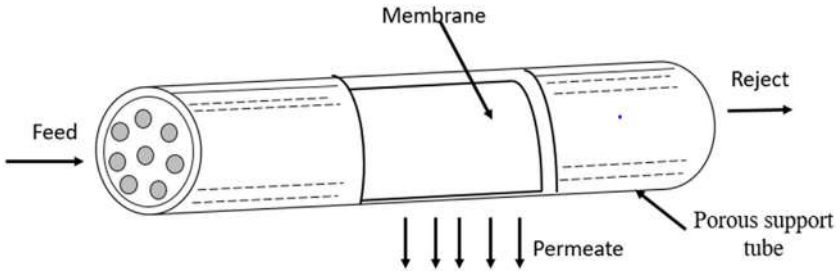

FIGURE 1.12 Schematic diagram of a tubular membrane module.

to the additional drag force generated by the spacer. The surface-to-volume area ratio is fair with low capital cost. For the filtration process of feed with minimum suspended particles, spiral-wound design membrane modules can be used. The membrane modules are selected for a particular application process depending on all these properties.

In a spiral configuration (Fig. 1.13), the flat membranes are rolled around the perforated center tube. In the spiral-wound membrane module, two membrane sheets are separated by a mesh-like spacer in between them. Here, the three edges are glued using epoxy, leaving the fourth end of the membrane open to a perforated cantered tube. The feed enters one end of the spiral and leaves at the other end. The permeate flows spirally through the permeate passage and enters through the holes on the central pipe, and leaves through an end of a pipe.

1.4.1.4 Hollow fiber/shell and tube module

A hollow-fiber membrane module (Fig. 1.14) can be defined as a bundle of many fibers inserted into a pipe of suitable diameter. In these membranes, the semipermeable nature of the capillary walls is utilized to flow the permeate. The hollow-fiber membranes are made from synthetic polymers, cellulose. The cellulose-based hollow fibers of the membranes are generally made of CTA. Due to the small fiber diameter, the fibers can withstand high (internal or external) pressure without any support. Compared to the above-discussed membrane module, the fouling is more frequent in the hollow-fiber membrane module due to fiber size and high packing density.

The economic consideration for any process primarily determines the basic concept behind the selection of the membrane module. However, apart from cost, membrane functionality plays a significant role in selecting the membrane module. For example, despite the expensive configuration, the tubular configuration is always best suited for application

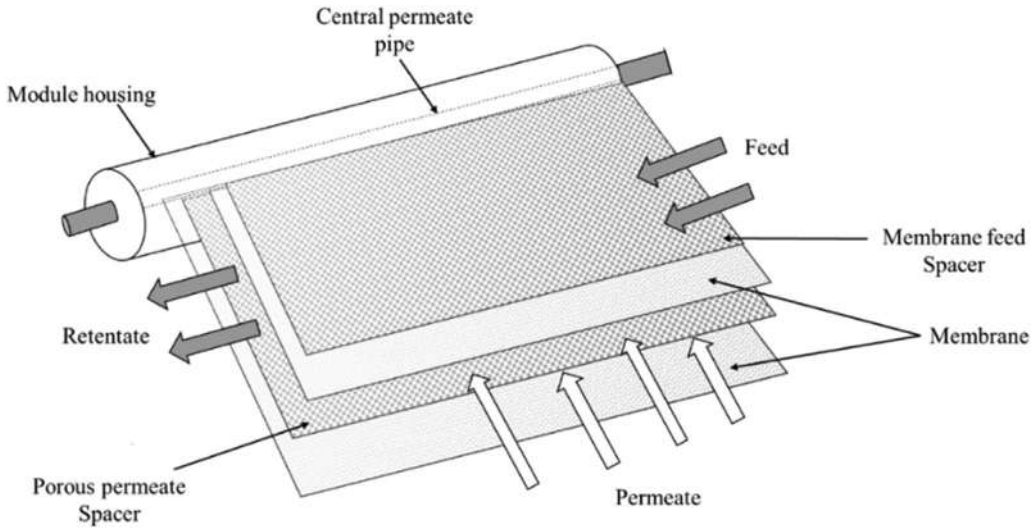

FIGURE 1.13 Schematic diagram of a spiral-wound membrane module.

with high fouling tendency because of its ease of membrane cleaning and good process control. It is often possible to choose between two or more types that are cumulatively used in practical application. For example, for desalination, gas separation, and pervaporation, both hollow-fiber and spiral-wound membrane modules are used. Table 1.2 provides a brief comparison among the above-mentioned membrane module design (Meneses, Stratton, & Flores, 2017).

1.4.2 Process configuration

For UF and MF membrane, the mode of operation and design is dependent on the membrane process's application. The continuous, batch and feed-and-bleed/fed-batch membrane process flow configurations are widely used in the industry concerning an application. In the membrane filtration process, two types of process flow configurations are adopted to increase the process's recovery; namely, single and multipass stage processes. Similarly, to improve the permeate water quality, the permeate collected from the first stage is treated again. This configuration is called a multipass system. Fig. 1.15 represents the single-pass and batch-type configuration of membrane filtration.

1.4.2.1 Continuous filtration process

In the continuous filtration process, the feed solution passes along the feed channel of membrane modules, and the permeate is collected in the permeate channel under applied feed pressure. It is one of the most straightforward membrane configurations.

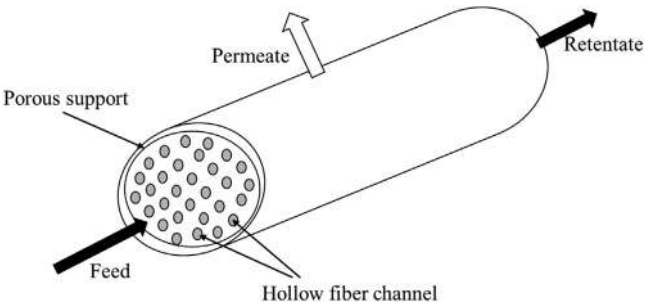

FIGURE 1.14 Schematic diagram of a hollow-fiber membrane module.

TABLE 1.2 Comparison of different membrane module designs.

Module design	Packing density ($m^2\ m^{-3}$)	Expected cost/area	Is pretreatment required?	Fouling efficiency	Is back-flushing possible?
Plate-and-frame	Moderate (200–400)	High	No	Medium	No
Tubular	Low (100–300)	High	Yes	Low	No
Spiral-wound	Moderate (300–1000)	Low	Yes	Medium	No
Hollow-fiber	High (1000–10,000)	Low	Yes	High	Yes

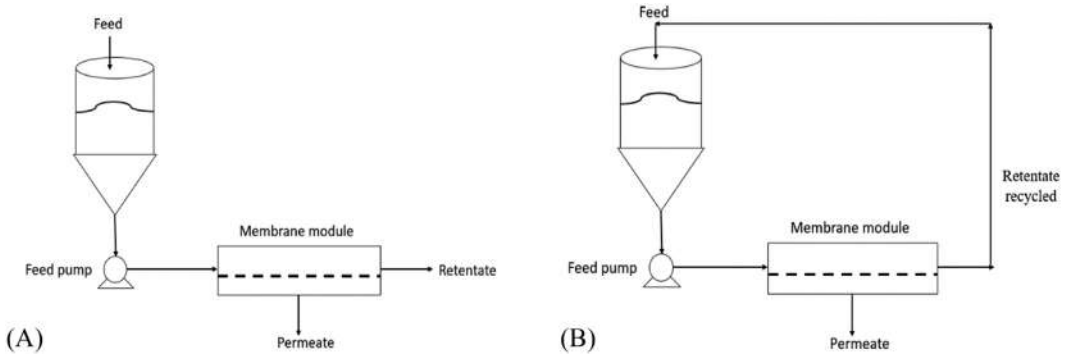

FIGURE 1.15 Schematic diagram of (A) single-pass membrane configuration and (B) batch-type configuration of membrane filtration.

1.4.2.2 Batch filtration

In the batch-type configuration (Fig. 1.15) of the membrane filtration process, the retentate is recycled back to the feed tank. Here, due to the recycling of the retentate to the feed tank, the retained solute concentration in the feed tank increases with time. The membrane flux declines with time because of the high concentration of feed, resulting from the recycling process of the retentate to the feed. In the batch process, the permeate recovery is smaller than in the single-pass process. The UF and MF batch filtration process can be used in small-scale and in the pilot plant application where permeate is the final product. The batch filtration is applied in various filtration processes such as effluent treatment and fruit juice filtration. But the batch process is not applicable when the concentrate is the product, because in the batch process, the concentrate is discarded. The constant recirculation of the retentate may result in the degradation of the final product.

1.4.2.3 Feed-and-bleed/fed-batch filtration

In feed-and-bleed/fed-batch filtration configuration, either:

1. a part of the retentate is recycled, and the remainder is separately collected, or
2. this collected retentate is used as feed for the next stage when the multistage operation is performed.

A feed-and-bleed configuration design is used in the multistage filtration operation process to reduce the required membrane area. These configurations are primarily applied in the large-scale commercial application process.

1.4.2.4 Single and multistage

In the multistage filtration process (Fig. 1.16) where a single pass has been applied, the reduction in volume loss is made by arranging the membrane module in a tapered design. In this system, the volume reduction factor is measured by the tapered structure, not by the pressure applied in the filtration process. The tapered structure is known as the Christmas tree design. In water recovery by UF membrane filtration, the permeate recovery is greater than 90% because CP is less due to water's high purity.

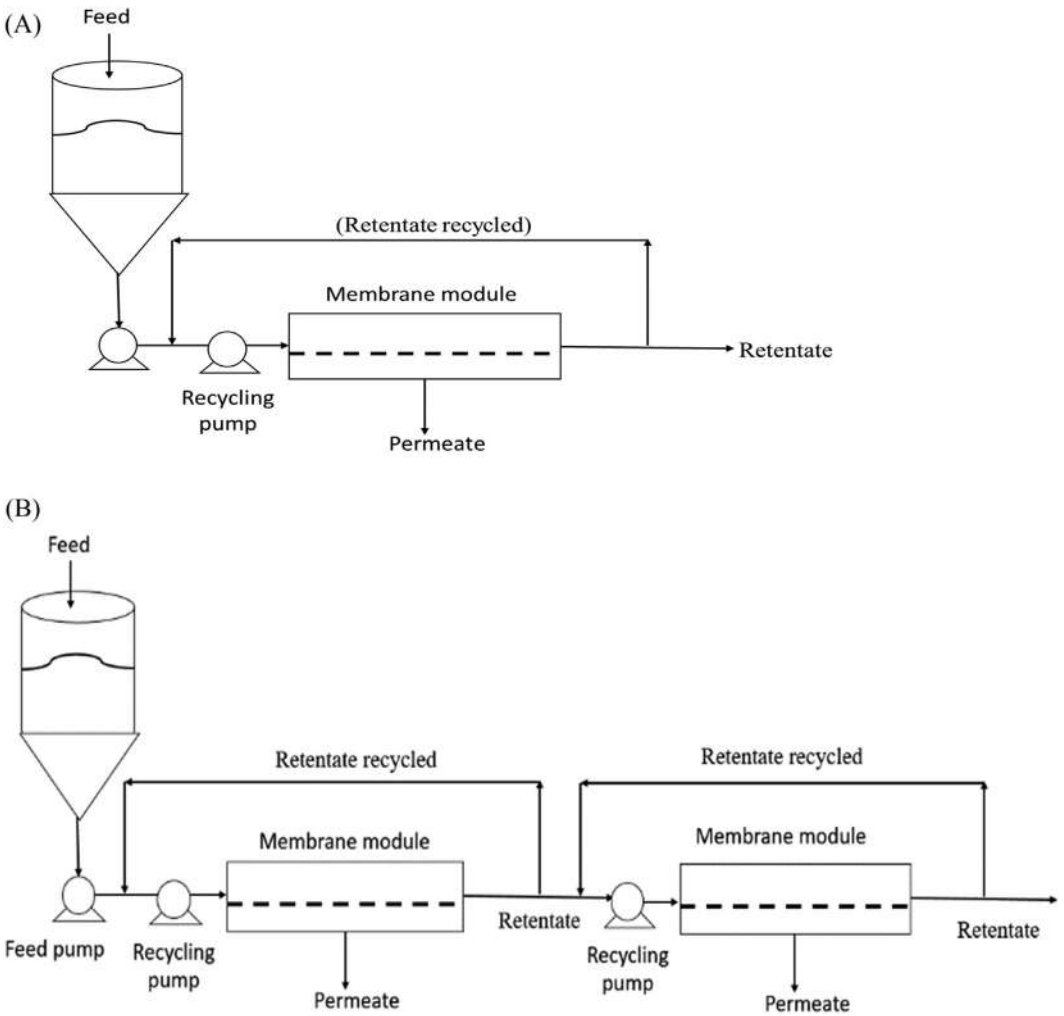

FIGURE 1.16 Schematic diagram of feed-and-bleed/fed-batch type configuration of (A) single-stage and (B) multistage.

1.4.2.5 Single and multipass

The single-pass UF membrane process (Fig. 1.17A) is used to recover high purity water in microelectronic plants. When the feed of nonhigh purity is used for filtration through single-pass membrane configuration, it requires a larger membrane area to achieve high permeate (95%–99%) recovery, resulting in high energy consumption. To minimize the CP and foul, the feed velocity increases and increases the pumping cost. In multipass UF membrane process (Fig. 1.17B), the permeate from the first pass becomes the feed water to the second pass, producing much higher permeate qualities.

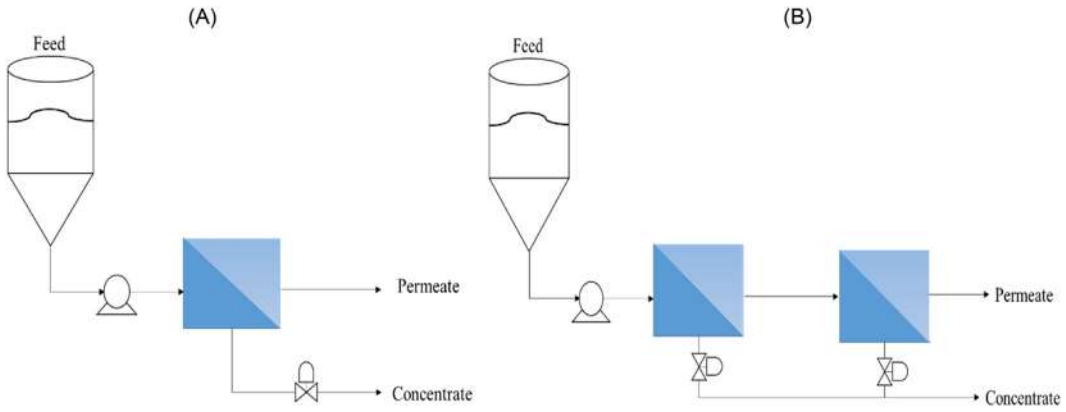

FIGURE 1.17 Schematic diagram of feed-and-bleed/fed-batch type configuration of (A) single pass and (B) multipass.

1.4.3 Commercial fabrication techniques employed for polymeric flat sheet and hollow-fiber membranes

1.4.3.1 Flat-sheet membranes

The casting technique is one of the well-established phase inversion techniques and is widely used to prepare flat sheet polymeric membranes. In this technique, first, a polymer is dissolved in a suitable solvent or a mixture of solvent and nonsolvent (in phase inversion) to form a homogeneous dope solution. As shown in Fig. 1.18, the dope solution is cast on a suitable support (glass or nonwoven polyester sheet) using a casting knife. The casting knife is made of a metal blade moving on two runners providing a sufficient gap between the blade support layers. The gap primarily determines the thickness of the membrane produced. The casted film is instantly dried, or the solvent is partially evaporated before the cast film is immersed in the coagulation bath. More than one coagulant bath is used with an appropriate temperature controller to control solvent evaporation rate, enabling a uniform pore size membrane. Finally, membrane is dried before packing them in the rolling unit. The resultant membrane can be used in commercial plate-and-frame and spiral-wound membrane systems (Membranes et al., 2019).

1.4.3.2 Hollow-fiber membranes

Compared to the flat-sheet membrane, the HF modules offer several beneficial features such as self-supporting property, good flexibility, and large specific surface area. Owing to the large surface area and high packing density, the unique configuration of HF membrane endows excellent mass-transfer properties, thus promoting numerous commercial applications in water and wastewater treatment. The hollow-fiber membrane can offer a significantly reduced footprint and equipment mass in comparison to a flat sheet membrane casting unit. (Moattari, Mohammadi, Rajabzadeh, Dabiryan, & Matsuyama, 2021) identified the standard fabrication method for HF membranes. It includes nonsolvent-induced phase separation (NIPS) as a wet spinning method,

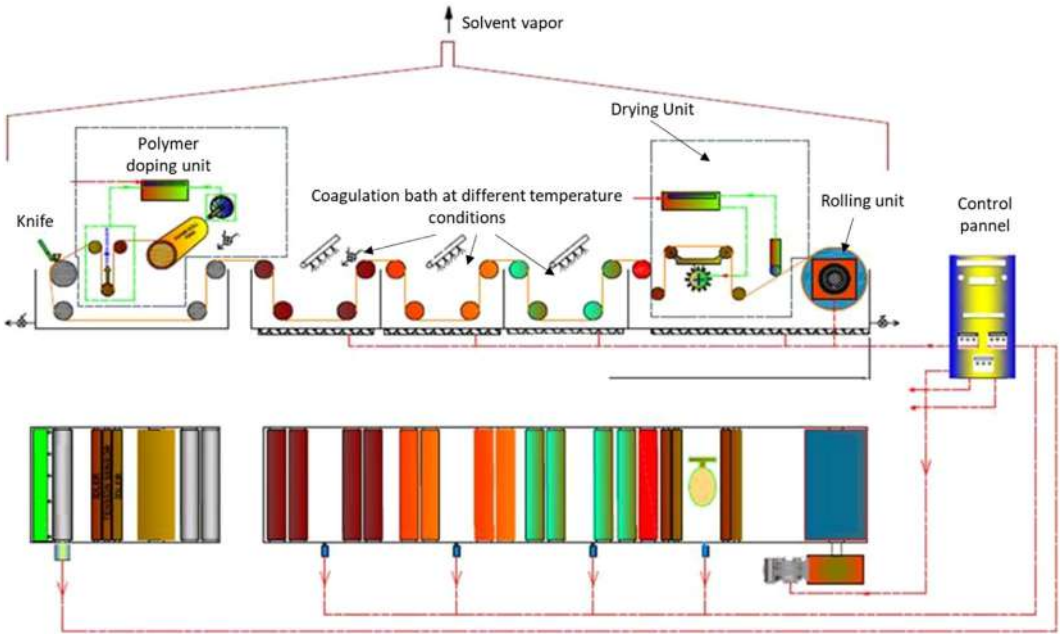

FIGURE 1.18 Flat-sheet membrane casting system.

thermally induced phase separation (TIPS), and melt-spinning cold stretching (MSCS) method. Reportedly, the TIPS and NIPS methods are commonly employed for HF membrane fabrication on a commercial or large scale. Compared to the NIPS method, the MSCS and TIPS method offers a more compact structure and narrow pore-size distribution in the cross-sectional direction of the membrane with better mechanical properties. Typically the primary material used in HF membranes fabrication includes the dope solution and bore fluid. The dope is a viscous solution prepared by mixing a polymer resin, additive, and an organic solvent for the polymer being used similar to flat sheet casting. Some of the commercial polymeric resin and organic solvent used are stated below:

1. Polymeric resin: PES, polyacrylonitrile, polyimide, PA-imide, polyvinylchloride, PSU, polyesterimide, and polyvinylidene difluoride.
2. Organic solvents: dimethylacetamide (DMAc), *N*-methyl pyrrolidone (NMP), dimethylformamide (DMF), or a mixture thereof.

The additives used in a dope solution can be categorized as (1) low molecular weight additives such as water, ethylene glycol, alcohol, glycerol, and inorganic salts ($LiClO_4$ and LiCl); (2) high molecular weight additives such as polyethylene glycol (PEG), and polyvinylpyrrolidone (PVP); and (3) additives such as a mixture of LiCl and water or PEG and LiCl.

Fig. 1.19 depicts an NIPS HF spinning line used for the fabrication of polymeric HF membranes. Initially, dope solution and bore fluid are metered through various

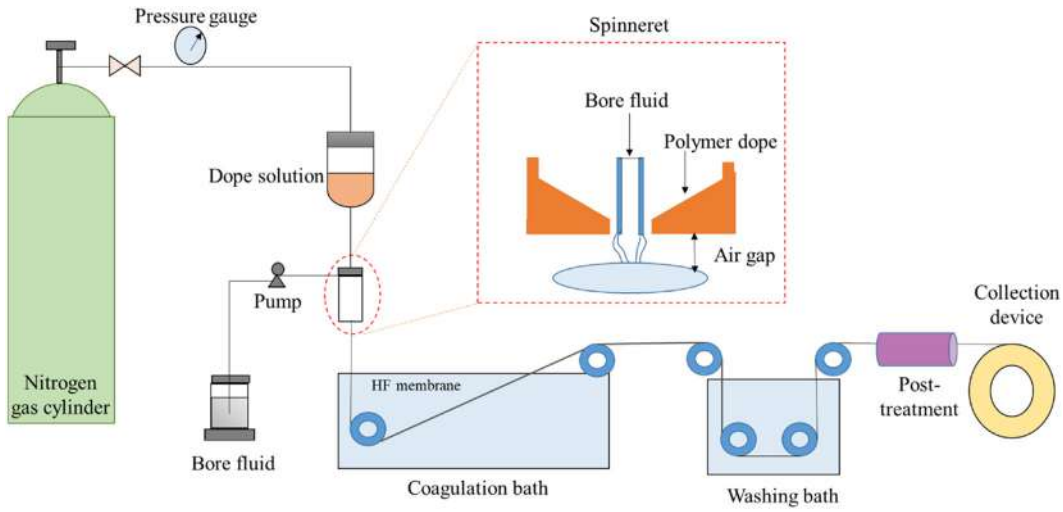

FIGURE 1.19 Nonsolvent-induced phase separation (NIPS) Hollow fiber (HF) spinning line for fabrication of polymeric HF membrane.

precision pumps followed by the extrusion through the spinneret. In this step, internal coagulation may occur during the dope contact with the bore fluid flowing out the Spinneret. Reportedly, solvent evaporation densifies the outer surface of the emerging fiber in the air gap, and the moisture triggers phase separation. The fiber is stretched due to the longitudinal tension and gravity by the take-up winder during the air-gap distance. An external coagulation bath is used to complete the phase separation, and the as-spun fibers are solidified. The as-spun fibers are collected using a roller. The roller speed plays a critical role in determining the take-up speed of the spinning process, solvent exchange, or any appropriate posttreatment to remove the residual solvents/additives.

The membranes fabricated using NIPS methods are usually asymmetric membranes with dense skin and porous support layers. These membranes exhibit high permeability, excellent separation performance, superior anti-fouling properties but poor mechanical strength. Apart from NIPS, another conventional method used for the fabrication of HF membrane is TIPS. Unlike NIPS, in TIPS, the mechanism of phase separation is achieved using thermal removal from high-temperature homogeneous polymer solutions. The membranes fabricated using this method have homogeneous pore structure, that is, uniform pore size and narrow pore size distribution. Thus it is challenging to produce acceptable permeation performance for industrial water treatment.

The UF/MF HF membranes are generally fabricated through the immersion precipitation method. The HF membrane has high permeability but suffers from low mechanical strength. To take care of this limitation, researchers suggested reinforced HF membranes. Typically, reinforced HF membranes are prepared by integrating the separation layer with a porous supported matrix. The comparison of different reinforced methods is tabulated in Table 1.3.

TABLE 1.3 Advantages and disadvantages of methods of reinforcing the hollow-fiber membranes.

Sl. No.	Reinforced method used for HF membranes	Advantages	Disadvantages
1.	Porous matric reinforcement	• Typically exhibit a tensile strength of more than 10 MPa • Provides mechanical strength without adverse effect (such as being dissolved and swelled)	• Dissolution/swelling of the porous support layer due to penetration of the casting solution in homogenous reinforcement method • The heterogeneous reinforcement fabrication process is very costly and complex
2.	Applying filaments or threads	• A relatively facile and low-cost fabrication process	
3.	Braid reinforcement	1. NIPS-based braid reinforcement • Easily applicable on an industrial scale • A wide range of tensile strength • Possibility to use a variety of braids	• The fabrication of round-stable braids on braiding machines is a slow and costly operation • Achieving a uniform polymeric coat on the braid is difficult • Low peeling strength for heterogeneous-braid reinforced HFMs • The possibility of biofouling formation
		2. Electrospinning-based braid reinforcement	The limited control of pore structure

1.5 Application of polymeric ultrafiltration and microfiltration membranes

UF/MF is a low-pressure operation; it reduces the capital and operating expenditure significantly. Additionally, these are low-temperature rate-governed processes and driven by the pressure differential across the membrane. Also, there is no state of equilibrium, that is, no change in phase or state of the solvent during membrane operation. Therefore the membrane separation technology is advantageous over the conventional dewatering processes with respect to huge energy (steam, electricity, etc.) as well as utility (cooling water to run condensers) consumption. The requirement of space as well as complicated heat transfer, heat generation, and steam generation equipment is minimum, which also reduces the thermal pollution as well as load in the sewage treatment plant. Table 1.4 summarizes the application of polymeric UF/MF membranes in water and wastewater treatment process.

1.5.1 Potable water reuse

Membranes, particularly polymeric membranes, play a crucial role in the purification of municipal wastewater to potable quality and are the core of almost all these systems

TABLE 1.4 Application of polymeric ultrafiltration (UF) and microfiltration (MF) membranes for water and wastewater treatment.

Sl. No.	Application	Membrane module/MWCO	Membrane material	Membrane nature	Membrane process	Recovered product	References
(i)	Textile dye wastewater	Tubular module/ >700 Da	Polysulfone	Hydrophobic	UF	>97% dye (direct green G, direct black metal, eriochrome black T) (M_w > 780)	Majewska-Nowak, Winnicki and Wiśniewski (1989)
		Flat-sheet	Polysulfone/ Polyetherimide	Hydrophobic	UF	68.5% and 64.7% rejection of acid-orange and methyl orange, respectively	Said, M'rabet, Hsissou and Harfi (2020)
		Flat-sheet/10 kDa (Cross-flow UF)	Regenerated cellulose	Hydrophobic	UF (MEUF)	>97% retention of anionic surfactants	Zaghbani, Hafiane and Dhahbi (2007)
		Flat sheet/1000 Da	Polyamide	Hydrophobic	UF (MEUF)	90% surfactant recovery	Purkait, DasGupta, and De (2004)
(ii)	Food processing industries						
	Olive mill wastewater	Spiral wound/ 25 kDa	Polysulfone	Hydrophobic	UF	Hydroxycinnamic acids and flavonols	Galanakis, Tornberg and Gekas (2010)
		• Flat sheet/3 kDa	Regenerated cellulose	Hydrophilic	UF	Phenolic compounds	Ochando-Pulido and Martínez-Férez (2017)
		• Flat sheet/4 kDa	Polyethersulfone	Hydrophobic	UF	Hydroxytyrosol, protocatechuic acid, caffeic acid tyrosol, and p-cumaric acid	Cassano, Conidi and Drioli (2011)
		• Flatsheet/10 kDa	Regenerated cellulose	Hydrophilic	UF		
	Winery sludge/ effluents	• Flat sheet/ 100 kDa	Polysulfone	Hydrophobic	UF	Hydroxycinnamic acids, o-diphenols	Galanakis, Markouli and Gekas (2013)
		• Flat sheet/ 20 kDa	Polysulfone	Hydrophobic	UF		
		• Flat sheet/1 kDa	Composite fluoropolymer	Hydrophobic	UF		
		• Hollow fiber/ 0.2 μm	Polyvinylidene fluoride	Hydrophobic	MF	Phenolic compounds	Giacobbo, Bernardes and de Pinho (2017)

		• Hollow fiber/ 0.4 μm	Polyimide	Hydrophilic	MF	Phenolic compounds	Giacobbo, do Prado, Meneguzzi, Bernardes and de Pinho (2015)
	Orange press liquor	Hollow fiber/ 100 kDa	Polysulphone	Hydrophilic	UF	Total polyphenols	Galanakis et al. (2013)
(iii)	Dairy processing industries	Flat-sheet/(30−50) kDa	Polyethersulfone	Hydrophilic	UF	Casein protein	Luo et al. (2012)
		Tubular	Polysulfone and polycarbonate	Hydrophilic	MF (cross-flow MF)	• Residual fat from whey or the clarification and the removal of bacteria from cheese brine • Separation of micellar casein and small milk fat	Saboya and Maubois (2004)
		Flat-sheet/10 kDa	Regenerated cellulose		UF	Complete rejection of whey protein from sweet whey	Butylina, Luque and Nyström (2006)
(iv)	Oil-water separation	Tubular/(100−200) kDa	Polyvinylidene fluoride	Hydrophilic	UF	99% permeate recovery, 54% aromatics rejection with 95% of rejection of both heavy metal and hydrocarbons.	Bilstad and Espedal (1996)
		Flat sheet/30 kDa	Cellulose acetate	Hydrophilic	UF	89%−95% oil rejection	Hussain and Al-Yaari (2021)
		Flat sheet/58 kDa	Polyethersulfone	Hydrophilic	UF	92.8% oil rejection	Adib and Raisi (2020)
		Flat sheet/30 kDa	Cellulose acetate and Nylon-66	Hydrophilic	UF	90% oil rejection	Hussain and Al-Yaari (2021)

MEUF, Micellar-enhanced UF.

(Ray, Iroegbu, & Bordado, 2020). The potable water reuse treatment commonly employs MF or UF to remove pathogens or pretreatment for NF or RO. MF membranes are commonly used to remove most fine suspended solids (>99% rejection) and some colloidal material. They can also provide 3−6 log removal of protozoan cysts and coliform bacteria. The UF membranes can typically reject all suspended solids, remove organic matter, reduce BOD_5 by at least 95%, and significantly reduce turbidity. In addition to the contaminants removed by MF, UF can provide up to 6-log removal of bacteria; and if the membrane modules are intact, they can eliminate protozoan cysts and coliform bacteria from the filtrate. Phosphorus, nitrogen, and total organic carbon (TOC) constituents in soluble and colloidal form can also be partially removed through UF (and less with MF), but the achieved rejection can vary widely, 10%−85%, depending on the phase of the contaminants (soluble or particulate). Increased removal can be achieved if chemical coagulants are dosed into the feed water. However, neither the MF nor UF process removes dissolved constituents such as salts and organic chemicals (Warsinger et al., 2018).

1.5.2 Recovery of dye and pigments

On a commercial-scale, the MF/UF membranes used for dye wastewater treatment are generally polymeric. The MF/UF membranes can potentially remove colloids, particles, and many biological molecules at significantly low pressure. The MF process has minimal application in textile wastewater treatment. The application of the MF process is restricted to the removal of suspended particles and colloidal dyes from the exhausted dye bath. The MF process is conventionally employed, and other concomitant processes (such as coagulation/flocculation/NF). Similar to the MF process, the UF process also has minimal application in textile dye wastewater treatment. This is because most dyes' molecular weights are significantly lower than the convention MWCO of UF membranes. Reportedly, UF membrane provides 90% rejection, although higher rejections have been reported using hydrophobic UF membranes (such as PES and PVDF membranes). The water reclaimed using the UF process can be reused for only subsidiary processes (such as washing and rinsing) and not for primary processes (such as dying of fibers). For the treatment of textile effluents, the use of polymeric membranes is usually not appreciated due to the low resistance to chemicals (such as organic solvents), acidic/caustic nature of the solution, and high temperature.

1.5.3 Treatment of effluent generated by dairy processing industries

A potential polluter releases a substantial amount of water for maintenance and hygiene conditions in the dairy industry. The membrane separation process is widely used to treat dairy industry effluents as an energy-saving and straightforward technique. Effluents generated by waste effluent generated by dairy processing industries majorly consist of sugar and protein. Reportedly, the effluent consists of an alarmingly high amount of lactose and whey protein that increases the level of both COD and BOD and causes pollution (Carvalho, Prazeres, & Rivas, 2013; Yadav et al., 2015). To control this pollution, membrane separation removes lactose and reduces organic load before draining the wastewater. The

UF (2−150 kDa) membranes remove almost all of the protein, fat, and some insoluble compounds and minerals in dairy wastewater; and only lactose, soluble salts, and ash content are allowed to pass (Luo et al., 2012). Similarly, MF (100−500 kDa) removes almost all pathogenic bacterial species and mold as well as a certain amount of halogenated salt (Mistry & Maubois, 2017; Saboya & Maubois, 2004). For preparation of whey protein concentrate (WPC), UF membranes (10-20 kDa) are typically used. These membranes allow the separation of lactose and minerals in the permeate from whey proteins in the retentate. Whereas, both MF and UF process is used for preparation of whey protein isolate (WPI). The MF process is used to lower the fat content in the whey-protein which is further concentrated using UF process.

1.5.4 Treatment of oily wastewater

Oily wastewater is generated by industrial processes such as food, chemical, pharmaceutical, textile, steel, leather, and petrochemical industries. For oil-water emulsions, the MF is primarily used as a pretreatment to separate TOC, COD, grease, and oil for the following treatment processes: UF, NF, and RO. The most common membrane materials used for the fabrication of MF for oil-water emulsions are PVDF, PSU, and CA. Electrospinning method is widely used for fabrication of polymer-based MF membranes with large porosity (>90%), highly interconnected pore structure, and better structure stability. A graphene oxide/polyacrylonitrile hierarchical structured superhydrophilic MF membrane with low oil adhesion was fabricated. Reported, the given membrane exhibited $\sim 10{,}000\ \mathrm{L\ m^{-2}\ h^{-1}}$ with >98% oil-removal efficiency (Zhang et al., 2017).

For treatment of waste effluent generated by oil and gas industries, polymeric UF membranes are most frequently used as a standalone or post separation process (Ahmad, Guria, & Mandal, 2020). Reportedly, oil-removal efficiency of MF and UF membranes are 97%−99% (oil-removal efficiency) and $<1\ \mathrm{mg\ L^{-1}}$ (oil content), respectively (Yu, Han, & He, 2017). Some commercially available polymers such as polyacrylonitrile (PAN), PES, polyvinylidene fluoride (PVDF), PSU, and polyvinyl chloride (PVC) are widely used for the treatment of oily wastewater. Some commercially available polymeric UF membranes marketed for oily wastewater treatment are Osmonics, Clean Water Tech PTE, Filtration Solutio Inc, and Koch.

1.5.5 Recovery of heavy metal from industry effluent

A significant amount of heavy metal is generated by plating/electroplating, mining, tanning, textiles, paper, and electrolysis industries. These heavy metals are nonbiodegradable and carcinogenic resulting in critical health issues to all living organisms.

UF is recognized as an effective method for separation of heavy metal ions. The selection of membrane material for preparation of UF membrane plays an important role in determining the efficiency of the given process. The selection of suitable membrane material for fabrication of UF membranes largely depends on the characteristics of the wastewater to be treated. Since, the UF membrane pores are conventionally larger than the heavy metal ions, the additives are bonded to the metal ions to enlarge the size of metal

TABLE 1.5 Removal of heavy metal using micellar enhanced ultrafiltration (MEUF) and polymer-enhanced ultrafiltration (PEUF) processes.

	Membrane material	Surfactant/complexing agent	Heavy metal	Removal efficiency (%)	References
MEUF	Polyethersulfone	Sodium dodecyl sulfate (SDS)	Cd^{2+}	86.13	Huang, Qi, et al. (2017)
		SDS at 8 mM concentration	Zn^{2+}, Cu^{2+}, Cd^{2+}, Pb^{2+}	>99.0% each	Huang, Yuan, et al. (2017)
		SDS at 0.8–8 mM	Cd^{2+}	99	Shi et al. (2019)
		SDS at 7 mM	Cu^{2+} and Cr^{3+}	66.64 and 26.02	Sum, Kok and Shalini (2021)
PEUF	Regenerated cellulose	Sodium alginate (10 mmol L^{-1})	Cr^{3+}, Cr^{6+}	100	Butter et al. (2021)
	Polyethersulfone	Polyethylenimine, chitosan and sodium polyacrylate	Sb^{5+}	85.8–94.7	Ren, Lin, Song, Sun and Shao (2021)
		Polyacrylic acid sodium (PAAS), polyacrylate (PAA)	Co^{2+}	>97	Gao, Qiu, Li and Le (2019)
		Carboxymethyl chitosan	Zn^{2+}, and Pb^{2+}	80 and 90	Edward, Dalmia, Mammen, Prabhakar and Mathur (2021)

TABLE 1.6 Heavy metal removal using microfiltration process.

Membrane material	Membrane type	Heavy metal	Removal efficiency (%)	References
Cellulose acetate	Crossflow	Pb^{2+}	98.3	Bayhan, Keskinler, Çakici, Levent and Akay (2001)
		Ni^{2+}	31.4	
		Cu^{2+}	56.2	
Polypropylene	Crossflow	Cr^{3+}	71	Brady, Rose and Duncan (1994)
		Cu^{2+}	31	
		Pb^{2+}	63	
		Cd^{2+}	7	
Polypropylene and polyethersulfone	Crossflow	Cd^{2+}	96.31	Enoch, van den Broeke and Spiering (1994)
		Cr^{2+}	99.98	
		As^{2+}	>94.83	
		Hg^{2+}	99.25	
		Pb^{2+}	98.54	
		Se^{2+}	91.88	
		Zn^{2+}	99.19	

ions. Thereby, the micellar-enhanced UF (MEUF) and polymer-enhanced UF (PEUF) membranes are suggested (Table 1.5).

MEUF membrane is formed by bonding UF and surfactant. It has high flux and high selectivity, leading to high removal efficiency, low-energy consumption, and less space demand. In MEUF, a surfactant is mixed with wastewater in a concentration above the critical micellar concentration (CMC). Reportedly, beyond CMC, the surfactant monomers assemble and create some micelles in the solution. PEUF is formed through the integration of UF and binding polymers. PEUF are also known as polymer-supported, complexation, polymer-assisted, size-enhanced, and complexation-enhanced UF. PEUF process blocks and extracts polymer-bonded metal ions while allowing permeation of water and uncomplexed components through the membrane pores.

In heavy metal removal, the application of MF membrane process has not drawn much attention because of its limited removal ability (Table 1.6).

1.6 Summary

Membrane processes that allow separating solutes from one another or the solvent with no phase change are interface mass transfers. This chapter provides a comprehensive insight into MF and UF membrane technology. The membrane technology is versatile and has vast application in the field of water remediation; despite the extensive applications of UF and MF membranes in numerous fields, the long-term stability of these membranes are restricted due to certain limitations. The membrane fouling and CP are among the most significant problems in pressure-driven membrane separation processes. The membrane module and process configuration play a significant role in the overall membrane performance. Based on application, the membranes can be characterized using both invasive and noninvasive methods. The current research focusing on technological developments offers increased system efficiency, higher quality effluent, and alternative water sources and helps end-users mitigate regional water quality and supply challenges.

References

Adib, H., & Raisi, A. (2020). Surface modification of a PES membrane by corona air plasma-assisted grafting of HB-PEG for separation of oil-in-water emulsions. *RSC Advances*, *10*, 17143–17153. Available from https://doi.org/10.1039/d0ra02032j.

Ahmad, T., Guria, C., & Mandal, A. (2020). A review of oily wastewater treatment using ultrafiltration membrane: A parametric study to enhance the membrane performance. *Journal of Water Process Engineering*, *36*, 101289. Available from https://doi.org/10.1016/j.jwpe.2020.101289.

Ahmed, I., Balkhair, K. S., Albeiruttye, M. H., & Shaibaan, A. A. J. (2020). Importance and significance of UF/MF membrane systems in desalination water treatment. *Desalination, INTECH*, 1–15. Available from https://doi.org/10.5772/intechopen.68694219.

Bayhan, Y. K., Keskinler, B., Çakici, A., Levent, M., & Akay, G. (2001). Removal of divalent heavy metal mixtures from water by Saccharomyces cerevisiae using crossflow microfiltration. *Water Research*, *35*, 2191–2200. Available from https://doi.org/10.1016/S0043-1354(00)00499-1.

Bilstad, T., & Espedal, E. (1996). Membrane separation of produced water. *Water Science and Technology: A Journal of the International Association on Water Pollution Research*, *34*, 239–246. Available from https://doi.org/10.1016/S0273-1223(96)00810-4.

Brady, D., Rose, P. D., & Duncan, J. R. (1994). The use of hollow fiber cross-flow microfiltration in bioaccumulation and continuous removal of heavy metals from solution by Saccharomyces cerevisiae. *Biotechnology and Bioengineering*, *44*, 1362–1366. Available from https://doi.org/10.1002/bit.260441113.

Butter, B., Santander, P., Pizarro, Gd. C., Oyarzún, D. P., Tasca, F., & Sánchez, J. (2021). Electrochemical reduction of Cr(VI) in the presence of sodium alginate and its application in water purification. *Journal of Environmental Sciences*, *101*, 304–312. Available from https://doi.org/10.1016/j.jes.2020.08.033.

Butylina, S., Luque, S., & Nyström, M. (2006). Fractionation of whey-derived peptides using a combination of ultrafiltration and nanofiltration. *Journal of Membrane Science*, *280*, 418–426. Available from https://doi.org/10.1016/j.memsci.2006.01.046.

Carvalho, F., Prazeres, A. R., & Rivas, J. (2013). Cheese whey wastewater: Characterization and treatment. *The Science of the Total Environment*, *445–446*, 385–396. Available from https://doi.org/10.1016/j.scitotenv.2012.12.038.

Cassano, A., Conidi, C., & Drioli, E. (2011). Comparison of the performance of UF membranes in olive mill wastewaters treatment. *Water Research*, *45*, 3197–3204. Available from https://doi.org/10.1016/j.watres.2011.03.041.

Chew, K. W., Show, P. L., Yap, Y. J., Juan, J. C., Phang, S. M., Ling, T. C., & Chang, J. S. (2018). Sonication and grinding pre-treatments on *Gelidium amansii* seaweed for the extraction and characterization of Agarose. *Frontiers of Environmental Science and Engineering*, *12*(4), 1–7. Available from https://doi.org/10.1007/s11783-018-1040-0.

Ebrahim, S. (1994). Cleaning and regeneration of membranes in desalination and wastewater applications: state-of-the-art. *Desalination*, *96*(1–3), 225–238. Available from https://doi.org/10.1016/0011-9164(94)85174-3.

Edward, K., Dalmia, M., Mammen, A., Prabhakar, S., & Mathur, S. (2021). Optimization of process conditions for the removal of zinc and lead by ultrafiltration using biopolymer. *Chemical Papers*, *75*, 3723–3737. Available from https://doi.org/10.1007/s11696-021-01613-y.

Enoch, G. D., van den Broeke, W. F., & Spiering, W. (1994). Removal of heavy metals and suspended solids from wastewater from wet lime (stone)—Gypson flue gas desulphurization plants by means of hydrophobic and hydrophilic crossflow microfiltration membranes. *Journal of Membrane Science*, *87*, 191–198. Available from https://doi.org/10.1016/0376-7388(93)E0146-B.

Galanakis, C. M., Markouli, E., & Gekas, V. (2013). Recovery and fractionation of different phenolic classes from winery sludge using ultrafiltration. *Seperation and Purification Technology*, *107*, 245–251. Available from https://doi.org/10.1016/j.seppur.2013.01.034.

Galanakis, C. M., Tornberg, E., & Gekas, V. (2010). Clarification of high-added value products from olive mill wastewater. *Journal of Food Engineering*, *99*, 190–197. Available from https://doi.org/10.1016/j.jfoodeng.2010.02.018.

Gao, J., Qiu, Y., Li, M., & Le, H. (2019). Removal of Co(II) from aqueous solution by complexation − ultrafiltration and shear stability of PAA − Co complex. *Transactions of Nonferrous Metals Society of China*, *29*, 1346–1352. Available from https://doi.org/10.1016/S1003-6326(19)65041-7.

Giacobbo, A., Bernardes, A. M., & de Pinho, M. N. (2017). Sequential pressure-driven membrane operations to recover and fractionate polyphenols and polysaccharides from second racking wine lees. *Seperation and Purification Technology*, *173*, 49–54. Available from https://doi.org/10.1016/j.seppur.2016.09.007.

Giacobbo, A., do Prado, J. M., Meneguzzi, A., Bernardes, A. M., & de Pinho, M. N. (2015). Microfiltration for the recovery of polyphenols from winery effluents. *Seperation and Purification Technology*, *143*, 12–18. Available from https://doi.org/10.1016/j.seppur.2015.01.019.

Hajibabania, S., Antony, A., Leslie, G., & Le-Clech, P. (2012). Relative impact of fouling and cleaning on PVDF membrane hydraulic performances. *Separation and Purification Technology*, *90*, 204–212. Available from https://doi.org/10.1016/j.seppur.2012.03.001.

Hilal, N., Kochkodan, V., Al-Khatib, L., & Levadna, T. (2004). Surface modified polymeric membranes to reduce (bio)fouling: A microbiological study using *E. coli*. *Desalination*, *167*, 293–300. Available from https://doi.org/10.1016/j.desal.2004.06.138.

Hoek, E. M. V. (2013). *Encyclopedia of membrane science and technology*. Wiley. Available from https://doi.org/10.1002/9781118522318.

Huang, J., Qi, F., Zeng, G., Shi, L., Li, X., Gu, Y., & Shi, Y. (2017). Repeating recovery and reuse of SDS micelles from MEUF retentate containing Cd2 + by acidification UF. *Colloids and Surfaces A: Physicochemical and Engineering Aspects*, *520*, 361–368. Available from https://doi.org/10.1016/j.colsurfa.2017.02.001.

Huang, J., Yuan, F., Zeng, G., Li, X., Gu, Y., Shi, L., ... Shi, Y. (2017). Influence of pH on heavy metal speciation and removal from wastewater using micellar-enhanced ultrafiltration. *Chemosphere*, *173*, 199–206. Available from https://doi.org/10.1016/j.chemosphere.2016.12.137.

Hussain, A., & Al-Yaari, M. (2021). Development of polymeric membranes for oil/water separation. *Membranes (Basel)*, *11*, 1–15. Available from https://doi.org/10.3390/membranes11010042.

Li, X., Jiang, L., & Li, H. (2018). Application of ultrafiltration technology in water treatment. *Earth and Environmental Science*, *186*, 012009.

Lin, J. C.-T., Lee, D.-J., & Huang, C. (2010). Membrane fouling mitigation: membrane cleaning. *Separation Science and Technology*, *45*(7), 858–872. Available from https://doi.org/10.1080/01496391003669403.

Luo, J., Cao, W., Ding, L., Zhu, Z., Wan, Y., & Jaffrin, M. Y. (2012). Treatment of dairy effluent by shear-enhanced membrane filtration: The role of foulants. *Seperation and Purification Technology*, *96*, 194–203. Available from https://doi.org/10.1016/j.seppur.2012.06.009.

Majewska-Nowak, K., Winnicki, T., & Wiśniewski, J. (1989). Effect of flow conditions on ultrafiltration efficiency of dye solutions and textile effluents. *Desalination*, *71*, 127–135. Available from https://doi.org/10.1016/0011-9164(89)80004-9.

Membranes, U. U. F., Moslehyani, A., Ismail, A. F., Matsuura, T., Rahman, M. A., & Goh, P. S. (2019). Recent progress of ultrafiltration (UF) membranes and processes in water treatment. *Membrane Seperation Principles and Applications* (pp. 85–110). Elsevier Inc. Available from https://doi.org/10.1016/B978-0-12-812815-2.00003-X.

Meneses, Y. E., Stratton, J., & Flores, R. A. (2017). Water reconditioning and reuse in the food processing industry: Current situation and challenges. *Trends in Food Science and Technology*, *61*, 72–79. Available from https://doi.org/10.1016/j.tifs.2016.12.008.

Mistry, V. V., & Maubois, J.-L. (2017). Application of membrane separation technology to cheese production. *Cheese: Chemistry, physics and microbiology* (4th ed., pp. 677–697). Academic Press. Available from https://doi.org/10.1016/B978-0-12-417012-4.00027-2.

Moattari, R. M., Mohammadi, T., Rajabzadeh, S., Dabiryan, H., & Matsuyama, H. (2021). Reinforced hollow fiber membranes: A comprehensive review. *Journal of the Taiwan Institute of Chemical Engineers*, *122*, 284–310. Available from https://doi.org/10.1016/j.jtice.2021.04.052.

Mulder, M. (1991). *Basic principles of membrane technology* (second ed.). Boston: Kluwer Academic. Available from https://doi.org/10.1524/zpch.1998.203.part_1_2.263.

Muthukumaran, S., Kentish, S. E., Stevens, G. W., & Ashokkumar, M. (2006). Application of ultrasound in membrane separation processes: A review. *Reviews in Chemical Engineering*, *22*, 155–194. Available from https://doi.org/10.1515/REVCE.2006.22.3.155.

Ning Koh, C., Wintgens, T., Melin, T., & Pronk, F. (2008). Microfiltration with silicon nitride microsieves and high frequency backpulsing. *Desalination*, *224*, 88–97. Available from https://doi.org/10.1016/j.desal.2007.04.081.

Ochando-Pulido, J. M., & Martínez-Férez, A. (2017). About the recovery of the phenolic fraction from olive mill wastewater by micro and ultracentrifugation membranes. *Chemical Engineering Transactions*, *60*, 271–276. Available from https://doi.org/10.3303/CET1760046.

Porcelli, N. J., & Judd, S. J. (2010). Effect of cleaning protocol on membrane permeability recovery: A sensitivity analysis. *American Water Works Association*, *102*(12), 78–86. Available from https://doi.org/10.2307/413147217.

Purkait, M. K., DasGupta, S., & De, S. (2004). Removal of dye from wastewater using micellar-enhanced ultrafiltration and recovery of surfactant. *Seperation and Purification Technology*, *37*, 81–92. Available from https://doi.org/10.1016/j.seppur.2003.08.005.

Ray, S. S., Iroegbu, A. O. C., & Bordado, J. C. (2020). Polymer-based membranes and composites for safe, potable, and usable water: A survey of recent advances. *Chemistry Africa*, *3*, 593–608. Available from https://doi.org/10.1007/s42250-020-00166-z.

Regula, C., Carretier, E., Wyart, Y., Gésan-Guiziou, G., Vincent, A., Boudot, D., & Moulin, P. (2014). Chemical cleaning/disinfection and ageing of organic UF membranes: A review. *Water Research*, *56*, 325–365. Available from https://doi.org/10.1016/j.watres.2014.02.050.

Ren, L.-F., Lin, Y., Song, H., Sun, H., & Shao, J. (2021). Efficient removal of antimony from aqueous solution by sustainable polymer assisted ultrafiltration process. *Seperation and Purification Technology*, *263*, 118418. Available from https://doi.org/10.1016/j.seppur.2021.118418.

Saboya, L. V., & Maubois, J.-L. (2004). Current developments of microfiltration technology in the dairy industry. *Membrane*, *29*, 328–332. Available from https://doi.org/10.5360/membrane.29.328.

Said, B., M'rabet, S., Hsissou, R., & Harfi, A. El (2020). Synthesis of new low-cost organic ultrafiltration membrane made from polysulfone/polyetherimide blends and its application for soluble azoic dyes removal. *Journal of Materials Research and Technology*, *9*, 4763–4772. Available from https://doi.org/10.1016/j.jmrt.2020.02.102.

Sangrola, S., Kumar, A., Nivedhitha, S., Chatterjee, J., Subbiah, S., & Narayanasamy, S. (2020). Optimization of backwash parameters for hollow fiber membrane filters used for water purification. *Journal of Water Supply: Research and Technology - AQUA*, *69*, 523–537. Available from https://doi.org/10.2166/aqua.2020.079.

Shi, L., Huang, J., Zhu, L., Shi, Y., Yi, K., & Li, X. (2019). Role of concentration polarization in cross flow micellar enhanced ultrafiltration of cadmium with low surfactant concentration. *Chemosphere*, *237*, 124859. Available from https://doi.org/10.1016/j.chemosphere.2019.124859.

Sum, J. Y., Kok, W. X., & Shalini, T. S. (2021). The removal selectivity of heavy metal cations in micellar-enhanced ultrafiltration: A study based on critical micelle concentration. *Materials Today: Proceedings*, *46*, 2012–2016. Available from https://doi.org/10.1016/j.matpr.2021.02.683.

Tarazaga, C. C, Campderros, M. E., & Padilla, A. P. (2006). Physical cleaning by means of electric field in the ultrafiltration of a biological solution. *Journal of Membrane Science*, *1*(2), 219–224. Available from https://doi.org/10.1016/J.MEMSCI.2005.11.004.

Wang, Y., Chen, X., Zhang, J., Yin, J., & Wang, H. (2009). Investigation of microfiltration for treatment of emulsified oily wastewater from the processing of petroleum products. *Desalination*, *249*, 1223–1227.

Warsinger, D., Chakraborty, S., Tow, E., Plumlee, M., Bellona, C., Loutatidou, S., … John, L. (2018). A review of polymeric membranes and processes for potable water reuse. *Progress in Polymer Science*, 81. Available from https://doi.org/10.1016/j.progpolymsci.2018.01.004.

Xu, Z. -K., Huang, X., & Wan, L. -S. (2009). *Surface engineering of polymer membranes*. Available from https://doi.org/10.1007/978-3-540-88413-2.

Yadav, JSS., Yan, S., Pilli, S., Kumar, L., Tyagi, R. D., & Surampalli, R. Y. (2015). Cheese whey: A potential resource to transform into bioprotein, functional/nutritional proteins and bioactive peptides. *Biotechnology Advances*, *33*, 756–774. Available from https://doi.org/10.1016/j.biotechadv.2015.07.002.

Yu, L., Han, M., & He, F. (2017). A review of treating oily wastewater. *Arabian Journal of Chemistry*, *10*, S1913–S1922. Available from https://doi.org/10.1016/j.arabjc.2013.07.020.

Zaghbani, N., Hafiane, A., & Dhahbi, M. (2007). Separation of methylene blue from aqueous solution by micellar enhanced ultrafiltration. *Seperation and Purification Technology*, *55*, 117–124. Available from https://doi.org/10.1016/j.seppur.2006.11.008.

Zhang, J., Xue, Q., Pan, X., Jin, Y., Lu, W., Ding, D., & Guo, Q. (2017). Graphene oxide/polyacrylonitrile fiber hierarchical-structured membrane for ultra-fast microfiltration of oil-water emulsion. *Chemical Engineering Journal*, *307*, 643–649. Available from https://doi.org/10.1016/j.cej.2016.08.124.

CHAPTER

2

Polymer-based microfiltration/ ultrafiltration membranes

Ananya Bardhan and Senthilmurugan Subbiah

Department of Chemical Engineering, Indian Institute of Technology, Guwahati, India

2.1 Introduction

Membrane-based separation processes have been most promising in efficiency, cost, applicability, and ease of operation for the environment pollution abatement and separation industry. Microfiltration (MF) and ultrafiltration (UF) are low-pressure-driven membrane processes conventionally used in treating wastewater, water treatment, pretreatment before advanced membrane filtration, industrial chemical separation, and food processing. These MF/UF membranes are either ceramic or polymeric, with their tailing inherent benefits and drawbacks. This chapter primarily focuses on the polymeric membrane for MF/UF-based applications. In recent years' polymeric membranes have gained unprecedented interest in the membrane-based separation industries and filtration markets because they are economical, easily applicable, handle large volumes of water, and lower carbon footprint. However, polymeric membrane limits its applied scale in adverse conditions owing to comparatively low chemical, mechanical, and thermal resistance. A continuous effort has been put in to circumvent these trade-offs by decorating desired properties on the polymeric membrane via material engineering and surface modification.

On the other hand, extensive research and many studies have been conducted to reduce time-based flux decline, heighten selectivity and reduce membrane fouling, which is the most crucial problem in applying polymeric membranes. MF/UF processes are usually the first line of treatment in membrane treatment processes and comparatively face a large water volume requiring high flux and surface area. The development of new materials and techniques for fabricating and modifying polymeric MF/UF membranes with controlled pore-size distribution, selectivity, and antifouling behavior has been the battleground for researchers, and substantial growth has been achieved the field. This chapter covers the most recent and applicable development regarding the preparation, modification, and performance of polymeric MF/UF membranes for the separation and purification industry.

Advancement in Polymer-Based Membranes for Water Remediation
DOI: https://doi.org/10.1016/B978-0-323-88514-0.00005-X

© 2022 Elsevier Inc. All rights reserved.

2.2 Polymers as raw material to synthesize microfiltration/ultrafiltration membranes

For polymeric MF/UF membrane preparation, polymers are considered one of the primary membrane materials. In MF/UF membranes, polymers with high hydrophilicity are more favored for their high permeability to water and are more resistant to fouling from negatively charged particles (such as protein and humic acid). In addition to hydrophilicity, permeability, strength, flexibility, and chemical resistance to the feed solution are essential properties that need to be considered during the selection of polymers as membrane material. For the preparation of porous (or microporous) membranes, both polymeric and ceramic membranes are used. However, considering a commercial application, polymeric membranes are most widely used. Some crucial polymers (both hydrophilic and hydrophobic) used as membrane material at the laboratory to commercial scale:

1. Hydrophilic polymers: poly(vinyl alcohol) (PVA), poly(vinyl chloride) (PVC), polyamide (PA), poly(acrylic acid) (PAA), poly(ethylene oxide) (PEOX), polyacrylonitrile (PAN), poly (vinyl acetate) (PVAC), poly(vinyl butyral) (PVB), poly(p-hydroxy styrene) (PHS), cellulose and its derivatives (such as cellulose acetate, CA; cellulose triacetate, CTA; cellulose acetate butyrate, CAB; cellulose acetate propionate, CAP; cellulose nitrate, CN; cellulose propionate, CP; ethyl cellulose, EC; carboxymethyl cellulose, CMC).
2. Hydrophobic polymers: polysulfone, PSF; polyethersulfone, PES; poly(vinylidene fluoride), PVDF; polycarbonate, PC; polypropylene, PP; poly(methyl methacrylate), PMMA; polytetrafluoroethylene, PTFE; polyethylene, PE; silicone, Si; polyphenylene oxide, PPO; polyphenylene sulfide, PPS; polystyrene, PS.

2.2.1 Classification

According to conventional methods, the membrane can be classified based on membrane materials (such as organic polymers, inorganic materials, mixed matrix), cross-section (such as symmetric, asymmetric, bi- or multilayer, a thin layer, or mixed matrix composite), preparation method (track etching, stretching, sol-gel process, phase inversion, and interface reaction), membrane shape [such as hollow fiber (HF), and flat-sheet]. Table 2.1 summarizes common polymeric materials used to fabricate UF/MF membranes for water and wastewater treatment processes.

2.2.2 Membrane fabrication method microfiltration/ultrafiltration

The polymeric membrane preparation techniques conventionally depend on the selected polymer and specification of the membrane structure. Several techniques are available to transform the polymeric material to achieve a polymer. This section discusses the basic working principle, advantages and disadvantages of membrane fabrication techniques, such as stretching, sintering, track etching, template leaching, interfacial polymerization, phase inversion [including immersion precipitation, thermally induced phase separation (TIPS), evaporation-induced phase separation, vapor-induced phase separation (VIPS), and precipitation by controlled evaporation], and electrospinning. The membrane fabrication technique can be broadly categorized as (1) mechanical and (2) chemical techniques.

TABLE 2.1 Common membrane material used for fabrication of polymeric microfiltration/ultrafiltration (MF/UF) membrane.

Polymer	Acronym	Advantages	Disadvantages	Mechanical strength	Hydrophilicity/ Contact angle	pH range	Chlorine resistance	Reference
Cellulose acetate	CA	Abundant availability, low-cost, high hydrophilicity, biocompatible	Poor chemical and thermal resistance, mechanical strength, biodegradability, and susceptible to greater compaction	Low−moderate	Hydrophilic; 20°−30°	4−8	Resistant	Lee, Heo, Jo, & Min (2016), Sossna, Hollas, Schaper, & Scheper (2007)
Chitosan	CS	Wide availability, low-cost, high hydrophilicity, biocompatible, multifunctional groups	Low solubility in solvents, easily agglomerate in an aqueous medium, brittle in nature	Low−moderate	Hydrophilic; 12°−30°	4−10	Resistant	Joshi & Kumar (2018), Salehi, Daraei, & Arabi Shamsabadi (2016)
Cyclodextrin derived from Starch	SH	High surface functionalities, hydrophilicity, porosity, and high permeability through cavities pf toroidal arrangement	Needs chemical derivatization, tend to retrograde, thermal decomposition, and low shear resistance	Low	Hydrophilic; 20°−30°	2−9	Resistant	Ahmadi, Javanbakht, Akbari-adergani, & Shabanian (2019), Wang, Guo, Zhang, Fang, & Zhu (2019)
Alginate	Alg	Biocompatibility, hydrophilicity, low toxicity, relatively low cost, good membrane-forming properties, multifunctional groups, and a plurality of charge	Soluble in aqueous solution hence needs derivatization, generally needs support layer	Low	Hydrophilic; 30°−40°	6−10	Resistant	Li et al. (2017), Meng, Winters, & Liu (2015), Mokhena & Luyt (2017)

(*Continued*)

TABLE 2.1 (Continued)

Polymer	Acronym	Advantages	Disadvantages	Mechanical strength	Hydrophilicity/ Contact angle	pH range	Chlorine resistance	Reference
Poly(lactic acid)	PLA	Natural hydrophilicity, higher mechanical and physical properties than other natural polymers, high water flux	Poor mechanical strength compared to the synthetic polymer membrane	Low to moderate	Hydrophilic; 20°–40°	2–10	Resistant	Li, Hashaikeh, & Arafat (2013), Moriya, Maruyama, Ohmukai, Sotani, & Matsuyama (2009)
Polysulfone	PSF	Good mechanical strength, thermal stability, and chemically resistant	Hydrophobic in natureCannot tolerate pressure above 7 bar	Good	Fair/ ~75°	1–13	Resistant	Tweddle, Kutowy, Thayer, & Sourirajan (1983)
Polyether sulfone	PES	Good thermal properties, rigid, compaction resistant, very permeable, oxidant tolerant, narrow pore-size distribution	Hydrophobic in natureCannot tolerate pressure above 7 bar	Good	Fair/ ~70°	1–13	Resistant	Ida (2021)
Polyvinylidiene fluoride	PVDF	Very oxidant tolerant, chlorine resistant	Broader pore-size distribution	Good	Poor/100°	2–11	Fair	Ji, Liu, Hashim, Abed, & Li (2015)
Polyethylene	PE	High resistance to organic solvents, low cost, oxidant tolerant	Poor thermal properties, weaker fouling resistance	Fair	Poor	1–14	Poor	Zaidi & Lakhi (2016)
Polypropylene	PP	High resistance to organic solvents, decent mechanical strength	Weaker fouling resistance, not oxidant tolerant	Fair	Fair	2–13	Poor	Ran (2015)
Polyamide	PA	Small pores, excellent rejection, selectivity	Poor acid and alkali resistance weak, experiences compaction	Fair	Good/ ~55°	1–13	Poor	Lau (2016)

2.2.2.1 *Mechanical techniques*

2.2.2.1.1 Stretching

Stretching is another relatively simple procedure for the preparation of a microporous membrane. This technique is employed with polyethylene or polytetrafluoroethylene films that have been extruded from a polymer powder and stretched perpendicular to the direction of extrusion. The applied mechanical stress results in minor rapture, resulting in a porous structure with a pore size of 0.1−3 μm.

The rate of stretching and the environment inside the system determines the pore and pore-size distribution. The stretched membranes made of polytetrafluoroethylene are frequently used as water-repellent textiles for clothing (such as tents, sleeping bags). This membrane reportedly has high porosity (up to 90%) and high permeability for gases and vapors. Therefore, the membrane repels rainwater but permits the water vapor from the body to permeate. Other applications of this membrane include removing ethanol from fermentation broth (or beer/wine) to produce low alcohol and medical applications (such as artificial blood vessels and burn dressing).

2.2.2.1.2 Sintering

The sintering can be used for the preparation of porous membranes both from organic and inorganic materials. This technique involves pressing powdered (polymeric) particles (of required particle size) sintered at an elevated temperature. The temperature required for sintering primarily depends on the material used. During the sintering process, the interface between the contacting particle disappears (Fig. 2.1).

The resulting membrane's pore size is controlled by selecting the polymer powder with suitable particle size and distribution. The sintering technique is suitable for producing membranes with pore sizes ranging from 0.1 to 10 μm (i.e., applicable for MF membrane only).

2.2.2.2 *Chemical techniques*

2.2.2.2.1 Track etching

The assembly of parallel cylindrical pores of uniform dimensions is obtained by track etching. The schematic representation of the track-etching technique is given in Fig. 2.2.

A polymeric foil or film (of polycarbonate) is subjected to high-energy particle radiation perpendicular to the film in this membrane preparation technique. The radiation particles damage the polymeric matrix, which subsequently results in tracks. The film is then immersed in an acid/alkali bath where the polymeric materials are etched away along these tracks resulting in uniform cylindrical pores (ranging between 0.2 and 10 μm) with narrow pore-size distribution. In this technique, the porosity and pore diameter is maintained

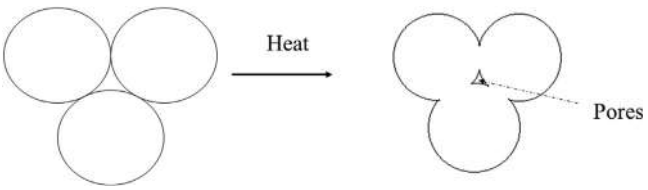

FIGURE 2.1 Schematic representation of the sintering process.

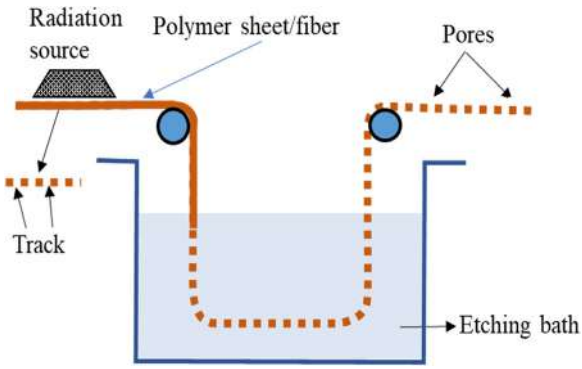

FIGURE 2.2 Schematic representation of track etching technique.

by manipulating radiation and etching time. The track-etched polymeric membranes are generally prepared using polycarbonate or poly(ethylene terephthalate) films. Due to their narrow pore-size distribution and low tendency to plug, capillary pore membranes made from polycarbonates and polyesters have found extensive-scale applications in analytical chemistry and microbiological laboratories, and medical diagnostic procedures. Capillary pore membranes are also used to produce ultrapure water for the electronic industry, showing certain advantages over other membrane products due to their short "rinse down" time and good long-term flux stability. Nevertheless, these membranes have limitations because pores' preparation with diameters in the lower nanometer range is not possible.

2.2.2.2.2 Template leaching

Template leaching is an essential fabrication technique for preparing isotropic microporous membranes by leaching out one component from the polymeric film. In this method, a homogeneous melt (at 1000°C–1500°C) of 3 components (polymeric membrane matrix material and a leachable component) is cooled, and as a consequence, the system separates into two-phase where one phase is soluble, and another is insoluble. The second phase is leached out using a suitable solvent (acid/alkaline wash) and, as a result, a microporous membrane. A wide range of pore diameter can be obtained using this technique with a minimum size of about 0.05 μm.

For example, a homogeneous film is prepared from a mixture of a membrane matrix material and leachable components such as a soluble low-molecular-weight substance or even a macromolecular material such as poly(vinyl alcohol) and poly(ethylene glycol). After film formation, the leachable component is removed with a suitable solvent (or chemical treatment), and a microporous membrane is acquired. This process is widely being used in the preparation of porous glass membranes.

2.2.2.2.3 Phase inversion

In the phase inversion technique, the membranes are prepared from any polymer–solvent mixture, which forms a homogeneous solution at a specific temperature and composition conditions but separates into two phases when these conditions are changed. The phase inversions can be induced by evaporating a volatile solvent from a homogeneous polymer (or casting) solution. When the solution is casted, the solvent is allowed to

evaporate due to which an increased polymer concentration at the solution/air interface is observed since the solvent is lost more rapidly from the surface. In asymmetric membranes, the polymer essentially leaches out of the solution and forms a skin layer on the surface. These membranes are used to prepare pressure-driven membrane processes, such as reverse osmosis (RO), nanofiltartion (NF) ultrafiltration (UF), or gas separation. For preparation of a symmetric polymeric membrane, the polymer is dissolved in an appropriate solvent and spread as a (20–200) μm thick film. A precipitant, such as water, is added to this liquid film from the vapor phase, causing the homogeneous polymer solution to separate into a solid polymer and a liquid solvent phase. The precipitated polymer forms a porous structure containing a network of more or fewer uniform pores.

A polymer is transformed in a controlled manner from a liquid to a solid phase in the phase transition technique. In this technique, a polymeric solution is precipitated into two phases: a solid polymer-rich phase that forms the membrane matrix and a liquid polymer–solvent phase that evaporates to form the membrane pores. The concept of phase inversion covers a range of different techniques (Das & Gebru, 2018).

Vapor-induced phase separation In the VIPS process, the nonsolvent phase is a gas. The nonvolatile nonsolvent is initially contained in the volatile solution, resulting in the nonsolvent being enriched in the casting solution during controlled solvent evaporation. This process implies that phase separation is a nonsolvent intake process rather than a solvent outflow. The polymer precipitates in the casting solution to form a membrane. The given method is primarily based on the casted film's exposure to a vapor chamber's nonsolvent (water) atmosphere (Fig. 2.3).

Here, the phase inversion occurs due to the inflow of the nonsolvent vapor into polymeric casted film and the outflow of solvent from the casted film. A PVDF membrane prepared via the VIPS method using various exposure times was reported (Peng, Fan, Dong, Song, & Han, 2012). This study demonstrated that long-time exposure facilitated the crystallization process leads to the formation of a porous membrane and increased hydrophilicity, thus high-water permeability.

Liquid-induced phase separation In liquid-induced phase separation (LIPS), dense or porous membranes can be fabricated by selecting appropriate monomer material, solvents, and nonsolvent mixtures. First, in this technique, a polymer solution is the first cast as a

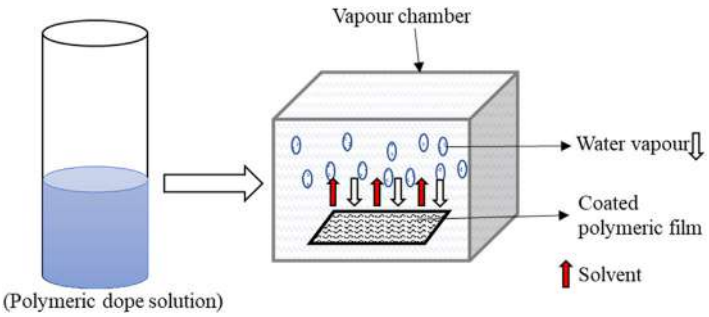

FIGURE 2.3 Schematic representation of vapor-induced phase separation method.

thin film on support and immersed into a nonsolvent bath. This technique is also known as immersion casting or wet casting. The precipitation occurs due to the potential chemical imbalance because the solvent from the polymer solution is exchanged for the nonsolvent. The polymeric phase is then solidified after the phase separation attains a certain degree to form the porous membrane. The entire immersion precipitation process includes both liquid−liquid demixing and solidification. This technique may be combined with VIPS for polymer solutions, for example, two solvents with different boiling points.

Thermally induced phase separation The material may solidify to a dense or porous product of a material solvent additive mixture by varying the solvent temperature during the casting process. As shown in Fig. 2.4, the polymeric dope solution is cast on a flat surface and then dipped in the cold-water bath, solidifying the polymer as a porous membrane having both polymer-rich and lean phases. This process is also known as melt casting.

Phase inversion techniques under progress in laboratory Colloidal-induced phase separation: A phase-separated colloidal solution performs structure arresting on the microfabricated mold. In this method, the pore morphology can be fine-tuned by adding a cosolvent to form smaller pores.

Pressure-induced phase separation (also known as "pressure casting"): the casting solution may contain a saturated dissolved gas, while the reduction of the pressure (or temperature increase) can induce growth of gas cells in the casting solution, with the obtaining of closed or open cell morphologies and typical sizes of 0.01−1000 microns.

Reaction-induced phase separation: a casting solution containing monomers starts to react and initiates phase separation due to an increase in molecular weight or production of a nonsolvent.

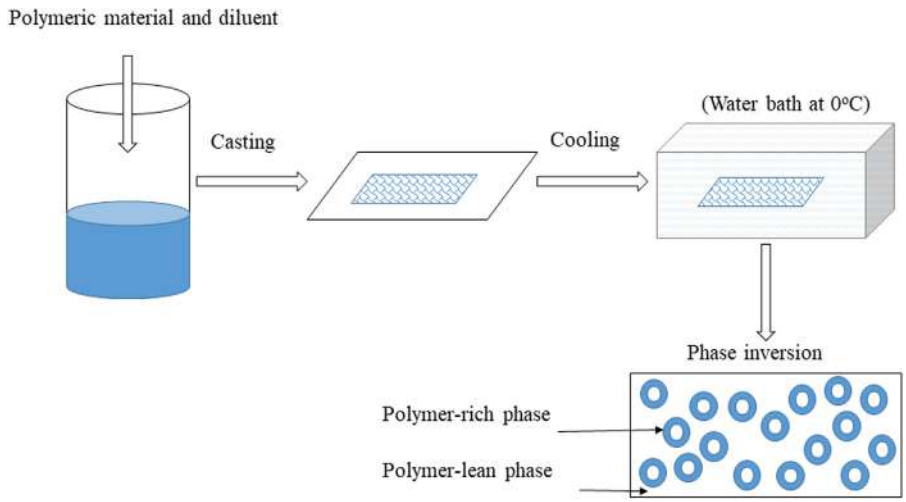

FIGURE 2.4 Schematic representation of thermally induced phase separation (TIPS) method.

2.2.2.2.4 Electrospinning

The electrospinning process involves fabricating fibers through an electrically charged jet of polymer solution (or melt). The electrospinning process is widely used to prepare highly porous membranes with high gravimetric porosity, low density, excellent pore interconnectivity, and high surface area to volume ratio with exceptional mechanical strength. The porous polymeric membrane fabricated using this technique can have a pore diameter ranging from micro- to nanoscale. During this process, a polymer solution is subjected to an electric field, and the voltage is increased until the electrical force is enough to overcome the surface tension of the solution. A typical electrospinning setup consists of four main parts: (1) a pump system, (2) a high voltage supply, (3) a syringe connected to a needle with a small diameter and, (4) a grounded metal collector (Fig. 2.5).

The electrospinning technique involves the drawing of a polymer fluid. Several types of polymer and precursor can be electrospun to form fibers. The materials to be electrospun depend on the application. For example, the materials such as polymer and polymer composites can be directly produced by electrospinning technique, whereas certain other materials such as ceramics and carbon nanotubes (CNT) require postprocessing of the electrospun fibers.

The polymer solution properties (such as surface tension, viscosity, and electrical properties) play an essential role in both the electrospinning and resultant membrane morphology. The surface tension determines the formation of a bead along the length of fiber formation. The viscosity and electrical properties determine the extent of elongation of the solution. The molecular weight of the polymer directly determines the viscosity of the solution. The molecular weight and viscosity of the solution affect the diameter of the resultant electrospun fibers. Reportedly, it was found that the electrospun fibers with cylindrical morphology were obtained with PVA content of about 6wt.% in the prespinning solute. The further increase of the polymer (PVA) concentration in the prespinning

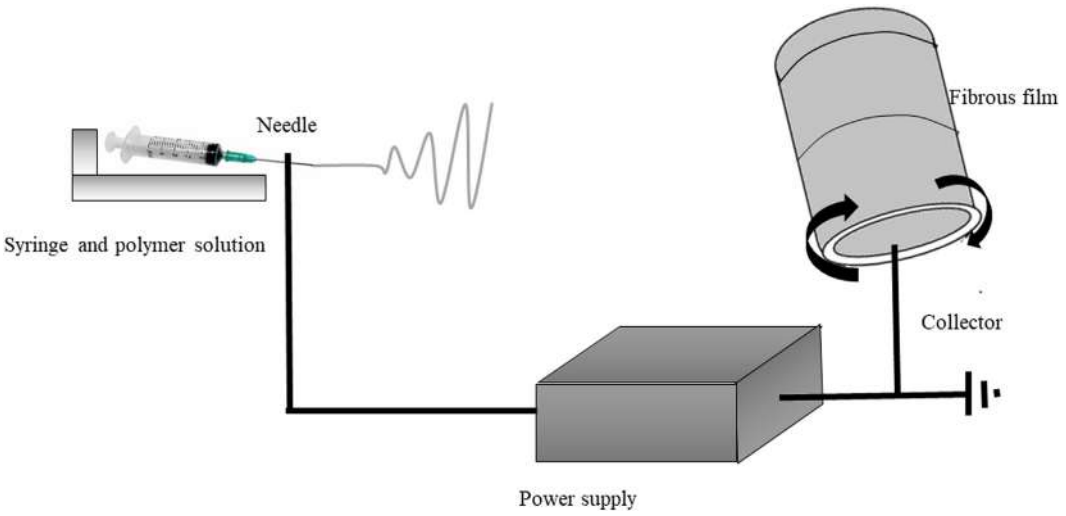

FIGURE 2.5 Schematic diagram of electrospinning process.

solution results in a mutilated nanofibers of flat and wide ribbon-like structure (Moheman, Alam, & Mohammad, 2016).

The processing parameters such as supplied voltage, the temperature of the solution, the diameter of the needle, feed rate, type of collector, and distance between the needle tip and collector are few critical process parameters that affect the electrospinning process. After that, a strong electrical field is applied between the capillary tip and the ground collector. The charge induced by the electric field opposes the surface tension of the polymer liquid, which is held at the tip of the capillary. By increasing the electric power, the polymer fluid's hemispherical shape at the tip changes to a conical shape called the Taylor cone. Once the applied electrical field reaches a critical value that exceeds the polymer liquid's surface tension, the solution is ejected from the tip of the Taylor cone. The path followed by the charged jet of the polymer solution can be electrically controlled; thus, continuous polymeric fibers can be collected to produce porous membranes.

2.2.2.2.5 3D-printing

The 3D-printing (also known as rapid prototyping) can be considered a relatively modern technique with enormous potential in biomedical membrane fabrication. This technique offers the ability to create complex shapes with a wide range of materials, including conventional thermoplastic, metals, ceramic, and graphene-based materials. This approach can be divided into four types:

1. Photopolymerization in which photoreactive polymers are cured with a laser or UV light.
2. Powder-based printing, in which the powder of the desired material is spread on a substrate followed by spurting a chemical binder to form a 3D object and selectively sinter it.
3. Material extrusion works by heating the thermoplastic higher than its T_g to melt and extrude a filament of the polymeric material to form the desired structure.
4. Lamination works by laminating the stacked thin layers of materials cut into the desired shape to form a prototype.

3D printing using stereolithography is currently the most widely used approach to produce polymeric membranes. In this technique, the UV-laser traces the desired structures and cure the photo-reactive polymers either on the top or bottom of the moving stage. Here, once the desired pattern is created on the surface of the photo-reactive polymer solution. The stage is moved vertically down into or up from the resin surface. UV-laser cures the resin on the surface to form a continuous 3D object.

The 3D-printing technique has great potential in various fields, including art, medicine, engineering, and manufacturing. However, its application is still constricted due to certain limitations: (1) material type, (2) high production cost, and (3) low mechanical strength without additional posttreatment.

2.2.2.2.6 Nanoimprint lithography

The nanoimprint lithography technique is one of the most common soft lithographic techniques applied to produce porous polymeric membranes. This mechanical lithographic technique involves pressing a template against a deformable resist layer deposited on a

substrate (Silicone, Si, or a metallic surface). The fabrication of the master mold is one of the most critical factors as its accuracy and definition of a structure is the key to define the pattern on the imprinted polymers. The master molds are usually fabricated using photolithography or electron-beam lithography (EBL) to create uniform nano- or microstructural patterns. Due to high technical application and operational cost, porous anodic aluminum oxide (pAAO) membranes are used as a template in practical application. As compared to EBL, it is relatively easy to fabricate pAAO membranes with uniform, straight nanochannels. The master molds are made of silicone, thermoset plastics, and nickel.

Thermal nanoimprint lithography A thin layer of thermoplastic polymer is deposited on a solid substrate using spin coating in thermal nanoimprint lithography. It is heated up to 20°C−40°C above its glass transition temperature (T_g) to soften the layer and emboss a patterned master mold with optimal pressure and time.

Photo nanoimprint lithography The photo nanoimprinting techniques involve embossing the desired patterns on a liquid photoresist layer and then curing it using UV exposure. The UV solidifies the resists by inducing polymer crosslinking. Compared to thermal nanoimprint lithography, photo nanoimprint lithography offers certain advantages. First, the photo nanoimprint lithography can be conducted at room temperature, which eventually resolves the issues resulting from thermal expansion variation between the mold, resists and, substrate. Also, the photoresist liquids are less viscous. The lower viscosity allows the fluid to fill the mold cavity quickly without vacuum.

2.2.3 Commercial status of membrane fabrication techniques

The membranes can be produced as flat-sheet and tubular/HF geometry. The flat-sheet membranes are packaged either in plate-and-frame or spiral-wound modules, whereas tubular membranes are packaged in HF modules. The HF is self-supporting, and they exhibit bidirectional strength that streamlines the manufacturing process of membrane modules (Munubarthi, Gautam, Reddy, & Subbiah, 2020).

HF membrane modules offer good mechanical stability, flexibility, and provide easy maintenance. The hollow cylindrical geometry offers a higher surface-to-volume ratio of fibers offers higher productivity per unit volume of the membrane module. The HF membrane has been primarily prepared using a melt-spinning process through TIPS or via solution spinning through wet or dry/wet spinning through EIPS/SNIPS/or combination.

Table 2.2 summarizes the advantages and disadvantages of the conventional methods used for fabrication, and Table 2.3 identifies the potential fabrication technology for the commercial UF/MF membranes.

MF, microfiltration; *SNIPS*, nonsolvent-induced phase separation; *TIPS*; thermally induced phase separation; *UF*, ultrafiltration; *VIPS*, vapor-induced phase separation.

The effect of membrane stretching on the permeability-selectivity trade-off for both MF and UF membranes was analyzed (Siddiqui, Muhammad Arif, & Bashmal, 2016). Reportedly, the stretching technique exhibited a positive shift in the permeability-selectivity trade-off curve of membranes with well-dispersed pores, whereas, in the case of pore clustering, a negative

TABLE 2.2 Advantages and disadvantages of conventional polymeric fabrication methods.

Sr. No.	Fabrication method	Polymer	Properties	Pore diameter (μm)/ Pore morphology	Advantages	Disadvantages	Reference
1	Sintering		Outstanding thermal, chemical, and mechanical stability; applicable for both organic and inorganic material can be used.	(10–20)/The sintering process controls the pore size	Widely used for the preparation of inorganic and some polymeric membranes	High processing costs. High sintering temperatures thereby results in limitation of material integration, material synthesis, and phase stability.	Guo et al. (2016), Maria et al. (2017), Tan & Rodrigue (2019)
2	Track etching	PET, PVDF, PC	Provides long-term flux-stability	(0.02–10)/ Cylindrical, conical, and funnel-shaped pores can be made. The pore size can be easily varied	Allows the preparation of membranes from chemically resistant polymer materialsProvides isoporous structure	Expensive technique due to the use of high-energy radiation	Apel (2001), Daubresse, Sergent-Engelen, Ferain, Schneider, & Legras (1995), Tan & Rodrigue (2019)
3	Phase inversion		Demixing of solvent with nonsolvent (SNIPS) or thermal evaporation of diluent (TIPS)	(0.21–20)/Pore size depends up on the preparation conditions such as dope solution concentration, casting, and posttreatment temperature			
	(i) Thermally induced-phase separation (TIPS)			The sites occupied by the diluent become micropores after their removal	Suitable for semicrystalline polymers that solvents cannot easily dissolve. Membranes are inherently reproducible and less prone to defects than other phase inversion methods	The low mutual affinity between the solvent and the nonsolvent results in the surface pore hardly being tuned.Expensive and the organic solvents used are usually not environmentally friendly	Lloyd, Kinzer, & Tseng (1990), Yang, Li, Xie, Wang, & Wang (2006), Zhang, Bai, Sun, Gu, & Xu (2010), Zhang et al. (2015), Yang, Li, Xie, Wang, & Wang (2006)

	(ii)	Vapor-induced phase separation (VIPS)		Resulting from the transfer at the interface, nonsolvent (gas) inflow and solvent outflow	This process allows modification and tailoring of both flat-sheet and hollow-fiber polymer membrane morphologies	The development of commercial polymer membranes remains limited	Benhabiles et al. (2019), Park, Kim, Kim, and Kang (1999), Su et al. (2009), Tsai et al. (2006), Zhang, Bai, Sun, Gu, & Xu (2010)
	(iii)	Nonsolvent-induced phase separation (SNIPS)		Resulting from liquid−liquid phase demixing	This process can effectively control the pore size, and other membranes surface characteristics with the help of additives	Difficult to precisely control the phase inversion process	Benhabiles et al. (2019), Kahrs & Schwellenbach (2020), Marino, Blasi, Tornaghi, Emanuele, & Figoli (2018), Zhang et al. (2015), Zhu & Zhang (2014)
4	Electrospinning	Gelatin, Chitosan, Silk, Silica-PVA, PVDF, PS, PLAGA, PAN-PMMA, PSF, PDO, PA-6	Resulting from the evaporation of the diluent	Porous/Allows the formation of interconnected pores with uniform pore size and above 90% porosity in a membrane.	• Simple, inexpensive, and high productivity method. • Produce superhydrophobic polymeric membranes and highly porous structures of smooth nonwoven nanofibers	Limited production capacity and low reproducibility	Mit-uppatham, Nithitanakul, & Supaphol (2004), Raghavan et al. (2012), Rivero and Redin (2020), Tijing, Woo, Yao, Ren, & Shon (2017)
5	3D-printing	Organometallic polymers, SCR500, PC, IP-Dip, MG37GR resin			Covers complex geometry fabrication	• High cost • Limited resolution and limited materials	
6	Nanoimprinting				• Low cost, and fast fabrication technique. • Can cover a wide range of pore size and density	Limited selection of materials and geometry	

PC, *polycarbonate;* PS, *polystyrene;* PSF, *polysulfone;* PVA, *poly(vinyl alcohol);* PVDF, *poly(vinylidene fluoride);* PET, *Polyethylene terephthalate;* PLAGA, *Poly [D(-)lactic-co-glycolic] acid;* PAN-PMMA, *polyacrylonitrile-poly(methyl methacrylate);* PDO, *Polydioxanone;* PA-6, *Polyamide 6*

TABLE 2.3 Technology and their commercial availability for fabrication of MF and UF membranes.

Sr. No.	Techniques	Large-scale production unit	Remarks	Reference
1	Stretching	No	The method used in lab-scale membrane production for special applications	Agung et al. (2018), Siddiqui, Muhammad Arif, & Bashmal (2016)
2	Sintering	No		Jia et al. (2017)
3	Phase inversion		Most widely used method for fabrication of industrial-scale polymeric MF/UF membranes	
	(i) SNIPS	Yes		Pedersen, Ireland, Gal, Examiner, and Phillip (2015), Zhang et al. (2015), Zhu & Zhang (2014)
	(ii) TIPS	Yes		Jeon et al. (2018), Yan, Wang, Mao, & Zhao (2019)
	(iii) VIPS	Yes		Peng, Fan, Dong, Song, & Han (2012)
4	Electrospinning	No	Further development in pore-size distribution, antifouling properties, cost reduction, and fabrication is large.	Ahmed, Lalia, & Hashaikeh (2015), Shiohara, Prieto-Simon, & Voelcker (2021)

change of the permeability-selectivity trade-off curve was observed. The application of both sintering and stretching is still limited to lab-scale application, and stretching is evolving for PP HF MF membrane fabrication.

On the other hand, phase inversion techniques are the most commonly used to prepare polymeric membranes on both small and large scales (Peng, Fan, Dong, Song, & Han, 2012; Zhang et al., 2015; Xu et al., 2009). The membrane structure is formed by bringing a thermodynamically stable polymer solution to an unstable state inversion technique. A change in temperature, composition, or pressure leads to a decrease in the Gibbs free energy of mixing of the solution causes phase separation of the initially stable solution into two or more phases with different compositions (Pinnau & Freeman, 2000). The extruded HF membrane function properties of polymer composition and temperature can be controlled more accurately using appropriate sensors and automation. The HF membranes formed via the phase inversion method exhibit specific physiochemical properties with favorable surface and mechanical properties. The progress of membrane science and technology, particularly in polymeric membranes, has attracted particular industrial interest because they have attracted particular industrial interest due to their comparatively small footprints, cost-effectiveness, and ease of production (Ismail et al., 2020). The solvents used in membrane fabrication are primarily toxic, dipolar aprotic solvents such as *N*-methyl-2-pyrrolidone (NMP) and *N*,*N*-dimethylformamide (DMF) for phase inversion. These solvents are mixed with water during membrane formation, and as a result, significant quantities of wastewater are produced during membrane production. In May 2020, the European Union (EU) restricted *N*-Methyl-2-pyrrolidone (NMP), the most popular solvent for membrane fabrication. The selection of the appropriate solvent greatly influences

the thermodynamic and kinetics of the overall membrane separation process. It subsequently affects the final membrane morphology and structure (i.e., symmetric, asymmetric, porous, or dense). The physicochemical characteristics of solvent heavily influence the interaction with the polymeric chains and affect the final membrane's physical morphology/structure.

The TIPS is the most straightforward phase inversion technique. In this fabrication technique, the polymer is dissolved in a solvent at a proper temperature and then cooled to induce phase separation, leading to the formation of a microporous structure (Agung et al., 2018).

The nonsolvent-induced phase separation (SNIPS) process is the most common commercially used HF membrane preparation. The organic solvent used in the given process of membrane preparation using the SNIPS method accounts for 80wt.% mass of the casting solution.

Table 2.4 suggests some nontoxic (or say "less"-toxic) solvents and diluents that can potentially prepare HF UF/MF membranes using the SNIPS, TIPS techniques, respectively.

Triethyl phosphate (TEP) is a widely used solvent to fabricate HF membranes due to its low toxicity and good affinity with PVDF. Compared to other "*toxic*" solvents, the TEP is likely to be a safer solvent as it is not classified as teratogenic, mutagenic, or carcinogenic. A typical HF membrane spinning line via the TIPS method includes a twin-screw extrusion in high temperature and extraction. Citroflex such as acetyl tributyl citrate (ATBC), acetyl triethyl citrate (ATEC), and triethyl citrate (TEC) are expected to be an environmental-friendly diluent for use in an HF membrane preparation. During the melt-spinning and cold-stretching (MSCS) process, a polymer melt is spun at a temperature close to its melting point, and then the micropores of the membrane are formed by the mechanical force acting on the membranes in a subsequent cold-stretching step. This technique is considered economical and clean compared to the SNIPS and TIPS methods since this process does not require any solvent diluents (or additives) (Kahrs & Schwellenbach, 2020; Liu et al., 2011). Reportedly, over a year, the membrane fabrication can cause the release of over 50 billion liters of contaminated water (Razali et al., 2015). According to a survey, the author also suggests that about 70% of industrial membrane fabricators flush generates effluent with a treatment directly to the environment without any treatment to assess the environmental impact of fabricating 1000 m^2 of polymeric HF (Yadav et al., 2021). The author reported the application of the most famous fossil and bio-based polymers such as polysulfone (PSF), polyvinylidene fluoride (PVDF), and cellulose acetate (CA). Solvents considered for use in polymer dope solution included polar aprotic solvents (*N*-methyl-2-pyrrolidone, *N*,*N*-dimethylacetamide, and dimethylformamide) that are widely used in industry and an alternative green solvent (ethylene carbonate). Reportedly, the choice of polymer, solvent, and source of electricity was identified as the significant determinants of the environmental impact and cost.

Electrospinning is a highly versatile technique in which operating conditions and solution parameters directly determine the resulting membranes' morphology. The electrospinning technique relies on the traction generated by the interaction of polymers with the external electric field force. However, electrospinning has the potential to produce functional nanostructures with attractive properties. The industrial upscaling of the process is still limited by low production capacity and low reproducibility. The lack of sufficient efforts in upscaling the process for mass production still presents a significant drawback in the commercialization of electrospinning (Ahmed, Lalia, & Hashaikeh, 2015). Table 2.5 summarizes some commercially available HF ultrafiltration membranes in water and wastewater treatment.

TABLE 2.4 Nontoxic (or, "less" toxic) solvent (for SNIPS method) and diluent (for TIPS method) for preparation of microfiltration/ultrafiltration (UF/MF) hollow-fiber membranes.

Method	Solvent	Solubility (in water)	Boiling point (°C)	Polymer	References
SNIPS	Triethyl phosphate (TEP)	Miscible	215–216	PVDF, PVDF/P(MMA-rPEGMA)	Abed, Kumbharkar, Groth, & Li (2012), Benhabiles et al. (2019), Chang, Zuo, Lu, & Chung (2018), Chang, Zuo, Zhang, O'Brien, & Chung (2017), Wang, Zhang, Xu, Zhu, and Xu (2014)
	Gamma-butyrolactone (GBL)	Miscible	204–205	PEEK-WC, PES	Abed, Kumbharkar, Groth, & Li (2012), Alsalhy et al. (2014)
	1-ethyl-3-ethylimidazolium dimethyl phosphate (EMIM)DEP	-	-	PES	Kim, Vovusha, Schwingenschlögl, & Nunes (2017)
	1,3-dimethylimidazolium dimethyl phosphate (MMIM)DMP	Miscible		PES	Kim, Vovusha, Schwingenschlögl, & Nunes (2017)
Method	**Diluent**	**Solubility (in water)**	**Boiling point (°C)**	**Polymer**	**References**
TIPS	Acetyl tributyl citrate (ATBC)	Insoluble	343	PVDF, Ethylene chlorotrifluoroethylene (ECTFE)	Cui et al. (2013), Hassankiadeh et al. (2014), Jung et al. (2018), Kim et al. (2016)
	Triethyl citrate (TEC)	Miscible	235	ECTFE	
	Glycerol triacetate (GTA or triacetin)	Miscible	258–260	PVDF, ECTFE	Fang et al. (2018), Ghasem, Al-Marzouqi, & Rahim (2012), Ghasem, Al-Marzouqi, & Duaidar (2011), Karkhanechi et al. (2016)
	Triethylene glycol (TEG)	Miscible	276	CA, CAB, CAP	Shibutani et al. (2011)
	Diethylene glycol monoethyl ether acetate (DCAC)	Miscible	218–219	PVDF	Wu & Sun (2015)
	Methyl-5-(dimethylamino)-2-methyl-5-oxopentanoate (Polarclean)	Miscible	278–282	PVDF/PES	Marino, Blasi, Tornaghi, Emanuele, & Figoli (2018)

CA, *cellulose acetate;* CAB, *cellulose acetate butyrate;* CAP, *cellulose acetate propionate,* PES, *polyethersulfone;* PVDF, *poly(vinylidene fluoride).*

2.2.3.1 *Fabrication of flat-sheet membranes*

The fabrication of a flat-sheet membrane involves dope preparation, the rheology of the casting solution, air gap, and immersion precipitation in the coagulant bath. The process mainly concerns three steps; namely, (1) the rheology of the dope solution at the casting window, (2) the formation of nascent flat-sheet membranes in the air gap, and solidification of flat-sheet membranes in the coagulation bath.

TABLE 2.5 Some commercially available hollow fiber-ultrafiltration membranes.

Brand	Manufacturer	Membrane material	MWCO	Application
DOW/FLMTEC	SFP and SFD	PVDF	0.03 μm	Wastewater
Membrane element	M-series	PAN	(0.03–1) μm	Oil-water separation
Nitto Denko, JP	Hydracap	PES (HF)	150 kDa	Wastewater
Toray, Switzerland	HFU, HFS, HSU	PVDF (HF)	150–200 kDa	RO feed water and Wastewater

PAN, polyacrylonitrile; *PES*, polyethersulfone; *PVDF*, polyvinylidene fluoride; *RO*, reverse osmosis.

2.2.3.2 *Fabrication of hollow-fiber membranes*

In 1966 the first polymeric HF membranes were prepared by extruding a polymer solution through an annular spinneret and a bore fluid flowing in the annular center. The fabrication of HF involves the thermodynamic of the polymer solution and the phase inversion, the rheology of the polymer solution inside the spinneret and at the air, and the other spinning conditions. The fabrication of HF membranes can be carried out using: (a) dry-jet spinning; (b) wet spinning, (c) dry-jet wet-spinning process. Being an extremely complex technique, the fabrication of HF membranes entails highly sophisticated mechanical, thermodynamic, and kinetic considerations.

For the dry-jet spinning process, the spun HF membranes are only exposed to a gaseous environment before vitrification, whereas the spun hollow finer membranes are exposed to a liquid environment before vitrification for the wet-spinning process. As for the dry-jet wet spinning process, there exists an air gap between the spinneret and the coagulation bath.

2.3 Effect of polymer-enhanced microfiltration/ultrafiltration membranes

2.3.1 Structural property

Typically, the membrane performance (in terms of flux, rejection, and fouling) is strongly influenced by Lalia, Kochkodan, Hashaikeh, & Hilal (2013).

2.3.1.1 *Crystallinity of the polymer*

The crystallinity of a polymer determines the mechanical stability and permeability of the polymer. The glass transition temperature and crystallinity are primarily defined in chain flexibility, chain interaction, and the polymer's molecular weight. In general, in the crystalline phase, the polymer chains are packed regularly due to solid intermolecular interactions such as hydrogen bonding. The effect of the degree of cross-linking of PVA on polysulfone (PS)-UF membrane was investigated. The study reported that an increase in PVA's degree of cross-linking improves pure-water permeability while decreasing the PVA film's crystallinity. The addition of plasticizers (such as glycerol) generally increases

the polymer chain's mobility in plasticized material, resulting in improved water molecule diffusion (Peng, Fan, Dong, Song, & Han, 2012).

2.3.1.2 Pore structure

In UF/MF membrane process, the water flux and solute rejection are controlled by the porosity, pore-size distribution, and pore tortuosity of the membrane. The pore geometry of a membrane can be controlled by choosing an appropriate fabrication technique. For example, membranes fabricated using track-etched techniques exhibit parallel cylindrical pores with pore lengths equal to the membrane thickness. For such pore geometry, the Hagen Poiseuille equation defines permeate flux. However, membranes prepared using phase inversion, stretching, solution casting, and electrospinning have irregular pore geometry and tortuosity. In such cases, the Kozeny Carman equations model the relationship between flux and geometrical parameters of membrane pores. In the phase transition technique, the composition of the membrane-forming system and coagulation media control the porosity, pore structure, and pore-size distribution of the membranes.

2.3.1.3 Surface properties

2.3.1.3.1 Hydrophilic and hydrophobic properties of the membrane

Based on surface wetting properties, the stability of the membrane for a given application can be defined. In general, the water liking hydrophilic membranes are expected to form the water layer between foulant and membrane surface, potentially enabling fouling protection than hydrophobic membranes. Similarly, in applications such as membrane distillation, the nonwetting property must achieve only vapor flux through membrane pores; therefore, the hydrophilic membranes are not suitable. CA membrane is hydrophilic and expected to provide $<$90-degree of the contact angle between membrane surface-water drop. Similarly, the membranes made of PVDF, PP, PS, PES are hydrophobic.

2.3.1.3.2 Surface charge

The electrostatic interaction between charged solutes and porous membranes depends on the membrane charge, usually quantified in zeta-potential measurements. Usually, the UF membrane's surface charge range carries a negative amount to increase the rejection of dissolved salts and minimize the adsorption of negatively charged organic foulants and microorganisms. The negative charge on the membrane surface resulted from the sulfonic and carboxylic acid groups in the skin membrane layer. Apart from inorganic solutes, the membrane charges also affect the rejection of charged organics.

In addition, it has been reported that salts present in the feed water could reduce the negative charge on a membrane surface by "shielding" the charge. It was found that the Debye length was small at higher ionic strengths, the zeta potential was positive, electrostatic interaction was minimized within the membrane, and the pore radii could shrink. When the Debye length is longer and the zeta potential is more harmful at low ionic strength, pore radii can increase in size to minimize electrostatic repulsion between the hostile functional groups in the membrane body. The electrostatic charge of membranes is an essential consideration for reducing membrane fouling where foulants are charged, which is often the case. When the surface and the foulant have similar charges,

electrostatic repulsion forces between the foulants and the membrane prevent the foulant deposition on the membrane, thereby reducing the fouling. Like the negatively charged surface, the positively charged membrane surfaces exhibited electrochemical repulsion against positively charged proteins and may even be used to remove heavy metals and dyes from water.

2.3.2 Functionalization methods for membrane surface

2.3.2.1 Surface functional modification

Usually, some polymeric membranes possesses excellent physical, chemical, and bulk properties. However, their application has been briefly restricted due to particular limitations in the membrane surface properties required for certain specific applications. In the MF/UF membrane process, the flux and rejection of a membrane are influenced by size exclusion. Thereby, the membrane surface properties play a significant role in determining the overall membrane performance. The surface modification of polymeric membrane offers a means to improve the membrane's surface properties (including hydrophilicity, hydrophobicity, antifouling, antibacterial, and antistatic properties) the bulk structure of the base membrane. In this section, we will be discussing the following methods of surface modification of polymeric membranes (Xu et al., 2009).

2.3.2.1.1 Self-assembly

Self-assembly is comparatively a newer technique in the field of membrane surface engineering. This involves self-assembled monolayers (SAMs) and layer-by-layer (LBL) assembly. SAM can be defined as an ordered molecular assembly formed by absorbing active surfactants on the membrane surface. Over other techniques conventionally used for preparing functional materials, the given mechanism offers numerous advantages. The assembly is based on spontaneous adsorptions, and no stoichiometric control is necessary to maintain surface functionality; the assembled molecular layers exhibit a much larger thermal and mechanical stability. Most of all, the method is not restricted to the substratum and can be used for designing a surface, even on a nanoscale.

2.3.2.1.2 Coating

The surface (or physical) coating for MF/UF membranes involves polymeric solution-bearing antifouling membrane properties. In this method, the hydrophilic (biocompatible) materials are physically deposited on membrane surface using one (or more) of the following mechanisms:

1. Casting: In coating via casting technique, the brush-like layer of the polymer (or copolymer), formed on the membrane surface, acts as a steric barrier to protein adsorption. It boosts the surface of the membrane with an exceptional fouling resistance with a slight reduction in flux.
2. Adsorption or filtration: The coating via adsorption usually imparts hydrophilicity to the membrane surface, whereas layer via filtration usually results in the deposition of hydrophilic additive polymers on the membrane surface and into the membrane pores.

By coating the functional material on the membrane surface, the surface properties can change from hydrophobic (nonbiocompatible) to hydrophilic (biocompatible). This mechanism's major disadvantage is that the given method cannot result in a stable membrane as the absorbing material can easily leach (or run) away with use. Table 2.6 summarizes the UF/MF membrane fouling mitigation effort via coating (Kumar & Ismail, 2015):

2.3.2.1.3 Chemical treatment

Chemical treatment is one of the standard methods of endowing membrane surfaces with functional groups. This mechanism helps retain the membrane's mechanical properties while the interfacial properties of the membrane have changed. The chemical treatment method provides a relatively stable membrane surface, which can also be applied to modify the chemical and physical properties of the (polymeric) membrane surface. The chemical treatments involve:

TABLE 2.6 Effect of surface modification using coating on MF/UF membranes.

Base membrane	Modifier group	Antifouling results	References
PSF	PVP, PVA, methylcellulose	Increased initial UF flux and lower flux decline	Kim, Fane, & Fell (1988)
PVDF	Chitosan	Good antifouling resistance with reduced irreversible membrane fouling	Boributh, Chanachai, and Jiraratananon (2009)
PSF	Anionic, cationic and nonionic polymers and surfactants	Significant reduction in protein adsorption on the surfactant-modified membranes	Brink & Romijn (1990)
PVDF	PEG	Drastic reduction in internal fouling caused by BSA protein molecules	Susanti, Han, Kim, Lee, & Carbonell (2013)
PSF	Nonionic and anionic surfactants	Reduced fouling potential of proteins at the pore entrance due to steric hindrance between the bulky ion surfactant and the protein	Chen, Fane, & Fell (1992)
PVDF	Block and random PEGylated copolymers of PEGMA and PS	BSA's protein resistance on PVDF membranes coated with block copolymers was much higher than that with random copolymers; the protein resistance was enhanced with the PEGMA content.	Chang et al. (2009)
PP, PDMS, PS, nylon, PVC, and PMMA	Zwitterionic sulfobetaine polymers with a catechol chain end (DOPA−PSB)	The polymer with the higher molecular weight was found to have better nonfouling than the low-molecular-weight polymer because of increased surface coverage	Chinpa, Quémener, Bèche, Jiraratananon, & Deratani (2010)

MF, microfiltration; *PMMA*, poly(methyl methacrylate); *PP*, polypropylene; *PS*, polystyrene; *PSF*, polysulfone; *PVA*, poly(vinyl alcohol); *PVC*, poly(vinyl chloride); *PVDF*, poly(vinylidene fluoride); *BSA*, Bovine serum albumin; *PDMS*, Polydimethylsiloxane; *PVP*, Polyvinylpyrrolidone; *PEG*, Polyethylene glycol; *PEGMA*, Poly(ethylene glycol) methacrylate; *UF*, ultrafilitration.

1. Oxidative treatment is the dominant means for chemically modified reactions, which generally involve dry or wet oxidation. In the dry-oxidation process, the oxygen-containing groups (such as carboxyl or hydroxyl) are introduced onto the membrane surface by flame (or corona discharge) treatment.
2. In wet-oxidation method involves nitric acid, sulfuric acid, phosphoric acid, alone or in combination with hydrogen peroxide, sodium hypochlorite, permanganate, chromate, or dichromate potassium, and transition metal nitrates.

2.3.2.1.4 Plasma treatment

Membrane surface modification with plasma is one of the practical and economical surface treatment techniques for a membrane. The advantage of plasma modification is that the surface properties and biocompatibility can be enhanced selectively while the bulk attributes of the membrane remain unchanged. For plasma-induced graft polymerization, an inert gas is used to produce radicals on the polymer surface. The plasma consists of a unique mixture of positively/negatively charged ions, electrons, atoms, molecules, or free molecules. The plasma treatment is usually used to increase the polarity, charge, hydrophobicity of the polymer surface.

2.3.2.1.5 Surface graft polymerization

Surface grafting is a chemical modification method. Here, the modification is achieved by tethering suitable macromolecular chains on the membrane surface through covalent bonding. The significant advantage of this technique is:

1. The membrane surface can be modified or tailored to acquire distinctive properties by choosing different grafting monomers while maintaining the substrate properties.
2. It also ensures an easy and controllable introduction of tethered chains with a high density and exact localization onto the membrane surface.
3. And most importantly, compared to the physical modification methods (such as coating), the covalent attachment of polymer chains onto the membrane surface avoids desorption and maintains the long-term chemical stability of the modified surface.

The grafting methods can be generally divided into two classes:

1. "*grafting-to*" processes (here, the preformed polymer chains carrying reactive groups at the end or side chains are covalently coupled onto the membrane surface),
2. "*grafting-from*" processes (this method utilizes active species existing on the membrane surfaces to initiate the polymerization of monomers from the surface toward the outside bulk phase).

According to different methods used generating the reactive groups, these can be classified as:

1. Grafting initiated by chemical means: Chemical grafting can activate functional groups on the membrane surface and react with monomers or macromolecules. The grafting process path, including free radical and ionic, is determined by the species of an initiator. In these two paths, active sites are produced from the initiators and transferred to the substrate to

react with the monomer and form grafted copolymers. Typical free radical grafting is generated by a redox reaction, viz. Mn + /H_2O_2, persulfates.

2. On the other hand, alkali metal suspensions in a Lewis base liquid, organometallic compounds, and sodium naphthalene are useful initiators in an ionic model. In recent years, "Living Polymerization" methods have been developed to provide great potential for grafting reactions. These cases provide living polymers with regulated molecular weights and low polydispersities, which means that a controlled and uniform polymer layer can be generated on the membrane surface.
3. Grafting initiated by radiation technique: Interaction of a membrane with irradiation can cause homolytic fission of polymer chains and form free radicals on the surface for further grafting polymerization. Radiation grafting proceeds in two significant ways:
   a. Preirradiation techniques (here, the membrane surface is first irradiated, and then the radical-possessing substrate is grafted with a monomer).
   b. Mutual irradiation techniques (here, membrane and monomer are irradiated simultaneously to form free radicals and subsequent graft polymerization).

   Properties of membrane/monomer, the monomer's concentration, duration of radiation, reaction temperature, and the medium are few examples of the factors that affect the results of radiation grafting. The high-energy radiation goes through the uppermost layer of the membrane, which may eventually change the substrate's physical or chemical properties.
4. Photochemical grafting: When groups on the membrane surface absorb light, they go to excited states. As a result, they generate reactive radicals and then initiate the grafting process. This technique's unique feature is that it takes place at the outmost surface of the membrane, and it does not change with the original polymer properties.
5. Plasma-grafting polymerization: When a polymeric membrane is exposed to plasma, radicals are created on the surface. These radicals can initiate polymerization reactions when put in contact with monomers in the liquid or gas phase. As a result, grafted copolymers are formed on the surface. Plasma-grafting polymerization is often used to alter the surface hydrophilicity of a membrane. The plasma treatment can change the membrane surface properties by introducing some polar groups (such as hydroxyl or amino groups). However, sometimes "hydrophobic recovery" is observed. This phenomenon alters the targeted surface properties with the time of storage. This causes gradual reorientation of surface chain segments in response to the interfacial forces when the membrane surface is exposed to air (or nonpolar media).

Apart from the mentioned polymeric membrane functionalization methods, the surface imprinting methods are the most efficient method. Similarly, for the immobilization of enzymes on membrane surfaces, synergizing the selective separation functions of polymeric membranes with the catalytic properties of enzymes provides hints for the preparation of biofunctional membranes.

2.3.2.2 Functionalization of polymeric membrane by molecular imprinting

2.3.2.2.1 Formation of imprinting sites by surface photo-grafting

In this technique, the starter radicals are commonly yielded on the membrane substrate under UV excitation. The imprinted layers are covalently anchored to cover the entire

surface of the support membrane. This can be explained as an intrinsic initiation of the photosensitive groups introduced to the membrane surface by graft (or block) polymerization. Despite high selectivity, this approach is not widely used as its application is limited to few polymers, and the efficiency is relatively very low. Therefore, another technique involves coated initiation via a hydrogen abstracting photoinitiator yielding polymer starter radicals on the substrate. This approach can be adapted to any kind of membrane with the presence of a C-H bond. This approach is widely used compared to intrinsic initiation due to its extensive applicability and simplicity in preparation.

2.3.2.2.2 Formation of imprinting sites by surface deposition

A surface deposition is an approach used to prepare a thin-layer MIP composite membrane using an efficient-coated α-scission photoinitiator yielding starter radical close to the membrane surface under UV excitation. This approach is usually considered a deposition process because the support membrane is relatively inert to a photoinitiator. No chemical bond is formed between the imprinted layer and the base membrane.

2.3.2.2.3 Formation of imprinting sites by emulsion polymerization on the surface

A porous membrane is dipped into a water-in-oil emulsion containing functional polymers and templates followed by a photo-induced polymerization in this approach. The advantage of this approach is that the imprinted sites are all near or at the surface, reducing mass transfer limitation. Since this imprinting process can be carried out in an aqueous medium rather than an organic solvent, therefore, provides a possible approach for imprinting large molecules of biological interest such as protein.

2.3.2.3 Functionalization of polymeric membrane by enzyme immobilization

2.3.2.3.1 Enzyme immobilization by physical absorption

For enzyme immobilization, physical absorption is one of the straightforward methods. In this technique, the enzyme, due to interactions of H-binding, static interaction, hydrophobic force, and electron or ion affinity, gets absorbed on the membrane surface. This method operates under mild operating conditions, and the residual activity of the immobilized enzyme is high compared to chemical immobilization. However, since the binding force is weak, and can easily change with a change in temperature or pH, the amount of enzyme incorporated is relatively small.

2.3.2.3.2 Enzyme immobilization by chemical binding

The method of immobilization by chemical binding also involves crosslinking. In this technique, the enzyme or biomacromolecules are joined together using a coupling agent. Here, the enzyme or biomacromolecules are joined together using a coupling agent. An enzyme immobilized by the chemical binding has higher stability but has lower residual activity than an enzyme immobilized by physical absorption due to the denaturalization of enzyme protein during the chemical reaction.

2.3.2.3.3 Enzyme immobilization by entrapment

The entrapment involves network-like and microcapsule-like methods. The enzyme is entrapped in a polymer gel network in the network-like form, whereas the enzyme is embedded in a semipermeable microcapsule in a microcapsule-like manner. Since giant molecules (such as protein) cannot diffuse into the polymer gel (or network), this immobilization method can only be applied to the enzyme that prefers a small substrate and product. Low stability is one of the significant disadvantages of this method. Therefore, to improve the strength of the immobilized enzyme, the crosslinking technique is always used. The two most common coupling methods involve adsorption/crosslinking and entrapment/crosslinking.

2.3.2.3.4 Other methods for enzyme immobilization

Apart from the procedures mentioned above for enzyme immobilization in recent years, many novel methods such as electrochemical and site-specific immobilization methods have been developed.

1. Electrochemical entrapment is one of the electrochemical methods. In this method, an electrode coated with a porous polymer is placed into an enzyme solution. When a suitable voltage has been applied, the enzyme with a negative charge moves toward the anode and gets entrapped in the membrane forming an enzyme-immobilized electrode. One major disadvantage is that the immobilized enzyme activity is often significantly decreased because the active site may be blocked from substrate accessibility, multiple point-binding may occur, or the enzyme protein may be denatured.
2. In the site-specific immobilization method, the enzymes are attached to the membrane surface in a highly ordered array using the power of molecular recognition. The active sites of the enzymes are away from the attached point, which benefits the diffusion of the substrate. These enzymes have superior catalytic properties compared to enzymes that have been immobilized randomly.

2.3.3 Physiochemical properties

In pressure-driven membrane processes (such as MF and UF), the reduction of water permeance over time is observed. This causes inconvenience in practical application, but it also causes increased operating cost (required for membrane cleaning and replacement) and increased energy input to decrease the permeance. Due to porous structure, the MF and UF membrane suffers both external and internal fouling. The fouling can be both reversible and irreversible. The reversible fouling is derived from external fouling, and these weakly bound foulants can be easily removed by physical cleaning (e.g., backwashing). In the irreversible fouling, the foulants due to solid affinity to the membrane surface are firmly attached to the membrane surface. These foulants cannot be removed using physical and chemical treatment.

The most effective strategy to mitigate membrane fouling in membranes is to enhance the antifouling properties of the membrane using surface modification. The two most widely explored surface modification approaches are (1) coating a thin film on the membrane surface; (2) grafting of polymer chain on the surface. The material chosen for coating/grafting must be

selected. It should not have affinity toward foulants (including protein, organic compounds, and emulsions) in order to avoid any interaction between membrane surface and foulants.

The membrane surface roughness and charge also play a significant role in the overall antifouling property and membrane surface chemistry. Reportedly, a membrane with a rough surface is more susceptible to membrane fouling than a membrane with a smooth surface. Similarly, it has been observed that the surface charge can promote fouling from foulants with counter-current charges due to favorable electrostatic interaction. Therefore to improve antifouling properties of membrane coating/grafting techniques are performed. However, this also results in an additional resistance layer for water transport and significantly decreases the water permeation rate. This can be avoided by designing thin coating/grafting materials with high permeance properties. This material can be broadly categorized as hydrophilic, hydrophobic, and amphiphilic materials.

2.3.3.1 *Membrane surface modification using hydrophilic materials*

Hydrophilic materials build additional hydration on the membrane surface. This layer serves as a physical and energy barrier that prevents foulant from attaching to the surface and eventually reduces fouling. The membrane surface can be grafted and coated with hydrophilic materials [such as poly(ethylene glycol), polydopamine, and zwitterions] to enhance the hydrophilicity antifouling properties of the membrane.

1. PEG-based coatings

   Reportedly, poly(ethylene glycol) (PEG) processes good antifouling properties toward protein and oil emulsions. PEG can potentially form hydration layers due to the hydrogen bond with water, which acts as an energy barrier for protein adhesion. Using, following approach, the PEG-based materials can be used to modify the membrane surface to enhance antifouling properties:
   - **a.** The first approach is to design PEG-based polymers that are insoluble in water and then directly coated on the surface of the membrane (Ju, Bryan, Sagle, Kusuma, & Freeman, 2009; Louie et al., 2006; Sagle et al., 2009).
   - **b.** The second approach is to graft PEG chains on the membrane surface. The PEG-based materials contain functional groups covalently bound on membrane surface (BD et al., 2010; McCloskey et al., 2012; Miller, Dreyer, Bielawski, Paul, & Freeman, 2017).
2. Polydopamine

   Polydopamine (PDA) coated on UF, MF, and reverse osmosis (RO) membrane surface decrease the water contact angle and increased surface hydrophilicity for all membranes. The PDA layer thickness increases with an increase in the coating layer and, as a result, due to the added transport resistance and decreases porosity/pore-size distribution. This technique has been evaluated for scaled-up industrial-scale spiral-wound UF membranes for wastewater treatment due to its simplicity in operation. Using the solution-dipping method, the PDA coating has also been successfully applied to the HF membrane module. In a study, the author reportedly coated the surface of polysulfone (PS) (MWCO, 20 kDa) and polyethersulfone (PES) (MWCO, 20 kDa) membrane with PDA for 75 and 5/30 minutes, respectively (Miller, Paul, & Freeman, 2014). When wastewater containing oil/water emulsion was allowed to pass through both coated and uncoated membranes in a constant permeate flux crossflow system. It

was observed that the PDA-coated membranes demonstrated lower transmembrane pressure compared to uncoated membranes, thereby indicating enhanced antifouling properties by PDA coatings. The membrane surface modification using PDA grafted-on PEG (PDA-g-PEG) layer exhibited less adhesion of protein and bacteria than the unmodified membrane. Compared to unmodified membranes, the PDA-gPEG-modified UF membrane modules show improved flux and decreased transmembrane pressure.

3. Zwitterionic materials

Zwitterions can also be grafted from the membrane surface, that is, zwitterionic monomers are polymerized from the surface-functionalized with initiators. Different polymerization can be utilized depending on the type of initiators, such as photo-initiated, ozone-initiated, plasma-initiated, and physisorption radical graft polymerization. To better control the grafting density, zwitterionic monomers can be polymerized using living polymerization, such as ATRP and reversible addition-fragmentation chain-transfer polymerization. Zwitterions can also be grafted to the membrane surface via glue, such as PDA. The antifouling properties can be affected by the packing density, polymer chain conformation, chemistry, and grafting coverage. Due to the versatility of ionic groups in the zwitterionic materials, they present a promising platform to improve antifouling properties for membranes.

2.3.3.2 *Membrane surface modification using hydrophobic/amphiphilic materials*

1. Fluoropolymers

Application of low-energy surfaces have been investigated as resistant to the adhesion of bacteria, micro/macromolecules, and precipitated salts such as $CaSO_4$. Due to their nonsticky nature, the accumulated matter on low-energy surfaces (with 10–20 mN m^{-1}) can be easily washed off. Membranes can also be directly fluorinated to enhance antifouling properties. The surface fluorination of polyamide-based NF membranes reduced the surface energy from 60.0 to 44.4 mN m^{-1}.

2. Amphiphilic polymers

Amphiphilic materials consisting of both hydrophilic and nonsticky components are explored to enhance antifouling properties. Thin films of amphiphilic materials are coated on membrane surfaces via chemical vapor deposition (CVD). Reportedly, when copolymers of hydrophilic hydroxyethyl methacrylate (HEMA) and hydrophobic perfluorodecyl acrylate (PFA) were deposited on an RO membrane, the adhesion of *Escherichia coli* bacteria on the RO membrane surface was reduced (Matin et al., 2014).

2.4 Recent advances made in polymeric microfiltration/ultrafiltration membranes for water remediation application

The use of polymeric membranes for water and wastewater treatment can be justified as a promising tool. For example, market share polymeric membranes lead the membrane separation industries and markets due to their economical and practical benefits.

Different types of natural and synthetic polymers are used for water and wastewater treatment to fabricate polymeric membranes. In a recent article, an overview of the

advantages and disadvantages of polymers used to design membrane systems for wastewater treatment (Nasir, Masood, Yasin, & Hameed, 2019). It was observed that even though the membrane separation process has unique advantages in terms of easy installation and energy efficiency, efficient large-scale application is still restricted. Few identified limitations of polymeric membranes includes: fouling, lower lifetime, limited mechanical and thermal resistance. To eliminate these obstacles, new membrane development activities have been recently conducted to obtain novel membrane material and methods of fabricating/modifying polymeric membranes. Reportedly, the polymeric nanocomposite membranes are considered an ideal choice for wastewater treatment due to their superior flexibility, improved chemical/mechanical stability, high removal capability, and modular approach for scale-up, leading to less installation space requirement. For example, the incorporation of novel metallic and metallic oxide nanoparticles in the polymeric matrix can improve salt rejection, water flux, mechanical–thermal stability, and antifouling properties to the membranes. Considering the scope of this chapter, the given section attempts to briefly summarize the recent advances made in the field of preparation, modification, and performance of polymeric membranes for water and wastewater treatment.

2.4.1 Polymeric nanocomposite membranes

The nanocomposite membranes (also known as nano-enhanced membranes) are an approach for developing innovative membranes to achieve properties such as fouling resistance and high chemical and mechanical strength. In this process, the researchers focus on incorporating nanoparticles to polymeric materials resulting in nanocomposite membranes with enhanced mechanical and physiochemical properties. The nanoparticles increase the hydrophilicity of the membranes. As a result, it helps in minimizing the fouling tendency without compromising the water flux (Sarkar & Chakraborty, 2021). According to the literature, for the fabrication of nanocomposite membranes, two different approaches have been adopted by the researchers, namely:

1. Surface coating of the membrane using nanoparticle

   The coating on the polymeric membrane is a common and effective method of surface modification. In this method, the membrane is dipped into the desired concentration of the nanoparticle for a specified period of time. The attachment of nanoparticles on membrane surface can be further improved by specific means such as pressure, UV, and irradiation. Sometimes the membrane surface can be modified using in situ interfacial polymerization technique. In this technique, a secondary polymer (or adhesive) is used for polymerization with the membrane surface, and as a result, the nanoparticle binds on the membrane surface. Using SEM and FTIR analysis, the surface modifications on the membrane surface are usually ensured. As discussed in Section 3 of this chapter, the surface coating can also be performed using the sol-gel and chemical vapor deposition methods. The method of surface modification using surface coating is usually straightforward, less time-consuming, but equally effective in membrane science. However, the major limitation of this method is the leaching of nanoparticles after specific cycles since they are loosely attached on the membrane surface.
2. Entrapment of the nanoparticles inside the polymeric structure during membrane fabrication via phase inversion method

Compared to surface coating, the method of entrapment of nanoparticles inside membrane matrix during fabrication process is more complex and tedious in nature. In this process, initially, the selected nanoparticle is dispersed in polymeric solution by introducing enhanced polymer mixing techniques to form a homogeneous casting solution. The polymeric casting solution is then casted over a clean, smooth surface using a casting knife followed by a posttreatment method to produce nanocomposite membranes. During this method, the phase inversion method can be broadly categorized as in situ and ex situ. In the in situ method, the nanomaterial is synthesized during the membrane fabrication, whereas during ex situ the synthesis of the nanoparticle is carried out prior to fabrication. The key objective of the preparation of the modified membrane is to enhance the membrane's performance and improve the separation effectiveness of the given process. The table below (Table 2.7) summarizes few nanocomposite membranes for water and wastewater treatment.

From the above discussion, it is evident that the nanomaterials have unique properties that can contribute to the development of high-end new composite membranes with enhanced potentials for water and wastewater treatments. Despite these stated advantages, the cost and potential risk associated with leaching nanoparticles to the treated water may lead to environmental pollution risk. Therefore, the application of nanocomposite membranes for industrial application cannot be extended until long-term studies are available to explore the membrane's stability and reduce the environmental pollution risk.

TABLE 2.7 Summary of TiO_2 and SiO_2 nanocomposite membranes for water and wastewater treatment process.

Nanomaterial	Modification technique	Purpose of modification	Reference
TiO_2	Surface coating	Thermal stability, permeability, selectivity, and salt rejection were improved to a satisfactory level. At a higher concentration of TiO_2 water flux became doubled compared to pure polyamide membrane	Rajaeian, Rahimpour, Tade, & Liu (2013)
	Sol-gel surface coating method	Improved hydrophilicity of the membrane surface showed better antifouling property however, the water flux was decreased	Razmjou, Mansouri, Chen, Lim, & Amal (2011)
	Dip coating	TiO_2 nanoparticles (in situ generated) were coated on a PES membrane at different temperatures, and polyacrylic acid was used to ensure fill coverage of nanoparticles on the membrane surface.	Fischer et al. (2018)
SiO_2	Phase inversion method	The composite membrane was applied for the separation of oil from the oil-water emulsion. It provided improved permeability and antifouling property.	Ahmad, Majid, & Ooi (2011)
	Phase inversion casting method	The modified membranes had improved hydrophilicity, porosity, water uptake, thermal stability, and antifouling properties.	Huang et al. (2012)

2.4.2 Literature review on the recent advances made in the field of polymeric microfiltration/ultrafiltration for water remediation application

The membrane separation process represents one of the most promising purification strategies for the purification of water sources. The existing commercially available UF membrane consists of broad pore-size distribution, thus limiting their size selectivity and making them prone to fouling. In a study the author suggested the improvements in the size selectivity to maximize the potential utilization of UF membranes (Hampu, Werber, Chan, Feinberg, & Hillmyer, 2020). The author reported, block polymers as a transformative solution since these materials can potentially self-assemble into a well-defined domain of uniform size. However, commercialization of block polymer UF membranes requires continuous production at a large scale and low costs. Here, the author suggested that the membrane fabricated through non-solvent-induced phase separation (SNIPS) technique is expected to be advantageous in the given context. In this method, a concentrated block polymer solution is casted into a film and immersed in a nonsolvent after a short evaporation time to induce phase separation and pore-formation. Reportedly, the SNIPS technique can reduce the consumption of block polymer by up to 95% while producing block polymer UF membrane. As a result, the overall production cost will be reduced. In another aspect, the block polymer membrane can be easily fabricated into a highly permeable membrane system using a blade-coating technique. The SNIPS process can be easily integrated into a conventional fiber spinning process, and this integrated process can enable industry-scale production capacity for HF membrane modules. However, the high material cost may limit block polymer membranes to high-value UF applications (such as bioprocessing, virus filtration) where the complete separation between the solute of similar size is crucial. A facile and up-scale fabrication strategy for PSF/PEG (polysulfone/polyethylene glycol) triblock polymer membranes was suggested (Ma, Wang, Liu, Hu, & Wang, 2021). In this method, the polymer triblock consists of PSF as the majority middle block tethered with a shorter block of PEG on both ends. Reportedly, this technique consists of spray coating dilute homogeneous triblock polymer solution on the top of macroporous support, resulting in a uniform polymer coating (thickness $\sim$ 1.2 μm) followed by immersion in an ethanol/acetone resulting in mesoporous triblock polymer coating as the selective layers. The author suggested the combination of spray coating and selective swelling is upscalable for the production of high-performance PSF-UF membranes.

The PES and PVDF are widely used for the production of polymeric UF membranes. Reportedly, these materials are intrinsically hydrophobic and are alarmingly prone to foul by both natural/artificial organic matter present in water and wastewaters. The membrane manufacturers usually address this issue by incorporating hydrophilic additives (such as PVP or PEG) during the early stages of membrane fabrication (i.e., before phase separation or during the dope preparation). However, due to the weak bond between the hydrophobic membrane matrix and hydrophilic additives. These hydrophilic additives have poor resistance to oxidants (such as chlorine and chlorine derivatives, conventionally used for membrane disinfection). To address these issues, a new generation PVDF membrane UF "Neophil" membrane for water filtration was developed using Kynar resin and new-block copolymer as hydrophilic additive (Lorain et al., 2020). Compared to the conventional additives, this type of block copolymers are resistant to oxidation and are not modified

during aging. The author suggested substantial benefits of Neophil membrane for pilot scale or large-scale units.

The membrane prepared using SNIPS process produces large amounts of organic solvents that are toxic to both humans and the environment. In an attempt of developing a green and sustainable method of membrane fabrication (Xie et al., 2021). The author utilized methyl-5-(dimethylamino)-2-methyl-5-oxopentanoate (PolarClean) as a green solvent for fabrication of poly(vinyl chlorine), PVC UF membranes. In the posttreatment process, the zwitterionic polymer, [2-(methacryloyloxy) ethyl] dimethyl-(3-sulfopropyl) ammonium hydroxide (DAMPS) was grafted onto the membrane surface to enhance the membranes antifouling properties using a green surface-initiated activator regenerated by an electron transfer-atom transfer radical polymerization (ARGET-ATRP) reaction.

Similarly, a sustainable polymeric membrane fabrication technique without using any hazardous organic solvent or crosslinker was also proposed (Kamp, Emonds, Borowec, Restrepo Toro, & Wessling, 2021). In this study, the author reportedly fabricated PES membrane using the salt dilution-induced phase separation method. Here, the complexation of the polyanions and polycations are suppressed by an overcritical salt concentration resulting in a homogeneous liquid solution. Due to the diffusion-induced subsequent dilution, the salt concentration in the homogeneous, stable polymer solution decreases until the composition reaches the demixing gap. The author suggested that the proposed salt dilution-induced polyelectrolyte complex membrane formation from the overcritical liquid polymer solution represents an easy-to-implement polymeric membrane fabrication method using commercially available polyelectrolytes.

The recent progress on the use of polymeric UF/MF membranes to remove dye and pigments from industrial waste effluent effectively (Ibrahim, Isloor, & Lakshmi, 2020). A new approach is proposed by using PES as a polymer blend with PPSU to improve membrane performance. The PES-PPSU UF membranes were prepared to remove dye from the simulated leather and tanning industry wastewater. The author tailored the morphology and performance of the PES-UF membranes using SNIPS method for dye and salt selective separation purposes. Reportedly, the dye removal efficiency was found to be higher than 99.65% (Hu et al., 2021).

To treat oily wastewater (oil/water emulsion), membrane technology is considered an effective method because of high separation with relatively simple operating conditions (Zhu, Wang, Jiang, & Jin, 2014). In a recent published article, the application of UF membrane process in oily wastewater treatment was briefly discussed (Ahmad, Guria, & Mandal, 2020). The author highlighted the challenges faced for commercial applications of UF membranes covering both the economic and strategic aspects. For the treatment of oily wastewaters (or oil/water emulsions) the polymers such as PVDF and PSF are widely used to prepare UF/MF membrane preparation. Most polymeric membranes are oleophilic in nature and thus cause the fouling as mentioned above and decline in flux. Reportedly, the polymeric membranes' hydrophilicity and antifouling performance can be improved by either blending with hydrophilic components or surface modification. Reportedly, a PVA-modified PVDF MF membranes to treat oil-in-water emulsion using a simple one-step approach to modify the surface of the PVDF membrane to produce good hydrophilicity with underwater superoleophobicity and accessible cleaning properties (Gu et al., 2021). In this method, PVA was directly and covalently anchored on PVDF membranes through an unconventional radiation method.

2.5 Microplastics and polymeric membranes

Current analytical practices for assessing and elucidating membrane degradation and its impact on atomic to macroscopic levels can be broadly classified to access changes in the filtration characteristics, surface characteristics, chemical/structural characteristics, morphological, mechanical, and thermochemical characteristics.

1. Filtration characteristics

   Filtration characteristics, such as permeability, membrane resistance, and solute rejection, are fundamental, real-time tests, and nondestructive methods for tracing the changes in membrane properties after degradation. The membrane permeability represents intrinsic membrane hydraulic resistance and, thus, is commonly referred to as the extent of the membrane flux restoration after cleaning. However, hydraulic permeability is a decisive measurement of membrane filtration; it cannot be considered a reliable tool for routine monitoring of membrane aging or degradation. Similarly, a change in rejection performance and pore size is usually measured by a solute rejection test using molecular weight markers (such as dextran, PEG, and polystyrene) of varying ranges. The direct pore-size measurements based on the bubble point and gas transport methods are comparatively more accurate methods for measuring the changes in pore-size distribution caused by pore enlargement due to membrane degradation.
2. Surface characteristics

   In polymeric membranes, the hydrophilicity and surface charge are parameters that affect the fouling propensity of the membranes. Reportedly, a hydrophilic uncharged membrane surface is considered to be resistant to fouling. Certain chemicals in contact with membranes may alter the hydrophilicity and surface charge properties of the membrane. The membrane hydrophilicity can be characterized using the sessile drop technique. The electrokinetic aspect of the membrane is measured in terms of streaming potential, which is conventionally used to indicate the potential of the membrane surface (or zeta).
3. Chemical/structural characteristics

   The ATR-FTIR and XPS are the two most widely used techniques to elucidate the chemical modification mechanism and membrane degradation. The ATR-FTIR technique is used to detect the bond between the membranes' functional group and chemical structure. The XPS techniques determine the surface composition of membrane samples and demonstrate their relative changes upon chemical treatment. XPS analysis of virgin and aged membrane allows the detection of chemical agent depositions on membrane surfaces and missing functional groups resulting from a chemical reaction between chemical agents and the membrane surface. In general, ATR-FTIR is conventionally adopted as a qualitative measurement of change in the chemical structure, whereas XPS is qualitative. Reportedly, increased exposure of membrane with hypochlorite results in decreased molar mass distribution, therefore exhibiting the formation of low molar mass polymers as a consequence of the polymeric chain breaking. The structural and operational deterioration of the PES-UF membrane due to chemical cleaning was analyzed using SEM microscopy, FTIR spectroscopy, contact angle measurement, and hydraulic membrane performance evaluation (Malczewska & Żak, 2019).

4. Morphological characteristics

   In membrane degradation studies, various microscopic methods such as scanning electron microscopy (SEM), transmission electron microscopy (TEM), field emission scanning electron microscopy (FESEM), scanning probe microscope (SPM), and atomic force microscopy (AFM) were used to visualize the degradation on the membrane surface. AFM is one of the surface probe microscope techniques in which a precision tip interacts with the sample, and the forces acting between them are measured. AFM produces micrograph images of the membrane surface and provides valuable information about pore-size distribution (MF/UF), surface roughness (NF/RO), surface forces, electrical properties, and interactions between membrane and foulant. Surface smoothness is an essential factor affecting membrane fouling; a smooth surface is comparatively resistant to membrane fouling. AFM is a valuable supportive tool that provides an insight into the surface roughness and porosity of the membrane.

5. Mechanical and thermochemical characteristics

   In polymeric membranes, physical aging is expected to be characterized by increased yield stress, whereas cross-linking is characterized by the rise in stress in the plastic zone, and a decrease in yield stress describes plasticization. Thermogravimetric analysis (TGA) is used to detect the mass of the sample as a function of temperature and time. TGA is commonly used to determine the degradation temperatures of the polymer materials; however, its application in membrane degradation studies is limited.

According to definition, microplastics (MPs) are plastic particles less than 5 mm in size (Frias & Nash, 2019; Yaranal, Subbiah, & Mohanty, 2021). However, from the above discussion, the release of degraded polymeric membranes can aid another subsequent source of environmental pollution. Similar to plastic bottles and carry bags, the degradation of polymeric membranes can also lead to the generation of micro- and nanolevel particles, which may further contribute to secondary MPs (Herbort & Schuhen, 2017; Jiang, 2018). Thereby, alongside advanced low-fouling, high propensity membrane fabrication techniques, the advanced study on optimizing the application and operating condition of polymeric membranes to control the release of degraded polymers to the environment are equally essential.

2.6 Prospective

Polymeric membranes have emerged significantly from 1855 to 2021. Different fabrication techniques for porous polymeric membranes were presented and discussed briefly in this chapter. However, the impact of membrane fabrication and challenges associated with polymeric degradation are still the prime challenges related to applying polymeric membranes for future innovation. These include better (polymeric) material. Thereby, this section is primarily intended to highlight the obstacles polymeric membranes are still facing. This consists of the chemical/biological contaminant removal, membrane fouling, and awareness highlighted as areas needing further research and development.

References

Agung, A., Agung, I., Komaladewi, S., Teta, P., Aryanti, P., Lugito, G., ... Gede, I. (2018). Recent progress in microfiltration polypropylene membrane fabrication by stretching method. In *E3S web of conferences, 3rd i-TREC 2018* (pp. 1–7).

Abed, M. R. M., Kumbharkar, S. C., Groth, A. M., & Li, K. (2012). Ultrafiltration PVDF hollow fibre membranes with interconnected bicontinuous structures produced via a single-step phase inversion technique. *Journal of Membrane Science*, *407–408*, 145–154. Available from https://doi.org/10.1016/j.memsci.2012.03.029.

Ahmad, A. L., Majid, M. A., & Ooi, B. S. (2011). Functionalized PSf/SiO_2 nanocomposite membrane for oil-in-water emulsion separation. *Desalination*, *268*, 266–269. Available from https://doi.org/10.1016/j.desal.2010.10.017.

Ahmad, T., Guria, C., & Mandal, A. (2020). A review of oily wastewater treatment using ultrafiltration membrane: A parametric study to enhance the membrane performance. *Journal of Water Process Engineering*, *36*, 101289. Available from https://doi.org/10.1016/j.jwpe.2020.101289.

Ahmadi, H., Javanbakht, M., Akbari-adergani, B., & Shabanian, M. (2019). Photo-grafting of β-cyclodextrin onto the polyethersulfone microfiltration-membrane: Fast surface hydrophilicity improvement and continuous phthalate ester removal. *Journal of Applied Polymer Science*, *136*, 47632. Available from https://doi.org/10.1002/app.47632.

Ahmed, F. E., Lalia, B. S., & Hashaikeh, R. (2015). A review on electrospinning for membrane fabrication: Challenges and applications. *Desalination*, *356*, 15–30. Available from https://doi.org/10.1016/j.desal.2014.09.033.

Alsalhy, Q. F., Salih, H. A., Simone, S., Zablouk, M., Drioli, E., & Figoli, A. (2014). Poly(ether sulfone) (PES) hollow-fiber membranes prepared from various spinning parameters. *Desalination*, *345*, 21–35. Available from https://doi.org/10.1016/j.desal.2014.04.029.

Apel, P. (2001). Track etching technique in membrane technology. *Radiation Measurements*, *34*, 559–566. Available from https://doi.org/10.1016/S1350-4487(01)00228-1.

BD, M., HB, P., Ju, H., BW, R., DJ, M., BJ, C., ... BD, F. (2010). *Polymer*, *51*, 3472–3485.

Benhabiles, O., Galiano, F., Marino, T., Mahmoudi, H., Lounici, H., & Figoli, A. (2019). Preparation and characterization of TiO2-PVDF/PMMA blend membranes using an alternative non-toxic solvent for UF/MF and photocatalytic application. *Molecules (Basel, Switzerland)*, *24*, 1–20. Available from https://doi.org/10.3390/molecules24040724.

Boributh, S., Chanachai, A., & Jiraratananon, R. (2009). Modification of PVDF membrane by chitosan solution for reducing protein fouling. *Journal of Membrane Science*, *342*, 97–104. Available from https://doi.org/10.1016/j.memsci.2009.06.022.

Brink, L. E. S., & Romijn, D. J. (1990). Reducing the protein fouling of polysulfone surfaces and polysulfone ultrafiltration membranes: Optimization of the type of presorbed layer. *Desalination*, *78*, 209–233. Available from https://doi.org/10.1016/0011-9164(90)80044-C.

Bryan D. Mc Closkey, Ho Bum Park, Hao Ju, Brandon W.Rowe, Daniel J.Miller, Byeong Jae Chun, Katherine Kin, Benny D. Freeman. (2010). *Polymer 51*:3472–85. Available from https://doi.org/10.1016/j.polymer.2010.05.008.

Chang, J., Zuo, J., Lu, K., & Chung, T.-S. (2018). Membrane development and energy analysis of freeze desalination-vacuum membrane distillation hybrid systems powered by LNG regasification and solar energy. *Desalination*, *449*, 16–25. Available from https://doi.org/10.1016/j.desal.2018.10.008.

Chang, J., Zuo, J., Zhang, L., O'Brien, G. S., & Chung, T.-S. (2017). Using green solvent, triethyl phosphate (TEP), to fabricate highly porous PVDF hollow fiber membranes for membrane distillation. *Journal of Membrane Science*, *539*. Available from https://doi.org/10.1016/j.memsci.2017.06.002.

Chang, Y., Ko, C.-Y., Shih, Y.-J., Quémener, D., Deratani, A., Wei, T.-C., et al. (2009). Surface grafting control of PEGylated poly(vinylidene fluoride) antifouling membrane via surface-initiated radical graft copolymerization. *Journal of Membrane Science*, *345*, 160–169. Available from https://doi.org/10.1016/j.memsci.2009.08.039.

Chen, V., Fane, A. G., & Fell, C. J. D. (1992). The use of anionic surfactants for reducing fouling of ultrafiltration membranes: their effects and optimization. *Journal of Membrane Science*, *67*, 249–261. Available from https://doi.org/10.1016/0376-7388(92)80028-I.

Chinpa, W., Quémener, D., Bèche, E., Jiraratananon, R., & Deratani, A. (2010). Preparation of poly(etherimide) based ultrafiltration membrane with low fouling property by surface modification with poly(ethylene glycol). *Journal of Membrane Science*, *365*, 89–97. Available from https://doi.org/10.1016/j.memsci.2010.08.040.

Cui, Z., Hassankiadeh, N. T., Lee, S. Y., Lee, J. M., Woo, K. T., Sanguineti, A., et al. (2013). Poly(vinylidene fluoride) membrane preparation with an environmental diluent via thermally induced phase separation. *Journal of Membrane Science*, *444*, 223–236. Available from https://doi.org/10.1016/j.memsci.2013.05.031.

Das, C., & Gebru, K. A. (2018). *Polymeric Membrane Synthesis, Modification, and Applications. Polymeric membrane synthesis, modification, and applications, polymeric membrane synthesis, modification, and applications electro-spun and phase inverted membranes*. CRC Press.

Daubresse, C., Sergent-Engelen, T., Ferain, E., Schneider, Y.-J., & Legras, R. (1995). Characterisation of energetic heavy ion track in PVDF: Production of PVDF track-etched membrane and application. *Nuclear Instruments and Methods in Physics Research Section B: Beam Interactions with Materials and Atoms*, *105*, 126–129. Available from https://doi.org/10.1016/0168-583X(95)00529-3.

Fang, C., Jeon, S., Rajabzadeh, S., Cheng, L., Fang, L., & Matsuyama, H. (2018). Tailoring the surface pore size of hollow fiber membranes in the TIPS process. *Journal of Materials Chemistry A*, *6*, 535–547.

Fischer, K, Schulz, P, Atanasov, I, Latif, AA, Thomas, I, Kühnert, M, et al. (2018). Synthesis of High Crystalline TiO_2 Nanoparticles on a Polymer Membrane to Degrade Pollutants from. *Water*. Available from https://doi.org/10.3390/catal8090376

Frias, J. P. G. L., & Nash, R. (2019). Microplastics: Finding a consensus on the definition. *Marine Pollution Bulletin*, *138*, 145–147. Available from https://doi.org/10.1016/j.marpolbul.2018.11.022.

Ghasem, N., Al-Marzouqi, M., & Duaidar, A. (2011). Effect of quenching temperature on the performance of poly (vinylidene fluoride) microporous hollow fiber membranes fabricated via thermally induced phase separation technique on the removal of CO_2 from CO_2-gas mixture. *International Journal of Greenhouse Gas Control*, *5*, 1550–1558. Available from https://doi.org/10.1016/j.ijggc.2011.08.012.

Ghasem, N., Al-Marzouqi, M., & Rahim, N. (2012). Effect of polymer extrusion temperature on poly(vinylidene fluoride) hollow fiber membranes: Properties and performance used as gas–liquid membrane contactor for CO_2 absorption. *Separation and Purification Technology*, *99*, 91–103. Available from https://doi.org/10.1016/j.seppur.2012.07.021.

Gu, Y., Zhang, B., Fu, Z., Li, J., Yu, M., Li, L., & Li, J. (2021). Poly (vinyl alcohol) modification of poly(vinylidene fluoride) microfiltration membranes for oil/water emulsion separation via an unconventional radiation method. *Journal of Membrane Science*, *619*, 118792. Available from https://doi.org/10.1016/j.memsci.2020.118792.

Guo, J., Berbano, S. S., Guo, H., Baker, A. L., Lanagan, M. T., & Randall, C. A. (2016). Cold Sintering Process of Composites: Bridging the Processing Temperature Gap of Ceramic and Polymer Materials. *Advanced Functional Materials*, *26*, 7115–7121. Available from https://doi.org/10.1002/adfm.201602489.

Hampu, N., Werber, J. R., Chan, W. Y., Feinberg, E. C., & Hillmyer, M. A. (2020). Next-Generation Ultrafiltration Membranes Enabled by Block Polymers. *ACS Nano*, *14*, 16446–16471. Available from https://doi.org/10.1021/acsnano.0c07883.

Hassankiadeh, N. T., Cui, Z., Kim, J. H., Shin, D. W., Sanguineti, A., Arcella, V., et al. (2014). PVDF hollow fiber membranes prepared from green diluent via thermally induced phase separation: Effect of PVDF molecular weight. *Journal of Membrane Science*, *471*, 237–246. Available from https://doi.org/10.1016/j.memsci.2014.07.060.

Herbort, A. F., & Schuhen, K. (2017). A concept for the removal of microplastics from the marine environment with innovative host-guest relationships. *Environmental Science and Pollution Research*, *24*, 11061–11065. Available from https://doi.org/10.1007/s11356-016-7216-x.

Hu, M., Cui, Z., Yang, S., Li, J., Shi, W., Zhang, W., et al. (2021). Pregelation of sulfonated polysulfone and water for tailoring the morphology and properties of polyethersulfone ultrafiltration membranes for dye/salt selective separation. *Journal of Membrane Science*, *618*, 118746. Available from https://doi.org/10.1016/j.memsci.2020.118746.

Huang, J., Zhang, K., Wang, K., Xie, Z., Ladewig, B., & Wang, H. (2012). Fabrication of polyethersulfone-mesoporous silica nanocomposite ultrafiltration membranes with antifouling properties. *Journal of Membrane Science*, *423–424*, 362–370. Available from https://doi.org/10.1016/j.memsci.2012.08.029.

Ibrahim, G. P. S., Isloor, A. M., & Lakshmi, B. (2020). *Synthetic polymer-based membranes for dye and pigment removal. Synthetic polymeric membranes for advanced water treatment, gas separation, and energy sustainability* (pp. 39–52). Elsevier.

Ida, S. (2021). PES (Poly(ether sulfone)), Polysulfone BT. In S. Kobayashi, & K. Müllen (Eds.), *Encyclopedia of polymeric nanomaterials* (pp. 1–8). Berlin, Heidelberg: Springer.

Ismail, N., Venault, A., Mikkola, J.-P., Bouyer, D., Drioli, E., & Tavajohi Hassan Kiadeh, N. (2020). Investigating the potential of membranes formed by the vapor induced phase separation process. *Journal of Membrane Science*, *597*, 117601. Available from https://doi.org/10.1016/j.memsci.2019.117601.

Jeon, S., Nishitani, A., Cheng, L., Fang, L. F., Kato, N., Shintani, T., & Matsuyama, H. (2018). One-step fabrication of polyamide 6 hollow fibre membrane using non-toxic diluents for organic solvent nanofiltration. *RSC Advances*, *8*, 19879–19882. Available from https://doi.org/10.1039/c8ra03328e.

Ji, J., Liu, F., Hashim, N. A., Abed, M. R. M., & Li, K. (2015). Poly(vinylidene fluoride) (PVDF) membranes for fluid separation. *Reactive and Functional Polymers*, *86*, 134–153. Available from https://doi.org/10.1016/j.reactfunctpolym.2014.09.023.

Jia, J., Kang, G., Zou, T., Li, M., Zhou, M., & Cao, Y. (2017). Sintering process investigation during polytetrafluoroethylene hollow fibre membrane fabrication by extrusion method. *High Performance Polymers*, *29*. Available from https://doi.org/10.1177/0954008316669409, 095400831666940.

Jiang, J.-Q. (2018). Occurrence of microplastics and its pollution in the environment: A review. *Sustainable Production and Consumption*, *13*, 16–23. Available from https://doi.org/10.1016/j.spc.2017.11.003.

Joshi, P., & Kumar, D. (2018). The role of polymer nanocomposite-based membranes for environmental remediation. In Chaudhery Mustansar Hussain, & Ajay Kumar Mishra (Eds.), *New polymer nanocomposites for environmental remediation* (pp. 437–456). Elsevier, for E.R.

Ju, H., Bryan, M., Sagle, A. C., Kusuma, V. A., & Freeman, B. D. (2009). Preparation and characterization of cross-linked poly(ethylene glycol) diacrylate hydrogels as fouling-resistant membrane coating materials. *Journal of Membrane Science*, *330*, 180–188. Available from https://doi.org/10.1016/j.memsci.2008.12.054.

Jung, J. T., Wang, H. H., Kim, J. F., Lee, J., Kim, J. S., Drioli, E., & Lee, Y. M. (2018). Tailoring nonsolvent-thermally induced phase separation (N-TIPS) effect using triple spinneret to fabricate high performance PVDF hollow fiber membranes. *Journal of Membrane Science*, *559*, 117–126. Available from https://doi.org/10.1016/j.memsci.2018.04.054.

Kahrs, C., & Schwellenbach, J. (2020). Membrane formation via non-solvent induced phase separation using sustainable solvents: A comparative study. *Polymer*, *186*, 122071. Available from https://doi.org/10.1016/j.polymer.2019.122071.

Kamp, J., Emonds, S., Borowec, J., Restrepo Toro, M. A., & Wessling, M. (2021). On the organic solvent free preparation of ultrafiltration and nanofiltration membranes using polyelectrolyte complexation in an all aqueous phase inversion process. *Journal of Membrane Science*, *618*, 118632. Available from https://doi.org/10.1177/2055207619871808.

Karkhanechi, H., Rajabzadeh, S., Di Nicolò, E., Usuda, H., Shaikh, A. R., & Matsuyama, H. (2016). Preparation and characterization of ECTFE hollow fiber membranes via thermally induced phase separation. *Polymer*, *97*, 515–524. Available from https://doi.org/10.1016/j.polymer.2016.05.067.

Kim, D. L., Vovusha, H., Schwingenschlögl, U., & Nunes, S. P. (2017). Polyethersulfone flat sheet and hollow fiber membranes from solutions in ionic liquids. *Journal of Membrane Science*, *539*, 161–171. Available from https://doi.org/10.1016/j.polymer.2016.05.067.

Kim, J. F., Jung, J. T., Wang, H. H., Lee, S. Y., Moore, T., Sanguineti, A., et al. (2016). Microporous PVDF membranes via thermally induced phase separation (TIPS) and stretching methods. *Journal of Membrane Science*, *509*, 94–104. Available from https://doi.org/10.1016/j.memsci.2016.02.050.

Kim, K. J., Fane, A. G., & Fell, C. J. D. (1988). The performance of ultrafiltration membranes pretreated by polymers. *Desalination*, *70*, 229–249. Available from http://dx.doi.org/10.1016/0011-9164(88)85057-4.

Kumar, R., & Ismail, A. F. (2015). Fouling control on microfiltration/ultrafiltration membranes: Effects of morphology, hydrophilicity, and charge. *Journal of Applied Polymer Science*, *132*. Available from https://doi.org/10.1002/app.42042.

Lalia, B. S., Kochkodan, V., Hashaikeh, R., & Hilal, N. (2013). A review on membrane fabrication: Structure, properties and performance relationship. *Desalination*, *326*, 77–95. Available from https://doi.org/10.1016/j.desal.2013.06.016.

Lau, W. J. (2016). Polyamide membrane BT. In E. Drioli, & L. Giorno (Eds.), *Encyclopedia of membranes* (pp. 1588–1590). Berlin, Heidelberg: Springer.

Lee, J. S., Heo, S. A., Jo, H. J., & Min, B. R. (2016). Preparation and characteristics of cross-linked cellulose acetate ultrafiltration membranes with high chemical resistance and mechanical strength. *Reactive and Functional Polymers*, *99*, 114–121. Available from https://doi.org/10.1016/j.reactfunctpolym.2015.12.014.

Li, L., Hashaikeh, R., & Arafat, H. A. (2013). Development of eco-efficient micro-porous membranes via electrospinning and annealing of poly (lactic acid). *Journal of Membrane Science*, *436*, 57–67. Available from https://doi.org/10.1016/j.memsci.2013.02.037.

Li, Q., Li, Y., Ma, X., Du, Q., Sui, K., Wang, D., et al. (2017). Filtration and adsorption properties of porous calcium alginate membrane for methylene blue removal from water. *Chemical Engineering Journal*, *316*, 623–630. Available from https://doi.org/10.1016/j.cej.2017.01.098.

Liu, X. D., Ni, L., Zhang, Y. F., Liu, Z., Feng, X. S., & Ji, L. (2011). Technology Study of Polypropylene Hollow Fiber Membranes-Like Artificial Lung Made by the Melt-Spinning and Cold-Stretching Method. *Advanced Materials Research*, *418–420*, 26–29. Available from https://doi.org/10.4028/www.scientific.net/AMR.418-420.26.

Lloyd, D. R., Kinzer, K. E., & Tseng, H. S. (1990). Microporous membrane formation via thermally induced phase separation. I. Solid-liquid phase separation. *Journal of Membrane Science*, *52*, 239–261. Available from https://doi.org/10.1016/S0376-7388(00)85130-3.

Lorain, O., Marcellino, S., Deratani, A., Gassara, S., Duchemin, I., & Espenan, J.-M. (2020). New ultrafiltration (UF) membrane made with a new polymer material for long lasting and rejections performances, Neophil®. *Water Practice and Technology*, *15*. Available from https://doi.org/10.2166/wpt.2020.022.

Louie, J. S., Pinnau, I., Ciobanu, I., Ishida, K. P., Ng, A., & Reinhard, M. (2006). Effects of polyether–polyamide block copolymer coating on performance and fouling of reverse osmosis membranes. *Journal of Membrane Science*, *280*, 762–770. Available from https://doi.org/10.1016/j.memsci.2006.02.041.

Ma, D., Wang, Z., Liu, T., Hu, Y., & Wang, Y. (2021). Spray coating of polysulfone/poly(ethylene glycol) block polymer on macroporous substrates followed by selective swelling for composite ultrafiltration membranes. *Chinese Journal of Chemical Engineering*, *29*, 85–91. Available from https://doi.org/10.1016/j.cjche.2020.05.002.

Malczewska, B., & Żak, A. (2019). Structural Changes and Operational Deterioration of the Uf Polyethersulfone (Pes) Membrane Due to Chemical Cleaning. *Scientific Reports*, *9*, 1–14. Available from https://doi.org/10.1038/s41598-018-36697-2.

Maria, J.-P., Kang, X., Floyd, R. D., Dickey, E. C., Guo, H., Guo, J., et al. (2017). Cold sintering: Current status and prospects. *Journal of Materials Research*, *32*, 3205–3218. Available from https://doi.org/10.1557/jmr.2017.262.

Marino, T., Blasi, E., Tornaghi, S., Emanuele, D. N., & Figoli, A. (2018). Polyethersulfone membranes prepared with Rhodiasolv (R) Polarclean as water soluble green solvent. *Journal of Membrane Science*, *549*, 192–204. Available from https://doi.org/10.1016/j.memsci.2017.12.007.

Matin, A., Shafi, H. Z., Khan, Z., Khaled, M., Yang, R., Gleason, K., & Rehman, F. (2014). Surface modification of seawater desalination reverse osmosis membranes: Characterization studies & performance evaluation. *Desalination*, *343*, 128–139. Available from https://doi.org/10.1016/j.desal.2013.10.023.

McCloskey, B. D., Park, H. B., Ju, H., Rowe, B. W., Miller, D. J., & Freeman, B. D. (2012). A bioinspired fouling-resistant surface modification for water purification membranes. *Journal of Membrane Science*, *413–414*, 82–90. Available from https://doi.org/10.1016/j.memsci.2012.04.021.

Meng, S., Winters, H., & Liu, Y. (2015). Ultrafiltration behaviors of alginate blocks at various calcium concentrations. *Water Research*, *83*, 248–257. Available from https://doi.org/10.1016/j.watres.2015.06.008.

Miller, D. J., Dreyer, D. R., Bielawski, C. W., Paul, D. R., & Freeman, B. D. (2017). Surface Modification of Water Purification Membranes. *Angewandte Chemie - International Edition*, *56*, 4662–4711. Available from https://doi.org/10.1002/anie.201601509.

Miller, D. J., Paul, D. R., & Freeman, B. D. (2014). An improved method for surface modification of porous water purification membranes. *Polymer*, *55*, 1375–1383. Available from https://doi.org/10.1016/j.polymer.2014.01.046.

Mit-uppatham, C., Nithitanakul, M., & Supaphol, P. (2004). Ultrafine Electrospun Polyamide-6 Fibers : Effect of Solution Conditions on Morphology and Average Fiber Diameter. *Macromolecular chemistry and Physics*, *6*, 2327–2338. Available from https://doi.org/10.1002/macp.200400225.

Moheman, A., Alam, M. S., & Mohammad, A. (2016). Recent trends in electrospinning of polymer nanofibers and their applications in ultra thin layer chromatography. *Advances in Colloid and Interface Science*. Available from https://doi.org/10.1016/j.cis.2015.12.003.

Mokhena, T., & Luyt, A. S. (2017). Development of multifunctional nano/ultrafiltration membrane based on a chitosan thin film on alginate electrospun nanofibres. *Journal of Cleaner Production*, *156*, 470–479. Available from https://doi.org/10.1016/j.jclepro.2017.04.073.

Moriya, A., Maruyama, T., Ohmukai, Y., Sotani, T., & Matsuyama, H. (2009). Preparation of poly(lactic acid) hollow fiber membranes via phase separation methods. *Journal of Membrane Science*, *342*, 307–312. Available from https://doi.org/10.1016/j.memsci.2009.07.005.

Munubarthi, K. K., Gautam, D. K., Reddy, K. A., & Subbiah, S. (2020). Distributed parameter system modeling approach for the characterization of a high flux hollow fiber forward osmosis (HFFO) membrane. *Desalination*, *496*, 114706. Available from https://doi.org/10.1016/j.desal.2020.114706.

Nasir, A., Masood, F., Yasin, T., & Hameed, A. (2019). Progress in polymeric nanocomposite membranes for wastewater treatment: Preparation, properties and applications. *Journal of Industrial and Engineering Chemistry*, 29–40. Available from https://doi.org/10.1016/j.jiec.2019.06.052.

Park, H., Kim, Y. P., Kim, H., & Kang, Y. (1999). Membrane formation by water vapor induced phase inversion. *Journal of Membrane Science*, *156*, 169–178. Available from https://doi.org/10.1016/S0376-7388(98)00359-7.

Pedersen, K., Ireland, J. D., Gal, S. E., Examiner, P., & Phillip, W. (2015). Device and process for producing a reinforced hollow fibremembrane. US00899.9454B2.

Peng, Y., Fan, H., Dong, Y., Song, Y., & Han, H. (2012). Effects of exposure time on variations in the structure and hydrophobicity of polyvinylidene fluoride membranes prepared via vapor-induced phase separation. *Applied Surface Science*, *258*, 7872–7881. Available from https://doi.org/10.1016/j.apsusc.2012.04.108.

Pinnau, I., & Freeman, B. D. (2000). Formation and Modification of Polymeric Membranes : Overview. *Membrane Formation and Modification*, 1–22. Available from https://pubs.acs.org/doi/pdf/10.1021.

Raghavan, P., Lim, D.-H., Ahn, J.-H., Nah, C., Sherrington, D. C., Ryu, H.-S., & Ahn, H.-J. (2012). Electrospun polymer nanofibers: The booming cutting edge technology. *Reactive and Functional Polymers*, *72*, 915–930. Available from https://doi.org/10.1016/j.reactfunctpolym.2012.08.018.

Rajaeian, B., Rahimpour, A., Tade, M. O., & Liu, S. (2013). Fabrication and characterization of polyamide thin film nanocomposite (TFN) nanofiltration membrane impregnated with TiO2 nanoparticles. *Desalination*, *313*, 176–188. Available from https://doi.org/10.1016/j.desal.2012.12.012.

Ran, F. (2015). Polypropylene (PP) BT. In E. Drioli, & L. Giorno (Eds.), *Encyclopedia of membranes* (pp. 1–2). Berlin, Heidelberg: Springer.

Razali, M., Kim, J. F., Attfield, M., Budd, P. M., Drioli, E., Lee, Y. M., & Szekely, G. (2015). Sustainable wastewater treatment and recycling in membrane manufacturing. *Green Chemistry*, *17*, 5196–5205. Available from https://doi.org/10.1039/c5gc01937k.

Rivero, P. J., & Redin, D. M. (2020). Metals, 10, 350.

Razmjou, A., Mansouri, J., Chen, V., Lim, M., & Amal, R. (2011). Titania nanocomposite polyethersulfone ultrafiltration membranes fabricated using a low temperature hydrothermal coating process. *Journal of Membrane Science*, *380*, 98–113. Available from https://doi.org/10.1016/j.memsci.2011.06.035.

Sagle, A. C., Van Wagner, E. M., Ju, H., McCloskey, B. D., Freeman, B. D., & Sharma, M. M. (2009). PEG-coated reverse osmosis membranes: Desalination properties and fouling resistance. *Journal of Membrane Science*, *340*, 92–108. Available from https://doi.org/10.1016/j.memsci.2009.05.013.

Salehi, E., Daraei, P., & Arabi Shamsabadi, A. (2016). A review on chitosan-based adsorptive membranes. *Carbohydrate Polymers*, *152*, 419–432. Available from https://doi.org/10.1016/j.carbpol.2016.07.033.

Sarkar, S., & Chakraborty, S. (2021). Nanocomposite polymeric membrane a new trend of water and wastewater treatment: A short review. *Groundwater for Sustainable Development*. Available from https://doi.org/10.1016/j.gsd.2020.100533.

Shibutani, T., Kitaura, T., Ohmukai, Y., Maruyama, T., Nakatsuka, S., Watabe, T., & Matsuyama, H. (2011). Membrane fouling properties of hollow fiber membranes prepared from cellulose acetate derivatives. *Journal of Membrane Science*, *376*, 102–109. Available from https://doi.org/10.1016/j.memsci.2011.04.006.

Shiohara, A., Prieto-Simon, B., & Voelcker, N. H. (2021). Porous polymeric membranes: fabrication techniques and biomedical applications. *Journal of Materials Chemistry B*, *9*, 2129–2154. Available from https://doi.org/10.1039/d0tb01727b.

Siddiqui, M. U., Muhammad Arif, A. F., & Bashmal, S. (2016). Permeability-Selectivity Analysis of Microfiltration and Ultrafiltration Membranes : Effect of Pore Size and Shape Distribution and Membrane Stretching. *Membranes*, *6*, 1–14. Available from https://doi.org/10.3390/membranes6030040.

Sossna, M., Hollas, M., Schaper, J., & Scheper, T. (2007). Structural development of asymmetric cellulose acetate microfiltration membranes prepared by a single-layer dry-casting method. *Journal of Membrane Science*, *289*, 7–14. Available from https://doi.org/10.1016/j.memsci.2006.11.024.

Su, Y. S., Kuo, C. Y., Wang, D. M., Lai, J. Y., Deratani, A., Pochat, C., & Bouyer, D. (2009). Interplay of mass transfer, phase separation, and membrane morphology in vapor-induced phase separation. *Journal of Membrane Science*, *338*, 17–28. Available from https://doi.org/10.1016/j.memsci.2009.03.050.

Susanti, R. F., Han, Y. S., Kim, J., Lee, Y. H., & Carbonell, R. G. (2013). A new strategy for ultralow biofouling membranes: Uniform and ultrathin hydrophilic coatings using liquid carbon dioxide. *Journal of Membrane Science*, *440*, 88–97. Available from https://doi.org/10.1016/j.memsci.2013.03.068.

Tan, X. M., & Rodrigue, D. (2019). A Review on Porous Polymeric Membrane Preparation. Part I: Production Techniques with Polysulfone and Poly (Vinylidene Fluoride). *Polymers*, *11*(7), 1160. Available from https://doi.org/10.3390/polym11071160.

Tijing, L. D., Woo, Y. C., Yao, M., Ren, J., & Shon, H. K. (2017). Electrospinning for Membrane Fabrication: Strategies and Applications. In Drioli Giorno Fontananova (Ed.), *Comprehensive membrane science and engineering* (pp. 418–444). Elsevier.

Tsai, H. A., Kuo, C. Y., Lin, J. H., Wang, D. M., Deratani, A., Pochat-Bohatier, C., et al. (2006). Morphology control of polysulfone hollow fiber membranes via water vapor induced phase separation. *Journal of Membrane Science*, *278*, 390–400. Available from https://doi.org/10.1016/j.memsci.2005.11.029.

Tweddle, T. A., Kutowy, O., Thayer, W. L., & Sourirajan, S. (1983). Polysulfone ultrafiltration membranes. *Industrial & Engineering Chemistry Product Research and Development*, *22*, 320–326. Available from https://doi.org/10.1021/i300010a030.

Wang, J., Zhang, Y., Xu, Y., Zhu, B., & Xu, H. (2014). Chinese Journal of Polymer Science, *32*, 143–150.

Wang, Z., Guo, S., Zhang, B., Fang, J., & Zhu, L. (2019). Interfacially crosslinked β-cyclodextrin polymer composite porous membranes for fast removal of organic micropollutants from water by flow-through adsorption. *Journal of Hazardous Materials*, *384*. Available from https://doi.org/10.1016/j.jhazmat.2019.121187.

Wu, L., & Sun, J. (2015). An improved process for polyvinylidene fluoride membrane preparation by using a water soluble diluent via thermally induced phase separation technique. *Materials & Design*, *86*, 204–214. Available from https://doi.org/10.1016/j.matdes.2015.07.053.

Xie, W., Tiraferri, A., Ji, X., Chen, C., Bai, Y., Crittenden, J. C., & Liu, B. (2021). Green and sustainable method of manufacturing anti-fouling zwitterionic polymers-modified poly(vinyl chloride) ultrafiltration membranes. *Journal of Colloid and Interface Science*, *591*, 343–351. Available from https://doi.org/10.1016/j.jcis.2021.01.107.

Xu, Z.-K., Huang, X., & Wan, L.-S. (2009). Surface engineering of polymer membranes, surface engineering of polymer membranes. In *Advanced topics in science and technology in China*. Berlin, Heidelberg: Springer.

Yadav, P., Ismail, N., Essalhi, M., Tysklind, M., Athanassiadis, D., & Tavajohi, N. (2021). Assessment of the environmental impact of polymeric membrane production. *Journal of Membrane Science*, *622*, 118987. Available from https://doi.org/10.1016/j.memsci.2020.118987.

Yan, S.-Y., Wang, Y.-J., Mao, H., & Zhao, Z.-P. (2019). Fabrication of PP hollow fiber membrane: Via TIPS using environmentally friendly diluents and its CO_2 degassing performance. *RSC Advances*, *9*, 19164–19170. Available from https://doi.org/10.1039/c9ra02766a.

Yang, Z., Li, P., Xie, L., Wang, Z., & Wang, S.-C. (2006). Preparation of iPP hollow-fiber microporous membranes via thermally induced phase separation with co-solvents of DBP and DOP. *Desalination*, *192*, 168–181. Available from https://doi.org/10.1016/j.desal.2005.10.016.

Yaranal, N. A., Subbiah, S., & Mohanty, K. (2021). Identification, extraction of microplastics from edible salts and its removal from contaminated seawater. *Environmental Technology & Innovation*, *21*, 101253. Available from https://doi.org/10.1016/j.eti.2020.101253.

Zaidi, S. M. J., & Lakhi, K. S. (2016). Polyethylene membrane BT. In E. Drioli, & L. Giorno (Eds.), *Encyclopedia of membranes* (pp. 1–2). Berlin, Heidelberg: Springer.

Zhang, C., Bai, Y., Sun, Y., Gu, J., & Xu, Y. (2010). Preparation of hydrophilic HDPE porous membranes via thermally induced phase separation by blending of amphiphilic PE-b-PEG copolymer. *Fuel and Energy Abstracts*, *365*, 216–224. Available from https://doi.org/10.1016/j.memsci.2010.09.007.

Zhang, R.-X., Liu, T.-Y., Braeken, L., Liu, Z., Wang, X.-L., & van der Bruggen, B. (2015). A design of composite hollow fiber membranes with tunable performance and reinforced mechanical strength. *Journal of Applied Polymer Science*, *132*, 1–9. Available from https://doi.org/10.1002/app.41247.

Zhu, Y., Wang, D., Jiang, L., & Jin, J. (2014). Recent progress in developing advanced membranes for emulsified oil/water separation. *NPG Asia Materials*. Available from https://doi.org/10.1038/am.2014.23.

Zhu, Y., & Zhang, Z. (2014). PVDF hollow fiber formation via modified NIPS method: Evolution elucidation of phase separation mechanism, structure and properties of membrane with coagulation strength varied. *Macromolecular Research*, *22*, 1275–1281.

CHAPTER

3

Polymer-based nano-enhanced microfiltration/ultrafiltration membranes

Amalia Gordano

Research Institute on Membrane Technology, Rende, Italy

3.1 Introduction

The terms "treatment" and "purification" of water are widely used for any operation and process-involving methods and processing steps for the removal of harmful contaminants such as particulates, bacteria, minerals, organic pollutants, chemicals, pharmaceuticals, salts dissolved, etc. present in the water. These contaminants can be of a physical, chemical, or biological nature. There are three major classes of technologies for water treatment: physical separation (sedimentation, thermal distillation, filtration, and membrane separation), chemical processes (disinfection, coagulation, ion exchange), and biological processes (slow sand filtration). Within this classification, membrane processes alone contribute 53% to clean-water production, wastewater treatment, and water recycling (Gohil, 2009) due to its simplicity of operation, no addition of additive chemicals, cost-effective, no phase change, high productivity, easy scalability, and high-removal capacity (Zhaid, Rashid, Akram, Rehan, & Razzaq, 2018).

The range of applications of membrane technology, especially in the field of water treatment, is acquiring a new perspective and expanding thanks to recent advances in nanotechnology. According to the International Organization for Standardization (ISO/TS0.80004-1:2010, 2010), a nanostructured material is defined as "material having an internal nanostructure or surface nanostructure," where nanostructure is defined as a "composition of related constituent parts, in which one or more of those parts is a nanoscale region" and the nanoscale is defined as "size range from about 1 nm to 100 nm" (Salim & Winston Ho, 2015). Thus nanostructured membranes take shape which can be defined as membranes with internal or surface nanostructure (Mueller et al., 2012). The nanostructured

Advancement in Polymer-Based Membranes for Water Remediation
DOI: https://doi.org/10.1016/B978-0-323-88514-0.00015-2

© 2022 Elsevier Inc. All rights reserved.

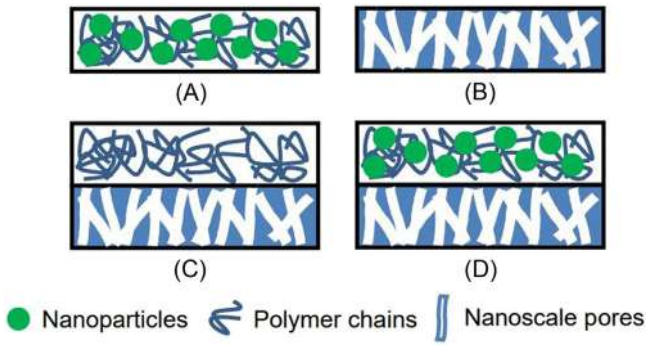

FIGURE 3.1 Schematic representation of nanostructured membranes, (A) dense membrane incorporated with nanomaterials, that is, nanoparticles (NPs), (B) porous membrane with nanoscale pores, (C) dense membrane on a porous membrane with nanoscale pores, (D) dense membrane incorporated with nanomaterials, that is, NPs, on a porous membrane with nanoscale pores (Salim & Winston Ho, 2015).

membrane can be a dense membrane embedded with nanomaterials, a porous membrane with nanoscale pores, or a combination of both, as shown in Fig. 3.1.

In the 1990s nanocomposite membranes were originally developed for gas separation processes (Ahmadizadegan, Esmaielzadeh, Ranjbar, & Marzban, 2018; Robeson, 1991), polymeric matrices were filled with highly selective zeolites to improve permeability and selectivity (Li, Ding, Zhang, & Liu, 2017). Later they were also used in the field of sensors (Jiang, Markutsya, Pikus, & Tsukruk, 2004; Pandey, Pandey, Agrawal, & Das, 2018), proton exchange membrane fuel cells (Boaretti et al., 2017; Jalani, Dunn, & Datta, 2005), pervaporation (Yang, Li, Jiang, Lu, & Chen, 2009), NF (nanofiltration) with organic solvents (Sorribas, Gorgojo, Téllez, Coronas, & Livingston, 2013), and water treatment.

Generally nanocomposite membranes are prepared by introducing nanoparticulate materials (filler) into a sample material (matrix). The nanoparticles can coat the surface of the membrane or be dispersed in the polymeric solution of origin (Al Aani, Wright, Atieh, & Hilal, 2017), in the latter case we speak of mixed matrix membranes (Environ, Pendergast, & Hoek, 2011) or nanopowered membranes (Mueller et al., 2012). The preparation and use of these membranes is one of the current challenges of nanotechnology applied to water treatment (Kim & van der Bruggen, 2010). For example, membranes based on nanoparticles have shown a reduction in fouling by adding inorganic particles (Kim & van der Bruggen, 2010; Sheikh et al., 2020), but the objective also includes an improvement in performance such as permeability and selectivity (Madaeni, Ghaemi, & Rajabi, 2015). Typically, the addition of fillers tends to modify the surface properties, positively influencing the performance of the separation in terms of high permeability, due to the greater porosity and the narrower pore size distribution created by the nanofillers, stable flow, good rejection of foulants, and better antifouling behavior (Kabsch-korbutowicz, Majewska-nowak, & Winnicki, 1999; Yan, Shui, & Bao, 2005; Yong, Wahab, Peng, & Hilal, 2013), due to the antimicrobial properties of the nanoparticles and the reduced surface roughness. The presence of nanoparticles results in a decrease in surface roughness and this positively affects performance, as the tendency to fouling decreases.

In the development of new nanocomposite membranes for water treatment applications there are numerous studies that have used different types of nanoparticles, such as silver (Ag) (Prince, Bhuvana, Boodhoo, Anbharasi, & Singh, 2014), titanium (TiO_2) (Shi, Ma, Ma, Wang, & Sun, 2012), zinc (ZnO) (Balta et al., 2012), copper oxide (CuO) (García et al., 2017),

carbon nanotubes (CNT) (Celik, Park, Choi, & Choi, 2011), graphene oxide (GO) (Xia & Ni, 2015), aluminum (Al_2O_3) (Arsuaga et al., 2013), silicon (SiO_2) (Yu et al., 2009), iron (Fe_3O_4) (Alam et al., 2016), cobalt (Co) (Gzara et al., 2016), zirconium (ZrO_2) (Maximous, Nakhla, Wan, & Wong, 2010), clay nanoparticles (Mierzwa, Arieta, Verlage, Carvalho, & Vecitis, 2013), and zeolite (NaX) (Fathizadeh, Aroujalian, & Raisi, 2011).

The concentration of the nanofillers changes the performance of the membranes and the optimal concentration depends on both the properties of the nanoparticles and the composition of the membrane. Higher concentrations of nanofillers above the optimal value result in poor performance, due to the aggregation of the nanoparticles. It follows that many studies are limited to the laboratory scale and that studies in this area are aimed at preparing nanocomposite membranes to be applied on an industrial scale, which show high selectivity, competitive flow, low tendency to fouling, and at the same time, respect the sustainability criteria in terms of environmental impact, ease of use, and adaptability (Le & Nunes, 2016).

3.2 Nanocomposite membranes

Among the various membrane processes in which nanocomposite membranes have been tested, UF is the most applied technology, as seen in Fig. 3.2. In the field of water treatment, the use of a nanocomposite is a promising alternative and the growing number of scientific publications on the subject testifies to its importance and growing interest. We will discuss the various fillers used for the preparation of nanocomposite membranes, with reference to their performance (Ursino et al., 2018).

Nanocomposite polymer membranes are polymer membranes modified with fillers, which can be organic materials, hybrid materials (two or more types of material), and biomaterials. The phase inversion technique is used to prepare the membranes, both in the case of a flat configuration and a hollow fiber (HF) one and, generally, the nanomaterial is dispersed in the casting solution (Fig. 3.3) (Yin & Deng, 2015).

Polymer nanocomposite membranes can be divided into thin-film nanocomposite membranes and blended nanocomposite membranes. In the case of blended nanocomposite membranes, the nanofillers are dispersed together with the polymer in a casting solution before the membrane is cast. In thin-film nanocomposite membranes, on the other hand, the nanoparticles form a thin film on the surface of the membrane, either through

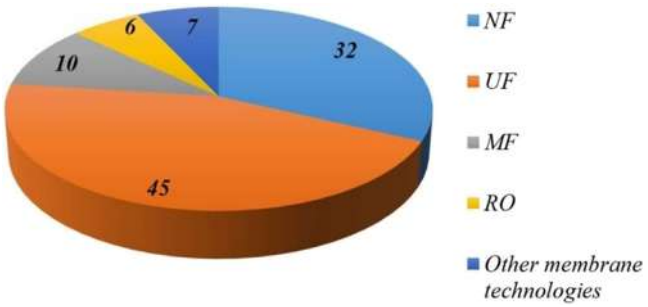

FIGURE 3.2 Overview about the use of nanocomposite membrane in pressure-driven membrane technologies for water treatment (Ursino et al., 2018) (https://www.scopus.com).

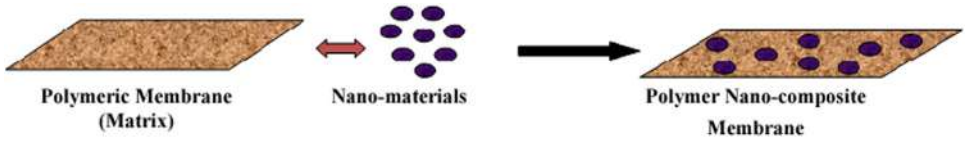

FIGURE 3.3 Representation of polymer nanocomposite membrane (Zhaid et al., 2018).

self-assembly, with a dip-coating method, or pressure deposited on the surface of the prepared membrane (Vatanpour, Madaeni, Khataee, Salehi, & Zinadini, 2012). The literature (Pourjafar, Rahimpour, & Jahanshahi, 2012) reports the preparation of thin-film membranes starting from polyethersulfone (PES) with TiO_2 nanoparticles, using additives such as poly(vinyl alcohol) (PVA) and glutaraldehyde and using an immersion-coating method. They have prepared PES-mixed matrix membranes in which TiO_2 nanoparticles have been trapped, after dissolution of TiO_2 in DMAc (dimethylacetamide), together with the polyvinylpyrrolidone (PVP) additive. The phase inversion was then performed in a coagulum bath that pulls away the PVP, with the consequent formation of pores and TiO_2 trapped in the pores of the resulting membrane. Through the homogeneous dispersion of the nanofillers, chemical–physical bonds are generated with the membrane. While the agglomeration of particles, due to interfacial tension and any incompatibility between organic and inorganic components, can cause inappropriate dispersion. This problem can be minimized by treating the membrane surface in order to obtain a more homogeneous distribution, or by employing a dispersing agent to favor the bond between inorganic particles and organic (immiscible) polymers (Kang & Cao, 2014).

The nanofillers commonly used for nanocomposite membranes are carbon nanotubes, titanium dioxide, silver, copper, zinc oxide, graphene oxide. Table 3.1 shows the main uses of nano-enhanced membrane in water and wastewater treatment (Ursino et al., 2018).

3.3 Hollow fiber nano-enhanced membranes

A special mention is deserved by HF membranes in water treatment for their high potential, even if, still, with many limitations. In the water sector, the concept of submerged system is well established in which the feed enters the tank at atmospheric pressure and the permeate is removed by sucking from the permeate side of the membrane. HF membranes are increasingly used in these systems, which have the advantages of higher packing density, the ability to induce motion by mechanisms such as bubbles and the feasibility of backwashing (Chellam, Jacangelo, & Bonacquisti, 1998; Di Profio, Ji, Curcio, & Drioli, 2011; Günther, Schmitz, Albasi, & Lafforgue, 2010; Nakatsuka, Nakate, & Miyano, 1996; Ye, Le Clech, Chen, Fane, & Jefferson, 2005). The key parameters that influence the fouling of submerged HF are the characteristics of the membrane (material, structure, diameter, length, tension), the operating conditions (temperature, flow), and the hydrodynamic conditions (flow rate, shear) (Chang & Fane, 2002; Wicaksana, Fane, & Chen, 2006). An important development that coincided with the introduction of submerged HF was the realization that dead-end filtration was attractive for some

TABLE 3.1 Application of different nanoparticles into polymeric membranes for water treatment.

Nanoparticle	Membrane process	Application	Polymer
ZnO	MF	Treatment of synthetic wastewater	
		Removal of copper ions	PVDF
		Removal of COD from wastewater	
		Removal of HA	PES
	UF	Removal of HA	PSF
		Removal of salt	PA
		Evaluation of antifouling properties in composite membranes for water treatment	PVDF
		Removal of micelle from aqueous solutions	PES
		Removal of pollutants sodium alginate	
		Evaluation of antifouling properties in composite membranes for water treatment	PES-PVA
		Treatment of wastewaters	
		Bacterial removal from aqueous solutions	PSF
		Evaluation of antifouling properties in composite membranes for water treatment	PVC
GO	MF	Treatment of effluents with high dyes content	PSF
		Filtration of wastewaters	PVDF
	UF	Evaluation of antifouling properties in composite membranes for water treatment	PSF
		Evaluation of antifouling properties in composite membranes for water treatment	PVP-PVDF
		Natural organic matter removal	PVDF
		Natural organic matter removal	PA
		Wastewater treatment	PSF
		Degradation of organic pollutants in salty water	Cellulose ester
		Treatment of distillery effluent	PES
Graphene	UF	Wastewater treatment	PSF
$AgNO_3$	UF	Reduction of the microbial load of raw milk during the concentration process by the UF process	PES
		Evaluation of antifouling properties in composite membranes for water treatment	PSF

(*Continued*)

TABLE 3.1 (Continued)

Nanoparticle	Membrane process	Application	Polymer
AgNPs	MF/UF	Evaluation of antifouling properties in composite membranes for water treatment	PSF
	UF	Water purification	PES
		Evaluation of antifouling and antibacterial properties in composite membranes for water treatment	PES, PSF, CA
Bio-Ag	UF	Evaluation of antifouling and antibacterial properties in composite membranes for water treatment	PES
Cu-NPs	UF	Evaluation of antifouling and antibacterial properties in composite membranes for water treatment	PSF
CuAc2		Evaluation of antifouling and antibacterial properties in composite membranes for water treatment	PAN/PEI
Cu-NP2		Treatment of wastewater and evaluation of antifouling properties in composite membranes for water treatment	PES
AgNPsCu-NPs		Evaluation of antifouling and antibacterial properties in composite membranes for water treatment	PSF
TiO_2-NPs	MF	Evaluation of antifouling properties using whey solution	
	UF	Evaluation of antifouling properties in composite membranes for water treatment	PVDF
		Treatment of wastewaters	
		Evaluation of UV-cleaning properties	
		Evaluation of UV-cleaning and antifouling properties	
		Evaluation of antifouling properties	PP
		Evaluation of antifouling properties and removal of salts	PSF
		Water treatment	CA
CNTs	UF	Water treatment and biofouling control application	PES
		Water treatment of UF application	PSF
		Wastewater treatment by membrane bioreactor	PSF
	MF	Bleach effluent treatment by membrane bioreactor	PSF

CA, cellulose acetate; *PSF*, polysulfone; *PES*, polyethersulfone; *PAN*, polyacrylonitrile; *PP*, polypropylene; *PTFE*, polytetrafluoroethylene; *PVDF*, polyvinylidine fluoride; *PEI*, polyethyleneimine; *PVC*, polyvinyl chloride.

applications, such as water pretreatment. In this case the filtration takes place in cycles, with the dead end forward, interrupted by backwashing and periodic washing of the surface (Hilal, Ogunbiyi, Miles, & Nigmatullin, 2005). Submerged HF systems are becoming increasingly attractive for water treatment, particularly in membrane bioreactors (MBRs)

(Aslam, Charfi, Lesage, Heran, & Kim, 2017; Krzeminski, Leverette, Malamis, & Katsou, 2017). The greater strength and flexibility of the HF modules are, however, counterbalanced by the studies to design the module and optimize the geometry of the fibers, the looseness, the packing density, the bubbling characteristics, the backwashing protocol. The current design of submerged HFs is very effective, but they are still under further development to optimize all parameters.

In the field of membrane filtration, HFs deserve a separate mention, as they represent an important and advanced process of purification and desalination of water. Colloidal Ag smaller than 10 nm inserted in appropriate matrices is very effective in the development of disinfection systems (Madhumathi et al., 2010; Sureshkumar, Siswanto, & Lee, 2010). Various studies have been reported on membranes incorporated with Ag nanoparticles. In these studies, the membranes are prepared by in situ reduction of silver nitrate which has been added to the initial polymeric solution or by mixing of Ag nanoparticles prepared ex situ. In both cases, the membrane preparation method is phase inversion (Basri et al., 2010; Yu, Teng, Chou, & Yang, 2003). Under continuous filtration, Taurozzi et al. reported that the Ag/PSF membrane did not show any significant difference in the inhibition of the biofilm, compared to the unmodified membrane, because the Ag ions were carried away convectively by the bacteria on the membrane from the permeate side (Taurozzi et al., 2008). More recently, Mauter et al. reported the grafting of polyethyleneimine-coated Ag nanoparticles on the surface of a plasma-treated polysulfone (PSF) membrane. He showed that the active layer had excellent antimicrobial activity against *Escherichia coli* (Mauter et al., 2011). These results indicate that it is important that the Ag nanoparticles are at the membrane/water interface, to allow direct contact between Ag and bacterial cells and therefore have optimal performance (Gunawan et al., 2011). Gunawan et al. also developed a nanocomposite coating of multi-walled carbon nanotubes (MWNTs) and Ag nanoparticles on a commercial hollow fiber PAN membrane (Gunawan et al., 2011).

In addition to functioning as a support for Ag nanoparticles, the nanoscale diameter and one-dimensional morphology of the MWNTs enable an open-network structure on the membrane surface to minimize the impact on water flow and also facilitate contact of Ag nanoparticles with pathogens. Both the deposition of Ag nanoparticles on MWNT and coating of Ag/MWNT on PAN were achieved by covalent grafting to achieve a strong bond between the various components. The Ag/MWNT layer has been shown to be effective in killing bacteria and controlling biofilm growth during filtration. The unique system developed in this work could potentially be used as a file disinfection system for antimicrobial water treatment. The methodology can also be extended to other membrane disinfectant systems for wide applications. Ag nanoparticles of controlled size (2 5 nm) were successfully coated on MWNT which were first modified with PEG (polyethylene glycol). PEG not only acted as a reducing agent by converting silver ions into metal Ag nanoparticles, leading to their immobilization on MWNTs, but also increased the hydrophilicity of MWNTs for less adverse effect on the resulting composite membrane flow. The relative flux decreases for the Ag/MWNTs/PAN membrane was significantly smaller than that over the pristine PAN. Effective killing of bacteria and inhibition of biofouling is believed to depend on Ag ions released by the Ag/MWNTs layer as well as on direct contact between Ag nanoparticles and cells.

3.4 Main aspects in membrane performances

3.4.1 Fouling membranes

Fouling of the membrane is caused by the attack of foulants on the surface of the membrane or in the internal structure. Based on the characteristics of the foulants, fouling is classified into crystalline fouling (e.g., mineral precipitates), organic encrustations (e.g., oils, polyelectrolytes), colloidal encrustations (e.g., clay), and biofouling (e.g., bacteria and fungi) (Flemming, 1997), as shown in Fig. 3.4.

Biofouling is the most worrying type of membrane fouling. The electrostatic and hydrophobic interactions between the surface and the microorganisms determine the efficiency of the attack. In general, the attachment is more favorable for more hydrophobic, nonpolar, and rough surfaces, making the pristine polymer membrane vulnerable to biofouling. Fig. 3.5 schematizes the goal of modifying the membranes to counter fouling.

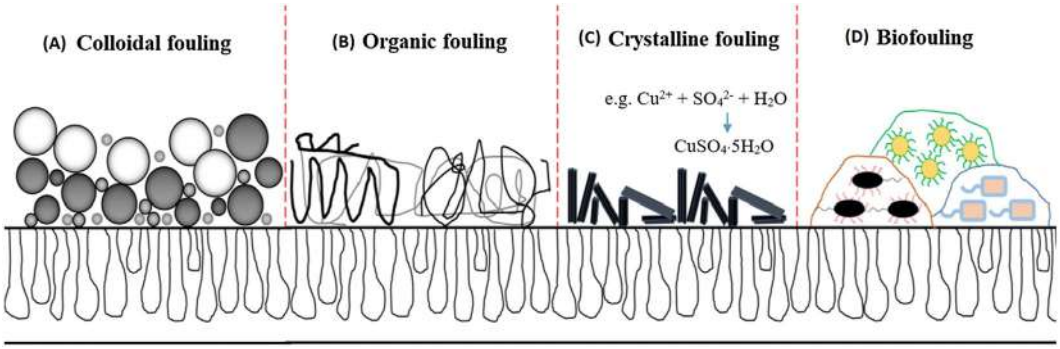

FIGURE 3.4 Four types of fouling mechanisms: (A) colloidal fouling, (B) organic fouling, (C) crystalline fouling, and (D) biofouling (Wen, Yuan, Ma, Wang, & Liu, 2019).

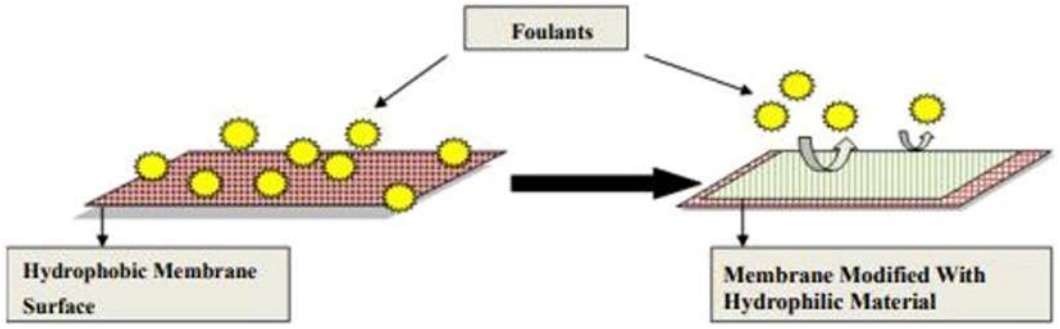

FIGURE 3.5 (A) Before modification foulants attached to hydrophobic membrane surface. (B) Repelling of foulants after modification with hydrophilic-material coating on membrane surface (Zhaid et al., 2018).

3.4.2 Permeability and selectivity

The permeability of a membrane refers to its flow capacity and a high permeability requires that the membrane be highly porous, ultrathin, and have a low tortuosity of the channel. The selectivity of a membrane refers to its ability to separate target molecules from the rest of the fluid and a high selectivity requires small and uniform pores and an appropriate surface chemistry (Bazhin, 2015). Almost all membranes have a trade-off relationship between permeability and selectivity, with the exception of biological membranes, which are both highly permeable and selective due to their unique structure and cellular regulation. Based on the understanding of biological and synthetic membranes, key membrane characteristics useful for overcoming the trade-off include adequately sized pores, narrow pore size distribution, a thin active layer, and a highly tuned interaction between the target compounds and the membrane (Zhang, Ren, Wang, & Liu, 2010).

Natural organic matter is composed of a heterogeneous mixture of humic substances, hydrophilic acids, proteins, lipids, carbohydrates, and hydrocarbons and is a main target of membrane filtration. Membranes for MF and UF reject only 20%–50% of natural organic substances with average dimensions below 1 nm. NF and RO (reverse osmosis) membranes, however, can block over 90% of organic substances by size exclusion. The rejection of saline ions depends on the hydration energy of the individual ions. The greater the hydration of the solute, the greater is the rejection of the solute. High valence ions typically have a higher rejection rate due to the stronger electrostatic repulsion of charged membranes (Garba, Taha, Cabon, & Dorange, 2003; Murthy & Gaikwad, 2013). To minimize the trade-off ratio, it is necessary to improve the selectivity of the low pressure membranes and the permeability of the high pressure membranes.

3.4.3 Physical properties

Although fouling and membrane permeability and selectivity are key parameters of membrane performance, these parameters are strongly influenced by the physical properties of the membrane which are also modified by nanofillers in the membrane (Lee, Elam, & Darling, 2016; Lee, Jeong, & Liu, 2016; Lee, Ye et al., 2016). These physical parameters include the average pore size of the membrane, porosity, and mechanical strength. Currently, two parameters are used to indicate the mechanical strength of membranes, including Young's modulus and tensile strength.

3.5 Carbon nanotubes and graphene oxide

Carbon nanotubes (CNTs) have attracted the attention of researchers for their extraordinary electrical, mechanical, and thermal properties and for their partial antibacterial activity. In fact, they alter the physico-chemical properties of membranes. Typically, the internal pores of CNTs tend to act as selective nanopores. For this reason, membranes filled with CNT show an increase in permeability without the selectivity being affected as well as improved mechanical and thermal properties (Fontananova et al., 2017). Gzara et al. (2016) improved the hydrophilicity of PES membranes, by introducing CNT.

The resulting membranes (wt./wt.%) show higher water flow values and lower fouling rates, compared to neat PES membranes. Similarly, Daraei et al. (2013) improved the hydrophilicity of PES membranes, again by incorporating chemically modified CNTs. The use of hyperbranched polycitric acid on CNTs is fundamental, as it has offered many functional groups and significantly improved the resistance of the membrane to fouling due to milk proteins. The acid-modified CNTs have increased hydrophilicity since they have developed surface functional groups, also increasing the resistance to hydrophobic foulants. Kim, Liu, and Gamal El-Din (2013) studied the incorporation of this filler in composite PA thin-film membranes, in a prefiltration by low-pressure-driven membranes, such as MF and UF processes, commonly selected to remove particles, colloids, and turbidity during municipal and industrial wastewater treatment, biopharmaceutical industry for wastewater treatment, distillation plant for water desalination, and food industries for water purification and wastewater treatment.

A thin-film layer improved the pure water permeability of the n-TFN membrane by 23% (Kim, Hwang, El-Din, & Liu, 2012). Furthermore, the membranes showed better antiadhesive and antibacterial properties, using *Pseudomonas aeruginosa*. At the same time, nitrocellulose membranes coated with a nanocomposite containing 3% by weight of single-walled CNTs showed significant antimicrobial activity (80%–90%) against Gram-positive and Gram-negative bacteria, as well as virus removal (Ahmed, Santos, Mangadlao, Advincula, & Rodrigues, 2013). These membranes did not show any toxicity to fibroblasts and this makes them excellent candidates for water purification, as well as for the treatment of drinking water.

Shah and Murthy (2013) prepared multiwalled amino-functionalized CNTs-PSF composite membranes and tested them in removing heavy metals, reaching values of 94.2% and 78.2% for Cr (II) and Cd (II), respectively, while they were 10.2% and 9.9%, respectively, in untreated PSF membranes. The percentage of metal rejection, for these membranes, increases as the MWNT load increases. Shen, Yu, Ruan, Gao, and van der Bruggen (2013) prepared hydrophobic membranes of thin-film PMMA nanocomposite with multiple-walled CNTs, by interfacial polymerization and obtained 99% Na_2SO_4 rejection, while improving the flow to water by 62%, compared to pristine thin-film composite membrane.

The introduction of polar functional groups in multiwalled CNTs was positive because it has a good dispersion of the filler, associated with the formation of hydrogen bonds between the solvents, the multiwalled CNTs, and the polymer (Grosso et al., 2014). This was highlighted in the study of composite membranes filled with oxidized and aminated multiwalled CNTs, and the functionalized filler reduced fouling in dye filtration and increased permeability (Grosso et al., 2014). Generally, multiwalled CNTs, before being used in the preparation of membranes, are treated with acid to increase their hydrophilicity; however, the structure of the CNT walls are damaged by acid treatments, therefore Sianipar, Kim, Min, Tijing, and Shon (2016) suggested coating the multiwalled CNTs with polydopamine (PDA), to increase hydrophilicity and avoid structural damage. PSF membranes filled with these multiwalled dopamine CNTs were prepared and resulted in an increase in water permeability of 19%–50%, a rejection performance greater than 99% and better mechanical strength than membranes treated with acids.

In wastewater treatment, the use of MBRs is also developing, even if they show fouling problems. Khalid, Abdel-Karim, Atieh, Javed, and McKay (2018) developed membranes in

PEG-CNT composite PSF and used them in MBR for water treatment. The presence of functionalized CNTs reduced the interaction between proteins and the membrane surface, improving resistance to fouling by 79%, while a fourfold increase was recorded in performance in terms of water and protein permeability. Using CNTs-PSF membranes in MBR, Mulopo (2017) treated the effluent of the bleach plant, obtaining an increase in flow up to 0.6 from 0.15 $L\,m^{-2}\,h^{-1}\,kPa^{-1}$, due to the presence of O−H bonds. The approaches are varied, but all demonstrate the versatility of CNT-filled nanocomposite membranes for water treatment applications.

Graphene oxide (GO) is a carbon nanomaterial which is obtained in the oxidized form of graphene. It has a hydrophilic nature, unlike graphene which is hydrophobic (Jhaveri, Murthy, Jhaveri, & Murthy, 2016). The use of GO in the preparation of nanocomposite membranes is aimed at improving the thermal and mechanical properties of the polymeric membranes (Ionita, Pandele, Crica, & Pilan, 2014). Typically, GO has functional groups that offer many possibilities to modify surfaces since they have many hydrophilic functional groups, including $-NH_2$, $-OH$, $-SO_3H$ (Enotiadis, Angjeli, Baldino, & Nicotera, 2012; Liu et al., 2017), useful for producing functionalized GO and graphene-based materials (Jhaveri & Murthy, 2016). In the preparation of nanocomposite membranes for water treatment, GO plays an important role in various fields, including the desalination of water, the removal of toxic ions and organic molecules from polluted water, and the potential use in the removal of traces of drugs from water and wastewater (Sophia et al., 2016) as well as other fillers. The incorporation of GO into polymeric membranes can cause an increase in hydrophilicity and an improvement in permeability (Xia, Yao, Zhao, Li, & Zheng, 2015). The synergistic effects of GO and PVP on membrane performance from UF to PVDF were investigated by Chang et al. (2014) and the result was that the addition of GO and PVP results in an increase in hydrophilicity and an improvement in antifouling performance, due to the formation of hydrogen bonds between PVP and GO.

The addition of GO to polyamide membranes (m-phenylene isophthalamide, PMIA) improved the flow to the water and the antifouling properties, showing a retention of the dye equal to 90% (Yang, Zhao, Zhang, Li, & Hou, 2017). The use of GO with other fillers such as oxidized MWCNT tends to cause a synergistic effect on the antifouling properties of PVDF polymeric membranes (Zhang et al., 2013). The use of GO-TiO_2 compounds may also prove useful in water purification, as they are capable of removing dye molecules, such as methyl orange and rhodamine (Gao, Liu, Tai, Delai, & Ng, 2013; Xu, Cui, Xu, & Fu, 2013). For water treatment, it has also been proposed to use a mixture of copper oxide (Cu_xO) and GO nanofillers based on PVDF (Zhao et al., 2017). The incorporation of the filler has improved the base polymer in several ways: antifouling properties, antibacterial activity, and permeability.

Goh et al. (2015) studied a possible application of GO-filled PSF membranes in desalination, the resulting membrane gave up to 72% removal of Na_2SO_4 from the feed solution and improvement in water flux. A poly(amide-imide)-polyethylenimine (PAI-PEI) membrane filled with GO rejected the NaCl salt at 60% and $CaCl_2$ by more than 95%, in water softening processes. The GO-filled polypiperazine-amide (PPA) composite membrane excellently rejected several salts: 98.2% Na_2SO_4, 96.5% $MgSO_4$, 56.8% NaCl, 50.5% $MgCl_2$ (Wang, Zhao et al., 2016).

Other studies also show the usefulness of membranes filled with GO in the removal of heavy metals as well as salts (Ghasemi, Marjani, Mahmoudian, & Farhadi, 2017), and a reduction in the surface roughness of the membranes (Yin & Deng, 2015) which limits the absorption of proteins and, therefore, reduces the fouling of the membrane.

3.5.1 Fouling

To minimize encrustations, different types of nanoparticles have been incorporated into the matrix of the polymer membrane to reduce the hydrophobicity of the membrane, reduce the roughness of the membrane, and modify the properties of the surface. CNTs and GO can introduce reactive oxygen species (ROS) in direct contact with microorganisms, and are antimicrobial (Kang & Cao, 2012). However, the high hydrophobicity of uncontaminated CNTs makes them less ideal as membrane nanofillers. Significant efforts have been made to functionalize their surfaces to improve their hydrophilicity (Lee, Elam et al., 2016; Lee, Jeong et al., 2016; Lee, Ye et al., 2016). Acid treatment using a mixture of concentrated sulfuric acid (H_2SO_4) and nitric acid (HNO_3) increases its hydrophilicity by providing oxygen-containing functional groups. Furthermore, oxygen-rich groups tend to deprotonate at circumneutral pH, making functionalized CNTs negatively charged and more hydrophilic. Cross-flow permeation tests with bovine serum albumin and ovalbumin showed greater resistance to protein soiling than CNT-containing PES membranes. As the concentration of oxygen-containing CNTs increased, the adsorbed bovine serum albumin quantities decreased both at pH 3 and at pH 7 due to increased hydrophilicity of the nanocomposite membrane and electrostatic repulsion at pH 7. Also the capacity of the nanocomposite membrane to recover protein fouling was greater than with bare polymeric membranes. The flow recovery ratio went from 40% for the uncontaminated membrane to a maximum of 80% for the nanocomposite membrane containing 2% of CNT. However, the surface roughness has increased. CNTs are likely to agglomerate one on top of the other at relatively high concentrations. Functionalization of CNT surfaces can lead to better antifouling properties and less roughness. The functional groups successfully applied for this purpose include the carboxylic functional group, the polyethylene glycol groups, and the amino group (Bai et al., 2015; Rahimpour et al., 2012). The total fouling resistance of the nanocomposite membrane containing amine-functionalized CNTs decreased by 20.2%, compared to bare PES membranes. Other functional groups that lead to varying degrees of improvement in the antifouling properties of nanocomposite membranes include 5-isocyanate-isophthaloyl chloride (Qiu et al., 2009), the hyperbranched polyamine ester (Zhao et al., 2012), aluminosilicate (Baroña, Lim, Choi, & Jung, 2013), and hydroxyl functional group (Majeed et al., 2012).

GO refers to the layer of graphene intercalated with different functional groups rich in oxygen, such as carboxyl, hydroxyl, and epoxy groups (Kang, Herzberg, Rodrigues, & Elimelech, 2008). Hu et al. (2010) reported that GO and graphene nanosheets inhibited the metabolic activities of *E. coli* by approximately 80% and 70%, respectively, compared to the control group. Sharp edges of GO are considered the main reason for cell membrane perforation (Zhao et al., 2013). The aggregated graphene nanosheets could also envelop single *E. coli* cells and isolate them from the microbial environment (Krishnamoorthy,

Umasuthan, Mohan, Lee, & Kim, 2012). The GO-filled PA membrane effectively inhibited the growth of *E. coli* (Perreault, Tousley, & Elimelech, 2013). Colony forming units (CFUs) of *E. coli* decreased by 64.5% after 1 hour of contact with the PA nanocomposite membrane with GO.

The CNT/GO complex has also been proposed as a solution to overcome the drawbacks of individual nanomaterials, such as the poor dispersion of CNTs in polymeric membranes (Lee, Elam et al., 2016; Lee, Jeong et al., 2016; Lee, Ye et al., 2016). GO can function as a surfactant to facilitate the dispersion of CNTs in aqueous solutions through noncovalent interactions (Akhavan, Ghaderi, & Esfandiar, 2011; Qiu et al., 2010). A nanocomposite membrane with a ratio of 5:5 (GO/CNT) showed superior antifouling performance compared to membranes having GO/CNT content in 1:1 ratio (Zhang et al., 2013).

3.5.2 Permeability and selectivity

Hinds et al. (2004) reported that fluid flow rates were increased from four to five orders of magnitude by incorporating aligned multiwalled CNTs into a polystyrene membrane (Yang, Wu, Wang, Cao, & Tang, 2016). Similarly, the permeability of the nanocomposite polycarbonate membrane with CNT was several orders of magnitude higher, despite having approximately one order of magnitude smaller pore sizes (Hinds et al., 2004). Subsequent analyses revealed that well-aligned CNTs function as highly efficient pores because the unique hollow structure allows for the frictionless transport of water molecules through the channels (Das, Ali, Hamid, Ramakrishna, & Chowdhury, 2014; Elimelech & Phillip, 2011; Holt et al., 2016). Theoretically, the strong hydrophobic interactions of CNTs with natural organic materials allow nanocomposite membranes with CNTs to obtain a better rejection of natural organic materials or hydrophobic organic compounds (Lee, Elam et al., 2016; Lee, Jeong et al., 2016; Lee, Ye et al., 2016). For inorganic ions, a number of interactions including size exclusion, steric hindrance, and electrostatic interaction contribute to their rejection by CNTs. Bulky hydrated salt ions can be excluded from the innermost tubes and interstitial voids between graphene sheets of CNT (Qiu et al., 2009). They are also hampered by functional groups on CNTs via steric effects. Depending on the functional groups, ions with the same charges are repelled and those with opposite charges are attracted. Electroneutrality prevents the random migration of ions and, therefore, both cations and anions are kept (Corry, 2008; Fornasiero et al., 2008).

Indeed, many studies have reported improvements in the trade-off relationship between permeability and selectivity by incorporating CNTs into membranes. For example, the permeation fluxes of the solutions of sodium chloride and purified terephthalic acid increased with increasing concentration of functionalized CNT in a PA/PES membrane, reaching a maximum of 71 and 41 L m^{-2} h^{-1}, respectively (Zhang, Shi, Qiu, Cheng, & Chen, 2011). In addition to the channels formed by the aligned nanotubes, the aggregation of the nanotubes could form intact networks interconnected with the original pores in the membrane, which further increase the flow as the concentration of CNTs increases. The optimized crosslinking density, polarity, and polymeric structure of the nanocomposite membrane are key factors for the increased permeability and selectivity of nanocomposite membranes (Kim et al., 2014). Proper functionalization of CNTs can often lead to better performance.

The pure water flow of the polynyline/PES membrane with 2% hydroxyl-functionalized CNTs was increased to a maximum of 1498.1 L m^{-2} h^{-1}, from 20.4 L m^{-2} h^{-1} at 0.1 MPa (Lee, Elam et al., 2016; Lee, Jeong et al., 2016; Lee, Ye et al., 2016). The enormous increase in water permeability has been attributed to the synergistic effects of the porosity of the membrane and hydrophilicity.

GO nanocomposite membranes also showed high permeability. However, the mechanisms for increased GO nanosheet permeability are not fully understood. Potential mechanisms include the passage of water molecules through the defects in GO sheets and through low-frictional hydrophobic channels formed between GO sheets (Nair, Wu, Jayaram, Grigorieva, & Geim, 2012), the defects on the GO nanosheets can function as aggregation points for the water molecules and the hydrophilic edges act as inputs for the passage of the accumulated water molecules. After passing through the defects, (Nair, Wu, Jayaram, Grigorieva, & Geim, 2012), both that the defects on the GO nanosheets can function as aggregation points for the water molecules and the hydrophilic edges act as inputs for the passage of the accumulated water molecules. After passing through the defects, the water molecules enter the hydrophobic 2D channels between the GO nanosheets and accelerate to a high speed due to the low friction, also known as the drag reduction effect. The larger lateral dimensions of the GO nanosheets can prolong the 2D hydrophobic channels and therefore lead to a greater speed of the water at the end of the channels (Wang, Zhang et al., 2016).

A PVDF nanocomposite membrane containing 1% GO functionalized with 3-aminopropyltriethoxylane achieved a maximum pure water flow of 401 L m^{-2} h^{-1} at 1.0 MPa, 11.1% and 70.8% higher than that of the nanocomposite membrane with GO nonfunctionalized and bare membrane, respectively. A similar result was obtained from a PES nanocomposite membrane with GO modified with O-(carboxymethyl)-chitosan. GO nanocomposite membranes also show better retention of organic contaminants. The addition of 0.1 g L^{-1} of polyethyleneamine-functionalized GO into the polyelectrolyte membrane led to the formation of a polymer−polymer hybrid membrane, resulting in 99.5%, 99.3%, and 87.6% rejection, respectively, for Congo red, methyl blue, and methyl orange. The results could be explained by the Donnan repulsion between the membrane surface and the anionic dye molecule. Furthermore, the rejection for $MgSO_4$ and NaCl was increased by 10.4% and 21.7%, respectively (Wang, Ji, Zhang, Li, & Wang, 2012; Wang, Yu et al., 2012).

3.5.3 Physical properties

At lower concentrations, the hydrophobicity of the CNTs improved the exchange of solvent and nonsolvent during phase inversion and allowed the CNTs to settle regularly in the matrix. However, the average pore size began to decrease when the concentration of the CNT additive increased, because the steric hindrance and electrostatic interactions between the CNTs and the polymer matrix became significant (Qiu et al., 2009). The narrowest pore size distribution was obtained at 0.5% wt./wt.% of CNT. These changes confirm with the studies on encrustation and membrane permeability that there is an optimal concentration of CNT to obtain maximum permeability and antifouling properties. Functionalization of CNTs generally leads to results similar to those of uncontaminated CNTs in terms of membrane pore size.

Significant improvements in pore size and porosity have also been reported for nanocomposite membranes with GO. The mean pore size of a GO/polyimide hybrid membrane increased from 0.71 to 0.98 nm with 3.5% wt./wt.% of GO (Zaman, Rohani, Mohammad, & Isloor, 2018). GO nanocomposite membranes also have excellent mechanical strength. The tensile strength and Young's modulus for a nanocomposite membrane were 27.3% and 22.0% higher than those of the bare membrane. When the concentration exceeded 3%, the crystallinity of GO in the membrane was compromised by its placement and irregular aggregation (Yu et al., 2013). The large specific surface and the good dispersion of GO at an optimal concentration could increase the bearing capacity of the membrane (Lee et al., 2015). The improvement in tensile strength has been attributed to the excellent mechanical properties of GO (Wang, Ji et al., 2012; Wang, Yu et al., 2012). In fact, GO is one of the strongest materials known, with a Young's modulus of 0.2−0.25 Tpa (Lee, Wei, Kysar, & Hone, 2008). It is likely that the modifications of the interactions between GO and polymer through hyperbranching and the covalent bond between the GO additives and the polymeric matrix will further improve the physical properties of the nanocomposite membrane (Wang, Ji et al., 2012; Wang, Yu et al., 2012; Xu et al., 2014; Zhao et al., 2012).

3.6 Metallic nanoparticles

3.6.1 Titanium dioxide

Titanium dioxide (TiO_2) is a photocatalytic material used in many applications, as a disinfectant, food-coloring additive, white pigment, and a flavor enhancer (Amini, Rahimpour, & Jahanshahi, 2016; Ghasemzadeh et al., 2014; Marino et al., 2017). It has three crystalline forms: anatase, rutile, and brookite. The rutile and anatase forms are preferred for photocatalytic processes and can be synthesized at low temperatures (Park, Lee, Jung, & Jung, 2009). They are less expensive nanomaterials than others and show good thermal and chemical stability and low toxicity (Marino et al., 2017). In addition to their photocatalytic properties, they are extensively studied to purify water and as antifouling agents. The main advantage of TiO_2-NP is an almost infinite duration, since, generally, TiO_2 remains unchanged during the degradation processes of organic compounds and microorganisms. UV radiation excites the electron of the photocatalyst and this energy promotes the electron to the TiO_2 conduction band, creating a negatively charged free electron and a positively charged electronic hole. The electrons and holes provide strong reducing and oxidizing activities and subsequently react with atmospheric water and oxygen to produce ROS, such as hydroxyl radicals, superoxide anions, and hydrogen peroxide (Liou & Chang, 2012). The hydroxyl radicals and superoxide ions generated can react with most biomolecules with bactericidal and virucidal activity. After a cycle of photocatalytic reaction, the photocatalyst returns to its original state, ready for another cycle.

In membrane processes, TiO_2 is very promising due to its high-oxidative power and induced hydrophilicity. Indeed, the development of self-cleaning membranes can be an approach to reduce fouling and maintain membrane permeability constant. The literature reports various methods for preparing membranes filled with TiO_2-NP, for example, immobilization on the membrane surface or the addition of TiO_2 in the casting solution.

Dip or spin coating, mixing, hot pressing, and physical or chemical crosslinking are some commonly used methods of incorporating NP onto the membrane surface (Nor et al., 2016; Romanos, Athanasekou, Likodimos, Aloupogiannis, & Falaras, 2013). One of the problems during the preparation of these nanocomposite membranes is the agglomeration of the NPs, which, due to their large surface area/particle size ratio, tend to form agglomerates and this reduces their efficiency, as well as negatively affecting performance of the membrane. Madaeni, Zinadini, and Vatanpour (2011) report a comparison between two membrane preparation procedures using TiO_2. In the first, the PAA-PVDF membranes are made by grafting a polymerization reaction in the aqueous phase, according to the green chemistry method. On the surface of prepared PAA-PVDF, 20 nm TiO_2-NP are self-assembled by immersing the membranes in a colloidal solution of 0.05% wt./wt.% TiO_2. Finally, the membranes were irradiated with UV light (160 W) to bind the nanoparticles to the surface of a hydrophobic PVDF membrane. In the second procedure, 0.05% wt./wt.% of TiO_2 was added to the acrylic acid monomer, then an initiator and crosslinking reagent were added to this solution. The PVDF membranes were immersed in this reactive solution, after which the same procedure was followed as in the first method. Using the first method, a low homogeneity and stability of the NPs was obtained due to the formation of agglomerates, as reported in Fig. 3.6. While, the grafting technique produced a covalent attachment of TiO_2 to the polyacrylic acid gel, reducing the agglomeration of NP and strengthening the interaction between NP and the polymer network. The authors report that the covalent bond increases the duration of the NPs on the surface of the modified membranes, confirming a better antifouling activity.

3.6.2 Silver

Compounds based on silver (Ag) include AgNP, stabilized Ag salts, metal oxide polymers and composites, silver dendrimer, Ag-impregnated zeolite, and activated carbon materials. In general, these Ag-based materials tend to offer antimicrobial properties, potentially exploitable in various applications, including water treatment. Zapata et al. (2016) prepared Ag nanofibers. Ag nanoparticles are among the most used nanoparticles for antimicrobial applications and the effects on health and the environment when Ag is released from the polymer membrane must be studied. Some reports on the incorporation of Ag NP into PE for medical applications indicate that Ag NPs are among the most used nanoparticles for antimicrobial applications. The guidelines of the World Health

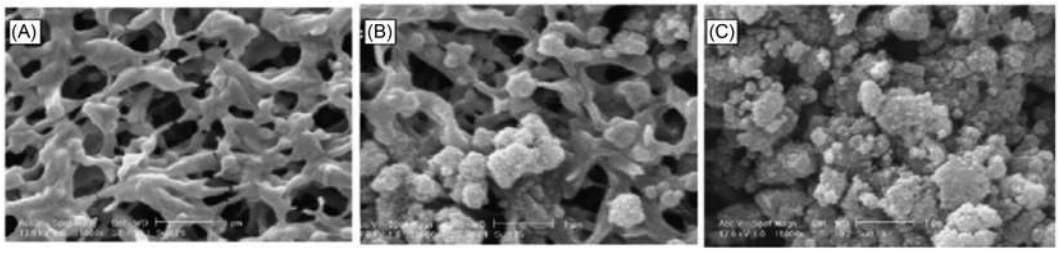

FIGURE 3.6 SEM images of (A) bare PVDF membrane, (B) PAA and self-assembling of TiO_2, and (C) grafted by mixture of PAA and TiO_2 (Madaeni et al., 2011; Ursino et al., 2018).

Organization (WHO) on drinking water report that Ag salts can be used as bacteriostatic agents; Ag levels up to 0.1 mg L^{-1} could be tolerated without any risk to human health (Gorchev & Ozolins, 2008).

In general, nano-Ag, with dimensions ranging from 1 to 100 nm, can be synthesized by various approaches using different precursors, reducing agents, and capping agents (Chaloupka, Malam, & Seifalian, 2010). López-Heras, Theodorou, Leo, Ryan, and Porter (2015) discussed the antibacterial activity of AgNPs, revealing that their activity depends on different physico-chemical properties of the particles, including size, shape, and chemistry. Typically, AgNPs reduce bacterial activity for a synergistic effect between the specific direct biological effects of the particles and the release of Ag^{+} ions. In addition, AgNPs can attach to the bacterial cell, which negatively affects the permeability and respiration of bacteria, but the particles affect the cell membrane resulting in cell lysis. In this way, the Ag particles can cross the bacterial cytoplasm, damaging the DNA (Kim & van der Bruggen, 2010; Koseoglu-Imer & Koyuncu, 2017; Wei et al., 2015). The preparation of nanocomposite membranes filled with Ag has been performed by several authors (Ahmad Rehan et al., 2016; Gorchev & Ozolins, 2008; López-Heras et al., 2015), and the most used polymeric materials for the preparation of nanocomposite membranes with Ag are cellulose acetate (CA), chitosan (CS), PAN, and PSF. Sile-Yuksel, Tas, Koseoglu-Imer, and Koyuncu (2014) studied the effects of the position of AgNPs in various types of polymers. Fig. 3.7 represents a detailed description by the authors of how AgNPs change position

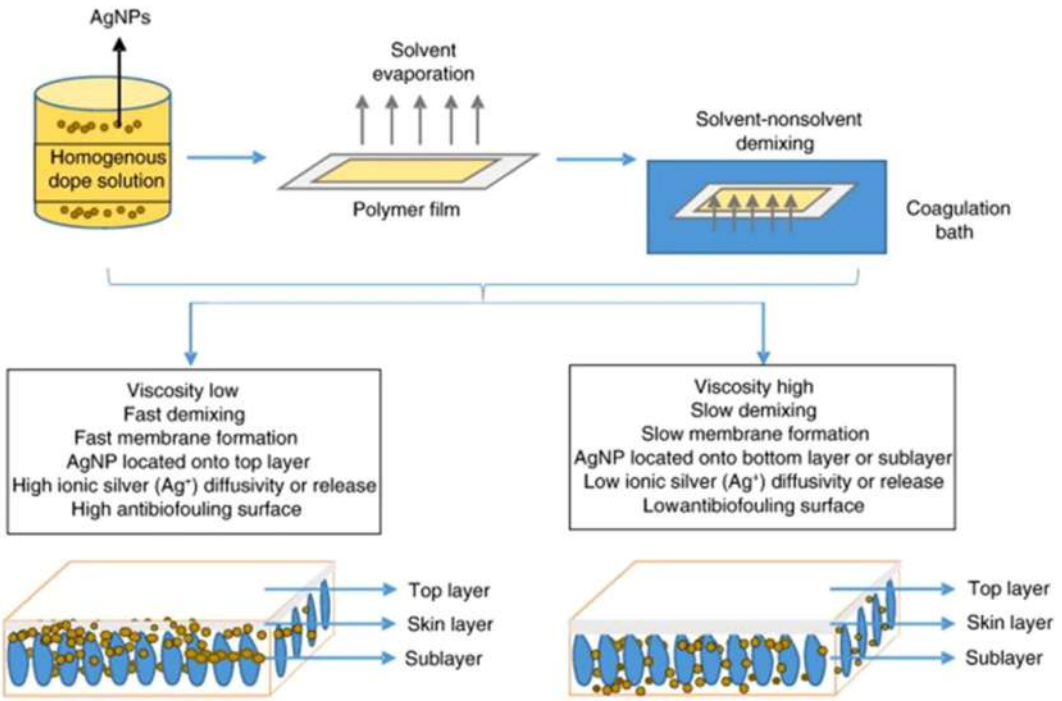

FIGURE 3.7 Description of the location of AgNP in the nanocomposite membranes (Sile-Yuksel et al., 2014; Ursino et al., 2018).

depending on the type of polymer and, subsequently, this position influences the antibacterial properties of nanocomposite membranes. Three different polymers, PES, PSF, and CA were used to prepare nanocomposite membranes with three different AgNP contents: 0.03, 0.06, and 0.09 wt./wt.%. The AgNPs are homogeneously positioned along the polymeric matrix, both on the surface and below it, but protruded from the surface of the PSF and PSE membranes. Furthermore, the increase in the AgNP/polymer ratio tended to increase water permeability in PSF membranes, while it decreased in PES and CA membranes.

The incorporation of AgNP on the surface of the membrane can be performed by reducing direct absorption, where the AgNPs are incorporated during the preparation of the casting solution or synthesis in situ. Basically, the ionic Ag is reduced during the phase inversion processes (Guo, Yuan, Lu, & Li, 2013). Zhu, Bai, Wee, Liu, and Tang (2010) reported a procedure to visualize the antibiofouling performance of CS membranes with immobilized ionic Ag and metallic Ag. The antibacterial effect was evaluated using *E. coli* and *Pseudomonas*, generally responsible for promoting biofouling, since they secrete an extracellular polysaccharide. Although the CS membrane could not inhibit the growth of both bacteria, both AG-functionalized membranes showed significant antibacterial performance. The antibiofouling properties were studied for 10 days, using a high concentration of bacterial suspensions, approximately 109 CFU mL^{-1}. Furthermore, the CS-based membrane with metallic Ag seemed to be more stable than the one with ionic Ag.

Haider et al. (2016) reported the immobilization of Ag NP on PES membranes by introducing amino groups, which contribute to form aminated PES (NH2-PES, APES). An overview of the immobilization mechanism is shown in Fig. 3.8. The antibacterial activity was evaluated against *E. coli*. The AgNPs attack on the surface of aminated PES improved by

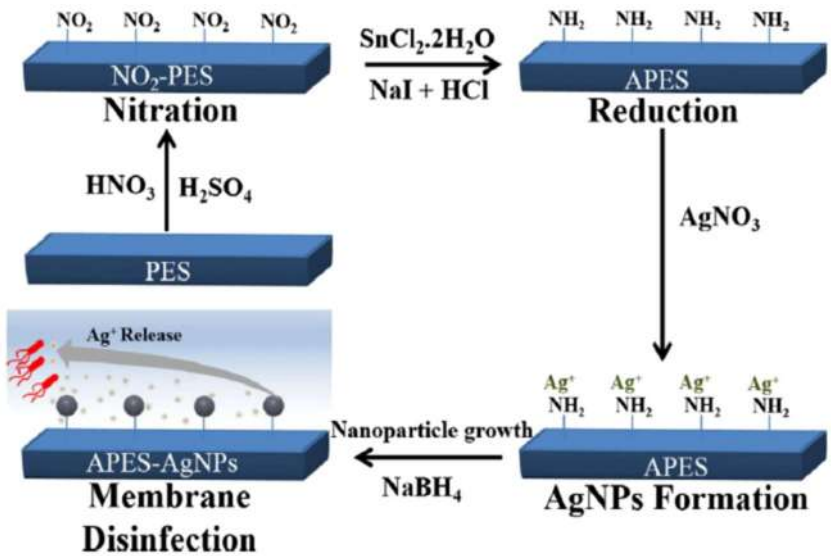

FIGURE 3.8 Schematic illustration of aminated-polyethersulfone (APES) membranes decorated with AgNPs (Haider et al., 2016; Ursino et al., 2018).

bacterial/Ag contact and the AgNPs-APES show the highest disinfection potential, reducing the colony count to zero.

Ahmad Rehan et al. (2016) report an ex situ method. The synthesis of AgNP was carried out using chemical reduction of Ag nitrate with fructose and using PVP as a covering agent. All membranes were prepared via NIPs process using PES as polymer. The amount of AgNO ranged from 0% to 0.64% wt., in order to homogeneously disperse the AgNPs in the polymer matrix and the addition of particles tended to eliminate the macrovoids of the native membrane.

The presence of AgNPs on the membrane surface resulted in an enhancement of the antibacterial effect. The authors reported that there could be a probable interaction between NP and the PES-SO_2 functional group, and this interaction could also prevent the release of AgNP into the permeate. In addition, the pristine and nanocomposite membranes were tested with filtration of bacteria-rich urban wastewater and bacteria-poor seawater and the incorporation of AgNPs into the PES matrix reduced the flow drop from 74% to 60. 3% for wastewater and 71% to 64% deal for sea water. The antibacterial and antibiofouling activity was evaluated against *P. aeruginosa* and *E. coli*. The zone of inhibition widened, increasing the concentration of AGNPs and the AGgNOs-PES membranes inhibited the formation of biofilm (Ahmad Rehan et al., 2016).

Tang and Cao (2012) report the preparation of PVDF nanocomposite membranes through the in situ formation of AgNP. In this work, the antibacterial activity of composite films with different amounts of Ag nitrate, 1.5%−10% wt./wt.%, was confirmed. Ag ions could spread by reducing the growth of bacteria. Yang, Lin, and Su (2016) and Ben-Sasson et al. (2014) prepared thin-film composite membranes for RO uses. In Yang's study, an environmentally friendly and easy method was suggested to immobilize Ag ions from reducing catechol groups in a PDA-coating layer, without using reducing agents and chemicals. The authors reported that electrons released from the oxidation of catechol to quinone can reduce Ag ions in the solution phase and, at the same time, O- and N-based binding sites in the PDA could serve as anchors that result in the formation of AgNPs. In addition, comparable high flux and NaCl rejection were achieved using the PDA coating; nanocomposite membranes also showed clear antimicrobial effects on model bacteria *Bacillus subtilis* and *E. coli*. An interesting study for the preparation of AgNPs-PSF nanocomposite membranes with enhanced permeate flow and antifouling properties was reported by Alpatova et al. (2013). The effect of PVP concentrations, from 1% to 5% wt./wt.%, and AgNP, 0.1% to 10% wt./wt.%, on morphology, performance, and antifouling/antibiofouling properties of nanocomposite membranes. Bacterial tests against *P. aeruginosa* showed that membranes loaded with 2.5% wt./wt.% of AgNP exhibited antibacterial activity. The authors also reported that permeate flux increases at high PVP concentrations of 1%−5% wt./wt.%, due to the formation of more macrovoid and more porous membrane structures (Ahmad Rehan et al., 2016). The addition of AgNPs decreased the rejection properties due to the increase in the size of the pores. Typically, the studies tended to use commercially available AgNp; however, there are several works on the use of Biogenic Silver NP (bio-AgO), synthesized by *Lactobacillus fermentum* LMG 8900 (Liu, Fang, Wu, & Zhang, 2015; Liu et al., 2016; Zhang, Field, & Zhang, 2014; Zhang, Zhang, de Gusseme, & Verstraete, 2012). The authors reported that Bio-AgO shows very high stability in aqueous solution and the attachment of fragment of the bacterium on the surface of the NPs helps to prevent AgNP

aggregation. In addition, the incorporation of bio-AgO increased the permeate flow and also the hydrophilicity. The use of the metal-organic structure based on Ag (MOF) has also been studied with the aim of mitigating biofouling in thin-film nanocompounds for TFC membranes by direct osmosis (FO) (Zirehpour, Rahimpour, Shamsabadi, Sharifian, & Soroush, 2017). Ag nanocrystals-MOFs provided biocidal activity for six months, showing an improvement in biofouling resistance, with a smaller decrease in flux of approximately 8% compared to 21% of the control membranes, in 24-hour tests.

Vermiculite nanoparticles (Verm NPs) incorporated PVDF flat sheet UF membrane for removal of organic pollutants from wastewater was prepared using phase inversion method and compared to aluminum oxide (Al_2O_3), silicon dioxide (SiO_2), and copper oxide (CuO) NPs incorporated PVDF (Isawi, 2019; Varyambath, Song, Singh, & Kim, 2021). The optimum concentration (wt./wt.%) used were 0.3% (Al_2O_3), 0.1% (SiO_2), 0.25 (CuO) and 0.2% (Verm). The nanocomposites PVDF membranes were modified via an ultrathin coating surface layer of a dilute PVA aqueous solution in order to provide sufficient hydrophilicity, rejection, and a reduced surface roughness. The highest permeate flux obtained with a modified ultrafiltration technique was in the order of Verm (628.7) > Al_2O_3 (598) < SiO_2 (590) > CuO (585 L m^{-2} h^{-1}) and the humic acid (HA) rejection was in order of Verm (94.56) > Al_2O_3 (91.7) > SiO_2 (89) > CuO (88.3%) based on an optimum concentration of 0.2, 0.3, 0.1, 0.2 wt.%. The results clearly showed that the incorporation of Verm NPs was favorable to the enhancement of antifouling properties, membrane performances, and the mechanical properties compared to other membranes at the identical condition.

3.6.3 Copper

Copper (Cu) and copper compounds possess bactericidal and fungicidal effects against various types of microorganisms, viruses, and algae, as demonstrated in the literature (Ren et al., 2009; Varkey & Dlamini, 2012). The mechanism of action of Cu ions is not yet clear, but there are some hypotheses that CuNPs can interact with bacteria by generating ROS, lipid peroxidation, protein oxidation, DN degradation, and generation of superoxide anions (Tamayo, Azócar, Kogan, Riveros, & Páez, 2016). Furthermore, Cu^{2+} ions can interact with phosphorus or −SH groups contained in biomolecules such as DNA and proteins, they can act by interrupting biochemical processes, driving the denaturation of proteins (Ruparelia, Chatterjee, Duttagupta, & Mukherji, 2008; Yoon, Byeon, Park, & Hwang, 2007). The antibacterial property of Cu, the low cost, and availability compared to Ag (Ben-Sasson et al., 2014) suggest its application in various sectors such as the production of medical devices, the textile industry (Yoon et al., 2007), food packaging, and decontamination of water, for example, using Cu to control biofouling (Araújo et al., 2012; Hausman, Gullinkala, & Escobar, 2010).

Several techniques have been used to preprepare antifungal nanocomposite membranes using CuNP. Xu, Feng, Chen, and Gao (2012) and Xu et al. (2015) studied antibacterial PAN membranes with Cu (II). The PAN membrane was immersed in the PEI solution to form a polyelectrolyte layer and, finally, the CuAc2 solution promoted the immobilization of Cu, since the PEI-Cu (II) complex in solution can be crosslinked on the membrane surface (Xu et al., 2012). The results of the morphological study show that the microporous

surface of the PAN-PEI-Cu membrane was more compact than the PAN-PEI membrane, agreeing with the results of the UF experiments. The PAN membrane is much more permeable than the PAN-PEI and PAN-PEI-CU membrane, respectively 1070, 507, and 594 L m^{-2} h^{-1} MPa^{-1}. Furthermore, the authors reported that the immobilization of Cu in PEI caused a decrease in surface hydrophilicity, but the PAN-PEI-CU membrane showed greater water permeability, despite its reduced hydrophilicity. The PAN-PEI-Cu membrane also showed good rejection toward HA (91% A 5 mg L^{-1}) and the efficiency against *E. coli* was 71.5% (Xu et al., 2012). The use of PAN-PEI-Cu (II) crosslinked membranes is able to modulate the release of Cu^{2+}, which is approximately below the threshold set by the WHO guidelines for drinking water (2 mg) (Xu et al., 2015). Thanks to the release of Cu^{2+}, the antibacterial efficiency was approximately 95%, while the formation of biofilm was prevented for up to six months of testing.

Akar, Asar, Dizge, and Koyuncu (2013) report an interesting study on the effect of the polymer concentration (14%−18% wt./wt.%), the evaporation time of the solvent (0−90 s), and the CuNP concentration (0.002%−0.05% wt./wt.%), for the preparation of CuNPs-PES membranes. As expected, water permeability decreased, from 606 to 231 L m^{-2} h^{-1} bar^{-1}, when the concentration of the polymer increases from 14% to 18% wt./wt.%. To increase permeability, the authors proposed that the addition of NP could cause changes in the structures of the membrane pores and in the surface electrical properties, attributed to the better hydrophilicity and higher density of electrostatic charges on the surface of the CuNPs. The antifouling property was evaluated using activated sludge as foulant solution and the nanocomposite membrane loaded with 0.05% wt./wt.% showed better antifouling performance than the uncontaminated one. Fig. 3.9 shows that the relative flux reduction (RFR) of the clean PES membrane was 93.8%, while the RFR of the nanocomposite membranes decreased with increasing NP concentration up to 76.2%.

3.6.4 Zinc oxide

Zinc oxide (ZnO) is another multifunctional inorganic nanoparticle that has attracted attention thanks to its physical and chemical properties, including catalytic, antibacterial, and bactericidal activities. Furthermore, ZnONPs can absorb hydrophilic hydroxyl groups (−OH) (Shi et al., 2012), while their surface area appears to be larger than other inorganic nanomaterials (Leo, Lee, Ahmad, & Mohammad, 2012). The incorporation of this inorganic filler leads to an increase in some properties of the polymers such as hydrophilicity, mechanical, and chemical properties (Lin, Xu, Ma, Shannon, & Chen, 2009; Shen et al., 2012). The use of the filler has improved resistance to fouling during the filtration of solutions containing HA, a typical foulant in natural waters (Balta et al., 2012). Shen et al. observed an improvement in the fouling resistance in the membranes of the ZnO-PES compounds, together with the improvement of hydrophilicity, thermal properties, and water permeability (Shen et al., 2012). The PSF membranes were also filled using this inorganic material, demonstrating an antivegetative effect on the surface of the membrane, as well as inside the pores of the composite membranes (Leo et al., 2012). Liang, Xiao, Mo, and Huang (2012) prepared PVDF nanocomposite membranes filled with ZnONPs. The

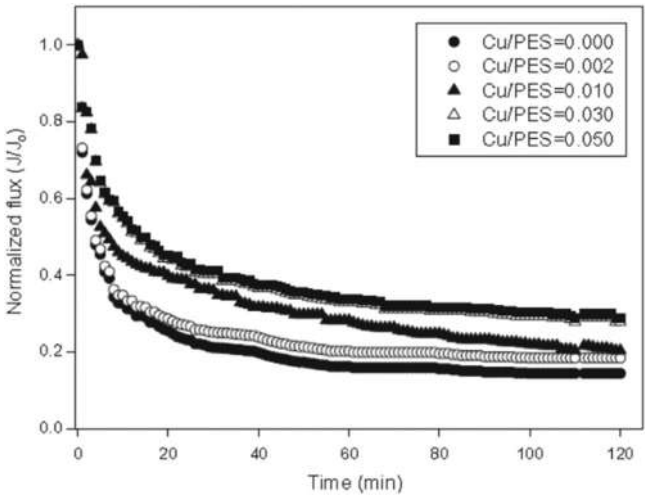

FIGURE 3.9 The biofouling properties of Cu containing polyethersulfone (PES) composite membranes (Akar et al., 2013; Ursino et al., 2018).

prepared membranes showed an initial recovery of 100% water permeability after cleaning the membrane, which means that irreversible fouling, generally found in membrane processes, was avoided. The nanocomposite membranes based on PVP and ZnP also showed antifouling properties during the removal of methylene blue and HA in water purification (Bai, Liu, & Sun, 2012). ZnO has the ability to be mixed with other fillers, such as GO, to form the GO-PSF (Tao et al., 2017) hybrid. These ZnO-GO composite membranes are more hydrophilic than other GO-PSF membranes, exhibiting excellent antifouling and antibacterial properties when filtering HA solutions.

By adding ZnO to the polymeric membranes, fouling resistance is improved and this can be a way to extend the shelf life of the membranes (Jhaveri et al., 2016). On the other hand, the addition of ZnONPs in membranes for wastewater treatment also tends to show a high efficiency of removal of the metals present (Bahadar et al., 2015). This absorbing capacity is totally attributed to ZnO materials due to their electropositive nature (Anjum, Miandad, Waqas, Gehany, & Barakat, 2016; Gupta, Tyagi, Sadegh, & Shahryari-ghoshekandi, 2015).

3.6.5 Fouling

Antimicrobial metal-based particles are widely incorporated into polymeric membranes (Mauter et al., 2011). These metal-based nanoparticles can reduce the adsorption or attachment of foulants on the surface of the membrane or on the internal structure (Zhang et al., 2016) or actively destroy cellular structures to eliminate proliferative encrustations. The PSF membrane filled with Ag nanoparticles, at 1% wt./wt., showed greater hydrophilicity and less roughness, as indicated by a 20% reduction in the contact angle to water, compared to the bare membrane (Koseoglu-Imer, Kose, Altinbas, & Koyuncu, 2013). The PE nanocomposite membrane with titanium oxide nanoparticle also exhibited antifouling performance, which is better than bare membranes. In particular, the hydrophilicity of the

nanocomposite membrane containing TiO_2 increases under UV radiation, because UV radiation creates superficial oxygen voids in the bridge site, which makes the surface more favorable for the dissociative adsorption of water (Wang et al., 1997). A 100% sterilization was obtained for a nanocomposite membrane of PA with TiO_2 under UV illumination, while only 63% reduction was obtained for the same membrane without UV (initial concentration at 6×104 CFU mL^{-1}) (Kim, Kwak, Sohn, & Park, 2003). ZnO nanoparticles can absorb light with the wavelength from 350 to 470 nm, while TiO_2 can only absorb light from 400 to 420 nm (Sakthivel et al., 2003). The self-cleaning efficiency of the PVDF membrane with ZnO nanoparticles increased from 62% to 93% with the increase in the nanoparticle content from 0% to 1.5% wt./wt.% (Hong & He, 2014). The increased hydrophilicity under UV illumination plays an essential role in the improved self-cleaning antifouling property. By varying the ZnO ratio in the nanocomposite membrane from 0.5% to 1.5% up to 3.0% wt./wt.%, the decolonization efficiency increased from 55% to 77%, up to 86%, respectively. The increased decolonization activity was mainly attributed to the production of ROS induced by ZnO nanoparticles (Laohaprapanon, Vanderlipe, Doma, & You, 2017). The detailed mechanisms for improving the antifouling performance of nanocomposite membranes are illustrated in Fig. 3.10.

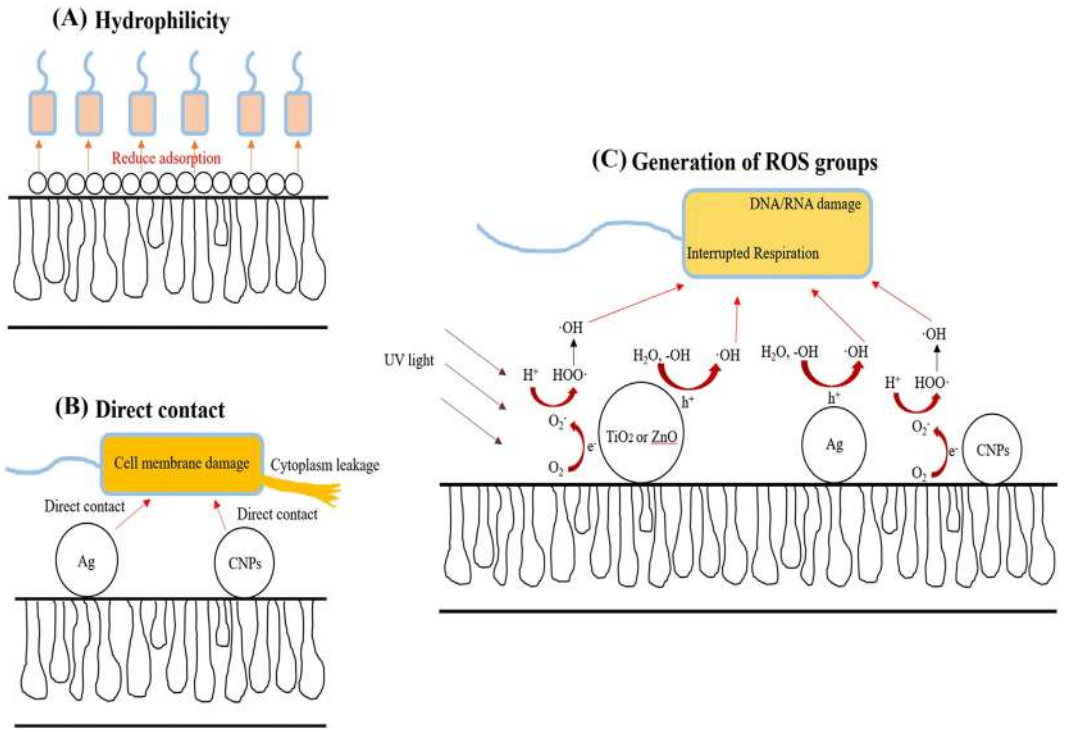

FIGURE 3.10 Three antifouling mechanisms (A) increasing hydrophilicity of membrane surface to minimize hydrophobic interaction, (B) piercing membranes of microorganisms causing cytoplasm leakage, and (C) reactive oxygen species (ROS) production leads to in vitro apoptosis (Wen et al., 2019).

In addition to the composition and concentration of the nanoparticles, the physicochemical properties of metal nanoparticles, such as their shape and surface properties, are important factors which influence the performance of the nanocomposite membrane. The shape of the particles is a primary factor. For example, the ZnO nanorod in the PES membrane produced a lower contact angle to water than the spherical ZnO nanoparticles, due to the greater migration of the ZnO nanorods toward the membrane surface (Rajabi et al., 2015).

3.6.6 Permeability and selectivity

The optimal content of metal nanoparticles in membranes depends on both the properties of the polymer membranes and the nanoparticles. For example, adding 0.5% wt./wt.% 70 nm Ag nanoparticles to a PSF membrane resulted in a lower water flow (−20%), while adding 0.5% wt./wt.% of Ag nanoparticles at 30 nm led to an increase in water flow of 186.7% (Mollahosseini, Rahimpour, Jahamshahi, Peyravi, & Khavarpour, 2012). The relatively lower performance of the larger Ag nanoparticles was likely due to pore blocking. Smaller nanoparticles also produced a smoother membrane surface and smaller pore size (Mollahosseini et al., 2012). For photoactive nanoparticles, UV radiation often leads to better performance. The molecular weight limit of the PES nanocomposite membrane with UV irradiated ZnO nanoparticles was 5275 Da, 13.7% higher than the same nanocomposite membrane without UV radiation (Kusworo et al., 2018). Of all metal oxide nanoparticles, zirconium oxide nanoparticles are chemically more stable and therefore more suitable for membrane filtration under harsh conditions. The PES nanocomposite membrane with zirconium oxide nanoparticles had a water permeability 20 times higher than the bare PES membrane (Gzara et al., 2016).

3.6.7 Physical properties

The increased hydrophilicity of metal nanoparticles can accelerate the exchange of solvent-nonsolvent in the casting solution, leading to a more porous membrane structure (Mulder, 2012). The mean pore size of the ZnO/PVDF membrane increased from 28.1 nm for the bare membrane to 33.6 nm for the nanocomposite membrane, with 6.7% wt./wt.% of ZnO, and the pore density (number of pores per unit area) increased from 44.1 to 49.8 μm^2 (Liang et al., 2012). A significant 180% increase in the average size of the macrovacuums was observed when 1% wt./wt. of hematite was incorporated into the PES membrane.

Metallic nanoparticles can also act as a crosslinking agent and cause an increase in membrane stiffness (Ogoshi & Chujo, 2005). It has been reported that the 0.1% wt./wt.% ZnO/PES nanocomposite membrane has a tensile strength of 2.1 MPa, 90.9% higher than the bare membrane, and also the elongation of the membrane to failure increased from 1.15% to 2.2% (Hong & He, 2014). Other nanoparticles such as aluminum oxide and TiO_2 nanoparticles could also lead to more resistant and porous membranes. The optimal concentration required for metal nanoparticles is generally higher than that of carbon-based nanoparticles.

3.7 Stability of nanocomposite membranes

Although nanocomposite membranes have shown many remarkable properties, the long-term stability of these membranes still matters (Som et al., 2010). A 10% loss of Ag nanoparticles has been reported for a nanocomposite membrane after a relatively short filtration period, resulting in a significant reduction in antifouling and antibacterial activity due to the release of Ag^+ from the membrane surface (Zodrow et al., 2009). The most common routes for the escape of nanoparticles from nanocomposite membranes include direct leaching and release of trapped nanoparticles along with the degradation of the polymer matrix. The chemistry of the polymer matrix is essential for determining the stability of nanoparticles in nanocomposite membranes because the matrix fixes the nanoparticles and acts as a barrier to protect them from the external environment. Well-dispersed CNTs are tightly bound to PA membranes and show good stability (Kingston et al., 2014). Reports on the leaching of CNTs from nanocomposite membranes are rare. Hence, it is reasonable to assume that CNTs are unlikely to leach unless the polymer membrane undergoes structural or chemical changes. The main mechanisms for membrane degradation include UV degradation, extreme temperatures, mechanical stresses, and chemical erosion, as illustrated in Fig. 3.11 (Kingston et al., 2014). The PA nanocomposite membrane with CNT

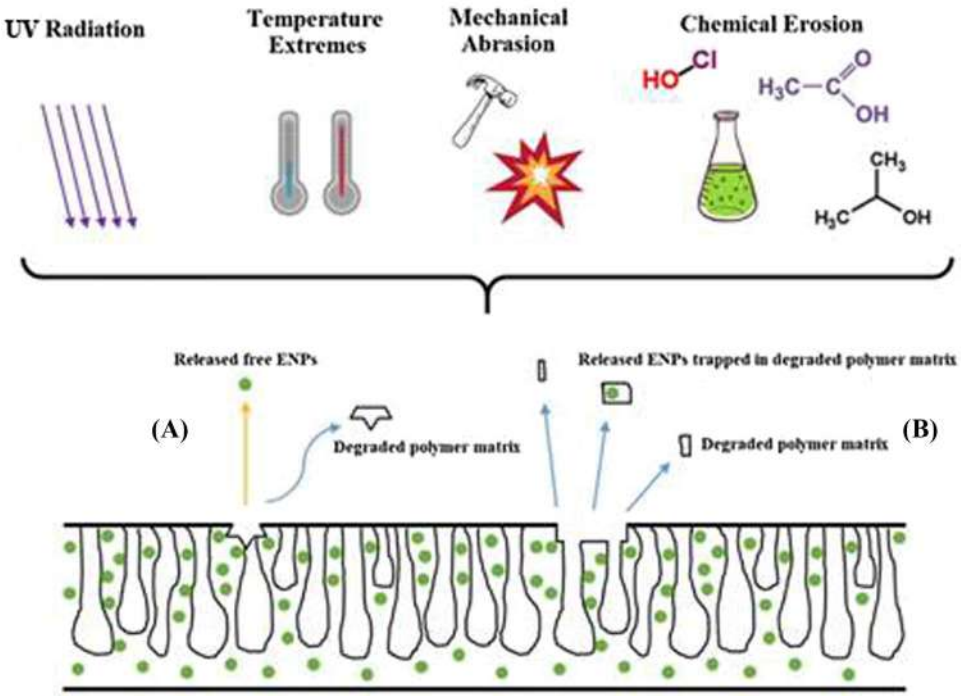

FIGURE 3.11 Four mechanisms of polymer matrix degradation, UV radiation, temperature extremes, mechanical abrasion, and chemical erosion. Two ways of engineered nanoparticle (ENP) release: (A) release of free ENPs due to polymer matrix degradation and (B) release of ENPs along with degraded polymer matrix (Wen et al., 2019).

actually showed significantly improved stability under UV irradiation and a higher temperature than the raw membrane (Vilar et al., 2013). Furthermore, CNTs function as nucleating agents that modify the lamellar orientation, dispersion, and viscosity of the PA membrane and, therefore, improve the thermal and mechanical properties (Vilar et al., 2013). Therefore chemical erosion due to chlorine disinfection is probably the most possible process resulting in the release of nanoparticles from degraded membranes (Kingston et al., 2014).

In addition to physical stability, the chemical stability of nanoparticles also affects the stability and performance of nanocomposite membranes. In particular, GO can act as a terminal electron acceptor and can be reduced to graphite by Shewanella, a group of heterotrophic and metal-reducing anaerobes present in a variety of environments (Salas, Sun, Lüttge, & Tour, 2010). The uniform reduction of nanoparticles in the polymer matrix is another major challenge for the production of high-performance nanocomposite membranes. Nanoparticles tend to aggregate due to strong interactions with each other and weak interfacial polymer−nanoparticle interactions. Poor dispersion and aggregation of the nanoparticles could lead to low improvements in the membrane performance of the nanocomposites (Liu, Gao, Cao, Zhang, & Guo, 2011).

3.8 Future research

Despite the impressive progress made in the synthesis of nanocomposite membranes, more research is needed to overcome existing challenges. First of all, the understanding of nanoscale phenomena of nanoparticles in membranes is still incomplete. Efforts to incorporate two or more nanoparticles or multielement nanostructures into the same polymer matrix can potentially improve the long-term stability and performance of membranes by compensating for the shortcomings of individual ones. Organic metal structures (MOFs) are particularly interesting as nanofillers because they allow the selective removal of some contaminants from source water (Abdi, Vossoughi, Mahmoodi, & Alemzadeh, 2017; Jabbari, Veleta, Zarei-Chaleshtori, Gardea-Torresdey, & Villagrán, 2016; Torad et al., 2014). Second, the agglomeration of nanoparticles is still hindering the progress of nanocomposite membranes. Current solutions include surface modification and optimization of manufacturing processes, but only work for specific nanoparticle and polymer matrix. Third, the long-term stability of nanocomposite membranes requires more attention. For example, it has been reported that several carbon-based nanoparticles could protect PA membranes from chlorine attack, but the direct interactions between these nanoparticles and free chlorine are not well studied (Wen et al., 2019). The long-term effects of exposure to chlorine on the alteration of functional groups on nanoparticles require more attention. Furthermore, studies on the potential release of nanoparticles from polymer membranes are very limited and the release mechanisms are not fully known. Nanomaterials possess unique size-dependent properties related to their high specific surface area; this feature contributes to the development of new high-tech materials for more efficient water and wastewater treatment processes (Gehrke, Geiser, & Somborn-Schulz, 2015). However, the widespread use of nanomaterials depends on the potential risk involved and cost effectiveness. The WHO has reported in its guidelines the limit and risk related to the use

of NP, as reported in this paper (Chaloupka et al., 2010). The approach to minimize the release of NP during the membrane process is to check the effective adhesion on the polymer matrix and to evaluate the stability over time. Therefore one of the challenges is to develop easy and inexpensive methods to immobilize NPs on membranes without reducing their performance (Qu, Alvarez, & Li, 2013). Many studies focus on NP release, which is an important technical hurdle for risk assessment, and on detection techniques, which are few, generally sophisticated, expensive, and with many limitations (Boccuni, Gagliardi, Ferrante, Rondinone, & Iavicoli, 2017). Finally, the successful applications of nanocomposite membranes in the literature are mostly limited to the laboratory scale. There is still a lack of large-scale manufacturing methods and long-term testing required for industrial applications.

3.9 Challenges and future perspectives

Compared to usual treatment processes, membrane technologies have the potential to produce better quality water, reduce disinfectant requirement, need less space due to their compact design, require simpler operating mechanism and less maintenance, and generate less sludge (Collivignarelli, Abbà, Benigna, Sorlini, & Torretta, 2018; Gao, Yu, Chen, Xin, & Zang, 2021; Zeng et al., 2021). Thus in addition to water clarification, MF- and UF-based membrane filters are used for water disinfection and sterilization. Sterilizing membrane filters are able to retain organisms in both the laboratory and industry, producing sterile filtrate. Membrane- and nano-based water disinfection technologies have been advantageously combined in nano-enhanced membranes. Nano-enhanced membranes are promising for achieving high water disinfection through the killing/inhibiting of microorganisms and physical capture through the sieving mechanism. In this regard, most of the nano-enhanced membranes prepared for RO, NF, UF, and MF application are intended to produce antifouling properties by imparting antimicrobial/hydrophilic properties to membranes. Using RO and NF membranes, molecular level separation can be possible, thereby producing water free from any toxic microorganisms, while the extent of disinfection achieved by UF and MF membrane depends on the feed water composition and amount of retention and/or inactivation of microbial cells. Thus pore size and surface charge of MF and UF membranes are important factors in the retention and inhibition of microorganisms.

Nanoscale materials have wide potential for water treatment through nano-enhanced membranes. The key issues facing nano-enhanced membranes which need to be addressed are nanoparticles cost effectiveness and toxicity and the production scalability and stability of nano-enhanced membranes.

The industrial production of nanoparticles of precise size and functionality requires state-of-the-art production facilities and specific chemicals, which ultimately increase the cost of the particles, so water purification has a considerably high cost.

Conventional industrial membrane manufacturing processes are not suitable for preparing large-scale nano-enhanced membranes, because they require optimization of membrane manufacturing parameters and equipment design.

The long-term stability of nano-enhanced membranes for water purification is a key concern as it is limited, as nanoparticles can seep into the water, not only decreasing the functional efficiency of the membrane over time, but also polluting water flow, posing a serious health risk to aquatic life and water consumers due to the toxic nature of nanoparticles.

A comprehensive study of the properties of nanoparticles, polymers, solvents, and binding agents and membrane fabrication techniques is required to devise a proper membrane structure for end use.

Nanotechnology would enable the development of next-generation membrane technology for the removal of specific micropollutants from water through integration with futuristic water-treatment approaches such as solar desalination, microbial desalination, direct osmosis, and nanotechnology MBR. The development of MOF-based nanofillers would have a leap potential for next generation antifouling membranes with a mechanically robust structure. There is an urgent need to prepare membranes with high selectivity and high water permeability based on bioinspired nanoscale materials and bio-derived nanoparticles, in order for sustainable membrane processes to acquire broad social acceptability.

3.10 Conclusions

Overall, nanocomposite membranes show superior performance compared to bare membranes. The properties of nanoparticles, including size and shape, surface properties and composition, as well as the type of polymers, have a strong impact on the final performance of nanocomposite membranes. For any combination of nanoparticles and polymer membrane materials, the literature suggests that there is an optimal concentration of nanoparticles and membrane materials. A higher concentration of nanofillers does not necessarily translate into better performance. Therefore full experimental evaluations are always required for specific combinations of nanoparticles and polymer membranes to achieve optimal results.

Although publications abound, most studies of nanocomposite membranes are limited to short-term tests. The long-term stability and performance of nanocomposite membranes remain uncertain. Furthermore, the large-scale production of nanocomposite membranes has not been thoroughly investigated. Advances in the mechanistic understanding of the interactions between polymer arrays of nanoparticles and the scalable production of nanocomposite membranes will greatly improve their applications. Future efforts should aim at developing more stable, highly performing, and usable nanocomposite membranes in different applications.

References

Abdi, J., Vossoughi, M., Mahmoodi, N., & Alemzadeh, I. (2017). Synthesis of metal-organic framework hybrid nanocomposites based on GO and CNT with high adsorption capacity for dye removal. *Chemical Engineering Journal*, *326*, 1145–1158.

Ahmad Rehan, Z., Gzara, L., Bahadar Khan, S., A Alamry, K., El-Shahawi, M. S., H Albeirutty, M., … M Asiri, A. (2016). Synthesis and characterization of silver nanoparticles-filled polyethersulfone membranes for antibacterial and anti-biofouling application. *Recent Patents on Nanotechnology*, *10*, 231–251.

Ahmadizadegan, H., Esmaielzadeh, D., Ranjbar, M., & Marzban, Z. (2018). Synthesis and characterization of polyester bionanocomposite membrane with ultrasonic irradiation process for gas permeation and antibacterial activity. *Ultrasonics Sonochemistry*, *41*, 538–550.

Ahmed, F., Santos, C. M., Mangadlao, J., Advincula, R., & Rodrigues, D. F. (2013). Antimicrobial PVK: SWNT nanocomposite coated membrane for water purification: Performance and toxicity testing. *Water Research*, *47* (12), 3966–3975.

Akar, N., Asar, B., Dizge, N., & Koyuncu, I. (2013). Investigation of characterization and biofouling properties of PES membrane containing selenium and copper nanoparticles. *Journal of Membrane Science*, *437*, 216–226.

Akhavan, O., Ghaderi, E., & Esfandiar, A. (2011). Wrapping bacteria by graphene nanosheets for isolation from environment, reactivation by sonication, and inactivation by near-infrared irradiation. *The Journal of Physical Chemistry. B*, *115*(19), 6279–6288.

Al Aani, S., Wright, C. J., Atieh, M. A., & Hilal, N. (2017). Engineering nanocomposite membranes: Addressing current challenges and future opportunities. *Desalination*, *401*, 1–15.

Alam, J., Alhoshan, M., Dass, L. A., Shukla, A. K., Muthumareeswaran, M. R., Hussain, M., & Aldwayyan, A. S. (2016). Atomic layer deposition of TiO_2 film on a polyethersulfone membrane: Separation applications. *Journal of Polymer Research*, *23*, 183.

Alpatova, A., Kim, E. S., Sun, X., Hwang, G., Liu, Y., & El-Din, M. G. (2013). Fabrication of porous polymeric nanocomposite membranes with enhanced anti-fouling properties: Effect of casting composition. *Journal of Membrane Science*, *444*, 449–460.

Amini, M., Rahimpour, A., & Jahanshahi, M. (2016). Forward osmosis application of modified TiO_2-polyamide thin film nanocomposite membranes. *Desalination and Water Treatment*, *57*, 14013–14023.

Anjum, M., Miandad, R., Waqas, M., Gehany, F., & Barakat, M. A. (2016). Remediation of wastewater using various nano-materials. *Arabian Journal of Chemistry*.

Araújo, P. A., Miller, D. J., Correia, P. B., van Loosdrecht, M. C. M., Kruithof, J. C., Freeman, B. D., … Vrouwenvelder, J. S. (2012). Impact of feed spacer and membrane modification by hydrophilic, bactericidal and biocidal coating on biofouling control. *Desalination*, *295*, 1–10.

Arsuaga, J. M., Sotto, A., del Rosario, G., Martínez, A., Molina, S., Teli, S. B., & de Abajo, J. (2013). Influence of the type, size, and distribution of metal oxide particles on the properties of nanocomposite ultrafiltration membranes. *Journal of Membrane Science*, *428*, 131–141.

Aslam, M., Charfi, A., Lesage, G., Heran, M., & Kim, J. (2017). Membrane bioreactors for wastewater treatment: A review of mechanical cleaning by scouring agents to control membrane fouling. *Chemical Engineering Journal*, *307*, 897–913.

Bahadar, S., Alamry, K. A., Bifari, E. N., Asiri, A. M., Yasir, M., Gzara, L., & Zulfiqar, R. (2015). Assessment of antibacterial cellulose nanocomposites for water permeability and salt rejection. *Journal of Industrial and Engineering Chemistry*, *24*, 266–275.

Bai, H., Liu, Z., & Sun, D. D. (2012). A hierarchically structured and multifunctional membrane for water treatment. *Applied Catalysis B: Environmental*, *111–112*, 571–577.

Bai, L., Liang, H., Crittenden, J., Qu, F., Ding, A., Ma, J., … Li, G. (2015). Surface modification of UF membranes with functionalized MWCNTs to control membrane fouling by NOM fractions. *Journal of Membrane Science*, *492*, 400–411.

Balta, S., Sotto, A., Luis, P., Benea, L., van der Bruggen, B., & Kim, J. (2012). A new outlook on membrane enhancement with nanoparticles: The alternative of ZnO. *Journal of Membrane Science*, *389*, 155–161.

Baroña, G., Lim, J., Choi, M., & Jung, B. (2013). Interfacial polymerization of polyamide-aluminosilicate SWNT nanocomposite membranes for reverse osmosis. *Desalination*, *325*, 138.

Basri, H., Ismail, A. F., Aziz, M., Nagai, K., Matsuura, T., Abdullah, M. S., & Ng, B. C. (2010). Silver-filled polyethersulfone membranes for antibacterial applications—Effect of PVP and TAP addition on silver dispersion. *Desalination*, *261*, 264–271.

Bazhin, N. (2015). Water flux in pressure retarded osmosis. *Desalination*, *375*, 21–23.

Ben-Sasson, M., Lu, X., Bar-Zeev, E., Zodrow, K. R., Nejati, S., Qi, G., … Elimelech, M. (2014). In situ formation of silver nanoparticles on thin-film composite reverse osmosis membranes for biofouling mitigation. *Water Research*, *62*, 260–270.

Ben-Sasson, M., Zodrow, K. R., Genggeng, Q., Kang, Y., Giannelis, E. P., & Elimelech, M. (2014). Surface functionalization of thin-film composite membranes with copper nanoparticles for antimicrobial surface properties. *Environmental Science & Technology*, *48*, 384–393.

Boaretti, C., Pasquini, L., Sood, R., Giancola, S., Donnadio, A., Roso, M., ... Cavaliere, S. (2017). Mechanically stable nanofibrous sPEEK/Aquivion® composite membranes for fuel cell applications. *Journal of Membrane Science*, *545*, 66–74.

Boccuni, F., Gagliardi, D., Ferrante, R., Rondinone, B. M., & Iavicoli, S. (2017). Measurement techniques of exposure to nanomaterials in the workplace for low- and medium-income countries: A systematic review. *International Journal of Hygiene and Environmental Health*, *220*, 1089–1097.

Celik, E., Park, H., Choi, H., & Choi, H. (2011). Carbon nanotube blended polyethersulfone membranes for fouling control in water treatment. *Water Research*, *45*, 274–282.

Chaloupka, K., Malam, Y., & Seifalian, A. M. (2010). Nanosilver as a new generation of nanoproduct in biomedical applications. *Trends in Biotechnology*, *28*, 580–588.

Chang, S., & Fane, A. G. (2002). Filtration of biomass with laboratory-scale submerged hollow fibre modules—Effect of operating conditions and module configuration. *Journal of Chemical Technology and Biotechnology*, *77*, 1030–1038.

Chang, X., Wang, Z., Quan, S., Xu, Y., Jiang, Z., & Shao, L. (2014). Applied surface science exploring the synergetic effects of graphene oxide (GO) and polyvinylpyrrodione (PVP) on poly (vinylylidenefluoride) (PVDF) ultrafiltration membrane performance. *Applied Surface Science*, *316*, 537–548.

Chellam, S., Jacangelo, J. G., & Bonacquisti, T. P. (1998). Modeling and experimental verification of pilot-scale hollow fiber, direct flow microfiltration with periodic backwashing. *Environmental Science & Technology*, *32*, 75–81.

Collivignarelli, M. C., Abbà, A., Benigna, I., Sorlini, S., & Torretta, V. (2018). Overview of the main disinfection processes for wastewater and drinking water treatment plants. *Sustainability*, *9*, 86.

Corry, B. (2008). Designing carbon nanotube membranes for efficient water desalination. *The Journal of Physical Chemistry B*, *112*(5), 1427–1434.

Daraei, P., Madaeni, S. S., Ghaemi, N., Khadivi, M. A., Astinchap, B., & Moradian, R. (2013). Enhancing antifouling capability of PES membrane via mixing with various types of polymer modified multi-walled carbon nanotube. *Journal of Membrane Science*, *444*, 184–191.

Das, R., Ali, M., Hamid, S., Ramakrishna, S., & Chowdhury, Z. (2014). Carbon nanotube membranes for water purification: A bright future in water desalination. *Desalination*, *336*, 97–109.

Di Profio, G., Ji, X., Curcio, E., & Drioli, E. (2011). Submerged hollow fiber ultrafiltration as seawater pretreatment in the logic of integrated membrane desalination systems. *Desalination*, *269*, 128–135.

Elimelech, M., & Phillip, W. (2011). The future of seawater desalination: Energy, technology, and the environment. *Science*, *333*(6043), 712–717.

Enotiadis, A., Angjeli, K., Baldino, N., & Nicotera, I. (2012). Graphene-based nafion nanocomposite membranes: Enhanced proton transport and water retention by novel organo-functionalized graphene oxide nanosheets. *Small*, *8*, 3338–3349.

Environ, E., Pendergast, M. M., & Hoek, E. M. V. (2011). A review of water treatment membrane nanotechnologies. *Energy & Environmental Science*, *4*, 1946–1971.

Fathizadeh, M., Aroujalian, A., & Raisi, A. (2011). Effect of added NaX nano-zeolite into polyamide as a top thin layer of membrane on water flux and salt rejection in a reverse osmosis process. *Journal of Membrane Science*, *375*, 88–95.

Flemming, H. (1997). Reverse osmosis membrane biofouling. *Experimental Thermal and Fluid Science*, *14*(4), 382–391.

Fontananova, E., Grosso, V., Aljlil, S. A., Bahattab, M. A., Vuono, D., Nicoletta, F. P., ... Di Profio, G. (2017). Effect of functional groups on the properties of multiwalled carbon nanotubes/polyvinylidenefluoride composite membranes. *Journal of Membrane Science*, *541*, 198–204.

Fornasiero, F., Park, H., Holt, J., Stadermann, M., Grigoropoulos, N. A., & Bakajin, O. (2008). Ion exclusion by sub-2-nm carbon nanotube pores. *Proceedings of the National Academy of Sciences*, *105*(45), 17250–17255.

Gao, N., Yu, J., Chen, S., Xin, X., & Zang, L. (2021). Interfacial polymerization for controllable fabrication of nanostructure conducting polymers and their composites. *Synthetic Metals*, 116693.

Gao, P., Liu, Z., Tai, M., Delai, D., & Ng, W. (2013). Applied catalysis B: Environmental multifunctional graphene oxide—TiO_2 microsphere hierarchical membrane for clean water production. *Applied Catalysis B: Environmental*, *138–139*, 17–25.

Garba, Y., Taha, S., Cabon, J., & Dorange, G. (2003). Modeling of cadmium salts rejection through a nanofiltration membrane: Relationships between solute concentration and transport parameters. *Journal of Membrane Science*, *211*(1), 51–58.

García, A., Rodríguez, B., Oztürk, D., Rosales, M., Diaz, D. I., & Mautner, A. (2017). Incorporation of CuO nanoparticles into thin-film composite reverse osmosis membranes (TFC-RO) for antibiofouling properties. *Polymer Bulletin*, 1–17.

Gehrke, I., Geiser, A., & Somborn-Schulz, A. (2015). Innovetions in nantotechnology for water treatment. *Nanotechnology, Science and Applications*, *8*, 1–17.

Ghasemi, M., Marjani, A., Mahmoudian, M., & Farhadi, K. (2017). Grafting of diallyldimethylammonium chloride on graphene oxide by RAFT polymerization for modification of nanocomposite polysulfone membranes using in water treatment. *Chemical Engineering Journal*, *309*, 206–221.

Ghasemzadeh, G., Momenpour, M., Omidi, F., Hosseini, M. R., Ahani, M., & Barzegari, A. (2014). Applications of nanomaterials in water treatment and environmental remediation. *Frontiers of Environmental Science & Engineering*, *8*, 471–482.

Goh, K., Setiawan, L., Wei, L., Si, R., Fane, A. G., Wang, R., & Chen, Y. (2015). Graphene oxide as effective selective barriers on a hollow fiber membrane for water treatment process. *Journal of Membrane Science*, *474*, 244–253.

Gohil, J. M., & Choudhury, R. R. (2009). Introduction to nanostructured and nano-enhanced polymeric membranes: preparation, function, and application for water purification. *Nanoscale Materials in Water Purification*, 25–57.

Gorchev, H. G., & Ozolins, G. (2008). WHO guidelines for drinking-water quality. *WHO Chronicle*, *38*, 564.

Grosso, V., Vuono, D., Bahattab, M. A., Di Profio, G., Curcio, E., Al-Jilil, S. A., … Fontananova, E. (2014). Polymeric and mixed matrix polyimide membranes. *Separation and Purification Technology*, *132*, 684–696.

Gunawan, P., Guan, C., Song, X., Zhang, Q., Leong, S. S. J., Tang, C., … Xu, R. (2011). Hollow fiber membrane decorated with Ag/MWNTs: Toward effective water disinfection and biofouling control. *ACS Nano*, *5*(12), 10033–10040.

Guo, L., Yuan, W., Lu, Z., & Li, C. M. (2013). Polymer/nanosilver composite coatings for antibacterial applications. *Colloids and Surfaces*, *439*, 69–83.

Gupta, V. K., Tyagi, I., Sadegh, H., & Shahryari-ghoshekandi, R. (2015). Nanoparticles as adsorbent; a positive approach for removal of noxious metal ions: A review. *Science & Technology Development*, *34*, 195–214.

Gzara, L., Rehan, Z. A., Khan, S. B., Alamry, K. A., Albeirutty, M. H., El-Shahawi, M. S., … Asiri, A. M. (2016). Preparation and characterization of PES-cobalt nanocomposite membranes with enhanced anti-fouling properties and performances. *Journal of the Taiwan Institute of Chemical Engineers*, *65*, 405–419.

Günther, J., Schmitz, P., Albasi, C., & Lafforgue, C. (2010). A numerical approach to study the impact of packing density on fluid flow distribution in hollow fiber module. *Journal of Membrane Science*, *348*, 277–286.

Haider, M. S., Shao, G. N., Imran, S. M., Park, S. S., Abbas, N., Tahir, M. S., … Kim, H. T. (2016). Aminated polyethersulfone-silver nanoparticles (AgNPs-APES) composite membranes with controlled silver ion release for antibacterial and water treatment applications. *Materials Science and Engineering: C*, *62*, 732–745.

Hausman, R., Gullinkala, T., & Escobar, I. C. (2010). Development of copper-charged polypropylene feedspacers for biofouling control. *Journal of Membrane Science*, *358*, 114–121.

Hilal, N., Ogunbiyi, O. O., Miles, N. J., & Nigmatullin, R. (2005). Methods employed for control of fouling in mf and uf membranes: A comprehensive review. *Separation Science and Technology*, *40*, 1957–2005.

Hinds, B., Chopra, N., Rantell, T., Andrews, R., Gavalas, V., & Bachas, L. (2004). Aligned multiwalled carbon nanotube membranes. *Science*, *303*(5654), 62–65.

Holt, J., Park, H., Wang, Y., Stadermann, M., Artyukhin, A., Grigoropoulos, C., & Bakajin, O. (2016). Fast mass transport through sub-2-nanometer carbon nanotubes. *Science*, *312*(5776), 1034–1037.

Hong, J., & He, Y. (2014). Polyvinylidene fluoride ultrafiltration membrane blended with nano-ZnO particle for photo-catalysis self-cleaning. *Desalination*, *332*(1), 67–75.

Hu, W., Peng, C., Luo, W., Lv, M., Li, X., Li, D., & Fan, C. (2010). Graphene-based antibacterial paper. *ACS Nano*, *4*(7), 4317–4323.

Ionita, M., Pandele, A. M., Crica, L., & Pilan, L. (2014). Improving the thermal and mechanical properties of polysulfone by incorporation of graphene oxide. *Composites Part B*, *59*, 133–139.

Isawi, H. (2019). Evaluating the performance of different nano-enhanced ultrafiltration membranes for removal of organic pollutants from wastewater. *Journal of Water Process Engineering*, *31*, 100833.

ISO/TS.80004-1:2010. (2010). *ISO nanotechnologies, vocabulary, core terms*. Geneva: International Organization for Standardization (ISO).

Jabbari, V., Veleta, J., Zarei-Chaleshtori, M., Gardea-Torresdey, J., & Villagrán, D. (2016). Green synthesis of magnetic MOF@ GO and MOF@ CNT hybrid nanocomposites with high adsorption capacity towards organic pollutants. *Chemical Engineering Journal*, *304*, 774–783.

Jalani, N. H., Dunn, K., & Datta, R. (2005). Synthesis and characterization of Nafion®-MO2 (M = Zr, Si, Ti) nanocomposite membranes for higher temperature PEM fuel cells. *Electrochimica Acta*, *51*, 553–560.

Jhaveri, J. H., & Murthy, Z. V. P. (2016). A comprehensive review on anti-fouling nanocomposite membranes for pressure driven membrane separation processes. *Desalination*, *379*, 137–154.

Jhaveri, J. H., Murthy, Z. V. P., Jhaveri, J. H., & Murthy, Z. V. P. (2016). Nanocomposite membranes. *Desalination and Water Treatment*, *57*, 26803–26819.

Jiang, C., Markutsya, S., Pikus, Y., & Tsukruk, V. V. (2004). Freely suspended nanocomposite membranes as highly sensitive sensors. *Nature Materials*, *3*, 721–728.

Kabsch-korbutowicz, M., Majewska-nowak, K., & Winnicki, T. (1999). Analysis of membrane fouling in the treatment of water solutions containing humic acids and mineral salts. *Desalination*, *126*, 179–185.

Kang, G., & Cao, Y. (2012). Development of antifouling reverse osmosis membranes for water treatment: A review. *Water Research*, *46*(3), 584–600.

Kang, G., & Cao, Y. (2014). Application and modification of poly (vinylidene fluoride) (PVDF) membranes-a review. *Journal of Membrane Science*, *463*, 145–165.

Kang, S., Herzberg, M., Rodrigues, D., & Elimelech, M. (2008). Antibacterial effects of carbon nanotubes: Size does matter!. *Langmuir: The ACS Journal of Surfaces and Colloids*, *24*(13), 6409–6413.

Khalid, A., Abdel-Karim, A., Atieh, M. A., Javed, S., & McKay, G. (2018). PEG-CNTs nanocomposite PSU membranes for wastewater treatment by membrane bioreactor. *Separation and Purification Technology*, *190*, 165–176.

Kim, E. S., Hwang, G., El-Din, M. G., & Liu, Y. (2012). Development of nanosilver and multi-walled carbon nanotubes thin-film nanocomposite membrane for enhanced water treatment. *Journal of Membrane Science*, *394–395*, 37–48.

Kim, E. S., Liu, Y., & Gamal El-Din, M. (2013). An in-situ integrated system of carbon nanotubes nanocomposite membrane for oil sands process-affected water treatment. *Journal of Membrane Science*, *429*, 418–427.

Kim, H., Choi, K., Baek, Y., Kim, D., Shim, J., Yoon, J., & Lee, J. (2014). High performance reverse osmosis CNT/polyamide nanocomposite membrane by controlled interfacial interactions. *ACS Applied Materials & Interfaces*, *6*(4), 2819–2829.

Kim, J., & van der Bruggen, B. (2010). The use of nanoparticles in polymeric and ceramic membrane structures: Review of manufacturing procedures and performance improvement for water treatment. *Environmental Pollution*, *158*, 2335–2349.

Kim, S., Kwak, S., Sohn, B., & Park, T. (2003). Design of TiO_2 nanoparticle self-assembled aromatic polyamide thin-film-composite (TFC) membrane as an approach to solve biofouling problem. *Journal of Membrane Science*, *211*(1), 157–165.

Kingston, C., Zepp, R., Andrady, A., Boverhof, D., Fehir, R., Hawkins, D., & Vejins, V. (2014). Release characteristics of selected carbon nanotube polymer composites. *Carbon*, *68*, 33–57.

Koseoglu-Imer, D., Kose, B., Altinbas, M., & Koyuncu, I. (2013). The production of polysulfone (PS) membrane with silver nanoparticles (AgNP): Physical properties, filtration performances, and biofouling resistances of membranes. *Journal of Membrane Science*, *428*, 620–628.

Koseoglu-Imer, D., & Koyuncu, I. (2017). Fabrication and application areas of mixed matrix flat-sheet membranes. In A. Figoli, J. Hoinkis, S. A. Altinkaya, & J. Bundschuh (Eds.), *Application of nanotechnology in membranes for water treatment*. London: CRC Press (Taylor & Francis Group).

Krishnamoorthy, K., Umasuthan, N., Mohan, R., Lee, J., & Kim, S. (2012). Antibacterial activity of graphene oxide nanosheets. *Science of Advanced Materials*, *4*(11), 1111–1117.

Krzeminski, P., Leverette, L., Malamis, S., & Katsou, E. (2017). Membrane bioreactors—A review on recent developments in energy reduction, fouling control, novel configurations, lca and market prospects. *Journal of Membrane Science*, *527*, 207–227.

Kusworo, T., Soetrisnanto, D., Aryanti, N., Utomo, D., Tambunan, V., & Simanjuntak, N. (2018). Evaluation of Integrated modified nanohybrid polyethersulfone-ZnO membrane with single stage and double stage system for produced water treatment into clean water. *Journal of Water Process Engineering*, *23*, 239–249.

Laohaprapanon, S., Vanderlipe, A., Doma, B., Jr, & You, S. (2017). Self-cleaning and antifouling properties of plasma-grafted poly (vinylidene fluoride) membrane coated with ZnO for water treatment. *Journal of the Taiwan Institute of Chemical Engineers*, *70*, 15–22.

Le, N. L., & Nunes, S. P. (2016). Materials and membrane technologies for water and energy sustainability. *Sustainable Materials and Technologies*, *7*, 1–28.
Lee, A., Elam, J., & Darling, S. (2016). Membrane materials for water purification: Design, development, and application. *Environmental Science: Water Research & Technology*, *2*(1), 17–42.
Lee, C., Wei, X., Kysar, J., & Hone, J. (2008). Measurement of the elastic properties and intrinsic strength of monolayer graphene. *Science*, *321*(5887), 385–388.
Lee, J., Jang, J., Chae, H., Lee, S., Lee, C., Park, P., & Kim, I. (2015). A facile route to enhance the water flux of a thin-film composite reverse osmosis membrane: Incorporating thickness-controlled graphene oxide into a highly porous support layer. *Journal of Materials Chemistry A*, *3*(44), 22053–22060.
Lee, J., Jeong, S., & Liu, Z. (2016). Progress and challenges of carbon nanotube membrane in water treatment. *Critical Reviews in Environmental Science and Technology*, *46*(11–12), 999–1046.
Lee, J., Ye, Y., Ward, A., Zhou, C., Chen, V., Minett, A., & Shi, J. (2016). High flux and high selectivity carbon nanotube composite membranes for natural organic matter removal. *Separation and Purification Technology*, *163*, 109–119.
Leo, C. P., Lee, W. P. C., Ahmad, A. L., & Mohammad, A. W. (2012). Polysulfone membranes blended with ZnO nanoparticles for reducing fouling by oleic acid. *Separation and Purification Technology*, *89*, 51–56.
Li, H., Ding, X., Zhang, Y., & Liu, J. (2017). Porous graphene nanosheets functionalized thin film nanocomposite membrane prepared by interfacial polymerization for CO_2/N_2 separation. *Journal of Membrane Science*, *543*, 58–68.
Liang, S., Xiao, K., Mo, Y., & Huang, X. (2012). A novel ZnO nanoparticle blended polyvinylidene fluoride membrane for anti-irreversible fouling. *Journal of Membrane Science*, *394–395*, 184–192.
Lin, W., Xu, Y., Ma, Y., Shannon, K. B., & Chen, D. (2009). Toxicity of nano- and micro-sized ZnO particles in human lung epithelial cells. *Journal of Nanoparticle Research*, *11*, 25–39.
Liou, J. W., & Chang, H. H. (2012). Bactericidal effects and mechanisms of visible light-responsive titanium dioxide photocatalysts on pathogenic bacteria. *Archivum Immunologiae et Therapiae Experimentalis*, *60*, 267–275.
Liu, G., Han, K., Ye, H., Zhu, C., Gao, Y., Liu, Y., & Zhou, Y. (2017). Graphene oxide/triethanolamine modified titanate nanowires as photocatalytic membrane for water treatment. *Chemical Engineering Journal*, *320*, 74–80.
Liu, J., Gao, Y., Cao, D., Zhang, L., & Guo, Z. (2011). Nanoparticle dispersion and aggregation in polymer nanocomposites: insights from molecular dynamics simulation. *Langmuir: The ACS Journal of Surfaces and Colloids*, *27*(12), 7926–7933.
Liu, S., Fang, F., Wu, J., & Zhang, K. (2015). The anti-biofouling properties of thin-film composite nanofiltration membranes grafted with biogenic silver nanoparticles. *Desalination*, *375*, 121–128.
Liu, S., Zhang, M., Fang, F., Cui, L., Wu, J., Field, R., & Zhang, K. (2016). Biogenic silver nanocomposite TFC nanofiltration membrane with antifouling properties. *Desalination and Water Treatment*, *57*, 10560–10571.
López-Heras, M., Theodorou, I. G., Leo, B. F., Ryan, M. P., & Porter, A. E. (2015). Towards understanding the antibacterial activity of Ag nanoparticles: Electron microscopy in the analysis of the materials-biology interface in the lung. *Environmental Science: Nano*, *2*, 312–326.
Madaeni, S. S., Ghaemi, N., & Rajabi, H. (2015). *Advances in polymeric membranes for water treatment*. Amsterdam: Elsevier.
Madaeni, S. S., Zinadini, S., & Vatanpour, V. (2011). A new approach to improve antifouling property of PVDF membrane using in situ polymerization of PAA functionalized TiO2 nanoparticles. *Journal of Membrane Science*, *380*, 155–162.
Madhumathi, K., Kumar, P. T. S., Abhilash, S., Sreeja, V., Tamura, H., Manzoor, K., ... Jayakumar, R. (2010). Development of novel chitin/nanosilver composite scaffolds for wound dressing applications. *Journal of Materials Science. Materials in Medicine*, *21*, 807–813.
Majeed, S., Fierro, D., Buhr, K., Wind, J., Du, B., Boschetti-de-Fierro, A., & Abetz, V. (2012). Multi-walled carbon nanotubes (MWCNTs) mixed polyacrylonitrile (PAN) ultrafiltration membranes. *Journal of Membrane Science*, *403*, 101–109.
Marino, A. F. T., Boerrigter, M., Faccini, M., Chaumette, C., Arockiasamy, L., & Bundschuh, J. (2017). Photocatalytic activity and synthesis procedures of TiO_2 nanoparticles for potential applications in membranes. In J. B. A. Figoli, J. Hoinkis, & S. A. Altinkaya (Eds.), *Application of nanotechnology in membranes for water treatment*. Abingdon: CRC Press (Taylor & Francis Group).
Mauter, M., Wang, Y., Okemgbo, K., Osuji, C., Giannelis, E., & Elimelech, M. (2011). Antifouling ultrafiltration membranes via post-fabrication grafting of biocidal nanomaterials. *ACS Applied Materials & Interfaces*, *3*(8), 2861–2868.

Maximous, N., Nakhla, G., Wan, W., & Wong, K. (2010). Performance of a novel ZrO_2/PES membrane for wastewater filtration. *Journal of Membrane Science*, *352*, 222–230.

Mierzwa, C., Arieta, V., Verlage, M., Carvalho, J., & Vecitis, C. D. (2013). Effect of clay nanoparticles on the structure and performance of polyethersulfone ultra fi ltration membranes. *Desalination*, *314*, 147–158.

Mollahosseini, A., Rahimpour, A., Jahamshahi, M., Peyravi, M., & Khavarpour, M. (2012). The effect of silver nanoparticle size on performance and antibacteriality of polysulfone ultrafiltration membrane. *Desalination*, *306*, 41–50.

Mueller, N. C., Van der Bruggen, B., Keuter, V., Luis, P., Melin, T., Pronk, W., … Nowack, B. (2012). Nanofiltration and nanostructured membranes—Should they be considered nanotechnology or not? *Journal of Hazardous Materials*, *211–212*, 275–280.

Mulder, J. (2012). *Basic principles of membrane technology*. New York: Springer.

Mulopo, J. (2017). Bleach plant effluent treatment in anaerobic membrane bioreactor (AMBR) using carbon nanotube/polysulfone nanocomposite membranes. *Journal of Environmental Chemical Engineering*, *5*, 4381–4387.

Murthy, Z. V. P., & Gaikwad, M. S. (2013). Preparation of chitosan-multiwalled carbon nanotubes blended membranes: Characterization and performance in the separation of sodium and magnesium ions. *Nanoscale and Microscale Thermophysical Engineering*, *17*, 245–262.

Nair, R., Wu, H., Jayaram, P., Grigorieva, I., & Geim, A. (2012). Unimpeded permeation of water through helium-leak-tight graphene-based membranes. *Science*, *335*(6067), 442–444.

Nakatsuka, S., Nakate, I., & Miyano, T. (1996). Drinking water treatment by using ultrafiltration hollow fiber membranes. *Desalination*, *106*, 55–61.

Nor, N. A. M., Jaafar, J., Ismail, A. F., Mohamed, M. A., Rahman, M. A., Othman, M. H. D., … Yusof, N. (2016). Preparation and performance of PVDF-based nanocomposite membrane consisting of TiO_2 nanofibers for organic pollutant decomposition in wastewater under UV irradiation. *Desalination*, *391*, 89–97.

Ogoshi, T., & Chujo, Y. (2005). Synthesis of poly (vinylidene fluoride) (PVdF)/silica hybrids having interpenetrating polymer network structure by using crystallization between PVDF chains. *Journal of Polymer Science Part A-Polymer Chemistry*, *43*(16), 3543–3550.

Pandey, I., Pandey, A. K., Agrawal, P. C., & Das, N. R. (2018). Synthesis and characterization of dendritic polypyrrole silver nanocomposite and its application as a new urea biosensor. *Journal of Applied Polymer Science*, *135*, 45705.

Park, J. Y., Lee, C., Jung, K. W., & Jung, D. (2009). Structure related photocatalytic properties of TiO_2. *Bulletin of the Korean Chemical Society*, *30*, 402–404.

Perreault, F., Tousley, M., & Elimelech, M. (2013). Thin-film composite polyamide membranes functionalized with biocidal graphene oxide nanosheets. *Environmental Science & Technology Letters*, *1*(1), 71–76.

Pourjafar, S., Rahimpour, A., & Jahanshahi, M. (2012). Synthesis and characterization of PVA/PES thin film composite nanofiltration membrane modified with TiO_2 nanoparticles for better performance and surface properties. *Journal of Industrial and Engineering Chemistry*, *18*, 1398–1405.

Prince, J. A., Bhuvana, S., Boodhoo, K. V. K., Anbharasi, V., & Singh, G. (2014). Synthesis and characterization of PEG-Ag immobilized PES hollow fiber ultrafiltration membranes with long lasting antifouling properties. *Journal of Membrane Science*, *454*, 538–548.

Qiu, L., Yang, X., Gou, X., Yang, W., Ma, Z., Wallace, G., & Li, D. (2010). Dispersing carbon nanotubes with graphene oxide in water and synergistic effects between graphene derivatives. *Chemistry—A European Journal*, *16*(35), 10653–10658.

Qiu, S., Wu, L., Pan, X., Zhang, L., Chen, H., & Gao, C. (2009). Preparation and properties of functionalized carbon nanotube/PSF blend ultrafiltration membranes. *Journal of Membrane Science*, *342*(1–2), 165–172.

Qu, X., Alvarez, P. J. J., & Li, Q. (2013). Applications of nanotechnology in water and wastewater treatment. *Water Research*, *47*, 3931–3946.

Rahimpour, A., Jahanshahi, M., Khalili, S., Mollahosseini, A., Zirepour, A., & Rajaeian, B. (2012). Novel functionalized carbon nanotubes for improving the surface properties and performance of polyethersulfone (PES) membrane. *Desalination*, *286*, 99–107.

Rajabi, H., Ghaemi, N., Madaeni, S., Daraei, P., Astinchap, B., Zinadini, S., & Razavizadeh, S. (2015). Nano-ZnO embedded mixed matrix polyethersulfone (PES) membrane: Influence of nanofiller shape on characterization and fouling resistance. *Applied Surface Science*, *349*, 66–77.

Ren, G., Hu, D., Cheng, E. W. C., Vargas-Reus, M. A., Reip, P., & Allaker, R. P. (2009). Characterisation of copper oxide nanoparticles for antimicrobial applications. *International Journal of Antimicrobial Agents*, *33*, 587–590.

Robeson, L. M. (1991). Correlation of separation factor vs permeability for polymeric membranes. *Journal of Membrane Science*, *62*, 165–185.

Romanos, G. E., Athanasekou, C. P., Likodimos, V., Aloupogiannis, P., & Falaras, P. (2013). Hybrid ultrafiltration/photocatalytic membranes for efficient water treatment. *Industrial & Engineering Chemistry Research*, *52*, 13938–13947.

Ruparelia, J. P., Chatterjee, A. K., Duttagupta, S. P., & Mukherji, S. (2008). Strain specificity in antimicrobial activity of silver and copper nanoparticles. *Acta Biomaterialia*, *4*, 707–716.

Sakthivel, S., Neppolian, B., Shankar, M., Arabindoo, B., Palanichamy, M., & Murugesan, V. (2003). Solar photocatalytic degradation of azo dye: Comparison of photocatalytic efficiency of ZnO and TiO_2. *Solar Energy Materials & Solar Cells*, *77*(1), 65–82.

Salas, E., Sun, Z., Lüttge, A., & Tour, J. (2010). Reduction of graphene oxide via bacterial respiration. *ACS Nano*, *4* (8), 4852–4856.

Salim, W., & Winston Ho, W. S. (2015). Recent developments on nanostructured polymer-based membranes. *Current Opinion in Chemical Engineering*, *8*, 76–82.

Shah, P., & Murthy, C. N. (2013). Studies on the porosity control of MWCNT/polysulfone composite membrane and its effect on metal removal. *Journal of Membrane Science*, *437*, 90–98.

Sheikh, M., Pazirofteh, M., Dehghani, M., Asghari, M., Rezakazemi, M., Valderrama, C., & Cortina, J. L. (2020). Application of ZnO nanostructures in ceramic and polymeric membranes for water and wastewater technologies: A review. *Chemical Engineering Journal*, 123475.

Shen, J. N., Yu, C. C., Ruan, H. M., Gao, C. J., & van der Bruggen, B. (2013). Preparation and characterization of thin-film nanocomposite membranes embedded with poly(methyl methacrylate) hydrophobic modified multi-walled carbon nanotubes by interfacial polymerization. *Journal of Membrane Science*, *442*, 18–26.

Shen, L., Bian, X., Lu, X., Shi, L., Liu, Z., Chen, L., … Fan, K. (2012). Preparation and characterization of ZnO/polyethersulfone (PES) hybrid membranes. *Desalination*, *293*, 21–29.

Shi, F., Ma, Y., Ma, J., Wang, P., & Sun, W. (2012). Preparation and characterization of PVDF/TiO_2 hybrid membranes with different dosage of nano-TiO_2. *Journal of Membrane Science*, *389*, 522–531.

Sianipar, M., Kim, S. H., Min, C., Tijing, L. D., & Shon, H. K. (2016). Potential and performance of a polydopamine-coated multiwalled carbon nanotube/polysulfone nanocomposite membrane for ultrafiltration application. *Journal of Industrial and Engineering Chemistry*, *34*, 364–373.

Sile-Yuksel, M., Tas, B., Koseoglu-Imer, D. Y., & Koyuncu, I. (2014). Effect of silver nanoparticle (AgNP) location in nanocomposite membrane matrix fabricated with different polymer type on antibacterial mechanism. *Desalination*, *347*, 120–130.

Som, C., Berges, M., Chaudhry, Q., Dusinska, M., Fernandes, T., Olsen, S., & Nowack, B. (2010). The importance of life cycle concepts for the development of safe nanoproducts. *Toxicology*, *269*(2–3), 160–169.

Sophia, A. C., Lima, E. C., Allaudeen, N., Rajan, S., Sophia, A. C., Lima, E. C., … Rajan, S. (2016). Application of graphene based materials for adsorption of pharmaceutical traces from water and wastewater—A review. *Desalination and Water Treatment*, *3994*, 1–14.

Sorribas, S., Gorgojo, P., Téllez, C., Coronas, J., & Livingston, A. G. (2013). High flux thin film nanocomposite membranes based on metal-organic frameworks for organic solvent nanofiltration. *Journal of the American Chemical Society*, *135*, 15201–15208.

Sureshkumar, M., Siswanto, D. Y., & Lee, C. K. (2010). Magnetic antimicrobial nanocomposite based on bacterial cellulose and silver nanoparticles. *Journal of Materials Chemistry*, *20*, 6948–6955.

Tamayo, L., Azócar, M., Kogan, M., Riveros, A., & Páez, M. (2016). Copper-polymer nanocomposites: An excellent and cost-effective biocide for use on antibacterial surfaces. *Materials Science and Engineering: C*, *69*, 1391–1409.

Tang, X., & Cao, X. (2012). Preparation and characterization of antibacterial poly(vinylidene fluoride)-silver composites. *High Performance Polymers*, *24*, 135–139.

Tao, Y., Mahmoudi, E., Wahab, A., Benamor, A., Johnson, D., & Hilal, N. (2017). Development of polysulfonenanohybrid membranes using ZnO-GO composite for enhanced antifouling and antibacterial control. *Desalination*, *402*, 123–132.

Taurozzi, J. S., Arul, H., Bosak, V. Z., Burban, A. F., Voice, T. C., Bruening, M. L., & Tarabara, V. V. (2008). Effect of filler incorporation route on the properties of polysulfone-silver nanocomposite membranes of different porosities. *Journal of Membrane Science*, *325*, 58–68.

Torad, N., Hu, M., Ishihara, S., Sukegawa, H., Belik, A., Imura, M., & Yamauchi, Y. (2014). Direct synthesis of MOF-derived nanoporous carbon with magnetic Co nanoparticles toward efficient water treatment. *Small*, *10* (10), 2096–2107.

Ursino, C., Castro-Munoz, R., Drioli, E., Gzara, L., Albeirutty, M. H., & Figoli, A. (2018). Progress of nanocomposite membranes for water treatment. *Membrane*, *8*, 18.

Varkey, A. J., & Dlamini, D. (2012). Point-of-use water purification using clay pot water filters and copper mesh. *Water SA*, *38*, 721–726.

Varyambath, A., Song, W. L., Singh, S., & Kim, S. K. (2021). Tunable construction of biphenyl-based porous polymeric nanostructures and their synergistically enhanced performance in pollutant adsorption and energy storage. *Microporous and Mesoporous Materials*, 110800.

Vatanpour, V., Madaeni, S. S., Khataee, A. R., Salehi, E., Zinadini, S., & Monfareda, H. A. (2012). TiO_2 embedded mixed matrix PES nanocomposite membranes: Influence of different sizes and types of nanoparticles on antifouling and performance. *Desalination*, *292*, 19–29.

Vilar, G., Fernández-Rosas, E., Puntes, V., Jamier, V., Aubouy, L., & Vázquez-Campos, S. (2013). Monitoring migration and transformation of nanomaterials in polymeric composites during accelerated aging. In *Paper presented at the Journal of Physics: Conference series*.

Wang, J., Zhang, P., Liang, B., Liu, Y., Xu, T., Wang, L., & Pan, K. (2016). Graphene oxide as an effective barrier on a porous nanofibrous membrane for water treatment. *ACS Applied Materials & Interfaces*, *8*(9), 6211–6218.

Wang, J., Zhao, C., Wang, T., Wu, Z., & Li, J. (2016). Graphene oxide polypiperazine-amide nanofiltration membrane for improving flux and anti-fouling in water purification. *RSC Advances*, *85*, 82174–82185.

Wang, N., Ji, S., Zhang, G., Li, J., & Wang, L. (2012). Self-assembly of graphene oxide and polyelectrolyte complex nanohybrid membranes for nanofiltration and pervaporation. *Chemical Engineering Journal*, *213*, 318–329.

Wang, R., Hashimoto, K., Fujishima, A., Chikuni, M., Kojima, E., Kitamura, A., & Watanabe, T. (1997). Light-induced amphiphilic surfaces. *Nature*, *388*(6641), 431.

Wang, Z., Yu, H., Xia, J., Zhang, F., Li, F., Xia, Y., & Li, Y. (2012). Novel GO blended PVDF ultrafiltration membranes. *Desalination*, *299*, 50–54.

Wei, L., Lu, J., Xu, H., Patel, A., Chen, Z. S., & Chen, G. (2015). Silver nanoparticles: Synthesis, properties, and therapeutic applications. *Drug Discovery*, *20*, 595–601.

Wen, Y., Yuan, J., Ma, X., Wang, S., & Liu, Y. (2019). Polymeric nanocomposite membranes for water treatment: A review. *Environmental Chemistry Letters*, *17*, 1539–1551.

Wicaksana, F., Fane, A. G., & Chen, V. (2006). Fibre movement induced by bubbling using submerged hollow fibre membranes. *Journal of Membrane Science*, *271*, 186–195.

Xia, S., & Ni, M. (2015). Preparation of poly(vinylidene fluoride) membranes with graphene oxide addition for natural organic matter removal. *Journal of Membrane Science*, *473*, 54–62.

Xia, S., Yao, L., Zhao, Y., Li, N., & Zheng, Y. (2015). Preparation of graphene oxide modified polyamide thin film composite membranes with improved hydrophilicity for natural organic matter removal. *Chemical Engineering Journal*, *280*, 720–727.

Xu, C., Cui, A., Xu, Y., & Fu, X. (2013). Graphene oxide—TiO_2 composite filtration membranes and their potential application for water purification. *Carbon*, *62*, 465–471.

Xu, J., Feng, X., Chen, P., & Gao, C. (2012). Development of an antibacterial copper (II)-chelated polyacrylonitrile ultrafiltration membrane. *Journal of Membrane Science*, *413–414*, 62–69.

Xu, J., Zhang, L., Gao, X., Bie, H., Fu, Y., & Gao, C. (2015). Constructing antimicrobial membrane surfaces with polycation-copper(II) complex assembly for efficient seawater softening treatment. *Journal of Membrane Science*, *491*, 28–36.

Xu, Z., Zhang, J., Shan, M., Li, Y., Li, B., Niu, J., & Qian, X. (2014). Organosilane-functionalized graphene oxide for enhanced antifouling and mechanical properties of polyvinylidene fluoride ultrafiltration membranes. *Journal of Membrane Science*, *458*, 1–13.

Yan, L., Shui, Y., & Bao, C. (2005). Preparation of poly (vinylidene fluoride)(pvdf) ultrafiltration membrane modified by nano-sized alumina (Al_2O_3) and its antifouling research. *Polymer*, *46*, 7701–7706.

Yang, D., Li, J., Jiang, Z., Lu, L., & Chen, X. (2009). Chitosan/TiO_2 nanocomposite pervaporation membranes for ethanol dehydration. *Chemical Engineering Science*, *64*, 3130–3137.
Yang, M., Zhao, C., Zhang, S., Li, P., & Hou, D. (2017). Preparation of graphene oxide modified poly (m-phenylene isophthalamide) nanofiltration membrane with improved water flux and antifouling property. *Applied Surface Science*, *394*, 149–159.
Yang, Q., Lin, X., & Su, B. (2016). Molecular filtration by ultrathin and highly porous silica nanochannel membranes: Permeability and selectivity. *Analytical Chemistry*, *88*(20), 10252–10258.
Yang, Z., Wu, Y., Wang, J., Cao, B., & Tang, C. Y. (2016). In situ reduction of silver by polydopamine: A novel antimicrobial modification of a thin-film composite polyamide membrane. *Environmental Science & Technology*, *50*, 9543–9550.
Ye, Y., Le Clech, P., Chen, V., Fane, A. G., & Jefferson, B. (2005). Fouling mechanisms of alginate solutions as model extracellular polymeric substances. *Desalination*, *175*, 7–20.
Yin, J., & Deng, B. (2015). Polymer-matrix nanocomposite membranes for water treatment. *Journal of Membrane Science*, *479*, 256–275.
Yong, L., Wahab, A., Peng, C., & Hilal, N. (2013). Polymeric membranes incorporated with metal/metal oxide nanoparticles: A comprehensive review. *Desalination*, *308*, 15–33.
Yoon, K. Y., Byeon, J. H., Park, J. H., & Hwang, J. (2007). Susceptibility constants of *Escherichia coli* and *Bacillus subtilis* to silver and copper nanoparticles. *The Science of the Total Environment*, *373*, 572–575.
Yu, D. G., Teng, M. Y., Chou, W. L., & Yang, M. C. (2003). Characterization and inhibitory effect of antibacterial PAN-based hollow fiber loaded with silver nitrate. *Journal of Membrane Science*, *225*, 115–123.
Yu, L., Zhang, Y., Zhang, B., Liu, J., Zhang, H., & Song, C. (2013). Preparation and characterization of HPEI-GO/PES ultrafiltration membrane with antifouling and antibacterial properties. *Journal of Membrane Science*, *447*, 452–462.
Yu, S., Zuo, X., Bao, R., Xu, X., Wang, J., & Xu, J. (2009). Effect of SiO_2 nanoparticle addition on the characteristics of a new organic-inorganic hybrid membrane. *Polymer*, *50*, 553–559.
Zaman, N., Rohani, R., Mohammad, A., & Isloor, A. (2018). Polyimidegraphene oxide nanofiltration membrane: Characterizations and application in enhanced high concentration salt removal. *Chemical Engineering Science*, *177*, 218–233.
Zapata, P. A., Larrea, M., Tamayo, L., Rabagliati, F. M., Azócar, M. I., & Páez, M. (2016). Polyethylene/silver-nanofiber composites: A material for antibacterial films. *Materials Science and Engineering: C*, *69*, 1282–1289.
Zeng, M., Guo, H., Wang, G., Shang, L., Zhao, C., & Li, H. (2021). Nanostructures high-performance electrolyte membranes based on polymer network post-assembly for high-temperature supercapacitors. *Journal of Colloid and Interface Science*, 408–417.
Zhaid, M., Rashid, A., Akram, S., Rehan, Z. A., & Razzaq, W. (2018). A comprehensive review on polymerice nano-composite membranes for water treatment. *Journal of Membrane Science and Technology*, *8*, 1.
Zhang, C., Ren, L., Wang, X., & Liu, T. (2010). Graphene oxide-assisted dispersion of pristine multiwalled carbon nanotubes in aqueous media. *Journal of Physical Chemistry C*, *114*(26), 11435–11440.
Zhang, J., Xu, Z., Shan, M., Zhou, B., Li, Y., Li, B., & Qian, X. (2013). Synergetic effects of oxidized carbon nanotubes and graphene oxide on fouling control and anti-fouling mechanism of polyvinylidene fluoride ultrafiltration membranes. *Journal of Membrane Science*, *448*, 81–92.
Zhang, L., Shi, G., Qiu, S., Cheng, L., & Chen, H. (2011). Preparation of highflux thin film nanocomposite reverse osmosis membranes by incorporating functionalized multi-walled carbon nanotubes. *Desalination and Water Treatment*, *34*(1–3), 19–24.
Zhang, M., Zhang, K., de Gusseme, B., & Verstraete, W. (2012). Biogenic silver nanoparticles (bio-Ag0) decrease biofouling of bio-Ag0/PES nanocomposite membranes. *Water Research*, *46*, 2077–2087.
Zhang, M., Field, R. W., & Zhang, K. (2014). Biogenic silver nanocomposite polyethersulfone UF membranes with antifouling properties. *Journal of Membrane Science*, *471*, 274–284.
Zhang, R., Liu, Y., He, M., Su, Y., Zhao, X., Elimelech, M., & Jiang, Z. (2016). Antifouling membranes for sustainable water purification: Strategies and mechanisms. *Chemical Society Reviews*, *45*(21), 5888–5924.
Zhao, C., Lv, J., Xu, X., Zhang, G., Yang, Y., & Yang, F. (2017). Highly antifouling and antibacterial performance of poly (vinylidene fluoride) ultrafiltration membranes blending with copper oxide and graphene oxide nanofillers for effective wastewater treatment. *Journal of Colloid and Interface Science*, *505*, 341–351.
Zhao, X., Ma, J., Wang, Z., Wen, G., Jiang, J., Shi, F., & Sheng, L. (2012). Hyperbranched-polymer functionalized multi-walled carbon nanotubes for poly (vinylidene fluoride) membranes: From dispersion to blended fouling-control membrane. *Desalination*, *303*, 29–38.

Zhao, Y., Xu, Z., Shan, M., Min, C., Zhou, B., Li, Y., & Qian, X. (2013). Effect of graphite oxide and multi-walled carbon nanotubes on the microstructure and performance of PVDF membranes. *Separation and Purification Technology*, *103*, 78–83.

Zhu, X., Bai, R., Wee, K. H., Liu, C., & Tang, S. L. (2010). Membrane surfaces immobilized with ionic or reduced silver and their anti-biofouling performances. *Journal of Membrane Science*, *363*, 278–286.

Zirehpour, A., Rahimpour, A., Shamsabadi, A. A., Sharifian, M. G., & Soroush, M. (2017). Mitigation of thin-film composite membrane biofouling via immobilizing nano-sized biocidal reservoirs in the membrane active layer. *Environmental Science & Technology*, *51*, 5511–5522.

Zodrow, K., Brunet, L., Mahendra, S., Li, D., Zhang, A., Li, Q., & Alvarez, P. (2009). Polysulfone ultrafiltration membranes impregnated with silver nanoparticles show improved biofouling resistance and virus removal. *Water Research*, *43*(3), 715–723.

Further reading

Shao, W., Wang, S., Wu, J., Huang, M., Liu, H., & Min, H. (2016). Synthesis and antimicrobial activity of copper nanoparticle loaded regenerated bacterial cellulose membranes. *RSC Advances*, *6*, 65879–65884.

CHAPTER

4

Nanofiltration membrane technologies

Tina Chakrabarty[1], *Arnab Kanti Giri*[2] *and Supriya Sarkar*[1]

[1]The Environmental Research Group, R&D, Tata Steel, Jamshedpur, India [2]Department of Chemistry, Karim City College, Jamshedpur, India

4.1 Introduction

An interesting class of advanced membrane separation is nanofiltration (NF). Among all pressure-driven membrane technologies, NF having molecular weight cut-off (MWCO) between 200 and 1000 g mol^{-1} for pore diameters in the range of 0.5–2.0 nm has attracted increasing attention in the last few decades (Wang, Shang, Wang, Wu, & Tu, 2009). Most NF membranes are moderately charged (either positively or negatively charged) due to the dissociation of surface functional groups or the adsorption of charged solutes. Fabrication methods for NF membranes include interfacial polymerization (IP), phase inversion, dip coating, and grafting. Polymeric NF membrane are usually charged due to the presence of ionizable groups like sulfonic acid or carboxylic acid group, which results in charged surface in the presence of aqueous feed solution and operates in moderate pressure range.

Due to charged surface, in aqueous environment, NF shows good capacity for retention of multivalent ions and small organic molecules, permitting their application in water treatment, chemical, pharmaceutical, and food industries. In industry, some uses of NF process are to separate colors in textile and dye industry, metal recovery, and olive mill wastewater treatment. NF was also used in coke wastewater treatment, pulp and paper, oily wastewater treatment from oil and petroleum industries, and acid sulfate removal from mine water. Textile industries are always most concerned because of huge wastewater generation during dye manufacturing and processing, which contains toxic compound, heavy metals, salts, and chemicals and causes water pollution (Lin et al., 2015).

Due to the presence of special features, NF can precisely separate ionic species and small organic molecules from different aqueous composition. Selective layer of NF membranes is usually a three-dimensional network made by polymer chains, and their

Advancement in Polymer-Based Membranes for Water Remediation
DOI: https://doi.org/10.1016/B978-0-323-88514-0.00012-7

© 2022 Elsevier Inc. All rights reserved.

TABLE 4.1 Polymer used for surface material of different nanofiltration membrane and their operating range.

Sl. number	Membrane name	Manufacturer	Surface polymer	pH range	Max. temp (°C)	Max. pressure (bar)
1	NF 90	Dow Filmtec	Polyamide	2–11	45	31
2	NF270	Dow Filmtec	Semiaromatic piperazine-based polyamide	3–10	45	31
3	Desal 5DL	GE Osmonics	Polyamide	2–11	90	41
4	CK	GE Osmonics	Cellulose acetate	3–8	30	31
5	FMNP010	Microdyn Nadir GmbH	Polyether sulfone	0–14	95	40

separation and filtration behavior depends on pore size and surface charge. Polymer used as surface materials for different commercial NF membranes synthesis is mentioned in Table 4.1. Since the pore size of membrane and the presence of electrical charge on polymeric material play a vital role, the small changes in the surface property of NF would have a high impact on its permeability. Transport phenomena carried out by NF membranes are categorized into two sections: (1) In the case of electrolyte solute separation, the mass transfer is affected by interaction electrolytes, and membrane surface and models are known as fixed-charged and space-charged models (Luo & Wan, 2013). In this case, NF membrane performance is measured by determining the selectivity, which is generally calculated as the permeance ratio of one component to the other. (2) On the other side, for separation of nonelectrolyte component through NF membrane, transport model is typically steric hindrance pore model for some cases, assuming the whole membrane has uniform pore structure. For a few cases it is solution diffusion model, which adopts dissolved solute-solvent passes through membrane driven by chemical potential caused by concentration difference as well as pressure difference.

It has been identified that a number of sectors where NF membranes find application are wastewater treatment, solid-waste management, chemical, and petrochemical industries. Global market for NF is expected to grow up to $1.2 billion by 2024 with 18.2% annual market growth rate (Global, 2019). Expected relevant factors that may contribute to this market expansion are the following: (1) demand for affordable water purification technologies to obtain potable water; (2) an increasing demand to recycle and reuse of industrial processed water; (3) increasing need for the recovery of relatively rare metals from aqueous stream; (4) high demand in treatment of different organic solvents. At present NF membrane having MWCO <500 Da, are known as tight NF, are dominant in the market due to their performance and excellent stability.

There are some popular commercially available tight NF membrane like NF270, NF90, DL, and DK (Chen et al., 2016; Guo, Chen, Wan, Feng, & Luo, 2020; Song, Gan, & Qi, 2020). In contrast, loose NF membranes are still in developing stage and still not applied widely in real applications due to lacking in performance and limited demand. Even though there are some commercial loose NF, such as TriSep SBNF, having MWCO $\sim$2000 Da; NFPES10, having

MWCO 1000 Da; and NTR7450 having MWCO 800−1000 Da. These NF membranes have water permeability in the range of 12−17 L m^{-2} h^{-1} bar^{-1}. GE, GH, and GK are also commercially available loose NF made up of polyamide and possess very low flux (Cissé, Vaillant, Pallet, & Dornier, 2011; Sterlitech Corporation; Jincai, Qian, Fuat, & Tai-Shung, 2010; Lin, Tang, & Ye, 2015). Due to weak performance in terms of separation factor, permeability, and fouling behavior, there is still hindrance to large-scale application in NF. Thus most advanced research is focused on improving NF membrane performances by following representative strategies such as reducing thickness of selective layer and adjusting the morphology for better performance (Jiang, Tian, & Zhai, 2019; Wentao, Feiyun, & Wei, 2020; Wu, Yuan, & Wu, 2019). NF membrane separation selectivity is governed by steric hindrance as well as charge interaction. Thus pore size distribution is an effective route for outstanding separation efficiency. Additionally, NF membrane performance will be reduced indirectly by unavoidable membrane fouling because pore sizes of membranes get narrower with foulant accumulation on surface and inside the pores over time (Yao-Shen, Yan-Li, & Bin, 2020; Zhang, Li, & Su, 2016).

So, polymeric NF membrane has limitations such as fouling and trade-off between selectivity and permeability. In a review, Mohammad et al. (2015) has reported about many commercial NF membranes, available for salt removal applications and their transport properties. With the very fast development of nanomaterials with desired pore sizes, good mechanical strength, superior resistance, and antifouling properties, thin-film nanocomposite membrane (TFNM) paid great attention for their applications in water purification due to having good pH tolerance, low energy consumption, and low cost (Subramani, Voutchkov, & Jacangelo, 2014). The aim of this chapter is to highlight the research progress in NF membrane technology over the past decade. Total research progressed and articles published on water treatment by using NF membrane during the period 2010−2020, according to Scopus, have been summarized in Fig. 4.1. In this chapter we will discuss on

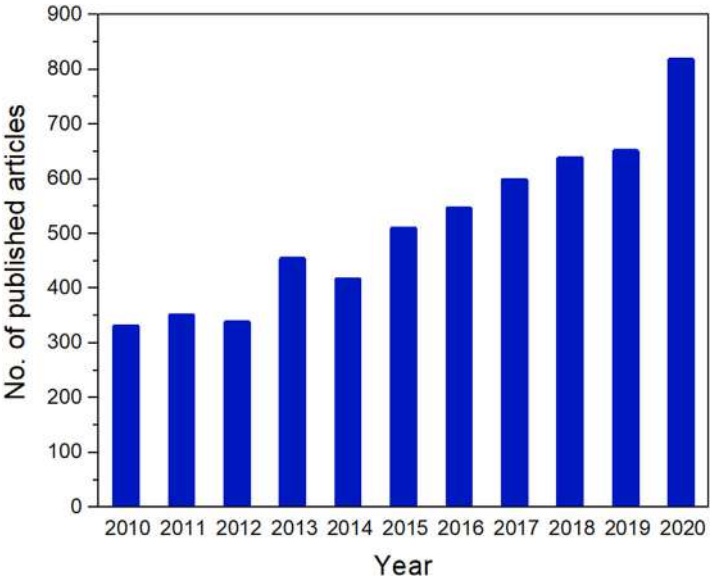

FIGURE 4.1 Number of articles published on "nanofiltration membrane" according to Scopus.

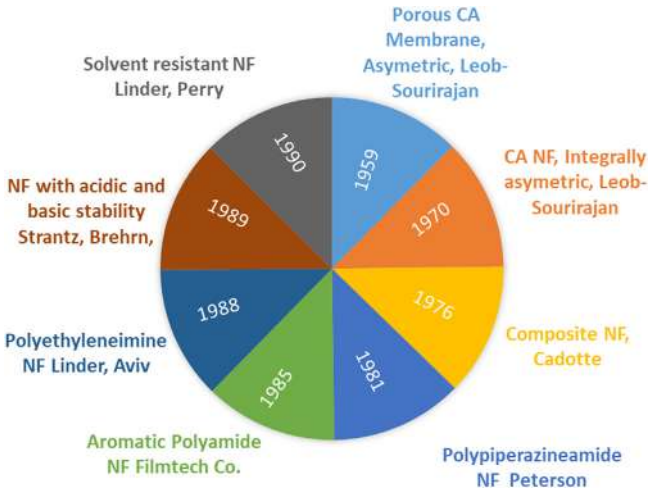

FIGURE 4.2 Historical development of nanofiltration membranes.

principle and transport mechanisms involved through NF separation. We will also focus on commercial availability of NF, NF membranes that are in piloting stage, maturity of technology, different conventional materials used in NF synthesis, membrane preparation, determination of configuration, and their applications domain. An overview of historical development of NF membranes from 1959 to 1990 (considered as golden era in NF invention) is highlighted in Fig. 4.2. Our discussion will also be focused on technical aspects of the NF mechanism and their limitations in water treatment. Finally, outlooks are offered on future potential opportunities for NF research in aqueous system.

4.2 Operation principle and transport mechanism

4.2.1 Nanofiltration pore model development and progress

The development of "pore model" for NF technology and its progress with time will be briefly discussed in this section. Fig. 4.3 summarizes the complete milestone of "pore model" establishment with key modifications. Schlogl (1965) has mentioned about extended Nernst–Planck equation to describe the ion transport or the transport of uncharged solute through ion-exchange membranes. For irreversible thermodynamics, this is a simplified version of Nernst–Planck equation.

After observation of hindered transport due to liquid-filled pores with similar size of solute molecules, Deen (1987) has added about hindered transport coefficients from solute and pore properties. Later on, in the case of NF and RO membranes, Xiao-Lin, Toshinori, Shin-ichi, and Shoji (1997) have proposed a model for mixed electrolyte system for calculation of ion rejection. Teorell–Meyer–Sievers (TMS) model explained the uniform distribution of fixed charge in membrane matrix (Tarsten, 1953). TMS model is the simplifying form of uniform charge distribution in the case of small pore size and small charge density. In 1998 DSPM model was applied to predict diafiltration result for dye and salt

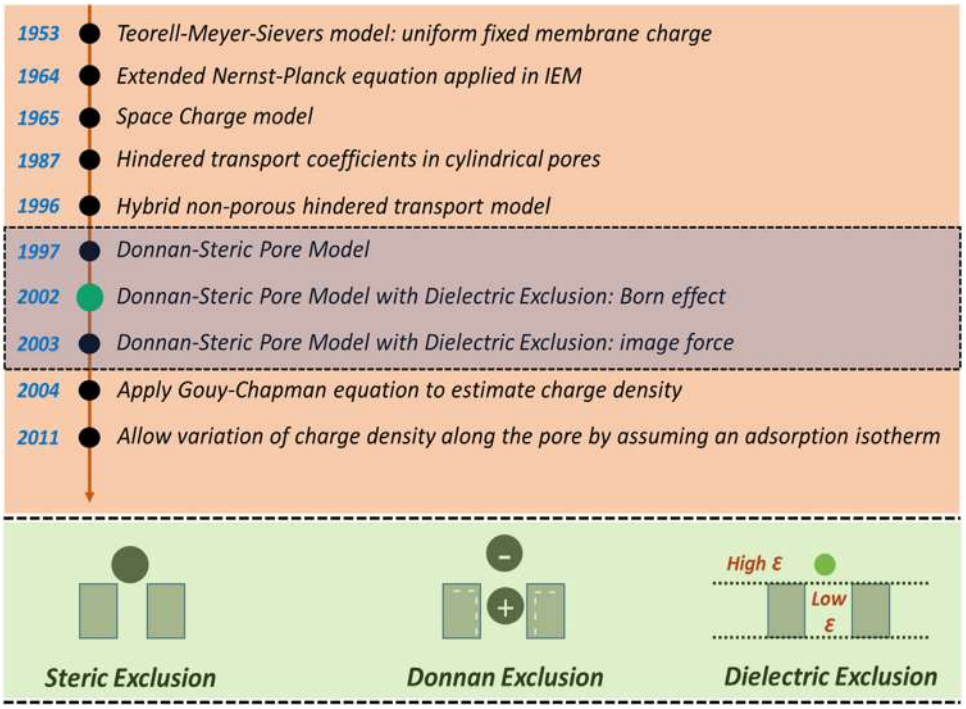

FIGURE 4.3 Pore model of membrane milestone.

separation (Bowen & Mohammad, 1998). Different parameters like membrane charge density and dielectric constant have been considered by many scientists during the past decades for a detailed membrane transportation study (Déon, Escoda, Fievet, & Salut, 2013; Montalvillo, Silva, & Palacio, 2014).

4.2.2 Diffusion and filtration mechanism

For removal of solute and electrostatic exclusions, two different mechanisms can result from membrane surface charge and solute charge of NF membranes. In this case, proper investigation of transport phenomena through membrane pores is very important. While transport phenomena through reverse osmosis (RO) and ultrafiltration (UF) have been investigated thoroughly, the transport and separation mechanism still remain hazy in the case of NF. Therefore in this chapter, we have tried to throw light on transport mechanism for NF separation to understand the phenomena in much depth.

Donan model has been used to estimate the diffusive flux (J) of different organic molecules through NF. Eq. (4.1) represents the above model across the charged membranes.

$$J = \frac{D -}{\partial}\left(\frac{C^2 - C'^2}{C^M}\right) \tag{4.1}$$

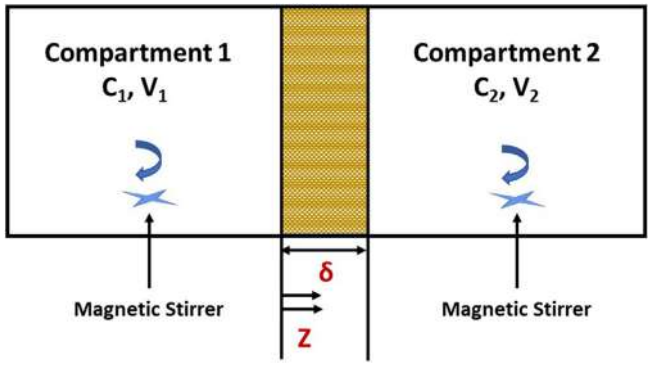

FIGURE 4.4 Schematic diagram of diffusion cell.

In this equation, J represents the diffusive flux through membrane (mol m^{-2} s^{-1}), C and C' are the concentration of the salt solution at feed and permeate side in mol m^{-3}, D is diffusion coefficient in m^{-2} s^{-1}, and membrane thickness is represented by ∂ (m). C_M represents the uniform concentration of fixed and negative charges in mol m^{-3}. In the case of Debye length is larger than pore size of membrane, transport will be dominated by electrostatic interactions rather than steric hindrance (Elimelech, Chen, & Waypa, 1994; Fairbrother & Mastin, 1924).

Total flux is determined by both diffusive transport and convective transport. In the case of filtration experiments, the solute flux (J) is calculated from permeate concentration and total flux through membrane. In Eq. (4.1), the term "diffusive flux" was modified and corrected with a factor f or p ($C_{2f} - C_{2p}$), to represent feed and permeance, respectively. However, during diffusion experiments, the diffusive flux obtained, which can only be used as an approximation of filtration experiment's diffusive flux, because for diffusion experiments, support layer and top portion of membranes were treated as a whole as active part. Due to the presence of large pores on support layer, the convective transport is much important in the case of support layers. A schematic diagram for diffusion cell has been given in Fig. 4.4.

4.2.3 Role of membrane charge on NF performance

Steric hindrance and solute–membrane nonelectrostatic interaction are the principal factors for NF separation. Besides this, membrane surface charge also plays an important role in performance (Van Der Bruggen, Schaep, Wilms, & Vandecasteele, 1999). In the case of charged molecules steric hindrance as well as electrostatic interaction, both have important role in NF separation performance (Chaufer, Rabiller-Baudry, Guihard, & Daufin, 1996; Childress & Elimelech, 2000). In principle, membranes in contact with solution gains some electric charge by following one of the following mechanisms: adsorption of ions from solution, dissociation of membranes-surface functional group, and polyelectrolyte and macromolecules adsorption. Interaction between ions and surface charge is actually electrostatic interaction, which is ruled by Donan-exclusion mechanism (Childress & Elimelech, 2000). In this mechanism, the coions, that is, the same-charged molecules with

membrane surface charge are repulsed by membranes to maintain the electroneutrality condition. At the same time, an equivalent number of counter ions will be retained to membrane surface, resulting in salt/other ionic species build-up on membrane surface (known as retentate species).

NF transport also get impacted by streaming potential, which is in principle opposite to electroosmotic phenomena. An electrical potential difference develops between the two ends of the pores, when oppositely charged ionic species are forced to get carried away by solvent through pores. By using Helmholtz–Smoluchowski equation (Elimelech, Chen, & Waypa, 1994; Fairbrother & Mastin, 1924),

$$\zeta = \frac{U_s}{\Delta_p}\frac{\mu}{\varepsilon\varepsilon_0}\frac{L}{A}\frac{1}{R} \tag{4.2}$$

$\frac{U_s}{\Delta_p}$ is obtained from the slope of the potential versus pressure graph. L/A value is calculated from Fairbrother and Mastin approach (Fairbrother & Mastin, 1924) for solutions with electrolyte concentration $>10^{-3}$ M:

$$\frac{L}{A} = \kappa R \tag{4.3}$$

In this equation, R is the resistance of the channel and can be calculated from streaming potential to streaming current ratio. Now with the help of Fairbrother and Mastin approach, Eq. (4.2) becomes

$$\zeta = \frac{U_s}{\Delta_p}\frac{\mu}{\varepsilon\varepsilon_0}\kappa \tag{4.4}$$

In this equation, "κ" is the specific conductivity ($\Omega^{-1}\,m^{-1}$). From this equation, streaming potential "U_s" as well as zeta potential "ζ" can be calculated. Based on the zeta potential value, surface charge "σ" can be calculated. Table 4.2 summarizes the zeta potential ζ and charge density (volumetric C_M and surface charge σ_s) at different pH for different commercial membranes (Braeken, Bettens, & Boussu, 2006).

Thus, to explain the NF membrane transport mechanism phenomena, diffusive transport and convective transport both are influenced by molecular weight of solute as well as electrostatic repulsion between solute and membrane surface. Braeken et al. (2006) have found that during NF of dissolved organic solutes in aqueous media, convection plays the dominant mechanism than diffusion phenomena, but if convective transport get hindered due to the presence of steric hindrance or other physical obstacles, then contribution of diffusion plays important role over convection mechanism.

4.3 Types of polymeric membranes and application domain

There are different types of NF membranes. Types of NF membrane are classified as per membrane structure and pore shapes, such as dense, thin-film composites, electrically charged membrane, isotropic, and nonisotropic.

TABLE 4.2 Zeta potential (ζ), surface charge density (σ_s), and volumetric charge density (C_M) at pH 3, 7, and 11 for different commercial membranes.

Membrane	pH	ζ (mV)	σ_s (10^{-3} C m^{-2})	C_M (mol m^{-3})
UTC	3	7.6	1.8	8.5
	7	−8.4	−2.0	−9.4
	11	−17.1	−4.0	−19.2
Desal-HL-51	3	3.5	0.8	35.2
	7	−14.2	−3.3	−142.7
	11	−17.4	−4.0	−174.8
NF270	3	2.4	0.6	34.0
	7	−21.6	−5.0	−306.4
	11	−26	−6.0	−368.8
NTR7450	3	1.2	0.3	8.3
	7	−16.6	−3.9	−114.4
	11	−19.3	−4.5	−133.0
NF-PES-010	3	0.65	0.2	3.1
	7	−12.4	−2.9	−59.8
	11	−15	−3.5	−72.3

4.3.1 Polymer used in membrane synthesis

IP is a widely used technique for NF membrane synthesis. There are various types of monomers that have been used in NF synthesis, such as trimesoyl chloride (TMC), isophthaloyl chloride, m-phenylenediamine, and polyvinylamine. Li, Cao, and Yu (2014) have mentioned about a new material polyhexamethylene guanidine hydrochloride, useful for bacteria removal and successfully used in NF synthesis. In addition to this, other monomer polyetherimide was modified with silica nanoparticle. A silica coupling agent was used for the amino functionalization of silica nanoparticles. Solvent separation and oil rejection performance was checked with this membrane and high performance was achieved (Namvar-Mahboub & Pakizeh, 2013). Some organic acid such as citric acid, ascorbic acid, and malic acid was studied for modification and fabrication of polysulfone-based NF membrane that helped to improve retention performance in separation (Ghaemi, Madaeni, & Alizadeh, 2012).

Till date, polyamide is the widely used polymer for NF membrane preparation. Recently, Chen, Wang, and Zhu (2021) have reported a graphene oxide (GO) based modified polyamide membrane, formed via IP, in which a novel electric-field-based strategy has been applied to fabricate GO-functionalized NF membrane. This membrane was found suitable in water purification with high flux and separation performance with great influence of electric field assistance. Sheng, Ming-Bang, and Cheng-Ye (2019) reported cellulose

nanocrystal incorporated polyamide NF membrane, which showed great performance in water purification with chlorine resistance and antifouling property. In another research, heavy ion irradiation and sequential UV illumination were used to create artificial nanopores of 0.3 nm size in polyethylene terephthalate membranes to make it suitable for highly selective ion transport. Due to such small pore size, these series of membrane can separate most of the hydrated ions selectively (Wang et al., 2018). Codeposition of polydopamine (PDA) and polyethylenimine (PEI) was used to prepare NF membrane which was used by Du and coworkers to filter a solution of small molecules (Du, Lv, Qiu, Wu, & Xu, 2016). There are several modifications applied to different polyamide NF membranes per its desire for different applications. To enhance water flux and chlorine resistance, cellulose nanocrystals were incorporated in polyamide NF membranes (Huang et al., 2019). In some studies, polyamide NF membranes were embedded with various GO content to improve the membrane flux as well as antifouling properties for desalination application (Bano, Mahmood, Kim, & Lee, 2015; Ma et al., 2019).

4.3.2 Other types of NF membranes

In the area of water softening and removal of organic matter, NF membrane replaces RO, owing to lower energy consumption. A range of hollow fiber as well as flat sheet NF membranes have been commercialized in the last few years.

Since the last decade, the development of high-performance nanomaterials-based NF membrane showed a great progress. In this chapter, we have reviewed the recent advanced studies on types of nanoparticle-based NF membranes, comprising different nanomaterials including metal oxide-based, metal−organic framework (MOF) based, covalent organic framework based, and carbon-based nanoparticles. In Fig. 4.5, the recent progress in nanoparticle-based NF membranes with improved selectivity, permeability, and antifouling properties has been overviewed. Here, we intend to summarize the types of NF membranes such as TFNM, mixed-matrix membranes, and self-assembly membranes.

4.3.2.1 Carbon nanomaterials-based NF

Carbon nanotubes (CNTs) having hollow structure and consisting of folded graphene layers are arranged in hexagonal form. Single-walled carbon nanotubes (SWCNTs) and multiwalled carbon nanotubes (MWCNTs) are important nanomaterials used in NF synthesis. Similarly, GO, a by-product of graphite oxide, is produced by treating graphite with a strong oxidizer.

To maintain the conductivity of graphene, reduced GO (RGO) is synthesized and both forms of GO are well-known materials for NF synthesis (Al-Anzi & Siang, 2017; Das, Ali, Hamid, Ramakrishna, & Chowdhury, 2014). Due to the presence of hydrophilic with strongly polarized functional groups, GO has capability to form good adhesion with most of the polymers and thus it has been widely used as hydrophilic membrane preparation. A PDA-based RGO composite novel lightweight and antifouling membrane was synthesized by Liu, Zhang, and Zhang (2015) with very high separation efficiency. CNTs have good hydrophobicity, smooth inner walls, and are able to transport water nicely. Wu, Tang, and Wu (2010) fabricated a TFNM with TMC, triethanolamine, and MWCNT

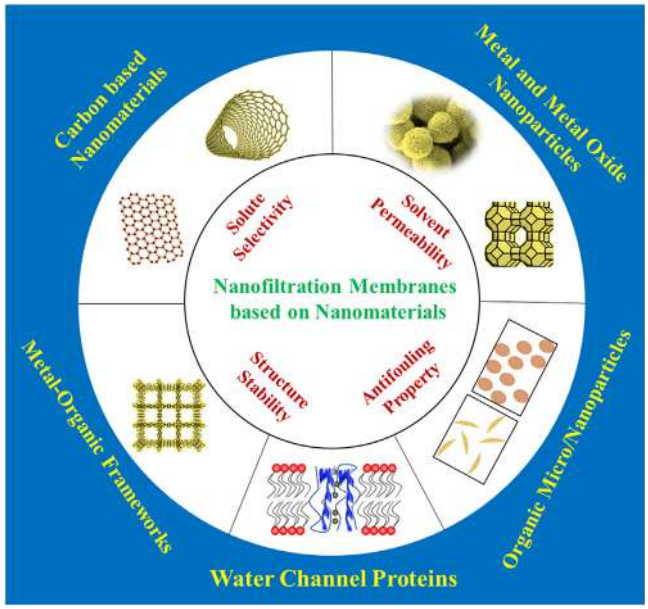

FIGURE 4.5 Nanoparticle-based nanofiltration membranes with improved selectivity, permeability, and antifouling properties.

via a reverse IP, which resulted in high flux but low salt rejection. Zhao, Ji, and Weng (2016) used PDA imbedded with MWCNTs into PEI/TMC polyamide thin-film composite (TFC) membranes. The compatibility and interfacial interaction between modified MWCNTs and polyamide matrix were improved; as a result in comparison to TMC/PEI bare membrane, the water flux of nanocomposite membrane increased up to 1.6 times. It has been found that CNT with vertical alignment forms straight pore channels in nanocomposite membranes and thus it performs better in terms of separation than the other variations of CNTs (Maschmann, Franklin, Amama, Zakharov, & Stach, 2006; Terrones et al., 1997). A new type of NF membrane based on stacked GO nanosheets, was reported by Kim, Hwang, Gamal El-Din, and Liu (2012). PDA-coated polysulfone support was used to prepare this membrane by using layer-by-layer (LbL) method and then crosslinked with TMC. This new type of membrane has flux in the range of 80–275 $L\,m^{-2}\,h^{-1}\,MPa^{-1}$, which is much higher than other commercially available NF membranes, but monovalent and divalent salt rejection capability is relatively low (around 46%). So, this result prove that further research is necessary for satisfying the salt separation.

4.3.2.2 Metal–organic framework-based NF

In the last few years, MOFs have been developed as great potential porous nanomaterials for preparing NF membranes. In 1995 first MOF concept was developed and proposed by Yaghi, Li, and Li (1995) and in 1999 they developed famous MOF-5 and published in *Nature*; since then these kinds of nanomaterials became research hotspot. A wide range of MOFs are modifying to meet the separation target for NF (Sorribas, Gorgojo, Téllez, Coronas, & Livingston, 2013; Van Goethem, Verbeke, Hermans, Bernstein, & Vankelecom, 2016; Wang et al., 2015; Xu et al., 2016). It has been found that porous MOFs provide a

good flow path for solvent, and due to this property, MOF-polyamide composite NF membrane, which has been prepared by IP, gives high solute rejection (Wang et al., 2015; Wang, Liu, Shen, Ji, & Li, 2016). Wu et al. (2010) synthesized ceramic tubular MOF-hybrid NF membrane through in situ LbL self-assembly. In this work, membranes prepared with optimized condition have shown very good performance with flux of around 200 L m^{-2} h^{-1} MPa^{-1} and rejection of methyl blue 98%, thus have showed an easy approach for fabrication of MOF-hybrid membrane on porous substrate suitable for commercial applications. A schematic diagram of different MOF membranes prepared by in situ method has been highlighted in Fig. 4.6 (Deng et al., 2021). Several other MOF-based membranes synthesized using in situ method have been reported as useful membranes for gas separation (Binling, Zhuxian, Yanqiu, & Yongde, 2014; Kang, Xue, & Fan, 2013; Wang, Liu, & Qiao, 2015).

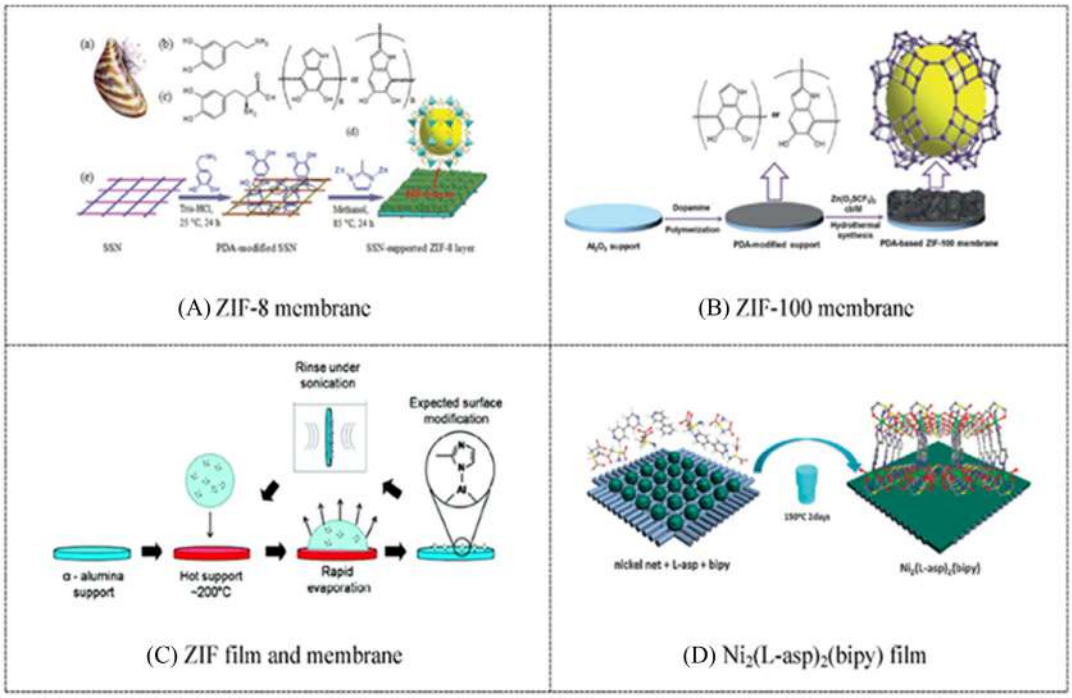

FIGURE 4.6 Schematic diagram of different metal–organic framework (MOF) membranes preparation by in situ growth method. (A) The preparation of a ZIF-8 molecular sieve membrane on a polydopamine (PDA)-functionalized stainless-steel-nets (SSN). (B) The synthesis process of ZIF-100 membranes on a polydopamine modified Al_2O_3 support. (C) The preparation of a ZIF-7 and ZIF-8 membrane on imidazole ligands modified α-alumina support. (D) The homochiral MOF membranes preparation by in situ growth on nickel nets. Source: *Part B reproduced with permission from Deng, Y., Wu, Y., Chen, G., Zheng, X., Dai, M., & Peng, C. (2021). Metal-organic framework membranes: Recent development in the synthesis strategies and their application in oil-water separation.* Chemical Engineering Journal, 405, *127004 (Copyright obtained).*

4.3.3 Application of NF membrane

Membrane separation process stands out as alternative to many conventional separation and purification process in chemical, food, pharmaceutical, and biotechnological industries. NF membranes are relatively recent development, having property in between RO and UF separation process. It allows most of the monovalent ions, like sodium chloride, potassium chloride through permeance, while rejects multivalent ions like calcium sulphate, magnesium sulphate, etc. Such exciting property and flexibility opens its opportunity for various process applications including textile industry, dyeing industry, food and chemicals processing, paper, and biotechnological applications. Due to NF properties like low energy consumption, reduction in number of processing steps, greater separation efficiency, and improved final product quality, NF technology became much popular for separation and processing industries (Baker, 2004). The main reported applications of NF separation are: separation of by-product in chemical industry, desalination of food, dyes desalination and brighteners of optical, removals of metals like nickel, and chrome plating from metal finishing industries, leather industry, pharmaceutical, and biotechnology applications (Cassano et al., 2003). Various industrial applications of NF technology have been discussed in this chapter.

4.3.3.1 Dye containing wastewater treatment in textile industry

Across the globe, textile industries follow the common production stages, where long complex chains are involved and "dyeing" is the key of this chain. Textile industries release a wide range of pollutants from different stages of fibers and garments processing, such as printing paste, dyeing bath residue, liquid paints, and solvents, which is an environmental concern. There are two types of dyes generally used in textile industries: (1) natural dyes (extracted from plant or animal organs) and (2) synthetic dyes (azo dye, non-azo dye, etc.). Azo dyes are used to offer color intensities and variations in shades (Collivignarelli, Abbà, Carnevale Miino, & Damiani, 2019). Acid dyes are generally used for silk, nylon, and wool garment materials. Synthetic dyes are most harmful to aquatic life as well as for groundwater. Some processes like chemical treatment (Meerbergen et al., 2017; Natarajan, Bajaj, & Tayade, 2018), biological treatment (Chinwetkitvanich, 2000), and physical treatment using RO and NF (Drewes, Reinhard, & Fox, 2003) are available to dye containing effluent treatment. Marcucci, Ciardelli, Matteucci, Ranieri, and Russo (2002) have studied and investigated the use of NF technology with the help of microfiltration (MF) pretreatment, for treatment of two different types of textile effluents: (1) a secondary effluent coming from a biological activated plant and (2) wastewater coming directly from several textile departments.

In this case, most interesting experimental results were obtained from treatment of wastewater from the carbonizing process. Kaan Morali, Uzal, and Yetis (2016) have revealed in a denim-producing plant, the wastewater treatment and reuse of indigo dyeing wastewater via application of membrane filtration. In a recent research, Thong, Gao, Lim, Wang, and Chung (2018) have mentioned about the development of a NF hollow fiber membrane which can effectively remove indigo carmine dye (MW: 466 gm mol^{-1}) with 94.9% rejection with high sustainability up to 72 h operation. Hybrid NF membranes are also explored in various

research for dye separation with >98% rejection and maximum efficiency (Gai, Li, Xiong, Wan, & Chung, 2016; Peydayesh, Mohammadi, & Bakhtiari, 2018).

4.3.3.2 NF in food processing industry

In food processing applications, NF has great potential. Due to many advantages like low thermal damage to product, low energy consumption, low maintenance cost over other traditional technologies, NF became popular in food processing industries. Food processing such as in plants and roots extraction, clarification, juice concentrator, wine application, dairy, and sugar processing are the main application area of NF. Vacuum-assisted evaporation process is used traditionally across food industries to make the fruit juices concentrated. But during process fragrance, color and taste are lost due to thermal degradation. In contrast, membrane technology works wonder to maintain aroma and juice flavor (Acosta, Vaillant, Perez, & Dornier, 2017). In food industries, color of soy sauce can be controlled by blending NF membrane-process with existing process. A sulfonated polysulfone NF membrane with a lower MWCO was used in the decolorization of Japanese soy sauce (shoyu) (Miyagi, Suzuki, Nabetani, & Nakajima, 2013). Machado, Trevisan, Pimentel-Souza, Pastore, and Hubinger (2016) have mentioned a process with NF and MF for clarification and concentration of oligosaccharides from artichoke by a sequential process.

In another research, NF is also used recently in removing undesirable components. Benedetti, Prudêncio, Mandarino, Rezzadori, and Petrus (2013) have mentioned the use of modified NF in concentrating soybean isoflavones and the aqueous defatted soy flour in their advanced research. NF can be useful in the purification of xylo-oligosaccharides (XOs) syrups. Beside this research, separation of XOs by NF has been carried out with reference to the mass transport phenomena by a combined Nernst−Planck equation and film theory.

4.3.3.3 NF in heavy metals removal from industrial waste

Discharge from various industries containing heavy metals not only pollute the groundwater but also threatens the human health by concentrating in food chain. Mining and hydrometallurgical industries are large generators of heavy metals and acidic liquid wastes. Besides traditional methods, membrane separation technology has been explored and applied recently for its high separation performances and cost effectiveness (Shao et al., 2020). Li et al. (2021) have explored the efficiency of the removal of heavy metals by using thin-film GO composite NF membranes. This study further explored its efficiency and stability for heavy metal ions removal during 30 h in the simulated tap water and mining wastewater, which indicated that the GO/PA-HFC (hollow fiber ceramic) membrane has great application potential in heavy metal rich wastewater treatment. Tian, Chang, Gao, and Zhang (2020) have fabricated a negatively charged NF membrane recently for the removal of heavy metal via IP. They have reached $MgCl_2$ rejection >94% in this study and after several experiments with Zn^{2+}, Cu^{2+}, Ni^{2+}, and Pb^{2+} samples, it was concluded that recently developed charged NF is suitable for metal removal from wastewater. Acid-containing wastewater was studied in another research (Niewersch, Meier, Wintgens, & Melin, 2010). Different NF membranes (Desal DL, DK, and NF270) were used and explored to treat pretreated sewage and sewage sludge ash at pH ranging

from 1 to 4 and minimum acid rejection was observed at pH 1, which was related to low degree of acid dissociation. In order to overcome the stability of membranes in acidic media, researchers are developing a new generation of NF membranes. For example, Zeng, Wang, Zhang, and Yu (2018) developed a poly(amide-s-triazine-amine) NF membrane that showed a similar performance before and after being immersed in 5 g L^{-1} H_2SO_4 for 720 h ($MgSO_4$ rejection of 94%).

In the past few decades, deteriorating water quality and increasing water crisis throughout the world became a serious problem. To solve this issue, NF became popular for water purification, brackish water desalination, and generation of ultrapure water (Loo, Fane, Krantz, & Lim, 2012). NF with MWCO 10,000 proved its effectiveness also in pyrogen removal. A unique membrane technique has been developed by Oh, Yamamoto, and Kitawaki (2000), which uses NF module coupled to a stationary bicycle to generate energy for reduction of feed pressure of system. Unfortunately, fouling of membrane prohibits it from long-run commercial applications. For many years, membrane process has been employed in dairy industries and nowadays, NF plays a great role in this field and at the same time it helps in developing new dairy products by reducing process cost and developing new process design. Thus currently, NF has become a popular alternative approach in many process and separation industries.

4.4 Polymeric membrane structure and configurations

IP is the most used technique for NF membrane preparation. The structure of IP membrane consists of a nonoven support layer and a selective TFC layer, and in most of the cases to add extra adhesion, other polymeric discriminating layer is present on top of the TFC layer, or in few cases, it may be present below this layer. A complete configuration of a commercial polyamide NF membrane is illustrated in Fig. 4.7, which consists a web for

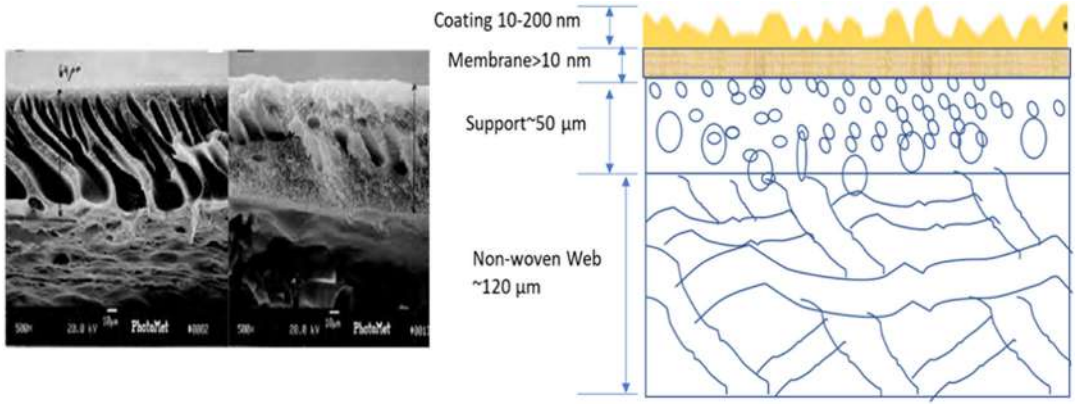

FIGURE 4.7 Configuration of a commercial polyamide nanofiltration membrane, which consists a web for strength layer of ~120 µm, a support layer of ~50 µm, thin-film composite membrane layer >10 nm, and a very thin polymeric layer coating (10–200 nm).

strength layer of ~100 μm, a support layer of ~50 μm, TFC membrane layer >10 nm, and a very thin polymeric layer. Engineering of almost all layers is possible as chemical composition varies for all layers as well as they are different for different membranes. Component of discriminating layers helps to improve the overall process performance with proper engineering. Structure and composition of a composite layer of NF membrane is mentioned below in details.

Composite NF membranes are prepared on a nonwoven support, which is made on fibrous, paper web to provide extra support (tensile strength) to membrane polymeric layer. There are nonwoven fabric manufacturers worldwide like Kavon Filter Products, Hirose Paper, Ahlstrom, and Awa Paper Mfg., which are the fabric suppliers for commercial polymeric membranes. In the case of TFC membrane, porous support and membrane layer can be modified separately to improve the membrane performance. In spiral wound elements, to avoid the deformation into channels, this web layer provides good support. Since NF is a pressure-depending process, thus to give stability in wide pressure range during operation, selection of web and their compatibility with the support is important. Most commercial supports are made of polyether sulfone (PES) or polyester web but sometimes at extremely higher pH and high temperature operating range, polyester does not work properly, thus as an alternative web polypropylene is used sometimes (Back-Flushable Spiral Wound Filter & Methods of Making and Using Same, 2004; Vilakati, Wong, Hoek, & Mamba, 2014).

During IP process, a porous support layer needs to be applied on web of strength. Support layer pore size plays an important role in polymer property as well as overall performance. Huang and McCutcheon (2015) have studied and explored a wide range of available nylon membrane as porous support and effect of pore size on forward osmosis TFC membrane preparation and related process. By varying pore size of supports for TFC preparation, they have found: (1) pore size of support layer has an impact on polyamide layer formation and crosslinking density; (2) with increasing pore size of support layer stability of membrane reduces at higher pressure; (3) it impacts on structural parameter; and (4) changes on pore size has impact on thickness and permeability of the resulting polyamide barrier layer. Some researchers have invented that changes of solvents like DMF, di-methyl sulphoxide (DMSO), or N-methyl-2-pyrolidone (NMP) used in casting solution also affect polyamide structure (Lu, Arias Chavez, Romero-Vargas Castrillón, Ma, & Elimelech, 2015). Crosslinking of support layer or polyamide layer also helps to improve the membrane texture made by phase-inversion method (Jimenez Solomon, Bhole, & Livingston, 2013). Crosslinked NF are useful for separation in nonaqueous media. Van Goethem, Mertens, and Vankelecom (2019), in a new study, mentioned about crosslinking of polyvinylidene fluoride (PVDF) membrane where one-pot diamine reaction was carried out for crosslinking process to achieve desired MWCO. After crosslinking, PVDF membrane became very stable in extreme pH condition, when bare PVDF is not stable in similar conditions. It also showed promising performance in terms of separation and flux in extreme basic and acidic conditions. Musale and Kumar (2000) crosslinked the surface of chitosan/poly (acrylonitrile) composite NF membrane with glutaraldehyde and some other varieties of glutaraldehyde. Crosslinked membrane was found to be stable over 10 h operation for pure water production. Kosaraju and Sirkar (2008) reported a use of polypropylene support for IP process of PEI and isophthaloyl dichloride. Good stability of these membrane was found in both methanol and ethanol.

Monomer has an active role in NF membrane performance. Although it is common that piperazine and TMC are the main components of solvent-resistant NF membrane, many other alternatives have been explored parallelly with aiming that it may improve conventional performance properties. Use of functional monomers has changed the property of NF in terms of hydrophilicity or charge and finally it impacts on flux and separation performance. Wang, Zhang, and Zhang (2011) prepared a positively charged NF membrane by using an IP on PAN support with 3,30,5,50-biphenyl tetraacyl chloride and piperazine in two different ways, only by changing solvent to toluene from cyclohexane. They found piperazine monomer diffuses more in toluene than cyclohexane, resulting in good compactness due to higher precipitation of monomer to interfacial layer. Due to lack in chlorine stability, polyamide membranes are modified by changing monomers many times for application. Some research areas in polyamide modification have been explored heavily, such as use of such monomers having tertiary amine groups or sometimes secondary amine groups.

There are some applications where NF needs to work in extreme pH stability conditions. Therefore lot of investigations are ongoing with monomers stability in extreme pH ranges, mainly in the field of metal separation in acidic solution, pulp, and paper-making industry. Similarly, solvent stable NF synthesis is also becoming an important area of research. In near future more extensive progress is needed in this part.

4.5 NF membrane preparation technologies

There are several approaches for polymeric NF membrane preparation technique. Most common approaches are IP, phase inversion, surface coating, grafting, etc. The method employed to fabricate the membrane mainly depends on membrane application, structure of membrane required (pore size, structure, selective layer thickness, etc.), and selection of polymers and their solubility. Depending on applications, like for gas-phase or liquid-phase separation, membrane texture needs to be decided, which leads to different approaches in membrane-casting technique. Besides flat sheet membranes, hollow fiber NF membranes are also getting attention for their wide application in filtration. Apart from these techniques, some emerging methods like incorporation of aquaporins, LbL casting, and use of glassy polymer are also available and used widely. Focusing on polymeric membrane, in this summary, we have lost chances to explain ceramic membrane preparation technology.

4.5.1 Interfacial polymerization

Most significant technique for NF and RO membrane preparation is IP. The first invention of interfacially polymerized TFC membranes was groundbreaking in terms of the performance of membranes in water purification applications (Lau, Ismail, Misdan, & Kassim, 2012; Petersen, 1993). To understand the mechanism of IP process in depth, it can be explained as follows: at the boundary of two immiscible solution phase (organic and aqueous), a polycondensation reaction happens between two monomers. In practice,

piperazine or m-phenylenediamine is used as the aqueous phase monomer, which often encompasses is first imbibed in a porous support and after that excess solution is removed carefully from surface, whereas TMC is used as an organic solvent. In most of the cases, it is found that use of m-phenylenediamine indicates the formation of tight RO and use of piperazine indicates the formation of NF membrane. It has been found that majority of NF and RO membranes formed using IP technique have polyamide thin layer on membrane support (Lind, Jeong, Subramani, Huang, & Hoek, 2009; Roh, Greenberg, & Khare, 2006). The important advantages of IP process over other techniques are: (1) Very thin selective layer can be formed at the interface of two different solution phase and can be tuned by adjusting the polymer concentration and other parameters. (2) Since the technique/process has shelf limitation it is reliable for commercial applications. Most of the interfacially polymerized NF membranes are found to be suitable for water purification and wastewater management application that proves its better suitability in aqueous applications. Solomon, Bhole, and Livingston (2012) synthesized a unique TFC membrane by IP process on P84-PI support and as a result, it showed higher permeability in polar solvents like dimethyl formamide (DMF) and acetone than the DuraMem 150 commercial membrane. One research in this field has confirmed the addition of additive in aqueous phase ease the polymerization reaction but the membrane posttreatment maintains the membrane porosity by increasing the free volume (Sun, Chung, Lu, & Chan, 2014). Thus low thickness and high permeability are the main attractive outputs of the IP technique. Fig. 4.8 has described different approaches of membrane preparation technique.

4.5.2 Phase inversion

Phase inversion is the easiest technique for NF membrane preparation. An advantage of this approach is a less complicated process and requires fewer number of steps than IP. The barrier layer of most of the interfacially polymerized composite membranes is formed on a phase-inverted support layer, thus phase-inversion process is typically applicable for NF preparation. This technique not only produces flat sheet membranes but also allows facile hollow fibers membrane formation. Thus a wide range of polymers are suitable for this technique. In phase-inversion technique, liquid−liquid demixing is the main principle which can occur in several ways such as: (1) vapor-induced phase separation, (2) thermal-induced phase separation, (3) evaporation-induced phase separation, and (4) immersion precipitation. Though in most of the cases, phase-separation-induced NF membranes are formed by immersion precipitation, sometime rest of the phase-separation techniques are also involved together. For immersion precipitation, polymer solution is immersed in nonsolvent coagulation bath, which is usually water. In this case, solvent and nonsolvent have to be miscible with each other and in coagulation bath exchange of polymer solution happens with this nonsolvent and then precipitation occurs (Drioli & Giorno, 2009; Mulder, 1996). There are many advantages of this technique, such as it can be used for a wide variety of polymers, can fabricate flat sheet and in tubular membranes form, simple to prepare and easy to scale up, membrane pores and membrane thickness are easy to optimize (Shao et al., 2020). To improve the morphology and membrane property, sometimes high molecular weight organic substances like polyethylene glycol, polyvinyl pyrolidone, or inorganic

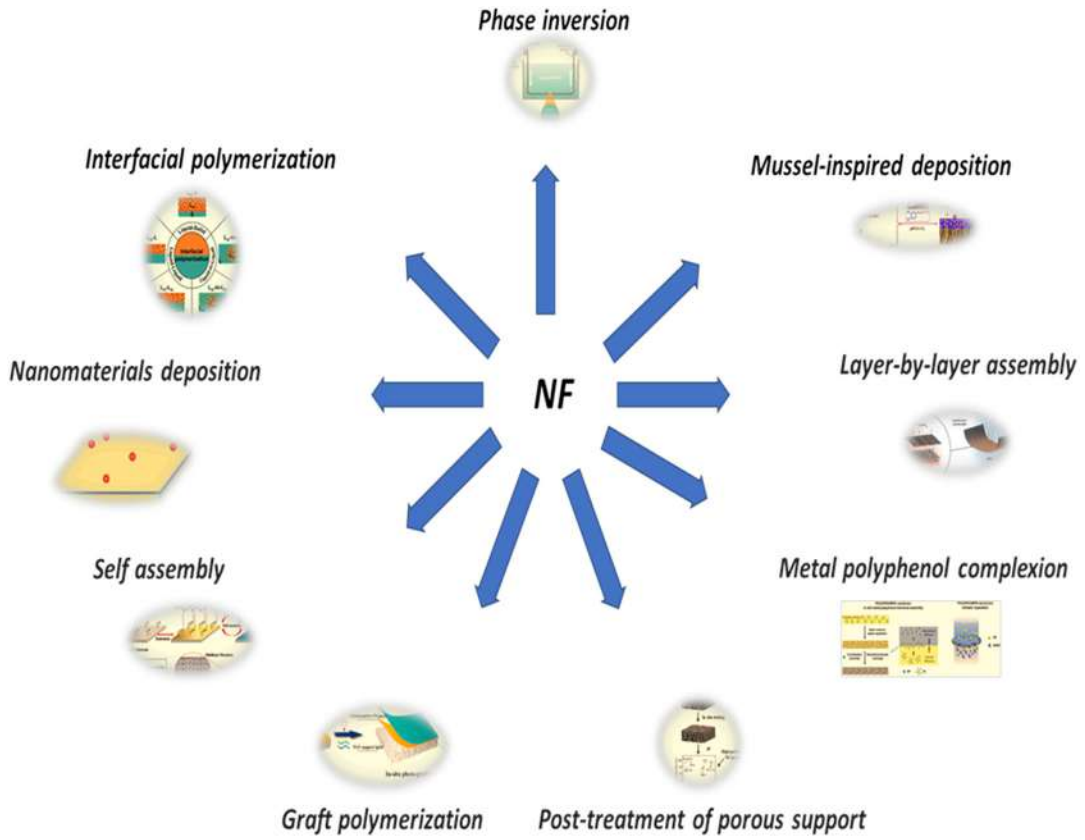

FIGURE 4.8 Different techniques for nanofiltration membrane preparation.

particles of LiCl are needed to be added (Liu, Hashim, Liu, Abed, & Li, 2011; P & FB, 1999). Poly dimethoxy siloxane microporous membranes have been created first by employing this method (Ren et al., 2020). In this case, membrane pore structure and pore size were tuned by varying the liquid paraffin concentration and casting temperature.

4.5.3 Posttreatment of porous support

Posttreatment of UF or MF membrane support layer like nonwoven, polyolefins, electrospun filament is also an important parameter to synthesize NF membranes (phase-inverted NF membrane). In several cases, this technique has been implemented by using any of the approaches such as spin coating, dip coating, spraying, and doctor blade casting. Peng, Huang, Jawor, and Hoek (2010) reported a use of multiple coating to obtain defectless superthin coating. This type of coating is attached with support surface through physical interaction (adsorption) or through electrostatic interaction and in some cases, coating reacts with support chemically. To maximize the permeability, it is typically desirable that the discriminating layer

should be separately created on the surfaces of support (Jun, Yoon, & Park, 2019). To stabilize the NF membrane for longer period or to enhance performance in terms of selectivity, modification of polymer is desirable. Considering the advantages of posttreatment of support to a wide range of polymers can be used as per applications. It has been found that polyvinyl alcohol (PVA) is the basis of first invented RO membrane and nowadays has become attractive as NF material and has been used onto polysulfone or PES support membrane followed by crosslinking (Gohil & Ray; Jahanshahi, Rahimpour, & Peyravi, 2010). In another report, Zhang, Guo, and Pan (2015) used coating on PVA and on 3-mercaptoropyltriethoxysilane crosslinker onto polysulfone support and further oxidized to introduce sulfonic acid group to TFC membrane, resulting in pH stable high performance in terms of selectivity and chlorine tolerance. Newly formed PVA-based coated membrane proved its better performance characteristics than base PVA membranes. Freger et al. (2005) reported another coated NF membrane with high acid stability and good separation performances. Beyond above classes, there was a wide variety of polymeric coatings with different properties and have been applied onto many supports. To improve fouling, both amphiphilic copolymers and a crosslinked terpolymer were used in some cases (Ji, An, & Zhao, 2012). Chakrabarty, Pérez-Manríquez, Neelakanda, and Peinemann (2017) have reported a unique coating method by using copper−tannic acid complex on PAN support. Copper−tannic acid complexes have good adhesion with PAN and achieved NF property, having MWCO 600 Da with low salt rejection.

Charged monomers also have an impact on membrane flux, reduction of fouling, and overall performances. Sometimes, increased charge may effect on swelling, which may favorably impact on membrane flux but may reduce the neutrally charged molecule's rejection property. Ahmad, Ooi, and Choudhury (2003) have invented a unique preparation technique for copolyimide TFC membrane from piperazine and 3,5-diaminobenzoic acid.

4.5.4 Layer-by-layer assembly

Multilayering, using polyelectrolytes, is an advanced technique to fabricate NF membranes. However, separation performance, fouling, and stability of membranes are necessary to improve large-scale application. Besides other coating techniques, LbL technique has been explored because of this technique's ability to control the membrane composition and membrane nanostructure (Guo et al., 2015; Ng, Mohammad, Ng, Leo, & Rohani, 2014). The traditional material for LbL assembly is anionic and cationic polyelectrolytes. Decher (1997) first reported using the LbL method to make films from polyelectrolytes and carried out further research and successfully prepared NF membranes. A special polyelectrolyte multilayer membrane was synthesized by Ng et al. (2014), by depositing poly(sodium 4-styrenesulfonate) and poly(diallyldimethyl ammonium chloride) having good NF performances. Under complicated condition, this polyelectrolyte chains may migrate and rearrange during NF process and, unfortunately, decrease the separation performances. A number of polyelectrolyte pairs could be suitable, such as PEI, chitosan, and poly(diallyldimethylammonium chloride). Polyacrylic acid, sodium alginate, and sodium carboxymethyl cellulose are the negatively charged polymers that have been used as suitable polyelectrolyte as NF material. Some researchers had found advantage of utilizing more than one pair of monomers, which provides greater flexibility to tune selectivity for separations of protein, enzymes, aminoamides, sugars, etc.

In an invention, Deng et al. (2008) have stated about the incorporation of copolymers into polyelectrolytes matrix, which gives a good opportunity to optimize membrane chemistry and structure. Thus a series of NF membranes were synthesized by shelf-copolymer, polyelectrolyte-based self-assembled method. Composite NF membrane, having high flux, was fabricated as hollow fibers through LbL assembly technique using oppositely charged crosslinked polyelectrolytes for dye removal (Chen et al., 2015). In another case, with the cellulose acetate NF system, Lajimi et al. noticed for 15 layers pairs, maximum flux and highest charge density (Lajimi, Abdallah, Ferjani, Roudesli, & Deratani, 2004) was observed and declination in flux with increase in number of bilayers was found. To understand the mechanism, for LbL assembly in the case of multilayered thin-film membranes (which was coated on inside the pores), water and ionic transport is ruled by convective flow. Rejection of ions depends on their size and as a result permeability decreases. In the case of thick film, transport mechanism is governed by through-layers diffusion mechanism and rejection of ions gets influenced by surface charge of these layers and membrane bulk charge. So, during the fabrication process of the LbL assembly, architecture on membrane surface charge is essential to optimize the ionic strength.

4.5.5 Hollow fiber NF membrane

Due to high separation and selectivity, hollow fiber membranes have great potential in several applications such as water purification, brackish water treatment, biomolecules separation, and gas separation. Similar to TFC membranes, hollow fiber membranes are prepared by phase-inversion method, thermally induced phase separation, or diffusion-induced phase separation method. In the last decade, there are many patents made on hollow fiber membrane fabrication techniques and production (Klotzer, 1999). An interesting research done by Sun, Wang, Rajarathnam, Hatton, and Chung (2010) on newly developed Torlon polyamide-imide (PAI) polymer is that they prepared hollow fiber NF membrane by phase-inversion process. Membrane was synthesized from a polymer/solvent binary system in the absence of additives without any modification and dry-jet spinning was adapted to control the membrane pore size; as a result pore size was reduced but membrane permeability increased. Setiawan, Wang, Li, and Fane (2011) have invented a microporous hollow fiber membrane with positively charge. NF-like selective layer was prepared by using asymmetric microporous hollow fibers, developed from Torlon PAI-based fabric, followed by PEI polyelectrolyte posttreatment. This PAI-based NF-like hollow fiber membrane showed a pure water permeability of 2.19–2.25 L m^{-2} h^{-1} bar^{-1} and salt reject for NaCl and $MgCl_2$ was also promising, 49% and 94%, respectively, at 1 bar pressure. Thus PAI-based NF-like hollow fiber membrane showed very good performance in multivalent heavy metal removal. Hence these types of membranes can be applied in water softening as well as heavy metal containing wastewater treatment using forward osmosis process. Cellulose acetate-based NF hollow fiber membrane was developed by Su, Yang, Teo, and Chung (2010) with MWCO of resultant membrane 186 Da. Though newly developed cellulose acetate-based membrane had relatively lower permeability for pure water but the rejection level for NaCl and $MgCl_2$ was 90.2% and 96.6%, respectively. Han, Chung, Weber, and Maletzko (2018) have developed a low pressure hollow fiber NF membrane having MWCO 1000 Da, with very high water permeability of 80 L m^{-2} h^{-1} bar^{-1} and found suitable in effective fractionation and wastewater treatment of textile industries.

Though fabrication and synthesis of hollow fiber is mature for industrial applications in gas separation, it is still less explored in pressure-driven separation like NF or RO and in membrane distillation.

4.6 Commercially available membranes

In this chapter, we have tried to highlight and gather an overall knowledge on the commercially available NF membranes and other NF membranes which are either in laboratory stage or in piloting stage. Table 4.3 has summarized the commercially available membranes along with the name of the manufacturer, their characteristics such as polymer used, MWCO, and pore size. Jiří, Edwin, and Petr (2020) have worked on commercially available tubular NF membranes from PCI, Poland (AFC 80, AFC 40, AFC 30) and focused on their characterizations and application in separation of heavy metals, drugs, micropollutants, etc. MWCO for AFC80, AFC30, and AFC 40 are 80, 100−150, and 200−400, respectively. Detailed characteristic study of tested membranes are summarized in Table 4.4. Stability in flux and high rejection of drug molecules was obtained and proved their potentiality in drug recovery and zinc from wastewater. Among these three, it was found that AFC 80 can be a good choice, in case feed contains monovalent anions such as chloride or nitrate as this membrane is denser than AFC30 and AFC40. For the removal of organic contaminants, AFC40 was used efficiently in Hartbeespoort dam, South Africa.

Another set of commercially available polyamide-based thin-film NF membranes NF270, NF90, NF, and NP010 from Dow Filmtec having MWCO in the range of 200−400 Da and for NP010 is 1000 Da, are well known for their excellence in beverage and juices extraction and separation. Vieira et al. (2018) have studied NF270, NF90, and PES-based NP010 for jussara ethanolic extraction (*Euterpe edulis*) in anthocyanins. They have parallelly checked the performance with Desal 5-DK (from GE Osmonics) membrane and found that Desal 5-DK showed the highest efficiency for jussara extract NF due to its highest flux with the smallest flux decline, in addition to the highest anthocyanins retention capacity in relation to the other commercial NF membranes. Suez (GE) has commercialized another polyamide-TFC membrane called Duracid, having MWCO 100−150 Da and shows high performance for industrial or sea water treatment. Apart from this, DL, HL, and DK are the other commercially available NF polyamide-based TFC membrane and CK (cellulose acetate based) from Suez (GE) and all are applicable in industrial water purification and sometimes in food industries. TriSep has launched two piperazine-amide-based flat sheet TFC membrane, TS40 and TS80, having MWCO 150−200 Da that are very useful in industrial wastewater purification. These flat sheet membranes offer high solute rejection of both salt and uncharged organic solute while operating in lower pressure than a RO. TS 80 is known as softening membrane and both are available in wet as well as in dry form. Synder filtration has commercialized a full range of wet and dry NF flat sheet membrane for pilot plant testing, process research, and for use in plate and frame module system with model name NFX, NFS, NFG, and NFW. Two polyamide-based TFC membranes are NDX and NFG, from Synder, having MWCO 500−800 Da and provide optimal performance in flux and rejection. The manufacturer claims that as per customers' requirement, small tuning on pore size and small modification on these membranes can be possible to the specific application. Synder launched two other NF membranes, namely NFX and NFW, which

TABLE 4.3 Commercially available membranes along with the name of manufacturer, their characteristics such as polymer used, MWCO, and pore size.

Sl. number	Membranes	Manufacturer	Pore size/MWCO (Da)	Polymer	Flux (GFD)/psi, permeability	References
1	AFC80 AFC40 AFC 30	PCI membrane system, Poland	80 200–400 100–150	Polyamide-TFC	7.1 L m^{-2} h^{-1} bar^{-1}	Van Goethem, Mertens, & Vankelecom (2019)
2	NF270	Dow Filmtec	~200–400	Polyamide-TFC	72–98/130	https://www.sterlitech.com/
	NF90				46–60/130	
	NF				26.5–39.5/130	
3	NP010	Microdyn Nadir	~1000	PES	200/40	
4	NP030	Microdyn Nadir	~500	PES	40/40	
5	Duracid	Suez (GE)	~150–200	Polyamide-TFC	10–19/225	
	DL	Suez (GE)	~150–300	Polyamide-TFC	28/220	
	HL	Suez (GE)	~150–300	Polyamide-TFC	39/100	
	DK	Suez (GE)	~150–300	Polyamide-TFC	22/100	
6	CK	Suez (GE)	~2000	Cellulose acetate	28/200	
7	TS80	TriSep	~150	Polyamide-TFC	20/110	
8	SB90	TriSep	~150	Cellulose acetate Biend	30/225	
9	SBNF		~2000	Cellulose acetate	NA	
10	TS40		~200	Polypiperazine amide-TFC	20/110	
11	XN45		~500	Polypiperazine amide-TFC	35/100	
12	NDX	Synder	500–700	—	35–45/110	
13	NFG	Synder	600–800	—	55–60/110	
14	NFW	Synder	300–500	—	45–50/110	
15	NFX	Synder	150–300	—	20–25/110	
16	N30F	Nadir Filtration GmbH, Wiesbaden, Germany	400	PES	1.0–1.8	*Separation and Purification Technology* 63 (2008), 251–263.

17	NF-PES-010	Nadir Filtration GmbH, Wiesbaden, Germany	1000	PES	5−10	*Separation and Purification Technology*
18	MPF-44	Koch	250	PDMS	1.3	
19	MPF-50	Koch	700	PDMS	1.0	
20	Desal 5-DK	Osmonics	150−300	PA	5.4	
	Desal 5-DL	Osmonics	150−300	PA	9.0	
	SS-030505	SolSep	—	—	1.0	
	SS-169	SolSep	—	—	10	
	SS-01	SolSep	—	—	10	
	HITK-1T	HITK	—	TiO_2	5	
	StarMem-120	MET	200	PI	1.0	
	StarMem-122	MET	220	PI	1.0	
	StarMem-128	MET	280	PI	0.26	
	CK	GE Osmonics	∼2000	Cellulose acetate	3.45	*Chemical Engineering Journal*, 127376. https://doi.org/10.1016/j.cej.2020.127376
	GE	GE Osmonics	1000	Polyamide	1.11	
	GH	GE Osmonics	2000	Polyamide	3.29	
	GK	GE Osmonics	2000	Polyamide	10.0	
	TriSep SBNF	Microdyn Nadir	2000	Cellulose acetate	12−17.7	
	NFPES10	Microdyn Nadir	1000	PES	15.4	
	NTR7450	Nitto Denko	600−800	Sulfonated polyether sulfone	5.7	
	Sepro NF2A	Ultura	530	Polyamide	10.1	
	Sepro NF6	Ultura	850	Polyamide	16.7	
	ETNA 01PP	Alfa Laval	1000	Fluoropolymer	29.4	

TABLE 4.4 Characteristics of the tested membrane.

Structural parameters	AFC 80	AFC 40	AFC 30
Membrane type material	Tubular polyamide film	Tubular polyamide film	Tubular polyamide film
Maximum pH range	1.5–10.5	1.5–9.5	1.5–9.5
Maximum pressure (bar)	60	60	60
Maximum temperature (°C)	70	60	60
NaCl or $CaCl_2$ retention (%)	80	60	75
MWCO (Da)	−80	200–400	100–150
Membrane surface change (pH = 7)	Negative	Negative	Negative
Effective membrane area (cm^2)	240	240	240
Length of one tube (cm)	30	30	30
Internal diameter (cm)	1.25	1.25	1.25

belong to lower MWCO range, that is, 150–300 and 300–500 Da, respectively, and provide excellent lactose and $MgSO_4$ rejection, while NFG partially removes monosaccharides from oligosaccharides. Hilal, Al-Zoubi, Darwish, and Mohammad (2005) have worked with a range of commercially available NF membranes NF90, NF270, and N30F to treat highly concentrated salt water (salinity similar to sea water or brackish water) containing $MgCl_2$, Na_2CO_3, and $CaSO_4$. Mainly, performance of each membrane was checked at 2–9 bar transmembrane pressure range and found that NF90 has high rejection at low flux while NF270 has lower rejection at high flux. These range of NF membranes can be used as alternative of pretreatment on sea water or brackish water desalination. LENNTECH has offered a special range of NF membranes with model name DK series, DK400, DL, Dura Slick, NF1 series, HP series, suitable in wide pH range and shows good performance in dairy production, pretreatment to desalination process, generation of high purity water. A complete range of NF membrane was offered by Ultura Inc., a few years ago. Newly launched low-charge SNF-20 membrane by Ultura Inc. has high performance and makes significant strides for selective separation. Sepro NF2A, Sepro NF6, polyamide-based NF flat sheet membrane having MWCO range 530–850 Da are manufactured by Ultura Inc. A group of researchers (Chen & Luo, 2018) have done the physicochemical characteristics for these membranes and studied their suitability in dairy wastewater treatment. A good interrelationship between physicochemical characteristics and performance was found. Particularly in this work, researchers have studied membrane properties of nine commercially available NF and surface charge, cross-sectional morphology, surface morphology, roughness, hydrophilicity, and permeability. It was found that semiaromatic polyamide membranes, NF270, DF30, and NF40-I, have high lactose retention and negligible salt retention. Outcome of this study improves our understanding about correlation between commercial NF membrane characteristics and their performance. There are several existing pilot plants based on NF technology throughout the world and some are upcoming to pilot-scale stage. In this chapter we have also highlighted such NF membranes used in pilot scale. In one study, Lau et al. (2012) have shown pilot-scale fabrication of NF membrane in spiral wound module.

Membrane was PES and piperazine based and complete procedure of membrane fabrication for pilot-scale spiral wound module is mentioned in their article, and the fabrication parameters and optimization studies are also done very systematically. This study claims that the optimized MWCO of prepared NF membrane is around 185 Da and possesses >95% rejection of $MgSO_4$, while flux is 75 L m^{-2} h^{-1} in specified modules, which is higher than many available commercial membranes. Bo-Zhi, Xiaohui, and Ning (2020) have reported a pilot-scale study with specific NF membrane for wastewater management from dye house effluent of textile industry. They have performed in pilot scale with Aquaset 9712 membrane filtration equipment in spiral wound module at 1−70 bar pressure. Result of this pilot study proves recycling of industrial wastewater containing organic substance inside their industry will be economical. Some pilot-scale study was found to be utilized in fertilizer-drawn forward osmosis desalination and its performance proves that it has possibility for full-scale upgradation in near future (Koyuncu, Kural, & Topacik, 2001). Defluorination is also an important area where NF has performed well. Some commercially available NF membranes such as NF90 and NF270 showed their excellent performance in F-removal. Textile industries generate effluent which contains different type of dyes with high molecular weight. Due to complex structures these dyes have low levels of biodegradability. For treatment of dye-rich industrial effluents, NF membranes are found to be very effective. NF90 was used to investigate the treatment of secondary effluent for wastewater reuse in the textile industry (Abid, Zablouk, & Abid-Alameer, 2012). In this research, it was showed that NF90 yielded a carbon oxygen demand (COD) reduction of 99% and the highest salt rejection of 75%-−95%.

4.7 Limitations and key mitigation strategies

In the field of membrane separations, NF technique has an active and very important role. High recovery and low energy consumption is the main reason of its success. Because of its potential, NF has attracted good attention in the area of desalination, brackish water treatment, petrochemical processing, sewage treatment, recovery, etc. Since 1980, application of NF has increased tremendously and has been providing solution to new challenges like drinking water production, arsenic removal, removal of insecticides, and chemicals. Among these, drinking water production is still the largest application of NF. To use NF membrane in diversified applications, several challenges need to be solved. Though NF is well known for its potential (Frenzel, Stamatialis, & Wessling, 2006; Kim, Phuntsho, & Shon, 2013), due to membrane fouling, process efficiency gets hindered. Thus understanding of fouling phenomena, that is, the interaction of feed stream with membrane surface need to understand very well.

4.7.1 Nexus between NF properties: fouling and antifouling

Performance of any membrane is reduced by polarization phenomena, but the effect of this phenomena may be different for different cases. Continuous flux decline is observed for MF and UF membrane operations, which is the result of irreversible deposition of suspension, colloids, emulsion on membrane surface and inside pores, but in the case of NF membranes, the fouling problem may somewhat be much complex as the interaction

happens at nanoscale and thus difficult to handle. Control on membrane fouling would reduce the chances of membrane cleaning and replacement (Mantt, 2006; Peng & Escobar, 2005). Formation of colloidal fouling or cake formation occurs depending on relative size of colloidal particles and their affinity to surface, texture of membrane surface, pore size, pore structure, etc. (Elimelech, Zhu, Childress, Hong; Lee, Cho, & Elimelech, 2005; Tarabara, Koyuncu, & Wiesner, 2004). Vrijenhoek et al. have explored the influence of membrane surface properties on rate of colloidal fouling (Warczok, Ferrando, López, & Güell, 2004). In these works, some experimental studies and AFM images proved that more particles are deposited on rough membrane than on smooth membrane surfaces and particularly on "valleys" of rough membranes, resulting severe flux decline due to "valley clogging." Concentration of colloids also influence the fouling of NF membrane. Apart from this, size, charge, and nature of particles or colloids also impact on fouling. Other two types of fouling such as biofouling and inorganic fouling also affect the membrane performance. Biofouling happens due to biologically active bacteria or fungi. Most of the commercially available polyamide NF membranes are exposed to biofouling which reduces the membrane performance with time (Vrijenhoek, Hong, & Elimelech, 2001). It has been observed that more hydrophobic and relatively rough membrane surfaces such as polyamide surfaces are prone to colloidal fouling than smoother surface-based membranes. Available polyamide membranes are mostly TFC membrane and selective layer is formed on porous support, thus many researchers are working on support modification as well as in selective layer modification to control the biofouling (Peng, Tang, Tang, Gong, & Zhao, 2019; Ren, Chen, Lu, Han, & Wu, 2021). Guo et al. have invented a process to resist the biofouling of polyamide membranes by covalent attachment of organic biocide on membrane surface (Guo, Weng, & Wu, 2019). Some researchers mentioned the modification of polyamide membranes with hydrophilic polymers to enhance the antibiofouling property (Guo et al., 2019; Zhang, Luo, Ding, & Jaffrin, 2015). Ren et al. (2021) highlighted a novel way for construction of antibiofouling NF membrane with high performance, by in situ photo grafting hydrophilic polymers. This approach also gives a common platform for selective layer preparation in membrane synthesis. Inorganic fouling is another type of fouling which forms scaling due to deposition of inorganic different salts on membrane surface. Common salts like gypsum, silica, calcium carbonate, and other salts are generally responsible in cake formation. Fig. 4.9 shows an overview of types of membrane fouling and fouling mechanism.

In reality, it is almost impossible to get rid of membrane fouling completely, but it can be minimized. Some approaches have come up to address the membrane fouling. These procedures can be divided into two categories: (1) techniques/methods applied during or prior to membrane separation to reduce the membrane fouling and (2) different strategies that can minimize the attachment of foulants on membrane surface by membrane modification (Park, Hwang, & Kim, 2018). Membrane pretreatment like using sand filter, optimization of feed water flow, membrane cleaning periodically are the usual procedure for membrane fouling treatment in RO and NF plant (Kang & Cao, 2012; Yang, Saeki, Wu, Yoshioka, & Matsuyama, 2019). In the case of heavy fouling, coagulation-based separation techniques by air flotation, sedimentation, etc. are used. Membrane module design and mass transport phenomena are also important that needs proper control for UF/NF processes. In practice, cleaning of NF membrane became an area of research in itself. There

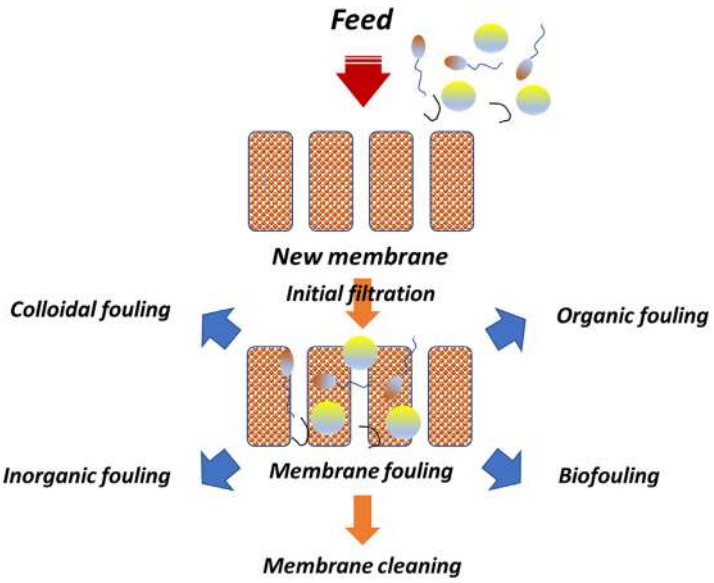

FIGURE 4.9 Types of membrane fouling and its mechanism.

are two types of cleaning such as physical cleaning hydraulic and pneumatic approaches (flushing, back flush, forward flush, scrubbing, etc.) and chemical cleaning (washing using acid, base, surfactant, etc.) which are the most attractive cleaning methods in fouling treatment, though chemical cleaning is more effective in the case of RO membrane (Zhang et al., 2015). Thus based on membrane characteristic and their influence on fouling, treatment procedure can be developed, hence building antifouling membrane surface by proper engineering can address the fouling issue.

4.7.2 Generation of membrane retentate

In pressure-driven membrane processes, generation of concentrate stream is a big hurdle for the whole process, as concentrate usually has to be discharged or further treated. Further treatment of concentrate is always expensive and energy intensive. In the case of NF, the membrane rejection is mainly due to accumulation of organic compound of molecular weight around 500 (depending on pore size of membrane) (Lin, Lee, & Huang, 2010). Characteristics of membrane reject depends on pretreatment and feed quality, process used, and permeance quality.

$$C_{\mathrm{r,i}} = \frac{\left(Q_f C_{f,i}\right) - \left(Q_p C_{p,i}\right)}{Q_r} \tag{4.5}$$

$$\mathrm{CF} = \frac{C_{r,i}}{C_{f,i}} = \frac{Q_f}{Q_r}\left[1 - R\frac{C_{p,i}}{C_{f,i}}\right] \tag{4.6}$$

Eqs. (4.5) and (4.6) help to calculate concentrate factor (CF), where Q is the volumetric flow and C is the concentration. CF can be calculated from i, the mass balance of each

component and its value depends on R value and I value. CF is the ratio of reject compartment concentration and feed compartment concentration. In the case of 100% rejection, CF can be calculated as

$$\mathrm{CF} = \frac{1}{1-R} \tag{4.7}$$

Handle of membrane reject can be done by different means such as: (1) reuse, (2) direct or indirect discharge into surface water, and (3) discharge into groundwater or on landfill. NF concentrates are more difficult to treat because of increased salt concentration or high concentrated organic compounds. Among all options, reuse of membrane reject is most attractive but applicable in only few cases, if the concentrated salt/compound matches with our desired product. In food and beverage industries, the concentrated stream is used as their desired product although some flavor may be lost after sometime. In textile or dye industries, concentrate generates during purification process is recycled systematically and separates all constituents for further use (Nguyen, Roddick, & Fan, 2012). Some of the membrane rejects get discharged for irrigation, some are deeply injected to groundwater, and less than 5% are discharged to evaporation pond. Though among all other applications, the first and most speeded application of membrane technology is in water industry. For sea water desalination and brackish water desalination, total use of membrane technology was surveyed in the United States and found that 73% of all technologies are RO installation and 11% is NF installation, and rest is electrodialysis (Semiat, 2000; Van der Bruggen, Curcio, & Drioli, 2004; Van Der Bruggen, Lejon, & Vandecasteele, 2003). The concentrate generates from half of the installation, gets discharged on surface water, and only 22%–23% concentrates are treated further in wastewater treatment plant, though with time the number of reject treatment plants have increased throughout the world.

4.8 Summary and future directions

Because of high efficiency and low energy consumption, NF technology became a very effective solution in the advanced field of water treatment. It has also increased researchers' attention in the field of desalination, sewage recovery, clean water production, petrochemical processing, etc.

In this chapter, we have summarized membrane transport mechanism, types of NF membranes, use of different approaches for NF synthesis, and identifying their specific application in each area. However, the primary focus was the use of specific NF membranes in water treatment, finding out their structural differences, and differences in performance in terms of permeation and selectivity. Maturity of this technology has been elaborated in a separate section by summarizing the availability of commercial NF membranes along with NF membranes that have passed laboratory developing stages and are entering the industrial scale development step. We have also summarized the limitations of NF technology such as membrane fouling–antifouling mechanism, problem with membrane concentrate (reject), and its treatment options.

Since selectivity is the key factor that determines the overall separation performance, researches have been carried out extensively in selectivity improvement techniques. In

principle, selectivity of NF membrane is controlled by steric hindrance, dielectric exclusion, and Donan effect. Many methods have been developed (based on these phenomena) and applied successfully to enhance the membrane selectivity by improving membrane permeance and membrane operation procedure.

Growth of NF research is so rapid that more than two-thirds of total publications on this field have been published in the last decade only. Not only in wastewater treatment, but solvent-resistant NF is also becoming very popular in this domain (Awerbuch & Weekes, 1990). Loose nanofiltration (LNF) membrane is popular for their extensive use in the removal of micropollutants including cyanobacterial metabolites. Due to low salt rejection capability and high permeability, LNF membrane has special advantage for recovery of resources from natural products and wastewater (Hacıfazlıoğlu, Tomasini, Bertin, Pek, & Kabay, 2019). Based on comprehensive article review, it is noted that some NF membranes are getting importance due to having sufficient flux and rejection capacity and overall performance in low energy, whereas other NF are gaining importance due to having ability in selective separation with high performance. Thus based on these studies, we can say there are still lot of challenges in NF research area, which can be focused for future development. Besides this, in the field of resource recovery from complicated industrial liquid mixture can be another future research scope. Since NF performance is mainly based on size exclusion and Donan phenomena, so by tailoring these two phenomena performance of process can be improved further. Membrane material development such as development of 2D material will be the future focus of research as this class of material has good potential to improve membrane selectivity. In this scope, besides other applications, though it is challenging to develop 2D materials in industrial scale. Like atomic layer deposition and related techniques, there are few methods available to improve the interfacial property of NF membrane, but still there is good scope where further research is needed to fulfill the industrial demand. Formation of new NF membrane architectures, having two faces with opposite, electrostatic attractions, wettability, and morphology, can be useful as ionic rectifiers, water diodes, and elsewhere.

During operation process, change in pH, transmembrane pressure, concentration change, and recycling ratio in feed stream can put a big impact on overall process performance, thus any innovativeness in membrane operating and separation process can play an important role to achieve high selectivity and separation ability (Lim & Bae, 2017). In conclusion, there are surely many exciting strategies which can be identified to meet the real challenges by better discussion between academicians and manufacturers.

References

Abid, M. F., Zablouk, M. A., & Abid-Alameer, A. M. (2012). Experimental study of dye removal from industrial wastewater by membrane technologies of reverse osmosis and nanofiltration. *Iranian Journal of Environmental Health Science & Engineering*, *9*(1), 17.

Acosta, O., Vaillant, F., Perez, A. M., & Dornier, M. (2017). Concentration of polyphenolic compounds in blackberry (*Rubus adenotrichos* Schltdl.) juice by nanofiltration. *Journal of Food Process Engineering*, *40*, 123–143.

Ahmad, A. L., Ooi, B. S., & Choudhury, J. P. (2003). Preparation and characterization of co-polyamide thin film composite membrane from piperazine and 3,5-diaminobenzoic acid. *Desalination*, *158*(1–3), 101–108. Available from https://doi.org/10.1016/S0011-9164(03)00440-5.

Al-Anzi, B. S., & Siang, O. C. (2017). Recent developments of carbon-based nanomaterials and membranes for oily wastewater treatment. *RSC Advances*, *7*, 20981–20994.

Awerbuch, L., & Weekes, M. C. (1990). Disposal of concentrates from brackish water desalting plants by means of evaporation technology. *Desalination*, *78*, 71.

Baker, R. W. (2004). *Membrane technology and applications* (2nd ed.). England: John Wiley and Sons, Ltd.

Bano, S., Mahmood, A., Kim, S. J., & Lee, K. H. (2015). Graphene oxide modified polyamide nanofiltration membrane with improved flux and antifouling properties. *Journal of Materials Chemistry A*, *3*, 2065–2071.

Benedetti, S., Prudêncio, E. S., Mandarino, J. M. G., Rezzadori, K., & Petrus, J. C. C. (2013). Concentration of soybean isoflavones by nanofiltration and the effects of thermal treatments on the concentrate. *Food Research International*, *50*(2), 625–632.

Binling, C., Zhuxian, Y., Yanqiu, Z., & Yongde, X. (2014). Zeolitic imidazolate framework materials: Recent progress in synthesis and applications. *Journal of Materials Chemistry A*, 16811–16831. Available from https://doi.org/10.1039/C4TA02984D.

Bowen, W. R., & Mohammad, A. W. (1998). Diafiltration by nanofiltration: Prediction and optimization. *AIChE Journal*, *44*(8), 1799–1812. Available from https://doi.org/10.1002/aic.690440811.

Bo-Zhi, C., Xiaohui, J., Ning, L., Chang-Hui, C., Jin-Peng, L., Chen, W., & Shi-Peng, S. (2020). Pilot-scale fabrication of nanofiltration membranes and spiral-wound modules. *Chemical Engineering Research and Design*, *160*, 395–404. Available from https://doi.org/10.1016/j.cherd.2020.06.011.

Braeken, L., Bettens, B., Boussu, K., Van der Meeren, P., Cocquyt, J., Vermant, J., & Van der Bruggen, B. (2006). Transport mechanisms of dissolved organic compounds in aqueous solution during nanofiltration. *Journal of Membrane Science*, *279*(1–2), 311–319. Available from https://doi.org/10.1016/j.memsci.2005.12.024.

Cassano, A., Adzet, J., Molinari, R., Buonomennac, M. G., Roig, J., & Drioli, E. (2003). Membrane treatment by nanofiltration of exhausted vegetable tannin liquors from the leather industry. *Water Research*, *37*(10), 2426–2434.

Chakrabarty, T., Pérez-Manríquez, L., Neelakanda, P., & Peinemann, K.-V. (2017). Bioinspired tannic acid-copper complexes as selective coating for nanofiltration membranes. *Separation and Purification Technology*, *184*, 188–194.

Chaufer, B., Rabiller-Baudry, M., Guihard, L., & Daufin, G. (1996). Retention of ions in nanofiltration at various ionic strength. *Desalination*, *104*(1–2), 37–46. Available from https://doi.org/10.1016/0011-9164(96)00024-0.

Chen, Q., Yu, P., Huang, W., Yu, S., Liu, M., & Gao, C. (2015). High-flux composite hollow fiber nanofiltration membranes fabricated through layer-by-layer deposition of oppositely charged crosslinked polyelectrolytes for dye removal. *Journal of Membrane Science*, *492*, 312–321. Available from https://doi.org/10.1016/j.memsci.2015.05.068.

Chen, X., Wang, W., Zhu, L., Liu, C., Cui, F., Li, N., & Zhang, B. (2021). Graphene oxide/polyamide-based nanofiltration membranes for water purification. *ACS Applied Nano Materials*, *4*(1), 673–682. Available from https://doi.org/10.1021/acsanm.0c02980.

Chen, Z., Luo, J., Hang, X., & Wan, Y. (2018). Physicochemical characterization of tight nanofiltration membranes for dairy wastewater treatment. *Journal of Membrane Science*, *547*, 51.

Chen, Z., Luo, J., Chen, X., Hang, X., Shen, F., & Wan, Y. (2016). Fully recycling dairy wastewater by an integrated isoelectric precipitation-nanofiltration-anaerobic fermentation process. *Chemical Engineering Journal*, *283*, 476–485. Available from https://doi.org/10.1016/j.cej.2015.07.086.

Childress, A. E., & Elimelech, M. (2000). Relating nanofiltration membrane performance to membrane charge (electrokinetic) characteristics. *Environmental Science and Technology*, *34*(17), 3710–3716. Available from https://doi.org/10.1021/es0008620.

Chinwetkitvanich, S. (2000). Anaerobic decolorization of reactive dyebath effluents by a two-stage UASB system with tapioca as a co-substrate. *Water Research*, *34*, 2223–2232.

Cissé, M., Vaillant, F., Pallet, D., & Dornier, M. (2011). Selecting ultrafiltration and nanofiltration membranes to concentrate anthocyanins from roselle extract (*Hibiscus sabdariffa* L.). *Food Research International*, *44*(9), 2607–2614. Available from https://doi.org/10.1016/j.foodres.2011.04.046.

Collivignarelli, M. C., Abbà, A., Carnevale Miino, M., & Damiani, S. (2019). Treatments for color removal from wastewater: State of the art. *Journal of Environmental Management*, *236*, 727–745.

Das, R., Ali, M. E., Hamid, S. B. A., Ramakrishna, S., & Chowdhury, Z. Z. (2014). Carbon nanotube membranes for water purification: A bright future in water desalination. *Desalination*, *336*(1), 97–109. Available from https://doi.org/10.1016/j.desal.2013.12.026.

Decher, G. (1997). Fuzzy nanoassemblies: Toward layered polymeric multicomposites. *Science*, *277*, 1232–1327.

Deen, W. M. (1987). Hindered transport of large molecules in liquid-filled pores. *AIChE Journal*, *33*(9), 1409–1425. Available from https://doi.org/10.1002/aic.690330902.

Deng, H. Y., Xu, Y. Y., Zhu, B. K., Wei, X. Z., Liu, F., & Cui, Z. Y. (2008). Polyelectrolyte membranes prepared by dynamic self-assembly of poly (4-styrenesulfonic acid-co-maleic acid) sodium salt (PSSMA) for nanofiltration (I). *Journal of Membrane Science*, *323*(1), 125–133. Available from https://doi.org/10.1016/j.memsci.2008.06.028.

Deng, Y., Wu, Y., Chen, G., Zheng, X., Dai, M., & Peng, C. (2021). Metal-organic framework membranes: Recent development in the synthesis strategies and their application in oil-water separation. *Chemical Engineering Journal*, *405*, 127004.

Déon, S., Escoda, A., Fievet, P., & Salut, R. (2013). Prediction of single salt rejection by NF membranes: An experimental methodology to assess physical parameters from membrane and streaming potentials. *Desalination*, *315*, 37–45. Available from https://doi.org/10.1016/j.desal.2012.09.005.

Drewes, J. E., Reinhard, M., & Fox, P. (2003). Comparing microfiltration-reverse osmosis and soil-aquifer treatment for indirect potable reuse of water. *Water Research*, *37*, 3612–3621.

Drioli, E., & Giorno, L. (2009). *Membrane operations: Innovative separations and transformations* (pp. 1–551). Italy: Wiley-VCH. Available from http://doi.org/10.1002/9783527626779.

Du, Y., Lv, Y., Qiu, W. Z., Wu, J., & Xu, Z. K. (2016). Nanofiltration membranes with narrowed pore size distribution via pore wall modification. *Chemical Communications*, *52*(55), 8589–8592.

Elimelech, M., Chen, W. H., & Waypa, J. J. (1994). Measuring the zeta (electrokinetic) potential of reverse osmosis membranes by a streaming potential analyzer. *Desalination*, *95*(3), 269–286. Available from https://doi.org/10.1016/0011-9164(94)00064-6.

Elimelech, M., Chen, W. H., & Waypa, J. J. (1994). Measuring the (electrokinetic) potential of reverse osmosis membranes by a streaming potential analyzer. *Desalination*, *95*, 269–286.

Elimelech, M., Zhu, X., Childress, A. E., & Hong, S. (1997). Role of membrane surface morphology in colloidal fouling of cellulose acetate and composite aromatic polyamide reverse osmosis membranes. *Journal of Membrane Science*, *127*, 101.

Fairbrother, F., & Mastin, H. (1924). Studies in electro-endosmosis: Part I. *Journal of the Chemical Society*, *125*, 2319–2330.

Fairbrother, F., & Mastin, H. (1924). CCCXII—Studies in electro-endosmosis. Part I. *Journal of the Chemical Society, Transactions*, *125*, 2319–2330. Available from https://doi.org/10.1039/CT9242502319.

Freger, V., Bottino, A., Capannelli, G., Perry, M., Gitis, V., & Belfer, S. (2005). Characterization of novel acid-stable NF membranes before and after exposure to acid using ATR-FTIR, TEM and AFM. *Journal of Membrane Science*, *256*(1–2), 134–142. Available from https://doi.org/10.1016/j.memsci.2005.02.014.

Frenzel, I., Stamatialis, D. F., & Wessling, M. (2006). Water recycling from mixed chromic acid waste effluents by membrane technology. *Separation and Purification Technology*, *49*(1), 76–83. Available from https://doi.org/10.1016/j.seppur.2005.08.010.

Gai, W., Li, X., Xiong, J. Y., Wan, C. F., & Chung, T.-S. (2016). Evolution of micro-deformation in inner-selective thin film composite hollow fiber membranes and its implications for osmotic power generation. *Journal of Membrane Science*, *516*, 104–112.

Ghaemi, N., Madaeni, S. S., Alizadeh, A., Daraei, P., Badieh, M. M. S., Falsafi, M., & Vatanpour, V. (2012). Fabrication and modification of polysulfone nanofiltration membrane using organic acids: Morphology, characterization and performance in removal of xenobiotics. *Separation and Purification Technology*, *96*, 214–228. Available from https://doi.org/10.1016/j.seppur.2012.06.008.

NF Global. (2019). *Membranes market set to reach $445.1 million by*. 70200–70209. Available from https://doi.org/10.1016/S0958-2118.

Gohil, J. M., & Ray, P. (2009). Polyvinyl alcohol as the barrier layer in thin film composite nanofiltration membranes: Preparation, characterization, and performance evaluation. *Journal of Colloid and Interface Science*, *338*, 121–127.

Guo, H., Chen, M., Liu, Q., Wang, Z., Cui, S., & Zhang, G. (2015). LbL assembly of sulfonated cyclohexanone-formaldehyde condensation polymer and poly(ethyleneimine) towards rejection of both cationic ions and dyes. *Desalination*, *365*, 108–116. Available from https://doi.org/10.1016/j.desal.2015.01.021.

Guo, S., Chen, X., Wan, Y., Feng, S., & Luo, J. (2020). Custom-tailoring loose nanofiltration membrane for precise biomolecule fractionation: New insight into post-treatment mechanisms. *ACS Applied Materials and Interfaces*, *12*(11), 13327–13337. Available from https://doi.org/10.1021/acsami.0c00259.

Guo, Y. S., Weng, X. D., Wu, B., Mi, Y.-F., Zhu, B.-K., & Ji, Y.-L., ... Gao, C. (2019). Construction of nonfouling nanofiltration membrane via introducing uniformly tunable zwitterionic layer. *Journal of Membrane Science*, *583*, 152–162. Available from https://doi.org/10.1016/j.memsci.2019.04.055.

Hacıfazlıoğlu, M. C., Tomasini, H. R., Bertin, L., Pek, T., & Kabay, N. (2019). Concentrate reduction in NF and RO desalination systems by membrane-in-series configurations-evaluation of product water for reuse in irrigation. *Desalination*, *466*, 89–96. Available from https://doi.org/10.1016/j.desal.2019.05.011.

Han, G., Chung, T.-S., Weber, M., & Maletzko, C. (2018). Low-pressure nanofiltration hollow fiber membranes for effective fractionation of dyes and inorganic salts in textile wastewater. *Environmental Science & Technology*, *52*(6), 3676–3684.

Hilal, N., Al-Zoubi, H., Darwish, N. A., & Mohammad, A. W. (2005). Nanofiltration of magnesium chloride, sodium carbonate, and calcium sulphate in salt solutions. *Separation Science and Technology*, *40*(16), 3299–3321. Available from https://doi.org/10.1080/01496390500423680.

Huang, L., & McCutcheon, J. R. (2015). Impact of support layer pore size on performance of thin film composite membranes for forward osmosis. *Journal of Membrane Science*, *483*, 25–33. Available from https://doi.org/10.1016/j.memsci.2015.01.025.

Huang, S., Wu, M. B., Zhu, C. Y., Ma, M. Q., Yang, J., Wu, J., & Xu, Z. K. (2019). Polyamide nanofiltration membranes incorporated with cellulose nanocrystals for enhanced water flux and chlorine resistance. *ACS Sustainable Chemistry & Engineering*, *7*, 12315–12322.

Jahanshahi, M., Rahimpour, A., & Peyravi, M. (2010). Developing thin film composite poly(piperazine-amide) and poly(vinyl-alcohol) nanofiltration membranes. *Desalination*, *257*(1–3), 129–136. Available from https://doi.org/10.1016/j.desal.2010.02.034.

Ji, Y. L., An, Q. F., Zhao, Q., Sun, W.-D., Lee, K.-R., Chen, H.-L., & Gao, C. (2012). Novel composite nanofiltration membranes containing zwitterions with high permeate flux and improved anti-fouling performance. *Journal of Membrane Science*, *390–391*, 243–253. Available from https://doi.org/10.1016/j.memsci.2011.11.047.

Jiang, C., Tian, L., Zhai, Z., Shen, Y., Dong, W., & He, M., ..., Niu, Q. J. (2019). Thin-film composite membranes with aqueous template-induced surface nanostructures for enhanced nanofiltration. *Journal of Membrane Science*, *589*. Available from https://doi.org/10.1016/j.memsci.2019.117244.

Jimenez Solomon, M. F., Bhole, Y., & Livingston, A. G. (2013). High flux hydrophobic membranes for organic solvent nanofiltration (OSN) – Interfacial polymerization, surface modification and solvent activation. *Journal of Membrane Science*, *434*, 193–203. Available from https://doi.org/10.1016/j.memsci.2013.01.055.

Jincai, S., Qian, Y., Fuat, T. J., & Tai-Shung, C. (2010). Cellulose acetate nanofiltration hollow fiber membranes for forward osmosis processes. *Journal of Membrane Science*, *355*, 36–44. Available from https://doi.org/10.1016/j.memsci.2010.03.003.

Jiří, C., Edwin, W., & Petr, M. (2020). Removal of micropollutants from water by commercially available nanofiltration membranes. *Science of the Total Environment*, *720*, 137474. Available from https://doi.org/10.1016/j.scitotenv.2020.137474.

Jun, B. M., Yoon, Y., & Park, C. M. (2019). Post-treatment of nanofiltration polyamide membrane through alkali-catalyzed hydrolysis to treat dyes in model wastewater. *Water*, *11*(8). Available from https://doi.org/10.3390/w11081645.

Kaan Morali, E., Uzal, N., & Yetis, U. (2016). Ozonation pre and post-treatment of denim textile mill effluents: Effect of cleaner production measures. *Journal of Cleaner Production*, *137*, 1–9.

Kang, G. d, & Cao, Y. M. (2012). Development of antifouling reverse osmosis membranes for water treatment: A review. *Water Research*, *46*(3), 584–600. Available from https://doi.org/10.1016/j.watres.2011.11.041.

Kang, Z., Xue, M., Fan, L., Ding, J., Guo, L., Gaob, L., & Qiu, S. (2013). Single nickel source in situ fabrication of a stable homochiral MOF membrane with chiral resolution properties. *Chemical Communications*, *49*(90). Available from https://doi.org/10.1039/c3cc42376j.

Kim, E. S., Hwang, G., Gamal El-Din, M., & Liu, Y. (2012). Development of nanosilver and multi-walled carbon nanotubes thin-film nanocomposite membrane for enhanced water treatment. *Journal of Membrane Science*, *394–395*, 37–48. Available from https://doi.org/10.1016/j.memsci.2011.11.041.

Kim, J. E., Phuntsho, S., & Shon, H. K. (2013). Pilot-scale nanofiltration system as post-treatment for fertilizer-drawn forward osmosis desalination for direct fertigation. *Desalination and Water Treatment*, *51*(31–33), 6265–6273. Available from https://doi.org/10.1080/19443994.2013.780804.

Klotzer, R., & Hamburg, D. (1999). *Method of producing hollow fiber polymer membranes*. US Patent 5980795.

Knappe, P. H., Kremen, S. S., Thomason, H. A., & Tanner, M. B. (2004). Back-flushable spiral wound filter and methods of making and using same. WO2000078436A1.

Kosaraju, P. B., & Sirkar, K. K. (2008). Interfacially polymerized thin film composite membranes on microporous polypropylene supports for solvent-resistant nanofiltration. *Journal of Membrane Science*, *321*(2), 155–161.

Koyuncu, I., Kural, E., & Topacik, D. (2001). Pilot scale nanofiltration membrane separation for waste management in textile industry. *Water Science and Technology*, *43*(10), 233–240. Available from https://doi.org/10.2166/wst.2001.0629.

Lajimi, R. H., Abdallah, A. B., Ferjani, E., Roudesli, M. S., & Deratani, A. (2004). Change of the performance properties of nanofiltration cellulose acetate membranes by surface adsorption of polyelectrolyte multilayers. *Desalination*, *163*(1–3), 193–202. Available from https://doi.org/10.1016/S0011-9164(04)90189-0.

Lau, W. J., Ismail, A. F., Misdan, N., & Kassim, M. A. (2012). A recent progress in thin film composite membrane: A review. *Desalination*, *287*.

Lee, S., Cho, J., & Elimelech, M. (2005). Combined influence of natural organic matter (NOM) and colloidal particles on nanofiltration membrane fouling. *Journal of Membrane Science*, *262*(1–2), 27–41. Available from https://doi.org/10.1016/j.memsci.2005.03.043.

Li, P., Li, Y.-X., Wu, Y. Z., Xu, Z. L., Zhang, H. Z., Gao, P., & Xu, S. J. (2021). Thin-film nanocomposite NF membrane with GO on macroporous hollow fiber ceramic substrate for efficient heavy metals removal. *Environmental Research*, *197*, 111040.

Li, X., Cao, Y., Yu, H., Kang, G., Jie, X., Liu, Z., & Yuan, Q. (2014). A novel composite nanofiltration membrane prepared with PHGH and TMC by interfacial polymerization. *Journal of Membrane Science*, *466*, 82–91. Available from https://doi.org/10.1016/j.memsci.2014.04.034.

Lim, G. T.-H., & Bae, R. W. (2017). Polymer-based membranes for solvent-resistant nanofiltration: A review. *Chinese Journal of Chemical Engineering*, 25.

Lin, J., Tang, C. Y., Ye, W., Sun, S.-P., Hamdan, S. H., & Volodin, A., ..., Van der Bruggen, B. (2015). Unraveling flux behavior of superhydrophilic loose nanofiltration membranes during textile wastewater treatment. *Journal of Membrane Science*, *493*, 690–702. Available from https://doi.org/10.1016/j.memsci.2015.07.018.

Lin, J. C. T., Lee, D. J., & Huang, C. (2010). Membrane fouling mitigation: Membrane cleaning. *Separation Science and Technology*, *45*(7), 858–872. Available from https://doi.org/10.1080/01496391003666940.

Lin, J., Ye, W., Huang, J., Ricard, B., Baltaru, M.-C., Greydanus, B., ... Van der Bruggen, B. (2015). Toward resource recovery from textile wastewater: Dye extraction, water and base/acid regeneration using a hybrid NF-BMED process. *ACS Sustainable Chemistry & Engineering*, *3*(9), 1993–2001.

Lind, M. L., Jeong, B. H., Subramani, A., Huang, X., & Hoek, E. M. V. (2009). Effect of mobile cation on zeolite-polyamide thin film nanocomposite membranes. *Journal of Materials Research*, *24*(5), 1624–1631. Available from https://doi.org/10.1557/jmr.2009.0189.

Liu, F., Hashim, N. A., Liu, Y. T., Abed, M. R. M., & Li, K. (2011). Progress in the production and modification of PVDF membranes. *Journal of Membrane Science*, *375*, 1.

Liu, N., Zhang, M., Zhang, W., Cao, Y., Chen, Y., & Lin, X., ..., Wei, Y. (2015). Ultralight free-standing reduced graphene oxide membranes for oil-in-water emulsion separation. *Journal of Materials Chemistry A*, *3*(40), 20113–20117. Available from https://doi.org/10.1039/c5ta06314k.

Loo, S., Fane, A. G., Krantz, W. B., & Lim, T. (2012). Emergency water supply: A review of potential technologies and selection criteria. *Water Research*, *46*(10), 3125–51.

Lu, X., Arias Chavez, L. H., Romero-Vargas Castrillón, S., Ma, J., & Elimelech, M. (2015). Influence of active layer and support layer surface structures on organic fouling propensity of thin-film composite forward osmosis membranes. *Environmental Science and Technology*, *49*(3), 1436–1444. Available from https://doi.org/10.1021/es5044062.

Luo, J., & Wan, Y. (2013). Effects of pH and salt on nanofiltration – A critical review. *Journal of Membrane Science*, *438*, 18–28. Available from https://doi.org/10.1016/j.memsci.2013.03.029.

Ma, W., Chen, T., Nanni, S., Yang, L., Ye, Z., & Rahaman, M. S. (2019). Zwitterion-functionalized graphene oxide incorporated polyamide membranes with improved antifouling properties. *Langmuir: The ACS Journal of Surfaces and Colloids*, *35*, 1513–1525.

Machado, M. T. C., Trevisan, S., Pimentel-Souza, J. D. R., Pastore, G. M., & Hubinger, M. D. (2016). Clarification and concentration of oligosaccharides from artichoke extract by a sequential process with microfiltration and nanofiltration membrane. *Journal of Food Engineering*, *180*, 120–128.

Manttäri, M., Viitikko, K., & Nystrom, M. (2006). Nanofiltration of biologically treated effluents from the pulp and paper industry. *Journal of Membrane Science*, *272*(1–2), 152–160.

Marcucci, M., Ciardelli, G., Matteucci, A., Ranieri, L., & Russo, M. (2002). Experimental campaigns on textile wastewater for reuse by means of different membrane processes. *Desalination*, *149*, 137–143.

Maschmann, M. R., Franklin, A. D., Amama, P. B., Zakharov, D. N., & Stach, E. A. (2006). Vertical single- and double-walled carbon nanotubes grown from modified porous anodic alumina templates. *Nanotechnology*, *17* (15), 3925–3929. Available from https://doi.org/10.1088/0957-4484/17/15/052.

Meerbergen, K., Crauwels, S., Willems, K. A., Dewil, R., Van Impe, J., Appels, L., & Lievens, B. (2017). Decolorization of reactive azo dyes using a sequential chemical and activated sludge treatment. *Journal of Bioscience and Bioengineering*, *124*, 668–673.

Miyagi, A., Suzuki, T., Nabetani, H., & Nakajima, M. (2013). Color control of Japanese soy sauce (shoyu) using membrane technology. *Food and Bioproducts Processing*, *91*, 507–514.

Mohammad, A. W., Teow, Y. H., Ang, W. L., Chung, Y. T., Oatley-Radcliffe, D. L., & Hilal, N. (2015). Nanofiltration membranes review: Recent advances and future prospects. *Desalination*, *356*, 226–254. Available from https://doi.org/10.1016/j.desal.2014.10.043.

Montalvillo, M., Silva, V., Palacio, L., Calvo, J. I., Carmona, F. J., Hernandez, A., & Pedro, P. (2014). Charge and dielectric characterization of nanofiltration membranes by impedance spectroscopy. *Journal of Membrane Science*, *454*, 163–173. Available from https://doi.org/10.1016/j.memsci.2013.12.017.

Mulder, M. (1996). *Basic principles of membrane technology*. Springer link.

Musale, D. A., & Kumar, A. (2000). Effects of surface crosslinking on sieving characteristics of chitosan/poly(acrylonitrile) composite nanofiltration membranes. *Separation and Purification Technology*, *21*(1–2), 27–37. Available from https://doi.org/10.1016/S1383-5866(00)00188-X.

Namvar-Mahboub, M., & Pakizeh, M. (2013). Development of a novel thin film composite membrane by interfacial polymerization on polyetherimide/modified SiO_2 support for organic solvent nanofiltration. *Separation and Purification Technology*, *119*, 35–45. Available from https://doi.org/10.1016/j.seppur.2013.09.003.

Natarajan, S., Bajaj, H. C., & Tayade, R. J. (2018). Recent advances based on the synergetic effect of adsorption for removal of dyes from waste water using photocatalytic process. *Journal of Environmental Sciences*, *65*, 201–222.

Ng, L. Y., Mohammad, A. W., Ng, C. Y., Leo, C. P., & Rohani, R. (2014). Development of nanofiltration membrane with high salt selectivity and performance stability using polyelectrolyte multilayers. *Desalination*, *351*, 19–26. Available from https://doi.org/10.1016/j.desal.2014.07.020.

Nguyen, T., Roddick, F. A., & Fan, L. (2012). Biofouling of water treatment membranes: A review of the underlying causes, monitoring techniques and control measures. *Membranes*, *2*(4), 804–840. Available from https://doi.org/10.3390/membranes2040804.

Niewersch, C., Meier, K., Wintgens, T., & Melin, T. (2010). Selectivity of polyamide nanofiltration membranes for cations and phosphoric acid. *Desalination*, *250*, 1021–1024.

Oh, J. I., Yamamoto, K., Kitawaki, H., Nakao, S., Sugawara, T., Rahman, M. M., & Rahman, M. H. (2000). Application of low-pressure nanofiltration coupled with a bicycle pump for the treatment of arsenic-contaminated groundwater. *Desalination*, *132*(1–3), 307–314. Available from https://doi.org/10.1016/S0011-9164(00)00165-X.

Pinnau, I., & Freeman, B. D. (1999). Formation and modification of polymeric membranes: Overview. *American Chemical Society (ACS)*, 1–22. Available from https://doi.org/10.1021/bk-2000-0744.ch001.

Park, S. H., Hwang, S. O., Kim, T. S., Cho, A., Kwon, S. J., & Kim, K. T., ..., Lee, J. H. (2018). Triclosan-immobilized polyamide thin film composite membranes with enhanced biofouling resistance. *Applied Surface Science*, *443*, 458–466.

Peng, F., Huang, X., Jawor, A., & Hoek, E. M. V. (2010). Transport, structural, and interfacial properties of poly (vinyl alcohol)-polysulfone composite nanofiltration membranes. *Journal of Membrane Science*, *353*(1–2), 169–176. Available from https://doi.org/10.1016/j.memsci.2010.02.044.

Peng, H., Tang, Q., Tang, S., Gong, J., & Zhao, Q. (2019). Surface modified polyamide nanofiltration membranes with high permeability and stability. *Journal of Membrane Science*, 592. Available from https://doi.org/10.1016/j.memsci.2019.117386.

Peng, W., & Escobar, I. C. (2005). Evaluation of factors influencing membrane performance. *Environmental Progress*, *24*(4), 392–399. Available from https://doi.org/10.1002/ep.10109.

Petersen, R. J. (1993). Composite reverse osmosis and nanofiltration membranes. *Journal of Membrane Science*, *83*, 81–150. Available from https://doi.org/10.1016/0376-7388.

Peydayesh, M., Mohammadi, T., & Bakhtiari, O. (2018). Effective treatment of dye wastewater via positively charged TETA-MWCNT/PES hybrid nanofiltration membranes. *Separation and Purification Technology*, *194*, 488–502.

Ren, L., Chen, J., Lu, Q., Han, J., & Wu, H. (2021). Anti-biofouling nanofiltration membrane constructed by in-situ photo-grafting bactericidal and hydrophilic polymers. *Journal of Membrane Science, 617*, 118658.

Ren, L.-F., Liu, C., Xu, Y., Zhang, X., Shao, J., & He, Y. (2020). High-performance electrospinning-phase inversion composite PDMS membrane for extractive membrane bioreactor: Fabrication, characterization, optimization and application. *Journal of Membrane Science*, 597.

Roh, I. J., Greenberg, A. R., & Khare, V. P. (2006). Synthesis and characterization of interfacially polymerized polyamide thin films. *Desalination, 191*, 279–290.

Schlogl, R. (1965). Membrane permeation in systems far from equilibrium. *Berichte der Bunsengesellschaft für physikalische Chemie*, 400–414. Available from https://doi.org/10.1002/bbpc.19660700403.

Semiat, R. (2000). Present and future. *Water International*, *25*(1), 54–65. Available from https://doi.org/10.1080/02508060008686797.

Setiawan, L., Wang, R., Li, K., & Fane, A. G. (2011). Fabrication of novel poly(amide-imide) forward osmosis hollow fiber membranes with a positively charged nanofiltration-like selective layer. *Journal of Membrane Science, 369*, 196–205.

Shao, W., Liu, C., Yu, T., Xiong, Y., Hong, Z., & Xie, Q. (2020). constructing positively charged thin-film nanocomposite nanofiltration membranes with enhanced performance. *Polymers, 12*, 2526–2535.

Sheng, H., Ming-Bang, W., Cheng-Ye, Z., Ma, M.-Q., Yang, J., Wu, J., & Xu, Z.-K. (2019). Polyamide nanofiltration membranes incorporated with cellulose nanocrystals for enhanced water flux and chlorine resistance. *ACS Sustainable Chemistry & Engineering*, *7*, 14. Available from https://doi.org/10.1021/acssuschemeng.9b01651.

Solomon, M. F. J., Bhole, Y., & Livingston, A. G. (2012). High flux membranes for organic solvent nanofiltration (OSN)—Interfacial polymerization with solvent activation. *Journal of Membrane Science, 423–424*, 371–382.

Song, X., Gan, B., Qi, S., Guo, H., Tang, C. Y., & Zhou, Y., ..., Gao, C. (2020). Intrinsic nanoscale structure of thin film composite polyamide membranes: Connectivity, defects, and structure-property correlation. *Environmental Science and Technology*, *54*(6), 3559–3569. Available from https://doi.org/10.1021/acs.est.9b05892.

Sorribas, S., Gorgojo, P., Téllez, C., Coronas, J., & Livingston, A. G. (2013). High flux thin film nanocomposite membranes based on metal-organic frameworks for organic solvent nanofiltration. *Journal of the American Chemical Society*, *135*(40), 15201–15208. Available from https://doi.org/10.1021/ja407665w.

Su, J., Yang, Q., Teo, J. F., & Chung, T. S. (2010). Cellulose acetate nanofiltration hollow fiber membranes for forward osmosis processes. *Journal of Membrane Science, 355*(1–2), 36–44.

Sterlitech Corporation, Flat sheet membranes. Ultrafiltration membranes. https://www.sterlitech.com/flat-sheet-membranes.html.

Subramani, A., Voutchkov, N., & Jacangelo, J. G. (2014). Desalination energy minimization using thin film nanocomposite membranes. *Desalination*, *350*, 35–43. Available from https://doi.org/10.1016/j.desal.2014.07.011.

Sun, S.-P., Chung, T.-S., Lu, K.-J., & Chan, S.-Y. (2014). Enhancement of flux and solvent stability of matrimid® thin-film composite membranes for organic solvent nanofiltration. *Separations: Materials, Devices and Processes, 60*, 3623–3633.

Sun, S. P., Wang, K. Y., Rajarathnam, D., Hatton, T. A., & Chung, T. S. (2010). Polyamide-imide nanofiltration hollow fiber with elongation-induced nano-pore evolution. *AIChE Journal. American Institute of Chemical Engineers, 56*(6), 1481–1494.

Tarabara, V. V., Koyuncu, I., & Wiesner, M. R. (2004). Effect of hydrodynamics and solution ionic strength on permeate flux in cross-flow filtration: Direct experimental observation of filter cake cross-sections. *Journal of Membrane Science*, *241*(1), 65–78. Available from https://doi.org/10.1016/j.memsci.2004.04.030.

Tarsten, T. (1953). Transport processes and electrical phenomena in ionic membranes. *Progress in Biophysics and Biophysical Chemistry*, *3*, 305–369. Available from https://doi.org/10.1016/s0096-4174(18)30049-0.

Terrones, M., Grobert, N., Olivares, J., Zhang, J. P., Terrones, H., & Kordatos, K., ..., Walton, D. R. M. (1997). Controlled production of aligned-nanotube bundles. *Nature*, *388*(6637), 52–55. Available from https://doi.org/10.1038/40369.

Thong, Z., Gao, J., Lim, J. X. Z., Wang, K.-Y., & Chung, T.-S. (2018). Fabrication of loose outer-selective nanofiltration (NF) polyethersulfone (PES) hollow fibers via single-step spinning process for dye removal. *Separation and Purification Technology, 192*, 483–490.

Tian, J., Chang, H., Gao, S., & Zhang, R. (2020). How to fabricate a negatively charged NF membrane for heavy metal removal via the interfacial polymerization between PIP and TMC? *Desalination, 491*, 114499.

Van der Bruggen, B., Curcio, E., & Drioli, E. (2004). Process intensification in the textile industry: The role of membrane technology. *Journal of Environmental Management*, *73*(3), 267–274. Available from https://doi.org/10.1016/j.jenvman.2004.07.007.

Van Der Bruggen, B., Lejon, L., & Vandecasteele, C. (2003). Reuse, treatment, and discharge of the concentrate of pressure-driven membrane processes. *Environmental Science and Technology*, *37*(17), 3733–3738. Available from https://doi.org/10.1021/es0201754.

Van Der Bruggen, B., Schaep, J., Wilms, D., & Vandecasteele, C. (1999). Influence of molecular size, polarity and charge on the retention of organic molecules by nanofiltration. *Journal of Membrane Science*, *156*(1), 29–41. Available from https://doi.org/10.1016/S0376-7388(98)00326-3.

Van Goethem, C., Mertens, M., & Vankelecom, I. F. J. (2019). Crosslinked PVDF membranes for aqueous and extreme pH nanofiltration. *Journal of Membrane Science*, *572*, 489–495. Available from https://doi.org/10.1016/j.memsci.2018.11.036.

Van Goethem, C., Verbeke, R., Hermans, S., Bernstein, R., & Vankelecom, I. F. J. (2016). Controlled positioning of MOFs in interfacially polymerized thin-film nanocomposites. *Journal of Materials Chemistry A*, *4*(42), 16368–16376. Available from https://doi.org/10.1039/c6ta05175h.

Vieira, G. S., Moreira, F. K. V., Matsumoto, R. L. S., Michelon, M., Filho, F. M., & Hubinger, M. D. (2018). Influence of nanofiltration membrane features on enrichment of jussara ethanolic extract (*Euterpe edulis*) in anthocyanins. *Journal of Food Engineering*, *226*, 31–41. Available from https://doi.org/10.1016/j.jfoodeng.2018.01.013.

Vilakati, G. D., Wong, M. C. Y., Hoek, E. M. V., & Mamba, B. B. (2014). Relating thin film composite membrane performance to support membrane morphology fabricated using lignin additive. *Journal of Membrane Science*, *469*, 216–224. Available from https://doi.org/10.1016/j.memsci.2014.06.018.

Vrijenhoek, E. M., Hong, S., & Elimelech, M. (2001). Influence of membrane surface properties on initial rate of colloidal fouling of reverse osmosis and nanofiltration membranes. *Journal of Membrane Science*, *188*, 115.

Warczok, J., Ferrando, M., Löpez, F., & Güell, C. (2004). Concentration of apple and pear juices by nanofiltration at low pressures. *Journal of Food Engineering*, 63–70. Available from https://doi.org/10.1016/s0260-8774(03)00283-8.

Wang, H., Zhang, Q., & Zhang, S. (2011). Positively charged nanofiltration membrane formed by interfacial polymerization of 3,3′,5,5′-biphenyl tetraacyl chloride and piperazine on a poly(acrylonitrile) (PAN) support. *Journal of Membrane Science*, *378*(1–2), 243–249. Available from https://doi.org/10.1016/j.memsci.2011.05.015.

Wang, L. Y., Fang, M. Q., Liu, J., He, J., & Li, J. D. (2015). Layer-by-layer fabrication of high performance polyamide/ZIF-8 nanocomposite membrane for nanofiltration applications. *ACS Applied Materials & Interfaces*, *7*, 24082–24093.

Wang, N., Liu, Y., Qiao, Z., Diestel, L., Zhou, J., & Huang, A., ..., Caroa, J. (2015). Polydopamine-based synthesis of a zeolite imidazolate framework ZIF-100 membrane with high H_2/CO_2 selectivity. *Journal of Materials Chemistry A*, *3*(8), 4722–4728. Available from https://doi.org/10.1039/c4ta06763k.

Wang, N. X., Liu, T. J., Shen, H. P., Ji, S. L., & Li, J. R. (2016). Ceramic tubular MOF Hybrid membrane fabricated through in situ layer-by-layer self-assembly for nanofiltration. *AIChE Journal. American Institute of Chemical Engineers*, *62*, 538–546.

Wang, X. L., Shang, W. J., Wang, D. X., Wu, L., & Tu, C. H. (2009). Characterization and applications of nanofiltration membranes: State of the art. *Desalination*, *236*(1–3), 316–326. Available from https://doi.org/10.1016/j.desal.2007.10.082.

Wang, P., Wang, M., Liu, F., Ding, S., Wang, X., Du, G., ... Wang, Y. (2018). Ultrafast ion sieving using nanoporous polymeric membranes. *Nature Communications*, *9*(1), 569.

Wentao, S., Feiyun, S., Wei, J., Guo, J., Yin, S., & Wai, P., ..., Kyoungjin, A. A. (2020). High-performance nanofiltration membrane structured with enhanced stripe nano-morphology. *Journal of Membrane Science*, 117852. Available from https://doi.org/10.1016/j.memsci.2020.117852.

Wu, H., Tang, B., & Wu, P. (2010). MWNTs/polyester thin film nanocomposite membrane: An approach to overcome the trade-off effect between permeability and selectivity. *Journal of Physical Chemistry C*, *114*(39), 16395–16400. Available from https://doi.org/10.1021/jp107280m.

Wu, M., Yuan, J., Wu, H., Wu, M., Yuan, J., & Wu, H., ..., Jiang, Z. (2019). Ultrathin nanofiltration membrane with polydopamine-covalent organic framework interlayer for enhanced permeability and structural stability. *Journal of Membrane Science*, *576*, 131–141. Available from https://doi.org/10.1016/j.memsci.2019.01.040.

Xiao-Lin, W., Toshinori, T., Shin-ichi, N., & Shoji, K. (1997). The electrostatic and steric-hindrance model for the transport of charged solutes through nanofiltration membranes. *Journal of Membrane Science*, 19–32. Available from https://doi.org/10.1016/s0376-7388(97)00125-7.

Xu, Y., Gao, X., Wang, Q., Wang, X., Ji, Z., & Gao, C. (2016). Highly stable MIL-101(Cr) doped water permeable thin film nanocomposite membranes for water treatment. *RSC Advances*, *6*(86), 82669–82675. Available from https://doi.org/10.1039/c6ra16896e.

Yaghi, O. M., Li, G., & Li, H. (1995). Selective binding and removal of guests in a microporous metal–organic framework. *Nature*, *378*(6558), 703–706. Available from https://doi.org/10.1038/378703a0.

Yang, Z., Saeki, D., Wu, H. C., Yoshioka, T., & Matsuyama, H. (2019). Effect of polymer structure modified on RO membrane surfaces via surface-initiated ATRP on dynamic biofouling behavior. *Journal of Membrane Science*, *582*, 111–119. Available from https://doi.org/10.1016/j.memsci.2019.03.094.

Yao-Shen, G., Yan-Li, J., Bin, W., Wang, N.-X., Yin, M. J., An, Q.-F., & Gao, C. (2020). High-flux zwitterionic nanofiltration membrane constructed by in-situ introduction method for monovalent salt/antibiotics separation. *Journal of Membrane Science*, 117441. Available from https://doi.org/10.1016/j.memsci.2019.117441.

Zeng, Y., Wang, L., Zhang, L., & Yu, J. Q. (2018). An acid resistant nanofiltration membrane prepared from a precursor of poly(s-triazine-amine) by interfacial polymerization. *Journal of Membrane Science*, *546*, 225–233.

Zhang, R., Li, Y., Su, Y., Xueting, Z., Yanan, L., & Xiaochen, F., ..., Zhongyi, J. (2016). Engineering amphiphilic nanofiltration membrane surfaces with a multi-defense mechanism for improved antifouling performances. *Journal of Materials Chemistry A*, *4*(20), 7892–7902. Available from https://doi.org/10.1039/c6ta02885c.

Zhang, W., Luo, J., Ding, L., & Jaffrin, M. Y. (2015). A review on flux decline control strategies in pressure-driven membrane processes *Industrial & Engineering Chemistry Research*, 54.

Zhang, Y., Guo, M., Pan, G., Yan, H., Xu, J., & Shi, Y., ..., L.iy, Y. (2015). Preparation and properties of novel pH-stable TFC membrane based on organic-inorganic hybrid composite materials for nanofiltration. *Journal of Membrane Science*, *476*, 500–507. Available from https://doi.org/10.1016/j.memsci.2014.12.011.

Zhao, F. Y., Ji, Y. L., Weng, X. D., Mi, Y.-F., Ye, C. C, An, Q.-F., & Gao, C.-J. (2016). High-flux positively charged nanocomposite nanofiltration membranes filled with poly(dopamine) modified multiwall carbon nanotubes. *ACS Applied Materials and Interfaces*, *8*(10), 6693–6700. Available from https://doi.org/10.1021/acsami.6b00394.

CHAPTER

5

Polymer-based nanofiltration membranes

Abdulaziz Alammar[1] *and Gyorgy Szekely*[2]

[1]Department of Chemical Engineering and Analytical Science, The University of Manchester, Manchester, United Kingdom [2]Advanced Membranes and Porous Materials Center, King Abdullah University of Science and Technology, Thuwal, Saudi Arabia

5.1 Introduction

Since the revolutionization of the polymer industry by Hermann Staudinger and Wallace Carothers in the 1920s–1930s, synthetic polymers have become a big part of industrialization, and it would be impossible to imagine the world without them (Abd-El-Aziz, Antonietti, & Barner-Kowollik, 2020). Advances in polymer science have made membrane technology increasingly competitive to the well-established separation technologies commonly used in the industry, such as distillation, extraction, adsorption/absorption, and crystallization. Membranes are usually classified as selective barriers that allow only specific molecules to pass through while rejecting other molecules. Membrane technology is environmentally friendly, energy-efficient, simple, and easy to integrate with other technologies. For example, using membranes over heat-driven technologies, such as distillation and evaporation, can minimize energy consumption by orders of magnitude (Sholl & Lively, 2016). Membranes have been successfully demonstrated in the context of environmental remediation and improved quality of life. Polymeric membranes have been favored over their counterpart (ceramic membranes) owing to their ease of fabrication, lower cost, chemical tunability, and controllable hydrophobicity/hydrophilicity, which enable different driving forces for various types of separation. As there is a growing body of literature on polymer-based membranes, they have been classified on the basis of the type of the driving force of separation (e.g., pressure, voltage, temperature, and concentration).

Increased awareness about sustainable separations, booming population, demand for clean water, and strict environmental regulations has created a huge market for membrane technology. It is projected that polymeric membranes will continue to be the leading

Advancement in Polymer-Based Membranes for Water Remediation
DOI: https://doi.org/10.1016/B978-0-323-88514-0.00018-8

© 2022 Elsevier Inc. All rights reserved.

membrane technology for the upcoming decade (Lin & Ding, 2020). Membrane technology covers 8 of the 17 sustainability goals set by the United Nations, as illustrated by Nunes, Culfaz-Emecen, and Ramon (2020) indicating a huge potential boost for its global market share in the future.

The nanofiltration (NF) membrane technology is a distinct pressure-driven process that emerged in the 1980s. The concept of NF was investigated by Peter Eriksson (Eriksson, 1988) and he is considered a pioneer of the NF membrane technology. NF membranes were originally developed for aqueous applications, particularly for water softening and dye removal, but some polymers were found to be stable in a number of organic solvents and therefore can be used for organic solvent applications (Chuntanalerg, Bureekaew, Klaysom, Lau, & Faungnawakij, 2018). Interestingly, NF membranes were shadowed by the reverse osmosis (RO) membrane market in the early days; RO membranes rejected during production because of quality control failures were sold as NF membranes at a lower cost (Pearce, 2011). NF has remained a niche technology for years; however, it has been gradually improving. In 1984 FilmTec (now a subsidiary of DuPont de Nemours Inc.) used NF to describe their RO process, which was designed to partially separate ions in the feed to make it more efficient for water purification (Van der Bruggen, Hoek, & Tarabara, 2013). Mery-sur-Oise, located in the northern region of Paris, was the first large-scale NF membrane plant for drinking water production (Ventresque, Gisclon, Bablon, & Chagneau, 2000). Although Lonsdale prepared RO membranes with properties similar to that of NF membranes, denoted as "loose RO" or "advance RO" membranes, to minimize the energy requirement of the RO process (Van der Bruggen et al., 2013), there is still confusion about NF membranes as a new classification. Some argue that "loose RO" or "tight ultrafiltration" (UF) is adequate to describe the filtration properties. We advise the reader not to be confused about the terminology used in the literature or industry but to focus on the filtration characteristics of the NF membrane. It is reasonable to describe NF membranes as having multiple separation properties in tandem (e.g., molecular sieving, electrostatic exclusion, and Donnan exclusion). The NF membrane has the property of a UF membrane for the rejection of uncharged organic matter realized by the molecular weight cutoff (MWCO), which is the most commonly used indicator by the membrane community to approximate the pore size characteristics. The MWCO of NF membranes is between 100 and 1000 g mol^{-1} (with pore diameters of <2 nm). In addition, the surface charge of polymer-based NF membranes in aqueous solutions depends on the functional groups (e.g., carboxylic and sulfonic acids) (Oatley-Radcliffe et al., 2017); thus, the separation mechanism cannot be limited to only one driving force. NF membranes have certain advantages over RO membranes in terms of productivity and energy requirements and exhibit better separation performance compared to UF membranes, which increases the industrial applicability of NF membranes. As such, NF membranes have been investigated for an extensive range of applications such as the separation of oil emulsions, triacylglycerols, sugars, amino acids, dyes, heavy metals, divalent salts, pesticides, and pathogens used for solvent recovery and challenging debottlenecking processes, such as catalysis and crystallization (Islam, Hassan-uz-Zaman, Islam, Clemens, & Ahmed, 2020). The market for polymer-based NF membranes is expected to have the highest growth during the forecast period of 2018–27 owing to their potential in the food, beverage, and pharmaceutical industries as well as their flexibility for use with the RO process for desalination and water treatment (BusinessWire, 2020).

Environmental regulations are becoming stricter and the emergence of challenging separations requires further advancements in membrane materials and preparation as well as process optimization to elevate the state-of-art of the polymer-based NF membranes. The overall direction of current research can be summarized as follows: (1) developing novel materials, (2) optimizing membrane preparation methods, and (3) understanding and modeling membrane transport mechanisms at the molecular level. Recent breakthroughs in polymer-based NF membrane studies related to novel materials are associated with incorporating emerging 2D materials and metal organic frameworks (MOFs) while minimizing the separation layer to be $\leq$10-nm thick (denoted as ultrathin). Ultrathin NF membranes with microporous properties have potential in various separation applications, including water treatment, desalination, and organic solvent nanofiltration (OSN) (Jimenez-Solomon, Song, Jelfs, Munoz-Ibanez, & Livingston, 2016), as well as hydrocarbon separation in the oil and gas industry (Thompson, Mathias, & Kim, 2020). This chapter discusses the research and industrial efforts toward solving these separation challenges and the types of polymer-based NF membranes, including their different preparation methods, the current state-of-art, with a focus on their potential application in water remediation and OSN, commercial viability, and future direction.

5.2 Polymer-based nanofiltration membranes

NF membranes have a porous separation layer with nanoscale pore size. The separation mechanism, which is mainly driven by electrostatic repulsion, dielectric effect, and size exclusion, is complex because of the small pore size (Fig. 5.1).

Energy-efficient liquid separation requires highly permeable and molecularly selective membranes to achieve a feasible timeframe and excellent purity. Two approaches are available for the fabrication of NF membranes that satisfy these criteria: (1) tuning the polymer microporosity at the molecular level via techniques such as physical dispersion, polymer blending, hybridization, network interpenetration, and organic framework controlling and (2) reducing the thickness of the separation layer to the nanometer level (Zhao, Li, Shen, Gao, & Van Der Bruggen, 2020). Elimelech's group reviewed the state-of-the-art and progress of membrane materials (i.e., morphologies, surface modifications, and chemical functionalities) to develop next-generation, high-performance NF membranes for desalination and water treatment that can be easily extended to other applications (e.g., OSN). Some recent advances include developing artificial water channels (AWCs), block copolymers, graphene-based materials, and polymerizable surfactants (Werber, Osuji, & Elimelech, 2016).

For industrial scale, polymer-based NF membranes are prepared in the form of several membrane modules, for example, hollow fiber, spiral wound, plate and frame, tubular, and capillary. Hollow-fiber modules have the highest packing density compared to other membrane module designs. In addition, hollow-fiber modules may be more suitable than spiral-wound modules, the most widely used membrane module for RO and NF, for high-permeance membranes. Further, spacers help in optimizing the membrane performance and energy efficiency of the process, for example, avoiding high-pressure drop and concentration polarization. In general, increasing the shear rates in the feed stream decreases the concentration polarization and improves the mass transfer rates. This section

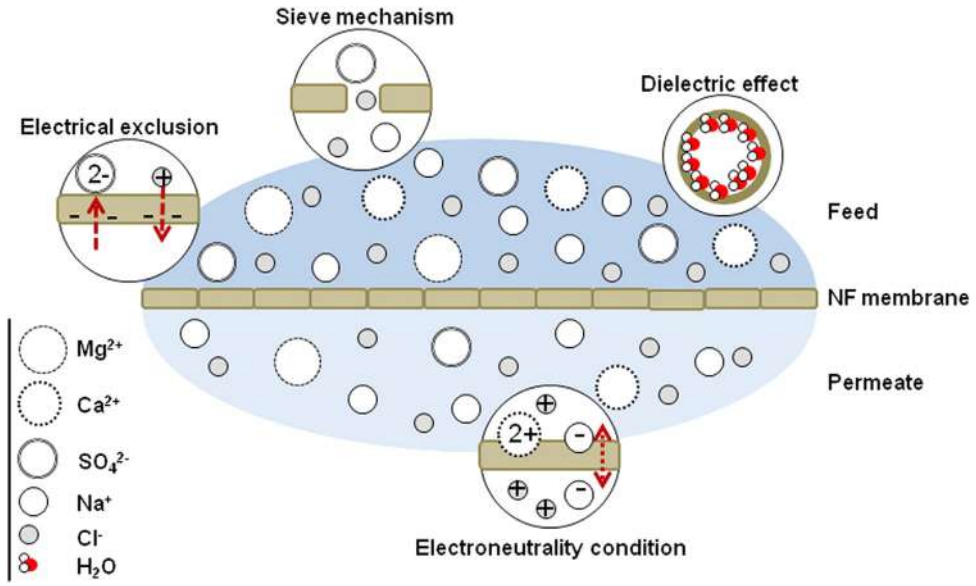

FIGURE 5.1 Separation mechanisms of a polymer-based nanofiltration (NF) membrane. Source: *From Nicolini, J. V., Borges, C. P., Ferraz, H. C. (2016). Selective rejection of ions and correlation with surface properties of nanofiltration membranes.* Separation and Purification Technology, *171, 238–247. https://doi.org/10.1016/j.seppur.2016.07.042.*

focuses on the current state-of-the-art polymer-based materials for preparing advanced NF membranes.

Before discussing the types and advances made in polymer-based NF membranes, the intrinsic properties and separation mechanisms of NF membranes are discussed. Mass transfer region divisions of an NF membrane were summarized by Van der Bruggen's group, as depicted in Fig. 5.2. In this figure, the first region is assigned to solution-diffusion models that describe the mass transfer of RO membranes, which govern the nonporous zone. The porous zone is divided into two regions depending on pore size: (1) partial salt passage region (PSR) and (2) absolute salt passage region (ASR). The final mass transfer region is based on the idea of a "water molecule channel" and is assigned to the water molecule passage region (WMR). Fig. 5.2 shows a conceptual approach for describing the mass transfer of NF membranes, which is very complex to be easily differentiated. This can be applied to the separation of solute, in general, and not just for desalination; however, for OSN, it may not be suitable to group them with aqueous-based separations due to the notable differences in the properties of organic solvents (Marchetti, Peeva, & Livingston, 2017; Zhang, Tian, Gao, & Van Der Bruggen, 2020). The solution-diffusion region (SDR) can well explain the mass transfer of RO membranes. For example, mass transfer starts with the absorption of solutes or ions from feed solutions into the separation layer of the NF membrane. Then, diffusion from the separation top layer to the permeate occurs, followed by desorption from the membrane structure and ending with the permeate. The solution-diffusion model describes the mass transfer of solutes and water independently for aqueous solution separations. The WMR represents the mass transfer of

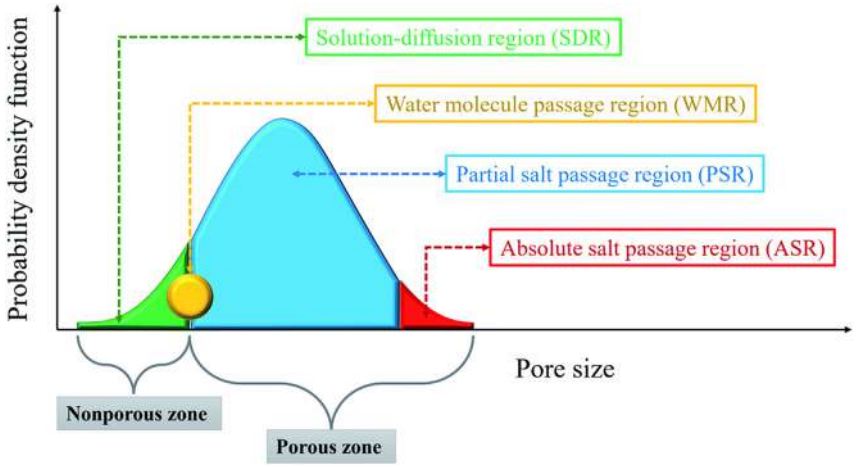

FIGURE 5.2 Mass transfer region of polymer-based nanofiltration (NF) membranes. Source: *From Zhang, R., Tian, J., Gao, S., & Van Der Bruggen, B. (2020). How to coordinate the trade-off between water permeability and salt rejection in nanofiltration?* Journal of Materials Chemistry A, 8*(18), 8831–8847*. https://doi.org/10.1039/d0ta02510k

water molecules, that is, "water channeling" across the NF membrane, in both nonporous and porous zones. Only water molecules pass through due to their intermolecular forces that repel solutes (i.e., salt ions). For example, increasing the WMR improves the water permeability while maintaining the salt rejection performance at an acceptable level. Moreover, the PSR lies in the porous zone, wherein salt ions can be effectively rejected due to their larger hydrated ionic diameter compared to the pore size of the NF membranes and/or due to the same electrostatic charge of the NF membrane as a result of electrostatic repulsion. Therefore, increasing the PSR leads to increased water permeance. Finally, the ASR also lies in the porous zone of the NF membrane, where the pore size is too large and both water and solutes (salt ions) pass through. Thus the charge of the NF membrane has no effect on the ASR because its pores have a larger diameter than the Debye length (i.e., the minimum distance where the electrical field has an effect). Hence, increasing the ASR increases the water permeance but deteriorates the salt rejection performance. Increasing the SDR, WMR, and PSR while decreasing the ASR can lead to optimum NF membrane performance.

Surface hydrophilicity is one of the key parameters that enhances the water mass transfer of NF membranes. Many approaches have been reported in the literature to improve hydrophilicity, such as surface grafting, surface coating, chemical modification, and irradiation. However, a limitation of surface coating is that it usually drastically decreases the water permeance due to increased membrane thickness. This decrease in water permeance can be termed as hydraulic resistance. Incorporating inorganic nanomaterials or cosolvents is challenging due to their varying interfacial properties (i.e., incompatibility), which may result in defects in the polymer matrix (i.e., voids at the polymer–inorganic interface), increasing the membrane permeance at the expense of deteriorated solute rejection performance. The following subsections highlight the main breakthroughs in polymer-based NF membranes.

5.2.1 Natural and bioinspired nanofiltration membranes

Among natural polymers, cellulose has attracted the most attention owing to its biocompatibility and abundance in nature. Research has shown the promising potential of cellulose in selective liquid separation for materials reinforcement and biofuel utilization. In addition, cellulose has already been adopted in various industries, such as pharmaceutical, textile, and paper. The main challenge that hampers cellulose from widespread industrial adoption is the difficulty in solubilizing it in common organic solvents. However, recent studies have demonstrated a number of sustainable processes to develop defect-free flat-sheet and hollow-fiber membranes for OSN using ionic liquids (Falca, Musteata, Behzad, Chisca, & Nunes, 2019; Kim, Livazovic, Falca, & Nunes, 2019), as well as by extracting cellulose fibers and separating them into small fibrils with diameters of <4 nm (Li, Chen, & Brozena, 2021). The utilization of cellulose nanofibers (CNFs) and cellulose nanocrystals (CNCs) is emerging as a potential technique for developing high-performance NF membranes. Although both CNFs and CNCs are derived from nanoscale cellulose fibers, they differ in shape, size, structure, and dispersion properties (Xu et al., 2013). Tan et al. developed a sustainable process to extract virgin silk nanofibrils (SNFs) using green deep eutectic solvents comprising urea and guanidine hydrochloride (GuHCl). They also developed a freestanding CNF membrane with strong mechanical properties, chemical resistance, and good separation performance for dyes, ions, and proteins in an aqueous environment (Tan, Zhao, & Mu, 2018). Incorporating CNCs into the aqueous solution of piperazine using the conventional interfacial polymerization (IP) method enhanced the hydrophilicity and surface area of the prepared thin-film nanocomposite (TFN) NF membranes, thereby increasing the water permeance while maintaining the rejection of Na_2SO_4 ($>98\%$) (Huang, Wu, & Zhu, 2019). Similarly, Zhang et al. prepared cellulose-based membranes by depositing CNFs under vacuum on a filter paper containing hydroxyapatite (HAP) nanowires as porous support, which resulted in high separation performance for various dyes (i.e., rejections of 65.8% and 75.7% for Na_2SO_4 and NaCl, respectively) (Zhang, Zhu, Wu, & Dong, 2019). This concept of combining the self-assembly of SNFs and in situ biomineralization to develop multilayer NF membranes (i.e., SNF/HAP) was simulated and proven experimentally to have high permeance and rejection of various containments for water remediation (Ling et al., 2017).

Mussel-inspired polydopamine (PDA) has been widely studied for improving membrane rejection, antifouling, and antibacterial properties. Meng et al. demonstrated the use of bioinspired catechol chemistry in PDA-assisted polyelectrolyte layer by layer (PDA-a-LBL) to enhance the long-term stability of the resultant NF membranes in harsh alkaline and acidic conditions (Meng, Song, Yao, Liu, & Zhao, 2020). Moreover, Qiu et al. demonstrated the possibility of aggregating green tea catechin/chitosan at the nanoscale on a polysulfone (PSf) support by oxidizing their catechol groups using natural oxidizing agents such as tyrosinase and laccase and cross-linking with chitosan to form a dense separation layer mimicking the self-polymerization of dopamine. The prepared thin-film composite (TFC) membranes showed high rejection of Na_2SO_4 and stable water permeance of 7.5 L m^{-2} h^{-1} bar^{-1} over 10 days of operation (Qiu, Zhong, Du, Lv, & Xu, 2016). However, surface modification using PDA usually decreases the membrane permeance due to the extra layer of hydraulic resistance formed by the molecular aggregation of PDA oligomers.

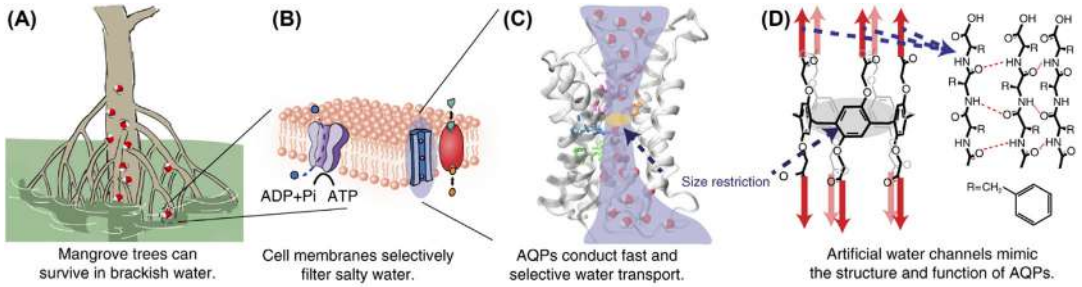

FIGURE 5.3 Bioinspiration for molecularly precise and highly permeable water channels and the process of assembly and preparation of nanofiltration (NF) membranes. Source: *From Shen, Y. X., Song, W. C., Ryan Barden, D., et al. (2018). Achieving high permeability and enhanced selectivity for Angstrom-scale separations using artificial water channel membranes.* Nature Communications, 9, 2294–2294. https://doi.org/10.1038/s41467-018-04604-y.

In contrast, bioinspired aquaporins (AQPs) have inspired much research interest given their unique features of selective water molecule passage and total ionic rejection, as illustrated in Fig. 5.3. These biological proteins channel water at a very fast rate when inserted into phospholipid membranes and are essential for cellular function. Kumar et al. demonstrated a novel strategy for developing AQP-based membranes by incorporating bacterial aquaporin Z (AQPZ) into block copolymer vesicles to form an ultrathin bilayer on a porous support, thereby shifting the paradigm from mechanically less-stable lipid vesicles for water purification (Kumar, Grzelakowski, Zilles, Clark, & Meier, 2007). Few studies have investigated routes to improve the mechanical stability of AQPZ-based membranes and the vesicle rupture process to immobilize AQ PZs (Xie He et al., 2013; Wang et al., 2015). Yet, scaling-up AQP-based membranes without generating defects remains challenging. Moreover, protein stability should not be overlooked because it can hamper practical applications as low-temperature storage is required to maintain its activity for long-term continuous operation (Werber et al., 2016). Vincenzo et al. proposed a novel approach for scalable biomimetic membranes using hexylureido-ethyl-imidazole (HC6) as an AWC. This includes the addition of a preliminary step to the conventional IP method to incorporate the AWC into the polyamide layer. The biomimetic membrane, TFC–HC6, realized a relatively high water permeance of $\sim 1.2\ \mathrm{L\ m^{-2}\ h^{-1}\ bar^{-1}}$ while maintaining 99.5% rejection of NaCl (i.e., minimizing the energy requirement of desalination by ~12%) (Di Vincenzo, Tiraferri, & Musteata, 2021).

5.2.2 Mixed-matrix nanofiltration membranes

Mixed-matrix membranes have attracted the attention of academia and industry for the engineering of various inorganic fillers such as porous and nonporous nanomaterials, MOFs, zeolitic imidazolate frameworks, and covalent organic frameworks (COFs) (Kandambeth, Biswal, & Chaudhari, 2017; Liu et al., 2020) to improve the capability of polymeric NF membranes.

Well-defined porous materials, such as MOFs, COFs, porous organic cages, and coordination polymers, are ideal in terms of both selectivity and permeability. However, COF-based

NF membranes are usually prepared via phase inversion [e.g., integrally skinned asymmetric (ISA) membranes] with thick and rigid separation layers due to the high molecular orientation of COF, resulting in decreased mass transfer and increased possibility of fractures or defects (Li, Zhu, Li, Guo, & Van Der Bruggen, 2020). Moreover, the fabrication of these materials is challenging technically and economically. Controlling the pore size of the NF membrane is difficult, and most studies report the average pore size; thus, increasing the pore size without a uniform or narrow size distribution will promote water permeance at the expense of membrane rejection (Park, Kamcev, Robeson, Elimelech, & Freeman, 2017). Surwade et al. developed nanoporous graphene membranes with small and uniform size distribution (0.5–1 nm) using plasma etching, with extraordinary water permeance of at least 252 L m^{-2} h^{-1} bar^{-1} and almost complete rejection of KCl. However, this technique is not feasible for scale-up (Surwade, Smirnov, & Vlassiouk, 2016).

The introduction of superhydrophilic nanomaterials, such as GO and carbon nanotubes (CNTs), creates water molecule channels in the top separation layer of NF membranes, increasing the favorable WMR and, therefore, enhancing the water permeance. In addition, graphene is used for constructing water channels to enlarge the WMR. However, these nanomaterials fail to resolve the incompatibility, as mentioned previously in this section (Zhang et al., 2020).

5.2.3 Block-copolymer nanofiltration membrane

A block copolymer is a polymer that comprises two or more monomers that are covalently bonded with distinctive chemical sequences prepared as nanoscale self-assembly building blocks or amphiphilic macromolecular surfactants. The most promising approach to develop tailored NF membranes is engineering self-assembled block polymers with embedded functional groups on the external and/or interior pore walls (i.e., direct incorporation, postsurface grafting, and coupling reactions), as shown in Fig. 5.4 (Jin et al., 2020; Zhang et al., 2020). Peinemann's group developed asymmetric isoporous NF membranes with a narrow pore-size distribution and an average pore size of 1.5 nm for the separation of solutes bigger than an MWCO of 600 in aqueous solutions via self-assembly of block copolymers combined with the simplicity of phase separation for membrane preparation (Peinemann, Abetz, & Simon, 2007; Qiu et al., 2013; Yu, Qiu, & Moreno, 2015). Recently, high-flux NF membranes for dye/salt separation (water permeance = 49.3 $\pm$ 0.9 L m^{-2} h^{-1} bar^{-1}, MWCO = 655 Da) were reported by Liu et al. using polysulfone-*block*-polyethylene glycol (PSf-*b*-PEG) membranes prepared via the phase inversion method; the loose NF membrane allowed complete salt passage while achieving ~98% dye rejection, which is attractive for practical water remediation (Liu, Wang, & Wang, 2021). Zwitterionic polymers contain opposite-charge functional groups with zero net charge for the entire molecule. Blocks of zwitterionic copolymers have been incorporated on the surface of a thin polyamide layer via the IP reaction of amines (Duong, Daumann, Hong, Ulbricht, & Nunes, 2019). The high cost of block copolymers is a concern for large-scale production, especially for water treatment, where monetization is limited compared to OSN. Nevertheless, the cost can be reduced over time through automation and increased interest in sustainable water treatment (Radjabian & Abetz, 2020).

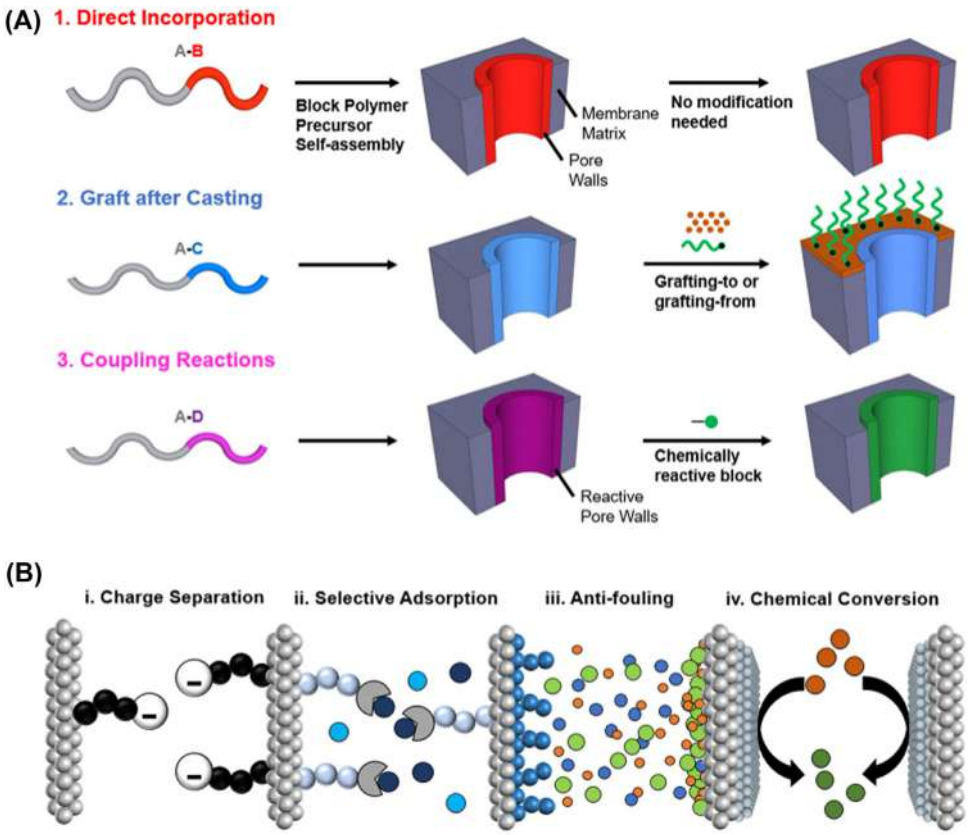

FIGURE 5.4 (A) Block polymer precursors molecularly engineered to achieve different pore wall chemistries. (B) Illustration of various capabilities enabled by functionalizing the pore walls within the membrane matrix. Source: *From Zhang, Y., Almodovar-Arbelo, N. E., Weidman, J. L., Corti, D. S., Boudouris, B. W., & Phillip, W. A. (2018). Fit-for-purpose block polymer membranes molecularly engineered for water treatment*. npj Clean Water, 1, 2–2. https://doi.org/10.1038/s41545-018-0002-1a.

5.2.4 Intrinsic microporous polymer-based nanofiltration membrane

Enhancement of the microporosity of polymer-based NF membranes to increase permeance without sacrificing membrane rejection has attracted much research interest. For example, polymers of intrinsic microporosity (PIMs) have promising features, including a rigid backbone and contorted polymer chains that result in inefficient packing; thus, nanometer-sized voids act as micropores, which are suitable for gas separation but limited to liquid separation due to their solubility in certain solvents (e.g., not ideal for OSN). It has been challenging to develop an ultrathin PIM-1 NF membrane without compromising the separation performance due to physical aging. In general, most polymers used in the preparation of NF membranes are glassy polymers that experience aging over time. Polymer aging can be defined as the rearrangement of polymer chains from a nonequilibrium state to a nonachievable equilibrium state as a function of time without any external influence. This effect leads to polymer chain

packing and collapse of pores, which is more pronounced in the case of high free-volume polymers, such as PIMs (Low, Budd, McKeown, & Patterson, 2018). Unexpected reduction in solvent permeance was observed when the membrane thickness was decreased to <140 nm (Gorgojo et al., 2014). This phenomenon has been extensively studied for PIM-based membranes; the lower the glass transition temperature (T_g) and the more flexible the polymer chains, the more efficient the packing (close to the equilibrium) and hence lower permeance. Thus this phenomenon can limit linear macromolecules in the fabrication of ultrathin NF membranes. Jimenez-Solomon et al. demonstrated an ultrathin TFC NF membrane (i.e., a cross-linked polyarylate layer with a thickness of ~ 20 nm) with interconnected microporosity that can be realized using the conventional IP method without compromising the rejection performance. They suggested the use of rigid contorted monomers in noncoplanar orientation to enhance the interconnectivity between intermolecular voids to achieve higher permeance and stability for organic solvents than when incorporating rigid moieties such as tetraphenylsilane (TPS) and tetraphenylmethane (TPM) as building blocks (Jimenez-Solomon et al., 2016). Furthermore, nontoxic cavity structures such as cyclodextrins (CDs) have been used recently as monomers via IP to prepare ultrathin TFC NF membranes with enhanced interconnected microporosity; the prepared polyamide-CD membrane is stable for a wide range of organic solvents with an MWCO of ~ 560 g mol^{-1} (Huang, Puspasari, Nunes, & Peinemann, 2020).

Thompson et al. evinced the superior functionalities of tuning polymer microporosity for the fractionation of crude oil mixtures, which is traditionally realized via energy-extensive distillations in the petrochemical industry. This was achieved by developing a novel polymer structure similar to PIM-1 but without its shortcomings, that is, plasticization and swelling due to "motion-enabled zones" or "flexible breathing motions" in the polymer network, thereby resulting in a higher free volume. The developed spirobifluorene aryl diamine (SABD) polymer is based on flexible C−N connections between the aromatic building blocks and spirocyclic, enabling $\pi-\pi$ stacking interactions and efficient chain packing, which results in noninterconnected microporosity structure owing to the absence of ladder-like morphology. The SABD TFC membranes were prepared on cross-linked polyetherimide supports and showed good hydrocarbon separation (i.e., an MWCO of 253 g mol^{-1} and a permeance of 0.1−0.7 L m^{-2} h^{-1} bar^{-1}) (Thompson et al., 2020).

5.3 Preparation of polymer-based nanofiltration membranes

5.3.1 Phase inversion

Membrane preparation methods have been established and optimized for decades. In the 1960s, the development of ISA membranes via phase inversion opened new horizons for the application of the polymeric membrane technology in industrial commercialization (Loeb & Sourirajan, 1963). It is still the most widely used method for preparing polymer-based NF membranes owing to its simplicity, scalability, and relatively low cost. Phase inversion can be described as the control solidification of a solvent-polymer solution (or a dope solution), wherein it transforms from liquid phase to solid phase. This phase transformation can be induced by a number of driving forces: nonsolvent-induced phase separation (NIPS), thermal-induced phase separation, nonsolvent-vapor-induced phase

separation, and evaporation-induced phase separation (Guillen, Pan, Li, & Hoek, 2011). Among these, NIPS is the most popular for the preparation of an NF membrane with an asymmetric structure comprising a dense top layer (or separation layer) with small pores propagating to larger pores to form a support sublayer (Kahrs & Schwellenbach, 2020). In a typical preparation procedure, a dope solution is cast on a nonwoven polymeric support using a casting knife and the cast film is then immersed into a nonsolvent coagulation bath (usually water), as shown in Fig. 5.5.

The thermodynamic and kinetic properties of the dope solution are two key aspects that strongly affect the morphology and properties of the resultant membrane. The ternary phase diagram is often used as a simplified representation of the thermodynamic behavior of the three components (polymer, solvent, and nonsolvent). Demixing between solvent and nonsolvent is initiated upon contacting the cast film with the nonsolvent, resulting in a polymer-rich phase with high polymer concentration and a polymer-lean phase with low polymer concentration to achieve thermodynamic equilibrium. The kinetic aspect of the phase inversion can be explained by the exchange rate (mass transfer) between the solvent and nonsolvent caused by the difference in the chemical potential. At initial contact with the nonsolvent, the difference in chemical potential is the largest and hence greater mass transfer. As demixing progresses, solidification of the polymer at the interference and the change in concentration profile results in the slowing of mass transfer. Different types of demixing can be simplified into slow demixing rates, also referred to as "delayed demixing," resulting in membranes with sponge-like morphologies; in contrast, fast demixing rates, also referred to as "instantaneous demixing," results in membranes with finger-like morphologies (large macrovoids in the sublayer) (Hołda & Vankelecom, 2015). The demixing process can be influenced by various parameters, such as the molecular weight and concentration of the

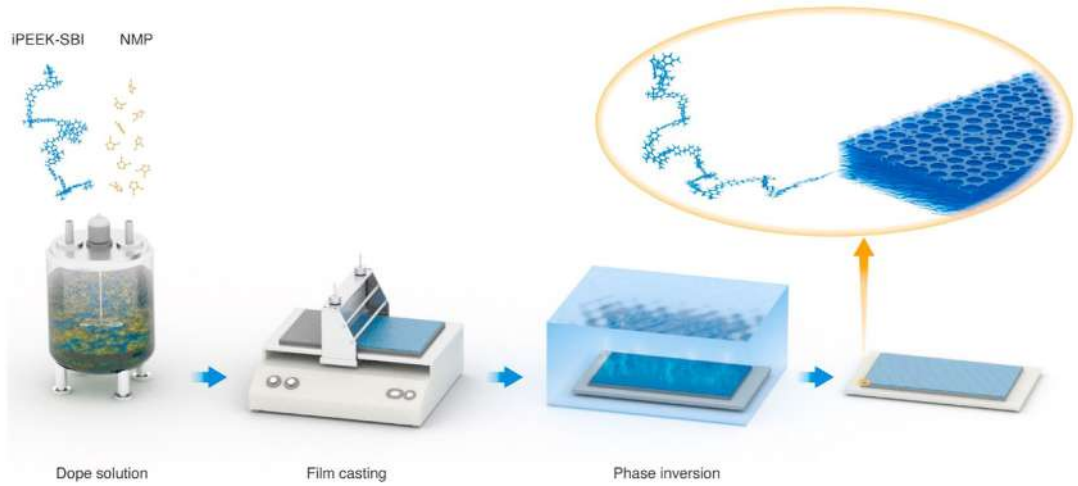

FIGURE 5.5 Schematic representation of phase inversion via the nonsolvent-induced phase separation method using a water coagulation bath. Source: *From Abdulhamid, M. A., Park, S. H., Zhou, Z., Ladner, D. A, & Szekely, G. (2021). Surface engineering of intrinsically microporous poly(ether-ether-ketone) membranes: From flat to honeycomb structures.* Journal of Membrane Science, 621, *118997*. https://doi.org/10.1016/j.memsci.2020.118997.

polymer (Soroko, Sairam, & Livingston, 2011), pore-forming additives (Kahrs & Schwellenbach, 2020), viscosity of the dope solution (Mousavi & Zadhoush, 2017), temperature and humidity (Marino, Russo, & Figoli, 2018), and use of a cosolvent and evaporation step before immersion (Soroko, Lopes, & Livingston, 2011), resulting in unique membrane morphologies that have different separation properties for various applications. Despite the simplicity and low cost of the phase inversion method, ISA NF membranes generally exhibit low permeance due to the thickness and morphology of the dense top layer. Increasing the number of macrovoids in the finger-like structure is usually unfavorable as these macrovoids become the weakest spots under high operating pressures, compromising the stability of the NF membrane. However, many approaches can be applied to enhance the permeance of ISA NF membranes. In addition to adjusting the thermodynamics and kinetics of the casting solution as mentioned earlier, hyperbranched polymers (HBPs) and dendrimers can be used to create free volume within the polymer matrix and hinder chain entanglement (Paul & Jons, 2016; Wang, Wang, & Zhang, 2015). An innovative approach for membrane preparation based on a pH switch of the aqueous phase separation was demonstrated by Baig et al. to develop a water-insoluble NF polyelectrolyte membrane (Baig, Durmaz, Willott, & de Vos, 2020). The unique feature of block copolymers to self-assemble into various morphologies depending on the degree of polymerization, type of blocks, composition, and molecular weight can be combined with the NIPS method to produce tailored isoporous NF membranes (Radjabian & Abetz, 2015; Zhang, Rahman, Abetz, & Abetz, 2020). Overall, applying phase inversion to prepare the NF membranes using NIPS as an example is a trial and error approach; therefore, a fundamental understanding is required for better optimization (Hołda & Vankelecom, 2015).

5.3.2 Interfacial polymerization

Another popular preparation method for developing polymer-based NF membranes is IP. The first commercial RO membrane was prepared in the 1970s by Cadotte and Riley (Sforca, Nunes, & Peinemann, 1997). Currently, IP is becoming the default method for developing TFC NF membranes with an ultrathin separation layer ($\sim$10–100 nm). In a typical preparation procedure, suitable porous support (i.e., polysulfone) is soaked in an aqueous solution of amine-containing monomer; then, the impregnated support is immersed in a solution of acid-chloride-containing monomer in an organic solvent where the two monomers polymerize to form a cross-linked thin layer at the interface of the two immiscible solvents. Aromatic polyamide TFC NF membranes are developed using the most commonly used monomers, such as m-phenylenediamine (MPD) and trimesoyl chloride (TMC), with hexane as the organic phase (Purkait, Sinha, Mondal, & Singh, 2018). Other commonly used reactive monomers include piperazine (PIP), diaminopiperazine (DAP), phenylenediamine (PPD), polyethyleneimine (PEI), and triethylenetetramine (TETA) as amine-containing monomers and 5-isocyanatoisophthaloyl chloride (ICIC), 5-chloroformyloxy-isophthaloyl chloride (CFIC), and isophthaloyl chloride (IPC) as acid chloride-containing monomers. The morphology and thickness of the top separation layer can be modified according to the required separation properties by tuning various parameters, such as monomer concentration, type of solvent, reaction condition,

surface chemistry, and type of support (Chen, Luo, Hang, & Wan, 2018) (discussed in detail in Section 5.4).

Overall, TFC NF membranes prepared via the IP method have higher permeance without sacrificing rejection compared to ISA NF membranes. However, obtaining an ultrathin separation layer comes at the cost of compromising the mechanical properties and increases the possibility of defects that can deteriorate the separation performance. Thus the IP method has the advantage of independently optimizing the separation layer and porous support.

5.3.3 Layer-by-layer assembly

Layer-by-layer (LBL) assembly is a simple and versatile method developed by Gero Decher in 1997 to prepare TFC membranes comprising thin multilayers of polyelectrolytes with tunable nanoscale thickness and efficient separation properties (Decher, 1997). The LBL method is illustrated in Fig. 5.6; a porous support is dip-coated in polycation and polyanion solutions in an alternating manner, followed by a rinsing step after each coating to remove excess and weakly bound polymer chains. The LBL assembly method has the main advantage of minimizing the additional hydraulic-resistance layer and can be controlled more efficiently than conventional surface-coating techniques (e.g., PDA, zwitterionic, and PEG-based coatings) (Xu, Wang, & Li, 2013). The polyelectrolyte layer is formed through surface adsorption due to electrostatic interactions between positive and negative charges, as well as other intermolecular interactions such as hydrophobic interactions, hydrogen bonding, and other specific interactions (e.g., surface sol–gel, host–guest, and change-transfer complexes) (Borges & Mano, 2014). Other coatings or deposition techniques are also used, such as spray coating and spin coating; their main advantage over the dip-coating technique include reduced processing time and usage of less volume (Joseph, Ahmadiannamini, Hoogenboom, & Vankelecom, 2014). Other promising coating techniques have been studied to improve the efficiency and assembly of multilayer architectures (i.e., from 2D to 3D), such as inkjet printing and high-gravity field-assisted LBL (Andres & Kotov, 2010; Ma, Cheng, & Jia, 2012). There are various parameters that can be controlled to achieve the optimum thickness for specific separation, such as the choice of polyelectrolytes, ionic strength, molecular weight and concentration, number of coating

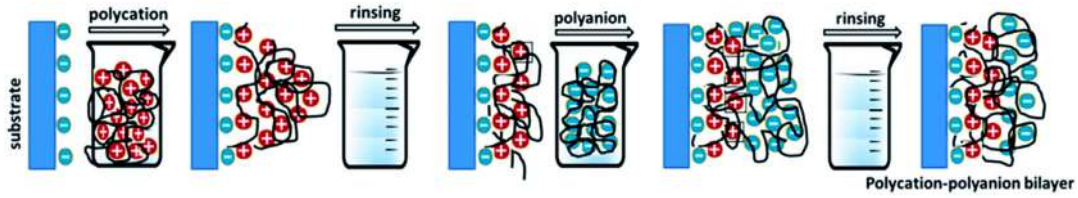

FIGURE 5.6 Schematic illustration of the layer-by-layer assembly method for preparing polyelectrolyte multilayer membranes via dip coating. Source: *From Joseph, N., Ahmadiannamini, P., Hoogenboom, R., & Vankelecom, I. F. J. (2014). Layer-by-layer preparation of polyelectrolyte multilayer membranes for separation.* Polymer Chemistry, 5*(6), 1817–1831.* https://doi.org/10.1039/c3py01262j.

cycles, and pH and temperature of the aqueous solution (Zhu, Feng, & Penlidis, 2007). LBL-based NF membranes have been studied extensively for the removal of dyes, multivalent ions, and micropollutants such as antibiotics, hormones, and plasticizers (Li, Xu, Goh, Chong, & Wang, 2020). The most common polyelectrolytes for preparing LBL-based NF membranes are polystyrene sulfonate (PSS), polyallylamine hydrochloride (PAH), and polydiallyldimethylammonium (PDADMAC). NF membranes prepared via the LBL method can be symmetric or asymmetric depending on the difference in the hydration of the capped separation layer with respect to the bottom layer (Gresham et al., 2020). Depending on the type of polyelectrolytes, LBL-based NF membranes exhibit good physical stability against repetitive backwashes and better chemical stability against hypochlorite (de Grooth et al., 2015) than conventional IP-based polyamide NF membranes (Do, Tang, Reinhard, & Leckie, 2012). In a recent study, Elshof et al. investigated the potential use of PDADMAC/PSS NF membranes at extreme pH conditions (Elshof, de Vos, de Grooth, & Benes, 2020) as well as using thin separation layers <5-nm thick (te Brinke, Reurink, Achterhuis, de Grooth, & de Vos, 2020).

5.3.4 Posttreatment

A major hurdle for extending the industrial adoption of polymer-based NF membranes is the development of membranes with high chemical and thermal stability. Common membrane posttreatment approaches, such as cross-linking, solvent treatment, and surface grafting, can improve the membrane stability in both harsh organic solvents and extreme pH conditions and can tune the separation performance. Cross-linking involves covalent bonding between two or more reactive groups through a range of chemical reactions and creates an interconnected network of polymer chains. Cross-linking strategies include chemical, thermal, and UV irradiation cross-linking, which are widely used to enhance the solvent resistance of polymer-based NF membranes and are usually combined with temperature resistance capabilities (Jin, Li, & Xu, 2018). A plethora of research has been conducted on cross-linking common polymers (e.g., PDMS, PI, PBI, and PSf) for polar and nonpolar solvent resistance, reduced swelling (Tarleton, Robinson, & Salman, 2006), and increased membrane rejection, for example, the enhancement of the chemical stability of PI membranes via cross-linking modification. More sustainable approaches have been studied, such as cross-linking during phase inversion by adding the cross-linker into the aqueous coagulation bath to reduce the number of steps and thus the amount of solvent used during membrane fabrication (Vanherck, Cano-Odena, Koeckelberghs, Dedroog, & Vankelecom, 2010). Furthermore, optimization of the diamine-based (i.e., hexamethylenediamine) cross-linking procedure has been performed by combining the role of the cross-linker, base, and solvent into a single compound via the addition of MgO as an acid acceptor (Van Goethem et al., 2020). However, cross-linking is often counterproductive in terms of decreased membrane permeance as it usually leads to a denser separation layer, thus decreasing the pore size (Valtcheva, Marchetti, & Livingston, 2015).

Solvent treatment or activation is illustrated in Fig. 5.7, which shows the solvent-induced effect after incorporating the aliphatic chains in which the organic solvent enhanced the mobility of the polymer chains of the cross-linked polyamide TFC membrane, thus leading to increased

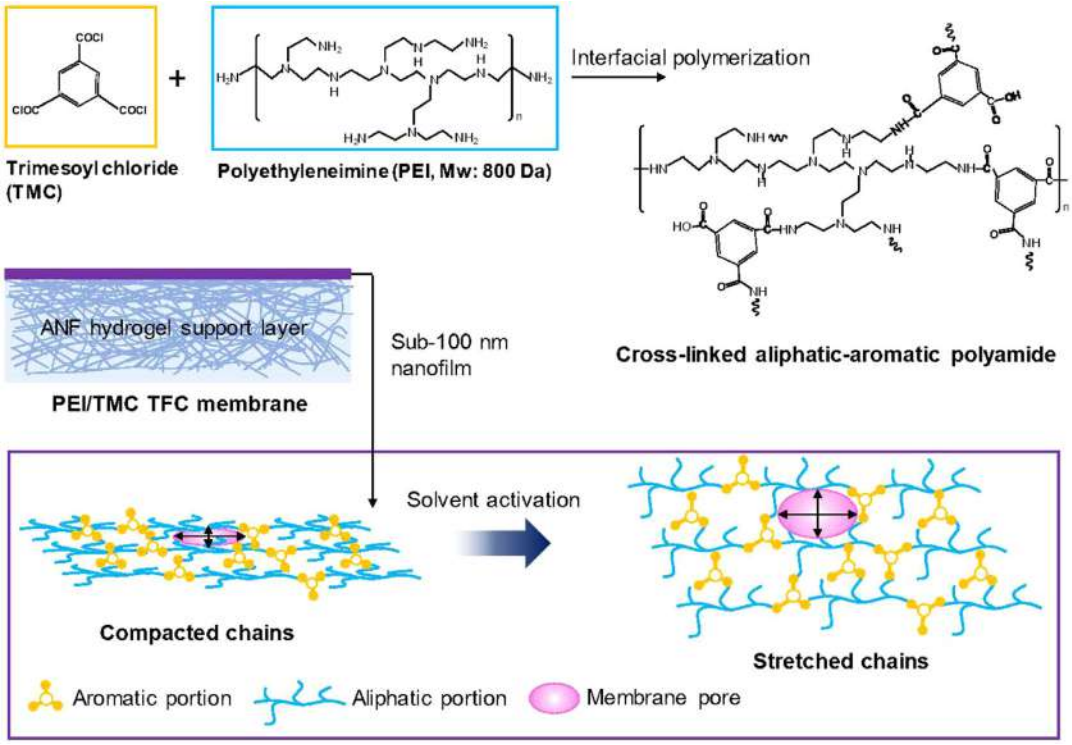

FIGURE 5.7 Schematic representation of the preparation of a semiaromatic thin-film composite membrane (i.e., PEI/TMC) followed by solvent activation. Source: *From Li, Y., Zhu, J., Li, S., Guo, Z., & Van Der Bruggen, B. (2020). Flexible aliphatic-aromatic polyamide thin film composite membrane for highly efficient organic solvent nanofiltration.* ACS Applied Materials and Interfaces, 12*(28), 31962–31974.* https://doi.org/10.1021/acsami.0c07341.

pore-size average (Li et al., 2020). This is a more promising approach owing to its simplicity, as investigated by Livingston's group, in utilizing strong polar aprotic solvents such as *N*,*N*-dimethylformamide (DMF) to improve membrane performance for OSN applications and aqueous solution separations (i.e., desalination) using benzyl alcohol as a solvent activator (Shin et al., 2019). A recent study demonstrated that swelling the polyamide layer of MPD-based TFC RO, which has been proven to be more durable under acidic conditions than the semiaromatic PIP-based TFC RO, can produce an acid-resistance NF membrane using polar aprotic solvents such as dimethyl sulfoxide (DMSO), *N*-methyl-2-pyrrolidone (NMP), and DMF with high water permeance and divalent salt rejection compared to commercial NF membranes (Shin, Kwon, Park, Park, & Lee, 2020). Further, Guo et al. investigated the solvent treatment of PIP-based NF membranes to produce a loose NF membrane with a high MWCO range of 300–1000 g mol^{-1} using different types of solvents such as organic solvents, ionic liquid, organic bases, and acids that can tune various physicochemical properties (i.e., hydrophilicity and roughness). This depends on their solvency and miscibility with the residual molecules (i.e., TMC, PIP) and their facilitation or prevention of hydrolysis of the TMC molecules (Guo, Chen, Wan, Feng, & Luo, 2020). Conversely, solvent treatment can rearrange and mobilize polymer chains into a denser

structure, promoting additional cross-linking via favorable interactions such as hydrogen bonding and π stacking. For example, the solvent treatment of cross-linked PI UF membrane (i.e., ISA) using DMF produced an NF membrane with an MWCO of $\sim 500\ g\ mol^{-1}$ (Mariën & Vankelecom, 2017). However, more research is needed to fine-tune the solvent activation approach in regard to the choice of solvent and time of immersion.

Other posttreatments mainly focus on improving the separation performance and antifouling properties. For example, surface grafting of hydrophilic molecules such as triethanolamine (TEOA) (Yan, Chen, & Lü, 2016) and amphibian-inspired amino acid ionic liquid (Xiao, Chu, & Xu, 2019) is more effective in increasing the water permeance while maintaining salt rejection compared to pristine TFC membranes. Another surface modification approach to enhance hydrophilicity and better coordinate the trade-off of the NF membrane was presented by Kim et al.; commercial NF membranes were modified using low-pressure NH_3 plasma, resulting in increased water permeance and membrane rejection depending on the intensity and duration of the plasma treatment (Kim, Yu, & Deng, 2011). Moreover, polyethylene glycol (PEG) grafted onto cross-linked polyimide UF support via argon plasma led to solvent-resistant NF membranes for OSN with increased membrane rejection (i.e., Rose Bengal in isopropanol) (Gao, Shi, Cui, & Chung, 2018). Further, Reis et al. utilized argon plasma to activate the surface of the TFC membrane; the results were promising as the water permeance was enhanced without compromising salt rejection via the application of a short period (<5 minutes) of low-power density, which led to membrane surface thinning without severely altering the surface morphology (Reis, Dumée, & Tardy, 2016). Surface plasma grafting has potential owing to its simplicity and has exhibited promising results in improving the separation performance and antifouling properties. However, plasma reactors are currently expensive and difficult to scale up.

5.4 Thin-film polymer composite nanofiltration membranes

TFC NF membranes are usually prepared via IP and LBL assembly (see Section 5.3) (Lin, Zhang, & Qu, 2017). The state-of-art of TFC NF membranes is diverse as countless optimizations have been achieved for each specific separation (Huang et al., 2020; Jin, Zhu, & Yuan, 2021). In 2004 Drioli et al. proposed a new approach of implementing loose NF (LNF) membranes, which has attracted attention for dye/salt separation, by permeating divalent salts to increase the rejection of organics (Van der Bruggen, Curcio, & Drioli, 2004). Recent work by Van der Bruggen's group on loose NF-based membranes included polyester-based TFC LNF membranes, with high rejection of dyes and high salt passage (i.e., rejection of 11% and 5.6% for Na_2SO_4 and NaCl, respectively), successfully prepared using hydroxyl-containing monomers such as mesoerythritol and TMC with sodium hydroxide (NaOH) as a catalysis to promote the esterification via the IP method on polyethersulfone (PES) supports (Jin et al., 2021). Furthermore, Li et al. demonstrated improved antifouling and antibacterial performance of LNF membranes for dye/salt separation using a rapid codeposition of polydopamine (PDA) and a zwitterionic polymer (SBMA) (Li, Liu, & Bai, 2020).

Blending thermally rearranged polymers with a polyamide separation layer resulted in chemically robust TFC membranes comprising a polybenzoxazole-co-imide thin layer via

the IP of MPD and TMC PDA-coated thermally rearranged polymeric supports for OSN and pressure-retarded osmosis (PRO) applications (Kim et al., 2018). Another approach was to blend o-hydroxyazo porous organic polymers (o-POPs) and piperazine (PIP) monomers in PES dope solutions and cast via phase inversion, followed by IP with TMC to fabricate TFN membranes. The o-POP incorporation improved the water permeance without sacrificing dye and divalent salt rejection (Liu, Zhu, & Zheng, 2020).

Overcoming the limitations of the porous support is essential to achieve an ultrathin TFC NF membrane with enhanced separation performance (see Section 5.5). Karan et al. demonstrated that an ultrathin separation layer, prepared via the IP method using MPD and TMC monomers, with a thickness of <10 nm is achievable using a cadmium hydroxide nanostrand as an interlayer to minimize the filtration resistance of the porous support (Karan, Jiang, & Livingston, 2015). Goa et al. introduced a novel technique to produce an ultrathin PA TFC NF membrane (i.e., a separation layer thickness of $\sim$15 nm) with 96.5% rejection of Na_2SO_4 and high water permeance of $\sim 40\ L\ m^{-2}\ h^{-1}\ bar^{-1}$ (Gao et al., 2019). Their preparation method included surface coating of single-wall carbon tube (SWCNT) dispersion onto a PES microfiltration support, followed by the IP of PIP and TMC to achieve the ultrathin PA layer, as shown in Fig. 5.8.

The sustainability and greenness of manufacturing TFC NF membranes have attracted a lot of attention as the organic phase usually involves volatile organic solvents, for example, hexane, cyclohexane, heptane, benzene, and ethylene dichloride. Recently, researchers have replaced these toxic solvents with more environmental-friendly solvents such as cyrene, rhodiasolv polarclean, dimethyl isosorbide, diethyl adipate, ionic liquid [$(C_4$mim$)(Tf_2N)$], and decanoic or capric acid. The latter was used as the organic phase by Ong et al. to develop an ultrathin polyamide layer on a polyacrylonitrile (PAN) support using TMC and PEI as the reactive monomers (Ong, Falca, & Huang, 2020).

5.5 Effect of polymeric support

The effect of the porous polymeric support has not captured the same amount of attention as the separation layer of NF membranes in the literature (Jimenez-Solomon, Gorgojo, Munoz-Ibanez, & Livingston, 2013; Liu, Wang, Li, Liu, & Deng, 2019). The physicochemical properties of the porous support, including hydrophilicity, roughness, porosity, and pore size, have a direct impact on the NF membrane performance. TFC membranes are usually supported by two layers: a nonwoven fabric to give structural support and increase the mechanical strength of the membrane, and a porous interlayer to withstand high operating pressures. For ISA membranes, the porous support sublayer cannot be independently manipulated as the optimization of the various fabrication parameters, as discussed in Section 5.3, controls the overall thickness and uniformity of the final NF membrane. Therefore, this section focuses on the effect of the porous support in TFC NF membranes.

Porous support is a critical factor for achieving ultrathin separation layers (Ramon, Wong, & Hoek, 2012). Dilute concentrations of the monomer solution are preferred to achieve the thinnest separation layer possible. However, the intrusion of the solution into a conventional UF support creates defects and drastically deteriorates the separation performance. Therefore, optimizing the physicochemical properties of the UF support and the

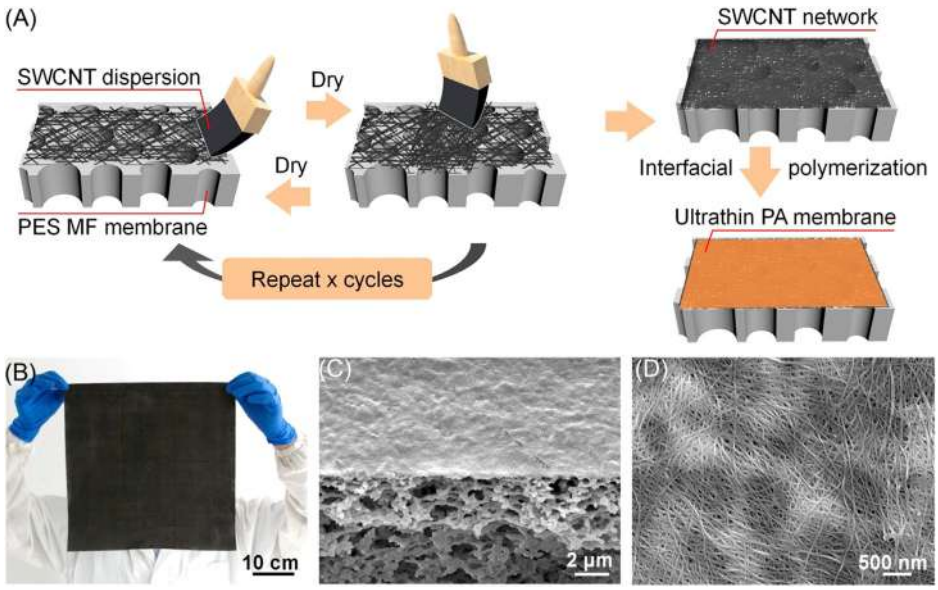

FIGURE 5.8 (A) Schematic illustrating the surface-coating cycles of a single-wall carbon tube (SWCNT) dispersion on a polyethersulfone (PES) MF support using a brush and the interfacial polymerization (IP) method to produce an ultrathin polyamide (PA) thin-film composite (TFC) membrane. (B–D) Photograph and cross-sectional and top surface SEM images of the PA/SWCNT TFC membrane (i.e., X = 3). Source: *From Gao, S., Zhu, Y., Gong, Y., Wang, Z., Fang, W., & Jin, J. (2019). Ultrathin polyamide nanofiltration membrane fabricated on brush-painted single-walled carbon nanotube network support for ion sieving*. ACS Nano, 13*(5), 5278–5290. https://doi.org/10.1021/acsnano.8b09761*.

type and concentration of monomers as well as the reaction and drying times is important to achieve defect-free TFC NF membranes, as shown in Fig. 5.9. Researchers have modified the UF support membranes to be smooth and uniform so that the IP reaction takes place between the dilute monomer solutions and ultrathin TFC membranes can be obtained (Wang, Guo, Jiang, & Pan, 2020; Zhu, Xie, & Gao, 2016). Many research reports have focused on modifying the surface wettability by incorporating hydrophilic additives and increasing the porosity to minimize the filtration resistance of the porous support (Gao et al., 2019; Karan et al., 2015). Moreover, few efforts have focused on improving the sustainability aspect of manufacturing polymeric porous supports. For example, Pulido et al. demonstrated the possibility of utilizing recyclable polymers from plastic waste such as polyethyleneterephthalate (PET) as the UF porous support with a pore-size range (35–100 nm) that is ideal for preparing TFC NF membranes (Pulido, Habboub, Aristizabal, Szekely, & Nunes, 2019). In addition to using dilute monomer concentrations, lowering the organic phase temperature to decrease the thickness of the selective layer of the TFC NF membranes was pursued by Liu et al. Their results showed high water permeance and salt rejection (Liu, Wu, Hung, Lu, & Lee, 2017). Further, incorporating hydrophilic additives and increasing the porosity minimizes the filtration resistance of the porous support. Recently, the use of an MF porous support has received a lot of attention, although it is well known that increasing the pore size of the porous support results in increased separation layer roughness, the possibility of defects, and, hence, decreased

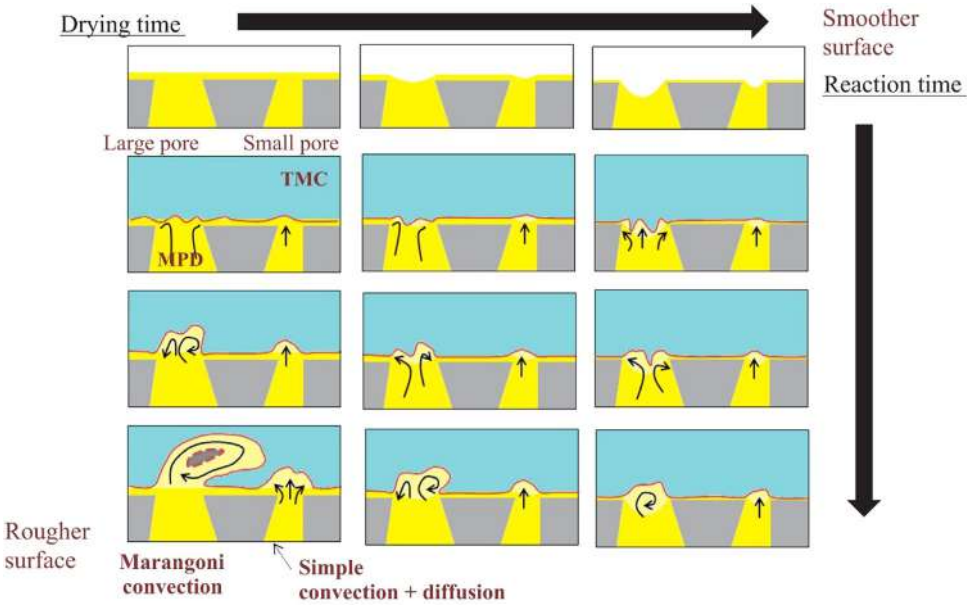

FIGURE 5.9 Schematic illustrating the formation mechanism of a typical polyamide thin-film composite membrane. Source: *From Klaysom, C., Hermans, S., Gahlaut, A., Van Craenenbroeck, S., & Vankelecom, I. F. J. (2013). Polyamide/polyacrylonitrile (PA/PAN) thin film composite osmosis membranes: Film optimization, characterization and performance evaluation.* Journal of Membrane Science, 445, 25–33. https://doi.org/10.1016/j.memsci.2013.05.037.

membrane rejection (Sharabati, Guclu, & Erkoc-Ilter, 2019). Preparing a TFC NF membrane with an ultrathin separation layer directly on an MF support allows for faster mass transfer compared to conventional NF membranes prepared on similar UF supports (Zhang et al., 2019). As an example, Karan et al. developed an ultrathin PA separation layer with a thickness of <10 nm on a porous support with an average pore size of 200 nm using cadmium hydroxide that minimizes the filtration resistance induced by the support and exhibits high acetonitrile permeance of 112 L m^{-2} h^{-1} bar^{-1} (Karan et al., 2015). Similar approaches were proposed to modify and deposit an interlayer onto MF-based porous supports to achieve uniform porosity and develop ultrathin PA membranes, such as using CNC (Wang, Yang, Wu, Zhang, & Xu, 2017). and carbon nanotubes (Gao et al., 2019; Zhou, Hu, & Boo, 2018; Zhu et al., 2016). Another approach is to repeat the IP reaction on a conventional support membrane to form a multilayer defect-free ultrathin separation layer (Zhang et al., 2019). A recent study investigated the presence of foulants on an MF PES porous support (i.e., the fouled MF support acts as an interlayer) and obtained ultrathin TFC PA membranes with no defects (Dai et al., 2021).

Interestingly, asymmetric polyelectrolyte NF membranes with ultrathin separation layers ($\sim$4 nm) were successfully developed via the LBL method using a multilayer coating of loose PSS/PAH on a porous support to prevent defects and capped by a thin layer of dense PAA/PAH, which provides the required separation properties (te Brinke et al., 2020). The same preparation method was proposed by Bruening's group using a porous alumina support (Liu & Bruening, 2004).

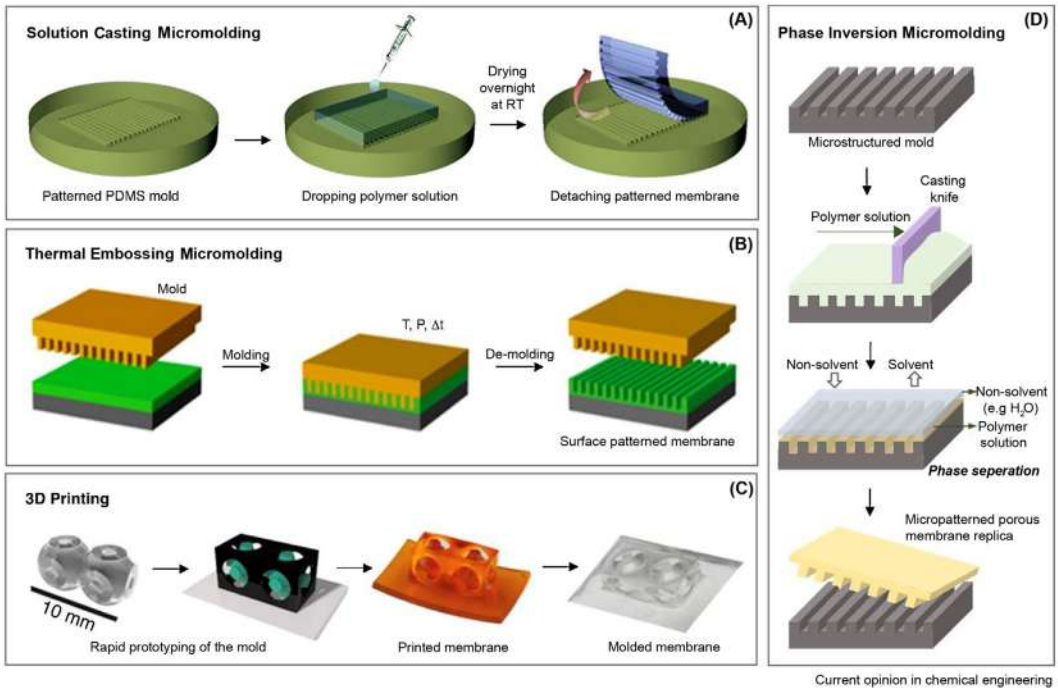

FIGURE 5.10 Schematic representation of the preparation of patterned membranes via (A) solution-casting micromolding, (B) thermal micromolding, (C) 3D-printing stages for the preparation of patterned membranes, and (D) phase inversion micromolding. Source: *From Heinz, O., Aghajani, M., Greenberg, A. R., & Ding, Y. (2018). Surface-patterning of polymeric membranes: Fabrication and performance.* Current Opinion in Chemical Engineering, 20, 1–12. https://doi.org/10.1016/j.coche.2018.01.008.

Researchers have developed a support-free IP (SIPF) technique to successfully develop ultrathin TFC membranes with a thickness of <12 nm (Park et al., 2017; Park, Ahn, & Choi, 2017; Zhu, Hou, & Zhang, 2018). Other approaches that showed promising results were also used, such as spray technology (Ma et al., 2018; Shan, Gu, Fan, Ji, & Zhang, 2017); micromolding and 3D printing can be used to tailor surface-patterned porous supports (Heinz, Aghajani, Greenberg, & Ding, 2018), as shown in Fig. 5.10. Overall, two main routes led to optimum separation properties and prevention of defect generation: (1) improving the method of casting the polymer on the porous support and (2) tailoring the properties of the porous support for minimum filtration resistance and compatible physicochemical properties, including high surface area and effective filtration pathways.

5.6 Potential of polymer-composite nanofiltration membranes for water desalination

Worldwide challenges associated with clean water scarcity are now well defined: (1) 1.2 billion people do not have access to drinkable water, (2) 2.6 billion people have little or no

sanitation facilities, (3) and millions of people die because of water contamination. The demand for freshwater is expected to increase with increasing population and industrial growth (Gassert, Landis, Luck, Reig, & Shiao, 2014; Mancosu, Snyder, Kyriakakis, & Spano, 2015). In the coming decades, water scarcity may trigger wars unless new ways to supply clean water are found (Shannon et al., 2008). The increase in water usage (1% increase per year) and the rise in extreme natural events caused by climate change, such as wildfires, storms, and floods, are making the situation even worse (United Nations, 2020). Up to 300 L of wastewater per person is produced daily; therefore, water scarcity is a genuine threat to sustainable development.

By 2025, almost half of the world population will experience water stress conditions. Increasing the production of clean water is essential to fight poverty, create food security, and minimize international conflicts. According to the World Water Assessment Program, more than 80% of the global wastewater is disposed of untreated into the environment. Therefore, treatment and reuse of wastewater is attracting much interest and has been highlighted in the United Nations' goals for sustainable development. Wastewater is generated by a wide range of industries, such as the food industry, power plants, textile dyeing, and the oil and gas industry, as an unwanted byproduct. Furthermore, the stringent environmental regulations for water discharge to surface and groundwater are among the primary drivers of the current market. High temperature, high salinity, and organic solvents are challenging for polymeric membranes in particular and limit their industrial application.

Conventional polymer-based NF membranes suffer in harsh conditions, that is, very acidic/alkaline solutions (extreme pH) and strong organic solvents. Therefore, many studies have focused on developing new materials to enhance membrane chemical stability and separation performance. High water flux can be achieved using NF membranes by enhancing the membrane hydrophilicity, antifouling properties, and chemical stability (Chen, Li, & Chen, 2018). Furthermore, NF membranes have shown promising phosphorus recovery from sewage sludge. Thong et al. developed NF TFC membranes involving PEI and TMC that can achieve 90% phosphorus recovery by efficiently rejecting heavy metals, particularly under the acidic condition of sewage sludge owing to the coupling of the Donnan exclusion (i.e., positively charged membrane surface) and size exclusion while permeating phosphoric acid (Thong, Cui, Ong, & Chung, 2016).

Recent studies have focused on utilizing sustainable starting materials and solvents to develop advanced NF membranes, which is much appreciated and encouraged by the scientific community to reach a cyclic economy. Van der Bruggen's group utilized glucose, maltose, and raffinose as aqueous monomers to fabricate a selective polyester layer prepared via the IP method with NaOH as the catalyst. These monomers replaced the typical petroleum-based monomers such as PIP and MPD that are primarily synthesized from benzene and ethylene, respectively. Among the chosen carbohydrates, glucose has higher potential owing to its availability and low cost. The fabricated sugar-based NF membranes showed high water permeance and divalent salt rejection (Zheng, Liu, & Zhu, 2021). Dilute concentrations and high volume of impurities (i.e., Se and As) make the contaminated stream difficult to treat.

Electrodialysis-based membranes are considered a niche market because of their high cost and weak feasibility for high-salinity streams. Currently, they are only feasible for brackish water as transporting more ions through the membranes requires more electricity. However, in recent years, advancements in the field have made electrodialysis-based membranes suitable for high-salinity streams, for example, BMED an integrated process

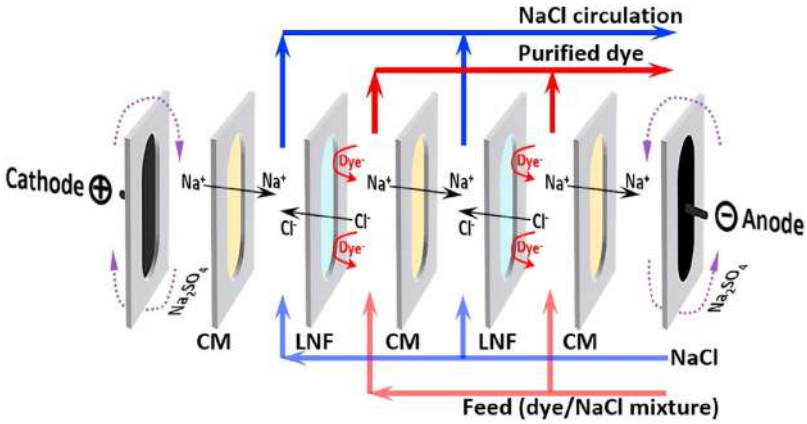

FIGURE 5.11 Configuration of the integration of loose nanofiltration (LNF) polymer-based membranes using the electrodialysis (ED) process, including a cation exchange membrane for dye/salt separation. Source: *From Ye, W., Liu, R., Chen, X., et al. (2020). Loose nanofiltration-based electrodialysis for highly efficient textile wastewater treatment.* Journal of Membrane Science, 608, *118182–118182. https://doi.org/10.1016/j.memsci.2020.118182*.

and sequestration of CO_2 into a valuable product. The sustainability of the process depends on the source of electricity used to have a net positive process. The key factors in the progress of current electromembranes are developing novel materials, such as bipolar membranes, and designing selective membranes for anions that have the same charging densities (chlorine, nitrate, and phosphate ions) as well as for cations (sodium, magnesium, and lithium ions). Loose NF membranes coupled with electrodialysis (ED) have the potential for textile wastewater treatment and desalination as they can separate dyes and salts more efficiently and reduce the fouling propensity compared to the conventional ED processes with ion exchange membranes (Fig. 5.11) (Ye, Liu, & Chen, 2020).

5.7 Polymers for solvent-resistant nanofiltration membranes

OSN, also called solvent-resistant nanofiltration (SRNF), is simply a continuous liquid–liquid separation that does not involve any phase transition and can be adopted by many industries (e.g., pharmaceutical, food, petrochemical, and other industries that utilize organic solvents). OSN processes have already been employed in the lubricant industry, such as in the Max–Dewax process. Polymer-based NF membranes are ideal for OSN processes in terms of the pore size (0.4–2.0 nm) necessary to achieve satisfactory separation performance and efficient recovery of most common organic solvents (Chen et al., 2018; Davood Abadi Farahani & Chung, 2018). OSN has been successfully demonstrated for industrial concentrations and applied in pharmaceuticals, solvent exchange, catalysis recovery, purification, and enrichment of consumer and specialty chemicals. However, OSN is considered an emerging application compared to desalination. High permeance and molecular selectivity to organic solvents with different polarities are highly sought after. Solvent-resistant polymers have improved significantly in recent decades; polymers such as polybenzimidazole (PBI),

polyether etherketones (PEEKs), polyarylenesulfidesulfone (PASS), and polyoxindolebiphenylylene (POXI) have been explored for OSN. However, efficient molecular separation of DMSO and DMF is still challenging, even for state-of-the-art polymeric membranes. Fabrication of PEI/TMC with a flexible aliphatic, aromatic polyamide TFC membrane via in situIP is followed by a solvent activation process. The activation effect in polar aprotic solvents (i.e., DMF, NMP, and DMSO) increases the permeance of methanol and acetone; in contrast, activation of the membrane separation layer with the latter solvents does not improve the permeance. An order of magnitude increase in water permeance was reported using solvent activation with DMF (Li et al., 2019), whereas only a marginal improvement in permeance caused by DMF treatment was reported by Livingston's group (Karan et al., 2015). Zhao et al. reported composite membranes prepared through self-polymerization and IP of dopamine with TMC on PES UF supports, which exhibited improved chemical stability and increased rejection for dyes and salts; however, the water permeance decreased drastically (Zhao, Su, & He, 2014). Szekely et al. reported NF membranes prepared via in situ polymerization of dopamine in PBI membranes and demonstrated improved stability in seven polar aprotic solvents and increased permeance while maintaining the MWCO due to an interpenetrating polymer network. However, a longer PDA deposition time increased the rejection (i.e., improved the hydrophobic properties and decreased the pore size from 1.4 nm to 0.8 nm at 300 Da) and decreased the permeance (Zhao et al., 2019).

Molecular dynamics simulations have been recommended by many researchers and are regarded as a promising solution to better understand the relationship between performance and polymeric properties of NF membranes at the molecular level, which is an essential tool for engineering any nano-based technology. Emerging high-performance polymers such as PIMs and PEEKs have attracted a lot of attention. PEEK is especially promising because of its negligible physical aging property. However, PEEK is insoluble in organic solvents and needs strong acidic conditions to be solubilized, thereby making it challenging to prepare membranes. Recently, Szekely's group modified PEEK through a high-temperature aromatic nucleophilic substitution reaction (S_NAr) between 4,4′-difluorobenzophenone and various diol contorted compounds. These contorted structures, such as triptycene, spirobisindane, and Tröger's base, resulted in an increase in the free volume, surface area, and, hence, porosity, as well as solubility in a few common organic solvents such as NMP. They utilized molecular dynamics simulations to understand and optimize the MWCO of intrinsic microporous poly(ether-ether-ketones) (iPEEKs) by varying either the contorted structure or the dope solution concentration, which resulted in high permeance and better thermal and chemical stability (Abdulhamid, Park, & Vovusha, 2020).

5.8 Commercialization status and commercial viability

Separation technologies are crucial in any industrial process compromising at least 70% of energy consumption. We can confidently say that polymeric membrane technology has developed from the lab to the industry with a pronounced positive impact on the efficiency of the separation process. This is because of superior scalability and lower footprint, operating cost, and chemical usage, as well as minimum energy requirements. NF membranes have shown advantages over RO and MF membranes. Examples include larger pore size, which has a

lower-energy requirement, than that of RO membranes and having better permeate water quality than that of MF membranes. However, large membrane areas are usually required for industrial applications due to the low permeance of conventional NF membranes, including TFC and ISA membrane types. Next-generation NF membranes have potential due to their advanced separation performance and sustainability (He, Zhao, & Chung, 2018). This is reflected by the increased research activity and growth of the polymer-based NF membrane market, which is expected to be approximately 49% (2017–2025). Solvent-stable NF membranes (e.g., GE Osmonics Desal DK, Koch MPF, and Evonik product line-ups) are of great interest for crude oil purification in the oil and gas industry. New advanced materials have already been commercialized, such as PolyCera membranes, and have gained market traction. Novel nanostructured, diamond-like carbon nanosheet membranes have been successfully scaled up to commercial applications for water remediation, achieving relatively higher permeance while maintaining high rejection, as shown in Table 5.1.

Increasing the polymer-based NF membrane permeance without sacrificing its rejection is not an easy task. The trade-off between permeance and rejection is one of the main obstacles in achieving a wider industrial adoption. The stability of the polymer-based NF membranes in both aqueous solutions and organic solvents is another obstacle hindering its life cycle (i.e., maintaining the membrane performance over several years). In addition, fouling and concentration polarization are considered major operational obstacles to sustain the permeance (Chidambaram, Oren, & Noel, 2015; Syed I, Arun, & Lakshmi, 2020). Fouling may increase the operation cost and deteriorate the membrane performance by decreasing the membrane permeance. The additional operating costs are due to the different treatment protocols followed to reduce membrane fouling, such as chemical cleaning, coagulation, and oxidation using either ozone, UV/H_2O_2, or Fenton (Yu, Liu, Crawshaw, Liu, & Graham, 2018). The physicochemical characteristics of NF membranes provide insight into the interactions between the membrane surface and feed solution, which directly affect the separation performance. The impact of important industrial parameters on membrane performance requires more attention from researchers; these parameters include pressure drop across the membrane, actual industrial concentrations, concentration polarization, and module and process design. Shi et al. demonstrated that membranes with ultrahigh permeance cannot improve the overall efficiency of the separation process without tailoring the membrane module and process (Shi, Marchetti, Peshev, Zhang, & Livingston, 2017).

In a recent study, Le Phuong et al. highlighted the main shortcomings of the current state of research in OSN that hamper its industrial and scientific advancement. They recommended a series of best practices and guidelines for researchers based on a comprehensive survey and critical analysis of studies published during 2015–19 (Le Phuong, Blanford, & Szekely, 2020). Fig. 5.12 shows a map of the essential parameters highlighted in the survey compared to parameters reported in the literature for OSN application. Feed flow rate, temperature, stirring or mixing speed, crossflow velocity, process configuration, and system volume have not been studied in detail. Without a standardized protocol covering the operating conditions and solute/solvent types, it will be difficult to reproduce and compare with other membranes. Most importantly, the operating conditions (i.e., temperature, pressure, solute concentrations, and filtration time) must be relevant to an industrial case; otherwise, the gap between academia and industry will not be narrowed. Another approach was implemented to standardize osmotic-driven membranes for

TABLE 5.1 Summary of commercial NF membranes used for desalination and OSN.

Membrane	Manufacturer	Material	Solute/solvent	Rejection (%)	Permeance ($L\ m^{-2}\ h^{-1}\ bar^{-1}$)	pH	Ref.
NF70	Dow-Filmtec	PA	Na_2SO_4/water	99	2.4	n.a.	Krieg et al. (2005)
NF90	Dow-Filmtec	PA	$MgSO_4$/water	>97	11.7 ± 0.3	2–11	Chen et al. (2018)
NF270	Dow-Filmtec	PA	$MgSO_4$/water	97	17.6 ± 0.4	3–10	Chen et al. (2018)
NT103	Microdyn-Nadir	Polypiperazine	$MgSO_4$/water	98	8.1 ± 0.1	n.a.	Chen et al. (2018)
NT102	Microdyn-Nadir	Polypiperazine	$MgSO_4$/water	95	10.0 ± 0.1	n.a.	Chen et al. (2018)
NF70	HWTT	Polypiperazine	$MgSO_4$/water	98	10.6	n.a.	Chen et al. (2018)
NF40-I	HWTT	Polypiperazine	$MgSO_4$/water	95	14.5 ± 0.2	n.a.	Chen et al. (2018)
NF40-II	HWTT	Polypiperazine	$MgSO_4$/water	98	11.2 ± 0.3	n.a.	Chen et al. (2018)
Desal DK	GE Osmonics	PA	$MgSO_4$/water	98	n.a.	3–9	Szymczyk et al. (2010)
GMT-oNF-2	Borsig GmbH	PDMS	4-chloroaniline (127 g mol^{-1})/toluene	~35–40	~5	n.a.	Razali et al. (2017)
DuraMem 150	Evonik MET	Cross-linked PI	BB (~826 g mol^{-1})/DMF	99.9	0.15–0.2	7	Sereewatthanawut et al. (2010)
DuraMem 200	Evonik MET	Cross-linked PI	BB (~826 g mol^{-1})/DMF	99.3–99.9	0.2–0.37	7	Sereewatthanawut et al. (2010)
DuraMem 300	Evonik MET	Cross-linked PI	BB (~826 g mol^{-1})/DMF	99.6–99.9	0.85–1.8	7	Sereewatthanawut et al. (2010)
DuraMem 500	Evonik MET	Cross-linked PI	BB (~826 g mol^{-1})/DMF	91.4–94.6	0.85–0.9	7	Sereewatthanawut et al. (2010)
PuraMem 280	Evonik MET	Cross-linked PI	API (~600 g mol^{-1})/IPAc	99.6–99.8	0.9–1.5	7	Rundquist et al. (2012)
StarMem 122	Evonik MET	PI	Styrene (236 g mol^{-1})/toluene	87	0.6	7	Marchetti et al. (2014)

(*Continued*)

TABLE 5.1 (Continued)

Membrane	Manufacturer	Material	Solute/solvent	Rejection (%)	Permeance ($L\ m^{-2}\ h^{-1}\ bar^{-1}$)	pH	Ref.
StarMem 240	Evonik MET	PI	Styrene (380 g mol^{-1})/ toluene	90	0.7	7	Fritsch et al. (2012)
MPF-44	Koch	PDMS	Daidzin (410 g mol^{-1})/ methanol	71.9	0.25	n. a.	Zhao and Yuan (2006)
NE4040-HRM/SRM	CSM Toray	PA	$MgSO_4$/water	99.0–99.5	6.2–8.8	3–10	Toray Advanced Materials Korea Inc (2020)
NE8040-HRM/SRM	CSM Toray	PA	$MgSO_4$/water	99.0–99.5	6.1–9.0	3–10	Toray Advanced Materials Korea Inc (2020)
dNF40	NX Filtration	Modified PES	$MgSO_4$/water	91	20–40 ($L\ m^{-2}\ h^{-1}$)	2–12	NX Filtration B.V. (2020a)
dNF80	NX Filtration	Modified PES	$MgSO_4$/water	76	20–50 ($L\ m^{-2}\ h^{-1}$)	2–12	NX Filtration B.V. (2020b)
PolyCera Titan	PolyCera	Not specified	RB/water	99	46–48	n.a.	Haan et al. (2020)

NF, nanofiltration; OSN, organic solvent nanofiltration; *PA*, polyamide; *PDMS*, polydimethylsiloxane; *BB*, brilliant blue R; *DMF*, dimethylformamide; *PI*, polyimide; *API*, active pharmaceutical ingredient; *IPAc*, isopropyl acetate; *PES*, polysulfone; *RB*, rose Bengal.

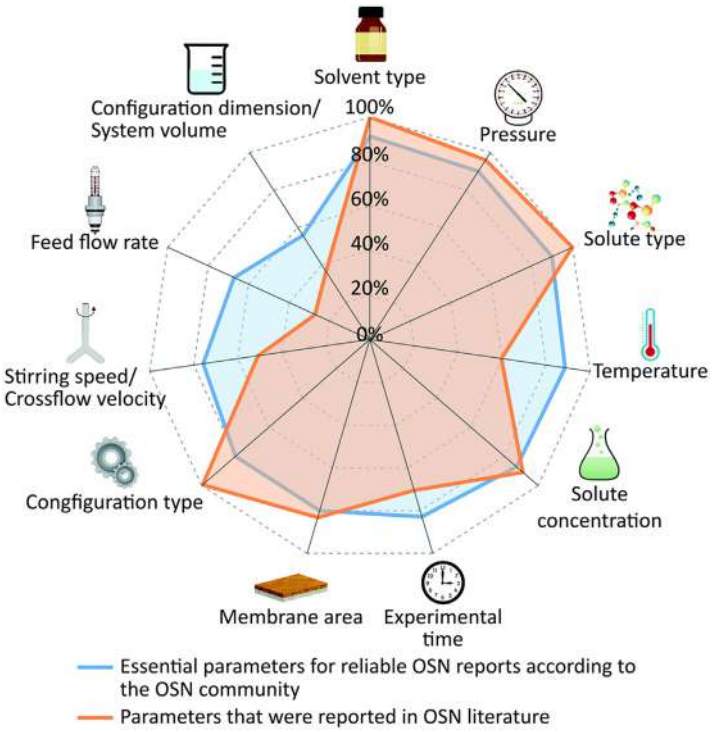

FIGURE 5.12 Percentage distribution of responses from surveying the OSN community about essential parameters required to ensure reproducibility (blue, it is virtually much broader in covering the parameters) and compared to the reported parameters in OSN literature (orange, it is narrower and concentrated in covering specific parameters such as the configuration type). Source: *From Le Phuong, H. A., Blanford, C. F., & Szekely, G. (2020). Reporting the unreported: The reliability and comparability of the literature on organic solvent nanofiltration.* Green Chemistry, 22*(11), 3397–3409.* https://doi.org/10.1039/d0gc00775g.

desalination by testing two commercial osmotic-driven membranes (i.e., RO, PRO, and FO) in seven independent laboratories. The study concluded that TFC membrane evaluation and reproduction are more challenging than for asymmetric membranes owing to the concentration polarization effect. The authors recommended several characterization techniques (e.g., SEM, AFM, and porosity) to check membrane integrity prior and after filtration to improve reproducibility (Cath, Elimelech, & McCutcheon, 2013).

There has been an exponential increase in the number of research papers on polymer-based NF membranes. However, we should not rely on research interest as a "number" but rather on the advancements made to revolutionize the status of NF membrane technology to shorten the path from laboratory to industry. Industrial membrane manufacturing is limited (i.e., phase separation, interfacial polymerization, and surface coating) to the production of flat-sheet and hollow-fiber NF membranes (Ulbricht, 2020). Comprehensive studies on translating the advances in polymer-based NF membranes (highlighted in Section 5.2) for industrial manufacturing are lacking.

5.9 Summary and future direction

In summary, two approaches for the development of membranes have been established by researchers and the membrane community. First, polymer-based NF membranes are

being engineered with the thinnest possible separation layer. Second, the intrinsic properties of the polymer are being designed at the molecular level (e.g., interconnected microporosity). Many breakthroughs, as mentioned in earlier sections, have encouraged novel material development, such as the introduction of PIMs with their unique ladder-like, contorted, and rigid monomers that create inefficient packing of their polymer chains, resulting in membranes with high free volumes. However, PIMs are not chemically stable in various polar solvents, which limits their applicability for OSN. Incorporating microporous organic materials (e.g., MOFs, COFs, zeolites, carbonous materials, and clay) into a polymer matrix is challenging due to weak compatibility, creation of defects, large voids, and nonuniform filler distribution, which decrease membrane rejection.

Improving the trade-off relationship between rejection and permeance can unlock new separation applications that were not possible before. However, the fabrication route of these novel membranes must be economical, scalable, and designed with operating process parameters in mind. Shi et al. suggested that further research on ultrafast permeance might not have a significant practical impact on membrane processes. Instead, we must consider directing membrane research away from the search for ultrahigh permeance in favor of prioritizing three related areas: (1) designing membrane module, (2) improving NF selectivity, and (3) reducing physical aging and fouling in modules (Shi et al., 2017). Furthermore, it is time to shift the focus of research on replacing these materials with renewable materials eligible for biodegradation or by satisfying the 3Rs system (reduce, reuse, and recycle). It is very important to emphasize which materials can be considered "green materials." Some polymers derived from fossil fuels are biodegradable, for example, polycaprolactone (PCL) and polybutylene adipate terephthalate (PBAT). In contrast, some materials derived from natural sources are not biodegradable, for example, bio-based polyethylene (bio-PE) and bio-polycarbonate (bio-PC) made from sugarcane and corn, respectively. Moreover, sustainable polymers need to outperform or at least match the conventional polymers to replace them; general properties include thermal stability, adequate mechanical strength, and high industrial scalability. Most sustainable polymers reported in academic works were not subjected to life-cycle assessment to quantify their impact and compare with existing fossil-fuel based polymers (Zhu, Romain, & Williams, 2016). More research is needed to study the replacement of organic solvents and monomers with green and sustainable alternatives since the current IP preparation method for ultrathin TFC NF membranes requires (1) large amounts of toxic solvents, such as hexane, and (2) dilute concentrations for organic and aqueous phases (as low as 0.05 wt.%). A cradle-to-grave approach, which includes membrane materials, modules, preparation, the overall process, and recyclability after usage, is recommended to ensure the sustainability of the membrane technology. Yadav et al. conducted a life cycle assessment of the production of 1000 m^2 of a polymeric hollow-fiber membrane to investigate its environmental impacts. Their study showed that the type of polymer, solvent, and electricity source have a significant effect on the environmental impact and cost. In particular, the use of green solvents (i.e., ethylene carbonate) over NMP can reduce the environmental costs by up to 35%. However, replacing a fossil-fuel-based polymer with a bio-based polymer, such as replacing PSf with bio-based CA, is not always favorable as it would increase the environmental costs mainly due to the environmentally unfriendly synthesis of acetic acid used in the CA production process (Yadav, Ismail, Essalhi, & Tysklind, 2021).

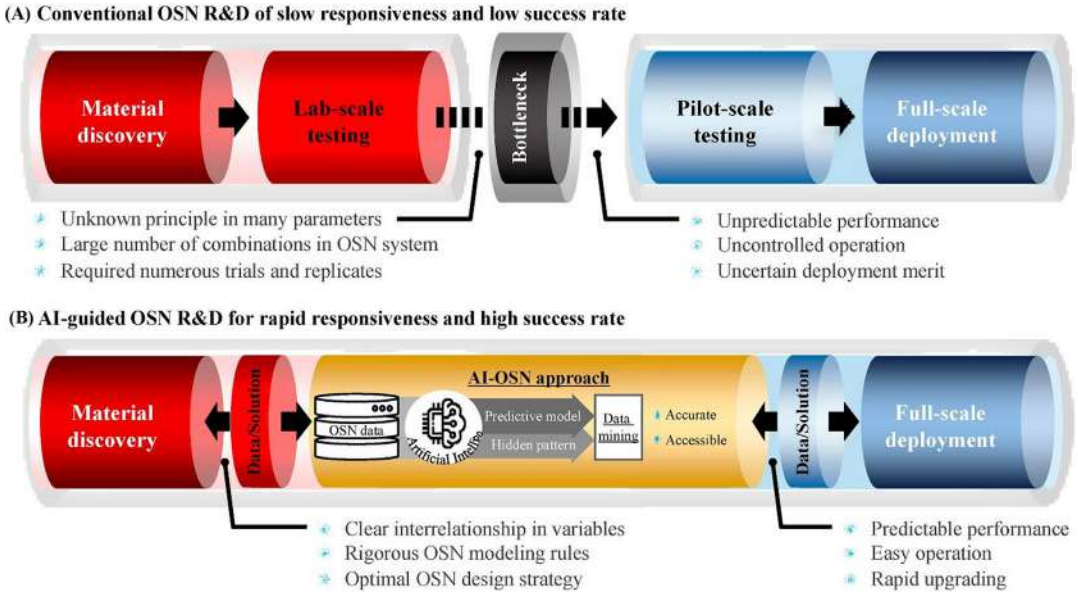

FIGURE 5.13 (A) Conventional organic solvent nanofiltration (OSN) R&D flowchart with slow responsiveness and a bottleneck in performance prediction; (B) proposed artificial intelligence (AI) guided OSN R&D with performance prediction and rapid responsiveness. Source: *From Hu, J., Kim, C., Halasz, P., Kim, J. F., Kim, J., & Szekely, G. (2021). Artificial intelligence for performance prediction of organic solvent nanofiltration membranes.* Journal of Membrane Science, 619, *118513*. https://doi.org/10.1016/j.memsci.2020.118513.

In addition, the empirical trial-and-error approach, which has been followed thus far for preparing NF membranes for different separation applications, must be upgraded to a tailor-made approach designed specifically for each application. One of the tools that could help reduce this gap is artificial intelligence (AI). AI is a broad computer science that focuses on creating systems that function independently and intelligently without human interference. For example, researchers used deep learning tools to analyze a large dataset (38,430 data points and 18 dimensions) using principal component analysis and three AI algorithms (i.e., artificial neural network, support vector machine, and random forest model) to extract the key parameters and predict/classify the membrane performance (i.e., permeance and rejection) for OSN application (Fig. 5.13) (Hu et al., 2021). This work can replace the conventional tools used to predict membrane performance, such as the solution-diffusion model that is limited regarding the compatibility of polymer-based membranes with many different solvents, to shorten the path from laboratory to industry.

References

Abd-El-Aziz, A. S., Antonietti, M., Barner-Kowollik, C., Binder, W. H., Böker, A., Boyer, C., … Zhang, G. (2020). The next 100 years of polymer science. *Macromolecular Chemistry and Physics*, *221*(16), 2000216. Available from https://doi.org/10.1002/macp.202000216.

Abdulhamid, M. A., Park, S.-H., Vovusha, H., Akhtar, F. H., Ng, K. C., Schwingenschlogl, U., & Szekely, G. (2020). Molecular engineering of high-performance nanofiltration membranes from intrinsically

microporous poly(ether-ether-ketone). *Journal of Materials Chemistry A*. Available from https://doi.org/10.1039/d0ta08194a.

Andres, C. M., & Kotov, N. A. (2010). Inkjet deposition of layer-by-layer assembled films. *Journal of the American Chemical Society*, *132*(41), 14496–14502. Available from https://doi.org/10.1021/ja104735a.

Baig, M. I., Durmaz, E. N., Willott, J. D., & de Vos, W. M. (2020). Sustainable membrane production through polyelectrolyte complexation induced aqueous phase separation. *Advanced Functional Materials*, *30*(5), 1907344. Available from https://doi.org/10.1002/adfm.201907344.

Borges, J., & Mano, J. F. (2014). Molecular interactions driving the layer-by-layer assembly of multilayers. *Chemical Reviews*, *114*(18), 8883–8942. Available from https://doi.org/10.1021/cr400531v.

BusinessWire. (2020). Membranes - Global Market Outlook (2018–2027). https://www.businesswire.com/news/home/20200406005374/en/Global-Membranes-Market-Outlook-to-2027-A-12.68-Billion-Opportunity-Assessment-ResearchAndMarkets.com.

Cath, T. Y., Elimelech, M., McCutcheon, J. R., McGinnis, R. L., Achilli, A., Anastasio, D., … Yip, N. Y. (2013). Standard methodology for evaluating membrane performance in osmotically driven membrane processes. *Desalination*, *312*, 31–38. Available from https://doi.org/10.1016/j.desal.2012.07.005.

Chen, L., Li, Y., Chen, L., Li, N., Dong, C., Chen, Q., … Ci, L. (2018). A large-area free-standing graphene oxide multilayer membrane with high stability for nanofiltration applications. *Chemical Engineering Journal*, *345*, 536–544. Available from https://doi.org/10.1016/j.cej.2018.03.136.

Chen, Z., Luo, J., Hang, X., & Wan, Y. (2018). Physicochemical characterization of tight nanofiltration membranes for dairy wastewater treatment. *Journal of Membrane Science.*, *547*, 51–63. Available from https://doi.org/10.1016/j.memsci.2017.10.037.

Chidambaram, T., Oren, Y., & Noel, M. (2015). Fouling of nanofiltration membranes by dyes during brine recovery from textile dye bath wastewater. *Chemical Engineering Journal*, *262*, 156–168. Available from https://doi.org/10.1016/j.cej.2014.09.062.

Chuntanalerg P., Bureekaew S., Klaysom C., Lau W. J., & Faungnawakij K. (2018). Nanomaterial-incorporated nanofiltration membranes for organic solvent recovery. In *Advanced nanomaterials for membrane synthesis and its applications* (pp. 159–181). doi: 10.1016/B978-0-12-814503-6.00007-0

Dai, R., Han, H., Wang, T., Li, J., Tang, C., & Wang, Z. (2021). Fouling is the beginning: Upcycling biopolymer-fouled substrates for fabricating high-permeance thin-film composite polyamide membranes. *Green Chemistry*. Available from https://doi.org/10.1039/d0gc03340e.

Davood Abadi Farahani, M. H., & Chung, T. S. (2018). Solvent resistant hollow fiber membranes comprising P84 polyimide and amine-functionalized carbon nanotubes with potential applications in pharmaceutical, food, and petrochemical industries. *Chemical Engineering Journal*, *345*, 174–185. Available from https://doi.org/10.1016/j.cej.2018.03.153.

de Grooth, J., Haakmeester, B., Wever, C., Potreck, J., de Vos, W. M., & Nijmeijer, K. (2015). Long term physical and chemical stability of polyelectrolyte multilayer membranes. *Journal of Membrane Science.*, *489*, 153–159. Available from https://doi.org/10.1016/j.memsci.2015.04.031.

Decher, G. (1997). Fuzzy nanoassemblies: Toward layered polymeric multicomposites. *Science*. Available from https://doi.org/10.1126/science.277.5330.1232.

Di Vincenzo, M., Tiraferri, A., Musteata, V. E., Chisca, S., Sougrat, R., Huang, L. B., … Barboiu, M. (2021). Biomimetic artificial water channel membranes for enhanced desalination. *Nature Nanotechnology*, *16*, 190–196. Available from https://doi.org/10.1038/s41565-020-00796-x.

Do, V. T., Tang, C. Y., Reinhard, M., & Leckie, J. O. (2012). Degradation of polyamide nanofiltration and reverse osmosis membranes by hypochlorite. *Environmental Science and Technology*. Available from https://doi.org/10.1021/es203090y.

Duong, P. H. H., Daumann, K., Hong, P. Y., Ulbricht, M., & Nunes, S. P. (2019). Interfacial polymerization of zwitterionic building blocks for high-flux nanofiltration membranes. *Langmuir: The ACS Journal of Surfaces and Colloids*, *35*(5), 1284–1293. Available from https://doi.org/10.1021/acs.langmuir.8b00960.

Elshof, M. G., de Vos, W. M., de Grooth, J., & Benes, N. E. (2020). On the long-term pH stability of polyelectrolyte multilayer nanofiltration membranes. *Journal of Membrane Science.*, *615*, 118532. Available from https://doi.org/10.1016/j.memsci.2020.118532.

Eriksson, P. (1988). Nanofiltration extends the range of membrane filtration. *Environmental Progress*, *7*(1), 58–62. Available from https://doi.org/10.1002/ep.3300070116.

Falca, G., Musteata, V. E., Behzad, A. R., Chisca, S., & Nunes, S. P. (2019). Cellulose hollow fibers for organic resistant nanofiltration. *Journal of Membrane Science*., *586*, 151–161. Available from https://doi.org/10.1016/j.memsci.2019.05.009.

Fritsch, D., Merten, P., Heinrich, K., Lazar, M., & Priske, M. (2012). High performance organic solvent nanofiltration membranes: Development and thorough testing of thin film composite membranes made of polymers of intrinsic microporosity (PIMs). *Journal of Membrane Science*, *401–402*, 222–231. Available from https://doi.org/10.1016/j.memsci.2012.02.008.

Gao, S., Zhu, Y., Gong, Y., Wang, Z., Fang, W., & Jin, J. (2019). Ultrathin polyamide nanofiltration membrane fabricated on brush-painted single-walled carbon nanotube network support for ion sieving. *ACS Nano*, *13*(5), 5278–5290. Available from https://doi.org/10.1021/acsnano.8b09761.

Gao, Z. F., Shi, G. M., Cui, Y., & Chung, T. S. (2018). Organic solvent nanofiltration (OSN) membranes made from plasma grafting of polyethylene glycol on cross-linked polyimide ultrafiltration substrates. *Journal Membrane Science*, *565*, 169–178. Available from https://doi.org/10.1016/j.memsci.2018.08.019.

Gassert F., Landis M., Luck M., Reig P., & Shiao T. (2014). *Aqueduct Global Maps 2.1: Constructing decision-relevant global water risk indicators*. World Resources Institute.

Gorgojo, P., Karan, S., Wong, H. C., Jimenez-Solomon, M. F., Cabral, J. T., & Livingston, A. G. (2014). Ultrathin polymer films with intrinsic microporosity: Anomalous solvent permeation and high flux membranes. *Advanced Functional Materials*, *24*(30), 4729–4737. Available from https://doi.org/10.1002/adfm.201400400.

Gresham, I. J., Reurink, D. M., Prescott, S. W., Nelson, A. R. J., De Vos, W. M., & Willott, J. D. (2020). Structure and hydration of asymmetric polyelectrolyte multilayers as studied by neutron reflectometry: Connecting multilayer structure to superior membrane performance. *Macromolecules*, *53*, 10644–10654. Available from https://doi.org/10.1021/acs.macromol.0c01909.

Guillen, G. R., Pan, Y., Li, M., & Hoek, E. M. V. (2011). Preparation and characterization of membranes formed by nonsolvent induced phase separation: A review. *Industrial and Engineering Chemistry Research*, *50*(7), 3798–3817. Available from https://doi.org/10.1021/ie101928r.

Guo, S., Chen, X., Wan, Y., Feng, S., & Luo, J. (2020). Custom-tailoring loose nanofiltration membrane for precise biomolecule fractionation: New insight into post-treatment mechanisms. *ACS Applied Materials and Interfaces*, *12*(11), 13327–13337. Available from https://doi.org/10.1021/acsami.0c00259.

Haan, T.Y., Chean, L.W., Mohammad, A.W. (2020). Thermo-responsive antifouling study of commercial PolyCera® membranes for POME treatment. *Membrane Water Treatment*, 11, 97–109. Available from https://doi.org/10.12989/mwt.2020.11.2.097.

He, Y., Zhao, D. L., & Chung, T. S. (2018). Na^+ functionalized carbon quantum dot incorporated thin-film nanocomposite membranes for selenium and arsenic removal. *Journal of Membrane Science.*, *564*, 483–491. Available from https://doi.org/10.1016/j.memsci.2018.07.031.

Heinz, O., Aghajani, M., Greenberg, A. R., & Ding, Y. (2018). Surface-patterning of polymeric membranes: Fabrication and performance. *Current Opinion in Chemical Engineering*, *20*, 1–12. Available from https://doi.org/10.1016/j.coche.2018.01.008.

Hołda, A. K., & Vankelecom, I. F. J. (2015). Understanding and guiding the phase inversion process for synthesis of solvent resistant nanofiltration membranes. *Journal of Applied Polymer Science*, *132*(27), 42130. Available from https://doi.org/10.1002/app.42130.

Hu, J., Kim, C., Halasz, P., Kim, J. F., Kim, J., & Szekely, G. (2021). Artificial intelligence for performance prediction of organic solvent nanofiltration membranes. *Journal of Membrane Science*, *619*, 118513. Available from https://doi.org/10.1016/j.memsci.2020.118513.

Huang, S., Wu, M. B., Zhu, C. Y., Ma, M. Q., Yang, J., Wu, J., & Xu, Z. K. (2019). Polyamide nanofiltration membranes incorporated with cellulose nanocrystals for enhanced water flux and chlorine resistance. *ACS Sustainable Chemistry and Engineering*, *7*(14), 12315–12322. Available from https://doi.org/10.1021/acssuschemeng.9b01651.

Huang, T., Puspasari, T., Nunes, S. P., & Peinemann, K. V. (2020). Ultrathin 2D-layered cyclodextrin membranes for high- performance organic solvent nanofiltration. *Advanced Functional Materials*, *30*(4), 1906797. Available from https://doi.org/10.1002/adfm.201906797.

Islam, Md. S., Hassan-uz-Zaman, Md., Islam, Md. S., Clemens, J. D., & Ahmed, N. (2020). Waterborne pathogens. In *Waterborne pathogens* (pp. 463–489). https://doi.org/10.1016/b978-0-12-818783-8.00003-7.

Jimenez-Solomon, M. F., Gorgojo, P., Munoz-Ibanez, M., & Livingston, A. G. (2013). Beneath the surface: Influence of supports on thin film composite membranes by interfacial polymerization for organic solvent nanofiltration. *Journal of Membrane Science*, *448*, 102–113. Available from https://doi.org/10.1016/j.memsci.2013.06.030.

Jimenez-Solomon, M. F., Song, Q., Jelfs, K. E., Munoz-Ibanez, M., & Livingston, A. G. (2016). Polymer nanofilms with enhanced microporosity by interfacial polymerization. *Nature Materials*, *15*, 760–767. Available from https://doi.org/10.1038/nmat4638.

Jin, P., Yuan, S., Zhang, G., Zhu, J., Zheng, J., Luis, P., & Van der Bruggen, B. (2020). Polyarylene thioether sulfone/sulfonated sulfone nanofiltration membrane with enhancement of rejection and permeability via molecular design. *Journal of Membrane Science*, *608*, 118241. Available from https://doi.org/10.1016/j.memsci.2020.118241.

Jin, P., Zhu, J., Yuan, S., Zhang, G., Volodine, A., Tian, M., … Van der Bruggen, B. (2021). Erythritol-based polyester loose nanofiltration membrane with fast water transport for efficient dye/salt separation. *Chemical Engineering Journal*, *406*, 126796. Available from https://doi.org/10.1016/j.cej.2020.126796.

Jin, X., Li, L., Xu, R., Liu, Q., Ding, L., Pan, Y., … Wang, T. (2018). Effects of thermal cross-linking on the structure and property of asymmetric membrane prepared from the polyacrylonitrile. *Polymers*, *10*(5), 539. Available from https://doi.org/10.3390/polym10050539.

Joseph, N., Ahmadiannamini, P., Hoogenboom, R., & Vankelecom, I. F. J. (2014). Layer-by-layer preparation of polyelectrolyte multilayer membranes for separation. *Polymer Chemistry*, *5*(6), 1817–1831. Available from https://doi.org/10.1039/c3py01262j.

Kahrs, C., & Schwellenbach, J. (2020). Membrane formation via non-solvent induced phase separation using sustainable solvents: A comparative study. *Polymer*, *186*, 122071. Available from https://doi.org/10.1016/j.polymer.2019.122071.

Kandambeth, S., Biswal, B. P., Chaudhari, H. D., Rout, K. C., Kunjattu, H. S., Mitra, S., … Banerjee, R. (2017). Selective molecular sieving in self-standing porous covalent-organic-framework membranes. *Advanced Materials*, *29*(2). Available from https://doi.org/10.1002/adma.201603945.

Karan, S., Jiang, Z., & Livingston, A. G. (2015). Sub-10 nm polyamide nanofilms with ultrafast solvent transport for molecular separation. *Science*, *348*(6241), 1347–1351. Available from https://doi.org/10.1126/science.aaa5058.

Kim, D., Livazovic, S., Falca, G., & Nunes, S. P. (2019). Oil-water separation using membranes manufactured from cellulose/ionic liquid solutions. *ACS Sustainable Chemistry and Engineering*, *7*(6), 5649–5659. Available from https://doi.org/10.1021/acssuschemeng.8b04038.

Kim, E. S., Yu, Q., & Deng, B. (2011). Plasma surface modification of nanofiltration (NF) thin-film composite (TFC) membranes to improve anti organic fouling. *Applied Surface Science*, *257*(23), 9863–9871. Available from https://doi.org/10.1016/j.apsusc.2011.06.059.

Kim, J. H., Moon, S. J., Park, S. H., Cook, M., Livingston, A. G., & Lee, Y. M. (2018). A robust thin film composite membrane incorporating thermally rearranged polymer support for organic solvent nanofiltration and pressure retarded osmosis. *Journal of Membrane Science*, *550*, 322–331. Available from https://doi.org/10.1016/j.memsci.2018.01.008.

Krieg, H. M., Modise, S. J., Keizer, K., & Neomagus, H. W. J. P. (2005). Salt rejection in nanofiltration for single and binary salt mixtures in view of sulphate removal. *Desalination*, *171*, 205–215. Available from https://doi.org/10.1016/j.desal.2004.05.005.

Kumar, M., Grzelakowski, M., Zilles, J., Clark, M., & Meier, W. (2007). Highly permeable polymeric membranes based on the incorporation of the functional water channel protein Aquaporin Z. *Proceedings of the National Academy of Sciences of the United States of America*, *104*(52), 20719–20724. Available from https://doi.org/10.1073/pnas.0708762104.

Le Phuong, H. A., Blanford, C. F., & Szekely, G. (2020). Reporting the unreported: The reliability and comparability of the literature on organic solvent nanofiltration. *Green Chemistry*, *22*(11), 3397–3409. Available from https://doi.org/10.1039/d0gc00775g.

Li, G., Liu, B., Bai, L., Shi, Z., Tang, X., Wang, J., … Van der Bruggen, B. (2020). Improving the performance of loose nanofiltration membranes by poly-dopamine/zwitterionic polymer coating with hydroxyl radical activation. *Separation and Purification Technology*, *238*, 116412. Available from https://doi.org/10.1016/j.seppur.2019.116412.

Li, T., Chen, C., Brozena, A. H., Zhu, J. Y., Xu, L., Driemeier, C., … Hu, L. (2021). Developing fibrillated cellulose as a sustainable technological material. *Nature*, *590*, 47–56. Available from https://doi.org/10.1038/s41586-020-03167-7.

Li, X., Xu, Y., Goh, K., Chong, T. H., & Wang, R. (2020). Layer-by-layer assembly based low pressure biocatalytic nanofiltration membranes for micropollutants removal. *Journal of Membrane Science*, *615*, 118514. Available from https://doi.org/10.1016/j.memsci.2020.118514.

Li, Y., Wong, E., Volodine, A., Van Haesendonck, C., Zhang, K., & Van Der Bruggen, B. (2019). Nanofibrous hydrogel composite membranes with ultrafast transport performance for molecular separation in organic solvents. *Journal of Materials Chemistry A*, *7*(33), 19269–19279. Available from https://doi.org/10.1039/c9ta06169j.

Li, Y., Zhu, J., Li, S., Guo, Z., & Van Der Bruggen, B. (2020). Flexible aliphatic-aromatic polyamide thin film composite membrane for highly efficient organic solvent nanofiltration. *ACS Applied Materials and Interfaces*, *12*(28), 31962–31974. Available from https://doi.org/10.1021/acsami.0c07341.

Lin, H., & Ding, Y. (2020). Polymeric membranes: Chemistry, physics, and applications. *Journal of Polymer Science*, *58*, 2433–2434. Available from https://doi.org/10.1002/pol.20200622.

Lin, Z., Zhang, Q., Qu, Y., Lin, Z., Zhang, Q., Qu, Y., … Liu, Q. (2017). LBL assembled polyelectrolyte nanofiltration membranes with tunable surface charges and high permeation by employing a nanosheet sacrificial layer. *Journal of Materials Chemistry A*, *5*, 14819–14827. Available from https://doi.org/10.1039/c7ta03183a.

Ling, S., Qin, Z., Huang, W., Cao, S., Kaplan, D. L., & Buehler, M. J. (2017). Design and function of biomimetic multilayer water purification membranes. *Science Advances*, *3*(4), e1601939. Available from https://doi.org/10.1126/sciadv.1601939.

Liu, F., Wang, L., Li, D., Liu, Q., & Deng, B. (2019). A review: The effect of the microporous support during interfacial polymerization on the morphology and performances of a thin film composite membrane for liquid purification. *RSC Advances*, *9*(61), 35417–35428. Available from https://doi.org/10.1039/c9ra07114h.

Liu, J., Han, G., Zhao, D., Lu, K., Gao, J., & Chung, T. S. (2020). Self-standing and flexible covalent organic framework (COF) membranes for molecular separation. *Science Advances*, *6*(41), eabb1110. Available from https://doi.org/10.1126/sciadv.abb1110.

Liu, S., Wu, C., Hung, W. S., Lu, X., & Lee, K. R. (2017). One-step constructed ultrathin Janus polyamide nanofilms with opposite charges for highly efficient nanofiltration. *Journal of Materials Chemistry A*, *5*(44), 22988–22996. Available from https://doi.org/10.1039/c7ta07582k.

Liu, X., & Bruening, M. L. (2004). Size-selective transport of uncharged solutes through multilayer polyelectrolyte membranes. *Chemistry of Materials*, *16*(2), 351–357. Available from https://doi.org/10.1021/cm034559k.

Liu, Y., Wang, J., Wang, Y., Zhu, H., Xu, X., Liu, T., & Hu, Y. (2021). High-flux robust PSf-b-PEG nanofiltration membrane for the precise separation of dyes and salts. *Chemical Engineering Journal*, *405*, 127051. Available from https://doi.org/10.1016/j.cej.2020.127051.

Liu, Y., Zhu, J., Zheng, J., Gao, X., Tian, M., Wang, X, … Van der Bruggen, B. (2020). Porous organic polymer embedded thin-film nanocomposite membranes for enhanced nanofiltration performance. *Journal of Membrane Science*, *602*, 117982. Available from https://doi.org/10.1016/j.memsci.2020.117982.

Loeb S., & Sourirajan S. (1963). Sea water demineralization by means of an osmotic membrane. In *Saline water conversion—II* (pp. 117–132). https://doi.org/10.1021/ba-1963-0038.ch009.

Low, Z. X., Budd, P. M., McKeown, N. B., & Patterson, D. A. (2018). Gas permeation properties, physical aging, and its mitigation in high free volume glassy polymers. *Chemical Reviews*, *118*(12), 5871–5911. Available from https://doi.org/10.1021/acs.chemrev.7b00629.

Ma, L., Cheng, M., Jia, G., Wang, Y, An, Q, Zeng, X, … Shi, F. (2012). Layer-by-layer self-assembly under high gravity field. *Langmuir: The ACS Journal of Surfaces and Colloids*, *28*(25), 9849–9856. Available from https://doi.org/10.1021/la301553w.

Ma, X. H., Yang, Z., Yao, Z. K., Guo, H., Xu, Z. L., & Tang, C. Y. (2018). Interfacial polymerization with electrosprayed microdroplets: Toward controllable and ultrathin polyamide membranes. *Environmental Science and Technology Letters*, *5*(2), 117–122. Available from https://doi.org/10.1021/acs.estlett.7b00566.

Mancosu, N., Snyder, R. L., Kyriakakis, G., & Spano, D. (2015). Water scarcity and future challenges for food production. *Water*, *7*(3), 975–992. Available from https://doi.org/10.3390/w7030975.

Marchetti, P., Jimenez Solomon, M. F., Szekely, G., & Livingston, A. G. (2014). Molecular separation with organic solvent nanofiltration: A critical review. *Chemical Reviews*, *114*, 10735–10806. Available from https://doi.org/10.1021/cr500006j

Marchetti, P., Peeva, L., & Livingston, A. (2017). The selectivity challenge in organic solvent nanofiltration: Membrane and process solutions. *Annual Review of Chemical and Biomolecular Engineering*, *8*, 473–497. Available from https://doi.org/10.1146/annurev-chembioeng-060816-101325.

Mariën, H., & Vankelecom, I. F. J. (2017). Transformation of cross-linked polyimide UF membranes into highly permeable SRNF membranes via solvent annealing. *Journal of Membrane Science*, *541*, 205–213. Available from https://doi.org/10.1016/j.memsci.2017.06.080.

Marino, T., Russo, F., & Figoli, A. (2018). The formation of polyvinylidene fluoride membranes with tailored properties via vapour/non-solvent induced phase separation. *Membranes*, *8*(3), 71. Available from https://doi.org/10.3390/membranes8030071.

Meng, F., Song, F., Yao, Y., Liu, G., & Zhao, S. (2020). Ultrastable nanofiltration membranes engineered by polydopamine-assisted polyelectrolyte layer-by-layer assembly for water reclamation. *ACS Sustainable Chemistry and Engineering*, *8*(29), 10928–10938. Available from https://doi.org/10.1021/acssuschemeng.0c03318.

Mousavi, S. M., & Zadhoush, A. (2017). Investigation of the relation between viscoelastic properties of polysulfone solutions, phase inversion process and membrane morphology: The effect of solvent power. *Journal of Membrane Science*, *532*, 47–57. Available from https://doi.org/10.1016/j.memsci.2017.03.006.

Nunes, S. P., Culfaz-Emecen, P. Z., Ramon, G. Z., Visser, T., Koops, G. H., Jin, W., & Ulbricht, M. (2020). Thinking the future of membranes: Perspectives for advanced and new membrane materials and manufacturing processes. *Journal of Membrane Science*, *598*, 117761. Available from https://doi.org/10.1016/j.memsci.2019.117761.

NX Filtration B. V. (2020a). WMC110 dNF40. Available from https://nxfiltration.com/app/uploads/WMC110-PVC-U-dNF40-TDS-20200611.pdf (access on 16 March 2021).

NX Filtration B. V. (2020b). WMC110 dNF80. Available from https://nxfiltration.com/app/uploads/WMC110-PVC-U-dNF80-TDS-20200611.pdf (access on 16 March 2021).

Oatley-Radcliffe, D. L., Walters, M., Ainscough, T. J., Williams, P. M., Mohammad, A. W., & Hilal, N. (2017). Nanofiltration membranes and processes: A review of research trends over the past decade. *Journal of Water Process Engineering*, *19*, 164–171. Available from https://doi.org/10.1016/j.jwpe.2017.07.026.

Ong, C., Falca, G., Huang, T., et al. (2020). Green synthesis of thin-film composite membranes for organic solvent nanofiltration. *ACS Sustainable Chemistry and Engineering*, *8*(31), 11541–11548. Available from https://doi.org/10.1021/acssuschemeng.0c02320.

Park, H. B., Kamcev, J., Robeson, L. M., Elimelech, M., & Freeman, B. D. (2017). Maximizing the right stuff: The trade-off between membrane permeability and selectivity. *Science*, *356*(6343), eaab0530. Available from https://doi.org/10.1126/science.aab0530.

Park, S. J., Ahn, W. G., Choi, W., Park, S. H., Lee, J. S., Jung, H. W., & Lee, J. H. (2017). A facile and scalable fabrication method for thin film composite reverse osmosis membranes: Dual-layer slot coating. *Journal of Materials Chemistry A*, *5*(14), 6648–6655. Available from https://doi.org/10.1039/c7ta00891k.

Park, S. J., Choi, W., Nam, S. E., Hong, S., Lee, J. S., & Lee, J. H. (2017). Fabrication of polyamide thin film composite reverse osmosis membranes via support-free interfacial polymerization. *Journal of Membrane Science*, *526*, 52–59. Available from https://doi.org/10.1016/j.memsci.2016.12.027.

Paul, M., & Jons, S. D. (2016). Chemistry and fabrication of polymeric nanofiltration membranes: A review. *Polymer*, *103*, 417–456. Available from https://doi.org/10.1016/j.polymer.2016.07.085.

Pearce, G. K. (2011). Nifty nanofiltration: New developments show promise. *Water and Wastewater International*. https://www.waterworld.com/international/desalination/article/16202187/nifty-nanofiltration-new-developments-show-promise.

Peinemann, K. V., Abetz, V., & Simon, P. F. W. (2007). Asymmetric superstructure formed in a block copolymer via phase separation. *Nature Materials*, *6*, 992–996. Available from https://doi.org/10.1038/nmat2038.

Pulido, B. A., Habboub, O. S., Aristizabal, S. L., Szekely, G., & Nunes, S. P. (2019). Recycled poly(ethylene terephthalate) for high temperature solvent resistant membranes. *ACS Applied Polymer Materials*, *1*(9), 2379–2387. Available from https://doi.org/10.1021/acsapm.9b00493.

Purkait, M. K., Sinha, M. K., Mondal, P., & Singh, R. (2018). Introduction to membranes, *in: Interface science and technology*, 1–37. Available from https://doi.org/10.1016/B978-0-12-813961-5.00001-2.

Qiu, W.-Z., Zhong, Q.-Z., Du, Y., Lv, Y., & Xu, Z.-K. (2016). Enzyme-triggered coatings of tea catechins/chitosan for nanofiltration membranes with high performance. *Green Chemistry*, *18*, 6205–6208. Available from https://doi.org/10.1039/c6gc02039a.

Qiu, X., Yu, H., Karunakaran, M., Pradeep, N., Nunes, S. P., & Peinemann, K. V. (2013). Selective separation of similarly sized proteins with tunable nanoporous block copolymer membranes. *ACS Nano*, *7*(1), 768–776. Available from https://doi.org/10.1021/nn305073e.

Radjabian, M., & Abetz, V. (2020). Advanced porous polymer membranes from self-assembling block copolymers. *Progress in Polymer Science*, *102*, 101219. Available from https://doi.org/10.1016/j.progpolymsci.2020.101219.

Radjabian, M., & Abetz, V. (2015). Tailored pore sizes in integral asymmetric membranes formed by blends of block copolymers. *Advanced Materials*, *27*, 352–355. Available from https://doi.org/10.1002/adma.201404309.

Ramon, G. Z., Wong, M. C. Y., & Hoek, E. M. V. (2012). Transport through composite membrane, Part 1: Is there an optimal support membrane? *Journal of Membrane Science*, *415-416*, 298–305. Available from https://doi.org/10.1016/j.memsci.2012.05.013.

Razali, M., Didaskalou, C., Kim, J.F., Babaei, M., Drioli, E., Lee, Y.M., Szekely, G. (2017). Exploring and exploiting the effect of Solvent treatment in membrane separations. *ACS Applied Materials & Interfaces*, 9, 11279–11289. Available from https://doi.org/10.1021/acsami.7b01879.

Reis, R., Dumée, L. F., Tardy, B. L., Dagastine, R., Orbell, J. D., Schutz, J. A., & Duke, M. C. (2016). Towards enhanced performance thin-film composite membranes via surface plasma modification. *Scientific Reports*, *6*, 29206. Available from https://doi.org/10.1038/srep29206.

Rundquist, E. M., Pink, C. J., & Livingston, A. G. (2012). Organic solvent nanofiltration: a potential alternative to distillation for solvent recovery from crystallisation mother liquors. *Green Chemistry*, *14*, 2197–2205. Available from https://doi.org/10.1039/c2gc35216h.

Sereewatthanawut, I., Lim, F.W., Bhole, Y.S., Ormerod, D., Horvath, A., Boam, A.T., & Livingston, A.G. (2010). Demonstration of molecular purification in polar aprotic solvents by organic solvent nanofiltration. *Organic Process Research & Development*, *14*, 600–611. Available from https://doi.org/10.1021/op100028p

Sforca, M. L., Nunes, S. P., & Peinemann, K. V. (1997). Composite nanofiltration membranes prepared by in situ polycondensation of amines in a poly(ethylene oxide-b-amide) layer. *Journal of Membrane Science*, *135*, 179–186. Available from https://doi.org/10.1016/S0376-7388(97)00141-5.

Shan, L., Gu, J., Fan, H., Ji, S., & Zhang, G. (2017). Microphase diffusion-controlled interfacial polymerization for an ultrahigh permeability nanofiltration membrane. *ACS Applied Materials and Interfaces*, *9*(51), 44820–44827. Available from https://doi.org/10.1021/acsami.7b14017.

Shannon, M. A., Bohn, P. W., Elimelech, M., Georgiadis, J. G., Marĩas, B. J., & Mayes, A. M. (2008). Science and technology for water purification in the coming decades. *Nature*, *452*, 301–310. Available from https://doi.org/10.1038/nature06599.

Sharabati, J. A. D., Guclu, S., Erkoc-Ilter, S., et al. (2019). Interfacially polymerized thin-film composite membranes: Impact of support layer pore size on active layer polymerization and seawater desalination performance. *Separation and Purification Technology*, *212*, 438–448. Available from https://doi.org/10.1016/j.seppur.2018.11.047.

Shi, B., Marchetti, P., Peshev, D., Zhang, S., & Livingston, A. G. (2017). Will ultra-high permeance membranes lead to ultra-efficient processes? Challenges for molecular separations in liquid systems. *Jornal of Membrane Science*, *525*, 35–47. Available from https://doi.org/10.1016/j.memsci.2016.10.014.

Shin, M. G., Kwon, S. J., Park, H., Park, Y. I., & Lee, J. H. (2020). High-performance and acid-resistant nanofiltration membranes prepared by solvent activation on polyamide reverse osmosis membranes. *Journal of Membrane Science*, *595*, 117590. Available from https://doi.org/10.1016/j.memsci.2019.117590.

Shin, M. G., Park, S. H., Kwon, S. J., Kwon, H. E., Park, J. B., & Lee, J. H. (2019). Facile performance enhancement of reverse osmosis membranes via solvent activation with benzyl alcohol. *Journal of Membrane Science*, *578*, 220–229. Available from https://doi.org/10.1016/j.memsci.2019.02.027.

Sholl, D. S., & Lively, R. P. (2016). Seven chemical separations to change the world. *Nature*, *532*(7600), 435–437. Available from https://doi.org/10.1038/532435a.

Soroko, I., Lopes, M. P., & Livingston, A. (2011). The effect of membrane formation parameters on performance of polyimide membranes for organic solvent nanofiltration (OSN): Part A. Effect of polymer/solvent/non-solvent system choice. *Journal of Membrane Science*, *381*(1-2), 163–171. Available from https://doi.org/10.1016/j.memsci.2011.07.027.

Soroko, I., Sairam, M., & Livingston, A. G. (2011). The effect of membrane formation parameters on performance of polyimide membranes for organic solvent nanofiltration (OSN). Part C. Effect of polyimide characteristics. *Journal of Membrane Science*, *381*(1-2), 172–182. Available from https://doi.org/10.1016/j.memsci.2011.07.029.

Surwade, S. P., Smirnov, S. N., Vlassiouk, I. V., Unocic, R. R, Veith, G. M., Dai, S., & Mahurin, S. M. (2016). Correction: Corrigendum:Water desalination using nanoporous single-layer graphene. *Nature Nanotechnology*, *11*(995). Available from https://doi.org/10.1038/nnano.2016.240.

Syed I, G. P., Arun, M. I., & Lakshmi, B. (2020). Synthetic polymeric membranes for advanced water treatment. *Gas Separation, and Energy Sustainability*, 39–52. Available from https://doi.org/10.1016/c2018-0-04133-x.

Szymczyk, A., Fievet, P., & Bandini, S. (2010). On the amphoteric behavior of Desal DK nanofiltration membranes at low salt concentrations. *Journal of Membrane Science*, *355*, 60–68. Available from https://doi.org/10.1016/j.memsci.2010.03.006.

Tan, X., Zhao, W., & Mu, T. (2018). Controllable exfoliation of natural silk fibers into nanofibrils by protein denaturant deep eutectic solvent: Nanofibrous strategy for multifunctional membranes. *Green Chemistry*, *20*(15), 3625–3633. Available from https://doi.org/10.1039/c8gc01609g.

Tarleton, E. S., Robinson, J. P., & Salman, M. (2006). Solvent-induced swelling of membranes - Measurements and influence in nanofiltration. *Journal of Membrane Science*, *280*(1-2), 442–451. Available from https://doi.org/10.1016/j.memsci.2006.01.050.

te Brinke, E., Reurink, D. M., Achterhuis, I., de Grooth, J., & de Vos, W. M. (2020). Asymmetric polyelectrolyte multilayer membranes with ultrathin separation layers for highly efficient micropollutant removal. *Applied Materials Today*, *18*, 100471. Available from https://doi.org/10.1016/j.apmt.2019.100471.

Thompson, K. A., Mathias, R., Kim, D., Kim, J., Rangnekar, N., Johnson, J. R., … Finn, M. (2020). N-Aryl–linked spirocyclic polymers for membrane separations of complex hydrocarbon mixtures. *Science*, *369*(6501), 310–315. Available from https://doi.org/10.1126/science.aba9806.

Thong, Z., Cui, Y., Ong, Y. K., & Chung, T. S. (2016). Molecular design of nanofiltration membranes for the recovery of phosphorus from sewage sludge. *ACS Sustainable Chemistry and Engineering*, *4*(10), 5570–5577. Available from https://doi.org/10.1021/acssuschemeng.6b01299.

Toray Advanced Materials Korea Inc. (2020). Product Specification Sheet. Available from http://www.csmfilter.com (access on 16 March 2021).

Ulbricht, M. (2020). Design and synthesis of organic polymers for molecular separation membranes. *Current Opinion in Chemical Engineering*, *28*, 60–65. Available from https://doi.org/10.1016/j.coche.2020.02.002.

United Nations. (2020). *The United Nations World Water Development Report 2020: Water and climate change*.

Valtcheva, I. B., Marchetti, P., & Livingston, A. G. (2015). Crosslinked polybenzimidazole membranes for organic solvent nanofiltration (OSN): Analysis of crosslinking reaction mechanism and effects of reaction parameters. *Journal of Membrane Science*, *493*, 568–579. Available from https://doi.org/10.1016/j.memsci.2015.06.056.

Van der Bruggen, B., Curcio, E., & Drioli, E. (2004). Process intensification in the textile industry: The role of membrane technology. *Journal of Environmental Management*, *73*(3), 267–274. Available from https://doi.org/10.1016/j.jenvman.2004.07.007.

Van der Bruggen B., Hoek E.M.V., Tarabara V.V. Nanofiltration. In Encyclopedia of membrane science and technology. John Wiley & Sons, Inc.; 2013. Available from https://doi.org/10.1002/9781118522318.

Van Goethem, C., Magboo, M. M., Mertens, M., Thijs, M., Koeckelberghs, G., & Vankelecom, I. F. J. (2020). A scalable crosslinking method for PVDF-based nanofiltration membranes for use under extreme pH conditions. *Journal of Membrane Science*, *611*, 118274. Available from https://doi.org/10.1016/j.memsci.2020.118274.

Vanherck, K., Cano-Odena, A., Koeckelberghs, G., Dedroog, T., & Vankelecom, I. (2010). A simplified diamine crosslinking method for PI nanofiltration membranes. *Journal of Membrane Science*, *353*(1-2), 135–143. Available from https://doi.org/10.1016/j.memsci.2010.02.046.

Ventresque, C., Gisclon, V., Bablon, G., & Chagneau, G. (2000). Outstanding feat of modern technology: The Mery-sur-Oise nanofiltration treatment plant (340,000 m3/d). *Desalination*, *131*(1-3), 1–16. Available from https://doi.org/10.1016/S0011-9164(00)90001-8.

Wang, J. J., Yang, H. C., Wu, M. B., Zhang, X., & Xu, Z. K. (2017). Nanofiltration membranes with cellulose nanocrystals as an interlayer for unprecedented performance. *Journal of Materials Chemistry A*, *5*(31), 16289–16295. Available from https://doi.org/10.1039/c7ta00501f.

Wang, M., Guo, W., Jiang, Z., & Pan, F. (2020). Reducing active layer thickness of polyamide composite membranes using a covalent organic framework interlayer in interfacial polymerization. *Chinese Journal of Chemical Engineering*, *28*(4), 1039–1045. Available from https://doi.org/10.1016/j.cjche.2019.11.007.

Wang, M., Wang, Z., Wang, X., Wang, S., Ding, W., & Gao, C. (2015). Layer-by-layer assembly of aquaporin z-incorporated biomimetic membranes for water purification. *Environmental Science and Technology*, *49*(6), 3761–3768. Available from https://doi.org/10.1021/es5056337.

Wang, L., Zhang, R., Li, J., Zhao, C., Wu, T., & Ji, S. (2015). Highly stable "pore-filling" tubular composite membrane by self-crosslinkable hyperbranched polymers for toluene/n-heptane separation. *Journal of Membrane Science*, *474*, 263–272. Available from https://doi.org/10.1016/j.memsci.2014.09.041.

Werber, J. R., Osuji, C. O., & Elimelech, M. (2016). Erratum: Materials for next-generation desalination and water purification membranes. *Nature Reviews Materials*, 16037. Available from https://doi.org/10.1038/natrevmats.2016.37.

Xiao, H. F., Chu, C. H., Xu, W. T., Chen, B. Z., Ju, X. H., Xing, W., & Sun, S. P. (2019). Amphibian-inspired amino acid ionic liquid functionalized nanofiltration membranes with high water permeability and ion selectivity for pigment wastewater treatment. *Journal of Membrane Science*, *586*, 44–52. Available from https://doi.org/10.1016/j.memsci.2019.05.038.

Xie, W., He, F., Wang, B., Chung, T. S., Jeyaseelan, K., Armugam, A., & Tong, Y. W. (2013). An aquaporin-based vesicle-embedded polymeric membrane for low energy water filtration. *Journal of Materials Chemistry A*, *1*(26), 7592–7600. Available from https://doi.org/10.1039/c3ta10731k.

Xu, G. R., Wang, J. N., & Li, C. J. (2013). Strategies for improving the performance of the polyamide thin film composite (PA-TFC) reverse osmosis (RO) membranes: Surface modifications and nanoparticles incorporations. *Desalination*, *328*, 83–100. Available from https://doi.org/10.1016/j.desal.2013.08.022.

Xu, X., Liu, F., Jiang, L., Zhu, J. Y., Haagenson, D., & Wiesenborn, D. P. (2013). Cellulose nanocrystals vs. cellulose nanofibrils: A comparative study on their microstructures and effects as polymer reinforcing agents. *ACS Applied Materials and Interfaces*, *5*(8), 2999–3009. Available from https://doi.org/10.1021/am302624t.

Yadav, P., Ismail, N., Essalhi, M., & Tysklind, M. (2021). Assessment of the environmental impact of polymeric membrane production. *Journal of Membrane Science*, *622*, 118987. Available from https://doi.org/10.1016/j.memsci.2020.118987.

Yan, F., Chen, H., Lü, Y., Lü, Z., Yu, S., Liu, M., & Gao, C. (2016). Improving the water permeability and antifouling property of thin-film composite polyamide nanofiltration membrane by modifying the active layer with triethanolamine. *Journal of Membrane Science*, *513*, 108–116. Available from https://doi.org/10.1016/j.memsci.2016.04.049.

Ye, W., Liu, R., Chen, X., Chen, Q., Lin, J., Lin, X., … Zhao, S. (2020). Loose nanofiltration-based electrodialysis for highly efficient textile wastewater treatment. *Journal of Membrane Science*, *608*, 118182. Available from https://doi.org/10.1016/j.memsci.2020.118182.

Yu, H., Qiu, X., Moreno, N., Ma, Z., Calo, V. M., Nunes, S. P., & Peinemann, K. V. (2015). Self-assembled asymmetric block copolymer membranes: Bridging the gap from ultra- to nanofiltration. *Angewandte Chemie - International Edition*, *54*(47), 13937–13941. Available from https://doi.org/10.1002/anie.201505663.

Yu, W., Liu, T., Crawshaw, J., Liu, T., & Graham, N. (2018). Ultrafiltration and nanofiltration membrane fouling by natural organic matter: Mechanisms and mitigation by pre-ozonation and pH. *Water Research*, *139*, 353–362. Available from https://doi.org/10.1016/j.watres.2018.04.025.

Zhang, Q. Q., Zhu, Y. J., Wu, J., & Dong, L. Y. (2019). Nanofiltration filter paper based on ultralong hydroxyapatite nanowires and cellulose fibers/nanofibers. *ACS Sustainable Chemistry and Engineering*, *7*(20), 17198–17209. Available from https://doi.org/10.1021/acssuschemeng.9b03793.

Zhang, R., Tian, J., Gao, S., & Van Der Bruggen, B. (2020). How to coordinate the trade-off between water permeability and salt rejection in nanofiltration? *Journal of Materials Chemistry A*, *8*(18), 8831–8847. Available from https://doi.org/10.1039/d0ta02510k.

Zhang, R., Yu, S., Shi, W., Zhu, J., & Van der Bruggen, B. (2019). Support membrane pore blockage (SMPB): An important phenomenon during the fabrication of thin film composite membrane via interfacial polymerization. *Separation and Purification Technology*, *215*, 670–680. Available from https://doi.org/10.1016/j.seppur.2019.01.045.

Zhang, Z., Rahman, M. M., Abetz, C., & Abetz, V. (2020). High-performance asymmetric isoporous nanocomposite membranes with chemically-tailored amphiphilic nanochannels. *Journal of Materials Chemistry A*, *8*(19), 9554–9566. Available from https://doi.org/10.1039/d0ta01023e.

Zhang, Z., Rahman, M. M., Abetz, C., Höhme, A. L., Sperling, E., & Abetz, V. (2020). Chemically tailored multifunctional Asymmetric Isoporous Triblock Terpolymer Membranes for Selective Transport. *Advanced Materials*, *32*(8), 1907014. Available from https://doi.org/10.1002/adma.201907014.

Zhao, D., Kim, J. F., Ignacz, G., Pogany, P., Lee, Y. M., & Szekely, G. (2019). Bio-inspired robust membranes nanoengineered from interpenetrating polymer networks of polybenzimidazole/polydopamine. *ACS Nano*, *13*(1), 125–133. Available from https://doi.org/10.1021/acsnano.8b04123.

Zhao, J., Su, Y., He, X., Zhao, X., Li, Y., Zhang, R., & Jiang, Z. (2014). Dopamine composite nanofiltration membranes prepared by self-polymerization and interfacial polymerization. *Journal of Membrane Science*, *465*, 41–48. Available from https://doi.org/10.1016/j.memsci.2014.04.018.

Zhao, Y., Li, X., Shen, J., Gao, C., & Van Der Bruggen, B. (2020). The potential of Kevlar aramid nanofiber composite membranes. *Journal of Materials Chemistry A*, *8*(16), 7548–7568. Available from https://doi.org/10.1039/d0ta01654c.

Zhao, Y., & Yuan, Q. (2006). A comparison of nanofiltration with aqueous and organic solvents. *Journal of Membrane Science*, *279*, 453–458. Available from https://doi.org/10.1016/j.memsci.2005.12.040

Zheng, J., Liu, Y., Zhu, J., Jin, P., Croes, T., & Volodine, A. (2021). Sugar-based membranes for nanofiltration. *Journal of Membrane Science*, *619*, 118786. Available from https://doi.org/10.1016/j.memsci.2020.118786.

Zhou, Z., Hu, Y., Boo, C., Liu, Z., Li, J., Deng, L., & An, X. (2018). High-performance thin-film composite membrane with an ultrathin spray-coated carbon nanotube interlayer. *Environmental Science and Technology Letters*, *5* (5), 243–248. Available from https://doi.org/10.1021/acs.estlett.8b00169.

Zhu, J., Hou, J., Zhang, R., Yuan, S., Li, J., Tian, M., . . . Van Der Bruggen, B. (2018). Rapid water transport through controllable, ultrathin polyamide nanofilms for high-performance nanofiltration. *Journal of Materials Chemistry A*, *6*(32), 15701–15709. Available from https://doi.org/10.1039/c8ta05687k.

Zhu, Y., Romain, C., & Williams, C. K. (2016). Sustainable polymers from renewable resources. *Nature*, *540*, 354–362. Available from https://doi.org/10.1038/nature21001.

Zhu, Y., Xie, W., Gao, S., et al. (2016). Single-walled carbon nanotube film supported nanofiltration membrane with a nearly 10 nm thick polyamide selective layer for high-flux and high-rejection desalination. *Small*, *12*(36), 5034–5041. Available from https://doi.org/10.1002/smll.201601253.

Zhu, Z., Feng, X., & Penlidis, A. (2007). Layer-by-layer self-assembled polyelectrolyte membranes for solvent dehydration by pervaporation. *Materials Science and Engineering C*, *27*(4), 612–619. Available from https://doi.org/10.1016/j.msec.2005.12.002.

CHAPTER

6

Polymer-based nanoenhanced nanofiltration membranes

Shaghayegh Goudarzi, Nahid Azizi, Reza Eslami and Hadis Zarrin

Nanoengineering Laboratory for Energy and Environmental Technologies, Department of Chemical Engineering, Ryerson University, Toronto, ON, Canada

6.1 Introduction

6.1.1 Introduction to nanoenhanced nanofiltration membranes

Clean water availability is a primary human demand and an essential factor for socio-economic development (UN World Water Development Report 2006 | UN-Water, n.d.). It is vital to reduce the universal burden of water-related diseases to promote the populations' health, productivity, and welfare. Therefore constant approachability to clean drinkable water is globally seen as a chief purpose since it is vital to a society's public health, economic efficiency, and national security (Elimelech & Phillip, 2011). Membrane-based technology carries profuse industrial, municipal, and residential processes and is considered as one of the greatest efficient means of scalable performing separations. NF membranes have a pore size of around 0.001 microns, while this size varies to 0.0001 and 0.01 for reverse osmosis (RO) and ultrafiltration (UF) membranes, respectively. Just like RO membranes, nanofiltration (NF) membranes can proficiently discharge small organic molecules and inorganic salt. More rejection of divalent ions, less rejection of monovalent ions, and high fluxes are the critical features for distinguishing between NF and RO membranes. These characteristics make NF membranes good candidates for wastewater treatment applications, such as seawater desalination (Ang et al., 2020), heavy metal ions removal (Jia et al., 2019), organic dyes separation (Soyekwo et al., 2019), bivalent/monovalent ions removal (Wang, Yang, Wu, Zhang, & Xu, 2017), and ionic liquids recovery (Wang et al., 2017). Notwithstanding the breakthrough technologies in NF membrane science, some challenges still need to be addressed for higher efficiency and improvement of their performance. Various NF modification processes have been reported to improve NF membranes features, which

Advancement in Polymer-Based Membranes for Water Remediation
DOI: https://doi.org/10.1016/B978-0-323-88514-0.00003-6

© 2022 Elsevier Inc. All rights reserved.

essentially fits into two strategies. One is to tune the polymeric membrane material and processing technique by optimizing the polymerization condition (Maruf, Greenberg, & Ding, 2016), and surfactant additive (Xiang, Xie, Hoang, & Zhang, 2013). The other one, as well as the most practical method, is to propose a hydrophilic nanofiller, such as silica (Li et al., 2015), amine-functionalized carbon nanotube (CNT) (Zarrabi, Yekavalangi, Vatanpour, Shockravi, & Safarpour, 2016), and graphene oxide (GO) (Safarpour, Vatanpour, Khataee, & Esmaeili, 2015) into the selective layer [polyamide (PA) layer] of the NF membranes, that is, nanoenhancement of the NF membranes. Nanoenhanced NF membrane technology aims at combining nanotechnology with membrane technology to improve membrane properties and thus increase their performance. Thin-film nanocomposite (TFN) NF membranes comprising an ultrathin separation layer fabricated by the interfacial polymerization (IP) of piperazine (PIP) and trimesoyl chloride (TMC), and mixed matrix NF membranes are the most popular nanoenhanced NF membranes which have been hugely investigated and studied to date. Figs. 6.1 and 6.2 are the two examples of TFN NF and MMM NF membranes, respectively. In the further subsections, these types of nanoenhanced NF membranes will be described in more detail (Hu, Zhang, He, Zhao, & Zhu, 2018; Daraei, Madaeni, Ghaemi, Ahmadi Monfared, & Khadivi, 2013).

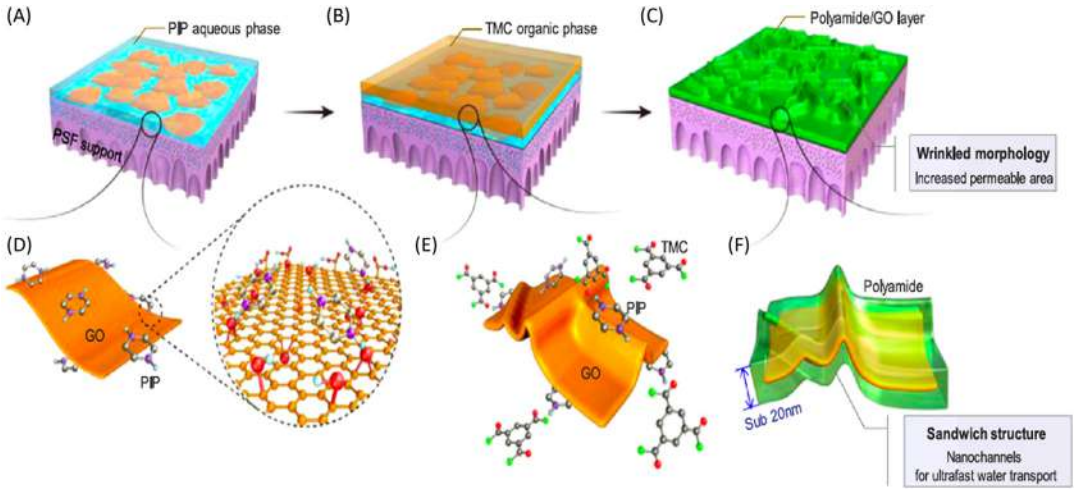

FIGURE 6.1 Graphene oxide (GO) embedded thin-film nanocomposite (TFN) nanofiltration (NF) membrane: schematics of the interfacial polymerization process and the as-prepared PIP-GO ultrathin composite membrane. (A)–(C) Preparation procedure of the PIP-GO membrane. (A) PIP-GO mixed aqueous solution covering on the Polysulfone (PSU) surface. (B) trimesoyl chloride (TMC) organic solution spreading on top of the PIP-GO covered PSU surface. (C) Wrinkled PIP-GO composite membranes. (D)–(F) Corresponding microstructure evolution. (D) PIP molecules attaching on the surfaces of GO nanosheets. (E) PIP monomers diffuse to the interface of two phases and reacted with TMC monomers via a condensation polymerization process. (F) Sandwich-structured membrane with an ultrathin thickness of sub-20 nm. Source: *Reprinted with permission from Hu, R., Zhang, R., He, Y., Zhao, G., & Zhu, H. (2018). Graphene oxide-in-polymer nanofiltration membranes with enhanced permeability by interfacial polymerization. Journal of Membrane Science, 564, 813–819. https://doi.org/10.1016/j.memsci.2018.07.087.*

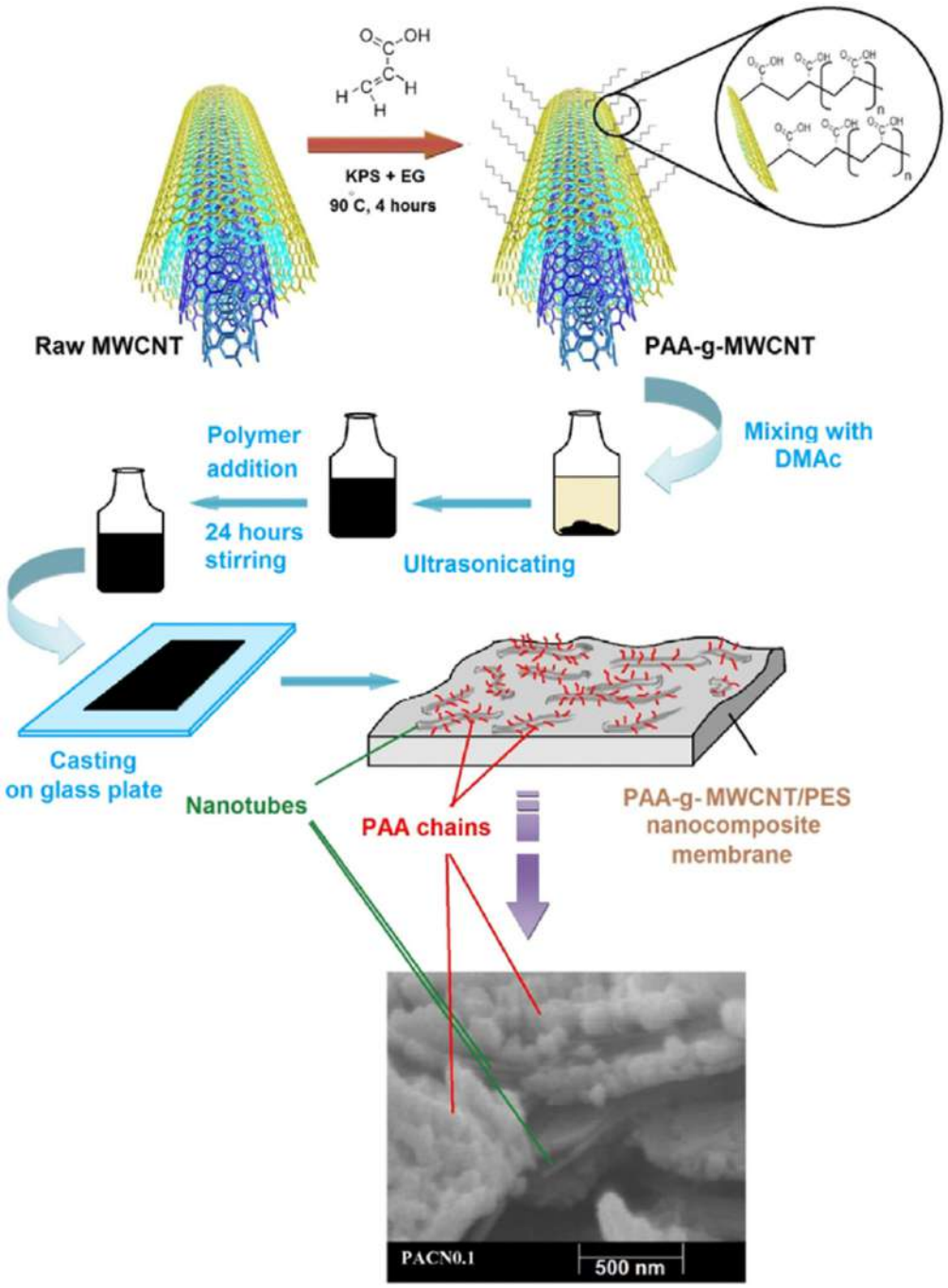

FIGURE 6.2 Schematic procedure of preparation of PAA-g-MWCNT/PES mixed matrix nanofiltration membrane. Source: *Adapted from Daraei, P., Madaeni, S. S., Ghaemi, N., Ahmadi Monfared, H., & Khadivi, M. A. (2013). Fabrication of PES nanofiltration membrane by simultaneous use of multi-walled carbon nanotube and surface graft polymerization method: Comparison of MWCNT and PAA modified MWCNT. Separation and Purification Technology, 104, 32–44. https://doi.org/10.1016/j.seppur.2012.11.004 (with permission from Elsevier).*

6.1.1.1 Preparation of nanoenhanced nanofiltration membranes

Polymeric and ceramic materials are the most commonly used substances for synthesizing NF membranes. Polymers are organic materials owning desirable features, that is, remarkable stiffness, chemical stability, and corrosion resistance capability. These properties make polymer composites great candidates for desalination and water treatment purposes. Most NF membranes are based on polymeric composites (Berber, 2020). A variety of different materials have been applied to fabricate NF membranes. These include various materials for the active layer and support layers (and various combinations of the two) and different elements used as fillers to modify the resultant membrane. Table 6.1 shows the top 20 materials for fabrication and modification of NF membranes. One of the most common materials for the fabrication of NF membranes is PA, typically employed as the membrane's active layer component. Polysulfone (PSU) is the most common materials used as a support layer in pure membranes or coupled with other materials.

TABLE 6.1 The top 20 frequently used polymers for the fabrication of nanofiltration membranes.

Abbreviation	Chemical term
PA	Polyamide
PSU	Polysulfone
PES	Polyethersulfone
PIP	Piperazine
PEI	Polyethyleneimine
PI	Polyimide
PAN	Polyacronitrile
CA	Cellulose acetate
PDMS	Poly(dimethylsiloxane)
PVA	Polyvinyl alcohol
PVDF	Poly(vinylidene fluoride)
CHI	Chitosan
AA	Acrylic acid
PSS	Poly(styrene sulfonate)
P84	Copolyimide
PSr	Polystyrene
PBI	Polybenzimidazole
PEsr	Polyester
PP	Polypropylene
PVP	Polyvinyl pyrrolidone

NF membranes can be classified into two categories typified as "tight" and "loose" NF membranes. Tight NF membranes also can be denoted as (loose) RO. The synthesis procedure is involved with preparing a composite substructure, normally a polysulfone sublayer, on a nonwoven support and a top layer made of mostly PA, which is made by IP. It is a synthesis technique in which the sublayer is immersed in an aqueous amine and further in an organic acyl chloride solution. This reaction produces a thin polymeric layer with excellent separation capacity. By managing the time of reaction, concentration and type of the monomers, top layer characteristics can still be modified to obtain more permeable membranes than RO membranes. On the other hand, loose NF membranes do not employ IP techniques to prepare the top layers (Bruggen, 2013). They are made by phase inversion (PI), which comprises a controlled alteration of a casted polymeric solution from a liquid form into a solid state. For achieving these membranes, the PI method can be done by immersion precipitation, that is, the immersion of the casted polymeric solution in a nonsolvent bath. The nonsolvent diffuses into the polymer-rich phase; simultaneously, the solvent diffuses to the polymer-lean phase. This process proceeds until the solvent is entirely extracted from the polymer-rich phase, leading to the NF membrane formation. The synthesizing procedure can be tuned by applying different factors naming the demixing pace (instantaneous or prolonged demixing), the structure of the casting solution (polymer concentration, the selection of solvent and nonsolvent, the use of nanofiller additives), and the postcasting treatment (curing of the membrane). This can lead to substantial differences and, therefore significant enhanced improvements. Accordingly, researchers (Xie et al., 2018), through their study, investigated the impacts of different casting solvents *N*-methylpyrrolidinone (NMP), *N*,*N*-dimethylacetamide (DMAc), and *N*,*N*-dimethylformamide (DMF) on the properties and performances of polysulfone (PSU) supports, which further was acted as the support for their GO-embedded TFN NF membranes (Fig. 6.3). The results exhibited that the physicochemical properties and PSU support performance were remarkably affected by the casting solvents. PSU support made from NMP exhibited a small surface pore size that restricted the penetration of poly(piperazineamide) (PPA) into the PSU pores, which lead to a defect-free active layer with exceptional permselectivity.

The support top layer's quality defines the membrane's ultimate quality; as such, the flaws and imperfections in the support layer usually induce defects in the top layer as well (Bruggen, 2013).

PSU, which has been broadly used to make porous membranes ranging from MF to NF, is an exemplary membrane material due to its chemical inertness toward the entire pH range, compressive strength, and thermal stabilities (Mulder, 1996). If controllable nanopore sizes of PSU membranes are achieved, NF will demonstrate excellent performance for separating multivalent and monovalent salts. Grafting polymerization on PSU UF membranes is one primary method which has led to access to NF membranes. Homayoonfal et al. achieved a separation efficiency of 91% for removing amoxicillin from pharmaceutical wastewater by application of NF membranes (Homayoonfal & Mehrnia, 2014). Their synthesis process comprised of polymerization of polyacrylic acid layer atop the PSU UF membrane, leading to a decrease in the PSU membrane pore sizes and, finally, the formation of the NF membrane. Wang et al. developed a gallic acid-grafted chitosan (GA-g-CS)/polysulfone composite membrane for dye/water separation (Wang et al., 2020). First, they grafted gallic acid onto the chitosan polymer by a free-radical grafting copolymerization reaction. Next, through the electrostatic

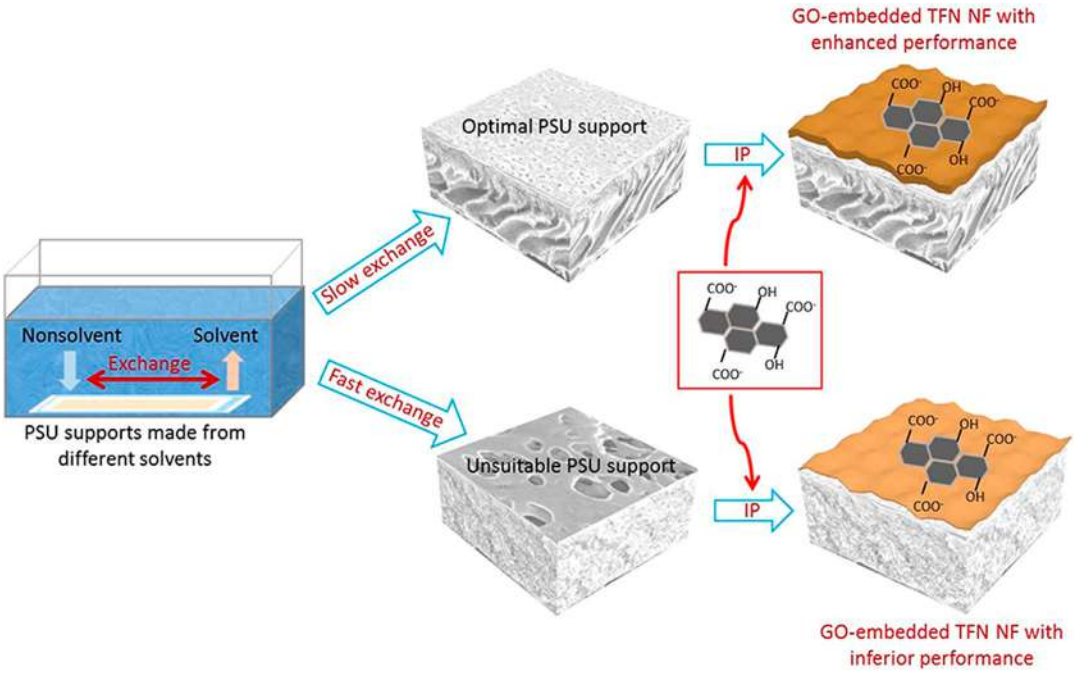

FIGURE 6.3 Graphical illustration of graphene oxide (GO) embedded thin-film nanocomposite (TFN) nanofiltration (NF) membranes. Source: *Reprinted with permission from Xie, Q., Zhang, S., Hong, Z., Ma, H., Liu, C., & Shao, W. (2018). Effects of casting solvents on the morphologies, properties, and performance of polysulfone supports and the resultant graphene oxide-embedded thin-film nanocomposite nanofiltration membranes. Industrial and Engineering Chemistry Research, 57(48), 16464–16475. https://doi.org/10.1021/acs.iecr.8b04515.*

interactions, the gallic acid-grafted chitosan conjugates were codeposited onto the top surface of the PSU substrate to convert the UF membrane to the thin NF membrane (average pore size of 17 nm) as shown in Fig. 6.4 The membrane displayed a high rejection of 97.2% for Congo red with a permeance of 14.0 L h^{-1} m^{-2} bar^{-1} and 97.3% for Evan blue, 97.6% for Acid red 94, and 98% for Alcian blue 8GX based on size segregation while maintaining the permeance of 12.9, 11.9, and 10.9 L h^{-1} m^{-2} bar^{-1}, respectively.

The complicated chemical reactions and multiple preparation steps of the grafting polymerization method, however, restrain their industrial production. Alternatively, a one-step method, nonsolvent-induced phase separation (NIPS) method has been broadly used to prepare PSU NF membranes with asymmetric structures. Nevertheless, one of the concerns in applying this method is the aggregation of nanoparticles (NPs), especially at high concentrations, resulting in a low dispensability in the casting solution and affects membrane properties and performance (Chen, Hu, Xie, & Wang, 2018). Moreover, due to the quick exchange between the solvent and nonsolvent, the skin layer shaped on the surface might not be dense enough to efficiently reject multivalent ions in some cases (Blanco, Sublet, Nguyen, & Schaetzel, 2006). In general, NF is a complex process as it is ruled by the hydrodynamic and interfacial phenomena happening at the membrane surface and

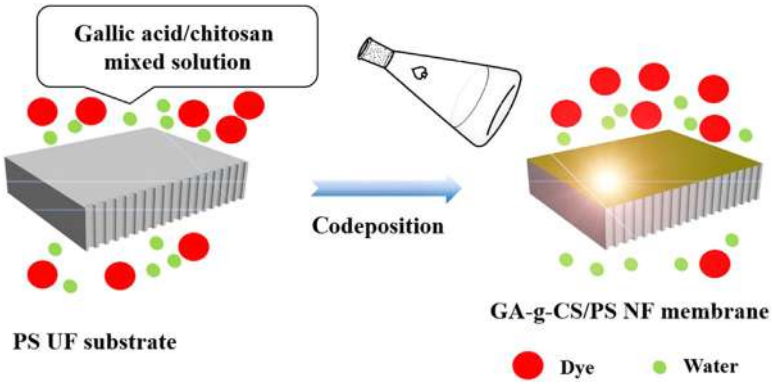

FIGURE 6.4 Schematic graphic of the fabricating process of GA-g-CS/PSU membrane. Source: *Reprinted with permission from Wang, J., Yang, X., Zheng, D., Yao, A., Hua, D., Srinivasapriyan, V., & Zhan, G. (2020). Fabrication of bioinspired gallic acid-grafted chitosan/polysulfone composite membranes for dye removal via nanofiltration. ACS Omega, 5 (22), 13077−13086. https://doi.org/10.1021/acsomega.0c01013. Copy right (2020) American Chemical Society.*

inside the membrane nanopores. The rejection performance in NF membranes is ascribed to several mechanisms; the most well-known of which are steric interactions (or size exclusion), charge exclusion (repulsion), and adsorption to the membrane surface depends on a combination of steric, Donnan, dielectric, and transport effects. The transport of neutral solutes is via the steric mechanism, whereas the classical Donnan effect defines the equilibrium and membrane potential synergies between a charged species and the charged membrane interface. The membrane charge derives from ionizable groups' dissociation on the membrane surface and the ones inside the membrane pores (Mohammad et al., 2015). Despite the breakthrough technologies, some challenges still remain, including improving water permeance while maintaining high rejection and fouling problems in NF membranes. One efficient method to reinforce the separation performances and membrane characteristics is to incorporate different additives such as nanofillers into NF membranes' polymeric matrix. The proper choice of either one additive or the integration of them to leverage from the synergic effectiveness they cause will result in more desirable mechanical properties and thermal stabilities. Fortunately, the advancement in nanotechnology has paved the way for producing nanoenhanced membranes (NEMs), that is, membrane functionalized with discrete nanomaterials/nanofillers. Tuning the NF membranes' polymeric matrix by NEMs is one practical approach to obtain well-performed NF membranes. In what follows we elaborate on different combinations of polymeric and inorganic materials with a focus on the mixed matrix NF membranes and electrospun nanofibrous polymers for nanofiltation applications.

6.2 Mixed matrix polymer-based nanoenhanced nanofiltration membranes

6.2.1 Introduction

Polymeric membranes attracted enormous attention due to their advantages, such as cost-effective fabricating materials and straightforward scale-up. However, there are some drawbacks, including flux decline during their operation stemming from membrane

compaction. Moreover, polymeric membranes have relatively low thermal and chemical stability. Ceramic membranes typically display decent properties such as more stable flux performance, well mechanical strength, high stability at extreme conditions, and higher resistance to organic solvents. Nevertheless, they possess the drawbacks of brittleness in scaling up (Yin & Deng, 2015). To fill these gaps, researchers have been trying to combine the useful features of both polymeric (organic), and ceramic (inorganic) materials in one new material called mixed matrix membranes (MMMs) (Shahzadi, Ahmed, & Siddiq, 2014). Using this methodology, both materials' advantageous traits can be obtained, and the performance of polymeric membranes will be boosted. A simple method to make these MMMs is the inclusion of inorganic materials in polymeric membranes. The linkage between the polymer and inorganic phases is formed by hydrogen bonding, van der Waals forces, and covalent bonds, thus fabricating membranes with different chemistries (Siddique, Rundquist, Bhole, Peeva, & Livingston, 2014). Two of the chief methods for the preparation of the mixed matrix NF membranes are covered in this section as follows: one by dispersing the NPs in the casting solution and preparation of membrane via PI method and the second is by incorporating NPs into the PA layer during IP. These strategies will be discussed hereinafter.

6.2.2 Asymmetric mixed matrix nanofiltration membranes prepared by phase inversion

Throughout the recent decades of intensive research on membrane preparation techniques, various methods have been proposed to generate selective and permeable films. The most studied and practical class of techniques is called PI. It is a method of controlled polymer transformation from a liquid phase to the solid phase. In this process, a casting solution consisting of polymer and solvent is immersed into a nonsolvent coagulation bath. The phase transition occurs due to the interchange of solvent and nonsolvent, which leads to the membrane's formation (Young & Chen, 1995).

Among several approaches of production of MMMs, compounding NPs in the casting solution of the PI technique is one of the most practical approaches. Table 6.2 summarizes some of the reported mixed matrix NF membranes incorporated by NPs and prepared via PI technique.

Researchers could come up with strategies for synthesizing NF membranes by embedment of various nanostructures such as GO (Ahmadi, Qanati, Seyed Dorraji, Rasoulifard, & Vatanpour, 2017; Huang et al., 2021; Kang et al., 2021; Nawaz et al., 2021), CNTs (Vatanpour, Madaeni, Moradian, Zinadini, & Astinchap, 2011; Xue, Xu, Tang, & Ji, 2016; Zinadini, Rostami, Vatanpour, & Jalilian, 2017), metal oxides (Bandehali, Moghadassi, Parvizian, Shen, & Hosseini, 2020; Fathy, Shahawy, El Moghny, & Nafady, 2020; Lee et al., 2008; Mansourpanah, Madaeni, Rahimpour, Farhadian, & Taheri, 2009; Mona Mirmousaei, Peyravi, Khajouei, Jahanshahi, & Khalili, 2019), and metal−organic frameworks (MOFs) (Cai et al., 2020; Gao, Naderi, Wei, & Chung, 2020; Separation, 2020; Yang et al., 2020) into the structure of the polymeric composites. Carbon-based nanomaterials have been employed as an efficient methodology to improve membrane surface hydrophilicity and its antifouling properties. Researchers studied the properties of mixed matrix NF membranes by embedding oxidized multiwalled carbon nanotubes (MWCNTs) into polyethersulfone (PES) as the matrix polymer (Vatanpour et al., 2011). They demonstrated that functionalization of MWCNTs could effectively improve the nanocomposite NF membranes' performance and its antifouling properties stemming from the hydrophilic

TABLE 6.2 Summary of mixed matrix nanofiltration membranes prepared via phase inversion technique.

Polymer	Nanomaterial	Solvent/ nonsolvent	Casting thickness (μm)	Separation performance		Reference
				Features	Description	
PVDF	hBN nanosheets	DMAC/ Distilled water	300	Permeability of 8 × 10^4 L m^{-2} h^{-1} bar^{-1}. For MB, up to 9.3 L g^{-1} of BNNSs, and for pharmaceuticals, up to 14.2 L g^{-1} of BNNSs in the composite membranes.	Permeability improved about 3 orders of magnitude higher than pure polymer. Super filter efficiencies for the dye methylene blue and pharmaceuticals of ciprofloxacin, chlortetracycline, and carbamazepine were achieved.	Liu et al. (2015)
PES + PEG	Different percentages of the GO nanofiller (1, 3, 5wt.%)	NMP Solvent/ Distilled water	–	Filler percentage up to 5wt.% showed higher hydrophilicity of the prepared nanocomposite membranes.	The addition of GO to the membrane significantly improved the pure water flux, salt rejection (NaCl, $MgSO_4$, and Na_2SO_4), heavy metals removal (zinc, cadmium and copper zinc, cadmium and copper ions), and dye removal (MB and MO).	Marjani, Nakhjiri, Adimi, Jirandehi, and Shirazian (2020)
PES (21wt.%)	Quaternized polyethylenimine (QPEI) soft nanoparticles (1.5wt.%).	DMAc/ Distilled water	1.67	The water flux of composite membranes was 75.37 L m^{-2} h^{-1} at 0.6 MPa. Overall flux of reactive red 49 and reactive black 5 dyes could reach a high value of 51 kg m^{-2} h^{-1} for NFM-3 at 0.4 MPa.	Higher water flux was due to the combination of relative loose interface structure and high membrane hydrophilicity. It was observed that increasing the PEI content from 0 to 1.5wt.% reduced the antifouling ration from 62%–7.07%.	Zhu, Zhang, Tian, and Liu (2015)
PES (15wt.%) + SDS surfactant (0.25–5wt.%) as pore forming agent	Titanate nanotubes	DMF	–	Membrane modified with 2.5wt.% SDS and 1wt.% (vs PES) of TNTs showed highest pure water flux.	The hybrid membranes showed superior antifouling properties toward bovine serum albumin (BSA) and sodium alginate (SA) compared with the pure PES one.	Mozia, Czyżewski, Sienkiewicz, and Darowna (2020)
PES (18wt.%) + PVP (1wt.%)	Ag_3PO_4/GO	DMAC/ Distilled water	170	The PES membrane containing 0.5wt.% of Ag_3PO_4/GO exhibited (83%) flux recovery ratio besides (13%) irreversible resistance during filtration of BSA protein. The membrane reduced 72% of viable *Escherichia coli* and 84% of *Staphylococcus aureus* in the bacterial suspensions.	In addition, the nanofiltration performance of the membranes in Lanasol Blue 3R dye separation was investigated. All the nanocomposite membranes had dye rejection higher than 85%.	Barzegar, Zahed, and Vatanpour (2020)

(*Continued*)

TABLE 6.2 (Continued)

Polymer	Nanomaterial	Solvent/ nonsolvent	Casting thickness (μm)	Separation performance		Reference
				Features	Description	
PES (18wt.%) + PVP (1wt.%) + Sodium citrate (0−0.5 wt.%)	Fe_3O_4 nanoparticles	DMAC/ Distilled water	150	The highest pure water flux (47 L m^{-2} h^{-1}) and Na_2SO_4 rejection (68%) was observed.	The pure water flux enhanced due to the increased porosity and mean pore size of membranes and the presence of more hydrophilic groups. The increased rejection can be attributed to creating more active sites for adsorption of Na_2SO_4 and the presence of negative charges and SO_4^{2-} repulsion.	Moghadassi, Moradi, and Bandehali (2020)
PEI (18wt.%) + PVP (1wt.%)	Glycidyl-polyhedral oligosilsesquioxane (POSS) functionalized-GO; PG	DMAC/ Distilled water	120	Pure water flux value of 74.77 L m^{-2} h^{-1}). The blended PEI/PG membranes showed outstanding Na_2SO_4 and Pb $(NO_3)_2$, $CrSO_4$, and Cu $(NO_3)_2$ rejection.	Highest pure water flux was measured for the blended membrane with 0.001wt.% of POSS-GO, whereas it was 51.06 L m^{-2} h^{-1} for the PEI/ GO membrane and 17.63 L m^{-2} h^{-1} for pristine membrane at 4.5 bar pressure.	Bandehali, Moghadassi, Parvizian, Zhang, et al. (2020)
PSU (15wt.%) + PVP (2wt.%)	Silver nanoparticle (AgNP) (2.0wt.%)	NMP/ Deionized water	200	Water flux of membrane containing 2.0wt.% in situ prepared AgNP was 121 ± 48 kg m^{-2} h^{-1}. Decrease in 90% *E. coli* adhered cells was observed compared to the pristine PSU membranes.	The nanocomposite membranes prepared by in situ method exhibited a better antibacterial activity, in comparison to those prepared by ex situ.	Andrade, de Faria, Oliveira, Arruda, and Gonçalves (2015)
PES (21wt.%) + PVP (1wt.%)	Graphene oxide/ TiO_2 (0.05%−0.2%)	DMAC/ Distilled water	150	Water flux value of 45.0 kg m^{-2} h^{-1}.	When the content of rGO/TiO_2 was 0.15wt.%, the water flux reached a maximum value 45.0 kg m^{-2} h^{-1} about twice of that of the bare PES membrane (23.1 kg m^{-2} h^{-1}). Fouling resistance of the membranes evaluated by bovine serum albumin (BSA) solution filtration showed that 0.1wt.% rGO/TiO_2 membrane had the best antifouling property.	Safarpour, Vatanpour, and Khataee (2016)

nature of the functional groups. The salt retention order with optimal value of 0.04wt.% MWCNT was Na_2SO_4 (75%) > $MgSO_4$(42%) > NaCl (17%) after 60 minutes filtration. The rejection of Na_2SO_4 for the PES membrane was 20% but it elevated to about 80%, 70%, and 40% for 0.04, 0.2, and 0.4wt.% of the MWCNT embedded membranes, respectively. In other study, mixed matrix PES membranes were prepared by incorporating Ag_3PO_4/GO nanomaterials into the PES NF membranes (Barzegar et al., 2020). They synthesized different structures by varying the Ag_3PO_4/GO composite wt.% added to the casting solution to achieve the best design and explore the Ag_3PO_4/GO nanocomposite's effect on the antibiofouling and permeation properties of PES NF membranes. The NF efficiency of the membrane toward Lanasol Blue 3R dye rejection was more than 80% for all the membranes. Besides, membrane antibacterial studies indicated that the PES membrane prepared with 0.5wt.% Ag_3PO_4/GO reduced 72% of viable *Escherichia coli* and 84% of *Staphylococcus aureus* in the bacterial suspensions. Researchers also came up with a design for increasing the hydrophilicity and filtration properties of membranes by utilizing PANI and GO to PVDF membranes (Nawaz et al., 2021). PVDF, PANI, and GO were dissolved in DMF and then the solution was stirred and heated at 59°C for 24 hours. The obtained solution was casted on a glass substrate through a doctor blade apparatus. Further, it was immediately immersed in a coagulation bath containing deionized water at 25°C. Fig. 6.5 gives the schematic for developing the membrane by the PI method. Membrane's removal

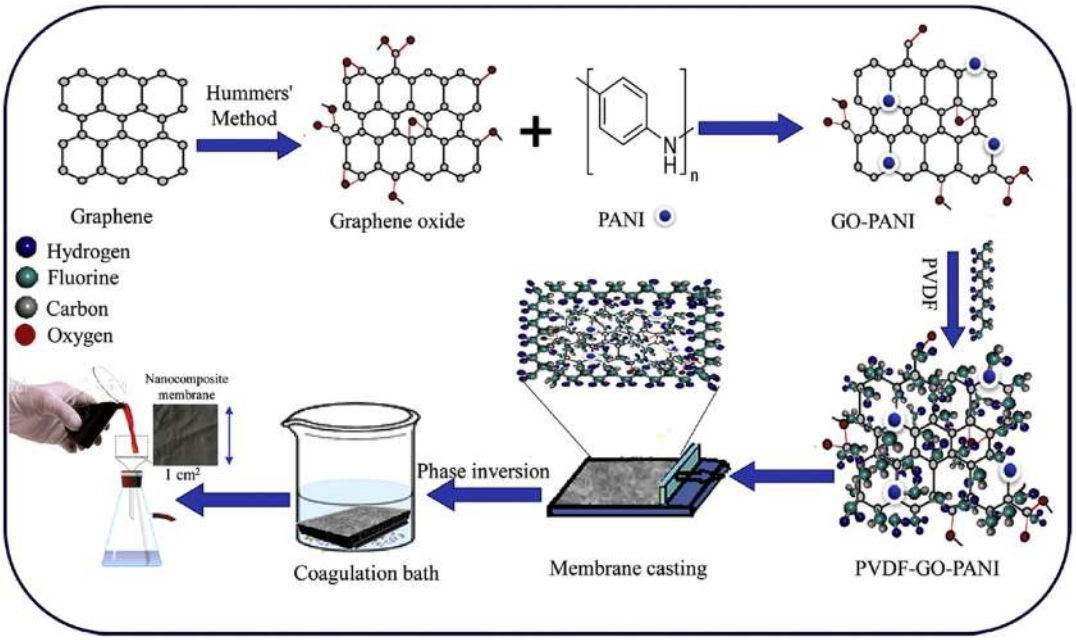

FIGURE 6.5 Schematic demonstration of membrane fabrication by phase inversion method. Source: *Reprinted with permission from Nawaz, H., Umar, M., Ullah, A., Razzaq, H., Zia, K. M., & Liu, X. (2021). Polyvinylidene fluoride nanocomposite super hydrophilic membrane integrated with polyaniline-graphene oxide nano fillers for treatment of textile effluents. Journal of Hazardous Materials, 403, 123587. https://doi.org/10.1016/j.jhazmat.2020.123587.*

efficiency toward removing methyl orange and Allura red is 95% and 98%, respectively. The as-prepared PVDF/PANI/GO membranes are beneficial for practical use in wastewater treatment, specifically for anionic dyes removal from textile industry's effluents.

6.2.3 Thin-film polymer nanocomposite nanofiltration membranes

NF and RO have played an essential role in water purification processes as a promising single-step method for cleaning up the contaminated water from multiple-sized solutes and organic pollutants. Most commercial plants operate with RO and NF with thin-film composite (TFC) membranes at the core of the separation systems. In general, TFC-NF membranes are used in water purification and wastewater treatment in pharmaceutical, food, and biotechnology industries, whereas TFC-RO membranes are mainly used in brackish water and seawater desalination process. Ever since the first TFC membrane was made by Cadotte, Petersen, Larson, and Erickson (1980), a vast of research work has focused on promoting TFCs performances for a breakthrough in industrial membrane expansion in desalination and water treatment applications. TFC, being viewed as the "golden standard" in the membrane industry for 40 years, is created by the IP of a liquid phase-organic phase system to make a thin (0.1−1 μm) selective PA layer deposited on a microporous support substrate membrane as follows. A TFC membrane consists of at least two layers: (1) the top thin selective layer made mostly of PA and (2) a bottom porous support layer mostly made of polysulfone (PSU) or PES (Gohil & Ray, 2017). Fig. 6.6A demonstrates the step-by-step procedure for preparing TFN membranes (Kumar, Khan, & Arafat, 2020). Fig. 6.6B also shows the preparation steps by IP technique for GO-TFN membranes (Lai et al., 2019). GO aqueous solution is deposited on the microporous substrate surface by vacuum filtration followed by a 2-minute contact time with piperazine (PIP) aqueous solution. The PIP solution was then discharged through vacuum filtration and the substrate deposited with GO and PIP later was contacted with trimesoyl chloride (TMC) organic solution for 1 minute to form the PA selective layer. Similar preparation technique, IP, was employed to fabricate silver nanoparticles (AgNPs) incorporated TFN membranes (Fig. 6.6C) (Liu, Qi, An, Liu, & Hu, 2017). AgNPs-functionalized membrane exhibited great antibacterial characteristics without losing their permeability and rejection capability. AgNPs incorporation had negligible impacts on surface roughness and charge of PA layer. Besides, the deposited AgNPs showed a low release rate (leakage) and excellent stability on PA surface.

Novel materials, different IP techniques, and surface modification methods have been adopted for developing what is believed to be the next generation of TFC membrane. One effective approach has been achieved through altering the performance characteristics of TFC via endowing the specific features of nanoscale materials (NMs) into the thin PA layer. Researchers have reported that the enhanced performance of TFC membranes can be gained by incorporating NPs into the PA layer to create TFN membranes (Gholami, López, Rezvani, Vatanpour, & Cortina, 2020). The concept of "thin-film nanocomposite (TFN)," which was first reported in 2007 by Cadotte et al. (1980), attributes to the application of NMs within or at the top surface of a PA layer. In this regard, several NMs prominently such as graphene, CNTs, metal/metal oxides,

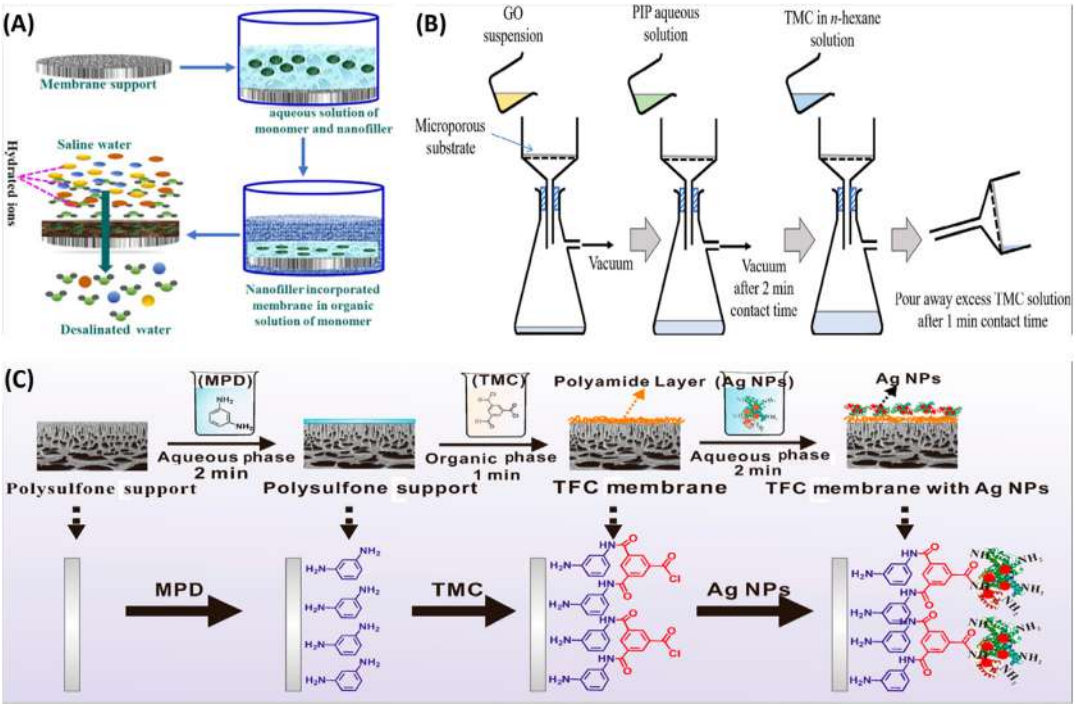

FIGURE 6.6 Schematic illustration of (A) preparing of TFN membranes incorporated with nanofiller by interfacial polymerization. (B) Fabrication of TFN-GO membrane via IP technique. (C) Layer-by-layer interfacial polymerization of polyamide TFN-silver nanoparticles onto polyamide surface. Source: *(A) From Kumar, M., Khan, M. A., & Arafat, H. A. (2020). Recent developments in the rational fabrication of thin film nanocomposite membranes for water purification and desalination. ACS Omega, 5(8), 3792–3800. https://doi.org/10.1021/acsomega.9b03975, Copy right (2020) American Chemical Society Omega. (B) Reprinted with permission from Lai, G. S., Lau, W. J., Goh, P. S., Tan, Y. H., Ng, B. C., & Ismail, A. F. (2019). A novel interfacial polymerization approach towards synthesis of graphene oxide-incorporated thin film nanocomposite membrane with improved surface properties. Arabian Journal of Chemistry, 12(1), 75–87. https://doi.org/10.1016/j.arabjc.2017.12.009. (C) Reprinted with permission from Liu, Z., Qi, L., An, X., Liu, C., & Hu, Y. (2017). Surface engineering of thin film composite polyamide membranes with silver nanoparticles through layer-by-layer interfacial polymerization for antibacterial properties. ACS Applied Materials and Interfaces, 9(46), 40987–40997. https://doi.org/10.1021/acsami.7b12314. Copy right (2017) American Chemical Society.*

and zeolite have been studied for their ability to enhance the TFN membranes' functionality. These enhancements were majorly but not limited to antifouling properties and membrane's breaking selectivity/permeability trade-off properties. Several NPs were demonstrated to endow the TFN membranes with an enhanced water permeability attributed to the hydrophilic nature and the negative surface charges of the incorporated NPs. The introduction of nanomaterials can improve the pore size and porosity, surface hydrophilicity, roughness of the TFN NF membrane and ultimately achieve the purpose of optimizing membranes' performance. In this chapter, we intend to introduce four main categories of these nanomaterials embedded in TFN membranes as follows.

6.2.3.1 *Fabrication of thin-film nanocomposite nanofiltration membranes*

6.2.3.1.1 Graphene oxide-based thin-film nanocomposite nanofiltration membranes

Due to unique characteristics, such as owing plenty of functional groups (oxygen) and atomic thickness, GO nanosheets have received increasing attention for the fabrication of TFN membranes. GO-revised membranes present improved surface hydrophilicity, leading to improved water flux and superior antifouling performance. Moreover, GO is able to interact with low concentration monomers due to the abundance number of functional groups that can interact with both piperazine (PIP) and organic trimesoyl chloride (TMC), two commonly used monomers for synthesis of active layer of NF membranes. Researchers have investigated the effects of the loadings of GO nanosheets in TFN membrane, and illustrated that permeate flux was elevated with increasing the concentration of GO (Yin, Zhu, & Deng, 2016). Their potential mechanism suggested that the GO-incorporated TFN membranes contribute to higher water permeability of the membranes. During the membrane filtration, an increased surface hydrophilicity will facilitate the solubilization of water molecules on membrane surface, and thus improve water permeability. Moreover, the interlayer space inside the layers of GO nanosheets can offer additional short paths for water permeation by PA selective thin-film layer.

In another study, researchers designed and fabricated zwitterionic polymer—poly sulfobetaine methacrylate (PSBMA)—grafted GO and incorporated it as a nanofiller into their TFN casting solutions to produce TFN desalination membranes with enhanced water affinity and antifouling characteristics (Ma et al., 2019) as depicted in Fig. 6.7 Zwitterionic PSBMA grafting improved the GO NPs' water affinity and partially neutralized the GO surface charge. Upon the incorporation of GO-PSBMA 0.3wt.% suspension in MPD (*m*-phenylenediamine), which used for making the aqueous solution for preparing the membrane's active layer (polyamide or PA), the PA membrane exhibited a decrease in water contact angle from 86.6 degrees $\pm$ 13.9 degrees to 58 degrees $\pm$ 6.1 degrees and a raise of zeta potential from -16.5 ± 2.1 to -5.6 ± 1.4 mV under pH 6.4. The PA/GO-PSBMA 0.3wt.% nanocomposite membrane exhibited a doubled water permeation flux compared to the control PA membrane with only 5% and 12% compromise in the rejection of divalent ($MgSO_4$) and monovalent ions (NaCl), respectively. With improved water affinity and reduced surface charge, the PA/GO-PSBMA 0.3wt.% membrane resisted bacterial attachment much better, with an $\sim$80% reduction in cell number than the control pure PA membrane after 48 hours.

One specific challenge regarding GO nanosheets' application is their disability of being homogenously dispersed at high concentrations in the top selective layer of TFN membranes; hence, lessening the GO-enabled TFN membranes' performances (Wang, Zhao, Tian, Li, & Ren, 2018). To overcome these challenges, the functionalized GO nanosheets have been prepared through chemical modifications and applied in the fabrication of TFN membranes. As an instance, GO nanosheets were functionalized via maleic anhydride to obtain functionalized GO thin-film nanocomposite membranes (TFN-MG). Compared with the TFN-GO membrane, the pure water fluxes of TFN-MG membranes showed a 76.7% higher value. The functionalized TFN-MG membrane exhibited superior hydrophilicity, water permeability, antifouling capability, and chlorine resistance over the nonfunctionalized GO TFN membranes. This was achieved potentially due to the enhanced hydrophilicity and charge density of MAH-GO nanosheets due to the increased number of carboxyl groups. TFN-MG membranes also preserved a high salt rejection rate of 97.6% toward Na_2SO_4, comparable to that of TFC-blank membrane (Xie et al., 2017).

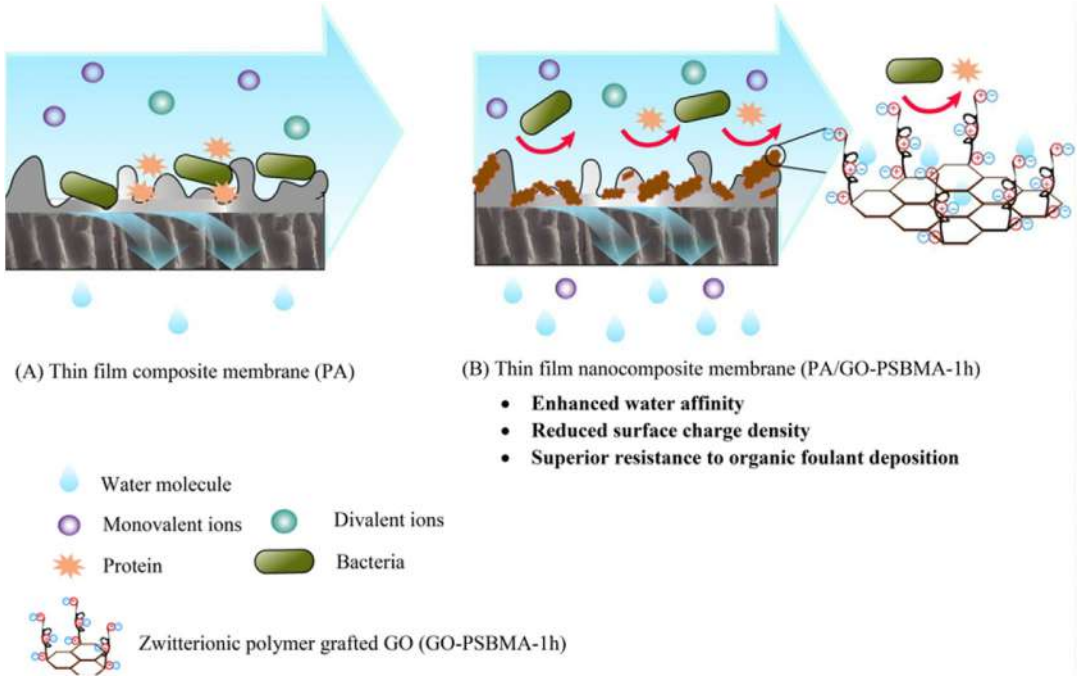

FIGURE 6.7 Schematic illustration of (A) A thin film composite membrane; (B) Thin film nanocomposite membrane incorporated with graphene oxide. Source: *Adapted with permission from Ma, W., Chen, T., Nanni, S., Yang, L., Ye, Z., & Rahaman, M. S. (2019). Zwitterion-functionalized graphene oxide incorporated polyamide membranes with improved antifouling properties. Langmuir: The ACS Journal of Surfaces and Colloids, 35(5), 1513–1525. https://doi.org/10.1021/acs.langmuir.8b02044.*

Another TFN NF membrane was prepared by incorporating sulfonated GO (SGO) nanosheets to the membranes' PA active layer (Izadmehr, Mansourpanah, Ulbricht, Rahimpour, & Omidkhah, 2020). As the result of loading 0.3wt.% of SGO, the water permeability of the functionalized TFN membrane increased to 87.3%, and this membrane was able to remove more than 95% of $MgSO_4$ (Kang, Obaid, Jang, & Kim, 2019). In another study, NH_2-end grafted molecules were induced to the GO TFN membrane structure via the functionalization of GO with triethylenetetramine (TETA). Consequently, the hydrophilicity of GO-TETA-embedded TFN membranes was drastically increased and the MWCO was decreased. The rejection rate toward some industrial dyes was studied; the retention ability of the modified membrane against direct red and Congo red was obtained to be over 99.6%. Therefore successful incorporation of some of functionalized GO nanosheets in the selective layer of TFN membrane is expected to result in higher water flux, enhanced antifouling resistance and improvement in the membrane surface characteristics.

6.2.3.1.2 Carbon nanotube-incorporated thin-film nanocomposite nanofiltration membranes

CNTs have been employed in the fabrication of TFN membranes by means of IP. The application of MWCNTs is explained by their properties, such as chemical strength, distinct

shape–structure, and compatibility with solvents (Andrews & Weisenberger, 2004; Bose, Khare, & Moldenaers, 2010; De Volder, Tawfick, Baughman, & Hart, 2013). The MWCNT–TFN-based membranes should be dispersed in an organic or inorganic solution during the IP reaction to develop such membranes. The inclination of MWCNTs to agglomerate in solvent media gives rise to the defect formation in the membrane surface. Therefore functionalization of MWCNTs by linking some hydrophilic functional groups onto the tube's wall can promote the dispersion ability. Xu et al. functionalized MWCNTs with carboxyl (MWCNTs–COOH), hydroxyl (MWCNTs–OH), and amine (MWCNTs–NH) groups (Xue et al., 2016). Due to the synergistic effect of MWCNT-OH and amino group in PIP monomer in the PA support the MWCNT-OH NF membrane had the highest pure water flux of 41.44 L m^{-2} h^{-1} bar^{-1} and the Na_2SO_4 rejection of 97.6%. MWCNT-NH showed higher rejecting capability and stability than NF MWCNT-COOH due to the strong adhesion of their amino and carboxyl group with the PA support layer. As mentioned before, PES is one of the most notable polymers for TFN membrane preparation in the area of water treatment applications. This stems from prominent chemical thermal and mechanical stabilities as well as an asymmetric structure which can be obtained by the PI method. Nevertheless, hydrophobicity, as a major factor of membrane fouling, is one main downside of PES (Zhao, Xue, Ran, & Sun, 2013). So, coating the PES support by a hydrophilic polymeric layer, membrane fouling can be minimized, and a higher water flux can be achieved. Polyether block amide (PEBA) with hard PA and soft polyether (PE) building blocks is a good candidate for this purpose due to the microbiphasic structure. In research conducted by Mousavi, Asghari, and Mahmoodi (2020), a facile pouring method was utilized to coat a very thin layer of chitosan-wrapped MWCNT (CWNT) incorporated PEBA (selective layer) on porous PES support layer. CWNT-PEBA/PES TFN membrane was then applied for removing Malachite green (MG) dye from water. The effects of adding 0, 0.1, 0.5, 1, and 2wt.% of CWNTs on the morphology and separation properties of the resulting membranes were examined systematically. The oil rejection of PSU/Pebax/2% F-MWCNT membrane is 99.79% and the flux recovery percentage of the 2wt.% F-MWCNT membrane was 97.79%. Fig. 6.8A and B shows cross-sectional FESEM images of PES-PEBA TFC membranes and PES-PEBA-chitosan wrapped MWNTs TFN membranes with 0.1wt.% CWNTs. A thin mixed matrix selective layer with an average thickness of 0.7 μm has developed such that it is overlapped well on the PES sublayer. The distinct split-free boundary between the PES sublayer and the PEBA top layer indicates this compatibility. The porous finger-like structure of PES presents a favorable passageway for selected molecules.

More rigorous studies on the effect of imparting functional groups on MWCNTs performance was studied recently. This research by Gholami et al. (2020), they functionalized aromatic amine MWCNTs (AAF-MWCNTs) and aliphatic amine MWCNTs (AF-MWCNTs) was compared for their performance efficiency toward rejection performance of inorganic pollutants from groundwater and acid and chlorine resistance. Results indicated that water permeates flux, and the arsenic rejection of the AAF–NF membrane improved by 15% compared with typical commercial semiaromatic PA NF membranes. According to these studies, the use of MWCNTs could be a route to increase membrane selectivity. Toxic mono-charged ions as NH_4^+ and NO_3^- reported low rejections values as most commercial NF membranes, and therefore it gives rise to the need to develop new active layers with increased rejections to mono-charged species. Investigation through the development of alternative NPs might be a potential direction.

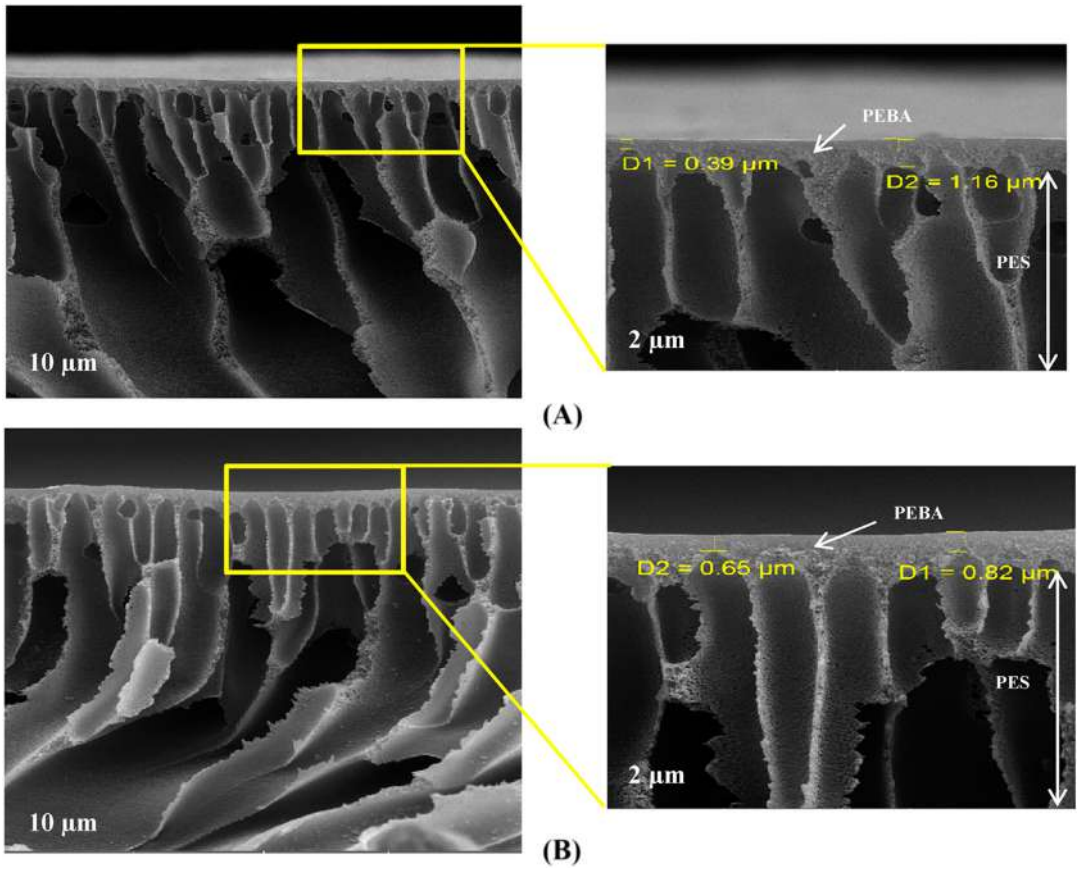

FIGURE 6.8 Cross-sectional FESEM images of (A) PES-PEBA and (B) PES-PEBA-CWNT. Source: *Reprinted with permission from Mousavi, S. R., Asghari, M., & Mahmoodi, N. M. (2020). Chitosan-wrapped multiwalled carbon nanotube as filler within PEBA thin film nanocomposite (TFN) membrane to improve dye removal. Carbohydrate Polymers, 237, 116128. https://doi.org/10.1016/j.carbpol.2020.116128.*

6.2.3.1.3 Metal–organic framework-integrated thin-film nanocomposite nanofiltration membranes

As previously described, the TFN membrane is generated by introducing NPs within the PA active layer via the IP process. Several NPs, other than the above-mentioned categories, including TiO_2 (Mollahosseini & Rahimpour, 2014), SiO_2 (Wei et al., 2019), and Ag (Singh, Ohlan, Saini, & Dhawan, 2008), have been employed to generate TFN membranes. Studies suggest that the incorporated NPs could improve membrane permeability by providing water channels within the nanoparticle pores or on the hydrophilic surfaces. Still, however, some problems predominate that threaten the performance of TFN membranes, such as the aggregation of these NPs, the incompatibility between rigid NPs and the polymer matrix, as well as the nonselective voids that deteriorate membrane selectivity. These demerits compelled researchers to exploit alternative categories of nanomaterials naming MOFs. Recently, MOFs have emerged as a novel substitute to conventional NPs. MOFs are a

type of organic–inorganic hybrid porous crystalline materials. With the assistance of metal ions—organic linkers bonds, MOFs exhibit high porosity, regular pore size, and tunable morphology, which are well qualified for separation purposes (Li et al., 2017). More importantly, organic–inorganic hybrid framework provides MOFs with better affinity with the polymeric matrix than fully inorganic NPs (Ma, Peh, Han, & Chen, 2017). ZIF-8, MIL-53(Al), NH_2-MIL-53(Al), and MIL-101(Cr) MOF-incorporated membranes were used for organic solvent NF (Sorribas, Gorgojo, Téllez, Coronas, & Livingston, 2013). The performance was evaluated on the basis of methanol (MeOH) and tetrahydrofuran (THF) permeances and rejection of styrene oligomers. When MOFs were embedded into the PA layer, MeOH and THF permeance increased and the rejection persisted higher than 90% (molecular weight cut off of less than 232 and 295 g mol^{-1} for MeOH and THF, respectively) through all the membranes. Similarly, other MOF types, such as HKUST-1 (Campbell, Davies, Braddock, & Livingston, 2015), UiO-66 (Qiao et al., 2012), ZF-11 and MIL-68(Al) (Echaide-Górriz, Sorribas, Téllez, & Coronas, 2016), and ZIF-8, ZIF-93, and UiO-66 (Paseta, Navarro, Coronas, & Téllez, 2019) were employed for organic solvent NF. The MOF-based NF membranes for water treatment began to emerge after year 2014 (Zhang et al., 2014). PA/ZIF-8 NF membranes were fabricated to remove dye from water (Wang et al., 2015). Membranes integrated with MOFs were prepared. Three different fabrication methods for dispersing ZIF-8 NPs were used to prepare the PA/ZIF-8 membranes in an aqueous phase, organic and in both the aqueous and organic phases, respectively. The PA/ZIF-8 membrane prepared in both phases revealed the best performance. The flux increased to two times that of the pure PA membrane, and the rejection was approximately 100%. They concluded that the membrane performance enhancement was achieved by the following factors: high ZIF-8 loading in the membrane composition, fair ZIF-8 distribution, and fewer ZIF-8 agglomerations in the PA/ZIF-8 selective layer. MOF-TFN membranes were also employed for desalination (Kadhom, Hu, & Deng, 2017; Zhu et al., 2017) and the result showed MOF NPs could reinforce the membrane water permeability while maintaining its selectivity.

Despite all the excellence, MOF materials' embedment in membranes for water treatment applications is limited to some key factors:

1. Precise choice of appropriate MOF. Selection of the appropriate MOF type should be accomplished by considering an ideal MOF which have high hydrophilicity, good water stability, moderate particle size, appropriate window size, and suitable compatibility with the substrate or PA layer.
2. The synthesis procedure should take place under mild and green conditions to avoid health and environmental risks.
3. A comprehensive perception of MOFs interaction with membrane polymers, which are a function of both MOF type and membrane fabrication method. Filling these knowledge gaps leads us to predict the properties of MOF-based TFN membranes, delivering smart membrane systems on the basis of both MOF and polymer functionalities.

6.2.3.1.4 Nanohybrid structure-based thin-film nanocomposite membranes

As discussed throughout the previous subsections, TFN membranes' performance with embedded nanomaterials has been considerably reinforced TFN membrane's filtration processes. We discussed that the critical physicochemical properties of TFN membranes could

notably improve by applying different nanomaterials. NPs each have a unique role in shaping the polymer membrane structures to modify the polymer-free volume characteristics by generating solvent pathways at the interface of the polymer matrix with the nanofiller. Their interesting properties are not limited to their individual impacts. Nanomaterials can also demonstrate synergistic effects when combining together. GO, for instance, is widely utilized for the fabrication of different hydrophilic membranes (Fathizadeh, Tien, Khivantsev, Chen, & Yu, 2017; Lai et al., 2016; Yin et al., 2016). The gaps between the GO sheets can act as a network of interconnected channels that aid the membranes' flux. Researchers have investigated the effects of the loadings of GO nanosheets in TFN membrane, and illustrated that permeate flux was increased with increasing the concentration of GO (Yin et al., 2016). However, the interactions between GO sheets, such as the ones through pi−pi interactions, compact the graphene-based films and narrow down the channel-like network, which adversely affects the membrane's permeation. Moreover, GO nanosheets' efficiency has been restricted due to its collapse of the two-dimensional channels. Injecting rigorous NPs onto the GO sheets prevents the collapse of the lamellar structure, generates spacious channels between the GO sheets and facilitates molecules permeation (Li et al., 2011). The GO−SiO_2 incorporated PA NF membrane was produced by the IP reaction between piperazine and trimesoyl chloride on a polysulfone support surface (Liu et al., 2019). For enhancing the water flux and antifouling properties, GO − SiO_2 nanocomposites were dispersed in piperazine solution. The composition of 0.01wt.% GO − SiO_2/TFN revealed the superior separation performance that the water flux was 43.55 L m^{-2} h^{-1} and salt rejection for NaCl, Na_2SO_4, $MgSO_4$ were 40.7%, 93.2%, 82.4%, respectively. Fig. 6.9A reveals the synthesis procedure; first, the mixed aqueous solution containing PIP (2wt.%) and different nanomaterials concentrations (0 − 0.02wt.%) was poured on the PSU support membrane's upper surface. With a soft rubber roller, the aqueous solution was removed until there were no aqueous droplets on the upper surface. Subsequently, the PSU membrane was coated between two acrylic frames by 0.01% (wt./v) TMC/*n*-hexane solution. After 1 minute, the excess TMC/*n*-hexane solution was discharged. For more polymerization, the fabricated membranes were posttreated by storing them under thermal conditions for 5 minutes at 80°C. The study revealed that SiO_2 was uniformly dispersed on the GO nanosheets and effectively lessened NPs' aggregation in the polymer matrix. At the same time, the interlayer spacing of GO can be enlarged by SiO_2, providing a unique channel for the water transmembrane.

Later, through another research study, the deposition of TiO_2 NPs on GO nanosheets was done. GO decorated with TiO_2 nanohybrids (TiO_2@rGO) were synthesized and incorporated into TFN membrane for organic solvent NF processes (Abadikhah et al., 2019). Fig. 6.9B demonstrates the preparation procedure TiO_2 and GO mixture were stirred and then transferred to microwave for 5 minutes at a power of 600 W. Microwave irradiation formed the rGO sheets, which in fact offered enough active sites of the GO sheets for TiO_2 NP decoration. For TFN membranes fabrications, the amino-functionalized TiO_2@rGO nanohybrids were dispersed in an aqueous solution employing an ultrasonic homogenizer for 30 minutes, followed by IP. Integration of TiO_2 into GO nanosheets enabled them to take full advantage of every aspect of nanostructures; they used GO for solvent channelization and TiO_2 for its super hydrophilicity. The incorporation of TiO_2@rGO altered the roughness by altering the mechanism of IP. The nanohybrids' hydrophilic nature led to a

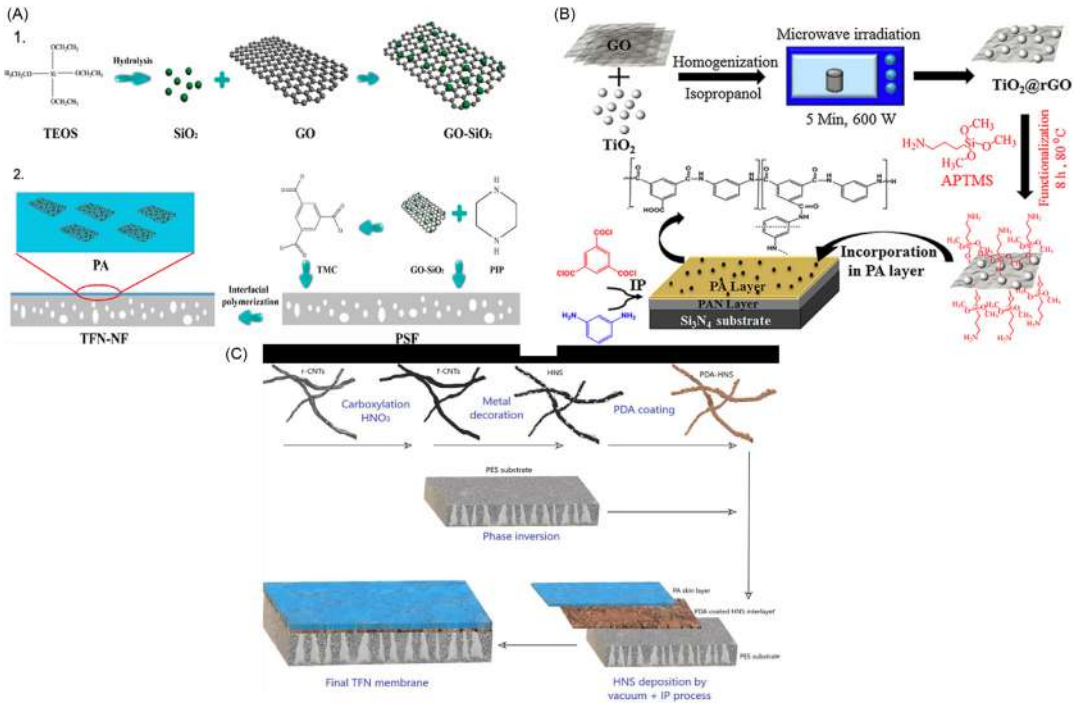

FIGURE 6.9 Schematic illustration of the fabrication of (A) (1) GO − SiO_2 nanocomposites and (2) GO − SiO_2/TFN-NF membrane. (B) TiO_2@rGO and incorporated TiO_2@rGO-TFN membrane. (C) Polydopamine-coated metals/carbon-nanostructures TFN membranes. *TFN*, thin-film nanocomposite; *NF*, nanofiltration. Source: *(A) Reprinted with permission from Liu, Y., Liu, J., Jiang, Y., Meng, M., Ni, L., Qiu, H., … Liu, H. (2019). Synthesis of novel high flux thin-film nanocomposite nanofiltration membranes containing GO-SiO2 via interfacial polymerization. Industrial and Engineering Chemistry Research, 58(49), 22324–22333. https://doi.org/10.1021/acs.iecr.9b03228. (B) Adapted with permission from Abadikhah, H., Kalali, E. N., Behzadi, S., Khan, S. A., Xu, X., Shabestari, M. E., & Agathopoulos, S. (2019). High flux thin film nanocomposite membrane incorporated with functionalized TiO2@reduced graphene oxide nanohybrids for organic solvent nanofiltration. Chemical Engineering Science, 204, 99–109. https://doi.org/10.1016/j.ces.2019.04.022. (C) Adapted from Al Aani, S., Haroutounian, A., Wright, C.J., & Hilal, N. (2018). Thin film nanocomposite (TFN) membranes modified with polydopamine coated metals/carbon-nanostructures for desalination applications. Desalination, 427, 60–74. https://doi.org/10.1016/j.desal.2017.10.011.*

considerable improvement of the wettability of the membrane surface and facilitated the permeability and polar solvent. The incorporation of TiO_2@rGO nanohybrids also improved the antifouling features and the rejection performance of the TFN membranes.

Furthermore, for improving the IP method to obtain higher water permeate, the hybrid nanostructure (HNS) of CNT/metallic NPs (Ag, TiO_2, Al_2O_3, Fe_2O_3) was prepared to fabricate TFN membranes for water desalination application (Al Aani, Haroutounian, Wright, & Hilal, 2018). Fig. 6.9C pictures a general scheme of the TFN preparation. The suspension of polydopamine (PDA) coated metals/carbon nanostructures was prepared and applied to deposit on the support membrane through vacuum filtration, forming a thin layer on the top surface. The MPD, aqueous solution, was then poured carefully to wet the deposited thin layer for 2 minutes. Then, vacuum pressure was applied again to remove excess solution from the

surface and wet the pores' internal wall. TMC in *n*-hexane, organic solution, was reacted with the top surface of the MPD-wetted substrate for 45 seconds. After the IP process, the membrane was rinsed with about 50 mL *n*-hexane to remove unreacted monomers, crosslinked in the oven at 70°C for 15 minutes and finally, stored in DI water. These four different metals/metal oxides were first deposited on the nanotube surfaces of CNTs and then coated with a PDA layer. Next, by vacuum filtration a thin layer of HNS was deposited on a porous substrate membrane and the PA layer was adjusted to entirely cover and robustly fix the HNS interlayer in order to produce a defect-free TFN membrane. The pure water flux was doubled for the TFN membrane compared to that of the TFC membrane without changing the permeability/selectivity trade-off relationship. Besides, greater than 90% monovalent removal and 94% divalent salts removals were obtained.

These studies show that introducing a second nanomaterial component to a TFN NF membrane's composition can positively affect the whole efficiency of the membrane. This phenomenon derives from the synergistic effect between the hybrid nanostructured materials. For preparing such TFN membranes incorporated with HNs, the nanomaterials can:

1. be added to the aqueous solution followed by the IP technique (Fig. 6.9A and B);
2. be coated by a thin-film polymer to create an intermediate layer between the support layer and the selective layer, a sandwiched layered structure (Fig. 6.9C).

The unique properties of HNS improve the membrane performance in terms of water permeability and salt rejection. However, the loading of these nanomaterials into the selective layer of membranes has always an optimum value as expected. Otherwise, the higher loading of these materials to the membrane's composition will decrease both water permeability and salt rejection due to the dense selective layer formation (Hibrid et al., 2017).

6.3 Electrospun nanofibrous polymers for nanofiltration applications

6.3.1 Introduction to electrospinning

The electrospinning technique can be considered as one of the efficient processes for producing fibers in micro- to nanosized fibers. This process is simply happening by pumping the polymer solution through the needle and applying a high voltage to create an electric field between a needle and collector. Then fiber electrospinning will start by initiating the jet from the needle tip to the collectors and will end by solidifying these macro/nanofibers on the collector (Mokhena, Jacobs, & Luyt, 2015; Ramakrishna & Shirazi, 2015; Ray, Chen, Nguyen, et al., 2016).

During the initiation of the jet, a charged droplet of polymer solution will form, which elongates toward the electric field to form a Taylor cone. This process enables us to control the aspect ratio (length/diameter) and morphology of nanofibers by adjusting the proper parameters related to the operation, polymer solution, and environmental conditions. This fact will lead to optimizing the pore-size distribution, porosity, surface area, smoothness of the fibers (beaded fibers or smooth fibers) and hydrophilicity/hydrophobicity (Feng et al., 2008; Zhao, Zheng, Wang, Zhang, & Han, 2012).

The role of each parameter in electrospinning process will be elaborated herein. The polymer solution parameter has a crucial impact on the diameter, smoothness, and morphology of the formed fibers. Moreover, the polymer solution directly defines viscosity and surface tension, which play an essential role in getting beaded or smooth fibers. These parameters can be discussed in terms of polymer molecular weight and concentration, conductivity, surface tension, and viscosity (Bhardwaj & Kundu, 2010; Liao, Loh, Tian, Wang, & Fane, 2018).

Too much low molecular weight or low concentration of polymers in the solutions results in a lack of physical entanglements and the deformation polymer network. Therefore the formed fibers will have resulted in the beaded form (Eda & Shivkumar, 2007; Khalf & Madihally, 2017; Stachewicz et al., 2017). Shenoy et al. in 2005 determined a condition for having smooth fibers based on solution entanglement number (Xue, Wu, Dai, & Xia, 2019):

$$(n_e)_{sol} = \frac{M_w}{(M_e)_{sol}} = \frac{\varnothing_p.M_w}{M_e} \tag{6.1}$$

where M_w, M_e, and $\varnothing_p$ are the molecular weight of the polymer, solution entanglement molecular weight, and the polymer volume fraction. Shenoy has proposed that whenever the solution entanglement number is between 2 and 3.5, the formed fibers will be beaded form. When this number is higher than 3.5, the smooth fibers will be obtained (Munir, Suryamas, Iskandar, & Okuyama, 2009; Xue et al., 2019).

On the other hand, there is a reverse proportionality between M_w and polymer solubility and direct promotionally between M_w and physical properties such as viscosity, flexibility, etc. Therefore for obtaining an ideal electrospun fiber, a polymer solution with the optimized property between the highest possible polymer fraction and optimized viscosity is needed. It is worth mentioning that beaded forms of fibers are happening due to the breakup of capillary waves below a critical concentration (Ghorani & Tucker, 2015; Shenoy, Bates, & Wnek, 2005). Therefore it is recommended to have a polymer solution with a concentration above the critical concentration, C^*, whereby the overlapping of polymer chains start. In addition, increasing in viscosity is causing higher fiber diameter, and lower orientation, crystallinity, and strength (Lasprilla-Botero, Álvarez-Láinez, & Lagaron, 2018; Lim, Tan, & Ng, 2008; Mendes, Stephansen, & Chronakis, 2017; Qasim et al., 2018; Sukigara, Gandhi, Ayutsede, Micklus, & Ko, 2003).

Another affecting parameter is conductivity. In general, by increasing the solution conductivity, the fiber diameter decreases. This conductivity can be controlled by the type of polymer, the type of solvent, and ionic salts. Wang et al. have studied this effect by adding sodium chloride salt to the polymer solution of polyethylene oxide. They have shown that by adding an optimum amount of this salt, the beads have been disappeared, and the smooth and uniform nanofibers of PEO have been achieved (Wang, Wang, & Wang, 2014).

Moreover, surface tension is another parameter that can affect the uniformity of the fibers. As the surface tension increases, the jet instability increases and therefore the electrospinning is prevented. Zuo et al. (2005) showed that increasing surface tension at a constant condition caused beaded fibers morphology. The summary of the effect of operation and environmental parameters on the electrospinning process and nanofibers have been shown in Table 6.3.

TABLE 6.3 Summary of the effect of operation and environmental parameters on the electrospinning process (Bhardwaj & Kundu, 2010; Ghorani & Tucker, 2015; Ray, Chen, Li, Nguyen, & Nguyen, 2016; Xue et al., 2019).

Parameter	Effect
Operational conditions	
Applied voltage	High voltage delivers needed charges and electrostatic repulsive force. In some polymers causes lower fiber diameter and in some other like PEO does not affect. Too much higher voltage decreases the flight time of fiber, resulting in the lower stretch before deposition on the collector.
Solution flow rate	There is an optimum flow rate. Deviation from that either decreasing or increasing will result in beaded fiber and/or higher diameter.
Needle tip diameter	There is an optimum flow rate. Deviation from that either decreasing or increasing will result in beaded fiber and/or higher diameter.
Collector rotating speed (for cylindrical collectors)	Increasing the rotating speed will increase stretching before deposition and more orientation of fibers on the collector.
Collector electrode	Often aluminum is a common substrate for collecting the fibers. Another conductive substrate such as conductive cloth, mesh and paper, gridded bare, etc., have been used for getting aligned fiber.
Distance (needle to collector)	The distance is controlling the fiber diameter and beaded form morphology. By increasing the distance, the diameter is first decreasing, and then it will increase due to the existence of optimum distance to favor the best solvent evaporation time.
Environmental conditions	
Temperature	Temperature can affect the solvent volatility, surface tension, and viscosity. Some studies showed a reduction in fiber diameter for polyamide-6 and cellulose acetate/poly(vinyl pyrrolidone) by increasing the temperature.
Humidity	Controlling the humidity can help to produce modified morphology of fibers by introducing pores to the surface. Also, very low humidity will speed up the solvent's evaporation and cause more often clogging of the needle tip.

6.3.2 Electrospun nanofiber application in nanofiltration

Electrospun membranes' pore sizes are in ranges of hundred nanometers that are too big to be used as nanofilters (Ahmed, Lalia, & Hashaikeh, 2015). Therefore the further modification should be considered in order to decrease pore sizes. Moreover, pore size and distribution quantification are crucial factors for evaluating the rejection percentage from feed water. The distribution of pore size can show the potential of the membrane for removing target substances from water. On the other hand, the surface charge of the membrane can greatly impact the removal procedure. For example, the negatively charged membranes are the candidate for negatively charged molecular rejection. In other words, solute rejection is highly correlated by the charge interaction of the membrane and solute (Lee et al., 2002).

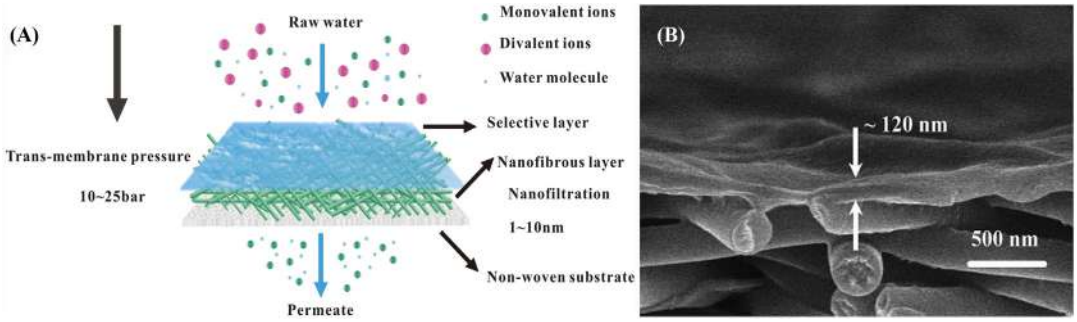

FIGURE 6.10 (A) Schematic of nanofiltration membrane using nanofibrous layer and (B) cross section of a membrane fabricated by interfacial polymerization method for nanofiltration. Source: *A: Reprinted by permission from Liu, Q., Chen, Z., Pei, X., Guo, C., Teng, K., Hu, Y., … Qian, X. (2020). Applications, effects and the prospects for electrospun nanofibrous mats in membrane separation. Journal of Materials Science, 55, pages 893–924 (2020). B: Reproduced from Yang, Y., Li, X., Shen, L., Wang, X. and Hsiao, B.S. (2017) with permission from the Royal Society of Chemistry. A durable thin-film nanofibrous composite nanofiltration membrane prepared by interfacial polymerization on a double-layer nanofibrous scaffold. RSC Adv.,2017,7,18001–18013.*

Thin-film nanofiber composite (TFC) membranes are the technique that the electrospun nanofiber substrates have been used to fabricate an NF membrane. In this design, the nanofiber support layer should satisfy the structural properties such as low thickness, high porosity, hydrophilicity, low curvature, and mechanical strength to tolerate crossflow pressure (Saleem, Trabzon, Kilic, & Zaidi, 2020). In addition, a selective layer can also be called the active layer, enhancing the retention effect of the membrane and selective permeability. Crosslinking and IP are two of the most well-known methods for creating active layers (Ahmed et al., 2015; Saleem et al., 2020). Based on this method, TFC membranes with the nanofiber supporting layers have attracted attention to a promising approach for modifying the electrospun nanofiber membranes (ENMs) owing to their interconnected pore cell structures, high porosity, high specific strength, easy control of pore distribution and membrane thickness, etc. (Lim et al., 2017; Woo et al., 2016). A schematic of NF membrane using nanofibrous layer is illustrated in Fig. 6.10 (Liu, Chen, et al., 2020; Yang, Li, Shen, Wang, & Hsiao, 2017).

In the cross-linking method, a functional monomer is used to have a functionalized polymer. A selective layer can then be made by networking the macromolecules on the surface of the nanofibers of the membrane (Huang et al., 2018). In a study by Yoon et al., they showed that crosslinking the poly(vinyl alcohol), PVA, on the electrospun polyacrylonitrile (PAN) supporting layer increased the flux and the rejection rate in oil–water separation tests (Yoon, Hsiao, & Chu, 2009b). Recently, Meng et al. fabricated an NF membrane by impregnating the electrospun polyvinylidene fluoride as a supporting layer with the sodium alginate (CaAlg), benefiting from the cross-linking procedure and $CaCl_2$ as the cross-linking solution. The results illustrated a dual thin TFC structure and high hydrophobicity, which had a water flux of 63.8 L m^{-2} h^{-1} bar^{-1} with a 98.5% rejection rate for methyl blue. Moreover, this membrane exhibited a suitable antifouling performance toward proteins such as bovine serum albumin and lactobacillus (Meng et al., n.d.).

On the other hand, using photoinitiators enables the free radical formation procedure during the ultraviolet radiation, and therefore a cross-linked network will form. Using this

method also suits the in situ cross-linking strategies to get good results (Kianfar, Vitale, Dalle Vacche, & Bongiovanni, 2019; Maciejewska et al., 2019). Moreover, the cross-linking process can help transfer water-soluble to an insoluble one by making a cross-linked network over it. Kianfar et al. have used PEO as a processing agent to help electrospun the chitosan. The electrospun mat was subjected to photocrosslinking as a fast and ecofriendly technique. The results showed that the photocured CS/PEO membrane has higher solvent stability (Kianfar et al., 2019). Zahran et al. recently used the photocrosslinking method for fabricating a tunable porous structure and nonbiofouling NF membrane out of polyvinylpyrrolidone (PVP)/lecithin. In order to enhance the mechanical properties, they added microcrystalline cellulose (MCC) to the PVP and photocrosslinked. Moreover, UV-curing helped to improve the hydrophobicity. Furthermore, the addition of 2%wt./v of lecithin has shown a remarkable reduction in the protein adhesion to almost zero (Zahran, Abdel-Halim, Mansour, & Nada, 2020).

On the other hand, in the IP method, a highly cross-linked network of a polymer film with ultrathin thickness will be formed at the surface of two immiscible solutions (Liu, Zhu, et al., 2020). This method has been used for the first time by Chu and his coworkers in 2009 (Yoon, Hsiao, & Chu, 2009a). In this research, the authors used electrospun PAN nanofibrous scaffold as a supporting layer and thin PA as the barrier layer. This newly fabricated TFC showed 2.4 times more permeate flux than the conventional TFC membranes without compromising $MgSO_4$ rejection. In this comparison, both membranes have been tested under the same conditions (Yoon et al., 2009a).

Moreover, the newly developed TFC membrane showed a 38% permeate flux increase than the commercial NF270 membrane at 70 psi. In both cases, the rejection was revealed to be the same as each other. As a matter of fact, the high permeate flux has related to the large and open-pore structure, nanofibrous support's low hydraulic resistance, and enhancement of the water transport capability due to the interfacial region has been created between nanofibers and PA caused an increment in permeability (Yoon et al., 2009a). This was a start for more investigation over the effect of electrospun nanofibrous support on the NF performance of TFC membranes. In a study, changing the nanofibers diameters has been evaluated, and the results showed that the pore size of TFC's nanofibers has a significant effect on the permeation and salt rejection of TFC NF membranes (Kaur, Sundarrajan, Rana, Matsuura, & Ramakrishna, 2012). Consequently, using the IP method and optimizing nanostructure and the nanofibers' physicochemical properties has revealed an efficient way to fabricate TFC NF membranes.

Furthermore, hot-pressing posttreatment is another method that has been used in combination with the electrospraying technique. Shen et al. fabricated a TFC NF membrane for anionic dye separation (Shen, Cheng, et al., 2016). In this study, they fabricated electrospun PAN nanofibers as a support layer and chitosan−polyethylene oxide−polytriethylene glycol dimethacrylate (CS−PEO−PTEGDMA) nanobeads electrospray as a hydrophilic top layer followed by an acidic moist-curing process. Then, they hot pressed the membrane to form an integrated barrier film on the PAN nanofibers. The acidic moist helps to soften the CS nanobeads and hence assists melting them. In the end, the top layer UV-cured to form an integrated CS/PEO/PTEGDMA layer physically crosslinked to CS without scarifying the amino/imino and hydroxyl

groups of CS. The optimized TFC membrane has shown an outstanding NF performance at high permeate flux ($\sim$117.5 L m^{-2} h^{-1}) and a high rejection rate ($\sim$99.9%) toward removing anionic dye. In this process, the low pressure of 0.2 MPa has been applied for energy saving purposes. The fabricated NF membranes showed good reusability with a simple process of regeneration. Furthermore, the 96% flux recovery ratio after three runs for 18 hours proved excellent antifouling (Shen, Cheng, et al., 2016). In another study, a TFC scaffold consists of a top ultrafine CN layer, a PAN electrospun nanofibrous midlayer and nonwoven fibrous substrate support. They have fabricated CN layer as a hydrophilic coating with controllable thickness over the electrospun nanofibrous substrate. After the IP process, a superior permeate flux of 44.7 L m^{-2} h^{-1} compared to the conventional PI substrate. Also, this combination showed a high rejection of >99% for $MgSO_4$ at 0.482 MPa. The higher permeation flux in this TFC membrane is reported to be related to the formation of the direct water channel in the interface between the CN and the PAN, which helps the water molecules transportation. Hence water flow resistance of the membrane was reduced (Wang, Fang, Hsiao, & Chu, 2014). Later, Shen et al. combined the advantages of both the highly porous electrospun nanofiber support layer and the controllable IP fabrication of PDA to enhance the TFC NF performance. The NF membrane in this study fabricated by IP on a PES electrospun nanofibrous scaffold modified by PDA and showed comparatively high flux ($\sim$63 L m^{-2} h^{-1}) and salt rejection of almost 99.4% to sodium sulfate (Na_2SO_4) solutions at a low pressure of 0.6 MPa. Furthermore, PDA has been known as a bioinspired polymer with naturally high adhesion properties and hydrophilicity. Therefore the PDA interlayer enhanced the structural stability and integral of the TFC membranes. On the other hand, PDA caused compatibility increment of the top active layer of PA and the substrate (Shen, Yang, Zhao, & Wang, 2016). To further enhance the functionality of the TFC NF, new research focused on creating a transitional midlayer on the supporting electrospun nanofibers. Guo et al. in 2016 used the three-layer composition of polyhydroxybutyrate/calcium alginate/carboxyl MWCNT (PHB/CaAlg/CMWCNT) in which the PHB was used for electrospinning and fabricating of the nanofibrous substrate, PHB/CaAlg as a transitional layer, and CaAlg/CMWCNT as the active layer. They have used these TFC NF membranes for low-pressure separation and removal of small organic substances in wastewater. During the fabrication of this membrane, the PHB/CaAlg was electrospun by synchronizing the PHB nanofibrous substrate to form the hydrophilic middle transitional layer, which actively participates in the top hydrogel layer (Guo, Zhang, Cai, & Zhao, 2016). Likewise, Yang et al. in 2017 utilized the IP method for fabricating the TFC NF membrane containing a thick layer of PAN nanofibrous as a support layer and an electrospun ultrathin PAN/AA nanofibrous layer as a transitional layer. Owing to the high hydrophilicity and swelling properties of the fabricated PAN/AA in amine solution, the membrane has shown container like behavior for capturing the amine monomer in the solution to create an ultrathin, uniform, and defect-free layer, which illustrated excellent separation performance due to improved interfacial bonding between active layer (PA) and the supporting layer (PAN nanofibrous) (Yang et al., 2017).

In an exciting work, Shen et al. in 2019 used the reverse IP (IP-R) method for forming the PA as an active layer on the gelatin side of the double-layer electrospun scaffold of the

gelatin/PAN supporting layer (Shen, Cheng, Zhang, & Wang, 2019). The resulted NF membrane showed a significant performance increment due to the synergistic interaction of gelatin interlayer and trimesoyl chloride (TMC). TMC has been used before the PA IP for both forward and reverse method. The results showed a permeate flux rate of 135.6 L m^{-2} h^{-1} with a rejection rate of 98.1% for Na_2SO_4 under 0.5 MPa pressure, which was almost three times more than the same membrane which has been prepared on the basis of the regular IP method (Shen et al., 2019).

Furthermore, modifying the electrospun supporting layer to get a smaller pore size and higher surface porosity not only can improve the mechanical properties of the layer but also can enhance the membrane structure and physicochemical properties. Liu et al. designed and fabricated tree-like PVDF electrospun nanofibrous membranes. They have used different amounts of tetrabutylammonium chloride (TBAC) alongside PVDF solution to get the tree-like nanofiber membrane after electrospinning and subjecting to hot-press process. These steps ended up with a 130−140 nm pore size and narrowest pore diameter distribution supporting layer. The PA matrix has then been synthesized on the tree-like electrospun PVDF membrane using IP to fabricate the final NF membrane. The water transporting speed has been increased by the "direct water channel" formed in ultrafine branches embedded into the PA film in which the highest permeate flux was 70.2 L m^{-2} h^{-1} MPa^{-1} with rejection rate of >97% for $MgSO_4$ (Liu, Wang, Li, Liu, & Deng, 2020).

As reviewed, TFC membranes, due to their high porosity and the ultrathin active layer, become a research hotspot for the NF membranes with high permeate flux and salt rejection. Therefore continuously the methods and materials for modifying the active or supporting layer are expanding in the research. Nevertheless, mechanical properties, reusability and durability performance and environmental resistance properties should be further investigated to gain a practical NF membrane using these methods. Moreover, incorporation of nanomaterials into the structure of electrospun-based NF membranes can add antibacterial activity to the membrane characteristics. Recently, Woranuch et al. fabricated a high efficiency NF membrane using rice flour-based nanofibers contain of polyvinyl alcohol (PVA). Electrospinning method was used to prepare rice flour-based biodegradable nanofibrous membrane with different amount of rice flour in solution. Only tiny particles with size of less than 0.1 micron can pass through rice flour nanofibrous membranes. Moreover, AgNPs and β-cyclodextrin incorporation into the nanofibrous membrane structure result in an improvement in antimicrobial properties and adsorption of volatile organic compounds, respectively. The prepared membrane made up of low-environmental impact rice flour blends has a great potential to be used as a high performance multipurpose nanofilters (Woranuch, Pangon, Puagsuntia, Subjalearndee, & Intasanta, 2017).

In another study, AgNPs were used to modify nanofibrous membrane based on cellulose acetate (CA) with high effective adsorption performance using the electrospinning method for removing dye from wastewater. Scanning electron microscopy (SEM) confirmed the highly porous structure of the CA nanofibrous membranes. Moreover, the adsorption of rhodamine B aqueous solution exhibited adsorption of dyes effectively, while the addition of AgNPs did not affect dye adsorption. The silver-loaded highly porous CA nanofibrous membrane's antimicrobial activity was compared with CA nanofibrous membrane without AgNPs, which the silver-loaded membrane displayed significant antimicrobial activity.

6.4 Nanoenhanced hollow-fiber nanofiltration membranes

NF membranes are fabricated in multiple geometries such as flat sheets, tubular, or hollow fiber (HF). HF membranes have several advantages as they demand less maintenance and pretreatment costs while having relatively high packing density (750–1700 $m^2\ m^{-3}$) (Urper et al., 2017). An HF module causes high surface area per unit volume that decreases manufacturing expenses. Therefore, there is also a growing interest in developing HF membranes for several NF applications such as membrane bioreactor (Choi, Dockko, Fukushi, & Yamamoto, 2002) and forward osmosis (Yang & Wang, 2009). The advantages of HF membranes from one side and the many unique properties offered by nanomaterials from the other side have inspired researchers to utilize nanostructured materials to enhance HF membranes' separation properties. As such, researchers electrostatically deposited negatively charged GO nanosheets onto the positively charged outer surfaces of the treated HF membranes by a dip-coating method (Goh et al., 2015). As a result, more desirable mechanical properties of the HF substrate were achieved. More importantly, better performance with up to 86% higher pure water permeability is observed compared with the HF membrane of similar selectivity. They observed that the deposited GO nanosheets could reduce the surface pore diameter and narrow the HF membrane's pore-size distribution. The GO nanosheets could withstand a 600 mL min^{-1} crossflow rate and a backwashing pressure of 1 bar that implied a stable electrostatic deposition. In another work, researchers intended to study nanoscale integration's role on the performance of HF TFN membranes on the rejection of natural organic matter (NOM) by incorporating TiO_2 NPs into the PA layer (Urper-Bayram et al., 2020). The nano-TiO_2-containing PA layer was formed on a support layer of MWCNT-blended polysulfone (PSU) in an HF geometry as shown in Figs. 6.7–6.11. The permeate flux of TFN 0.05 composite membranes was increased nearly 12 times by embedding TiO_2, displaying rejections of

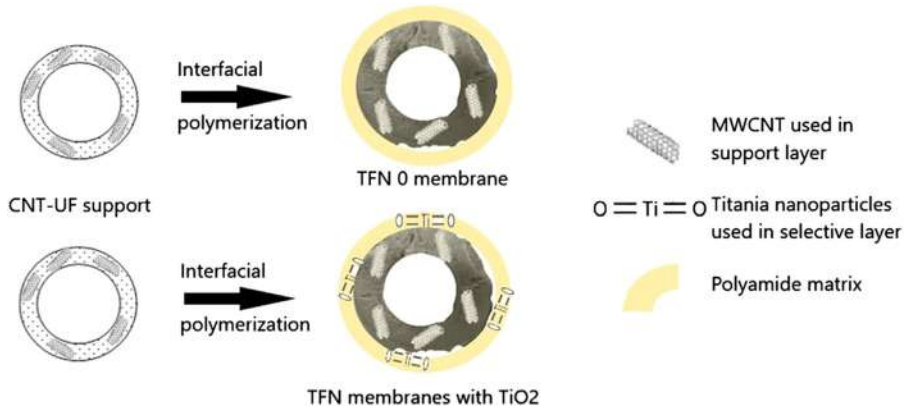

FIGURE 6.11 Schematic illustration of TFN nanocomposite membranes with the MWCNTs blended into the polysulfone hollow fiber support layer. Source: *Reprinted with permission from Urper-Bayram, G. M., Sayinli, B., Bossa, N., Ngaboyamahina, E., Sengur-Tasdemir, R., Ates-Genceli, E., ... Koyuncu, I. (2020). Thin film nanocomposite nanofiltration hollow fiber membrane fabrication and characterization by electrochemical impedance spectroscopy. Polymer Bulletin, 77(7), 3411–3427. https://doi.org/10.1007/s00289-019-02905-w.*

22% and 5% for $MgSO_4$ and NaCl salts, respectively. The NF membranes' rejections for humic acid and tannic acid were 84% and 74%, respectively, with improved antifouling properties compared to the bare TFC membrane without TiO_2.

Electrospun-base polymeric HF membranes are promising candidates for use in different fields such as desalination, water filtration, protein filtration, pervaporation, and gas separation. Producing filtration membranes using electrospinning can provide advantages such as low cost, ease of production, high surface area per unit volume, high packing density, more minor space requirements, and overall high efficiency. Moreover, altering the electrospinning parameters results in producing nanofibers with different pore sizes. It should be noted that HF's performance can be enhanced by a greater pressure differential (Anka & Balkus, 2013). According to a study by Anka and Balkus, core–shell electrospinning method was used to prepare HF PAN membrane with the potential to be used in water purification and desalination. The average inner and outer diameter of the relatively smooth PAN fibers were 530 and 890 nm, respectively. The membrane was tested for separation Indigo carmine dye and NaCl salt, which dye rejection and salt rejection were 100% and 97.7% ± 0.6%, respectively (Anka & Balkus, 2013).

6.5 Commercialization status and commercial viability

It is almost a decade that polymeric-based NF membrane for water treatment has been taken to the market, and it seems that the NEMs should step in from a laboratory scale to an industrial one. The addition of different types of nanomaterials increases NF properties such as salt rejection and water flux. On the other hand, there are challenges of using these nanoenhanced formulations for the industrial grades of the NFs. These challenges can be classified into the cost of the final product, long-term stability, scalability of the formulation, and toxicity of NEMs.

Industrial production of the NEMs comes with the mass production lines of the nanomaterials with specific properties such as size and functionality. This high-end nanomaterial mass production requires high-tech technology facilities and chemicals with reagent grades. All these lead the cost of these nanoenhanced NF membranes to become more expensive. For instance, CNTs are one of the highly attracted nanomaterials used for the membranes on the laboratory scale. However, the commercialization of the CNTs is still on-going; some fabrication methods such as catalytic chemical vapor deposition (CVD) have been modified to enable large-scale production of CNTs. Despite these improvements in the large-scale production of CNTs, some doubts in reproducibility and viability for using them in membranes have remained unsolved (Yang et al., 2019).

Moreover, the stability and long-term usability of the NEMs are limited due to the leaching of the NMs into the water (Bushra et al., 2014; Dimapilis, Hsu, Mendoza, & Lu, 2018). Releasing of NMs into the water despite the unknown environmental effect, reduces the performance of the membrane during the time. The leaching process decreases the stability in long-term usages, and therefore the efficiency of the membrane drops dramatically over time. On the other hand, to address this issue, some immobilizing methods of the NMs into the polymeric matrix, with different methods of functionalization or stabilization, are needed (Fathy et al., 2020; Paseta et al., 2020). These immobilizations of NMs in

the laboratory come with precision equipment, which scaling up the equipment and experiment design is always is the big challenge in all laboratory to industry scale-ups. Consequently, simulation of this process and transferring it from the laboratory scale to the industrial scale with a stable fabrication rate is a big challenge.

Another main challenge of using NMs in wastewater treatment is related to uncertainty about the safety of NMs for the health and its toxicity. Several studies have been conducted to evaluate the toxicity of the NMs in the water (Chaloupka, Malam, & Seifalian, 2010). Meanwhile, it is difficult to come up with a general conclusion on the toxicity of the NMs and more studies are required to evaluate the appropriate concentration and their toxicological effects (Ursino et al., 2018).

Overall, nanotechnology could be the next generation of NF membrane in the market if commercialization challenges can be addressed. To the authors' knowledge, no NEMs have been entered to the market for NFs; however, some recent studies and news showed that several types of commercial NEMs for RO has entered the market (e.g., LG chem—NanoH_2O nanocomposite membranes) (Ursino et al., 2018). This trend in the market reveals that commercialization challenges are aimed to be solved quickly in other types of membranes, and we will not be surprised if any NEM for NF enters the market soon by overcoming these challenges.

6.6 Summary and future directions

Membrane technology captivated lots of attention and could replace conventional water treatment technologies while maintaining the prices as low as possible. Polymeric materials are the perfect choice for applications in which a cost-effective filtration is highly preferred. Over time, increasing water demands, identifying new pollutants and their effective removal, and enforcing regulations have urged researchers to investigate new horizons to overcome the new challenges. Therefore it is essential to develop strategies by which the polymeric membranes' properties can be modified. One fruitful approach is to combine polymeric membranes with nanomaterials by incorporating them into the organic polymer matrix to leverage their synergist effects. Throughout this chapter, we discussed various blends of polymeric and inorganic materials with a focus on the mixed matrix NF membranes being classified into:

1. Asymmetric mixed matrix NF membranes (prepared by PI method)
2. TFN NF membranes (prepared by IP technique)

Further, we discussed electrospun nanofibrous polymers for NF membranes. Advancement in the development of these membranes for various applications has been eye-captivating in recent years. These new types of membranes have proved to be more efficient in terms of permeability and selectivity; yet, it has also developed its barriers, limiting its broader industrial application. These challenges include the high cost, the complexity of the synthesis process, identification of compatible inorganic particles, control of morphology and structural defects. Besides, the technique for better dispersion of nanomaterials needs to be further explored. Aggregation is the common problem that hinders nanomaterials from being homogeneously dispersed inside the polymeric backbone.

Lastly, incorporating inorganic particles into an organic membrane structure to treat water is recognized as a potential risk to the ecosystem and human health, which also needs to be addressed in the future. There are multiple laboratory-scale studies on polymer-based nanoenhanced NF membranes, but these membranes' industrial application is still not developed yet. More studies are needed to investigate the cost-effectiveness of large-scale fabrication, including nanomaterials' supply, additional enhanced methods for nanomaterial incorporation (preventing nanomaterial leakage) and monitoring membranes' long-term stability.

Abbreviations

CVD	chemical vapor deposition
CNT	carbon nanotube
DMAc	dimethylacetamide
DMF	dimethylformamide
GO	graphene oxide
HF	hollow fiber
IP	interfacial polymerization
MeOH	methanol
MF	microfiltration
MMM	mixed matrix membrane
MOF	metal organic framework
MPD	m-phenylenediamine
MWCNT	multiwall carbon nanotube
NF	nanofiltration
NIPS	nonsolvent-induced phase separation
NMP	*N*-methylpyrrolidinone
NPs	nanoparticles
PA	polyamide
PAN	polyacrylonitrile
PIP	piperazine
PPA	piperazineamide
PSBMA	poly(sulfobetaine methacrylate)
PSU	polysulfone
PVAc	poly(vinylacetate);
PVDF	polyvinylidenefluoride
PWF	pure water flux
RO	reverse osmosis
TBAC	tetrabutylammonium chloride
TFC	thin-film composite
TFN	thin-film nanocomposite
TMC	trimesoylchloride
TOC	total organic carbon
UF	ultrafiltration

References

Abadikhah, H., Kalali, E. N., Behzadi, S., Khan, S. A., Xu, X., Shabestari, M. E., & Agathopoulos, S. (2019). High flux thin film nanocomposite membrane incorporated with functionalized TiO_2@reduced graphene oxide nanohybrids for organic solvent nanofiltration. *Chemical Engineering Science*, *204*, 99–109. Available from https://doi.org/10.1016/j.ces.2019.04.022.

Ahmadi, A., Qanati, O., Seyed Dorraji, M. S., Rasoulifard, M. H., & Vatanpour, V. (2017). Investigation of antifouling performance a novel nanofibrous S-PVDF/PVDF and S-PVDF/PVDF/GO membranes against negatively charged oily foulants. *Journal of Membrane Science*, *536*, 86–97. Available from https://doi.org/10.1016/j.memsci.2017.04.056.

Ahmed, F. E., Lalia, B. S., & Hashaikeh, R. (2015). A review on electrospinning for membrane fabrication: Challenges and applications. *Desalination*, *356*, 15–30.

Al Aani, S., Haroutounian, A., Wright, C. J., & Hilal, N. (2018). Thin film nanocomposite (TFN) membranes modified with polydopamine coated metals/carbon-nanostructures for desalination applications. *Desalination*, *427*, 60–74. Available from https://doi.org/10.1016/j.desal.2017.10.011.

Andrade, P. F., de Faria, A. F., Oliveira, S. R., Arruda, M. A. Z., & Gonçalves, Md. C. (2015). Improved antibacterial activity of nanofiltration polysulfone membranes modified with silver nanoparticles. *Water Research*, *81*, 333–342. Available from https://doi.org/10.1016/j.watres.2015.05.006.

Andrews, R., & Weisenberger, M. C. (2004). Carbon nanotube polymer composites. *Current Opinion in Solid State and Materials Science*, *8*(1), 31–37. Available from https://doi.org/10.1016/j.cossms.2003.10.006.

Ang, M. B. M. Y., Tang, C. L., De Guzman, M. R., Maganto, H. L. C., Caparanga, A. R., Huang, S. H., … Lai, J. Y. (2020). Improved performance of thin-film nanofiltration membranes fabricated with the intervention of surfactants having different structures for water treatment. *Desalination*, *481*, 114352. Available from https://doi.org/10.1016/j.desal.2020.114352.

Anka, F. H., & Balkus, K. J. (2013). Novel nanofiltration hollow fiber membrane produced via electrospinning. *Industrial and Engineering Chemistry Research*, *52*(9), 3473–3480. Available from https://doi.org/10.1021/ie303173w.

Bandehali, S., Moghadassi, A., Parvizian, F., Shen, J., & Hosseini, S. M. (2020). Glycidyl POSS-functionalized ZnO nanoparticles incorporated polyether-imide based nanofiltration membranes for heavy metal ions removal from water. *Korean Journal of Chemical Engineering*, *37*(2), 263–273. Available from https://doi.org/10.1007/s11814-019-0441-5.

Bandehali, S., Moghadassi, A., Parvizian, F., Zhang, Y., Hosseini, S. M., & Shen, J. (2020). New mixed matrix PEI nanofiltration membrane decorated by glycidyl-POSS functionalized graphene oxide nanoplates with enhanced separation and antifouling behaviour: Heavy metal ions removal. *Separation and Purification Technology*, *242*, 116745. Available from https://doi.org/10.1016/j.seppur.2020.116745.

Barzegar, H., Zahed, M. A., & Vatanpour, V. (2020). Antibacterial and antifouling properties of Ag3PO4/GO nanocomposite blended polyethersulfone membrane applied in dye separation. *Journal of Water Process Engineering*, *38*, 101638. Available from https://doi.org/10.1016/j.jwpe.2020.101638.

Berber, M. R. (2020). Current advances of polymer composites for water treatment and desalination. *Journal of Chemistry*, *2020*. Available from https://doi.org/10.1155/2020/7608423.

Bhardwaj, N., & Kundu, S. C. (2010). Electrospinning: A fascinating fiber fabrication technique. *Biotechnology Advances*, *28*(3), 325–347.

Blanco, J. F., Sublet, J., Nguyen, Q. T., & Schaetzel, P. (2006). Formation and morphology studies of different polysulfones-based membranes made by wet phase inversion process. *Journal of Membrane Science*, *283*(1–2), 27–37. Available from https://doi.org/10.1016/j.memsci.2006.06.011.

Bose, S., Khare, R. A., & Moldenaers, P. (2010). Assessing the strengths and weaknesses of various types of pretreatments of carbon nanotubes on the properties of polymer/carbon nanotubes composites: A critical review. *Polymer*, *51*(5), 975–993. Available from https://doi.org/10.1016/j.polymer.2010.01.044.

Bruggen, B.V.D. (2013). Bart Van der Bruggen. 6, 1–22.

Bushra, R., Shahadat, M., Ahmad, A., Nabi, S. A., Umar, K., Oves, M., … Muneer, M. (2014). Synthesis, characterization, antimicrobial activity and applications of polyanilineTi (IV) arsenophosphate adsorbent for the analysis of organic and inorganic pollutants. *Journal of Hazardous Materials*, *264*, 481–489.

Cadotte, J. E., Petersen, R. J., Larson, R. E., & Erickson, E. E. (1980). A new thin-film composite seawater reverse osmosis membrane. *Desalination*, *32*(C), 25–31. Available from https://doi.org/10.1016/S0011-9164(00)86003-8.

Cai, Y., Shi, D., Liu, G., Ying, Y., Cheng, Y., Wang, Y., … Zhao, D. (2020). Polycrystalline zirconium metal-organic framework membranes supported on flexible carbon cloth for organic solvent nanofiltration. *Journal of Membrane Science*, *615*, 118551. Available from https://doi.org/10.1016/j.memsci.2020.118551.

Campbell, J., Davies, R. P., Braddock, D. C., & Livingston, A. G. (2015). Improving the permeance of hybrid polymer/metal-organic framework (MOF) membranes for organic solvent nanofiltration (OSN)-development of MOF thin films via interfacial synthesis. *Journal of Materials Chemistry A*, *3*(18), 9668–9674. Available from https://doi.org/10.1039/c5ta01315a.

Chaloupka, K., Malam, Y., & Seifalian, A. M. (2010). Nanosilver as a new generation of nanoproduct in biomedical applications. *Trends in Biotechnology*, *28*(11), 580–588.

Chen, X., Hu, Y., Xie, Z., & Wang, H. (2018). Materials and design of photocatalytic membranes. In Current trends and future developments on (bio-) membranes: Photocatalytic membranes and photocatalytic membrane reactors (pp. 71–96). Elsevier Inc. <https://doi.org/10.1016/B978-0-12-813549-5.00003-7>

Choi, J. H., Dockko, S., Fukushi, K., & Yamamoto, K. (2002). A novel application of a submerged nanofiltration membrane bioreator (NF MBR) for wastewater treatment. *Desalination*, *146*(1–3), 413–420. Available from https://doi.org/10.1016/S0011-9164(02)00524-6.

Daraei, P., Madaeni, S. S., Ghaemi, N., Ahmadi Monfared, H., & Khadivi, M. A. (2013). Fabrication of PES nanofiltration membrane by simultaneous use of multi-walled carbon nanotube and surface graft polymerization method: Comparison of MWCNT and PAA modified MWCNT. *Separation and Purification Technology*, *104*, 32–44. Available from https://doi.org/10.1016/j.seppur.2012.11.004.

De Volder, M. F. L., Tawfick, S. H., Baughman, R. H., & Hart, A. J. (2013). Carbon nanotubes: Present and future commercial applications. *Science*, *339*(6119), 535–539. Available from https://doi.org/10.1126/science.1222453.

Dimapilis, E. A. S., Hsu, C.-S., Mendoza, R. M. O., & Lu, M.-C. (2018). Zinc oxide nanoparticles for water disinfection. *Sustainable Environment Research*, *28*(2), 47–56.

Echaide-Górriz, C., Sorribas, S., Téllez, C., & Coronas, J. (2016). MOF nanoparticles of MIL-68(Al), MIL-101(Cr) and ZIF-11 for thin film nanocomposite organic solvent nanofiltration membranes. *RSC Advances*, *6*(93), 90417–90426. Available from https://doi.org/10.1039/c6ra17522h.

Eda, G., & Shivkumar, S. (2007). Bead-to-fiber transition in electrospun polystyrene. *Journal of Applied Polymer Science*, *106*(1), 475–487.

Elimelech, M., & Phillip, W. A. (2011). The future of seawater desalination: Energy, technology, and the environment. *Science*, *333*(6043), 712–717. Available from https://doi.org/10.1126/science.1200488.

Fathizadeh, M., Tien, H. N., Khivantsev, K., Chen, J. T., & Yu, M. (2017). Printing ultrathin graphene oxide nanofiltration membranes for water purification. *Journal of Materials Chemistry A*, *5*(39), 20860–20866. Available from https://doi.org/10.1039/c7ta06307e.

Fathy, M., Shahawy, A., El Moghny, T. A., & Nafady, A. (2020). Enhanced desalination process using a Cu–ZnO-polyvinyl chloride-nylon nanofiltration membrane as a calcite antiscalant in reverse osmosis. *Materials Express*, *10*(5), 671–679. Available from https://doi.org/10.1166/mex.2020.1677.

Feng, C., Khulbe, K. C., Matsuura, T., Gopal, R., Kaur, S., Ramakrishna, S., & Khayet, M. (2008). Production of drinking water from saline water by air-gap membrane distillation using polyvinylidene fluoride nanofiber membrane. *Journal of Membrane Science*, *311*(1–2), 1–6.

Gao, Z. F., Naderi, A., Wei, W., & Chung, T. S. (2020). Selection of crosslinkers and control of microstructure of vapor-phase crosslinked composite membranes for organic solvent nanofiltration. *Journal of Membrane Science*, *616*, 118582. Available from https://doi.org/10.1016/j.memsci.2020.118582.

Gholami, S., López, J., Rezvani, A., Vatanpour, V., & Cortina, J. L. (2020). Fabrication of thin-film nanocomposite nanofiltration membranes incorporated with aromatic amine-functionalized multiwalled carbon nanotubes. Rejection performance of inorganic pollutants from groundwater with improved acid and chlorine resistance. *Chemical Engineering Journal*, *384*, 123348. Available from https://doi.org/10.1016/j.cej.2019.123348.

Ghorani, B., & Tucker, N. (2015). Fundamentals of electrospinning as a novel delivery vehicle for bioactive compounds in food nanotechnology. *Food Hydrocolloids*, *51*, 227–240.

Goh, K., Setiawan, L., Wei, L., Si, R., Fane, A. G., Wang, R., & Chen, Y. (2015). Graphene oxide as effective selective barriers on a hollow fiber membrane for water treatment process. *Journal of Membrane Science*, *474*, 244–253. Available from https://doi.org/10.1016/j.memsci.2014.09.057.

Gohil, J. M., & Ray, P. (2017). A review on semi-aromatic polyamide TFC membranes prepared by interfacial polymerization: Potential for water treatment and desalination. *Separation and Purification Technology*, *181*, 159–182. Available from https://doi.org/10.1016/j.seppur.2017.03.020.

Guo, J., Zhang, Q., Cai, Z., & Zhao, K. (2016). Preparation and dye filtration property of electrospun polyhydroxybutyrate–calcium alginate/carbon nanotubes composite nanofibrous filtration membrane. *Separation and Purification Technology*, *161*, 69–79.

Hibrid, K., Tiub, K., Pelbagai, N., Nano, D. T., Bagi, T., Penapisan, M., & Pengenyahmasin, N. (2017). The effect of novel multiwalled carbon nanotube-titania nanotube hybrid in polyamide active layer towards water permeability and high sodium chloride rejection performance of nanofiltration membrane desalination. *Malaysian Journal of Analytical Science*, *21*(2), 402–408. Available from https://doi.org/10.17576/mjas-2017-2102-15.

Homayoonfal, M., & Mehrnia, M. R. (2014). Amoxicillin separation from pharmaceutical solution by pH sensitive nanofiltration membranes. *Separation and Purification Technology*, *130*, 74–83. Available from https://doi.org/10.1016/j.seppur.2014.04.009.

Hu, R., Zhang, R., He, Y., Zhao, G., & Zhu, H. (2018). Graphene oxide-in-polymer nanofiltration membranes with enhanced permeability by interfacial polymerization. *Journal of Membrane Science*, *564*, 813–819. Available from https://doi.org/10.1016/j.memsci.2018.07.087.

Huang, L., Li, Z., Luo, Y., Zhang, N., Qi, W., Jiang, E., … He, G. (2021). Low-pressure loose GO composite membrane intercalated by CNT for effective dye/salt separation. *Separation and Purification Technology*, *256*, 117839. Available from https://doi.org/10.1016/j.seppur.2020.117839.

Huang, Y., Dan, N., Dan, W., Zhao, W., Bai, Z., Chen, Y., & Yang, C. (2018). Bilayered antimicrobial nanofiber membranes for wound dressings via in situ cross-linking polymerization and electrospinning. *Industrial & Engineering Chemistry Research*, *57*(50), 17048–17057.

Izadmehr, N., Mansourpanah, Y., Ulbricht, M., Rahimpour, A., & Omidkhah, M. R. (2020). TETA-anchored graphene oxide enhanced polyamide thin film nanofiltration membrane for water purification; performance and antifouling properties. *Journal of Environmental Management*, *276*, 111299. Available from https://doi.org/10.1016/j.jenvman.2020.111299.

Jia, T. Z., Lu, J. P., Cheng, X. Y., Xia, Q. C., Cao, X. L., Wang, Y., … Sun, S. P. (2019). Surface enriched sulfonated polyarylene ether benzonitrile (SPEB) that enhances heavy metal removal from polyacrylonitrile (PAN) thin-film composite nanofiltration membranes. *Journal of Membrane Science*, *580*, 214–223. Available from https://doi.org/10.1016/j.memsci.2019.03.015.

Kadhom, M., Hu, W., & Deng, B. (2017). Thin film nanocomposite membrane filled with metal-organic frameworks UiO-66 and MIL-125 nanoparticles for water desalination. *Membranes*, *7*(2), 31. Available from https://doi.org/10.3390/membranes7020031.

Kang, J., Choi, Y., Kim, J. H., Choi, E., Choi, S. E., Kwon, O., & Kim, D. W. (2021). Functionalized nanoporous graphene membrane with ultrafast and stable nanofiltration. *Journal of Membrane Science*, *618*, 118635. Available from https://doi.org/10.1016/j.memsci.2020.118635.

Kang, Y., Obaid, M., Jang, J., & Kim, I. S. (2019). Sulfonated graphene oxide incorporated thin film nanocomposite nanofiltration membrane to enhance permeation and antifouling properties. *Desalination*, *470*, 114125. Available from https://doi.org/10.1016/j.desal.2019.114125.

Kaur, S., Sundarrajan, S., Rana, D., Matsuura, T., & Ramakrishna, S. (2012). Influence of electrospun fiber size on the separation efficiency of thin film nanofiltration composite membrane. *Journal of Membrane Science*, *392*, 101–111.

Khalf, A., & Madihally, S. V. (2017). Recent advances in multiaxial electrospinning for drug delivery. *European Journal of Pharmaceutics and Biopharmaceutics*, *112*, 1–17.

Kianfar, P., Vitale, A., Dalle Vacche, S., & Bongiovanni, R. (2019). Photo-crosslinking of chitosan/poly(ethylene oxide) electrospun nanofibers. *Carbohydrate Polymers*, *217*, 144–151.

Kumar, M., Khan, M. A., & Arafat, H. A. (2020). Recent developments in the rational fabrication of thin film nanocomposite membranes for water purification and desalination. *ACS Omega*, *5*(8), 3792–3800. Available from https://doi.org/10.1021/acsomega.9b03975.

Lai, G. S., Lau, W. J., Goh, P. S., Ismail, A. F., Yusof, N., & Tan, Y. H. (2016). Graphene oxide incorporated thin film nanocomposite nanofiltration membrane for enhanced salt removal performance. *Desalination*, *387*, 14–24. Available from https://doi.org/10.1016/j.desal.2016.03.007.

Lai, G. S., Lau, W. J., Goh, P. S., Tan, Y. H., Ng, B. C., & Ismail, A. F. (2019). A novel interfacial polymerization approach towards synthesis of graphene oxide-incorporated thin film nanocomposite membrane with improved surface properties. *Arabian Journal of Chemistry*, *12*(1), 75–87. Available from https://doi.org/10.1016/j.arabjc.2017.12.009.

Lasprilla-Botero, J., Álvarez-Láinez, M., & Lagaron, J. M. (2018). The influence of electrospinning parameters and solvent selection on the morphology and diameter of polyimide nanofibers. *Materials Today. Communications*, *14*, 1–9.

Lee, H. S., Im, S. J., Kim, J. H., Kim, H. J., Kim, J. P., & Min, B. R. (2008). Polyamide thin-film nanofiltration membranes containing TiO_2 nanoparticles. *Desalination*, *219*(1–3), 48–56. Available from https://doi.org/10.1016/j.desal.2007.06.003.

Lee, S., Park, G., Amy, G., Hong, S.-K., Moon, S.-H., Lee, D.-H., & Cho, J. (2002). Determination of membrane pore size distribution using the fractional rejection of nonionic and charged macromolecules. *Journal of Membrane Science*, *201*(1–2), 191–201.

Li, Q., Wang, Y., Song, J., Guan, Y., Yu, H., Pan, X., … Zhang, M. (2015). Influence of silica nanospheres on the separation performance of thin film composite poly(piperazine-amide) nanofiltration membranes. *Applied Surface Science*, *324*, 757–764. Available from https://doi.org/10.1016/j.apsusc.2014.11.031.

Li, X., Liu, Y., Wang, J., Gascon, J., Li, J., & Van Der Bruggen, B. (2017). Metal-organic frameworks based membranes for liquid separation. *Chemical Society Reviews*, *46*(23), 7124–7144. Available from https://doi.org/10.1039/c7cs00575j.

Li, Z., Wang, J., Liu, X., Liu, S., Ou, J., & Yang, S. (2011). Electrostatic layer-by-layer self-assembly multilayer films based on graphene and manganese dioxide sheets as novel electrode materials for supercapacitors. *Journal of Materials Chemistry*, *21*(10), 3397–3403. Available from https://doi.org/10.1039/c0jm02650f.

Liao, Y., Loh, C.-H., Tian, M., Wang, R., & Fane, A. G. (2018). Progress in electrospun polymeric nanofibrous membranes for water treatment: Fabrication, modification and applications. *Progress in Polymer Science*, *77*, 69–94.

Lim, C. T., Tan, E. P. S., & Ng, S. Y. (2008). Effects of crystalline morphology on the tensile properties of electrospun polymer nanofibers. *Applied Physics Letters*, *92*(14), 141908.

Lim, S., Park, M. J., Phuntsho, S., Tijing, L. D., Nisola, G. M., Shim, W.-G., … Shon, H. K. (2017). Dual-layered nanocomposite substrate membrane based on polysulfone/graphene oxide for mitigating internal concentration polarization in forward osmosis. *Polymer*, *110*, 36–48.

Liu, D., He, L., Lei, W., Klika, K. D., Kong, L., & Chen, Y. (2015). Multifunctional polymer/porous boron nitride nanosheet membranes for superior trapping emulsified oils and organic molecules. *Advanced Materials Interfaces*, *2*(12), 1–6. Available from https://doi.org/10.1002/admi.201500228.

Liu, F., Wang, L., Li, D., Liu, Q., & Deng, B. (2020). Preparation and characterization of novel thin film composite nanofiltration membrane with PVDF tree-like nanofiber membrane as composite scaffold. *Materials & Design*, *196*, 109101.

Liu, Q., Chen, Z., Pei, X., Guo, C., Teng, K., Hu, Y., … Qian, X. (2020). Applications, effects and the prospects for electrospun nanofibrous mats in membrane separation. *Journal of Materials Science*, 1–32.

Liu, Y., Liu, J., Jiang, Y., Meng, M., Ni, L., Qiu, H., … Liu, H. (2019). Synthesis of novel high flux thin-film nanocomposite nanofiltration membranes containing GO-SiO_2 via interfacial polymerization. *Industrial and Engineering Chemistry Research*, *58*(49), 22324–22333. Available from https://doi.org/10.1021/acs.iecr.9b03228.

Liu, Y., Zhu, J., Zheng, J., Gao, X., Wang, J., Wang, X., … Van der Bruggen, B. (2020). A facile and scalable fabrication procedure for thin-film composite membranes: Integration of phase inversion and interfacial polymerization. *Environmental Science & Technology*, *54*(3), 1946–1954.

Liu, Z., Qi, L., An, X., Liu, C., & Hu, Y. (2017). Surface engineering of thin film composite polyamide membranes with silver nanoparticles through layer-by-layer interfacial polymerization for antibacterial properties. *ACS Applied Materials and Interfaces*, *9*(46), 40987–40997. Available from https://doi.org/10.1021/acsami.7b12314.

Ma, D., Peh, S. B., Han, G., & Chen, S. B. (2017). Thin-film nanocomposite (TFN) membranes incorporated with super-hydrophilic metal-organic framework (MOF) UiO-66: Toward enhancement of water flux and salt rejection. *ACS Applied Materials and Interfaces*, *9*(8), 7523–7534. Available from https://doi.org/10.1021/acsami.6b14223.

Ma, W., Chen, T., Nanni, S., Yang, L., Ye, Z., & Rahaman, M. S. (2019). Zwitterion-functionalized graphene oxide incorporated polyamide membranes with improved antifouling properties. *Langmuir: The ACS Journal of Surfaces and Colloids*, *35*(5), 1513–1525. Available from https://doi.org/10.1021/acs.langmuir.8b02044.

Maciejewska, B. M., Wychowaniec, J. K., Woźniak-Budych, M., Popenda, Ł., Warowicka, A., Golba, K., … Jurga, S. (2019). UV cross-linked polyvinylpyrrolidone electrospun fibres as antibacterial surfaces. *Science and Technology of Advanced Materials*, *20*(1), 979–991.

Mansourpanah, Y., Madaeni, S. S., Rahimpour, A., Farhadian, A., & Taheri, A. H. (2009). Formation of appropriate sites on nanofiltration membrane surface for binding TiO_2 photo-catalyst: Performance, characterization and fouling-resistant capability. *Journal of Membrane Science*, *330*(1–2), 297–306. Available from https://doi.org/10.1016/j.memsci.2009.01.001.

Marjani, A., Nakhjiri, A. T., Adimi, M., Jirandehi, H. F., & Shirazian, S. (2020). Effect of graphene oxide on modifying polyethersulfone membrane performance and its application in wastewater treatment. *Scientific Reports*, *10*(1), 1–11. Available from https://doi.org/10.1038/s41598-020-58472-y.

Maruf, S. H., Greenberg, A. R., & Ding, Y. (2016). Influence of substrate processing and interfacial polymerization conditions on the surface topography and permselective properties of surface-patterned thin-film composite membranes. *Journal of Membrane Science*, *512*, 50–60. Available from https://doi.org/10.1016/j.memsci.2016.04.003.

Mendes, A. C., Stephansen, K., & Chronakis, I. S. (2017). Electrospinning of food proteins and polysaccharides. *Food Hydrocolloids*, *68*, 53–68.

Meng, J., Xie, Y., Gu, Y.-H., Yan, X., Chen, Y., Guo, X.-J., & Lang, W.-Z. (n.d.). PVDF-CaAlg nanofiltration membranes with dual thin-film-composite (TFC) structure and high permeation flux for dye removal. *Separation and Purification Technology*, *255*, 117739.

Moghadassi, A., Moradi, S., & Bandehali, S. (2020). Fabrication of antifouling mixed matrix NF membranes by embedding sodium citrate surfactant modified-iron oxide nanoparticles. *Korean Journal of Chemical Engineering*, *37*(11), 1963–1974. Available from https://doi.org/10.1007/s11814-020-0599-x.

Mohammad, A. W., Teow, Y. H., Ang, W. L., Chung, Y. T., Oatley-Radcliffe, D. L., & Hilal, N. (2015). Nanofiltration membranes review: Recent advances and future prospects. *Desalination*, *356*, 226–254. Available from https://doi.org/10.1016/j.desal.2014.10.043.

Mokhena, T. C., Jacobs, V., & Luyt, A. S. (2015). A review on electrospun bio-based polymers for water treatment. eXPRESS Polymer Letters, 9(10), 839.

Mollahosseini, A., & Rahimpour, A. (2014). Interfacially polymerized thin film nanofiltration membranes on TiO_2 coated polysulfone substrate. *Journal of Industrial and Engineering Chemistry*, *20*(4), 1261–1268. Available from https://doi.org/10.1016/j.jiec.2013.07.002.

Mona Mirmousaei, S., Peyravi, M., Khajouei, M., Jahanshahi, M., & Khalili, S. (2019). Preparation and characterization of nano-filtration and its photocatalytic abilities via pre-coated and self-forming dynamic membranes developed by ZnO, PAC and chitosan. *Water Science and Technology*, *80*(12), 2273–2283. Available from https://doi.org/10.2166/wst.2020.044.

Mousavi, S. R., Asghari, M., & Mahmoodi, N. M. (2020). Chitosan-wrapped multiwalled carbon nanotube as filler within PEBA thin film nanocomposite (TFN) membrane to improve dye removal. *Carbohydrate Polymers*, *237*, 116128. Available from https://doi.org/10.1016/j.carbpol.2020.116128.

Mozia, S., Czyżewski, A., Sienkiewicz, P., & Darowna, D. (2020). Influence of sodium dodecyl sulfate on the morphology and performance of titanate nanotubes/polyethersulfone mixed-matrix membranes. *Desalination and Water Treatment*, *208*, 287–302. Available from https://doi.org/10.5004/dwt.2020.26504.

Mulder, M. (1996). Basic principles of membrane technology. Springer The Netherlands. <https://doi.org/10.1007/978-94-009-1766-8>.

Munir, M. M., Suryamas, A. B., Iskandar, F., & Okuyama, K. (2009). Scaling law on particle-to-fiber formation during electrospinning. *Polymer*, *50*(20), 4935–4943.

Nawaz, H., Umar, M., Ullah, A., Razzaq, H., Zia, K. M., & Liu, X. (2021). Polyvinylidene fluoride nanocomposite super hydrophilic membrane integrated with polyaniline-graphene oxide nano fillers for treatment of textile effluents. *Journal of Hazardous Materials*, *403*, 123587. Available from https://doi.org/10.1016/j.jhazmat.2020.123587.

Paseta, L., Luque-Alled, J. M., Malankowska, M., Navarro, M., Gorgojo, P., Coronas, J., & Téllez, C. (2020). Functionalized graphene-based polyamide thin film nanocomposite membranes for organic solvent nanofiltration. *Separation and Purification Technology*, *247*, 116995. Available from https://doi.org/10.1016/j.seppur.2020.116995.

Paseta, L., Navarro, M., Coronas, J., & Téllez, C. (2019). Greener processes in the preparation of thin film nanocomposite membranes with diverse metal-organic frameworks for organic solvent nanofiltration. *Journal of Industrial and Engineering Chemistry*, *77*, 344–354. Available from https://doi.org/10.1016/j.jiec.2019.04.057.

Qasim, S. B., Zafar, M. S., Najeeb, S., Khurshid, Z., Shah, A. H., Husain, S., & Rehman, I. U. (2018). Electrospinning of chitosan-based solutions for tissue engineering and regenerative medicine. *International Journal of Molecular Sciences*, *19*(2), 407.

Qiao, Z., Wang, Z., Zhang, C., Yuan, S., Zhu, Y., & Wang, J. (2012). PVAm–PIP/PS composite membrane with high performance for CO_2/N_2 separation. *AIChE Journal*, *59*(4), 215–228. Available from https://doi.org/10.1002/aic.

Ramakrishna, S., & Shirazi, M. M. A. (2015). Electrospun membranes: Next generation membranes for desalination and water/wastewater treatment. *Journal of Membrane Science and Research*, *1*, 46–47.

Ray, S. S., Chen, S.-S., Li, C.-W., Nguyen, N. C., & Nguyen, H. T. (2016). A comprehensive review: Electrospinning technique for fabrication and surface modification of membranes for water treatment application. *RSC Advances*, *6*(88), 85495–85514.

Ray, S. S., Chen, S.-S., Nguyen, N. C., Nguyen, H. T., Li, C.-W., Wang, J., & Yan, B. (2016). Forward osmosis desalination by utilizing chlorhexidine gluconate based mouthwash as a reusable draw solute. *Chemical Engineering Journal*, *304*, 962–969.

Safarpour, M., Vatanpour, V., & Khataee, A. (2016). Preparation and characterization of graphene oxide/TiO_2 blended PES nanofiltration membrane with improved antifouling and separation performance. *Desalination*, *393*, 65–78. Available from https://doi.org/10.1016/j.desal.2015.07.003.

Safarpour, M., Vatanpour, V., Khataee, A., & Esmaeili, M. (2015). Development of a novel high flux and fouling-resistant thin film composite nanofiltration membrane by embedding reduced graphene oxide/TiO_2. *Separation and Purification Technology*, *154*, 96–107. Available from https://doi.org/10.1016/j.seppur.2015.09.039.

Saleem, H., Trabzon, L., Kilic, A., & Zaidi, S. J. (2020). Recent advances in nanofibrous membranes: Production and applications in water treatment and desalination. *Desalination*, *478*, 114178.

Separation, S. (2020). Cu (I/II) metal – organic frameworks incorporated nanofiltration membranes for organic solvent separation.

Shahzadi, A., Ahmed, R., & Siddiq, M. (2014). Synthesis and characterization of Nafion/SiO_2-MO_x (M = Ti, Zr, W) nanocomposite membranes by sol-gel reaction for fuel cells. *IOP Conference Series: Materials Science and Engineering*, *60*(1), 012033. Available from https://doi.org/10.1088/1757-899X/60/1/012033.

Shen, K., Cheng, C., Zhang, T., & Wang, X. (2019). High performance polyamide composite nanofiltration membranes via reverse interfacial polymerization with the synergistic interaction of gelatin interlayer and trimesoyl chloride. *Journal of Membrane Science*, *588*, 117192.

Shen, L., Cheng, C., Yu, X., Yang, Y., Wang, X., Zhu, M., & Hsiao, B. S. (2016). Low pressure UV-cured CS–PEO–PTEGDMA/PAN thin film nanofibrous composite nanofiltration membranes for anionic dye separation. *Journal of Materials Chemistry A*, *4*(40), 15575–15588.

Shen, L., Yang, Y., Zhao, J., & Wang, X. (2016). High-performance nanofiltration membrane prepared by dopamine-assisted interfacial polymerization on PES nanofibrous scaffolds. *Desalination and Water Treatment*, *57*(21), 9549–9557.

Shenoy, S. L., Bates, W. D., & Wnek, G. (2005). Correlations between electrospinnability and physical gelation. *Polymer*, *46*(21), 8990–9004.

Siddique, H., Rundquist, E., Bhole, Y., Peeva, L. G., & Livingston, A. G. (2014). Mixed matrix membranes for organic solvent nanofiltration. *Journal of Membrane Science*, *452*, 354–366. Available from https://doi.org/10.1016/j.memsci.2013.10.012.

Singh, K., Ohlan, A., Saini, P., & Dhawan, S. K. (2008). Composite – super paramagnetic behavior and variable range hopping 1D conduction mechanism – synthesis and characterization. *Polymers for Advanced Technologies*, *November*, *2007*, 229–236. Available from https://doi.org/10.1002/pat.

Sorribas, S., Gorgojo, P., Téllez, C., Coronas, J., & Livingston, A. G. (2013). High flux thin film nanocomposite membranes based on metal-organic frameworks for organic solvent nanofiltration. *Journal of the American Chemical Society*, *135*(40), 15201–15208. Available from https://doi.org/10.1021/ja407665w.

Soyekwo, F., Liu, C., Zhao, L., Wen, H., Huang, W., Cai, C., … Hu, Y. (2019). Nanofiltration membranes with metal cation-immobilized aminophosphonate networks for efficient heavy metal ion removal and organic dye degradation. *ACS Applied Materials and Interfaces*, *11*(33), 30317–30331. Available from https://doi.org/10.1021/acsami.9b10208.

Stachewicz, U., Dijksman, J. F., Soudani, C., Tunnicliffe, L. B., Busfield, J. J. C., & Barber, A. H. (2017). Surface free energy analysis of electrospun fibers based on Rayleigh-Plateau/Weber instabilities. *European Polymer Journal*, *91*, 368–375.

Sukigara, S., Gandhi, M., Ayutsede, J., Micklus, M., & Ko, F. (2003). Regeneration of Bombyx mori silk by electrospinning—Part 1: Processing parameters and geometric properties. *Polymer*, *44*(19), 5721–5727.

UN World Water Development Report 2006 | UN-Water. (n.d.). <https://www.unwater.org/publications/water-shared-responsibility/>. Acessed 01.11.20.

Urper, G. M., Sengur-Tasdemir, R., Turken, T., Ates Genceli, E., Tarabara, V. V., & Koyuncu, I. (2017). Hollow fiber nanofiltration membranes: A comparative review of interfacial polymerization and phase inversion fabrication methods. *Separation Science and Technology (Philadelphia)*, *52*(13), 2120–2136. Available from https://doi.org/10.1080/01496395.2017.1321668.

Urper-Bayram, G. M., Sayinli, B., Bossa, N., Ngaboyamahina, E., Sengur-Tasdemir, R., Ates-Genceli, E., … Koyuncu, I. (2020). Thin film nanocomposite nanofiltration hollow fiber membrane fabrication and characterization by electrochemical impedance spectroscopy. *Polymer Bulletin*, *77*(7), 3411–3427. Available from https://doi.org/10.1007/s00289-019-02905-w.

Ursino, C., Castro-Muñoz, R., Drioli, E., Gzara, L., Albeirutty, M. H., & Figoli, A. (2018). Progress of nanocomposite membranes for water treatment. *Membranes*, *8*(2), 18.

Vatanpour, V., Madaeni, S. S., Moradian, R., Zinadini, S., & Astinchap, B. (2011). Fabrication and characterization of novel antifouling nanofiltration membrane prepared from oxidized multiwalled carbon nanotube/polyethersulfone nanocomposite. *Journal of Membrane Science*, *375*(1–2), 284–294. Available from https://doi.org/10.1016/j.memsci.2011.03.055.

Wang, B.-B., Wang, X.-D., & Wang, T.-H. (2014). Microscopic mechanism for the effect of adding salt on electrospinning by molecular dynamics simulations. *Applied Physics Letters*, *105*(12), 121906.

Wang, J., Yang, X., Zheng, D., Yao, A., Hua, D., Srinivasapriyan, V., & Zhan, G. (2020). Fabrication of bioinspired gallic acid-grafted chitosan/polysulfone composite membranes for dye removal via nanofiltration. *ACS Omega*, *5*(22), 13077–13086. Available from https://doi.org/10.1021/acsomega.0c01013.

Wang, J. J., Yang, H. C., Wu, M. B., Zhang, X., & Xu, Z. K. (2017). Nanofiltration membranes with cellulose nanocrystals as an interlayer for unprecedented performance. *Journal of Materials Chemistry A*, *5*(31), 16289–16295. Available from https://doi.org/10.1039/c7ta00501f.

Wang, L., Fang, M., Liu, J., He, J., Li, J., & Lei, J. (2015). Layer-by-layer fabrication of high-performance polyamide/ZIF-8 nanocomposite membrane for nanofiltration applications. *ACS Applied Materials and Interfaces*, *7*(43), 24082–24093. Available from https://doi.org/10.1021/acsami.5b07128.

Wang, X., Fang, D., Hsiao, B. S., & Chu, B. (2014). Nanofiltration membranes based on thin-film nanofibrous composites. *Journal of Membrane Science*, *469*, 188–197.

Wang, X., Zhao, Y., Tian, E., Li, J., & Ren, Y. (2018). Graphene oxide-based polymeric membranes for water treatment. *Advanced Materials Interfaces*, *5*(15), 1–20. Available from https://doi.org/10.1002/admi.201701427.

Wei, X., Xu, X., Wu, J., Li, C., Chen, J., Lv, B., … Xiang, H. (2019). SiO_2 -modified nanocomposite nanofiltration membranes with high flux and acid resistance. *Journal of Applied Polymer Science*, *136*(18), 1–11. Available from https://doi.org/10.1002/app.47436.

Woo, Y. C., Tijing, L. D., Shim, W.-G., Choi, J.-S., Kim, S.-H., He, T., … Shon, H. K. (2016). Water desalination using graphene-enhanced electrospun nanofiber membrane via air gap membrane distillation. *Journal of Membrane Science*, *520*, 99–110.

Woranuch, S., Pangon, A., Puagsuntia, K., Subjalearndee, N., & Intasanta, V. (2017). Starch-based and multipurpose nanofibrous membrane for high efficiency nanofiltration. *RSC Advances*, *7*(56), 35368–35375. Available from https://doi.org/10.1039/c7ra07484k.

Xiang, J., Xie, Z., Hoang, M., & Zhang, K. (2013). Effect of amine salt surfactants on the performance of thin film composite poly(piperazine-amide) nanofiltration membranes. *Desalination*, *315*, 156–163. Available from https://doi.org/10.1016/j.desal.2012.10.038.

Xie, Q., Shao, W., Zhang, S., Hong, Z., Wang, Q., & Zeng, B. (2017). Enhancing the performance of thin-film nanocomposite nanofiltration membranes using MAH-modified GO nanosheets. *RSC Advances*, *7*(86), 54898–54910. Available from https://doi.org/10.1039/c7ra11550d.

Xie, Q., Zhang, S., Hong, Z., Ma, H., Liu, C., & Shao, W. (2018). Effects of casting solvents on the morphologies, properties, and performance of polysulfone supports and the resultant graphene oxide-embedded thin-film nanocomposite nanofiltration membranes. *Industrial and Engineering Chemistry Research*, *57*(48), 16464–16475. Available from https://doi.org/10.1021/acs.iecr.8b04515.

Xue, J., Wu, T., Dai, Y., & Xia, Y. (2019). Electrospinning and electrospun nanofibers: Methods, materials, and applications. *Chemical Reviews*, *119*(8), 5298–5415.

Xue, S. M., Xu, Z. L., Tang, Y. J., & Ji, C. H. (2016). Polypiperazine-amide nanofiltration membrane modified by different functionalized multiwalled carbon nanotubes (MWCNTs). *ACS Applied Materials and Interfaces*, *8*(29), 19135–19144. Available from https://doi.org/10.1021/acsami.6b05545.

Yang, F., Sadam, H., Zhang, Y., Xia, J., Yang, X., Long, J., … Shao, L. (2020). A de novo sacrificial-MOF strategy to construct enhanced-flux nanofiltration membranes for efficient dye removal. *Chemical Engineering Science*, *225*, 115845. Available from https://doi.org/10.1016/j.ces.2020.115845.

Yang, Q., & Wang, K. Y. , Chung, T. S. (2009). Dual-layer hollow fibers with enhanced flux as novel forward osmosis membranes for water production. *Environmental Science & Technology*, *43*(8), 2800–2805.

Yang, Y., Li, X., Shen, L., Wang, X., & Hsiao, B. S. (2017). A durable thin-film nanofibrous composite nanofiltration membrane prepared by interfacial polymerization on a double-layer nanofibrous scaffold. *RSC Advances*, *7*(29), 18001–18013.

Yang, Z., Zhou, Y., Feng, Z., Rui, X., Zhang, T., & Zhang, Z. (2019). A review on reverse osmosis and nanofiltration membranes for water purification. *Polymers*, *11*(8), 1252.

Yin, J., & Deng, B. (2015). Polymer-matrix nanocomposite membranes for water treatment. *Journal of Membrane Science*, *479*, 256–275. Available from https://doi.org/10.1016/j.memsci.2014.11.019.

Yin, J., Zhu, G., & Deng, B. (2016). Graphene oxide (GO) enhanced polyamide (PA) thin-film nanocomposite (TFN) membrane for water purification. *Desalination*, *379*, 93–101. Available from https://doi.org/10.1016/j.desal.2015.11.001.

Yoon, K., Hsiao, B. S., & Chu, B. (2009a). High flux nanofiltration membranes based on interfacially polymerized polyamide barrier layer on polyacrylonitrile nanofibrous scaffolds. *Journal of Membrane Science*, *326*(2), 484–492.

Yoon, K., Hsiao, B. S., & Chu, B. (2009b). High flux ultrafiltration nanofibrous membranes based on polyacrylonitrile electrospun scaffolds and crosslinked polyvinyl alcohol coating. *Journal of Membrane Science*, *338*(1–2), 145–152.

Young, T. H., & Chen, L. W. (1995). Pore formation mechanism of membranes from phase inversion process. *Desalination*, *103*(3), 233–247. Available from https://doi.org/10.1016/0011-9164(95)00076-3.

Zahran, S. M. E., Abdel-Halim, A. H., Mansour, K., & Nada, A. A. (2020). Fabrication of nanofiltration membrane based on non-biofouling PVP/lecithin nanofibers reinforced with microcrystalline cellulose via needle and needle-less electrospinning techniques. *International Journal of Biological Macromolecules*, *157*, 530–543.

Zarrabi, H., Yekavalangi, M. E., Vatanpour, V., Shockravi, A., & Safarpour, M. (2016). Improvement in desalination performance of thin film nanocomposite nanofiltration membrane using amine-functionalized multi-walled carbon nanotube. *Desalination*, *394*, 83–90. Available from https://doi.org/10.1016/j.desal.2016.05.002.

Zhang, R., Ji, S., Wang, N., Wang, L., Zhang, G., & Li, J. R. (2014). Coordination-driven in situ self-assembly strategy for the preparation of metal-organic framework hybrid membranes. *Angewandte Chemie - International Edition*, *53*(37), 9775–9779. Available from https://doi.org/10.1002/anie.201403978.

Zhao, C., Xue, J., Ran, F., & Sun, S. (2013). Modification of polyethersulfone membranes—A review of methods. *Progress in Materials Science*, *58*(1), 76–150. Available from https://doi.org/10.1016/j.pmatsci.2012.07.002.

Zhao, Z., Zheng, J., Wang, M., Zhang, H., & Han, C. C. (2012). High performance ultrafiltration membrane based on modified chitosan coating and electrospun nanofibrous PVDF scaffolds. *Journal of Membrane Science*, *394*, 209–217.

Zhu, J., Qin, L., Uliana, A., Hou, J., Wang, J., Zhang, Y., … Van der Bruggen, B. (2017). Elevated performance of thin film nanocomposite membranes enabled by modified hydrophilic MOFs for nanofiltration. *ACS Applied Materials and Interfaces*, *9*(2), 1975–1986. Available from https://doi.org/10.1021/acsami.6b14412.

Zhu, J., Zhang, Y., Tian, M., & Liu, J. (2015). Fabrication of a mixed matrix membrane with in situ synthesized quaternized polyethylenimine nanoparticles for dye purification and reuse. *ACS Sustainable Chemistry and Engineering*, *3*(4), 690–701. Available from https://doi.org/10.1021/acssuschemeng.5b00006.

Zinadini, S., Rostami, S., Vatanpour, V., & Jalilian, E. (2017). Preparation of antibiofouling polyethersulfone mixed matrix NF membrane using photocatalytic activity of ZnO/MWCNTs nanocomposite. *Journal of Membrane Science*, *529*, 133–141. Available from https://doi.org/10.1016/j.memsci.2017.01.047.

Zuo, W., Zhu, M., Yang, W., Yu, H., Chen, Y., & Zhang, Y. (2005). Experimental study on relationship between jet instability and formation of beaded fibers during electrospinning. *Polymer Engineering & Science*, *45*(5), 704–709.

CHAPTER

7

Polymer-based bioinspired, biomimetic, and stimuli-responsive nanofiltration membranes

Nahid Azizi, Shaghayegh Goudarzi, Reza Eslami and Hadis Zarrin

Nanoengineering Laboratory for Energy and Environmental Technologies, Department of Chemical Engineering, Ryerson University, Toronto, ON, Canada

7.1 Introduction

The global water crisis is a challenging issue that draws great attention to develop new technologies (Yan et al., 2020). Membrane separation technologies have several advantages, including less energy demanding, having a small footprint, being less expensive, and high-quality effluent, making them appealing for applying for large-scale industrial usage as desalination (Meng, Song, Yao, Liu, & Zhao, 2020; Nabeel et al., 2020).

Between different types of membranes, nanofiltration (NF) technology is a practical water purification approach due to its efficiency in elimination of low molecular weight impurities, such as ions and small organic compounds (Sun, Chung, Jeyaseelan, & Armugam, 2013a).

As high-operation pressure and fouling troubles are the main problems of existing NF membranes for water reclamation, important efforts are needed to improve their performance (Meng et al., 2020). In water reclamation, an ideal NF membrane should meet features including (1) high water permeability; (2) high elimination efficiency of organic compounds and divalent/multivalent ions; (3) low rejection to monovalent ions which decreases the energy consumption and operating pressure; and (4) antifouling property and robust chemical stability which enables the stable performance of the membrane in a long-term operation (Meng et al., 2020).

Between different types of membranes, biomimetic and bioinspired membranes designed using natural or natural-like materials using bioinspired and biomimetic

Advancement in Polymer-Based Membranes for Water Remediation
DOI: https://doi.org/10.1016/B978-0-323-88514-0.00017-6

© 2022 Elsevier Inc. All rights reserved.

approaches including bioadhesion, biomineralization, self-assembly, etc. are between the emerging membranes that can be helpful in water treatment applications (Abdelrasoul, Doan, & Lohi, 2017).

Stimuli-responsive membranes are another type of membranes that can change their properties in response to changes in pH, light, temperature, etc., which can be used in various applications such as antifouling and bioseparation purposes (Wandera, Wickramasinghe, & Husson, 2010). Bioinspired, biomimetic, and stimuli-responsive membranes can be applied to design NF membranes. This chapter describes the polymer-based bioinspired, biomimetic, and stimuli-responsive NF membranes, their applications, and recent developments in these areas.

7.2 Bioinspired membranes and their applications

Bioinspiration relates science to applied engineering by extracting concept of biological systems to form a bridge to develop solutions to issues that conventionally have few connections with biology (Montero De Espinosa, Meesorn, Moatsou, & Weder, 2017; Vullev, 2011). Discovering and capturing a basic idea underpinning a biological system and its technological implementation is the aim of a bioinspired approach (Maletskyi, 2020).

As water scarcity and insufficient access to clean water is a global challenge, there is a vital need to use a combination of technology to develop a solution for water purification. In this scenario, utilizing bioinspired materials can play an essential role in developing membranes with high performance as an environmentally friendly solution (Gonzalez-Perez & Persson, 2016). For example, bioinspired adhesive materials like tannic acid, polydopamine (PDA), and other polyphenols can create coatings with several active groups on different surfaces, making them an excellent tool for use in biomedical, energy, surface modification, marine, and other fields (Feng, Weber, Maletzko, & Chung, 2019; Wang et al., 2020).

7.2.1 Dopamine-based nanofiltration membrane

Dopamine has been widely used to develop bioinspired NF membranes. Dopamine, 3,4-dihydroxyphenethylamine, with excellent biocompatibility and adhesion, mimics the adhesive protein (Li et al., 2014). Dopamine can be spontaneously oxidized and self-polymerized in a weakly alkaline situation (typically pH = 7.5 or 8.5) because of the existence of catechol groups and amine groups (Dai, Li, & Wang, 2020; Fang et al., 2020; Xu, Tang, Liu, Guo, & Shao, 2017; Yan et al., 2020). Dopamine self-polymerization leads to create a thin adherent PDA layer onto almost surfaces of all inorganic and organic materials like polymers, noble metals, ceramics, and semiconductors (Dai et al., 2020; Li et al., 2014; Xu et al., 2017; Yan et al., 2020). PDA can adhere to different supports through strong covalent and noncovalent bonds (Ji et al., 2018). The PDA film has high surface hydrophilicity, ultrathin and controllable film thickness, no damage to the substrate, the robust interfacial binding force between the substrate and the film through covalent bonds, and

strong intermolecular interactions. PDA provides many active groups, like abundantly amines and additional reactions with other molecules (Li et al., 2014).

Marine mussel-inspired PDA draws great attention owing to its unique properties such as strong adhesion on most materials, thermal, and chemical stability (Zhao et al., 2019). PDA is a widely used polymer to improve ultrafiltration, NF and reverse osmosis membranes' fouling resistance through the coating of surface, and increasing the hydrophilicity of membrane surface (Dai et al., 2020; Yan et al., 2020). Submerging the membranes into dopamine solutions introduces a hydrophilic PDA layer on the membrane's surface, altering polymeric membranes' mechanical characteristics via this adhesion procedure (Yan et al., 2020). Bioinspired PDA can be used to fabricate antifouling and high-flux NF membranes (Wang et al., 2020). Also, PDA-coated membranes can be applied in membrane separation because of their potential in improving stability (Xu et al., 2017). However, it must be considered that providing optimum synthesis conditions including dopamine concentration, substrate type of the membrane, reaction duration, pH, type of oxidant, and the solvent is required for incurring dopamine self-polymerization and the formation of uniform PDA layers (Yan et al., 2020). Modification of NF membranes with PDA for using in different water treatment applications will be discussed.

One of the important subcategories of NF membranes is thin-film composite (TFC) membranes, comprised of a selective layer on the ultrafiltration support. Selective layer structure directly has a critical function in the properties of TFC NF membranes (Du, Qiu, Lv, Wu, & Xu, 2016). TFC membranes have been used broadly because of their considerable salt rejection as well as high-water permeation flux. In this regard, an interlayer of PDA/polyethylenimine was codeposited on the ultrafiltration substrate to tune the piperazine and trimesoyl chloride's interfacial polymerization for preparing TFC NF membranes. Furthermore, TFC NF membrane has shown salt rejection sequence of $Na_2SO_4 \approx MgSO_4 > MgCl_2 > NaCl$. Also, high rejection of 97% Na_2SO_4 was achieved using this membrane (Yang, Du, Zhang, He, & Xu, 2017).

In another example, dopamine/trimesoyl chloride composite membranes were fabricated. Bioadhesion of PDA could increase the interaction between the thin film and the composite membrane's substrate. Temperature and reaction time were the useful factors in the performance of the dopamine/trimesoyl chloride composite membranes, while trimesoyl chloride concentration had a minor effect on dopamine/trimesoyl chloride composite membranes' performance. The rejection was increased for both inorganic salts and organic dyes, while water fluxes were reduced with dopamine concentration's increase in an aqueous solution. Also, a considerable increase in water fluxes was displayed after immersion of the membrane in sodium hypochlorite solution, while the separation property was still in the NF range. Finally, the composite membrane displayed chemical stability in sodium hypochlorite solution. Also, a long-term structural stability was seen by immersing the membrane in alcohol after 12 days (Zhao et al., 2014). In a study, an enhanced NF membrane was fabricated using covalent organic framework interlayer of PDA on polyacrylonitrile support via interfacial polymerization, as shown in Fig. 7.1. The covalent organic framework nanosheets acted as a multifunctional controller for optimizing the hybrid interlayer porous structure using physicochemical interactions. By controlling monomer diffusion behavior, a dense polyamide layer of 11 nm in thickness was generated by the PDA-covalent organic framework hybrid interlayer with high porosity

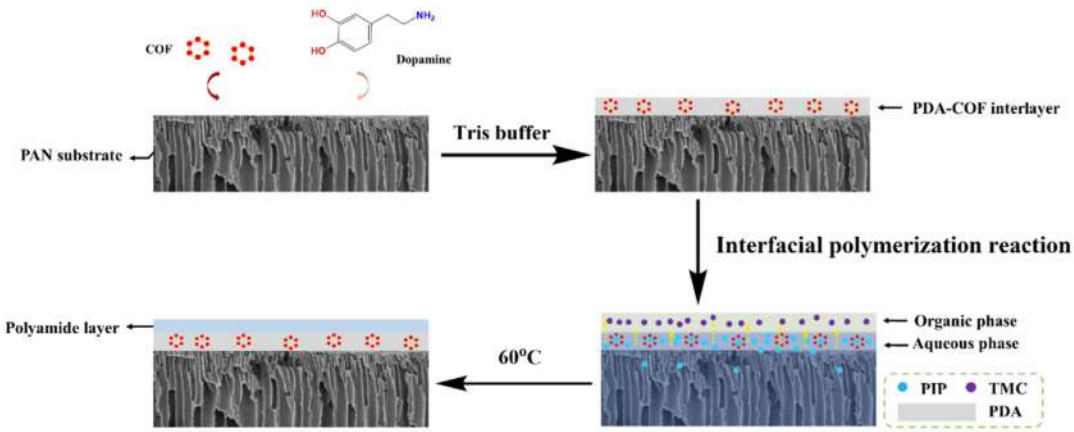

FIGURE 7.1 The schematic diagram to prepare the nanofiltration membranes. (Wu et al., 2019) Source: *Adapted with permission from Wu, M., Yuan, J., Wu, H., Su, Y., Yang, H., You, X., ... Jiang, Z. (2019). Ultrathin nanofiltration membrane with polydopamine-covalent organic framework interlayer for enhanced permeability and structural stability.* Journal of Membrane Science, 576, *131–141. Copyright (2019) Elsevier.*

and surface hydrophilicity, which resulted in improved water permeability by three times compared to commercial NF membranes with alike solute rejection. The adhesive PDA guaranteed the composite NF membranes stability by improving the interfacial interaction between the skin layer and support. The fabricated NF membrane demonstrated superior structural stability for 16 days (Wu et al., 2019).

Organic solvent NF membranes separate molecules with a molecular weight between 200 and 1000 g mol^{-1} from organic solvents (Huang et al., 2020; Xu, You, Sun, & Shao, 2017; Xu et al., 2017). One of the critical parameters effective in the permeances of organic solvent NF membranes toward different solvents is the interactions between solvents and membrane materials (Huang et al., 2020; Zhao et al., 2019).

So far, different polymers such as poly(ether block amide), polyimide, polybenzimidazole, etc. have been cross-linked by different methods for fabricating stable organic solvent NF membranes. Polyimide is the common polymer for applying in organic solvent NF application because of its ability to simply cross-linked by diamine via the reaction between amine groups and imide groups (Xu et al., 2017). According to a study, a PDA-coating layer was used as a separating layer on cross-linked polyimide support for organic solvent NF, as shown in Fig. 7.2. Then, the subsequent membrane was treated with 1,6-hexanediamine for cross-linking on both the PDA layer and polyimide support. The pure PDA-coating layer could perform as a separating layer for organic solvent NF, whereas cross-linking PDA by 1,6-hexanediamine can result in a denser compact layer of stability in the long-term performance testing the composite membrane, which increases dye rejection considerably. After coating time optimization of 4 h, the prepared membrane displayed ethanol permeance of 0.91 L m^{-2} h^{-1} bar^{-1} and a rejection of 99% for rose bengal. Moreover, the composite membrane demonstrated suitable structural stability in long-term performance testing and good performance toward dyes separation in various

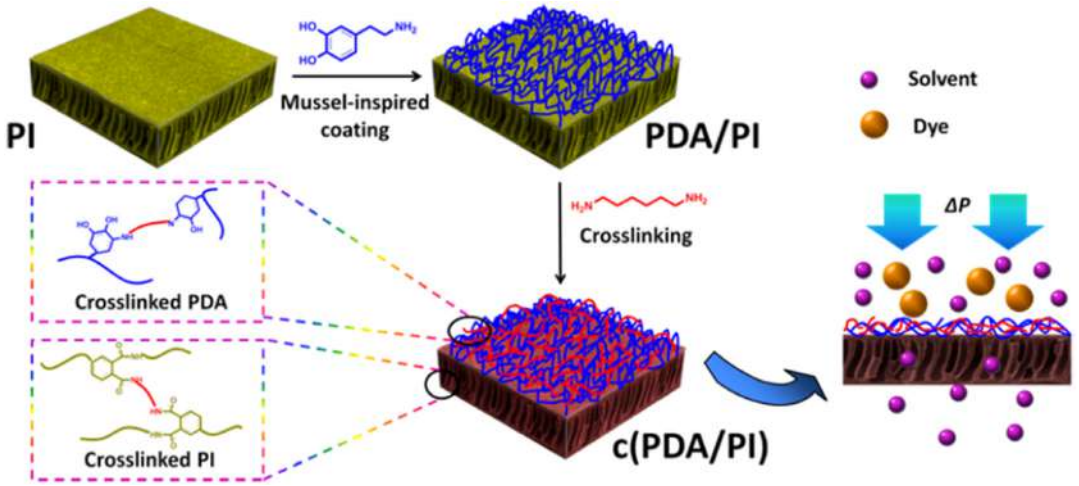

FIGURE 7.2 Illustration of mussel-inspired polydopamine-based nanofiltration membrane fabrication. Source: *Adapted with permission from Xu, Y., You, F., Sun, H., & Shao, L. (2017). Realizing mussel-inspired polydopamine selective layer with strong solvent resistance in nanofiltration toward sustainable reclamation.* ACS Sustainable Chemistry and Engineering, 5*(6), 5520–5528. Copyright (2017) American Chemical Society.*

solvents such as challenging polar aprotic and strongly swelling solvents such as acetone and dimethylformamide (Xu et al., 2017).

The polymers' stability in the presence of harsh organic solvents, such as toxic polar aprotic solvents, is another challenging issue in organic solvent NF fabrication. Chemical cross-linking such as covalent cross-linking is usually employed to enhance membranes' stability under harsh solvent and avoid dissolution in polar aprotic solvents (Zhao et al., 2019). A NF was developed based on interpenetrating polymer networks incorporating PDA and polybenzimidazole for organic solvent NF. Dopamine's in situ polymerization within polybenzimidazole support led to good polar aprotic solvents resistance and permeance without covalent cross-linking of polybenzimidazole backbone due to the formation of interpenetrating polymer networks. The molecular weight cut off and permeance of the membranes are tunable by altering the polymerization time. Also, permeance up to 12 L m^{-2} h^{-1} bar^{-1} in *N*,*N*-dimethylformamide was achieved. PDA in situ polymerization provided an alternative method to covalent cross-linking membranes without requiring usual cross-linking to make polybenzimidazole membranes stable in harsh environs. Generally, covalently cross-linked polymers in harsh conditions lead to obtaining solvent stability. The membrane separation performance and pore size were engineered by controlling PDA's polymerization time to fine-tune the membrane molecular weight cut off in the range of $190 - 850$ g mol^{-1}. Membranes with long-term stability and robustness were obtained in seven polar aprotic solvents in temperatures ranging from -10°C to $+100^{\circ}$C (Zhao et al., 2019).

The layer-by-layer electrostatic assembly is another facile, economical, scalable, and environmentally friendly method to fabricate NF membranes with high-performance. However, because of the compromising the structural integrity of the separated layers in

strong acid and alkaline conditions, their application has been limited in water reclamation. So, fabricating a robust chemically stable NF membrane is a challenge in membrane applications (Meng et al., 2020). In another attempt, an ultra-stable layer-by-layer-based NF membrane was designed on polyethersulfone ultrafiltration substrates with PDA-assisted polyelectrolytes and layer-by-layer deposition (PDA-a-LBL) technique, as illustrated in Fig. 7.3. Alternatively, deposition of PDA/polyethylenimine and poly(sodium 4-styrenesulfonate) layers onto polyethersulfone ultrafiltration substrates were led to tunable surface chemistry and tailorable pore size. The functionality of the outermost layer of the NF membranes was useful in the surface charge and hydrophilicity of the prepared NF membranes. The evaluation of the developed NF membranes' separation efficiencies was performed on a bench-scale crossflow NF apparatus using four kinds of salts and neutral solutes polyethylene glycol with different molecular weights. The PDA-a-LBL NF membranes with robust chemical stability had good rejections more than 94% against divalent anions along with 7–13 L m^{-2} h^{-1} bar^{-1} pure water permeability. The developed NF membrane (polyethersulfone-50–3L) has shown long-term operation stability in the pH range of 2–11, attributing to the synergistic effects of covalent bonds between PDA and polyethylenimine, electrostatic interaction and π-π stacking between PDA/polyethylenimine and poly(sodium 4-styrenesulfonate) layers. Besides, the optimized NF membrane had outstanding hydrophilicity, and the water contact angle was as low as 22.1 degrees. Additionally, the membrane's chemical stability and robust performance in a continuously one-week long-term operation demonstrated its ability to apply in sustainable water reclamation applications (Meng et al., 2020).

Co-deposition of PDA and polyetheylenimine was used to fabricate NF membranes, followed by cross-linking of glutaraldehyde. A robust, uniform, and defect-free selective layer was produced on the hydrolyzed polyacrylonitrile ultrafiltration membrane substrate, which endowed a NF membrane with a high separation of multivalent ions. Zeta potential measurements reveal the proposed NF membranes are somewhat positively

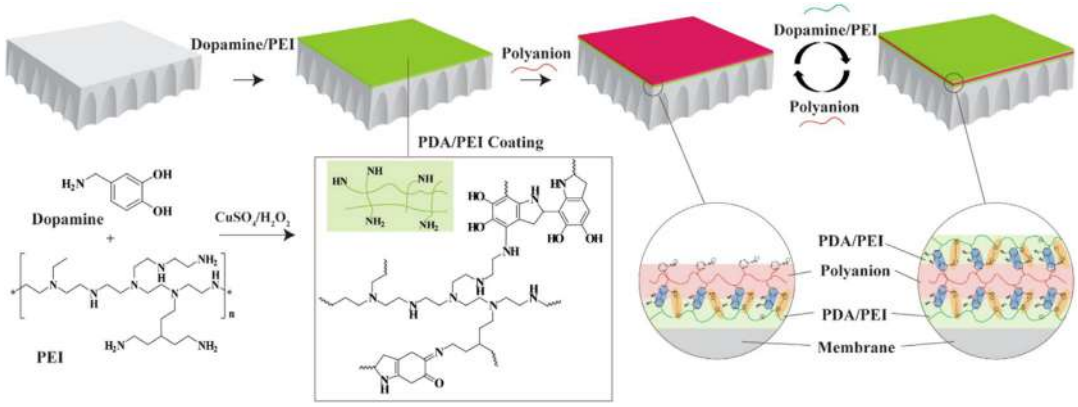

FIGURE 7.3 Schematic of PDA-a-LBL nanofiltration membrane fabrication. Source: *Adapted with permission from Meng, F., Song, F., Yao, Y., Liu, G., & Zhao, S. (2020). Ultrastable nanofiltration membranes engineered by polydopamine-assisted polyelectrolyte layer-by-layer assembly for water reclamation.* ACS Sustainable Chemistry and Engineering, 8*(29), 10928–10938. Copyright (2020) American Chemical Society.*

charged, leading to salts rejection of $MgCl_2 > CaCl_2 > MgSO_4 > Na_2SO_4 > NaCl$ at pH 5.5. The codeposition time of 4 h and the mass ratio of dopamine/polyetheylenimine (2/2) were the useful parameters in the optimum protocol to alter the NF performance. Moreover, the NF membrane displayed good structural stability for submerging in ethanol and long-term operation (Lv, Yang, Liang, Wan, & Xu, 2015).

Zhang et al. made positively charged composite NF membranes by deposition of bioinspired PDA, followed by grafting polyethylenimine on polyethersulfone substrates. Polyethylenimine grafting to the PDA surface can result in a dense and defect-free active layer in the composite membrane, which reduces PDA deposition time down to as short as 4 h. Moreover, tuning the PDA deposition time, polyethylenimine reaction temperature, polyethylenimine concentration, and time are also useful in the membrane's separation properties and surface properties, including morphology, surface charge, chemical composition, and hydrophilicity. By increasing PDA deposition time, polyethylenimine concentration, polyethylenimine reaction temperature and time, the pure water flux was decreased, while the rejection of salts was increased. The salts rejection sequence of the membrane was $MgCl_2 > CaCl_2 > MgSO_4 > Na_2SO_4$, which confirmed that the membranes were positively charged. The rejection for $MgCl_2$ and $CaCl_2$ could reach 73.7% and 57.1%, prospectively, and the membranes rejection for cationic dyes was up to 96.5% (Zhang et al., 2014).

Antibiotics are useful antimicrobial pharmaceuticals, but they also can act as organic pollutants in natural waters. With low NaCl rejection and high antibiotic rejection, NF technology can be used for antibiotic extraction (Cheng, Zhang, Wang, & Shao, 2016). Pores tailoring of hydrophilic polyethylene glycol-based NF membrane is required for proficiently sieving the active molecules to concentrate/purify antibiotics. A hydrophilic polyethylene glycol-based NF membrane can be modified through the coating with PDA to tailor the NF membranes' pores to have enhanced antibiotics separation performance (Cheng et al., 2016). Cheng et al. fabricated a coating layer using self-polymerization of dopamine on the hydrophilic polyethylene glycol-based NF membrane to tailor the NF membrane's pores for increasing the membrane performance in antibiotics separation as shown in Fig. 7.4. Coating the NF membrane with PDA decreased the NF membrane's pore radius from 0.42 to 0.33 nm, and the dual resistance to chlorine and fouling remained at a high level. The PDA formation around the pore of the hydrophilic polyethylene glycol-based NF membranes was confirmed by elements content results examined by X-ray photoelectron spectrometer indicate. The membrane displayed the stable tobramycin solution flux of 46 L m^{-2} h^{-1} and rejections up to 99%, 94%, and 93% for the tobramycin, clindamycin phosphate, and cephalexin, respectively, and with a low concentration of feed (50 mg L^{-1}) under 8.0 bar operating pressure. Surprisingly, the membrane still had high rejections to all antibiotics up to 90%, when the feed concentration increased up to 800 mg L^{-1}. So, coating the NF with PDA is a promising method to tailor hydrophilic polyethylene glycol-based membranes' pores toward separation performance. This efficient and cost-effective membrane can be applied to separating negative and amphiprotic charged antibiotics (Cheng et al., 2016).

Polymer–matrix nanocomposite NF membrane is an emerging field for applications like gas separation, desalination, and water purification in which the considerable interest is designing membranes with high permeability and salt rejection (Zhao et al., 2016).

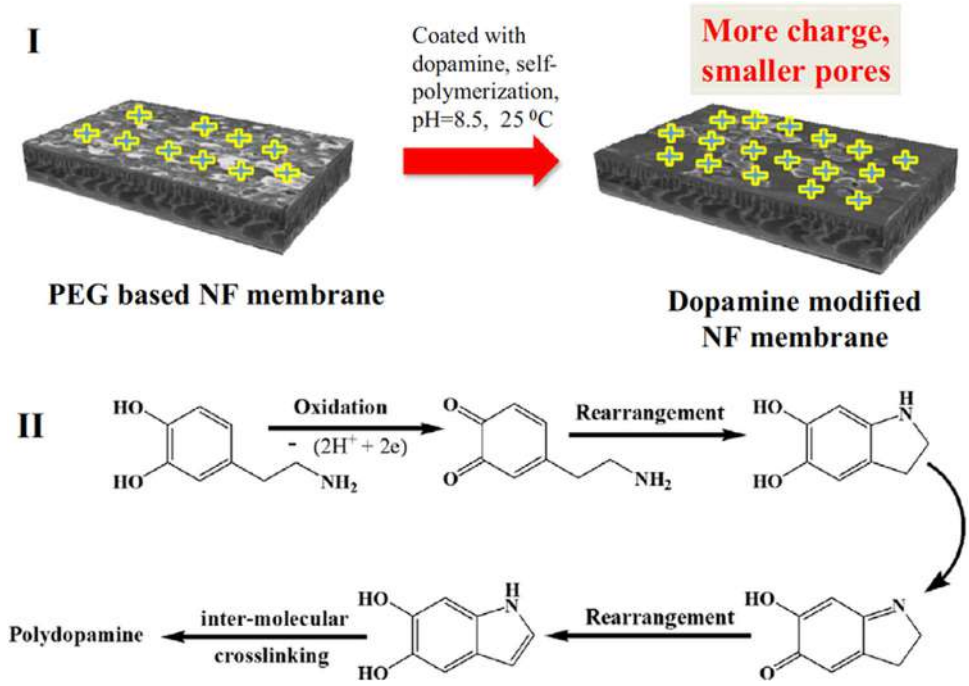

FIGURE 7.4 Surface modification process of polyethylene glycol-based nanofiltration membranes. Source: *Adapted with permission from Cheng, X. Q., Zhang, C., Wang, Z. X., & Shao, L. (2016). Tailoring nanofiltration membrane performance for highly efficient antibiotics removal by mussel-inspired modification*. Journal of Membrane Science, 499, 326–334. *Copyright (2016) Elsevier*.

However, the poor dispensability of nanocarbons such as the pristine carbon nanotubes in water is a barrier to their implantation in thin-film nanocomposite membranes for water purification applications. Zhao and coworkers prepared high-flux positively charged nanocomposite NF membranes using uniformly embedding PDA-modified multiwall carbon nanotubes in polyamide TFC membranes through interfacial polymerization between polyethylenimine and trimesoyl chloride, as shown in Fig. 7.5. PDA improved dispersion of carbon nanotubes in water and improved its interfaces with polyamide matrices, leading to facile preparation of mixed matrix NF membranes with enhanced separation performances. The prepared NF membranes were suitable for water softening, removing a heavy metal, and recovering valuable cationic molecules (Zhao et al., 2016).

Heavy metals are emerging carcinogenic or toxic pollutants due to the rapid development of industries such as mining operations, electroplating, batteries, aerospace, paper industries, atomic power plants, and tanneries, which can cause severe environmental issues. The presence of metal ions higher than the minimum hazardous limit can directly or indirectly threaten water resources and human health. Unlike microorganisms, suspended solids, organics, and other pollutants, heavy metals are resistant to biodegradation, accumulating in living organisms. The abundant toxic ions in industrial wastewater are mercury (Hg^{2+}), copper (Cu^{2+}), chromium (Cr^{3+} and Cr^{6+}), nickel (Ni^{2+}), cadmium

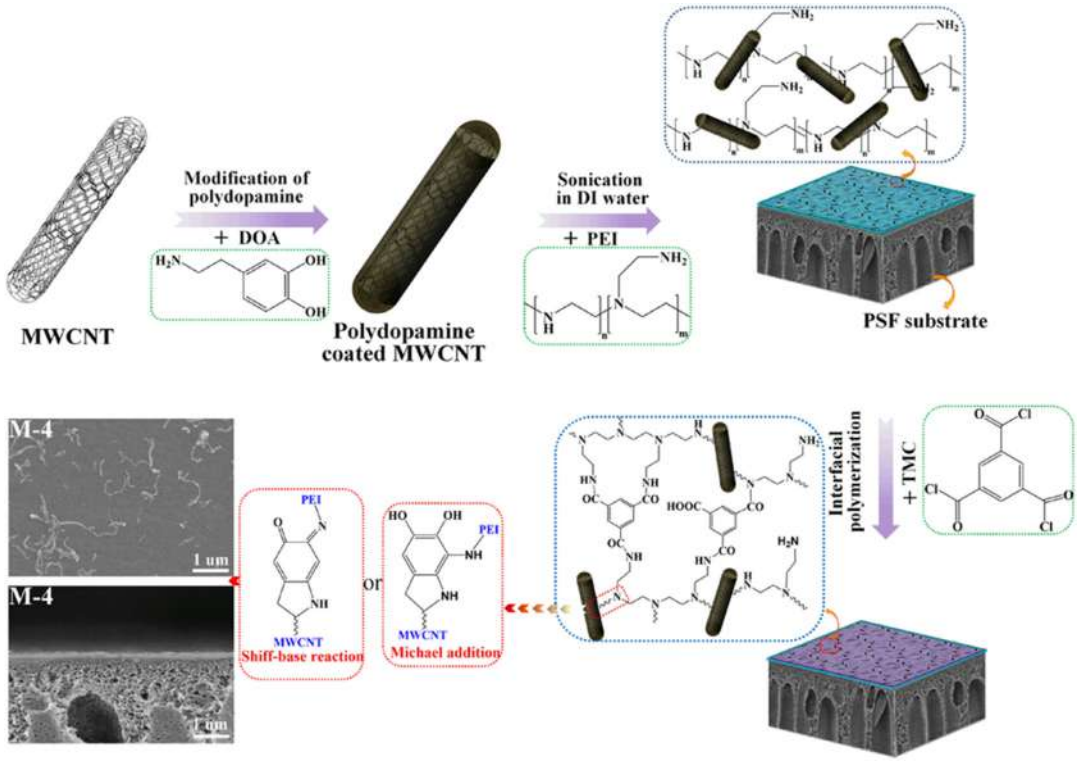

FIGURE 7.5 Schematic preparation of the nanofiltration membranes. Source: *Adapted with permission from Zhao, F. Y., Ji, Y. L., Weng, X. D., Mi, Y. F., Ye, C. C., An, Q. F., & Gao, C. J. (2016). High-flux positively charged nanocomposite nanofiltration membranes filled with poly(dopamine) modified multiwall carbon nanotubes.* ACS Applied Materials and Interfaces, *8(10), 6693–6700. Copyright (2016) American Chemical Society.*

(Cd^{2+}), etc. Conventional methods, including flotation, coagulation, adsorption, and flocculation for removing heavy metal ions from wastewater, are facing problems like high-energy consumption or low separation efficiency. NF membranes have been commonly reported for metal removal from wastewater (Liu, Feng, Zhang, & Chen, 2020). Since most heavy metal ions are multivalent, NF membranes are a promising method to remove heavy metals due to their unique rejection mechanisms—steric effect and Donnan exclusion. Moreover, in comparison to reverse osmosis, NF membranes need a lower pressure while providing a higher flux without much compromise in rejection (Gao, Sun, Zhu, & Chung, 2014). For example, the heavy metal ion elimination behavior and antifouling performance of NF membrane were investigated by Liu et al. Halloysite nanotubes were used to decorate commercial NF membranes via self-polymerization of dopamine. Different analyses confirmed the homogeneous halloysite nanotubes' distribution on the membrane's surface layer, and surface roughness was increased by enhancing the number of halloysite nanotubes adhered by dopamine. Halloysite nanotubes incorporation increased the membranes' hydrophilicity and enhanced the membrane's antifouling property and stability.

Moreover, the membrane rejection ratios were increased during the heavy metal ions removal from wastewater. Cu^{2+} and Ni^{2+} ions rejections were 74.3% and 70.1%, respectively, in feed solution removed by halloysite nanotubes modified membrane. The permeability of the modified NF membrane was 13.9 L m^{-2} h^{-1} bar^{-1}. The fabricated membrane can be used for desalination applications and removing the hazards from wastewater (Liu et al., 2020). Desalination is the process of removing salts from saline water such as brackish water, groundwater, or seawater to make it suitable for human, industrial, and agricultural uses (Nabeel et al., 2020). NF membranes can reject multivalent ions and low molecular weight organics, useful in desalination and wastewater reclamation (Wu et al., 2019; Yan et al., 2020).

7.2.2 Tannic acid-based nanofiltration membranes

Plant polyphenols such as tannic acid and gallic acid, epigallocatechin gallate with rich catechol or pyrogallol groups can be used to fabricate substrate-independent coatings through a simple dip-coating method in an aqueous solution, a procedure of which is easy-to-get, free from toxic reagents, green, and easy for operation (Chakrabarty, Pérez-Manríquez, Neelakanda, & Peinemann, 2017; Li et al., 2020; Zhang et al., 2019). Tannic acid, gallic acid, and catechol with alike structures to dopamine can undergo self-polymerization on the membrane surface (Yan et al., 2020). Moreover, some benefits of plant polyphenol-inspired coatings are comparable to the ones of PDA coatings like spontaneous polymerization under mild conditions, firm adhesion to different substrates, and covalently bonding with thiol and amine groups (Zhang et al., 2019).

Tannic acid is a typical plant-derived polyphenol found in natural materials like fruits, tea leaves, oak wood, and nettle (Chakrabarty et al., 2017; Li et al., 2020). Moreover, catechol or gallol groups in tannic acid provide excellent binding with surfaces of organic/inorganic/metallic through either of covalent and/or noncovalent bond interactions (Chakrabarty et al., 2017). So, tannic acid's abundant catechol groups can be mixed with polymer or organic containing amine groups to mimic dopamine self-polymerization to fabricate NF membrane selective layers through a codeposition strategy (Guo et al., 2020; Xiao et al., 2020).

Guo and coworkers prepared a NF membrane by a layer-by-layer process using plant-based polyphenol tannic acid and hydrophilic Jeffamine. This design was inspired by the mussel-adhesion mechanism because of the existence of catechol and amino groups in the following materials. The NF membrane selective layer without any pretreatment to the substrate was fabricated using alternately submerging a polyacrylonitrile substrate into individual tannic acid and Jeffamine buffer solutions. High pure water permeance of 37 L m^{-2} h^{-1} bar^{-1} was displayed for the optimized membrane while maintaining good rejection performance higher than 90% for dyes with molecular weights ranging from 269 to 1017 g mol^{-1}. Moreover, the membrane's good antifouling and long-term performance can be ascribed to the hydrophilic surface and the presence of covalent bonds in the selective layer (Guo et al., 2020).

Chakrabarty et al. prepared high-flux NF membranes by codeposition of a bio-polyphenolic coating from tannic acid and copper acetate on polyacrylonitrile ultrafiltration membranes, as displayed in Fig. 7.6A. The results confirmed that the modification of

membranes with tannic acid and cupric acetate (CuII) developed a thin-skin layer. The adhesion of the catechol- and gallol-rich tannic acid/cupric acetate (TA/CuII) coating on top of the polyacrylonitrile membrane support was excellent. The TA/CuII coated polyacrylonitrile membranes with TA/CuII 10, TA/CuII 20, and TA/CuII 30 polyacrylonitrile membranes were used to evaluate the inorganic salts rejection of NaCl, $MgSO_4$, and Na_2SO_4; the salt concentrations of which were measured using their conductivity magnitudes. The order of $Na_2SO_4 > MgSO_4 > NaCl$ was fallowed for the inorganic salt rejection using coated membranes. As illustrated in Fig. 7.6B, the membrane exhibited a low sodium chloride rejection of about 5%. The membrane was a suitable candidate for applications where organic solutes must be desalted. Moreover, the provided hydrophilic membrane exhibited no decline in water permeance over 20 days (Chakrabarty et al., 2017).

Zhang et al. used natural tannic acid as a polyphenol monomer to manufacture the composite NF membranes benefiting from phenol groups of tannic acid and acyl chloride groups of trimesoyl chloride to cross-link them in the water/oil interfacial zone. At a fixed trimesoyl chloride concentration, by increasing of tannic acid concentrations, the enhancement in the salt rejection ratios of the composite NF membranes has been observed. In contrast, at a fixed tannic acid concentration, the salt rejection ratios of the composite NF membranes were lowered with an increase of trimesoyl chloride concentrations. The prepared composite NF membranes' excellent chemical stability and antifouling properties made them suitable candidates in wastewater treatment (Zhang et al., 2013).

Recently, nonpolyamide TFC NF membranes have caught the attention of researchers. However, there are some barriers to developing nonpolyamide TFC NF membranes because of the complex fabrication process and the trade-off between selectivity and permeability. Liu et al. fabricated hydrolyzed polyacrylonitrile substrate-based membrane by modifying it with tannic acid and Fe^{3+} intermediated regulation. This membrane coordinate to develop a highly perm-selective nonpolyamide TFC NF membrane. The fabricated membrane owned an ultrathin selective film with a defect-free, negatively charged, and a molecular weight cut off of around 390 Da. It exhibited high rejections for inorganic salts in a sequence of $Na_2SO_4 > MgSO_4 > NaCl$ (50.0%) $> MgCl_2$ and good rejections toward organic pollutants and a pure water permeance of as high as 13.6 L m^{-2} h^{-1} bar^{-1} (Liu, Chen, Tran, & Zhang, 2020).

Another strategy for the fabrication of NF membranes is codeposition between plant polyphenol tannic acid and Fe^{3+}. This method has been described as a facile method for NF membranes fabrication. However, this method generates environmentally harmful aggregate wastes in solution. To solve this, a green layer-by-layer self-assembly method was used to prepare a TA-Fe^{3+} complex-based NF membrane. The suggested technique was free of toxic solvent or chemical for the pretreatment of the support. The membrane also displayed a water contact angle as low as 8 degrees, a sign of superhydrophilicity property, which was tested by a contact angle meter. The membrane displayed a stable pure water permeance and dye rejections in a 48 h filtration, which could be attributed to the strong coordination ability between TA and Fe^{3+}. Also, water permeance of 40.9 L m^{-2} h^{-1} bar^{-1} and rejections of 93.9% toward different dyes with 320−1017 Da molecular weight range was displayed in the fabricated membrane (Xiao et al., 2020).

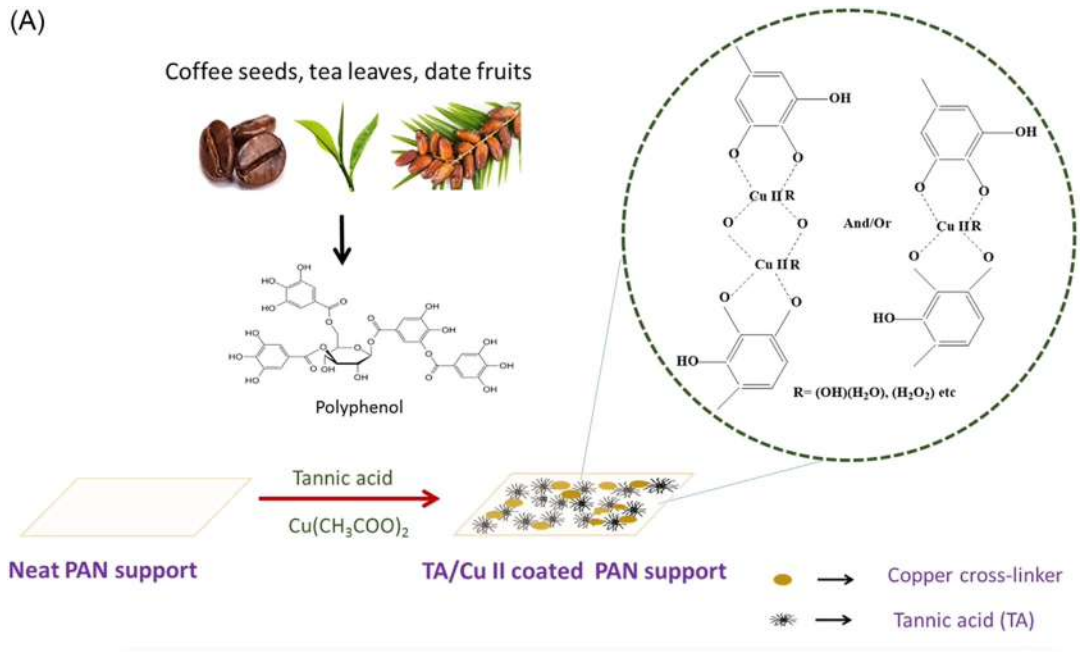

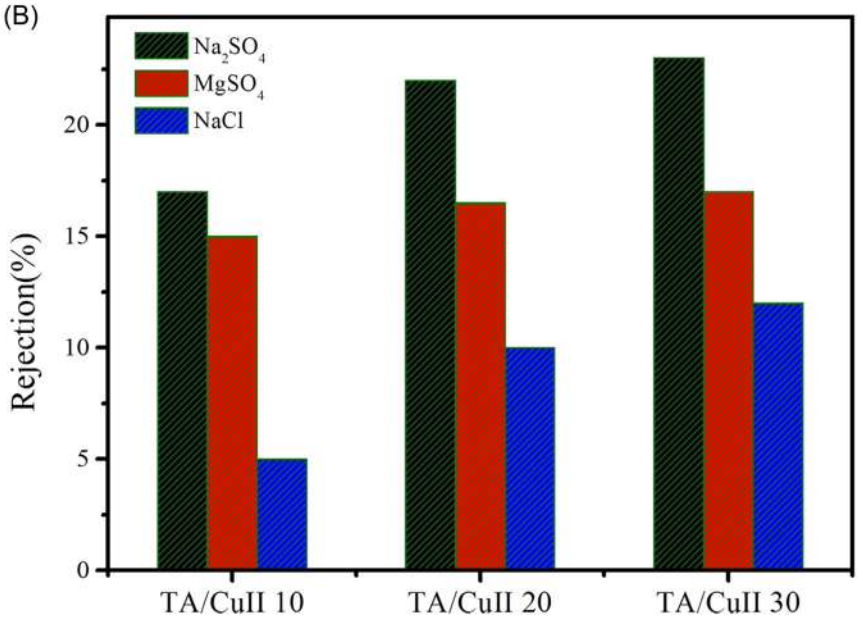

FIGURE 7.6 (A) Schematic of membrane coating process using one-step coordination assembly of tannic acid (TA) and cupric acetate (CuII) on polyacrylonitrile support. (B) Rejection performance of TA/CuII 10, TA/CuII 20, and TA/CuII 30 polyacrylonitrile membrane with various inorganic salts. Source*: Adapted with permission from Chakrabarty, T., Pérez-Manríquez, L., Neelakanda, P., & Peinemann, K. V. (2017). Bioinspired tannic acid-copper complexes as selective coating for nanofiltration membranes*. Separation and Purification Technology, *184, 188–194. Copyright (2017) Elsevier*.

7.2.2.1 *Tannic acid-based nanofiltration membranes with hollow fiber configuration*

Membranes with hollow fiber configuration have higher surface area per unit membrane volume, making them desirable to be used in different areas. However, despite being more favorable, hollow fiber membranes are rare due to their complex fabrication compared to flat sheets (Tham & Chung, 2020).

Tham and Chung reported using a single-step cross-linking and modification method which involves only an aqueous solution of the naturally occurring tannic acid and hydrazine for polyacrylonitrile-based hollow fibers. Hydrazine cross-linker was used for cross-linking polyacrylonitrile while it forms interactions with tannic acid, which results in a robust modification. Changing the amount of tannic acid in the process can lead in fabrication of hollow fibers with diverse filtration properties, which has been shown by standard pore size tests using aqueous feeds. Efficacy of the utilized one-step modification of these hollow fibers was evaluated by organic solvent feeds like dissolved dyes in methanol. A stable methanol permeance of 1.2 L m^{-2} h^{-1} bar^{-1} and sustained 100% rejection of Evans Blue (M_w = 960.81 g mol^{-1}) was seen for long-term tests (Tham & Chung, 2020).

7.2.3 Other bioinspired nanofiltration membranes and their application

Nature is an inspiration to tailor artificial surfaces with superhydrophilic or superhydrophobic properties. From a biological viewpoint, the *Bombina orientalis* can be adapted to both land and aquatic ecosystems using epidermal secretions, which can be attributed to the skin secretion akin to the mussels secreting of an adhesive protein. Additional investigation on skin of the *B. orientalis* showed the abundance of bioactive substances (i.e., biogenic amines, alkaloids, peptides, heterocyclic rings, and other proteins) (Xiao et al., 2019). Bioinspired NF membranes inspiring with amphibian skin of *B. orientalis* by grafting amino acid ionic liquids on the interfacially polymerized membrane was fabricated, as shown in Fig. 7.7. It is worth mentioning that amino acid ionic liquids contain similar amino and carboxyl residues to the residues in *B. orientalis* secretion. The hydrophilicity of

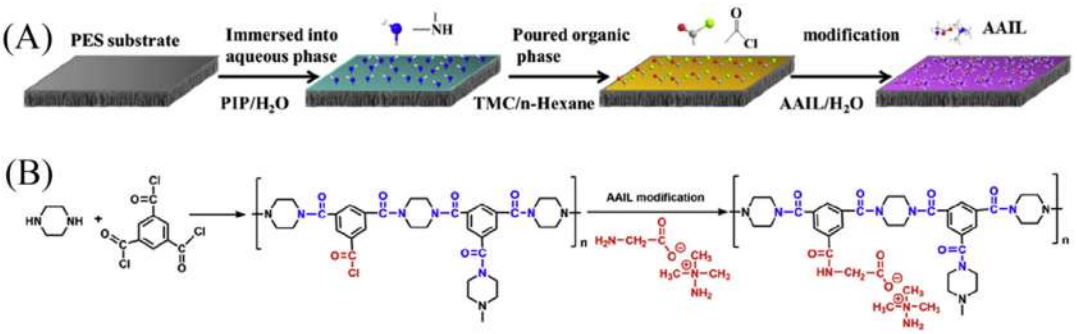

FIGURE 7.7 (A) Schematic diagram of amino acid ionic liquid-modified nanofiltration membrane and (B) the probable reaction formula. Source: *Adapted with permission from Xiao, H. F., Chu, C. H., Xu, W. T., Chen, B. Z., Ju, X. H., Xing, W., & Sun, S. P. (2019). Amphibian-inspired amino acid ionic liquid functionalized nanofiltration membranes with high water permeability and ion selectivity for pigment wastewater treatment*. Journal of Membrane Science, 586, 44–52. *Copyright (2019) Elsevier.*

the membrane surface could be enhanced using amino and carboxyl residues. Manufacture, modification, and characterization of the membrane for applying in real pigment wastewater to remove the chloride ions in the wastewater were assessed. It was found that amino acid ionic liquid helped tune the membrane hydrophilicity and charge characteristics. The amino acid ionic liquid functionalized membrane might effectively design high-performance NF membranes to be applied in waste decrease in pigment and other industries. Besides, the amino acid end groups (glycine) of amino acid ionic liquid, similar to the *B. orientalis*' epidermal secretion, act as a humectant that avoids pore shrinkage during heat-treatment, which is vital for storage and transport of membranes (Xiao et al., 2019).

The other method to fabricate bioinspired membranes is biomineralization, which can be utilized to manufacture bioinspired NF membranes (Sambudi & Sahoo, 2017). Since the 1990s, many processes inspired by biomineralization were developed to prepare the inorganic nanoparticles with controllable morphology in vitro by the induction of natural and synthesized polymers (Pan, Cheng, Jia, & Jiang, 2010). Biomineralization is a natural process of biomineral production by living organisms (Sambudi & Sahoo, 2017). Pearls in shells, vertebrate bones, conch shells, and eggshells are examples of synthesizing from minerals achieved by animals. Unparalleled biomineralization phenomenon in nature, like sponge organism silicon skeleton structure, can be a foundation to create loose and stable NF membranes (Qiang et al., 2020).

Qiang et al. fabricated a polyimide/SiO_2 membrane via one-step phase inversion inspired by the biomineralization phenomena and its unique structure with the siliceous framework, as illustrated in Fig. 7.8. The obtained membranes resulted in high pure water permeability of 65 L m^{-2} h^{-1}, and Na_2SO_4 and NaCl rejection at 0.4 MPa was 91.55% and

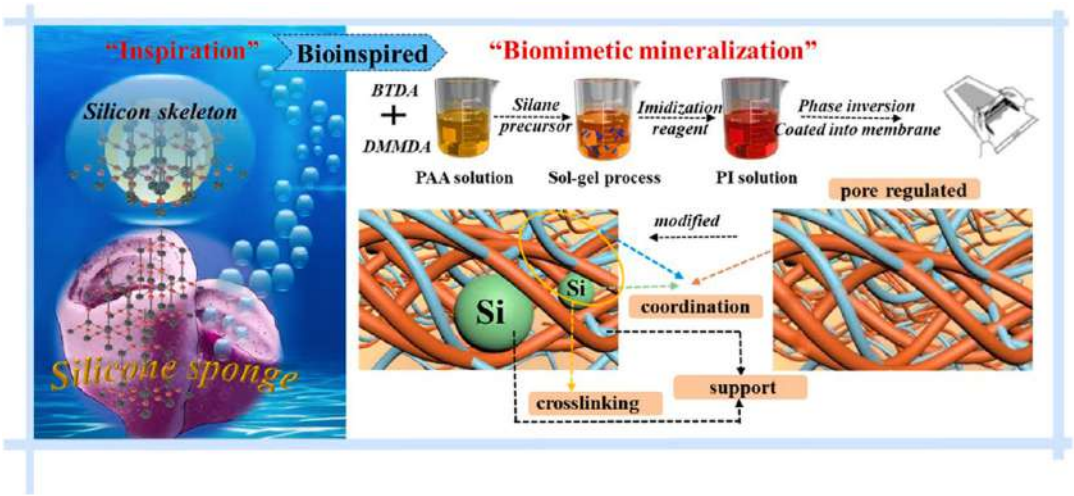

FIGURE 7.8 Illustration of 3D interwoven silicon sponge formation. Source: *Adapted with permission from Qiang, R., Wei, C., Lin, L., Deng, X., Zheng, T., Wang, Q., ... Zhang, Y. (2020). Bioinspired: A 3D vertical silicon sponge-inspired construction of organic-inorganic loose mass transfer nanochannels for enhancing properties of polyimide nanofiltration membranes.* Separation and Purification Technology, 259, *118038. Copyright (2020) Elsevier.*

30.21%, respectively. Moreover, membranes maintained their integrity and long-term stability for 72 h at 0.8 MPa using diverse organic solvents such as cyclohexane, acetone, *n*-heptane, methanol, absolute ethanol, ethyl acetate, and toluene. Therefore the polyimide/SiO_2 membrane with siliceous sponge biologically structure considerably enhanced the membrane's performance and structural stability, which is also a promising possibility for treating solutions in extreme environments (Qiang et al., 2020).

Zhang et al. used polyethylenimine as a polymer matrix, the $-NH_2/-NH-$ groups that catalyzed the inorganic precursor (tetraethoxysilane/tetra-n-butyl titanate) to synthesize inorganic nanoparticles (silica/titania) with tunable structure, inspired by biomineralization. The microstructures and physicochemical characteristics of the as-prepared membranes were tailored by altering the type and loading of inorganic precursors. The composite membranes' thermal stability was improved because of silica/titania nanoparticles' presence by inhibiting the polymer chain mobility. Moreover, incorporating the nanoparticles elevated the composite membranes' rejection abilities while remaining adequate solvent flux and good long-term operation stability (Zhang et al., 2014).

7.3 Biomimetic membranes

Biomimetics is an interdisciplinary field in which the principle of chemistry, biology, and engineering are applied to synthesize materials with functions of mimicking biological manners by generating the biological system's aspects (Maletskyi, 2020). Biomimetic membranes borrow concepts of biological systems by incorporating biological elements like aquaporin into synthetic materials, which, due to their advantages, can tackle the limitations of conventional membranes (Fuwad, Ryu, Malmstadt, Kim, & Jeon, 2019; Goh, Wong, Lim, Ismail, & Hilal, 2019; Maletskyi, 2020). Therefore developing high-performance membranes with new materials like aquaporins could help the design of novel NF membranes (Sun et al., 2013a). Moreover, most membrane technologies are struggling with fouling problems. This is mainly due to the inherent nature of conventional membranes' fabrication material and manufacturing method, which causes low pore density structure (Fuwad et al., 2019). Aquaporin-based biomimetic membranes can be a solution to these unsolved problems in conventional membranes.

7.3.1 Aquaporin-based biomimetic membranes

Aquaporin structures with a uniform pore size prevent pores' blockage by undesirable species, which render the membranes resistant to fouling. Fig. 7.9 displays the general problems of conventional membranes and the benefits of aquaporins. The hourglass shape of aquaporin, along with selective extracellular and intracellular vestibules, permits water molecules to pass while ejecting impurities (Fuwad et al., 2019).

Apart from the mentioned property, biomimetic aquaporin membranes took the scientific community's interest in water purification because of their properties, such as high selectivity and high permeability (Goh, Matsuura, Ismail, & Hilal, 2016; Martínez-Ballesta et al., 2018; Wagh & Escobar, 2019). Aquaporin membranes are low energy desalination

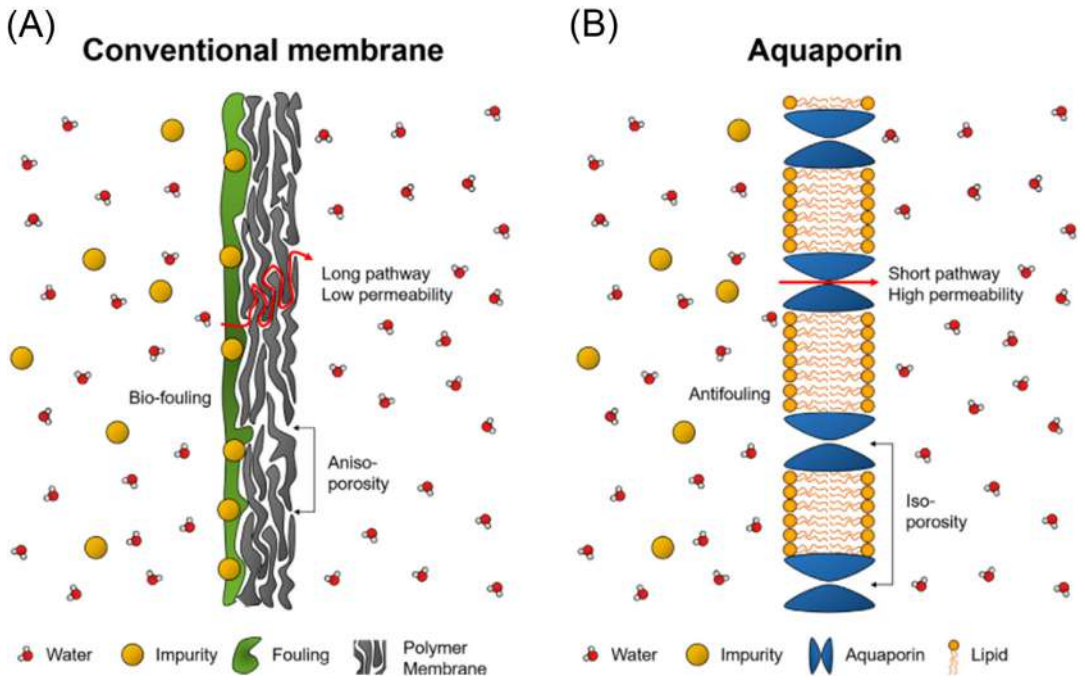

FIGURE 7.9 Schematic of (A) the drawbacks of regular membranes, with low flux and fouling problems due to their inherent structural characteristics and (B) the benefits of aquaporin membranes over traditional membranes. (Fuwad et al., 2019) Source: *Adapted with permission from Fuwad, A., Ryu, H., Malmstadt, N., Kim, S. M., & Jeon, T. J. (2019). Biomimetic membranes as potential tools for water purification: Preceding and future avenues.* Desalination, 458, *97–115. Copyright (2019) Elsevier.*

strategies, so they can play a crucial role in desalination technology, which has opened a new way in desalination approaches because of the high aquaporin water transport and remarkable selectivity (Goh et al., 2016). Aquaporins face stability challenges due to incompatibility with support material, which has to work at high pressures (Nabeel et al., 2020). Since 2012, many efforts have been adopted to retain aquaporins stable and functional to assemble the biomimetic membrane (Wagh & Escobar, 2019).

Usually, biomimetic membranes have three components: Aquaporin as the biological component in the assembly, amphiphilic carriers such as lipid bilayer or amphiphilic block copolymers for protein incorporation, and a polymeric support structure (Nabeel et al., 2020; Wagh & Escobar, 2019). There are several techniques for preparing biomimetic membranes, including vesicle fusion, the Langmuir–Blodgett method, interfacial polymerization, and ultraviolet cross-linking of proteoliposomes (Sengur-Tasdemir, Kilic, et al., 2018). The fabrication methods of aquaporin based membranes can be divided into two different categories, membranes with planar and vesicular structures, as shown in Table 7.1 (Nabeel et al., 2020; Ryu et al., 2019).

Aquaporins are transmembrane water channel proteins with three-dimensional structures that create pores to let water molecules' selective passage at a very high permeability

TABLE 7.1 Performance of aquaporin biomimetic. (Ryu et al., 2019)

Membrane design	Protein housing	Fabrication techniques	Limitations
Vesicles embedding	Synthetic lipids	Electrokinetic force, pressure force, magnetic adsorption	Small membrane size, harsh coating conditions, defects in large-area membrane
	Synthetic polymers	Adsorption chemical bonding, pressure-assisted coating	Low water desalination property shows high defects in the coating, no uniform surface coating
Planar bilayer	Synthetic lipids	Chemical bonding, vesicles fusion via electrostatic interactions	Incomplete surface coating, low performance, unstable under high pressure
	Synthetic polymers	Vesicles rupturing with disulfide-gold conjugation	Low water purification, incomplete surface coating

Adapted with permission from Ryu, H., Fuwad, A., Yoon, S., Jang, H., Lee, J. C., Kim, S. M., & Jeon, T. J. (2019). Biomimetic membranes with transmembrane proteins: State-of-the-art in transmembrane protein applications. International Journal of Molecular Sciences, 20*(6). Copyright (2019) MDPI.*

(Fuwad et al., 2019; Maletskyi, 2020). These proteins exist in nearly all alive organisms, including bacteria, archaea, eukaryotes, plants, and animals (Fuwad et al., 2019). They can operate as nanofilters to convey water molecules at high speeds and selectively through the living cells' membranes while blocking all other solutes, including gases, urea, boric acid, ions, and even protons, from going through (Figoli et al., 2017; Nabeel et al., 2020; Xie et al., 2013). Almost one billion water molecules per second can transport via a single aquaporin protein while rejecting solutes and ions larger than water molecules, making it permeable around three times higher than commercial one with polyamide membrane pore (Maletskyi, 2020; Nabeel et al., 2020).

Aquaporins require a cell membrane-like environment to perform their function correctly (Sengur-Tasdemir, Kilic, et al., 2018). Naturally, in aquaporin-based biomimetic membranes, aquaporins are embedded within cell membranes as integral proteins. While in engineering applications to mimic the cell structure, aquaporins must be embedded into amphiphilic carriers, such as lipid bilayers or block copolymers, with a similar amphiphilic structure to biological membranes to create *vesicles* or films for preserving their functionality in aqueous environments (Fuwad et al., 2019; Li et al., 2012, 2014; Qi et al., 2016). Therefore by considering different structure designs, there are two kinds of biomimetic aquaporin membranes. The first is aquaporin incorporated into a bilayer on membrane support, and the second is aquaporin immobilized into a dense polymer layer (Qi et al., 2016).

Aquaporins incorporation into the liposomes or polymersomes are vesicles that named proteoliposomes or proteopolymersomes (Li et al., 2014). Lipids are amphiphilic molecules that in aqueous environments form enclosed vesicular structures named liposomes (Fuwad et al., 2019). Lipids such as 1,2-diphytanoyl-sn-glycero-3-phosphocholine, 1,2-dioleoyl-sn-glycero-3-phosphocholine (DOPC), 1,2-dioleoyl-3-trimethylammonium-propane are the typical components in the biomimetic membranes' fabrication because the lipid membranes can offer the natural environment helping to keep both structure and function of the incorporated membrane proteins (Duong et al., 2012; Sengur-Tasdemir, Kilic, et al., 2018). However, an aquaporin-embedded lipid bilayer's construction is complicated because of the lipid bilayer's delicate nature (Nabeel et al., 2020).

TABLE 7.2 Properties of lipid- and polymer-based vesicle.

Lipidic membranes (liposomes)	Polymeric membranes (polymersomes)
• Low chemical stability and fluidity (because of low molecular weight) • High cost • Uncontrolled/high permeability • Short-membrane lifespan	• Higher stability (due to high molecular weight) • Low cost and tunable • Controlled/low permeability • Long-membrane life cycle

Adapted with permission from Fuwad, A., Ryu, H., Malmstadt, N., Kim, S. M., & Jeon, T. J. (2019). Biomimetic membranes as potential tools for water purification: Preceding and future avenues. Desalination, 458, *97–115. Copyright (2019) Elsevier.*

In contradiction of lipids, block copolymers are used to mimic cell membranes by forming polymersomes, with properties such as stability, durability, increased lifespan, the appropriate thickness, being inexpensive, and better exclusion of small molecules and permeation, which are controllable using extending the chain length, adding functional groups, choosing proper blocks, and conducting additional reactions for covalent cross-linking (Duong et al., 2012; Fuwad et al., 2019). Differences between polymeric and lipidic membranes are shown in Table 7.2 (Fuwad et al., 2019).

Since the required hydrostatic pressure are high, both lipidic and polymeric synthetic membranes are too fragile to tolerate it. The fragility of lipidic and polymeric synthetic membranes is mainly due to the low thickness of the membranes, which is not greater than a few nanometers, requiring solid support to enhance the membrane mechanical strength and stability. Solid supports can be fabricated by a porous structure of either inorganic or organic materials (Fuwad et al., 2019).

Compared to organic substrates, inorganic substrates have benefits including chemical, mechanical, and thermal stability, being resistant to solvents, having well-defined pore structure, and the ability to be sterilized. Though, compared to organic counterparts, inorganic substrates are more expensive (Duong et al., 2012; Fuwad et al., 2019). One example of common inorganic substrates is alumina, a uniform pore size material with a high pore density (Duong et al., 2012; Fuwad et al., 2019). Porous alumina membranes have some disadvantages, like possessing nonfunctionalized surface property (Duong et al., 2012).

Different stabilization and conjugation methods can be used to obtain defect-free, robust membranes based on the substrates' structural design and surface properties, including vesicle adsorption, vesicle fusion, and interfacial polymerization, chemical cross-linking, and magnetic-aided adsorption (Fuwad et al., 2019; Shenvi, Isloor, & Ismail, 2015). It must be noted that conjugation methodologies depend on the surface charge and the structure of both the vesicles and substrate (Fuwad et al., 2019). Biomimetic-based NF membranes can be used widely in wastewater treatment applications, which will be discussed in the following sections.

7.3.2 Application of aquaporin-based biomimetic nanofiltration membranes

Aquaporins can be chemically altered under high pressure and could not function properly, which leads to their failure in the assembly of synthetic membrane and the protein. Wagh et al. protected purified aquaporins with gum Arabic, followed by dispersing into a selective amphiphilic polyvinyl alcohol layer, which was cross-linked to a synthetic

polybenzimidazole membrane backbone with carbodiimide chemistry to reduce the disruptive effects of high hydraulic pressure. Schematic of the biomimetic membrane is shown in Fig. 7.10. Moreover, polyvinyl alcohol-alkyl acted as support for aquaporins to avoid their chemical change, giving the membranes mechanical strength. The modified membrane demonstrated lower flux declines, higher ion selectivity, higher flux recoveries, and higher protein and salt rejections compared to unmodified polybenzimidazole membranes (Wagh, Parungao, Viola, & Escobar, 2015).

According to a study conducted by Zhong et al., a planar biomimetic membrane with high flux and a reasonable salt rejection containing Aquaporin Z (AqpZ) were fabricated using methacrylate end groups functionalized cellulose acetate membrane substrate for water reuse application. A selective layer upon the substrate for NF was designed using ultraviolet polymerization and vesicle rupture of methacrylate end functionalized poly(2-methyloxazolineb-dimethylsiloxane-b-2-methyloxazoline) PMOXA(1000)-b-PDMS(4000)-PMOXA(1000) triblock copolymer (ABA) vesicles. The mechanical stability has been imparted by porous substrate and the polymeric layer upon it provided selective separation. The amount of aquaporin employed in membrane fabrication was vital to obtain excellent water permeability and salt rejection. So, the influence of AqpZ:ABA ratios on NF performance varying from 1:200 to 1:50 were clarified. The results have shown that the NF membranes containing AqpZ:ABA ratio of 1:50 can lead to water permeability of 34 L m^{-2} h^{-1} bar^{-1} and NaCl rejection of 30% (Zhong, Chung, Jeyaseelan, & Armugam, 2012). According to another study, to fabricate a NF membrane, Sun et al. used AqpZ, one

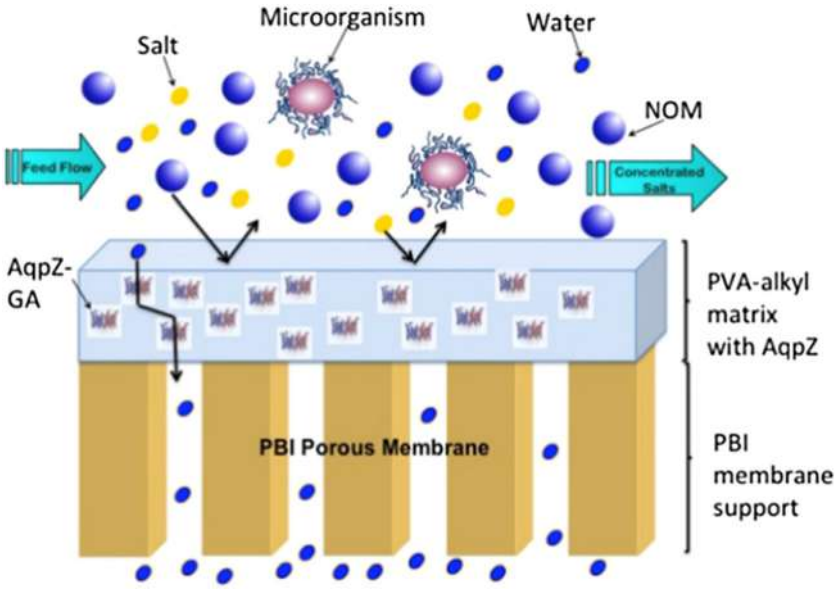

FIGURE 7.10 Schematic of biomimetic membranes. (Wagh et al., 2015) Source: *Adapted with permission from Wagh, P., Parungao, G., Viola, R. E., & Escobar, I. C. (2015). A new technique to fabricate high-performance biologically inspired membranes for water treatment.* Separation and Purification Technology, 156, *754–765. Copyright (2015) Elsevier.*

of the aquaporin family members, in a pressure-driven water purification process by immobilizing AqpZ-reconstituted liposomes on a PDA coated microporous membrane. Amine-functionalized proteoliposomes were deposited using vacuum suction and then conjugated on the PDA layer using formation of an amine-catechol adduct. The results have shown that the membrane with AqpZ incorporation can provide a higher pure water permeability and improved NaCl and $MgCl_2$ rejections (Sun, Chung, Jeyaseelan, & Armugam, 2013b). According to a study reported by Wagh et al., AqpZ was modified with a cysteine at the N-terminus for covalent attaching to the polymer membrane matrix. Compared to unmodified membranes, achieving a higher salt rejection can be done using Aqp-SH modified membranes. The obtained rejection using Aqp-SH membranes for 2 M NaCl and $CaCl_2$ solutions were almost 49% and 59%, respectively, while obtained rejection using unmodified membranes for 2 M NaCl and $CaCl_2$ solutions were almost 0.8% and 1.3%, respectively (Wagh et al., 2019).

Wang et al. fabricated biomimetic membranes using aquaporin 1 (AQP1) incorporation, which AQP1 was utilized as the water channel protein to evaluate the performance of the composite supported lipid bilayer in NF membranes. An essential factor in the performance of the AQP1 incorporated supported lipid bilayer membranes is lipid mobility. The study demonstrated that biomimetic membrane quality and lipid mobility are tunable by monoolein (MO) addition, which are related to the performance of the AQP1 incorporated supported lipid bilayers. The flux increment and salt rejection of the AQP1-embedded biomimetic membranes increased with lipid mobility (Wang et al., 2015). MO is a biocompatible and nontoxic monoglyceride that can enhance molecular mobility in a bilayer by adding to a lipid bilayer and providing extra free volume through its *cis*-double bond (Giwa et al., 2017; Sengur-Tasdemir, Tutuncu, Gul-Karaguler, Ates-Genceli, & Koyuncu, 2019). The results revealed that adding MO into 1,2-dipalmitoyl-sn-glycero-3-phosphocholine (DPPC) bilayers lead to a decrease in the phase transition temperature of the DPPC/MO system and improving lipid mobility due to MO's *cis*-double bond. While the DOPC and MO's hydrocarbon chain structure was similar, MO's adding did not lead to enhancing the DOPC/MO system's lipid mobility. Also, MO cubic liquid crystals in the DOPC supported lipid bilayer inhibit lipid motion and induce some defects. This study offered great insight into developing membranes for water purification purposes using biomimetic membranes (Wang et al., 2015).

7.3.3 Aquaporin-based biomimetic nanofiltration membranes with hollow fiber configuration

As discussed before, hollow fiber configuration of the membranes make them suitable for using in various fields (Tham & Chung, 2020). Sengur-Tasdemir designed a hollow fiber NF membrane by immobilizing AqpZ on the outer surface of the separation layer. Integration of AqpZ-embedded proteoliposomes into the polyamide layer was performed by interfacial polymerization. Evaluating the effects of three ultrafiltration's supports—polymeric, nanocomposite, and reinforced—was performed on the separation properties of membranes with AqpZ. Surface characterization confirmed integration of AqpZ-reconstituted proteoliposomes with the polyamide matrix leading to permeate flux improvement of up to 2.5 times (Sengur-Tasdemir, Sayinli, et al., 2018). Membranes with hollow fiber configuration have

higher surface area per unit membrane volume, making them desirable to use in different areas. However, despite being more favorable, hollow fiber membranes are rare due to their complex fabrication compared to flat sheets (Tham & Chung, 2020).

7.4 Stimuli-responsive/smart membranes

Conventional cleaning methods are effective to recover membrane original flux, but they can change the membranes surface chemistry because of using chemical cleaning agents. Therefore this adversely disturbs the permeate quality. As a result, recent efforts have been led to develop smart materials which their surface properties can be changed by different external stimuli (Low & Ng, 2019). Modified membranes with stimuli-responsive materials have outstanding antifouling properties and different sorts of foulants can be physically detached from the membrane surface. Therefore stimuli-responsive materials have caught the imagination of engineers and researchers and can be a novel water purification method (Woo, Yun, & Kwak, 2018).

Stimuli-responsive materials have caught the imagination of engineers and researchers because of their biometric behavior. Stimuli-responsive materials are any synthetic or natural material that can respond to environmental triggers including pH, temperature, color, ionic strength, magnetic field, electricity, etc. by alteration of their own characteristics such as shape, size, permeability, surface area, optical properties, and mechanical properties (Jiang, Ji, Li, Chen, & Lv, 2020; Purkait, Sinha, Mondal, & Singh, 2018a; Weng et al., 2016; Yang, Himstedt, Ulbricht, Qian, & Ranil Wickramasinghe, 2013). Grafting the responsive polymers inside the pore structure or surface of the membrane results in reversible membrane properties changes, realizing the controlled permeation of target molecules (Qian, Yang, Vu, & Wickramasinghe, 2016).

7.4.1 pH-responsive membranes

The pH-responsive membranes have attracted the attention of many researchers as pH is an easy parameter to be adjusted in membrane separation processes (Weng et al., 2016). Because of the pH-responsive membrane's applications in various areas, such as degrading toxic organics in water purification systems, metal recovery, oil and water separation, food processing, drug and gene delivery, pH sensors, etc., developing pH stimuli-responsive membranes is of crucial importance (Yang et al., 2017).

Ouyang et al. fabricated a dually charged polyelectrolyte multilayer membrane with an active skin layer and comprehensive rejection to personal care and pharmaceuticals products. In this study, the positively charged chitosan and negatively charged PDA has been used for fabricating the membrane, as shown in Fig. 7.11. In detail, quaternate chitosan was positively charged with glycidyl trimethyl ammonium chloride by a nucleophilic substitution reaction. The optimized membrane exhibited a molecular weight cut off of 935 Da, stokes radius of 0.68 nm, and pure water permeability of 15.665 L m^{-2} h^{-1} MPa^{-1}. Besides, the optimum membrane exhibited a higher rejection of 76.22%, 87.29%, and 89.85% to atenolol, carbamazepine, and ibuprofen, respectively. The results have shown salt rejection sequence of $K_2SO_4 > Na_2SO_4 > MgSO_4 > NaCl > KCl > MgCl_2$ at neutral pH.

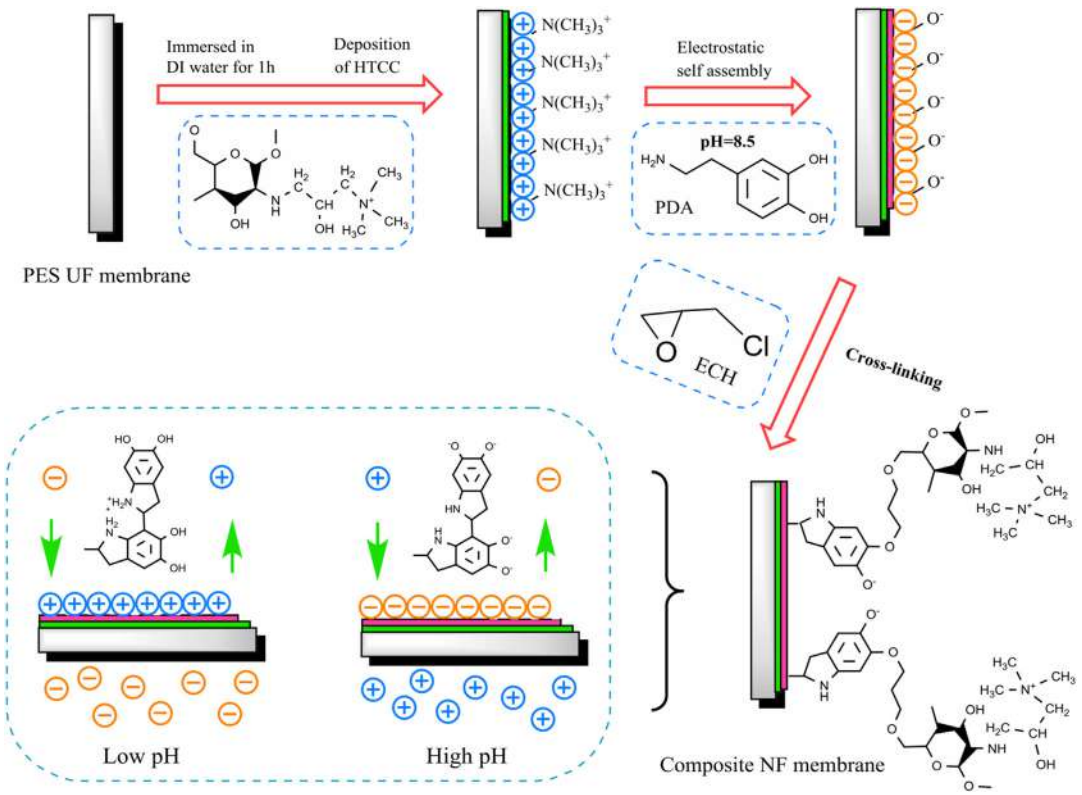

FIGURE 7.11 Illustration of fabrication steps and selective permeability mechanism of the membrane with multicharged nanofilms. Source: *Adapted with permission from Ouyang, Z., Huang, Z., Tang, X., Xiong, C., Tang, M., & Lu, Y. (2019). A dually charged nanofiltration membrane by pH-responsive polydopamine for pharmaceuticals and personal care products removal.* Separation and Purification Technology, 211, *90–97. Copyright (2019) Elsevier.*

Moreover, by pH adjusting, the retention of atenolol and carbamazepine could be enhanced to 81.67% and 92.50%, respectively, representing that the modified membrane's surface has a dually charged characteristic (Ouyang et al., 2019).

In another study, Weng et al. developed pH-responsive NF membranes with tunable ion selectivity. Poly(carboxybetaine methacrylamide-co-*N*-(Hydroxymethyl) acrylamide) were used to prepare membranes using surface-coating glutaraldehyde cross-linking technique. Ion selectivity of the membrane toward monovalent and divalent ions was tunable by pH adjustment of the feeding solution (Weng et al., 2016).

7.4.2 Magnetically responsive membranes

Polymeric magnetic-responsive membranes attracted researchers' attention due to their smart characteristics. Polymeric magnetic-responsive membranes can alter their morphology and porous nature under a magnetic field (Purkait et al., 2018a).

In order to address some problems of membranes, there is a vital need for such smart materials. Antifouling activity of the membrane is a significant parameter in the process of developing membranes. Embedding highly magnetic nanoparticles within the matrices of polymeric membranes can remove the fouling agents from wastewater. The foulants over the membrane surface can be removed quite easily through backwashing, as the pore shape and size of the magnetic-responsive smart membranes can be altered under a magnetic field (Purkait et al., 2018a). Changes in the polymer matrix's conformation occur instantaneously in the existence of a magnetic field, magnetophoretic forces and torques acting on the particles and vanish suddenly when the field is removed (Song, Wickramasinghe, & Qian, 2017). In another study, a magnetically responsive NF membranes was developed using superparamagnetic nanoparticles' attachment to the end of polymer chains grafted from the surface of commercially NF membranes. It was displayed that the movement of magnetically responsive polymer chains can help to disrupt the concentration polarization at the boundary layer and also can decrease the amount of foulants that aggregate, precipitate, or deposit on the membrane surface suppresses. One of the used performance-determining factors was the filtration time of feed solutions containing an organic salt, an inorganic salt, and synthetic oil to determine the influence on long-term membrane fouling by conducting experiments for periods of up to 6 h. The results show suppression of long-term fouling in the presence of an oscillating magnetic field (Song, Sengupta, Qian, & Wickramasinghe, 2018).

In another study, to design magnetically responsive membranes, Yang et al. fabricated a polyamide NF membrane using TFC method and grafting poly(2-hydroxyethyl methacrylate) chains to the surface of the membrane. Therefore superparamagnetic (Fe_3O_4) nanoparticles have been attached to the end of polymer chains through a modified Gabriel synthesis procedure. To control the density and length of the polymer chains during the synthesis, the surface-initiated atom transfer radical polymerization has been used. This method enables to control the polymer chain's length by altering the initiator density and duration of polymerization. Dead-end filtration experiments showed a reduction in permeate flux and a salt rejection increase in modified membranes in comparison to unmodified membranes in the lack of the magnetic field. Modified membranes displayed both increment of salt rejection and permeate fluxes in the presence of an oscillating magnetic field compared to their performance in the lack of an oscillating magnetic field. Moreover, attached nanoparticles with higher densities displayed a greater increase in salt rejection and permeate flux. For example, percentage improvement in flux for 500 ppm $CaCl_2$ for nanoparticles with higher densities was $\sim$63%, but percentage improvement in the same flux for nanoparticles with lower densities was $\sim$33% (Yang et al., 2013).

As discussed before, NF membranes' fouling is a challenging issue that limits the membranes' practical viability. Modifying the membrane's filtration surface and pores to minimize the adsorption of dissolved solutes is a fouling-minimizing method (Himstedt, Marshall, & Wickramasinghe, 2011). This issue becomes more challenging through produced water in oil and gas exploration extraction fields. One of the world's concerns is produced water, a by-product of oil and gas exploration, comprising elevated concentrations of inorganic and organic pollutants because of the contact with hydrocarbon products and geologic formations in underground basins (Tomer, Mondal, Wandera, Wickramasinghe, & Husson, 2009). Recently, filtration processes such as NF and reverse

osmosis have been proposed to treat produced water from oil and gas extraction plants (Tomer et al., 2009).

7.4.3 Temperature-responsive membrane

Membranes responsive to temperature have found a broad interest among researchers (Dutta & De, 2017). By subjecting temperature-responsive membranes composed of a porous membrane matrix to the external temperature, the polymer chain conformation and/or intramolecular forces will alter to adjust its structural performance. This altering in the structural performance is due to having a functional grafting layer. Therefore resizing the pores in the membrane leads to an apparent switching effect in operational processes. The composite membrane's responsive behavior depends on the properties of the grafted temperature-responsive polymers (Tang, Tang, & Wu, 2015). Also, it must be considered that temperature response can be controlled by altering the amount of hydrophilic or hydrophobic units in the temperature-responsive copolymers (Tang et al., 2015).

Between different types of polymers, poly(*N*-isopropylacrylamide) is one of the temperature-sensitive polymers by demonstrating a dramatic change in its volume at its lower critical solution temperature of ~32ºC, which results in its application as a thermo-responsive pore-controller in the temperature-responsive membrane (Dutta & De, 2017).

As mentioned before, filtration method can be used for the treatment of produced water (Tomer et al., 2009). However, the water flux declines because of the concentration polarization and subsequent membrane fouling which is a significant barrier to the membrane-based treatment of produced water. Forming a high concentration boundary layer of rejected species causes concentration polarizations while membrane fouling is because of the deposition of the rejected species on the surface. Membrane fouling could lead to a decrease in membrane permeability and shorten the membrane's life because of the aggressive chemical usage required for cleaning the retentates deposited on the membrane. Thereby, membranes need to be replaced frequently as the cleaning process becomes useless after several washing cycles. Accordingly, membrane fouling can turn into a significant economic challenge in membrane filtration operations. Moreover, membrane fouling can be both reversible and irreversible because of the interactions between suspended and dissolved solutes and the membrane surface. However, membrane fouling may probably be controlled by altering the membrane surface chemistry (Tomer et al., 2009).

Tomer et al. modified a NF membrane's surface with block copolymer nanolayers. This nanolayers consist of a temperature-responsive block and a foul-resistant block. This combination of the blocks in copolymer can limit fouling during filtration of coal-bed methane produced water and enable the chemical-free alternation to detach any accumulate foulants on the surface. In order to achieve this combination, the authors grafted the surface of commercial polyamide TFC NF membranes with poly(*N*-isopropylacrylamide) and poly (*N*-isopropylacrylamide-blockethylene glycol methacrylate). Compared to unmodified membranes, modified membranes exhibited enhanced permeate water quality, lower flux recovery, and higher hydrophobicity after modification. Results indicated that surface-initiated atom transfer radical polymerization yields lower surface roughness values than other modification methods (Tomer et al., 2009).

Production of block copolymer-based NF membranes with sharp molecular weight cut offs was addressed by Bar at al. Atom-transfer radical polymerization was utilized to synthesize pentablock copolymer comprising temperature-responsive Pluronic F127 poly (ethyleneoxide)-b-poly(propyleneoxide)-b-poly-(ethyleneoxide) middle blocks and pH-responsive poly(*N*,*N*-(diethylamino)ethyl methacrylate) end blocks. Then, the polymer was coated electrostatically to on top support membrane of polysulfone/sulfonated polyether-sulfone. The results revealed that the pore size remained constant in the presence of significant external stimuli of pH and temperature. It was shown that by increasing the stimulus, the permeability improved. Acidic and neutral environment long-term stability occurred in the membrane due to the strong electrostatic interactions between the copolymer and support. Findings suggested that the pentablock copolymer membrane provides a means to overcome the tradeoff between selectivity and permeability. The proposed membrane fabrication method was scalable and combined dynamic coating and classical nonsolvent-induced phase inversion without involving complicated synthetic paths (Bar, Çağlar, Uz, Mallapragada, & Altinkaya, 2019).

7.4.4 Photo-responsive membranes

Light-responsive membranes are among the less explored membranes for application in water treatment (Dutta & De, 2017). Proper wavelengths of photoirradiation of ultraviolet or visible can be exploited to induce a conformational change in polymer chains that carry photochromic moieties in a noninvasive manner by promoting or reversing their isomerization. Moreover, photo-responsiveness needs incorporating photochromic chromophores or their derivatives, such as spiropyran and azobenzene (Wee & Bai, 2013).

A light-responsive polyamide TFC was recently designed for water softening by Das, Kuehnert, Kazemi, Abdi, and Schulze (2019). Polyamide TFC-based NF membranes, because of their universal application, dominate the water softening debate. However, designing polyamide TFC-based NF membranes and optimizing their performance is still essential as most polyamide TFC membranes are static in both form and function. Therefore designing different types of stimuli-responsive dynamic NF membranes could be an innovative method. Different forms of external stimuli have a different impact on the behavior of a polyamide TFC membrane. As light possesses unique benefits, it can be used to design light-responsive membranes (Das et al., 2019). Das and coworkers used light-responsive spiropyran immobilization onto polyethersulfone/polyamide TFC (PES/PA-TFC) NF membranes through low-energy electron beam technology. Ultraviolet light irradiation was used to transform spiropyran into the zwitterionic merocyanine, which guaranteed >95% removal of $MgSO_4$ ions with water permeation rates of 6.5 L m^{-2} h^{-1} bar^{-1}. Alternatively, merocyanine converted to spiropyran using visible light, which achieved >95% of $MgSO_4$ retention with 5.25 L m^{-2} h^{-1} bar^{-1} water flux. The spiropyran immobilized PES/PA-TFC-based NF showed both a higher normalized water flux and higher chlorine resistance than the reference membrane without the loss of ion retention. Therefore the proposed inexpensive method could be applied to water softening applications (Das et al., 2019).

Light-responsive chemical groups such as diarylethenes, spiropyrans, azobenzenes, and semiconductor nanoparticles can be physically blended or chemically attached within the

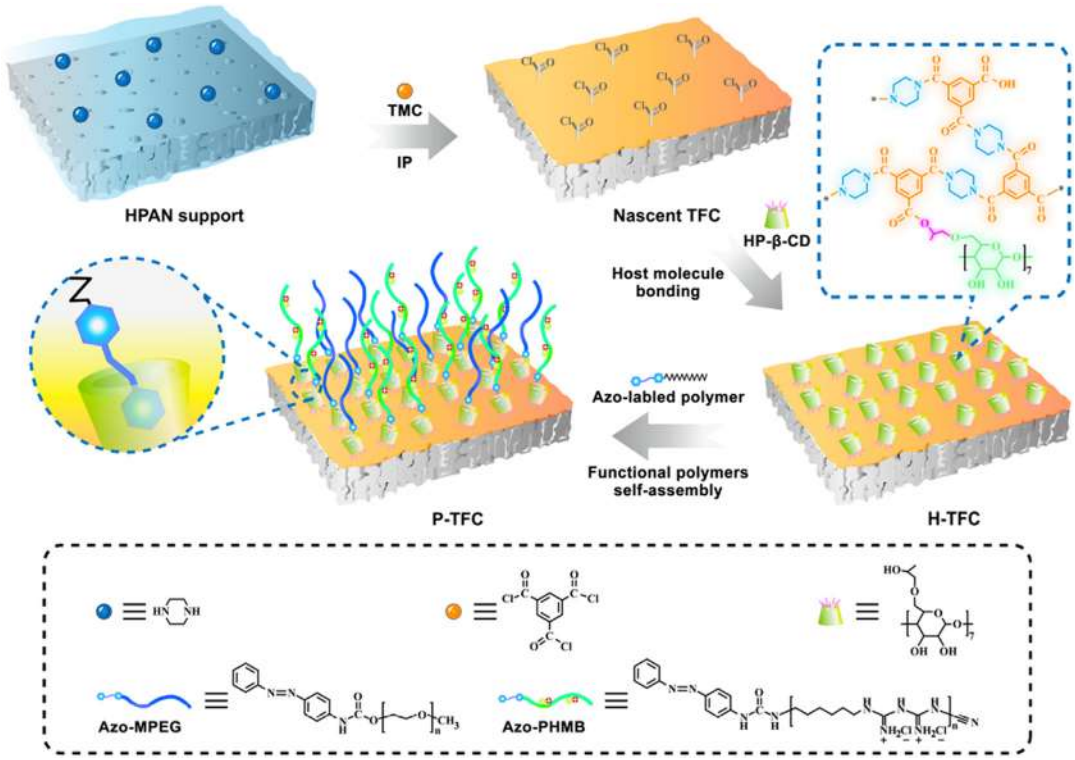

FIGURE 7.12 Schematic of thin-film composite nanofiltration membrane fabrication using interfacial polymerization process and surface modification via host–guest self-assembly. Source: *Adapted with permission from Ren, L., Chen, J., Lu, Q., Han, J., & Wu, H. (2020). Antifouling nanofiltration membrane fabrication via surface assembling light-responsive and regenerable functional layer.* ACS Applied Materials and Interfaces, 12, *52050–52058. Copyright (2020) American Chemical Society.*

bulk structure of the membrane or immobilized by grafting or coating onto the surface and/or pores of the membrane. According to a study conducted by Ren et al., a β-cyclodextrin bonded polyamide TFC NF membrane was prepared by the reaction between hydroxypropyl groups of 2-hydroxypropyl-β-cyclodextrin and residual acyl chloride groups on the nascent membrane. Then, to achieve membrane antifouling modification, host–guest self-assembly was used to attach the Azo-labeled methoxypolyethylene glycol, and Azo-labeled polyhexamethylene biguanide onto the membrane surface. The fabrication process of TFC NF membrane and surface modification has been illustrated in Fig. 7.12. Bonding β-cyclodextrin on the membrane's surface offers linking sites for guest labeled functional polymers and adjusts surface properties and the polyamide selective layer's pore structure. Furthermore, endowing the membrane with a light-responsive and regenerable antifouling layer was achieved by successful assembly of functional polymers on the surface of the membrane. The proposed surface modification method could be pragmatic, synchronously promoting antifouling ability, improve separation properties,

and enable the sustainable utilization of the polyamide TFC NF membrane (Ren, Chen, Lu, Han, & Wu, 2020).

7.4.5 CO_2-responsive nanofiltration membranes

CO_2 gas is a plentiful, nontoxic, and renewable resource studied as a green stimulus to develop switchable functional materials for use in switchable or tunable membrane technologies (Dong et al., 2018; Yin et al., 2019).

Dong et al. fabricated a smart NF membrane based on graphene oxide (GO) with poly (*N*,*N*-diethylaminoethyl methacrylate) bearing a pyrene end group (Py-PDEAEMA). GO is a 2D material with single-atom layers with promising properties such as excellent mechanical strength, easy accessibility, and high chemical and thermal stability for use as a membrane material for NF. The composite membranes displayed a potential for water treatment. Reversible, gas-tunable water permeability between the pore closure state under CO_2 stimulation and the pore opening state upon Ar bubbling was displayed in the membrane. The water permeability remained much higher compared to a pure GO membrane even at the pore closure state. In summary, Py-PDEAEMA/GO NFM combined both CO_2-responsive polymers and GO-based NF membranes' advantages to develop smart stimuli-responsive NF membranes (Dong et al., 2018).

Yin et al. fabricated a NF membrane, which upon CO_2 bubbling into the water, the membranes were positively charged. The membrane displayed high rejection to $MgCl_2$, while after bubbling Ar to eliminate CO_2, the membranes gradually transformed to negatively charged, and high rejection to Na_2SO_4 was obtained (Yin et al., 2019).

In another study, a CO_2-responsive copolymer polyacrylonitrile-co-poly(2-diethylaminoethyl methacrylate) (PAN-co-PDEAEMA) was synthesized. In this process, they used the free-radical copolymerization for synthesis of the copolymer and then the PAN/PAN-co-PDEAEMA blend membrane fabricated with a switchable flux and permeability properties to clean the membrane fouling efficiently. The results indicate that alternative aeration of N_2/CO_2 through the solution can remove protein foulant on the prepared membrane effectively without the aid of chemical agents. Therefore flux and permeability of CO_2-responsive PAN/PAN-co-PDEAEMA membrane can be reversibly switched simply by altering gas aeration. Upon CO_2/N_2 alternation, the flux recovery of the membrane reached 90%, which was comparable with acid cleaning or alkali cleaning. No damage to membrane structure and performance and no effluent emission consisting of chemical agents were the advantages of the proposed method (Zhang et al., 2020).

7.4.6 Stimuli-responsive membranes with hollow fiber configuration

Hollow fiber membranes have some advantages over flat sheet membranes, such as having less fouling and providing a larger effective surface area to volume ratios. Also, hollow fiber membranes are more favorable than flat sheet membranes at the industrial scale and commercial level as the low fouling gives them a longer life, and the area to volume ratio provides high packing densities. Therefore hollow fiber membranes can play a

vital role in developing membranes for various sectors (Purkait, Sinha, Mondal, & Singh, 2018b).

According to a study, interfacial polymerization of lysine and trimesoyl chloride on the outer surface of poly(m-phenylene isophthalamide) hollow fiber membrane was used to fabricate an ionic and pH-responsive TFC membrane. Lysine introduced a large number of −COOH groups in the cross-linked polyamide layer. These functional groups endorse hydrophilicity and strong negative electricity. After the increase of membrane pore size from 0.53 nm at low pH and salt concentration to 0.68 nm at high pH and salt concentration, the anionic dyes rejection with a molecular weight greater than 461 Da was still more than 95%. However, the salt rejection decreased severely (e.g., NaCl rejection reduced from 16.4% to 4.7%), and the water flux increased from 36.77 to 117.65 $L\,m^{-2}\,h^{-1}$ by increasing salt concentration from 1 to 4 $g\,L^{-1}$ and increased almost three times by increasing pH from 3 to 12. The TFC membrane could separate Coomassie bright blue G and methyl orange by changing the solution's pH or ionic strength, which shows the potential to separate dyes of different molecular weights. Therefore the responsive TFC membrane shows excellent performance in separating dye mixture and dye-salt mixture (Zhang, Yang, Chen, & Hu, 2020).

7.5 Commercial status and future directions

To date, an impressive number of laboratory-level research studies have confirmed the high performance of the modified bioinspired membranes with PDA. However, their commercial application in removing multipollutants from surface water, sewage, and industrial wastewater treatments is rare. Currently, moving the application of mussel-inspired membranes from lab scale to commercialized scale has been limited due to some obstacles. The first obstacle is the unclear composition of products and polymerization mechanisms. Several hours are needed for the natural deposition of pure dopamine solution. Thus different oxidants must be employed for accelerating the reaction of dopamine polymerization. This may lead to damages to the polymer film in the meantime. Therefore there is a need for developing mild and swift modification techniques to hasten the process. In a further step, figuring out the parameters that can be effective on the PDA structure at the molecular scale must be considered. The second obstacle is suspending the PDA particles in the solution rather than on the membrane surface, resulting in a high preparation cost and environmental pollution. Therefore the deposition process must be optimized and further modification strategies must be adopted to improve the membranes' performance in a wide variety of applications (Yan et al., 2020).

Another rising approach is biomimetic membranes. Biomimetic membranes will turn into superior technologies in the coming years, and research and development studies in these membranes are rapidly evolving (Shen, Saboe, Sines, Erbakan, & Kumar, 2014; Wagh & Escobar, 2019). Aquaporin-based membranes should be competitive with other regular membranes in terms of useful life and stability to enter the water and wastewater market (Gehrke, Geiser, & Somborn-Schulz, 2015). Moreover, extensive research is required to fully understand the structure−functional relationships of biological systems to expand the technological development in the biomimetic membranes field. The cost of large-scale

expression of biological molecules and biomimetic membranes' synthesis is another problem, as it is too high, which must be reduced significantly (Wagh & Escobar, 2019). Biomimetic membranes are facing some challenges that must be tackled before considering this technology as a mainstream. Three significant challenges of biomimetic membranes are: (1) the lack of a fundamental understanding of the interaction between functional molecules and matrix materials, (2) scaling up the existing approaches to synthesize biomimetic membranes, and (3) the high production cost of large quantities of biomimetic materials (Shen et al., 2014). Other challenges in producing the industrial-scale defect-free biomimetic membrane that must be solved are related to protein stability, membrane housing materials, and the surface chemistry of the substrate (Fuwad et al., 2019).

Producing aquaporin-based biomimetic membranes via interfacial polymerization recently has gained favorable results over stability for extended periods up to several months, and commercial products are available. A company established in Copenhagen, Denmark, used incorporation of the aquaporin protein into bilayer thin film based on porous support membrane to develop a technology named Aquaporin Inside. The technology is patented and is based on simulation for biomembrane water transport by Morten Østergaard Jensen. The technology operates well, ensuring the natural functionality of aquaporins held using a thin film. The thin film can be coated with hollow fibers or flat sheets. Hollow fibers or flat sheets coated the thin film. The company has produced flat sheets with 40 cm width and hollow fiber modules of a 0.6 m^2 active area for reverse osmosis and forward osmosis. The company also produced its first pilot spiral wound forward osmosis element under the testing phase (Nabeel et al., 2020).

Stimuli-responsive membranes has vast potentials to perform as smart separation systems in environmental applications such as water treatment (Dutta & De, 2017; Wee & Bai, 2013). As smart membranes are newcomers to the membrane family, their large-scale application is limited and further studies is needed (Chu, Xie, & Ju, 2011).

Stimuli-responsive filtration membranes can be tuned based on the internal or external existence of stimulus/stimuli, which as a result are desirable for removing contaminants from water. However, there is a vast scope of research activities ahead to scaling up these stimuli-responsive materials and understanding their real-life applicability in water treatment applications. Also, it must be noted that there are large numbers of pollutants in water ranging from dyes to heavy metals to phenolics to salts, etc. To find a suitable treatment solution, some challenges must be addressed. For example, regarding pH-responsive materials in a scaled-up operation, pH switching needs many chemicals. On the other hand, changing the pore size of materials with pH can easily fractionate solutes in the feed. Therefore optimizing the condition is essential. In the case of temperature-responsive materials, they respond in a narrow range of temperature, like 10°C−15°C, which seems easy to tune the smart materials' selectivity just by altering the temperature. Although, in this situation, there is no need of external chemicals, changing the temperature of the process streams needs investing in capital cost of the plant by installing proper heat exchangers. It can be afforded by plants if the plants have heat generation or cooling within themselves. Otherwise, fuel cost would be added to realizing the temperature change to the process fluid. Overall, by addressing critical parameters including scalability, design, efficiency, and reproducibility, smart materials can be a paradigm shift in water treatment applications (Dutta & De, 2017).

7.6 Summary

Membranes are among the globally high promising technologies for water purification. In this chapter, different types of polymer-based NF membranes, including bioinspired, biomimetic, and stimuli-responsive membranes and their application and performances in removing different types of pollutants have been reviewed. Applying a variety of materials and methods in fabrication approaches of bioinspired, biomimetic, and stimuli-responsive NF membranes through the recently conducted studies were presented thoroughly to understand their potential and possible future directions. However, it must be noted that most of these studies are in their early stages. Therefore optimizing the membranes' functionality and a long-term evaluation of their performances under industrial conditions is essential to make these NFs commercially available and to get a better perspective of their role in wastewater treatment applications. For example, nature is an inspiration for developing innovative biomimetic and bioinspired membranes. Along with the rapid development of this field in the fabrication of membranes in research studies, different challenges such as high production cost and scaling-up issues must be solved. Moreover, other challenges such as the design of the membrane, reproducibility, efficiency of the membranes, scalability, their high cost, the stability of the membranes, and sustainability of the membranes through bioinspired, biomimetic, and stimuli-responsive approaches must be addressed to bring these emerging novel membranes into the market. Therefore broad research studies and massive research and development efforts are needed to pave innovative membranes' road to their commercialization.

Nomenclature

1,2-dioleoyl-sn-glycero-3-phosphocholine (DOPC)
1, 2-dipalmitoyl-sn-glycero-3-phosphocholine (DPPC)
Aquaporin Z (AqpZ)
Aquaporin 1 (AQP1)
Copper (Cu^{2+})
Chromium (Cr^{3+} and Cr^{6+})
Cadmium (Cd^{2+})
Cupric acetate (CuII)
Graphene oxide (GO)
Mercury (Hg^{2+})
Monoolein (MO)
Nickel (Ni^{2+})
Nanofiltration (NF)
Polydopamine (PDA)
PDA-assisted polyelectrolytes layer-by-layer deposition (PDA-a-LBL)
Polyethersulfone/polyamide (PES/PA)
Polyacrylonitrile-co-poly(2-diethylaminoethyl methacrylate) (PAN-co-PDEAEMA)
Poly(*N*,*N*-diethylaminoethyl methacrylate) bearing a pyrene end group (Py-PDEAEMA)
Thin-film composite (TFC)
Tannic acid/cupric acetate (TA/CuII)

References

Abdelrasoul, A., Doan, H., & Lohi, A. (2017). Fabrication of biomimetic and bioinspired membranes. *Biomimetic and Bioinspired Membranes for New Frontiers in Sustainable Water Treatment Technology*. Available from https://doi.org/10.5772/intechopen.71718.

Bar, C., Çağlar, N., Uz, M., Mallapragada, S. K., & Altinkaya, S. A. (2019). Development of a high-flux thin-film composite nanofiltration membrane with sub-nanometer selectivity using a pH and temperature-responsive pentablock co-polymer. *ACS Applied Materials and Interfaces*, *11*(34), 31367–31377. Available from https://doi.org/10.1021/acsami.9b10273.

Chakrabarty, T., Pérez-Manríquez, L., Neelakanda, P., & Peinemann, K. V. (2017). Bioinspired tannic acid-copper complexes as selective coating for nanofiltration membranes. *Separation and Purification Technology*, *184*, 188–194. Available from https://doi.org/10.1016/j.seppur.2017.04.043.

Cheng, X. Q., Zhang, C., Wang, Z. X., & Shao, L. (2016). Tailoring nanofiltration membrane performance for highly-efficient antibiotics removal by mussel-inspired modification. *Journal of Membrane Science*, *499*, 326–334. Available from https://doi.org/10.1016/j.memsci.2015.10.060.

Chu, L., Xie, R., & Ju, X. (2011). Stimuli-responsive membranes: Smart tools for controllable mass-transfer and separation processes. *Chinese Journal of Chemical Engineering*, *19*(6), 891–903. Available from https://doi.org/10.1016/S1004-9541(11)60070-0.

Dai, R., Li, J., & Wang, Z. (2020). Constructing interlayer to tailor structure and performance of thin-film composite polyamide membranes: A review. *Advances in Colloid and Interface Science*, *282*, 102204. Available from https://doi.org/10.1016/j.cis.2020.102204.

Das, R., Kuehnert, M., Kazemi, A. S., Abdi, Y., & Schulze, A. (2019). Water softening using a light-responsive, spiropyran-modified nanofiltration membrane. *Polymers*, *11*(2), 1–10. Available from https://doi.org/10.3390/polym11020344.

Dong, L., Fan, W., Tong, X., Zhang, H., Chen, M., & Zhao, Y. (2018). A CO_2-responsive graphene oxide/polymer composite nanofiltration membrane for water purification. *Journal of Materials Chemistry A*, *6*(16), 6785–6791. Available from https://doi.org/10.1039/c8ta00623g.

Du, Y., Qiu, W. Z., Lv, Y., Wu, J., & Xu, Z. K. (2016). Nanofiltration membranes with narrow pore size distribution via contra-diffusion-induced mussel-inspired chemistry. *ACS Applied Materials and Interfaces*, *8*(43), 29696–29704. Available from https://doi.org/10.1021/acsami.6b10367.

Duong, P. H. H., Chung, T. S., Jeyaseelan, K., Armugam, A., Chen, Z., Yang, J., & Hong, M. (2012). Planar biomimetic aquaporin-incorporated triblock copolymer membranes on porous alumina supports for nanofiltration. *Journal of Membrane Science*, *409–410*, 34–43. Available from https://doi.org/10.1016/j.memsci.2012.03.004.

Dutta, K., & De, S. (2017). Smart responsive materials for water purification: An overview. *Journal of Materials Chemistry A*, *5*(42), 22095–22112. Available from https://doi.org/10.1039/c7ta07054c.

Fang, S. Y., Zhang, P., Gong, J. L., Tang, L., Zeng, G. M., Song, B., ... Ye, J. (2020). Construction of highly water-stable metal-organic framework UiO-66 thin-film composite membrane for dyes and antibiotics separation. *Chemical Engineering Journal*, *385*, 123400. Available from https://doi.org/10.1016/j.cej.2019.123400.

Feng, Y., Weber, M., Maletzko, C., & Chung, T. S. (2019). Fabrication of organic solvent nanofiltration membranes via facile bioinspired one-step modification. *Chemical Engineering Science*, *198*, 74–84. Available from https://doi.org/10.1016/j.ces.2019.01.008.

Figoli, A., Marino, T., Galiano, S., Dorraji, S. S., Di Nicolò, E., & He, T. (2017). *Sustainable route in preparation of polymeric membranes*. *Sustainable Membrane Technology for Water and Wastewater Treatment*. Springer. Available from https://link.springer.com/chapter/10.1007/978-981-10-5623-9_4.

Fuwad, A., Ryu, H., Malmstadt, N., Kim, S. M., & Jeon, T. J. (2019). Biomimetic membranes as potential tools for water purification: Preceding and future avenues. *Desalination*, *458*, 97–115. Available from https://doi.org/10.1016/j.desal.2019.02.003.

Gao, J., Sun, S. P., Zhu, W. P., & Chung, T. S. (2014). Chelating polymer modified P84 nanofiltration (NF) hollow fiber membranes for high efficient heavy metal removal. *Water Research*, *63*, 252–261. Available from https://doi.org/10.1016/j.watres.2014.06.006.

Gehrke, I., Geiser, A., & Somborn-Schulz, A. (2015). Innovations in nanotechnology for water treatment. *Nanotechnology, Science and Applications*, *8*, 1–17. Available from https://doi.org/10.2147/NSA.S43773.

Giwa, A., Hasan, S. W., Yousuf, A., Chakraborty, S., Johnson, D. J., & Hilal, N. (2017). Biomimetic membranes: A critical review of recent progress. *Desalination*, *420*, 403–424. Available from https://doi.org/10.1016/j.desal.2017.06.025.

Goh, P. S., Matsuura, T., Ismail, A. F., & Hilal, N. (2016). Recent trends in membranes and membrane processes for desalination. *Desalination*, *391*, 43–60. Available from https://doi.org/10.1016/j.desal.2015.12.016.

Goh, P. S., Wong, T. W., Lim, J. W., Ismail, A. F., & Hilal, N. (2019). Innovative and sustainable membrane technology for wastewater treatment and desalination application. *Innovation strategies in environmental science*. Elsevier Inc. Available from https://doi.org/10.1016/B978-0-12-817382-4.00009-5.

Gonzalez-Perez, A., & Persson, K. M. (2016). Bioinspired materials for water purification. *Materials*, *9*(6). Available from https://doi.org/10.3390/ma9060447.

Guo, D., Xiao, Y., Li, T., Zhou, Q., Shen, L., Li, R., … Lin, H. (2020). Fabrication of high-performance composite nanofiltration membranes for dye wastewater treatment: Mussel-inspired layer-by-layer self-assembly. *Journal of Colloid and Interface Science*, *560*, 273–283. Available from https://doi.org/10.1016/j.jcis.2019.10.078.

Himstedt, H. H., Marshall, K. M., & Wickramasinghe, S. R. (2011). pH-responsive nanofiltration membranes by surface modification. *Journal of Membrane Science*, *366*(1–2), 373–381. Available from https://doi.org/10.1016/j.memsci.2010.10.027.

Huang, J. H., Cheng, X. Q., Zhang, Y., Wang, K., Liang, H., Wang, P., … Shao, L. (2020). Polyelectrolyte grafted MOFs enable conjugated membranes for molecular separations in dual solvent systems. *Cell Reports Physical Science*, *1*(4), 100034. Available from https://doi.org/10.1016/j.xcrp.2020.100034.

Ji, Y. L., Ang, M. B. M. Y., Hung, H. C., Huang, S. H., An, Q. F., Lee, K. R., & Lai, J. Y. (2018). Bio-inspired deposition of polydopamine on PVDF followed by interfacial cross-linking with trimesoyl chloride as means of preparing composite membranes for isopropanol dehydration. *Journal of Membrane Science*, *557*, 58–66. Available from https://doi.org/10.1016/j.memsci.2018.04.023.

Jiang, P., Ji, H., Li, G., Chen, S., & Lv, L. (2020). Structure formation in pH-sensitive micro porous membrane from well-defined ethyl cellulose-g-PDEAEMA via non-solvent-induced phase separation process. *Journal of Macromolecular Science, Part A: Pure and Applied Chemistry*, *57*(6), 461–471. Available from https://doi.org/10.1080/10601325.2020.1722691.

Li, M., Xu, J., Chang, C. Y., Feng, C., Zhang, L., Tang, Y., & Gao, C. (2014). Bioinspired fabrication of composite nanofiltration membrane based on the formation of DA/PEI layer followed by cross-linking. *Journal of Membrane Science*, *459*, 62–71. Available from https://doi.org/10.1016/j.memsci.2014.01.038.

Li, T., Xiao, Y., Guo, D., Shen, L., Li, R., Jiao, Y., … Lin, H. (2020). In-situ coating TiO_2 surface by plant-inspired tannic acid for fabrication of thin film nanocomposite nanofiltration membranes toward enhanced separation and antibacterial performance. *Journal of Colloid and Interface Science*, *572*, 114–121. Available from https://doi.org/10.1016/j.jcis.2020.03.087.

Li, X., Wang, R., Tang, C., Vararattanavech, A., Zhao, Y., Torres, J., & Fane, T. (2012). Preparation of supported lipid membranes for aquaporin Z incorporation. *Colloids and Surfaces B: Biointerfaces*, *94*, 333–340. Available from https://doi.org/10.1016/j.colsurfb.2012.02.013.

Li, X., Wang, R., Wicaksana, F., Tang, C., Torres, J., & Fane, A. G. (2014). Preparation of high performance nanofiltration (NF) membranes incorporated with aquaporin Z. *Journal of Membrane Science*, *450*, 181–188. Available from https://doi.org/10.1016/j.memsci.2013.09.007.

Liu, D., Chen, Y., Tran, T. T., & Zhang, G. (2020). Facile and rapid assembly of high-performance tannic acid thin-film nanofiltration membranes via Fe^{3+} intermediated regulation and coordination. *Separation and Purification Technology*, *260*, 118228. Available from https://doi.org/10.1016/j.seppur.2020.118228.

Liu, X., Feng, P., Zhang, L., & Chen, Y. (2020). Mussel-inspired method to decorate commercial nanofiltration membrane for heavy metal ions removal. *Polymers for Advanced Technologies*, *31*(4), 665–674. Available from https://doi.org/10.1002/pat.4803.

Low., & Ng. (2019). *Chapter 4 - Progress of stimuli responsive membranes in water treatment*. *Advanced Nanomaterials for Membrane Synthesis and Its Applications*. Elsevier. Available from https://doi.org/10.1016/B978-0-12-814503-6.00004-5.

Lv, Y., Yang, H. C., Liang, H. Q., Wan, L. S., & Xu, Z. K. (2015). Nanofiltration membranes via co-deposition of polydopamine/polyethylenimine followed by cross-linking. *Journal of Membrane Science*, *476*, 50–58. Available from https://doi.org/10.1016/j.memsci.2014.11.024.

Maletskyi, Z. (2020). Advances in membrane materials and processes for water and wastewater treatment. *ACS Symposium Series*, *1348*, 3–35. Available from https://doi.org/10.1021/bk-2020-1348.ch001.

Martínez-Ballesta, M., del, C., García-Gomez, P., Yepes-Molina, L., Guarnizo, A. L., Teruel, J. A., & Carvajal, M. (2018). Plasma membrane aquaporins mediates vesicle stability in broccoli. *PLoS One*, *13*(2), 1–19. Available from https://doi.org/10.1371/journal.pone.0192422.

Meng, F., Song, F., Yao, Y., Liu, G., & Zhao, S. (2020). Ultrastable nanofiltration membranes engineered by polydopamine-assisted polyelectrolyte layer-by-layer assembly for water reclamation. *ACS Sustainable Chemistry and Engineering*, *8*(29), 10928–10938. Available from https://doi.org/10.1021/acssuschemeng.0c03318.

Montero De Espinosa, L., Meesorn, W., Moatsou, D., & Weder, C. (2017). Bioinspired polymer systems with stimuli-responsive mechanical properties. *Chemical Reviews*, *117*(20), 12851–12892. Available from https://doi.org/10.1021/acs.chemrev.7b00168.

Nabeel, F., Rasheed, T., Bilal, M., Li, C., Yu, C., & Iqbal, H. M. N. (2020). Bio-inspired supramolecular membranes: A pathway to separation and purification of emerging pollutants. *Separation and Purification Reviews*, *49*(1), 20–36. Available from https://doi.org/10.1080/15422119.2018.1500919.

Ouyang, Z., Huang, Z., Tang, X., Xiong, C., Tang, M., & Lu, Y. (2019). A dually charged nanofiltration membrane by pH-responsive polydopamine for pharmaceuticals and personal care products removal. *Separation and Purification Technology*, *211*, 90–97. Available from https://doi.org/10.1016/j.seppur.2018.09.059.

Pan, F., Cheng, Q., Jia, H., & Jiang, Z. (2010). Facile approach to polymer-inorganic nanocomposite membrane through a biomineralization-inspired process. *Journal of Membrane Science*, *357*(1–2), 171–177. Available from https://doi.org/10.1016/j.memsci.2010.04.017.

Purkait, M. K., Sinha, M. K., Mondal, P., & Singh, R. (2018a). Magnetic-responsive membranes. *Interface Science and Technology*, *25*, 193–219. Available from https://doi.org/10.1016/B978-0-12-813961-5.00007-3.

Purkait, M. K., Sinha, M. K., Mondal, P., & Singh, R. (2018b). pH-Responsive membranes. *Interface Science and Technology*, *25*, 39–66. Available from https://doi.org/10.1016/B978-0-12-813961-5.00002-4.

Qi, S., Wang, R., Chaitra, G. K. M., Torres, J., Hu, X., & Fane, A. G. (2016). Aquaporin-based biomimetic reverse osmosis membranes: Stability and long term performance. *Journal of Membrane Science*, *508*, 94–103. Available from https://doi.org/10.1016/j.memsci.2016.02.013.

Qian, X., Yang, Q., Vu, A., & Wickramasinghe, S. R. (2016). Localized heat generation from magnetically responsive membranes. *Industrial and Engineering Chemistry Research*, *55*(33), 9015–9027. Available from https://doi.org/10.1021/acs.iecr.6b01820.

Qiang, R., Wei, C., Lin, L., Deng, X., Zheng, T., Wang, Q., ... Zhang, Y. (2020). Bioinspired: A 3D vertical silicon sponge-inspired construction of organic-inorganic loose mass transfer nanochannels for enhancing properties of polyimide nanofiltration membranes. *Separation and Purification Technology*, *259*, 118038. Available from https://doi.org/10.1016/j.seppur.2020.118038.

Ren, L., Chen, J., Lu, Q., Han, J., & Wu, H. (2020). Antifouling nanofiltration membrane fabrication via surface assembling light-responsive and regenerable functional layer. *ACS Applied Materials and Interfaces*, *12*, 52050–52058. Available from https://doi.org/10.1021/acsami.0c16858.

Ryu, H., Fuwad, A., Yoon, S., Jang, H., Lee, J. C., Kim, S. M., & Jeon, T. J. (2019). Biomimetic membranes with transmembrane proteins: State-of-the-art in transmembrane protein applications. *International Journal of Molecular Sciences*, *20*(6). Available from https://doi.org/10.3390/ijms20061437.

Sambudi, N. S., & Sahoo, P. C. (2017). Biomineralization: An inspiration from nature for the synthesis of advanced materials. *Mineral processing: Methods, applications and technology* (pp. 1–17). Nova Science Publishers.

Sengur-Tasdemir, R., Kilic, A., Tutuncu, H. E., Ergon-Can, T., Gul-Karaguler, N., Ates-Genceli, E., ... Koyuncu, I. (2018). Characterization of aquaporin Z-incorporated proteoliposomes with QCM-D. *Surface Innovations*, *7*(2), 133–142. Available from https://doi.org/10.1680/jsuin.18.00057.

Sengur-Tasdemir, R., Sayinli, B., Urper, G. M., Tutuncu, H. E., Gul-Karaguler, N., Ates-Genceli, E., ... Koyuncu, I. (2018). Hollow fiber nanofiltration membranes with integrated aquaporin Z. *New Journal of Chemistry*, *42*(21), 17769–17778. Available from https://doi.org/10.1039/C8NJ04367A.

Sengur-Tasdemir, R., Tutuncu, H. E., Gul-Karaguler, N., Ates-Genceli, E., & Koyuncu, I. (2019). Biomimetic membranes as an emerging water filtration technology. *Biomimetic lipid membranes: Fundamentals, applications, and commercialization*. Available from https://doi.org/10.1007/978-3-030-11596-8_11.

Shen, Yx, Saboe, P. O., Sines, I. T., Erbakan, M., & Kumar, M. (2014). Biomimetic membranes: A review. *Journal of Membrane Science*, *454*, 359–381. Available from https://doi.org/10.1016/j.memsci.2013.12.019.

Shenvi, S. S., Isloor, A. M., & Ismail, A. F. (2015). A review on RO membrane technology: Developments and challenges. *Desalination*, *368*, 10–26. Available from https://doi.org/10.1016/j.desal.2014.12.042.

Song, G., Sengupta, A., Qian, X., & Wickramasinghe, S. R. (2018). Investigation on suppression of fouling by magnetically responsive nanofiltration membranes. *Separation and Purification Technology*, *205*, 94–104. Available from https://doi.org/10.1016/j.seppur.2018.05.022.

Song, G., Wickramasinghe, S. R., & Qian, X. (2017). The effects of salt type and salt concentration on the performance of magnetically activated nanofiltration membranes. *Industrial and Engineering Chemistry Research*, *56*(7), 1848–1859. Available from https://doi.org/10.1021/acs.iecr.6b04278.

Sun, G., Chung, T. S., Jeyaseelan, K., & Armugam, A. (2013a). A layer-by-layer self-assembly approach to developing an aquaporin-embedded mixed matrix membrane. *RSC Advances*, *3*(2), 473–481. Available from https://doi.org/10.1039/c2ra21767h.

Sun, G., Chung, T. S., Jeyaseelan, K., & Armugam, A. (2013b). Stabilization and immobilization of aquaporin reconstituted lipid vesicles for water purification. *Colloids and Surfaces B: Biointerfaces*, *102*, 466–471. Available from https://doi.org/10.1016/j.colsurfb.2012.08.009.

Tang, Y., Tang, B., & Wu, P. (2015). A polymeric ionic liquid functionalized temperature-responsive composite membrane with tunable responsive behavior. *Journal of Materials Chemistry A*, *3*(15), 7919–7928. Available from https://doi.org/10.1039/c5ta00212e.

Tham, H. M., & Chung, T. S. (2020). One-step cross-linking and tannic acid modification of polyacrylonitrile hollow fibers for organic solvent nanofiltration. *Journal of Membrane Science*, *610*, 118294. Available from https://doi.org/10.1016/j.memsci.2020.118294.

Tomer, N., Mondal, S., Wandera, D., Wickramasinghe, S. R., & Husson, S. M. (2009). Modification of nanofiltration membranes by surface-initiated atom transfer radical polymerization for produced water filtration. *Separation Science and Technology*, *44*(14), 3346–3368. Available from https://doi.org/10.1080/01496390903212540.

Vullev, V. I. (2011). From biomimesis to bioinspiration: What's the benefit for solar energy conversion applications? *Journal of Physical Chemistry Letters*, *2*(5), 503–508. Available from https://doi.org/10.1021/jz1016069.

Wagh, P., & Escobar, I. C. (2019). Biomimetic and bioinspired membranes for water purification: A critical review and future directions. *Environmental Progress and Sustainable Energy*, *38*(3). Available from https://doi.org/10.1002/ep.13215.

Wagh, P., Parungao, G., Viola, R. E., & Escobar, I. C. (2015). A new technique to fabricate high-performance biologically inspired membranes for water treatment. *Separation and Purification Technology*, *156*, 754–765. Available from https://doi.org/10.1016/j.seppur.2015.10.073.

Wagh, P., Zhang, X., Blood, R., Kekenes-Huskey, P. M., Rajapaksha, P., Wei, Y., & Escobar, I. C. (2019). Increasing salt rejection of polybenzimidazole nanofiltration membranes via the addition of immobilized and aligned aquaporins. *Processes*, *7*(2), 28–37. Available from https://doi.org/10.3390/pr7020076.

Wandera, D., Wickramasinghe, S. R., & Husson, S. M. (2010). Stimuli-responsive membranes. *Journal of Membrane Science*, *357*(1–2), 6–35. Available from https://doi.org/10.1016/j.memsci.2010.03.046.

Wang, Z., He, F., Guo, J., Peng, S., Cheng, X. Q., Zhang, Y., … Shao, L. (2020). The stability of a graphene oxide (GO) nanofiltration (NF) membrane in an aqueous environment: Progress and challenges. *Materials Advances*, *1*(4), 554–568. Available from https://doi.org/10.1039/d0ma00191k.

Wang, Z., Wang, X., Ding, W., Wang, M., Qi, X., & Gao, C. (2015). Impact of monoolein on aquaporin1-based supported lipid bilayer membranes. *Science and Technology of Advanced Materials*, *16*(4). Available from https://doi.org/10.1088/1468-6996/16/4/045005.

Wee, K., & Bai, R. (2013). *Stimuli-responsive membranes*. Encyclopedia of Membrane Science and Technology. Wiley Online Library. Available from https://onlinelibrary.wiley.com/doi/abs/10.1002/9781118522318.emst053.

Weng, X. D., Bao, X. J., Jiang, H. D., Chen, L., Ji, Y. L., An, Q. F., & Gao, C. J. (2016). pH-responsive nanofiltration membranes containing carboxybetaine with tunable ion selectivity for charge-based separations. *Journal of Membrane Science*, *520*, 294–302. Available from https://doi.org/10.1016/j.memsci.2016.08.002.

Woo, S. T., Yun, T., & Kwak, S. Y. (2018). Fouling-resistant microfiltration membrane modified with magnetite nanoparticles by reversible conjunction. *Separation and Purification Technology*, *202*, 299–306. Available from https://doi.org/10.1016/j.seppur.2018.04.002.

Wu, M., Yuan, J., Wu, H., Su, Y., Yang, H., You, X., … Jiang, Z. (2019). Ultrathin nanofiltration membrane with polydopamine-covalent organic framework interlayer for enhanced permeability and structural stability. *Journal of Membrane Science*, *576*, 131–141. Available from https://doi.org/10.1016/j.memsci.2019.01.040.

Xiao, H. F., Chu, C. H., Xu, W. T., Chen, B. Z., Ju, X. H., Xing, W., & Sun, S. P. (2019). Amphibian-inspired amino acid ionic liquid functionalized nanofiltration membranes with high water permeability and ion selectivity for pigment wastewater treatment. *Journal of Membrane Science*, *586*, 44–52. Available from https://doi.org/10.1016/j.memsci.2019.05.038.

Xiao, Y., Guo, D., Li, T., Zhou, Q., Shen, L., Li, R., … Lin, H. (2020). Facile fabrication of superhydrophilic nanofiltration membranes via tannic acid and irons layer-by-layer self-assembly for dye separation. *Applied Surface Science*, *515*, 146063. Available from https://doi.org/10.1016/j.apsusc.2020.146063.

Xie, W., He, F., Wang, B., Chung, T. S., Jeyaseelan, K., Armugam, A., & Tong, Y. W. (2013). An aquaporin-based vesicle-embedded polymeric membrane for low energy water filtration. *Journal of Materials Chemistry A*, *1*(26), 7592–7600. Available from https://doi.org/10.1039/c3ta10731k.

Xu, Y., You, F., Sun, H., & Shao, L. (2017). Realizing mussel-inspired polydopamine selective layer with strong solvent resistance in nanofiltration toward sustainable reclamation. *ACS Sustainable Chemistry and Engineering*, *5*(6), 5520–5528. Available from https://doi.org/10.1021/acssuschemeng.7b00871.

Xu, Y. C., Tang, Y. P., Liu, L. F., Guo, Z. H., & Shao, L. (2017). Nanocomposite organic solvent nanofiltration membranes by a highly-efficient mussel-inspired co-deposition strategy. *Journal of Membrane Science*, *526*, 32–42. Available from https://doi.org/10.1016/j.memsci.2016.12.026.

Yan, Z., Zhang, Y., Yang, H., Fan, G., Ding, A., Liang, H., … Van der Bruggen, B. (2020). Mussel-inspired polydopamine modification of polymeric membranes for the application of water and wastewater treatment: A review. *Chemical Engineering Research and Design*, *157*, 195–214. Available from https://doi.org/10.1016/j.cherd.2020.03.011.

Yang, B., Yang, X., Liu, B., Chen, Z., Chen, C., Liang, S., … Crittenden, J. (2017). PVDF blended PVDF-g-PMAA pH-responsive membrane: Effect of additives and solvents on membrane properties and performance. *Journal of Membrane Science*, *541*, 558–566. Available from https://doi.org/10.1016/j.memsci.2017.07.045.

Yang, Q., Himstedt, H. H., Ulbricht, M., Qian, X., & Ranil Wickramasinghe, S. (2013). Designing magnetic field responsive nanofiltration membranes. *Journal of Membrane Science*, *430*, 70–78. Available from https://doi.org/10.1016/j.memsci.2012.11.068.

Yang, X., Du, Y., Zhang, X., He, A., & Xu, Z. K. (2017). Nanofiltration membrane with a mussel-inspired interlayer for improved permeation performance. *Langmuir*, *33*(9), 2318–2324. Available from https://doi.org/10.1021/acs.langmuir.6b04465.

Yin, C., Dong, L., Wang, Z., Chen, M., Wang, Y., & Zhao, Y. (2019). CO_2-responsive graphene oxide nanofiltration membranes for switchable rejection to cations and anions. *Journal of Membrane Science*, *592*, 117374. Available from https://doi.org/10.1016/j.memsci.2019.117374.

Zhang, H., Mao, H., Wang, J., Ding, R., Du, Z., Liu, J., & Cao, S. (2014). Mineralization-inspired preparation of composite membranes with polyethylenimine-nanoparticle hybrid active layer for solvent resistant nanofiltration. *Journal of Membrane Science*, *470*, 70–79. Available from https://doi.org/10.1016/j.memsci.2014.07.019.

Zhang, J., Liu, Y., Guo, J., Yu, Y., Li, Y., & Zhang, X. (2020). A CO_2-responsive PAN/PAN-co-PDEAEMA membrane capable of cleaning protein foulant without the aid of chemical agents. *Reactive and Functional Polymers*, *149*, 2–9. Available from https://doi.org/10.1016/j.reactfunctpolym.2020.104503.

Zhang, K., Yang, K., Chen, Y., & Hu, Y. (2020). Ionic and pH responsive thin film composite hollow fiber nanofiltration membrane for molecular separation. *Desalination*, *496*, 114709. Available from https://doi.org/10.1016/j.desal.2020.114709.

Zhang, N., Jiang, B., Zhang, L., Huang, Z., Sun, Y., Zong, Y., & Zhang, H. (2019). Low-pressure electroneutral loose nanofiltration membranes with polyphenol-inspired coatings for effective dye/divalent salt separation. *Chemical Engineering Journal*, *359*, 1442–1452. Available from https://doi.org/10.1016/j.cej.2018.11.033.

Zhang, R., Su, Y., Zhao, X., Li, Y., Zhao, J., & Jiang, Z. (2014). A novel positively charged composite nanofiltration membrane prepared by bio-inspired adhesion of polydopamine and surface grafting of poly(ethylene imine). *Journal of Membrane Science*, *470*, 9–17. Available from https://doi.org/10.1016/j.memsci.2014.07.006.

Zhang, Y., Su, Y., Peng, J., Zhao, X., Liu, J., Zhao, J., & Jiang, Z. (2013). Composite nanofiltration membranes prepared by interfacial polymerization with natural material tannic acid and trimesoyl chloride. *Journal of Membrane Science*, *429*, 235–242. Available from https://doi.org/10.1016/j.memsci.2012.11.059.

Zhao, D., Kim, J. F., Ignacz, G., Pogany, P., Lee, Y. M., & Szekely, G. (2019). Bio-inspired robust membranes nanoengineered from interpenetrating polymer networks of polybenzimidazole/polydopamine. *ACS Nano*, *13*(1), 125–133. Available from https://doi.org/10.1021/acsnano.8b04123.

Zhao, F. Y., Ji, Y. L., Weng, X. D., Mi, Y. F., Ye, C. C., An, Q. F., & Gao, C. J. (2016). High-flux positively charged nanocomposite nanofiltration membranes filled with poly(dopamine) modified multiwall carbon nanotubes. *ACS Applied Materials and Interfaces*, *8*(10), 6693–6700. Available from https://doi.org/10.1021/acsami.6b00394.

Zhao, J., Su, Y., He, X., Zhao, X., Li, Y., Zhang, R., & Jiang, Z. (2014). Dopamine composite nanofiltration membranes prepared by self-polymerization and interfacial polymerization. *Journal of Membrane Science*, *465*, 41–48. Available from https://doi.org/10.1016/j.memsci.2014.04.018.

Zhong, P. S., Chung, T. S., Jeyaseelan, K., & Armugam, A. (2012). Aquapori n-embedded biomimetic membranes for nanofiltration. *Journal of Membrane Science*, *407–408*, 27–33. Available from https://doi.org/10.1016/j.memsci.2012.03.033.

CHAPTER

8

Reverse and forward osmosis membrane technologies

Soleyman Sahebi[1,2], *Mohammad Sheikhi*[2], *Mohammad Kahriz*[2], *Nasim Fadaie*[2], *Zahra Shabani*[2], *Sanaz Ghiasi*[2], *Norollah Kasiri*[2] *and Toraj Mohammadi*[2]

[1]Mana Energy and Sorin Refining Company Pty. Ltd., Tehran, Iran [2]Centre of Excellence for Membrane Science and Technology, School of Chemical, Petroleum and Gas Engineering, Iran University of Science and Technology (IUST), Tehran, Iran

8.1 Introduction

Although there are various industrialized membrane-based desalination processes, reverse osmosis (RO) process has been the prominent technology in this sector due to its obvious advantages. Forward osmosis (FO) has also attracted considerable interest of many investigators as an interesting alterative. FO operates based on the osmotic pressure differences between draw solution (DS) and feed solution (FS) as a driving force to transfer water across the membrane without external hydraulic pressure (Tijing, Choi, Lee, Kim, & Shon, 2014). Unlike RO, FO operates at no applied hydraulic pressure or just requires a very low pressure [in the case of pressure-assisted osmosis (PAO)]. Therefore it requires much lower energy and compared to the other pressure-driven membrane processes, it has lower membrane fouling tendency (Cath, Childress, & Elimelech, 2006; Zyaie, Sheikhi, Baniasadi, Sahebi, & Mohammadi, 2018).

Development of cellulose acetate (CA) asymmetric membranes for RO process revolutionized this technology and significant development has been made by utilizing other asymmetric membranes so far. However, development of FO membranes has been hindered by the lack of appropriate membranes and other obstacles. Many researches have been carried out to develop FO membranes, but they are limited to lab scale fabrication methods (Ren & McCutcheon, 2014; Zirehpour, Rahimpour, Seyedpour, & Jahanshahi, 2015).

Advancement in Polymer-Based Membranes for Water Remediation
DOI: https://doi.org/10.1016/B978-0-323-88514-0.00011-5

© 2022 Elsevier Inc. All rights reserved.

8.2 Classification of osmotic processes and basic concept

The osmotic processes can be classified into four types based on applied hydraulic pressure either on the DS side or the FS side (Sahebi, Phuntsho, Eun Kim, Hong, & Kyong Shon, 2015). Fig. 8.1 illustrates the difference between RO and the other different engineered osmosis. Regardless of different FO applications, the flow of water naturally is from lower concentrated solution (P1) to higher concentrated solution (P2), while in RO water flow requires applied hydraulic pressure to overcome osmotic pressure ($\Delta\pi$). Thus water flow is from (P2) to (P1). It also displays the relationship between PAO, FO, pressure-retarded osmosis (PRO), and RO for an ideal membrane. In FO mode, water molecules diffuse to the more concentrated side of the semipermeable membrane where ΔP is almost zero. PAO is comparable to FO, but extra pressure is applied on the FS side, while in PRO mode of operation, positive pressure ($\Delta\pi > \Delta P$) is applied and as a consequence, water disperses to the more brine liquid side. In RO, due to high hydraulic pressure ($\Delta P > \Delta\pi$), water molecules diffuse to the less or nonsaline liquid side. Fig. 8.2 validates the direction and extent of water flux as a function of the applied hydraulic pressure in RO, PRO, FO, and PAO process. Based on this figure, PRO and RO occur at $\Delta P > 0$; FO occurs at $\Delta P = 0$; and PAO occurs at $\Delta P < 0$ (Sahebi et al., 2015).

Defining Fig. 8.1 in more details, based on hydraulic pressure applied on the side, the osmotic processes can be categorized into four types, that can be defined by the circumstances detailed below. These processes are also depicted in Fig. 8.2.

Forward osmosis (FO): $\Delta P = 0$, driving force = $\pi_D - (\pi_F - \pi_p)$
Reverse osmosis (RO): $\Delta P > \Delta\pi$, driving force = $\Delta P - (\pi_F - \pi_p)$
Pressure retarded osmosis (PRO): $\Delta P < \Delta\pi$, driving force = $\pi_D - (\pi_F - \pi_p)$-ΔP
Pressure assisted osmosis (PAO): $\Delta P < 0$, driving force = $\Delta P - (\pi_F - \pi_p - \pi_D)$

In which, π_D is the DS osmotic pressure. Also the fundamental of the PRO and FO processes are alike but, in the PRO process, the pressure is applied on the DS side ($\Delta P < \Delta\pi$) contrary to the osmotic gradient that partly retards the water passage the FO membrane produced by the osmotic agent driving force. This generates hydraulic pressure inside the DS tank that in turn can be used to run a hydraulic turbine to generate power (Sahebi et al., 2015).

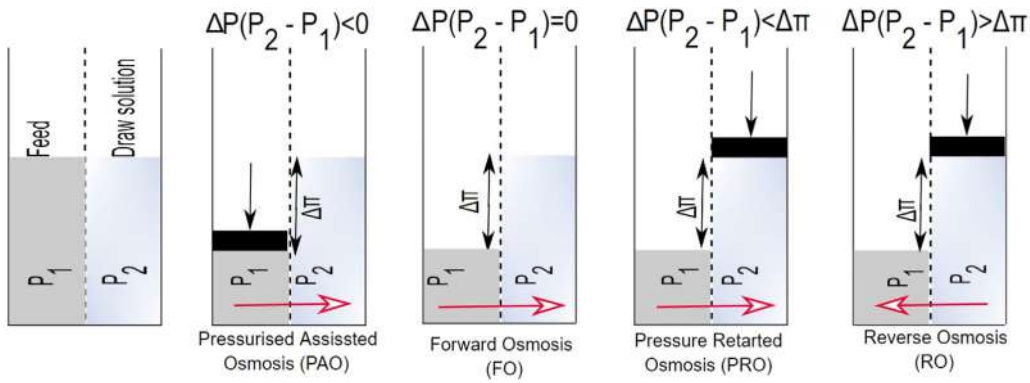

FIGURE 8.1 Relationship between reverse osmosis (RO), pressure-retarded osmosis (PRO), forward osmosis (FO), and pressure-assisted osmosis (PAO) and direction of water flow for an ideal semipermeable membrane.

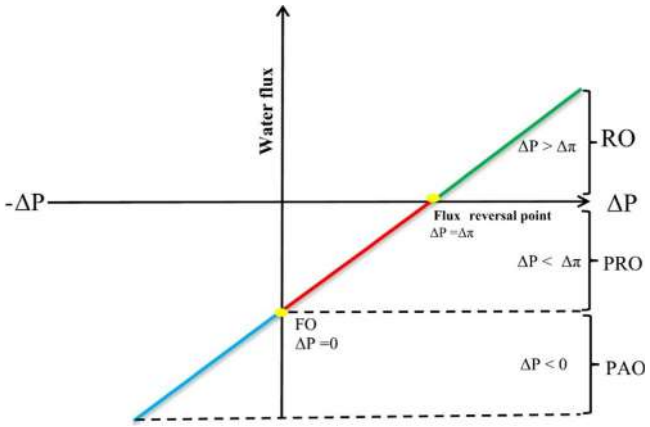

FIGURE 8.2 Theoretical relationship between the entire osmosis processes (Sahebi et al., 2015).

8.2.1 Transport membrane mechanism

Different mechanistic and mathematical models have been proposed to describe the performance of the osmosis process. These models are divided into three general categories: (1) irreversible thermodynamics models; (2) nonporous or homogeneous membrane models; and (3) pore models. Some of these models are based on simple concepts while others have been relatively complex. Models which can predict performance with high accuracy are crucial because they can minimize the number of experiments which should be conducted to characterize a specific system. All models focus on the membrane active layer because flux and selectivity are a function of the active layer properties (Chian, Chen, Sheng, Ting, & Wang, 2007; Strathmann, Winston, & Sirkar, 1992). It should be noted that most of these models have derived with assumption of steady-state conditions or equilibrium in membrane.

8.2.1.1 Irreversible thermodynamics models

Irreversible thermodynamic models are one of the most common methods for describing transmission phenomena in membrane systems. These models consider the membrane as a black box in which a slow process is performed very close to equilibrium. In these models, the transfer mechanism and the membrane structure were not considered. Additionally, the thermodynamic properties can be used to assume that the system can be divided into small subsystems, which all of them are near equilibrium.

$$Jw = Lp.(\Delta P - \sigma\Delta\pi) \tag{8.1}$$

$$Js = Cs.(1-\sigma)Jw + D\varepsilon\Delta C \tag{8.2}$$

where $\Delta\pi$ and ΔP are the osmotic pressure across membrane and transmembrane pressure, respectively; ΔC and C_s are solute concentration difference across membrane and average solute concentration, respectively; ε is the membrane porosity and D is the diffusion coefficient; L_p is the coefficient; σ is the reflection coefficient of the membrane which measure the solute−water coupling within the membrane and may often be considered as Eq. (8.1).

The main disadvantage of irreversible thermodynamic models is that they are developed with a Black-box view. Therefore they do not describe the transport membrane mechanisms with details; therefore irreversible thermodynamic models are not suitable for optimizing separation based on membrane structure and material properties. In addition, these models cannot predict the water flux with high accuracy for systems including organic matter and dilute.

8.2.1.2 Homogeneous models

As mentioned earlier, irreversible thermodynamics (Black-box) models cannot describe the transfer mechanism in the membrane in detail. To tackle this issue, the solution–diffusion models based on solvent and solute into the membrane was proposed. These models are divided into three categories (Soltanieh & Gill', 1981; Wijmans & Baker, 1995):

1. Solution–diffusion
2. Solution–diffusion imperfection
3. Extended solution–diffusion

The solution–diffusion models were derived based on this assumption that the osmosis membranes have a homogeneous and nonporous surface layer. The separation depends on the solubilities and diffusivities of the solvent and solute variance in the membrane phase. When the solute and solvent molecules reached the membrane surface, both molecules will dissolve in the surface layer. Thus solute distribution coefficient had a respective impact on solubilities of the solute molecules amid the solution and the membrane phase. Once in the membrane phase, these molecules will diffuse across the membrane. The flux and movement of these molecules are governed by transmembrane pressure variance and their particular concentration difference across the semipermeable membrane (collectively known as the molecular species' individual chemical potential gradient) (Chian et al., 2007).

The solution–diffusion model is the most common model which has been used to predict water and salt fluxes in FO and RO processes:

$$J_w = \frac{P_w}{\Delta x}(\Delta P - \Delta\pi) = Aw(\Delta P - \Delta\pi) \tag{8.3}$$

where Δx is the membrane thickness; P_w is the water permeability; A_w is the water permeability constant.

$$J_s = \frac{D_s K_s}{\Delta x}(Cp - Cf) = Bs(Cp - Cf) \tag{8.4}$$

K_s is the sorption coefficient between the membrane and solution; D_s is the diffusion coefficient of the solute; B_s is solute permeability; C_f is the solute concentration in the FS on the membrane surface; and C_p is the solute concentration in the permeate solution. The intrinsic membrane solute rejection (R) can be calculated by the following equation:

$$Bs = \frac{Aw(1-R)(\Delta P - \Delta\pi)}{R} = \frac{(1-R)J_w}{R} \tag{8.5}$$

It should be noted that equations based on solution–diffusion mechanism without considering effect of internal concentration polarization (ICP), external concentration

polarization (ECP), and fouling have overestimate water and reverse solute fluxes (RSF) in FO process. The below equations with considering the effect of ICP, ECP, and RFS were developed to predict water and RSF for FO and PRO modes (Bui, Arena, & McCutcheon, 2015; Suh & Lee, 2013):

$$J_w^{FO} = Aw\left[\frac{\pi_{db}\exp\left[-J_w\left(\frac{1}{k_d}+\frac{S}{D_d}\right)\right]-\pi_{fb}\exp\left(\frac{J_w}{k_f}\right)}{1+\frac{Bs}{J_w}\left\{\exp\left(\frac{J_w}{k_f}\right)-\exp\left[-J_w\left(\frac{1}{k_d}+\frac{S}{D_d}\right)\right]\right\}}\right] \tag{8.6}$$

$$J_w^{PRO} = Aw\left[\frac{\pi_{db}\exp\left(-\frac{J_w}{k_d}\right)-\pi_{fb}\exp\left[J_w\left(\frac{1}{k_f}+\frac{S}{D_f}\right)\right]}{1+\frac{Bs}{J_w}\left\{\exp\left[J_w\left(\frac{1}{k_f}+\frac{S}{D_f}\right)-\exp\left(\frac{J_w}{k_f}\right)\right]\right\}}-\Delta P\right] \tag{8.7}$$

$$J_s = Bs\left[\frac{C_{db}+\frac{J_s}{J_w}}{\exp\left(J_wK\right)\exp\left(\frac{J_w}{k_d}\right)}-\left(C_{fb}+\frac{J_s}{J_w}\right)\exp\left(\frac{J_w}{k_f}\right)\right] \tag{8.8}$$

π_{fb} and π_{db} are the bulk osmotic pressures of the feed and DS, respectively; k_f and k_d are the mass transfer coefficients of the feed and DS, respectively; D_d and D_f are the solute diffusivity in the DS and FS, respectively; C_{fb} and C_{db} are the bulk concentrations of the feed and draw channels, respectively; K is the support layer resistivity; and S is the membrane structure parameter.

8.2.1.3 Solution–diffusion–imperfection model

Although the solution–diffusion model was assumed the surface layer of ideal membrane without any pore, however, the actual membrane surface layer has pores. These pores can provide pathways by which the solvent and solute molecules can diffuse through the membrane. The solution–diffusion imperfection model is similar to the solution–diffusion model by considering one term for the pore existences. This model gives the water and solute fluxes as (Sherwood, Brian, & Fisher, 1967).

$$J_w = \frac{P_w}{\Delta x}(\Delta P - \Delta\pi) + \frac{P_3}{\Delta x}\Delta P \tag{8.9}$$

where $P_3/\Delta x$ is a coupling coefficient.

$$J_s = \frac{P2}{\Delta x}(Cp - Cf) + \frac{P_3}{\Delta x}\Delta PCp \tag{8.10}$$

It is obvious that Eqs. (8.9) and (8.10) compared to Eqs. (8.3) and (8.4) have an additional term relating to solvent flow through the imperfections in the membrane surfaces.

8.2.1.4 Extended solution–diffusion model

Extended solution–diffusion model has been mainly applied for organic solutes considering the pressure-dependent term. This model has two significant drawbacks: (1) To characterize the membrane system, it contains three parameters that must be determined by nonlinear regression. (2) The parameters described by the model are usually functions of both feed concentration and pressure. Additionally, the model cannot describe the

transport of some organic solutes well. Therefore it is not widely used in practice (Burghoff, Lee, & Pusch, 1980; Sobana & Panda, 2011).

8.2.1.5 Pore models

The preferential sorption capillary flow (PSCF) model, the first pore model, was introduced. In contrast to the solution–diffusion model, the membrane is microporous (capillary structure). The separation mechanism is recognized by both fluid transport via surface phenomena and membrane pores. According to the PSCF model, on the contact of the FS with the membrane, chemical properties of the active layer let for the preferential sorption of the solvent molecules and subsequently, the formation of a solvent layer on the surfaces and in the membrane pores. On the contrary, the solute molecules are rejected by the membrane; therefore, the solute molecules cannot form any surface layer. The solvent molecules in the solvent layer are then forced, under hydrostatic pressure, through the membrane capillary pores to the permeate side. This model gives the water and solute fluxes as (Sobana & Panda, 2011; Sourirajan, 1970):

$$Jw = Aw(\Delta P - (\pi(Cp) - \pi(Cf)) \tag{8.11}$$

$\pi(Cp)$ and $\pi(Cf)$ are the osmotic pressure at solute mole fraction p and f.

$$J_s = \frac{D_s K_s}{\Delta x}(Cp - Cf) \tag{8.12}$$

Another pore model is the finely porous model that assumed solvent transport would be accomplished by viscous flow through uniform membrane pores and that solute transport occurs by both diffusion and convection in these pores. It can prepare noteworthy insight into parameters, for instance, solute–membrane interaction, pore size, and partition coefficient that affect solute transport (Soltanieh & Gill', 1981). However, for some solute systems such as dilute organics, the model cannot participate water flux with high accuracy. This drawback limits the applicability of the finely porous models for water flux prediction in these systems.

8.3 Reverse osmosis and forward osmosis membranes

FO process suffers from suitable membrane. FO can run without hydraulic pressure as a driving force and needs only concentration gradient. As it is a unique process, it needs a unique membrane to fulfill the osmotic requirement. The process for making a suitable and durable FO membrane has not been yet discovered and fabricating a suitable membrane for FO is still a major challenge. A review of literature and history of research on FO process presents that there are mainly three pathways to membranes that can be used in FO process. The most common approach and the earliest one is using RO membranes for FO application (Sahebi et al., 2020; Sahebia, Sheikhic, & Ramavandid, 2019). The main obstacle is low water flux across the membrane due to the thick backing fabric support and the dense hydrophobic support polymer that hinder the water transport. Although there is limited published data on this approach, in recent studies, fluxes of up to 3.1 $L\,m^{-2}\,h^{-1}$ have been reported (Arena, McCloskey, Freeman, & McCutcheon, 2011). The low fluxes can be mainly related to the fact

that RO membranes possess a relatively thick polymer support and the support of a nonwoven fabric to withstand highly applied hydraulic pressure (Sahebi et al., 2020).

The second approach is to modify RO membranes for FO application. Although it is almost impossible to replace the thick backing fabric, further modification on the membrane polymer support structure is possible by improving its hydrophilicity nature. There are few works that mainly focus on increasing the membrane hydrophilicity. It has been performed through direct and indirect sulfonation, dopamine, and polyethylene glycol-coating treatment to increase the membrane wettability. Using dopamine for modification of RO membranes has been proved to be interesting to some extent. Although the results have not been promising for FO process, a very large improvement has been found for PRO process for energy production (Arena et al., 2011).

The third and final approach is to design and fabricate a membrane that is customized for FO process. Understanding the fundamentals of FO process and its dependency on osmotic pressure and the role of osmotic agent make it possible to design a membrane that can suit the process. So far a membrane that is robust, hydrophilic, thin with porous backing fabric support has been recommended based on fundamental findings (Gray, McCutcheon, & Elimelech, 2006). Although FO has already been exploited in several applications, designing a suitable membrane remains as a major challenge (Yip & Elimelech, 2011). FO desalination technologies can be viable in the coming years, if a proper high-performance membrane is carefully considered. There are a few considerations that need to be overseen regarding a suitable membrane for FO which are concentration polarization (CP) and fouling. CP is an existing problem in most of the membrane separation technologies. CP, however, is the main reason for low water flux in FO membranes and needs to be explained in more details.

8.4 Concentration polarization in an osmotic-driven membrane

The flux in an osmotic-driven membrane such as FO depends on osmotic pressure difference ($\Delta\pi$) across the membrane thin active layer. However, the osmotic pressure is lower across the active layer in comparison with the bulk osmotic pressure in FS and DS. This results in lower water flux which is often attributed to several phenomena (Cath et al., 2006). Two types of CP phenomena: (1) external CP and (2) internal CP in osmotic-driven membrane processes can take place as discussed in more details later.

8.4.1 External concentration polarization

In RO process, CP mostly occurs on the exterior surface of the membrane which is known as ECP (McCutcheon & Elimelech, 2006). Due to constant pressure and rejection of solute by the rejection layer of the membrane, the bulk osmotic pressure near the membrane surface increasingly builds up. This causes a reduction in water flux through the membrane (Hoek & Elimelech, 2003). The real osmotic pressure is higher than that in the bulk and water flux is consequently reduced. ECP is a well-known phenomenon in RO membranes. ECP also exists in FO process but it is not a major problem compared to RO

process, while existence of ICP is much more common in FO process (McCutcheon & Elimelech, 2007). In membranes with dense symmetric structure used as FO membrane, the ECP causes a dilutive effect on DS near the membrane surface, causing reduced osmotic pressure resulting in water flux decline. Unlike RO membranes, ECP effects depend on operational mode as well in other osmotic membranes (Tan & Ng, 2008).

FO process is divided into two operational modes known as FO and PRO modes shown in Fig. 8.3. In the FO mode, DS faces the support layer while in the PRO mode, DS faces the selective layer. Effects of ECP have been observed to be different in the two modes. However, in the both modes, it can reduce water flux through dilutive ECP in the PRO mode on DS side and concentrative ECP in the FO mode on FS side. Furthermore, regardless of the operational modes, it is well known that ECP can be limited by increasing water flow rate (McCutcheon & Elimelech, 2006).

8.4.2 Internal concentration polarization

ICP is a more severe problem in FO process which is related to the membrane structure (Hoek & Elimelech, 2003). This phenomenon occurs within the semipermeable membrane. Solute characteristics may play a role in the ICP effects as well. Solutes with different diffusivity and molecular size can affect ICP (Zhao & Zou, 2011). Thus ICP can be related to the membrane substrate morphology directly and the solute characteristics indirectly. It means ICP depends on both FO membrane morphology and solute diffusivity through FO membrane. Solute diffusivity is an element chemical property but it can be hindered by the membrane tortuosity (Mitragotri et al., 2011). Similar to ECP, there are different ICP effects depending on the operational modes. In the PRO mode, mostly concentrative ICP

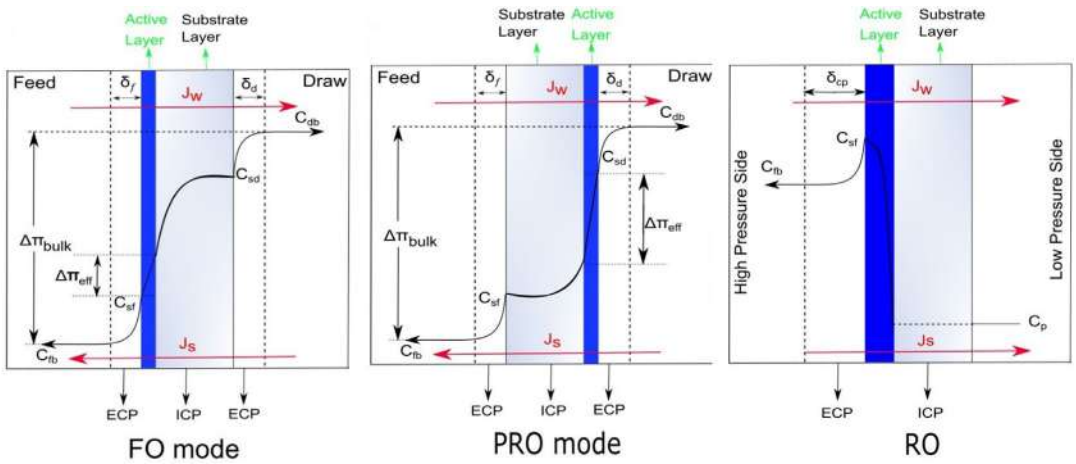

FIGURE 8.3 Water flux transport through pressure-retarded osmosis (PRO) and forward osmosis (FO) modes in FO and through reverse osmosis (RO) processes. J_w, water flux; J_s, reverse salt flux; C, concentration; C_{fb}, concentration of feed bulk; C_{sf}, concentration of feed at membrane surface on feed channel; C_p, concentration in permeate; C_{sm}, concentration at membrane surface on membrane channel; C_{db}, concentration of DS bulk; C_{sd}, concentration of DS at membrane surface on draw channel.

exists. Solutes accumulate in the membrane support structure through FS as well as RSF from DS. As a result, this increases the osmotic pressure within the membrane structure in FS side, resulting in water flux decline (Yip & Elimelech, 2011). Furthermore, dilutive ICP occurs in the FO mode resulting in reduced DS osmotic pressure and water flux decline. In conclusion, it may be revealed that, firstly ICP can cause more flux decline compared to ECP, secondly ICP is more obvious in the FO mode, and finally ICP is more severe at the higher DS concentration (Tang, She, Lay, Wang, & Fane, 2010). Unlike ECP, the ICP effects cannot be limited by hydrodynamic flow conditions such as increasing turbulence through applying spacer or water flow rate (Xu, Peng, Tang, Fu, & Nie, 2010). Through this fundamental limitation, a considerable effort has been made to design a suitable membrane for FO process to minimize the ICP effects in recent years. In summary, the desirable membrane structure needs to have thin substrate which is highly porous and possesses low structural parameter.

8.5 Reverse osmosis and forward osmosis membrane fabrication methods

It is common when woven or nonwoven backing support fabric is used for additional mechanical strength. Wrinkling can be related to the fabric used for the FO membrane fabrication since without it or using RO membrane thick nonwoven backing fabric, defect points and wrinkles disappear significantly. There are several factors that can create defect points and wrinkles. This may be the reason that most of the research groups have not used any backing fabrics for the FO membrane fabrication or if they used, there would be a lot of defect points which would make only a small piece of the fabricated membranes suitable for the test. Therefore making reproducible membranes (cast on woven or nonwoven backing fabrics) in the lab condition is very challenging. In summary, fabrication of FO, PAO, and PRO membranes reinforced with backing fabric support is still crucial in the laboratory condition for further research development on engineered osmosis.

It is worth noting that the FO fabrication method on commercial scale is quite different from the method for RO membranes and this may explain the FO membrane fabrication adoption for limiting the problem. The main reasons for the FO membrane unique fabrication style on the rotating roll are related to several factors involved in the fabrication. First of all, backing fabric support in RO membrane is thick nonwoven fabric, while for FO membrane, thin nonwoven or woven mesh can be used. Therefore due to more porous fabric with bigger pore size, polymer penetration is common during the FO membrane fabrication. Although it is not proven that this polymer penetration is the reason for the defect points appearance and membrane wrinkles during phase inversion, however, due to the nature of the backing fabric required for FO membrane and lower polymer concentration (less viscose casting solution) for FO membrane, the fabrication method in commercial scale is quite different to prevent and limit the casting solution strike through the backing fabric. Fig. 8.4A shows the membrane fabrication RO-style where the backing fabric turns on the rotating roll and then the polymer solution is poured on the top surface of the fabric. In contrast, Fig. 8.4B shows the membrane fabrication FO-style where the polymer solution is cast on the rotating roll and then the backing support fabric is pulled on the top surface of the casted polymer.

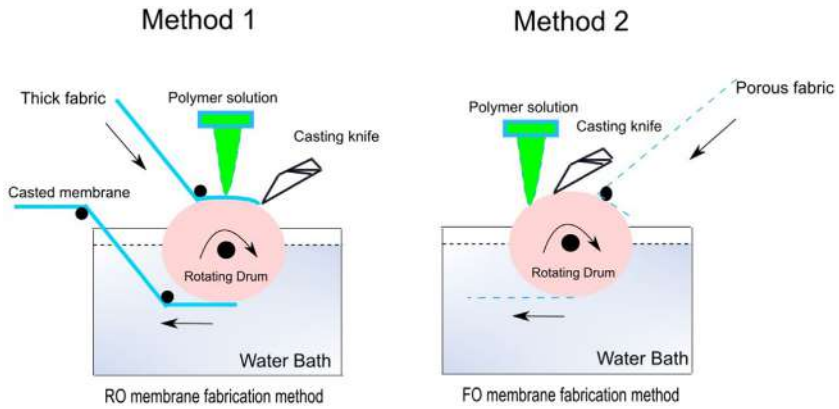

FIGURE 8.4 Diagram of reverse osmosis (RO) and forward osmosis (FO) membrane production methods in commercial scale.

Based on the literatures, there are suggestions for fabric pretreatment to increase polymer and backing fabric compatibility or changing precipitation bath component and temperature (Tiraferri, Yip, Phillip, Schiffman, & Elimelech, 2011).

Although wrinkles and defect points can be minimized by making the backing fabric compatible with the polymer solution or softening the precipitation bath by N-methyl-2-pyrrolidone (NMP), it still exists to the point that interfacial polarization becomes very difficult or impossible due to various defect points and wrinkles on the membrane top surface.

8.6 Advances in forward osmosis and reverse osmosis membranes' structures and properties

Membranes are the principal elements for desalination technologies such as conventional RO and FO processes. Membrane different physicochemical properties govern salt rejection, water flux, chemical stability, and fouling resistance which prominently impact energy consumption in these processes. Significant improvement has been made in the development of high-performance composite membranes for desalination applications in recent years, in terms of polymer and fabrication methods.

8.6.1 Reverse osmosis membrane development

The first membrane used in RO was made of cellulosic polymers back in 1960s. CA RO membranes were initially made of cellulose diacetate and triacetate.

To date, remarkable efforts have been made to explore proper RO polymeric membranes. Polymeric materials with low cost, mechanical strength, and chemical stability have been explored. In this regard, enhanced performance in terms of water permeability and salt rejection with antifouling tendency and chlorine resistance are the key objectives.

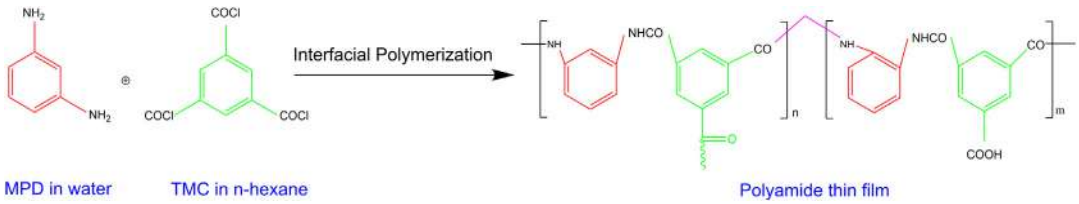

FIGURE 8.5 Schematic of the interfacial polymerization process.

Interfacial polymerization (IP) for thin-film composite (TFC) membranes was used to produce RO membranes with improved performance in terms of salt rejections and water fluxes compared to those fabricated by the Loeb–Sourirajan method in the early 1960s. A selective PA layer can be formed via IP. Rejection PA layer forms through the reaction of m-phenylenediamine (MPD) saturated membrane film when exposed to trimesoyl chloride (TMC) solution either in hexane or in ISOPAR-G solution (zinc salt of mono-2-butyloctyl phosphate). Fig. 8.5 shows the reaction of MPD and TMC at the interface of the two solutions (on the top surface of the membrane film), resulting in an extremely thin membrane rejection layer. Table 8.1 summarizes the most important monomers or reactants used for developing rejection layers of TFC-RO membranes based on literature review.

8.6.2 Forward osmosis membrane development

Improving the membrane material and the fabrication technique are two mutual methods to enhance the membrane performance. Based on previous studies, there are at least two different fabrication techniques to produce polymeric membranes for FO applications and one distinguished fabrication technique to produce nonpolymeric, inorganic membranes. Polymeric membranes are divided into: (1) integral asymmetric membranes which are fabricated via one-step nonsolvent-induced phase separation and (2) composite membranes which are fabricated via a two or more step preparation using phase inversion followed by IP (Fig. 8.6).

8.6.2.1 Phase inversion membranes

Fabrication of asymmetric and symmetric membranes through one stage precipitation of polymer solutions is called phase inversion. Phase inversion is one of the most versatile membrane fabrication techniques to prepare vast varieties of different polymeric membranes including FO. In the following section, the most popular membranes for FO process that is fabricated through phase inversion is being presented.

8.6.2.1.1 Cellulose acetate

Cellulose ester polymers, especially CA, have attracted attention in order to fabricate suitable membranes for FO process due to their availability, low cost, and high resistance to chlorine. Initially, CA has been used to fabricate RO membranes since Loeb-Sourirajan introduced it in the mid-1960s (Zhao, Zou, Tang, & Mulcahy, 2012). However, CA RO membranes could not perform in FO process due to their thick nonwoven fabric support

TABLE 8.1 Different monomers or reactants used in rejection layers of thin-film composite reverse osmosis (TFC-RO) membranes (Yang et al., 2019).

Monomer A	Monomer B	References
m-Phenylenediamine, 2,2′-benzidinedisulfonic acid	Trimesoyl chloride	Baroña, Lim, and Jung (2012)
m-Phenylenediamine, 3,3′-disulfonated-4,4′-dichlorodiphenyl sulfone	Trimesoyl chloride	Xie et al. (2012)
m-Phenylenediamine, 1,2-bis(2-aminoethoxy)ethane, triethylenetetramine	Trimesoyl chloride	Hung et al. (2014)
Isophthaloyl chloride	Trimesoyl chloride	Zhang et al. (2013)
Piperazine, ethylenediamine cored poly(amidoamine)	Trimesoyl chloride	Sum, Ahmad, and Ooi (2014)
Diethylenetriamine, triethylenetetramine, tetraethylenepentamine, piperazidine	Trimesoyl chloride	Li, Su et al. (2014)
Dopamine	Trimesoyl chloride	Zhao, Su et al. (2014)
Piperazine	2,2′,4,4′,6,6′-Biphenyl hexaacyl chloride	Wang, Yang, Zheng, Zhang, and Zhang (2013)
m-Phenylenediamine, 3,5-diamino-N-(4-aminophenyl) benzamide	Trimesoyl chloride	Wang, Li, Zhang, & Zhang (2010)
m-Phenylenediamine	Trimesoyl chloride, 2,4,6-pyridinetricarboxylic acid	Jewrajka, Reddy et al. (2013)
m-Phenylenediamine	2,4,4′,6-Biphenyl tetraacyl chloride, 2,3′,4,5′,6-biphenyl pentaacyl chloride and 2,2′,4,4′,6,6′-biphenyl hexaacyl chloride (BHAC)	Wang, Dai, Zhang, Li, and Zhang (2013)
Piperazine	Poly(sodium-p-styrene-sulfonate), trimesoyl chloride	Liu, Zhou et al. (2014)
m-Phenylenediamine, mphenylenediamine-5-sulfonic acid	Trimesoyl chloride	Yong, Sanchuan, Meihong, and Congjie (2006)
Polyhexamethylene guanidine hydrochloride	Trimesoyl chloride	Li, Cao et al. (2014)
1,3-Phenylenediamine	1,3,5-Benzene-tricarbonyl trichoride	Huang, Meng et al. (2019)
Piperazine	2,4,6-Trischlorosulfonylphenol	He, Yuan et al. (2019)
Polyallylamine	1,3-Benzenedisulfonyl chloride	Wang, Wei et al. (2019)
p-Phenylenediamine	1,3,5-Triformylphloroglucinol	

(*Continued*)

TABLE 8.1 (Continued)

Monomer A	Monomer B	References
		Wang, Shi, Xiao, Zhou, and Wang (2018)
n-Aminoethyl piperazine propane sulfonate	Trimesoyl chloride	Ma, Ji, Weng, An, and Gao (2016)
Pentaerythritol	Trimesoyl chloride	Cheng, Shi, Zhang, and Zhang (2017)

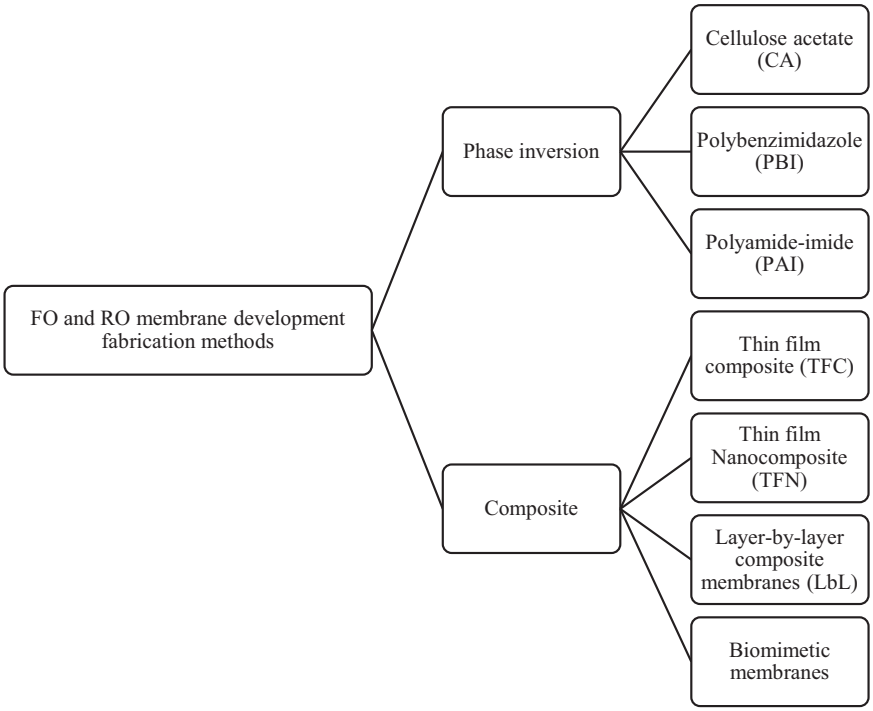

FIGURE 8.6 Categories and classifications of reverse osmosis (RO) and forward osmosis (FO) membranes according to their method of fabrication.

and low porosity of CA structure support. Therefore CA material was not implemented for FO until recently. The Hydration Technology Innovations (HTI) Company has improved a structure design and applied woven polyester mesh with high open area as backing support fabric (Herron, 2008). Cellulose triacetate (CTA) FO membrane has an asymmetric structure that is formed via phase inversion. The membrane is fabricated through a different fabrication method than CTA RO membrane. Therefore embedding a polyester mesh woven fabric with high open rate is successful without any appearance of

air bubbles or polymer penetration that can cause defect points on the membrane surface (Herron, 2008). The porous open polyester mesh and the thinner CA support material greatly reduce ICP compared to RO membranes. The HTI CTA membranes have been extensively evaluated in various FO applications in the past decade in lab and pilot scale studies (Cath et al., 2006).

Few research groups have tried to develop FO hollow fiber membranes based on CA material as well. In recent years, Chung's group developed CA hollow fiber membranes through phase inversion (Su, Yang, Teo, & Chung, 2010). Also, further studies and a few other groups have tried to modify the CA membranes in both flat sheet and hollow fiber. However, low water flux, low rejection, poor resistance to biological attach, and hydrolysis are the drawbacks for the CA-based membranes. These problems have diverted research focus from the CA material to screening better materials for FO membranes.

8.6.2.1.2 Polybenzimidazole

Hydrophilic polybenzimidazole (PBI) is another material that has been used to develop a membrane for FO through phase inversion (Wang, Yang, Chung, & Rajagopalan, 2009). Although, in terms of hydrophilicity, it is similar to CA materials, its excellent chemical stability and self-charged properties make it a promising material for making FO membranes. However, similar to CA materials, low rejection is common with PBI membrane and its industrial-scale membrane applications are also affected by high price and brittleness (Fu, Zhang, Sun, Wang, & Chung, 2013). Further modification has been applied through manufacturing a double skin PBI membrane or a dual-layer structure PBI-PES membrane to increase the membrane performance in terms of rejection (Yang, Wang, & Chung, 2009).

8.6.2.1.3 Polyamide-imide

Polyamide-imide (PAI) has been used as a base support material to fabricate FO hollow fiber and flat membranes through phase inversion in recent years (Setiawan, Wang, Li, & Fane, 2011). The advantage for this kind of membrane is that it has a capability to easily crosslink with materials like polyethyleneimide (PEI) molecules for further modifications. PAI crosslinking greatly depends on several conditions which include PEI molecular weight, concentration, casting temperature, and crosslinking time (Setiawan et al., 2011). Performance results for the flat sheet PAI membranes were better than the hollow fiber PAI membranes due to the ease of further modification. For instance, a positively charged selective layer using PAI on a woven fabric showed better performance compared to a similar hollow fiber membrane due to its better modification (Qiu, Setiawan, Wang, Tang, & Fane, 2012). Table 8.2 shows a summary of recent FO membranes made via phase inversion.

8.6.2.1.4 Composite membranes

Composite membranes are composed of multiple layers and fabricated in multiple stages. They are usually prepared in two steps: (1) fabrication of base support substrate and, (2) formation of selective layer on top of the support through the next step which can be via IP, spin coating, etc. (Kedem & Katchalsky, 1963). The main advantage for composite membranes is ability to modify and control both support and selective layers for

TABLE 8.2 Recent forward osmosis (FO) membranes made through phase inversion.

Membrane	Materials (substrate, active layer)	Feed	Draw solution	Flux ($L\ m^{-2}\ h^{-1}$)	References
(FO NF like) Hollow fiber	PBI	DI water	2.0 M $MgCl_2$	6.0	Wang, Chung, and Qin (2007)
(FO NF like) Hollow fiber with a thin wall	PBI	DI water	2.0 M $MgCl_2$	10.0	Wang, Yang et al. (2009)
Dual-layer (NF) hollow fiber	PBI-PES/PVP	DI water	2.0 M $MgCl_2$	15.0	Yang et al. (2009)
Double-skinned layer, flat sheet	CA	DI water	2.0 M $MgCl_2$	25.0	Wang, Ong, and Chung (2010)
Double dense-layer, flat sheet	CA	DI water	2.0 M $MgCl_2$	10.0	Zhang et al. (2010)
(FO NF like) Hollow fiber	CA	DI water	2.0 M $MgCl_2$	5.0	
Flat sheet composite	CA + Nylon fabric	0.6 M NaCl	1.2 M $MgSO_4$	1.3	Sairam, Sereewatthanawut, Li, Bismarck, and Livingston (2011)
Flat sheet	Cellulose ester	DI water	1.0 M NaCl	7.0	Zhang, Wang, Chung, Jean, and Chen (2011)
Positively charged (NF) hollow fiber	PAI substrate + posttreatment using PEI	DI water	0.5 M $MgCl_2$	8.0	Setiawan et al. (2011)
Cellulose esters with different degrees of substitution of functional groups, flat sheet	Cellulose ester	DI water	1 M NaCl	9.4	Wang, Yu et al. (2012)
Flat sheet	CTA/CA	DI water	1.0 M NaCl	10.4	
Flat sheet	CTA/CA + boehmite	0.01 M NaCl	2.0 M NaCl	23.0	Zirehpour, Rahimpour et al. (2015)
Flat sheet	CTA/CA + CNFs-COOH	0.01 M NaCl	1.0 M NaCl	15.0	Dabaghian and Rahimpour (2015)
Flat sheet	CA + CBA (as additives)	0.1 M NaCl	2.0 M Glucose	11.0–12.0	Xu, Li, Jiao, Shan, and Gao (2016)
Flat sheet	CTA/CA + CNF-NH_2	0.01 M NaCl	1.0 M NaCl	18.0	Dabaghian, Rahimpour, and Jahanshahi (2016)
Free-standing flat sheet	CTA + GO	DI water	0.5 M NaCl	18.0	Wang, Wang et al. (2016)
Flat sheet	CTA/CA + MOF	DI water	2.0 M NaCl	45.0	Zirehpour, Rahimpour, Khoshhal, Firouzjaei, and Ghoreyshi (2016)
Flat sheet	CTA + $ZnCl_2$-lactic acid (LA)	0.1 M NaCl	2 M Glucose	11.0	Chen, Xu, Lu, Shan, and Gao (2017)

membrane custom design. Based on selective layer formation methods, composite membranes for FO can be divided into three categories.

8.6.2.1.5 Thin-film composite membranes

TFC membranes are principally designed for use in water desalination or water purification. Also, they have other applications such as fuel cells and batteries (Baker, 2000; Lonsdale, 1982). A TFC membrane is fabricated through two or more multiple fabrication stages (Petersen, 1993). Developing TFC membranes for various applications including desalination was introduced by Cadotte in the 1970s (Cadotte, 1977). However, the earliest work on fabrication of TFC for FO membrane applications dated back to 2010 (Wei, Qiu, Tang, Wang, & Fane, 2011; Yip, Tiraferri, Phillip, Schiffman, & Elimelech, 2010). Generally, TFC FO membranes consist of porous membrane support and top thin rejection layer, mainly PA. This structure can be supported by backing support fabrics for additional mechanical strength. Formation of thin rejection layer of PA can be formed via IP. IP occurs between two monomer solutions such as MPD monomer dissolved in nonpolar organic solvent, for example, water and TMC monomer in a polar organic solvent, for example, hexane. Reaction occurs when the MPD-saturated membrane substrate is exposed to the TMC solution which results in forming a thin selective layer on the top of the membrane support (Cadotte, 1981).

Resulting TFC membranes exhibit high performance (Wei et al., 2011). However, TFC membranes typically suffer from compaction effects especially for the pressure-based membranes such as RO, PRO, and possibly PAO process. Due to constant applied hydraulic pressure, the polymers are compacted which results in lower porosity. In general, the higher the pressure, the greater the compaction and this can affect the membrane performance in the long term (Pendergast, Nygaard, Ghosh, & Hoek, 2010). Although the procedures for fabrication of FO and RO TFC membranes are similar, the fabrication schemes are quite different. They have different essential requirements for preparing the support structure that stands as cushion for the selective layer. Therefore the main differences between FO and RO TFC membranes are: (1) different polymeric support nature and structure, and (2) supporting backing fabric. Unlike RO with hydrophobic dense polymeric support, FO requires hydrophilic and porous support structure (Cath et al., 2006). Furthermore, FO membranes require very thin and porous support fabric which can be woven mesh or nonwoven PET fabrics. However, RO membranes require thick support fabric commonly nonwoven PET fabrics to withstand high hydraulic pressure. Therefore poor TFC RO membrane performance in FO application can be related to both RO support structure and thick backing fabric support (McCutcheon & Elimelech, 2008). Based on this fundamental, research groups have tried to develop TFC membranes that can perform in FO process. Initial efforts showed that finger-like support structure is preferred to form TFC FO membranes (Yip et al., 2010).

Further studies evaluated the porous support hydrophilicity and its effect on FO performance. The results confirmed the important role of hydrophilic support characteristics on FO performance (Wang, Chung, & Amy, 2012). Increased hydrophilicity can be achieved either by choosing more hydrophilic materials such as polyethersulfone (PES) or direct sulfnation posttreatment through thermal sulfonation or blending with sulfonated polymers (Ariza, Jones, & Rozière, 2002). Widjojo et al. demonstrated a new method to

synthesis high performance TFC FO membranes using sulfonated materials. From this finding, it can be concluded that the membrane hydrophilicity has more effect on the performance than the support structure morphology. The resultant hydrophilic membrane (sulfonated membrane) also showed fully sponge-like structure but attained higher performance in terms of salt reverse fluxes and water fluxes (Widjojo, Chung, Weber, Maletzko, & Warzelhan, 2011). Earlier research on TFC FO membranes has related the membrane performance to the membrane finger-like structure (Tiraferri et al., 2011). Also, this can be true for hydrophobic polysulfone (Psf) polymers used in that study but when other modification factors such as increasing the substrate hydrophilicity are considered, the role of membrane structure in terms of morphologies on the membrane performance may be less important. Furthermore, in addition to sulfonation, hydrophilic properties of the membrane enhanced for the Psf support layer when coated with polydopamine (PDA) (Arena et al., 2011, Han, Zhang, Li, Widjojo, & Chung, 2012). The TFC support membrane surface coated with PDA before IP showed improved performance (Han, Zhang et al., 2012). Also, earlier work using PDA on TFC RO membranes showed significant improvement. After removing their nonwoven fabric layer, the PDA-coated TFC RO membrane structure showed remarkable performance improvement. In comparison with the uncoated membranes, water flux enhanced by 8–15 fold (Arena et al., 2011).

These findings provided an opportunity for screening new hydrophilic materials for FO support. Few studies evaluated the capability of hydrophilic CA materials as support for fabricating TFC FO membranes (Li, Wang, Helmer, & Chung, 2012). Further studies confirmed that cellulose-based polymers can perform as reliable hydrophilic support for TFC FO membranes (Alsvik, Zodrow, Elimelech, & Hägg, 2013). In addition, an alternative concept of using electrospinning nanofibers as support structure for FO membranes can remarkably decrease ICP and the structural parameter. The lower structural parameter in those nanofibers supports is related to the low tortuosity and high-porosity characteristics of membrane films that are fabricated through electrospinning. The results showed relatively high water fluxes which are credited to high porosity and relatively thin thickness of the electrospun nanofibers supports. For instance, using the same types of CTA polymer material for producing nanofibers supports exhibited significantly improved water fluxes compared to the FO HTI-CTA commercial membranes (Song, Liu, & Sun, 2011). Furthermore, close performance in different modes of FO and PRO in FO processes indicated a significant reduction of ICP within the membrane substrate as a result of electrospinning. In conclusion, the TFC membranes show higher performance but unlike the CTA membranes, the TFC membranes consist of PA that is not tolerant to chlorine (Sagle & Freeman, 2004).

8.6.2.1.6 Thin-film nanocomposite membranes

Principally, TFN membranes are modified forms of TFC membranes through applying nanoparticles such as zeolites, carbon nanoparticulates, etc. on the membrane support structure or the selective layer to obtain higher performance (Jeong et al., 2007).

A wide variety of carbon-based nanomaterials can be used to fabricate TFN membranes. For instance, TFN FO membranes have been developed using multiwalled carbon nanotubes (MWCNT) in the membrane selective layer or graphene oxide (GO) in the membrane support structure (Amini, Jahanshahi, & Rahimpour, 2013).

8.6.2.1.7 Layer-by-layer composite membranes

The Layer-by-layer (LbL) self-assembly occurs through an electrostatic force hydrophobic attraction which is a covalent bonding force. This is a simple, robust, and flexible process to fabricate a membrane for specific separation purposes. LbL fabrication can be assembled via spin-coating, dip-coating, or spraying methods applying electrostatic interaction. The membrane performance properties can be controlled by deposition time, ionic strength of the polyelectrolyte solution, and pH of the polyelectrolyte solution (Decher, 1997). The results showed that an FO membrane fabricated through the LbL method has high performance. For instance, water flux up to 100 LMH was achieved using a 2 M $MgCl_2$ solution with high rejection (Duong, Zuo, & Chung, 2013; Saren, Qiu, & Tang, 2011). However, it showed poor performance in terms of monovalent ion rejection such as NaCl. Further studies showed the improved rejection performance for monovalent ions by applying an additional layer of polyelectrolyte (Duong et al., 2013).

8.6.2.1.8 Biomimetic membranes

Despite a promising result for CNT and vertically stand CNT membranes (Kar, Bindal, & Tewari, 2012; Wang, Xiang et al., 2013), currently the highest performance belongs to the successfully made biomimetic membranes (Honglei et al., 2012). Biomimetic membranes have been copied through the function of the biological membranes in the cells that are characterized by their high permeability and specific selectivity toward water and different solutes (Xie et al., 2013). Their unique performance is related to the proteins known as aquaporins. The membrane design has been achieved by mimicking nature through coating of vesicles and black lipid membranes on the top surface of the membrane substrate (Kaufman, Berman, & Freger, 2010). However, incorporation of aquaporin still remains important (Rigaud, Pitard, & Levy, 1995).

Regarding FO application, a novel study demonstrated an outstanding performance by coating aquaporin-containing proteoliposomes or proteopolymersome on the surface of the membrane support followed by IP (Sun, Chung, Jeyaseelan, & Armugam, 2013; Xie et al., 2013). Also, further study achieved mechanically robust Aquaporin Z-embedded biomimetic membranes for FO process with high performance (Xie et al., 2013). Fabricated flat sheet biomimetic FO membranes showed 142 LMH in PRO mode when 2 M NaCl solution was used as DS (Honglei et al., 2012). Table 8.3 shows a summary of recent FO composite membranes made via different materials.

8.7 Custom designs of flat sheet forward osmosis and reverse osmosis membranes

Based on the FO fundamentals and requirements, three factors can significantly affect water flux in FO process. As mentioned, TFC membranes usually consist of three distinct layers which include: (1) selective rejection layer, (2) support polymeric layer, and (3) support backing fabric for additional mechanical strength. There are several options for manufacturing high performance FO membranes via individual design and modification for each layer.

TABLE 8.3 Recent forward osmosis (FO) composite membranes.

Membrane	Materials (substrate, active layer)	FS	DS	Flux (L m^{-2} h^{-1})	References
Hollow fiber	PES, PA	DI water	5.0 M NaCl	Outer surface (#A-FO) = 5 inner surface (#B-FO) = 14	Wang, Shi et al. (2010)
Hollow fiber	PES, PA	DI water	2.0 M NaCl	29.0	Chou et al. (2010)
Flat sheet	PSf, PA, PET	DI water	1.5 M NaCl	18.2	Yip et al. (2010)
Flat sheet	Sulfonated PES, PA	DI water	2.0 M NaCl	21.0	Widjojo et al. (2011)
Flat sheet	PSf, PA	0.01 M NaCl	2.0 M NaCl	22.2	Wei et al. (2011)
Nanofiber composite	PES nanofiber + PET, PA	DI water	0.5 M NaCl	37.8	Song et al. (2011)
Flat sheet	Sulfonated poly(ether ketone) (SPEK), PA	DI water	2.0 M NaCl	35.0	Han, Chung, Toriida, and Tamai (2012)
Hollow fiber	PES, PA	DI water	2.0 M NaCl	32.1–34.5	Sukitpaneenit and Chung (2012)
Flat sheet TFN	PSf, PA + Zeolite	0.01 M NaCl	1.0 M NaCl	14.6	Ma, Wei, Liao, and Tang (2012)
Flat sheet	PES/multiwalled carbon nanotube (MWCNT), PA	0.01 M NaCl	2.0 M glucose	12.0 (PRO)	Wang, Ou, Ge, Wang, and Xu (2013)
Flat sheet	Sulfonated polyphenylenesulfone (sPPSU), PA	DI water	2.0 M NaCl	48.0	Widjojo, Chung, Weber, Maletzko, and Warzelhan (2013)
Flat sheet	PAN, PA	DI water	0.5 M NaCl	9.25	Klaysom, Hermans, Gahlaut, Van Craenenbroeck, and Vankelecom (2013)
Flat sheet	Carboxylated polysulfone (CPSf), PA	DI water	1.0 M $MgCl_2$	18.0	Cho, Han, Han, Guiver, and Park (2013)
Nanofiber thin film composite	Electrospun PET (polyethylene terephthalate)- PSf, PA	DI water	1.0 M NaCl	12.9	Hoover, Schiffman, and Elimelech (2013)

(*Continued*)

TABLE 8.3 (Continued)

Membrane	Materials (substrate, active layer)	FS	DS	Flux (L m^{-2} h^{-1})	References
Flat sheet	PVDF nanofiber, PA	DI water	1.0 M NaCl	11.6, 28.0	Tian, Qiu, Liao, Chou, and Wang (2013)
Nanofiber thin film composite (NTFC)	Crosslinked PVA nanofibers, PA	DI water	0.5 M NaCl	27.2	Puguan, Kim, Lee, and Kim (2014)
Hydrophobic/hydrophilic interpenetrating network composite nanofibers (HH-IPN-CNF)	Polyethylene terephthalate (PET)/PVA, PA	DI water	0.5 M NaCl	47.2 (PRO)	Tian et al. (2014)
Hollow fiber	PES, PA + CTAC 2% (cetyltrimethylammonium chloride)	DI water	2.0 M NaCl	5.3	Jia, Han et al. (2014)
Flat sheet	PSf + sulfonated poly (phenylene oxide) (SPPO, PA	DI water	2.0 M NaCl	39.0	Zhou, Lee, and Chung (2014)
Flat sheet	Cellulose ester, PA	DI water	2.0 M NaCl	80.1	Ong, Chung, de Wit, and Helmer (2015)
Flat sheet	Polyketone, PA	DI water	0.6 M NaCl	29.3	Yasukawa, Mishima et al. (2015)
Flat sheet (cocasting)	Silica + PSf, PA, PET	DI water	1.0 M NaCl	31.0	Liu and Ng (2015)
Flat sheet	PES, sulfonated polyethersulfone (SPES), PA	DI water	2.0 M NaCl	35.1	Sahebi et al. (2016)
TFC membranes based on PSf supports blended with nanostructured carbon materials	PSf + functionalized MWCNTs-TiO + PVP, PA	DI water	2.0 M NaCl	20.3	Morales-Torres, Esteves, Figueiredo, and Silva (2016)
Flat sheet	Polyketone, PA	DI water	0.6 M NaCl	24.8	Yasukawa, Mishima, Tanaka, Takahashi, and Matsuyama (2017)
Hollow fiber	Polyketone, PA	DI water	1.0 M NaCl	HF-A = ~51.0 (PRO) HF-B = ~36.0 (PRO)	Shibuya, Yasukawa et al. (2017)

Flat sheet (cocasting)	PEI + sulfonated poly (ether ether ketone) (SPEEK)/PSF, PA	DI water	0.5 M NaCl	22.4 ± 2.1	Chen, Liu et al. (2017)
LbL flat sheet	PAN substrate	DI water	1.0 M $MgCl_2$	28.7	Saren, et al. (2011)
Chemically crosslinked LbL flat sheet	PAN substrate	DI water	1.0 M $MgCl_2$	34.0	Qiu, Qi, and Tang (2011)
Double-skinned LbL flat sheet	PAN substrate	DI water	0.5 M $MgCl_2$	30.0	Qi, Qiu, Zhao, and Tang (2012)
Crosslinked LbL flat sheet	PAN substrate	DI water	0.5 M $MgCl_2$	14.5	Duong et al. (2013)
LbL hollow fiber	PES substrate	DI water	0.5 M $MgCl_2$	21.5	Liu, Shi, and Wang (2015)
Double-skinned hollow fiber	PES substrate	DI water	0.5 M NaCl	17.5	Fang, Liu, Shi, and Wang (2015)
CS/GO LbL flat sheet membranes	SPES-PES substrate (10 LbL)	DI water	1.0 M Na_2SO_4	25.0	Salehi, Rastgar, and Shakeri (2017)
LbL flat sheet	PVDF substrate	DI water	0.5 M $MgCl_2$	10.0	Liu et al.(2017)
Biomimetic flat sheet	—	DI water	0.5 M NaCl	30.0	Wang, Xiang et al. (2013)
Biomimetic hollow fiber	—	Pure water	0.5 M NaCl	55.2 (PRO)	Li, Chou et al. (2015)
Biomimetic hollow fiber	—	DI water	0.5 M NaCl	35.4	Li, Loh, Wang, Widjajanti, and Torres (2017)

8.7.1 Selective rejection layer

The ideal FO membranes should have a high water permeability and good ions rejection. Water permeability is mainly determined by properties of the support structure and the rejection layer, while ions rejection is mainly obtained by the PA selective layer. Therefore an ultrathin rejection layer is required to increase selectivity without hindering water flux. Depending on FO application and FS characteristics, the requirements for membranes' thin layer properties and selectivity are different. For example, for desalination proposes using brackish or sea water as feed, the selective layer should be more or less similar to RO membranes to allow the passage of water but reject most of the sodium and chloride ions (Wei et al., 2011; Yip et al., 2010). For this purpose, similar to RO, the suitable materials are limited. They include crosslinked PA formed by IP or CA/CTA through phase inversion (Lee, Arnot, & Mattia, 2011). Similarly, selective layer modification is limited as well. There are studies that have tried to improve selective layer by chemical modification, applying PDA or graphene nanosheets coating, or incorporating nanoparticles such as zeolites and CNTs on thin PA selective layer. Those modifications can occur during or after IP for increasing performance or improving the selective layer properties for fouling resistance. For example, Ning et al. developed a Zeolite-PA TFN membrane by incorporating 0.02−0.1 wt.% zeolite in PA layer. The TFN membrane performance with 0.1 wt./v% zeolite loading increased almost 80% higher compared to the baseline TFC membrane (Ma et al., 2012). Materials such as LbL polyelectrolytes and PBI with hydrophilic nature can be used for FO application other than desalination (Table 8.4).

TABLE 8.4 Recent forward osmosis (FO) membrane developments in selective rejection layer.

Membrane	Materials (substrate, active layer)	FS	DS	Flux ($L\ m^{-2}\ h^{-1}$)	References
Flat sheet TFN	PSf, PA + SiO_2	10 mM NaCl	2.0 M NaCl	22.5	Niksefat, Jahanshahi, and Rahimpour (2014)
Flat sheet TFC	PAN, PA + GO	DI water	2.0 M NaCl	32.0	Shen, Xiong, and Wang (2016)
Flat sheet TFC	Hydrolyzed PAN, PA + N- [3 (trimethoxysilyl) propyl] ethylenediamine (NPED)	DI water	0.5 M NaCl	16.7	Xiong, Zuo et al. (2016)
Flat sheet TFC	SPES-PES, (TMC + CS)	DI water	1.0 M NaCl	19.7	Shakeri, Salehi, and Rastgar (2017)
Flat sheet TFN	PES, PA + (MOF) consisting of silver (I) and 1,3,5-benzene tricarboxylic acid	DI water	2.0 M NaCl	46.0	Zirehpour, Rahimpour, and Ulbricht (2017)
PA-crosslinked GO membrane	PES, PA + GO	DI water	0.3 M TSC (trisodium citrate)	13.2	Jin, Wang, Zheng, and Mi (2018)
ST-modified TFC	PES, PA + sodium taurine (chemical modification)	DI water	2.0 M $MgCl_2$	26.7 ± 1.8	Xu and Ge (2018)

8.7.2 Support polymeric layer

In the phase inversion membranes such as CTA or PBI membranes, the support layer functions as both the support structure and the rejection layer (Zhang et al., 2010). However, regarding the composite membranes for FO, the support structure does not carry both burdens. The ideal TFC FO membrane can be semipermeable without the porous polymeric layer; however, without the support polymeric structure, the selective layer is not able to stand independently (Chou et al., 2010). The polymeric substrate gives the membrane its frame and mechanical strength and a cushion for the selective thin rejection layer and without it, the rejection layer is not able to be free-standing.

The main differences between RO and FO membranes are in support polymeric layer properties in addition to support backing fabrics characteristics. High-structural parameter (S value) and thick backing fabric support are the main factors that limit use of RO membranes for FO applications. S value for the RO membranes is usually bigger than a few millimeters, while it is a few hundred micrometers (200−700 μm) for FO membranes (McCutcheon & Elimelech, 2007; Yip et al., 2010).

Previous studies suggest that more hydrophilic membranes and finger-like structures can enhance the membrane performance (Yip et al., 2010). Furthermore, ICP and ECP play crucial role in FO membranes. Thus to minimize this effect especially ICP, the supporting FO membrane polymeric layer requires special designed chemical properties and structure (McCutcheon & Elimelech, 2006, 2007). Structural parameter which can be obtained through tortuosity, porosity, and thickness of the membrane supporting layer, is the main element to improve the FO membrane design. This can be achieved by designing a membrane with high porosity, small tortuosity, and lower thickness to reduce structural parameter (Yip et al., 2010).

The main approaches to decrease the S value for FO membranes can be achieved by fabricating a thin membrane which is supported by a highly porous woven/nonwoven backing fabric thus increasing porosity and improving hydrophilicity of the polymeric support by adding pore formers such as PEG. Furthermore, enhancing the membrane hydrophilic nature is possible through modification by a hydrophilic agent such as direct thermal sulfonation or blending with sulfonated polymers. This is in addition to the casting condition in phase inversion that has an obvious role in reducing ICP and structural parameter by producing a more porous membrane through precipitation bath components and conditions (Sheikhi, Mirshekar et al., 2021).

Regardless of the membrane finger or sponge like morphology, the substrate hydrophilicity plays greater role than the membrane morphology. A hydrophilic sulfonated membrane with sponge-like structure can perform better than a hydrophobic finger like structure FO membrane. Thus higher performance may depend more on support hydrophilicity than substrate morphology (Han, Chung et al., 2012; Widjojo et al., 2011, 2013).

In addition to support polymeric film fabrication via phase inversion, electrospinning has been recognized as an efficient versatile technique for fabrication of polymer nanofibers matrix in recent years (Ma, Kotaki, & Ramakrishna, 2005; Ramakrishna et al., 2006). The potential application is based on the use of such fibers as reinforcement in nanocomposite development for medical and separation industries (Ramakrishna, Fujihara, Teo, Lim, & Ma, 2005). Due to the specific control on the fiber size, shape, and morphology, these membranes fit well for filtration and MD processes (Tijing et al., 2014). Regarding electrospun nanofibers film for FO

application, the concept is relatively new. The nanofibers support layer has porous structure which provides direct routes for water and salt diffusion (Song et al., 2011).

Through (1) fabrication method (electrospinning), (2) choosing and modifying hydrophilic support materials, and (3) incorporating nanomaterials in membrane substrate during phase inversion, custom design of support layer for FO membranes is possible.

Firstly, TFC membranes possess polymeric sponge or finger-like structure substrates as support. Support membrane properties are the main cause for the membrane high ICP which results in poor water flux. Even using the same materials in an electrospun nanofibers FO membrane, the conventional polymeric support (sponge or finger-like structure) can be replaced with thinner, more porous, and less tortuous nanofibers film structure (Bui & McCutcheon, 2012). TFC membranes fabricated through nanofibers as their membrane support showed 2–5 times higher water flux depending on fabrication condition and posttreatment (Bui, Lind, Hoek, & McCutcheon, 2011). Xiaoxiao et al. reported that using PES nanofibers as support layer can greatly enhance the membrane performance. Using 1 M NaCl as DS, water flux of 46 LMH with a RSF of 0.6 GMH were achieved (Song et al., 2011). Diameters of the nanofibers were in the range of 50–150 nm for this PES nanofibers support layer with 45 μm thickness.

Further studies tried to use more hydrophilic materials such as nylon 6,6 to produce nanofibers matrices for FO applications (Bui & McCutcheon, 2012). Nylon 6,6 was the choice of material for the support layer, mainly due to its hydrophilicity, good mechanical strength, and excellent compatibility with the PA polyamide selective film (Huang, Bui, Meyering, Hamlin, & McCutcheon, 2013). This significantly reduced the structural parameter to 250 μm.

Secondly, the custom design of an FO membrane is possible by choosing more hydrophilic materials like CTA or PES than hydrophobic materials such as Psf. Furthermore, modifying support with hydrophilic nature through sulfonation can modify the substrate properties. Incorporating nanomaterials in support polymeric layer can enhance and specialize the membrane properties for a specific purpose which can include performance enhancement or fouling resistance. This kind of membrane is commonly called as TFN membrane. A summary of FO membrane developments in support polymeric layer is provided in Table 8.5.

8.7.3 Support backing fabric

Membrane mechanical strength is one the most important characteristics for the membranes to be industrialized (Yip et al., 2010). However, most of research works have not incorporated backing fabrics in their cast membranes. The support in composite membranes functions as support for the PA rejection layer and is contained of two basics, the backing fabric and the polymeric material (Lee & Liu, 1976). The backing fabric that is merged into the porous polymeric matrix is rather woven, but may be nonwoven as it is in most RO membranes. For FO membranes, a woven backing is favored over a nonwoven backing fabric for two key motives: (1) sufficient mechanical integrity and (2) minimizing water transport resistance due to the integral large openings in the woven mesh structure (Farr, Bharwada, & Gullinkala, 2013).

Based on FO fundamental requirements for achieving high flux, the backing fabrics should be thin and porous preferably woven. The CTA FO membrane from HTI shows better performance than the CTA FO membrane on nonwoven fabric (Wei et al., 2011).

TABLE 8.5 Recent forward osmosis (FO) membrane developments in support polymeric layer.

Membrane	Materials (substrate, active layer)	FS	DS	Flux ($L\ m^{-2}\ h^{-1}$)	References
Nylon 6,6 nanofiber	Nylon 6,6, PA	DI water	1.0 M NaCl	21.0	Huang and McCutcheon (2014)
Flat sheet TFN	PSf + TiO_2, PA	mM NaCl 10	M NaCl 2.0	29.7	Emadzadeh, Lau, Matsuura, Rahbari-Sisakht, and Ismail (2014)
Flat sheet TFC	SPES-PES + montmorilonite (MMT), PA	DI water	2.0 M NaCl	28.4	Wang and Xu (2015)
Flat sheet TFC	cellulose ester, PA posttreatments; (SDS) and glycerol followed by heat treatment	DI water	2.0 M NaCl	80.1	Ong et al. (2015)
Flat sheet TFC	PSf + GO, PA	DI water	2.0 M NaCl	35.0	Park et al. (2015)
Flat sheet TFN	PSf + layered double hydroxide nanoparticles (LDH-NPs), PA	DI water	1.0 M NaCl	18.1	Lu, Liang, Qiu, Gao, and Wang (2016)
Flat sheet TFC	PSf + $CaCO_3$, PA	DI water	2.0 M NaCl	17.0	Kuang et al. (2016)
Flat sheet TFC	substrate; SPES-PES, PA	DI water	2.0 M NaCl	35.1	Sahebi et al. (2016)
Flat sheet TFC	PSf + BPSH100-BPS0 25%wt. (disulfonated poly (arylene ether sulfone) hydrophilic-hydrophobic multiblock copolymer), PA	DI water	2.0 M NaCl	40.9	Zhang et al. (2016)
Flat sheet TFN	PSf + imogolite nanotubes (INTs), PA	DI water	1.0 M NaCl	7.5	Pan, Zhao, Gu, and Wu (2017)
Flat sheet TFC	PSf + Na type ion exchange resin (IER-Na), PA	DI water	1.5 M NaCl	25.0	Zuo, Lu et al. (2017)
Flat sheet TFC	PVDF/PFSA (polyvinylidene fluoride/perfluorosulfonic acid, PA	DI water	1.0 M NaCl	27.0	Zhang, Shen, Lang, and Wang (2017)
Flat sheet TFN (nanofibrous substrate)	PEI nanofibrous support + silica nanoparticles, PA	DI water	1.0 M NaCl	42.0	Tian, Wang, Wang, and Fane (2017)
Flat sheet TFC (dual-layered substrate)	PSf + GO, PA	DI water	1.0 M NaCl	33.8	Lim, Park et al. (2017)
Flat sheet TFC	PES/PAA (in situ crosslinked polymerization technique), PA	DI water	2.0 M NaCl	32.9	Qiu, Wang, and He (2018)
PVA- coating on hydrophobic electrospun nanofiber membrane (TFC)	PVDF nanofiber + PVA (dip coating), PA	DI water	0.5 M NaCl	24.8	Park, Gonzales, Abdel-Wahab, Phuntsho, and Shon (2018)

The woven reinforced membranes display distinct benefit over the nonwoven backing fabrics due to the inclusive thinness of the membranes that can be produced. Besides, it can reduce diffusional barrier to osmotic agent movement within the support layer (Farr, Bharwada, & Gullinkala, 2014). However, casting a FO membrane on fabrics with this property seems to be challenging due to certain obstacles including:

1. Firstly by removing any RO membrane backing fabric for quick observation and comparison with the conventional backing fabric used for FO membrane fabrication, it is clear that the RO backing fabric is thick nonwoven (200 μm) and more importantly it does not appear to be porous (similar to note taking paper with open pores ≈ 1 μm). However, conventional backing fabrics either woven or nonwoven for FO are thinner (40–70 μm) and more importantly they are porous with big open pores ≈100 μm.
2. Due to the FO membrane backing support fabric high porosity, polymer solution penetrates to the back of the fabric which can cause defect points, creasing and wrinkling on the membrane top surface skin layer.
3. Backing fabric pretreatment with NMP solution improves the casting and can remove the defect points to some extent, however, merging backing fabric and porous polymer-based support into an inseparable matrix to form a defect free composite support layer is still a challenge.

On commercial scale, FO membranes are fabricated by pouring the polymer solution on rotating drum and then pulling the woven mesh backing fabric into the cast solution from the top. In this case, polymer penetration through the fabric is limited because of the casting method (Herron, 2008). However, simulating this fabrication method under laboratory conditions is challenging. Therefore either using hand cast or automatic casting knife, the polymer solution is poured on top of the fabric similar to the commercial RO membranes fabrication method. For fabrication of FO, PAO, or PRO membranes to be able to be tested in a regular FO cell (2.7–8 cm), a large piece of membrane reinforced with backing fabric support is required.

Regarding the backing fabric custom design, various potential materials can be used for membrane backing support. So far, metal mesh (You et al., 2013), and woven and nonwoven fabrics have been used for developing FO membranes (Qiu et al., 2012; Yip et al., 2010). Also, there are patented works that suggest spacer fabric or polyaniline as backing support (Farr, Herron, Bharwada, & Gullinkala, 2013). Furthermore, there are materials like nanocellulose or microfibrillated cellulose (MFC) that may be suitable options as a backing fabric support for an engineered osmosis membrane. Nanocellulose stands out as a unique choice among those options. MFC has been around since the early 1980s and is composed of nanosized cellulose fibrils that can be extracted from wood. Due to good stability, durability, and high surface area, they are expected to be promising functional entity in the next generation of membrane separation technologies (Mathew, Karim, Liu, & Oksman, 2013), including MFC-enabled FO membranes, considering the following points:

1. There are a large number of functional groups that are present on surface of the nanocelluloses substrate that give a positive approach to modify the surface according to the needs.
2. MFC substrate is similar to electrospinning nanofibers. However, it may function both as a support polymeric structure and a backing fabric support due to its stiffness; this

TABLE 8.6 Recent forward osmosis (FO) membrane developments in support backing fabric.

Membrane	Materials (substrate, active layer)	FS	DS	Flux ($L\ m^{-2}\ h^{-1}$)	References
Flat sheet TFC	PSf + PET nonwoven fabric, PA	DI water	1.0 M NaCl	25.0	Tiraferri et al. (2011)
Positively charged flat sheet	PAI substrate, treated by PEI + PET woven fabric	DI water	0.5 M $MgCl_2$	19.2	Qiu et al. (2012)
Modified PVDF nanofiber	PVDF nanofibers coated with nylon 6,6 + PET nonwoven fabric, PA	DI water	1.0 M NaCl	22.0	Huang, Arena, and McCutcheon (2016)
Flat sheet TFC	PSf /SPSf + PET nonwoven fabric, PA	DI water	1.0 M NaCl	29.9	Ren, O'Grady, and McCutcheon (2016)
Flat sheet TFC	PES + compacted woven fabric mesh (with 5% open area), PA	DI water	0.5 M NaCl	FO = 6.7 PAO (10 bar) = 37.0	Sahebi et al. (2017)

may lead to a fully bio-based FO membrane for different FO applications. An overview of these membrane developments in support backing fabric is summarized in Table 8.6.

8.8 Concluding remarks and recommendations

RO process for desalination has been broadly used for decades and possibly for many more decades it will be used to tackle water scarcity worldwide. It is a relatively low cost and easy to operate technology. However, the demand to lowering carbon foot print in desalination technology has encouraged researchers to investigates, first, RO and FO membrane materials with superior properties, and second, FO and RO hybrid units for further energy saving. Hybrid units lower fouling in RO units, and consequently, reduce energy and maintenance cost. Engineered osmosis processes have risen as an emerging technology in recent years. It is unlikely for FO to take over the dominant desalination technology such as RO in the near future. However, it is still attractive considering its fast growing applications and hybrid FO systems for desalination and energy production due to FO advantages over pressure-based membrane technologies. Application of FO on hybrid systems is a very good opportunity to expand the engineered osmosis. Any successful FO application particularly in PAO and hybrid FO units depends on novel customized enhanced robust FO membranes.

References

Alsvik, I. L., Zodrow, K. R., Elimelech, M., & Hägg, M.-B. (2013). Polyamide formation on a cellulose triacetate support for osmotic membranes: Effect of linking molecules on membrane performance. *Desalination*, *312*, 2–9.

Amini, M., Jahanshahi, M., & Rahimpour, A. (2013). Synthesis of novel thin film nanocomposite (TFN) forward osmosis membranes using functionalized multi-walled carbon nanotubes. *Journal of Membrane Science*, *435*, 233–241.

Arena, J. T., McCloskey, B., Freeman, B. D., & McCutcheon, J. R. (2011). Surface modification of thin film composite membrane support layers with polydopamine: Enabling use of reverse osmosis membranes in pressure retarded osmosis. *Journal of Membrane Science*, *375*(1–2), 55–62.

Ariza, M. J., Jones, D. J., & Rozière, J. (2002). Role of post-sulfonation thermal treatment in conducting and thermal properties of sulfuric acid sulfonated poly (benzimidazole) membranes. *Desalination*, *147*(1), 183–189.

Baker, R. W. (2000). *Membrane technology*. Wiley Online Library.

Baroña, G. N. B., Lim, J., & Jung, B. (2012). High performance thin film composite polyamide reverse osmosis membrane prepared via m-phenylenediamine and 2,2′-benzidinedisulfonic acid. *Desalination*, *291*, 69–77.

Bui, N.-N., & McCutcheon, J. R. (2012). Hydrophilic nanofibers as new supports for thin film composite membranes for engineered osmosis. *Environmental Science & Technology*, *47*(3), 1761–1769.

Bui, N.-N., Arena, J. T., & McCutcheon, J. R. (2015). Proper accounting of mass transfer resistances in forward osmosis: Improving the accuracy of model predictions of structural parameter. *Journal of Membrane Science*, *492*, 289–302.

Bui, N.-N., Lind, M. L., Hoek, E., & McCutcheon, J. R. (2011). Electrospun nanofiber supported thin film composite membranes for engineered osmosis. *Journal of Membrane Science*, *385*, 10–19.

Burghoff, H. G., Lee, K., & Pusch, W. (1980). Characterization of transport across cellulose acetate membranes in the presence of strong solute–membrane interactions. *Journal of Applied Polymer Science*, *25*(3), 323–347.

Cadotte, J. E. (1977). *Reverse osmosis membrane*. Google Patents.

Cadotte, J. E. (1981). *Interfacially synthesized reverse osmosis membrane*. Google Patents.

Cath, T. Y., Childress, A. E., & Elimelech, M. (2006). Forward osmosis: Principles, applications, and recent developments. *Journal of Membrane Science*, *281*(1), 70–87.

Chen, G., Liu, R., Shon, H. K., Wang, Y., Song, J., Li, X.-M., … He, T. (2017). Open porous hydrophilic supported thin-film composite forward osmosis membrane via co-casting for treatment of high-salinity wastewater. *Desalination*, *405*, 76–84.

Chen, X., Xu, J., Lu, J., Shan, B., & Gao, C. (2017). Enhanced performance of cellulose triacetate membranes using binary mixed additives for forward osmosis desalination. *Desalination*, *405*, 68–75.

Cheng, J., Shi, W., Zhang, L., & Zhang, R. (2017). A novel polyester composite nanofiltration membrane formed by interfacial polymerization of pentaerythritol (PE) and trimesoyl chloride (TMC). *Applied Surface Science*, *416*, 152–159.

Chian, E. S., Chen, J. P., Sheng, P.-X., Ting, Y.-P., & Wang, L. K. (2007). Reverse osmosis technology for desalination. *Advanced physicochemical treatment technologies* (pp. 329–366). Springer.

Cho, Y. H., Han, J., Han, S., Guiver, M. D., & Park, H. B. (2013). Polyamide thin-film composite membranes based on carboxylated polysulfone microporous support membranes for forward osmosis. *Journal of Membrane Science*, *445*, 220–227.

Chou, S., Shi, L., Wang, R., Tang, C. Y., Qiu, C., & Fane, A. G. (2010). Characteristics and potential applications of a novel forward osmosis hollow fiber membrane. *Desalination*, *261*(3), 365–372.

Dabaghian, Z., & Rahimpour, A. (2015). Carboxylated carbon nanofibers as hydrophilic porous material to modification of cellulosic membranes for forward osmosis desalination. *Chemical Engineering Research and Design*, *104*, 647–657.

Dabaghian, Z., Rahimpour, A., & Jahanshahi, M. (2016). Highly porous cellulosic nanocomposite membranes with enhanced performance for forward osmosis desalination. *Desalination*, *381*, 117–125.

Decher, G. (1997). Fuzzy nanoassemblies: Toward layered polymeric multicomposites. *Science*, *277*(5330), 1232–1237.

Duong, P. H., Zuo, J., & Chung, T.-S. (2013). Highly crosslinked layer-by-layer polyelectrolyte FO membranes: Understanding effects of salt concentration and deposition time on FO performance. *Journal of Membrane Science*, *427*, 411–421.

Emadzadeh, D., Lau, W. J., Matsuura, T., Rahbari-Sisakht, M., & Ismail, A. (2014). A novel thin film composite forward osmosis membrane prepared from PSf–TiO_2 nanocomposite substrate for water desalination. *Chemical Engineering Journal*, *237*, 70–80.

Fang, W., Liu, C., Shi, L., & Wang, R. (2015). Composite forward osmosis hollow fiber membranes: Integration of RO- and NF-like selective layers for enhanced organic fouling resistance. *Journal of Membrane Science*, *492*, 147–155.

Farr, I. V., Bharwada, U. J., & Gullinkala, T. (2013). *Method to improve forward osmosis membrane performance*. Google Patents.

Farr, I. V., Bharwada, U. J., & Gullinkala, T. (2014). *Method to improve forward osmosis membrane performance*. Google Patents.

Farr, I. V., Herron, J. R., Bharwada, U. J., & Gullinkala, T. (2013). *Forward osmosis membrane based on an ipc spacer fabric*. Google Patents.

Fu, F.-J., Zhang, S., Sun, S.-P., Wang, K.-Y., & Chung, T.-S. (2013). POSS-containing delamination-free dual-layer hollow fiber membranes for forward osmosis and osmotic power generation. *Journal of Membrane Science*, *443*, 144–155.

Gray, G. T., McCutcheon, J. R., & Elimelech, M. (2006). Internal concentration polarization in forward osmosis: role of membrane orientation. *Desalination*, *197*(1), 1–8.

Han, G., Chung, T.-S., Toriida, M., & Tamai, S. (2012). Thin-film composite forward osmosis membranes with novel hydrophilic supports for desalination. *Journal of Membrane Science*, *423*, 543–555.

Han, G., Zhang, S., Li, X., Widjojo, N., & Chung, T.-S. (2012). Thin film composite forward osmosis membranes based on polydopamine modified polysulfone substrates with enhancements in both water flux and salt rejection. *Chemical Engineering Science*, *80*, 219–231.

He, M., Yuan, T., Dong, W., Li, P., Jason Niu, Q., & Meng, J. (2019). High-performance acid-stable polysulfonamide thin-film composite membrane prepared via spinning-assist multilayer interfacial polymerization. *Journal of Materials Science*, *54*(1), 886–900.

Herron, J. (2008). *Asymmetric forward osmosis membranes*. Google Patents.

Hoek, E. M., & Elimelech, M. (2003). Cake-enhanced concentration polarization: A new fouling mechanism for salt-rejecting membranes. *Environmental Science & Technology*, *37*(24), 5581–5588.

Honglei, W., Tai-Shung, C., Wah, T. Y., Kandiah, J., Arunmozhiarasi, A., Zaichun, C., … Wolfgang, M. (2012). Highly permeable and selective pore-spanning biomimetic membrane embedded with aquaporin Z. *Small*, *8*(8), 1185–1190.

Hoover, L. A., Schiffman, J. D., & Elimelech, M. (2013). Nanofibers in thin-film composite membrane support layers: Enabling expanded application of forward and pressure retarded osmosis. *Desalination*, *308*, 73–81.

Huang, L., & McCutcheon, J. R. (2014). Hydrophilic nylon 6,6 nanofibers supported thin film composite membranes for engineered osmosis. *Journal of Membrane Science*, *457*, 162–169.

Huang, L., Arena, J. T., & McCutcheon, J. R. (2016). Surface modified PVDF nanofiber supported thin film composite membranes for forward osmosis. *Journal of Membrane Science*, *499*, 352–360.

Huang, L., Bui, N.-N., Meyering, M. T., Hamlin, T. J., & McCutcheon, J. R. (2013). Novel hydrophilic nylon 6,6 microfiltration membrane supported thin film composite membranes for engineered osmosis. *Journal of Membrane Science*, *437*, 141–149.

Huang, M., Meng, L., Li, B., Niu, F., Lv, Y., Deng, Q., & Li, J. (2019). Fabrication of innovative forward osmosis membranes via multilayered interfacial polymerization on electrospun nanofibers. *Journal of Applied Polymer Science*, *136*(12), 47247.

Hung, W.-S., Lai, C.-L., An, Q., De Guzman, M., Shen, T.-J., Huang, Y.-H., … Lee, K.-R. (2014). A study on high-performance composite membranes comprising heterogeneous polyamide layers on an electrospun substrate for ethanol dehydration. *Journal of Membrane Science*, *470*, 513–523.

Jeong, B.-H., Hoek, E., Yan, Y., Subramani, A., Huang, X., Hurwitz, G., … Jawor, A. (2007). Interfacial polymerization of thin film nanocomposites: A new concept for reverse osmosis membranes. *Journal of Membrane Science*, *294*(1), 1–7.

Jewrajka, S. K., Reddy, A. V. R., Rana, H. H., Mandal, S., Khullar, S., Haldar, S., … Ghosh, P. K. (2013). Use of 2,4,6-pyridinetricarboxylic acid chloride as a novel co-monomer for the preparation of thin film composite polyamide membrane with improved bacterial resistance. *Journal of Membrane Science*, *439*, 87–95.

Jia, Q., Han, H., Wang, L., Liu, B., Yang, H., & Shen, J. (2014). Effects of CTAC micelles on the molecular structures and separation performance of thin-film composite (TFC) membranes in forward osmosis processes. *Desalination*, *340*, 30–41.

Jin, L., Wang, Z., Zheng, S., & Mi, B. (2018). Polyamide-crosslinked graphene oxide membrane for forward osmosis. *Journal of Membrane Science*, *545*, 11–18.

Kar, S., Bindal, R., & Tewari, P. (2012). Carbon nanotube membranes for desalination and water purification: Challenges and opportunities. *Nano Today*, *7*(5), 385–389.

Kaufman, Y., Berman, A., & Freger, V. (2010). Supported lipid bilayer membranes for water purification by reverse osmosis. *Langmuir: The ACS Journal of Surfaces and Colloids*, *26*(10), 7388–7395.

Kedem, O., & Katchalsky, A. (1963). Permeability of composite membranes. Part 1.—Electric current, volume flow and flow of solute through membranes. *Transactions of the Faraday Society*, *59*, 1918–1930.
Klaysom, C., Hermans, S., Gahlaut, A., Van Craenenbroeck, S., & Vankelecom, I. F. J. (2013). Polyamide/polyacrylonitrile (PA/PAN) thin film composite osmosis membranes: Film optimization, characterization and performance evaluation. *Journal of Membrane Science*, *445*, 25–33.
Kuang, W., Liu, Z., Yu, H., Kang, G., Jie, X., Jin, Y., … Cao, Y. (2016). Investigation of internal concentration polarization reduction in forward osmosis membrane using nano-$CaCO_3$ particles as sacrificial component. *Journal of Membrane Science*, *497*, 485–493.
Lee, K. P., Arnot, T. C., & Mattia, D. (2011). A review of reverse osmosis membrane materials for desalination—Development to date and future potential. *Journal of Membrane Science*, *370*(1–2), 1–22.
Lee, L. T., & Liu, K. -J. (1976). *Method of making permselective interpolymer membranes*. Google Patents.
Li, X., Cao, Y., Yu, H., Kang, G., Jie, X., Liu, Z., & Yuan, Q. (2014). A novel composite nanofiltration membrane prepared with PHGH and TMC by interfacial polymerization. *Journal of Membrane Science*, *466*, 82–91.
Li, X., Chou, S., Wang, R., Shi, L., Fang, W., Chaitra, G., … Fane, A. G. (2015). Nature gives the best solution for desalination: Aquaporin-based hollow fiber composite membrane with superior performance. *Journal of Membrane Science*, *494*, 68–77.
Li, X., Loh, C. H., Wang, R., Widjajanti, W., & Torres, J. (2017). Fabrication of a robust high-performance FO membrane by optimizing substrate structure and incorporating aquaporin into selective layer. *Journal of Membrane Science*, *525*, 257–268.
Li, X., Wang, K. Y., Helmer, B., & Chung, T.-S. (2012). Thin-film composite membranes and formation mechanism of thin-film layers on hydrophilic cellulose acetate propionate substrates for forward osmosis processes. *Industrial & Engineering Chemistry Research*, *51*(30), 10039–10050.
Li, Y., Su, Y., Dong, Y., Zhao, X., Jiang, Z., Zhang, R., … Zhao, J. (2014). Separation performance of thin-film composite nanofiltration membrane through interfacial polymerization using different amine monomers. *Desalination*, *333*(1), 59–65.
Lim, S., Park, M. J., Phuntsho, S., Tijing, L. D., Nisola, G. M., Shim, W.-G., … Shon, H. K. (2017). Dual-layered nanocomposite substrate membrane based on polysulfone/graphene oxide for mitigating internal concentration polarization in forward osmosis. *Polymer*, *110*, 36–48.
Liu, C., Lei, X., Wang, L., Jia, J., Liang, X., Zhao, X., … Zhu, H. (2017). Investigation on the removal performances of heavy metal ions with the layer-by-layer assembled forward osmosis membranes. *Chemical Engineering Journal*, *327*, 60–70.
Liu, C., Shi, L., & Wang, R. (2015). Enhanced hollow fiber membrane performance via semi-dynamic layer-by-layer polyelectrolyte inner surface deposition for nanofiltration and forward osmosis applications. *Reactive and Functional Polymers*, *86*, 154–160.
Liu, M., Zhou, C., Dong, B., Wu, Z., Wang, L., Yu, S., … Gao, C. (2014). Enhancing the permselectivity of thin-film composite poly(vinyl alcohol) (PVA) nanofiltration membrane by incorporating poly(sodium-p-styrenesulfonate) (PSSNa). *Journal of Membrane Science*, *463*, 173–182.
Liu, X., & Ng, H. Y. (2015). Fabrication of layered silica–polysulfone mixed matrix substrate membrane for enhancing performance of thin-film composite forward osmosis membrane. *Journal of Membrane Science*, *481*, 148–163.
Lonsdale, H. (1982). The growth of membrane technology. *Journal of Membrane Science*, *10*(2), 81–181.
Lu, P., Liang, S., Qiu, L., Gao, Y., & Wang, Q. (2016). Thin film nanocomposite forward osmosis membranes based on layered double hydroxide nanoparticles blended substrates. *Journal of Membrane Science*, *504*, 196–205.
Ma, N., Wei, J., Liao, R., & Tang, C. Y. (2012). Zeolite-polyamide thin film nanocomposite membranes: Towards enhanced performance for forward osmosis. *Journal of Membrane Science*, *405–406*, 149–157.
Ma, R., Ji, Y.-L., Weng, X.-D., An, Q.-F., & Gao, C.-J. (2016). High-flux and fouling-resistant reverse osmosis membrane prepared with incorporating zwitterionic amine monomers via interfacial polymerization. *Desalination*, *381*, 100–110.
Ma, Z., Kotaki, M., & Ramakrishna, S. (2005). Electrospun cellulose nanofiber as affinity membrane. *Journal of Membrane Science*, *265*(1), 115–123.
Mathew, A. P., Karim, Z., Liu, P., & Oksman, K. (2013). Nanocellulose for water purification membranes. *Nanomaterials*, *7*(3), 57.
McCutcheon, J. R., & Elimelech, M. (2008). Influence of membrane support layer hydrophobicity on water flux in osmotically driven membrane processes. *Journal of Membrane Science*, *318*(1), 458–466.

McCutcheon, J. R., & Elimelech, M. (2007). Modeling water flux in forward osmosis: implications for improved membrane design. *AIChE Journal*, *53*(7), 1736–1744.
McCutcheon, J. R., & Elimelech, M. (2006). Influence of concentrative and dilutive internal concentration polarization on flux behavior in forward osmosis. *Journal of Membrane Science*, *284*(1–2), 237–247.
Mitragotri, S., Anissimov, Y. G., Bunge, A. L., Frasch, H. F., Guy, R. H., Hadgraft, J., ... Roberts, M. S. (2011). Mathematical models of skin permeability: An overview. *International Journal of Pharmaceutics*, *418*(1), 115–129.
Morales-Torres, S., Esteves, C. M. P., Figueiredo, J. L., & Silva, A. M. T. (2016). Thin-film composite forward osmosis membranes based on polysulfone supports blended with nanostructured carbon materials. *Journal of Membrane Science*, *520*, 326–336.
Niksefat, N., Jahanshahi, M., & Rahimpour, A. (2014). The effect of SiO_2 nanoparticles on morphology and performance of thin film composite membranes for forward osmosis application. *Desalination*, *343*, 140–146.
Ong, R. C., Chung, T.-S., de Wit, J. S., & Helmer, B. J. (2015). Novel cellulose ester substrates for high performance flat-sheet thin-film composite (TFC) forward osmosis (FO) membranes. *Journal of Membrane Science*, *473*, 63–71.
Pan, Y.-H., Zhao, Q.-Y., Gu, L., & Wu, Q.-Y. (2017). Thin film nanocomposite membranes based on imologite nanotubes blended substrates for forward osmosis desalination. *Desalination*, *421*, 160–168.
Park, M. J., Gonzales, R. R., Abdel-Wahab, A., Phuntsho, S., & Shon, H. K. (2018). Hydrophilic polyvinyl alcohol coating on hydrophobic electrospun nanofiber membrane for high performance thin film composite forward osmosis membrane. *Desalination*, *426*, 50–59.
Park, M. J., Phuntsho, S., He, T., Nisola, G. M., Tijing, L. D., Li, X.-M., ... Shon, H. K. (2015). Graphene oxide incorporated polysulfone substrate for the fabrication of flat-sheet thin-film composite forward osmosis membranes. *Journal of Membrane Science*, *493*, 496–507.
Pendergast, M. T. M., Nygaard, J. M., Ghosh, A. K., & Hoek, E. (2010). Using nanocomposite materials technology to understand and control reverse osmosis membrane compaction. *Desalination*, *261*(3), 255–263.
Petersen, R. J. (1993). Composite reverse osmosis and nanofiltration membranes. *Journal of Membrane Science*, *83*(1), 81–150.
Puguan, J. M. C., Kim, H.-S., Lee, K.-J., & Kim, H. (2014). Low internal concentration polarization in forward osmosis membranes with hydrophilic crosslinked PVA nanofibers as porous support layer. *Desalination*, *336*, 24–31.
Qi, S., Qiu, C. Q., Zhao, Y., & Tang, C. Y. (2012). Double-skinned forward osmosis membranes based on layer-by-layer assembly—FO performance and fouling behavior. *Journal of Membrane Science*, *405–406*, 20–29.
Qiu, C., Qi, S., & Tang, C. Y. (2011). Synthesis of high flux forward osmosis membranes by chemically crosslinked layer-by-layer polyelectrolytes. *Journal of Membrane Science*, *381*(1), 74–80.
Qiu, C., Setiawan, L., Wang, R., Tang, C. Y., & Fane, A. G. (2012). High performance flat sheet forward osmosis membrane with an NF-like selective layer on a woven fabric embedded substrate. *Desalination*, *287*, 266–270.
Qiu, M., Wang, J., & He, C. (2018). A stable and hydrophilic substrate for thin-film composite forward osmosis membrane revealed by in-situ cross-linked polymerization. *Desalination*, *433*, 1–9.
Ramakrishna, S., Fujihara, K., Teo, W.-E., Lim, T.-C., & Ma, Z. (2005). *An introduction to electrospinning and nanofibers*. World Scientific.
Ramakrishna, S., Fujihara, K., Teo, W.-E., Yong, T., Ma, Z., & Ramaseshan, R. (2006). Electrospun nanofibers: Solving global issues. *Materials Today*, *9*(3), 40–50.
Ren, J., & McCutcheon, J. R. (2014). A new commercial thin film composite membrane for forward osmosis. *Desalination*, *343*, 187–193.
Ren, J., O'Grady, B., & McCutcheon, J. R. (2016). Sulfonated polysulfone supported high performance thin film composite membranes for forward osmosis. *Polymer*, *103*, 486–497.
Rigaud, J.-L., Pitard, B., & Levy, D. (1995). Reconstitution of membrane proteins into liposomes: Application to energy-transducing membrane proteins. *Biochimica et Biophysica Acta (BBA)-Bioenergetics*, *1231*(3), 223–246.
Sagle, A., & Freeman, B. (2004). Fundamentals of membranes for water treatment. *The Future of Desalination in Texas*, *2*, 137–154.
Sahebi, S., Phuntsho, S., Eun Kim, J., Hong, S., & Kyong Shon, H. (2015). Pressure assisted fertiliser drawn osmosis process to enhance final dilution of the fertiliser draw solution beyond osmotic equilibrium. *Journal of Membrane Science*, *481*, 63–72.
Sahebi, S., Phuntsho, S., Tijing, L., Han, G., Han, D. S., Abdel-Wahab, A., ... Shon, H. K. (2017). Thin-film composite membrane on a compacted woven backing fabric for pressure assisted osmosis. *Desalination*, *406*, 98–108.

Sahebi, S., Phuntsho, S., Woo, Y. C., Park, M. J., Tijing, L. D., Hong, S., ... Shon, H. K. (2016). Effect of sulphonated polyethersulfone substrate for thin film composite forward osmosis membrane. *Desalination*, *389*, 129–136.

Sahebi, S., Sheikhi, M., Ramavandi, B., Zhao, S., Baniasadi, J., Fadaie, N., ... Mohammadi, T. (2020). Developing novel thin film composite membrane on a permeate spacer backing fabric for forward osmosis. *Chemical Engineering Research and Design*, *160*, 326–334.

Sahebia, S., Sheikhic, M., & Ramavandid, B. (2019). A new biomimetic aquaporin thin film composite membrane for forward osmosis: Characterization and performance assessment. *Desalination and Water Treatment*, *148*, 42–50.

Sairam, M., Sereewatthanawut, E., Li, K., Bismarck, A., & Livingston, A. G. (2011). Method for the preparation of cellulose acetate flat sheet composite membranes for forward osmosis—Desalination using $MgSO_4$ draw solution. *Desalination*, *273*(2), 299–307.

Salehi, H., Rastgar, M., & Shakeri, A. (2017). Anti-fouling and high water permeable forward osmosis membrane fabricated via layer by layer assembly of chitosan/graphene oxide. *Applied Surface Science*, *413*, 99–108.

Saren, Q., Qiu, C. Q., & Tang, C. Y. (2011). Synthesis and characterization of novel forward osmosis membranes based on layer-by-layer assembly. *Environmental Science & Technology*, *45*(12), 5201–5208.

Setiawan, L., Wang, R., Li, K., & Fane, A. G. (2011). Fabrication of novel poly (amide–imide) forward osmosis hollow fiber membranes with a positively charged nanofiltration-like selective layer. *Journal of Membrane Science*, *369*(1), 196–205.

Shakeri, A., Salehi, H., & Rastgar, M. (2017). Chitosan-based thin active layer membrane for forward osmosis desalination. *Carbohydrate Polymers*, *174*, 658–668.

Sheikhi, M., Mirshekar, L., Kamarehie, B., Ghaderpoori, M., Ramavandi, B., Amini, F., ... Sahebi, S. (2021). Synthesis and characterization of thin film composite forward osmosis membranes reinforced on woven mesh and non-woven backing fabric supports. *Chemical Engineering & Technology*, *44*(7).

Shen, L., Xiong, S., & Wang, Y. (2016). Graphene oxide incorporated thin-film composite membranes for forward osmosis applications. *Chemical Engineering Science*, *143*, 194–205.

Sherwood, T., Brian, P., & Fisher, R. (1967). Desalination by reverse osmosis. *Industrial & Engineering Chemistry Fundamentals*, *6*(1), 2–12.

Shibuya, M., Yasukawa, M., Mishima, S., Tanaka, Y., Takahashi, T., & Matsuyama, H. (2017). A thin-film composite-hollow fiber forward osmosis membrane with a polyketone hollow fiber membrane as a support. *Desalination*, *402*, 33–41.

Sobana, S., & Panda, R. C. (2011). Review on modelling and control of desalination system using reverse osmosis. *Reviews in Environmental Science and Bio/Technology*, *10*(2), 139–150.

Soltanieh, M., & Gill', W. N. (1981). Review of reverse osmosis membranes and transport models. *Chemical Engineering Communications*, *12*(4–6), 279–363.

Song, X., Liu, Z., & Sun, D. D. (2011). Nano gives the answer: Breaking the bottleneck of internal concentration polarization with a nanofiber composite forward osmosis membrane for a high water production rate. *Advanced materials*, *23*(29), 3256–3260.

Sourirajan, S. (1970). *Reverse osmosis*. London, UK: Logos Press Ltd.

Strathmann, H., Winston, H. W., & Sirkar, K. (1992). *Membrane handbook*. New York: Vam Nostrand Reinhold.

Su, J., Yang, Q., Teo, J. F., & Chung, T.-S. (2010). Cellulose acetate nanofiltration hollow fiber membranes for forward osmosis processes. *Journal of Membrane Science*, *355*(1), 36–44.

Suh, C., & Lee, S. (2013). Modeling reverse draw solute flux in forward osmosis with external concentration polarization in both sides of the draw and feed solution. *Journal of Membrane Science*, *427*, 365–374.

Sukitpaneenit, P., & Chung, T.-S. (2012). High performance thin-film composite forward osmosis hollow fiber membranes with macrovoid-free and highly porous structure for sustainable water production. *Environmental Science & Technology*, *46*(13), 7358–7365.

Sum, J. Y., Ahmad, A. L., & Ooi, B. S. (2014). Synthesis of thin film composite membrane using mixed dendritic poly(amidoamine) and void filling piperazine monomers. *Journal of Membrane Science*, *466*, 183–191.

Sun, G., Chung, T.-S., Jeyaseelan, K., & Armugam, A. (2013). A layer-by-layer self-assembly approach to developing an aquaporin-embedded mixed matrix membrane. *RSC Advances*, *3*(2), 473–481.

Tan, C. H., & Ng, H. Y. (2008). Modified models to predict flux behavior in forward osmosis in consideration of external and internal concentration polarizations. *Journal of Membrane Science*, *324*(1), 209–219.

Tang, C. Y., She, Q., Lay, W. C., Wang, R., & Fane, A. G. (2010). Coupled effects of internal concentration polarization and fouling on flux behavior of forward osmosis membranes during humic acid filtration. *Journal of Membrane Science*, *354*(1), 123–133.

Tian, E. L., Zhou, H., Ren, Y. W., Mirza, Z. A., Wang, X. Z., & Xiong, S. W. (2014). Novel design of hydrophobic/hydrophilic interpenetrating network composite nanofibers for the support layer of forward osmosis membrane. *Desalination*, *347*, 207–214.

Tian, M., Qiu, C., Liao, Y., Chou, S., & Wang, R. (2013). Preparation of polyamide thin film composite forward osmosis membranes using electrospun polyvinylidene fluoride (PVDF) nanofibers as substrates. *Separation and Purification Technology*, *118*, 727–736.

Tian, M., Wang, Y.-N., Wang, R., & Fane, A. G. (2017). Synthesis and characterization of thin film nanocomposite forward osmosis membranes supported by silica nanoparticle incorporated nanofibrous substrate. *Desalination*, *401*, 142–150.

Tijing, L. D., Choi, J.-S., Lee, S., Kim, S.-H., & Shon, H. K. (2014). Recent progress of membrane distillation using electrospun nanofibrous membrane. *Journal of Membrane Science*, *453*, 435–462.

Tiraferri, A., Yip, N. Y., Phillip, W. A., Schiffman, J. D., & Elimelech, M. (2011). Relating performance of thin-film composite forward osmosis membranes to support layer formation and structure. *Journal of Membrane Science*, *367*(1), 340–352.

Wang, H., Li, L., Zhang, X., & Zhang, S. (2010). Polyamide thin-film composite membranes prepared from a novel triamine 3,5-diamino-*N*-(4-aminophenyl)-benzamide monomer and m-phenylenediamine. *Journal of Membrane Science*, *353*(1), 78–84.

Wang, H., Wei, Z., Wang, H., Jiang, H., Li, Y., & Wu, C. (2019). An acid-stable positively charged polysulfonamide nanofiltration membrane prepared by interfacial polymerization of polyallylamine and 1,3-benzenedisulfonyl chloride for water treatment. *RSC Advances*, *9*(4), 2042–2054.

Wang, H., Xiang, Z., Hu, C.-F., Pant, A., Fang, W., Alonso, S., … Lee, C. (2013). Development of stretchable membrane based nanofilters using patterned array of vertically grown carbon nanotubes. *Nanoscale*, *5*(18), 8488–8493.

Wang, K. Y., Chung, T. S., & Amy, G. (2012). Developing thin-film-composite forward osmosis membranes on the PES/SPSf substrate through interfacial polymerization. *AIChE Journal*, *58*(3), 770–781.

Wang, K. Y., Chung, T.-S., & Qin, J.-J. (2007). Polybenzimidazole (PBI) nanofiltration hollow fiber membranes applied in forward osmosis process. *Journal of Membrane Science*, *300*(1), 6–12.

Wang, K. Y., Ong, R. C., & Chung, T.-S. (2010). Double-skinned forward osmosis membranes for reducing internal concentration polarization within the porous sublayer. *Industrial & Engineering Chemistry Research*, *49*(10), 4824–4831.

Wang, K. Y., Yang, Q., Chung, T.-S., & Rajagopalan, R. (2009). Enhanced forward osmosis from chemically modified polybenzimidazole (PBI) nanofiltration hollow fiber membranes with a thin wall. *Chemical Engineering Science*, *64*(7), 1577–1584.

Wang, R., Shi, L., Tang, C. Y., Chou, S., Qiu, C., & Fane, A. G. (2010). Characterization of novel forward osmosis hollow fiber membranes. *Journal of Membrane Science*, *355*(1), 158–167.

Wang, R., Shi, X., Xiao, A., Zhou, W., & Wang, Y. (2018). Interfacial polymerization of covalent organic frameworks (COFs) on polymeric substrates for molecular separations. *Journal of Membrane Science*, *566*, 197–204.

Wang, T., Dai, L., Zhang, Q., Li, A., & Zhang, S. (2013). Effects of acyl chloride monomer functionality on the properties of polyamide reverse osmosis (RO) membrane. *Journal of Membrane Science*, *440*, 48–57.

Wang, T., Yang, Y., Zheng, J., Zhang, Q., & Zhang, S. (2013). A novel highly permeable positively charged nanofiltration membrane based on a nanoporous hyper-crosslinked polyamide barrier layer. *Journal of Membrane Science*, *448*, 180–189.

Wang, X., Wang, X., Xiao, P., Li, J., Tian, E., Zhao, Y., … Ren, Y. (2016). High water permeable free-standing cellulose triacetate/graphene oxide membrane with enhanced antibiofouling and mechanical properties for forward osmosis. *Colloids and Surfaces A: Physicochemical and Engineering Aspects*, *508*, 327–335.

Wang, Y., & Xu, T. (2015). Anchoring hydrophilic polymer in substrate: An easy approach for improving the performance of TFC FO membrane. *Journal of Membrane Science*, *476*, 330–339.

Wang, Y., Ou, R., Ge, Q., Wang, H., & Xu, T. (2013). Preparation of polyethersulfone/carbon nanotube substrate for high-performance forward osmosis membrane. *Desalination*, *330*, 70–78.

Wang, Z., Yu, H., Xia, J., Zhang, F., Li, F., Xia, Y., … Li, Y. (2012). Novel GO-blended PVDF ultrafiltration membranes. *Desalination*, *299*, 50–54.

Wei, J., Qiu, C., Tang, C. Y., Wang, R., & Fane, A. G. (2011). Synthesis and characterization of flat-sheet thin film composite forward osmosis membranes. *Journal of Membrane Science*, *372*(1), 292–302.
Widjojo, N., Chung, T.-S., Weber, M., Maletzko, C., & Warzelhan, V. (2011). The role of sulphonated polymer and macrovoid-free structure in the support layer for thin-film composite (TFC) forward osmosis (FO) membranes. *Journal of Membrane Science*, *383*(1), 214–223.
Widjojo, N., Chung, T.-S., Weber, M., Maletzko, C., & Warzelhan, V. (2013). A sulfonated polyphenylenesulfone (sPPSU) as the supporting substrate in thin film composite (TFC) membranes with enhanced performance for forward osmosis (FO). *Chemical Engineering Journal*, *220*, 15–23.
Wijmans, J. G., & Baker, R. W. (1995). The solution-diffusion model: A review. *Journal of Membrane Science*, *107*(1–2), 1–21.
Xie, W., Geise, G. M., Freeman, B. D., Lee, H.-S., Byun, G., & McGrath, J. E. (2012). Polyamide interfacial composite membranes prepared from m-phenylene diamine, trimesoyl chloride and a new disulfonated diamine. *Journal of Membrane Science*, *403–404*, 152–161.
Xie, W., He, F., Wang, B., Chung, T. S., Jeyaseelan, K., Armugam, A., & Tong, Y. W. (2013). An aquaporin-based vesicle-embedded polymeric membrane for low energy water filtration. *Journal of Materials Chemistry A*, *1*(26), 7592–7600.
Xiong, S., Zuo, J., Ma, Y. G., Liu, L., Wu, H., & Wang, Y. (2016). Novel thin film composite forward osmosis membrane of enhanced water flux and anti-fouling property with *N*-[3-(trimethoxysilyl) propyl] ethylenediamine incorporated. *Journal of Membrane Science*, *520*, 400–414.
Xu, J., Li, P., Jiao, M., Shan, B., & Gao, C. (2016). Effect of molecular configuration of additives on the membrane structure and water transport performance for forward osmosis. *ACS Sustainable Chemistry & Engineering*, *4*(8), 4433–4441.
Xu, W., & Ge, Q. (2018). Novel functionalized forward osmosis (FO) membranes for FO desalination: Improved process performance and fouling resistance. *Journal of Membrane Science*, *555*, 507–516.
Xu, Y., Peng, X., Tang, C. Y., Fu, Q. S., & Nie, S. (2010). Effect of draw solution concentration and operating conditions on forward osmosis and pressure retarded osmosis performance in a spiral wound module. *Journal of Membrane Science*, *348*(1), 298–309.
Yang, Q., Wang, K. Y., & Chung, T.-S. (2009). Dual-layer hollow fibers with enhanced flux as novel forward osmosis membranes for water production. *Environmental Science & Technology*, *43*(8), 2800–2805.
Yang, Z., Zhou, Y., Feng, Z., Rui, X., Zhang, T., & Zhang, Z. (2019). A review on reverse osmosis and nanofiltration membranes for water purification. *Polymers*, *11*(8), 1252.
Yasukawa, M., Mishima, S., Shibuya, M., Saeki, D., Takahashi, T., Miyoshi, T., … Matsuyama, H. (2015). Preparation of a forward osmosis membrane using a highly porous polyketone microfiltration membrane as a novel support. *Journal of Membrane Science*, *487*, 51–59.
Yasukawa, M., Mishima, S., Tanaka, Y., Takahashi, T., & Matsuyama, H. (2017). Thin-film composite forward osmosis membrane with high water flux and high pressure resistance using a thicker void-free polyketone porous support. *Desalination*, *402*, 1–9.
Yip, N. Y., & Elimelech, M. (2011). Performance limiting effects in power generation from salinity gradients by pressure retarded osmosis. *Environmental Science & Technology*, *45*(23), 10273–10282.
Yip, N. Y., Tiraferri, A., Phillip, W. A., Schiffman, J. D., & Elimelech, M. (2010). High performance thin-film composite forward osmosis membrane. *Environmental Science & Technology*, *44*(10), 3812–3818.
Yong, Z., Sanchuan, Y., Meihong, L., & Congjie, G. (2006). Polyamide thin film composite membrane prepared from m-phenylenediamine and m-phenylenediamine-5-sulfonic acid. *Journal of Membrane Science*, *270*(1), 162–168.
You, S., Tang, C., Yu, C., Wang, X., Zhang, J., Han, J., … Ren, N. (2013). Forward osmosis with a novel thin-film inorganic membrane. *Environmental Science & Technology*, *47*(15), 8733–8742.
Zhang, S., Wang, K. Y., Chung, T.-S., Chen, H., Jean, Y. C., & Amy, G. (2010). Well-constructed cellulose acetate membranes for forward osmosis: Minimized internal concentration polarization with an ultra-thin selective layer. *Journal of Membrane Science*, *360*(1), 522–535.
Zhang, S., Wang, K. Y., Chung, T.-S., Jean, Y. C., & Chen, H. (2011). Molecular design of the cellulose ester-based forward osmosis membranes for desalination. *Chemical Engineering Science*, *66*(9), 2008–2018.
Zhang, X., Shen, L., Lang, W.-Z., & Wang, Y. (2017). Improved performance of thin-film composite membrane with PVDF/PFSA substrate for forward osmosis process. *Journal of Membrane Science*, *535*, 188–199.

Zhang, X., Tian, J., Ren, Z., Shi, W., Zhang, Z., Xu, Y., ... Cui, F. (2016). High performance thin-film composite (TFC) forward osmosis (FO) membrane fabricated on novel hydrophilic disulfonated poly (arylene ether sulfone) multiblock copolymer/polysulfone substrate. *Journal of Membrane Science*, *520*, 529–539.

Zhang, Z., Wang, S., Chen, H., Liu, Q., Wang, J., & Wang, T. (2013). Preparation of polyamide membranes with improved chlorine resistance by bis-2,6-N,N-(2-hydroxyethyl) diaminotoluene and trimesoyl chloride. *Desalination*, *331*, 16–25.

Zhao, J., Su, Y., He, X., Zhao, X., Li, Y., Zhang, R., ... Jiang, Z. (2014). Dopamine composite nanofiltration membranes prepared by self-polymerization and interfacial polymerization. *Journal of Membrane Science*, *465*, 41–48.

Zhao, S., & Zou, L. (2011). Relating solution physicochemical properties to internal concentration polarization in forward osmosis. *Journal of Membrane Science*, *379*(1), 459–467.

Zhao, S., Zou, L., Tang, C. Y., & Mulcahy, D. (2012). Recent developments in forward osmosis: opportunities and challenges. *Journal of Membrane Science*, *396*, 1–21.

Zhou, Z., Lee, J. Y., & Chung, T.-S. (2014). Thin film composite forward-osmosis membranes with enhanced internal osmotic pressure for internal concentration polarization reduction. *Chemical Engineering Journal*, *249*, 236–245.

Zirehpour, A., Rahimpour, A., & Ulbricht, M. (2017). Nano-sized metal organic framework to improve the structural properties and desalination performance of thin film composite forward osmosis membrane. *Journal of Membrane Science*, *531*, 59–67.

Zirehpour, A., Rahimpour, A., Khoshhal, S., Firouzjaei, M. D., & Ghoreyshi, A. A. (2016). The impact of MOF feasibility to improve the desalination performance and antifouling properties of FO membranes. *RSC Advances*, *6*(74), 70174–70185.

Zirehpour, A., Rahimpour, A., Seyedpour, F., & Jahanshahi, M. (2015). Developing new CTA/CA-based membrane containing hydrophilic nanoparticles to enhance the forward osmosis desalination. *Desalination*, *371*, 46–57.

Zuo, H.-R., Lu, H., Cao, G.-P., Wang, M., Wang, Y.-Y., & Liu, J.-M. (2017). Ion exchange resin blended membrane: Enhanced water transfer and retained salt rejection for forward osmosis. *Desalination*, *421*, 12–22.

Zyaie, J., Sheikhi, M., Baniasadi, J., Sahebi, S., & Mohammadi, T. (2018). Assessment of a thermally modified cellulose acetate forward-osmosis membrane using response surface methodology. *Chemical Engineering & Technology*, *41*(9), 1706–1715.

CHAPTER

9

Polymer-based reverse osmosis membranes

Jasneet Kaur Pala[1], *Anirban Roy*[1] *and Asim K. Ghosh*[2]

[1]Water Energy Nexus Laboratory, Department of Chemical Engineering, BITS Pilani-Goa, Zuarinagar, India [2]Desalination and Membrane Technology Division, Bhabha Atomic Research Centre, Mumbai, India

9.1 Introduction

Sustainable water supply is a challenge plaguing human civilization. The concept of water has been treated as a utility more than a resource for the better part of the 21st Century, which has stressed water availability as well as rendered a lot of good water unavailable due to unrestricted pollution. Harvesting good water from seas and oceans is the only logical solution to this problem, but as producing water involves an energy penalty, hence specific energy consumption becomes a declining factor in the choice of desalination technologies. In this regard, thermal desalination technologies like Multi-Stage Flash and Multi-Effect Distillation are mature and well established. Reverse Osmosis (RO) is a membrane-based technology that utilizes work (not heat) and is inherently less energy-consuming. This is well documented in the literature that while thermal technologies consume 30–40 kWh/m^3, RO can work in as low as 2–3 kWh/m^3. RO has matured as a complete technology solution for seawater desalination over a period of 5 decades. The success of RO can not only be attributed to better membrane design but also process design including state of art energy-recovering devices. The advancement has been so profound that the current state of art RO plants operate near the thermodynamic limits of desalination (1.04 kWh/m^3 for 50% recovery) leaving very little scope for improvement in terms of energy. However, the membrane is definitely the 'heart' of the RO plant.

The foundation of the membrane was first built in the late 1950s by Reid and Breton by designing hand-cast symmetrical thin cellulose acetate (CA) membranes which unfortunately did not gain people's attention as its permeate flux was extremely low even though salts were 98% retained on the membrane surface. Later, Loeb and Sourirajan prepared an asymmetric membrane (200 nm thin layer over thick porous support) that outperformed the earlier work by giving better water flux after which the membranes for desalination purposes came into light, and

Advancement in Polymer-Based Membranes for Water Remediation
DOI: https://doi.org/10.1016/B978-0-323-88514-0.00004-8

© 2022 Elsevier Inc. All rights reserved.

research began intensively to attain high water flux and salt rejection. Many membranes were designed by using cellulose diacetate (CDA), cellulose triacetate (CTA), and a blend of CDA and CTA. Even though CTA proved to be very stable over a wide range of temperature and pH, it was prone to compaction which resulted in a major loss of flux. This problem was overcome when CDA was blended with CTA, which not only provided greater resistance to compaction but also gave high permeation and salt rejection. The major aim of the researchers was to develop asymmetric RO membranes which had improved transport properties and a simple manufacturing process for industrial applications. Until 1969, CA was considered the best type of polymer after which first non-cellulosic asymmetric membranes (aromatic polyamide hollow fiber membrane) were introduced by Richter & Hoehn that was later commercialized by DuPont for brackish water desalination. Despite the fact that the resultant membrane offered low water flux and salt rejection, its stability, durability, versatility was better than CA membranes.

A new era began when Francis cast the first Thin-Film Composite (TFC) membrane by float casting thin-film CA on a water surface that was later annealed and laminated onto a CA support. However, it did not gain recognition commercially because asymmetric membranes were better in terms of performance and operational costs. Cadotte and Peterson were the first who introduced efficient TFC membranes after which till today the research is taking place to enhance the performance of the membranes in terms of chlorine resistance, antifouling, etc. After detailed studies, polysulfone (PSU) was found out to be an optimal porous support with good resistance to compaction, stability in an acidic environment, reasonable performance, etc. Over time, preparation methods, for instance, acid polycondensation and interfacial polymerization, were introduced for the development of TFC membranes (Li, Yan, & Wang, 2016).

Overall, Loeb and Sourirajan's work on synthesizing RO membranes using the phase inversion process has truly revolutionized desalination technology. Low structured strength coupled with limited flux forced a move for better membranes, which led to the thin film composite technology, and later the groundbreaking work on thin film nanocomposite membranes proved that RO is a market leader. In this chapter, the authors discuss the RO technology from the perspective of membranes and membrane development. The first patented TFC membrane was NS-200, which suffered from hydrolysis and swelling of the sulfate linkage, followed by PEC-1000 by Toray which was susceptible to chlorine attacks.

9.2 Asymmetric polymer-based reverse osmosis membranes

In general, membranes are classified based on their retentivity and porosity difference. Water permeability is considered to be one of the most important characteristics of the membrane and is directly proportional to the pressure applied. At the same time, salt rejection is highly dependent on the surface chemistry of the membrane.

Researchers have worked for several decades on asymmetric membranes to improve the skin layer and porous support. Asymmetric membranes are those which have different porosity on both sides, unlike symmetric membranes that have the same porosity. There is a thin skin of the same pore size above the body of larger pores which enhances the flow rate of the water. Due to the uniform pores in symmetric membranes, fluids experience the same retentivity which eventually decreases the flow rate. Therefore, as the retentivity increases, water permeability decreases because the small pores offer high resistance to the flow rate

of the water. For that reason, asymmetric membranes are preferable to symmetric membranes due to their high flow rate and less resistance (Ismail, Khulbe, & Matsuura, 2019).

Cellulose acetate (CA) membranes (asymmetric membranes) were introduced in the late 1950s and were commercially available for large-scale plants in the 1960s. Similar to thin-film composite membranes, it consists of three layers, unlike in polyamide (PA) membrane, the top two layers in CA membrane are made of the same polymer with structural difference. Loeb and Sourirajan used the dry-wet phase inversion technique to transform the polymer from liquid to solid state during membrane preparation. In general, the solution of the polymer and solvent is poured into a thin-film/hollow-tube/hollow-fiber after which the polymer precipitates under controlled conditions. The composition of polymer solution, solvent, and nonsolvent affects the phase separation time, size, and number of droplets. The solubility of the polymer is dependent on a temperature called the critical miscibility temperature (T_c). The polymer is miscible in solvent only when the operating temperature is above T_c or phase separation will take place in the opposed case. The chemical properties of the solvent must be considered when choosing the solvent for the preparation of polymeric membranes. Good solvents are those which, when mixed with the solution of the polymer, interact with each other more than the forces of attraction among polymer molecules. Also, they can also provide proper viscosity. If the ratio of the solvent to the polymer is low, the mixture becomes very viscous and unfit for casting uniform films while on other hand, thin jelly-like films are formed when immersed in water.

The mixture of polymer, solvent, and nonsolvent is cast on an appropriate surface, and the film thickness is obtained with an inclined knife that is uniformly used across the top of the plane after which precipitation takes place. Two steps are involved in the formation of precipitate. First, the solvent evaporates from the top of the surface during which a layer of thin skin starts forming to govern selectivity and salt rejection, and secondly, polymer solution comes in contact with the nonsolvent which diffuses in, and solvent diffuses out at the same time from the thin solid layer formed at the top. At one point, the concentration of solvent in the solution is too low that the polymer is no longer in one phase and its droplets start dispersing in the other liquid phase (Kingsland, 1948).

During the rate of precipitation, two types of structure can be formed, a sponge-like structure and finger-like structure as shown in Fig. 9.1 and Fig. 9.2 (Hoek et al., 2011). Sponge-like structures are formed at a low precipitation rate when the polymer concentration is high. In that situation, membranes have high salt rejections and low water fluxes. If the precipitation rate is high due to low polymer concentration, in that case, finger-like pores are formed which have low salt rejections and high water fluxes. In both cases, sponge-like structures are preferred for the RO process at high pressure. The easiest way to reduce the precipitation rate to get a sponge-like structure is to reduce the chemical potential between solvent and precipitant (nonsolvent) which will eventually reduce the driving force. Another way is to increase the concentration of solvent so that the precipitation rate decreases (Strathmann, Kock, Amar, & Baker, 1975).

To understand the precipitation pathway concept clearly, the ternary diagram is illustrated in Fig. 9.3. Point 1 consists of an original casting solution that consists of solvent, polymer solution, and precipitant in one phase, whereas point 2 is the composition of the final membrane in two phases in equilibrium, solid (polymer-rich) and liquid (polymer-poor). Point 3 is the moment when the polymer starts precipitating and as the precipitation proceeds, the composition of

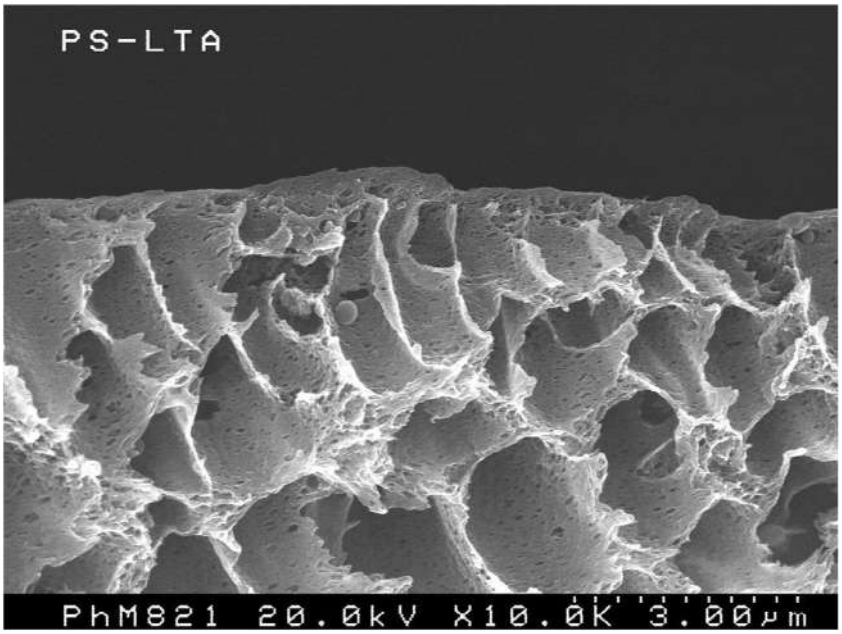

FIGURE 9.1 Sponge-like structure.

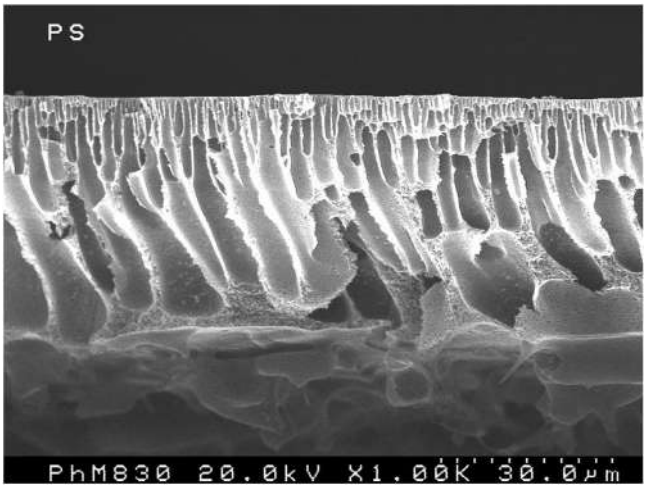

FIGURE 9.2 Finger-like structure.

solvent reduces and the membrane becomes polymer-rich as the viscosity increases and at point 4, polymer solidification takes place (Pinnau & Freeman, 1999; Broens, Altena, Smolders, & Koenhen, 1980; Purkait, Sinha, Mondal, & Singh, 2018; Koenhen, Mulder, & Smolders, 1977; Lanjewar, Mukherjee, Rehman, Abdelrasoul, & Roy, 2020; Broens et al., 1980).

Asymmetric membranes were not only prepared with cellulose acetate but also cellulose diacetate, cellulose triacetate, or their blend. They are mostly used in municipal applications for seawater which has high fouling potential. Also, they are used in the pharmaceutical and semiconductor industries for the production of ultra-pure water. Apart from the smooth surface of the membrane which makes them less susceptible to fouling, the surface has very little charge or uncharged, unlike polyamide membranes which are negatively charged and more prone to fouling if polymers are cationic. Moreover, these membranes can only be operated under low temperature and limited pH range. If pH increases and is exposed to high temperature, the membrane has a tendency towards hydrolysis and results in membrane failure. Additionally, the density of cellulose acetate is high because the separation process experiences high head-loss and is operated at high pressure which results in an increase in expenditure (Yang et al., 2019). The most common polymer, solvent, and nonsolvent for the preparation of asymmetric membranes are mentioned in Table 9.1 (Ismail et al., 2019; Kingsland, 1948). The performance of the membrane can be improved by varying its composition or by altering the non-solvents, etc. Currently, the Middle East and Japan are using cellulose acetate membranes despite

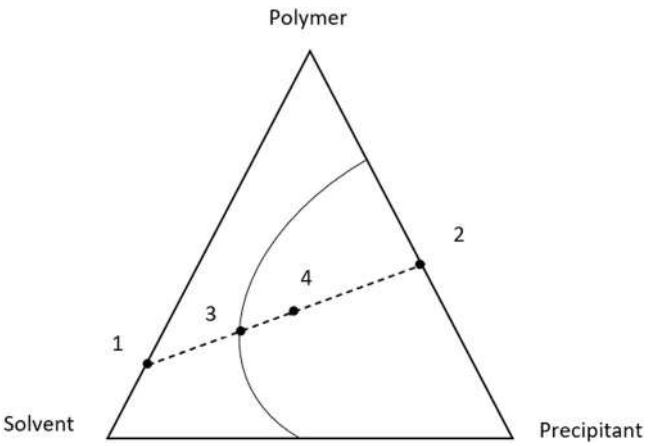

FIGURE 9.3 Ternary diagram depicting the phase inversion method.

TABLE 9.1 Polymer, solvent, and nonsolvent for the preparation of asymmetric membranes.

Polymer	Solvent	Nonsolvent
Polysulfone	DMF	Water
Cellulose acetate	Dioxane	Water
Cellulose acetate	Acetone-formamide	Water
Cellulose acetate	Acetone	Glycerol & n-Propanol
Cellulose acetate/cellulose acetate butyrate/cellulose acetate methacrylate/cellulose acetate propionate	Acetone	Formamide & Maleic acid
Cellulose triacetate	Acetic acid	Dioxane &Triacetin

their disadvantages because of the rich content of organics that are present in their source water and due to the reduced need for cleaning and pretreatment process. However, the introduction of low fouling polyamide membranes in the following years will eliminate the use of cellulose acetate membranes in the future.

9.3 Thin-film composite membrane

After an introduction to the Thin-film composite (TFC) membrane (Fig. 9.4) in the 1970s by Cadotte and his co-workers, the market shifted its focus to the production of a more similar membrane because of its economic feasibility and vast large-scale application (Lau, Ismail, Misdan, & Kassim, 2012). This is because aside from providing excellent mechanical strength and resistance to compaction, it can be operated at a wide temperature range, pH range, and low feed pressure which outweighs the drawbacks faced by the asymmetric membranes as discussed in the previous section. The TFC membrane consists of three layers:

1. Nonwoven fabric acts as a bottom layer (~100−150 μm)
2. The middle layer consists of finely microporous support (~50 μm)
3. Ultrathin barrier layer at the top (~0.01−0.2 μm)

Its preparation is a two-step process which, in turn, is more expensive than the one-step process used for the preparation of asymmetric membranes. The advantage of using the TFC membrane is that each layer can be altered and modified to attain the desired water permeability and salt rejection. However, researchers have focused on them to improve productivity, selectivity, and tolerance against chlorine, fouling, etc. (Yang et al., 2019; Liu, Wang, Yang, Xiao, & Zhao, 2021).

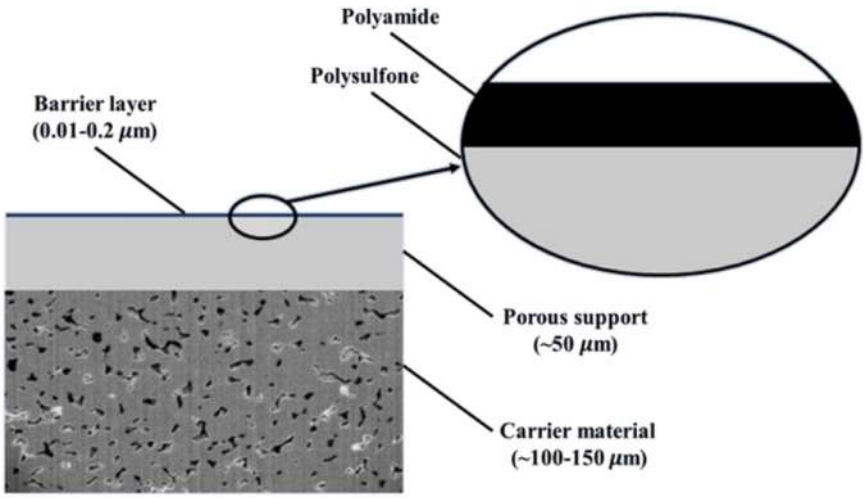

FIGURE 9.4 Thin-film composite (TFC) reverse osmosis (RO) membrane.

The nonwoven fabric is mainly composed of polyester, which is readily available in the market and is extremely porous and allows for high water permeability with no resistance. Its role is to provide mechanical strength to withstand high pressure during reverse osmosis while the middle layer (porous support) regulates the water flux and salt flux. Also, the porous support coupled with the polyamide layer plays a critical role in membrane overall performance (Karami, Khorshidi, Soares, & Sadrzadeh, 2020). Pore structure and chemistry are important factors that define the performance of water flux and salt rejections. Factors involved in affecting the performance of the TFC membrane could be polymer concentration, operating temperature, type of solvent, and additives that are used for the improvement in the performance (Jie, Lee, Bae, Torres, & Wang, 2020). Many polymers are used as backing supports, such as polysulfone (PSU), polycarbonate (PO), polyethersulfone (PES), polyacrylonitrile (PAN), polyetherimide (PEI), polypropylene (PP), poly (phthalazinone ether sulfone ketone) (PPESK), and polyphenylene oxides (PPO). For the commercial production of RO membranes, PSU and PES are the most common polymers used as porous supports due to easy fabrication, stability, and good thermal resistance. However, PSU has low mechanical strength, low-temperature resistance, and poor chemical resistance, that is, ketones, hydrocarbons, etc. Researchers have also acknowledged PAN as a porous support due to its strong chemical resistance and thermal stability, but they are mainly used as ultrafiltration membranes prepared by electrostatic spinning method or conventional casting method because it is difficult to prepare RO membranes with phase inversion technique due to the presence of large shin pore size of PAN membranes. However, there are reports on the preparation of TFC membrane with PAN as a porous support by plasma grafting method. Poly-tetrafluoroethylene (PTFE) and polyvinylidene fluoride (PVDF) are also considered polymers as porous support in the preparation of membranes due to their toughness and corrosive resistance. These fluorinated polymers, especially PTFE, have gained special attention in water treatment applications because of their high porosity, good flexibility, and uniform pore size. However, the big challenge still lies in the hydrophobicity of PTFE and PVDF due to the non-polar configuration of F and C atoms that can be overcome by surface modification (coating or blending hydrophilic material on the membrane surface) of the membrane. One of the published works also involves PP as a porous support in RO membranes that turned out to be hydrophobic after which it was treated with plasma to generate polar groups on the surface of the membrane that eventually improved the salt rejection (Li, Wei, & Wang, 2017; Liu, Wang, Li, Liu, & Deng, 2019).

Although polyamide materials are common in the preparation of TFC membranes, there are other polymeric materials that provide good performance. Some of the recognized polymeric materials include sulfonated polyfuran, polyether-polyfuran, sulfonated polysulfone, polyamide (aliphatic-aromatic), polyamide (via polydopamine), polypiperazine-amide, fully aromatic polyamide, etc. Moreover, researchers have done limited work on sulfonated poly(arylene ether sulfone), polyamide-imide, polyurethane-amide, etc for water treatment applications (Li, Zhang, Fu, & Chung, 2013; Park, Kim, Chun, Bang, & Kim, 2010; Pulyalina et al., 2020; Zhou, Yu, Liu, & Gao, 2005). A few polymer materials and their structural formulas are listed in Table 9.2 with their operating conditions and performance (Ghosh, Bindal, Prabhakar, & Tewari, n.d.; Lee, Arnot, & Mattia, 2011; Li et al., 2016).

TABLE 9.2 Polymer materials with their structure.

Support layer	Structure	Operational parameter	Performance
sulfonated poly (arylene ether sulfone)	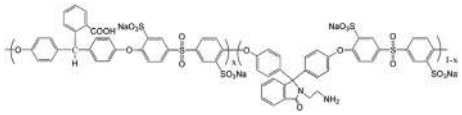	15.5 bar 2000ppm	-
polyamide-imide	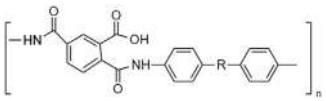	-	-
polyurethane-amide	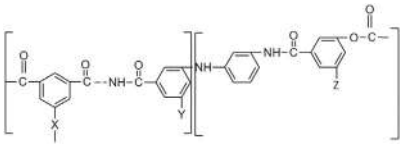	1–3 MPa 500–8000 mg/l	Water flux: 13.5–19 L/m^{2}h Salt rejection: 94.5–98%
Polyfurane (Commercial Membrane NS-200)	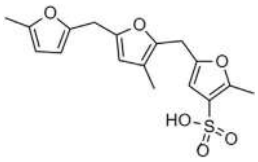	>100 bar 3.5% NaCl solution	Water flux: 0.8 m^3/m^{2}day^{-1} Salt rejection:99.8%
Sulfonated Polysulfone (Commercial Membrane Hi-FluxCP)	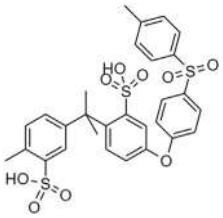	>69 bar 3.5% NaCl solution	Water flux: 0.06m^3/m^{-2}day^{-1} Salt rejection:98%
Polyvinylamine (Commercial Membrane WFX-X006)	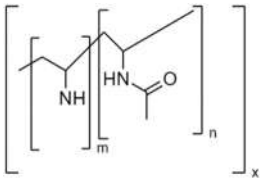	>40 bar	Water flux: 2m^3/m^{-2} day^{-1} Salt rejection:98.7%

Polymers used in the TFC membrane should be selected based on their molecular weight, chain interaction, and flexibility, and other properties such as density, melting point, change in temperature, and pH (Hailemariam et al., 2020). The only major drawback of the use of TFC membrane is that it is prone to chlorine attack present in water due to the treatment of disinfectant that would result in membrane deterioration. Table 9.3 represents the comparison between polyamide membrane and cellulose acetate membrane by using some parameters for which the checked membrane is preferred over another membrane to achieve high performance and better efficiency (Membrane, n.d.; Voutchkov, n.d.).

For the preparation of an ultrathin barrier layer, in addition to the type and concentration of monomer used, the polymerization process is also considered to be one of the important factors for superior performance. For maximum water flux and salt rejection, the membrane is supposed to be ultrathin, highly crosslinked, and hydrophilic. Moreover, it should be environmentally friendly, low cost, and easy to access for desalination. The well-recognized technique used for coating the ultrathin barrier layer on the top of porous support is interfacial polymerization that was introduced by Mogan in 1965. In general, a microporous support is soaked in an aqueous solution of polymeric amine which is later dipped in the solution of di-isocyanate or di/tri-acid chloride in hexane. Polymerization occurs at the interface between one monomer (aqueous solution) and a second monomer (organic solution). In the end, the membrane is heated to 90–110 °C to form a cross-linked polymer. Among all the monomers that are used to form the polyamide layer at the top, m-phenylenediamine (MPD) and trimethyl chloride (TMC) are preferred the most as shown in Fig. 9.5 (Ghernaout, 2017; Habib & Weinman, 2021). There are two drawbacks to using these two monomers; first, they are not highly hydrophilic when crosslinked which would eventually lead to poor water flux, and second, they are prone to fouling that would require a pretreatment process before polymerization. Both the drawbacks would

TABLE 9.3 Comparison of polyamide and cellulose acetate membranes.

Parameter	Polyamide membranes	Cellulose Acetate membranes
Higher Salt Rejection	✓	
Lower Feed Pressure	✓	
High Chlorine Tolerance		✓
Lower Cleaning Frequency		✓
Low Pretreatment Requirements		✓
pH Tolerance	✓	

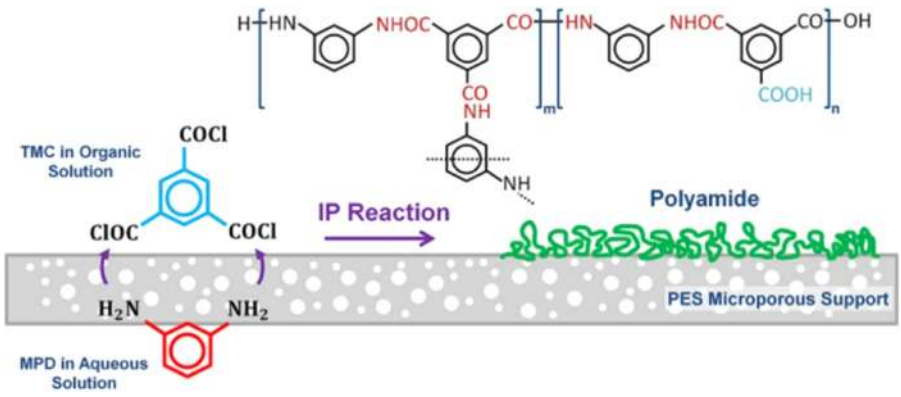

FIGURE 9.5 Interfacial polymerization.

eventually lead to a rise in energy and manufacturing costs for the desalination process. The other monomers that are preferred in the preparation of TFC membrane include p-phenylenediamine, N-(2-aminoethyl)-piperazine, piperazine, polyethyleneimine, and triethylenetetramine (Ji et al., 2020). The selection and combination of monomers for the formation of an active layer of TFC membrane and their properties from existing papers are summarized in Table 9.4 (Chiang, Hsub, Ruaan, Chuang, & Tung, 2009; Gol & Jewrajka, 2014; Jewrajka et al.,

TABLE 9.4 Summary of monomers for the preparation of the active layer of thin-film composite (TFC) membranes with its properties.

Aqueous phase monomers	Organic phase monomers	Operating conditions	Properties
MPD	TMC	Pressure-20 bar Salinity-2000ppm	WF: 37.5 LMH SR: 98.4-98.1%
MPD & DABA	TMC	Pressure-20 bar Salinity-2000ppm	Improved flexibility and hydrophilicity, WF increases to 55.4 LMH with 0.25 w/v% DABA concentration.
Dopamine	TMC	-	Hydrophilic surface; At pH > 6, higher rejection and lower flux; good chemical stability
MPD	BTAC/ BPAC/BHAC	Pressure-15.5 bar Salinity-2000ppm	MPD-BHAC had minimum film thickness and roughness followed by MPD-BPAC, MPD-BTAC, MPD-TMC. While MPD-BTAC and MPD-BPAC showed high hydrophilicity surfaces followed by MPD-TMC and MPD-BHAC. WF: MPD-BTAC-43.3 LMH; MPD-BPAC- 31.2 LMH; MPD-BHAC- 22.1 LMH SR: 99% in all cases
S-BAPS	TMC	Pressure-15.5 bar Salinity-2000ppm	WF: 55LMH; SR: 87.9% (Lower TMC and higher S-BAPS concentration); lower chlorine tolerance than MPD-TMC
EDA/DETA	TMC	Pressure-4 bar Salinity-1000ppm	Negatively charged surface; WF:EDA-TMC-7 LMH
PEI	TMC/TPC	Pressure-4 bar Salinity-1000ppm	Positively charged surface; WF: PEI-TMC- 35LMH; PEI-TMC-11LMH
MPD	TMC/CFIC/ ICIC	Pressure-16 bar Salinity-2000ppm	MPD-ICIC proved to be most chlorine resistant, high hydrophilicity and smooth surface with WF: 58 LMH followed by MPD-TMC -48LMH and MPD-CFIC- 40LMH
MMPD	HTC/TMC	Pressure-15 bar Salinity-1500ppm	WF: MMPD-HTC- 53.2 LMH; MMPD-TMC-34.8 LMH; SR: 98% (approx.)
MPD	PTC	Pressure-15 bar Salinity-1500ppm	Bacterial tendency reduced WF: 53 LMH; SR: 93%
MPD & DAHP	TMC	Pressure-15 bar Salinity-2000ppm	Reduced ultrathin thickness High flux with SR 96–98%
MPD-PEG-MPD	TMC	-	Improved hydrophilicity and antifouling
PIP	IPC/TMC	Pressure-20.7 bar Salinity-1462 ppm	WF- PIP-IPC- 60LMH; SR- 51.8% Strong antifouling property

2013; Liu, Wu, Yu, & Gao, 2009; Liu et al., 2011; Wang, Dai, Zhang, Li, & Zhang, 2013; Xie et al., 2012; Yu, Liu, Lü, Zhou, & Gao, 2009; Zhao et al., 2014). The most common mode of preparation of TFC membrane involves interfacial polymerization of MPD and TMC on porous support (i.e. PES in Fig. 9.5). First, 2% MPD is poured onto the PES sheet which is already placed on the glass plate. After some time (contact time varies to evaluate the performance of the membrane), 0.15% of TMC dissolved in isooctane solution is poured onto the sheet which, if present in excess, is removed with the casting knife. The resultant membrane is dried at high temperature (for instance 80°C) after which the membrane is soaked in deionized water (DI) and later stored for 20–24 hours at 4°C before it is used for application purposes.

Apart from interfacial polymerization, the other coating techniques used include photo grafting, dip coating, and plasma initiated polymerization. In the dip-coating process, the substrate is immersed in the solution of the coating material and while pulling up, a thin layer is deposited which is later formed when the solvent is evaporated from the surface. While in the photo-grafting process, the main objective is to covalently couple the polymer chains that carry reactive groups at the end. At the same time in plasma polymerization, a plasma source is used for the initiation of the polymerization process. Polymers formed on the surface are highly cross-linked and show strong adhesion on the porous surface (Hailemariam et al., 2020; Taylor, Kochkodan, & Sharma, n.d.).

9.3.1 Reverse osmosis membranes for boron removal

In 2011, World Health Organization (WHO) approved the presence of boron up to 2.4 mg/l in the potable water while the EU limited it to 1 mg/l. Even though boron is crucial in many applications, its excess presence can create toxicity and adversely affect human health and the environment. Removal of boron through reverse osmosis membranes has been one of the many challenges as boron is present in the form of uncharged boric acid ($B(OH)_3$) which easily passes along the water through the membranes. Therefore, multiple pass RO membranes are installed instead of single-pass as it is essential to remove for the drinking water application. pH plays a dominant role in boron rejection, for instance, with an increase in pH of feed water, boron gets negatively charged ($B(OH)_4)^-$) and because most of the polyamide RO membranes are negatively charged due to electrostatic repulsion, boron rejection rises. The other parameters, like temperature and pressure, are inversely proportional to the performance of the membrane (in terms of boron rejection). As temperature and pKa are indirectly proportional to each other, the elevation of temperature reduces the boron rejection. While with an increase in pressure, concentration polarization rises that eventually leads to an increase in boron concentration, hence boron diffusion rises. Earlier studies reveal that brackish water reverse osmosis (BWRO) rejects less than 65% of boron while seawater reverse osmosis (SWRO) rejects up to 90% of boron (Hailemariam et al., 2020; Tang, Luo, Thong, & Chung, 2017). Some of the commercial RO membranes for boron removal are mentioned in Table 9.5.

9.3.2 Reverse osmosis membranes for antifouling/chlorine tolerant

Fouling occurs when unwanted materials are present on the surface or they clog the pores of the membranes. They can be categorized as organic and inorganic fouling,

TABLE 9.5 Commercial membranes for boron removal.

Commercial membranes	Boron rejection	pH
TM820A-400	93	8
SW30XHR-400i	93	8
SWC4 + B	95	6.5–7

colloidal/particulate fouling, biofouling, and microbiological fouling. Fouling does not only affect the performance but reduces the membrane lifespan and significantly increases the operational cost. Moreover, hydrophilicity, surface charge, and roughness are the major factors that have a great impact on fouling. The best membrane that is least susceptible to fouling is the one that has high hydrophilicity, smooth surface, and low negative charge. However, fouling can be extensively reduced during the pretreatment, it generally involves the addition of chlorine to deactivate the microbial growth. Nevertheless, usage of chlorine is threatening for polymer-based membranes as it leads to impaired performances and membrane degradation. Some of the ways to reduce chlorination is to modify the surface of the polymer structure, protect or eliminate the chlorine-prone sites.

Inorganic fouling or scaling are formed when permeate water passes through the membranes. As the feed concentration increases, dissolved salts exceed the solubility limit which eventually precipitates and form scale. The compounds that form scaling include calcium sulfate, silica, calcium phosphate, barium sulfate, calcium carbonate, etc. Thus, the preparation of an anti-biofouling membrane is one of the biggest challenges that is still being studied. The most widely used polymer in the membrane is PSU because it has antifouling properties, chlorine resistance, wide availability, stability, economics, etc.

Recently, through metalation sulfochlorination of PSF, sulfochlorinated polysulfone membrane was designed to increase the chlorine resistance. The membrane provided long-term stability in terms of chlorine with 17.8 LMH of water permeability and 96.9% salt rejection. Also, poly(ethylene glycol) is a commonly used polymer that enhances the hydrophilic surface of the membrane which increases the antifouling resistance. They have long flexibility, large volume, and unique coordination with water molecules (Hailemariam et al., 2020).

9.3.3 Hollow fiber reverse osmosis membranes

Earlier, hollow fibers gained recognition for reverse osmosis applications. They are comprised of heavy-walled hollow cylindrical tubes formed from semipermeable polymeric material called fibers because of the small diameter (range 50–200 microns). U-shaped fibers are packed in shells and as the pressurized feed flows over the fibers, potable water permeates through the walls of the fibers towards an open end. The primary advantage of the hollow fiber membrane is that it provides a large area per unit volume and does not require a support tube. Moreover, due to the large surface area, concentration polarization is negligible and water flux is low. Also, the geometry is complicated and the pressure varies axially due to large frictional losses. However, the introduction of a spiral wound RO membrane provides high water flux and is more resistant to fouling and biofouling, so

researchers have shifted their attention away from hollow fibers and only the Toyobo company manufactures hollow fibers composed of cellulose triacetate (Cohen, Grable, & Riggleman, 1972; Gill & Bansal, 1973).

9.4 Potential of different polymer-based reverse osmosis membranes for brackish water desalination

Brackish water sources have salinities values of 500 mg/L up to 10,000−15,000 mg/L, and the membrane is designed for the optimal operation of 5000-10,000 mg/L. The performance is highly dependent on its fouling resistance and hydrophilic nature, which further assists in estimating the capital and energy demand for the desalination process. The poor performance of the membrane could limit the treatment of both brackish and seawater.

To make the membrane more hydrophilic, the blending of a hydrophilic polymer with a main membrane polymer is a common practice. Compared to the polymers that have been studied earlier, polyethylene glycol (PEG) turned out to be highly hydrophilic which would increase the fouling resistance when hydrogen bonding is coordinated between PEG and water molecules. To avoid the reduction of water flux on the surface, crosslinking PEG showed better performance thereby preventing the penetration of feedwater in the TFC membrane.

Other work on PA-TFC membranes involved the addition of four hydrophilic additives, m-aminobenzoic acid-triethylamine salt, 4-(2-hydroxyethyl) morpholine, 2-(2-hydroxyethyl) pyridine, and o-aminobenzoic acid-triethylamine salt in MPD (m-phenylenediamine) which further reacted with TMC (trimesoyl chloride), eventually the performance proved to outperform all other membranes [water flux-52.6 gallons/ft^2/day (gfd), salt rejection 98.8%] after the membrane was post-treated with sodium lauryl sulfate, glycerol, and camphor sulfonic acid-triethylamine salt. The commercial membrane, FT-30, was compared with the same membrane that was modified by PEG crosslinking, and the water flux improved from 24.5 gfd to 60.4 gfd while salt rejection decreased from 99.4% to 98.4% but it was acceptable for the treatment of brackish water (Zhao, Chang, Yen, & Ho, 2013).

Membrane manufacturers design membranes depending on the crucial performance parameters that are divided into four groups: (i) High rejection membranes; (ii) Low energy membranes; (iii) Low fouling membranes; and (iv) High productivity membranes. There are no standard test conditions for brackish water reverse osmosis membranes unlike seawater reverse osmosis membranes, like high rejection membranes that are able to reject salt to 99.5−99.7% compared to standard BWRO membranes which reject 99−99.3% of salt from water inputs. Low energy membranes are designed to produce potable water with low feed pressure, which significantly reduces the operating cost. These membranes are used when the source water has a low TDS (total dissolved salts) concentration, the unit energy costs are high, and the feed water is relatively cold. Another type of membrane is a low fouling membrane that is defined by the surface chemistry of the membrane, that is, neutral surface charge increases the fouling resistance. The last type of membrane is the high productivity membrane, which produces maximum water and high performance, and is achieved by increasing the surface area of the membrane. Some of the commercially used membranes for treating brackish seawater are mentioned in Table 9.6 (Voutchkov, n.d.).

TABLE 9.6 Commercial brackish water reverse osmosis (BWRO) membranes.

Commercial Membranes	Polymer layer	Permeate flow rate (m^3/day)	NaCl rejection (%)	Test Feed Pressure (bar)	Surface area (m^2)
High Rejection BWRO membranes					
ESPA 2 + Hydranautics	Composite polyamide	41.6	99.6	10.3	39.5
BW30−400 Dow Filmtec	Polyamide TFC	40	99.5	15.8	35
TM720-400 Toray	Cross linked fully aromatic polyamide composite	39	99.7	15.8	37.1
Low Energy BWRO membranes					
ESPA 4 Hydranautics	Composite polyamide	49.2	99.2	6.7	37.1
BW30 XLE-440 Dow Filmtec	Polyamide TFC	48.1	99	6.7	40.8
TMH20−400	Cross linked fully aromatic polyamide composite	49.2	99.4	6.7	37.1
Low Fouling BWRO membranes					
Espa 4-LD Hydranautics	Composite polyamide	45.4	99.2	6.7	39.5
BW30 XLE400/34I Dow Filmtec	Polyamide TFC	48.1	99.5	15.8	35
TM720D-400Toray	Cross linked fully aromatic polyamide composite	49.2	99.8	15.8	37.1
High Productivity BWRO membranes					
ESPA 4-MAX Hydranautics	Composite polyamide	50	99.2	10.3	40.8
BW30 LE440 Dow Filmtec	Polyamide TFC	48.1	99.3	10.3	40.8
TM720D-440Toray	Cross linked fully aromatic polyamide composite	45.8	99.8	15.8	40.8

9.5 Polymer-based reverse osmosis membranes for seawater desalination

The most common category of SWRO membranes are TFC polyamide type prepared from MPD (m-phenylenediamine) & TMC (trimesoyl chloride) systems over the polysulfone support. To date, researchers have focused on discovering polymeric material that would provide high permeability and salt rejection at a low cost and with good chemical stability, good mechanical strength, chlorine resistance and antifouling. Until now, many polymers have been acknowledged as reverse osmosis membranes. Apart from cellulose acetate and polyamide discussed in

previous sections, many polymers have been introduced for the preparation of membranes for SWRO, that is, poly(furfuryl alcohol), sulfonated poly(arylene ether sulfone), etc. for the treatment of saline water. Moreover, polyelectrolyte and biomimetic aquaporin membranes were also introduced and experimented with to achieve high membrane performance.

9.5.1 Polyelectrolyte membranes

Additional to cellulose derivatives and polyamide, polyelectrolytes have also bee studied for improved membrane performance. They consist of alternating layers of cationic and anionic electrolytes (also called layer by layer assembled polyelectrolyte membrane) on a porous support. The factors involved while preparing the membrane include thickness, hydrophilicity, surface charges, etc. The most common techniques preferred for the formation of the polyelectrolyte membrane is dip coating, overspray coating, and spin coating. To form the layer of positive and negative charges of polyionic compounds on solid substrates, a positively charged substrate is dipped in an aqueous solution of negatively charged polyelectrolyte which results in the adsorption of polymer on the surface of the substrate, and the surface charge is reversed. After washing, the same substrate is dipped in an aqueous solution of positively charged polyelectrolyte which is later adsorbed, and thereby, the second layer is formed as shown in Fig. 9.6. A polyelectrolyte multilayer is formed by the repetition of the procedure. One of the earlier works in the preparation of polyelectrolyte membrane consisted of 60 layers made from polyacrylonitrile (PAN) and polyethylene terephthalate (PET) which had a huge number of coatings and appeared to be time-consuming. One major drawback was found when the significant rise in the number of layers increased the mass transport resistance, which consequently reduced the water permeability. Another challenge to overcome was to improve the stability of the membrane, and this was later resolved by crosslinking the electrolyte membranes [i.e., poly(acrylic acid) (PAA) and poly(allylamine hydrochloride)] at high temperatures (around 180 °C), but this did not provide satisfactory results when compared to TFC membranes. However, it was observed that crosslinking did not apply to all polyelectrolyte membranes (Klitzing & Tieke, 2004; Yang, Huang, Wang, & Tang, 2018).

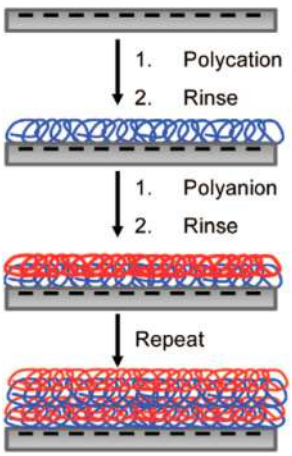

FIGURE 9.6 Formation of a polyelectrolyte membrane.

9.5.2 Aquaporin biomimetic membranes

Aquaporin biomimetic membranes are biological proteins that have natural water channels as water channels in the living cells. They are considered to have supreme water permeability and selectivity. There are two types of aquaporin (AQP) biomimetic membranes described below:

- Incorporation of AQP in bilayers on the top of the support membrane
- Immobilization of AQP in polymer layer

During the reverse osmosis process, due to hydraulic pressure, water passes through the membrane via narrow water channels that pass through the proteins and eventually exit from the porous support as shown in Fig. 9.7. The narrow channels exclude salts at the feed. For ideal performance, the support should not create resistance for water transportation and in that case, organic supports are preferred over inorganic supports because of their porous structure and flexibility. So, for the preparation of biomimetic membranes, lipids and polymers are used as building blocks where membrane vesicles are constructed using lipids to improve the strength and stability of biomimetic membranes. Defects that can be created during the preparation of membranes are avoided to reduce the escape of small molecules. Some of the earlier work also involved the addition of foreign polymers to enhance performance (Habel et al., 2015; Qi et al., 2016).

Some of the earlier work made the statement that very high water flux and salt rejection can be obtained by using an AQP membrane. The membrane was composed of Aquaporin Z (AqpZ) and achieved a water flux of 601 L/m^2 h bar, which showed superior performance over-commercial RO membranes. Another membrane with high water flux was fabricated using interfacial polymerization. Currently, these membranes are being studied at the lab scale, and there are still many challenges, that is, cost, stability, scalability, robustness that are yet to overcome before they are available in the market for wide operation (Tang, Zhao, Wang, Hélix-Nielsen, & Fane, 2013). The most common commercial membranes used for treating seawater are mentioned in Table 9.7 (Voutchkov, n.d.). Similar to BWRO membranes, SWRO membranes are also categorized into four categories but comparatively, they have high hydrophilicity, high salt rejection, and lower roughness compared to BWRO membranes. Moreover, because SWRO membranes are designed to handle high salinity feed, the feed pressure is high and the flow rate is low (Zhou & Gao, 2010).

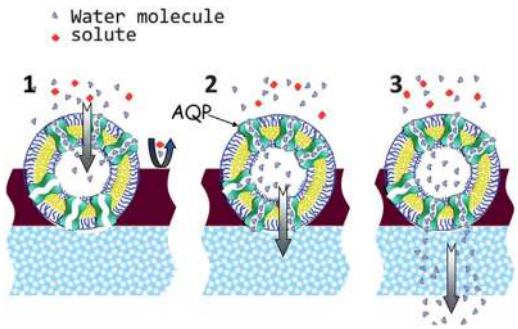

FIGURE 9.7 Aquaporin biomimetic membranes.

TABLE 9.7 Commercial seawater reverse osmosis (SWRO) membranes.

Commercial Membranes	Polymer layer	Permeate flow rate (m^3/day)	NaCl rejection (%)	Test Feed Pressure (bar)	Surface area (m^2)
High Rejection BWRO membranes					
SWC4 + Hydranautics	Composite polyamide	24.6	99.8	10.3	37.1
SW30 HR-380 Dow Filmtec	Polyamide TFC	22.7	99.7	10.3	35
TM820K-440 Toray	Cross linked fully aromatic polyamide composite	24.2	99.86	10.3	40.8
Low Energy BWRO membranes					
SWC6 Max Hydranautics	Composite polyamide	50	99.8	10.3	40.8
SW30 ULE-400I Dow Filmtec	Polyamide TFC	45.4	99.7	10.3	40.8
TM820L-440 Toray	Crosslinked fully aromatic polyamide composite	51.1	99.8	10.3	40.8
Low Fouling BWRO membranes					
SWC4-LD Hydranautics	Composite polyamide	24.6	99.8	10.3	37.1
SWC5-LD Hydranautics	Composite polyamide	34.1	99.8	10.3	37.1
SW30 HRLE-370/34I Dow Filmtec	Polyamide TFC	25	99.8	10.3	34.4
High Productivity BWRO membranes					
SWC6 Max Hydranautics	Composite polyamide	50	99.8	10.3	40.8
SW30 ULE-400I Dow Filmtec	Polyamide TFC	45.4	99.7	10.3	40.8
TM820L-440 Toray	Crosslinked fully aromatic polyamide composite	51.1	99.8	10.3	40.8

9.5.3 Supramolecular polymers and water-soluble polymers

Unlike polymers that are composed of long chains of molecules connected via covalent bonds, supramolecular polymers are made of arrays of monomers held together by secondary and reversible interactions, that is, non-covalent bonds (hydrogen bonds, Van der Waals forces). The reversible interaction ensures that the polymers are formed in thermodynamic equilibrium, and the concentration of monomer, temperature, and strength of

non-covalent bonds are directly proportional to the length of the chain. They provide satisfactory results in ultrafiltration and nanofiltration applications, but due to the formation of large pores, they were not a fit for desalination applications. However, researchers have introduced nano-sized porous materials for high permeation and salt rejection to fill in the literature gap. Furthermore, these supramolecular membranes could meet current separation demand by providing an economical desalination process with less use of antifouling chemicals, frequent cleaning, etc. One of the works in the formation of supramolecular assemblies is the combination of polystyrene-b-poly(4-vinyl pyridine) (PS-b-P4VP) and 2,4-hydroxybenzeneazo benzoic acid connected through non-covalent interactions (de Greef & Meijer, 2008; Nabeel, Rasheed, Bilal, & Iqbal, 2019).

As discussed earlier, polymers have significantly contributed in membrane technologies. Currently, polysulfone (PSU), polyethersulfone (PES), polyimide, polyacrylonitrile (PAN), polyvinylidene fluoride (PVDF), polyvinyl alcohol (PVA), polytetrafluoroethylene (PTFE), and polypropylene (PP) are the most commonly used membranes. However, existing polymeric membranes can cause fouling due to their hydrophobic nature. Therefore, researchers have focused on altering the membrane pore structure and surface properties that would impart hydrophilic characteristics and reduce fouling tendencies. Recently, water soluble polymers (WSPs) have introduced hydrophilic groups which, when dissolved in water, enhance the physical properties of solutions, that is, stability and strength. Poly(vinyl pyrrolidone) (PVP), poly(ethylene glycol) (PEG), and polyvinyl alcohol (PVA) are among the synthetic WSPs that are used to attain the hydrophilic character in the membranes. Some published work involves the addition of PVP to PES membranes and PEG in PSU membranes to enhance the porosity. Also, PVA is considered to have the best hydrophilicity and can be simply prepared. Moreover, PAA is another WSP that is biodegradable and has unique properties. For instance, at pH 5, it acts as a liquid, but at pH 7, it behaves like a gel (Malik et al., 2019).

9.6 Commercialization status and commercial viability

Some well-known membrane manufacturers that design RO membranes of large diameter for the production of freshwater with a capacity of 380,000 m^3/day or more are (i) Dow Filmtec, (ii) Hydranautics, (iii) Toray, (iv) Woongjin Chemical, (v) Koch Membrane system, etc. Large diameter membrane sizes are four or six times greater than conventional size (8 in). Table 9.8 represents the large diameter commercial membranes that can produce large volumes of potable water per day.

However, there are some membranes that have dominated industries since the 1980s. Manufacturers like Dow Filmtec, Toray, Hydranautics, Microdyn-Nadir use PA-TFC membranes for the production of potable water (SW30HRLE-400, SWC4 + , TM820C-370) while manufacturers like Koch, USA supply proprietary PA-TFC membranes (8040-SW-400-34, 4040-HR). GE Osmonics, USA is a manufacturer that products both TFC membranes (HL2540FM, AG4040C) cellulose acetate membranes (CK4040FM). Moreover, Toyobo in Japan makes membranes with selective layer cellulose triacetate (CTA) hollow fibers (HB10255) (Voutchkov, n.d.).

TABLE 9.8 Large diameter commercial reverse osmosis (RO) membrane.

Membranes manufacturers	Commercial membranes	Polymer layer	Permeate flow rate (gpd)	NaCl rejection (%)	Feed spacer thickness (mm)	Surface area (ft^2)
DOW/Filmtec	BW30−1724	Polyamide TFC	45,000	99.50	0.71	1725
	SW30HRLW-1725	Polyamide TFC	32000	99.75	0.71	1725
Hydranautics	ESPA2−1640	Composite Polyamide	38000	99.6	0.76	1600
	SWC5−1640	Composite Polyamide	34000	99.8	0.76	1600
Toray	TM740-160	Cross linked fully aromatic polyamide composite	40,700	99.7	0.79	1600
	TM840E-160	Cross linked fully aromatic polyamide composite	30,000	99.75	0.71	1600
Woongjin Chemical	CSM RE16040-BE	Polyamide TFC	41000	99.7	0.71	1600
	CSM RE16040-SHF	Polyamide TFC	36,000	99.7	0.71	1600
Koch Membrane System	19061-HR-3525	Polyamide TFC	98,900	99.55	0.70	3525
	18061-HF-3050	Polyamide TFC	69,500	99.7	0.7	3050

9.7 Summary and future direction

Reverse osmosis is a promising desalination technology. A productive RO membrane should offer simultaneously high solute rejection, water permeability, chemical stability, and good chlorine resistance. Cellulosic membranes are susceptible to microbiological attack, undergo compaction at higher pressures, and have limited chemical stability. On the other hand, TFC-polyamide membranes exhibit higher flux at a given applied pressure, less microorganism susceptible, and are more stable over a wider range of pH values than cellulosic membranes. Researchers are still investigating a multipurpose membrane even after asymmetric cellulosic/polyamide membrane and TFC-polyamide membrane dominated the market to not only enhance water flux and salt rejection but also resist chlorine attacks and increase mechanical and chemical stability. After more than a few decades, water flux and solute rejection of polyamide TFC membranes have continually improved, but these membranes are not fouling and chlorine resistant. Hence, the future direction of research in RO membrane is towards the development of more fouling and chlorine-resistant membranes with comparable or even better salt rejection and water permeability properties than presently available membranes. In addition, preparation of membranes having very narrow pore size distributions or precise pore sizes by techniques like 3-D printing is the future of RO membrane preparation technique.

Surface functionalization of ready-made RO membrane by chemical modification is one of the methods used to make a surface fouling resistant membrane but the chain breakage or degradation of polymer during the chemical reaction result to low compaction resistance in the final RO membrane. Similarly, blending of functional polymer with base polymer can also be used for the preparation of fouling-resistant membranes (in case of asymmetric membrane

making) but very few polymers are compatible with commonly-used RO membrane polymers. Properties and characteristics of many new polymers have been studied so far, but because the synthesis of the right kind of polymer is an enormous challenge, progress is being made day by day by researchers. The concept of a mixed-matrix membrane (a small filler material is dispersed throughout a larger polymeric matrix) has been adopted to develop membranes with improved mechanical, chemical, and thermal stability and enhanced separation performance. However, upon the incorporation of nanoparticles in polymer matrices, it is often found that the membrane pores get plugged by the aggregation of nanoparticles and unselective void formation takes place at the polymer-inorganic filler interface, which creates inhomogeneity within the membrane and restricts the scaling-up of these membranes from laboratory scale developments. The major practical challenges are still: (a) high cost of nanomaterials, (b) the extra energy required to effectively disperse the nanoparticles into the barrier layer, (c) health and safety issues for use of nanomaterials in the drinking water industry as these are toxic and (d) the difficulty in scaling up nanocomposite membrane manufacturing processes for commercial use. Hence, it is always desired and advantageous to develop novel organic polymeric RO membranes (preferably of TFC type) with chlorine resistant properties using properly selective reaction systems, which can be more readily adaptable to commercial use due to their similarities to current commercial RO membranes.

It is well-known that in the presence of free chlorine, TFC-polyamide RO membranes synthesized from aromatic primary diamines readily undergo N-chlorination in amide functional groups followed by the chlorination of the aromatic ring by Orton rearrangement. As a result, the chemical property of the thin polyamide layer of the membranes changes and the actual performance of the membranes decreases. So, two strategies proposed for the development of better chlorine-resistant RO membranes could be: (a) polyamide TFC membrane by use of commercially available aliphatic amine monomers with aliphatic or aromatic acid chloride (b) non-polyamide based TFC membranes like polyester (synthesized in-situ by polycondensation reaction between mutually reactive di/poly-alcohol and di/poly-carboxylic acid) or polyurethane (synthesized in-situ by polycondensation reaction between mutually reactive Di/poly-alcohol and Di-isocyanate) (Scheme 9.1, Scheme 9.2).

Probable amines are 1,6-Diaminohexane, 1,8-Diaminooctane, 1,4-Diaminobutane etc.; probable acid chlorides are decanedioyl dichloride & Sebacoyl chloride (aliphatic), isophthaloyl & terephthaloyl chloride (aromatic).

SCHEME 9.1 TFC-polyamide using amine in aqueous and acid chloride in organic medium.

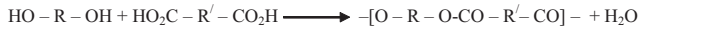

Probable amines are Hexane-1,6-Diol (aliphatic), Resorcinol (aromatic); probable carboxylic acid is adipic acid.

Probable amines are Hexane-1,6-Diol (aliphatic), Resorcinol (aromatic); probable Di-isocyanate is toluene diisocyanate.

SCHEME 9.2 TFC-polyester using alcohol in aqueous and carboxylic acids in the organic medium.

References

Broens, L., Altena, F. W., Smolders, C. A., & Koenhen, D. M. (1980). Asymmetric membrane structures as a result of phase separation phenomena. *Desalination*, *32*, 33–45. Available from https://doi.org/10.1016/S0011-9164(00)86004-X.

Chiang, Y. C., Hsub, Y. Z., Ruaan, R. C., Chuang, C. J., & Tung, K. L. (2009). Nanofiltration membranes synthesized from hyperbranched polyethyleneimine. *Journal of Membrane Science*, *326*, 19–26. Available from https://doi.org/10.1016/j.memsci.2008.09.021.

Cohen, M. E., Grable, M. A., & Riggleman, B. M. (1972). Hollow-fiber reverse osmosis membranes. In H. K. Lonsdale, & H. E. Podall (Eds.), *Reverse osmosis membrane research* (pp. 331–340). US, Boston, MA: Springer. Available from https://doi.org/10.1007/978-1-4684-2004-3_17.

de Greef, T. F. A., & Meijer, E. W. (2008). Supramolecular polymers. *Nature*, *453*, 171–173. Available from https://doi.org/10.1038/453171a.

Ghernaout, D. (2017). Short communication: Requiring reverse osmosis membranes modifications—An overview. *American Journal of Chemical Engineering*, *5*, 81. Available from https://doi.org/10.11648/j.ajche.20170504.15.

Ghosh, A.K., Bindal, R.C., Prabhakar, S., Tewari, P.K., n.d. Composite Polyamide Reverse Osmosis (RO) Membranes – Recent Developments and Future Directions 9.

Gill, W. N., & Bansal, B. (1973). Hollow fiber reverse osmosis systems analysis and design. *AIChE Journal. American Institute of Chemical Engineers*, *19*, 823–831. Available from https://doi.org/10.1002/aic.690190422.

Gol, R. M., & Jewrajka, S. K. (2014). Facile in situ PEGylation of polyamide thin film composite membranes for improving fouling resistance. *Journal of Membrane Science*, *455*, 271–282. Available from https://doi.org/10.1016/j.memsci.2013.12.058.

Habel, J., Hansen, M., Kynde, S., Larsen, N., Midtgaard, S. R., Jensen, G. V., … Hélix-Nielsen, C. (2015). Aquaporin-based biomimetic polymeric membranes: Approaches and challenges. *Membranes*, *5*, 307–351. Available from https://doi.org/10.3390/membranes5030307.

Habib, S., & Weinman, S. T. (2021). *A review on the synthesis of fully aromatic polyamide reverse osmosis membranes*. *Desalination*. Elsevier B.V. Available from https://doi.org/10.1016/j.desal.2021.114939.

Hailemariam, R. H., Woo, Y. C., Damtie, M. M., Kim, B. C., Park, K. D., & Choi, J. S. (2020). Reverse osmosis membrane fabrication and modification technologies and future trends: A review. *Advances in Colloid and Interface Science*, *276*, 102100. Available from https://doi.org/10.1016/j.cis.2019.102100.

Hoek, E. M. V., et al. (2011). Physical–chemical properties, separation performance, and fouling resistance of mixed-matrix ultrafiltration membranes. *Desalination*, *283*, 89–99. Available from http://dx.doi.org/10.1016/j.desal.2011.04.008.

Ismail, A. F., Khulbe, K. C., & Matsuura, T. (2019). RO Membrane Preparation. *Reverse Osmosis*. Available from https://doi.org/10.1016/b978-0-12-811468-1.00002-5.

Jewrajka, S. K., Reddy, A. V. R., Rana, H. H., Mandal, S., Khullar, S., Haldar, S., … Ghosh, P. K. (2013). Use of 2,4,6-pyridinetricarboxylic acid chloride as a novel co-monomer for the preparation of thin film composite polyamide membrane with improved bacterial resistance. *Journal of Membrane Science*, *439*, 87–95. Available from https://doi.org/10.1016/j.memsci.2013.03.047.

Ji, C., Zhai, Z., Jiang, C., Hu, P., Zhao, S., Xue, S., … Niu, Q. J. (2020). Recent advances in high-performance TFC membranes: A review of the functional interlayers. *Desalination*, 114869. Available from https://doi.org/10.1016/j.desal.2020.114869.

Jie, Y., Lee, J., Bae, T., Torres, J., & Wang, R. (2020). Feasibility and performance of a thin-film composite seawater reverse osmosis membrane fabricated on a highly porous microstructured support. *Journal of Membrane Science*, *611*, 118407. Available from https://doi.org/10.1016/j.memsci.2020.118407.

Karami, P., Khorshidi, B., Soares, J. B. P., & Sadrzadeh, M. (2020). Fabrication of highly permeable and thermally stable reverse osmosis thin film composite polyamide membranes. *ACS Applied Materials and Interfaces*, *12*, 2916–2925. Available from https://doi.org/10.1021/acsami.9b16875.

Kingsland, L. C. (1948). The United States patent office. *Law and Contemporary Problems*, *13*, 354. Available from https://doi.org/10.2307/1190003.

Klitzing, R. V., & Tieke, B. (2004). Polyelectrolyte Membranes. *Advances in Polymer Science*, *165*, 177–210. Available from https://doi.org/10.1007/b11270.

Koenhen, D. M., Mulder, M. H. V., & Smolders, C. A. (1977). Phase separation phenomena during the formation of asymmetric membranes. *Journal of Applied Polymer Science*, *21*, 199–215. Available from https://doi.org/10.1002/app.1977.070210118.

Lanjewar, S., Mukherjee, A., Rehman, L., Abdelrasoul, A., & Roy, A. (2020). Thermodynamics of casting solution in membrane synthesis. *Modeling in Membranes and Membrane-Based Processes* (pp. 9–45). John Wiley & Sons, Ltd. Available from https://doi.org/10.1002/9781119536260.ch2.

Lau, W. J., Ismail, A. F., Misdan, N., & Kassim, M. A. (2012). A recent progress in thin film composite membrane: A review. *Desalination*, *287*, 190–199. Available from https://doi.org/10.1016/j.desal.2011.04.004.

Lee, K. P., Arnot, T. C., & Mattia, D. (2011). A review of reverse osmosis membrane materials for desalination—Development to date and future potential. *Journal of Membrane Science*, *370*, 1–22. Available from https://doi.org/10.1016/j.memsci.2010.12.036.

Li, D., Yan, Y., & Wang, H. (2016). Recent advances in polymer and polymer composite membranes for reverse and forward osmosis processes. *Progress in Polymer Science*, *61*, 104–155. Available from https://doi.org/10.1016/j.progpolymsci.2016.03.003.

Li, J., Wei, M., & Wang, Y. (2017). Substrate matters: The influences of substrate layers on the performances of thin-film composite reverse osmosis membranes. *Chinese Journal of Chemical Engineering*, *25*, 1676–1684. Available from https://doi.org/10.1016/j.cjche.2017.05.006.

Li, X., Zhang, S., Fu, F., & Chung, T.-S. (2013). Deformation and reinforcement of thin-film composite (TFC) polyamide-imide (PAI) membranes for osmotic power generation. *Journal of Membrane Science*, *434*, 204–217. Available from https://doi.org/10.1016/j.memsci.2013.01.049.

Liu, C., Wang, W., Yang, B., Xiao, K., & Zhao, H. (2021). Separation, anti-fouling, and chlorine resistance of the polyamide reverse osmosis membrane: From mechanisms to mitigation strategies. *Water Research*. Elsevier Ltd. Available from https://doi.org/10.1016/j.watres.2021.116976.

Liu, F., Wang, L., Li, D., Liu, Q., & Deng, B. (2019). A review: The effect of the microporous support during interfacial polymerization on the morphology and performances of a thin film composite membrane for liquid purification. *RSC Advances*, *9*, 35417–35428. Available from https://doi.org/10.1039/c9ra07114h.

Liu, M., Wu, D., Yu, S., & Gao, C. (2009). Influence of the polyacyl chloride structure on the reverse osmosis performance, surface properties and chlorine stability of the thin-film composite polyamide membranes. *Journal of Membrane Science*, *326*, 205–214. Available from https://doi.org/10.1016/j.memsci.2008.10.004.

Liu, Y., He, B., Li, J., Sanderson, R. D., Li, L., & Zhang, S. (2011). Formation and structural evolution of biphenyl polyamide thin film on hollow fiber membrane during interfacial polymerization. *Journal of Membrane Science*, *373*, 98–106. Available from https://doi.org/10.1016/j.memsci.2011.02.045.

Malik, T., Razzaq, H., Razzaque, S., Nawaz, H., Siddiqa, A., Siddiq, M., & Qaisar, S. (2019). Design and synthesis of polymeric membranes using water-soluble pore formers: an overview. *Polymer Bulletin*, *76*, 4879–4901. Available from https://doi.org/10.1007/s00289-018-2616-3.

Membrane, R. O. n.d. Introduction to Reverse Osmosis Membrane 2. Cellulose 16–18.

Nabeel, F., Rasheed, T., Bilal, M., & Iqbal, H. M. N. (2019). Supramolecular membranes: A robust platform to develop separation strategies towards water-based applications. *Separation and Purification Technology*, *215*, 441–453. Available from https://doi.org/10.1016/j.seppur.2019.01.035.

Park, K. T., Kim, S. G., Chun, B. H., Bang, J., & Kim, S. H. (2010). Sulfonated poly(arylene ether sulfone) thin-film composite reverse osmosis membrane containing SiO2 nano-particles. *Desalination and Water Treatment*, *15*, 69–75. Available from https://doi.org/10.5004/dwt.2011.1669.

Pinnau, I., & Freeman, B. D. (1999). Formation and modification of polymeric membranes: Overview. *ACS Symposium Series*, *744*, 1–22. Available from https://doi.org/10.1021/bk-2000-0744.ch001.

Pulyalina, A., Rostovtseva, V., Minich, I., Silyukov, O., Toikka, M., Saprykina, N., & Polotskaya, G. (2020). Specific structure and properties of composite membranes based on the torlon® (polyamide-imide)/layered perovskite oxide. *Symmetry*, *12*, 1142. Available from https://doi.org/10.3390/sym12071142.

Purkait, M. K., Sinha, M. K., Mondal, P., & Singh, R. (2018). Introduction to membranes. *Interface Science and Technology*. Available from https://doi.org/10.1016/B978-0-12-813961-5.00001-2.

Qi, S., Wang, R., Chaitra, G. K. M., Torres, J., Hu, X., & Fane, A. G. (2016). Aquaporin-based biomimetic reverse osmosis membranes: Stability and long term performance. *Journal of Membrane Science*, *508*, 94–103. Available from https://doi.org/10.1016/j.memsci.2016.02.013.

Strathmann, H., Kock, K., Amar, P., & Baker, R. W. (1975). The formation mechanism of asymmetric membranes. *Desalination*, *16*, 179–203. Available from https://doi.org/10.1016/S0011-9164(00)82092-5.

Tang, C. Y., Zhao, Y., Wang, R., Hélix-Nielsen, C., & Fane, A. G. (2013). Desalination by biomimetic aquaporin membranes: Review of status and prospects. *Desalination*, *308*, 34–40. Available from https://doi.org/10.1016/j.desal.2012.07.007.

Tang, Y. P., Luo, L., Thong, Z., & Chung, T. S. (2017). Recent advances in membrane materials and technologies for boron removal. *Journal of Membrane Science*, *541*, 434–446. Available from https://doi.org/10.1016/j.memsci.2017.07.015.

Taylor, P., Kochkodan, V.M., Sharma, V.K., n.d. Journal of Environmental Science and Health, Part A: Toxic/Hazardous Substances and Environmental Graft polymerization and plasma treatment of polymer membranes for fouling reduction: A review Graft polymerization and plasma treatment of polymer memb 37–41. https://doi.org/10.1080/10934529.2012.689183.

Voutchkov, N., n.d. Desalination Engineering Planning and Design.

Wang, T., Dai, L., Zhang, Q., Li, A., & Zhang, S. (2013). Effects of acyl chloride monomer functionality on the properties of polyamide reverse osmosis (RO) membrane. *Journal of Membrane Science*, *440*, 48–57. Available from https://doi.org/10.1016/j.memsci.2013.03.066.

Xie, W., Geise, G. M., Freeman, B. D., Lee, H. S., Byun, G., & McGrath, J. E. (2012). Polyamide interfacial composite membranes prepared from m-phenylene diamine, trimesoyl chloride and a new disulfonated diamine. *Journal of Membrane Science*, *403–404*, 152–161. Available from https://doi.org/10.1016/j.memsci.2012.02.038.

Yang, Z., Huang, X., Wang, J., & Tang, C. Y. (2018). Novel polyethyleneimine/TMC-based nanofiltration membrane prepared on a polydopamine coated substrate. *Front. Chem. Sci. Eng.*, *12*, 273–282. Available from https://doi.org/10.1007/s11705-017-1695-2.

Yang, Z., Zhou, Y., Feng, Z., Rui, X., Zhang, T., & Zhang, Z. (2019). A review on reverse osmosis and nanofiltration membranes for water purification. *Polymers*, *11*, 1–22. Available from https://doi.org/10.3390/polym11081252.

Yu, S., Liu, M., Lü, Z., Zhou, Y., & Gao, C. (2009). Aromatic-cycloaliphatic polyamide thin-film composite membrane with improved chlorine resistance prepared from m-phenylenediamine-4-methyl and cyclohexane-1,3,5-tricarbonyl chloride. *Journal of Membrane Science*, *344*, 155–164. Available from https://doi.org/10.1016/j.memsci.2009.07.046.

Zhao, J., Su, Y., He, X., Zhao, X., Li, Y., Zhang, R., & Jiang, Z. (2014). Dopamine composite nanofiltration membranes prepared by self-polymerization and interfacial polymerization. *Journal of Membrane Science*, *465*, 41–48. Available from https://doi.org/10.1016/j.memsci.2014.04.018.

Zhao, L., Chang, P. C. Y., Yen, C., & Ho, W. S. W. (2013). High-flux and fouling-resistant membranes for brackish water desalination. *Journal of Membrane Science*, *425–426*, 1–10. Available from https://doi.org/10.1016/j.memsci.2012.09.018.

Zhou, Y., & Gao, C. (2010). Comparison between BWRO membrane and SWRO membrane. Huagong Xuebao/CIESC. *The Journal*, *61*, 2590–2595.

Zhou, Y., Yu, S., Liu, M., & Gao, C. (2005). Preparation and characterization of polyamide-urethane thin-film composite membranes. *Desalination*, *180*, 189–196. Available from https://doi.org/10.1016/j.desal.2004.12.037.

CHAPTER

10

Polymer-based nano-enhanced reverse osmosis membranes

Hiren D. Raval and Mrinmoy Mondal

Membrane Science and Separation Technology Division, CSIR-Central Salt and Marine Chemicals Research Institute, Bhavnagar, India

10.1 Introduction

Scarcity of freshwater has become a major concern for many countries in the 21st century. Due to population growth, economic development, and rapid industrialization, global freshwater demand is rising in recent years. Availability of freshwater from natural sources is only 2.5% of the global water quantity, whereas the rest is saline (Alkaisi, Mossad, & Sharifian-Barforoush, 2017). In order to address this problem, water desalination from saline water offers a viable alternative for natural source of freshwater. Several technologies, such as multistage flash distillation (Al-Mutaz & Al-Namlah, 2004), multiple-effect distillation (Ihm, Al-Najdi, Hamed, Jun, & Chung, 2016), membrane distillation (Hsu, Cheng, & Chiou, 2002), electro dialysis (Sadrzadeh & Mohammadi, 2008), vapor-compression distillation (Al-Karaghouli & Kazmerski, 2013), and capacitive deionization (Oren, 2008) are used for desalination. Most of these methods suffer from poor scalability and limited commercial availability.

Membrane technology can be a viable alternative for desalination due to various advantages, such as physical separation, no chemical use, easily scalable, and commercially available. Particularly, polymeric reverse osmosis (RO) is widely used membrane for desalination process throughout the world (Lee, Arnot, & Mattia, 2011). Due to low cost, energy efficiency, and simple operation, RO processes are gaining popularity worldwide for desalination. It is estimated that, globally more than 50% of operating desalination plant use RO membrane (Huang et al., 2013b). Generally, RO membranes are developed by thin-film composite (TFC) polyamide (PA) layer over the base polymer substrate (Ismail, Padaki, Hilal, Matsuura, & Lau, 2015). These TFC polyamide membranes comprise of three different layers. It consists a nonwoven structural support in the bottom, a porous polymeric layer at the middle, and ultra thin polyamide layer over the top to offer higher selectivity (Porter, 1990). This dense polyamide layer is usually created by the interfacial polymerization (IP) reaction between two

Advancement in Polymer-Based Membranes for Water Remediation
DOI: https://doi.org/10.1016/B978-0-323-88514-0.00007-3

© 2022 Elsevier Inc. All rights reserved.

monomers such as aromatic amine and acyl chloride (Cadotte, 1977). Apart from these advantages, some restrictions and challenges are still significant for the usefulness of RO membrane. One of the major difficulties for RO membrane is to achieve both higher throughput and selectivity at the same time. Several techniques are proposed to improve the permeability of TFC RO membrane. Membrane surface functionalization, synthesis of new PA layer using different monomer, post treatment, etc., are used for higher membrane throughput. Another major concern for TFC RO membrane is fouling. Fouling occurs due to the deposition of organic and inorganic particulate matter over the membrane. Due to fouling, throughput and efficiency of the membrane decreases and also it reduces the membrane lifetime. Several methods are proposed to increase the antifouling characteristics of the PA layer of TFC RO membrane. These include selection of new monomer, surface modification of PA layer, advance fabrication process. Therefore development of high flux, antifouling RO membranes along with high selectivity is an area of active research.

Nanoscale materials have been identified as functional materials for applications in water treatment and range of nanomaterials have been found to be effective in different water treatment applications (Raval & Gohil, 2010). Nanotechnology provides new approaches to increase the performance of RO membrane by incorporating nanomaterial within the PA thin selective layer. These nanomaterial-doped new category of composite membrane is known as thin-film nanocomposite (TFN) membrane. Nanomaterials are embedded within the thin PA dense layer of the TFC membrane can enhance the surface charge of the interfacially polymerized layer, resulting in high selectivity due to charge–charge interaction and high throughput of porous membranes. This new concept of TFN RO membrane was first reported by Jeong et al. (2007). They prepared TFN RO membrane by incorporating inorganic porous Sodium zeolite A (NaA) nanomaterials into the PA layer by IP. The resulting nanocomposite membrane showed improved permeate flux compared to nascent TFC membrane without changing the selectivity. Since then, many other nanomaterials including nonporous and porous has been utilized for TFN RO membrane preparation. The same research group, Pendergast, Nygaard, Ghosh, and Hoek (2010) embedded silica and zeolite nanomaterials into the PA layer over polysulfone (PSF) substrate to developed TFN RO membrane with higher permeate flux and enhanced mechanical stability. Several types of nanomaterials, such as silver (Kim, Hwang, Gamal El-Din, & Liu, 2012), graphene oxide (Crock, Rogensues, Shan, & Tarabara, 2013; Ganesh, Isloor, & Ismail, 2013; Zinadini, Zinatizadeh, Rahimi, Vatanpour, & Zangeneh, 2014), carbon nanotube (CNT) (Chan et al., 2013; Park et al., 2010b; Roy, Ntim, Mitra, & Sirkar, 2011), multiwalled carbon nanotube (MWCNT) (Amini, Jahanshahi, & Rahimpour, 2013), silica (Bao, Zhu, Wang, Wang, & Gao, 2013; Jadav & Singh, 2009; Yin, Kim, Yang, & Deng, 2012), metal oxide (Kong et al., 2011), TiO_2 (Lee et al., 2008), metal-organic framework (MOF) (Basu et al., 2009), alumina (Maximous, Nakhla, Wan, & Wong, 2010; Yan, Hong, Li, & Li, 2009), zeolites (Dong et al., 2011; Jeong et al., 2007; Fathizadeh, Aroujalian, & Raisi, 2011; Huang, Qu, Dong, Zhang, & Chen, 2013a; Lind et al., 2009a; Lind, Jeong, Subramani, Huang, & Hoek, 2009b; Lind, Eumine Suk, Nguyen, & Hoek, 2010; Ma, Wei, Liao, & Tang, 2012) were utilized for nano-enhanced RO membrane. These nanomaterials are distributed in the aqueous or organic phase depending on the hydrophilic/hydrophobic nature of the materials. Nanomaterials may exhibit enhanced membrane physical properties, such as mechanical, chemical, and thermal stability. Transport and separation

properties of TFN membrane depends on various factors such as size of nanomaterials, chemical function, surface hydrophilicity, dose of nanomaterials in PA layer, and thickness of the film. The technique of nanomaterials doped during interfacial polymerization has also been applied for the preparation of TFN RO membranes in hollow fiber module (Gai, Zhao, & Chung, 2019; Guo et al., 2020; Lin, Chen, & Wang, 2019). Low pressure TFN RO membrane can be developed by interfacial polymerization technique (Shen et al., 2019).

In this chapter, we discuss the various attempts and progress made on nano-enhanced RO membrane in recent years (Saleem & Zaidi, 2020; Zhao et al., 2020a). In addition, potential use of TFN RO membrane application in desalination, commercial viability, and further improvement is also reported.

10.2 Preparation strategies of polymer-based nano-enhanced reverse osmosis membranes

Polymer-based nano-enhanced membrane can be classified in four categories depending on location of nanomaterials and structure of membrane. These four types are:

1. Conventional nanocomposite or mixed matrix membrane (MMM)
2. TFC with nanocomposite substrate
3. TFN
4. Nanocomposite located at membrane surface.

The usual configurations of these membranes are presented in Fig. 10.1. It can be noted that in Fig. 10.1, spheres are used for representation of nanoparticles, nanotubes, nanofibers, or nanosheets.

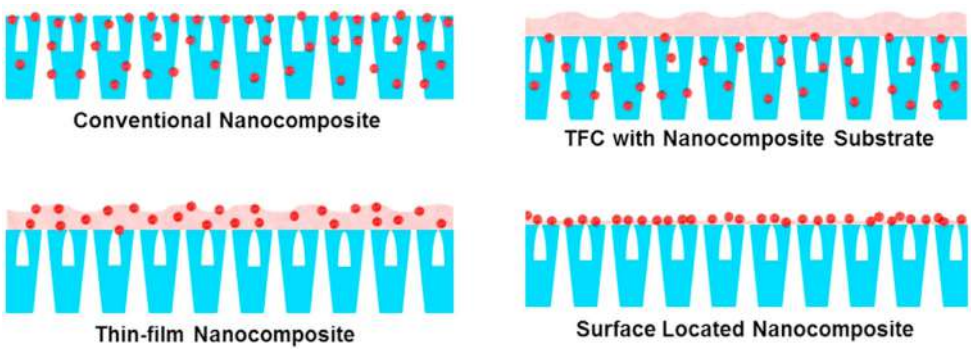

FIGURE 10.1 Various types of nanocomposite membranes (Yin & Deng, 2015). Source: *Adapted from Yin, J., & Deng, B. (2015). Polymer-matrix nanocomposite membranes for water treatment.* Journal of Membrane Science, 479, 256–275. https://doi.org/10.1016/j.memsci.2014.11.019.

10.2.1 Conventional nanocomposite or mixed matrix membrane

Conventional nanocomposite membranes or mixed matrix membrane (MMM) are fabricated by phase inversion technique, in which, nanomaterials are incorporated in the polymer solution. Different types of nanomaterials, such as inorganic, organic, or biomaterial can be used for conventional nanocomposite membrane or MMM. In recent years, various publications reported MMM or conventional nanocomposite membrane. These reported works have revealed that inclusion of different nanomaterials in polymer matrix enhanced the structure, physical, chemical properties, antibacterial and antifouling properties into the membrane. Due to typical porous structure, MMM is mostly utilized in microfiltration and ultrafiltration (UF) application. Ghaseminezhad, Barikani, and Salehirad (2019) developed conventional nanocomposite RO membrane by incorporation of graphene oxide (GO) nanosheets in cellulose acetate (CA) polymer matrix. Desalination performance of these nanocomposite CA-based RO membrane was enhanced due to the presence of GO nanosheets in polymer matrix.

10.2.2 Thin-film composite with nanocomposite substrate

In TFC with nanocomposite substrate membrane, nanomaterials are incorporated into the polymer substrate and then utilized to prepare TFC membrane by IP process. A few studies reveal that TFC with nanocomposite substrate provided higher permeate flux related to pristine TFC membrane. The nanocomposite substrates improved the hydrophilicity of the membrane. Very few reports are available on development of RO membrane using this process (Kim et al., 2012; Pendergast, Ghosh, & Hoek, 2013). Thin-film nanofibrous composite RO membrane was developed by incorporation of cellulose nanofibers into the polymer substrates followed by interfacial polymerization (Wang, Ma, Chu, & Hsiao, 2017). This technique is mainly used in forward osmosis membrane preparation to minimize the internal concentration polarization.

10.2.3 Thin-film nanocomposite

TFN membranes are prepared by IP, in which nanomaterial is incorporated in PA thin layer. Nanomaterials can be distributed either in organic or aqueous phase depending upon solubility nature of the materials. Membrane properties such as selectivity, permeability, and fouling resistance are mainly controlled by the PA thin layer in TFC membrane. Inclusion of nanomaterials into the PA thin layer may improve the physicochemical characteristics such as hydrophilicity, porosity, charge density and also enhance the permeability and selectivity of the membrane. Various nanomaterials such as nanoparticles, nanotubes, and nanofibers, which are used in conventional nanocomposite membrane, may be utilized in development of TFN membrane. TFN technique can be utilized for development of RO membrane for better performance over conventional TFC membrane. General fabrication process of TFN membrane by IP process between m-phenylenediamine (MPD) and trimesoyl chloride (TMC) solution is presented in Fig. 10.2.

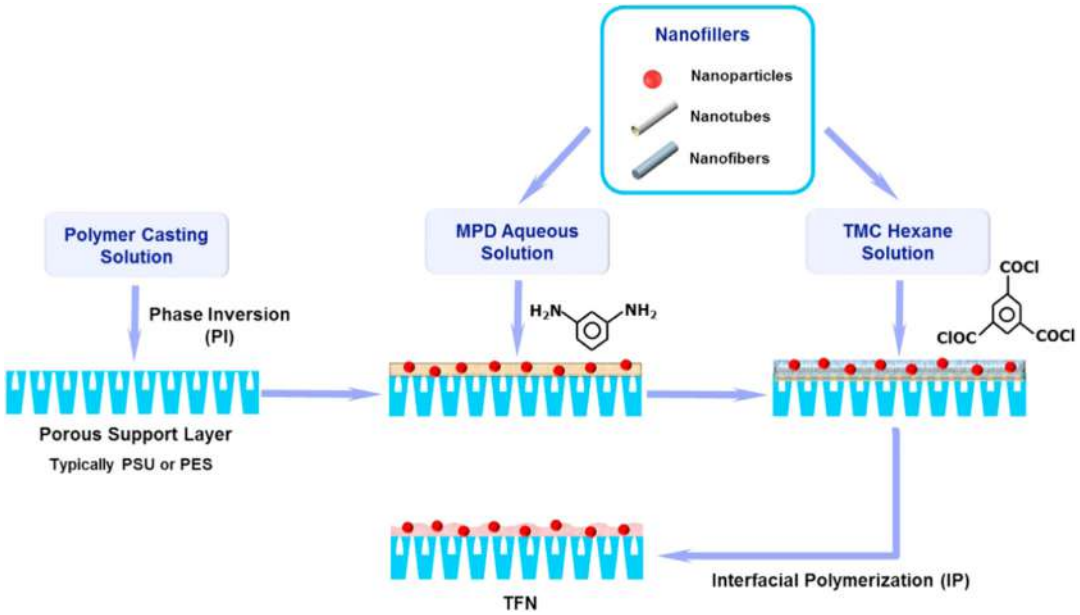

FIGURE 10.2 Fabrication process of thin-film nanocomposite (TFN) membrane by interfacial polymerization (IP) process. Source: *Adapted from Yin, J., & Deng, B. (2015). Polymer-matrix nanocomposite membranes for water treatment*. Journal of Membrane Science, 479, 256–275. https://doi.org/10.1016/j.memsci.2014.11.019.

10.2.4 Nanocomposite located at membrane surface

Membrane performance like separation and antifouling properties not only depends on membrane structure, porosity, and thickness but also depends on membrane surface characteristics, such as charge density, pore size, roughness, and hydrophilicity. Therefore, alteration of membrane surface could be enhanced by the effectiveness of membrane separation application in water treatment. Surface-located nanocomposite membranes are developed depending on the modification of membrane surface without affecting the intrinsic structure of the membrane. Several techniques such as chemical grafting, coating/deposition, and self-assembly are used to prepared surface-located nanocomposite membrane. Unique properties such as bonding force and bonding process are mainly utilized by the above-mentioned methods to prepared surface-located nanocomposite membrane. Few literatures are reported about RO membrane preparation using this process. RO membrane developed using surface-located nanocomposite membrane is summarized in Table 10.1.

TiO2 nanoparticles are attached on the specific surfaces consisting $-COOH$, $-SO_3^-H^+$ and sulfone groups by H-bonding and coordination interactions in self-assembly process (Kim et al., 2003; Luo, Zhao, Tang, & Pu, 2005). Addition of TiO2 nanoparticles on membrane surface may enhance hydrophilicity and antimicrobial property of the membrane.

To utilize the antimicrobial property of sliver, nanoparticles are attached onto the membrane surface by adsorption-reduction mechanism. Membrane surface adsorbed the silver ions and then reduced by the chemicals agents such as formaldehyde (Yang et al., 2009),

TABLE 10.1 Nanocomposite located at membrane surface.

Fabrication method	Nanomaterial	Pressure (bar)	Flux (LMH)	NaCl rejection (%)	Performance enhanced	References
Self-assembly	TiO_2	15.5	129.25	96	Hydrophilicity, fouling resistance, antimicrobial activity	Kwak, Kim, and Kim (2001)
		15.5	24.49	96.6		Kim, Kwak, Sohn, and Park (2003)
Adsorption-reduction	Ag	55.5	54.17	95	Antimicrobial activity	Yang, Lin, and Huang (2009)
		10	40	96		Zhang, Qiu, Ting, and Chung (2013)
Electrostatic attraction	Cu	27.6	69	98.6	Antimicrobial activity	Ben-Sasson et al. (2014b)
Layer-by-layer assembly	CNTs	15.5	13.6	92.5	Thermal stability, chlorine resistance	Park et al. (2010b)
	GO	3.44	68.8	60	Selectivity, chlorine resistance	Hu and Mi (2013)
		15.5	12.5	97.1		Choi, Choi, Bang, and Lee (2013)
Chemical grafting	CNTs	27.6	38.64	–	Antimicrobial activity	Tiraferri, Vecitis, and Elimelech (2011)
	Ag	20.7	69.4	93.6	Antimicrobial activity	Yin, Yang, Hu, and Deng (2013)

ascorbic acid (Cao, Tang, Liu, Nie, & Zhao, 2010; Zhu, Bai, Wee, Liu, & Tang, 2010), or under light irradiation (Zhang et al., 2013) to prepared RO membrane.

Positive-charged polyethyleneimine (PEI) encapsulated Cu nanoparticles are embedded onto the negative charge membrane surface by electrostatic attraction to enhanced membrane antimicrobial and antifouling property (Ben-Sasson et al., 2014b). RO membranes are prepared by this process to improve the antimicrobial property. But the main drawback of this process is leaching of nanoparticles from membrane surface.

In layer-by-layer assembly, several coatings of nanomaterials are incorporated on the membrane surface by electrostatic attraction, hydrogen bonding, and/or chemical bonding. Electrostatic attraction between polyanion and polycation are utilized to prepare this type of nanocomposite membrane. Thermal stability of the RO membrane are enhanced by poly (allylamine hydrochloride) as polycation and polyacrylic acid containing CNT as polyanion assembly on the PSF membrane surface (Park et al., 2010a). Novel RO membrane was prepared by layer-by-layer accumulation of GO nanosheets onto the polydopamine-coated PSF membrane to improved selectivity and chlorine resistance of the membrane (Hu & Mi, 2013). Layer-by-layer assemble of GO membrane fabrication process is presented in Fig. 10.3.

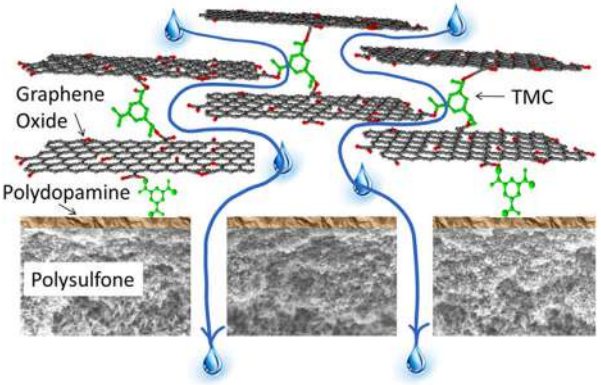

FIGURE 10.3 Fabrication procedures of layer-by-layer assemble of graphene oxide (GO) incorporated membrane. Source: *Adapted from Hu, M., & Mi, B. (2013). Enabling graphene oxide nanosheets as water separation membranes.* Environmental Science and Technology, 47, *3715–3723. https://doi.org/10.1021/es400571g*.

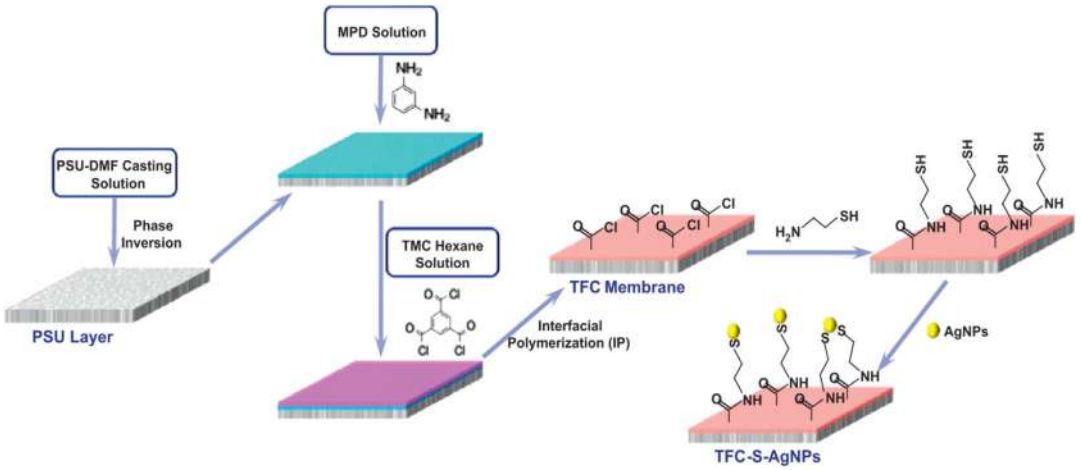

FIGURE 10.4 Schematic representation of chemical grafting of silver nanoparticles onto the surface of polyamide (PA) thin-film composite (TFC) membrane (Yin et al., 2013). Source: *Adapted from Yin, J., Yang, Y., Hu, Z., & Deng, B. (2013). Attachment of silver nanoparticles (AgNPs) onto thin-film composite (TFC) membranes through covalent bonding to reduce membrane biofouling.* Journal of Membrane Science, 441, *73–82. https://doi.org/10.1016/j.memsci.2013.03.060*.

Nanocomposite RO membrane can be developed by chemical grafting of nanomaterials onto the membrane surface by chemical bonding mechanism. For example, silver nanoparticles are embedded onto the PA TFC membrane surface by chemical bonding, where cysteamine $(H_2N-(CH_2)_2-SH)$ used as a linking agent. This fabrication process is represented in Fig. 10.4.

10.3 Polymer nanocomposite reverse osmosis membranes

Recently, TFN-based membrane is gaining interest over other nanocomposite-based RO membrane. Different hydrophilic nanomaterials, such as GO, CNT, metal and metal oxide are

used for preparation of TFN membrane. In the following section, utilization of different nanoparticles in the advancement of RO membranes, their fabrication, applications, and performance will be discussed. Antifouling behavior of modified RO membrane is also analyzed.

10.3.1 Carbon based

Numerous carbon-based nanoparticles such as CNTs, GO, reduced-GO, and carbon quantum dots (CQD) have been used to prepared TFN RO membrane. Carbon-based nanoparticles incorporated in TFN RO membranes are summarized in Table 10.2.

10.3.1.1 Carbon nanotubes

Recently, carbon nanotubes (CNTs) are utilized in membrane for water treatment due to quick transport of water molecules across the CNT and antifouling characteristics. CNTs exhibit quick transport over the other nano-porous materials, due to their exceptionally smooth inner wall (Kim et al., 2014; Lee et al., 2014; Raval & Gohil, 2009). These unique properties of CNTs are utilized in membrane to enhance the throughput without affecting the selectivity. Few studies show that water transport through the CNT with proper diameter can enhance the rejection of ions (Lee et al., 2014). MWCNT have been utilized for preparation of nanocomposite membrane due to their unique physicochemical properties. Various studies show that incorporation of MWCNT in nanocomposite membrane can enhance water permeability, rejection of salt, antifouling and antimicrobial characteristics of the membrane (Zhao et al., 2014a). MWCNT are doped in PA layer during IP process to prepared antifouling TFN RO membrane. Inukai et al. (2015) reports that high-performance RO nanocomposite membrane prepared by MWCNT is incorporated in PA layer. They used porous PSF substrate to prepare the nanocomposite RO membrane. MPD aqueous solution (2 wt.%) and TMC-hexane solution (0.1 wt.%) used to form PA layer over the membrane surface by IP process. 1 wt.% MWCNT are dispersed in MPD solution to prepared nanocomposite RO membrane. They found that 15.5 wt.% MWCNT in PA layer of the membrane which is to improve the membrane permeability, antifouling, and chlorine resistance. It is interesting to note that, MWCNT nanocomposite membrane exhibits permeate flux more than 2 times over the pristine PA membrane. At high pressure also it performs very well. MWCNT nanocomposite membrane shows 90% salt rejection, where pristine PA membrane exhibits 97% salt rejection.

Takizawa et al. (2017) prepared antifouling and low-protein adhesion RO nanocomposite membrane by incorporation of MWCNT in PA layer. They investigated membrane antifouling mechanism by experimentally as well as theoretically using molecular dynamics simulation. They used bovine serum albumin solution for fouling studies. They found that MWCNT PA membrane shows better antifouling characteristics compared to other pristine PA membranes. Due to incorporation of MWCNT in PA layer membrane surface are getting smoother resulting lower interaction between foulants and membrane surface. This leads to improve the antifouling mechanism of the MWCNT PA membrane. Fouling behavior of MWCNT incorporated PA membrane surface and pristine PA membrane surface are represented in Fig. 10.5Aand B, respectively. Also MWCNT PA-based membrane exhibits comparable water permeability and salt rejection to other commercial PA membrane.

TABLE 10.2 Carbon-based nanoparticles incorporated in thin-film nanocomposite (TFN) reverse osmosis (RO) membrane preparation by interfacial polymerization (IP) process.

Nanomaterial	Amount of NPs (wt.%)	Pressure (bar)	Flux (LMH)	Performance enhanced	NaCl rejection (%)	References
MWCNTs	0.1	50	71	Permeate flux, antifouling, chlorine resistance	90	Inukai et al. (2015)
	0.1	50	6.5	Hydrophilicity, permeate flux, antifouling, salt rejection	99.7	Takizawa et al. (2017)
	0.001	15.5	51.15	Permeate flux, antifouling	97	Baek, Kim, Kim, Lee, and Yoon (2017)
	0.005	15	25.9	Hydrophilicity, permeate flux, antifouling, salt rejection	98.1	Farahbakhsh, Delnavaz, and Vatanpour (2017)
	0.7	10	11.4	Permeate flux, permeate flux, salt rejection	97.04	Hu et al. (2020)
CNT	0.1	7	7	Permeate flux	96	Takeuchi et al. (2018)
	0.00375	15.5	51.3	Hydrophilicity, permeate flux	98.5	Lee, Kim, Cho, and Park (2014)
	0.002	15.5	44	Hydrophilicity, permeate flux	95.4	Kim et al. (2014)
Carboxy-functionalized MWCNT	0.1	16	28	Hydrophilicity, permeate flux, antifouling, chlorine resistance	>90	Zhao et al. (2014a)
Zwitterion functionalizedsingle-walled CNT (SWCNT)	0.2	36.5	48.5	Hydrophilicity, permeate flux, salt rejection	98.6	Chan et al. (2013)
GO	0.0038	15.5	16.5	Hydrophilicity, permeate flux, antifouling, chlorine resistance	99.3	Chae, Lee, Lee, Kim, and Park (2015)
	0.01	15	39	Hydrophilicity, permeate flux, antifouling chlorine resistance	≥97	Ali, Wang, Wang, and Feng (2016)

(*Continued*)

TABLE 10.2 (Continued)

Nanomaterial	Amount of NPs (wt.%)	Pressure (bar)	Flux (LMH)	Performance enhanced	NaCl rejection (%)	References
	0.06	20	31.8	Hydrophilicity, permeate flux, antifouling chlorine resistance	98.8	Hamdy and Taher (2020)
p-aminophenolmodified GO	0.005	15	23.6	Hydrophilicity, permeate flux, salt rejection	99.7	Zhang et al. (2020a)
Carbon dots(CD)	0.02	15.5	88.7	Hydrophilicity, permeate flux, antifouling, salt rejection	98.8	Li, Li, and Zhang (2017a)
Graphene oxide quantum dots (GOQD)	0.01	16	37.4	Hydrophilicity, permeate flux, antifouling chlorine resistance	98.8	Song, Zhou, Zhang, Xu, and Wang (2016)
Nitrogen-doped GOQD (N-GOQD),	0.02	15	24.9	Hydrophilicity, permeate flux	93	Fathizadeh et al. (2019)
Na-CQDs	1	15	64	Hydrophilicity, permeate flux, antifouling	98.6	Gai et al. (2019)
Sulfonic decoration on GOQD (S-d-GOQD)	0.5	15	88.35	Hydrophilicity, permeate flux, salt rejection	97.1	Shen et al. (2020)
Graphite carbon	0.004	16	73.4	Hydrophilicity, permeate flux, antifouling,salt rejection	99.04	Zhang, Wang, Wei, Gao, and Zhu (2020b)
Graphitic carbon nitride	0.005	15	91.8	Hydrophilicity, permeate flux, antifouling	98.1	Seyyed Shahabi, Azizi, Vatanpour, and Yousefimehr (2020)

Zhao et al. (2014a) developed the nanocomposite with MWCNTs functionalized by Carboxylic acid group in PA RO membrane. It was prepared by IP process of TMC (0.1 wt.%) and MPD (2 wt.%) solution. 0.1 wt.% MWCNT was added in MPD solution before IP process to prepared nanocomposite membrane. To improve the chemical activity and dispersity pure MWCNTs were processed with mixed acid and then adjusted with diisobutyryl peroxide. They reported that prepared nanocomposite membrane had 100–300 nm skin PA layer and

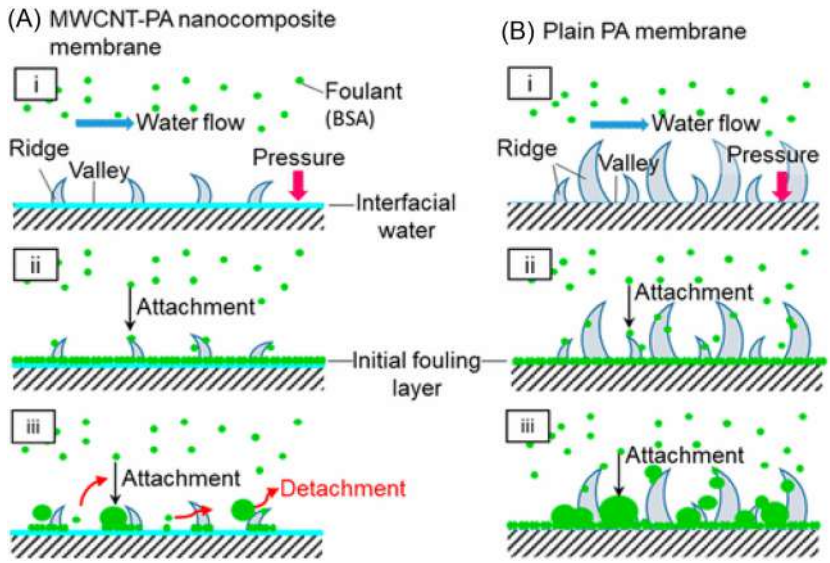

FIGURE 10.5 Foulants attachment over (A) the MWCNT-PA nanocomposite membrane, and (B) plain PA membrane. Source: *Adapted from Takizawa, Y., Inukai, S., Araki, T., Cruz-Silva, R., Uemura, N., Morelos-Gomez, A., … Endo, M. (2017). Antiorganic fouling and low-protein adhesion on reverse-osmosis membranes made of carbon nanotubes and polyamide nanocomposite.* ACS Applied Materials and Interfaces, 9, *32192–32201. https://doi.org/10.1021/acsami.7b06420*.

MWCNTs are incorporated in that layer. The incorporation of MWCNT in PA layer improves the membrane antifouling properties. They observed that MWCNT PA membrane surface have more negative charge compared to pristine PA membrane. They also found that increase concentration of MWCNT in PA layer leads to change the membrane morphology and enhanced permeated flux without compromising solute rejection. It is also noted that this MWCNT membrane shows better antifouling as well as antioxidative property compared to other PA membrane. This investigation indicates that incorporation of modified MWCNT in PA membrane is improving the performance of the membrane for salt rejection.

Baek et al. (2017) studied the effects of CNT in PA TFN RO membrane. They reported that surface characteristics and antifouling properties of membrane improved by incorporation of CNT in PA layer over the membrane surface. This membrane exhibits 30% increase in water flux, leads to low energy consumption. The illustrative of CNT-based PA TFC membrane is presented in Fig. 10.6.

It is interesting to note that specific energy consumption (SEC) of CNT TFN RO membrane is less as the permeate flux is high compared to other commercial TFC RO membrane. SEC is directly related to electric energy requirement for generating permeate. SEC versus different NaCl concentrations of the CNT-based PA TFN membrane with commercially used RO membrane and PA TFC RO membrane are presented in Fig. 10.7A. It is evident from Fig. 10.7A that CNT-based TFN RO membrane required less energy compared to other commercial RO membrane or PA TFC RO membrane. Kim et al. (2014) developed CNT incorporated in PA to prepared TFN RO membrane. Water transport through the PA-CNT membrane is presented in Fig. 10.7B.

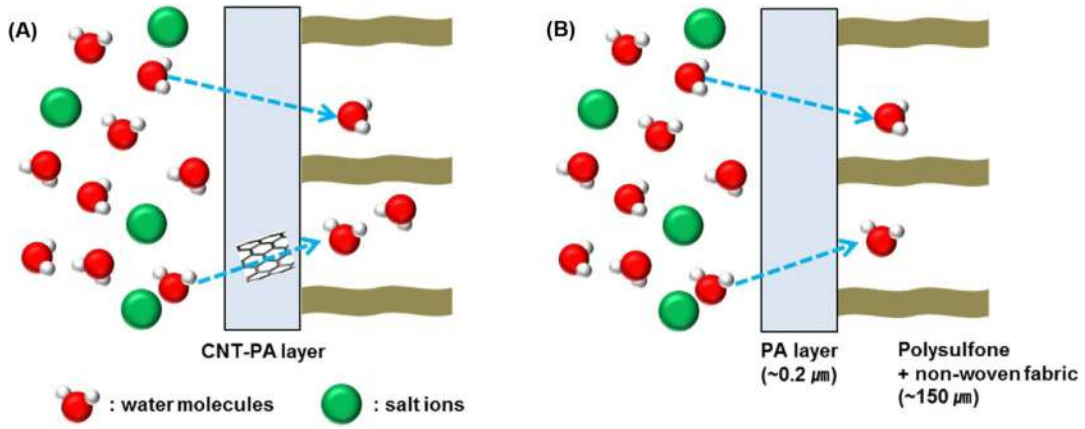

FIGURE 10.6 Illustrative of (A) carbon nanotube (CNT) based polyamide (PA) and (B) PA thin-film composite (TFC) reverse osmosis (RO) membrane. Source: *Adapted from Baek, Y., Kim, H. J., Kim, S.-H., Lee, J.-C., & Yoon, J. (2017). Evaluation of carbon nanotube-polyamide thin-film nanocomposite reverse osmosis membrane: Surface properties, performance characteristics and fouling behavior*. Journal of Industrial and Engineering Chemistry, 56, 327–334. https://doi.org/10.1016/j.jiec.2017.07.028.

Single-walled carbon nanotubes (SWCNTs) modified using chainlike zwitterion groups is also utilized to prepared TFN RO membrane (Chan et al., 2013). Zwitterions groups in SWCNT impart both negative and positive charge in the membrane surface by incorporating in PA layer. This leads to improve the membrane permeability, antifouling characteristics, and salt rejection.

10.3.1.2 Graphene oxide

Recent days, Graphene embedded membranes have been gaining interest to membrane scientists due to several unique features such as excellent water transport in graphene nanochannels and charge imparted by Graphene. These nanomaterials have been extensively used in membrane for water treatment, mainly used in desalination. Additionally graphene-based nanomaterials exhibit antifouling and antimicrobial properties, which is utilized for the fabrication of TFC membrane (Chae et al., 2015; Fathizadeh et al., 2019). Graphene oxide (GO) is prepared by Hummers or Staudenmaier technique (Lomeda, Doyle, Kosynkin, Hwang, & Tour, 2008). GO exhibits better hydrophilicity and forms suspension in water and therefore it is regarded as a promising candidate for making nanocomposite MMM (Zhan et al., 2015; Zhao, Xu, Chen, & Yang, 2014b). GO can also be used for preparing TFN PA RO membrane for desalination. Several studies are reported preparation and application of TFN RO membrane by incorporation of GO in PA layer. Both antifouling and antimicrobial properties of GO have been utilized in TFN membrane to minimized biofoluing (Perreault et al., 2016). Additionally, membrane mechanical strength can be enhanced by incorporation of GO in polymer matrix. Several researches show that addition of GO in PA layer can improve the permeability of the TFN RO membrane. Chae et al. (2015) reported high permeate flux, anti-biofouling, and chorine resistance GO-embedded TFC RO membrane. They prepared the PA nanocomposite membrane by IP between MPD and TMC solution, where optimized

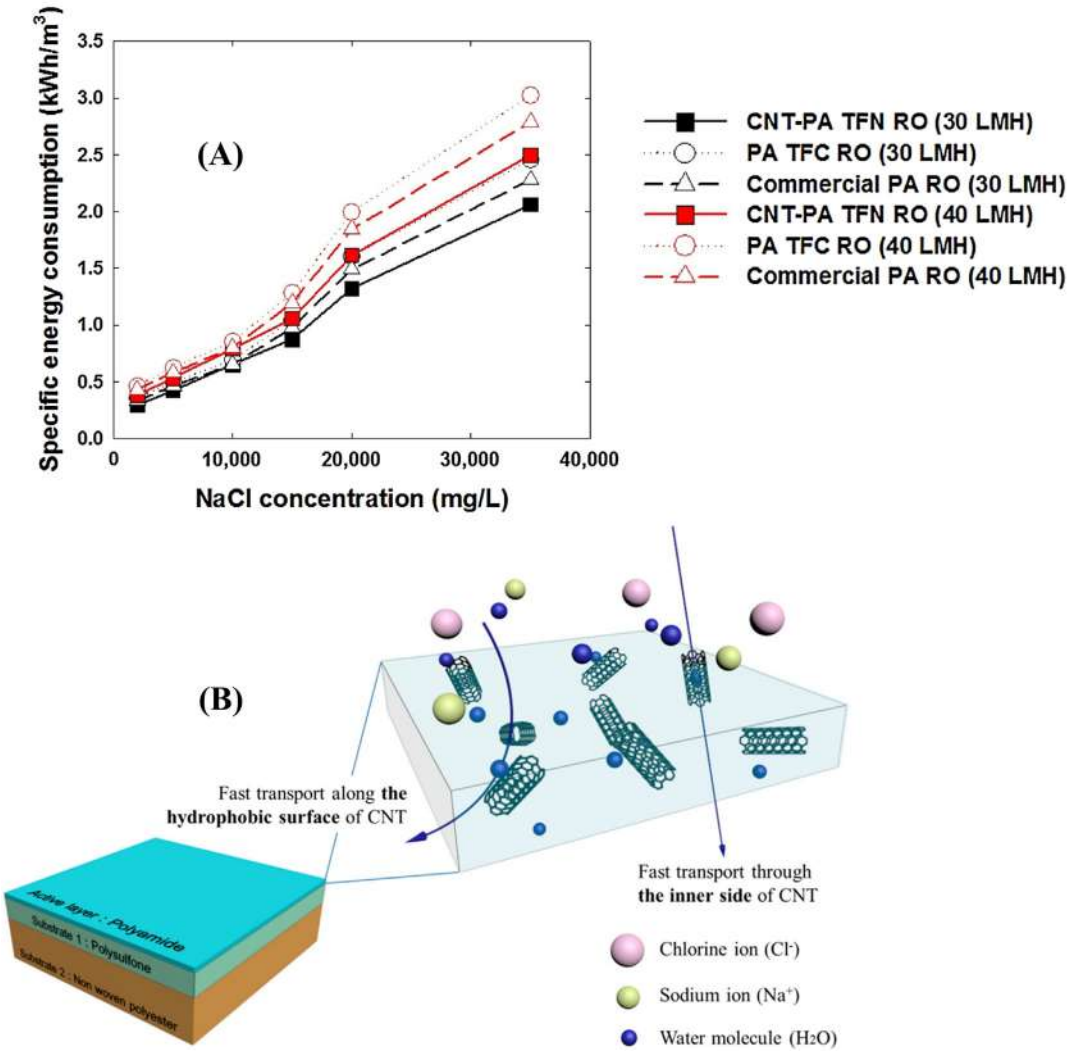

FIGURE 10.7 (A) Specific energy consumption (SEC) of different membranes; (B) schematic representation of transport of water molecules through polyamide (PA) carbon nanotube (CNT) membrane. Source: *Adapted from (A) Baek, Y., Kim, H. J., Kim, S.-H., Lee, J.-C., & Yoon, J. (2017). Evaluation of carbon nanotube-polyamide thin-film nanocomposite reverse osmosis membrane: Surface properties, performance characteristics and fouling behavior.* Journal of Industrial and Engineering Chemistry, 56, 327–334. https://doi.org/10.1016/j.jiec.2017.07.028; *(B) Kim, H. J., Choi, K., Baek, Y., Kim, D.-G., Shim, J., Yoon, J., & Lee, J.-C. (2014). High-performance reverse osmosis CNT/polyamide nanocomposite membrane by controlled interfacial interactions.* ACS Applied Materials and Interfaces, 6, 2819–2829. https://doi.org/10.1021/am405398f.

concentration of GO (40 ppm) are included in MPD solution. They found that incorporation of GO in PA layer increases the water flux and antifouling characteristics of the membrane. Salt rejection by these membranes is almost comparable with the pristine TFC membrane. It

is interesting to note that membrane surface roughness, surface charge, hydrophilicity, and thickness of PA layer change due to inclusion of GO in TFC, leads to enhance the membrane performance. GO-based TFN membrane exhibits enhanced antifouling characteristics due to membrane surface smoothness, surface charge, and hydrophilicity (Bernstein, Belfer, & Freger, 2011; Goosen et al., 2005; Pang, Hong, Guo, & Liu, 2005). Permeate flux of the GO-based TFC membrane increased to 32.5 from 9.18 L m^{-2} h. Salt rejection of the both with or without GO TFC membrane is comparable.

Ali et al. (2016) developed GO-embedded TFC membrane for water desalination. These composite membranes are prepared by IP process between MPD and TMC solution, where optimized concentration of GO (100 ppm) are added in MPD solution to prepared nanocomposite membrane. The interaction between MPD and TMC during IP process as well as incorporation of GO in PA layer is illustrated in Fig. 10.8. Incorporation of GO in PA layer enhance hydrophilicity of the membrane leads to enhance permeate flux of the membrane.

Yin, Zhu, and Deng (2016) developed a GO-enhanced PA TFN membrane by IP process between aqueous MPD and organic TMC-GO solution. They dispersed the GO nanosheets in the TMC-hexane solution during the IP process and vary the concentration of GO from 0 to 0.02 wt.%. They found that up to 0.015 wt.% GO embedded in PA enhanced the permeability of the membrane because inclusion of GO in PA layer enhanced hydrophilicity; hence, permeate flux increases. Schematic of hypothesized mechanism of GO TFNC membrane is represented in Fig. 10.9. It is evident from Fig. 10.9 that interlayer spacing within GO nanosheets may help the pass of water through the PA thin-film layer leads to enhanced flux. Numerous studies show that GO-incorporated PA TFN membrane may enhance antifouling, antimicrobial, physicochemical properties, as well as transport properties. These types of membranes can be used for desalination application.

Raval and Das reported the novel approach to bind GO over polyamide layer by posttreatment. The polyamide membrane was treated with sodium hypochlorite solution and subsequently subjected to aqueous suspension of GO. It was anchored by crosslinking with *N*-hydroxysuccinimide. This approach did not require any modification in membrane making but imparted GO by posttreatment (Raval & Das, 2017).

10.3.1.3 Quantum dots

Quantum dots are the recent development in the area. The preparation procedure of CQD is easy and inexpensive compared to other carbon nanomaterials. CQD can be utilized for TFN membrane preparation due to their unique feature such as small size, excellent biocompatibility, flexible hydrophilicity, and ample surface functional group. Many research groups have utilized CQD in RO TFN preparation due to these unique advantages.

Song et al. (2016), utilized Graphene oxide quantum dots (GOQDs) in TFN RO membrane preparation by IP process. They dispersed GOQD in MPD solution, and formed PA over PSF substrate by IP reaction between MPD and TMC solution for TFN RO preparation. GOQD/MPD suspension was first filtered by vacuum filtration onto the PSF substrate, in order to obtain a cushion layer over the membrane surface. Schematic of preparation process of GOQD-embedded RO membranes with the applied of pressure is presented in Fig. 10.10A. GOQD-incorporated TFN RO membrane exhibits better permeate flux without compromise the solute rejection compared to pristine TFC membrane. They also found that antifouling and chlorine resistance properties are enhance by inclusion of GOQD in PA layer.

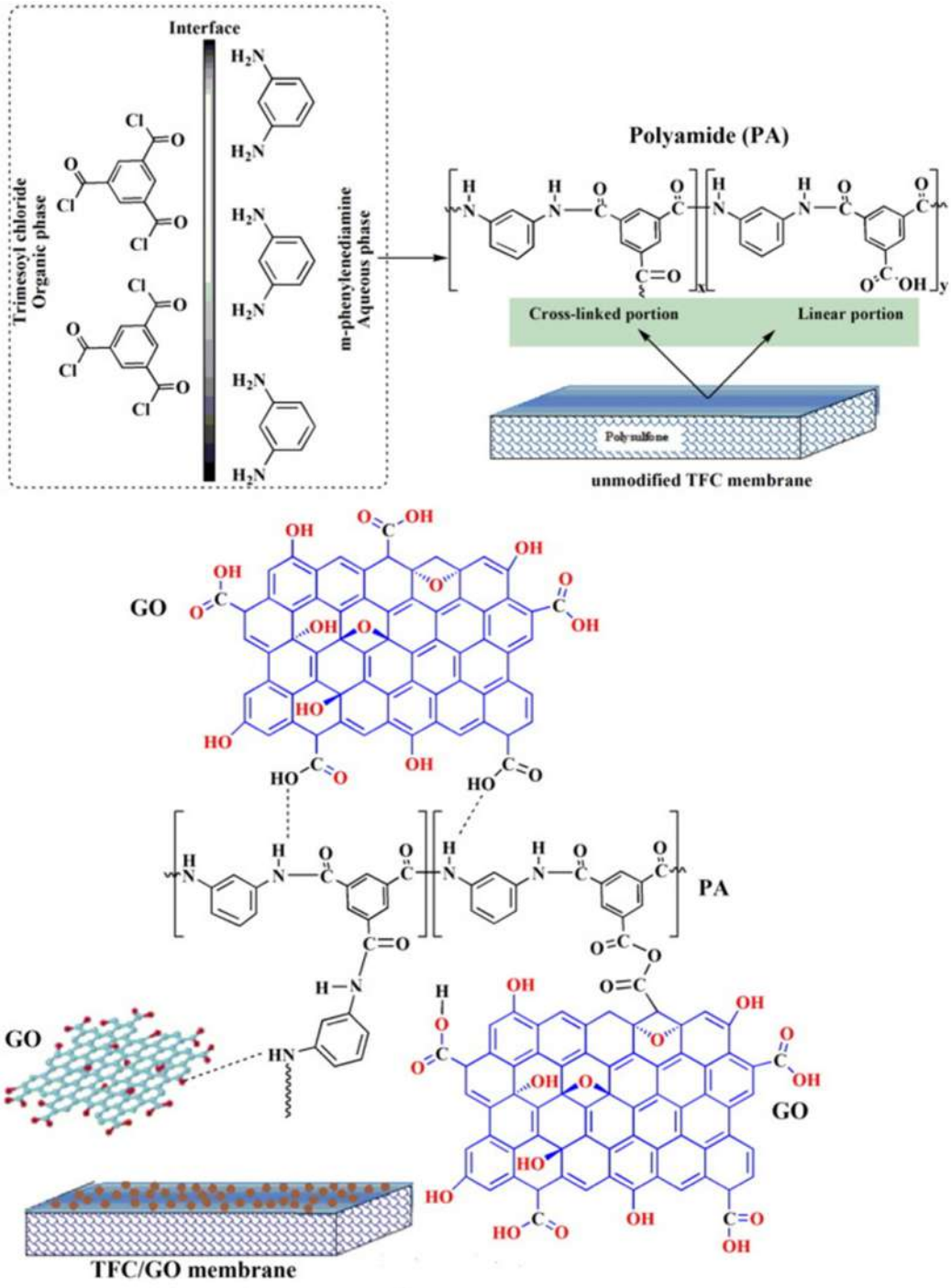

FIGURE 10.8 Schematic views of interfacial polymerization. Source: *Adapted from Ali, M. E. A., Wang, L., Wang, X., & Feng, X. (2016). Thin film composite membranes embedded with graphene oxide for water desalination.* Desalination, 386, 67–76. https://doi.org/10.1016/j.desal.2016.02.034.

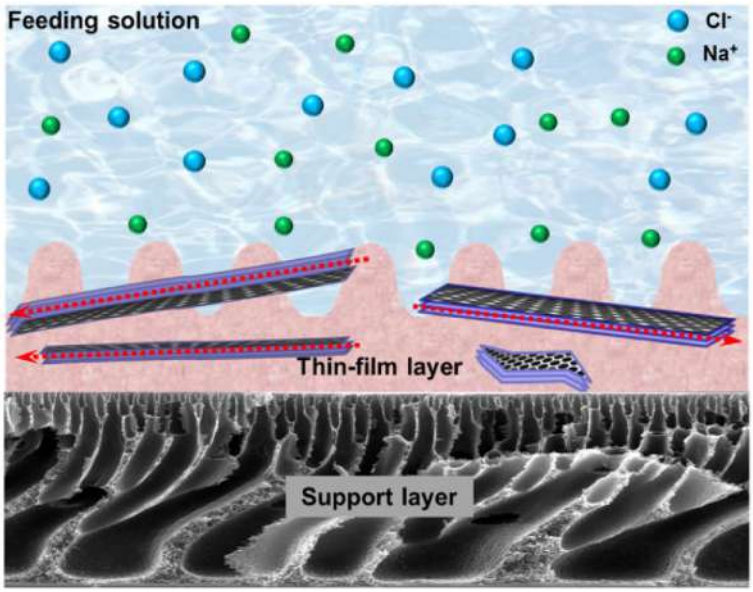

FIGURE 10.9 Illustrative representation of mechanism of graphene oxide (GO) thin-film nanocomposite (TFN) membrane. Source: *Adapted from Yin, J., Zhu, G., & Deng, B. (2016). Graphene oxide (GO) enhanced polyamide (PA) thin-film nanocomposite (TFN) membrane for water purification.* Desalination, 379, 93–101. https://doi.org/10.1016/j.desal.2015.11.001.

Li et al. (2017a) investigated the influence of CQD on PA TFN RO membrane. CQDs are dispersed in MPD solution followed by IP between MPD and TMC solution to prepared nanocomposite membrane. They found that incorporation of CQDs in PA layer enhanced permeate flux without affecting the solute rejection. CQDs contain carboxyl group which interact with the amine group of MPD solution and remaining carboxyl group formed covalent bond with the terminal acyl chloride groups of TMC in the IP to prepared TFN membrane. Schematic of interaction between CQD and PA layer is illustrated in Fig. 10.10B.

Fathizadeh et al. (2019) developed a high flux TFN RO membrane by utilizing nitrogen-doped GOQD (N-GOQD) as nanomaterials which in incorporated in PA layer. They prepared these novel N-GOQD nanoparticles and first time used these nanoparticles for the preparation of TFN RO for desalination application. They found that incorporation of 0.02 wt.% N-GOQD in PA membrane increased permeate flux 3 times compared to nascent PA membrane and the salt rejection is comparable. Different concentrations varying from 0 to 0.1 wt.% N-GOQD are dispersed in MPD solution to prepared PA TFN membrane by IP process. Concentration variation of N-GOQD in PA layer is represented in Fig. 10.10C. It can be note that from Fig. 10.10C at higher N-GOQD concentration, hydrophilicity is enhanced to enhance the permeate flux. In addition, incorporation of N-GOQD increases the thermal stability of the membrane.

10.3.2 Metal and metal oxides based

Metal oxides are also important nanomaterials being used in membrane. Metal- and metal oxides-based nanoparticles incorporated in TFN RO membranes are summarized in Table 10.3.

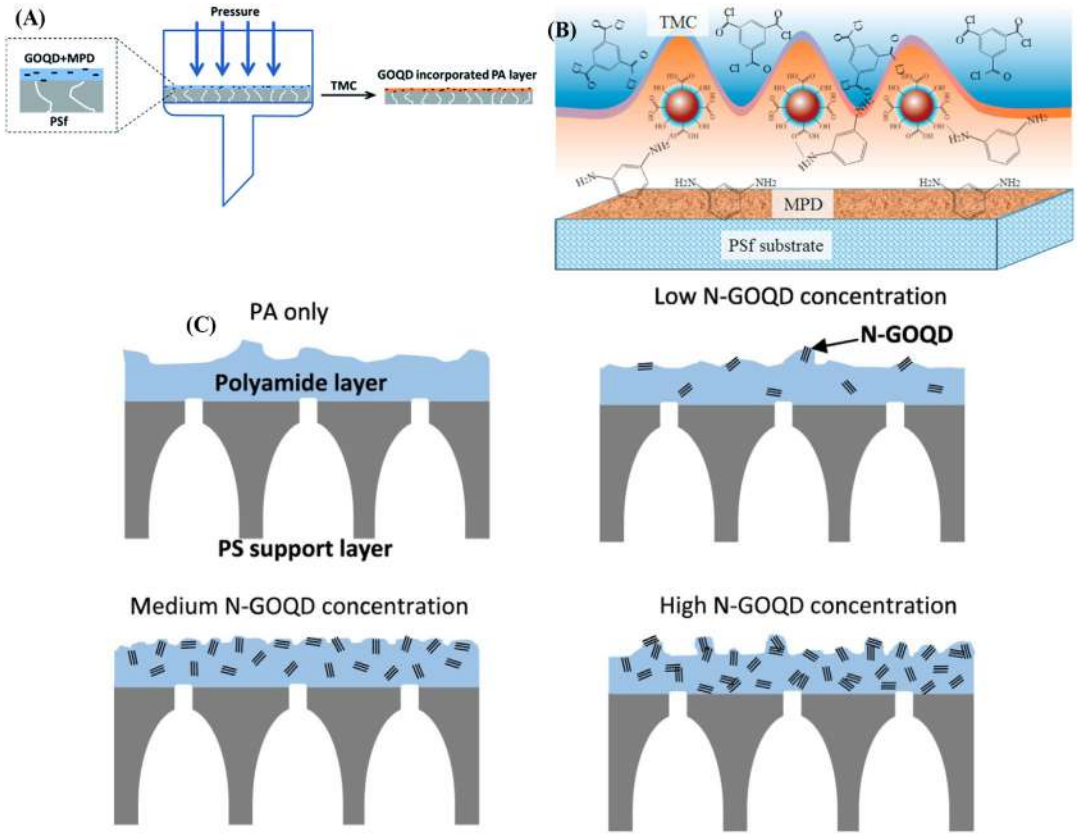

FIGURE 10.10 (A) Schematic representation of preparation process of graphene oxide quantum dots (GOQD) embedded reverse osmosis (RO) membranes with the applied pressure; (B) schematic representation of interaction between carbon quantum dots (CQD) and polyamide (PA) layer; (C) schematic representation of quantum dots. Source: *Adapted from (A) Song, X., Zhou, Q., Zhang, T., Xu, H., & Wang, Z. (2016); (B) Li, Y., Li, S., & Zhang, K. (2017a). Influence of hydrophilic carbon dots on polyamide thin film nanocomposite reverse osmosis membranes.* Journal of Membrane Science, 537, *42–53. https://doi.org/10.1016/j.memsci.2017.05.026; (C) Fathizadeh, M., Tien, H. N., Khivantsev, K., Song, Z., Zhou, F., & Yu, M. (2019). Polyamide/nitrogen-doped graphene oxide quantum dots (N-GOQD) thin film nanocomposite reverse osmosis membranes for high flux desalination.* Desalination, 451, *125–132. https://doi.org/10.1016/j.desal.2017.07.014. Pressure-assisted preparation of graphene oxide quantum dot-incorporated reverse osmosis membranes: Antifouling and chlorine resistance potentials.* Journal of Materials Chemistry A, 4, *16896–16905. https://doi.org/10.1039/C6TA06636D*.

10.3.2.1 Silver

Silver (Ag) nanoparticles have tremendous antimicrobial property. Recent days Ag nanoparticles have been utilized for antifouling membrane preparation (Ben-Sasson et al., 2014a; Park et al., 2016). Several studies reported that Ag nanoparticles are doped over the PA layer of TFC membrane. Different methods are applied for Ag nanoparticles impregnated onto the PA TFC membrane. One of the methods is chemical immobilization of Ag nanoparticles onto the PA membrane surface with enhanced antimicrobial properties

TABLE 10.3 Metal- and metal oxides-based nanoparticles incorporated thin-film nanocomposite (TFN) reverse osmosis (RO) membrane preparation by interfacial polymerization (IP) process.

Nanomaterial	Amount of NPs (wt.%)	Pressure (bar)	Flux (LMH)	Performance enhanced	NaCl rejection (%)	References
Silver	–	27.5	58.3	Antifouling	98.64	Ben-Sasson et al. (2014a)
	–	20	50	Permeate flux, salt rejection	99.1	Yang, Guo, Yao, Mei, and Tang (2019)
	–	15.5	52.91	Hydrophilicity, permeate flux, salt rejection	99.18	Dong et al. (2017)
	–	15.5	31	Hydrophilicity, permeate flux, antifouling	99.4	Jeon and Lee (2020)
Copper	–	27.5	82.5	Permeate flux	98.31	Ben-Sasson, Lu, Nejati, Jaramillo, and Elimelech (2016)
	1	20.7	45.12	Hydrophilicity, permeate flux, antifouling	97.4	García et al. (2018)
Titanium dioxide (TiO_2)	0.015	15.5	40.14	Hydrophilicity, permeate flux,salt rejection	99.72	El-Aassar (2014)
	0.0125	15.2	24.3	Hydrophilicity, permeate flux, antifouling	97.7	Khorshidi, Biswas, Ghosh, Thundat, and Sadrzadeh (2018)
Titanate nanotubes (TNT)	0.05	15	36.74	Hydrophilicity, permeate flux,salt rejection, antifouling	96.53	Emadzadeh et al. (2015)
Zinc oxide (ZnO)	0.009	15.5	48	Permeate flux, salt rejection	99	Ghoul, Ghiloufi, Al-Hobaib, and El Mir (2017)
	0.03	20	25.6	Hydrophilicity, permeate flux, antifouling, chlorine resistance, salt rejection	99.3	Rajakumaran et al. (2019)
	0.02	20	23.85	Hydrophilicity, permeate flux, antifouling	97	Rajakumaran, Kumar, and Chetty (2020)
Alumina (Al_2O_3)	1	10	4	Hydrophilicity, permeate flux, antifouling, salt rejection	88	Saleh and Gupta (2012)
MOF-based-ZIF-8	0.4	15.5	52	Hydrophilicity, permeate flux, salt rejection	99.5	Duan et al. (2015)
	0.4	15	34.5	Hydrophilicity, permeate flux, salt rejection	99.4	Aljundi (2017)
	0.2	15.5	61.2	Permeate flux, salt rejection	99.2	Lee et al. (2019)

(*Continued*)

TABLE 10.3 (Continued)

Nanomaterial	Amount of NPs (wt.%)	Pressure (bar)	Flux (LMH)	Performance enhanced	NaCl rejection (%)	References
0.005	16	17.6		Hydrophilicity, permeate flux	99.8	Li et al. (2020)
0.15	20	52.2		Hydrophilicity, permeate flux, salt rejection	98.6	Zhao, Zhao, and Chung (2021)
MOF-based UiO-66	0.05	15.5	56.9	Hydrophilicity, Permeate flux, salt rejection	99.35	Liu et al. (2019)
MOF-based UiO-66-NH_2	0.02	20	40	Hydrophilicity, permeate flux, salt rejection,chlorine resistance	99.2	Zhao, Yeung, Zhao, and Chung (2020b)
MOF-based MIL-101	0.05	16	36	Hydrophilicity, permeate flux, salt rejection	99.1	Xu et al. (2016)
MOF-based MIL-125	0.3	20.7	74.9	Hydrophilicity, permeate flux, salt rejection	>98.5	Kadhom, Hu, and Deng (2017)
MOF-based PCN-222	0.01	17.2	5.8	Permeate flux	94.5	Bonnett et al. (2020)
Zirconium metal − organic cages (Zr-MOCs)	0.06	15.5	22.79	Hydrophilicity, permeate flux	94.7	Liu et al. (2021)

(Wijnhoven et al., 2009). Other studies reported that Ag nanoparticles were attached to PA TFC membrane by covalent bonding, where cysteamine was used as a linking agent.

The aforementioned method is ex situ process for impregnation of Ag nanoparticles in PA TFC membrane. These ex situ processes have some drawbacks such as required extra capping agents, difficulty in the presynthesis process, and cost-expensive. Therefore in situ impregnation of Ag nanoparticles in PA layer of TFC membrane is important. Ben-Sasson et al. (2014a) reported new procedure for inclusion of Ag nanoparticles on TFC RO membrane. They irreversibly bound the Ag nanoparticles on the membrane by reacting silver salt ($AgNO_3$) reduction with $NaBH_4$ followed by IP process. These Ag nanoparticles embedded TFC membrane shows better antimicrobial activity compared to virgin TFC membrane.

Similar methods have been used by Yang et al. (2019) for incorporation of Ag nanoparticles on TFC RO membrane. Schematic of this procedure is illustrated in Fig. 10.11A and B. It is noted that from Fig. 10.11A and B, the formation of nanochannels in PA layer due to Ag nanoparticles enhances water permeability 3 times compared to pristine PA membrane.

Dong et al. (2017) presented an approach for the in situ immobilization of Ag nanoparticles on the TFC RO membrane via two-step surface modifications. This procedure is presented in Fig. 10.11C. Presence of Ag nanoparticles in RO membrane exhibits better antimicrobial characteristics over pristine RO membrane. Also flux and salt rejection enhance by immobilization of Ag nanoparticles on the RO membrane surface.

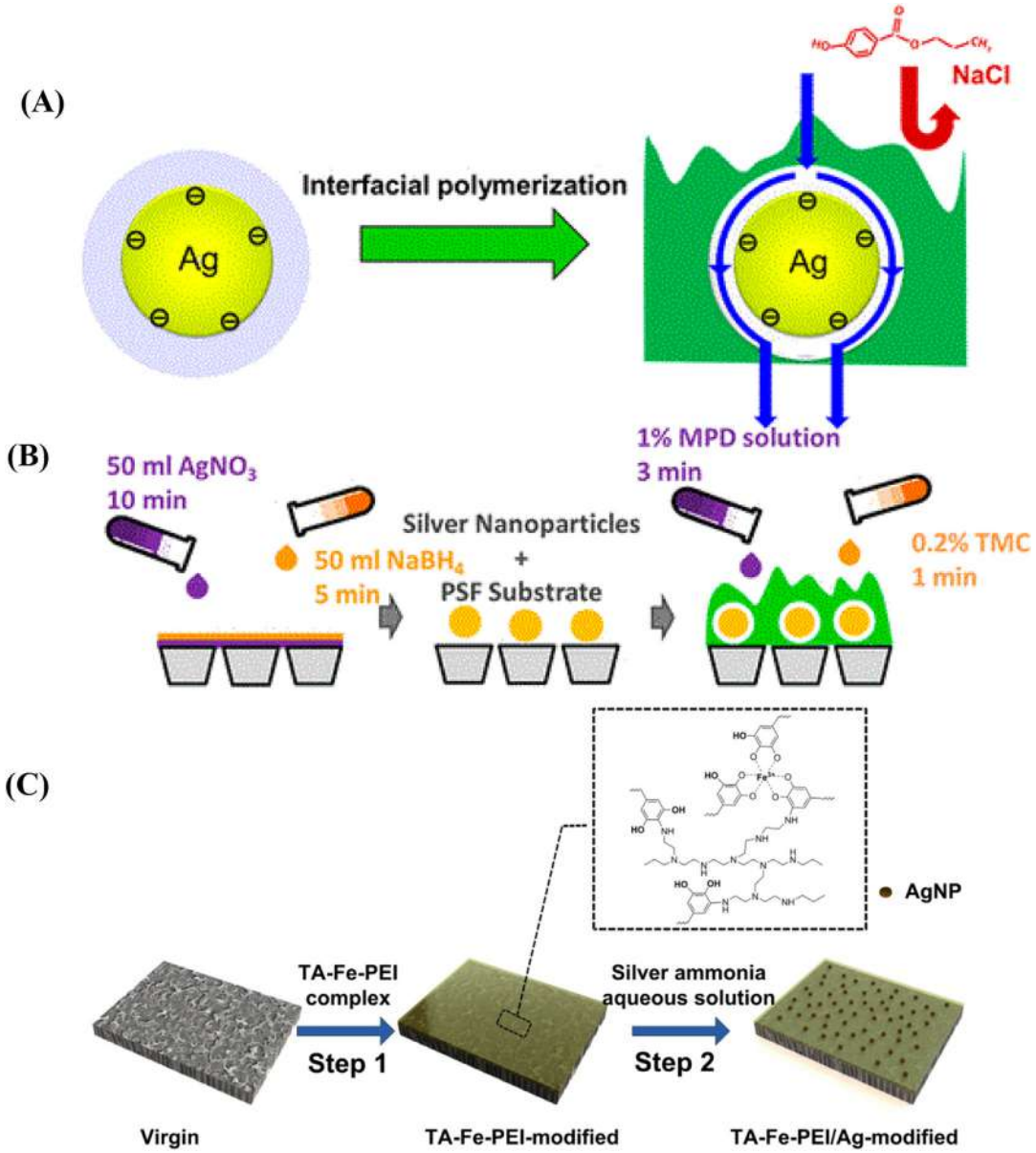

FIGURE 10.11 (A) Illustrative representation of mechanism of Ag nanoparticles-induced nanochannels in the polyamide (PA) layer for efficient water transport; (B) illustrative representation of fabricating Ag nanoparticles incorporated thin-film nanocomposite (TFN) membranes; (C) illustrative representation of the in situ immobilization of Ag nanoparticles onto the reverse osmosis (RO) membrane surface. Source: *Adapted from (A-B) Yang, Z., Guo, H., Yao, Z., Mei, Y., & Tang, C. Y. (2019). Hydrophilic silver nanoparticles induce selective nanochannels in thin film nanocomposite polyamide membranes.* Environmental Science and Technology, 53, *5301–5308; (C) Dong, C., Wang, Z., Wu, J., Wang, Y., Wang, J., & Wang, S. (2017). A green strategy to immobilize silver nanoparticles onto reverse osmosis membrane for enhanced anti-biofouling property.* Desalination, 401, *32–41.* https://doi.org/10.1016/j.desal.2016.06.034. https://doi.org/10.1021/acs.est.9b00473.

10.3.2.2 Copper

Copper (Cu) nanoparticles have tremendous antimicrobial property and it is abundantly found hence, economical compared to silver nanoparticles. Recently, Cu nanoparticles have been extensively utilized in membrane technology for improving antifouling and antimicrobial properties (Akar, Asar, Dizge, & Koyuncu, 2013; Ben-Sasson et al., 2014b). Generally, Cu nanoparticles are used in membrane technology as nanofiltration or UF application (Isloor et al., 2013; Zareei & Hosseini, 2019). Few literatures are available for use of Cu nanoparticles in RO membrane application. One study reported incorporation of Cu nanoparticles in PA TFC membrane by dip-coating technique (Ben-Sasson et al., 2014b). In other studies in situ immobilization of Cu nanoparticles in TFC membrane is reported. Ben-Sasson et al. (2016) developed a novel technique for immobilization of biocidal Cu nanoparticles over the TFC RO membrane surface. Effects of in situ Cu nanoparticles modification in membrane for salt permeability as well as water permeability are minimal due to Cu nanoparticles presence over the membrane surface providing enhanced antimicrobial property. Cu nanoparticles embedded membrane exhibits 90% reduction in the amount of attached live *Escherichia coli*, compared to pristine membrane.

García et al. (2018) reported antifouling TFC RO membrane developed by incorporation of copper oxide (CuO) nanoparticles into PA layer. Resultant membranes have been utilized for desalination application. They found that water permeability of newly membrane enhanced, relative to pristine TFC membrane. Hydrophilicity of membrane also increases by inclusion of CuO nanoparticles in PA layer. Antifouling properties are also enhanced by this CuO nanoparticles embedded TFC membrane without affecting the salt rejection.

10.3.2.3 Titanium dioxide

Recently, titanium dioxide (TiO_2) nanoparticles have been extensively utilized in membrane modification due to their antifouling properties (Keshmiri, Mohseni, & Troczynski, 2004; Wu, 2004). Additionally, TiO_2 nanoparticles can be used as photo-catalytic material, which can disintegrate the organic compounds and reduce the generation of biofilms over the membrane surface. Several studies reported the utilization of TiO_2 nanoparticles in TFN RO membrane modification to enhance antifouling properties. El-Aassar (2014) reported that TiO_2 nanoparticles incorporated in PA layer of TFN membrane. They dispersed TiO_2 nanoparticles either in organic solution (TMC-hexane) or aqueous solution (MPD) for before IP process. Newly developed TFN membrane permeability, salt rejection, as well as antifouling property enhance due to incorporation of TiO_2 nanoparticles in PA layer. Hydrophilicity of the TFN membrane also enhanced.

Khorshidi et al. (2018) prepared a thermally stable and antifouling TFN RO membrane by incorporation of TiO_2 nanoparticles in PA matrix. They performed the filtration test under room temperature as well as 65°C temperatures to investigate the thermal stability of the newly synthesized TFN membrane. They found that permeate flux and salt rejections of TFN membrane is higher at high operating temperature. Thermal stability of the TFN membrane is represented in Fig. 10.12A and B. It can be found that permeate flux and salt rejection of the TFN membrane is enhanced compared to nascent TFC membrane. Antibiofouling properties of these membrane is also investigated. Biofouling can be quantified in terms of number of *E. coli* colonies count over the membrane surface.

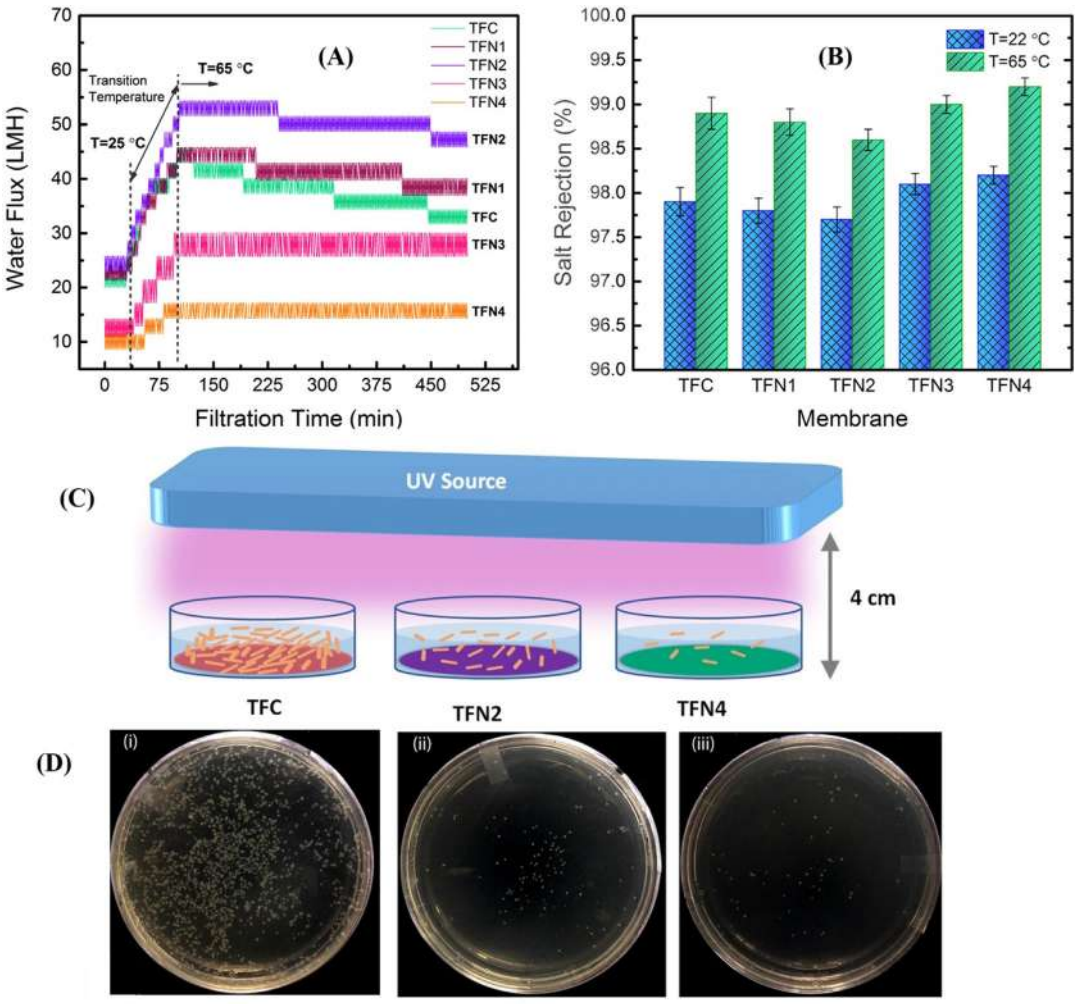

FIGURE 10.12 (A) Profile of water flux and (B) salt rejection of thin-film composite (TFC) and thin-film nanocomposite (TFN) membrane operated at room and 65°C temperatures; (C) antibacterial property of TFN membranes; (D) photograph of the *Escherichia coli* colonies formed in the plate of UV-treated (i) TFC, (ii) TFN2, and (iii) TFN4 membranes. Source*: Adapted from Khorshidi, B., Biswas, I., Ghosh, T., Thundat, T., & Sadrzadeh, M. (2018). Robust fabrication of thin film polyamide-TiO_2 nanocomposite membranes with enhanced thermal stability and anti-biofouling propensity*. Scientific Reports, 8, *784*. https://doi.org/10.1038/s41598-017-18724-w.

Antibacterial activity of TFC and TFN membrane is showed in Fig. 10.12C and D. It is found that under UV light TiO_2 nanoparticles embedded TFN membrane exhibit lower *E. coli* count relative to TFC membrane. This can be concluded that TiO_2 nanoparticles can be utilized as antifouling agent for membrane modification.

Emadzadeh et al. (2015) developed a TFN RO membrane by amino-functionalized titanate nanotubes (NH_2-TNT) nanoparticles doped in PA layer. NH_2-TNT nanoparticles

interact with acid chloride (-COCl) groups of TMC during IP process. Reaction between NH_2-TNT and acid chloride groups of polyamide is demonstrated in Fig. 10.13.

10.3.2.4 Zinc oxide

Zinc oxide (ZnO) nanoparticles can be utilized in membrane modification due to its antibacterial and photo-catalysis property. Several studies reported use of ZnO nanoparticles in TFN RO membrane preparation to enhanced antifouling property. ZnO nanoparticles preparation is very inexpensive compared to other biocidal nanoparticles. In addition, incorporation of ZnO nanoparticles in TFN membrane can enhanced the hydrophilicity of the membrane resulting permeate flux increases. Ghoul et al. (2017) developed a high flux

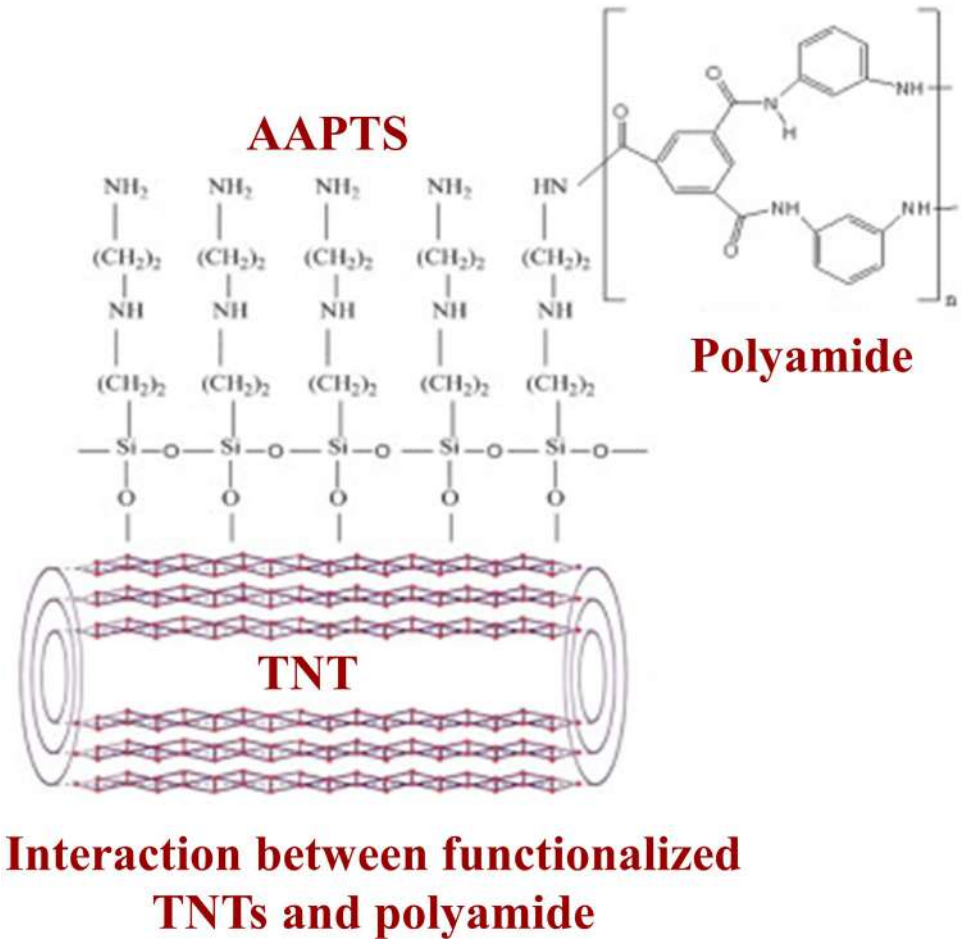

FIGURE 10.13 Illustrative of titanate nanotubes (NH_2-TNTs) incorporated polyamide (PA) layer formation. Source: *Adapted from Emadzadeh, D., Lau, W. J., Rahbari-Sisakht, M., Daneshfar, A., Ghanbari, M., Mayahi, A., … Ismail, A. F. (2015). A novel thin film nanocomposite reverse osmosis membrane with superior anti-organic fouling affinity for water desalination.* Desalination, 368, *106–113.* https://doi.org/10.1016/j.desal.2014.11.019.

antifouling TFN RO membrane by incorporation of ZnO nanoparticles in the PA layer using IP process. Hydrophilicity of the TFN membrane drastically improves by inclusion of ZnO nanoparticles in membrane surface. Therefore permeability of the membrane enhanced due to existence of the ZnO nanoparticles over membrane surface. It is also noted that salt rejection of TFN membrane is almost same as TFC membrane.

Rajakumaran et al. (2019) investigate the effects of different nanoparticles incorporation in TFN membrane with various morphology of polymer-based RO membrane. They developed different TFN RO membrane by inclusion of GO and amino-functionalized ZnO nanoparticles with different morphology, such as rod shaped (ZnO-R), flower (ZnO-F), and spherical (ZnO-S) nanostructure. They found that 0.02 wt.% of GO-ZnO TFN membranes exhibit enhanced permeability and hydrophilicity compared to pristine TFC membrane.

10.3.2.5 Alumina

Alumina (Al_2O_3) nanoparticles have been utilized for TFN RO membrane preparation for enhanced antifouling and hydrophilicity characteristics. Saleh and Gupta (2012) investigated the effects of Al_2O_3 nanoparticles incorporated in PA layer of TFN membrane. They found that salt rejection performance of Al_2O_3 nanoparticles-doped TFN membrane is better relative to pristine TFC membrane. They also reported that TFN membrane exhibit higher hydrophilicity due to inclusion of Al_2O_3 nanoparticles in PA layer, hence permeability of the membrane also enhanced. Antifouling characteristics of the TFN membrane increases because of Al_2O_3 nanoparticles presence on the membrane surface. In another study reported that hydrophilicity of the membrane enhanced by addition of zeolite in PA layer of the TFC membrane leads to enhanced permeate flux and antifouling property of the membrane (Jeong et al., 2007). Thus Al_2O_3 nanoparticles can be a promising candidate for the modification of TFN membrane.

10.3.2.6 Metal-organic frameworks

Metal-organic frameworks (MOFs) are recently developed hybrid materials which contain inorganic metal clusters or centers connected by organic linkers. These materials have variable framework with one, two, and three dimensional porous structure (Li et al., 2017b). MOFs can be utilized as porous filler because of their unique properties such as high surface area, high porosity, tuneable pore size, and convenient surface functionality. Several studies report that MOFs are used in MMM preparation for gas separation application. MOF can also be utilized in liquid separation application by MMM. Few studies show that development of TFN RO membrane by utilization of MOF in PA layer. MOF-incorporated PA membranes have some unique advantages, such as (1) pore structure and size of MOFs can be tuneable by altering the metal salt and organic ligands and (2) compatibility of MOFs with polymer is better due to organic linker present in MOFs have strong interactions with polymer (Li et al., 2017b; Zhu et al., 2017).

ZIFs is used in liquid separation membrane modification due to high water permeability, large surface area, and highly stable in water. Duan et al. (2015) prepared a high flux TFN RO membrane by incorporating ZIF-8 as nanofillers in PA layer. They found that inclusion of ZIF-8 in TFN membrane increases water permeate flux 162% higher than pristine PA membrane. In another study, Aljundi (2017) reported that addition of 0.4 wt.% ZIF-8 in PA layer enhanced the hydrophilicity of the membrane leads to enhanced permeate flux without affecting the ions

rejection. They also found that TFN membrane exhibit better antifouling relative to pristine PA membrane. Lee et al. (2019) reported the influence of ZIF-8 particle size incorporated in PA layer TFN membrane performance. They used different particle size (60, 150, 250 nm) of ZIF-8 nanoparticles for TFN preparation. TFN membrane was prepared by IP process on PSF substrate, where ZIF-8 nanoparticles were scattered in aqueous solution. Deposition of ZIF on PSF substrate is presented in Fig. 10.14.

Another, Zirconium-based MOF UiO-66 made by the central Zr (IV) ions and terephthalic acid ligands, has been utilized as a nanomaterials in TFN RO membrane preparation because of their good water stability (He, Tang, Ma, & Chung, 2017; Liu et al., 2019; Ma, Peh, Han, & Chen, 2017). Liu et al. (2019) prepared a high flux TFN by incorporating UiO-66 in PA layer. They found the presence of UiO-66 in PA layer enhanced water flux around 50% and comparable salt rejection relative to TFC membrane. Chromium-based MOF MIL-101 can also be utilized for the TFN RO membrane preparation due to good water stability. MIL-101 MOF provides bigger pore size along with surface area leads to extensive water flow channels (Duan et al., 2015). Xu et al. (2016) utilized MIL-101 for preparation of TFN RO membrane. These newly TFN have been tested for desalination application. They found that incorporation of 0.05 wt.% MIL-101 in TFN membrane enhanced water flux around 44% relative to pristine TFC membrane. Salt rejection by the novel TFN membrane is above 99%. Due to good water stability of MIL-101 nanoparticles have been extensively used in membrane modification for water purification. However, further research should be required to identify suitable MOF for chlorine resistance and antifouling membrane preparation.

Titanium-based MOFs MIL-125 has also been used to developed TFN membrane. Kadhom et al. (2017), utilized both MIL-125 and UiO-66 nanoparticles to prepared novel

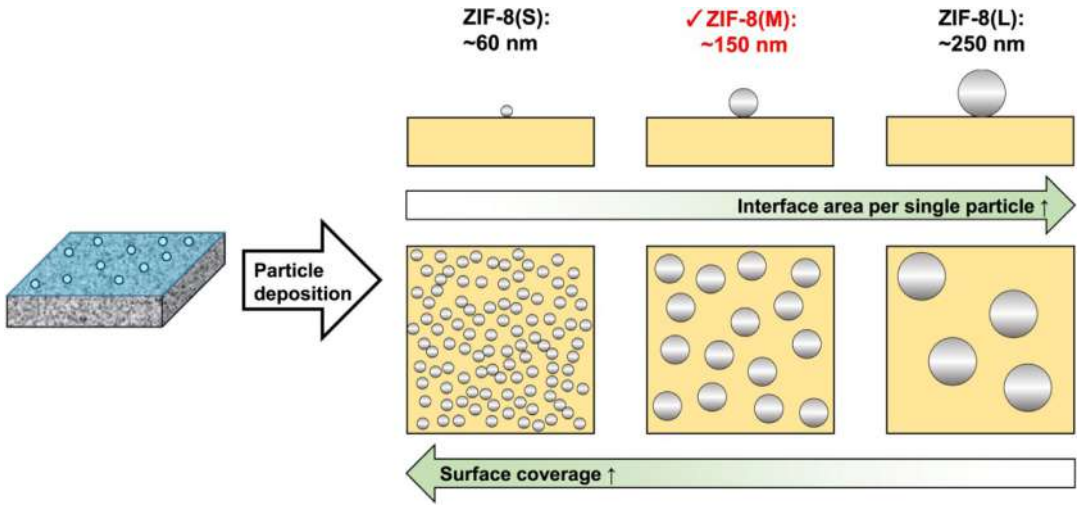

FIGURE 10.14 Schematic representation of ZIF-8 deposition on polysulfone (PSF) substrate. Source: *Adapted from Lee, T. H., Oh, J. Y., Hong, S. P., Lee, J. M., Roh, S. M., Kim, S. H., & Park, H. B. (2019). ZIF-8 particle size effects on reverse osmosis performance of polyamide thin-film nanocomposite membranes: Importance of particle deposition*. Journal of Membrane Science, 570–571, 23–33. *https://doi.org/10.1016/j.memsci.2018.10.015*.

TFN membrane. They also found that TFN membrane shows better permeate flux and salt rejection related to virgin TFC membrane. Thus these advanced MOF nanoparticles have great potential for preparation of TFN RO membrane and its application in water purification specifically desalination application.

10.3.3 Other nanoparticles

Different nanoparticles incorporated in TFN RO membranes are summarized in Table 10.4.

10.3.3.1 Silica

Silica (SiO_2) nanoparticles have been utilized in TFN RO membrane preparation for enhanced membrane performance, such as thermal stability, permeate flux. Generally, silica nanoparticles are low cost, thermally stable, and chemically inert. Jadav and Singh (2009) prepared thermally stable TFN membrane by addition of silica nanoparticles in situ into the PA layer. They found that pore size of PA layer can be adjustable depending on the concentration of silica nanoparticles. In another study, Peyki et al. (2015) incorporated SiO_2 nanoparticles into the PA layer to developed indigenous TFN RO membrane, which is tested with high pressure desalination application. They found that permeate flux increases from 30 to 50 L m^{-2} h^{-1} with SiO_2 nanoparticles concentration. Salt rejection of the membrane initially increases with SiO_2 nanoparticles concentration but after certain concentration it decreases. This can be noted that at higher concentration nanoparticles may agglomerate in PA layer resulting decreases in salt rejection. Pang and Zhang (2018) used hydrophobic fluorinated silica nanoparticles in TFN RO membrane preparation to enhanced salt rejection and water flux. They dispersed the nanoparticles in organic phase for IP process. They investigate the effects of fluorinated silica nanoparticles loading in PA layer with salt rejection and permeate flux. Salt rejection initially increases with nanoparticles concentration up to 0.1 wt.% but after that salt rejection decreases. They found that water flux continuously decreases with nanoparticles loading, due to hydrophobic nature of the fluorinated silica nanoparticles.

Shen, Wang, Xu, Zhou, and Gao (2018) proposed a new method for SiO_2- incorporated PA TFN membrane preparation. They prepared the TFN membrane by in situ IP process of aqueous amine and silicon tetrachloride ($SiCl_4$) solutions. This fabrication process is presented in Fig. 10.15. They found that water permeability of the membrane remarkably improved by addition of nanoparticles with minimal loss in the salt rejection.

10.3.3.2 Halloysite (aluminosilicate)

Several reports are available on utilization of HNT in MMM preparation for UF or nanofiltration application. Use of HNT in TFN RO application has very limited reported. Ghanbari et al. (2015) utilized the hydrophilic HNTs to developed high flux and antifouling TFN membrane. TFN membranes are prepared by the IP process where HNT nanoparticles are dispersed in organics phase. They found that HNT-incorporated TFN exhibit higher flux compared to pristine TFC membrane with comparable salt rejection (95.6%).

TABLE 10.4 Nanoparticles incorporated in thin-film nanocomposite (TFN) reverse osmosis (RO) membrane preparation by interfacial polymerization (IP) process.

Nanomaterial	Amount of NPs (wt.%)	Pressure (bar)	Flux (LMH)	Performance enhanced	NaCl rejection (%)	References
Silica (SiO_2)	0.04	17	21.3	Permeate flux, salt rejection	91.1	Jadav and Singh (2009)
	0.1	44	50	Hydrophilicity, permeate flux, antifouling	95	Peyki, Rahimpour, and Jahanshahi (2015)
Silica SBA-15	0.1	15	74.17	Hydrophilicity, permeate flux, salt rejection	98.5	Kalash, Kadhom, and Al-Furaiji (2020)
Alkyl capped silica	0.1	15.5	55.3	Permeate flux, salt rejection	99.6	Wu et al. (2020)
Halloysite nanotube (HNT)	0.05	15	36	Hydrophilicity, permeate flux, antifouling	95.6	Ghanbari, Emadzadeh, Lau, Matsuura, and Ismail (2015)
Zeolite A nanocrystals	0.4	12.4	17	Hydrophilicity, permeate flux, antifouling, salt rejection	93.9	Jeong et al. (2007)
Sodium zeolite Y (NaY)	0.75	15.5	74	Hydrophilicity, permeate flux, salt rejection	98.8	Dong et al. (2015)
NaA nano-zeolites	0.1	16	35	Permeate flux, salt rejection	97.5	Huang et al. (2013a)
Zeolite (NaX) nanocrystals	0.2	12	14.6	Hydrophilicity, permeate flux, salt rejection	96.4	Fathizadeh et al. (2011)
S-beta zeolite	0.05	20.7	65.25	Hydrophilicity, permeate flux, salt rejection	97.33	Marioryad et al. (2020)
Cellulose nanocrystals (CNC)	0.1	20	63	Hydrophilicity, permeate flux, antifouling	97.8	Asempour, Emadzadeh, Matsuura, and Kruczek (2018)
Laponite nanoclays (NC-LAP)	0.3	20	54	Hydrophilicity, permeate flux, salt rejection	98.18	Zhao, Zhao, and Chung (2020c)
Boron nitride nanosheets	0.02	15.5	64	Hydrophilicity, permeate flux, salt rejection	96.4	Wang et al. (2020a)
Two-dimensional (2D) MXene $Ti_3C_2T_x$	0.015	16	40.5	Hydrophilicity, permeate flux, antifouling, chlorine resistance		Wang et al. (2020b)

Water flux may be enhanced due to hydrophilicity of the membrane increases by HNT. They also found that antifouling properties also enhanced due to presence of HNT in PA layer.

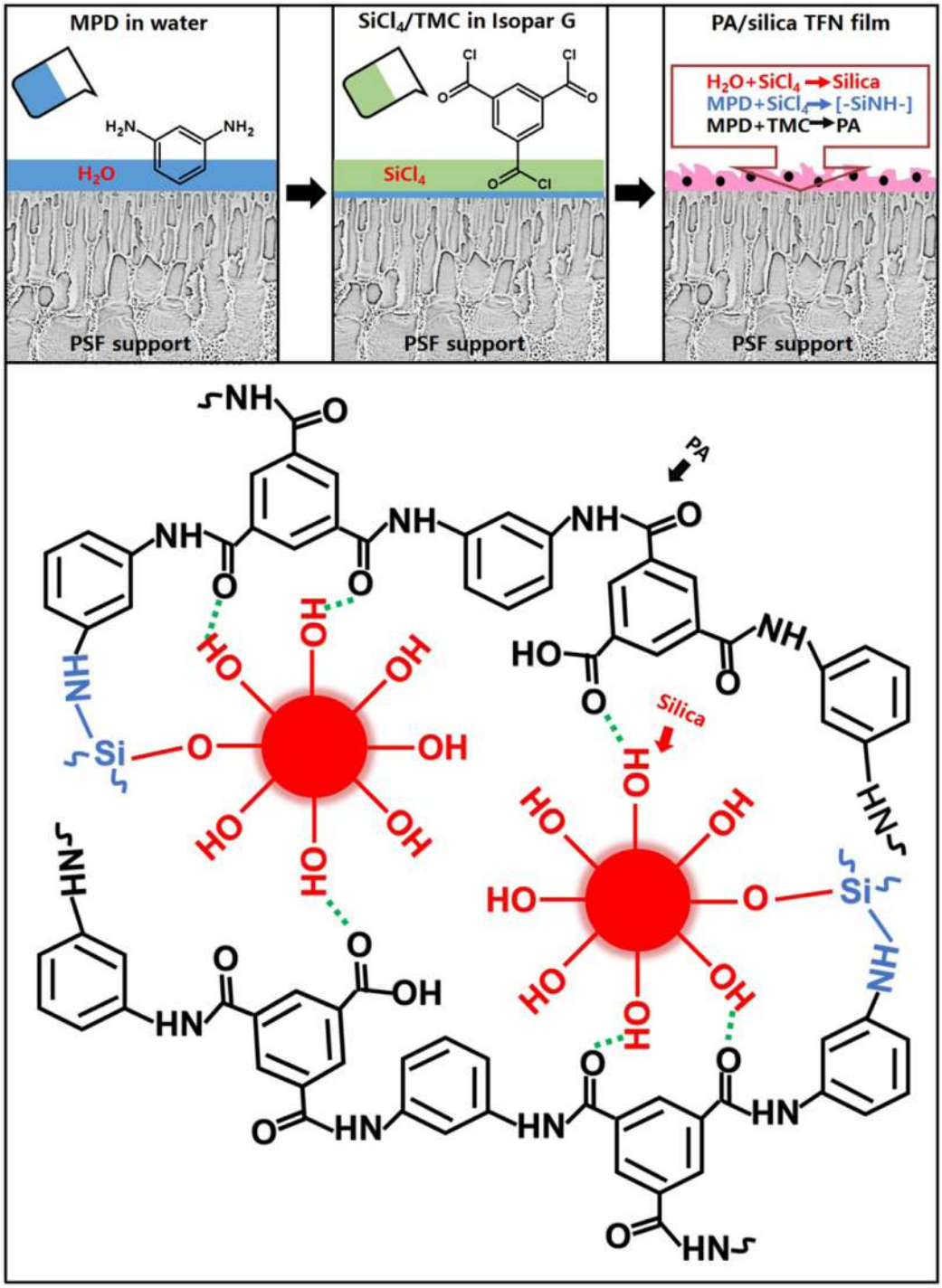

FIGURE 10.15 Schematic representation of polyamide (PA)/silica thin-film nanocomposite (TFN) membranes via an in situ polymerization reaction. Source*: Adapted from Shen, H., Wang, S., Xu, H., Zhou, Y., & Gao, C. (2018). Preparation of polyamide thin film nanocomposite membranes containing silica nanoparticles via an in-situ polymerization of $SiCl_4$ in organic solution.* Journal of Membrane Science, 565, 145–156. https://doi.org/10.1016/j.memsci.2018.08.016.

10.3.3.3 Zeolite

Recent days zeolites have been extremely utilized in RO membrane modification due to their chemical stability as well as ions rejection capability (Daer, Kharraz, Giwa, & Hasan, 2015; Dong et al., 2015; Zhu et al., 2014). TFN RO membrane can be modified by incorporation of zeolite to enhance membrane performance. Dong et al. (2015) developed a high flux TFN RO membrane by IP process between MPD and TMC with incorporation of NaY zeolite in PA layer. They found that addition of NaY zeolites in TFN membrane enhanced the permeate flux without affecting the salt rejection. They noticed that newly posttreated TFN membrane showing 2 times greater flux than pristine NaY-doped TFN membrane. Several studies reported development of TFN RO by incorporation of zeolites. These zeolites not only enhance permeability of the membrane but also modified the interfacial properties, such as charge density, hydrophilicity, pore structure, antimicrobial properties, chemical, and mechanical stability. Huang et al. (2013a) investigate the effects of NaA nano-zeolites incorporation in PA layer of by IP process of TFN RO membrane. They found that zeolites dispersed in organic solution TFN membrane exhibit better performance relative to aqueous dispersed zeolites TFN membrane.

10.3.3.4 Cellulose nanocrystals

One of the main drawbacks of TFN RO membrane is leaching of nanoparticles in retentate as well as permeate stream, which will be harmful in environment. Incorporation of cellulose nanocrystals (CNCs) in PA layer to prepared TFN membrane can address this issue. CNCs are prepared from natural cellulose by acid hydrolysis and regarded to be rod-/needle-like particles (Souza Lima & Borsali, 2004). CNCs have negative surface charge and high surface area. These are generally nontoxic, biodegradable, and ecofriendly. Due to this, features of CNC have been utilized for TFN membrane preparation. Asempour et al. (2018) prepared a TFN RO membrane by incorporation of 0.05−0.1 wt.% CNCs into the PA. They tested this newly developed membrane for brackish water desalination. They found that flux of TFN membrane enhanced 2 times relative to pristine TFC membrane. These TFN membrane also exhibits antifouling property. Several studies reported CNCs surface can be functionalized by surface modification (Habibi, Lucia, & Rojas, 2010). For example, CNC surface is altered by 2,2,6,6-Tetramethylpiperidine-1-oxyl (TEMPO)-mediated oxidation (Kong et al., 2014). Smith, Hendren, Haag, Foster, and Martin (2019) developed high flux RO membrane by utilizing CNCs and TEMPO oxidized cellulose nanocrystals in PA layer.

10.4 Potential of different polymer-based nanocomposite reverse osmosis membranes for water desalination

Nanoparticles impregnated TFN RO membranes have been enormously utilized for desalination application due to their ion rejection capability, antifouling behavior, better chlorine resistance, and enhanced water permeability. Several studies have reported desalination application by TFN RO membrane and are listed in Table 10.5. Ions are rejected by TFN membrane due to existence of nanoparticles in the membrane surface.

TABLE 10.5 Thin-film nanocomposite (TFN) reverse osmosis (RO) membrane used for desalination application.

Nanomaterials	Amount of nanoparticles (wt. %)	RO test conditions		Specific flux (LMH bar^{-1})[a]	NaCl rejection (%)[b]	References
		Feed concentration of NaCl (g L^{-1})	Pressure (bar)			
MWCNTs	0.1	35	50	0.54→1.42	97→90	Inukai et al. (2015)
	0.1	0.58	7	0.85→0.79	99.7→99.7	Takizawa et al. (2017)
	0.001	35	55	0.49→0.64	98→97	Baek et al. (2017)
	0.005	2	15	1.33→1.93	97.4→98	Farahbakhsh et al. (2017)
	0.7	2	10	0.7→1.14	96→97.04	Hu et al. (2020)
CNT	0.1	2	7	0.2→1	99.7→96	Takeuchi et al. (2018)
	0.00375	2	15.5	2.5→3.31	98.7→98.5	Lee et al. (2014)
	0.002	2	15.5	2.4→2.84	97.5→95.4	Kim et al. (2014)
Carboxy-functionalized MWCNT	0.1	2	16	0.92→1.75	95→90	Zhao et al. (2014a)
Zwitterion functionalized single-walled CNT (SWCNT)	0.2	2.5	36.5	0.32→1.33	97.6→98.6	Chan et al. (2013)
GO	0.0038	2	15.5	0.58→1.06	99.3→99.3	Chae et al. (2015)
	0.01	2	15	1.97→2.6	97.6→97	Ali et al. (2016)
	0.06	2	20	0.85→1.6	98→98.8	Hamdy and Taher (2020)
p-aminophenol modified GO	0.005	2	15	1.2→1.6	99.5→ 99.7	Zhang et al. (2020a)
CD	0.02	2	15.5	4.61→5.72	98.5→99	Li et al. (2017a)

GOQD	0.01	2	16	1.56→2.34	98.5→98.1	Song et al. (2016)
N-GOQD	0.02	2	15	0.62→1.66	93→92.1	Fathizadeh et al.,(2019)
Na-CQDs	1	2	15	2.61→4.27	98.7→98.6	Gai et al. (2019)
S-d-GOQD	0.5	2	15	1.88→5.89	96.3→97.1	Shen et al. (2020)
Graphite carbon	0.004	2	16	1.96→4.585	96.3→97.1	Zhang et al. (2020b)
Graphitic carbon nitride	0.05	2	15	4→6.12	98.1→98.1	Seyyed Shahabi et al. (2020)
Silver	–	2	10	2.41→2.12	98.85→98.64	Ben-Sasson et al. (2014a)
	–	2	20	0.93→2.5	97.4→99.1	Yang et al. (2019)
	–	2	15.5	2.95→3.39	98.95→99.15	Dong et al. (2017)
	–	2	15.5	1.4→2	99. 5→99.4	Jeon and Lee (2020)
Copper	–	3	27.5	2.5→3	99→98.4	Ben-Sasson et al. (2016)
	1	1	21	1.21→2.18	96.9→97.4	García et al. (2018)
TiO_2	0.015 (a)0.04 (o)	2	15.5	2.17→2.592.17→2.55	99.75→99.7299.75→99.83	El-Aassar (2014)
	0.0125 (o)	2	15.2	1.41→1.6	97.9→97.7	Khorshidi et al. (2018)
Titanate nanotubes (TNT)	0.05	2	15	1.27→2.45	94.05→96.53	Emadzadeh et al. (2015)

(*Continued*)

TABLE 10.5 (Continued)

Nanomaterials	Amount of nanoparticles (wt. %)	RO test conditions		Specific flux (LMH bar^{-1})[a]	NaCl rejection (%)[b]	References
		Feed concentration of NaCl (g L^{-1})	Pressure (bar)			
ZnO	0.009	2	15.5	1.67→3.09	98→99	Ghoul et al. (2017)
	0.02	2	20	0.71→1.57	99.2→99.3	Rajakumaran et al. (2019)
	0.02	2	20	0.71→1.19	99.2→97	Rajakumaran et al. (2020)
Al_2O_3	1	1	10	0.25→0.4	85→88	Saleh and Gupta (2012)
MOF-based ZIF-8	0.4	2	15.5	1.28→3.35	98.1→99.5	Duan et al. (2015)
	0.4	2	15	1.11→2.3	98.4→99.4	Aljundi (2017)
	0.2	2	15.5	2.76→3.95	98.9→99.2	Lee et al. (2019)
	0.005	2	16	0.7→1.1	99.8→99.8	Li et al. (2020)
	0.15	2	20	1.72→2.61	98.2→98.6	Zhao et al. (2021)
MOF-based UiO-66	0.05	2	15.5	2.37→3.67	99.08→99.35	Liu et al. (2019)
MOF-based UiO-66-NH_2	0.02	2	20	1.4→2	98.5→99.2	Zhao et al. (2020b)
MOF-based MIL-101	0.05	2	16	1.5→2.2	99.2→99.3	Xu et al. (2016)
MOF-based MIL-125	0.3	2	21	2.97→4.04	98.5→99	Kadhom et al. (2017)
MOF-based PCN-222	0.01	2	17.2	0.24→0.34	97.5→94.5	Bonnett et al. (2020)
Zirconium metal − organic cages (Zr-MOCs)	0.06	2	15.5	0.5→1.47	94.9→94.7	Liu et al. (2021)

SiO_2	0.02	2	17.2	0.53→1.24	90→91.1	Jadav and Singh (2009)
	0.1	11	44	0.72→1.14	92→92	Peyki et al. (2015)
SilicaSBA-15	0.1	2.5	15	2.66→4.94	95.1→98.5	Kalash et al. (2020)
Alkyl cappedSilica	0.1	2	15.5	1.2→3.57	99.49→99.6	Wu et al. (2020)
HNT	0.05	2	15	1.27→2.41	97.2→95.6	Ghanbari et al. (2015)
Zeolite A nanocrystals	0.4	2	12.4	0.76→1.37	93.4→93.9	Jeong et al. (2007)
NaY zeolite	0.75	2	15.5	2.55→4.8	93.4→98.8	Dong et al. (2015)
NaA nanozeolites	0.1	2	16	1.26→2.18	91.4→98.8	Huang et al. (2013a)
Zeolite (NaX) nanocrystals	0.2	2	12	0.67→2.48	97→96.4	Fathizadeh et al. (2011)
S-beta zeolite	0.05	1.5	20.7	1.22→3.15	97→97.33	Marioryad et al. (2020)
Cellulosenanocrystals (CNC)	0.1	3	20	1.35→3.15	98.6→97.8	Asempour et al. (2018)
Laponite nanoclays(NC-LAP)	0.3	2	20	1.76→2.7	98→98.18	Zhao et al. (2020c)
Boron nitridenanosheets	0.02	2	15.5	3→4	96→96.4	Wang et al. (2020a)
Two-dimensional (2D)MXene $Ti_3C_2T_x$	0.015	2	16	1.74→2.53	97.1→98.5	Wang et al. (2020b)

[a]*The left value is the specific flux of nascent RO membrane and the right value is the best specific flux of TFN RO membrane.*
[b]*The left value is the NaCl rejection of nascent RO membrane and the right value is the best NaCl rejection of TFN RO membrane.*

TABLE 10.6 Thin-film nanocomposite (TFN) reverse osmosis (RO) membrane used for seawater desalination.

		RO test conditions				
Nanomaterials	**Amount of nanoparticles (wt.%)**	**Feed concentration of NaCl (g L^{-1})**	**Pressure (bar)**	**Specific flux (LMH/bar)[a]**	**NaCl rejection (%)[b]**	**References**
Zeolite	5	32	59	1.4→1.94	99.3→99.4	Lind et al. (2010)
Silica	1	32	55	0.4→0.63	98→97.7	Kim, Chun, Chun, and Kim (2013)
MOF UiO-66-NH_2	0.02	32	50	0.56→0.8	98.5→99.2	Zhao et al. (2020b)

[a]*The left value is the specific flux of nascent RO membrane and the right value is the best specific flux of TFN RO membrane.*
[b]*The left value is the NaCl rejection of nascent RO membrane and the right value is the best NaCl rejection of TFN RO membrane.*

TABLE 10.7 Thin-film nanocomposite (TFN) reverse osmosis (RO) membrane used for other applications.

Pollutants	**Nanomaterials**	**Amount of NPs (wt.%)**	**Pressure (bar)**	**Flux (LMH)**	**Rejection (%)**	**References**
Boron	MOF UiO-66	0.05	15.5	51.46	91.2	Liu et al. (2019)
	TNT	0.05	15	49.5	75.56	Ng, Chong, Lau, Karaman, and Ismail (2019)
N-nitrosodimethylamine (NDMA)	Zeolite	–	17	20	70	Hofs et al. (2013)

Nanoparticles generally impart negative charge in the PA layer of the TFN membrane resulting enhanced charge–charge repulsion (Donnan mechanism) between membrane surface and solute. TFN membrane rejected salts by this Donnan exclusion mechanism. Several studies show that, TFN RO membranes have also been utilized for seawater desalination and are tabulated in Table 10.6.

10.5 Potential other applications of polymer nanocomposite reverse osmosis membranes in water treatment

Numerous studies reported other applications of TFN RO membrane apart from desalination. TFN RO membranes are used for removal of specific ions (such as arsenic, boron, bromide, chloride, heavy metals, selenium, etc.), organic pollutant from water. Pollutant removal by TFN RO membranes are listed in Table 10.7.

10.6 Commercialization status and viability

Last few decades, various developments were attempted for commercializing seawater desalination by membrane-based process. Several analyses in laboratory scale have been executed to overcome different disadvantages.

Due to durability, superior productivity, and scalability zeolite-embedded TFN membrane can be utilized in commercial application. The zeolite-based TFN membrane technology has adapted in the early phase of commercialization. QuantumFlux membranes of NanoH_2O was the first commercial TFN RO grade membrane used in seawater desalination (https://tdg.ucla.edu/quantumflux-reverse-osmosis; https://www.lenntech.com/Data-sheets/Nano-H2O-Qfx-SW-400-R-L.pdf). LG Chem acquired NanoH_2O to provide the nano-enhanced RO membrane-based solutions (https://www.prnewswire.com/news-releases/nanoh2o-acquired-by-lg-chem-258855911.html). Major problem is the production cost of such kind of membrane. Therefore substantial development is required in TFN membrane for its commercial use in near future.

Incorporation of nanomaterial in the membrane involves significant cost. Thus the affordable and scalable solution should take the cost in consideration for economic viability and large-scale implementation.

Several strategies have been taken to reducing the complication in TFN membrane for large-scale commercialization. The advanced desalination membrane should be apt to minimize the operating cost and tackle the environmental concerns. The costs of desalinating seawater are generally higher than the alternates due to higher energy consumption in desalination operation. Therefore, desalination technology has reached upto certain limit in deveoping countries. The major ecological concern from desalination technology is the release of highly concentrated salt that can affects the local ecosystem as well as biodiversity. Leaching of nanomaterial in permeate is also a concern and needs to be addressed to match the permeate water quality requirements.

10.7 Way forward

Substantial research is needed to develop TFN membrane with improve efficiency, reliability, and stability for its commercial as well as industrial application. It is important to synthesize advanced nanoparticles having distinct pore structure and charge features, which can simply be distributed in any organic solvent or aqueous solution to improve the IP process. So that nanoparticles are uniformly distributed in PA layer. Following points should be inspected for improving the feasibility for used in the desalination application in the future works:

Most of the reports on TFN RO membrane for desalination are not showing the long-term performance. Performance, maintenance and cleaning protocol can be identified by long run of the membrane. Therefore long-term performance of TFN membrane with real feed must be one of the important topics of future research. Another important point for long-term performance of the membrane is proper planning for membrane maintenance and cleaning.

Majority of the findings in TFN membrane are based on lab-scale studies. Major challenges for researchers are manufacturing of industrial-scale nanoparticles, TFN membrane and modules for seawater desalination. A few reports show the scaling up procedure for nanoparticles manufacturing. Commercial scale fabrication techniques for TFN membrane are several orders of magnitude larger than laboratory scale fabrication, thus, it needs to be conducted in a more economical and efficient way.

TFN membrane technology effectively implemented with consideration of economical aspects as well as environmental aspects. Details inspection should be needed to estimate the cost effective and environmental effects of the process. Most of the studies reported short-term effects of nanoparticles on the surroundings. Hence, future research must be directed to longer term impact of nanoparticles in the surroundings. Moreover, the nanoparticle concentration in the permeate stream should be nil or within stipulated limit.

It was found that the metal oxide nanoparticles are incorporated in TFN membrane to enhance the antifouling properties by enhancing the hydrophilicity in membrane surface. Future research should be directed to surface modification of membrane for long-term performance of the membrane and stability of the coating on the membrane surface for actual feed solution. Future studies should be directed to GO-based TFN membrane for utilized in long-term performance to make the membrane competent for large-scale manufacturing. Various nanoparticles such as TiO_2, Ag, SiO_2, and MWCNT have been utilized in TFN membrane. New nanomaterial such as MOF will also be utilized for TFN membrane development. Further development is required in large scale production of the above-mentioned nanoparticles and development of sustainable solutions without any adverse environmental impact.

10.8 Conclusion

Thus polymer-based nano-enhanced RO membranes show the potential for widening the membrane applications in the areas, such as wastewater treatment and reuse, where the propensity of fouling is high. Moreover, these membranes offer an advantage of increased permeate flux. Higher hydrophilicity of these membranes indicates greater resistance to fouling and they are easier to clean as compared hydrophobic membranes. Future development in this area will help the industry widen their horizons for developing the highly efficient desalination and advanced water treatment solutions.

Acknowledgment

CSIR-CSMCRI PRIS no. 31/2021. Authors acknowledge Council of Scientific and Industrial Research-Central Salt and Marine Chemicals Research Institute (CSIR-CSMCRI) library facility.

References

Akar, N., Asar, B., Dizge, N., & Koyuncu, I. (2013). Investigation of characterization and biofouling properties of PES membrane containing selenium and copper nanoparticles. *Journal of Membrane Science*, *437*, 216–226. Available from https://doi.org/10.1016/j.memsci.2013.02.012.

Al-Karaghouli, A., & Kazmerski, L. L. (2013). Energy consumption and water production cost of conventional and renewable-energy-powered desalination processes. *Renewable and Sustainable Energy Reviews*, *24*, 343–356. Available from https://doi.org/10.1016/j.rser.2012.12.064.

Al-Mutaz, I. S., & Al-Namlah, A. M. (2004). Characteristics of dual purpose MSF desalination plants. *Desalination*, *166*, 287–294. Available from https://doi.org/10.1016/j.desal.2004.06.083.

Ali, M. E. A., Wang, L., Wang, X., & Feng, X. (2016). Thin film composite membranes embedded with graphene oxide for water desalination. *Desalination*, *386*, 67–76. Available from https://doi.org/10.1016/j.desal.2016.02.034.

Aljundi, I. H. (2017). Desalination characteristics of TFN-RO membrane incorporated with ZIF-8 nanoparticles. *Desalination*, *420*, 12–20. Available from https://doi.org/10.1016/j.desal.2017.06.020.

Alkaisi, A., Mossad, R., & Sharifian-Barforoush, A. (2017). A review of the water desalination systems integrated with renewable energy. *Energy Procedia*, *110*, 268–274. Available from https://doi.org/10.1016/j.egypro.2017.03.138.

Amini, M., Jahanshahi, M., & Rahimpour, A. (2013). Synthesis of novel thin film nanocomposite (TFN) forward osmosis membranes using functionalized multi-walled carbon nanotubes. *Journal of Membrane Science*, *435*, 233–241. Available from https://doi.org/10.1016/j.memsci.2013.01.041.

Asempour, F., Emadzadeh, D., Matsuura, T., & Kruczek, B. (2018). Synthesis and characterization of novel cellulose nanocrystals-based thin film nanocomposite membranes for reverse osmosis applications. *Desalination*, *439*, 179–187. Available from https://doi.org/10.1016/j.desal.2018.04.009.

Baek, Y., Kim, H. J., Kim, S.-H., Lee, J.-C., & Yoon, J. (2017). Evaluation of carbon nanotube-polyamide thin-film nanocomposite reverse osmosis membrane: Surface properties, performance characteristics and fouling behavior. *Journal of Industrial and Engineering Chemistry*, *56*, 327–334. Available from https://doi.org/10.1016/j.jiec.2017.07.028.

Bao, M., Zhu, G., Wang, L., Wang, M., & Gao, C. (2013). Preparation of monodispersed spherical mesoporous nanosilica–polyamide thin film composite reverse osmosis membranes via interfacial polymerization. *Desalination*, *309*, 261–266. Available from https://doi.org/10.1016/j.desal.2012.10.028.

Basu, S., Maes, M., Cano-Odena, A., Alaerts, L., De Vos, D. E., & Vankelecom, I. F. J. (2009). Solvent resistant nanofiltration (SRNF) membranes based on metal-organic frameworks. *Journal of Membrane Science*, *344*, 190–198. Available from https://doi.org/10.1016/j.memsci.2009.07.051.

Ben-Sasson, M., Lu, X., Bar-Zeev, E., Zodrow, K. R., Nejati, S., Qi, G., … Elimelech, M. (2014a). In situ formation of silver nanoparticles on thin-film composite reverse osmosis membranes for biofouling mitigation. *Water Research*, *62*, 260–270. Available from https://doi.org/10.1016/j.watres.2014.05.049.

Ben-Sasson, M., Zodrow, K. R., Genggeng, Q., Kang, Y., Giannelis, E. P., & Elimelech, M. (2014b). Surface functionalization of thin-film composite membranes with copper nanoparticles for antimicrobial surface properties. *Environmental Science and Technology*, *48*, 384–393. Available from https://doi.org/10.1021/es404232s.

Ben-Sasson, M., Lu, X., Nejati, S., Jaramillo, H., & Elimelech, M. (2016). In situ surface functionalization of reverse osmosis membranes with biocidal copper nanoparticles. *Desalination*, *388*, 1–8. Available from https://doi.org/10.1016/j.desal.2016.03.005.

Bernstein, R., Belfer, S., & Freger, V. (2011). Bacterial attachment to RO membranes surface-modified by concentration-polarization-enhanced graft polymerization. *Environmental Science and Technology*, *45*, 5973–5980. Available from https://doi.org/10.1021/es1043694.

Bonnett, B. L., Smith, E. D., De La Garza, M., Cai, M., Haag, J. V., Serrano, J. M., … Morris, A. J. (2020). PCN-222 metal–organic framework nanoparticles with tunable pore size for nanocomposite reverse osmosis membranes. *ACS Applied Materials and Interfaces*, *12*, 15765–15773. Available from https://doi.org/10.1021/acsami.0c04349.

Cao, X., Tang, M., Liu, F., Nie, Y., & Zhao, C. (2010). Immobilization of silver nanoparticles onto sulfonated polyethersulfone membranes as antibacterial materials. *Colloids Surfaces B Biointerfaces*, *81*, 555–562. Available from https://doi.org/10.1016/j.colsurfb.2010.07.057.

Chae, H.-R., Lee, J., Lee, C.-H., Kim, I.-C., & Park, P.-K. (2015). Graphene oxide-embedded thin-film composite reverse osmosis membrane with high flux, anti-biofouling, and chlorine resistance. *Journal of Membrane Science*, *483*, 128–135. Available from https://doi.org/10.1016/j.memsci.2015.02.045.

Chan, W.-F., Chen, H., Surapathi, A., Taylor, M. G., Shao, X., Marand, E., & Johnson, J. K. (2013). Zwitterion functionalized carbon nanotube/polyamide nanocomposite membranes for water desalination. *ACS Nano*, *7*, 5308–5319. Available from https://doi.org/10.1021/nn4011494.

Choi, W., Choi, J., Bang, J., & Lee, J.-H. (2013). Layer-by-layer assembly of graphene oxide nanosheets on polyamide membranes for durable reverse-osmosis applications. *ACS Applied Materials and Interfaces*, *5*, 12510–12519. Available from https://doi.org/10.1021/am403790s.

Crock, C. A., Rogensues, A. R., Shan, W., & Tarabara, V. V. (2013). Polymer nanocomposites with graphene-based hierarchical fillers as materials for multifunctional water treatment membranes. *Water Research*, *47*, 3984–3996. Available from https://doi.org/10.1016/j.watres.2012.10.057.

Daer, S., Kharraz, J., Giwa, A., & Hasan, S. W. (2015). Recent applications of nanomaterials in water desalination: A critical review and future opportunities. *Desalination*, *367*, 37–48. Available from https://doi.org/10.1016/j.desal.2015.03.030.

Dong, H., Qu, X.-Y., Zhang, L., Cheng, L.-H., Chen, H.-L., & Gao, C.-J. (2011). Preparation and characterization of surface-modified zeolite-polyamide thin film nanocomposite membranes for desalination. *Desalination and Water Treatment*, *34*, 6–12. Available from https://doi.org/10.5004/dwt.2011.2789.

Dong, H., Zhao, L., Zhang, L., Chen, H., Gao, C., & Winston Ho, W. S. (2015). High-flux reverse osmosis membranes incorporated with NaY zeolite nanoparticles for brackish water desalination. *Journal of Membrane Science*, *476*, 373–383. Available from https://doi.org/10.1016/j.memsci.2014.11.054.

Dong, C., Wang, Z., Wu, J., Wang, Y., Wang, J., & Wang, S. (2017). A green strategy to immobilize silver nanoparticles onto reverse osmosis membrane for enhanced anti-biofouling property. *Desalination*, *401*, 32–41. Available from https://doi.org/10.1016/j.desal.2016.06.034.

Duan, J., Pan, Y., Pacheco, F., Litwiller, E., Lai, Z., & Pinnau, I. (2015). High-performance polyamide thin-film-nanocomposite reverse osmosis membranes containing hydrophobic zeolitic imidazolate framework-8. *Journal of Membrane Science*, *476*, 303–310. Available from https://doi.org/10.1016/j.memsci.2014.11.038.

El-Aassar, A. M. A. (2014). Improvement of reverse osmosis performance of polyamide thin-film composite membranes using TiO 2 nanoparticles. *Desalination and Water Treatment*, 1–12. Available from https://doi.org/10.1080/19443994.2014.940206.

Emadzadeh, D., Lau, W. J., Rahbari-Sisakht, M., Daneshfar, A., Ghanbari, M., Mayahi, A., ... Ismail, A. F. (2015). A novel thin film nanocomposite reverse osmosis membrane with superior anti-organic fouling affinity for water desalination. *Desalination*, *368*, 106–113. Available from https://doi.org/10.1016/j.desal.2014.11.019.

Farahbakhsh, J., Delnavaz, M., & Vatanpour, V. (2017). Investigation of raw and oxidized multiwalled carbon nanotubes in fabrication of reverse osmosis polyamide membranes for improvement in desalination and antifouling properties. *Desalination*, *410*, 1–9. Available from https://doi.org/10.1016/j.desal.2017.01.031.

Fathizadeh, M., Aroujalian, A., & Raisi, A. (2011). Effect of added NaX nano-zeolite into polyamide as a top thin layer of membrane on water flux and salt rejection in a reverse osmosis process. *Journal of Membrane Science*, *375*, 88–95. Available from https://doi.org/10.1016/j.memsci.2011.03.017.

Fathizadeh, M., Tien, H. N., Khivantsev, K., Song, Z., Zhou, F., & Yu, M. (2019). Polyamide/nitrogen-doped graphene oxide quantum dots (N-GOQD) thin film nanocomposite reverse osmosis membranes for high flux desalination. *Desalination*, *451*, 125–132. Available from https://doi.org/10.1016/j.desal.2017.07.014.

Gai, W., Zhao, D. L., & Chung, T.-S. (2019). Thin film nanocomposite hollow fiber membranes comprising Na + -functionalized carbon quantum dots for brackish water desalination. *Water Research*, *154*, 54–61. Available from https://doi.org/10.1016/j.watres.2019.01.043.

Ganesh, B. M., Isloor, A. M., & Ismail, A. F. (2013). Enhanced hydrophilicity and salt rejection study of graphene oxide-polysulfone mixed matrix membrane. *Desalination*, *313*, 199–207. Available from https://doi.org/10.1016/j.desal.2012.11.037.

García, A., Rodríguez, B., Oztürk, D., Rosales, M., Diaz, D. I., & Mautner, A. (2018). Incorporation of CuO nanoparticles into thin-film composite reverse osmosis membranes (TFC-RO) for antibiofouling properties. *Polymer Bulletin*, *75*, 2053–2069. Available from https://doi.org/10.1007/s00289-017-2146-4.

Ghanbari, M., Emadzadeh, D., Lau, W. J., Matsuura, T., & Ismail, A. F. (2015). Synthesis and characterization of novel thin film nanocomposite reverse osmosis membranes with improved organic fouling properties for water desalination. *RSC Advances*, *5*, 21268–21276. Available from https://doi.org/10.1039/C4RA16177G.

Ghaseminezhad, S. M., Barikani, M., & Salehirad, M. (2019). Development of graphene oxide-cellulose acetate nanocomposite reverse osmosis membrane for seawater desalination. *Composites Part B Engineering*, *161*, 320–327. Available from https://doi.org/10.1016/j.compositesb.2018.10.079.

Ghoul, J. El, Ghiloufi, I., Al-Hobaib, A. S., & El Mir, L. (2017). Efficiency of polyamide thin-film nanocomposite membrane containing ZnO nanoparticles. *Journal of Ovonic Research*, *13*, 83–90.

Goosen, M. F. A., Sablani, S. S., Al-Hinai, H., Al-Obeidani, S., Al-Belushi, R., & Jackson, D. (2005). Fouling of reverse osmosis and ultrafiltration membranes: A critical review. *Separation Science and Technology*, *39*, 2261–2297. Available from https://doi.org/10.1081/SS-120039343.

Guo, B.-Y., Li, F., Japip, S., Yang, L., Shang, C., & Zhang, S. (2020). Double cross-linked POSS-containing thin film nanocomposite hollow fiber membranes for brackish water desalination via reverse osmosis. *Industrial and Engineering Chemistry Research*, *59*, 22272–22280. Available from https://doi.org/10.1021/acs.iecr.0c05191.

Habibi, Y., Lucia, L. A., & Rojas, O. J. (2010). Cellulose nanocrystals: Chemistry, self-assembly, and applications. *Chemical Reviews*, *110*, 3479–3500. Available from https://doi.org/10.1021/cr900339w.

Hamdy, G., & Taher, A. (2020). Enhanced chlorine-resistant and low biofouling reverse osmosis polyimide-graphene oxide thin film nanocomposite membranes for water desalination. *Polymer Engineering and Science*, *60*, 2567–2580. Available from https://doi.org/10.1002/pen.25495.

He, Y., Tang, Y. P., Ma, D., & Chung, T.-S. (2017). UiO-66 incorporated thin-film nanocomposite membranes for efficient selenium and arsenic removal. *Journal of Membrane Science*, *541*, 262–270. Available from https://doi.org/10.1016/j.memsci.2017.06.061.

Hofs, B., Schurer, R., Harmsen, D. J. H., Ceccarelli, C., Beerendonk, E. F., & Cornelissen, E. R. (2013). Characterization and performance of a commercial thin film nanocomposite seawater reverse osmosis membrane and comparison with a thin film composite. *Journal of Membrane Science*, *446*, 68–78. Available from https://doi.org/10.1016/j.memsci.2013.06.007.

Hsu, S. T., Cheng, K. T., & Chiou, J. S. (2002). Seawater desalination by direct contact membrane distillation. *Desalination*, *143*, 279–287. Available from https://doi.org/10.1016/S0011-9164(02)00266-7.

Hu, M., & Mi, B. (2013). Enabling graphene oxide nanosheets as water separation membranes. *Environmental Science and Technology*, *47*, 3715–3723. Available from https://doi.org/10.1021/es400571g.

Hu, X., Sun, J., Peng, R., Tang, Q., Luo, Y., & Yu, P. (2020). Novel thin-film composite reverse osmosis membrane with superior water flux using parallel magnetic field induced magnetic multi-walled carbon nanotubes. *Journal of Cleaner Production*, *242*, 118423. Available from https://doi.org/10.1016/j.jclepro.2019.118423.

Huang, H., Qu, X., Dong, H., Zhang, L., & Chen, H. (2013a). Role of NaA zeolites in the interfacial polymerization process towards a polyamide nanocomposite reverse osmosis membrane. *RSC Advances*, *3*, 8203. Available from https://doi.org/10.1039/c3ra40960k.

Huang, H., Qu, X., Ji, X., Gao, X., Zhang, L., Chen, H., & Hou, L. (2013b). Acid and multivalent ion resistance of thin film nanocomposite RO membranes loaded with silicalite-1 nanozeolites. *Journal of Materials Chemistry A*, *1*, 11343. Available from https://doi.org/10.1039/c3ta12199b.

Ihm, S., Al-Najdi, O. Y., Hamed, O. A., Jun, G., & Chung, H. (2016). Energy cost comparison between MSF, MED and SWRO: Case studies for dual purpose plants. *Desalination*, *397*, 116–125. Available from https://doi.org/10.1016/j.desal.2016.06.029.

Inukai, S., Cruz-Silva, R., Ortiz-Medina, J., Morelos-Gomez, A., Takeuchi, K., Hayashi, T., ... Endo, M. (2015). High-performance multi-functional reverse osmosis membranes obtained by carbon nanotube polyamide nanocomposite. *Scientific Reports*, *5*, 13562. Available from https://doi.org/10.1038/srep13562.

Isloor, A. M., Ganesh, B. M., Isloor, S. M., Ismail, A. F., Nagaraj, H. S., & Pattabi, M. (2013). Studies on copper coated polysulfone/modified poly isobutylene alt-maleic anhydride blend membrane and its antibiofouling property. *Desalination*, *308*, 82–88. Available from https://doi.org/10.1016/j.desal.2012.07.021.

Ismail, A. F., Padaki, M., Hilal, N., Matsuura, T., & Lau, W. J. (2015). Thin film composite membrane—Recent development and future potential. *Desalination*, *356*, 140–148. Available from https://doi.org/10.1016/j.desal.2014.10.042.

Cadotte, J. E. (1977). *Reverse osmosis membrane*. Patent Application No. 4039440.

Jadav, G. L., & Singh, P. S. (2009). Synthesis of novel silica-polyamide nanocomposite membrane with enhanced properties. *Journal of Membrane Science*, *328*, 257–267. Available from https://doi.org/10.1016/j.memsci.2008.12.014.

Jeon, S., & Lee, J.-H. (2020). Rationally designed in-situ fabrication of thin film nanocomposite membranes with enhanced desalination and anti-biofouling performance. *Journal of Membrane Science*, *615*, 118542. Available from https://doi.org/10.1016/j.memsci.2020.118542.

Jeong, B.-H., Hoek, E. M. V., Yan, Y., Subramani, A., Huang, X., Hurwitz, G., ... Jawor, A. (2007). Interfacial polymerization of thin film nanocomposites: A new concept for reverse osmosis membranes. *Journal of Membrane Science*, *294*, 1–7. Available from https://doi.org/10.1016/j.memsci.2007.02.025.

Kadhom, M., Hu, W., & Deng, B. (2017). Thin film nanocomposite membrane filled with metal-organic frameworks UiO-66 and MIL-125 nanoparticles for water desalination. *Membranes*, *7*, 31. Available from https://doi.org/10.3390/membranes7020031.

Kalash, K., Kadhom, M., & Al-Furaiji, M. (2020). Thin film nanocomposite membranes filled with MCM-41 and SBA-15 nanoparticles for brackish water desalination via reverse osmosis. *Environmental Technology and Innovation*, *20*, 101101. Available from https://doi.org/10.1016/j.eti.2020.101101.

Keshmiri, M., Mohseni, M., & Troczynski, T. (2004). Development of novel TiO2 sol–gel-derived composite and its photocatalytic activities for trichloroethylene oxidation. *Applied Catalysis B: Environmental*, *53*, 209–219. Available from https://doi.org/10.1016/j.apcatb.2004.05.016.

Khorshidi, B., Biswas, I., Ghosh, T., Thundat, T., & Sadrzadeh, M. (2018). Robust fabrication of thin film polyamide-TiO2 nanocomposite membranes with enhanced thermal stability and anti-biofouling propensity. *Scientific Reports.*, *8*, 784. Available from https://doi.org/10.1038/s41598-017-18724-w.

Kim, S. H., Kwak, S.-Y., Sohn, B.-H., & Park, T. H. (2003). Design of TiO2 nanoparticle self-assembled aromatic polyamide thin-film-composite (TFC) membrane as an approach to solve biofouling problem. *Journal of Membrane Science*, *211*, 157–165. Available from https://doi.org/10.1016/S0376-7388(02)00418-0.

Kim, E.-S., Hwang, G., Gamal El-Din, M., & Liu, Y. (2012). Development of nanosilver and multi-walled carbon nanotubes thin-film nanocomposite membrane for enhanced water treatment. *Journal of Membrane Science*, *394–395*, 37–48. Available from https://doi.org/10.1016/j.memsci.2011.11.041.

Kim, S. G., Chun, J. H., Chun, B.-H., & Kim, S. H. (2013). Preparation, characterization and performance of poly (aylene ether sulfone)/modified silica nanocomposite reverse osmosis membrane for seawater desalination. *Desalination*, *325*, 76–83. Available from https://doi.org/10.1016/j.desal.2013.06.017.

Kim, H. J., Choi, K., Baek, Y., Kim, D.-G., Shim, J., Yoon, J., & Lee, J.-C. (2014). High-performance reverse osmosis CNT/polyamide nanocomposite membrane by controlled interfacial interactions. *ACS Applied Materials and Interfaces*, *6*, 2819–2829. Available from https://doi.org/10.1021/am405398f.

Kong, C., Koushima, A., Kamada, T., Shintani, T., Kanezashi, M., Yoshioka, T., & Tsuru, T. (2011). Enhanced performance of inorganic-polyamide nanocomposite membranes prepared by metal-alkoxide-assisted interfacial polymerization. *Journal of Membrane Science*, *366*, 382–388. Available from https://doi.org/10.1016/j.memsci.2010.10.026.

Kong, L., Zhang, D., Shao, Z., Han, B., Lv, Y., Gao, K., & Peng, X. (2014). Superior effect of TEMPO-oxidized cellulose nanofibrils (TOCNs) on the performance of cellulose triacetate (CTA) ultrafiltration membrane. *Desalination*, *332*, 117–125. Available from https://doi.org/10.1016/j.desal.2013.11.005.

Kwak, S.-Y., Kim, S. H., & Kim, S. S. (2001). Hybrid organic/inorganic reverse osmosis (RO) membrane for bactericidal anti-fouling. 1. Preparation and characterization of TiO 2 nanoparticle self-assembled aromatic polyamide thin-film-composite (TFC) membrane. *Environmental Science and Technology*, *35*, 2388–2394. Available from https://doi.org/10.1021/es0017099.

Lee, H. S., Im, S. J., Kim, J. H., Kim, H. J., Kim, J. P., & Min, B. R. (2008). Polyamide thin-film nanofiltration membranes containing TiO2 nanoparticles. *Desalination*, *219*, 48–56. Available from https://doi.org/10.1016/j.desal.2007.06.003.

Lee, K. P., Arnot, T. C., & Mattia, D. (2011). A review of reverse osmosis membrane materials for desalination—Development to date and future potential. *Journal of Membrane Science*, *370*, 1–22. Available from https://doi.org/10.1016/j.memsci.2010.12.036.

Lee, H. D., Kim, H. W., Cho, Y. H., & Park, H. B. (2014). Experimental evidence of rapid water transport through carbon nanotubes embedded in polymeric desalination membranes. *Small*, *10*, 2653–2660. Available from https://doi.org/10.1002/smll.201303945.

Lee, T. H., Oh, J. Y., Hong, S. P., Lee, J. M., Roh, S. M., Kim, S. H., & Park, H. B. (2019). ZIF-8 particle size effects on reverse osmosis performance of polyamide thin-film nanocomposite membranes: Importance of particle deposition. *Journal of Membrane Science*, *570–571*, 23–33. Available from https://doi.org/10.1016/j.memsci.2018.10.015.

Li, Y., Li, S., & Zhang, K. (2017a). Influence of hydrophilic carbon dots on polyamide thin film nanocomposite reverse osmosis membranes. *Journal of Membrane Science*, *537*, 42–53. Available from https://doi.org/10.1016/j.memsci.2017.05.026.

Li, X., Liu, Y., Wang, J., Gascon, J., Li, J., & Van der Bruggen, B. (2017b). Metal–organic frameworks based membranes for liquid separation. *Chemical Society Reviews*, *46*, 7124–7144. Available from https://doi.org/10.1039/C7CS00575J.

Li, M.-P., Zhang, X., Zhang, H., Liu, W.-L., Huang, Z.-H., Xie, F., … Xu, Z.-L. (2020). Hydrophilic yolk-shell ZIF-8 modified polyamide thin-film nanocomposite membrane with improved permeability and selectivity. *Separationand Purification Technology*, *247*, 116990. Available from https://doi.org/10.1016/j.seppur.2020.116990.

Lin, Y., Chen, Y., & Wang, R. (2019). Thin film nanocomposite hollow fiber membranes incorporated with surface functionalized HKUST-1 for highly-efficient reverses osmosis desalination process. *Journal of Membrane Science*, *589*, 117249. Available from https://doi.org/10.1016/j.memsci.2019.117249.

Lind, M. L., Ghosh, A. K., Jawor, A., Huang, X., Hou, W., Yang, Y., & Hoek, E. M. V. (2009a). Influence of zeolite crystal size on zeolite-polyamide thin film nanocomposite membranes. *Langmuir: the ACS Journal of Surfaces and Colloids*, *25*, 10139–10145. Available from https://doi.org/10.1021/la900938x.

Lind, M. L., Jeong, B.-H., Subramani, A., Huang, X., & Hoek, E. M. V. (2009b). Effect of mobile cation on zeolite-polyamide thin film nanocomposite membranes. *Journal of Materials Research*, *24*, 1624–1631. Available from https://doi.org/10.1557/jmr.2009.0189.

Lind, M. L., Eumine Suk, D., Nguyen, T.-V., & Hoek, E. M. V. (2010). Tailoring the structure of thin film nanocomposite membranes to achieve seawater RO membrane performance. *Environmental Science and Technology*, *44*, 8230–8235. Available from https://doi.org/10.1021/es101569p.

Liu, L., Xie, X., Qi, S., Li, R., Zhang, X., Song, X., & Gao, C. (2019). Thin film nanocomposite reverse osmosis membrane incorporated with UiO-66 nanoparticles for enhanced boron removal. *Journal of Membrane Science*, *580*, 101–109. Available from https://doi.org/10.1016/j.memsci.2019.02.072.

Liu, G., Zhang, X., Di Yuan, Y., Yuan, H., Li, N., Ying, Y., … Zhao, D. (2021). Thin-film nanocomposite membranes containing water-stable zirconium metal–organic cages for desalination. *ACS Materials Letters*, *3*, 268–274. Available from https://doi.org/10.1021/acsmaterialslett.0c00511.

Lomeda, J. R., Doyle, C. D., Kosynkin, D. V., Hwang, W.-F., & Tour, J. M. (2008). Diazonium functionalization of surfactant-wrapped chemically converted graphene sheets. *Journal of the American Chemical Society*, *130*, 16201–16206. Available from https://doi.org/10.1021/ja806499w.

Luo, M.-L., Zhao, J.-Q., Tang, W., & Pu, C.-S. (2005). Hydrophilic modification of poly(ether sulfone) ultrafiltration membrane surface by self-assembly of TiO2 nanoparticles. *Applied Surface Science*, *249*, 76–84. Available from https://doi.org/10.1016/j.apsusc.2004.11.054.

Ma, N., Wei, J., Liao, R., & Tang, C. Y. (2012). Zeolite-polyamide thin film nanocomposite membranes: Towards enhanced performance for forward osmosis. *Journal of Membrane Science*, *405–406*, 149–157. Available from https://doi.org/10.1016/j.memsci.2012.03.002.

Ma, D., Peh, S. B., Han, G., & Chen, S. B. (2017). Thin-film nanocomposite (TFN) membranes incorporated with super-hydrophilic metal–organic framework (MOF) UiO-66: Toward enhancement of water flux and salt rejection. *ACS Applied Materials and Interfaces*, *9*, 7523–7534. Available from https://doi.org/10.1021/acsami.6b14223.

Marioryad, H., Ghaedi, A. M., Emadzadeh, D., Baneshi, M. M., Vafaei, A., & Lau, W. (2020). A thin film nanocomposite reverse osmosis membrane incorporated with S-beta zeolite nanoparticles for water desalination. *Chemistry Select*, *5*, 1972–1975. Available from https://doi.org/10.1002/slct.201904084.

Maximous, N., Nakhla, G., Wan, W., & Wong, K. (2010). Effect of the metal oxide particle distributions on modified PES membranes characteristics and performance. *Journal of Membrane Science*, *361*, 213–222. Available from https://doi.org/10.1016/j.memsci.2010.05.051.

Ng, Z., Chong, C., Lau, W., Karaman, M., & Ismail, A. F. (2019). Boron removal and antifouling properties of thin-film nanocomposite membrane incorporating PECVD-modified titanate nanotubes. *Journal of Chemical Technology and Biotechnology*, *94*, 2772–2782. Available from https://doi.org/10.1002/jctb.6044.

Oren, Y. (2008). Capacitive deionization (CDI) for desalination and water treatment—Past, present and future (a review). *Desalination*, *228*, 10–29. Available from https://doi.org/10.1016/j.desal.2007.08.005.

Pang, C. M., Hong, P., Guo, H., & Liu, W.-T. (2005). Biofilm formation characteristics of bacterial isolates retrieved from a reverse osmosis membrane. *Environmental Science and Technology*, *39*, 7541–7550. Available from https://doi.org/10.1021/es050170h.

Pang, R., & Zhang, K. (2018). Fabrication of hydrophobic fluorinated silica-polyamide thin film nanocomposite reverse osmosis membranes with dramatically improved salt rejection. *Journal of Colloid and Interface Science*, *510*, 127–132. Available from https://doi.org/10.1016/j.jcis.2017.09.062.

Park, J., Choi, W., Cho, J., Chun, B. H., Kim, S. H., Lee, K. B., & Bang, J. (2010a). Carbon nanotube-based nanocomposite desalination membranes from layer-by-layer assembly. *Desalination and Water Treatment*, *15*, 76–83. Available from https://doi.org/10.5004/dwt.2010.1670.

Park, J., Choi, W., Kim, S. H., Chun, B. H., Bang, J., & Lee, K. B. (2010b). Enhancement of chlorine resistance in carbon nanotube based nanocomposite reverse osmosis membranes. *Desalination and Water Treatment*, *15*, 198–204. Available from https://doi.org/10.5004/dwt.2010.1686.

Park, S.-H., Ko, Y.-S., Park, S.-J., Lee, J. S., Cho, J., Baek, K.-Y., ... Lee, J.-H. (2016). Immobilization of silver nanoparticle-decorated silica particles on polyamide thin film composite membranes for antibacterial properties. *Journal of Membrane Science*, *499*, 80–91. Available from https://doi.org/10.1016/j.memsci.2015.09.060.

Pendergast, M. T. M., Nygaard, J. M., Ghosh, A. K., & Hoek, E. M. V. (2010). Using nanocomposite materials technology to understand and control reverse osmosis membrane compaction. *Desalination*, *261*, 255–263. Available from https://doi.org/10.1016/j.desal.2010.06.008.

Pendergast, M. M., Ghosh, A. K., & Hoek, E. M. V. (2013). Separation performance and interfacial properties of nanocomposite reverse osmosis membranes. *Desalination*, *308*, 180–185. Available from https://doi.org/10.1016/j.desal.2011.05.005.

Perreault, F., Jaramillo, H., Xie, M., Ude, M., Nghiem, L. D., & Elimelech, M. (2016). Biofouling mitigation in forward osmosis using graphene oxide functionalized thin-film composite membranes. *Environmental Science and Technology*, *50*, 5840–5848. Available from https://doi.org/10.1021/acs.est.5b06364.

Peyki, A., Rahimpour, A., & Jahanshahi, M. (2015). Preparation and characterization of thin film composite reverse osmosis membranes incorporated with hydrophilic SiO2 nanoparticles. *Desalination*, *368*, 152–158. Available from https://doi.org/10.1016/j.desal.2014.05.025.

Porter, M. C. (1990). *Handbook of industrial membrane technology*. New Jersey: Noyes Publications.

Rajakumaran, R., Boddu, V., Kumar, M., Shalaby, M. S., Abdallah, H., & Chetty, R. (2019). Effect of ZnO morphology on GO-ZnO modified polyamide reverse osmosis membranes for desalination. *Desalination*, *467*, 245–256. Available from https://doi.org/10.1016/j.desal.2019.06.018.

Rajakumaran, R., Kumar, M., & Chetty, R. (2020). Morphological effect of ZnO nanostructures on desalination performance and antibacterial activity of thin-film nanocomposite (TFN) membrane. *Desalination*, *495*, 114673. Available from https://doi.org/10.1016/j.desal.2020.114673.

Raval, H. D., & Gohil, J. M. (2009). Carbon nanotube membrane for water desalination. *International Journal of Nuclear Desalination*, *3*, 360. Available from https://doi.org/10.1504/IJND.2009.028863.

Raval, H. D., & Gohil, J. M. (2010). Nanotechnology in water treatment: an emerging trend. *International Journal of Nuclear Desalination*, *4*, 184. Available from https://doi.org/10.1504/IJND.2010.035176.

Raval, H. D., & Das, R. K. (2017). A novel approach to bind graphene oxide to polyamide for making high performance reverse osmosis membrane. *Membrane Water Treatment*, *8*, 613–623. Available from https://doi.org/10.12989/mwt.2017.8.6.613.

Roy, S., Ntim, S. A., Mitra, S., & Sirkar, K. K. (2011). Facile fabrication of superior nanofiltration membranes from interfacially polymerized CNT-polymer composites. *Journal of Membrane Science*, *375*, 81–87. Available from https://doi.org/10.1016/j.memsci.2011.03.012.

Sadrzadeh, M., & Mohammadi, T. (2008). Sea water desalination using electrodialysis. *Desalination*, *221*, 440–447. Available from https://doi.org/10.1016/j.desal.2007.01.103.

Saleem, H., & Zaidi, S. J. (2020). Nanoparticles in reverse osmosis membranes for desalination: A state of the art review. *Desalination*, *475*, 114171. Available from https://doi.org/10.1016/j.desal.2019.114171.

Saleh, T. A., & Gupta, V. K. (2012). Synthesis and characterization of alumina nano-particles polyamide membrane with enhanced flux rejection performance. *Separationand Purification Technology*, *89*, 245–251. Available from https://doi.org/10.1016/j.seppur.2012.01.039.

Seyyed Shahabi, S., Azizi, N., Vatanpour, V., & Yousefimehr, N. (2020). Novel functionalized graphitic carbon nitride incorporated thin film nanocomposite membranes for high-performance reverse osmosis desalination. *Separationand Purification Technology*, *235*, 116134. Available from https://doi.org/10.1016/j.seppur.2019.116134.

Shen, H., Wang, S., Xu, H., Zhou, Y., & Gao, C. (2018). Preparation of polyamide thin film nanocomposite membranes containing silica nanoparticles via an in-situ polymerization of SiCl4 in organic solution. *Journal of Membrane Science*, *565*, 145–156. Available from https://doi.org/10.1016/j.memsci.2018.08.016.

Shen, H., Wang, S., Li, Y., Gu, K., Zhou, Y., & Gao, C. (2019). MeSiCl3 functionalized polyamide thin film nanocomposite for low pressure RO membrane desalination. *Desalination*, *463*, 13–22. Available from https://doi.org/10.1016/j.desal.2019.04.006.

Shen, Q., Lin, Y., Kawabata, Y., Jia, Y., Zhang, P., Akther, N., ... Matsuyama, H. (2020). Engineering heterostructured thin-film nanocomposite membrane with functionalized graphene oxide quantum dots (GOQD) for highly efficient reverse osmosis. *ACS Applied Materials and Interfaces*, *12*, 38662–38673. Available from https://doi.org/10.1021/acsami.0c10301.

Smith, E., Hendren, K., Haag, J., Foster, E., & Martin, S. (2019). Functionalized cellulose nanocrystal nanocomposite membranes with controlled interfacial transport for improved reverse osmosis performance. *Nanomaterials*, *9*, 125. Available from https://doi.org/10.3390/nano9010125.

Song, X., Zhou, Q., Zhang, T., Xu, H., & Wang, Z. (2016). Pressure-assisted preparation of graphene oxide quantum dot-incorporated reverse osmosis membranes: antifouling and chlorine resistance potentials. *Journal of Materials Chemistry A*, *4*, 16896–16905. Available from https://doi.org/10.1039/C6TA06636D.

Souza Lima, M. M. de, & Borsali, R. (2004). Rodlike cellulose microcrystals: Structure, properties, and applications. *Macromolecular Rapid Communications*, *25*, 771–787. Available from https://doi.org/10.1002/marc.200300268.

Takeuchi, K., Takizawa, Y., Kitazawa, H., Fujii, M., Hosaka, K., Ortiz-Medina, J., ... Endo, M. (2018). Salt rejection behavior of carbon nanotube-polyamide nanocomposite reverse osmosis membranes in several salt solutions. *Desalination*, *443*, 165–171. Available from https://doi.org/10.1016/j.desal.2018.04.021.

Takizawa, Y., Inukai, S., Araki, T., Cruz-Silva, R., Uemura, N., Morelos-Gomez, A., ... Endo, M. (2017). Antiorganic fouling and low-protein adhesion on reverse-osmosis membranes made of carbon nanotubes and polyamide nanocomposite. *ACS Applied Materials and Interfaces*, *9*, 32192–32201. Available from https://doi.org/10.1021/acsami.7b06420.

Tiraferri, A., Vecitis, C. D., & Elimelech, M. (2011). Covalent binding of single-walled carbon nanotubes to polyamide membranes for antimicrobial surface properties. *ACS Applied Materials and Interfaces*, *3*, 2869–2877. Available from https://doi.org/10.1021/am200536p.

Wang, X., Ma, H., Chu, B., & Hsiao, B. S. (2017). Thin-film nanofibrous composite reverse osmosis membranes for desalination. *Desalination*, *420*, 91–98. Available from https://doi.org/10.1016/j.desal.2017.06.029.

Wang, R., Low, Z.-X., Liu, S., Wang, Y., Murthy, S., Shen, W., & Wang, H. (2020a). Thin-film composite polyamide membrane modified by embedding functionalized boron nitride nanosheets for reverse osmosis. *Journal of Membrane Science*, *611*, 118389. Available from https://doi.org/10.1016/j.memsci.2020.118389.

Wang, X., Li, Q., Zhang, J., Huang, H., Wu, S., & Yang, Y. (2020b). Novel thin-film reverse osmosis membrane with MXene Ti3C2T embedded in polyamide to enhance the water flux, anti-fouling and chlorine resistance for water desalination. *Journal of Membrane Science*, *603*, 118036. Available from https://doi.org/10.1016/j.memsci.2020.118036.

Wijnhoven, S. W. P., Peijnenburg, W. J. G. M., Herberts, C. A., Hagens, W. I., Oomen, A. G., Heugens, E. H. W., ... Geertsma, R. E. (2009). Nano-silver – a review of available data and knowledge gaps in human and environmental risk assessment. *Nanotoxicology*, *3*, 109–138. Available from https://doi.org/10.1080/17435390902725914.

Wu, N. (2004). Enhanced TiO2 photocatalysis by Cu in hydrogen production from aqueous methanol solution. *International Journal of Hydrogen Energy*, *29*, 1601–1605. Available from https://doi.org/10.1016/j.ijhydene.2004.02.013.

Wu, B., Wang, S., Wang, J., Song, X., Zhou, Y., & Gao, C. (2020). Facile fabrication of high-performance thin film nanocomposite desalination membranes imbedded with alkyl group-capped silica nanoparticles. *Polymers*, *12*, 1415. Available from https://doi.org/10.3390/polym12061415.

Xu, Y., Gao, X., Wang, X., Wang, Q., Ji, Z., Wang, X., ... Gao, C. (2016). Highly and stably water permeable thin film nanocomposite membranes doped with MIL-101 (Cr) nanoparticles for reverse osmosis application. *Materials*, *9*, 870. Available from https://doi.org/10.3390/ma9110870.

Yan, L., Hong, S., Li, M. L., & Li, Y. S. (2009). Application of the Al2O3–PVDF nanocomposite tubular ultrafiltration (UF) membrane for oily wastewater treatment and its antifouling research. *Separationand Purification Technology*, *66*, 347–352. Available from https://doi.org/10.1016/j.seppur.2008.12.015.

Yang, H.-L., Lin, J. C.-T., & Huang, C. (2009). Application of nanosilver surface modification to RO membrane and spacer for mitigating biofouling in seawater desalination. *Water Research*, *43*, 3777–3786. Available from https://doi.org/10.1016/j.watres.2009.06.002.

Yang, Z., Guo, H., Yao, Z., Mei, Y., & Tang, C. Y. (2019). Hydrophilic silver nanoparticles induce selective nanochannels in thin film nanocomposite polyamide membranes. *Environmental Science and Technology*, *53*, 5301–5308. Available from https://doi.org/10.1021/acs.est.9b00473.

Yin, J., Kim, E.-S., Yang, J., & Deng, B. (2012). Fabrication of a novel thin-film nanocomposite (TFN) membrane containing MCM-41 silica nanoparticles (NPs) for water purification. *Journal of Membrane Science*, *423–424*, 238–246. Available from https://doi.org/10.1016/j.memsci.2012.08.020.

Yin, J., Yang, Y., Hu, Z., & Deng, B. (2013). Attachment of silver nanoparticles (AgNPs) onto thin-film composite (TFC) membranes through covalent bonding to reduce membrane biofouling. *Journal of Membrane Science*, *441*, 73–82. Available from https://doi.org/10.1016/j.memsci.2013.03.060.

Yin, J., & Deng, B. (2015). Polymer-matrix nanocomposite membranes for water treatment. *Journal of Membrane Science*, *479*, 256–275. Available from https://doi.org/10.1016/j.memsci.2014.11.019.

Yin, J., Zhu, G., & Deng, B. (2016). Graphene oxide (GO) enhanced polyamide (PA) thin-film nanocomposite (TFN) membrane for water purification. *Desalination*, *379*, 93–101. Available from https://doi.org/10.1016/j.desal.2015.11.001.

Zareei, F., & Hosseini, S. M. (2019). A new type of polyethersulfone based composite nanofiltration membrane decorated by cobalt ferrite-copper oxide nanoparticles with enhanced performance and antifouling property. *Separationand Purification Technology*, *226*, 48–58. Available from https://doi.org/10.1016/j.seppur.2019.05.077.

Zhan, X., Zhang, G., Chen, X., He, R., Zhang, Q., & Chen, F. (2015). Improvement of antifouling and antibacterial properties of poly(ether sulfone) UF membrane by blending with a multifunctional comb copolymer. *Industrial and Engineering Chemistry Research*, *54*, 11312–11318. Available from https://doi.org/10.1021/acs.iecr.5b03416.

Zhang, S., Qiu, G., Ting, Y. P., & Chung, T.-S. (2013). Silver–PEGylated dendrimer nanocomposite coating for anti-fouling thin film composite membranes for water treatment. *Colloids and Surfaces A: Physicochemical and Engineering Aspects*, *436*, 207–214. Available from https://doi.org/10.1016/j.colsurfa.2013.06.027.

Zhang, Y., Ruan, H., Guo, C., Liao, J., Shen, J., & Gao, C. (2020a). Thin-film nanocomposite reverse osmosis membranes with enhanced antibacterial resistance by incorporating p-aminophenol-modified graphene oxide. *Separationand Purification Technology*, *234*, 116017. Available from https://doi.org/10.1016/j.seppur.2019.116017.

Zhang, H., Wang, Y., Wei, Y., Gao, C., & Zhu, G. (2020b). Fabrication of polyamide thin film nanocomposite reverse osmosis membrane incorporated with a novel graphite-based carbon material for desalination. *Journal of Applied Polymer Science*, *137*, 49030. Available from https://doi.org/10.1002/app.49030.

Zhao, H., Qiu, S., Wu, L., Zhang, L., Chen, H., & Gao, C. (2014a). Improving the performance of polyamide reverse osmosis membrane by incorporation of modified multi-walled carbon nanotubes. *Journal of Membrane Science*, *450*, 249–256. Available from https://doi.org/10.1016/j.memsci.2013.09.014.

Zhao, C., Xu, X., Chen, J., & Yang, F. (2014b). Optimization of preparation conditions of poly(vinylidene fluoride)/graphene oxide microfiltration membranes by the Taguchi experimental design. *Desalination*, *334*, 17–22. Available from https://doi.org/10.1016/j.desal.2013.07.011.

Zhao, D. L., Japip, S., Zhang, Y., Weber, M., Maletzko, C., & Chung, T.-S. (2020a). Emerging thin-film nanocomposite (TFN) membranes for reverse osmosis: A review. *Water Research*, *173*, 115557. Available from https://doi.org/10.1016/j.watres.2020.115557.

Zhao, D. L., Yeung, W. S., Zhao, Q., & Chung, T.-S. (2020b). Thin-film nanocomposite membranes incorporated with UiO-66-NH2 nanoparticles for brackish water and seawater desalination. *Journal of Membrane Science*, *604*, 118039. Available from https://doi.org/10.1016/j.memsci.2020.118039.

Zhao, Q., Zhao, D. L., & Chung, T. (2020c). Nanoclays-incorporated thin-film nanocomposite membranes for reverse osmosis desalination. *Advanced Materials Interfaces*, *7*, 1902108. Available from https://doi.org/10.1002/admi.201902108.

Zhao, Q., Zhao, D. L., & Chung, T.-S. (2021). Thin-film nanocomposite membranes incorporated with defective ZIF-8 nanoparticles for brackish water and seawater desalination. *Journal of Membrane Science*, *625*, 119158. Available from https://doi.org/10.1016/j.memsci.2021.119158.

Zhu, B., Hong, Z., Milne, N., Doherty, C. M., Zou, L., Lin, Y. S., … Duke, M. (2014). Desalination of seawater ion complexes by MFI-type zeolite membranes: Temperature and long term stability. *Journal of Membrane Science*, *453*, 126–135. Available from https://doi.org/10.1016/j.memsci.2013.10.071.

Zhu, X., Bai, R., Wee, K.-H., Liu, C., & Tang, S.-L. (2010). Membrane surfaces immobilized with ionic or reduced silver and their anti-biofouling performances. *Journal of Membrane Science*, *363*, 278–286. Available from https://doi.org/10.1016/j.memsci.2010.07.041.

Zhu, J., Qin, L., Uliana, A., Hou, J., Wang, J., Zhang, Y., ... Van der Bruggen, B. (2017). Elevated performance of thin film nanocomposite membranes enabled by modified hydrophilic MOFs for nanofiltration. *ACS Applied Materials and Interfaces*, *9*, 1975–1986. Available from https://doi.org/10.1021/acsami.6b14412.

Zinadini, S., Zinatizadeh, A. A., Rahimi, M., Vatanpour, V., & Zangeneh, H. (2014). Preparation of a novel anti-fouling mixed matrix PES membrane by embedding graphene oxide nanoplates. *Journal of Membrane Science*, *453*, 292–301. Available from https://doi.org/10.1016/j.memsci.2013.10.070.

CHAPTER

11

Reuse and recycling of end-of-life reverse osmosis membranes

J. Contreras-Martínez[1], *J.A. Sanmartino*[1], *M. Khayet*[1,2] *and M.C. García-Payo*[1]

[1]Department of Structure of Matter, Thermal Physics and Electronics, Faculty of Physics, Complutense University of Madrid, Madrid, Spain [2]Madrid Institute of Advances Studies of Water (IMDEA Water Institute), Madrid, Spain

11.1 Introduction

It is an unquestionable issue that climate change is one of the biggest problems of the coming years. Human activity generates a large number of greenhouse gases, which is one of the main causes of climate change (Sarja, Onkila, & Mäkelä, 2021; Schöggl, Stumpf, & Baumgartner, 2020; Stocker, 2013). Therefore mitigating the climatic impact of human activity is a necessity today. One of the emerging tools to carry out this task is the circular economy based on reduction, reuse, recycling, and recovering, so that the use of resources is established within a closed loop, reducing pollution and at the same time maintaining the growth of economy (Sarja et al., 2021; Schöggl et al., 2020). This tool must be applied to all aspects of human activity. One of these aspects under study nowadays is the discarded reverse osmosis (RO) membrane modules in desalination plants (García-Pacheco, Lawler, Landaburu-Aguirre, García-Calvo, & Le-Clech, 2017; Landaburu-Aguirre et al., 2016; Lawler, Bradford-Hartke, & Cran, 2012).

The lack of accessibility to drinking water for human consumption is a problem in numerous countries all around the world. According to the report published by the World Health Organization (WHO) and the United Nations Children's Fund (UNICEF) (WHO UNICEF, 2017), this problem affected 29% of the world's population in 2017. In 2020 the report by United Nations (UN) (United-Nations-World-Water-Assessment-Programme, 2020) included other than the problems of deforestation, water pollution, industrialization, and agricultural activities, the consequences of climate change. This new report not only does not present any improved vision compared to the previous report, but it also adds

Advancement in Polymer-Based Membranes for Water Remediation
DOI: https://doi.org/10.1016/B978-0-323-88514-0.00010-3

© 2022 Elsevier Inc. All rights reserved.

greater uncertainty about access of people to adequate drinking water sources. This shows that water stress is increasing and the prospects for the future are dramatic because water demand exceeds its availability.

Among the different measures adopted by authorities, RO desalination has been presented for years as a viable and mature solution to supply fresh water. Its growth since the first sustainable desalination plants during the period 1929–38 (Rahimi & Chua, 2017) has been exponential. In 2019 142 million of m^3 per day of drinkable water was produced by RO desalination (IDA G, desalData, 2019). Even though it is a technology with a high energy consumption, it is by far more competitive than other traditional thermal, evaporation, and condensation technologies. Various techniques have been adopted to reduce the energy consumption and water production cost including the use of renewable energy sources (Khan, Rehman, & Al-Sulaiman, 2018). If the growth and volume of desalination by RO separation process are compared to those of other desalination technologies, RO is the most widely implemented technology with the greatest water production capacity (Haidari, Heijman, & van der Meer, 2018; Panagopoulos & Haralambous, 2020).

Although RO is a mature and extensively implemented technology, it also has various drawbacks to overcome other than the reduction of energy consumption (Khan et al., 2018), such as the discharge of brines (Panagopoulos & Haralambous, 2020) and the management of the high volume of wastes generated by the discarded membrane modules. This last disadvantage is caused by the short average life span of RO membrane modules (5–8 years) (Lawler, Alvarez-Gaitan, Leslie, & Le-Clech, 2015). More than 14,000 tonnes of membrane modules are disposed annually around the world (Landaburu-Aguirre et al., 2016).

In this chapter, an overview of the different procedures adopted and techniques developed, to avoid the disposal of discarded RO membrane modules in landfills and to recycle or reuse them in other applications, are presented.

11.2 Reverse osmosis membrane technology

RO separation process makes use of a permeable and selective membrane that separates a solute from its solvent using an external hydrostatic pressure greater than the osmotic pressure (π) of the feed solution (Fig. 11.1). The mechanism of separation and the related transport theories have been widely reviewed (Greenlee, Lawler, Freeman, Marrot, & Moulin, 2009; Ismail & Matsuura, 2018; Malaeb & Ayoub, 2011; Qasim, Badrelzaman, Darwish, Darwish, & Hilal, 2019).

RO separation process is used in numerous applications, for instance, wastewater and leachate of landfill treatment, medical, pharmaceutical, food, and hydrogen production industries to obtain clean water. However, the main application of this process is the sea or brackish water desalination (Ahsan & Imteaz, 2018). In 2019 74% of the world's desalination plants used RO technology (Panagopoulos & Haralambous, 2020). Nevertheless, RO desalination presents some environmental problems that are already being addressed by the scientific community. Different configurations and combinations with other technologies have been developed to improve the desalination performance and reduce the environmental impact of RO technology (Peñate & García-Rodríguez, 2012). Fig. 11.2 shows, as an example, the general operating schema of a typical RO desalination plant.

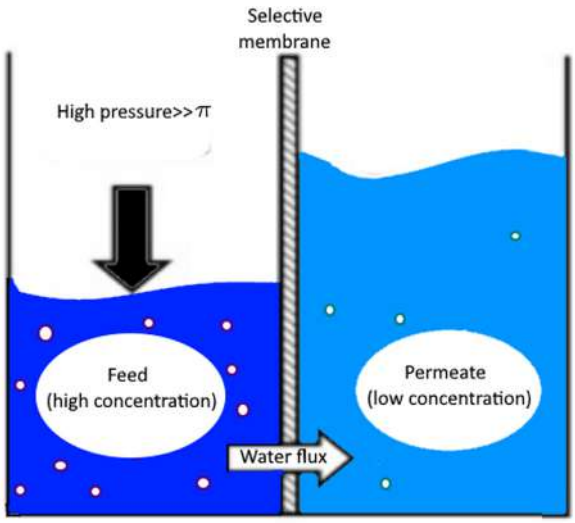

FIGURE 11.1 Schematic of reverse osmosis (RO) membrane process.

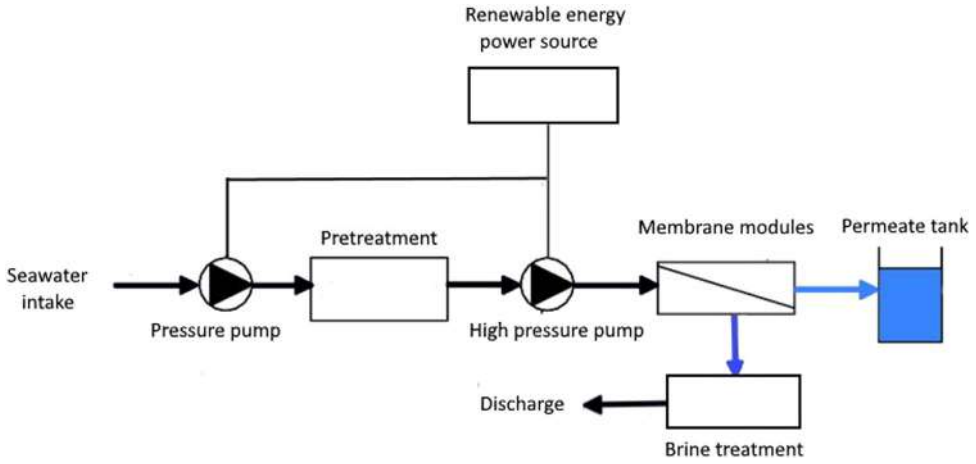

FIGURE 11.2 Operational schema of a typical reverse osmosis (RO) desalination plant.

Microfiltration (MF) and ultrafiltration (UF) are commonly considered as pretreatment methodologies to the RO process. These permit to remove a large part of major components from feed solutions so that the efficiency of the RO process is enhanced as both the working hydrostatic pressure at the entrance of the RO membrane modules and membrane fouling are reduced, extending their useful life as a consequence (Ahmed, Hashaikeh, & Hilal, 2020; Henthorne & Boysen, 2015; Joo & Tansel, 2015; Kavitha, Rajalakshmi, Phani, & Padaki, 2019). With the same purpose, other conventional pretreatment methods are also used in RO plants such as disinfection, pH adjustment, coagulation, flocculation, sedimentation, flotation, filtration, and dechlorination (Kavitha et al., 2019).

Different procedures and technologies have been tested for the treatment of RO brines looking at the creation of a sustainable process. Currently, the most common disposal methods are the surface water discharge in open water bodies, the sewer discharge, the deep-well injection, and the evaporation pond; but these methods have environmental disadvantages that should be solved without increasing water production costs (Panagopoulos, Haralambous, & Loizidou, 2019). Different membrane technologies, such as forward osmosis, pressure retarded osmosis, membrane distillation, electrodialysis, and reverse electrodialysis have been proposed for the treatment of RO brines (Ahmed et al., 2020; Lee et al., 2019; Mavukkandy, Chabib, Mustafa, Al Ghaferi, & AlMarzooqi, 2019; Panagopoulos & Haralambous, 2020; Panagopoulos et al., 2019).

In order to reduce costs and environmental impacts due to consumption of fossil fuels, different configurations for energizing by renewable energies and energy recovery systems have been proposed. Khan et al. (2018) reviewed the potential of wind and photovoltaic technologies as possible electrical energization technologies for RO desalination. It was stated that the difficulty of the direct application of both technologies lay in the intermittency of both natural resources, either wind or sun, and it was claimed that the best energy solution was the mixture of different technologies (i.e., renewable, nonrenewable, and storage systems), which guaranteed a stable and continuous electricity supply. As energy recovery systems, the Pelton wheel turbine and the pressure exchanger are widely coupled at the brine outlets of RO membrane modules (Nassrullah, Anis, Hashaikeh, & Hilal, 2020). The use of solar thermal energy coupled to RO membrane process has also been proposed, but it is still far from commercialization (Kosmadakis, Manolakos, Kyritsis, & Papadakis, 2010; Nafey & Sharaf, 2010).

11.3 Reverse osmosis membranes and modules

In 1959 Reid and Breton (1959) successfully synthesized the first cellulose acetate membrane for water desalination. This membrane exhibited a high salt rejection factor, but it showed an extremely low water permeate flux. Later, in 1963, Loeb and Sourirajan (Loeb & Sourirajan, 1963) presented an asymmetric cellulose diacetate membrane that improved both the salt rejection factor and the water permeate flux obtained by Reid and Breton. In the following years, cellulose triacetate membranes were developed with greater resistance to chemical and biological attacks, but prone to compaction even at low pressures ($<$30 bar) (Lee, Arnot, & Mattia, 2011). Later on, Richter, Square, and Hoehn (Richter, Square, & Hoehn, 1971) proposed the use of polyamide (PA) as a material to manufacture membranes. In 1968, Rozelle and coworkers (Rozelle, Cadotte, Corneliussen, & Erickson, 1968) developed the first thin-film composite (TFC) membrane that consisted a porous substrate as a support or a backing material and a thin selective layer of PA. Up to date, the TFC PA membranes remain the most widely used commercial RO membranes and are present in 95% of RO desalination plants in the world (Geise et al., 2010).

A typical TFC PA membrane (Fig. 11.3) is composed of a mechanical support of a nonwoven polyester material over which a porous substrate of polysulfone is deposited by phase inversion (PI) method. The active PA layer is then formed by interfacial polymerization (IP) method as a thin film on the porous polysulfone layer (Hailemariam et al., 2020;

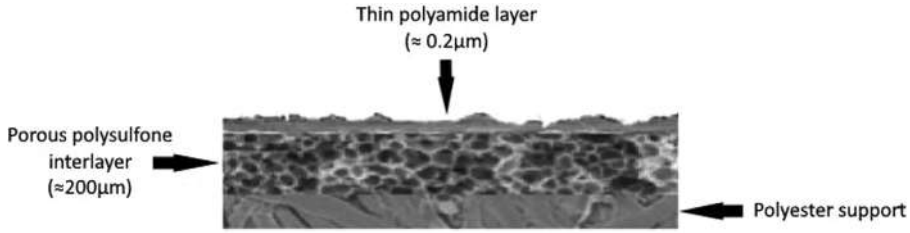

FIGURE 11.3 Schematic illustration of common thin-film composite polyamide (TFC PA) membrane. Source: *Adapted and modified from Shenvi, S. S., Isloor, A. M., & Ismail A. F. (2015). A review on RO membrane technology: Developments and challenges.* Desalination, 368, 10–26. https://doi.org/10.1016/j.desal.2014.12.042.

Otitoju, Saari, & Ahmad, 2018; Shenvi, Isloor, & Ismail, 2015). The latest generations of commercial TFC PA membranes exhibit water permeabilities for seawater and brackish water between 1–2 and 2–8 LMH bar^{-1}, respectively. The salt rejection factors of these membranes are higher than 99.7% (Okamoto & Lienhard, 2019).

To improve the permeate flux of water together with the salt rejection factor, different monomers have been investigated. In 1981, Cadotte (Cadotte, 1981) was able to synthesize a high-water permeability (0.75 LMH bar^{-1}) and high salt rejection factor (99.5%) membrane by IP using 1,3-diaminobenzene (m-phenylenediamine, MPDA) and trimesoyl chloride (TMC). Currently, the TFC PA membranes produced by IP of MPD and TMC are the most commercially used ones (Lawler et al., 2012). Different studies propose the use of other combinations of monomers for the synthesis of the PA layer. In very few cases, it was possible to increase the water permeate flux without scarifying the salt rejection factor achieved by Cadotte. Uemura et al. (Uemura, Yoshio, & Masaru, 1988) by using MPDA and 1,3,5-trisaminobenzene and a mixture of TMC and terephthaloyl chloride obtained a water permeability of 2.8 LMH bar^{-1} and a salt rejection factor of 99.6%. Liu, Wu, Yu, and Gao (2009) synthesized the PA layer using MPDA and 5-isocyanate-isophthaloyl chloride and obtained a higher water permeability (3.65 LMH bar^{-1}) but a value of the salt rejection factor (98.6%) lower than that reported by Cadotte.

In recent years, different modification strategies have been proposed to improve the performance of the TFC PA membranes. These look at the increase of the water permeate fluxes without reducing the salt rejection factors and the improvement of the antifouling properties of the membranes as well. For this purpose, various manufacturing control technologies have been applied to fix specific thicknesses for the different layers of the membrane as well as their porosities and hydrophilic properties, surface modifications of both the support layer and the PA active layer, and the addition of nano-additives in the different layers among others (Asadollahi, Bastani, & Musavi, 2017; Hailemariam et al., 2020; Otitoju et al., 2018; Xu, Wang, & Li, 2013; Zhao et al., 2020).

In general, in RO desalination plants, TFC PA membranes are packed in a spiral wound membrane (SWM) module configuration as can be seen in Fig. 11.4 (Johnson & Busch, 2010). Inside the module, membranes are packed together with the feed and permeate spacers , which are designed adequately to allow the liquid circulation while minimizing the concentration polarization layer as much as possible (Karabelas, Kostoglou, & Koutsou, 2015). The spacer for the permeate is located between two membranes with their

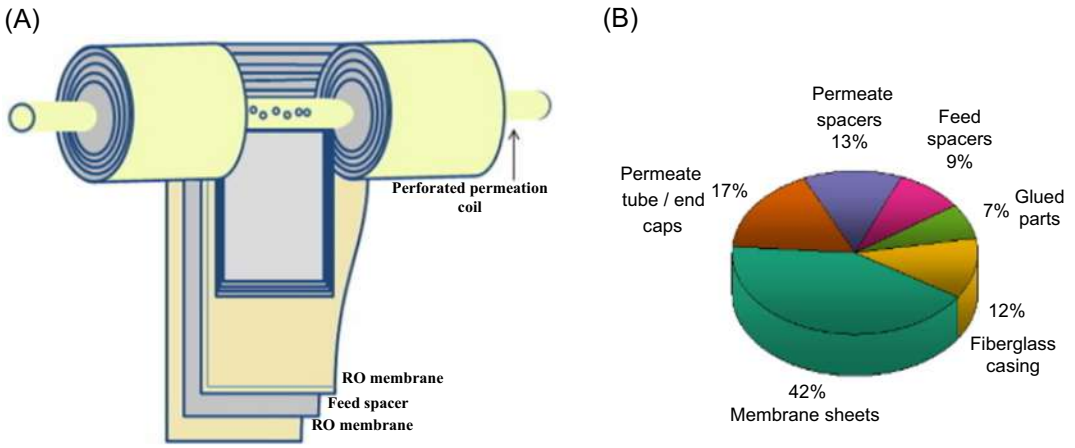

FIGURE 11.4 (A) Configuration of spiral wound membrane modules and (B) its composition. Source: *Adapted and modified from (A) Shenvi, S. S., Isloor, A. M., & Ismail, A. F. (2015). A review on RO membrane technology: Developments and challenges.* Desalination, *368, 10–26; (B) Lawler, W., Bradford-Hartke, Z., Cran, M. J., et al. (2012). Towards new opportunities for reuse, recycling and disposal of used reverse osmosis membranes.* Desalination, *299, 103–112. https://doi.org/10.1016/j.desal.2012.05.030.*

active layers facing each other. The membrane sheets are sealed with glue on three of their edges. The open edge is connected to the perforate central collector tube. Between each of these sets of two membranes and a permeate spacer is located the feed spacer. The configuration of the SWM module and its material composition are presented in Fig. 11.4A and B, respectively.

Currently, the standard dimension of these types of membrane modules is 8-inch diameter and 40-inch length. Efforts are currently being made to fabricate larger modules (16-, 18-, and 24-inch) in order to increase the performance of the RO membrane process because these modules would reduce the energy required per liter of produced fresh water (Karabelas et al., 2015).

11.4 Fouling in reverse osmosis separation process: problem, prevention, and cleaning protocols

It is already known that the RO membrane separation process is limited by the increase of the osmotic pressure of the feed solution to be treated due to the corresponding increase of the feed solution concentration and the concentration polarization during the desalination process. However, there are some limiting factors like membrane fouling and membrane deterioration (Fritzmann, Löwenberg, Wintgens, & Melin, 2007) that reduce considerably the RO performance. Membrane deterioration refers to the damage of the membrane active layer due to the utilization of different oxidants in the feed water pretreatment and chemicals during the cleaning procedures (Fritzmann et al., 2007). This results in a decline of the rejection capability and an irreversible membrane destruction.

Membrane fouling, which is an unavoidable phenomenon affecting both membrane surface and its pores, leads to severe permeability losses and drastic enhancements of water production costs in RO desalination (Daly, Allen, Koutsos, & Semião, 2020; Matin, Khan, Zaidi, & Boyce, 2011; Matin, Laoui, Epalath, & Eparoouue, 2020). Generally, fouling depends on membrane characteristics, feed solution, and RO operating conditions. During the RO process, the convective and diffusive transport of nondissolved colloidal or biologic matter and precipitated inorganic material creates a continuous fouling layer on the membrane surface (i.e., surface fouling) or within the pores of the membrane (i.e., internal fouling), as shown in Fig. 11.5 (Hong & Elimelech, 1997; Matin et al., 2011). When RO membranes get fouled, the developed fouling layer increases the pressure loss along the membrane and induces an additional resistance to water permeation together with a reduction of the rejection factor affecting, therefore, the membrane lifetime (Fritzmann et al., 2007; Hong & Elimelech, 1997; Matin et al., 2011; Zhao, Song, & Ong, 2010).

As RO membranes are relatively compact in comparison to microporous membranes, the major fouling mechanism is often associated with surface fouling in contrast to internal fouling (Goh, Lau, Othman, & Ismail, 2018). Fouling includes precipitation of inorganic salts, accumulation of suspended particulate matter, and formation of biofilms (Goh et al., 2018; She et al., 2016). Hence, four major types of membrane fouling can be distinguished based on the foulant type, namely: crystalline or inorganic fouling, particulate or colloidal fouling, organic fouling, and microbiological fouling or biofouling (Andrews et al., 2008; Fritzmann et al., 2007; Goh et al., 2018; Jiang, Li, & Ladewig, 2017; Kang & Cao, 2012; Kim et al., 2019; Malaeb & Ayoub, 2011; Matin, Rahman, Shafi, & Zubair, 2019; Vrouwenvelder, van Paassen, Wessels, van Dam, & Bakker, 2006; Yu, Song, Chen, & Yang, 2020).

11.4.1 Inorganic fouling

Crystalline or inorganic fouling, which generally refers to mineral scaling, consists in the deposition of inorganic material precipitating on a membrane surface (Matin et al., 2011), causing one of the major membrane fouling problems in water treatment and membrane desalination processes (Karabelas et al., 2015) due to the high amount of total dissolved solids in feed aqueous solutions and the very high salt rejection factors (Andrews et al., 2008).

Common scaling substances can be mainly categorized into metal ions and silica-based scales due to their chemical components (Fritzmann et al., 2007; Matin et al., 2019; Oh, Lee, Elimelech, Lee, & Hong, 2014; Yu et al., 2020). Carbonates like $CaCO_3$, phosphates like $Ca_3(PO_4)_2$, and sulfates like $CaSO_4$ and $BaSO_4$, among others, are usually formed by crystallization. Crystal growth is usually divided into three stages as shown in Fig. 11.6A. The starting step takes place when salts concentration is over their solubility and the ions start colliding to form ion pairs and clusters. Then, some ion clusters align in an orderly way to

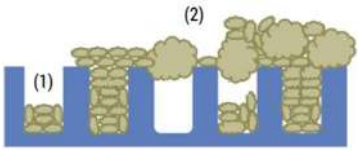

FIGURE 11.5 (1) Internal (within membrane pores) and (2) external (on membrane surface) membrane fouling. Source: *Adapted and modified from She, Q., Wang, R., Fane, A. G., & Tang, C. Y. (2016). Membrane fouling in osmotically driven membrane processes: A review.* Journal of Membrane Science, 499, 201–233. https://doi.org/10.1016/j.memsci.2015.10.040.

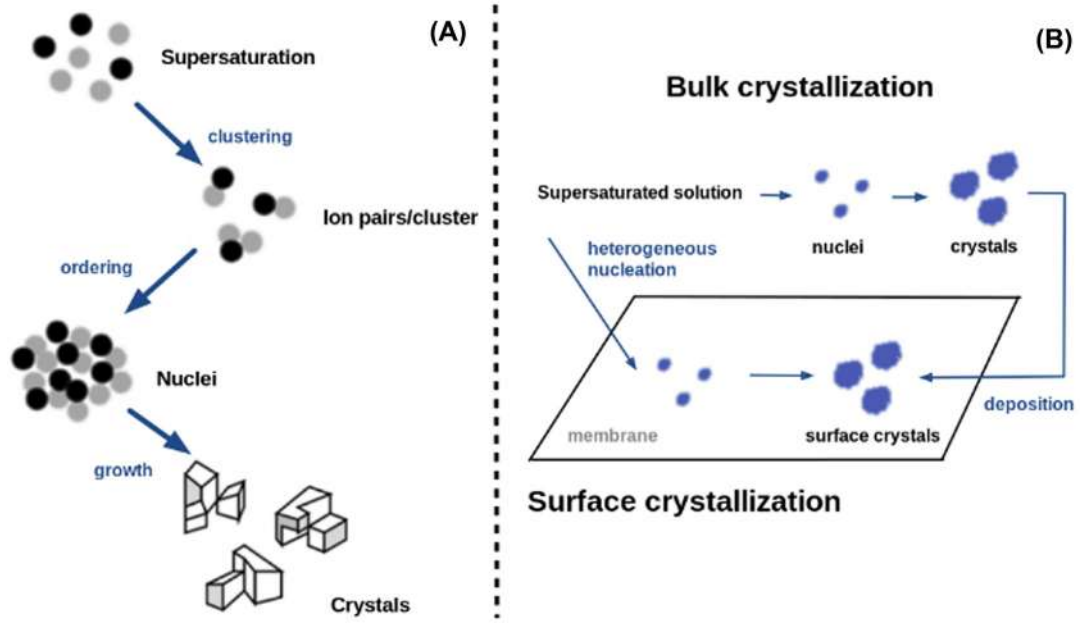

FIGURE 11.6 Stages of crystals growth (A) and bulk and surface crystallization processes (B).

form stable nuclei. Finally, crystals grow gradually from nuclei in an irreversible process (Fritzmann et al., 2007; Matin et al., 2019; Yu et al., 2020). The formation of silica-based scale is complex, which depends on multiple factors, including pH, temperature, ionic strength, multivalent ions, silica concentration, etc. (Yu et al., 2020).

In RO processes, membrane scaling can be divided into bulk (homogeneous) and surface (heterogeneous) crystallization, as shown in Fig. 11.6B (Goh et al., 2018; Matin et al., 2019; Oh et al., 2014; Qasim et al., 2019; Yu et al., 2020). It is known that the high recovery rates of RO in water desalination result in high concentration of sparingly soluble salts from feed water over their solubility limit, favoring the formation of salt crystals in the bulk solution and their subsequent deposition on the membrane surface causing membrane blocking and deterioration of membrane performance (Jawor & Hoek, 2009; Matin et al., 2019; Tran, Bolto, Gray, Hoang, & Ostarcevic, 2007; Yu et al., 2020). On the other hand, salt crystals can be directly formed and grown on the membrane surface under a high concentration polarization and salt supersaturation (Matin et al., 2019; Yu et al., 2020). Regardless of their origin, scaling dramatically reduces the RO membrane permeate flux.

11.4.2 Colloidal fouling

Particulate or colloidal fouling refers to the accumulation of particles, intermediate in size between suspended solids and true dissolved solids, on membrane surface and within its pores (Flemming, 1997; Fritzmann et al., 2007; Matin et al., 2011, 2020). Colloidal particles are difficult to remove by filtration pretreatment procedures because of their small

size. These accumulate on the membrane surface causing a fouling layer (Aimar & Bacchin, 2010). It is worth noting that despite of the well-known pretreatments in RO plants that remove most of the particulate matter, this type of fouling still occurs in RO seawater desalination (Gutiérrez Ruiz et al., 2020). The most common colloidal particles can be divided into inorganic colloids (i.e., silica, iron, and aluminum oxides), organic colloids (i.e., proteins, natural organic matter (NOM), and polysaccharides), and biological colloids (i.e., microorganisms) (Flemming, 1997; Fritzmann et al., 2007; Matin et al., 2011, 2020).

This type of fouling and its reversibility or irreversibility can be controlled by foulant–foulant and foulant–membrane interactions (Matin et al., 2019; Tang, Chong, & Fane, 2011; Vrijenhoek, Seungkwan, & Menachem, 2001). The colloidal fouling layer increases the concentration polarization near the membrane surface, enhances the corresponding osmotic pressure, and reduces the water permeate flux (Ju & Hong, 2014; Matin et al., 2020). Additionally, the increase of the overall thickness through which the water must permeate reduces the membrane permeability, making necessary a higher operational hydrostatic pressure to maintain a constant permeate flux (Matin et al., 2020).

11.4.3 Organic fouling

Seawater RO desalination membranes are mainly fouled by organic matter (Daly et al., 2020; Greenlee et al., 2009). Organic fouling results from the deposition of NOM on the membrane surface (Flemming, 1997; Laqbaqbi, Sanmartino, Khayet, García-Payo, & Chaouch, 2017; Matin et al., 2011). The principal components of NOM are humic substances, in particular humic acid (HA), produced by the degradation of NOM (Fritzmann et al., 2007; Laqbaqbi et al., 2017), followed by carbohydrates (including polysaccharides), proteins, and a variety of acidic and low molecular weight species (Laqbaqbi et al., 2017; She et al., 2016). HA, which is usually present in natural waters, surface and ground waters and seawater, can form chelates with metal ions and generates a gel like fouling layer by complexation of multivalent ions (Fritzmann et al., 2007). It has been identified as one of the major foulants for RO membranes (Tang, Kwon, & Leckie, 2007).

HA follows an adsorption–desorption mechanism to migrate through the membrane pores, as shown in Fig. 11.7. It involves an initial deposition on the membrane governed by the interactions between HA and the membrane surface, and the subsequent development of a gel or cake layer governed by the interactions between the deposited HA and HA in the bulk solution (Fritzmann et al., 2007; Zhao et al., 2010). Later, hydrogen bonding formed between water and HA is weakened as water vapor moves through the membrane, causing readsorption of HA onto the membrane and inducing pore wetting (Laqbaqbi et al., 2017).

The adsorption of these organics on the membrane surface is further influenced by the physicochemical properties of organic foulant(s) and the membrane and the operating conditions (Zhao et al., 2010). In general, this type of fouling results in permeability decline, which can be an irreversible process.

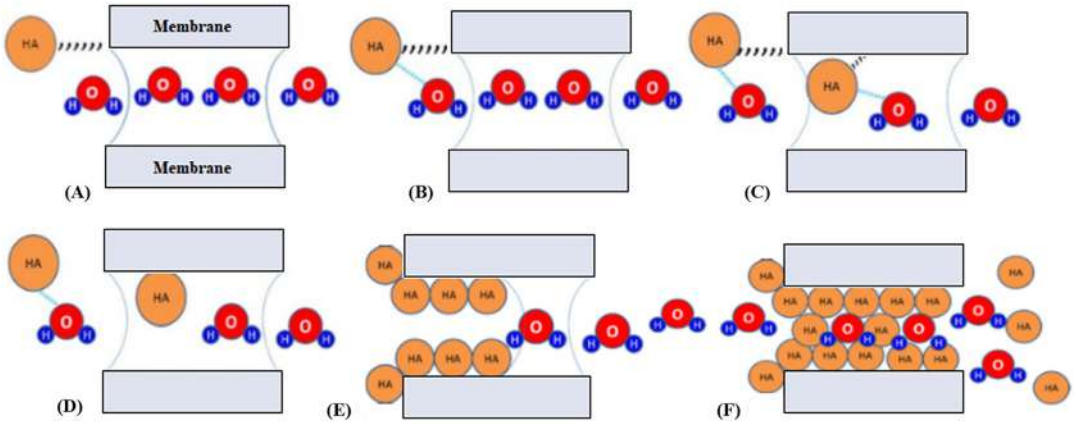

FIGURE 11.7 Adsorption–desorption mechanism for humic acid (HA) migration through a membrane pore. (A) Adsorption of HA onto membrane surface; (B) hydrogen bonding between water and HA; (C and D) weakening of hydrogen bond as water vapor moves through the membrane; (E) readsorption of HA onto the membrane; and (F) pore wetting phenomenon. Source: *From Laqbaqbi, M., Sanmartino, J. A., Khayet, M., García-Payo, C., & Chaouch, M. (2017). Fouling in membrane distillation, osmotic distillation and osmotic membrane distillation.* Applied Sciences, 7(4). *https://doi.org/10.3390/app7040334*.

11.4.4 Biofouling

Biofouling or microbiological fouling of RO membranes has been recognized as one of the most severe problems that reduces the efficiency of the RO desalination process (Kim et al., 2019; Lee, Seo, Kim, & Lee, 2017; Matin et al., 2011). This type of fouling is referred to as the unwanted reversibly or irreversibly deposition (adhesion and accumulation) and growth of microorganisms onto the membrane surface or within its pores (Kim et al., 2019; Matin et al., 2011). While reversibly attached microorganisms (i.e., planktonic organisms) can be removed easily by chemical treatments that cause microbial inactivation, irreversibly attached microorganisms induce biofilms formation that cannot be removed by gentle rinsing or water circulation. Among the microorganisms that have potential to form biofilm on the membrane surface are mycobacterium, flavobacterium, pseudomonas, bacillus, cytophaga, and lactobacillus (Matin et al., 2011). A biofilm is an assemblage of surface-associated microbial cells covered by self-produced extracellular polymeric substances (EPS), resistant to biocides and antibiotics (Flemming, Schaule, Griebe, Schmitt, & Tamachkiarowa, 1997; Kim et al., 2019; Laqbaqbi et al., 2017; Matin et al., 2011; She et al., 2016). EPS are composed of polysaccharides, proteins, glycoproteins, lipoproteins, and other macromolecules of microbial origin, forming a slime matrix which glues the cells to the membrane surface and keep the biofilm together (Flemming et al., 1997). The general development of a biofilm takes place in three phases (Flemming, 1997; Matin et al., 2011) as is schematized in Fig. 11.8.

The first step, named the induction phase, is probably the most important for the prevention of any biofilm development. This stage is characterized by an initial rapid primary colonization, followed by a primary plateau. The adhesion is essentially proportional to the cell density in water phase and it occurs owing to weak physicochemical interactions

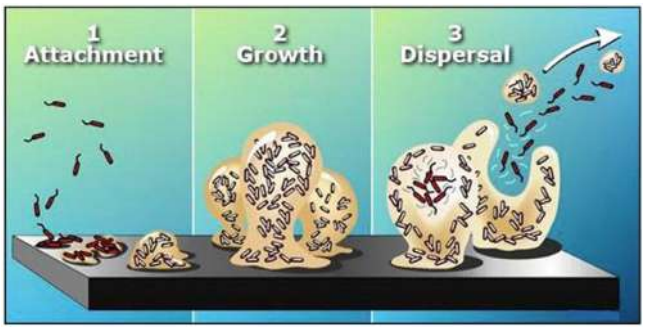

FIGURE 11.8 Biofilm formation process. (1) Attachment of microorganisms to membrane surface, colonization, and extracellular polymeric substances (EPS) production. (2) EPS development and biofilm growth. (3) Plateau phase and biofilm propagation. Source: *From Matin, A. Khan, Z., Zaidi, S. M. J., & Boyce, M. C. (2011). Biofouling in reverse osmosis membranes for seawater desalination: Phenomena and prevention.* Desalination, 281*(1), 1–16. https://doi.org/10.1016/j.desal.2011.06.063*.

(Flemming, 1997; Matin et al., 2011). Then, a logarithmical growth takes place when cell growth on the membrane surface contributes more to biofilm accumulation than does the adhesion of planktonic cells. When biofilm grows (adhesion and multiplication), the cell detachment and cellular senescence are in balance. This last phase is mainly known as plateau phase and when it is reached, the original surface properties of the membrane are masked by the biofilm (Flemming, 1997; Matin et al., 2011).

It can be stated that biofouling takes place when biofilms are present in the wrong place and at the wrong time. For example, on a separation membrane, the biofilm acts as a secondary membrane that participates in water purification process, producing a long-term flux decline and enhanced concentration polarization resulting in a decrease of the salt rejection factor that cannot be recovered fully by the hydraulic cleaning of the membrane (Matin et al., 2011). Thus while the first three types of fouling can be reduced by means of pretreatments, it is difficult to effectively control biofouling by any pretreatment in RO process because the deposited microbial cells can grow, multiply, and relocate (Flemming, 1997).

11.4.5 Fouling prevention and mitigation

As it is already mentioned in the previous section, membrane fouling is unavoidable in membrane separation processes. However, there exist some strategies to prevent or reduce it such as the application of a specific pretreatment of the feed solution, the optimization of the RO operating conditions, the development of adequate membranes using materials resistant to fouling, and the development of surface modification of membranes using nanomaterials with structural and chemical properties less prone to fouling (Goh et al., 2018; She et al., 2016).

Feed water pretreatment prior to RO desalination to minimize membrane fouling by removing foulants and/or adjusting the feed water chemistry is widely considered and studied by numerous researchers. The typical or conventional pretreatment approaches include screening, coagulation-flocculation, media filtration, UF/MF, and their combinations (Goh et al., 2018; She et al., 2016). Screening is a prior step to remove large and suspended solids in water. Coagulants and flocculants are mainly utilized to enhance the settlement of suspended solids in the feed water in order to achieve higher removal rates. Typical coagulants and flocculants include ferric chloride, ferric

sulfate, and cationic polymers (Goh et al., 2018). Their efficiency was confirmed in different studies. For instance, Mitrouli, Yiantsios, Karabelas, and Mitrakas (2008), who used polyaluminum chloride, ferric chloride, and ferric chlorosulfate as coagulants, observed up to 88% reduction of water turbidity. To control biofouling, Ma, Zhao, and Wang (2007) proposed coagulation with Fe (VI) followed by UF and achieved 98% of algae and microbial removal rate.

Media filtration is employed to eliminate different types of particles smaller than those removed by screening. Various type of materials can be utilized like activated carbon, expanded clay, and anthracite coal, among others. For example, Mitrouli et al. (2008) and Flemming et al. (1997) observed a reduction of water turbidity and silt by using different filters like expanded clay and anthracite coal with similar particle range to pretreat seawater under different operating conditions. Moreover, Van der Hoek, Hofman, Bonné, Nederlof, and Vrouwenvelder (2000), who used biologically activated carbon and slow sand filtration, observed an excellent RO feed water and a very stable operating RO parameters overtime, with only a 16% permeate flux reduction in 11 months.

MF/UF are the most popular for the pretreatment of feed water as both can remove a variety of foulants, such as biomass flocs, individual bacterial cells, colloidal particles, and macromolecular organics depending on the membrane pore size and the foulant molecular weight (Goh et al., 2018; She et al., 2016). After a previous coagulation, a UF membrane was used by Ma et al. (2007) as a pretreatment step to diminish RO feed water pollution, achieving a 98% reduction of algae and microbes. Kim et al. (2019) carried out a comparative study of the MF and UF membranes as pretreatment method for high-pressure membranes for the reclamation of biologically treated wastewater effluents. Compared to MF pretreatment, it was found that the UF pretreatment allowed a lower permeate flux reduction in the subsequent RO process and less RO membrane fouling due to a higher rejection of colloidal substances, organic matter, and polysaccharides.

The above-mentioned methods are focused on the feed water foulants removal. Nevertheless, other methodologies aim to optimize the feed water chemistry (i.e., pH, hardness, ionic strength, etc.) because the solution chemistry influences the interactions between foulant and membrane and between foulants with each other, in addition to the influence of the inorganic scale precipitation and the biological activity of microorganisms (She et al., 2016). For example, the pH adjustment is extensively considered to control the inorganic scaling. Van der Hoek et al. (2000) tried to avoid scaling problems with barium sulfate ($BaSO_4$) and calcium carbonate ($CaCO_3$) by acidifying the feed water with hydrochloric acid (HCl), achieving a recovery of 85% in the RO separation process. Maartens, Swart, and Jacobs (1999) achieved a significant reduction of NOM adsorption on membrane surface by adjusting the pH at 7 with HCl and sodium hydroxide (NaOH).

Another way to reduce fouling risk, both organic and inorganic, is to remove or diminish water hardness (i.e., reduce calcium and magnesium salts concentrations). In this case, the ionic exchange is the most followed technique. Huang, Cho, Schwab, and Jacangelo (2011) by using magnetic ion exchange, coagulation, and UF, could reduce organic fouling in RO membranes to values between 87% and 99.9% when treating humic substances. Moreover, Apell and Boyer (2010) combined both anion and cation exchange treatments in a single and completely mixed reactor for the simultaneous removal of 70% of dissolved organic carbon in feed water and at least a 55% of water hardness.

It must be mentioned that the limitation of nutrients present in water is an effective strategy for biofouling control. For this purpose, Kim et al. (2014) discovered that the phosphate limitation in feed water greatly reduced microbial growth and biofilm formation.

Most of the used chemicals in the pretreatment processes are coagulants/flocculants for the enhancement of suspended solids removal, and acids for the pH adjustment. Scaling inhibitors or antiscalants are also mostly considered. These are formulated using polyacrylic acid, carboxylic acid, or phosphonates (Goh et al., 2018). Lyster, Kim, Au, and Cohen (2010) used two different commercial antiscalants (PC-504T and Flocon 260) to retard the nucleation and crystal growth of a RO feed water. Van der Hoek et al. (2000) added Flocon 100 antiscalant in combination with sulfuric acid (H_2SO_4) dosage to recover up to 90% of RO water. However, some antiscalants in feed water showed risks of increasing biofouling potential as well as an enhancement of organic fouling (Sweity, Ronen, & Herzberg, 2014; Van der Hoek et al., 2000).

Besides feed water pretreatments, RO operational conditions must be chosen and optimized, within the design limitations of different RO membrane modules, in terms of temperature, operating pressure, and feed flow rate to mitigate fouling phenomenon (Goh et al., 2018; She et al., 2016). Separation performance is improved with temperature in RO systems. However, an elevated temperature also affects fouling formation on the membrane surface, favoring crystal nucleation (Jawor & Hoek, 2009) and biofilms growth (Chiu, Thiyagarajan, Tsoi, & Qian, 2005; Toleti, 2010). In addition, the operating hydrostatic pressure in RO separation process is also a very important parameter that allows to control membrane fouling (Oh et al., 2014; She, Jin, Li, & Tang, 2012). A high pressure result in a higher initial permeate flux, hence promoting fouling development due to an increase in the concentration polarization effect (Goh et al., 2018). Furthermore, a high-pressure may result in the compaction of foulants onto the membrane surface by increasing the hydraulic resistance of the foulant(s) layer (Wang & Tang, 2011), making irreversible their removal by any subsequent physical cleanings (Xie, Lee, Nghiem, & Elimelech, 2015). In general, membrane fouling can be reduced at high feed flow rate or low permeate flux. A greater feed flow rate induces a high shear force on the membrane surface that can result in less foulant(s) deposition and concentration polarization effect (She et al., 2016). In addition, the permeate flux decline overtime is lower for higher feed flow rates. This fact can be directly related to lower organic fouling, inorganic fouling, and biofilms development (Mattaraj, Phimpha, Hongthong, & Jiraratananon, 2010; Radu, Vrouwenvelder, van Loosdrecht, & Picioreanu, 2012).

TFC membranes, which is generally composed of an ultrathin PA layer on a porous support, are the widely used RO membranes because of the excellent physicochemical properties of PA (Wang, Wang, Han, Wang, & Wang, 2017). It was reported that membrane fouling is closely related to membrane surface characteristics such as smoothness and hydrophilicity (Asadollahi et al., 2017). Accordingly, membrane modification is considered one of the main strategies followed to reduce membrane fouling. Among the considered approaches to design fouling resistant TFC membranes, one can find the increase of the hydrophilic character of the RO membrane active layer with reduced roughness and the nano-enhanced TFC membranes (NEMs) by incorporating nano-additives (nanoparticles or nanotubes) in their active layer due to their excellent antifouling properties as well as the impressive water transport properties.

To date, surface modification is the most promising way of biofouling control in RO systems and includes physical modification (adsorption or coating) and chemical modification (covalent attachment of antifouling polymer chains or grafting) (Goh et al., 2018; Nguyen, Azari, & Zou, 2013; Yu, Kang, Liu, & Mi, 2014). While the most promising technique for membrane surface coating is plasma treatment (Goh et al., 2018; Zou et al., 2011), surface grafting can be achieved by using a single or a mixture of monomers. Different methods like atom transfer radical polymerization, chemical coupling, and free radical graft polymerization, among others, are considered (Goh et al., 2018). However, most of the proposed studies are based on the active layer modification and only few researches consider the support layer modification (Otitoju et al., 2018). This is because membrane fouling occurs mainly at the membrane surface and in the active layer near the feed solution. Surface modification can be effective to mitigate external fouling, but may have little effect on the internal fouling control and sometimes reduces membrane water permeability because an additional layer is formed on the membrane surface (She et al., 2016).

As it is mentioned previously, some research studies were focused on the improvement of the membrane surface by adding nanomaterials into the PA layer to produce NEMs, such as carbon nanotubes or halloysite nanotubes (Ghanbari, Emadzadeh, Lau, Matsuura, & Ismail, 2015; Lee et al., 2017). Another way to tune the structure and physicochemical properties of RO membranes to improve the permeate flux and the fouling resistance is by adding nanosized ceramic and metal particles, such as TiO_2 (Nguyen, Zou, & Priest, 2014), silver (Liu et al., 2013), and silica (Kim, Chun, Chun, & Kim, 2013), among others. A complete study on surface modification and incorporation of nanoparticles in membrane surfaces for the improvement of antifouling properties was reported by Goh et al. (2018).

Some research studies were also carried out on feed spacers (i.e., thickness) (Valladares Linares et al., 2014), geometry (Haaksman et al., 2017), or even surface modification (Araújo, Kruithof, Van Loosdrecht, & Vrouwenvelder, 2012), as an integrated part in RO spiral wound modules (Goh et al., 2018). In fact, spacers inserted in the feed flow play an important role in fouling mitigation. These help to provide turbulent flow and less concentration polarization effect (Mo & Ng, 2010; She et al., 2016), resulting in an enhancement in mass transfer, better mixing, and less membrane fouling initiated by particle depositions (Neal, Li, Fane, & Wiley, 2003; Suwarno et al., 2012).

11.5 End-of-life reverse osmosis membrane modules: reuse and recycling techniques

A membrane module reaches the end of its useful life when its performance, both water permeate flux or salt rejection factor, declines below the minimum operating levels established by the manufacturer and it is no longer possible to apply any cleaning treatment to recover the required values of production. A common indicator of the decline in an RO system performance is an increase in the feed inlet pressure to keep constant the water permeate flux. This degradation in membrane performance is generally due to irreversible fouling and chemical damage of the membrane material suffered during its operational life (Landaburu-Aguirre et al., 2016). Therefore the annual module replacement rate in RO plants was estimated to be between 10% and 20% (Greenlee et al., 2009; Muñoz, Frank,

Pilar, Perez, & Simón, 2014). Consequently, thousands of tons of wastes are generated per year. It is worth noting that prior to the disposal of discarded RO membrane modules, cleaning protocols are being developed to extend the useful life of these modules or finally to prepare them for reuse or recycling.

11.5.1 Cleaning strategies adopted for reverse osmosis fouled membranes and discarded modules

Because of the nature of filtration, fouling in RO membrane separation process is unavoidable and shortens membrane life imposing, therefore is a large economic burden on RO membrane plant operation (Fritzmann, Löwenberg, Wintgens, & Melin, 2007; Matin, Khan, Zaidi, & Boyce, 2011; Matin, Laoui, Epalath, & Eparoouue, 2020). One of the major goals of the RO desalination industry has been the enhancement, or at least the maintenance of the water permeate flux without sacrificing the salt rejection factor over long periods in order to increase the efficiency and reduce the operation costs. For that, effective, sustainable, and periodical cleaning strategies of each RO desalination plant must be programmed and performed (Daly et al., 2020). Cleaning processes aim to restore the membrane performance when the expected permeate flux decreases by about 10% (Fritzmann et al., 2007; Matin et al., 2011).

RO membrane cleaning is usually performed in three different ways: physical, chemical, and biological (Madaeni & Samieirad, 2010; She et al., 2016). The physical cleaning methods mainly include membrane surface flushing and backwashing (Matin et al., 2020; Mi & Elimelech, 2010; She et al., 2016). The first one is based on an enhanced crossflow velocity along the membrane surface. Even though it has been demonstrated to be effective against membrane fouling, this cleaning method consumes high amount of clean water during flushing, which would in turn reduce the actual water recovery (She et al., 2016). On the other hand, membrane backwashing consists on reversing the water permeation direction and using the permeation drag force to detach and remove the deposited foulant(s) on the membrane surface (She et al., 2016). This is carried out by applying a larger pressure on the permeate side, hence the osmotic pressure causes the permeate water to flow in the opposite direction with a given force to remove the deposited foulant(s) (Matin et al., 2020). For this reason, RO membranes must withstand hydrostatic pressures in both directions. Finally, ultrasonic techniques have also been applied for membrane cleaning. Ultrasound causes cavitation, which refers to the formation of bubbles in liquid, that grow and lastly collapse, aiding membrane cleaning. However, one drawback of this applied technique is the cost while the other is the vulnerability of the RO membrane to be damaged due to the high cavitational collapse depending on the applied power density, frequency, and time of ultrasound (Matin et al., 2020).

Chemical cleaning aims to remove impurities by means of chemical agents that weaken the adhesion force between foulant(s) and membrane (She et al., 2016). A large number of chemical cleaning agents have been used: alkalis, acids (HCl, nitric acid—HNO_3, H_2SO_4), bases (like NaOH), metal chelating agents (such as sodium ethylene diamine tetra acetic acid—EDTA), surfactants (such as sodium dodecyl sulfate—SDS), oxidation agents (like sodium hypochlorite—NaClO or hydrogen peroxide—H_2O_2), and their combinations

(Madaeni & Samieirad, 2010; Matin et al., 2020; She et al., 2016; Wang et al., 2014). Despite the fact that chemical cleaning is able to achieve a high efficiency against organic fouling and biofouling, it could not remove foulant(s) from membrane pores.

Although it has been claimed that both physical and chemical cleaning are effective against membrane fouling, the former consumes a large amount of water and can cause damage to membrane integrity, while the later generates a large waste of chemical reagents that can cause environmental problems, and uses corrosive substances such as NaClO or H_2O_2 that may be detrimental to membranes and also exert negative influences on microbial community (She et al., 2016; Wang et al., 2014). To overcome these impacts, biological cleaning that involves the use of bioactive agents for foulant(s) removal has been suggested (Maartens, Swart, & Jacobs, 1996; She et al., 2016). Among the different biological cleaning strategies reported in the literature, enzymatic cleaning is the most widely used (She et al., 2016; Wang et al., 2014). In this case, environmental-friendly enzymes can specifically interact with the biopolymeric foulant(s) (i.e., proteins and lipids) and break up the foulant(s) layer on the membrane surface, thus preventing the physical and chemical destruction of the membrane materials (Wang et al., 2014). One advantage of using enzymes for membrane cleaning is its normal operation conditions (i.e., pH, temperature, and concentration) that are not harmful for RO membranes (Argüello, Álvarez, Riera, & Álvarez, 2005). Nevertheless, the use of enzymes alone for cleaning RO fouled membranes can result in more of a liability than a solution since enzymes could become additional foulants on the membrane surface reducing its permeability as well. Therefore enzymatic cleaning should be combined with other cleaning procedures (physical and/or chemical) to address other types of fouling for an effective cleaning of RO modules used in seawater desalination (Matin et al., 2020). Table 11.1 summarizes different cleaning strategies of RO fouled membranes.

To study and verify the causes of performance loss of the discarded RO membrane modules at the end of their useful life, autopsies of the modules were performed by different authors (Butt, Rahman, & Baduruthamal, 1995; Butt, Rahman, & Baduruthamal, 1997; Carnahan, Bolin, & Suratt, 1995; Dudley & Darton, 1996; Dudley, 1998; Karime, Bouguecha, & Hamrouni, 2008; Vrouwenvelder & Van Der Kooij, 2001). Pontié, Rapenne, and Thekkedath (2005) described different tools available for the characterization of discarded RO membrane modules such as gravimetry, permeability, and rejection of solutes as well as different scanning and microscopy techniques necessary for the analysis and surface characterization of RO membranes.

In specific studies aimed at the possible recycling of the discarded RO membrane modules, a clear difference has been observed for the type of fouling existing in the discarded modules depending on the type of feed water used, seawater or brackish water. The characterization of the membranes discarded during autopsy of the end-of-life RO modules has shown similar characteristics to UF membranes (García-Pacheco et al., 2017; Ould Mohamedou, Penate Suarez, Vince, Jaouen, & Pontie, 2010; Pontié, Awad, Tazerout, Chaouachi, & Chaouachi, 2017; Pontié, 2015; Prince, Cran, Le-Clech, Uwe-Hoehn, & Duke, 2011). When seawater was used as feed, the type of membrane fouling was more organic and biofouling, while for brackish water used as feed, the most abundant fouling type was clay matrix (Fortunato et al., 2020; García-Pacheco et al., 2017; Karime et al., 2008; Molina et al., 2018).

TABLE 11.1 Cleaning procedures of reverse osmosis fouled membranes.

Fouling type	Membrane	Cleaning method	Cleaning agents	Procedure	Improvement	References
Organic fouling/ biofouling	TFC polyamide	Osmotic backwashing	NaCl	1.5 M NaCl flushes into the feed water, at 13.8 bar	70%–90% Reduction of biofouling. 63% Original flux recovery	Bar-Zeev and Elimelech (2014)
Organic fouling/ biofouling	TFC polyamide	Surface flushing + chemical + osmotic backwashing	EDTA and NaCl	Flushing with DI water (45 min) + chemical cleaning with 5 mM (EDTA) at pH 11 (45 min) + osmotic backwashing with 32–96 g L^{-1} NaCl (10 min) + flushing with DI water	Increase permeate flux and permeation rates after cleaning increased with solution salinity (32, 64, and 96 g L^{-1} NaCl)	Ramon, Nguyen, and Hoek (2013)
Organic fouling/ biofouling	TFC polyamide	Surface flushing	NaCl	50 mM NaCl cleaning solution (15 min)	70% Permeate flux recovery	Mi and Elimelech (2010)
Organic fouling/ biofouling	LFC polyamide		Monovalent cations (Na^+, K^+, Cs^+, NH_4^+)	25 and 100 mM	75% Cleaning efficiency for NaCl at 25 mM and ~90% for all the salts at 100 mM	Lee and Elimelech (2007)
Organic fouling/ biofouling	Cellulose acetate	Chemical and biological	Enzyme + EDTA + dispersant. Bactericidal agent + anionic detergent	Chemicals dissolved in a 100 mM phosphate buffer at pH 7.	70%–90% Biofilm removal	Whittaker, Ridgway, and Olson (1984)
Organic fouling/ biofouling	BTESE-derived organosilica membranes	Physical (immersion and agitation)	DI water	Three cleaning steps at 1000 rpm. First at 298K and the others at 353K	Total recovery of membrane	Ibrahim, Nagasawa, Kanezashi, and Tsuru (2020)

(*Continued*)

TABLE 11.1 (Continued)

Fouling type	Membrane	Cleaning method	Cleaning agents	Procedure	Improvement	References
Organic fouling/ biofouling	TFC polyamide	Biological	Subtilisin (protease and lipase) + dextranase + polygalacturonase	Doses of 50, 100, and 150 ppm at neutral pH (~7) during 18–36 h	Restored the hydrophobicity and roughness of the TFC RO surface to its initial condition	Khan et al. (2013)
Inorganic fouling ($CaCO_3$)	TFC polyamide	Osmotic backwashing	NaCl	Backwashing immediately after salt precipitation	Initial permeate flux recovery	Sagiv and Semiat (2005)
Inorganic and organic fouling/ biofouling	Polyamide	Physical and chemical	NaOH + SDS + HCl	10 min DI water + 10 min chemicals at 0.5 bar	Removal of most of the deposited materials from the membrane surface	Madaeni and Samieirad (2010)
Inorganic and organic fouling/ biofouling	Polyamide	Physical (ultrasounds)	—	20 kHz Frequency and 2.8 W cm^{-2} power intensity	50%–250% Permeate flux increase with no compromise in salt rejection	Feng, Deventer, and van, Aldrich (2006)

TFC, Thin-film composite; *EDTA*, ethylene diamine tetra acetic acid; *LFC*, low fouling composite; *BTESE*, bis(triethoxysilyl)ethane; *DI*, deionized water.

11.5.2 Reuse of discarded reverse osmosis membrane modules

Following the waste management hierarchy shown in Fig. 11.9, reduction together with reuse or recycling should be prioritized for an adequate management of RO discarded membrane modules. Nevertheless, it is not always possible to reduce wastes. Therefore strategies to reuse and recycle discarded RO membrane modules become of great importance.

The potential reuse of discarded RO membrane modules is very scarce as only few reports have been found in the membrane literature (Ould Mohamedou et al., 2010; Pontié, 2015; Prince et al., 2011). For example, Ould Mohamedou et al. (2010) verified that a discarded RO membrane could be a useful nanofiltration (NF) membrane valid in less-demanding filtration processes. It also proposed the use of spacers and the discarded RO membrane as a geotextile in gardens (root entry protective layer in drainage sublayer). Prince et al. (2011), after studying the characteristics of discarded RO membranes from seawater RO modules, proposed their reuse in RO separation of lower solute concentrations (i.e., for selective demineralization of brackish water or NF as RO pretreatment). The external and internal elements of the RO membrane modules have been proposed for reuse in various applications such as geotextile, mouse pad, support for children drawings, protection from snake attack, and aromatic herbs containers in familial kitchen (Pontié, 2015).

11.5.3 Recycling discarded reverse osmosis membrane modules

Different chemical procedures have been proposed to recycle discarded RO membrane modules. The degradation of the PA layer of TFC membranes by certain oxidizing agents has been widely investigated (Kang et al., 2007; Mitrouli, Karabelas, & Isaias, 2010). This method has been used for the total or partial elimination of the PA layer where the irreversible fouling is located (Araújo et al., 2012). NaClO is one of the most used chemical agent (Coutinho de Paula et al., 2018; Lawler et al., 2012). Other considered chemical agents for PA layer degradation are H_2O_2, SDS, acetone, *N*-methyl-2-pyrrolidone, potassium permanganate ($KMnO_4$), tannic acid, and NaOH (Ambrosi & Tessaro, 2013; Da Silva, Ambrosi, Dos Ramos, & Tessaro, 2012; García-Pacheco et al., 2015; Landaburu-Aguirre et al., 2016; Lawler, 2011; Muñoz et al., 2014; Pontié et al., 2017; Rodríguez, Jiménez, Trujillo, & Veza, 2002). Any of these chemicals can be applied following an active

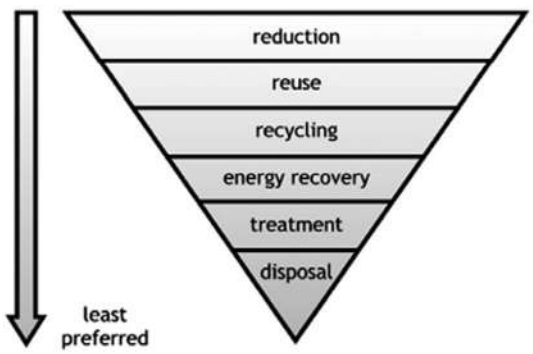

FIGURE 11.9 Waste management hierarchy. Source: *From Lawler, W., Bradford-Hartke, Z., & Cran, M. J., et al. (2012). Towards new opportunities for reuse, recycling and disposal of used reverse osmosis membranes.* Desalination, 299, 103–112. https://doi.org/10.1016/j.desal.2012.05.030.

procedure in which the oxidant solutions are pumped through the discarded RO membrane modules, or a passive procedure by immersing the discarded RO membrane modules in the oxidizing solution without any type of pumping. The exposure time of the discarded membrane modules in the oxidant solution and its concentration determines the degradation speed of the PA layer. For this reason, both parameters (exposure time and oxidant concentration) have been investigated in the following studies (Ambrosi & Tessaro, 2013; Da Silva et al., 2012; García-Pacheco, Landaburu-Aguirre, & Lejarazu-Larrañaga, 2019; Lawler, 2011; Molina et al., 2018). Both parameters were merged as the exposure dose (ppm · h) defined as the concentration of the oxidizing agent in parts per million (ppm) multiplied by the exposure time in hours (h). In addition, it was reportedthat the basic pH of the oxidant solutions plays a decisive role in the degradation of the PA layer (García-Pacheco et al., 2015; Lawler et al., 2013; Raval, Chauhan, Raval, & Mishra, 2012). Fig. 11.10 shows the degradation schema of the PA layer of the discarded RO TFC membrane as a function of the applied dose of the oxidizing agent.

By analyzing the attenuated total reflectance-Fourier transform infrared (ATR-FTIR) spectra of RO discarded membranes subjected to different exposure doses in the recycling process, it was confirmed that the dependence of the degradation of the PA layer depends on the exposure dose of the oxidizing agent. Fig. 11.11 shows the spectra of seawater and brackish water discarded membranes and those exposed to different exposure doses. If the characteristic peaks of PA amide I and amide II are observed at 1664 and 1542 cm^{-1}, respectively, the different degrees of degradation of the PA layer are clearly detected. Due to the difference of fouling layers present on the discarded membranes that generally depend on the type of feed water used, for the same exposure dose, the discarded membrane from brackish water desalination suffers greater degradation of the PA layer than the membrane previously used in seawater desalination. It was claimed a complete degradation of the PA layer around 300,000 ppm h exposure doses for the discarded membranes previously used in seawater desalination and 50,000 ppm h for those applied in brackish water desalination (Molina et al., 2018).

The surface of discarded RO membranes and those subjected to a recycling process with different exposure doses of NaClO were studied by SEM. Fig. 11.12 shows the removal of fouling and the progressive degradation of the PA layer from the surface of the RO membrane with the increase of the exposure dose of the oxidizing agent (Moradi, Pihlajamäki, Hesampour, Ahlgren, & Mänttäri, 2019).

It is worth noting that most of the above-mentioned recycling procedures have been reported on a laboratory scale. However, a pilot plant has been proposed for passive

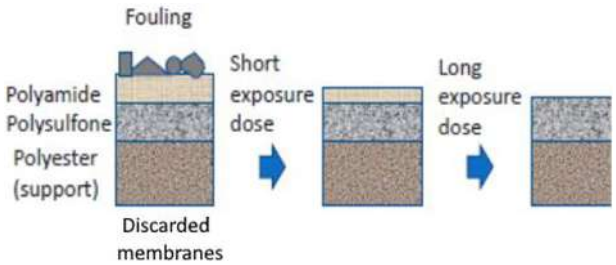

FIGURE 11.10 Degradation of the polyamide (PA) layer of discarded reverse osmosis thin-film composite (RO TFC) membrane as a function of the oxidizing agent dose.

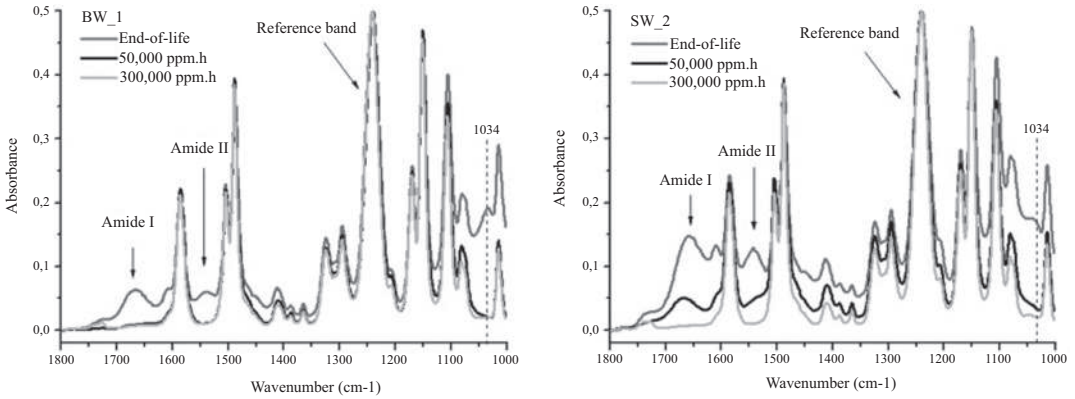

FIGURE 11.11 Attenuated total reflectance-Fourier transform infrared (ATR-FTIR) spectra of recycled membranes from brackish water and seawater desalination plants after different exposure doses. Source: *From Molina, S., Landaburu-Aguirre, J., Rodríguez-Sáez, L., García-Pacheco, R., de la Campa, J. G., & García-Calvo, E. (2018). Effect of sodium hypochlorite exposure on polysulfone recycled UF membranes and their surface characterization*. Polymer Degradation and Stability, 150, 46–56. https://doi.org/10.1016/j.polymdegradstab.2018.02.012.

simultaneous recycling of six membrane modules (García-Pacheco et al., 2018). As can be seen in Fig. 11.13, this consists of a cylindrical polypropylene container filled with the oxidizing solutions. It is equipped with low pressure pumps, valve circuits, a container to store the oxidant solutions, and a container to carry out the neutralization of NaClO with sodium bisulfite in order to maintain constant the NaClO concentration.

Headed for the industrialization and standardization of membrane module recycling, García-Pacheco, Li, Comas, Taylor, and Le-Clech (2021) developed and tested two other housing designs for recycling membrane modules. This design only replaces the endcaps (lids for feed and permeate inlet and outlet of the RO modules) adapting the recycled end-of-life RO modules to use in ultra-low-pressure gravity-driven membrane systems with acceptable results.

In addition to the chemical recycling processes mentioned earlier, various transformations have been adopted to the discarded RO membranes for their use in other applications. These transformations were carried out directly on the discarded membranes or after the chemical recycling process (Lejarazu-Larrañaga, Molina, Ortiz, Navarro, & García-Calvo, 2020; Moradi et al., 2019; Morón-López, Nieto-Reyes, Aguado, El-Shehawy, & Molina, 2019; Morón-López, Nieto-Reyes, Senán-Salinas, Molina, & El-Shehawy, 2019; Morón-López, Nieto-Reyes, Molina, & Lezcano, 2020; Rodríguez-Sáez, Landaburu-Aguirre, Molina, García-Payo, & García-Calvo, 2021). For instance, Moradi et al. (2019) investigated the deposition of polyelectrolyte multilayers after chemical recycling using NaClO aqueous solution and could improve the performance of recycled membranes in UF separation process. With the same purpose, Rodríguez-Sáez et al. (2021) reported on the modification of the active layer of recycled membranes by passive cleaning with NaClO dissolution and dip-coating technique using catechol and polyethyleneimine. Morón-López et al. (2019, 2020) used both discarded and recycled membranes treated with NaClO to grow a cyanobacterial biofilm in its active layer for use in membrane biofilms reactor process (MBfR). Lejarazu-Larrañaga et al.

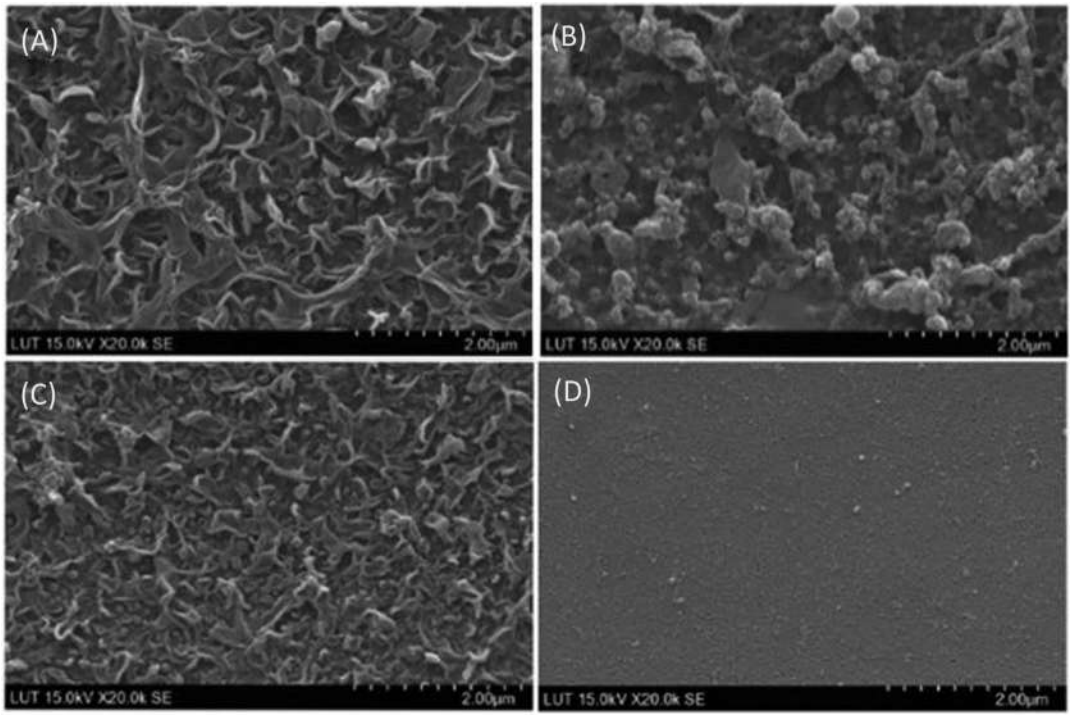

FIGURE 11.12 Scanning electron microscopy (SEM) images of polyamide (PA) thin-film composite (TFC) reverse osmosis (RO) seawater desalination membrane surface: (A) pristine, (B) end-of-life, (C) exposed to 94,250 ppm h of NaClO solution, and (D) exposed to 240,500 ppm h of NaClO solution. Source: *Adapted and modified from Moradi, M. R., Pihlajamäki, A., Hesampour, M., Ahlgren, J., & Mänttäri, M. (2019). End-of-life RO membranes recycling: Reuse as NF membranes by polyelectrolyte layer-by-layer deposition*. Journal of Membrane Science, 584, 300–308. https://doi.org/10.1016/j.memsci.2019.04.060.

(2020) used membranes recycled by passive cleaning with NaClO as a support to prepare anion exchange membranes for electrodialysis separation process.

Few reports have evaluated energy recovery as an alternative to the disposal of modules discarded in landfills (Pontié et al., 2017; Prince et al., 2011). Pontié et al. (2017) reported the use of pyrolysis and show a reduction of 48.5% in the mass of waste and an energy recovery of 2210 kWh. These results showed an environmental improvement with respect to landfill disposal but not with respect to reuse or recycling for the modules.

Nowadays, discarded RO membrane modules are disposed in landfills and it is necessary to propose other alternatives. It is necessary to study whether recycling, reuse, or any of the proposed techniques improve current procedures environmentally and economically. Lawler et al. (2015) presented a comparative life cycle assessment (LCA) study reporting the environmental impact produced by the different alternatives to landfill disposal of discarded RO membrane modules. It was claimed that reuse is the most environmentally friendly option. Recycling also seems a favorable option, but it is necessary to know its new useful life in order to assess it properly. The disposal of discarded membrane modules in landfills is presented as the least favorable alternative for the environment.

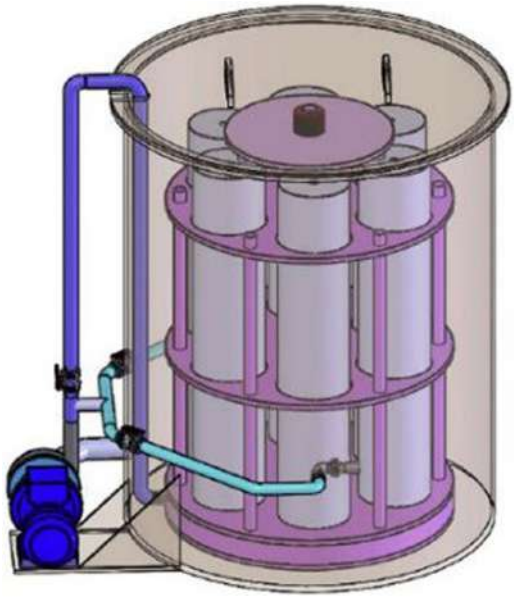

FIGURE 11.13 Pilot scale used to recycle simultaneously six membrane modules. Source: *From García-Pacheco, R., Landaburu-Aguirre, J., Terrero-Rodríguez, P., et al. (2018). Validation of recycled membranes for treating brackish water at pilot scale.* Desalination, 433, *199–208. https://doi.org/10.1016/j.desal.2017.12.034.*

11.6 Applications of reverse osmosis recycled membranes in other membrane processes

Taking into consideration the type of membranes commonly used in the RO process, a relatively simple conversion of the dense membrane into a porous material is possible through the degradation of the PA active layer (Lawler et al., 2012). In this way, recycled RO membranes could then be expected to comply with the characteristics, hydraulic permeabilities, and separation performances comparable to commercially available filtration membranes (Lawler et al., 2012). The application of RO recycled membrane modules and membranes in filtration processes mainly refers to NF and UF technologies. The difference between these two membranes, NF or UF, lies in the PA layer degradation. For NF only a low degradation of the PA layer is necessary, thus a low exposure dose to the oxidizing agent is needed. However, for UF membranes, a higher exposure dose is needed to ensure the total degradation of the PA layer (Ambrosi & Tessaro, 2013; Da Silva et al., 2012; García-Pacheco et al., 2019; Lawler, 2011; Mitrouli et al., 2010; Molina et al., 2018).

Few authors have reported on the use of recycled RO membranes in MBfR, membrane distillation (MD), ED, and photocatalytic membrane reactor (PMR). For these applications, RO recycled membranes require some additional transformations to adapt their characteristics to those of the new application. These are explained in detail in Section 11.5.3. Table 11.2 summarizes the different alternatives reported in literature for the application of recycled RO membranes in other membrane separation processes.

TABLE 11.2 Different alternatives reported for the application of recycled reverse osmosis membranes in other membrane separation processes.

RO membrane	Oxidant agent	Cleaning type	Transformation	New application	Results	References
—	$KMnO_4$	Peeling by oxidizing solution (1000 mg L^{-1}) at 4.4 bar (1–2 h) + neutralization by SBS (18 h)	—	Filtration prior to RO desalination	94% Suspended solids reduction (turbidity) before further RO treatment	Rodríguez et al. (2002)
TFC PA	NaClO	Exposure to NaClO solution of 6.25 g L^{-1} (48 h), equivalent to 300,00 ppm h	—	UF	MWCO between 10 and 100 kDa. Similar protein rejection than UF commercial of PES (10 kDa)	Lawler (2011), Lawler et al. (2013)
TFC PA	NaClO	62,500 ppm for 3 h	—	UF	UF 10 kDa MWCO membrane was prepared	Pontié (2015)
TFC PA	NaClO, acetone, or NMP	124 ppm NaClO, 10,000 ppm acetone, 10,000 ppm NMP for 0.8, 20, and 92 h + NaClO 124 ppm from 1 to 410 h	—	UF and NF	NaClO was the most effective reagent. Up to 122 h of NaClO, membranes showed NF properties and from 242 h, MF properties	García-Pacheco et al. (2015)
TFC PA	—	—	Old RO spacers of PP + low density PP to elaborate a new flat sheet membrane by IP	MD	Membrane characteristics (contact angle, porosity, thickness, and roughness) were those of a typical MD membrane	Pontié et al. (2017)
TFC PA	NaClO	Passive process in pilot scale plant at different exposure doses from 6200 to 1,700,000 ppm h	—	NF and MF	80% Salt rejection factor in long-term experiments with UF-like recycled membranes	García-Pacheco et al. (2018)
TFC PA	NaClO	Exposure dose ranging from 13,000 to 240,500 ppm h	Deposition of polyelectrolyte multilayers	NF	Mg SO_4 rejection 98.3%. The permeability and rejection greater than those values for commercial membranes	Moradi et al. (2019)

(*Continued*)

TABLE 11.2 (Continued)

RO membrane	Oxidant agent	Cleaning type	Transformation	New application	Results	References
TFC PA	NaClO	Exposure dose at 6200 and 300,000 ppm h	—	MBfR	Chlorination process could eliminate previous incrustations and improve the binding of the desired bacteria in MBfR	Morón-López et al. (2019)
TFC PA	—	—	Discarded RO membranes as a support material to biofilm layer of microcystins	MBfR	Microcystins-degrading biofilm on discarded RO membranes removed 2 mg L^{-1} of microcystin in 24 h	Morón-López et al. (2019)
TFC PA	NaClO	Exposure dose at 6200 ppm h	Discarded RO membranes as a support material to grow natural cyanobacterial bloom	MBfR	Microcystins removal rate of 0.021 h^{-1}	Morón-López et al. (2020)
TFC PA	NaClO	Passive immersion at ~300,000 ppm h at room temperature	PMR composed of TiO_2 nanoparticles and UF-like recycled RO membrane	PMR and MBR	60% of organic matter of the MBR permeate was discomposed in the PMR	de Oliveira et al. (2020)
TFC PA	NaClO	Passive process at 800,000 ppm h	Recycled anion exchange membranes prepared by casting and phase inversion using discarded RO modules as membrane support. Use of PP components (feed spacers, end plates, and compartments) as ED stacks	ED	Highly permselective (87% higher than commercial membrane). 84.5% salt rejection of membranes tested by brackish water desalination experiments in the assembled electrodialysis	Lejarazu-Larrañaga et al. (2020)
TFC PA	NaClO	Passive immersion at 6000–26,500 ppm h for NF-like recycled membranes and 300,000 ppm h for UF-like recycled membranes	Housing (end caps) designs for NF and UF gravity-driven recycled membrane-based systems	NF and UF	NF-like recycled membranes: ~1.7 L m^{-2} h^{-1} bar^{-1} permeability and >81% DOC rejection UF-like recycled membranes: >74% biopolymers rejection and 18-fold higher permeate rate than NF-like recycled membranes	García-Pacheco et al. (2021)

(*Continued*)

TABLE 11.2 (Continued)

RO membrane	Oxidant agent	Cleaning type	Transformation	New application	Results	References
TFC PA	NaClO	Passive process at 350,000 ppm h	Active layer modification by dip-coating using CA and PEI	UF	Flow recovery ratio of 1.38 and a relative permeability (individual permeability over average permeability) of 1.12	Rodríguez-Sáez et al. (2021)

CA, Catechol; *DOC*, dissolved organic carbon; *ED*, electrodialysis; *MBfR*, membrane biofilms reactors; *MBR*, membrane bioreactor; *MD*, membrane distillation; *MF*, microfiltration; *MWCO*, molecular weight cut-off; *NF*, nanofiltration; *NMP*, *N*-methyl-2-pyrrolidone; *PEI*, polyethyleneimine; *PES*, polyethersulfone; *PMR*, photocatalytic membrane reactor; *PP*, polypropylene; *RO*, reverse osmosis; *SBS*, sodium bisulfite solution; *TFC PA*, thin-film composite polyamide; *UF*, ultrafiltration.

11.6.1 Reverse osmosis recycled membranes in ultrafiltration and microfiltration process

The most considered applications for RO recycled membranes have been UF and MF. These applications do not require any transformation of the membranes after recycling by means of an oxidizing agent. Since the first published paper on the recycling of discarded RO membrane modules in 2002 and 2003 (Rodríguez et al., 2002; Veza & Rodriguez-Gonzalez, 2003), some researchers proposed improvements to the recycling process in order to improve the performance of these membranes in their subsequent filtration applications. Rodríguez et al. (2002) reported their best results for the recycling process using $KMnO_4$ in aqueous solution at 1000 mg L^{-1} as an oxidizing agent. In the first step, the oxidant solution was circulated at 4.4 bar during 1−2 h, then a sodium bisulfite solution was circulated to neutralize the oxidant solution. Later, Veza and Rodriguez-Gonzalez (2003) tested recycled membrane modules for wastewater secondary effluent filtration treatment prior to RO treatment. In addition to the reduction of suspended solids by 94%, the RO unit reduced 98.5% the electrical conductivity at a 60% recovery ratio.

During the past decade (2010−20) and due to the implementation of the waste treatment method based on circular economy, the idea of membrane recycling was recovered. Lawler et al. (Lawler, 2011; Lawler et al., 2013; Mitrouli et al., 2010) reported similar properties of the recycled membranes to those of the commercial Pall Omega 10 kDa PES-UF membrane by using an exposure dose of 300,000 ppm h of NaClO as an oxidizing agent to the discarded RO membranes. It was emphasized as the remarkable importance of the storage conditions of the discarded RO membrane modules. The storage of the membrane modules before and after recycling in dry conditions produced an irrecoverable decrease of the permeate flux. Similarly, for the same RO membrane modules, it was observed a variable membrane performance caused by differences in fouling. García-Pacheco et al. (2016) defined a gravimetric method that allows the classification of the discarded RO membrane modules according to their fouling degree, in order to apply the most suitable recycling procedure, and thus the recycled modules could present a more homogeneous performance. García-Pacheco et al. (Fortunato et al., 2020; García-Pacheco et al., 2015, 2019) made optimized

studies of the adequate exposure dose in NaClO solutions as an oxidizing agent together with the adequate pH in the recycling processes. They also reported the first pilot scale plant for recycling end-of-life RO membrane modules (García-Pacheco et al., 2018). Based on the operating data of this pilot plant, Senán-Salinas, García-Pacheco, Landaburu-Aguirre, and García-Calvo (2019) reported a comparative LCA and cost-effectiveness analysis. This comparison highlighted the environmental and economic viability of recycling discarded RO membrane modules.

Recently, two research studies have been published (Moradi et al., 2019; Rodríguez-Sáez et al., 2021) with the main objective to improve the filtration performance by transforming the recycled RO membranes using NaClO as an oxidizing solution. Moradi et al. (2019) deposited multilayers of SC498/KE253 polyelectrolyte after the recycling process of the RO membrane. The electrolyte layers were deposited by circulation of the polyelectrolytic solution (1 g L^{-1} polyelectrolyte and 0.05 M NaCl) through the RO membrane module by fluidic assembly technique. The NF membrane composed of eight bilayers of polyelectrolytes deposited on the recycled RO membrane exhibited an improved saltwater permeability of 11 L m^{-2} h^{-1} bar^{-1} with maximum NaCl and $MgSO_4$ rejection factors of 92% and 98%, respectively. By applying the dip-coating technique, Rodríguez-Sáez et al. (2021) modified recycled RO membranes (350,000 ppm h of exposure dose) transforming it into NF membranes. The best parameters reported for the transformation of the active layer of the recycled membranes was using catechol (1 g L^{-1}) and polyethyleneimine (1 g L^{-1}) at 30°C for 2 h. Under these conditions, a flow recovery ratio of 1.38 and a relative permeability (individual permeability over average permeability) of 1.12 were obtained.

11.6.2 Reverse osmosis recycled membranes in membrane distillation, membrane biofilms reactors, and electrodialysis separation processes

In recent years, several reports have been focused on the application of recycled RO membranes in other membrane separation processes rather than filtration systems. In this case, transforming the recycled RO membranes in order to adapt their characteristics to those required by the new applications is necessary.

Morrón et al. (Morón-López et al., 2019; Morón-López et al., 2019; Morón-López et al., 2020) reported the use of discarded and recycled RO membranes as a support material to create a biofilm layer of microcystins-degrading. The feasibility of using recycled RO membranes as supports to prepare biofilm reactor membranes was analyzed in their first report (Morón-López et al., 2019), confirming finally their suitability. In their second report (Morón-López et al., 2019), a biofilm layer of microcystins-degrading (*Sphingopyxis* sp. strain IM-1) was prepared on the active layer of a discarded RO membrane. These new recycled membranes, when tested for microcystin-degradation in an MBfR system, were able to remove 2 mg L^{-1} of microcystin in 24 h. In their latest report (Morón-López et al., 2020), both discarded and recycled RO membranes were used to generate a biofilm layer using natural cyanobacterial bloom. In MBfR system, these membranes exhibited a removal rate of 0.021 h^{-1}.

Lejarazu-Larrañaga et al. (2020) proposed the application of recycled RO membranes in ED process. These were used as a support material for the preparation of anion

exchange membranes. The necessary transformation was performed using two combined methods: casting and PI. A mixture of anion exchange resin with a solution of polymerized polyvinylchloride in tetrahydrofuran (1:1 (w/w)) was used. After studying the impact of various manufacturing parameters (i.e., thickness and solvent evaporation time) on the membrane performance, the membrane prepared with 800 μm thickness and 60 min solvent evaporation time was the one that presented the best characteristics and performance (84.5% salt removal) comparable to those of commercial membranes (AMH-PES for anion exchange and CMH-PES for cation exchange from RALEX).

For these applications, a more advanced development is still necessary to make feasible the evaluation of economic and environmental costs produced by the transformations carried out based on the performance and new useful life provided to the discarded RO membranes. In addition, developing more standardized protocols for the transformed and/or recycled membranes is necessary.

In addition to the use of recycled RO membranes in the above-mentioned water remediation processes, future research trends should be focused on the direct reuse of end-of-life RO membrane modules as part of the prefiltration step in RO desalination plants, making the process more sustainable. Furthermore, their other plastic parts of the modules should be reused for the manufacture of new RO modules. There is also an open window for new development and transformation of discarded membranes and their reutilization as supports. Current membrane recycling methodologies must be improved in terms of ecology and performance in order to open the range of use of recycled RO membranes in other water remediation processes for their implementation at an industrial level.

11.7 Conclusions

RO is the most common technology applied for desalination worldwide due to its low cost and high-water production rate compared to other available techniques. It is expected that from 2025 around 2 million of RO spiral-wound modules will be discarded per year due to membrane fouling and other associated problems. Based on an adequate waste management hierarchy, different strategies have been adopted since years to revalue discarded RO membrane modules. These alternatives include reuse and recycling of RO membrane modules for their use in other membrane processes, such as NF, UF, biofilm-membrane reactors, or ED. In this sense, the oxidation and removal of the PA layer by means of different chemicals is the most studied method to convert the dense RO membrane into a porous one. Moreover, the recycling of discarded RO membrane modules as prefilters in RO desalination plants, the utilization of the support layer of RO membranes for new membrane development, or even the use of plastic parts for other purposes have been considered. Nevertheless, these other ways are still under study.

Research efforts should be focused on the following lines: i) direct reutilization of RO discarded membrane modules within the desalination plants themselves as prefilters, contributing to a circular economy, since less waste and lower associated costs would be generated; ii) development of effective recycling techniques and protocols in order to be able

to use the discarded RO membrane modules and the recycled membranes in other membrane processes, and iii) improvement of the performance of current recycling procedures to make the leap from labs to industry.

Acknowledgments

We appreciate the financial support from the Spanish Ministry of Economy and Competitiveness through its project CTM2015-65348-C2-2-R and the Spanish Ministry of Science, Innovation, and Universities through its project RTI2018-096042-B-C22.

References

Ahmed, F. E., Hashaikeh, R., & Hilal, N. (2020). Hybrid technologies: The future of energy efficient desalination – A review. *Desalination*, 495. Available from https://doi.org/10.1016/j.desal.2020.114659.

Ahsan, A., & Imteaz, M. (2018). *Application and future prospects of reverse osmosis process*. *Nanotechnology in water and wastewater treatment: Theory and applications* (pp. 297–301). Bangladesh: Elsevier. Available from http://doi.org/10.1016/B978-0-12-813902-8.00015-0.

Aimar, P., & Bacchin, P. (2010). Slow colloidal aggregation and membrane fouling. *Journal of Membrane Science*, *360*(1–2), 70–76. Available from https://doi.org/10.1016/j.memsci.2010.05.001.

Ambrosi, A., & Tessaro, I. C. (2013). Study on potassium permanganate chemical treatment of discarded reverse osmosis membranes aiming their reuse. *Separation Science and Technology*, *48*(10), 1537–1543. Available from https://doi.org/10.1080/01496395.2012.745876.

Andrews, B., Davé, B., López-Serrano, P., Tsai, S. P., Frank, R., Wilf, M., & Koutsakos, E. (2008). Effective scale control for seawater RO operating with high feed water pH and temperature. *Desalination*, *220*(1–3), 295–304. Available from https://doi.org/10.1016/j.desal.2007.02.041.

Apell, J. N., & Boyer, T. H. (2010). Combined ion exchange treatment for removal of dissolved organic matter and hardness. *Water Research*, *44*(8), 2419–2430. Available from https://doi.org/10.1016/j.watres.2010.01.004.

Araújo, P. A., Kruithof, J. C., Van Loosdrecht, M. C. M., & Vrouwenvelder, J. S. (2012). The potential of standard and modified feed spacers for biofouling control. *Journal of Membrane Science*, *403–404*, 58–70. Available from https://doi.org/10.1016/j.memsci.2012.02.015.

Argüello, M. A., Álvarez, S., Riera, F. A., & Álvarez, R. (2005). Utilization of enzymatic detergents to clean inorganic membranes fouled by whey proteins. *Separation and Purification Technology*, *41*(2), 147–154. Available from https://doi.org/10.1016/j.seppur.2004.05.005.

Asadollahi, M., Bastani, D., & Musavi, S. A. (2017). Enhancement of surface properties and performance of reverse osmosis membranes after surface modification: A review. *Desalination*, *420*, 330–383. Available from https://doi.org/10.1016/j.desal.2017.05.027.

Bar-Zeev, E., & Elimelech, M. (2014). Reverse osmosis biofilm dispersal by osmotic back-flushing: Cleaning via substratum perforation. *Environmental Science and Technology Letters*, *1*, 162–166. Available from https://doi.org/10.1021/ez400183d.

Butt, F. H., Rahman, F., & Baduruthamal, U. (1997). Characterization of foulants by autopsy of RO desalination membranes. *Desalination*, *114*(1), 51–64. Available from https://doi.org/10.1016/S0011-9164(97)00154-9.

Butt, F. H., Rahman, F., & Baduruthamal, U. (1995). Identification of scale deposits through membrane autopsy. *Desalination*, *101*(3), 219–230. Available from https://doi.org/10.1016/0011-9164(95)00025-W.

Cadotte, J. E. (1981). *Interfacially synthesized reverse osmosis membranes, US Patent 4* (277). MN: FilmTec Corporation, Minetonka.

Carnahan, R. P., Bolin, L., & Suratt, W. (1995). Biofouling of PVD-1 reverse osmosis elements in the water treatment plant of the City of Dunedin, Florida. *Desalination*, *102*(1–3), 235–244. Available from https://doi.org/10.1016/0011-9164(95)00059-B.

Chiu, J. M. Y., Thiyagarajan, V., Tsoi, M. M. Y., & Qian, P. Y. (2005). Qualitative and quantitative changes in marine biofilms as a function of temperature and salinity in summer and winter. *Biofilms*, *2*(3), 183–195. Available from https://doi.org/10.1017/S147905050500195X.

Coutinho de Paula, E., & Santos Amaral, M. C. (2018). Environmental and economic evaluation of end-of-life reverse osmosis membranes recycling by means of chemical conversion. *Journal of Cleaner Production*, *194*, 85–93. Available from https://doi.org/10.1016/j.jclepro.2018.05.099.

Da Silva, M. K., Ambrosi, A., Dos Ramos, G. M., & Tessaro, I. C. (2012). Rejuvenating polyamide reverse osmosis membranes by tannic acid treatment. *Separation and Purification Technology*, *100*, 1–8. Available from https://doi.org/10.1016/j.seppur.2012.07.027.

Daly, S., Allen, A., Koutsos, V., & Semião, A. J. C. (2020). Influence of organic fouling layer characteristics and osmotic backwashing conditions on cleaning efficiency of RO membranes. *Journal of Membrane Science*, 616. Available from https://doi.org/10.1016/j.memsci.2020.118604.

de Oliveira, C. P. M., Viana, M. M., Silva, G. R., Frade Lima, L. S., Coutinho de Paula, E., & Amaral, M. C. S. (2020). Potential use of green TiO_2 and recycled membrane in a photocatalytic membrane reactor for oil refinery wastewater polishing. *Journal of Cleaner Production*, *257*, 120526. Available from https://doi.org/10.1016/j.jclepro.2020.120526.

Dudley, L. (1998). Membrane autopsies for reversing fouling in reverse osmosis. *Membrane Technology*, *95*, 9–12.

Dudley, L. Y., & Darton, E. G. (1996). Membrane autopsy—A case study. *Desalination*, *105*(1–2), 135–141. Available from https://doi.org/10.1016/0011-9164(96)00067-7.

Feng, D., Deventer, J. S. J., & van, Aldrich, C. (2006). Ultrasonic defouling of reverse osmosis membranes used to treat wastewater effluents. *Separation and Purification Technology*, *50*, 318–323. Available from https://doi.org/10.1016/j.seppur.2005.12.005.

Flemming, H. C. (1997). Reverse osmosis membrane biofouling. *Experimental Thermal and Fluid Science*, *14*(4), 382–391. Available from https://doi.org/10.1016/S0894-1777(96)00140-9.

Flemming, H. C., Schaule, G., Griebe, T., Schmitt, J., & Tamachkiarowa, A. (1997). Biofouling—The Achilles heel of membrane processes. *Desalination*, *113*(2–3), 215–225. Available from https://doi.org/10.1016/S0011-9164(97)00132-X.

Fortunato, L., Alshahri, A. H., Farinha, A. S. F., Zakzouk, I., Jeong, S., & Leiknes, T. O. (2020). Fouling investigation of a full-scale seawater reverse osmosis desalination (SWRO) plant on the Red Sea: Membrane autopsy and pretreatment efficiency. *Desalination*, 496. Available from https://doi.org/10.1016/j.desal.2020.114536.

Fritzmann, C., Löwenberg, J., Wintgens, T., & Melin, T. (2007). State-of-the-art of reverse osmosis desalination. *Desalination*, *216*(1–3), 1–76. Available from https://doi.org/10.1016/j.desal.2006.12.009.

García-Pacheco, R., Landaburu-Aguirre, J., Lejarazu-Larrañaga, A., Rodríguez-Sáez, L., Molina, S., Ransome, T., & García-Calvo, E (2019). Free chlorine exposure dose (ppm · h) and its impact on RO membranes ageing and recycling potential. *Desalination*, *457*, 133–143. Available from https://doi.org/10.1016/j.desal.2019.01.030.

García-Pacheco, R., Landaburu-Aguirre, J., Molina, S., Rodríguez-Sáez, L., Teli, S. B., & García-Calvo, E. (2015). Transformation of end-of-life RO membranes into NF and UF membranes: Evaluation of membrane performance. *Journal of Membrane Science*, *495*, 305–315. Available from https://doi.org/10.1016/j.memsci.2015.08.025.

García-Pacheco, R., Landaburu-Aguirre, J., Terrero-Rodríguez, P., Campos, E., Molina-Serrano, F., Rabadán, J., … García-Calvo, E. (2018). Validation of recycled membranes for treating brackish water at pilot scale. *Desalination*, *433*, 199–208. Available from https://doi.org/10.1016/j.desal.2017.12.034.

García-Pacheco, R., Lawler, W., Landaburu-Aguirre, J., García-Calvo, E., & Le-Clech, P. (2017). End-of-life membranes: Challenges and opportunities. In E. Drioli, L. Giorno, & E. Fontananova (Eds.), *Comprehensive membrane science and engineering* (2nd ed., pp. 293–310). Oxford: Elsevier, ISBN 978-0-444-63796-3.

García-Pacheco, R., Li, Q., Comas, J., Taylor, R. A., & Le-Clech, P. (2021). Novel housing designs for nanofiltration and ultrafiltration gravity-driven recycled membrane-based systems. *Science of the Total Environment*, *767*. Available from https://doi.org/10.1016/j.scitotenv.2020.144181.

García-Pacheco, R., Terrero, P., Molina Martínez, S., Martínez, D., Campos, E., García-Pacheco, R., … Zarzo, D. E. (2016). García-Calvo. In Life + 13 transfomem: A recycling example within the desalination world, . (XI). Valencia: AEDYR Int Congr. Available from https://aedyr.com/congresos/xi-congreso-internacional-aedyr/.

Geise, G. M., Lee, H. S., Miller, D. J., Freeman, B. D., McGrath, J. E., & Paul, D. R. (2010). Water purification by membranes: The role of polymer science. *Journal of Polymer Science, Part B: Polymer Physics*, *48*(15), 1685–1718. Available from https://doi.org/10.1002/polb.22037.

Ghanbari, M., Emadzadeh, D., Lau, W. J., Matsuura, T., & Ismail, A. F. (2015). Synthesis and characterization of novel thin film nanocomposite reverse osmosis membranes with improved organic fouling properties for water desalination. *RSC Advances*, *5*(27), 21268–21276. Available from https://doi.org/10.1039/c4ra16177g.

Goh, P. S., Lau, W. J., Othman, M. H. D., & Ismail, A. F. (2018). Membrane fouling in desalination and its mitigation strategies. *Desalination*, *425*, 130–155. Available from https://doi.org/10.1016/j.desal.2017.10.018.

Greenlee, L. F., Lawler, D. F., Freeman, B. D., Marrot, B., & Moulin, P. (2009). Reverse osmosis desalination: Water sources, technology, and today's challenges. *Water Research*, *43*(9), 2317–2348. Available from https://doi.org/10.1016/j.watres.2009.03.010.

Gutiérrez Ruiz, S., López-Ramírez, J. A., Hassani Zerrouk, M., Egea-Corbacho Lopera, A., & Quiroga Alonso, J. M. (2020). Study of reverse osmosis membranes fouling by inorganic salts and colloidal particles during seawater desalination. *Chinese Journal of Chemical Engineering*, *28*(3), 733–742. Available from https://doi.org/10.1016/j.cjche.2019.10.004.

Haaksman, V. A., Siddiqui, A., Schellenberg, C., Kidwell, J., Vrouwenvelder, J. S., & Picioreanu, C. (2017). Characterization of feed channel spacer performance using geometries obtained by X-ray computed tomography. *Journal of Membrane Science*, *522*, 124–139. Available from https://doi.org/10.1016/j.memsci.2016.09.005.

Haidari, A. H., Heijman, S. G. J., & van der Meer, W. G. J. (2018). Optimal design of spacers in reverse osmosis. *Separation and Purification Technology*, *192*, 441–456. Available from https://doi.org/10.1016/j.seppur.2017.10.042.

Hailemariam, R. H., Woo, Y. C., Damtie, M. M., Kim, B. C., Park, K. D., & Choi, J. S. (2020). Reverse osmosis membrane fabrication and modification technologies and future trends: A review. *Advances in Colloid and Interface Science*, 276. Available from https://doi.org/10.1016/j.cis.2019.102100.

Henthorne, L., & Boysen, B. (2015). State-of-the-art of reverse osmosis desalination pretreatment. *Desalination.*, *356*, 129–139. Available from https://doi.org/10.1016/j.desal.2014.10.039.

Hong, S., & Elimelech, M. (1997). Chemical and physical aspects of natural organic matter (NOM) fouling of nanofiltration membranes. *Journal of Membrane Science*, *132*(2), 159–181. Available from https://doi.org/10.1016/S0376-7388(97)00060-4.

Huang, H., Cho, H., Schwab, K., & Jacangelo, J. G. (2011). Effects of feedwater pretreatment on the removal of organic microconstituents by a low fouling reverse osmosis membrane. *Desalination*, *281*(1), 446–454. Available from https://doi.org/10.1016/j.desal.2011.08.018.

Ibrahim, S. M., Nagasawa, H., Kanezashi, M., & Tsuru, T. (2020). Chemical-free cleaning of fouled reverse osmosis (RO) membranes derived from bis(triethoxysilyl) ethane (BTESE). *Journal of Membrane Science*, *601*, 117919.

IDA G, desalData. (2019). *The IDA water security handbook 2019–2020 (ed.)*. Media Analytics Ltd.

Ismail, A. F., & Matsuura, T. (2018). Progress in transport theory and characterization method of Reverse Osmosis (RO) membrane in past fifty years. *Desalination.*, *434*, 2–11. Available from https://doi.org/10.1016/j.desal.2017.09.028.

Jawor, A., & Hoek, E. M. V. (2009). Effects of feed water temperature on inorganic fouling of brackish water RO membranes. *Desalination.*, *235*(1–3), 44–57. Available from https://doi.org/10.1016/j.desal.2008.07.004.

Jiang, S., Li, Y., & Ladewig, B. P. (2017). A review of reverse osmosis membrane fouling and control strategies. *Science of the Total Environment*, *595*, 567–583. Available from https://doi.org/10.1016/j.scitotenv.2017.03.235.

Johnson, J., & Busch, M. (2010). Engineering aspects of reverse osmosis module design. *Desalination and Water Treatment*, *15*(1–3), 236–248. Available from https://doi.org/10.5004/dwt.2010.1756.

Joo, S. H., & Tansel, B. (2015). Novel technologies for reverse osmosis concentrate treatment: A review. *Journal of Environmental Management*, *150*, 322–335. Available from https://doi.org/10.1016/j.jenvman.2014.10.027.

Ju, Y., & Hong, S. (2014). Nano-colloidal fouling mechanisms in seawater reverse osmosis process evaluated by cake resistance simulator-modified fouling index nanofiltration. *Desalination*, *343*, 88–96. Available from https://doi.org/10.1016/j.desal.2014.03.012.

Kang, G. D., & Cao, Y. M. (2012). Development of antifouling reverse osmosis membranes for water treatment: A review. *Water Research*, *46*(3), 584–600. Available from https://doi.org/10.1016/j.watres.2011.11.041.

Kang, G. D., Gao, C. J., Chen, W. D., Jie, X. M., Cao, Y. M., & Yuan, Q. (2007). Study on hypochlorite degradation of aromatic polyamide reverse osmosis membrane. *Journal of Membrane Science*, *300*(1–2), 165–171. Available from https://doi.org/10.1016/j.memsci.2007.05.025.

Karabelas, A. J., Kostoglou, M., & Koutsou, C. P. (2015). Modeling of spiral wound membrane desalination modules and plants—Review and research priorities. *Desalination*, *356*, 165–186. Available from https://doi.org/10.1016/j.desal.2014.10.002.

Karime, M., Bouguecha, S., & Hamrouni, B. R. O. (2008). Membrane autopsy of Zarzis brackish water desalination plant. *Desalination*, *220*(1–3), 258–266. Available from https://doi.org/10.1016/j.desal.2007.02.040.

Kavitha, J., Rajalakshmi, M., Phani, A. R., & Padaki, M. (2019). Pretreatment processes for seawater reverse osmosis desalination systems—A review. *Journal of Water Process Engineering*, 100926. Available from https://doi.org/10.1016/j.jwpe.2019.100926.

Khan, M., Danielsen, S., Johansen, K., Lorenz, L., Nelson, S., & Camper, A. (2013). Enzymatic cleaning of biofouled thin-film composite reverse osmosis (RO) membrane operated in a biofilm membrane reactor. *Biofouling*, *30*, 153–167. Available from https://doi.org/10.1080/08927014.2013.852540.

Khan, M. A. M., Rehman, S., & Al-Sulaiman, F. A. (2018). A hybrid renewable energy system as a potential energy source for water desalination using reverse osmosis: A review. *Renewable and Sustainable Energy Reviews*, *97*, 456–477. Available from https://doi.org/10.1016/j.rser.2018.08.049.

Kim, C. M., Kim, S. J., Kim, L. H., Shin, M. S., Yu, H. W., & Kim, I. S. (2014). Effects of phosphate limitation in feed water on biofouling in forward osmosis (FO) process. *Desalination*, *349*, 51–59. Available from https://doi.org/10.1016/j.desal.2014.06.013.

Kim, H. S., Lee, J. Y., Ham, S. Y., Lee, J. H., Park, J. H., & Park, H. D. (2019). Effect of biofilm inhibitor on biofouling resistance in RO processes. *Fuel*, *253*, 823–832. Available from https://doi.org/10.1016/j.fuel.2019.05.062.

Kim, S. G., Chun, J. H., Chun, B. H., & Kim, S. H. (2013). Preparation, characterization and performance of poly (aylene ether sulfone)/modified silica nanocomposite reverse osmosis membrane for seawater desalination. *Desalination*, *325*, 76–83. Available from https://doi.org/10.1016/j.desal.2013.06.017.

Kosmadakis, G., Manolakos, D., Kyritsis, S., & Papadakis, G. (2010). Design of a two stage Organic Rankine Cycle system for reverse osmosis desalination supplied from a steady thermal source. *Desalination.*, *250*(1), 323–328. Available from https://doi.org/10.1016/j.desal.2009.09.050.

Landaburu-Aguirre, J., García-Pacheco, R., Molina, S., Rodríguez-Sáez, L., Rabadán, J., & García-Calvo, E. (2016). Fouling prevention, preparing for re-use and membrane recycling. Towards circular economy in RO desalination. *Desalination*, *393*, 16–30. Available from https://doi.org/10.1016/j.desal.2016.04.002.

Laqbaqbi, M., Sanmartino, J. A., Khayet, M., García-Payo, C., & Chaouch, M. (2017). Fouling in membrane distillation, osmotic distillation and osmotic membrane distillation. *Applied Sciences*, *7*(4). Available from https://doi.org/10.3390/app7040334.

Lawler, W. (2011). *Reuse of reverse osmosis desalination membranes*. IDA World Congress Perth Convention.

Lawler, W., Alvarez-Gaitan, J., Leslie, G., & Le-Clech, P. (2015). Comparative life cycle assessment of end-of-life options for reverse osmosis membranes. *Desalination.*, *357*, 45–54. Available from https://doi.org/10.1016/j.desal.2014.10.013.

Lawler, W., Antony, A., Cran, M., Duke, M., Leslie, G., & Le-Clech, P. (2013). Production and characterisation of UF membranes by chemical conversion of used RO membranes. *Journal of Membrane Science*, *447*, 203–211. Available from https://doi.org/10.1016/j.memsci.2013.07.015.

Lawler, W., Bradford-Hartke, Z., Cran, M. J., et al. (2012). Towards new opportunities for reuse, recycling and disposal of used reverse osmosis membranes. *Desalination*, *299*, 103–112. Available from https://doi.org/10.1016/j.desal.2012.05.030.

Lee, H. J., Seo, J., Kim, M. S., & Lee, C. (2017). Inactivation of biofilms on RO membranes by copper ion in combination with norspermidine. *Desalination*, *424*, 95–101. Available from https://doi.org/10.1016/j.desal.2017.09.034.

Lee, K. P., Arnot, T. C., & Mattia, D. (2011). A review of reverse osmosis membrane materials for desalination—Development to date and future potential. *Journal of Membrane Science*, *370*(1–2), 1–22. Available from https://doi.org/10.1016/j.memsci.2010.12.036.

Lee, S., Choi, J., Park, Y. G., Shon, H., Ahn, C. H., & Kim, S. H. (2019). Hybrid desalination processes for beneficial use of reverse osmosis brine: Current status and future prospects. *Desalination*, 104–111. Available from https://doi.org/10.1016/j.desal.2018.02.002.

Lee, S., & Elimelech, M. (2007). Salt cleaning of organic-fouled reverse osmosis membranes. *Water Research*, *41*, 1134–1142.

Lee, T. H., Lee, M. Y., Lee, H. D., Roh, J. S., Kim, H. W., & Park, H. B. (2017). Highly porous carbon nanotube/polysulfone nanocomposite supports for high-flux polyamide reverse osmosis membranes. *Journal of Membrane Science*, *539*, 441–450. Available from https://doi.org/10.1016/j.memsci.2017.06.027.

Lejarazu-Larrañaga, A., Molina, S., Ortiz, J. M., Navarro, R., & García-Calvo, E. (2020). Circular economy in membrane technology: Using end-of-life reverse osmosis modules for preparation of recycled anion exchange membranes and validation in electrodialysis. *Journal of Membrane Science*, 593. Available from https://doi.org/10.1016/j.memsci.2019.117423.

Liu, M., Wu, D., Yu, S., & Gao, C. (2009). Influence of the polyacyl chloride structure on the reverse osmosis performance, surface properties and chlorine stability of the thin-film composite polyamide membranes. *Journal of Membrane Science*, *326*(1), 205–214. Available from https://doi.org/10.1016/j.memsci.2008.10.004.

Liu, X., Qi, S., Li, Y., Yang, L., Cao, B., & Tang, C. Y. (2013). Synthesis and characterization of novel antibacterial silver nanocomposite nanofiltration and forward osmosis membranes based on layer-by-layer assembly. *Water Research*, *47*(9), 3081–3092. Available from https://doi.org/10.1016/j.watres.2013.03.018.

Loeb, S., & Sourirajan, S. (1963). *Sea water demineralization by means of an osmotic membrane*, . *Saline Water Conversion-II* (38, pp. 117–132). American Chemical Society. Available from http://doi.org/10.1021/ba-1963-0038.ch009.

Lyster, E., Kim, M. m, Au, J., & Cohen, Y. (2010). A method for evaluating antiscalant retardation of crystal nucleation and growth on RO membranes. *Journal of Membrane Science*, *364*(1–2), 122–131. Available from https://doi.org/10.1016/j.memsci.2010.08.020.

Ma, W., Zhao, Y., & Wang, L. (2007). The pretreatment with enhanced coagulation and a UF membrane for seawater desalination with reverse osmosis. *Desalination*, *203*(1–3), 256–259. Available from https://doi.org/10.1016/j.desal.2006.02.020.

Maartens, A., Swart, P., & Jacobs, E. P. (1996). An enzymatic approach to the cleaning of ultrafiltration membranes fouled in abattoir effluent. *Journal of Membrane Science*, *119*(1), 9–16. Available from https://doi.org/10.1016/0376-7388(96)00015-4.

Maartens, A., Swart, P., & Jacobs, E. P. (1999). Feed-water pretreatment: Methods to reduce membrane fouling by natural organic matter. *Journal of Membrane Science*, 51–62. Available from https://doi.org/10.1016/s0376-7388(99)00155-6.

Madaeni, S. S., & Samieirad, S. (2010). Chemical cleaning of reverse osmosis membrane fouled by wastewater. *Desalination*, *257*(1–3), 80–86. Available from https://doi.org/10.1016/j.desal.2010.03.002.

Malaeb, L., & Ayoub, G. M. (2011). Reverse osmosis technology for water treatment: State of the art review. *Desalination*., *267*(1), 1–8. Available from https://doi.org/10.1016/j.desal.2010.09.001.

Matin, A., Khan, Z., Zaidi, S. M. J., & Boyce, M. C. (2011). Biofouling in reverse osmosis membranes for seawater desalination: Phenomena and prevention. *Desalination*, *281*(1), 1–16. Available from https://doi.org/10.1016/j.desal.2011.06.063.

Matin, A., Laoui, T., Epalath, W., & Eparoouue, M. (2020). Fouling control in reverse osmosis for water desalination & reuse: Current practices and emerging environment-friendly technologies. *Science of the Total Environment*, *765*, 142721. Available from https://doi.org/10.1016/j.scitotenv.2020.142721.

Matin, A., Rahman, F., Shafi, H. Z., & Zubair, S. M. (2019). Scaling of reverse osmosis membranes used in water desalination: Phenomena, impact, and control; future directions. *Desalination*, *455*, 135–157. Available from https://doi.org/10.1016/j.desal.2018.12.009.

Mattaraj, S., Phimpha, W., Hongthong, P., & Jiraratananon, R. (2010). Effect of operating conditions and solution chemistry on model parameters in crossflow reverse osmosis of natural organic matter. *Desalination*, *253*(1–3), 38–45. Available from https://doi.org/10.1016/j.desal.2009.11.039.

Mavukkandy, M. O., Chabib, C. M., Mustafa, I., Al Ghaferi, A., & AlMarzooqi, F. (2019). Brine management in desalination industry: From waste to resources generation. *Desalination*, 472. Available from https://doi.org/10.1016/j.desal.2019.114187.

Mi, B., & Elimelech, M. (2010). Organic fouling of forward osmosis membranes: Fouling reversibility and cleaning without chemical reagents. *Journal of Membrane Science*, *348*(1–2), 337–345. Available from https://doi.org/10.1016/j.memsci.2009.11.021.

Mitrouli, S. T., Karabelas, A. J., & Isaias, N. P. (2010). Polyamide active layers of low pressure RO membranes: Data on spatial performance non-uniformity and degradation by hypochlorite solutions. *Desalination*, *260*(1–3), 91–100. Available from https://doi.org/10.1016/j.desal.2010.04.061.

Mitrouli, S. T., Yiantsios, S. G., Karabelas, A. J., Mitrakas, M., Fóllesdal, M., & Kjolseth, P. A. (2008). Pretreatment for desalination of seawater from an open intake by dual-media filtration: Pilot testing and comparison of two different media. *Desalination*, *222*(1–3), 24–37. Available from https://doi.org/10.1016/j.desal.2007.02.062.

Mo, H., & Ng, H. Y. (2010). An experimental study on the effect of spacer on concentration polarization in a long channel reverse osmosis membrane cell. *Water Science and Technology*, *61*(8), 2035–2041. Available from https://doi.org/10.2166/wst.2010.116.

Molina, S., Landaburu-Aguirre, J., Rodríguez-Sáez, L., García-Pacheco, R., de la Campa, J. G., & García-Calvo, E. (2018). Effect of sodium hypochlorite exposure on polysulfone recycled UF membranes and their surface

characterization. *Polymer Degradation and Stability*, *150*, 46–56. Available from https://doi.org/10.1016/j.polymdegradstab.2018.02.012.

Moradi, M. R., Pihlajamäki, A., Hesampour, M., Ahlgren, J., & Mänttäri, M. (2019). End-of-life RO membranes recycling: Reuse as NF membranes by polyelectrolyte layer-by-layer deposition. *Journal of Membrane Science*, *584*, 300–308. Available from https://doi.org/10.1016/j.memsci.2019.04.060.

Morón-López, J., Nieto-Reyes, L., Aguado, S., El-Shehawy, R., & Molina, S. (2019). Recycling of end-of-life reverse osmosis membranes for membrane biofilms reactors (MBfRs). Effect of chlorination on the membrane surface and gas permeability. *Chemosphere*, *231*, 103–112. Available from https://doi.org/10.1016/j.chemosphere.2019.05.108.

Morón-López, J., Nieto-Reyes, L., Molina, S., & Lezcano, M. Á. (2020). Exploring microcystin-degrading bacteria thriving on recycled membranes during a cyanobacterial bloom. *Science of the Total Environment*, 736. Available from https://doi.org/10.1016/j.scitotenv.2020.139672.

Morón-López, J., Nieto-Reyes, L., Senán-Salinas, J., Molina, S., & El-Shehawy, R. (2019). Recycled desalination membranes as a support material for biofilm development: A new approach for microcystin removal during water treatment. *Science of the Total Environment*, *647*, 785–793. Available from https://doi.org/10.1016/j.scitotenv.2018.07.435.

Muñoz, S., Frank, R., Pilar, I., Perez, C., & Simón, F. X. (2014). Life + Remembrane: End-of-life recovery of reverse osmosis. *FuturENVIRO*, 1–5. Available from https://futurenviro.es/en/liferemembrane-recuperacion-de-las-membranas-de-osmosis-inversa-al-final-de-su-vida-util/.

Nafey, A. S., & Sharaf, M. A. (2010). Combined solar organic Rankine cycle with reverse osmosis desalination process: Energy, exergy, and cost evaluations. *Renewable Energy*, *35*(11), 2571–2580. Available from https://doi.org/10.1016/j.renene.2010.03.034.

Nassrullah, H., Anis, S. F., Hashaikeh, R., & Hilal, N. (2020). Energy for desalination: A state-of-the-art review. *Desalination*, 491. Available from https://doi.org/10.1016/j.desal.2020.114569.

Neal, P. R., Li, H., Fane, A. G., & Wiley, D. E. (2003). The effect of filament orientation on critical flux and particle deposition in spacer-filled channels. *Journal of Membrane Science*, *214*(2), 165–178. Available from https://doi.org/10.1016/S0376-7388(02)00500-8.

Nguyen, A., Azari, S., & Zou, L. (2013). Coating zwitterionic amino acid l-DOPA to increase fouling resistance of forward osmosis membrane. *Desalination*, *312*, 82–87. Available from https://doi.org/10.1016/j.desal.2012.11.038.

Nguyen, A., Zou, L., & Priest, C. (2014). Evaluating the antifouling effects of silver nanoparticles regenerated by TiO_2 on forward osmosis membrane. *Journal of Membrane Science*, *454*, 264–271. Available from https://doi.org/10.1016/j.memsci.2013.12.024.

Oh, Y., Lee, S., Elimelech, M., Lee, S., & Hong, S. (2014). Effect of hydraulic pressure and membrane orientation on water flux and reverse solute flux in pressure assisted osmosis. *Journal of Membrane Science*, *465*, 159–166. Available from https://doi.org/10.1016/j.memsci.2014.04.008.

Okamoto, Y., & Lienhard, J. H. (2019). How RO membrane permeability and other performance factors affect process cost and energy use: A review. *Desalination.*, 470. Available from https://doi.org/10.1016/j.desal.2019.07.004.

Otitoju, T. A., Saari, R. A., & Ahmad, A. L. (2018). Progress in the modification of reverse osmosis (RO) membranes for enhanced performance. *Journal of Industrial and Engineering Chemistry*, *67*, 52–71. Available from https://doi.org/10.1016/j.jiec.2018.07.010.

Ould Mohamedou, E., Penate Suarez, D. B., Vince, F., Jaouen, P., & Pontie, M. (2010). New lives for old reverse osmosis (RO) membranes. *Desalination*, *253*(1–3), 62–70. Available from https://doi.org/10.1016/j.desal.2009.11.032.

Panagopoulos, A., & Haralambous, K. J. (2020). Environmental impacts of desalination and brine treatment—Challenges and mitigation measures. *Marine Pollution Bulletin*, 161. Available from https://doi.org/10.1016/j.marpolbul.2020.111773.

Panagopoulos, A., Haralambous, K. J., & Loizidou, M. (2019). Desalination brine disposal methods and treatment technologies—A review. *Science of the Total Environment*, 693. Available from https://doi.org/10.1016/j.scitotenv.2019.07.351.

Peñate, B., & García-Rodríguez, L. (2012). Current trends and future prospects in the design of seawater reverse osmosis desalination technology. *Desalination*, *284*, 1–8. Available from https://doi.org/10.1016/j.desal.2011.09.010.

Pontié, M. (2015). Old RO membranes: Solutions for reuse. *Desalination and Water Treatment*, *53*(6), 1492–1498. Available from https://doi.org/10.1080/19443994.2014.943060.

Pontié, M., Awad, S., Tazerout, M., Chaouachi, O., & Chaouachi, B. (2017). Recycling and energy recovery solutions of end-of-life reverse osmosis (RO) membrane materials: A sustainable approach. *Desalination*, *423*, 30–40. Available from https://doi.org/10.1016/j.desal.2017.09.012.

Pontié, M., Rapenne, S., Thekkedath, A., et al. (2005). Tools for membrane autopsies and antifouling strategies in seawater feeds: A review. *Desalination*, *181*(1–3), 75–90. Available from https://doi.org/10.1016/j.desal.2005.01.013.

Prince, C., Cran, M., Le-Clech, P., Uwe-Hoehn, K., & Duke, M. (2011). *Reuse and recycling of used desalination membranes*. https://www.researchgate.net/publication/246549314_Reuse_and_recycling_of_used_desalination_membranes.

Qasim, M., Badrelzaman, M., Darwish, N. N., Darwish, N. A., & Hilal, N. (2019). Reverse osmosis desalination: A state-of-the-art review. *Desalination*, *459*, 59–104. Available from https://doi.org/10.1016/j.desal.2019.02.008.

Radu, A. I., Vrouwenvelder, J. S., van Loosdrecht, M. C. M., & Picioreanu, C. (2012). Effect of flow velocity, substrate concentration and hydraulic cleaning on biofouling of reverse osmosis feed channels. *Chemical Engineering Journal*, *188*, 30–39. Available from https://doi.org/10.1016/j.cej.2012.01.133.

Rahimi, B., & Chua, H. T. (2017). *Low grade heat driven multi-effect distillation and desalination* (pp. 1–194). Iran: Elsevier Inc. Available from http://www.sciencedirect.com/science/book/9780128051245.

Ramon, G. Z., Nguyen, T. V., & Hoek, E. M. V. (2013). Osmosis-assisted cleaning of organic-fouled seawater RO membranes. *Chemical Engineering Journal*, *218*, 173–182.

Raval, H. D., Chauhan, V. R., Raval, A. H., & Mishra, S. (2012). Rejuvenation of discarded RO membrane for new applications. *Desalination and Water Treatment*, *48*(1–3), 349–359. Available from https://doi.org/10.1080/19443994.2012.704727.

Reid, C. E., & Breton, E. J. (1959). Water and ion flow across cellulosic membranes. *Journal of Applied Polymer Science*, 133–143. Available from https://doi.org/10.1002/app.1959.070010202.

Rodríguez, J. J., Jiménez, V., Trujillo, O., & Veza, J. (2002). Reuse of reverse osmosis membranes in advanced wastewater treatment. *Desalination*, *150*(3), 219–225. Available from https://doi.org/10.1016/S0011-9164(02)00977-3.

Rodríguez-Sáez, L., Landaburu-Aguirre, J., Molina, S., García-Payo, C., & García-Calvo, E. (2021). Study of surface modification of recycled ultrafiltration membranes using statistical design of experiments. *Surfaces and Interfaces*, *23*, 100978. Available from https://doi.org/10.1016/j.surfin.2021.100978.

Rozelle, L. T., Cadotte, J. E., Corneliussen, R. D., & Erickson, E. E. (1968). *Development of new reverse osmosis membranes for desalination, Progress Report No. 359*. Washington, DC: Office of Saline Water Research and Development.

Sagiv, A., & Semiat, R. (2005). Backwash of RO spiral wound membranes. *Desalination*, *179*, 1–9. Available from https://doi.org/10.1016/j.desal.2004.11.050.

Sarja, M., Onkila, T., & Mäkelä, M. (2021). A systematic literature review of the transition to the circular economy in business organizations: Obstacles, catalysts and ambivalences. *Journal of Cleaner Production*, *286*. Available from https://doi.org/10.1016/j.jclepro.2020.125492.

Schöggl, J. P., Stumpf, L., & Baumgartner, R. J. (2020). The narrative of sustainability and circular economy—A longitudinal review of two decades of research. *Resources, Conservation and Recycling*, *163*. Available from https://doi.org/10.1016/j.resconrec.2020.105073.

Senán-Salinas, J., García-Pacheco, R., Landaburu-Aguirre, J., & García-Calvo, E. (2019). Recycling of end-of-life reverse osmosis membranes: Comparative LCA and cost-effectiveness analysis at pilot scale. *Resources, Conservation and Recycling*, *150*. Available from https://doi.org/10.1016/j.resconrec.2019.104423.

She, Q., Jin, X., Li, Q., & Tang, C. Y. (2012). Relating reverse and forward solute diffusion to membrane fouling in osmotically driven membrane processes. *Water Research*, *46*(7), 2478–2486. Available from https://doi.org/10.1016/j.watres.2012.02.024.

She, Q., Wang, R., Fane, A. G., & Tang, C. Y. (2016). Membrane fouling in osmotically driven membrane processes: A review. *Journal of Membrane Science*, *499*, 201–233. Available from https://doi.org/10.1016/j.memsci.2015.10.040.

Shenvi, S. S., Isloor, A. M., & Ismail, A. F. (2015). A review on RO membrane technology: Developments and challenges. *Desalination*, *368*, 10–26. Available from https://doi.org/10.1016/j.desal.2014.12.042.

Stocker, T. F. (2013). *IPCC, 2013: Climate Change 2013: The physical science basis*. Contribution of Working Group I to the Fifth Assessment Report of the Intergovernmental Panel on Climate Change, p. 1535.

Suwarno, S. R., Chen, X., Chong, T. H., et al. (2012). The impact of flux and spacers on biofilm development on reverse osmosis membranes. *Journal of Membrane Science*, *405–406*, 219–232. Available from https://doi.org/10.1016/j.memsci.2012.03.012.

Sweity, A., Ronen, Z., & Herzberg, M. (2014). Induced organic fouling with antiscalants in seawater desalination. *Desalination*, *352*, 158–165. Available from https://doi.org/10.1016/j.desal.2014.08.018.

Tang, C. Y., Chong, T. H., & Fane, A. G. (2011). Colloidal interactions and fouling of NF and RO membranes: A review. *Advances in Colloid and Interface Science*, *164*(1–2), 126–143. Available from https://doi.org/10.1016/j.cis.2010.10.007.

Tang, C. Y., Kwon, Y. N., & Leckie, J. O. (2007). Fouling of reverse osmosis and nanofiltration membranes by humic acid—Effects of solution composition and hydrodynamic conditions. *Journal of Membrane Science*, *290* (1–2), 86–94. Available from https://doi.org/10.1016/j.memsci.2006.12.017.

Toleti, S. R. (2010). Comparative effect of temperature on biofilm formation in natural and modified marine environment. *Aquatic Ecology*, 463–478. Available from https://doi.org/10.1007/s10452-009-9304-1.

Tran, T., Bolto, B., Gray, S., Hoang, M., & Ostarcevic, E. (2007). An autopsy study of a fouled reverse osmosis membrane element used in a brackish water treatment plant. *Water Research*, *41*(17), 3915–3923. Available from https://doi.org/10.1016/j.watres.2007.06.008.

United-Nations-World-Water-Assessment-Programme. (2020). *The United Nations World Water Development Report*.

Uemura, T. K., Yoshio, H., & Masaru, K. (1988). Interfacially Synthesized Reverse Osmosis Membrane. *Patent Application, No.*, 4761234.

Valladares Linares, R., Bucs, S. S., Li, Z., AbuGhdeeb, M., Amy, G., & Vrouwenvelder, J. S. (2014). Impact of spacer thickness on biofouling in forward osmosis. *Water Research*, 223–233. Available from https://doi.org/10.1016/j.watres.2014.03.046.

Van der Hoek, J. P., Hofman, J. A. M. H., Bonné, P. A. C., Nederlof, M. M., & Vrouwenvelder, H. S. (2000). RO treatment: Selection of a pretreatment scheme based on fouling characteristics and operating conditions based on environmental impact. *Desalination*, *127*(1), 89–101. Available from https://doi.org/10.1016/S0011-9164(99)00195-2.

Veza, J. M., & Rodriguez-Gonzalez, J. J. (2003). Second use for old reverse osmosis membranes: Wastewater treatment. *Desalination*, *157*(1–3), 65–72. Available from https://doi.org/10.1016/S0011-9164(03)00384-9.

Vrijenhoek, E. M., Seungkwan, H., & Menachem, E. (2001). Influence of membrane surface properties on initial rate of colloidal fouling of reverse osmosis and nanofiltration membranes. *Journal of Membrane Science*, 115–128. Available from https://doi.org/10.1016/s0376-7388(01)00376-3.

Vrouwenvelder, J. S., & Van Der Kooij, D. (2001). Diagnosis, prediction and prevention of biofouling of NF and RO membranes. *Desalination*, *139*(1–3), 65–71. Available from https://doi.org/10.1016/S0011-9164(01)00295-8.

Vrouwenvelder, J. S., van Paassen, J. A. M., Wessels, L. P., van Dam, A. F., & Bakker, S. M. (2006). The membrane fouling simulator: A practical tool for fouling prediction and control. *Journal of Membrane Science*, *281*(1–2), 316–324. Available from https://doi.org/10.1016/j.memsci.2006.03.046.

Wang, Y., Wang, Z., Han, X., Wang, J., & Wang, S. (2017). Improved flux and anti-biofouling performances of reverse osmosis membrane via surface layer-by-layer assembly. *Journal of Membrane Science*, *539*, 403–411. Available from https://doi.org/10.1016/j.memsci.2017.06.029.

Wang, Y. N., & Tang, C. Y. (2011). Protein fouling of nanofiltration, reverse osmosis, and ultrafiltration membranes—The role of hydrodynamic conditions, solution chemistry, and membrane properties. *Journal of Membrane Science*, *376*(1–2), 275–282. Available from https://doi.org/10.1016/j.memsci.2011.04.036.

Wang, Z., Ma, J., Tang, C. Y., Kimura, K., Wang, Q., & Han, X. (2014). Membrane cleaning in membrane bioreactors: A review. *Journal of Membrane Science*, *468*, 276–307. Available from https://doi.org/10.1016/j.memsci.2014.05.060.

Whittaker, C., Ridgway, H., & Olson, B. (1984). Evaluation of cleaning strategies for removal of biofilms from reverse-osmosis membranes. *Applied and Environmental Microbiology*, *48*, 395–403. Available from https://doi.org/10.1128/AEM.48.2.395-403.1984.

WHO UNICEF. (2017). *Progress on drinking water, sanitation and hygiene*.

Xie, M., Lee, J., Nghiem, L. D., & Elimelech, M. (2015). Role of pressure in organic fouling in forward osmosis and reverse osmosis. *Journal of Membrane Science*, *493*, 748–754. Available from https://doi.org/10.1016/j.memsci.2015.07.033.

Xu, G. R., Wang, J. N., & Li, C. J. (2013). Strategies for improving the performance of the polyamide thin film composite (PA-TFC) reverse osmosis (RO) membranes: Surface modifications and nanoparticles incorporations. *Desalination*, *328*, 83–100. Available from https://doi.org/10.1016/j.desal.2013.08.022.

Yu, H. Y., Kang, Y., Liu, Y., & Mi, B. (2014). Grafting polyzwitterions onto polyamide by click chemistry and nucleophilic substitution on nitrogen: A novel approach to enhance membrane fouling resistance. *Journal of Membrane Science*, *449*, 50–57. Available from https://doi.org/10.1016/j.memsci.2013.08.022.

Yu, W., Song, D., Chen, W., & Yang, H. (2020). Antiscalants in RO membrane scaling control. *Water Research*, 183. Available from https://doi.org/10.1016/j.watres.2020.115985.

Zhao, D. L., Japip, S., Zhang, Y., Weber, M., Maletzko, C., & Chung, T. S. (2020). Emerging thin-film nanocomposite (TFN) membranes for reverse osmosis: A review. *Water Research*, 173. Available from https://doi.org/10.1016/j.watres.2020.115557.

Zhao, Y., Song, L., & Ong, S. L. (2010). Fouling of RO membranes by effluent organic matter (EfOM): Relating major components of EfOM to their characteristic fouling behaviors. *Journal of Membrane Science*, *349*(1-2), 75–82. Available from https://doi.org/10.1016/j.memsci.2009.11.024.

Zou, L., Vidalis, I., Steele, D., Michelmore, A., Low, S. P., & Verberk, J. Q. J. C. (2011). Surface hydrophilic modification of RO membranes by plasma polymerization for low organic fouling. *Journal of Membrane Science*, *369*(1-2), 420–428. Available from https://doi.org/10.1016/j.memsci.2010.12.023.

Richter, J.W., Square, K. & Hoehn H.H. (1971). Perm-selective, aromatic, nitrogen-containing polymeric membranes, US Patent 3 567 632, E. I. du Pont de Nemours and Company,Wilmington, DE.

CHAPTER

12

Polymer-based forward osmosis membranes

Soheila Shokrollahzadeh and Yasamin Bide

Department of Chemical Technologies, Iranian Research Organization for Science and Technology (IROST), Tehran, Iran

Polymeric materials are the most common materials used to make membranes. The name forward osmosis (FO) is derived from the mass transfer processes that occur through nature's osmotic phenomenon. One of the FO process challenges is the production of high water fluxes in water and wastewater treatment compared to reverse osmosis membranes. For this reason, researchers have always tried to overcome this problem in the last thirty years by modifying polymer type and fabrication methods. An ideal FO membrane should have high hydrophilicity (water permeability), high selectivity (rejection), lower membrane fouling, chemical stability, good mechanical strength to fit in the high-density module for various applications easily.

12.1 Introduction

12.1.1 Important notes in forward osmosis membrane transport

Osmosis refers to the transfer of water through a selective semipermeable membrane due to the difference in water chemical potential (osmotic pressure difference) between the sides of the membrane rather than hydraulic pressure difference. Water transports from the side with higher water chemical potential to the side with lower water chemical potential. The semipermeable membrane allows water to pass through but prevents the transfer of most soluble materials.

To understand this phenomenon, early researchers studied the mechanism of osmosis in natural materials. However, from the 1960s, their attention turned to synthetic materials to develop the science of making synthetic membranes. This phenomenon application in

Advancement in Polymer-Based Membranes for Water Remediation
DOI: https://doi.org/10.1016/B978-0-323-88514-0.00016-4

© 2022 Elsevier Inc. All rights reserved.

the FO process was introduced in the 1970s when the fabrication of semipermeable membranes was developing (Kessler & Moody, 1975; Moody & Kessler, 1975).

Forward or direct osmosis, unlike RO, is performed without external pressure. The driving force of many applications in the FO phenomenon is osmotic pressure. Its main advantages are performance at low or zero hydraulic pressure, low inlet energy, high membrane rejection to solutes and less membrane fouling, and easier removal of foulants than the processes whose driving force is external pressure (such as RO, nanofiltration, and ultrafiltration).

The FO process was initially introduced for the water transfer from useless water resources (e.g., brackish solution) to a useful fertilizer (Moody & Kessler, 1971) and the production of emergency potable water for humans in the lifeboats or satellites (Capital & West, 2004; Flynn et al., 2007). Then, the concentration of pharmaceuticals and foodstuffs (Jiao, Cassano, & Drioli, 2004), energy production (Loeb, 2001; Seppälä & Lampinen, 1999), and portable water recovery equipment were also introduced (Cath, Adams, & Childress, 2005). With the development of suitable membrane and draw solutions, its applications were extended to the controlled release of pharmaceutical products, direct irrigation, wastewater treatment, and saline water desalination.

The water-soluble synthetic substances are usually used for the production of high osmotic pressure called draw solutions. The FO system consists of three main components: (1) feed solution whose volume decreases and becomes more concentrated during the FO process, (2) draw solution is a solution whose salinity or osmotic pressure is higher than the feedwater solution, and (3) the FO membrane, whose primary function is to pass the maximum amount of water from the feed solution to the draw solution and not to pass solutes on both sides of the membrane to the opposite side.

The most influential factors in the FO process are membrane type and concentration of draw solution, the concentration of feed, and temperature (Nematzadeh, Samimi, & Shokrollahzadeh, 2016). Research on FO has identified two significant challenges: access to a high-performance membrane and a high-osmotic draw solution with easy recovery and reuse. Although much research has been done in the last two decades, optimization and improvement of conditions in these two aspects are still under research to improve the FO process's economic conditions.

12.1.2 Concentration polarization

Concentration polarization is a common and unavoidable phenomenon in osmotic-driven membrane processes due to the difference in concentration between feedwater solution and draw solution on both sides of the membrane. The occurrence of concentration polarization reduces the water flux in the process (Akther et al., 2015).

Eq. (12.1) is a general formula that shows the water flux in FO and RO processes (Cath, Childress, & Elimelech, 2006; Zhao, Zou, Tang, & Mulcahy, 2012):

$$J_W = A(\sigma\Delta\pi - \Delta P) \tag{12.1}$$

where J_w is the water flux through the membrane (L m^{-2} h^{-1}, LMH), A is the permeability coefficient of pure water (LMH/bar), $\Delta\pi$ is the osmotic pressure difference across the

membrane (bar), ΔP is the external pressure difference (bar), and σ is the reflection coefficient. In the FO process, the difference in external pressure is considered insignificant. Experimental results have shown that the difference in osmotic pressure across the FO membrane is much less than the difference in osmotic pressure between the two solutions on both sides of the membrane, making the water flow much lower than expected (McCutcheon, McGinnis, & Elimelech, 2005; Seppälä & Lampinen, 1999). This result is due to the effects of several transport phenomena on the membrane that is shown in Fig. 12.1.

The FO membrane consists typically of a selective (active) layer supported by a porous layer (support layer). The selective layer is a thin layer that determines the membrane's separation properties. The selective layer of the membrane is permeable to water. It prevents solutes' passage, which causes solute accumulation near the active layer and creates a concentration gradient between the solution bulk and the interface between the membrane and solution. This accumulation ultimately results in an osmotic pressure difference on both sides of the active membrane layer being slightly less than the osmotic pressure difference between the draw solution and feed bulks.

Consequently, the resulting water flux will be less than the predicted flux [Eq. (12.1)]. This concentration gradient is called concentration polarization. If this phenomenon occurs in the membrane support layer, it is known as internal concentration polarization (ICP). When a layer occurs outside the membrane near the active layer, it is called external concentration polarization (ECP) (Cath et al., 2006; McCutcheon, McGinnis, & Elimelech, 2006). The result of these two phenomena will be a reduction in the osmotic pressure difference and a reduction in water flux. ECP can be almost removed by applying turbulence near the membrane surface; however, ICP is very difficult to deal with because it occurs inside the membrane.

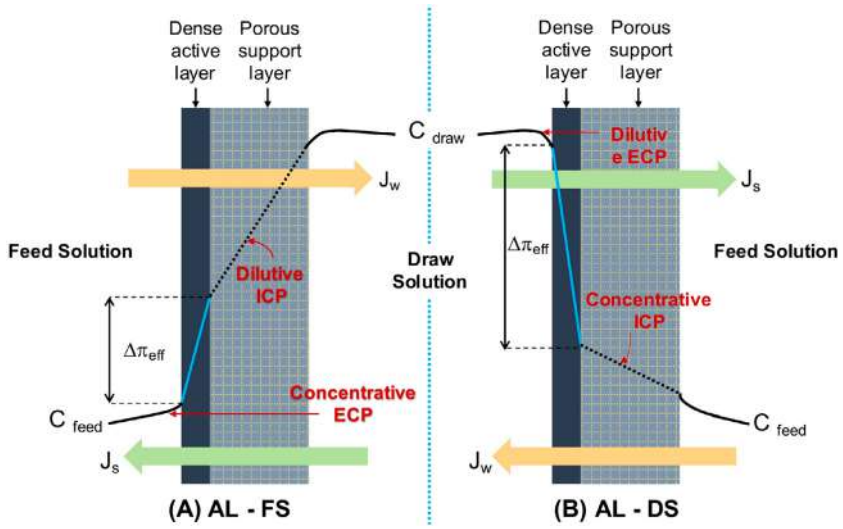

FIGURE 12.1 Internal concentration polarization phenomenon at FO (A) and PRO (B) membrane orientations (Suzaimi et al., 2020).

As shown in Fig. 12.1, there are two types of membrane orientation in the FO process: (1) FO orientation, where the active layer faces the feed solution and (2) PRO (pressure-retarded osmosis) orientation the active layer faces the draw solution. The formation of the concentration polarization phenomenon and its effect on process performance is different in each orientation depending on the type of feed and draw solutions and their concentrations.

The effect of ICP on the FO process for each membrane orientation has been experimentally verified by the researchers (Ahmadizadeh, Shokrollahzadeh, & Latifi, 2019). The lower water flux in FO orientation compared to the PRO mode is attributed to the adverse effect of ICP in the porous support (Gray, McCutcheon, & Elimelech, 2006; Jiao et al., 2004; Loeb, Titelman, Korngold, & Freiman, 1997; McCutcheon, & Elimelech, 2006, 2007; Mehta & Loeb, 1978; Wang, Chung, & Qin, 2007a; Yang, Wang, & Chung, 2009a).

Zhang, Wang, et al. (2010) experimentally showed that ICP could be greatly reduced by synthesizing a highly porous support layer (Zhang, Wang, et al., 2010). Therefore the design of the support layer is critical in the performance of FO membranes. The degree of ICP in the support layer is shown by the structural parameter S, which is a good indicator of the support layer's resistance against water penetration (Eq. 12.2). The ICP degree is reduced by decreasing the number of structural parameters, and subsequently, water fluxes increase. The S parameter is defined by

$$S = \frac{L \cdot \tau}{\varepsilon} \tag{12.2}$$

where L is the thickness, τ is the tortuosity, and ε is the porosity of the support layer. Generally, thin-film composite (TFC) membranes offer a more water flux than membranes constructed by the phase inversion method. The reverse solute permeation of the draw solution to the feed side is one of the most significant tasks of the selective layer. This reversal permeation influences the FO process's performance concerning water flux, osmotic pressure dissipation, and membrane fouling.

12.2 Polymer-based flat sheet forward osmosis membranes

Flat sheets are the typical type of membranes that are designed in plate-and-frame modules. The flat sheet membranes can be categorized into single-layer and dual-layer polymer-based membranes.

12.2.1 Single-layer membranes

12.2.1.1 Cellulosic membranes

Cellulose acetate (CA) has been a common material for various membrane separation applications, including RO (Matsuura & Sourirajan, 1985) since Loeb and Sourirajan invented the phase inversion process to make asymmetric polymeric membranes (Carter, Psaras, & Price, 1973; Loeb & Sourirajan, 1962; Michaels, Bixler, & Hodges, 1965; Wang, Lau, & Sourirajan, 1994). This choice is due to CA hydrophilicity that enhances water flux,

good mechanical strength, environment-friendly, and wide availability. The early studies showed the CA's low fouling tendency than polyamide (PA) membranes in FO applications (Mi & Elimelech, 2010).

The RO membranes of hydrophilic CA and cellulose triacetate (CTA) were first used as the FO membranes, indicating the low water flux because of the porous support layer and consequently great ICP. Therefore an FO membrane should consist of a single thin and dense layer without any support layer that leads to mechanical weakness and limiting their wide application. Various modifications were applied to obtain the flat sheet cellulosic membranes with excellent salt resistance to remove ICP.

Cellulose triacetate (CTA) membrane was the first commercial FO membrane that researchers initially used to study the FO process for different applications (Bide & Shokrollahzadeh, 2020; Khazaie, Shokrollahzadeh, Bide, Sheshmani, & Shahvelayati, 2021; Nematzadeh et al., 2016; Shokrollahzadeh, Bide, & Gholami, 2020). This membrane was a unique membrane that was specifically developed for the FO process by Hydration Technologies Inc. (HTI).

A hybrid system constructed from FO (using HTI's CTA membrane), RO, and membrane distillation followed by catalytic oxidation of the permeated products as a posttreatment stage was used to treat gray water, humidity condensate, and urine in spacecraft. The FO water flux and salt rejection of the membrane were reported as 10 LMH (at 50 mg L^{-1} brine osmotic agent) and 98%, respectively. The authors reported the successful results for this preliminary stage of the project; however, they proposed a validation and optimization stage for reducing power consumption and maximizing the whole system's water recovery (Flynn et al., 2007).

In a project between NASA Ames Research Center and HTI company, namely Lightweight Contingency Water Recovery System (LWC-WRS), its X-Pack/SeaPack commercial product was used to purify urine and other nonpotable waters without the need for electricity. A CTA membrane and fructose nutrient draw solution were used in SeaPack to treat water sources produced in spacecraft. For this, a combination of activated carbon and FO membrane was examined. It was shown that this method was successful, and about 75% of the feed urine would be recovered. The final product could supply the water, electrolytes, and caloric requirements for crew consumption (Gormly, Richardson, Flynn, & Kliss, 2008).

McCutcheon *et al*. presented an FO process for seawater desalination to recover water from a saline feedwater (0.5 M NaCl), where a highly soluble ammonium bicarbonate draw solution yielded high water flux and high water recovery. Previous studies were unsuccessful or uneconomical because of the lack of a suitable draw solution and semipermeable membrane. However, the FO membrane of this study was not either specified for desalination. A commercial flat sheet CTA membrane (HTI) applied in this study demonstrated high product water flux and relatively high salt rejection. Two commercial flat sheet brackish water RO membranes were also used in the FO experiment for comparison: an interfacial-polymerized polyamide-polysulfone TFC membrane and a CA asymmetric membrane. Both membranes had thick fabric backing layers to provide mechanical strength. This experiment showed that the RO membrane, formerly used as the semipermeable membrane in the FO process, was not suitable for FO application because of relatively low water fluxes. The lower water flux was attributed to severe ICP in the porous support and fabric layers of the RO membrane, reducing the effective driving force and

resulting water flux. The main difference between the RO and FO membranes was the membrane structure. They showed by scanning electron microscope (SEM) that the overall thickness of commercial CTA was 50 μm and composed of two layers of CTA polymer and a polyester mesh embedded between these layers as a support of the membrane (McCutcheon et al., 2005).

Ng, Tang, and Wong (2006) studied the performance of an FO process to elucidate the effect of membrane structure and orientation on water flux. Two types of RO membranes (flat sheet) and a flat sheet FO membrane were used, while three draw solutions, including glucose, ammonium bicarbonate, and fructose, were used to recover water from a feed solution. Different NaCl concentrations were used as feed solutions. Under the same experimental conditions, the FO membrane achieved a higher water flux than the RO membranes. The high salt rejection (greater than 97%) was obtained for the FO membrane. The effect of membrane orientation on water flux was also tested in both PRO and FO orientations in the FO membrane. They found the process's better performance when the membrane was used in PRO orientation due to lesser ICP. The authors suggested that an ideal FO membrane should consist of a thin dense selective layer without any loose fabric support layer (Ng et al., 2006).

Cartinella et al. (2006) used the process for removal of natural steroid hormones endocrine-disrupting chemicals as emerging water contaminants (excreted in urine) from wastewater that would be applied for space missions and other life-support systems. The CTA FO (HTI Co.) membrane contact angle was measured to be 61 degrees, and the membrane was found to be negatively charged at pH 6.5. The membrane provided from 77%–99% hormone rejection depending on experiment duration and feed solution composition (Cartinella et al., 2006).

Zhang, Wang, et al. (2010) tried to manipulate the FO membrane structure to minimize ICP and salt leakage. They fabricated both the CA single-dense and double-dense layers by phase inversion using different casting substrates and coagulant baths. Different substrate's hydrophilicity was used for casting, and the effect of membrane structure and pore size distribution on the FO performance was tested. The double-dense layer membrane showed ICP mitigation and less salt leakage in seawater desalination via the FO process compared to the single-layer membrane. The membrane structural parameter was reduced by the use of high-porosity membrane. Besides, the double-dense layer membrane showed good resistance to the large particles (200 nm) foulants in an FO-MBR system as compared to the single-dense layer (Zhang, Wang, et al., 2010).

Tang and Ng (2008) studied the potential application of the FO process in the concentration of brine. An HTI-CTA FO membrane and two dense selective layers of RO membranes (asymmetric CA and PA composite) were used. The support layers of RO membranes were peeled off to decrease the membrane support layer resistance to water permeation. They found a better water flux in the dense selective layer of the CA-RO membrane attributed to the hydrophilicity and less thickness compared to the other FO and RO membranes. At the same time, the rejection was reported as 99.7%. The CA membrane performance showed 1.5 times better than the FO membrane due to the thin structure and similar hydrophilicity that minimized concentration polarization. They proved the FO potential in brine (1 M) treatment using fructose 5 M as draw solution. However, they suggested an improvement in both FO membrane and draw solution to make FO a viable technology for brine treatment (Tang & Ng, 2008).

McCutcheon and Elimelech (2008) investigated the role of wetting characteristics of support layer in water flux using three commercial membranes: two RO membranes (designed for brackish and seawater desalination) and an HTI's CTA FO membrane. Both RO membranes had a polyester fabric support that was used as a substrate to cast cellulosic and polysulfone support layer by phase inversion. The fabric layer was removed by peeling before use, but the integrity of the membrane was saved. A polysulfone-supported TFC did not get wet fully when exposed to water; therefore the water flux decreased. On the other hand, cellulosic membranes exhibited a marked higher water flux. They concluded that the support layer's hydrophobicity hindered water flux in the FO process due to increasing the ICP and disruption of water continuity within the membrane that reduced the pathways for water transport. These findings showed that both the structural properties and chemistry of the support layer should be focused on the design of membrane for osmotically driven processes (McCutcheon & Elimelech, 2008).

For different applications, various morphologies of CA are required. Different CA membranes' morphologies have been synthesized by changing the demixing point and polymer concentration in the phase separation process, and the SEM images are presented in Fig. 12.3 (Cardea & De Marco, 2020). Beginning with a high polymer concentration led to obtaining a cellular membrane (Fig. 12.2A). If the starting solution contained less polymer concentration, spinodal membrane morphology was observed (Fig. 12.2B). With the low polymerization concentration, the liquid–liquid binodal demixing and polymer growth occurred in the polymer-lean phase, and a bead-like morphology was preferred (Fig. 12.2C).

Chen, Xu, Lu, Shan, and Gao (2017) used a single additive modification using acetic acid–lactic acid, acetic acid–maleic acid, and zinc chloride–lactic acid as binary mixed pore-forming additives to simultaneously enhance the salt rejection and water flux. In another work, a defect-free flat sheet composite membrane consisted of a thin layer of CTA cast on a nylon fabric was synthesized through a phase inversion method. CA membranes with determined thickness were prepared with lactic acid, maleic acid, and zinc chloride as pore-forming agents upon various annealing temperatures (Sairam, Sereewatthanawut, Li, Bismarck, & Livingston, 2011).

Nguyen, Yun, Kim, and Kwon (2013) studied the morphologies of woven and nonwoven fabrics microscopically. The effect of the support layer morphology on the FO performance was investigated and compared with commercial FO membranes. They synthesized CTA/CA-based membranes by immersion precipitation under different conditions, including solvent, casting composition, thickness, and annealing temperature. The presented membrane indicated a more hydrophilic and smoother surface than the commercial FO membrane (Nguyen et al., 2013).

The CA membranes were also modified by polyethylene terephthalate (PET) mesh via a phase inversion process. The effect of different concentrations, casting composition and temperature, and each step's time on the membrane performance was explored. A typical asymmetric sandwich structure was obtained and used in the FO process. The use of 0.2-M NaCl as the feed solution and 1.5-M glucose as the draw solution led to a water flux of 3.47 and 4.74 LMH in the FO and PRO modes, respectively. According to their results, the prepared membrane showed a lower degree of ICP than comparable membranes (Li, Wang, Hou, Bai, & Liu, 2016).

12.2.1.2 *Polyamide-imide-based membranes*

Polyamide-imides (PAIs) represent a positive synergy of properties from both PAs and polyimides such as excellent chemical resistance and superior thermal and mechanical properties. These amorphous thermoplastics show many applications in the aerospace industry, bearings, gears, and oil & gas industry (Scheme 12.1).

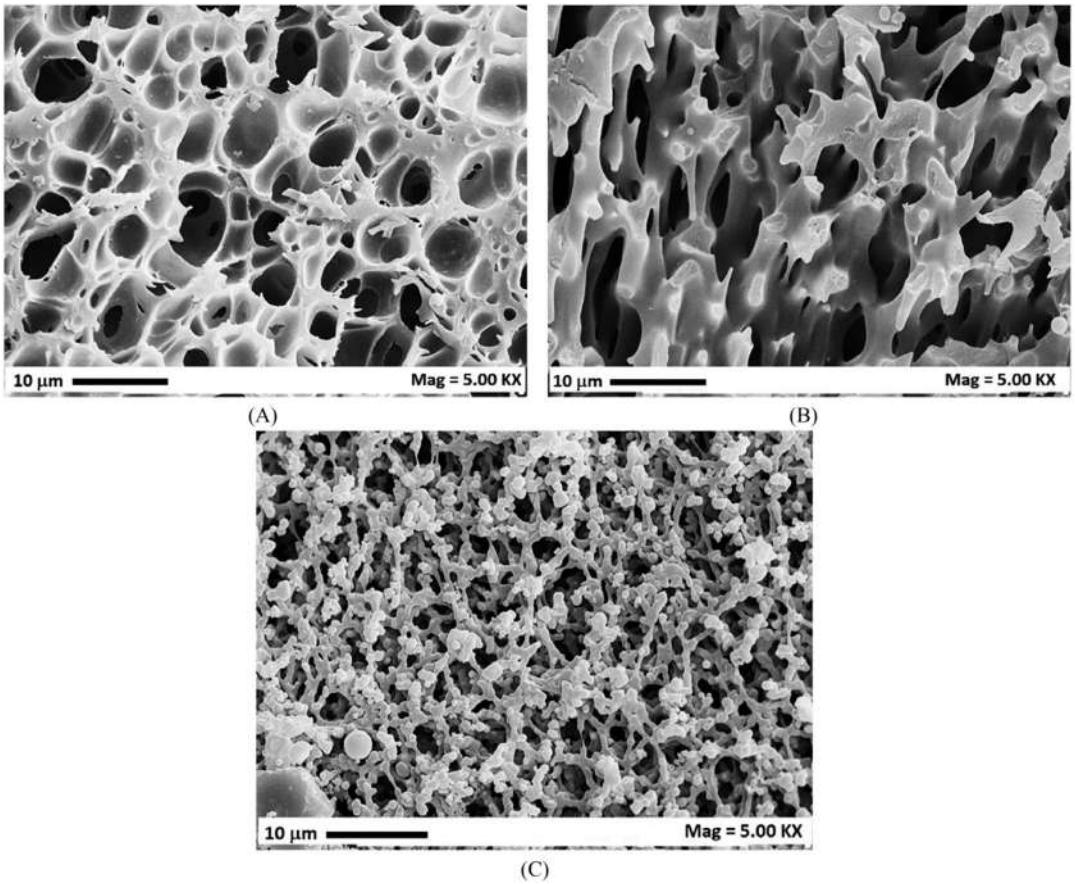

FIGURE 12.2 Cellular (A), spinodal (B), and (C) beads-like morphologies of cellulose acetate (CA) membrane prepared by Cardea and De Marco (2020).

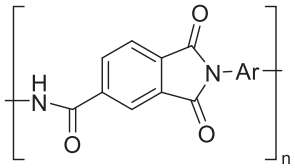

SCHEME 12.1 Chemical structure of polyamide-imide (PAI).

There are rare reports on using PAIs in the flat sheet FO membrane. For example, Qiu *et al*. reported the use of Torlon PAI materials to produce the flat sheet FO membranes by phase inversion method. The modification with polyethyleneimine was then carried out to attain a positively charged nanofiltration (NF)-like rejection layer. The influence of casting conditions and immersing methods on the structure and charge of the FO membrane was investigated. According to their results, PAI microporous support embedded with a woven fabric exhibited enhanced mechanical strength with a thinner substrate and higher water flux (Qiu, Setiawan, Wang, Tang, & Fane, 2012).

12.2.1.3 Polybenzimidazole membranes

One of the common FO membranes is polybenzimidazole (PBI) based membranes which suggest several advantages over cellulosic membranes such as high mechanical and thermal stability, charged features, and superior chemical resistance. The structure of PBI is shown in Scheme 12.2.

The low hydrophilicity and surface charge neutrality are disadvantages of using PBI as the membrane material. Therefore several works have been carried out to functionalize the PBI membranes with various modifying agents to enhance the hydrophilicity and surface charge of PBI flat sheet membranes. Increasing hydrophilicity results in lower fouling, while the negative charge on the membrane causes more ions rejection. Flanagan et al. reported PBI membrane synthesis by phase inversion procedure, followed by the surface activation with 4-(chloromethyl) benzoic acid. The taurine, para-phenylenediamine, and ethylenediamine were employed as modifying agents to supply a charge of the PBI membrane at neutral pH values (Flanagan et al., 2011). In another work, p-phenylenediamine, ethylenediamine, taurine, and poly(acrylamide-co-acrylic acid) were employed as a modifying agent for the FO applications showed enhanced membrane performance concerning water flux and salt rejection (Flanagan & Escobar, 2013).

12.2.1.4 Others

Other polymeric materials have been employed as the flat sheet FO membrane precursor that has not been used widely and are not included in the above sections. We just mention a couple of them. For instance, Li et al. synthesized a support-free symmetric membrane using poly(triazole-co-oxadiazole-co-hydrazine) through a solution casting method. The presented membrane possesses a dense structure, negative surface charge, and smooth surface that demonstrates low fouling and reverse solute flux (RSF) in the FO process (Li et al., 2019).

The synthesis of COOH-derived polyoxadiazole copolymer has been carried out to produce a support-free, symmetric, and self-standing FO membrane. The membrane thickness was altered to optimize the water permeability and salt rejection using Na_2SO_4 draw solution. Because of the absence of ICP in the symmetric FO membrane, the prepared membrane's structural parameter was zero (Li, Karanikola, Zhang, Wang, & Elimelech, 2018).

The performance of some reported single-layer flat sheet FO membrane was compared and summarized in Table 12.1.

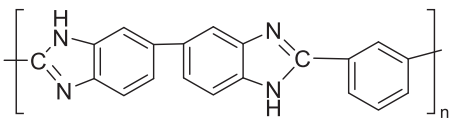

SCHEME 12.2 Chemical structure of polybenzimidazole (PBI).

TABLE 12.1 Comparing the performance of reported single-layer flat sheet forward osmosis (FO) membranes.

Entry	Membrane	Feed solution	Draw solution	Water flux (LMH)	RSF	*S* parameter/ thickness (μm)	Mode	References
Polymer-based flat sheet forward osmosis membranes								
Single-layer membranes								
Cellulosic membranes								
1	Zinc chloride–lactic acid/ CTA	0.1 M NaCl	2 M glucose	11.5	98.3%	–	FO	Chen et al. (2017)
2	Zinc chloride/CA, annealing temp. 70°C	35 g L^{-1} NaCl	150 g L^{-1} $MgSO_4$	0.27	95.0%	–/70–80	FO	Sairam et al. (2011)
3	CTA:CA (1:2 wt./wt.), AT: 85°C	Milli-Q water	1 M NaCl	10.39	0.084 mol m^{-2} h	–/250	FO	Nguyen et al. (2013)
4	Polyethylene terephthalate mesh/CTA	0.2 M NaCl	1.5 M glucose	3.47	95.48%	–/148.2	FO	Li et al. (2016)
Polyamide-imide (PAI)-based membranes								
5	Polyethyleneimine/PAI	Deionized (DI) water	0.5 M $MgCl_2$	29.65	64.8%	–/55	PRO	Qiu et al. (2012)
Polybenzimidazole (PBI) membranes								
6	p-Phenylenediamine/PBI	0.1 M NaCl	2 M $(NH_4)HCO_3$	~5.5	~90%	–/8	FO	Flanagan and Escobar (2013)
7	Ethylenediamine/PBI	0.1 M NaCl	2 M $(NH_4)HCO_3$	~2.4	~89%	–/8	FO	Flanagan and Escobar (2013)
8	Taurine/PBI	0.1 M NaCl	2 M $(NH_4)HCO_3$	~4.1	~90%	–/8	FO	Flanagan and Escobar (2013)
9	Poly(acrylamide-co-acrylic acid)/PBI	0.1 M NaCl	2 M $(NH_4)HCO_3$	~5.5	~90%	–/8	FO	Flanagan and Escobar (2013)
Others								
10	Poly(triazole-co-oxadiazole-co-hydrazine)	1.0 g L^{-1} Congo Red	1.5 M Na_2SO_4	11.7	0.0275 mol m^{-2} h	–	FO	Li et al. (2019)
12	COOH-derived polyoxadiazole copolymer	DI water	Na_2SO_4	12.3	~0.03 mol m^{-2} h	–/8	FO	Li et al. (2018)

12.2.2 Dual-layer membranes

The forward osmosis membrane requires a dense selective layer to highly reject the feed and draw solutes to maintain the osmotic difference as a driving force for mass transport. Extensive research on the synthesis of polymeric membrane proved that TFC prepared by interfacial polymerization (IP) produced a high salt rejection and high water permeability for different applications. Despite the useful properties of cellulosic materials for making FO membranes, researchers tried to use other polymers and synthesis methods to make FO membranes due to the possibility of their degradation under process conditions.

TFC membranes synthesized by IP include a porous support layer and a thin selective layer on the top. A typical TFC membrane and some properties of each layer are given in Fig. 12.3 (Idarraga-Mora et al., 2018).

The first TFC membranes used in the FO process were membranes made for RO. Using TFC membranes, the concept of forward osmosis was proven for dewatering and desalination applications, but due to the high thickness of these membranes, the resulting water flux was low. Therefore a very large membrane area would be required to reach the desired concentration, increasing the capital costs for commercial applications (Tinge et al., 2007).

The TFC FO membranes exhibited higher water permeability, solute rejection, and nonbiodegradability than conventional CTA membranes. Nevertheless, the ICP in the porous substrate and subsequent reduced osmotic driving force and osmotic pressure is the main

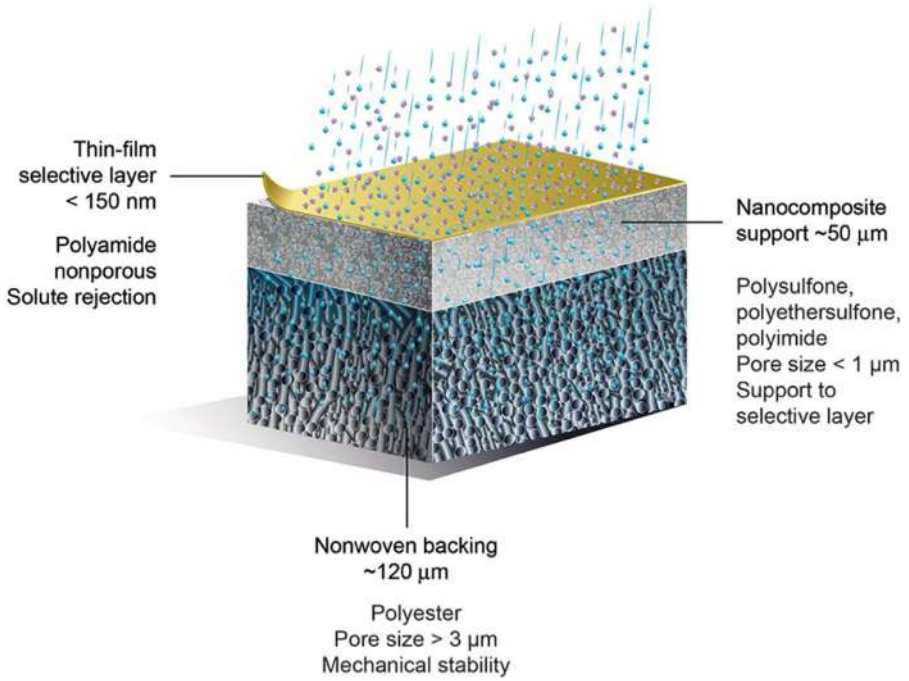

FIGURE 12.3 A schematical representation of typical thin-film composite (TFC) membranes (Idarraga-Mora et al., 2018).

drawback of TFC FO membranes. Different modifications on the support or/and selective layer have been carried out to enhance its hydrophilicity, leading to a more wetted surface and improved effective area for water transportation and, consequently, enhanced FO membrane performance.

12.2.2.1 Support layer

Various polymer materials were used as the support layer, which for the simplicity of the discussion, they were mainly categorized as polysulfone, polyethersulfone, polyacrylonitrile, cellulosic membrane, polyvinyl chloride, polyvinylidene fluoride, etc.

12.2.2.1.1 Polysulfone-based membranes

Polysulfone (PSf) is one of the essential polymers for membrane production due to its outstanding properties, such as good mechanical and thermal properties, chemical stability, and various functionalization procedures for different applications (Serbanescu, Voicu, & Thakur, 2020; Tajik, Moini Jazani, Shokrollahzadeh, & Latifi, 2016).

Yip, Tiraferri, Phillip, Schiffman, and Elimelech (2010) developed a TFC membrane tailored for FO operation by optimizing the casting process. The membrane consisted of a PA active layer synthesized by IP on a phase-inverted polysulfone support layer onto a thin polyester nonwoven fabric. By manipulating the casting polysulfone solution (polymer concentration; DMF:NMP solvent ratio), they fabricated a new support layer structure with a mix of finger-like and sponge-like morphologies. This novel membrane improved the membrane water flux compared to the commercially available FO and RO membranes, while the rejection was more than 97% against 1.5 M NaCl draw solution. This behavior was attributed to the decrease in the membrane structural parameter (S) of the support layer and providing a solution direct path in the support layer to the membrane's active surface. The membrane structural parameter and resistance to mass transfer were reduced by increasing the porosity and decreasing the support layer's thickness and tortuosity. The synthesized membrane stability was also demonstrated in an ammonium bicarbonate solution indicated its potential application in the FO process using this draw solution. They suggested improving the hydrophilicity of the support layer by the use of different polymers (such as polyethersulfone) and the addition of hydrophilic additives (such as polyethylene oxide or poly-4-vinylpyrrolidone) to the casting solution (Yip et al., 2010).

The introduction of hydrophilic groups into hydrophobic polymer backbones frequently decreases mechanical strength because of the high water swelling. Cho et al. reported the synthesis of carboxylated polysulfone as a hydrophilic microporous support membrane. In this work, despite the functionalization of polysulfone with hydrophilic groups, the mechanical strength was retained. The obtained water flux and salt passage were improved for carboxylated PSf compared to the conventional PSf FO membrane at the same conditions, probably due to the higher hydrophilicity and low ICP (Cho, Han, Han, Guiver, & Park, 2013). The hydrophilic−hydrophobic multiblock copolymer, including different amounts of disulfonated poly(arylene ether sulfone), was synthesized by Zhang et al. to improve the substrate hydrophilicity, porosity, and mechanical strength. The addition of copolymer to PSf with 25 wt.% significantly improved the FO performance of the TFC membrane (Zhang, Tian, Ren, et al., 2016). Combining a sulfonated polymer with various polyester (PET) nonwoven backings was used in the support materials of TFC membranes to improve the hydrophilicity and

mechanical properties with low the structural parameter for the FO process. These properties resulted in a membrane with desalination capacity and chlorine tolerance. This report proposes the combination of sulfonated polymer middle layer with PET nonwovens for forward and pressure-retarded osmosis (Ren, O'Grady, deJesus, & McCutcheon, 2016).

Several groups have modified the PSf support layer by dopamine under different conditions. For example, Han et al. functionalized the top surface of PSf with bio-inspired polymer polydopamine (PDA), which led to a hydrophilic smooth membrane including slighter surface pores and uniformly distributed pore size. This functionalization enhanced the pore wall's hydrophilicity inside the substrate and, consequently, the interaction of the PDA layer with trimesoyl chloride (TMC) during the polymerization and, consequently, a high salt rejection of the PA layer. The water permeability and salt rejection were enhanced compared to the pristine PSf substrate (Han, Zhang, Li, Widjojo, & Chung, 2012). In another work, norepinephrine was employed as an alternative monomer to dopamine for support layer modification that causes a broader array of coating conditions and better control of deposition. According to their results, polynorepinephrine performs similarly to polydopamine under ambient conditions on the TFC membrane for FO application (Chwatko, Arena, & McCutcheon, 2017).

The hydrophilic and microporous PSf layer synthesis through a sacrificial-layer approach followed by poly(3-sulfopropyl methacrylate potassium salt) grafting under UV irradiation was reported recently. The synthesized TFC membrane showed enhanced FO performance and separation selectivity and good antifouling properties due to improved hydrophilicity (Wang et al., 2019).

Recently, using responsive materials in various fields has attracted researchers' attention. The synthesis of a polysulfone-graft-poly(2-dimethylaminoethyl methacrylate) through a click reaction and atom-transfer radical polymerization was reported. Introducing a pH-responsive graft copolymer to the polysulfone improved both water flux and selectivity of the TFC membrane in the FO process. Moreover, the as-prepared membrane showed a reversible pH-dependence water flux (Salehi, Shakeri, Mahdavi, & Lammertink, 2020).

12.2.2.1.2 Polyethersulfone-based membranes

Polyethersulfone is a common substrate for TFC membranes due to its high chemical resistance, mechanical strength, and thermal stability. As polyethersulfone (PES) is hydrophobic, its modification is necessary for enhancing hydrophilicity and reducing ICP.

Using an alloy porous structure containing PES/sulfonated PSf was from the initial works for substrate FO membrane modification which enhanced the hydrophilicity. The IP reaction between p-phenylenediamine and 1,3,5-trimesoylchloride on this support led to a thin PA selective layer of 150 nm. The S parameter of the membrane was 238 μm. The obtained membrane was employed in the FO process using 5.0 M NaCl as the draw solution and deionized (DI) water as feed solution, which showed a water flux of 69.8 LMH (Wang, Chung, & Amy, 2012). Montmorillonite (MMT) was used to interact with sulphonated polyethersulfone (SPES) followed by mixing with PES dope solution to inhibit the hydrophilic polymer's leaching in a nonsolvent-induced phase separation procedure. The prepared substrate showed enhanced wettability, hydrophilicity, water permeability, and narrower pore size distribution. The water flux of the membrane containing MMT increased four folds compared to PES/SPES substrate at a similar thickness, and the reverse salt flux was halved (Wang & Xu, 2015).

Qiu et al. reported an in situ cross-linked acrylic acid polymerization on PES with enhanced hydrophilicity. The structural parameter was decreased four times, and water flux increased considerably compared to the pristine membrane. The ionic bonds between polyacrylic acid and m-phenylenediamine (MPD) during IP led to the PA layer with higher salt rejection and long-term stability (Qiu, Wang, & He, 2018).

In continuation to synthesize stimuli-responsive membranes, Salehi et al. synthesized carboxylic PES via acylation and oxidation reaction as a hydrophilic substrate for TFC membrane. The casting of modified polymer solution in a coagulation bath converts the sponge-like structure of PES to a long finger-like one. The carboxylic groups were deprotonated under this condition, which led to electrostatic repulsion and consequently the substrate with open pores and a less dense structure. The membrane showed pH-reversible properties for the FO process. Therefore the water permeability and selectivity could be controlled by changing the draw solution's pH or coagulation bath (Salehi, Shakeri, & Rastgar, 2018).

12.2.2.1.3 Polyacrylonitrile (PAN)-based membranes

Polyacrylonitrile (PAN) is a synthetic thermoplastic polymer used as the membrane substrate with higher hydrophilicity than PSf and PES. Besides, PAN indicates high thermal and chemical stability as well as solvent resistance. Klaysom et al. investigated the effect of different parameters, including the monomer mixture's composition, time, and drying on the PAN-based TFC FO membrane. According to their results, the addition of surfactant and drying time of amine solution on the support before adding the second monomer affects selective layer properties. The salt retention was increased from 56.8% to 95.6% by adding sodium dodecyl sulfate surfactant with retained water permeability. The extra amine removal increased the salt retention from 84.2% to 94.5%. The obtained membrane outperforms compared to commercial FO membrane (Klaysom, Hermans, Gahlaut, Van Craenenbroeck, & Vankelecom, 2013).

Conventional IP is carried out on hydrophobic substrates like PSf and PES. For the PAN as hydrophilic support, the strong affinity to amine monomer decreased amine diffusion to the organic phase, which causes the formation of a less cross-linked PA layer. Therefore an amine aqueous solution limits the formation of a dense and permeable PA layer. Various modifications have been accomplished to overcome this problem (Shokrollahzadeh & Tajik, 2018). For example, Kwon et al. accomplished the IP in an aromatic solvent (toluene) on the PAN substrate that enhanced amine diffusion toward the organic phase and consequently the formation of PA layer with high water permeability and selectivity. The mass transport was simplified due to the thin and finger-like structure of porous support on a nonwoven fabric. According to their results, the water flux was increased 2.3 times, and specific salt flux decreased 68% compared to those of membrane prepared by the conventional solvent in the IP. Using toluene as the solvent can overcome the challenge of hydrophilic support in the TFC membranes (Kwon et al., 2019).

12.2.2.1.4 Cellulosic membranes

The hydrophilic cellulose acetate propionate was used as microporous support to prepare TFC FO membranes that were first conducted by Li et al. in 2012. According to their results, the support's surface and skin morphology affect the PA layer, and FO

performance and the finger-like structure are not vital. They suggested that substrates with larger pores and broader distributions can simplify the fast migration of amine molecules and led to a rougher but more compact PA layer in TFC membranes. However, smaller surface pores result in smoother and less dense structures with fewer defects (Li, Wang, Helmer, & Chung, 2012).

Adding polyvinyl butyral (PVB) to cellulose acetate butyrate (CAB) substrate for preparing the TFC FO membrane was investigated by Ma et al. They proposed that PVB enhances the hydrophilicity and changes the substrate's pore formation mechanism that causes to decrease ICP in the FO process. Very low total mass transfer resistance was reported for this membrane, making it suitable for the FO membrane application (Ma, Xiao, Long, & Yang, 2020).

12.2.2.1.5 Polyvinyl chloride based membranes

One of the most attractive membrane materials is polyvinyl chloride (PVC) because of the thermal and chemical stability, mechanical resistance, film-making properties, easy modification, solubility in various organic solvents, and low cost compared to most membrane substrates materials. Nevertheless, using a hydrophilic additive to increase the porosity and wettability is necessary. In the report by Pardeshi, layered double hydride (LDH) was added to PVC to obtain a substrate material for the FO process. The hydrophilicity, pore size, surface free energy, and porosity were increased by elevating the concentration of LDH in PVC (Pardeshi, Mungray, & Mungray, 2017).

Among various modifications, using sulfonated polysulfone (SPSf) was from the attractive works. The SPSf/PVC substrate possesses different advantages like low cost, high porosity, water permeability, and hydrophilicity. The field emission scanning electron microscopy (FESEM) images of the substrates with different ratios of SPSf to PVC are exhibited in Fig. 12.4. According to the results, introducing SPSf led to improve the porosity of the substrates. The less cross-linked PA layer with a rougher and looser structure was obtained using the low ratio of SPSf to PVC membrane (Zheng, Zhou, & Zhou, 2018).

Very recently, the effect of adding cellulose carbamate to PVC has been explored for the TFC FO membrane that showed the enhanced performance. The porosity, hydrophilicity, and pore structure of the substrate were improved. The selective layer showed a less cross-linked structure (Zheng, Zhou, Cheng, & Huang, 2021b).

12.2.2.1.6 Poly(vinylidene difluoride) (PVDF)-based membranes

Another polymer material used as the substrate for the TFC FO membrane is PVDF. The high hydrophobicity, chemical and mechanical resistance, and thermal stability are some features of this material. As mentioned in previous sections, introducing a hydrophilic additive to enhance the hydrophilicity and reducing the ICP of the substrate is crucial for the FO application.

There are rare reports on using PVDF in flat sheet FO membrane. Zhang et al. reported using hydrophilic perfluorosulfonic acid (PFSA) with small content to PVDF substrate to improve the FO performance of the TFC membrane. The hydrophilicity and good consistency of PFSA with PVDF caused the enhanced wettability, morphology, pore size, and consequently the better formation of PA layer during IP and higher water flux and membrane selectivity (Zhang, Shen, et al., 2017).

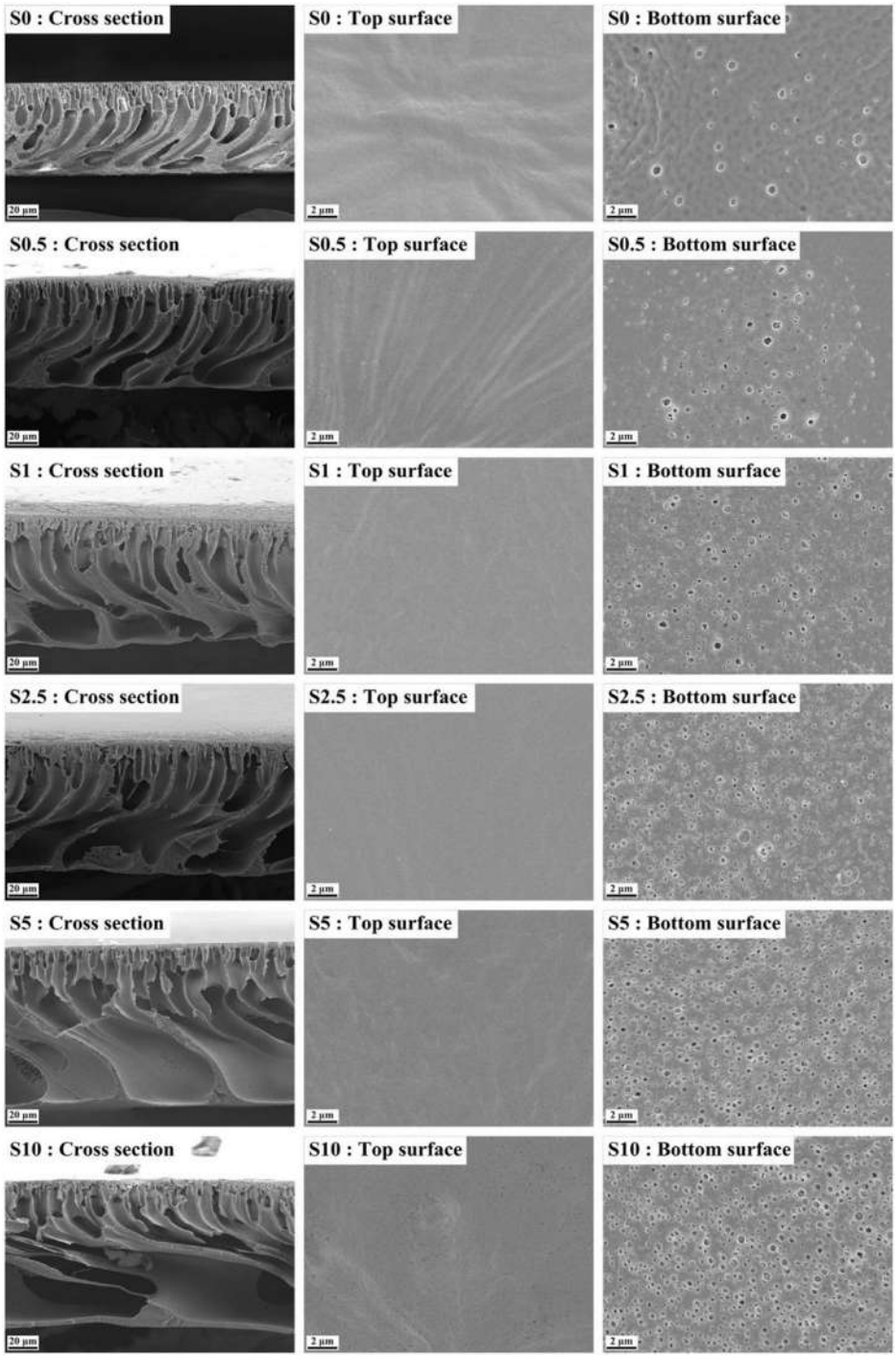

FIGURE 12.4 Field emission scanning electron microscopy (FESEM) images of the support layers with different sulfonated polysulfone (SPSf) to the polyvinyl chloride (PVC) mixing ratio (S denotes to SPSf/PVC blend ratio).

12.2.2.1.7 Polyazole-based membranes

The excellent mechanical and thermal stability make polyoxadiazoles (PODs) another choice for membrane materials. Nevertheless, the hydrophobicity of this polymer restricts its application for the FO membranes. Polytriazoles are more hydrophilic than PODs with aromatic and heterocyclic structures. These membranes can be used as antifouling membranes because of the antibiofouling properties of oxadiazoles and antifouling of triazoles. These polymers' low solubility in the common casting solvents and lower hydrophilicity is the drawback of these polymers. To overcome this problem, Duong et al. (2015) suggested hydroxyl functionalization, which enhanced the hydrophilicity and polymer processibility.

12.2.2.2 Active layer

Usually, the researchers use the IP of two monomers containing amine and acyl chloride groups to synthesize the selective layer of TFC membranes. The PA layer usually exhibits low water permeability due to its hydrophobicity and high fouling propensity. Different modifications on the active layer have been reported with altering the monomers, solvents, additives, and conditions during the IP reaction. In some cases, the post-modifications have been carried out to obtain the desired properties.

12.2.2.2.1 Monomers

Different aliphatic or aromatic amines, including piperazine, MPD, and p-phenylenediamine have been used as amine monomer. The monomers containing acyl chlorides such as TMC, isophthaloyl chloride, and 5-isocyanatoisophthaloyl chloride have been employed to react with amine monomers and formation of PA layer. The most common monomers for this reaction are MPD and TMC, which led to efficient water desalination. However, using other materials as monomers or using a third monomer along with components has been suggested by various researchers to improve the FO performance.

Xiong et al. used N-[3-(trimethoxysilyl)propyl]ethylenediamine as an organic–inorganic hybrid amine monomer mixed with MPD to form the PA layer. The obtained TFC FO membrane showed enhanced hydrophilicity and water flux along with antifouling properties (Xiong et al., 2016). In another work, tris(2-aminoethyl) amine was used both as the amine monomer and the catalyst for amidation reaction with TMC. The synthesized TFC FO membrane's performance was improved compared to conventional TFC membrane in terms of water flux, antifouling properties, and RSF (Shen & Wang, 2018). The influence of adding dopamine as the monomer along with MPD to mix with TMC in the IP reaction was investigated by another group. According to their results, the structural parameter was significantly decreased compared to conventional TFC membrane. Besides, low ICP, less flux decline, and enhanced antifouling properties were obtained using a dopamine-based TFC membrane (Wang et al., 2018).

In recent work, 4-aminophenyl sulfone (APS) was used instead of MPD as an amine monomer to react with TMC on the filter paper substrate for the formation of the TFC FO membrane. The stability of selective layer coating was studied by the monomer interaction. Based on the results, the interconnected cross-linked structure of two monomers was obtained after the IP. The synthesized TFC membrane was compared with the control

membrane (MPD and TMC as the monomers), which exhibited higher rejection and comparable water flux (Nayak et al., 2020).

12.2.2.2.2 Solvent

Among different factors affecting the IP reaction and the PA layer's properties, the reaction solvent is a facile way to control the membrane features. In 2017, Liang et al. proposed the addition of acetone in the aqueous phase, which simplifies the IP reaction on the support layer with vertical pores. They found that the synthesized membrane has a thicker and denser selective layer compared to conventional FO membrane with asymmetric substrates. The lower structure parameter and ICP were obtained by using this membrane (Liang et al., 2017).

Very recently, 1-butyl-3-methylimidazolium bis (trifluoromethylsulfonyl) imide ionic liquid was employed as an organic reagent phase instead of hexane in IP reaction on the polyimide (PI) support layer to obtain TFC FO membranes. Compared to the traditional TFC FO membrane, similar performance was obtained but without any additives. The phase inversion and PI cross-linking and amine monomer impregnation were carried out at the same time. The concentration of PI and solvent compositions were optimized. A mixture of ionic liquid/hexyl acetate with 0.5 wt.% MPD and 0.3 wt./vol.% TMC showed J_s/J_w of 0.25 g L^{-1} and a Jw/$\Delta\pi$ of 0.41 LMH/bar using 0.5 M NaCl draw solution (Hartanto, Corvilain, Mariën, Janssen, & Vankelecom, 2020a).

12.2.2.2.3 Postmodification

The rough surface of the PA layer and increased surface for foulant interaction cause the high fouling. The electrostatic interaction of deprotonated carboxylic acid groups with metal ions of the feed solution is another problem of conventional TFC FO membranes. To overcome this problem, various antifouling materials have been incorporated into the membranes, such as nanostructures and hydrophilic materials (Chiao et al., 2020; Li et al., 2018; Shen, Xiong, & Wang, 2016). However, most of the reports are on in situ modifications that could affect the selective layer structure. In the following, several examples of the postmodification of the PA layer were discussed.

Ni and Ge (2018) presented chemically modified FO membranes, including aniline sulfonate/bisulfonate covalently functionalized PA layer on PES support through the acylation reaction between primary amine and acyl chloride groups. The more hydrophilic and smoother membrane surface and consequently enhanced water flux and antifouling properties were obtained by this modification (Ni & Ge, 2018). In another work, ethane diamine was used to accomplish the second IP leading to a modified FO membrane with high fouling resistance. The sodium salt of 2-[(2-aminoethyl)amino]-ethane sulfonic acid was also investigated by this group to obtain an improved FO membrane in terms of wettability and water flux due to the introduction of the hydrophilic group ($-SO_3Na$) (Wang et al., 2016).

To improve fouling resistance, poly(ethylene glycol) was incorporated into the TFC FO membrane. A second IP was carried out between acyl chloride groups of the nascent PA layer and ethylenediamine to enrich amino groups. Then, epoxide groups of PEG diglycidyl ether were reacted with amine groups, leading to a more hydrophilic membrane surface which PEG prevents the foulant adsorption (Castrillón, Lu, Shaffer, & Elimelech, 2014). Recently, polyamidoamine dendrimer with lots of easily protonated amine groups

was covalently attached to the TFC FO membrane to improve the fouling resistance and ammonia rejection. Due to the electrostatic repulsion of amino groups and concentration-induced diffusion resistance, the rejection and antifouling properties of the TFC FO membrane were enhanced, using NH_4Cl as the feed solution (Bao et al., 2019).

The zwitterionic species have been widely used to modify the AL of TFC FO membranes. For example, Chen and Ge (2019) introduced bifunctional zwitterion of (1-(3-aminopropyl)-imidazole) propane-sulfonate (APIS) to the membrane via an amidation reaction. The membrane with higher water flux and fouling resistance, smaller flux decline, and stronger renewability was obtained, and its application for water production and protein enrichment was investigated. Moreover, APIS was also employed as a draw solution with an easily pH regulation method for its regeneration. Besides, APIS does not damage the protein structure, making it an excellent choice for protein enrichment applications (Chen & Ge, 2019). Another report to enhance antifouling properties was grafting a zwitterionic polymer brush through an initiator immobilized on the membrane. The obtained TFC FO membrane showed higher hydrophilicity, lower surface charge, decreased roughness, and improved fouling resistance, which was explained by the controlled architecture of polymer brush on the membrane surface formed by the atom-transfer radical polymerization (Liu et al., 2017). Chiao et al. proposed a zwitterionic PA species for the second IP reaction to achieve an asymmetric TFC FO membrane with enhanced antifouling and antibacterial features. The zwitterionic moieties led to a more hydrophilic membrane surface with shielded negative charge distribution (Chiao et al., 2019).

12.2.2.2.4 Additive

The TFC FO membranes obtained by the IP between MPD and TMC have some drawbacks, such as low water permeability and fouling tendency because of aromatic groups. The incorporation of additives such as surfactants, nanomaterials, and suitable solutions has been employed as another modification method to enhance the membrane's hydrophilicity and water permeability. For example, Jia et al. used cetyltrimethylammonium chloride (CTAC) on the TFC FO membrane's selective layer. In the aqueous solution, CTAC micelles showed ionic interactions with MPD molecules affecting the IP reaction between MPD and TMC. As the concentration of CTAC increased, the linear structure of the selective layer and microcrystalline structure also increased. This structure caused a lower water flux but higher salt rejection and selectivity than the control membrane without CTAC (Jia et al., 2014). In another work, polyethyleneimine (PEI) was employed as a cationic hydrophilic material to introduce the PA layer via the IP reaction. The PEI-modified TFC FO membranes exhibited higher water permeability, salt rejection, and antifouling properties due to the introduction of positive charges and hydrophilicity to the membrane. The skin layer's surface roughness and thickness were decreased as the PEI content was increased (Chiao et al., 2020).

In a recent report, polyoxometalate-based open frameworks (POM-OFs), including POM coordinated by organic cationic ligands, were used as nanofiller due to their high surface area, thermal stability, hydrophilicity, and uniform tubular pores. The surface of POM was functionalized with tetramethylammonium bromide to enhance the computability of nanofiller with the polymer matrix. The hydrophilicity, water permeability, and

selectivity of the modified TFC FO membranes were improved (Shakeri, Mighani, Salari, & Salehi, 2019).

12.2.2.2.5 Reaction conditions

Among the modifications used to enhance the TFC FO membrane's characteristics, altering the reaction conditions seems to be more straightforward. Khorshidi et al. investigated the effect of temperature of the organic solution in the IP reaction between TMC and MPD on the PES substrate. According to their results, reducing the temperature of organic solution to −20°C decreased the PA layer thickness, leading to higher water permeability and lower specific solute flux. The boiler feedwater of the steam-assisted gravity drainage process was also treated by the synthesized membrane. The water flux and specific solute flux were improved compared to the commercial membrane (Khorshidi, Bhinder, Thundat, Pernitsky, & Sadrzadeh, 2016).

The influence of ultrasonication in the IP reaction was recently investigated. Based on the results, ultrasonication can enhance monomer mixing, leading to a complete IP reaction. When a high-ultrasonication power (480−600 W) was employed, a higher amount of cavitation bubbles led to more cross-linking, greater free volume pore size, rougher, and thicker PA layer, and consequently, the efficient separation of the membrane was obtained using 60 kHz ultrasonication frequency compared to 40 kHz. Using low ultrasonication power (360 W), more enhancements were obtained at a lower frequency (40 Hz) because of the higher sonochemical effect of acoustical cavitation. The effect of ultrasonication time on the water flux and RDF was also studied, which displayed monotonically and nonmonotonic changes, respectively (Shen et al., 2020).

The comparison between different reported dual-layer flat sheet FO membranes is presented in Table 12.2.

12.2.3 Layer-by-layer membranes

The layer-by-layer (LbL) procedure has been widely used to obtain an ultrathin and uniform separation layer by depositing various cation and anion polyelectrolytes by a straightforward synthetic procedure. The controllable thickness, flexibility, and hydrophilicity are advantages of this modification method compared to conventional chemical procedures. In a report by Liu et al., a multilayer polymer network was prepared by deposition of PEI and sodium alginate bilayers on a polydopamine-functionalized PVDF substrate to remove heavy metal ions. According to their results, various heavy metal ions were efficiently rejected by the modified membrane. The reaction parameters and the number of bilayers and the hydrated radii of metal ions affect the heavy metal rejection (Liu et al., 2017). In another work, the PEI cross-linked hexadecafluorodecanedioic acid polyelectrolyte was deposited on a PES UF membrane substrate resulting in a positively charged modified FO membrane. The composition, reaction time, and temperature were optimized. Based on their results, the membrane deposited with 3.5 bilayers and cured at 60°C for 1 hour showed enhanced water flux and RSF compared to the neat membrane (Suwaileh, Johnson, Khodabakhshi, & Hilal, 2019b).

TABLE 12.2 Comparing the performance of reported dual-layer flat sheet forward osmosis (FO) membranes.

Entry	Membrane	Feed solution	Draw solution	Water flux (LMH)	RSF	*S* parameter/ thickness (μm)	Mode	References
Polymer-based flat sheet forward osmosis membranes								
Dual-layer membranes								
Support layer modification								
Polysulfone								
1	Porous finger-like polysulfone–PA TFC	DI water	2 M NaCl	54	–	670–710/–	PRO	Wei, Qiu, Tang, Wang, & Fane (2011)
2	Carboxylated polysulfones–PA TFC	DI water	1 M $MgCl_2$	18	2.2 gMH	–/68	FO	Cho et al. (2013)
3	Mesh-embedded polysulfone/sulfonated polysulfone–PA TFC	DI water	1 M NaCl	31.76	6.03 gMH	220/–	FO	Zhao, Wang, Ren, and Pei (2018)
4	Sulfonated polysulfone/ polyester nonwoven	DI water	1 M NaCl	70	6.87 gMH	277/–	PRO	Ren et al. (2016)
5	Polysulfone-graft-poly (2-dimethylaminoethyl methacrylate)–PA TFC FS, pH = 3.0	DI water	1 M NaCl	25	–	–	PRO	Salehi et al. (2020)
6	Polysulfone-graft-poly (2-dimethylaminoethyl methacrylate)–PA TFC FS, pH = 10.0	DI water	1 M NaCl	30	–	–	PRO	Salehi et al. (2020)
7	Polysulfone-graft-poly (2-dimethylaminoethyl methacrylate)–PA TFC DS, pH = 3.0	DI water	1 M NaCl	18	–	–	FO	Salehi et al. (2020)
8	Polysulfone-graft-poly (2-dimethylaminoethyl methacrylate)–PA TFC DS, pH = 10.0	DI water	1 M NaCl	16.4	2.5 gMH	546/–	FO	Salehi et al. (2020)

(*Continued*)

TABLE 12.2 (Continued)

Entry	Membrane	Feed solution	Draw solution	Water flux (LMH)	RSF	*S* parameter/ thickness (μm)	Mode	References
Polyethersulfone								
9	Amine-terminated sulfonated poly(arylene ether sulfone)—PA TFC	40,000 ppm soybean oil/ water emulsion	2 M NaCl	11.5	98.7%	–	FO	Zhang, Tian, Gao, et al. (2017)
10	Carboxylic polyethersulfone—PA TFC, pH = 3	DI water	1 M NaCl	14.23	–	1423.54/–	FO	Salehi et al. (2018)
11	Carboxylic polyethersulfone—PA TFC, pH = 12	DI water	1 M NaCl	28.03	–	653.94/–	FO	Salehi et al. (2018)
12	Carboxylic polyethersulfone—PA TFC, pH = 3	DI water	1 M NaCl	27.8	86.47%	653.94/–	PRO	Salehi et al. (2018)
13	Carboxylic polyethersulfone—PA TFC, pH = 12	DI water	1 M NaCl	46.17	80.2%	1423.54/–	PRO	Salehi et al. (2018)
14	Polyethersulfone/poly (acrylic acid)—PA TFC	DI water	2 M NaCl	32.9	96.6%	346/–	FO	Qiu et al. (2018)
15	Polyethersulfone/poly (acrylic acid)—PA TFC	DI water	2 M NaCl	56.3	–	–	PRO	Qiu et al. (2018)
16	Polyethersulfone/sulfonated polysulfone—PA TFC	DI water	0.5 M NaCl	24.1	4.5 gMH	238/–	PRO	Wang et al. (2012)
17	Polyethersulfone/sulfonated polysulfone—PA TFC	DI water	0.5 M NaCl	14.0	3.6 gMH	238/–	FO	Wang et al. (2012)
Polyacrylonitrile								
18	PAN—PA TFC	DI water	1 M NaCl	31.3	5.11 gMH	112.1/–	FO	Hajighahremanzadeh, Abbaszadeh, Mousavi, Soltanieh, and Bakhshi (2016)
19	Polydopamine/PAN—PA TFC	DI water	3.5 wt.% NaCl	38.0	0.4 LMH	600 ± 80/–	PRO	Zhang, Fu, and Chung (2013)

Cellulosic membranes								
20	Cellulose acetate propionate–PA TFC	DI water	2 M NaCl	35.0	1.9 gMH	–	PRO	Li et al. (2012)
21	Cellulose acetate butyrate/ polyvinyl butyral–PA TFC	DI water	1 M NaCl	27.5	9.62 gMH	363.5/–	PRO	Ma et al. (2020)
Polyvinyl chloride								
22	Polyvinyl chloride/cellulose carbamate–PA TFC	DI water	1 M NaCl	40.4	4.0 gMH	337/–	PRO	Zheng et al. (2021b)
23	Polyvinyl chloride/layered double hydroxide–PA TFC	DI water	1 M NaCl	37.46	3.57	303/–	FO	Pardeshi et al. (2017)
24	Polyvinyl chloride/layered double hydroxide–PA TFC	DI water	1 M NaCl	50.89	14.28	303/–	PRO	Pardeshi et al. (2017)
25	Polydopamine/polyvinyl chloride–PA TFC	DI water	1 M NaCl	18.9	3.35 gMH	–	FO	Shabani, Kahrizi, Mohammadi, Kasiri, and Sahebi (2021)
26	Polyvinyl chloride/ quaternized poly phenylene oxide–PA TFC	DI water	1 M NaCl	71.21	5.6 gMH	187 ± 7/–	PRO	Zheng, Zhou, Cheng, and Huang (2021a)
Poly(vinylidene difluoride)								
27	Perfluorosulfonic acid/ PVDF–PA TFC	DI water	1 M NaCl	54.4	10.9 gMH	–	PRO	Zhang, Shen, et al. (2017)
28	Perfluorosulfonic acid/ PVDF–PA TFC	DI water	1 M NaCl	27.0	8.4 gMH	334.6 ± 3.5/–	FO	Zhang, Shen, et al. (2017)
29	Electrospun PVDF nanofibers–PA TFC	DI water	1 M NaCl	30.4	6.38 gMH	812/–	PRO	Tian, Qiu, Liao, Chou, and Wang (2013)
30	PVDF nanofibers coated with nylon 6,6–PA TFC	DI water	1 M NaCl	31	14.33 gMH	–	PRO	Huang, Arena, and McCutcheon (2016)
31	PVDF nanofibers coated with nylon 6,6–PA TFC	DI water	1 M NaCl	22	3.74 gMH	193 ± 22/–	FO	Huang et al. (2016)

(*Continued*)

TABLE 12.2 (Continued)

Entry	Membrane	Feed solution	Draw solution	Water flux (LMH)	RSF	*S* parameter/ thickness (μm)	Mode	References
Polyazole								
32	Hydroxyl functionalized polytriazole-co-polyoxadiazole	DI water	1 M NaCl	24.9	4.1 gMH	236/–	FO	Duong et al. (2015)
33	Hydroxyl functionalized polytriazole-co-polyoxadiazole	DI water	1 M NaCl	47.2	8.2 gMH	–	PRO	Duong et al. (2015)
Active layer modification								
Monomers								
34	PSf/filter paper –4-aminophenyl sulfone and trimesoyl chloride (TMC)	1000ppm NaCl	1 M NH_4HCO_3	2.5	3.7	160/–	FO	Nayak et al. (2020)
35	PSf/filter paper –4-aminophenyl sulfone and TMC	1000ppm NaCl	1 M NH_4HCO_3	3.23	4.7	–	PRO	Nayak et al. (2020)
36	PSf/tris(2-aminoethyl) amine and TMC	DI water	2 M NaCl	42.4 ± 1.2	~18.3 gMH	–	FO	Shen & Wang (2018)
37	PSf/tris(2-aminoethyl) amine and TMC	DI water	2 M NaCl	74.4 ± 2.2	~28.5 gMH	–	PRO	Shen and Wang (2018)
38	PAN/N-[3-(trimethoxysilyl) propyl]ethylenediamine, MPD, and TMC	DI water	0.5 M NaCl	16.67	10.7 gMH	290 ± 29/–	FO	Xiong et al. (2016)
39	Mixed cellulose ester/ dopamine, MPD, and TMC	DI water	1 M NaCl	50	8.19 gMH	135.2/–	FO	Xu, Xu, Shan, Wang, and Gao (2017)
40	PSf/dopamine, MPD, and TMC	DI water	1 M NaCl	22.08	32.77 mmol m^{-2} h	176/–	FO	Wang et al. (2018)
41	PSf/N-aminoethyl piperazine propane sulfonate, MPD, and TMC	DI water	0.5 M NaCl	9.1	5.27 gMH	–	FO	Wang et al. (2018)

Solvent								
42	PVDF/MPD (acetone addition in the aqueous phase) and TMC	DI water	2 M NaCl	93.6	10 gMH	99.1 ± 3.7/–	FO	Liang et al. (2017)
43	PVDF/MPD (acetone addition in the aqueous phase) and TMC	DI water	2 M NaCl	122	12 gMH	–	PRO	Liang et al. (2017)
44	PSf/MPD and TMC (1-butyl-3-methylimidazolium bis(trifluoromethylsulfonyl) imide/hexyl acetate as organic phase)	DI water	0.5 M NaCl	8.4–12.5	2.3 gMH	–	FO	Hartanto, Corvilain, Mariën, Janssen, and Vankelecom (2020b)
45	PSf/MPD & TMC (1-butyl-3-methylimidazolium bis (trifluoromethylsulfonyl) imide/hexyl acetate as organic phase)	DI water	0.5 M NaCl	11.2–14.7	3.9 gMH	–	PRO	Hartanto et al. (2020b)
Postmodification								
46	PES/Aniline sulfonate/ bisulfonate-functionalized PA	DI water	0.5 M NaCl	16	1.81 gMH	–	PRO	Ni and Ge (2018)
47	PES/aniline sulfonate/ bisulfonate-functionalized PA	DI water	0.5 M NaCl	12.6	1.6 gMH	–	FO	Ni and Ge (2018)
48	PES/ethane diamine (EDA) and 2-[(2-aminoethyl) amino]-ethane sulfonic acid monosodium salt	DI water	3 M NaCl	19	~0.22 mol m^{-2} h	301/–	FO	Wang et al. (2016)
49	PSf/poly(ethylene glycol)–PA	DI water	2 M NaCl	~20	–	–	FO	Romero-Vargas Castrillón, Lu, Shaffer, and Elimelech (2014)
50	Sulfonated PES/ polyamidoamine dendrimer PA	DI water	1 M NaCl	~34	~0.167 gMH	–	FO	Bao et al. (2019)

(*Continued*)

TABLE 12.2 (Continued)

Entry	Membrane	Feed solution	Draw solution	Water flux (LMH)	RSF	*S* parameter/ thickness (μm)	Mode	References
51	PES/(1-(3-aminopropyl) imidazole) propanesulfonate PA	DI water	0.5 M NaCl	~18.7	~2.4 gMH	–	FO	Chen and Ge (2019)
52	PES/(1-(3-aminopropyl) imidazole) propanesulfonate PA	DI water	0.5 M NaCl	~20.3	~2.5 gMH	–	PRO	Chen and Ge (2019)
53	PSf/N-aminoethyl piperazine propane sulfonate PA	DI water	1 M NaCl	18.9	2.5 gMH	560/–	FO	Chiao et al. (2019)
54	CA/[2-(methacryloyloxy)-ethyl] dimethyl-(3-sulfopropyl) ammonium hydroxide zwitterionic polymer brush PA	DI water	0.8 M NaCl	20	–	~280/–	FO	Liu et al. (2017)
Additive								
55	PSf/ cetyltrimethylammonium chloride PA	DI water	2 M NaCl	5.32	98%	–/225	FO	Jia et al. (2014)
56	PES/polyoxometalate-based open frameworks PA	DI water	1 M NaCl	29.9	9.3 gMH	–	FO	Shakeri et al. (2019)
57	PES/polyoxometalate-based open frameworks PA	DI water	1 M NaCl	41.7	15.8 gMH	–	PRO	Shakeri et al. (2019)
58	PSf/halloysite nanotubes PA	DI water	1 M NaCl	24.1	6.2 gMH	–	FO	Ghanbari et al. (2015)
59	PSf/halloysite nanotubes PA	DI water	1 M NaCl	33.6	9.1 gMH	–	PRO	Ghanbari et al. (2015)
60	PSf/Zirconium (IV)-carboxylate metal–organic framework (MOF) UiO-66 nanoparticles PA	DI water	1 M NaCl	20.7	4.3 gMH	–	FO	Ma, Peh, Han, and Chen (2017)

61	PSf/Zirconium (IV)-carboxylate metal−organic framework (MOF) UiO-66 nanoparticles PA	DI water	1 M NaCl	36.7	7.1 gMH	–	PRO	Ma et al. (2017)
62	PSf/graphene oxide PA	DI water	1 M NaCl	34.7	4.66 gMH	–	PRO	Shokrgozar Eslah, Shokrollahzadeh, Moini Jazani, and Samimi (2018)
Reaction conditions								
63	PES/PA, organic solution temperature: 25°C	DI water	3 M NaCl	17.6	~5.2 gMH	1770/–	FO	Khorshidi et al. (2016)
64	PES/PA, organic solution temperature: −20°C	DI water	3 M NaCl	38.5	~2.1 gMH	451 ± 13/–	FO	Khorshidi et al. (2016)
65	PSf/ultrasonication PA	DI water	2 M NaCl	120.1 ± 2.1	12.1 ± 0.7 gMH	465−482/–	PRO	Shen et al. (2020)

Recently, the synthesis of positively charged FO membranes through the combination of homogeneous polyelectrolyte complex membranes and the LbL method was reported to prepare an effective selective layer on PES substrate for brackish water desalination. Due to hydrophilicity and positively charged properties, the modified membrane exhibited very low RSF of positively charged ions and good water flux (Suwaileh, Johnson, Khodabakhshi, & Hilal, 2019a). Table 12.3 shows the FO performance of some reported LbL flat sheet FO membranes.

12.2.4 Double-skinned membranes

Recently, double-skinned FO membranes with two active layers, a dense and a loose active layer, on the two sides of the substrate were introduced, which possess the FO and PRO modes' benefits in the FO process. The osmotic gradient for water transport was kept by the dense active layer, while the loose active layer prevents the contaminants from passing into the substrate. The lower water flux and inevitable RSF are some drawbacks of double-skinned compared to single-skinned FO membranes.

Wang et al. (2010) fabricated a highly porous support layer sandwiched between two active layers to mitigate the concentration polarization. Because internal polarization could not be eliminated by increasing flow velocity and turbulence, these researchers prevented the salt and draw solute penetration to the membrane porous layer by forming two active layers on either side of it. The synthesized double-skinned membrane was made of CA material by phase inversion and showed a high water flux and low reverse solute diffusion against $MgCl_2$ draw solution. This high performance was attributed to the salt rejection of active layers as well as the low water transport resistance of the porous layer. They concluded that although the formation of another layer creates new resistance to water transport, it significantly mitigates the adverse effects of ICP. This study showed that by modifying the membrane structure, FO membrane performance could be improved (Wang et al., 2010).

In 2012 a double-skinned cross-linked layer-by-layer membrane was first prepared by coating oppositely charged polyelectrolyte layers to obtain the rejection skin on a porous support. This group studied the FO performance and fouling properties of the modified membrane. According to their results, the double-skinned membrane showed better solute rejection and fouling resistance (Qi, Qiu, Zhao, & Tang, 2012).

The double-skinned membrane consisting of a porous support layer sandwiched between a dense PAN layer for solute rejection and a fairly loose dense zwitterionic polyelectrolyte brush for emulsified oil particle elimination was synthesized by Ong et al. for the emulsified oil–water treatment (Fig. 12.5). Using the double-skinned membrane and 2 M NaCl draw solution, high rejection and good water flux were obtained with a lower fouling tendency than a single one. The polyelectrolyte brush played a critical role as an antifouling layer due to its hydrophilic nature, leading to decreased ICP effect (Ong et al., 2017).

12.2.5 Impregnated membranes

The common FO membranes include thick microporous support and a thin selective layer that led to ICP and water transport resistance. Another approach to improve the FO performance and water flux is the design of a thin porous substrate impregnated with a hydrophilic

TABLE 12.3 Comparing the performance of reported layer-by-layer flat sheet forward osmosis (FO) membranes.

Entry	Membrane	Feed solution	Draw solution	Water flux (LMH)	RSF	*S* parameter/ thickness (μm)	Mode	References
Polymer-based flat sheet forward osmosis membranes								
Layer-by-layer membranes								
1	PES/poly(ethylenimine) cross-linked hexadecafluorodecanedioic acid polyelectrolyte (3.5 bilayers)	DI water	1 M NaCl	21.9	1.6 LMH	–	FO	Suwaileh et al. (2019b)
2	Polydopamine-functionalized PVDF/ polyethylenimine and sodium alginate bilayers (3 layers)	2 g L^{-1} heavy metal ions	1.0 M $MgCl_2$	14	99.32%	–	FO	Liu et al. (2017)
3	Polydopamine-functionalized PVDF/ polyethylenimine and sodium alginate bilayers (3 layers)	2 g L^{-1} heavy metal ions	1.0 M $MgCl_2$	23.5	95.93%	–	PRO	Liu et al. (2017)
4	PES/MPDADMAC, MCMCNa polyelectrolyte complex (2.5 bilayers)	DI water	1 M NaCl	23.1	1.54 LMH	–	FO	Suwaileh et al. (2019a)
5	PAN/PA molecular layer-by-layer (10 cycles)	DI water	0.5 M NaCl	24.6	2.36 gMH	350/–	FO	Kwon et al. (2015)
6	PAN/PA molecular layer-by-layer (10 cycles)	DI water	0.5 M NaCl	32.9	3.77	350/–	PRO	Kwon et al. (2015)
7	PAN/poly(allylamine hydrochloride) and poly(sodium 4-styrene-sulfonate) (3 layers)	DI water	3 M $MgCl_2$	105.4	–	–	PRO	Qiu, Qi, and Tang (2011)

polymer to altogether remove the open-pore structures in the membranes, which are called impregnated membranes. For instance, Zhao et al. suggested using porous hydrophobic Solupor substrate impregnated with a hydrophilic cross-linked poly(ethylene glycol) diacrylate for the FO process. The membrane performance of impregnated membranes was increased compared to the commercial FO membranes (Zhao, Huang, & Lin, 2015). Very recently, the synthesis of a porous membrane impregnated with highly cross-linked PAs on both sides through a gel–liquid IP was reported. The elimination of pores led to lowering the effect of ICP. The PA layer presented high solute rejection and water flux compared to the hydrogels (Tran et al., 2020). The impregnated flat sheet FO membranes are given in Table 12.4.

12.2.6 Biomimetic membranes

The membranes that are inspired by the biological membranes are called biomimetic membranes. Among these membranes, aquaporin attracted much attention. Due to the

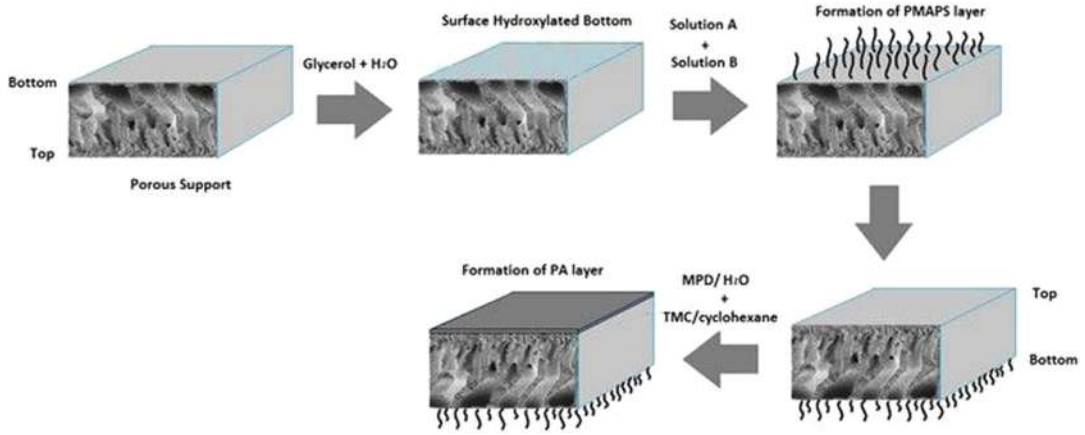

FIGURE 12.5 Synthesis of double-skinned forward osmosis (FO) membrane (Ong et al., 2017).

TABLE 12.4 Comparing the performance of reported impregnated flat sheet forward osmosis (FO) membranes.

Entry	Membrane	Feed solution	Draw solution	Water flux (LMH)	RSF	*S* parameter/ thickness (μm)	Mode	References
Polymer-based flat sheet forward osmosis membranes								
Impregnated membranes								
1	Solupor/cross-linked poly (ethylene glycol) diacrylate impregnated membrane	DI water	1 M NaCl	–	7.1 gMH	–	FO	Zhao et al. (2015)
2	Zwitterionic hydrogels impregnated in porous membranes/PA	DI water	1 M Na_2SO_4	0.14 ± 0.05 LMH/bar	21 ± 7 gMH	–/35	FO	Tran et al. (2020)

high water transport capacity and exceptional solute selectivity that is not observed in any artificial polymeric membranes, aquaporins have been used as inspiration for designing biomimetic membranes. Despite the unique features and application of AquaporinZ (AqpZ) in water treatments, the synthesis of defect-free-supported lipid bilayer biomimetic membranes has some problems. Ding et al. proposed the formation of amide bonds between the lipid bilayer and microporous support layer to obtain the biomimetic FO membrane with good stability and durability. They also investigated the effect of the addition of positively charged phospholipid 1,2-dioleoyl-3-trimethylammonium-propane mixed in the 1,2-dioleoyl-sn-glycero-3-phosphoethanolamine bilayer on the water flux and RSF. The water flux was enhanced in the alter because of more AqpZ in the mixed bilayer (Ding et al., 2015). Chun et al. employed aquaporin inside membrane (AIM) for the FO process, and the surface properties and fouling tendency were compared with commercial FO membrane. The prototype AIM membrane consisted of a semiaromatic PA layer instead of a wholly aromatic structure in commercial FO membranes, which led to higher water flux. The lower RSF caused the lower organic fouling sodium alginate solution using calcium chloride as the draw solution. After several runs, the retained membrane integrity showed the possible application of this membrane for harsh feed solution treatments (Chun et al., 2018). Some reported biomimetic flat sheet FO membranes are compared in Table 12.5.

12.3 Polymer-based hollow fiber forward osmosis membranes

It has been proposed that tubular/hollow fiber membranes may possess an FO membrane's desired properties and are more suitable than flat sheet FO membranes due to the self-supported structure, having a flow pattern vital for the FO process, and a higher ratio of membrane area per module volume. Besides, the preparation of a hollow fiber module with a high packing density is easier (Xu, Peng, Tang, Fu, & Nie, 2010).

12.3.1 Single-layer membranes

In the early stages of the FO process, researchers tried to prove the FO concept using available commercial membranes. NF membrane was of interest due to its high rejection of divalent ions that could fractionate the ionic mixture in the FO process. The asymmetric membranes, including PBI and CA, have been selected as the first hollow fiber FO membranes due to their outstanding NF properties (Wang, Yang, Chung, & Rajagopalan, 2009). Various treatments were accomplished to improve the selectivity of the membranes. Despite the relatively good performance of the membranes for divalent ions, the lack of selectivity for monovalent ions restricted their applications in the desalination process. In continuation, dual-layer membranes were used to improve the water permeability of the membrane. Wang et al. (2007a, 2007b) explored the fabrication of polybenzimidazole (PBI) NF hollow fiber membrane with desirable pore size and its application in the FO experiment. The chemical and thermal stability, robust mechanical strength, charged property, and hydrophilicity, and antifouling behavior made it the right candidate for membrane

TABLE 12.5 Comparing the performance of reported biomimetic flat sheet forward osmosis (FO) membranes.

Entry	Membrane	Feed solution	Draw solution	Water flux (LMH)	RSF	*S* parameter/ thickness (μm)	Mode	References
Polymer-based flat sheet forward osmosis membranes								
Biomimetic membranes								
1	Prototype FO AIM	Milli-Q water	1 M NaCl	23.1 ± 0.9	4.4 ± 0.4 gMH	420/–	FO	Chun et al. (2018)
2	Aquaporin Asia Pte. Ltd in Singapore	DI water	1 M KCl	12.8	14.8 gMH	735/–	FO	Sahebi, Sheikhi, and Ramavandi (2019)
3	Aquaporin Asia Pte. Ltd in Singapore	DI water	1 M KCl	17.1	17.5 gMH	735/–	PRO	Sahebi et al. (2019)
4	AqpZ-incorporated supported lipid bilayer	DI water	2 M $MgCl_2$	19.2	3.2 gMH	–	FO	Ding et al. (2015)
5	AqpZ-1,2-dioleoyl-3-trimethylammonium-propane blended in the 1,2-dioleoyl-sn-glycero-3-phosphoethanolamine bilayer	DI water	2 M $MgCl_2$	23.1	3.1 gMH	981/–	FO	Ding et al. (2015)
6	AIM by Aquaporin A/S Denmark	DI water	1 M NaCl	8.8	4.0 gMH	630/–	FO	Xia, Andersen, Hélix-Nielsen, and McCutcheon (2017)
7	AIM by Aquaporin A/S Denmark	DI water	1 M NaCl	14.0	4.6 gMH	630/–	PRO	Xia et al. (2017)

synthesis in aqueous separation. The microstructure of the membrane consisted of four morphologies: asymmetric selective layer, finger-like macrovoids, spongey substructure, and porous inner skin layer. The narrow pore size distribution (mean effective pore radius of 0.32 nm), high water permeation flux, and low good salt selectivity to divalent ions were reported at different concentrations of NaCl and $MgCl_2$ draw solutions. The effect of membrane orientations of asymmetric PBI hollow fiber membrane was also studied, where the PRO mode showed much higher water permeation. Thus it was suggested for the recovery and concentration of various feed solutions by the FO process (Wang, Chung, & Qin, 2007b).

NF membranes that are suitable for FO application should have a negative charge at most pHs. As PBI is neutrally charged at a pH of 7, it reduces the electrostatic repulsion between the membrane surface and aqueous ions and harms membrane separation. To overcome this problem, the surface of the PBI NF membrane was functionalized with short hydrophilic charged groups, and the positive effect on water flux was shown (Mettu, Escobar, Coleman, & Chung, 2008).

Wang et al. (2009) tried to develop a high-flux and high-rejection PBI NF hollow fiber membrane with a thin wall and desired pore size. They used the phase inversion method and chemical modification of the membrane. For tuning the pore size distribution and improve the salt selectivity, cross-linking was done by p-xylene dichloride. The narrow pore size distribution of the membrane resulted in high water permeation and low salt permeation. Similar to their last investigation (Wang et al., 2009), different types of morphologies were formed in the support layer. The study demonstrated that the modified PBI NF membrane might be used for water recovery from wastewater, and a longer cross-linking time might enhance the membrane for desalination purposes. Thin wall formation enhanced the water flux due to a reduction in water transfer resistance. Besides, the effects of membrane morphology and process conditions on water and salt permeation were investigated. They reported that the draw solution concentration ($MgCl_2$) and membrane orientation were the most influential parameters on water flux (Wang et al., 2009).

Su et al. fabricated CA NF hollow fiber membrane and used it in the FO process. They used a two-step heat treatment to shrink the mean pore radius of the membrane to reach a denser outer skin layer and a high salt rejection similar to FO membranes. The fabricated fibers rejected 90.2% of NaCl and 96.7% of $MgCl_2$; however, the water permeability was low. By increasing the feedwater salinity, the osmotic pressure efficiency decreased due to the more severe ICP (Su, Yang, Teo, & Chung, 2010). Then, Su et al. studied the effect of annealing on the microstructure of FO performance of CA hollow fiber membranes. The depth profiles of the free volume, the mean radius, and the radius distribution of free volume in the CA membrane's outer skin were measured. The mean pore radius was reduced by increasing the annealing temperature because heat treatment caused shrinkage of the large voids between nodule aggregates to smaller cavities and reduced spaces between intra-molecular chain segments. They showed that water and salt permeabilities are affected mainly by thermal annealing. At optimum temperature, the annealed CA membrane demonstrated a relatively high water flux and low reverse salt flux using $MgCl_2$ draw solution in PRO membrane orientation (Su, Zhang, et al., 2010). The FO performance of some reported single-layer hollow fiber FO membranes is given in Table 12.6.

TABLE 12.6 Comparing the performance of reported single-layer hollow fiber forward osmosis (FO) membranes.

Entry	Membrane	Feed solution	Draw solution	Water flux (LMH)	RSF	*S* parameter/ thickness (μm)	Mode	References
Polymer-based hollow fiber forward osmosis membranes								
Single-layer membranes								
1	Polybenzimidazole	DI water	5 M $MgCl_2$	11.2	–	–	PRO	Wang et al. (2007b)
2	Polybenzimidazole via nonsolvent-induced phase inversion	DI water	5 M $MgCl_2$	36.5	–	–	PRO	Wang et al. (2009)
3	Polybenzimidazole via nonsolvent-induced phase inversion and 2-h cross-linking	DI water	5 M $MgCl_2$	32.4	–	–	PRO	Wang et al. (2009)
4	Cellulose acetate	DI water	2 M $MgCl_2$	5.0	–	–	FO	Su, Yang, et al. (2010)
5	Cellulose acetate	DI water	2 M $MgCl_2$	7.3	0.53 gMH	–	PRO	Su, Yang, et al. (2010)
6	Cellulose acetate annealed at 80°C	DI water	2 M $MgCl_2$	30.98	0.37 gMH	–	PRO	Su, Zhang, et al. (2010)

12.3.2 Dual-layer membranes

Yang et al. (2009a, 2009b) investigated the synthesis of a dual-layer polybenzimidazole-polyethersulfone (PBI-PES) NF hollow fiber membrane and its application in the FO process. Their objective was the concentration of pharmaceutical products (lysozyme) to prevent denaturing of the components. To obtain a very thin selective layer of PBE (10 μm), they used the coextrusion method, and a sharp pore size distribution was obtained. Their FO experiments showed that a suitable water flux and less fouling were obtained by protein. Magnesium ion reaction was also higher than 90%. They used PBI polymer and LiCl stabilizer to make the self-charged outer layer of the membrane. At the same time, a mixture of PES and polyvinylpyrrolidone (PVP) was applied to make the inner porous layer. The morphological studies of the obtained membrane showed that the selective outer layer of PBI had a thickness of 10 μm with an effective pore size of 0.4 nm and the substrate of PES/PVP was completely spongy. Numerous macro-cavities were formed beneath the selective layer that was connected to the surface of the layer through channels, while the outer surface was utterly porous. They concluded that there was little mass transfer resistance in the membrane. Compared to their previous work on single-layer membranes (Yang et al., 2009a), they claimed that this membrane not only had a suitable selective layer, but the addition of PVP to PES resulted in a higher porosity layer.

In another study, the concept of using NF membranes in the FO process was tested to concentrate pharmaceutical dilute solutions using $MgCl_2$ as a draw solution. The reverse salt flux of this membrane was low. To continue the work, they suggested that reduction of the active layer thickness, minimization of porosity and thickness of the support layer, and optimizing the hydrodynamic conditions would increase the water flux (Yang, Wang, & Chung, 2009b).

Chou et al. (2010) tried to synthesize a hollow fiber thin-film composite membrane without outer ultrafiltration (UF) skin for FO applications. The support layer was made of PES, and the RO-like PA active layer with a thickness of 300 nm was fabricated by IP on the inner surface of a commercial PES layer. The membrane showed good intrinsic separation properties and water flux. The ratio of salt flux to water flux in PRO membrane orientation was lower than the other published articles. The application of membrane in water desalination was successfully reported using different NaCl feed solution concentrations (up to 3.5%) and 2 M NaCl as draw solution. By formulating the skin and resistances to membrane transport in PRO using NaCl in both feed and draw solutions, they suggested that if the feed concentration was low and the draw solution concentration was almost low, the controlling step of mass transfer was the water permeability through the skin layer. In this case, the value of water permeability (A) becomes more critical than S's value in FO membrane transport. However, suppose the salt concentration in the feed is relatively high. In that case, the support layer's mass transfer will control the membrane transfer, and lower S values will play a much more important role in osmotic performance (Wang et al., 2010).

Wang et al. (2010) examined TFC membrane performance by fabricating two types of TFC FO hollow fiber membrane with a thin active layer on either side of the phase-inverted PES porous substrate. The prepared substrate layer membrane was hydrophilic and highly porous with long needle-like pores and narrow pore size distribution. The

dense layer thickness was 300−600 nm for either of the synthesized membranes. The membrane's intrinsic separation properties were found superior compared to the commercial FO flat sheet, while the S value was comparable with the HTI's FO flat sheet. They concluded that a suitable FO membrane structure should have a thin layer of spongy structure and a highly porous substrate (Chou et al., 2010).

Setiawan et al. synthesized NF-like selective layer by using PAI as microporous hollow fiber and then polyelectrolyte posttreatment with cationic polymer PEI (Setiawan, Wang, Li, & Fane, 2011a). This membrane showed good water flux but was still limited to NF selectivity.

In another work, hydrophilic PAN was used as the substrate to obtain a TFC FO hollow fiber membrane, which showed a water flux of 36.6 LMH with 1 M NaCl draw solution (Ren & McCutcheon, 2015). Very recently, PVDF membrane was synthesized at high temperature rapid nonsolvent-induced phase separation upon different conditions. According to their results, the stock solution's temperature should be adjusted which gelation did not occur. Moreover, the temperature of the outer coagulation solution should be maintained higher than the upper critical solution. A solution containing PVDF, butyrolactone, and PVP was used under this condition to prepare a hollow fiber membrane, which showed a higher water permeability than other reported PVDF membranes (Yabuno et al., 2020). Dual-layer hollow fiber membranes are compared in Table 12.7.

12.3.3 Layer-by-layer membranes

An LBL polyelectrolyte on a PES substrate hollow fiber membrane was fabricated with different coating layers by Liu et al. The performance of obtained FO membrane was investigated using $MgCl_2$ draw solution in both FO and PRO modes. Based on their results, with six layers of coated membrane, the higher membrane performance was obtained in the PRO mode with a small concentration of draw solution (Liu et al., 2013).

12.3.4 Double-skinned membranes

To overcome the problem of foulants diffusion into the substrate, various solutions have been proposed. For example, altering synthesis conditions to obtain a smaller pore size of the substrate is one procedure, but it caused decreased porosity of the support layer and consequently more ICP effect. The fabrication of double-skinned FO membranes with a substrate sandwiched between two skin layers, one selective to draw solute and the other as the barrier for fouling diffusion, is another approach (Han, Cheng, & Chung, 2017; Su, Chung, Helmer, & de Wit, 2012).

Su et al. (2012) prepared the double-skinned hollow fiber FO membrane consisting of CA deposited by two dense skins to decrease ICP and fouling tendency. When 0.5 M sucrose as draw solute at the shell side and 200−2000 mg L^{-1} mixed metal ions wastewater as feed solutions at the lumen side were utilized, the good water flux with minimum RSF was obtained (Su et al., 2012). In another work, PAI was utilized as the UF substrate followed by IP to obtain a PA RO-like selective layer and a positively charged NF-like

TABLE 12.7 Comparing the performance of reported dual-layer hollow fiber forward osmosis (FO) membranes.

Entry	Membrane	Feed solution	Draw solution	Water flux (LMH)	RSF	*S* parameter/ thickness (μm)	Mode	References
Polymer-based hollow fiber forward osmosis membranes								
Dual-layer membranes								
1	Polybenzimidazole-polyethersulfone/ polyvinylpyrrolidone	DI water	3.125 M $MgCl_2$	17.7	–	–	FO	Yang et al. (2009b)
2	Polybenzimidazole-polyethersulfone/ polyvinylpyrrolidone	DI water	3.125 M $MgCl_2$	23.3	–	–	PRO	Yang et al. (2009b)
3	Ultrathin PA-based RO-like skin layer on the inner surface of a porous hollow fiber substrate	DI water	0.5 M NaCl	32.2	3.7 gMH	–	PRO	Wang et al. (2010)
4	PES/PA	DI water	0.5 M NaCl	42.6	4.0 gMH	–	PRO	Chou et al. (2010)
5	Torlon® polyamide-imide/polyethyleneimine	DI water	0.5 M $MgCl_2$	8.36	92.7%	–	FO	Setiawan, Wang, Li, and Fane (2011b)
6	Torlon® polyamide-imide/polyethyleneimine	DI water	0.5 M $MgCl_2$	9.74	91.1%	–	PRO	Setiawan et al. (2011b)
7	Polyacrylonitrile	DI water	1 M NaCl	36.6	18.75 gMH	~300/–	PRO	Setiawan et al. (2011b)
8	PVDF/PA	DI water	1 M NaCl	18.9	8.4 gMH	216/–	FO	Yabuno et al. (2020)
9	PSf commercial UF supports TFC FO	DI water	1 M NaCl	10.3	2.2 gMH	725/–	FO	Ren et al. (2017)
10	TFC tri-bore	DI water	1 M NaCl	9.4	2.1 gMH	1100/–	FO	Luo, Wang, Zhang, Han, and Chung (2014)
10	PES/PA using dual-layer coextrusion technology	DI water	2 M NaCl	34.5	9.9 gMH	261/–	FO	Sukitpaneenit and Chung (2012)
11	CTA/PA	DI water	1 M NaCl	8.0	0.6 gMH	639/–	FO	Shibuya et al. (2015)

secondary layer. The obtained double-skinned hollow fiber showed enhanced FO performance (Fang, Wang, Chou, Setiawan, & Fane, 2012b).

To minimize fouling and ICP, the PES fiber support layer deposited by an inner PA skin layer and outer PA sealing layer was synthesized through double IP. Because of the rejection of the PA sealing layer, salts and foulants diffusion into the support layer is considerably blocked, and consequently, ICP and fouling were decreased, and the FO performance was improved (Han et al., 2017).

One-step preparation of dual-layer PES substrate coated by a thin inner skin layer via IP reaction was reported to fabricate a double-skinned hollow fiber TFC FO membrane for the sludge concentration application. The support layer includes a fairly dense UF outer layer and a porous UF inner layer. The water permeability of the synthesized double-skinned membrane was enhanced. Based on their results, UF outer layer led to reject organic foulants with higher sizes (>300 Da) (Ng, Wu, Chen, Dong, & Wang, 2019).

In a recent report, the PSf inner layer is sandwiched between the layers of PSf/aminosilanized poly(methyl methacrylate) (N-PMMA) with finger-like structures coating towards the center of the membrane. The results displayed that the urea adsorption capacity of the membrane depends on the N-PMMA amount, which under the optimal condition, considerable urea removal was observed (Abidin et al., 2020).

12.3.5 Biomimetic membranes

Up to 2018, there are few reports on the fabrication of aquaporins hollow fiber platform for full-scale production. The AqpZ-based hollow fiber membranes reported by Li et al. were synthesized by immobilization of aquaporin-incorporated proteoliposomes on the substrate's inner surface coating with PA layer. This membrane showed high FO performance but was limited to the lab-scale application (Li et al., 2015).

In 2018, the first full-scale fabrication of aquaporin-based hollow fiber membrane was presented from Aquaporin A/S (Denmark) in a continuous process. The synthesized membrane's FO performance was investigated, which showed a water flux of 21 LMH and RSF of 3.6 gMH. The structural parameter of the membrane was measured as $210.5 \pm 55.5\,\mu m$ (Ren & McCutcheon, 2018). In a study by Engelhardt et al., the rejection of three trace organic contaminants was tested by an FO process using an aquaporin-based membrane in which high rejection rates were obtained (Engelhardt, Sadek, & Duirk, 2018).

Recently, the combination of polyelectrolyte multilayer and biomimetic membranes was carried out to obtain proteopolymersomes multilayers using proteopolymersomes (PP +) with the incorporated aquaporin as the polycation and poly(styrene 4-sulfonate) (PSS) and poly(acrylic acid) (PAA) as the polyanions. The prepared membrane obtained a similar FO performance with other biomimetic membranes. However, this one was prepared by a desired hollow fiber geometry having features of both biomimetic and polyelectrolytes (Reurink, Du, Górecki, Roesink, & De Vos, 2020). Table 12.8 represents the performance of reported LbL, double-skinned, and biomimetic hollow fiber FO membranes.

TABLE 12.8 Comparing the performance of reported layer-by-layer, double-skinned, and biomimetic hollow fiber forward osmosis (FO) membranes.

Entry	Membrane	Feed solution	Draw solution	Water flux (LMH)	RSF	*S* parameter/ thickness (μm)	Mode	References
Polymer-based hollow fiber forward osmosis membranes								
Layer-by-layer membranes								
1	PES/layer-by-layer polyelectrolyte	DI water	1 M $MgCl_2$	25.9	1.7 gMH	–/200	PRO	Liu et al. (2013)
Double-skinned membranes								
2	PES/double-skinned PA TFC	DI water	1 M NaCl	–	–	996	FO	Han et al. (2017)
3	CA/double-skinned membranes with an inner dense layer	DI water	2 M $MgCl_2$	17.1	–	–	FO	Su et al. (2012)
4	Poly(amide–imide)/RO- and NF-like selective layers	DI water	2 M NaCl	41.3	5.2 gMH	–	PRO	Fang, Wang, Chou, Setiawan, and Fane (2012a)
5	Relatively dense UF outer layer and a porous UF inner layer/PA	Humic acid (50 mg L^{-1})	0.5 M NaCl	14.1	–	–	PRO	Ng et al. (2019)
6	Relatively dense UF outer layer and a porous UF inner layer/PA	DI water	0.5 M NaCl	24.1	8.4 gMH	–	PRO	Ng et al. (2019)
Biomimetic membranes								
7	Aquaporine-incorporated proteoliposomes immobilized on the inner surface	DI water	0.5 M NaCl	55.2 ± 4.5	4.5 ± 0.2 gMH	–	PRO	Li et al. (2015)
8	AIM from A/S, Denmark	DI water	1 M NaCl	21	3.6	210.5 ± 55.5/–	PRO	Ren and McCutcheon (2018)

12.4 Commercialization status and commercial viability

Given that well-established RO membranes have a high market share, and many efforts have been made to make RO membranes more economical, at present, FO membranes cannot replace them. FO is currently considered as a technology in the following cases in the water and wastewater sector:

- in situations where the possibility of using RO is not technically or economically possible, such as feeds with a high tendency for membrane fouling;
- in cases where feed salinity is high and cannot be desalinated by RO;
- in cases where there is no need to regenerate the draw solution, such as fertigation;
- in wastewaters that are difficult to treat by other membranes, such as brines.

A complementary technique and RO is a pretreatment or posttreatment to achieve high water quality and more water recovery from saline or contaminated feedwater.

Since FO technology is based on natural processes, which consume less energy, it is hoped that FO will gradually expand further with the development of suitable membranes and draw solutions.

It has been about two decades since the first manufacture of FO membranes. HTI was a leading company that commercially produced flat sheet membranes for specific applications. This company's membranes were used in the first FO pilot plants and semicommercial FO units for water purification and water desalination. HTI is no longer commercially available due to economic problems. Oasys Water is currently one of the active companies in FO membrane application in various industries. This company introduced the first commercial TFC FO membrane with reasonable water flux (Goh, Ismail, Ng, & Abdullah, 2019). In recent years, Oasys Company has developed integrated FO and other membrane processes to design high-recovery desalination systems for brine management, and zero liquid discharge (ZLD) systems for water recycling of power plant wastewater, as well as desalination of highly saline solutions. Following them, several international companies have been added to the list of FO membrane production companies, which their information is summarized in Table 12.9. The companies' characteristics are obtained from their websites and other related websites (https://www.forwardosmosistech.com). Although the name of FO membrane is not seen in the product catalogs of several companies, the membrane and membrane modules made by them are mentioned in published scientific articles. Among them, CSM (Korea), Toray Group (Japan), and Samsung (Korea) are pointed out.

As can be seen, more companies have entered the production of FO membranes in recent years, which shows the positive attitude of the market to the future of this technology. These companies produce a variety of membrane configurations, including hollow fiber, spiral wound, and tubular. However, several companies have focused on developing hollow fiber membranes for the FO application due to their benefits in high surface area, uniform water flow, and mechanical strength. Undoubtedly, in the future, we will observe the expansion of companies producing FO membranes for various applications.

TABLE 12.9 List of existing suppliers of commercial forward osmosis (FO) membranes.

Company	Membrane	Configuration	Membrane characteristics	Target sector/applications	Country
Aromatec Pte Ltd	–	Hollow fiber 2-inch (6 L h^{-1}) and 4-inch (30 L h^{-1})	High water flux with low reverse salt flux	Product concentration in food & beverage, flavor & fragrance, pharmaceutical, and oil & gas wastewater treatment	Singapore
Aquaporin	Biomimetic membrane using natural aquaporins	Hollow fiber 11 LMH, 0.15 g L^{-1} RSF	High selectivity, retain difficult treat-contaminants to reuse more water with better quality and use fewer chemicals	Water reuse, concentration of natural compounds	Denmark
Asahi Kasei	–	Hollow fiber	Concentration rate three-times higher than RO	Concentration of aromas and active ingredients in food, beverage, and pharmaceuticals	Japan
Berghof Membranes Technology	–	Tubular (in collaboration with Aquaporin)	Ideal for the treatment of challenging process and wastewater streams	Industrial process streams and wastewaters treatment	Germany
FTSH2O-Fluid Technology Solutions	CTA	Flat sheet, 4- and 8-inch spiral-wound elements, flux 3.5 LMH, rejection > 99.9% (joint with Aquaporin)	High rejection, high resistance to fouling and abrasion, ideal for treating dirty waste streams	Wastewater treatment (ZLD/high brine concentration), product concentration in food & beverage and pharmaceutical, personal hydration	United States
Koch Membrane Systems	–	Spiral wound 4 and 8-in. elements	–	Trial for product concentration in food, beverage, and life science markets	United States
Porifera	–	Flat sheet stacked elements		Product concentration in food and beverage industries, water reuse, waste minimization, industrial and municipal water, oil & gas wastewater	United States
Oasys Water	TFC	Spiral wound	–	Wastewater treatment	United States
Toyobo	CTA	hollow fiber	Uniform water flow with minimum pressure loss, fouling resistant	Desalination of seawater, osmotic power production, industrial wastewater concentration	Japan

12.5 Summary and future directions

In this chapter, the development process of FO polymeric membranes using different polymer solutions and monomers was reviewed, and the advantages and disadvantages of each of them were explained. In the past few decades, a great effort has been made to design superior performance FO membrane concerning materials and structural properties. Several scientific articles have been published on the synthesis of FO membranes that mainly focused on reducing concentration polarization and enhancing the water permeability and lower ICP and decreasing the reverse salt diffusion through the membrane. Fabrication of fouling-resistant membranes was another objective of the researchers that can be used explicitly in wastewater treatment.

In the design of high-performance FO membranes, the scientists tried to synthesize a thin and hydrophilic support layer with optimal porosity to provide higher water flux and less internal polarization. Lowering the structural parameter of the support is a goal for the synthesis of an appropriate FO membrane. Besides, the active layer should be very thin and selective to provide high water flux and low RSF.

To achieve these goals, the researchers adopted the following strategies in the last few years:

- using more hydrophilic polymers for the support layer
- application of various monomers for polymerization of the active layer
- functionalization of the membrane
- synthesis of double-skinned membranes
- using different fabrication methods
- manipulating the porosity of the support layer
- inspired by nature to fabricate efficient membranes

The membranes were synthesized thinner through developmental research, but the selective layer remained similar to the RO membrane for not passage of the other solutes except water.

There are different methods to manufacture a membrane with a selective layer, such as IP, LbL assembly, conventional phase inversion (asymmetric membranes), blending, and surface grafting.

To date, several types of FO membranes have been introduced, which include:

- flat sheet membrane
- hollow fiber membranes
- LbL membranes
- impregnated membranes
- biomimetic membranes

This chapter shows that many efforts have been made in the synthesis of suitable membrane, but researchers are still looking to improve the performance of FO membranes. A competitive relationship exists between water flux and membrane selectivity (rejection) in polymeric membranes; therefore high water flux and high rejection cannot be achieved simultaneously. On the other hand, high water flux also means increased

concentration polarization and a higher fouling tendency. One way to solve this problem might be the design of specific FO membranes for each application. For instance, when the product's high quality is desired, a membrane with high rejection but not very high water flow can be used and vice versa.

Another challenge in FO membranes, like other polymeric membranes, is scaling and fouling (organic and bio-based). Due to the low pressure in this process, the fouling layer is less compacted and can be removed more easily, but fouling will ultimately reduce the membrane's lifetime. Over the past decade, fouling in FO membranes has been widely investigated, and their removal methods have been explored, but more studies are still needed to understand this phenomenon better.

Despite many advances in the production of FO membranes, for mass production and widespread use of FO membranes, it is still necessary to prove that the specific energy consumption of water production with this technology is less than similar technologies as RO. The low-pressure FO process itself has a lower energy consumption than other pressure-driven membrane processes. Nevertheless, the required energy for the regeneration of the draw solution is still very decisive. If the produced water is used for drinking water, quantities of draw solution even at deficient concentrations in the product will be significant. Therefore to achieve the quality of drinking water, high-efficiency regeneration methods must be used, which increases the energy consumption for water production.

Forward osmosis technology has been shown to have great potential for use in various applications of water desalination, wastewater treatment, dehydration of food and pharmaceutical products, and energy production. The new subjects are added continuously to this list of applications. In the synthesis of FO membranes, more attention has been paid to water desalination. However, it is necessary to consider the fabrication and modification of membranes for wastewater treatment or dehydration of food and pharmaceuticals.

Undoubtedly, synthesizing a suitable membrane will not be effective without introducing a draw solution that can generate high osmotic pressure, needs low-energy recovery methods, and be nontoxic. The manufacture of new draw solutions besides the appropriate FO membrane could expand FO process applications in the near future.

Abbreviations

AIM	aquaporin inside membrane
APIS	1-(3-Aminopropyl)-imidazole propane-sulfonate
AqpZ	aquaporinZ
APS	4-Aminophenyl sulfone
BFW	boiler feedwater
CA	cellulose acetate
CAB	cellulose acetate butyrate
CTA	cellulose triacetate
CTAC	cetyltrimethylammonium chloride
DI	deionized
DMF	dimethylformamide
ECP	external concentration polarization
FESEM	field emission scanning electron microscopy

FO	forward osmosis
ICP	internal concentration polarization
IP	interfacial polymerization
LbL	layer by layer
LDH	layered double hydride
LMH	L m^{-2} h^{-1}
MMT	montmorillonite
MPD	m-Phenylenediamine
NF	nanofiltration
NMP	*N*-Methyl-2-pyrrolidone
PA	polyamide
PAI	polyamide-imide
PAMAM	polyamidoamine
PAN	polyacrylonitrile
PBI	polybenzimidazole
PDF	polydopamine
PEI	polyethyleneimine
PET	polyethylene terephthalate
PES	polyehtersulfone
PFSA	perfluorosulfonic acid
PI	polyimide
POD	polyoxadiazole
POM	polyoxometalate
PRO	pressure-retarded osmosis
PSf	polysulfone
PVB	polyvinyl butyral
PVC	polyvinyl chloride
PVDF	poly(vinylidene difluoride)
PVP	polyvinylpyrrolidone
RO	reverse osmosis
RSF	reverse solute flux
SAGD	steam-assisted gravity drainage
SEC	specific energy consumption
SEM	scanning electron microscopy
SL	support layer
SLB	supported lipid bilayer
SPSf	sulfonated polysulfone
TFC	thin-film composite
TMC	trimesoyl chloride
UV	ultraviolet

Nomenclature

J_w	water flux L m^{-2} h^{-1} (LMH)
A	permeability coefficient of pure water LMH/bar
$\Delta\pi$	osmotic pressure difference across the membrane bar
ΔP	external pressure difference bar
σ	reflection coefficient
S	structural parameter μm
L	thickness, μm
τ	tortuosity
ε	porosity of the support layer %

References

Abidin, M. N. Z., Goh, P. S., Said, N., Ismail, A. F., Othman, M. H. D., Abdullah, M. S., … Kamal, F. (2020). Polysulfone/amino-silanized poly (methyl methacrylate) dual layer hollow fiber membrane for uremic toxin separation. *Separation and Purification Technology*, *236*, 116216.

Ahmadizadeh, R., Shokrollahzadeh, S., & Latifi, S. M. (2019). Mass transfer study in brine water treatment by forward osmosis process. *Advances in Environmental Technology*, *5*(3), 141–148.

Akther, N., Sodiq, A., Giwa, A., Daer, S., Arafat, H., & Hasan, S. (2015). Recent advancements in forward osmosis desalination: A review. *Chemical Engineering Journal*, *281*, 502–522.

Bao, X., Wu, Q., Shi, W., Wang, W., Yu, H., Zhu, Z., … Cui, F. (2019). Polyamidoamine dendrimer grafted forward osmosis membrane with superior ammonia selectivity and robust antifouling capacity for domestic wastewater concentration. *Water Research*, *153*, 1–10.

Bide, Y., & Shokrollahzadeh, S. (2020). Toward tailoring of a new draw solute for forward osmosis process: Branched poly(deep eutectic solvent)-decorated magnetic nanoparticles. *Journal of Molecular Liquids*, *320*, 114409. Available from https://doi.org/10.1016/j.molliq.2020.114409.

Capital, C., & West, V. (2004). HTI receives $6.3 million in US defence bill. *Filtration Industry Analyst*, *9*, 3. https://doi.org/10.1016/S1365-6937(04)00414-9.

Cardea, S., & De Marco, I. (2020). Cellulose acetate and supercritical carbon dioxide: Membranes, nanoparticles, microparticles and nanostructured filaments. *Polymers*, *12*(1), 162.

Carter, J., Psaras, G., & Price, M. (1973). The effect of precipitating media on the performance of porous cellulose acetate reverse osmosis membranes. *Desalination*, *12*(2), 177–188.

Cartinella, J. L., Cath, T. Y., Flynn, M. T., Miller, G. C., Hunter, K. W., & Childress, A. E. (2006). Removal of natural steroid hormones from wastewater using membrane contactor processes. *Environmental Science & Technology*, *40*(23), 7381–7386.

Castrillón, S. R.-V., Lu, X., Shaffer, D. L., & Elimelech, M. (2014). Amine enrichment and poly (ethylene glycol) (PEG) surface modification of thin-film composite forward osmosis membranes for organic fouling control. *Journal of Membrane Science*, *450*, 331–339.

Cath, T. Y., Adams, D., & Childress, A. E. (2005). Membrane contactor processes for wastewater reclamation in space: II. Combined direct osmosis, osmotic distillation, and membrane distillation for treatment of metabolic wastewater. *Journal of Membrane Science*, *257*(1–2), 111–119.

Cath, T. Y., Childress, A. E., & Elimelech, M. (2006). Forward osmosis: Principles, applications, and recent developments. *Journal of Membrane Science*, *281*(1–2), 70–87.

Chen, X., Xu, J., Lu, J., Shan, B., & Gao, C. (2017). Enhanced performance of cellulose triacetate membranes using binary mixed additives for forward osmosis desalination. *Desalination*, *405*, 68–75.

Chen, Y., & Ge, Q. (2019). A bifunctional zwitterion that serves as both a membrane modifier and a draw solute for forward osmosis wastewater treatment. *ACS Applied Materials & Interfaces*, *11*(39), 36118–36129.

Chiao, Y.-H., Chen, S.-T., Patra, T., Hsu, C.-H., Sengupta, A., Hung, W.-S., … Chang, Y. (2019). Zwitterionic forward osmosis membrane modified by fast second interfacial polymerization with enhanced antifouling and antimicrobial properties for produced water pretreatment. *Desalination*, *469*, 114090.

Chiao, Y.-H., Chen, S.-T., Patra, T., Hsu, C.-H., Sengupta, A., Hung, W.-S., … Lai, J.-Y. (2019). Zwitterionic forward osmosis membrane modified by fast second interfacial polymerization with enhanced antifouling and antimicrobial properties for produced water pretreatment. *Desalination*, *469*, 114090. Available from https://doi.org/10.1016/j.desal.2019.114090.

Chiao, Y.-H., Sengupta, A., Chen, S.-T., Hung, W.-S., Lai, J.-Y., Upadhyaya, L., … Wickramasinghe, S. R. (2020). Novel thin-film composite forward osmosis membrane using polyethylenimine and its impact on membrane performance. *Separation Science and Technology*, *55*(3), 590–600.

Cho, Y. H., Han, J., Han, S., Guiver, M. D., & Park, H. B. (2013). Polyamide thin-film composite membranes based on carboxylated polysulfone microporous support membranes for forward osmosis. *Journal of Membrane Science*, *445*, 220–227.

Chou, S., Shi, L., Wang, R., Tang, C. Y., Qiu, C., & Fane, A. G. (2010). Characteristics and potential applications of a novel forward osmosis hollow fiber membrane. *Desalination*, *261*(3), 365–372. Available from https://doi.org/10.1016/j.desal.2010.06.027.

Chun, Y., Qing, L., Sun, G., Bilad, M. R., Fane, A. G., & Chong, T. H. (2018). Prototype aquaporin-based forward osmosis membrane: Filtration properties and fouling resistance. *Desalination*, *445*, 75–84.

Chwatko, M., Arena, J. T., & McCutcheon, J. R. (2017). Norepinephrine modified thin film composite membranes for forward osmosis. *Desalination*, *423*, 157–164.

Ding, W., Cai, J., Yu, Z., Wang, Q., Xu, Z., Wang, Z., & Gao, C. (2015). Fabrication of an aquaporin-based forward osmosis membrane through covalent bonding of a lipid bilayer to a microporous support. *Journal of Materials Chemistry A*, *3*(40), 20118–20126.

Duong, P. H. H., Chisca, S., Hong, P.-Y., Cheng, H., Nunes, S. P., & Chung, T.-S. (2015). Hydroxyl functionalized polytriazole-co-polyoxadiazole as substrates for forward osmosis membranes. *ACS Applied Materials & Interfaces*, *7*(7), 3960–3973. Available from https://doi.org/10.1021/am508387d.

Engelhardt, S., Sadek, A., & Duirk, S. (2018). Rejection of trace organic water contaminants by an Aquaporin-based biomimetic hollow fiber membrane. *Separation and Purification Technology*, *197*, 170–177.

Fang, W., Wang, R., Chou, S., Setiawan, L., & Fane, A. G. (2012a). Composite forward osmosis hollow fiber membranes: Integration of RO- and NF-like selective layers to enhance membrane properties of anti-scaling and anti-internal concentration polarization. *Journal of Membrane Science*, *394–395*, 140–150. Available from https://doi.org/10.1016/j.memsci.2011.12.034.

Fang, W., Wang, R., Chou, S., Setiawan, L., & Fane, A. G. (2012b). Composite forward osmosis hollow fiber membranes: Integration of RO-and NF-like selective layers to enhance membrane properties of anti-scaling and anti-internal concentration polarization. *Journal of Membrane Science*, *394*, 140–150.

Flanagan, M., Hausman, R., Digman, B., Escobar, I. C., Coleman, M., & Chung, T.-S. (2011). Surface functionalization of polybenzimidazole membranes to increase hydrophilicity and charge. *Modern applications in membrane science and technology* (pp. 303–321). ACS Publications.

Flanagan, M. F., & Escobar, I. C. (2013). Novel charged and hydrophilized polybenzimidazole (PBI) membranes for forward osmosis. *Journal of Membrane Science*, *434*, 85–92.

Flynn, M., Gormly, S., Cath, T. Y., Adams, V. D., & Childress, A. E. (2007). *Direct osmotic concentration system for spacecraft wastewater recycling* (pp. 0148–7191).

Ghanbari, M., Emadzadeh, D., Lau, W. J., Lai, S. O., Matsuura, T., & Ismail, A. F. (2015). Synthesis and characterization of novel thin film nanocomposite (TFN) membranes embedded with halloysite nanotubes (HNTs) for water desalination. *Desalination*, *358*, 33–41. Available from https://doi.org/10.1016/j.desal.2014.11.035.

Goh, P. S., Ismail, A. F., Ng, B. C., & Abdullah, M. S. (2019). Recent progresses of forward osmosis membranes formulation and design for wastewater treatment. *Water*, *11*(10), 2043.

Gormly, S., Richardson, T.-M. J., Flynn, M., & Kliss, M. (2008). Lightweight contingency water recovery system concept development. *SAE International Journal of Aerospace*, *1*(1), 444–453.

Gray, G. T., McCutcheon, J. R., & Elimelech, M. (2006). Internal concentration polarization in forward osmosis: Role of membrane orientation. *Desalination*, *197*(1–3), 1–8.

Hajighahremanzadeh, P., Abbaszadeh, M., Mousavi, S. A., Soltanieh, M., & Bakhshi, H. (2016). Polyamide/polyacrylonitrile thin film composites as forward osmosis membranes. *Journal of Applied Polymer Science*, *133*, 42.

Han, G., Cheng, Z. L., & Chung, T.-S. (2017). Thin-film composite (TFC) hollow fiber membrane with double-polyamide active layers for internal concentration polarization and fouling mitigation in osmotic processes. *Journal of Membrane Science*, *523*, 497–504.

Han, G., Zhang, S., Li, X., Widjojo, N., & Chung, T.-S. (2012). Thin film composite forward osmosis membranes based on polydopamine modified polysulfone substrates with enhancements in both water flux and salt rejection. *Chemical Engineering Science*, *80*, 219–231.

Hartanto, Y., Corvilain, M., Mariën, H., Janssen, J., & Vankelecom, I. F. (2020a). Interfacial polymerization of thin-film composite forward osmosis membranes using ionic liquids as organic reagent phase. *Journal of Membrane Science*, *601*, 117869.

Hartanto, Y., Corvilain, M., Mariën, H., Janssen, J., & Vankelecom, I. F. J. (2020b). Interfacial polymerization of thin-film composite forward osmosis membranes using ionic liquids as organic reagent phase. *Journal of Membrane Science*, *601*, 117869. Available from https://doi.org/10.1016/j.memsci.2020.117869.

https://www.forwardosmosistech.com.

Huang, L., Arena, J. T., & McCutcheon, J. R. (2016). Surface modified PVDF nanofiber supported thin film composite membranes for forward osmosis. *Journal of Membrane Science*, *499*, 352–360. Available from https://doi.org/10.1016/j.memsci.2015.10.030.

Idarraga-Mora, J. A., Childress, A. S., Friedel, P. S., Ladner, D. A., Rao, A. M., & Husson, S. M. (2018). Role of nanocomposite support stiffness on TFC membrane water permeance. *Membranes*, *8*(4), 111. Available from https://doi.org/10.3390/membranes8040111.

Jia, Q., Han, H., Wang, L., Liu, B., Yang, H., & Shen, J. (2014). Effects of CTAC micelles on the molecular structures and separation performance of thin-film composite (TFC) membranes in forward osmosis processes. *Desalination*, *340*, 30–41.

Jiao, B., Cassano, A., & Drioli, E. (2004). Recent advances on membrane processes for the concentration of fruit juices: A review. *Journal of Food Engineering*, *63*(3), 303–324.

Kessler, J. O., & Moody, C. D. (1975). Applications of Direct Osmosis: Design Characteristics for Hydration and Dehydration. In: Arizona-Nevada Academy of Science.

Khazaie, F., Shokrollahzadeh, S., Bide, Y., Sheshmani, S., & Shahvelayati, A. S. (2021). Forward osmosis using highly water dispersible sodium alginate sulfate coated-Fe_3O_4 nanoparticles as innovative draw solution for water desalination. *Process Safety and Environmental Protection*, *146*, 789–799. Available from https://doi.org/10.1016/j.psep.2020.12.010.

Khorshidi, B., Bhinder, A., Thundat, T., Pernitsky, D., & Sadrzadeh, M. (2016). Developing high throughput thin film composite polyamide membranes for forward osmosis treatment of SAGD produced water. *Journal of Membrane Science*, *511*, 29–39.

Klaysom, C., Hermans, S., Gahlaut, A., Van Craenenbroeck, S., & Vankelecom, I. F. (2013). Polyamide/polyacrylonitrile (PA/PAN) thin film composite osmosis membranes: Film optimization, characterization and performance evaluation. *Journal of Membrane Science*, *445*, 25–33.

Kwon, H.-E., Kwon, S. J., Park, S.-J., Shin, M. G., Park, S.-H., Park, M. S., ... Lee, J.-H. (2019). High performance polyacrylonitrile-supported forward osmosis membranes prepared via aromatic solvent-based interfacial polymerization. *Separation and Purification Technology*, *212*, 449–457.

Kwon, S.-B., Lee, J. S., Kwon, S. J., Yun, S.-T., Lee, S., & Lee, J.-H. (2015). Molecular layer-by-layer assembled forward osmosis membranes. *Journal of Membrane Science*, *488*, 111–120.

Li, G., Wang, J., Hou, D., Bai, Y., & Liu, H. (2016). Fabrication and performance of PET mesh enhanced cellulose acetate membranes for forward osmosis. *Journal of Environmental Sciences*, *45*, 7–17.

Li, M., Karanikola, V., Zhang, X., Wang, L., & Elimelech, M. (2018). A self-standing, support-free membrane for forward osmosis with no internal concentration polarization. *Environmental Science & Technology Letters*, *5*(5), 266–271.

Li, M., Wang, X., Porter, C. J., Cheng, W., Zhang, X., Wang, L., & Elimelech, M. (2019). Concentration and recovery of dyes from textile wastewater using a self-standing, support-free forward osmosis membrane. *Environmental Science & Technology*, *53*(6), 3078–3086.

Li, M.-N., Sun, X.-F., Wang, L., Wang, S.-Y., Afzal, M. Z., Song, C., & Wang, S.-G. (2018). Forward osmosis membranes modified with laminar MoS2 nanosheet to improve desalination performance and antifouling properties. *Desalination*, *436*, 107–113.

Li, X., Chou, S., Wang, R., Shi, L., Fang, W., Chaitra, G., ... Fane, A. G. (2015). Nature gives the best solution for desalination: Aquaporin-based hollow fiber composite membrane with superior performance. *Journal of Membrane Science*, *494*, 68–77.

Li, X., Wang, K. Y., Helmer, B., & Chung, T.-S. (2012). Thin-film composite membranes and formation mechanism of thin-film layers on hydrophilic cellulose acetate propionate substrates for forward osmosis processes. *Industrial & Engineering Chemistry Research*, *51*(30), 10039–10050.

Liang, H.-Q., Hung, W.-S., Yu, H.-H., Hu, C.-C., Lee, K.-R., Lai, J.-Y., & Xu, Z.-K. (2017). Forward osmosis membranes with unprecedented water flux. *Journal of Membrane Science*, *529*, 47–54.

Liu, C., Fang, W., Chou, S., Shi, L., Fane, A. G., & Wang, R. (2013). Fabrication of layer-by-layer assembled FO hollow fiber membranes and their performances using low concentration draw solutions. *Desalination*, *308*, 147–153. Available from https://doi.org/10.1016/j.desal.2012.07.027.

Liu, C., Lee, J., Ma, J., & Elimelech, M. (2017). Antifouling thin-film composite membranes by controlled architecture of zwitterionic polymer brush layer. *Environmental Science & Technology*, *51*(4), 2161–2169.

Liu, C., Lei, X., Wang, L., Jia, J., Liang, X., Zhao, X., & Zhu, H. (2017). Investigation on the removal performances of heavy metal ions with the layer-by-layer assembled forward osmosis membranes. *Chemical Engineering Journal*, *327*, 60–70.

Loeb, S. (2001). One hundred and thirty benign and renewable megawatts from Great Salt Lake? The possibilities of hydroelectric power by pressure-retarded osmosis. *Desalination*, *141*(1), 85–91.

Loeb, S., & Sourirajan, S. (1962). *Sea water demineralization by* means *of an osmotic membrane*. ACS Publications.

Loeb, S., Titelman, L., Korngold, E., & Freiman, J. (1997). Effect of porous support fabric on osmosis through a Loeb-Sourirajan type asymmetric membrane. *Journal of Membrane Science*, *129*(2), 243–249.

Luo, L., Wang, P., Zhang, S., Han, G., & Chung, T.-S. (2014). Novel thin-film composite tri-bore hollow fiber membrane fabrication for forward osmosis. *Journal of Membrane Science*, *461*, 28–38. Available from https://doi.org/10.1016/j.memsci.2014.03.007.

Ma, D., Peh, S. B., Han, G., & Chen, S. B. (2017). Thin-film nanocomposite (TFN) membranes incorporated with super-hydrophilic metal–organic framework (MOF) UiO-66: Toward enhancement of water flux and salt rejection. *ACS Applied Materials & Interfaces*, *9*(8), 7523–7534. Available from https://doi.org/10.1021/acsami.6b14223.

Ma, J., Xiao, T., Long, N., & Yang, X. (2020). The role of polyvinyl butyral additive in forming desirable pore structure for thin film composite forward osmosis membrane. *Separation and Purification Technology*, *242*, 116798.

Matsuura, T., & Sourirajan, S. (1985). Materials science of reverse-osmosis-ultrafiltration membranes. In Reverse osmosis and ultrafiltration. *American Chemical Society*, *281*, 1–19. https://doi.org/10.1021/bk-1985-0281.ch001.

McCutcheon, J. R., & Elimelech, M. (2006). Influence of concentrative and dilutive internal concentration polarization on flux behavior in forward osmosis. *Journal of Membrane Science*, *284*(1–2), 237–247.

McCutcheon, J. R., & Elimelech, M. (2007). Modeling water flux in forward osmosis: Implications for improved membrane design. *AIChE Journal*, *53*(7), 1736–1744.

McCutcheon, J. R., & Elimelech, M. (2008). Influence of membrane support layer hydrophobicity on water flux in osmotically driven membrane processes. *Journal of Membrane Science*, *318*(1–2), 458–466.

McCutcheon, J. R., McGinnis, R. L., & Elimelech, M. (2005). A novel ammonia—carbon dioxide forward (direct) osmosis desalination process. *Desalination*, *174*(1), 1–11.

McCutcheon, J. R., McGinnis, R. L., & Elimelech, M. (2006). Desalination by ammonia–carbon dioxide forward osmosis: Influence of draw and feed solution concentrations on process performance. *Journal of Membrane Science*, *278*(1–2), 114–123.

Mehta, G. D., & Loeb, S. (1978). Internal polarization in the porous substructure of a semipermeable membrane under pressure-retarded osmosis. *Journal of Membrane Science*, *4*, 261–265.

Mettu, D., Escobar, I., Coleman, M., & Chung, T.-S. (2008). Surface functionalization of polybenzimidazole nanofiltration membranes for forward osmosis. *In 2008 AIChE Annual Meeting, AIChE 100*.

Mi, B., & Elimelech, M. (2010). Gypsum scaling and cleaning in forward osmosis: Measurements and mechanisms. *Environmental Science & Technology*, *44*(6), 2022–2028.

Michaels, A. S., Bixler, H. J., & Hodges, R. M., Jr (1965). Kinetics of water and salt transport in cellulose acetate reverse osmosis desalination membranes. *Journal of Colloid Science*, *20*(9), 1034–1056.

Moody, C., & Kessler, J. (1971, June). An initial investigation into the use of direct osmosis as a means for obtaining agricultural water from brackish *water*. Unpublished paper, Department of Physics, University of Arizona, Tucson.

Moody, C. D., & Kessler, J. O. (1975). April). Application of Direct Osmosis: Possibilities for Reclaiming Wellton-Mohawk Drainage Water. *Arizona-Nevada Academy of Science*.

Nayak, V., MS, J., Balakrishna, R. G., Padaki, M., Zadorozhnyy, V. Y., & Kaloshkin, S. D. (2020). 4-Aminophenyl sulfone (APS) as novel monomer in fabricating paper based TFC composite for forward osmosis: Selective layer optimization. *Journal of Environmental Chemical Engineering*, *8*(2), 103664. Available from https://doi.org/10.1016/j.jece.2020.103664.

Nematzadeh, M., Samimi, A., & Shokrollahzadeh, S. (2016). Application of sodium bicarbonate as draw solution in forward osmosis desalination: Influence of temperature and linear flow velocity. *Desalination and Water Treatment*, *57*(44), 20784–20791.

Ng, D. Y. F., Wu, B., Chen, Y., Dong, Z., & Wang, R. (2019). A novel thin film composite hollow fiber osmotic membrane with one-step prepared dual-layer substrate for sludge thickening. *Journal of Membrane Science*, *575*, 98–108.

Ng, H. Y., Tang, W., & Wong, W. S. (2006). Performance of forward (direct) osmosis process: Membrane structure and transport phenomenon. *Environmental Science & Technology*, *40*(7), 2408–2413.

Nguyen, T. P. N., Yun, E.-T., Kim, I.-C., & Kwon, Y.-N. (2013). Preparation of cellulose triacetate/cellulose acetate (CTA/CA)-based membranes for forward osmosis. *Journal of Membrane Science*, *433*, 49–59.

Ni, T., & Ge, Q. (2018). Highly hydrophilic thin-film composition forward osmosis (FO) membranes functionalized with aniline sulfonate/bisulfonate for desalination. *Journal of Membrane Science*, *564*, 732–741.

Ong, C. S., Al-Anzi, B., Lau, W. J., Goh, P. S., Lai, G. S., Ismail, A. F., & Ong, Y. S. (2017). Anti-fouling double-skinned forward osmosis membrane with zwitterionic brush for oily wastewater treatment. *Scientific Reports*, *7*(1), 1–11.

Pardeshi, P. M., Mungray, A. K., & Mungray, A. A. (2017). Polyvinyl chloride and layered double hydroxide composite as a novel substrate material for the forward osmosis membrane. *Desalination*, *421*, 149–159.

Qi, S., Qiu, C. Q., Zhao, Y., & Tang, C. Y. (2012). Double-skinned forward osmosis membranes based on layer-by-layer assembly—FO performance and fouling behavior. *Journal of Membrane Science*, *405*, 20–29.

Qiu, C., Qi, S., & Tang, C. Y. (2011). Synthesis of high flux forward osmosis membranes by chemically crosslinked layer-by-layer polyelectrolytes. *Journal of Membrane Science*, *381*(1–2), 74–80.

Qiu, C., Setiawan, L., Wang, R., Tang, C. Y., & Fane, A. G. (2012). High performance flat sheet forward osmosis membrane with an NF-like selective layer on a woven fabric embedded substrate. *Desalination*, *287*, 266–270.

Qiu, M., Wang, J., & He, C. (2018). A stable and hydrophilic substrate for thin-film composite forward osmosis membrane revealed by in-situ cross-linked polymerization. *Desalination*, *433*, 1–9.

Ren, J., Chowdhury, M. R., Qi, J., Xia, L., Huey, B. D., & McCutcheon, J. R. (2017). Relating osmotic performance of thin film composite hollow fiber membranes to support layer surface pore size. *Journal of Membrane Science*, *540*, 344–353. Available from https://doi.org/10.1016/j.memsci.2017.06.024.

Ren, J., & McCutcheon, J. R. (2015). Polyacrylonitrile supported thin film composite hollow fiber membranes for forward osmosis. *Desalination*, *372*, 67–74.

Ren, J., & McCutcheon, J. R. (2018). A new commercial biomimetic hollow fiber membrane for forward osmosis. *Desalination*, *442*, 44–50.

Ren, J., O'Grady, B., deJesus, G., & McCutcheon, J. R. (2016). Sulfonated polysulfone supported high performance thin film composite membranes for forward osmosis. *Polymer*, *103*, 486–497.

Reurink, D. M., Du, F., Górecki, R., Roesink, H. D., & De Vos, W. M. (2020). Aquaporin-containing proteopolymersomes in polyelectrolyte multilayer membranes. *Membranes*, *10*(5), 103.

Romero-Vargas Castrillón, S., Lu, X., Shaffer, D. L., & Elimelech, M. (2014). Amine enrichment and poly(ethylene glycol) (PEG) surface modification of thin-film composite forward osmosis membranes for organic fouling control. *Journal of Membrane Science*, *450*, 331–339. Available from https://doi.org/10.1016/j.memsci.2013.09.028.

Sahebi, S., Sheikhi, M., & Ramavandi, B. (2019). A new biomimetic aquaporin thin film composite membrane for forward osmosis: Characterization and performance assessment. *Desalination and Water Treatment*, *148*, 42–50.

Sairam, M., Sereewatthanawut, E., Li, K., Bismarck, A., & Livingston, A. (2011). Method for the preparation of cellulose acetate flat sheet composite membranes for forward osmosis—desalination using $MgSO_4$ draw solution. *Desalination*, *273*(2–3), 299–307.

Salehi, H., Shakeri, A., Mahdavi, H., & Lammertink, R. G. (2020). Improved performance of thin-film composite forward osmosis membrane with click modified polysulfone substrate. *Desalination*, *496*, 114731.

Salehi, H., Shakeri, A., & Rastgar, M. (2018). Carboxylic polyethersulfone: A novel pH-responsive modifier in support layer of forward osmosis membrane. *Journal of Membrane Science*, *548*, 641–653.

Seppälä, A., & Lampinen, M. J. (1999). Thermodynamic optimizing of pressure-retarded osmosis power generation systems. *Journal of Membrane Science*, *161*(1–2), 115–138.

Serbanescu, O., Voicu, S., & Thakur, V. (2020). Polysulfone functionalized membranes: Properties and challenges. *Materials Today Chemistry (Weinheim an der Bergstrasse, Germany)*, *17*, 100302.

Setiawan, L., Wang, R., Li, K., & Fane, A. G. (2011a). Fabrication of novel poly (amide–imide) forward osmosis hollow fiber membranes with a positively charged nanofiltration-like selective layer. *Journal of Membrane Science*, *369*(1–2), 196–205.

Setiawan, L., Wang, R., Li, K., & Fane, A. G. (2011b). Fabrication of novel poly(amide–imide) forward osmosis hollow fiber membranes with a positively charged nanofiltration-like selective layer. *Journal of Membrane Science*, *369*(1), 196–205. Available from https://doi.org/10.1016/j.memsci.2010.11.067.

Shabani, Z., Kahrizi, M., Mohammadi, T., Kasiri, N., & Sahebi, S. (2021). A novel thin film composite forward osmosis membrane using bio-inspired polydopamine coated polyvinyl chloride substrate: Experimental and computational fluid dynamics modelling. *Process Safety and Environmental Protection*, *147*, 756–771.

Shakeri, A., Mighani, H., Salari, N., & Salehi, H. (2019). Surface modification of forward osmosis membrane using polyoxometalate based open frameworks for hydrophilicity and water flux improvement. *Journal of Water Process Engineering*, *29*, 100762.

Shen, L., Hung, W.-s, Zuo, J., Tian, L., Yi, M., Ding, C., & Wang, Y. (2020). Effect of ultrasonication parameters on forward osmosis performance of thin film composite polyamide membranes prepared with ultrasound-assisted interfacial polymerization. *Journal of Membrane Science*, *599*, 117834.

Shen, L., & Wang, Y. (2018). Efficient surface modification of thin-film composite membranes with self-catalyzed tris (2-aminoethyl) amine for forward osmosis separation. *Chemical Engineering Science*, *178*, 82–92.

Shen, L., Xiong, S., & Wang, Y. (2016). Graphene oxide incorporated thin-film composite membranes for forward osmosis applications. *Chemical Engineering Science*, *143*, 194–205.

Shibuya, M., Yasukawa, M., Takahashi, T., Miyoshi, T., Higa, M., & Matsuyama, H. (2015). Effect of operating conditions on osmotic-driven membrane performances of cellulose triacetate forward osmosis hollow fiber membrane. *Desalination*, *362*, 34–42. Available from https://doi.org/10.1016/j.desal.2015.01.031.

Shokrgozar Eslah, S., Shokrollahzadeh, S., Moini Jazani, O., & Samimi, A. (2018). Forward osmosis water desalination: Fabrication of graphene oxide-polyamide/polysulfone thin-film nanocomposite membrane with high water flux and low reverse salt diffusion. *Separation Science and Technology*, *53*(3), 573–583. Available from https://doi.org/10.1080/01496395.2017.1398261.

Shokrollahzadeh, S., Bide, Y., & Gholami, S. (2020). Enhancing forward osmosis performance via an oligomeric deep eutectic solvent as a draw solute. *Desalination*, *491*, 114473. Available from https://doi.org/10.1016/j.desal.2020.114473.

Shokrollahzadeh, S., & Tajik, S. (2018). Fabrication of thin film composite forward osmosis membrane using electrospun polysulfone/polyacrylonitrile blend nanofibers as porous substrate. *Desalination*, *425*, 68–76.

Su, J., Chung, T.-S., Helmer, B. J., & de Wit, J. S. (2012). Enhanced double-skinned FO membranes with inner dense layer for wastewater treatment and macromolecule recycle using sucrose as draw solute. *Journal of Membrane Science*, *396*, 92–100. Available from https://doi.org/10.1016/j.memsci.2012.01.001.

Su, J., Yang, Q., Teo, J. F., & Chung, T.-S. (2010). Cellulose acetate nanofiltration hollow fiber membranes for forward osmosis processes. *Journal of Membrane Science*, *355*(1), 36–44. Available from https://doi.org/10.1016/j.memsci.2010.03.003.

Su, J., Zhang, S., Chen, H., Chen, H., Jean, Y. C., & Chung, T.-S. (2010). Effects of annealing on the microstructure and performance of cellulose acetate membranes for pressure-retarded osmosis processes. *Journal of Membrane Science*, *364*(1), 344–353. Available from https://doi.org/10.1016/j.memsci.2010.08.034.

Sukitpaneenit, P., & Chung, T.-S. (2012). High performance thin-film composite forward osmosis hollow fiber membranes with macrovoid-free and highly porous structure for sustainable water production. *Environmental Science & Technology*, *46*(13), 7358–7365. Available from https://doi.org/10.1021/es301559z.

Suwaileh, W., Johnson, D., Khodabakhshi, S., & Hilal, N. (2019a). Development of forward osmosis membranes modified by cross-linked layer by layer assembly for brackish water desalination. *Journal of Membrane Science*, *583*, 267–277. Available from https://doi.org/10.1016/j.memsci.2019.04.052.

Suwaileh, W., Johnson, D., Khodabakhshi, S., & Hilal, N. (2019b). Superior cross-linking assisted layer by layer modification of forward osmosis membranes for brackish water desalination. *Desalination*, *463*, 1–12.

Suzaimi, N. D., Goh, P. S., Ismail, A. F., Mamah, S. C., Malek, N. A. N. N., Lim, J. W., … Hilal, N. (2020). Strategies in forward osmosis membrane substrate fabrication and modification: A review. *Membranes*, *10*(11), 332. Available from https://doi.org/10.3390/membranes10110332.

Tajik, S., Moini Jazani, O., Shokrollahzadeh, S., & Latifi, S. M. (2016). Thin film nanocomposite forward osmosis membrane prepared by graphene oxide embedded PSf substrate. *Journal of Particle Science & Technology*, *2*(2), 103–117.

Tang, W., & Ng, H. Y. (2008). Concentration of brine by forward osmosis: Performance and influence of membrane structure. *Desalination*, *224*(1–3), 143–153.

Tian, M., Qiu, C., Liao, Y., Chou, S., & Wang, R. (2013). Preparation of polyamide thin film composite forward osmosis membranes using electrospun polyvinylidene fluoride (PVDF) nanofibers as substrates. *Separation and Purification Technology*, *118*, 727–736. Available from https://doi.org/10.1016/j.seppur.2013.08.021.

Tinge, J. T., Krooshof, G. J. P., Smeets, T. M., Vergossen, F. H. P., Krijgsman, J., Hoving, E., & Altink, R. M. (2007). Direct osmosis membrane process to de-water aqueous caprolactam with concentrated aqueous ammonium

sulphate. *Chemical Engineering and Processing: Process Intensification*, *46*(6), 505–512. Available from https://doi.org/10.1016/j.cep.2006.08.002.

Tran, T., Pan, S., Chen, X., Lin, X.-C., Blevins, A. K., Ding, Y., & Lin, H. (2020). Zwitterionic hydrogel-impregnated membranes with polyamide skin achieving superior water/salt separation properties. *ACS Applied Materials & Interfaces*, *12*(43), 49192–49199. Available from https://doi.org/10.1021/acsami.0c13363.

Wang, J., Xiao, T., Bao, R., Li, T., Wang, Y., Li, D., … He, T. (2018). Zwitterionic surface modification of forward osmosis membranes using N-aminoethyl piperazine propane sulfonate for grey water treatment. *Process Safety and Environmental Protection*, *116*, 632–639. Available from https://doi.org/10.1016/j.psep.2018.03.029.

Wang, K. Y., Chung, T. S., & Amy, G. (2012). Developing thin-film-composite forward osmosis membranes on the PES/SPSf substrate through interfacial polymerization. *AIChE Journal*, *58*(3), 770–781.

Wang, K. Y., Chung, T.-S., & Qin, J.-J. (2007a). Polybenzimidazole (PBI) nanofiltration hollow fiber membranes applied in forward osmosis process. *Journal of Membrane Science*, *300*(1–2), 6–12.

Wang, K. Y., Chung, T.-S., & Qin, J.-J. (2007b). Polybenzimidazole (PBI) nanofiltration hollow fiber membranes applied in forward osmosis process. *Journal of Membrane Science*, *300*(1), 6–12. Available from https://doi.org/10.1016/j.memsci.2007.05.035.

Wang, K. Y., Ong, R. C., & Chung, T.-S. (2010). Double-skinned forward osmosis membranes for reducing internal concentration polarization within the porous sublayer. *Industrial & Engineering Chemistry Research*, *49*(10), 4824–4831. Available from https://doi.org/10.1021/ie901592d.

Wang, K. Y., Yang, Q., Chung, T.-S., & Rajagopalan, R. (2009). Enhanced forward osmosis from chemically modified polybenzimidazole (PBI) nanofiltration hollow fiber membranes with a thin wall. *Chemical Engineering Science*, *64*(7), 1577–1584.

Wang, L., Ma, F., Jia, J., Lei, X., Zhao, X., & Liu, C. (2019). Investigation of forward osmosis performance and anti-fouling properties of the novel hydrophilic polymer brush-grafted TFC-type FO membranes. *Journal of Chemical Technology & Biotechnology*, *94*(7), 2198–2211.

Wang, R., Shi, L., Tang, C. Y., Chou, S., Qiu, C., & Fane, A. G. (2010). Characterization of novel forward osmosis hollow fiber membranes. *Journal of Membrane Science*, *355*(1), 158–167. Available from https://doi.org/10.1016/j.memsci.2010.03.017.

Wang, Y., Fang, Z., Zhao, S., Ng, D., Zhang, J., & Xie, Z. (2018). Dopamine incorporating forward osmosis membranes with enhanced selectivity and antifouling properties. *RSC Advances*, *8*(40), 22469–22481.

Wang, Y., Lau, W. W., & Sourirajan, S. (1994). Effects of pretreatments on morphology and performance of cellulose acetate (formamide type) membranes. *Desalination*, *95*(2), 155–169.

Wang, Y., Li, X., Cheng, C., He, Y., Pan, J., & Xu, T. (2016). Second interfacial polymerization on polyamide surface using aliphatic diamine with improved performance of TFC FO membranes. *Journal of Membrane Science*, *498*, 30–38.

Wang, Y., & Xu, T. (2015). Anchoring hydrophilic polymer in substrate: An easy approach for improving the performance of TFC FO membrane. *Journal of Membrane Science*, *476*, 330–339.

Wei, J., Qiu, C., Tang, C. Y., Wang, R., & Fane, A. G. (2011). Synthesis and characterization of flat-sheet thin film composite forward osmosis membranes. *Journal of Membrane Science*, *372*(1–2), 292–302.

Xia, L., Andersen, M. F., Hélix-Nielsen, C., & McCutcheon, J. R. (2017). Novel commercial aquaporin flat-sheet membrane for forward osmosis. *Industrial & Engineering Chemistry Research*, *56*(41), 11919–11925.

Xiong, S., Zuo, J., Ma, Y. G., Liu, L., Wu, H., & Wang, Y. (2016). Novel thin film composite forward osmosis membrane of enhanced water flux and anti-fouling property with N-[3-(trimethoxysilyl) propyl] ethylenediamine incorporated. *Journal of Membrane Science*, *520*, 400–414.

Xu, L., Xu, J., Shan, B., Wang, X., & Gao, C. (2017). Novel thin-film composite membranes via manipulating the synergistic interaction of dopamine and m-phenylenediamine for highly efficient forward osmosis desalination. *Journal of Materials Chemistry A*, *5*(17), 7920–7932.

Xu, Y., Peng, X., Tang, C. Y., Fu, Q. S., & Nie, S. (2010). Effect of draw solution concentration and operating conditions on forward osmosis and pressure retarded osmosis performance in a spiral wound module. *Journal of Membrane Science*, *348*(1–2), 298–309.

Yabuno, Y., Mihara, K., Miyagawa, N., Komatsu, K., Nakagawa, K., Shintani, T., … Yoshioka, T. (2020). Preparation of polyamide–PVDF composite hollow fiber membranes with well-developed interconnected bicontinuous structure using high-temperature rapid NIPS for forward osmosis. *Journal of Membrane Science*, *612*, 118468.

Yang, Q., Wang, K. Y., & Chung, T.-S. (2009a). Dual-layer hollow fibers with enhanced flux as novel forward osmosis membranes for water production. *Environmental Science & Technology*, *43*(8), 2800–2805.

Yang, Q., Wang, K. Y., & Chung, T.-S. (2009b). A novel dual-layer forward osmosis membrane for protein enrichment and concentration. *Separation and Purification Technology*, *69*(3), 269–274. Available from https://doi.org/10.1016/j.seppur.2009.08.002.

Yip, N. Y., Tiraferri, A., Phillip, W. A., Schiffman, J. D., & Elimelech, M. (2010). High performance thin-film composite forward osmosis membrane. *Environmental Science & Technology*, *44*(10), 3812–3818. Available from https://doi.org/10.1021/es1002555.

Zhang, S., Fu, F., & Chung, T.-S. (2013). Substrate modifications and alcohol treatment on thin film composite membranes for osmotic power. *Chemical Engineering Science*, *87*, 40–50.

Zhang, S., Wang, K. Y., Chung, T.-S., Chen, H., Jean, Y., & Amy, G. (2010). Well-constructed cellulose acetate membranes for forward osmosis: Minimized internal concentration polarization with an ultra-thin selective layer. *Journal of Membrane Science*, *360*(1–2), 522–535.

Zhang, X., Shen, L., Lang, W.-Z., & Wang, Y. (2017). Improved performance of thin-film composite membrane with PVDF/PFSA substrate for forward osmosis process. *Journal of Membrane Science*, *535*, 188–199.

Zhang, X., Tian, J., Gao, S., Zhang, Z., Cui, F., & Tang, C. Y. (2017). In situ surface modification of thin film composite forward osmosis membranes with sulfonated poly (arylene ether sulfone) for anti-fouling in emulsified oil/water separation. *Journal of Membrane Science*, *527*, 26–34.

Zhang, X., Tian, J., Ren, Z., Shi, W., Zhang, Z., Xu, Y., … Cui, F. (2016). High performance thin-film composite (TFC) forward osmosis (FO) membrane fabricated on novel hydrophilic disulfonated poly (arylene ether sulfone) multiblock copolymer/polysulfone substrate. *Journal of Membrane Science*, *520*, 529–539.

Zhao, S., Huang, K., & Lin, H. (2015). Impregnated membranes for water purification using forward osmosis. *Industrial & Engineering Chemistry Research*, *54*(49), 12354–12366.

Zhao, S., Zou, L., Tang, C. Y., & Mulcahy, D. (2012). Recent developments in forward osmosis: Opportunities and challenges. *Journal of Membrane Science*, *396*, 1–21.

Zhao, Y., Wang, X., Ren, Y., & Pei, D. (2018). Mesh-embedded polysulfone/sulfonated polysulfone supported thin film composite membranes for forward osmosis. *ACS Applied Materials & Interfaces*, *10*(3), 2918–2928.

Zheng, K., Zhou, S., Cheng, Z., & Huang, G. (2021a). Polyvinyl chloride/quaternized poly phenylene oxide substrates supported thin-film composite membranes: Enhancement of forward osmosis performance. *Journal of Membrane Science*, *623*, 119070. Available from https://doi.org/10.1016/j.memsci.2021.119070.

Zheng, K., Zhou, S., Cheng, Z., & Huang, G. (2021b). Thin-film composite forward osmosis membrane prepared from polyvinyl chloride/cellulose carbamate substrate and its potential application in brackish water desalination. *Journal of Applied Polymer Science*, *138*(9), 49939.

Zheng, K., Zhou, S., & Zhou, X. (2018). A low-cost and high-performance thin-film composite forward osmosis membrane based on an SPSU/PVC substrate. *Scientific Reports*, *8*(1), 1–13.

CHAPTER

13

Polymer-based nano-enhanced forward osmosis membranes

Salam Bakly[1], *Ibrar Ibrar*[1], *Haleema Saleem*[2], *Sudesh Yadav*[1], *Raed Al-Juboori*[3], *Osamah Naji*[1], *Ali Altaee*[1] *and Syed Javaid Zaidi*[2]

[1]Centre for Green Technology, School of Civil and Environmental Engineering, University of Technology Sydney, Broadway, NSW, Australia [2]Center for Advanced Materials (CAM), Qatar University, Doha, Qatar [3]Water and Environmental Engineering Research Group, Department of Built Environment, Aalto University, Aalto, Espoo, Finland

13.1 Introduction

In recent years, forward osmosis (FO) technology has attracted considerable attention from different industrial applications due to its low energy demand, high recovery rate, and low fouling propensity (Eyvaz, Arslan, Yüksel, & Koyuncu, 2018). However, FO technology has some shortcomings that limit its potential, such as reverse solute diffusion (RSD), internal concentration polarization (ICP), and lower flux compared to pressure-driven membranes (Grylewicz & Mozia, 2020; Rezaei-DashtArzhandi, Sarrafzadeh et al., 2018). Many solutions have been proposed to mitigate the impact of these problems, including operational strategies in the form of low hydraulic pressure (<10 bar), electrolysis, or ultrasound and membrane structure modification (Zou, Qin, & He, 2019). The latter method captured the interest of many studies due to its effects on water flux, membrane fouling, and selectivity. Adding nanoparticles to active layer and substrate of thin-film composite (TFC) membranes can improve the membrane properties. Researching in this space has resulted in the emergence of a new class of membranes known as mixed matrix membranes (MMMs), which is the focus of this chapter. The structural modification aspects of conventional polymeric membranes will succinctly be addressed in this chapter by paying special attention to FO applications. The common preparation and modification methods will be discussed, and the pros and cons of each method will be highlighted.

Advancement in Polymer-Based Membranes for Water Remediation
DOI: https://doi.org/10.1016/B978-0-323-88514-0.00006-1

© 2022 Elsevier Inc. All rights reserved.

The most tested filling materials will also be reviewed. Examples of successful attempts of using MMMs with FO technology will be presented, and headline results will be highlighted. The synthesis of flat sheet and hollow fiber membranes embedded with various nanaomaterials will be described. The utilization of the unique characteristics of stimuli-responsive polymeric membranes for FO applications will be discussed. The chapter will conclude by pinpointing commercialization opportunities and challenges of nano-enhanced FO membranes and providing future research directions.

13.2 Polymer-based mixed matrix forward osmosis membranes

13.2.1 Overview

Several research efforts have been directed towards improving the FO membranes properties to prolong their working life and enhance their throughput. MMMs are believed to offer the solution for the most common challenges in FO (e.g., RSD and ICP). The first version of MMMs was produced in the 1970s to provide interconnected flow paths of high diffusion rate materials, leading to boosting gas separation using membranes (Klaysom & Shahid, 2019).

MMMs consist of a continuous phase, which is typically a polymer-modified, with a dispersed phase (commonly referred to as nanomaterials), which can be organic, inorganic, or biological (Qadir, Mukhtar, & Keong, 2017; Zornoza, Tellez, Coronas, Gascon, & Kapteijn, 2013). The nanomaterials are primarily added to overcome the upper bound trade-off between the permeability and selectivity (Galizia, Chi et al., 2017). They can also enhance polymeric membranes' chemical and physical stability. MMMs have a unique nature that combines the strengths and functionalities of the two phases. Fig. 13.1 shows an illustration of the separation capacity of MMMs compared to membranes made of their

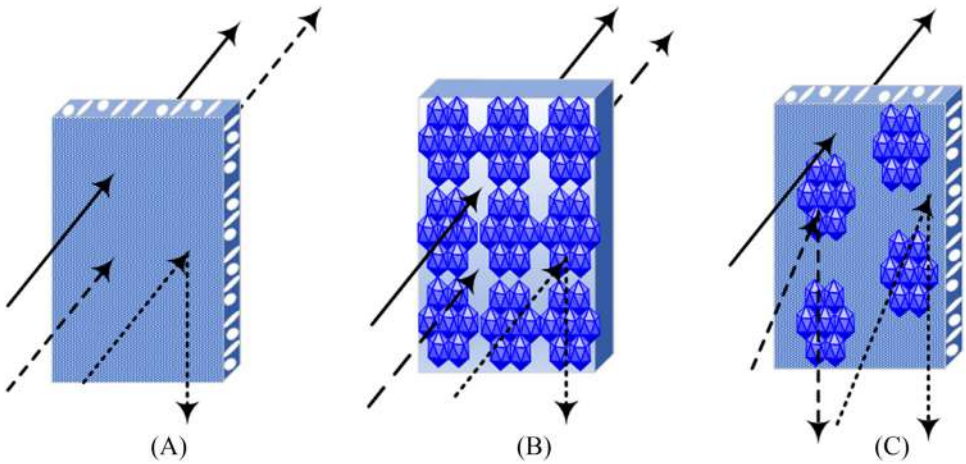

FIGURE 13.1 Schematic illustrating three membrane systems: (A) pure polymer membrane, (B) pure inorganic membrane, and (C) mixed matrix membrane (MMM) composed. Solid arrow represents water, dashed arrow represents contaminant, and dotted arrow represents contaminant.

continuous and dispersed phases separately. There is a range of techniques and a broad spectrum of nanomaterials that are used for synthesizing MMMs. It can be seen from this illustration that MMMs have selectivity superior to unmodified membranes. The standard techniques and filling materials used specifically for preparing membranes for FO technology will be discussed in the following sections.

13.2.2 Common membrane preparation and modification approaches

The methods for membrane modification can generally be classified into physical and chemical. Common examples for physical methods include blending and in situ interfacial polymerization (IP). The popular chemical methods applied for preparing/modifying MMMs encompass layer-by-layer (LbL) assembly and surface grafting (Sun, Shi et al., 2018). Blending is the simplest and most used technique for preparing MMMs. Blending membranes are basically produced by mixing the dispersed phase of nanomaterials with the continuous polymeric phase, and then casting to obtain the final product. The blending method is normally applied for mixing nanomaterials with the support layer of MMMs. However, this method is easy to apply; its disadvantages include nanomaterials agglomeration (Sun, Shi et al., 2018). This phenomenon may lead to voids in the nanomaterials cluster that a polymer chain cannot bridge. This negatively affects the selectivity of the produced MMMs (Dong, Li, & Chen, 2013). Several solutions have been suggested in the literature to resolve this issue. For instance, Mahajan, Burns, Schaeffer, and Koros (2002) proposed a protocol termed "prime," where a small portion of the well-mixed polymer solution is added to the nanomaterials to coat them prior to mixing them with the final volume of the solution (Mahajan, Burns et al., 2002). Another approach involves adding the nanomaterials to the solvents instead of the polymer solution, where low viscosity of the solvent helps in achieving good dispersion of the nanomaterials with the aid of mixing (Kusworo, Ismail, Mustafa, & Matsuura, 2008). Other solutions suggested for avoiding agglomeration include solubilizing or addition of cross-linking agents to improve the consistency of the mixture (Sun, Shi et al., 2018), and the use of ultrasonication and evaporation to restrict nanomaterials movement by increasing the viscosity of the mixture while maintaining nanomaterials dispersion (Kusworo, Ismail et al., 2008).

The in situ IP method entails mixing nanomaterials with monomers, followed by polymerization of the mixture at the desired conditions to produce the membrane active layer (Cheng, Ding et al., 2017). In situ IP techniques include dispersion polymerization, suspension polymerization, emulsion polymerization, and the polymerization between monomers and functional groups of nanomaterials (Sun, Shi et al., 2018). This technique also has its challenges, such as facile agglomeration and uneven dispersion (Sun, Shi et al., 2018), that can be alleviated by applying the solutions suggested for blending membranes. In addition to these challenges, there are problems observed with the physical methods, such as low adhesion between nanomaterials and polymer, partial nanomaterials blockage by polymer chain, and polymer rigidification (Dong, Li et al., 2013). The ineffective interaction between the dispersion and continuous phase is likely to be attributed to polymer dewater at the nanomaterial surface (Duval, Folkers, Mulder, Desgrandchamps, & Smolders, 1993). Several strategies have been tested to tackle this issue, such as the use of mesoporous

nanomaterials (Zornoza, Téllez, & Coronas, 2011), application of silane coupling agent (Fryčová, Sysel et al., 2012), thermal annealing to overcome the tensile strength (Moghadam, Lee, Park, & Park, 2020), and wetting of both polymers and nanomaterials (Hudiono, Carlisle et al., 2010).

Surface grafting method involves adding nanomaterials to the membrane-active surface using techniques such as photoinitiation and induction by radiation (Sun, Shi et al., 2018). The application of such techniques on monomers induces free radicals' active sites that facilitate the binding between nanomaterials and polymeric membrane. Although surface grafting offers the right solution for immobilizing nanomaterials through the formation of strong chemical bonds (Zhang, Su et al., 2014), it is limited by the sensitivity of polymers to the activation technique. For example, ultraviolet irradiation is only effective in photosensitive polymers (Sun, Shi et al., 2018).

The LbL method is used to prepare MMMs to encompass polyelectrolyte thin films of opposite charge connected by electrostatic and van der Waals forces (Salehi, Rastgar, & Shakeri, 2017; Wu, Shi, Liu, Fan, & Yu, 2020). LbL can be conducted by repeating the dip coating of the layers on the substrate. This method has attractive features that make it of a great potential in MMMs field, such as the capacity to precisely control the components and the structure for produced membranes, simplicity and environmental friendliness, and versatility as it can be used with different coating techniques, including dip/rinse and spin and spray processing (Hong, Malaisamy, & Bruening, 2006; Kolasinska, Krastev, Gutberlet, & Warszynski, 2009). The success of the LbL method relies on the conditions of the layering components, polyelectrolytes, substrate, and operating conditions of the process (Nikolaeva & Luis, 2020). For a comprehensive overview of this method, readers are referred to the work done by Xu, Wang et al. (2015). Nanomaterials properties are one of the essential factors that impact the quality and characterization of the produced MMMs. The following section is dedicated to addressing the general classification of nanomaterials, their materials' specific properties, and their reported effects on the separation process with the FO process. In general, the nanomaterials in their different categories enhance the membrane performance by improving the water flux, salt rejection, fabrication simplicity, mechanical and thermal stability, tunable selectivity, hydrophilicity, mechanical strength, cationic dye removal from wastewater, catalytic activity, specific area, and antifouling behavior. Also, nanomaterials can be incorporated for various purposes, like disinfection, alleviating membrane fouling, water purification, and biofouling (Pendergast & Hoek, 2011, Qadir, Mukhtar et al., 2017).

13.2.3 Nanomaterials classification

Researchers have been using different nanomaterials for preparing MMMs; Fig. 13.2 illustrates these nanomaterials' general categories. There are three nanomaterials categories: organic, inorganic, and bionanomaterials. Incorporating nanomaterials into the membrane structure could involve using either one category or the combination of two or three categories. Inorganic nanomaterials are believed to bind to the continuous phase through covalent or hydrogen bonds or by van der Waals forces. The inorganic nanomaterials can be synthesized by a number of techniques, such as sol–gel, gas condensation, spark

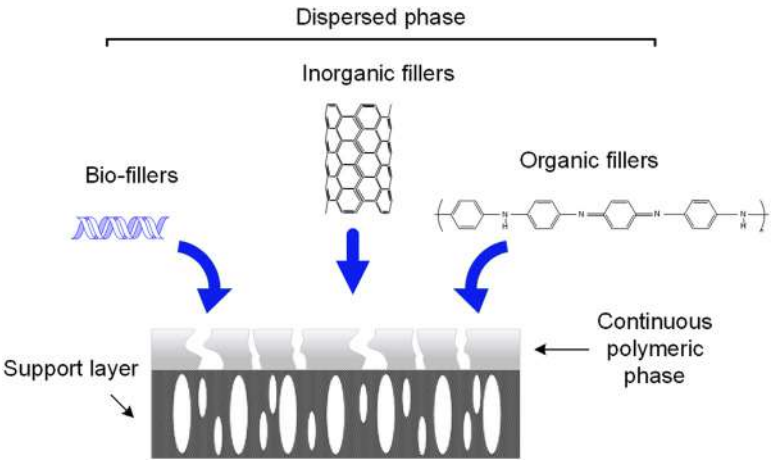

FIGURE 13.2 Nanomaterials categories in mixed matrix membranes (MMMs).

discharge generation, pyrolysis electrodeposition, ion sputtering, and thermal plasma. Common inorganic nanomaterials include elemental oxides (e.g., ZnO, SiO_2), nanoparticles [e.g., carbon nanotubes (CNTs), titanium dioxide, halloysite nanotubes (HNTs)], graphene oxide (GO), metal-organic frameworks (MOFs), and metal nanoparticles (Ag). Organic and bionanomaterials are less commonly applied in FO compared to the inorganic nanomaterials. Examples for these two categories include polyaniline, chitosan, and Aquaporin. There are many successful attempts reported in the literature for improving FO performance using different nanomaterials. A summary of the outcome of some of these attempts is provided in Table 13.1. There are some dedicated reviews for certain nanomaterials that can be a great source of information for readers, such as the recent work on GO applications development with FO (Wu, Shi et al., 2020), the progress of HNTs embedment into different membrane types, including FO (Grylewicz & Mozia, 2020), and the up-to-date MOFs-membranes advancement (Yuan & Zhu, 2020). In addition to the nanomaterials presented in Table 13.1, some studies applied activated carbon (AC) (Lewis, Al-sayaghi, Buelke, & Alshami, 2019) and waste materials (Arjmandi, Peyravi, Arjmandi, & Altaee, 2020) to enhance FO performance.

13.3 Polymer-based nanocomposite flat sheet forward osmosis membranes

Polyamide (PA) TFC membranes are now the most commonly used membranes for water treatment and desalination in the industry. A schematic representation of a three-layered membrane is presented in Fig. 13.3.

Recently, nanomaterials have found significant applications in different fields and its application in desalination and water treatment is noted to be very significant. Incorporating nanomaterials to the active layer and substrate of TFC membranes is a new technique in the FO desalination field that efficiently varies the resultant membrane properties. This nanomaterial incorporation method influences the hydrophilicity, permeability, porosity, thickness, and roughness of the surface of the substrate. This also influences the

TABLE 13.1 Comparison of different nanomaterials, including the advantages of each filler.

Nanomaterials									
Class	**Materials**	**Properties**	**Continuous phase**	**Feed solution**	**Draw solution**	**Flux LMH**	**Salt rejection (%)**	**Altered characteristics**	**References**
Inorganic	Zeolite	Particle size: 40–150 nm	Polyamide on polysulfone substrate	10 mM NaCl	1 M NaCl and deionized (DI) water	21.5	95.6	Improved permeability for nanomaterials loading of up to 0.1 wt.%/vol.%	Ma, Wei, Liao, and Tang (2012)
		Gel, particle size 40–63, pore size: 5.8–17.3 nm, surface area: 68–433 $m^2\ g^{-1}$	Polyacrylonitrile	DI water	0.1–3.0 M $MgCl_2$	42.3–126	99	Enhanced permeability due to the improved surface porosity and reduced structural parameter	Lee, Wang, Tang, and Huo (2015)
	Silica	Particle size 1–20 nm effective membrane area of 36 cm^2	Polybenzimidazole	DI water	0.6–2 M NaCl	16.9	99.5	Enhanced permeability, reduced structural parameter and increased tensile strength	Daer, Akther, Wei, Shon, and Hasan (2020)
	Ag	Pore size 24.3–47.2 nm, particle size 160–240 nm in diameter	Polysulfone	DI water	1 M NaCl	31.0	97.1	Improved water flux and reduced structural parameter with maintaining relatively low RSD	Liu and Ng (2015)
		Effective area of membrane 38.52 cm^2, particle size 20 nm	Polyacrylonitrile	DI water	0.5 M NaCl	21.58	–	Mitigated the ICP and improved water flux	Pan, Ke et al. (2018)
									Liu and Hu (2016)
Inorganic	GO	Particle size 269–1245 nm at 5–50 degrees respectively, MA 6.25 cm^2	Polyethersulfone	DI water	0.33 M $MgCl_2$	13.2	98	Improved water flux and reduced RSD	Jin, Wang, Zheng, and Mi (2018)

	Effective area 15.8 cm^2	Polysulfone-graphene oxide (PSf-GO)	DI water	1.0 M NaCl	37.74	98.6	Enhanced water flux and reduced ICP	Tajik, Moini Jazani, Shokrollahzadeh, and Latifi (2016)
	Effective area 30 cm^2	Polyethersulfone	DI water	1.0 M NaCl	6.1	–	Enhanced water flux and increased slightly ICP	Kang, Wang et al. (2019)
Nanotubes (CNTs and HNTs)	Effective area 20 cm^2	Polyethersulfone	DI water	0.6 M NaCl	11.98	97	Improved water flux and enhanced reverse salt flux selectivity (RSFS)	Choi, Son, and Choi (2017)
	Effective area 12.57 cm^2, average pore size 5 nm	Polyethersulfone	DI water	1.0 M NaCl	42	–	Enhanced water flux and reduced the structural parameter	Samieirad, Mousavi, and Saljoughi (2020)
Nanotubes (CNTs and HNTs)	Effective area 20.02 cm^2, pore size 3.2 nm	Polysulfone substrate	DI water	2.0 M NaCl	21.34	–	Minimized the ICP effect and improved the water permeability	Rezaei-DashtArzhandi, Sarrafzadeh et al. (2018), Rezaei-DashtArzhandi, Sarrafzadeh et al. (2020)
MOF	Pore size 0.1 μm, particle size 60–72 nm, effective membrane area of 11.34 cm^2	Polydopamine/ metal-organic framework thin-film nanocomposite	DI water	1.0 M NaCl	64.2	90	Enhanced water flux and lower reverse flux selectivity	Xu, Yang, Li, Chang, and Xu (2020)
	Particle size 50–150 nm	Polyacrylonitrile (PAN)	DI water	1.0 M NaCl	16	93.5	Improved the water permeation and salt rejection	He, Wang et al. (2020)
	Pore size 0.39–0.48 nm, area 12.5 cm^2, particle size 75 nm	Poly (ethyleneimine)/ 1,3,5-benzenetricarboxylic acid chloride [PEI/ trimesoyl chloride (TMC)] cross-linked matrix	DI water	1.0 M $MgCl_2$	20.8	96	Improved flux with slight increase in RSD for nanomaterials loading of up to 0.05 wt.%	Qiu and He (2019)

(*Continued*)

TABLE 13.1 (Continued)

Nanomaterials									
Class	Materials	Properties	Continuous phase	Feed solution	Draw solution	Flux LMH	Salt rejection (%)	Altered characteristics	References
		Particle size 196.72−1401, pore size 0.34 nm, effective membrane area of 14.6 cm^2	m-Phenylenediamine	DI water	1 M NaCl	5.688	88.6	Enhanced permeability and chemical stability improved when nanomaterials were coated with poly (sodium 4-styrenesulfonate)	Beh, Ooi, Lim, Ng, and Mustapa (2020)
Organic	Polyaniline	Exposed area of membrane 4.25 cm^2, pores range of c. <100 nm	Polysulfone and polyaniline (PAni)	DI water	5% wt./vol. NaCl	12.7	–	Improved membrane permeability and incorporated antifouling properties	Cruz-Tato, Rivera-Fuentes, Flynn, and Nicolau (2019)
		Effective area of membrane 9.6 cm^2	Polyethersulfone-polyethersulfone (SPES-PES)	DI water	1 M of NaCl	19.7	94.52	Improved water permeability	Shakeri, Salehi, and Rastgar (2017)
		Effective area of membrane 19.6 cm^2, particle size 180−240 nm	Polyvinylidene fluoride (PVDF)	DI water	1.5 M NaCl	55.05	97	Improved flux – low reverse salt flux	Shi, Kang et al. (2019)
	Chitosan	Effective area of membrane 9.62 cm^2	Polyethersulfone (SPES)	Polysulfone	1 M Na_2SO_4	25	91.11	Improved water flux	Salehi, Rastgar et al. (2017)
Bio-fillers	Aquaporin	Effective area of membrane 20 cm^2	Polysulfone	Secondary wastewater effluent	Seawater	4.6	98.5	Improved water flux and reduced ICP	Li, Linares et al. (2017)
		Pore size 0.5 μm, active area 0.6 m^2	Polyethersulfone (PES)	DI water	1 M of NaCl	7	99	Improved water flux	Engelhardt, Sadek, and Duirk (2018)

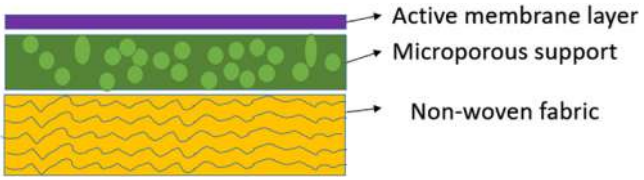

FIGURE 13.3 Diagrammatic representation of a thin-film composite membrane.

active layer structure. The incorporation of nanomaterials in either organic or aqueous solution generates nano-sized pores in the PA selective layer. Hence, the thin-film nanocomposite (TFNC) membranes for the FO application are typically manufactured in the flat-sheet configuration. The following section discusses different nanocomposite FO membranes preparation methods and nanomaterials incorporation to the selective and substrate layers of flat-sheet FO membranes.

13.3.1 Methods for nanocomposite forward osmosis membrane preparation

Phase inversion is considered a significant and very effective method employed to fabricate hollow-fiber and flat-sheet FO membranes. In this method, the polymer is mixed with a solvent and, subsequently, the polymer suspension is cast on a substrate layer. The succeeding phase is the substrate layer immersion precipitation, described as soaking a polymer solution in a nonsolvent coagulant bath.

Electrospinning (ES) is a different method employed for the preparation of fibrous polymer in different configurations and functions. The ES method has been used to fabricate the flat-sheet membrane and hollow-fiber membranes. In this method, a higher electrical field is applied to a polymer suspension in a syringe. This will lead to an ejection and deposition of fine fibers on a collector (Fig. 13.4). Even though the phase inversion technique is the most commonly used method for the synthesis of the FO membrane substrate, it has been recommended in recent times to apply the ES technique for producing the nanofiber polymer substrate in place of the phase inversion technique, because it generates more suitable results concerning the FO flux. The ES method uses a higher electric field for preparing nanofibers from a dope solution.

Fig. 13.4 illustrates the synthesis process of the FO membrane (Xu et al., 2020). The LbL coating technique is another method employed for the fabrication of FO membranes. A prefabricated sublayer is exposed to a polyelectrolyte having an opposite charge for a specified time period in this method. By the addition of alternately charged polyelectrolytes, it is possible to develop multilayers. The active layer is prepared using IP process, that is, the interaction between trimesoyl chloride (TMC) and m-phenylenediamine monomers to develop an extremely thin layer.

13.3.2 Nanomaterials-incorporated support/substrate layer

The substrate of the TFC flat-sheet membrane plays a significant role in the FO process performance. In the following section, we discuss the modification of substrates using carbon-based nanoparticles and metal-based nanoparticles. Table 13.2 shows the

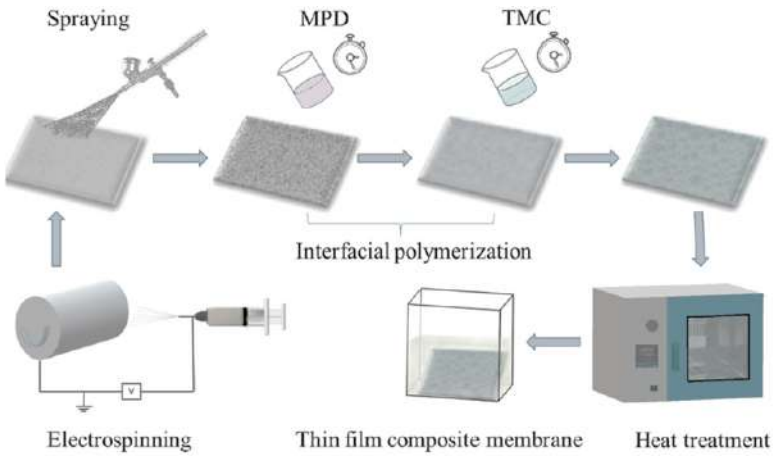

FIGURE 13.4 Synthesis process of the forward osmosis (FO) membrane, in a study by Xu et al. (2020). Source: *Reproduced from Xu, L., Yang, T., Li, M., Chang, J., & Xu, J. (2020). Thin-film nanocomposite membrane doped with carboxylated covalent organic frameworks for efficient forward osmosis desalination. Journal of Membrane Science, 118111.*

different studies carried out on flat-sheet membranes by the modification of substrate with nanoparticles.

13.3.2.1 Substrate layer containing carbon-based nanomaterials

Different carbon-based nanomaterials such as graphene oxide and CNTs have been used in the substrate layer to improve the flat sheet FO membrane's performance. Out of the different studies reviewed, graphene-based nanomaterials have demonstrated to be the best to improve the membrane performance while incorporated in the membrane supports. Because of its exclusive properties, the carbon-based nanomaterial GO is a perfect material choice for modifying the substrate of TFC FO membranes. This is due to abundant oxygen-containing functional groups like hydroxyl, epoxy, and carboxyl groups.

The manufacturing and performance of the fabricated TFC FO membranes with GO-modified substrate are examined in the study by Park et al. (2015). GO nanosheets were included in PSF for obtaining the GO−PSF nanocomposite membrane substrate. PA selective layer was successively prepared on the GO−PSF substrate by the IP process for obtaining the TFC FO membranes. The test results revealed that at an optimum quantity of GO incorporation (0.25 wt.%), a GO-PSF nanocomposite membrane substrate with suitable structural property, pore size, porosity, and the thickness could be accomplished. The optimal inclusion of GO in the PSF substrate considerably increased the permeability of water. It permitted the PA layer's effective formation compared to that of the pristine PSF substrate with extremely less water permeability.

CNTs are renowned nanomaterials used in membrane-based water treatment because of its increased strength and other benefits of being a nanomaterial. In a study by Tian et al. (2015a), the team effectively manufactured an advanced TFNC FO membrane comprising a polyetherimide nanofibrous support layer strengthened by functionalized MWCNTs and an ultrathin PA selective layer. Along with the higher interconnected porous configuration of the nanofiber support layer, the properly distributed functionalized MWCNTs in the nanofibers enhanced the support layer porosity by almost 18%. They decreased the structural parameter

TABLE 13.2 Different studies carried out on flat-sheet membranes containing nanomaterials-embedded substrate.

			Experimental conditions			Performance				
						AL-FS (FO)		AL-DS (PRO)		
Support layer	**Selective layer**	**Nanomaterial**	**Draw solution**	**Feed solution**	**Cross-flow velocity**	**Reverse salt flux (g L^{-1})**	**Water flux (LMH)**	**Reverse salt flux (g L^{-1})**	**Water flux (LMH)**	**References**
Polysulfone	Polyamide	TiO_2	2 M NaCl	10 mM NaCl	32.72 cm s^{-1}	0.24	29.76	0.25	56.27	
Polysulfone	Polyamide	Zeolite	2 M NaCl	Deionized water	500 mL min^{-1}	0.7	40.00	0.66	86.00	
Polysulfone	Polyamide	Halloysite nanotubes	2 M NaCl	10 mM NaCl	350 mL min^{-1}	0.52	27.71	0.63	43.25	
Polysulfone	Polyamide	Silica	1 M NaCl	Deionized water	25 cm s^{-1}	0.24	31.00	0.26	60.5	
Polyetherimide	Polyamide	Carbon nanotubes	1 M NaCl	Deionized water	9 cm s^{-1}	0.12	32.80	0.07	61.3	Tian et al. (2015a)

AL-FS, active layer facing feed solution; *AL-DS*, active layer facing draw solution; *LMH*, L m^{-2} h^{-1}; *NaCl*, sodium chloride.

of the membrane by 30%, and considerably increased the support layer tensile modulus by approximately 53%. The increased mechanical strength offered by the incorporated functionalized MWCNTs contributed to the additional increase in the substrate porosity and pore size for mitigating the ICP.

13.3.2.2 Substrate layer containing metal-based nanomaterials

Out of the different metal-based nanomaterials examined, titanium dioxide has demonstrated better improvement in the performance of the membrane when incorporated in the substrate layer of flat sheet FO membrane, either individually or in hybrid form. Titanium dioxide nanoparticle is considered one of the most commonly used nanomaterials to prepare nanocomposite membranes. The extreme hydrophilic surface of titanium dioxide nanoparticle and its exceptionally small particle size (less than 21 nm) are the foremost features truly considered for the preparation of nanocomposite membranes.

In a work by Emadzadeh et al. (2014), titanium dioxide (TiO_2)/polysulfone nanocomposite support layers were fabricated by the addition of various quantities of TiO_2 nanoparticles (0−1 wt.% range) into the polysulfone matrices. The fabricated nanocomposite support layers were subsequently characterized for surface roughness, overall porosity, hydrophilicity, and cross-sectional structure. The team noted that both porosity and hydrophilicity of the support layer increased by incorporating TiO_2. Moreover, long finger-shaped structures have been prepared by enhancing the concentration of TiO_2, increasing the water permeability. To fabricate the nanomaterial-incorporated TFC membrane for FO process, a thin PA selective layer was prepared by IP of 1,3,5-benzenetricarbonyl trichloride 1,3-phenylendiamine on the topmost surface of TiO_2/polysulfone nanocomposite support layer. The FO performance assessment was carried out with 0.5 and 2.0 M NaCl concentration in draw solution, 10 mM NaCl concentration in the feed solution, both the active layers facing the draw solution (AL−DS orientations) and the active layers facing the feed solution (AL−FS). The TFNC membrane manufactured using polysulfone substrate incorporated with 0.5 wt.% TiO_2 nanoparticles demonstrated the most favorable results by having a lower reverse solute flux and higher water permeability.

Moreover, in a study performed by Sirinupong et al. (2018), a nanocomposite substrate was prepared using a TiO_2/GO hybrid into polysulfone matrices. Before carrying out the performance analysis, the support layer fabricated was characterized by surface roughness, surface chemistry, and cross-sectional structure. The test results confirmed that both surface roughness and hydrophilicity of the polysulfone-based substrates were enhanced by nanomaterials. Support layers with longer finger-shaped voids, prolonged from top to bottom, can be developed by adding TiO_2 or TiO_2/GO hybrid. Higher surface hydrophilicity and satisfactory structure development are the major factors for increasing water flux in the nanocomposite supporting layer. Additionally, the water flux in the FO process, using TFC membranes can be increased by employing this nanocomposite supporting layer. As compared to the control TFC membrane, the membranes with TiO_2 substrate and TiO_2/GO hybrid demonstrated increased water flux with minimal increase in the reverse draw solute flux. From the obtained results, it can be confirmed that the addition of TiO_2 and TiO_2/GO hybrid into the polysulfone supporting layer can potentially enhance the performance of the TFC membrane towards the FO applications.

13.3.3 Nanomaterials-incorporated selective/active layer

Different nanomaterials have been extensively used in the PA active layer of the TFC flat-sheet membrane to improve the membrane performance in the membrane-based separation process. Table 13.3 presents different studies on flat-sheet membranes by modifying the selective layer with nanoparticles.

13.3.3.1 Active layer containing carbon-based nanomaterials

Out of the carbon-based nanomaterials used in the active layer of membranes, GO has been considered as the best one for improving the performance of the flat sheet FO membrane. GO has exclusive feature characteristics that have made it an ideal material for water purification applications. In a study by Shen et al. (2016), GO nanosheets are prepared and incorporated into the PA active layer for developing an advanced TFC membrane for the FO process. As compared to the control TFC membrane, the GO-incorporated TFC membranes exhibited increased water flux and acceptable draw solute rejection. The GO loading impacts on the morphology of the membrane and FO performance of the GO-incorporated TFC membrane were examined for different characterizations and intrinsic separation performance. Moreover, the GO-incorporated TFC membrane also possessed low fouling propensity in the FO process compared to the membrane having no embedded GO.

Shokrgozar et al. (2018) investigated the preparation of GO-added PA TFC flat-sheet membranes on polysulfone supporting layer for FO process. The GO nanosheets were incorporated into the PA layer employing various amounts (ranging from 0.05 to 0.2 wt.%). The test results confirmed the modification of PA surface by GO nanosheets and increased surface hydrophilicity by enhancing GO concentration. The results confirmed that the water flux of the 0.1 wt.% GO-included composite membrane was about 34.7 L m^{-2} h^{-1}, demonstrating an increase of 90% relative to the TFC. In contrast, salt reverse diffusion decreased to 39%. Fig. 13.5 showed the FO fouling test result of the control TFC membrane and GO-embedded TFC membrane. Moreover, it was noted that the water flux reduction of GO-embedded TFC membrane with time is very slow, relative to the control TFC membrane, signifying the low fouling propensity.

13.3.3.2 Active layer containing metal-based nanomaterials

Different metal-based nanomaterials such as titanate nanotubes and MOFs have been used in the selective layer for improving the membrane performance of flat sheet FO membrane. Out of the different studies reviewed, titanate nanotubes have been demonstrated to be the best to improve the membrane performance while incorporated in the membrane active layer. Generally, the titanate nanotubes developed from TiO_2 nanoparticles using hydrothermal technique exhibit the hydrophilic properties of TiO_2 nanoparticles and provide a very large specific surface area pore volume. In a study by Emadzadeh et al. (2015), a self-synthesized thin-film nanocomposite membrane embedded with hydrophilic functionalized titanate nanotubes was developed subsequently tested for FO desalination. The team used different analytical instruments to study the prepared amine-functionalized titanate nanotubes' properties, and they confirmed its exclusive interactions with PA functional groups (Fig. 13.6). The test results confirmed that the membrane water flux was considerably increased from 11.58 L m^{-2} h^{-1} for the control TFC membrane to 20.79 L m^{-2} h^{-1} in the FO mode with the incorporation of 0.05 wt.% amine-functionalized titanate nanotubes into the PA matrix. It was

TABLE 13.3 Different studies carried out on flat-sheet membrane with nanomaterials-embedded selective later.

			Experimental conditions			Performance				
						AL-FS (FO)		AL-DS (PRO)		
Support layer	**Selective layer**	**Nanomaterial**	**Draw solution**	**Feed solution**	**Cross-flow velocity**	**Reverse salt flux (g L^{-1})**	**Water flux (LMH)**	**Reverse salt flux (g L^{-1})**	**Water flux (LMH)**	**References**
Polysulfone	Polyamide	Silicon dioxide	2 M NaCl	10 mM NaCl	800 mL min^{-1}	0.10	15.00	0.14	25.00	
Polysulfone	Polyamide	Zeolite	1 M NaCl	Deionized water	500 mL min^{-1}	0.45	17.40	0.37	38.2	Ma et al. (2012)
Polyacrylonitrile	Polyamide	GO	2 M NaCl	Deionized water	300 mL min^{-1}	0.21	31.7	0.24	47.0	
Polysulfone	Polyamide	MOF	2 M NaCl	Deionized water	1.1 cm s^{-1}	0.23	27.0	0.24	51.3	
Polysulfone	Polyamide	TiO_2	0.5 M NaCl	10 mM NaCl	300 mL min^{-1}	0.19	26.0	0.18	34.4	

AL-FS, active layer facing feed solution; *AL-DS*, active layer facing draw solution; *LMH*, L m^{-2} h^{-1}; *NaCl*, sodium chloride.

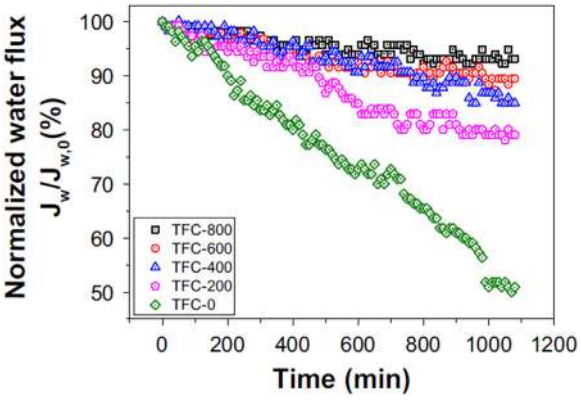

FIGURE 13.5 Forward osmosis fouling test of the control and graphene oxide (GO) incorporated thin-film composite membranes. Source: *Reproduced from S. Shokrgozar Eslah, S. Shokrollahzadeh, O. Moini Jazani & A. Samimi, Forward osmosis water desalination: Fabrication of graphene oxide-polyamide/polysulfone thinfilm nanocomposite membrane with high water flux and low reverse salt diffusion, Separation Science and Technology, 53 (3), 2018.*

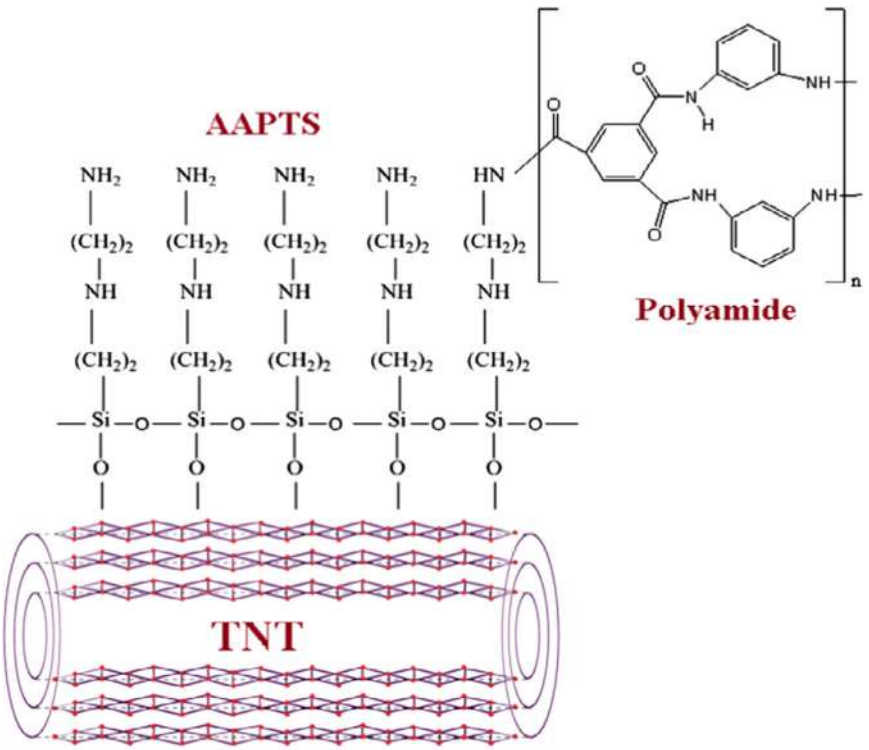

FIGURE 13.6 Interaction between modified titanate nanotubes and the polyamide active layer of composite membrane for forward osmosis (FO) application. Source: *Reproduced from D. Emadzadeh, W.J. Lau, T. Matsuura, M. Rahbari-Sisakht, A.F. Ismail, A novel thin film composite forward osmosis membrane prepared from PSf–TiO2 nanocomposite substrate for water desalination, Chemical Enigneerign Journal, 237, 2014, 70–80.*

also confirmed that the finest performing thin-film nanocomposite membrane (with 0.05 wt.% amine-functionalized titanate nanotubes in the PA matrix) was able to overcome the trade-off effect between reverse solute flux and water permeability, as this membrane exhibited higher water permeability as well as a lower reverse solute flux as compared to control TFC membrane when these membranes were tested under two dissimilar orientations.

Another study successfully synthesized Zirconium (IV)-carboxylate MOF-UiO-66 nanoparticles and incorporated these nanoparticles into the PA active layer for fabricating advanced TFNC membrane. As compared to pure PA TFC membrane, the addition of UiO-66 nanomaterials remarkably changed the chemistry and morphology of the membrane, resulting in an increase in the intrinsic separation properties because of the molecular sieving and the extremely hydrophilic nature of these nanoparticles. The finest performing TFNC (0.1 wt.% nanoparticle loading) membrane demonstrated a 52% increment in the water permeability. It also maintained salt rejection levels of almost 95%, as same as the benchmark. The impact of this nanoparticle incorporation on the FO performance was also examined. The addition of 0.1 wt.% of nanoparticle generated an ultimate water flux enhancement of 25% over the TFC control under the FO mode when 1 M NaCl was employed as the draw solution and deionized water as the feed solution.

13.3.4 Nanomaterials-incorporated support/substrate and selective/active layers

It was noted that the nanomaterials when incorporated with both the support layer and active layer showed improved membrane performance, as compared to when used with either a support layer or a selective layer. TFC flat-sheet membranes' characteristics can be enhanced by introducing extremely hydrophilic nanomaterials into the PA selective layer and/or the supporting layer. In a study by Rezaei-DashtArzhandi, Sarrafzadeh et al. (2018), TFNC membranes were prepared by incorporating extremely hydrophilic HNTs and self-synthesized graphitic carbon nitride nanoparticles into the polysulfone supporting and the topmost PA layers, respectively. The TFNC membranes were examined for their performance in FO application. HNTs possess a combination of exclusive characteristics, like strong mechanical strength, excellent biocompatibility, availability of functional groups, t natural abundance, high aspect ratio, and tubular nanostructure. The impacts of nanomaterials on the supporting and active layers were examined in terms of hydrophilicity, membrane surface morphology, and separation performance. When 0.05 wt.%/vol.% of graphitic carbon nitride nanoparticles were incorporated into the PA active layer, the membrane surface water-drop contact angle considerably decreased from 68 degrees in the control membrane to less than 10 degrees in the TFNC membrane, resulting in a higher water flux of 18.88 L m^{-2} h^{-1} (almost 270% greater than the TFC membrane). The test results have confirmed the influence of PA layer modification on the support modification to enhance FO performance.

13.4 Polymer-based nanocomposite hollow fiber forward osmosis membranes

Hollow fiber membranes are considered more appropriate for the FO process than thin flat-sheet membranes due to their self-supported mechanical characteristics. It permits

denser packing density and increased effective membrane surface area for both draw and feed solutions. Furthermore, the preparation of the hollow fiber module is rather easy, and it offers a larger surface area per volume ratio. Moreover, it can be noted that the hollow fiber structure might contribute to the flow pattern exactly necessary for the FO process. However, hollow fiber membrane fabrication methods suffer from certain drawbacks, like restricting suitable materials. Currently, the polymer-based nanocomposites are extensively used in water treatment applications along with its application in different other fields. The following section discusses modifying the active layer of the hollow-fiber FO membranes (using carbon-based and metal-based nanomaterials) and biomimetic membranes.

13.4.1 Active layer modifications

The active layer of the hollow-fiber FO membranes can be modified using carbon-based and metal-based nanomaterials.

13.4.1.1 Active layer containing carbon-based nanomaterials

Out of the different studies reviewed, GO has been demonstrated to be the best nanomaterial used to improve the membrane performance while incorporated in the active layer of hollow-fiber FO membranes. In TFC membranes, the carbon-based nanomaterial GO can be incorporated into the thin selective PA layer to improve the membranes' performance. The addition of GO into the selective PA layer can increase the PA layer internal free volume because of GO's incompatibility with the polymeric structure. The enhanced surface smoothness and the hydrophilicity of the PA selective layer led to lower surface tension towards water molecules, thus improving water transport.

The outer selective hollow-fiber TFC membrane was fabricated successfully by Lim et al. (2019). The size-controlled GO nanosheets, with a size smaller than 2 μm, have been effectively added by Lim et al. (2020a) into the selective PA layer to prepare an outer selective hollow-fiber TFNC membrane for FO process by vacuum-assisted IP method. In this study, the team particularly demonstrated that the size-controlled GO nanosheets in aqueous amine solution were aligned horizontally and stacked on the membrane substrate surface by vacuum suction from exterior to interior in the vacuum-assisted IP. The size-controlled GO nanosheets were subsequently incorporated into the thin selective PA layer with lesser physical damage. Moreover, the effective loading of the size-controlled GO nanosheets inside the PA layer under the vacuum-assisted IP was more than that under the standard IP process. Also, there was no concern about the particle loss from blowing nitrogen or air for separation of excess amine solution. The advantage is that it will be extremely economical concerning nanomaterials used in a TFNC membrane fabrication. Fig. 13.7 presents the FO performance (specific reverse solute flux and water flux) of outer selective hollow-fiber TFNC membrane incorporated with GO in the range from 0 to 10 g m^{-3}. The FO operation was carried out with deionized water as a feed solution and a 1 M sodium chloride solution as a draw solution. This study confirmed that the optimal outer selective hollow-fiber TFNC membrane could be the most appropriate candidate to improve the membrane performance due to its scalability in different wastewater treatments and water reuse applications.

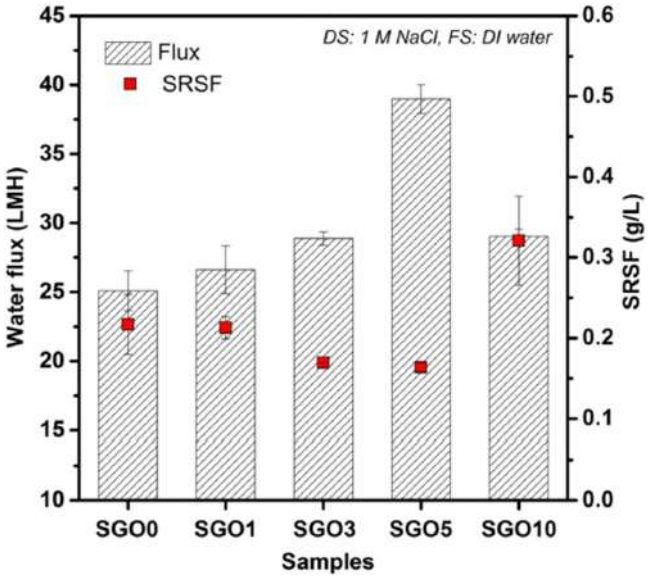

FIGURE 13.7 Forward osmosis performance (specific reverse solute flux and water flux) of outer selective hollow-fiber thin-film nanocomposite membrane incorporated with GO in the loading range from 0 to 10 g m^{-3}. The forward osmosis operation was carried out with deionized water as a feed solution and 1 M sodium chloride solution as a draw solution. Source: *Reproduced from Beh, J., Ooi, B., Lim, J., Ng, E., & Mustapa, H. (2020). Development of high water permeability and chemically stable thin film nanocomposite (TFN) forward osmosis (FO) membrane with poly (sodium 4-styrenesulfonate)(PSS)-coated zeolitic imidazolate framework-8 (ZIF-8) for produced water treatment. Journal of Water Process Engineering, 33, 101031.*

In a study by Jang et al. (2020), it was noted that the reverse salt flux was considerably decreased to 0.06 mol m^{-2} h^{-1} using 2.0 M NaCl draw solution when GO was employed in the selective layer of the hollow-fiber membrane. Even though there have been random reports of GO utilization for improving the reverse salt flux performance instead of improving water flux performance, the aforestated study confirmed that GO was used only in the localized selective layer leading to an unusually decreased reverse salt flux results.

13.4.1.2 Active layer containing metal-based nanomaterials

Different types of framework-based materials, like zeolitic imidazolate frameworks, covalent organic frameworks (COFs), and MOFs, have been examined as an advanced category of nanomaterials to develop nanocomposite membranes for FO process. Out of the different studies reviewed, Schiff-based network nanomaterials have demonstrated to be the best to improve the membrane performance while incorporated in the active layer of hollow fiber FO membranes. COFs have adjustable chemical functionalities, extremely microporous configurations, and selective grafting capability with different chemistries because of the organic linkers on the building blocks. In the study by Lim et al. (2020b), an advanced outer selective hollow fiber thin-film nanocomposite FO membrane embedded with a type of COFs, amine-rich Schiff-based network nanomaterials, was prepared by a vacuum-assisted IP process. The Schiff-based network nanomaterials possess porous internal structures and hydrophilic nature, which are adequate to produce extremely permeable and effective FO membranes. The Schiff-based network nanomaterials have been conformally packed across the exterior surface of the hollow-fiber substrate by vacuum pressure used at the time of the vacuum-assisted IP process, resulting in defect-free coatings.

Moreover, covalent bonding between secondary amines across the Schiff-based network nanomaterials and carboxylic groups available from the monomer employed for the IP step supported the adhesion of the Schiff-based network nanomaterials to the native PA layer present across the surface of the TFNC membrane. Thus the loading of Schiff-based network nanomaterials at 0.001 wt.% displayed the maximum FO performance with increased water flux (greater than 23% of the pure one) and comparatively lower specific reverse solute flux at 0.18 g L^{-1} employing 1 M sodium chloride and deionized water in a series of TFC membranes. The optimal loading at 0.001 wt.% was much less than other TFNC membranes (usually higher than 0.05 wt.%) because of the minimum loss of Schiff-based network nanomaterials in the vacuum-assisted IP process. Moreover, this TFNC membrane showed superior FO operation stability when tested for 72 h. This advanced technique is ideal for optimizing the FO processes for water treatment and desalination in the upcoming years.

13.4.1.3 *Biomimetic forward osmosis membranes*

Biomimetic membranes with Aquaporin pave an advanced way for the progress in membrane-based purification technique. In recent times, several methods are developed for producing membranes with Aquaporin. In the study by Ren and McCutcheon (2018), the team studied the Aquaporin Inside hollow-fiber FO membrane (Fig. 13.8) developed by Aquaporin A/S, Denmark. The aforestated membranes were examined in miniature modules in distinct osmotic testing conditions. By incorporating biomimetic aquaporin proteins as water channels in the active layer, the membranes showed superior performance with a reverse salt flux of 3.6 g m^{-2} h^{-1}, and water flux of 21 L m^{-2} h^{-1}, with deionized water and 1 M NaCl as feed and draw solutions, respectively.

Generally, the biomimetic membranes utilize the superior water permeability and selectivity of aquaporin proteins incorporated into the membrane selective layer. In a work by Engelhardt et al. (2018), a 0.6 m^2 hollow-fiber aquaporin-based membranes module was examined for its rejection of two types of trace organic contaminants: the preservative methylparaben, the plastic component bisphenol A, and the herbicide 2,4-dichlorophenoxyacetic acid. With the hollow-fiber aquaporin-based membranes module, almost 95% of methylparaben was separated by the membrane. In contrast, for 2,4-dichlorophenoxyacetic

FIGURE 13.8 Photograph of Aquaporin Inside hollow fiber membrane module. Source: *Reproduced from Ren, J., & McCutcheon, J. R. (2018). A new commercial biomimetic hollow fiber membrane for forward osmosis.* Desalination, 442, *44–50.*

acid and plastic component bisphenol A rejection rates of approximately 99% were obtained. On the other hand, it was also noted that methylparaben and bisphenol A were adsorbed on the aquaporin membrane and subsequently flushed out again in the course of succeeding tests.

13.5 Nanofibrous-based forward osmosis membranes

Electrospun nanofibrous mats are extensively employed as substrate for developing advanced FO membranes because of its ultralow structure parameter. Nanofiber support layer with incorporated nanomaterials, such as CNTs, is also developed to improve membrane performance. The ES process generates polymer fibers with a diameter in a range of 5–500 nm and a large surface area. The scaffold-like nanofibers could be converted to an extremely porous structure to obtain less tortuosity and S value. The aspect ratio, diameters, and prepared nanofiber orientation could be achieved by adjusting the applied voltage, solution flow rate, solution viscosity, and environment conditions.

Hydrophilic/hydrophobic interpenetrating network composite nanofibers was employed for the FO membrane substrate layer, which was effectively designed and manufactured by (Tian et al., 2014) with the ES technique. The hydrophilic polymer is polyvinyl alcohol, and the hydrophobic polymer is polyethylene terephthalate. The FO membrane's flux showed a remarkable enhancement because of the hydrophilic/hydrophobic interpenetrating network composite nanofiber substrate layer. It was noted that with the rise in polyvinyl alcohol nanofiber content in the hydrophilic/hydrophobic interpenetrating network composite nanofiber substrate layer, the membrane flux was increased. As the ratio of polyethylene terephthalate/polyvinyl alcohol composite nanofibers was 1/4, the membrane showed the lowest salt leakage (9.5 g m^{-2} h^{-1}) and the greatest water flux (47.2 L m^{-2} h^{-1}). In the FO experiment, 0.5 M NaCl solution was used as a draw solution, and deionized (DI) water was used as feed s olution, and when the active layer faces the draw solution. The increase in the flow was due to the rise in the wetting performance of the substrate layer and the water-transferring function. The hydrophilic/hydrophobic interpenetrating network composite nanofiber structure developed between polyvinyl alcohol and polyethylene terephthalate nanofibers resulted in decreased ICP. Bui et al. (2013) studied the polymer composition properties by mixing cellulose acetate and polyacrylonitrile polymers for preparing the nanofiber substrate. The team noted that a uniform and homogenous nanofiber support with hollow peaks nanopores was connected firmly with the active layer.

A beneficial alternative design for support layer of FO membrane is a thin and fine nanofiber upper layer having compatibility with the active layer and rough fibrous layer in the lower most part for improving the strength of the support layer. Tian et al. (2015b) manufactured a polyetherimide nanofiber support layer with incorporated functionalized MWCNTs. Because of the uniform dispersion of functionalized MWCNTs, substrate stiffness and tensile strength were increased remarkably. Bui and McCutcheon (2016) developed a nanofiber support layer by incorporating 15% mesoporous silica nanomaterials into polyacrylonitrile nanofiber-supporting layer. The silica particles were properly distributed within the supporting layer, thus offering extra water pathways using porous channels in the particles and enhanced water-holding capacity.

Despite its beneficial features, the higher porosity might result in a severe rise in salt flux for some fabricated membranes. These membranes can significantly demonstrate inadequate mechanical strength for withstanding an applied pressure while examining the intrinsic performance parameters for commercial-scale operations. The fabrication process is complicated and can take an extended time. An additional serious problem exists, that is, the compatibility between the active and nanofibrous supporting layers.

13.6 Nanomaterials used in surface modification of forward osmosis membranes

Surface modification of membrane is one of the well-studied techniques for the prevention of the development of biofilm. Out of the different nanomaterials used for the surface modification of FO membranes, GO has been demonstrated to be the best one, due to its exclusive features. Due to its extremely functionalized edges and basal planes, the nanomaterial GO offers exclusive characteristics when employed as a support for silver and gold. For biofouling issue related to the TFC FO membranes, Soroush et al. (2015) fabricated advanced surface coatings through covalent bonding of silver-decorated GO. This nano-functionalization of TFC FO membranes offers a proper antimicrobial surface with excellent features than silver nanoparticles or the GO separately. This improved efficiency was due to the synergetic impact of the capture–killing mechanism demonstrated by the system.

Because of the appropriate features of both GO flakes and polyvinyl alcohol as a coating for membrane, the study by Akther et al. (2020) analytically explored the impact of cross-linked hydrophilic polyvinyl alcohol hydrogel and GO flakes composite coating on the antifouling, physicochemical properties, and selectivity of commercial TFC PA flat-sheet FO membranes. This coating was noted to enhance the hydrophilicity and smoothness of the surface of the membrane. The polyvinyl alcohol hydrogel-coated TFC membrane with a 0.02 wt.% GO demonstrated a decrease in specific reverse solute flux. However, the antifouling property with a 58% greater flux recovery than the pure TFC membrane was noted. The remarkable increase in the modified membranes' selectivity signified that hydrogel coating could be employed for sealing PA defects.

13.7 Polymer-based stimuli-responsive forward osmosis membranes

A variety of polymers are sensitive to their external environment and always respond to external stimuli (Wandera, Wickramasinghe, & Husson, 2010). The rise and decrease in swelling behavior of these polymers have been especially useful in drug delivery, as the drug release can be caused by changing the environmental conditions. These polymers are termed stimuli-responsive polymers and have attracted tremendous attention in recent years. Researchers have focused on using these polymers to design and fabricate smart membranes or artificial/synthetic membranes (lab-fabricated). Stimuli-responsive membranes are membranes that can be controlled, adapted, or manipulated by applying an external stimulus control, such as pH, temperature, heat, biochemicals (enzymes or antigens),

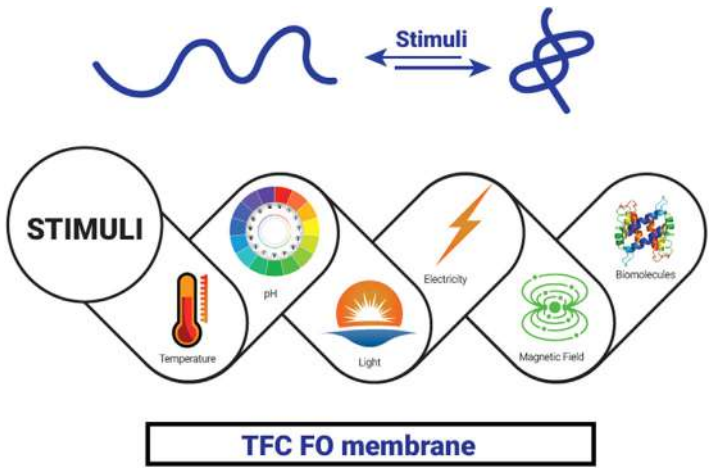

FIGURE 13.9 Various stimuli for stimulus-responsive membranes.

electric or magnetic field, ultraviolet light, ionic strength of the solution, or any other external stimuli (Fig. 13.9). The stimuli-responsive membranes can be used in various practical applications, such as water treatment, drug delivery, and concentrating juices.

External stimuli can be broadly divided into direct stimulation, indirect stimulation, and field stimulation (Darvishmanesh, Qian, & Wickramasinghe, 2015). Direct stimulation occurs when a membrane is in direct contact with the stimulus. In indirect stimulation, some responsive sites on the membrane surface respond to the external stimulus. For instance, temperature-responsive groups can respond to change in the temperature, while pH-responsive groups will respond to the pH change. Similarly, field-responsive stimulation occurs when the membrane responds to an external electromagnetic field.

During the fabrication process of stimuli-responsive membranes, a stimuli-responsive species is introduced using a blend of the main polymer and the stimuli-responsive polymer (Miao, Tu et al., 2017). By changing the external stimuli during the process of membrane filtration, the membrane performance can be manipulated. There is scarce literature concerning FO stimuli-responsive membranes, as much of the research is focussed on stimuli-responsive draw solutions.

Several methods have been reported in the literature for synthesizing stimulus-responsive membranes. The first step in membrane preparation usually involves the synthesis of the responsive polymer or copolymer. Subsequently, these synthesized materials are processed into membranes. Commercially available TFC membranes can also be modified by incorporating stimulus-responsive polymers. Wandera, Wickramasinghe et al. (2010) showed that stimulus-responsive membranes could be developed through phase inversion method, radiation-based methods, solvent casting, and formation of interpenetrating polymer networks. The surface of the membranes can be modified using either "Grafting from" or "Grafting to" methods. The Grafting from method includes photo-initiated polymerization, redox-initiated polymerization, radiation-induced polymerization, plasma-graft-filling polymerization, and atom-transfer radical polymerization (ATRP). The "Grafting to" methods include physical adsorption, or coating and (photo) chemical drafting.

TABLE 13.4 pH-responsive groups and materials.

Group	Property manipulated	References
Carboxyl	The pore size of the membrane can be adjusted by varying the pH	Darvishmanesh, Qian et al. (2015)
Pyridine	Membranes can become positive charge or swell at low pH, or pores can open at low pH and close at high pH	Shevate, Karunakaran, Kumar, and Peinemann (2016)
Polyacrylic acid nanobrushes	At low pH, the membrane collapses, whereas at high pH, the membrane is deprotonated and swells	Himstedt, Marshall, and Wickramasinghe (2011)
Methacrylic acid	Membrane responds rapidly to external pH	Wang, An, Wu, Mo, and Gao (2007)

Among the various external stimuli, pH sensitivity gives more choices for both the materials and the material environment, making it a powerful technique (Zhao, Nie, Tang, & Sun, 2011). Table 13.4 lists the different pH-responsive groups or materials, and how they respond to change in pH. In pH-sensitive FO membranes, the membrane flux, solute rejection, reverse salt flux, and pore size may be manipulated by making the membrane respond to external pH stimulus.

Numerous preparation methods have been proposed in the literature for pH-responsive membranes, but the traditional phase inversion method has been the most commonly used (Kademoglou, Williams, & Collins, 2018). In the phase inversion process, the stimulus-responsive polymer casting solution is cast on a flat surface, such as a glass sheet, and then immersed in a coagulation bath containing solvent, such as water, to facilitate membrane formation. Another method reported, particularly for the FO membrane fabrication, is ATRP. ATRP is gaining huge popularity in recent years in the field of stimulus-responsive membrane fabrication. ATRP involves the controlled growth of polymer chains from a membrane surface. For the first time, Salehi, Shakeri, Mahdavi, and Lammertink (2020) synthesized a TFC-FO membrane by blending hydrophilic polysulfone-graft-poly 2-dimethylaminoethyl methacrylate (PSf-g-PDMA) copolymer in the PSf support layer. This membrane exhibited superior performance compared to a normal PSf-based TFC membrane (Table 13.5). In the FO mode, the modified membrane achieved a water flux of 28.03 LMH compared to 14.23 LMH for the pristine TFC membrane, whereas, in the PRO mode, the modified membrane exhibited a flux of 46.1 LMH compared to 27.80 LMH for the pristine membrane.

Membrane surface for pH-responsive membranes can also be modified using UV-initiated grafted polymerization and redox-initiated grafted polymerization. The former has several advantages, including low cost and simplicity, and has been utilized in various applications (Hilal, Al-Khatib, Atkin, Kochkodan, & Potapchenko, 2003). Although redox-initiated grafted polymerization was used to modify nanofiltration (NF) and ultrafiltration (UF) membranes' surface, the reaction time was too long (Abu Seman, Khayet, Bin Ali, & Hilal, 2010). Himstedt, Marshall et al. (2011) modified commercially available NF membrane using UV-initiated grafted polymerization with polyacrylic acid nanobrushes. The membrane responded to change in the feed solution pH, switching between swollen and collapsed state. At the feed pH value of 7 and 8, the membrane is expected to be deprotonated and swelled, thus exhibiting good antifouling behavior. On the other hand, at a low

TABLE 13.5 Advancements in the forward osmosis (FO) membranes in terms of stimulus-responsive membranes.

Stimulus	Application	Technique	Modification	Property manipulated	Results	References
pH	Forward osmosis	Grafting (atom-transfer radical polymerization; ATRP)	PSf-g-PDMA was blended in the PSf support layer of the TFC FO membrane	Water flux or permeability	Modified membrane showed higher water flux without compromising selectivity	Salehi, Shakeri et al. (2020)
pH	Nanofiltration	UV-initiated graft polymerization	Acrylic acid nanobrushes are grown from the membrane surface	Antifouling	Membrane flux and rejections are dependent on the pH	Himstedt, Marshall et al. (2011)
Electric field	Forward osmosis	Loeb–Sourirajan phase inversion method	A carbon paper is incorporated in the membrane substrate by the phase inversion method	Antifouling/ flux recovery	Membrane showed good antifouling behavior and mechanical stability	Liu, Qiu et al. (2016)
Salt	Forward osmosis	Grafting ATRP	TFC-FO membranes with PSBMA poly (sulfobetaine methacrylate) brushes	Antifouling/ flux recovery	Water permeability of the membrane can be recovered after long-term fouling operation by using salt cleaning	Zhang, Tian et al. (2017)
Temperature	Forward osmosis	Interfacial polymerization (IP) reaction	PNIPAM (poly (N-isopropyl acrylamide) microgels was incorporated in the substrate)	Water flux	Significant decrease in ICP occurred for the fabricated membrane	Zhang, Xiong et al. (2021)

pH value, such as 3.15, the polyacrylic acid collapses; and thus the grafted layer has little effect on the membrane performance. Wang, An et al. (2007) used *in situ* redox-initiated grafted polymerization to graft methacrylic acid to the pores of a commercially available TFC PA UF membrane. The reported membrane exhibited a rapid and reversible response to a pH stimulus. At a high pH value, the membrane exhibited a decrease in permeability, whereas the membrane collapsed at a low pH value.

Another stimulus commonly applied in most FO membranes is an electric field or an external voltage. These membranes are also termed as conductive FO membranes and are fabricated by embedding an electrode, such as CNTs, in the membrane substrate (Liu, Qiu et al., 2016). An external electric field is then applied or coupled with the membrane

during the membrane filtration, which generates electrostatic repulsion between the membrane surface and the charged foulants, thus effectively mitigating membrane fouling (Busalmen & De Sanchez, 2001; Van der Borden, Van der Mei, & Busscher, 2005). The conductive FO membrane modified with metal, carbon, or other materials can be used as a negative electrode (Li, Guo et al., 2018). Rastgar, Bozorg, Shakeri, and Sadrzadeh (2019) experimentally demonstrated that an outstanding resistance to microbial fouling and organic fouling was achieved by electroactive membrane by applying an external voltage to a conductive FO membrane. Besides, applying an electric field to the membrane surface is easy to operate and automate (Li, Guo et al., 2018).

Salt-responsive and temperature-responsive FO membranes have been reported in the literature. Fabricating salt responsive self-cleaning or easy-cleaning FO membranes can be a more efficient way to deal with membrane fouling.

Zwitterions polymers, such as poly(4-(2-sulfoethyl)-1-(4-vinylbenzyl) pyridinium betaine), are insoluble in water but are readily soluble in the presence of halide salts (Meng, Cao et al., 2014). These membranes can exhibit good antifouling behavior when exposed to a halide salt. Zhang, Xiong et al. (2021) incorporated PNIPAM (poly-*N*-isopropyl acrylamide) microgels in polyvinylidene fluoride substrate for fabricating a thermoresponsive TFC membrane. At elevated temperature, the PNIPAM microgels undergo shrinkage leading to decreased tortuosity of the substrate. At higher operating temperature, the modified TFC membrane exhibited remarkably good water flux and reduced reverse salt flux than a pristine TFC membrane at elevated temperatures.

13.8 Commercialization status of the forward osmosis membranes

The preparation of ideal FO membranes is an active research field for academia and several industrial companies (Yadav, Saleem et al., 2020). FO membrane manufacturing and modification has experienced a boom in recent years. To commercialize FO membranes, we first need to identify how much economic value there is in the FO process and the technological obstacles companies must address to commercialize the FO process. For instance, in desalination, we should pay particular attention to the recovery of the draw solution and drawing out the fresh water in the process (Chung, Zhang, Wang, Su, & Ling, 2012). Hydration Technology Innovations (HTI) brought the earliest commercial evolution of FO technology in 2002, for emergency drinking water supply to the US military. The HTI membranes have also explored FO process feasibility for wastewater minimization (Hutchings, Appleton, & McGinnis, 2010; Thompson & Nicoll, 2011). The company HTI has been developing cellulose-based asymmetric membranes on woven/nonwoven support for almost 20 years (Basile, Cassano, & Rastogi, 2015). In 2008, thin-film PA FO membrane was introduced by Osmotic Applications and Systems (Oasys) Water; later, similar membranes were used by Modern Water in 2010 (Awad, Jalab et al., 2019). While Oasys Water has focused on spiral wound configuration, Porifera has mainly focused on developing flat sheet membranes from 2014 (Ren & McCutcheon, 2014, 2018). Further, Toray Industries Korea has developed a spiral wound TFC PA membrane with 85% rejection for salt ions in 2012 (Kim, Blandin et al., 2017). Aquaporin Inside has also prepared a TFC membrane, but they have modified the skin layer with aquaporin proteins. In FO

mode, the prepared membrane shows low reverse salt flux ($4\ g^{-2}\ h^{-1}$) with moderate water flux of 8.8 LMH (Xia, Andersen, Hé lix-Nielsen, & McCutcheon, 2017). In 2017, Aquaporin A/S introduced a new FO hollow fiber (HF) membrane, which offers higher packing density than the spiral wound configuration. Afterwards, Toyobo and Cheil Industries have also developed HF membrane for FO (Lotfi, Phuntsho et al., 2015). Current commercial membrane manufactures and suppliers are listed in Table 13.6. Despite many publications on FO membranes' preparation, industrial applications and commercialization studies are still rare and lacking in details.

13.9 Summary and future directions

It is crucial to have a robust FO membrane of desired specifications for a successful desalination process. A plethora of research is available on new membranes showing excellent performance in the laboratory-scale experiments. However, these membranes either have intricate fabrication process or are too costly to commercialize. Most commercial FO membranes exhibit lower selectivity than the RO process; hence, efficiency is a key factor in improving the FO process. The RO process was suffering from the same drawbacks, such as low water flux, till Sidney Loeb and Srinivasa Sourirajan were able to design high-performing RO membranes in the 1950s. Novel stimulus-responsive membranes using novel and responsive materials demonstrated excellent water flux and low fouling; however, there is a lack of research in this field, probably due to the high cost of such membranes. Therefore only few FO membranes are reported in the literature in this area.

For successful commercialization of FO membranes, their cost should be comparable or cheaper compared to the RO membrane. At present, the FO membrane is at least 4.5 times more expensive than a RO membrane. Further investment is required to reduce the cost of the membrane to promote FO applications (Altaee, Zaragoza, & Sharif, 2014). Another critical issue regarding the FO membrane is a lack of antifouling properties and mechanical strength of newly fabricated membranes. Most of the high-performance FO membranes have a very thin support structure or lower "S" value to alleviate the effects of ICP. Although these ultrathin membranes exhibit excellent performance, they lack the mechanical strength and can be damaged if a small hydraulic pressure builds up across the membrane. Similarly, to achieve a successful commercial FO desalination process, inputs from the industry are required. Water flux and recovery rate of FO membranes are the most significant parameters to be considered before commercialization (Qasim, Darwish, Sarp, & Hilal, 2015).

Further, FO membranes' application for wastewater treatment has been identified as one of the most effective industrial applications. In recent years, the interest in removing various organic matters using the FO processes has risen. In addition to being feasible, the energy and cost advantages of the FO processes must be critically analyzed before going to market. With its potential for low energy consumption and effective recovery system, FO has great promise.

TABLE 13.6 Commercial status of forward osmosis membrane development.

Manufacturer or supplier	Membrane	Flux (LMH)	Specific Flux (LMH/bar)	RSF (g L^{-1})	Structural parameter S (μm)	Contact angle (°)	System	Configuration	Commercial status
Aquaporin A/S	Aquaporin	7	0.15	0.29	NA	TS: 96 ± 5	No	SWo, HF	Commercial
						BS: 35 ± 2			
Modern Water	Undefined	NA	NA	NA	NA	NA	Yes	SWo	Commercial
Oasys Water	TFC	30	0.64	1.67	375	NA	Yes	SWo	Commercial
Porifera	TFC	33	0.70	0.40	215	TS: 65 ± 5	Yes	SWo	Commercial
						BS: 70 ± 5			
Toyobo	NA	NA	NA	NA	NA	NA	No	HF	Commercial
Trevi Systems	NA	NA	NA	NA	NA	NA	Yes	SWo	Commercial
Green Centre Canada	NA	NA	NA	NA	NA	NA	No	SWo	Development
Idaho National Lab	NA	NA	NA	NA	NA	NA	No	NA	Development
Fluid Technology solutions	CTA	12	0.26	0.58	500	TS: 68 ± 2	NA	SWo	Commercial
						BS: 60 ± 5			
Toray	TCK-N	27.59	NA	NA	461	NA	No	SWo	Development
Toray	TCK-W	37.75	NA	NA	266	NA	No	Swo	Development
IDE Technologies	NA	NA	NA	NA	NA	NA	Yes	SWo	Precommercial
Samsung	NA	NA	NA	NA	NA	NA	No	NA	Development
GKSS	Polymeric	NA	NA	NA	NA	NA	No	NA	Development
Fuji	NA	NA	NA	NA	NA	NA	No	NA	Development

CTA, cellulose triacetate; *TFC*, thin-film composite; *NA*, not available; *RSF*, reverse salt flux; *TCK-N*, TCF membrane prepared on polyester nonwoven fabric; *TCK-W*, TFC membrane prepared on a polyester-woven fabric; *TS*, top surface; *BS*, bottom surface; *HF*, hollow fiber; *SWo*, spiral wound.

Data collected from Cath, T.Y., Elimelech, M., McCutcheon, J.R., McGinnis, R.L., Achilli, A., Anastasio, D., ... Hancock, N.T. (2013). Standard methodology for evaluating membrane performance in osmotically driven membrane processes. Desalination, 312, *31–38 (Cath, Elimelech, et al., 2013), Nguyen, T.P.N., Jun, B.-M., Lee, J.H., & Kwon, Y.-N. (2015). Comparison of integrally asymmetric and thin film composite structures for a desirable fashion of forward osmosis membranes.* Journal of Membrane Science, 495, *457–470 (Nguyen, Jun, Lee, & Kwon, 2015), Awad, A.M., Jalab, R., Minier-Matar, J., Adham, S., Nasser, M.S., & Judd, S. (2019). The status of forward osmosis technology implementation.* Desalination, 461, *10–21, and Xia, L., Andersen, M.F., Hélix-Nielsen, C., & McCutcheon, J.R. (2017). Novel commercial aquaporin flat-sheet membrane for forward osmosis.* Industrial & Engineering Chemistry Research, 56*(41), 11919–11925.*

References

Abu Seman, M. N., Khayet, M., Bin Ali, Z. I., & Hilal, N. (2010). Reduction of nanofiltration membrane fouling by UV-initiated graft polymerization technique. *Journal of Membrane Science*, *355*(1), 133–141.

Altaee, A., Zaragoza, G., & Sharif, A. (2014). Pressure retarded osmosis for power generation and seawater desalination: Performance analysis. *Desalination*, *344*, 108–115.

Arjmandi, A., Peyravi, M., Arjmandi, M., & Altaee, A. (2020). Exploring the use of cheap natural raw materials to reduce the internal concentration polarization in thin-film composite forward osmosis membranes. *Chemical Engineering Journal*, 125483.

Awad, A. M., Jalab, R., Minier-Matar, J., Adham, S., Nasser, M. S., & Judd, S. (2019). The status of forward osmosis technology implementation. *Desalination*, *461*, 10–21.

Basile, A., Cassano, A., & Rastogi, N. K. (2015). *Advances in membrane technologies for water treatment: Materials, processes and applications*. Elsevier.

Beh, J., Ooi, B., Lim, J., Ng, E., & Mustapa, H. (2020). Development of high water permeability and chemically stable thin film nanocomposite (TFN) forward osmosis (FO) membrane with poly (sodium 4-styrenesulfonate) (PSS)-coated zeolitic imidazolate framework-8 (ZIF-8) for produced water treatment. *Journal of Water Process Engineering*, *33*, 101031.

Busalmen, J., & De Sanchez, S. (2001). Adhesion of *Pseudomonas fluorescens* (ATCC 17552) to nonpolarized and polarized thin films of gold. *Applied and Environmental Microbiology*, *67*(7), 3188–3194.

Cath, T. Y., Elimelech, M., McCutcheon, J. R., McGinnis, R. L., Achilli, A., Anastasio, D., ... Hancock, N. T. (2013). Standard methodology for evaluating membrane performance in osmotically driven membrane processes. *Desalination*, *312*, 31–38.

Cheng, X., Ding, S., Guo, J., Zhang, C., Guo, Z., & Shao, L. (2017). In-situ interfacial formation of TiO_2/polypyrrole selective layer for improving the separation efficiency towards molecular separation. *Journal of Membrane Science*, *536*, 19–27.

Choi, H.-g, Son, M., & Choi, H. (2017). Integrating seawater desalination and wastewater reclamation forward osmosis process using thin-film composite mixed matrix membrane with functionalized carbon nanotube blended polyethersulfone support layer. *Chemosphere*, *185*, 1181–1188.

Chung, T.-S., Zhang, S., Wang, K. Y., Su, J., & Ling, M. M. (2012). Forward osmosis processes: Yesterday, today and tomorrow. *Desalination*, *287*, 78–81.

Cruz-Tato, P., Rivera-Fuentes, N., Flynn, M., & Nicolau, E. (2019). Anti-fouling electroconductive forward osmosis membranes: Electrochemical and chemical properties. *ACS Applied Polymer Materials*, *1*(5), 1061–1070.

Daer, S., Akther, N., Wei, Q., Shon, H. K., & Hasan, S. W. (2020). Influence of silica nanoparticles on the desalination performance of forward osmosis polybenzimidazole membranes. *Desalination*, *491*, 114441.

Darvishmanesh, S., Qian, X., & Wickramasinghe, S. R. (2015). Responsive membranes for advanced separations. *Current Opinion in Chemical Engineering*, *8*, 98–104.

Dong, G., Li, H., & Chen, V. (2013). Challenges and opportunities for mixed-matrix membranes for gas separation. *Journal of Materials Chemistry A*, *1*(15), 4610–4630.

Duval, J.-M., Folkers, B., Mulder, M., Desgrandchamps, G., & Smolders, C. (1993). Adsorbent filled membranes for gas separation. Part 1. Improvement of the gas separation properties of polymeric membranes by incorporation of microporous adsorbents. *Journal of Membrane Science*, *80*(1), 189–198.

Engelhardt, S., Sadek, A., & Duirk, S. (2018). Rejection of trace organic water contaminants by an Aquaporin-based biomimetic hollow fiber membrane. *Separation and Purification Technology*, *197*, 170–177.

Eyvaz, M., Arslan, S., İmer, D., Yüksel, E., & Koyuncu, İ. (2018). *Forward osmosis membranes—A review: Part I. Osmotically driven membrane processes—Approach, development and current status*. IntechOpen.

Fryčová, M., Sysel, P., Kočiřík, M., Brabec, L., Hrabánek, P., Prokopová, O., ... Zikánová, A. (2012). Mixed matrix membranes based on 3-aminopropyltriethoxysilane endcapped polyimides and silicalite-1. *Journal of Applied Polymer Science*, *124*(S1), E233–E240.

Galizia, M., Chi, W. S., Smith, Z. P., Merkel, T. C., Baker, R. W., & Freeman, B. D. (2017). 50th anniversary perspective: Polymers and mixed matrix membranes for gas and vapor separation: A review and prospective opportunities. *Macromolecules*, *50*(20), 7809–7843.

Grylewicz, A., & Mozia, S. (2020). Polymeric mixed-matrix membranes modified with halloysite nanotubes for water and wastewater treatment: A review. *Separation and Purification Technology*, 117827.

He, M., Wang, L., Lv, Y., Wang, X., Zhu, J., Zhang, Y., ... Liu, T. (2020). Novel polydopamine/metal organic framework thin film nanocomposite forward osmosis membrane for salt rejection and heavy metal removal. *Chemical Engineering Journal*, *389*, 124452.

Hilal, N., Al-Khatib, L., Atkin, B. P., Kochkodan, V., & Potapchenko, N. (2003). Photochemical modification of membrane surfaces for (bio)fouling reduction: A nano-scale study using AFM. *Desalination*, *158*(1), 65–72.

Himstedt, H. H., Marshall, K. M., & Wickramasinghe, S. R. (2011). pH-responsive nanofiltration membranes by surface modification. *Journal of Membrane Science*, *366*(1), 373–381.

Hong, S. U., Malaisamy, R., & Bruening, M. L. (2006). Optimization of flux and selectivity in Cl^-/SO_4^{2-} separations with multilayer polyelectrolyte membranes. *Journal of Membrane Science*, *283*(1–2), 366–372.

Hudiono, Y. C., Carlisle, T. K., Bara, J. E., Zhang, Y., Gin, D. L., & Noble, R. D. (2010). A three-component mixed-matrix membrane with enhanced CO_2 separation properties based on zeolites and ionic liquid materials. *Journal of Membrane Science*, *350*(1–2), 117–123.

Hutchings, N. R., Appleton, E. W., & McGinnis, R. A. (2010). Making high quality frac water out of oilfield waste. In *SPE annual technical conference and exhibition*. Society of Petroleum Engineers.

Jin, L., Wang, Z., Zheng, S., & Mi, B. (2018). Polyamide-crosslinked graphene oxide membrane for forward osmosis. *Journal of Membrane Science*, *545*, 11–18.

Kademoglou, K., Williams, A. C., & Collins, C. D. (2018). Bioaccessibility of PBDEs present in indoor dust: A novel dialysis membrane method with a Tenax TA® absorption sink. *Science of The Total Environment*, *621*, 1–8.

Kang, H., Wang, W., Shi, J., Xu, Z., Lv, H., Qian, X., ... Niu, J. (2019). Interlamination restrictive effect of carbon nanotubes for graphene oxide forward osmosis membrane via layer by layer assembly. *Applied Surface Science*, *465*, 1103–1106.

Kim, J., Blandin, G., Phuntsho, S., Verliefde, A., Le-Clech, P., & Shon, H. (2017). Practical considerations for operability of an 8″ spiral wound forward osmosis module: Hydrodynamics, fouling behaviour and cleaning strategy. *Desalination*, *404*, 249–258.

Klaysom, C., & Shahid, S. (2019). Zeolite-based mixed matrix membranes for hazardous gas removal. In *Advanced nanomaterials for membrane synthesis and its applications* (pp. 127–157). Elsevier.

Kolasinska, M., Krastev, R., Gutberlet, T., & Warszynski, P. (2009). Layer-by-layer deposition of polyelectrolytes. Dipping versus spraying. *Langmuir: The ACS Journal of Surfaces and Colloids*, *25*(2), 1224–1232.

Kusworo, T. D., Ismail, A. F., Mustafa, A., & Matsuura, T. (2008). Dependence of membrane morphology and performance on preparation conditions: The shear rate effect in membrane casting. *Separation and Purification Technology*, *61*(3), 249–257.

Lee, J.-Y., Wang, Y., Tang, C. Y., & Huo, F. (2015). Mesoporous silica gel–based mixed matrix membranes for improving mass transfer in forward osmosis: Effect of pore size of filler. *Scientific Reports*, *5*, 16808.

Lewis, J., Al-sayaghi, M. A., Buelke, C., & Alshami, A. (2019). Activated carbon in mixed-matrix membranes. *Separation & Purification Reviews*, 1–31.

Li, C., Guo, X., Wang, X., Fan, S., Zhou, Q., Shao, H., ... Kumar, R. R. (2018). Membrane fouling mitigation by coupling applied electric field in membrane system: Configuration, mechanism and performance. *Electrochimica Acta*, *287*, 124–134.

Li, Z., Linares, R. V., Bucs, S., Fortunato, L., Hélix-Nielsen, C., Vrouwenvelder, J. S., ... Amy, G. (2017). Aquaporin based biomimetic membrane in forward osmosis: Chemical cleaning resistance and practical operation. *Desalination*, *420*, 208–215.

Liu, Q., Qiu, G., Zhou, Z., Li, J., Amy, G. L., Xie, J., & Lee, J. Y. (2016). An effective design of electrically conducting thin-film composite (TFC) membranes for bio and organic fouling control in forward osmosis (FO). *Environmental Science & Technology*, *50*(19), 10596–10605.

Liu, X., & Ng, H. Y. (2015). Fabrication of layered silica–polysulfone mixed matrix substrate membrane for enhancing performance of thin-film composite forward osmosis membrane. *Journal of Membrane Science*, *481*, 148–163.

Liu, Z., & Hu, Y. (2016). Sustainable antibiofouling properties of thin film composite forward osmosis membrane with rechargeable silver nanoparticles loading. *ACS Applied Materials & Interfaces*, *8*(33), 21666–21673.

Lotfi, F., Phuntsho, S., Majeed, T., Kim, K., Han, D. S., Abdel-Wahab, A., ... Shon, H. K. (2015). Thin film composite hollow fibre forward osmosis membrane module for the desalination of brackish groundwater for fertigation. *Desalination*, *364*, 108–118.

Ma, N., Wei, J., Liao, R., & Tang, C. Y. (2012). Zeolite-polyamide thin film nanocomposite membranes: Towards enhanced performance for forward osmosis. *Journal of Membrane Science*, *405*, 149–157.

Mahajan, R., Burns, R., Schaeffer, M., & Koros, W. J. (2002). Challenges in forming successful mixed matrix membranes with rigid polymeric materials. *Journal of Applied Polymer Science*, *86*(4), 881–890.
Meng, J., Cao, Z., Ni, L., Zhang, Y., Wang, X., Zhang, X., & Liu, E. (2014). A novel salt-responsive TFC RO membrane having superior antifouling and easy-cleaning properties. *Journal of Membrane Science*, *461*, 123–129.
Miao, L., Tu, Y., Yang, Y., Lin, S., Hu, J., Zhang, M., … Mo, Y. (2017). Robust stimuli-responsive membranes prepared from a blend of polysulfone and a graft copolymer bearing binary side chains with thermo- and pH-responsive switching behavior. *Chemistry – A European Journal*, *23*(32), 7737–7747.
Moghadam, F., Lee, T. H., Park, I., & Park, H. B. (2020). Thermally annealed polyimide-based mixed matrix membrane containing ZIF-67 decorated porous graphene oxide nanosheets with enhanced propylene/propane selectivity. *Journal of Membrane Science*, 118019.
Nguyen, T. P. N., Jun, B.-M., Lee, J. H., & Kwon, Y.-N. (2015). Comparison of integrally asymmetric and thin film composite structures for a desirable fashion of forward osmosis membranes. *Journal of Membrane Science*, *495*, 457–470.
Nikolaeva, D., & Luis, P. (2020). Top-down polyelectrolytes for membrane-based post-combustion CO_2 capture. *Molecules*, *25*(2), 323.
Pan, S.-F., Ke, X.-X., Wang, T.-Y., Liu, Q., Zhong, L.-B., & Zheng, Y.-M. (2018). Synthesis of silver nanoparticles embedded electrospun PAN nanofiber thin-film composite forward osmosis membrane to enhance performance and antimicrobial activity. *Industrial & Engineering Chemistry Research*, *58*(2), 984–993.
Pendergast, M. M., & Hoek, E. M. (2011). A review of water treatment membrane nanotechnologies. *Energy & Environmental Science*, *4*(6), 1946–1971.
Qadir, D., Mukhtar, H., & Keong, L. K. (2017). Mixed matrix membranes for water purification applications. *Separation & Purification Reviews*, *46*(1), 62–80.
Qasim, M., Darwish, N. A., Sarp, S., & Hilal, N. (2015). Water desalination by forward (direct) osmosis phenomenon: A comprehensive review. *Desalination*, *374*, 47–69.
Qiu, M., & He, C. (2019). Efficient removal of heavy metal ions by forward osmosis membrane with a polydopamine modified zeolitic imidazolate framework incorporated selective layer. *Journal of Hazardous Materials*, *367*, 339–347.
Rastgar, M., Bozorg, A., Shakeri, A., & Sadrzadeh, M. (2019). Substantially improved antifouling properties in electro-oxidative graphene laminate forward osmosis membrane. *Chemical Engineering Research and Design*, *141*, 413–424.
Ren, J., & McCutcheon, J. R. (2014). A new commercial thin film composite membrane for forward osmosis. *Desalination*, *343*, 187–193.
Ren, J., & McCutcheon, J. R. (2018). A new commercial biomimetic hollow fiber membrane for forward osmosis. *Desalination*, *442*, 44–50.
Rezaei-DashtArzhandi, M., Sarrafzadeh, M. H., Goh, P. S., Lau, W. J., Ismail, A. F., Wong, K. C., … Mohamed, M. A. (2020). Enhancing the desalination performance of forward osmosis membrane through the incorporation of green nanocrystalline cellulose and halloysite dual nanofillers. *Journal of Chemical Technology & Biotechnology*.
Rezaei-DashtArzhandi, M., Sarrafzadeh, M., Goh, P., Lau, W., Ismail, A., & Mohamed, M. (2018). Development of novel thin film nanocomposite forward osmosis membranes containing halloysite/graphitic carbon nitride nanoparticles towards enhanced desalination performance. *Desalination*, *447*, 18–28.
Salehi, H., Shakeri, A., Mahdavi, H., & Lammertink, R. G. H. (2020). Improved performance of thin-film composite forward osmosis membrane with click modified polysulfone substrate. *Desalination*, *496*, 114731.
Salehi, H., Rastgar, M., & Shakeri, A. (2017). Anti-fouling and high water permeable forward osmosis membrane fabricated via layer by layer assembly of chitosan/graphene oxide. *Applied Surface Science*, *413*, 99–108.
Samieirad, S., Mousavi, S. M., & Saljoughi, E. (2020). Alignment of functionalized multiwalled carbon nanotubes in forward osmosis membrane support layer induced by electric and magnetic fields. *Powder Technology*, *364*, 538–552.
Shakeri, A., Salehi, H., & Rastgar, M. (2017). Chitosan-based thin active layer membrane for forward osmosis desalination. *Carbohydrate Polymers*, *174*, 658–668.
Shevate, R., Karunakaran, M., Kumar, M., & Peinemann, K.-V. (2016). Polyanionic pH-responsive polystyrene-b-poly(4-vinyl pyridine-N-oxide) isoporous membranes. *Journal of Membrane Science*, *501*, 161–168.
Shi, J., Kang, H., Li, N., Teng, K., Sun, W., Xu, Z., … Liu, Q. (2019). Chitosan sub-layer binding and bridging for nanofiber-based composite forward osmosis membrane. *Applied Surface Science*, *478*, 38–48.
Sun, W., Shi, J., Chen, C., Li, N., Xu, Z., Li, J., … Zhao, L. (2018). A review on organic–inorganic hybrid nanocomposite membranes: A versatile tool to overcome the barriers of forward osmosis. *RSC Advances*, *8*(18), 10040–10056.

Tajik, S., Moini Jazani, O., Shokrollahzadeh, S., & Latifi, S. M. (2016). Thin film nanocomposite forward osmosis membrane prepared by graphene oxide embedded PSf substrate. *Journal of Particle Science & Technology*, *2*(2), 103–117.

Thompson, N. A., & Nicoll, P. G. (2011). Forward osmosis desalination: A commercial reality. In *IDA world congress*. Perth Convention and Exhibition Centre (PCEC), Perth, Western Australia.

Van der Borden, A., Van der Mei, H., & Busscher, H. (2005). Electric block current induced detachment from surgical stainless steel and decreased viability of Staphylococcus epidermidis. *Biomaterials*, *26*(33), 6731–6735.

Wandera, D., Wickramasinghe, S. R., & Husson, S. M. (2010). Stimuli-responsive membranes. *Journal of Membrane Science*, *357*(1), 6–35.

Wang, M., An, Q.-F., Wu, L.-G., Mo, J.-X., & Gao, C.-J. (2007). Preparation of pH-responsive phenolphthalein poly (ether sulfone) membrane by redox-graft pore-filling polymerization technique. *Journal of Membrane Science*, *287*(2), 257–263.

Wu, W., Shi, Y., Liu, G., Fan, X., & Yu, Y. (2020). Recent development of graphene oxide based forward osmosis membrane for water treatment: A critical review. *Desalination*, *491*, 114452.

Xia, L., Andersen, M. F., Hélix-Nielsen, C., & McCutcheon, J. R. (2017). Novel commercial aquaporin flat-sheet membrane for forward osmosis. *Industrial & Engineering Chemistry Research*, *56*(41), 11919–11925.

Xu, G.-R., Wang, S.-H., Zhao, H.-L., Wu, S.-B., Xu, J.-M., Li, L., … Liu, X.-Y. (2015). Layer-by-layer (LBL) assembly technology as promising strategy for tailoring pressure-driven desalination membranes. *Journal of Membrane Science*, *493*, 428–443.

Xu, L., Yang, T., Li, M., Chang, J., & Xu, J. (2020). Thin-film nanocomposite membrane doped with carboxylated covalent organic frameworks for efficient forward osmosis desalination. *Journal of Membrane Science*, 118111.

Yadav, S., Saleem, H., Ibrar, I., Naji, O., Hawari, A. A., Alanezi, A. A., … Zhou, J. (2020). Recent developments in forward osmosis membranes using carbon-based nanomaterials. *Desalination*, *482*, 114375.

Yuan, Q., & Zhu, G. (2020). A review on metal organic frameworks (MOFs) modified membrane for remediation of water pollution. *Environmental Engineering Research*, *26*(3), 190435.

Zhang, R., Su, Y., Zhao, X., Li, Y., Zhao, J., & Jiang, Z. (2014). A novel positively charged composite nanofiltration membrane prepared by bio-inspired adhesion of polydopamine and surface grafting of poly (ethylene imine). *Journal of Membrane Science*, *470*, 9–17.

Zhang, X., Tian, J., Gao, S., Shi, W., Zhang, Z., Cui, F., … Liu, D. (2017). Surface functionalization of TFC FO membranes with zwitterionic polymers: Improvement of antifouling and salt-responsive cleaning properties. *Journal of Membrane Science*, *544*, 368–377.

Zhang, X., Xiong, S., Liu, C.-X., Shen, L., Wang, S.-L., Lang, W.-Z., … Wang, Y. (2021). Smart TFC membrane for simulated textile wastewater concentration at elevated temperature enabled by thermal-responsive microgels. *Desalination*, *500*, 114870.

Zhao, C., Nie, S., Tang, M., & Sun, S. (2011). Polymeric pH-sensitive membranes—A review. *Progress in Polymer Science*, *36*(11), 1499–1520.

Zornoza, B., Téllez, C., & Coronas, J. (2011). Mixed matrix membranes comprising glassy polymers and dispersed mesoporous silica spheres for gas separation. *Journal of Membrane Science*, *368*(1–2), 100–109.

Zornoza, B., Tellez, C., Coronas, J., Gascon, J., & Kapteijn, F. (2013). Metal organic framework based mixed matrix membranes: An increasingly important field of research with a large application potential. *Microporous and Mesoporous Materials*, *166*, 67–78.

Zou, S., Qin, M., & He, Z. (2019). Tackle reverse solute flux in forward osmosis towards sustainable water recovery: Reduction and perspectives. *Water Research*, *149*, 362–374.

CHAPTER

14

Electrodialysis, electrodialysis reversal and capacitive deionization technologies

Tatiane Benvenuti[1], *Alexandre Giacobbo*[2], *Carolina de Moraes da Trindade*[3], *Kayo Santana Barros*[2] *and Tatiana Scarazzato*[2]

[1]Science, Innovation, and Modeling in Materials Post-Graduation Programm – PROCIMM, Department of Exact and Technologic Sciences, State University of Santa Cruz – UESC, Ilhéus, Brazil [2]Department of Materials Engineering, Federal University of Rio Grande do Sul - UFRGS, Porto Alegre, Brazil [3]Federal Institute of Pará -IFPA - Campus Óbidos, Óbidos, Brazil

14.1 Introduction

A broad range of water remediation technologies have been developed in the last decades (Campione, Cipollina, & Bogle, 2019). Among which electromembrane processes have gained prominence in predesalination, desalination, and brine treatment (Koseoglu-Imer & Karagunduz, 2018); as well as in the management of wastewater from mining (Martí-Calatayud, Buzzi & García-Gabaldón, 2014), electroplating (Benvenuti, Siqueira Rodrigues, Bernardes, & Zoppas-Ferreira, 2017; da Trindade, Giacobbo, Ferreira, Rodrigues, & Bernardes, 2015), petrochemical (Venzke, Giacobbo, Ferreira, Bernardes, & Rodrigues, 2018), pharmaceutical (Ravikumar, Sridhar, & Satyanarayana, 2013), and pulp and paper (Souza, Benvenuti, Buzzi, Rodrigues, & Amado, 2020) industries, in addition to the preparation of ultrapure water (Lee & Choi, 2012), and water (Bacher, de Oliveira, & Giacobbo, 2017) and sewage (Albornoz, Marder, Benvenuti, & Bernardes, 2019) processing.

In fact, electromembrane processes are an increasingly important group of separation methods, widely used for the removal of charged components from solutions. The separation is

Advancement in Polymer-Based Membranes for Water Remediation
DOI: https://doi.org/10.1016/B978-0-323-88514-0.00014-0

© 2022 Elsevier Inc. All rights reserved.

based on ion migration across ion-exchange membranes (IEMs), that is, charged membranes (a polymeric matrix with fixed charged groups, counterbalanced with mobile counter-ions), placed in an electric field. Thus the IEMs are the key components of electromembrane processes (Mitko & Turek, 2015).

A precursor of the electromembrane processes is electrodialysis (ED), and it has been researched since 1930s. However, the main applications started in 1960s; and the improvement achieved by polarity reversion with electrodialysis reversal (EDR) appeared only in 1970s. EDR development is very important for water treatment and low-conductivity wastewater. The changes and advances in ED will be presented in topic 14.3. For both ED and EDR, the number of publications in the last 20 years has been expressively increased, reporting from water treatment to different wastewater treatment and materials recovery (Bernardes, Rodrigues, Zoppas, & Ferreira, 2014).

The origin of the IEMs was the ion-exchange resins. Presenting superior advantages, the membranes do not demand chemicals for regeneration; while for the resin, a large volume of water and chemicals are needed to clean it. When ED is applied aiming to remove some components to very low values in water and wastewater treatment, aiming to meet legal parameters for drinking or discharge, respectively, the association of ED and ion-exchange resins may be effective. Similar to ED, the publications about electrodeionization (EDI) in the last 10 years have increased (Koseoglu-Imer & Karagunduz, 2018).

The development of IEMs—presented in topic 14.2 of this chapter—allowed the modification of ED to recover products by applying bipolar membranes (BPMs). About this theme, 112 documents are listed in the Scopus database since 1984. However, the last 10 years revealed the growing interest in the association of ED and BPMs for water and also wastewater treatment, recovering materials (Handojo, Wardani, Regina, & Bella, 2019). Additional advances in membrane synthesis allow the selectivity for specific ionic charges, improving the efficiency of ED, presented by some researchers as selective ED (Reig, Vecino, Valderrama, Gibert, & Cortina, 2018).

Electrochemical reactions using porous electrodes associated with IEMs opened a new electromembrane process. From capacitive deionization techniques, the addition of membranes allows an alternative process for water and wastewater treatment, water recovery, and chemical savings reported since 2005 and increasing (Van Limpt & van der Wal, 2014).

Electromembrane processes have also been applied for organic acid recovery/production, associated with fermentation processes, allowing effectiveness in recovery rates and product purity. The number of publications related to this application has been increased since 2000s, highlighting advantages as high yield and without the requirement of solvent addition, commonly mandatory in conventional acid recovery processes (Handojo et al., 2019).

To understand how electromembrane processes are able to treat water, wastewater, recover materials, and produce clean water for industrial and human consumption, an explanation about IEMs, the key piece of electromembrane processes, its structure and properties, is reported in the next section. Following, this chapter will present an overview of the main electromembrane processes used for water remediation, that is, for the treatment of water and wastewater. The processes were evaluated on theoretical and technological backgrounds, presenting and discussing aspects such as applications, operating principles, configurations and flow patterns, limitations and main mitigation strategies, transport equations, as well as the commercial viability of these technologies and their prospects for future directions.

14.2 Structure of ion-exchange membranes

In the membrane process for water or wastewater treatment with IEMs, such as ED and EDR, the IEMs are the main components of the system that must comply with the desired degree of treatment. The IEMs must have properties that demonstrate their efficiency in use in the above-mentioned processes: high permselectivity, low electrical resistance, high mechanical and chemical resistance, and low water diffusion. The selectivity and ion transfer of the IEMs may cause limitations in electromembrane processes. These two characteristics are affected by the affinity between the ions and the membrane exchange groups, the concentration of the exchange groups, ion valence, electrolyte concentration, membrane hydrophobicity, degree of membrane cross-linking, and morphology (Kim, Kim & Kwak, 2021; Lee, Meng, & Wang, 2021).

IEMs used in electromembrane processes are classified into three main groups: cation-exchange membranes (CEMs), anion-exchange membranes (AEMs), and BPMs. This classification depends on ionic groups attached to the membrane matrix. Other membrane groups are the monovalent ion permselective membranes and mixed matrix membranes (Liao, Chen, & Pan, 2020).

The ED membranes are effectively ion-exchange resins in a laminar form with specific permselectivity for ions. The CEMs present negative functional groups at the polymeric matrix, while the AEMs present positive functional groups. These functional groups are directly related to the flow of ions present in solution through the membranes by electrostatic interactions (Ran, Wu, & He, 2017).

According to the functional group, the IEMs may have specific developments for particular applications: monoselective membranes (selective only to monovalent ions, retaining upper valence ions) and BPMs (developed for the salt production by acid and basic compounds). In the last type, the IEM present in one face is an AEM and, in the other, a CEM (Irfan, Xu, Ge, Wang, & Xu, 2019.

The matrix of an IEM can be polymeric (organic), nonpolymeric (inorganic), or hybrid (organic−inorganic). For the manufacture of polymeric IEM, cellulose acetate, polysufoned, polyethersulfonated, polyacrylonitrile, polyetherimide, and polycarbonate are generally used. Nonpolymeric materials, on the other hand, usually consist of ceramic material, carbon, metal oxides, and metals; while the hybrid membranes are a mix of polymeric and nonpolymeric material (Ran et al., 2017).

Another classification to IEM is homogeneous or heterogeneous, illustrated in Fig. 14.1. This classification is made according to the distribution of charges by the structure of the film and the method of preparing the membrane (Lee et al., 2021).

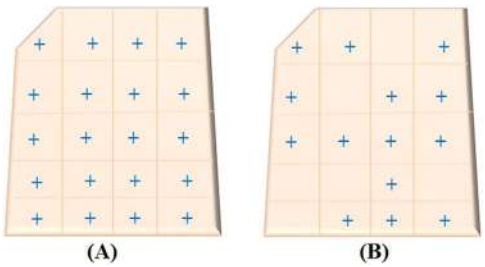

FIGURE 14.1 Schematic representation of functional groups distribution in (A) homogeneous membrane and (B) heterogeneous membrane.

The main characteristics of homogeneous IEM are high mechanical strength, excellent permselectivity, and low electrical resistance when compared to heterogeneous membranes. Homogeneous membranes present functional groups inserted in the polymeric matrix due to the process used for membrane synthesis. The functional groups, which are responsible for the cation- or anion-exchange, or both (bipolar) characters of the membranes, are directly fixed to the polymer by chemical reactions. In this case, as the ions are added directly to the polymeric matrix structure of the membrane, the charges are arranged more evenly throughout the film, so its character is homogeneous (Lee et al., 2021).

The insertions of the functional groups can be done in three ways. The first is the copolymerization of a monomer containing anionic or cationic groups with a nonfunctionalized monomer. Another possibility is the introduction of functional groups directly into a polymeric film by inserting a functional or nonfunctional monomer, followed by a functionalization reaction. The third is the introduction of functional groups in a solid polymer or polymer blends subsequently dissolved in a solvent and processed into a film (Shukla & Shahi, 2019).

Homogeneous CEMs can be obtained by first monomer polymerization with subsequent sulfonation reaction, while AEMs can be obtained by introducing functional groups in two steps—first by the chloromethylation reaction and subsequent quaternary amination reaction (Vogel 7 Meier-Haack, 2014).

The heterogeneous IEM uses polyvinyl chloride (PVC), polyethylene, fluorinated polymers, or phenolic resins as support (polymeric matrix) (Bazrgar Bajestani, Moheb, & Dinari, 2020; Vogel & Meier-Haack, 2014; Zabolotskii, Sheldeshov, & Melnikov, 2014). The manufacture of these membranes can be by mixing a base polymer with an ion-exchange resin in an extruder and subsequent pressing to form the membrane. Other possibility is by dispersing the ion-exchange resin or polymer that presents exchange groups in powder form in a polymer solution (the membrane is created after evaporation of the solvent—casting method). In addition, the membrane manufacture can be by fusion or compression of the resin with the polymeric matrix (Ran et al., 2017; Vogel & Meier-Haack, 2014; Xu, 2005).

The conductive phase of the homogeneous and/or heterogeneous membranes is responsible for allowing the ion transport from one side of the membrane to the other. For this purpose, the ion transfer occurs in homogeneous membranes due to groups chemically inserted into the polymeric matrix; and in heterogeneous ones, due to the presence of ion-exchange resin particles dispersed in the base polymer (Fan, Huang, & Yip, 2020).

When producing the heterogeneous IEM, or when choosing the membrane to use in ED or EDR processes, it is interesting to know that some species have a high affinity for the resin/polymeric matrix/backbone polymer, such as F^{-}, Cl^{-}, HCO_3^{-}, SO_4^{-2}, $HSiO^{-3}$, Li^{+}, Na^{+}, K^{+}, Mg^{+2}, Ca^{+2}, Al^{+3}, and Fe^{+3}. This affinity makes the transportation of these ions through the membrane difficult (Ferreira, Müller, & Amado, 2014).

IEMs can present in their structure conductive and/or conventional polymers. The advantage of using conductive polymers in IEMs is the fact that the transport properties can be reversibly altered. Another attraction of this type of material in the manufacture of membranes is the wettability and selectivity characteristics (Ferreira et al., 2014).

Conductive polymers are organic materials able to conduct the electric current. Also known as synthetic metals, conductive polymers can combine mechanical properties

and processability of conventional polymers with electrical, optical, and magnetic behavior similar to that of metals and inorganic semiconductors (Pärnamäe, Mareev, & Nikonenko, 2021).

The molecular structure of this material forms a conjugated system of alternating double and single bonds between the carbon atoms of the polymer. This phenomenon confers a difference between the conductive properties of conjugated polymers, doped or nondoped, of polymers with saturated chains (only simple bonds in carbon atoms chains) (Ferreira et al., 2014).

The polymers used for ion-selective membranes synthesis, after preparation procedure, present cross-linked bonds and pores/channels with molecular level sizes. These characteristics allow no significant water flow, even under pressure, but allow the ion flow (Ran et al., 2017).

The pores/channels present inside the membrane, forming an interconnected network (cross-linked) provide the ionic conduction from one side to the other of the membrane. This pores'/channels' network has groups assigned positive (AEMs) or negative (CEMs), or both (BPMs) chemically linked to the polymeric matrix (Pärnamäe et al., 2021; Ran et al., 2017; Xu, 2005).

The main functional groups (ions chemically linked to the polymeric matrix) at CEMs are: $-SO_3^-$, $-COO^-$, $-PO_3^{-2}$, $-PO_3H^-$, $-C_6H_4O^-$, $-SeO_3^-$, and $-AsO_3^{-2}$; therefore this type of membrane allows the passage of positive ions [cations (counter-ions)] and retains negative ions [anions (co-ions)]. AEMs have the main functional groups $-NH_3^+$, $-RNH_2^+$, $-R_2NH^+$, $-NR_3^+$, $-PR_3^+$, and $-SR_2^+$; so, contrary to CEM, AEMs allow the passage of ions with negative charges (counter-ions) and retain positively charged ions (co-ions) (Ferreira et al., 2014; Ran et al., 2017). A CEM structure is represented in Fig. 14.2

Morphology is one structural characteristic that can be analyzed in membranes used at separation processes, classifying them in dense or porous (Liao et al., 2019; Strathmann, 2011). The IEMs used in ED or EDR are classified as dense membranes, because of the presence of interconnected pores or channels, with angstroms sizes, that promote one of the main characteristics of IEMs: prevent the water transport through membrane channels. The water that can flow through the IEMs is the ion hydration water (solvation). It gives us an idea about the maximum molecule size that can flow through the channels of the IEMs (Díaz & Kamcev, 2021; Mareev, Evdochenko, & Wessling, 2020).

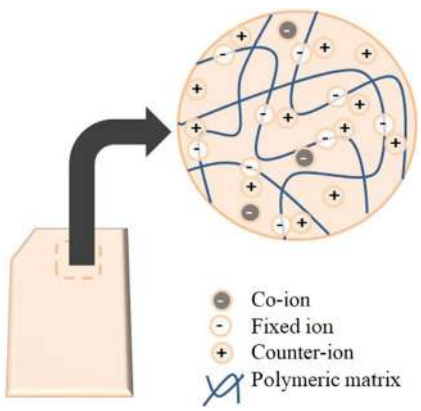

FIGURE 14.2 Representation of cation-exchange membrane (CEM) internal structure.

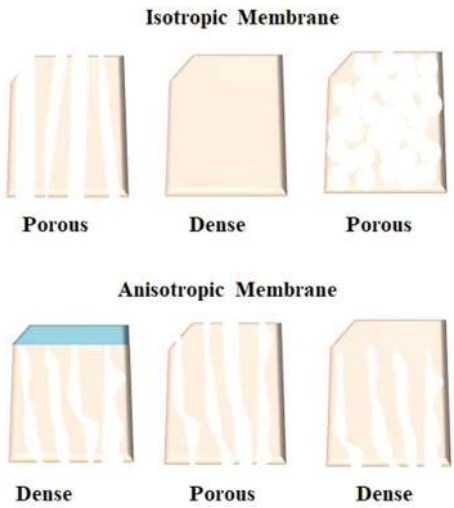

FIGURE 14.3 Schematic representation of isotropic and anisotropic membranes.

Dense IEMs can be isotropic or anisotropic, as schematically represented in Fig. 14.3. Anisotropic membranes are characterized by an upper (superficial) region around 1 μm thickness, with or without pores, supported on the membrane structure (polymeric matrix). When both regions are made of one material, the membrane is integral anisotropic. If different materials are used in the preparation of each region, the membrane will be composite anisotropic. In dense membranes, the physicochemical characteristics of the polymer, thickness of the polymeric film, as well as type and method of functionalization are important parameters (Ferreira et al., 2014; Mareev et al., 2020).

The development of new materials and methods for the modification of IEMs have been enough explored within the scientific field. The modification in the membrane structure aims to promote better selectivity; less electrical resistance; and good chemical, mechanical, and thermal stability. Ways to obtaining superior IEMs include the use of various additives, the variation of functional groups, alteration of cross-link density and surface modifications, selection of different polymeric matrices, and polymer blending. These characteristics promote new areas of activity for the treatment processes that use IEMs (Ahangar & Mir, 2020; Shukla & Shahi, 2019).

IEMs are usually composed of hydrophobic substrates, groups functionalized with immobilized ions, and mobile counter-ions, and are classified into two large groups: CEMs and AEMs (Chen, Zhang, Liu, & Jian, 2021; Ferreira et al., 2014; Strathmann, 2011).

After the penetration of sufficient water molecules, the ion-functionalized groups attached to the IEMs will dissociate and cations or anions are released for the transfer of corresponding ions. The most common functional groups in CEMs contain sulfonic acid, phosphoric acid, and carboxylic acid groups. In AEMs, the quaternary ammonium cations, imidazole cations, and guanidinium cations are generally anchored onto the polymer backbones (Chen et al., 2021).

IEMs can be used to solve problems associated with energy and the environment. Several electrochemical technologies use IEMs, such as polymer electrolyte membrane,

fuel cells, redox flow batteries, reverse ED cells, and water electrolysis. These technologies separate and transport ions between the anode and the cathode to balance the electron flow in the external circuit, directly relating IEMs to the creation of new renewable energy sources. Specifically, in ED, IEMs are part of the system for the concentration or dilution of aqueous or nonaqueous electrolyte systems and in the diffusion-dialysis to recover acid or alkali from acid waste/residues or alkaline solutions (İpekçi, Kabay, & Bunani, 2020; Shukla & Shahi, 2019).

Several researchers have been dedicated to the development of new IEMs or the modification of original IEMs. Particularly, with the rapid progress in nanoscience, the regulation and control of polymeric structures favor the formation of ion channels, which is a new development in this field (Chen et al., 2021; Fan et al., 2020; İpekçi et al., 2020; Shukla & Shahi, 2019).

Most IEMs consist of polymeric backbones prepared by either polymerization of preexisting polymers or direct polymerization of functional monomers. To convert the prepared polymers into IEMs, suitable membrane-forming techniques are required. In the field of IEMs, materials, preparation methods and final applications are crucial to improve the quality of IEMs. Then, IEMs with excellent qualities can be mounted on various devices and processes. (Ran et al., 2017).

14.2.1 Anion-exchange membranes

AEMs are designed to conduct anions while being impermeable to neutral species and/or cations. The properties required for AEMs are good anion conductivity, good chemical stability (main problem found in AEMs), and good dimensional stability, which has a direct relationship with the positively charged polyelectrolytes present in the membrane structure and with the architecture and structure of the polymeric matrix (Hosseini, Jeddi, Nemati, Madaeni, & Moghadassi, 2014; Ran et al., 2017).

The AEMs are classified as AEMs with new cationic head groups (De Schepper, Moraru, Jacobs, Oudshoorn, & Helsen, 2019; Fan et al., 2020) and AEMs with new polymer architecture (Shen, Sana, & Pu, 2020; Zhu et al., 2016). The study of the synthesis of new anion-conducting groups (ACGs) and the design of a particular polymer architecture are two branches of research that aims to improve the characteristics present in existing AEMs and develop new properties (to expand the use of AEMs) (Kotoka, Merino-Garcia, & Velizarov, 2020).

14.2.2 Cation-exchange membranes

The most reported types of CEMs are block CEMs, side chain type CEMs, comb-shaped CEMs, and densely functionalized CEMs. Several polymeric materials to be used as backbones for CEMs have already been investigated, as the overall performance of CEMs is directly affected by the organizational architecture of the polymer. Examples of polymeric materials used include: polyethersulfone (PES), polyether ketone (PEK), polybenzimidazole (PBI), polyimide (PI), polyphenylene, polyphosphazene, and polyvinylidene fluoride (PVDF); all of these showing the presence of sulfonic acid groups, phosphoric acid groups, sulfonamides, and azole derivatives—characteristic species present in CEMs (Bazrgar Bajestani et al., 2020; Zhao, Ren, Chen, Li, & Wang, 2020).

14.2.3 Bipolar membranes

Bipolar membranes are a special polymeric membrane class of IEMs constituted by two layers—a negatively charged cation-exchange layer (CEL) and a positively charged anion-exchange layer (AEL). The interface between CEL and AEL is referred to as bipolar junction (Pärnamäe et al., 2021; Ran et al., 2017).

In contrast to CEMs and AEMs, the main function of a BPM is to electrodissociate water into protons and hydroxide ions at the bipolar junction, without any gas formation. BPMs are gaining attention for the production of acid and base and local pH control due to their technical, environmental, and economical advancements compared to conventional processes (İpekçi et al., 2020; Liao et al., 2020; Ran et al., 2017).

The electrochemical properties of a BPM are mainly determined by the properties/characteristics presented by each layer of the BPM (Ferreira et al., 2014; Liu & Wang, 2020).

Commercial BPMs have AEL with quaternary ammonium groups in a polystyrene matrix and the CEL with sulfonic acid groups; some have phosphonic acid groups and, recently, membranes with carboxyl groups have appeared in the market (Kotoka et al., 2020; Pärnamäe et al., 2021; Ran et al., 2017).

Three types of interfaces (contact region) can be present in BPMs: a smooth interface (characteristic of homogeneous BPMs), a corrugated interface (also present in homogeneous BPMs), and a heterogeneous interface. These types of bipolar junctions are due to the membrane production method (Pärnamäe et al., 2021). There are also multilayer BPMs, which are obtained by deposition of polyelectrolytes (layer-by-layer technique—LBL).

A special BPMs type is asymmetric BPMs, made of a CEL and an AEL with different thicknesses. Use one layer membrane with reduced thickness to decrease the overall membrane resistance (Mareev et al., 2020; Pärnamäe et al., 2021; Zabolotskii et al., 2014).

The total permselectivity of BPMs is greater than monopolar membranes. The monolayers with opposite charges tend to exclude co-ions (which are counter-ions for the neighboring layer), decreasing diffusion (as well as overall leakage) (Pärnamäe et al., 2021; Yu, Yan, Freeman, & Chen, 2021).

The applicability of BPM in ED process (BMED) for different areas is limited for this permselectivity. Owing to a decrease in the Donnan exclusion, the permselectivity is reduced at high product concentrations, decreasing the purity of the product obtained in the electromembrane process. For a BPM to have good applicability in BMED, in different areas, it must also have thermal stability (functional groups and stable matrix) in a temperature range of 20°C−80°C (Han, Jeong, & Kim, 2019).

Dissociation of solvent in BPMs is not limited to water. Alcohols can be also dissociated into BPMs, producing alkoxides and acids. The use of BPMs to dissociate solvents through a protonation−deprotonation mechanism can probably be used in other protic solvents, thus promoting new fields of application for BPMs (Pärnamäe et al., 2021).

Advances in techniques for membrane synthesis achieved improvement in mechanical properties, thermal stability, and selectivity. Thus the development of IEMs has enabled their application in different electromembrane processes for water remediation, allowing high efficiency in water and wastewater treatment, and for water and materials recovery, as presented in the next sections.

14.3 Electrodialysis, electrodialysis reversal, and selective electrodialysis

The application of ED was first proposed in 1890 by Maigrot and Sabates, who used permanganate paper as membranes to demineralize sugar syrup; and since the 1950s, it has been mostly used to produce drinking water from brackish water sources (Scarazzato et al., 2020). Because of its high versatility, conventional and adapted ED systems have also been often applied at bench and industrial scale to solve problems related to water treatment, wastewater treatment, sewage treatment, water and chemicals recovery, and others. The search in *Scopus* platform indicated that, in the last 10 years, 3018 papers were published considering ED, EDR, and selective ED. In this section, these processes are described concerning system configuration, operation principles, transport equations, efficiency evaluation, applications, and obtained results.

14.3.1 General description of electrodialysis cells: configuration and operating principles

Electrodialysis is an electrically driven process in which charged species are transported through IEMs toward electrodes as a result of the application of a direct current (DC) and concentration gradients established between both sides of the membranes. The system is composed of CEMs and AEMs arranged in an alternating pattern. Two electrodes placed at the side compartments of the cell and connected to a power source accomplish the function of cathode and anode. When an electric field is imposed between the electrodes, cations are attracted by the cathode, whereas anions are attracted by the anode due to potential gradients. Thus the feed solution is converted into product streams of two types: one more diluted and another more concentrated than the feed solution. The repeating unit of ED is called cell pair, which is composed of an AEM, a CEM, a dilute, and a concentrated channel. Industrial ED stacks may contain several hundred of cell pairs, depending mainly on the feed solution composition (Strathmann, 2004).

The transfer of ions across IEMs occurs as a result of the Donnan exclusion effect (Strathmann, 2004). As detailed in Section 14.2, for CEMs, cations in the solution are called counter-ions, whereas anions are co-ions; in an ideal system, CEMs allow only the transfer of cations while retaining anions. For AEMs, the inverse phenomenon occurs, where anions are counter-ions and cations are co-ions; in theory, AEMs allow only the passage of anions and retain cations. Fig. 14.4 shows a representation of an ED system.

The ED performance is influenced mainly by membrane properties, presented in Section 14.2, feed solution composition, equipment design, and operational parameters. Concerning the feed solution, the factors that most affect the ED performance are concentration and charge of ions, solution pH, electrolyte strength, the presence of complexing agents, and its tendency of forming precipitates (Barros, Martí-Calatayud, Ortega, Pérez-Herranz, & Espinosa, 2020). Finally, the equipment design and operational parameters that most influence ED processes are the cell geometry, the spacer configuration, feed flow velocity, and the applied current density (Lee, Sarfert, Strathmann, & Moon, 2002). The latter is generally chosen in function of the occurrence of the concentration polarization phenomenon.

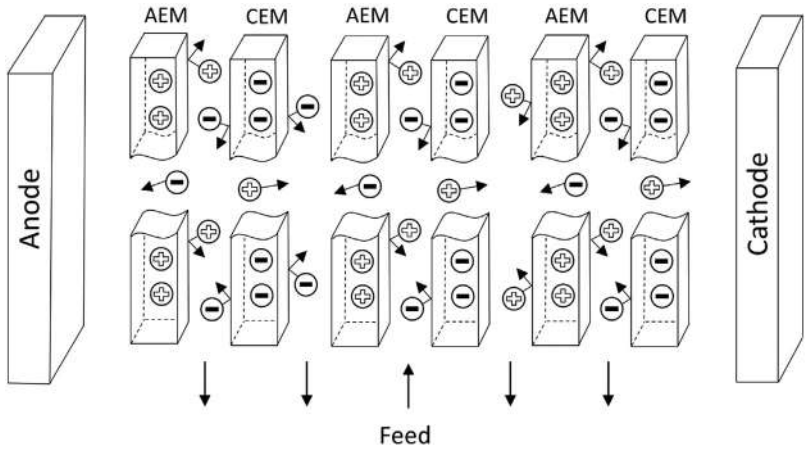

FIGURE 14.4 Representation of an electrodialysis system composed of cation-exchange membranes (CEMs) and anion-exchange membranes (AEMs).

Concentration polarization takes place in membrane processes due to a difference established between the fraction of current density carried by counter-ions (transport number) in the bulk solution and near the membrane/solution interface (Nikonenko, Kovalenko, & Urtenov, 2014). This thin region that comprises the membrane surface and the solution adjacent to it is called diffusion boundary layer (DBL). When the applied current density is sufficiently high for a given membrane system, intense concentration polarization occurs at the DBL, which may hinder considerably the ED performance. At this condition, the concentration of counter-ions in the DBL is virtually zero and the resistance of ion transfer tends to infinity; thus the mass transfer is limited. In general, the energy supplied to the membrane system at this condition is spent in reactions of water dissociation at the membrane surface, leading to unnecessary energy consumption. Besides, operating under intense concentration polarization may cause the deposition of organic and inorganic materials at the membrane surface, which is called fouling and scaling phenomena, respectively. Therefore it is crucial to determine the current density from which intense concentration polarization occurs, which is called limiting current density (*ilim*). The *ilim* may be estimated using the Peers equation (Barros, Scarazzato, & Espinosa, 2018) when single salt solutions are considered, or it may be experimentally determined by obtaining current–voltage curves for any membrane/electrolyte system (Barros & Espinosa, 2018).

In conventional ED operations, the applied current density is generally 80% of the limiting current density of the membrane system to avoid operating under intense concentration polarization, which may lead to fouling/scaling occurrence and increase considerably the energy consumption of the process (Strathmann, 2004). Conversely, in the last years, some authors have verified several advantages in operating ED in overlimiting current regimes, such as the reduction of effective membrane area, reduction of apparatus dimensions, reduction in operating time, and increase in ion transport (Barros, Scarazzato, Pérez-Herranz, & Espinosa, 2020; Bukhovets, Eliseeva, Dalthrope, & Oren, 2011).

Considering the above-mentioned limitations caused by fouling/scaling in ED systems, the process may be operated as an EDR, which may reduce considerably the deposition of insoluble species at membranes. The apparatus of an EDR system is very similar to that of the conventional ED, except for the presence of reversal valves. In this case, the polarity of the DC power is periodically reversed in certain time intervals simultaneously to the flow streams. Thus the anode is converted into cathode, and the diluate cells become the concentrated ones, and vice versa (Strathmann, 2010). This alternative mode of ED operation started to be applied industrially in the 1970s and has been shown to be very effective in many industrial applications for removing precipitated colloidal materials and precipitated salts deposited on membrane surfaces (Hansima, Makehelwala, & Jinadasa, 2021).

Another emerging electromembrane technique often used as a water remediation method is selective ED, also known as selectrodialysis. The apparatus of this hybrid ED system is identical to the conventional ED, but ion-selective membranes are used to separate ions in function of their charge. Selective ED is used when some ions are desired and need to be kept or concentrated, but other ions must be removed from the feed solution.

14.3.2 Transport equations and driving forces

The flux of an ion being transported in membrane/solution systems can be expressed by the extended Nernst–Planck equation with a convective term (Nikonenko et al., 2014), as shown in Eq. (14.1), where $\vec{J}_j$, D_j, z_j, and C_j represent the flux, diffusion coefficient, charge, and concentration of a species j, respectively; φ is the electric potential, $\vec{v}$ is the velocity vector; F, R, and T are the Faraday constant, the gas constant, and the temperature, respectively. As shown in Eq. (14.1), the total flux of ions is given by the sum of diffusive (the first term in the right-hand side), migrative (the second term), and convective flux (the third term).

$$\vec{J}_j = -D_j\left(\nabla C_j + z_j C_j \frac{F}{RT}\nabla\varphi\right) + C_j\vec{v} \tag{14.1}$$

As shown in detail in the work of Nikonenko et al. (2014), Eq. (14.1) can be converted into Eq. (14.2) when the local electroneutrality (LEN) assumption is considered; the current density $\vec{i}$ shown in Eq. (14.2) can be expressed by Eq. (14.3). In Eq. (14.2), D is the electrolyte diffusion coefficient; for strong binary electrolytes, this can be determined by Eq. (14.4) by using the individual diffusion coefficients of counter-ions ($D_{counter}$) and co-ions in solution (D_{co}). The term t_j in Eq. (14.2) is the transport number of a species j in the solution, which can be calculated by Eq. (14.5).

$$\vec{J}_j = -D\nabla C_j + \frac{t_j\vec{i}}{z_j F} + C_j\vec{v} \tag{14.2}$$

$$\vec{i} = F\sum\nolimits_j z_j\vec{J}_j \tag{14.3}$$

$$D = \frac{2D_{\text{counter}}D_{\text{co}}}{(D_{\text{counter}} + D_{\text{co}})} \tag{14.4}$$

$$t_j = \frac{D_j}{(D_{\text{counter}} + D_{\text{co}})} \tag{14.5}$$

When binary electrolytes are transported without convective flux, in a regime governed by Ohm's Law, the third term in the right-hand side of Eq. (14.2) can be neglected. Thus the flux of ions migrating by diffusion–migration in the solution can be expressed by Eq. (14.6) (Nikonenko, Pismenskaya, & Belova, 2010).

$$\vec{J}_j = -D\nabla C_j + \frac{t_j\vec{i}}{z_jF} \tag{14.6}$$

The flux of ions migrating in the membrane phase (J_j^m) can be expressed by Eq. (14.7), where $\overline{t_j}$ is the transport number of a species j in the membrane phase (Nikonenko et al., 2010). This equation comes from the definition of permselectivity, which relates the transport of a specific species to the total transport of electric charges through the membrane (Strathmann, 2004).

$$J_j^m = \frac{\overline{t}_j i}{z_jF} \tag{14.7}$$

For calculating the material balance at the membrane/solution interface, the flux of ions migrating at the solution side [Eq. (14.6)] is equalized to the flux at the membrane side [Eq. (14.7)]. This is mathematically expressed by Eq. (14.8), by considering the transport of ions occurring only in the direction of the component normal to the membrane surface (x coordinate) (Nikonenko et al., 2010). By rearranging Eq. (14.8), Eq. (14.9) is obtained, which expresses the concentration profile of ions at the membrane/solution interface (Nikonenko et al., 2014).

$$-D\left(\frac{\partial C_j}{\partial x}\right) + \frac{t_j i}{z_jF} = \frac{\overline{t}_j i}{z_jF} \tag{14.8}$$

$$\left(\frac{\partial C_j}{\partial x}\right) = -\frac{i}{z_jFD}(\overline{t}_j - t_j) \tag{14.9}$$

The equation describing mass transfer in the membrane/solution interface may also be written in the Nernstian form, which considers the thickness (δ) of the DBL, as shown in Eq. (14.10); this is the most common expression that describes ion mass transfer in membrane systems (Campione et al., 2018; Larchet, Nouri, Auclair, Dammak, & Nikonenko, 2008; Nikonenko et al., 2010). In the equation, C_j^m and C_j^{bulk} are the concentrations of j at the membrane surface and in the bulk solution, respectively. The term δ can be calculated by the Levich equation (Campione et al., 2018) or via chronopotentiometry associated with mathematical models (Larchet et al., 2008). The term $\overline{t_j}$ can be experimentally determined via chronopotentiometry (Barros et al., 2018), Hittorf (Zabolotsky, Novak, & Kovalenko, 2017), or emf methods (Kim, Seo, & Lee, 2014). Finally, note in Eq. (14.10) that as the

current density increases, the concentration gradient at the membrane/solution interface increases and C_j^m decreases. Thus it is reasonable to assume that when intense concentration polarization occurs ($i = i_{lim}$) in a membrane system with strong binary electrolytes, the concentration of ions at the membrane surface is zero; in this case, Eq. (14.11) is obtained (Peers equation), which allows estimating the limiting current density of membrane/solution systems.

$$\left(\frac{\partial C_j}{\partial x}\right)_{x=\delta} = \frac{C_j^m - C_j^{bulk}}{\delta} = -\frac{i}{z_j F D}(\bar{t}_j - t_j) \tag{14.10}$$

$$i_{lim} = \frac{z_j D C_0 F}{\delta(\bar{t}_j - t_j)} \tag{14.11}$$

14.3.3 Achievements in the use of electrodialysis, electrodialysis reversal, and selective electrodialysis as water remediation methods

In recent years, ED has been shown to be useful in several applications in addition to the production of drinking water from brackish water sources, such as in the treatment of industrial (Barros, Ortega, Pérez-Herranz, & Espinosa, 2020) and municipal wastewater (Rotta, Bitencourt, Marder, & Bernardes, 2019), in the pharmaceutical and food industry (Van der Bruggen, 2018), and in the production of organic acids and ultrapure water (Bazinet & Geoffroy, 2020). Electrodialysis has been especially used as a water remediation method due to its environmental and technical advantages compared to other techniques and due to the growing concerns about water quality. Thus in recent years, many efforts have been made to make this process viable on an industrial scale.

One of the promising directions in the development of ED processes is the operation in overlimiting current regimes. Until a few years ago, this process was associated only with intense occurrence of fouling/scaling due to water dissociation taking place at the membrane surface, as verified in the treatment of industrial wastewater (Barros et al., 2018). However, several authors have verified that ED in overlimiting conditions is also able to mitigate fouling/scaling occurrence. Recently, wastewater from the brass electroplating industry was treated by ED in underlimiting and overlimiting conditions (Barros et al., 2020). The authors noted that in overlimiting regimes, ion transfer across the membranes was enhanced, and fouling/scaling occurrence at both CEMs and AEMs was mitigated; this occurred mainly due to the occurrence of electroconvection and water dissociation on the surface of the membranes. In addition to intensifying ion transfer, ED operation time has also been shown to be strongly influenced by the current regime.

On the other hand, controversial results regarding overlimiting ED operations have also been reported in the literature. In the recent work of Rotta et al. (2019), the application of overlimiting current densities to an ED system operated to treat solutions emulating municipal wastewater led to intense water dissociation, hampering phosphate transfer through the AEM (Rotta et al., 2019). Bak, Yun, Kim, and Kang (2019) tested the use of ED in underlimiting and overlimiting conditions to recover volatile fatty acids from the hydrogen fermentation broth of food wastes (Bak et al., 2019). Considerable improvements were

not verified in the species recovery due to the intense occurrence of water dissociation at the AEM. Thus several aspects still need to be evaluated in detail before operating ED industrially in overlimiting current regimes, such as the influence of water dissociation on the transfer of ions, costs associated with energy consumption, heat production by Joule effect, and impacts of water dissociation and electroconvection on the membrane integrity after long-term operations (Barros, Martí-Calatayud, Pérez-Herranz, & Espinosa, 2020; Bazinet & Geoffroy, 2020).

Electrodialysis reversal has also been used in water remediation processes since it mitigates fouling and scaling occurrence and requires practically no adaptation to the design of conventional ED plants. In the work of Bacher et al. (2017), EDR was installed in a municipal water treatment plant to obtain desalted water suitable for human consumption and industrial uses. EDR was applied as a tertiary treatment, after the river water has been treated by coagulation with a tannin-based product. High-quality water was obtained, achieving percent removal of 60% and 70% for cations and anions, respectively. Fouling occurrence affected the EDR efficiency, but a procedure of membrane cleaning conducted with an acidic solution associated with manual washing was able to restore the process performance (Bacher et al., 2017).

Chao and Liang (2008) evaluated the use of EDR to treat wastewater from a metallurgical company and obtained the following results: 92% of desalination rate, 98% of chlorine ion removal, 80% of sulfate removal, and 99% of calcium ion removal (Chao & Liang, 2008). Unfortunately, the authors did not evaluate fouling occurrence. The use of EDR in the recovery of nutrients (nitrogen and phosphorus) from pig manure containing two types of antibiotics (sulfadiazine and tetracycline) was evaluated recently. Synthetic and real wastewater were tested, and the results were compared to a conventional ED operation conducted in parallel to the EDR (Shi, Hu, & Simplicio, 2020). In the EDR with real wastewater, the particles, organic foulants, and antibiotics in the fouling zone were mostly released back to the feed solution due to the reversal operation. At the end of the long-term EDR operations, the used membranes presented separation performances almost identical to the virgin ones.

Electrodialysis reversal has also been used in the treatment of municipal wastewater (sewage). In the work of Goodman, Taylor, Xie, Gozukara, and Clements (2013), the EDR process reduced the total dissolved solids in the feed solution from 1104 mg L^{-1} to 328 mg L^{-1} and decreased the solution conductivity by 72%. Additionally, the treatment removed 84% of calcium, 76% of chloride, 59% of fluoride, 60% of phosphate, and reduced the alkalinity by 64%, suggesting that EDR may be a viable method for treating municipal wastewater (Goodman et al., 2013).

Another ED system that has been frequently used as a water remediation method is selective ED. Tran, Zhang, and De Corte (2014) tested this technique as a pretreatment of wastewater rich in phosphate ions, followed by a crystallization process; the current efficiencies to transport phosphate and chloride ions were 26.6% with a conventional AEM and 63% with a monovalent selective AEM, achieving a desalination efficiency of 87% (Tran et al., 2014). Liu, Wang, Wu, Luo, and Wang (2017) used selective ED to treat a secondary effluent and recover nitrogen and phosphorus nutrients; the recovery efficiency of N (NO_3^-) in the feed solution and P (HPO_4^{-2}) in the product solution was 62.1% and 86.5%, respectively (Liu et al., 2017).

Selective ED has also been used to treat wastewater from metallurgical processes. Chen et al. (2009) tested a two-stage ED process using monovalent selective membranes to separate chromate present as $HCrO_4^-$ in the first stage (pH 2.2) and as CrO_4^{-2} in the second stage (pH 8.5) from $NH_2SO_3^-$, Na^+, and Cl^-; a percent concentration of 191% for chromate was obtained (Chen et al., 2009). Reig et al. (2018) used selective ED with conventional and monovalent selective membranes to separate arsenic from copper and zinc ions present in acidic wastewater from a metallurgical process; around 80% of copper, 87% of zinc, and 95% of arsenic ions were recovered in different compartments by selective ED (Reig et al., 2018). Therefore selective ED has been shown to be a promising technique in water remediation applications, allowing water treatment and the recovery of metals and nutrients.

In recent years, several mathematical models able to describe the transport of ions and water across IEMs have been proposed to improve the performance of ED processes. The models present different levels of complexity, depending on the phenomena considered, such as concentration polarization, overlimiting mass transfer phenomena (water dissociation, electroconvection, gravitational convection, current-induced membrane discharge), shifts of chemical equilibrium at the DBL and inside the membranes, etc. The simplest models neglect all nonideal phenomena and consider average concentrations of the compartments to estimate all process variables. These models are used, in general, to conduct a simple economic analysis of the process. Another class of models, which are widely used in ED studies, includes the rigorous Nernst–Plank (NP) and Stefan–Maxwell (SM) based models. These models describe a variety of phenomena occurring inside IEMs at a microscopic level, generating accurate results close to real ED processes. In this case, thermodynamics and mass transfer models, including the description of the fluid dynamics, are generally used. The major limitation of NP and SM based models is the very large computational power required to conduct the simulations. Therefore some considerations are generally made to simplify the ED system, such as dividing the process into several small parts. Thus these rigorous models are generally unfeasible to simulate the whole stack. To overcome this limitation, semiempirical models may be used, which allow a plant-scale description. In these models, transfer phenomena occurring at a microscopic level in membrane systems are described using empirical information or small-scale theoretical analysis; for this, computational fluid dynamics tools are used. A critical review of the mathematical models that have been developed can be found in the work of Campione et al. (2018).

As described, in ED, EDR, and selective ED, the function of the electrodes is to conduct the applied electric current and to establish an electric potential gradient, providing the direction for ion transport across the IEMs. Alternately, for treatments based on electrochemical demineralization of water—as capacitive deionization (CDI)—high-surface-area electrodes, if electrically charged, can quantitatively adsorb ionic components from water; thereby resulting in desalination. CDI processes have also been improved by the inclusion of membranes, leading to new processes for water remediation. These technologies are presented in the next section.

14.4 Capacitive deionization-based technologies

The beginning of the CDI dates back to the early 1960s when a research group from the University of Oklahoma introduced the concept of electrochemical demineralization of water (Arnold & Murphy, 1961; BLAIR & MURPHY, 1960). In that system, saline water

was pumped between charged electrode sheets made of activated carbon powder. The authors assumed that the ions held in the pores of the electrode sheets as a result of physical adsorption and static electrical force. In the late 1960s, Abbas et al. (1968) demonstrated the applicability of this technique on a commercial scale with long-term trials (Abbas et al., 1968). However, it was from the 1990s that the technique gained more attention, mainly due to the development of new materials for making the electrodes, such as carbon aerogels and carbon nanotubes. Afterward, Farmer, Fix, Mack, Pekala, and Poco (1996) were the first to introduce the term capacitive deionization and the abbreviation CDI commonly used today (Farmer et al., 1996). Since then, other variants of the CDI have been developed and improved, such as the membrane capacitive deionization (MCDI) and flow-electrode capacitive deionization (FCDI), for example.

14.4.1 General description of capacitive deionization cells: configuration, operating principles, and flow patterns

CDI can be defined as an electrochemical process used for desalting water with low to moderate salt concentration (Koseoglu-Imer & Karagunduz, 2018). A CDI cell unit consists of two electrodes made of activated carbon separated by a spacer acting as a flow channel for a solution containing ions (Strathmann, 2010). Thus the ions are removed from the solution by applying an electric potential gradient between the electrodes, where they will be electroadsorbed. After a certain period of operation, the storage capacity is reached with the saturation of the electrode pores. Then, they can be regenerated, releasing the adsorbed ions (Porada, Zhao, Van Der Wal, Presser, & Biesheuvel, 2013).

Indeed, the CDI process is fundamentally divided into two steps: (1) adsorption, first producing a stream of desalinated water and (2) desorption, generating a brine stream (concentrated in ions) (AlMarzooqi, Al Ghaferi, Saadat, & Hilal, 2014). In the first step (sorption), represented in Fig. 14.5A, the feed solution to be treated (water or wastewater) flows through one or more porous electrode pairs, which, after the application of an electrical potential, display poles with positive (anode) and negative (cathode) charges. Therefore the applied potential forms the electric double layer (EDL) on the pore surfaces of the electrodes (Suss,

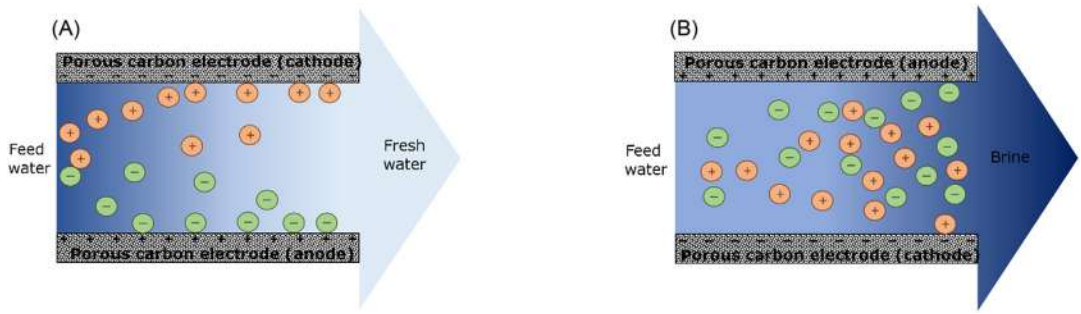

FIGURE 14.5 Schematic illustration of basic capacitive deionization (CDI) cell configuration and operation: (A) sorption, freshwater production and (B) electrode regeneration by reversing polarity, brine production. *Source: Adapted from (Koseoglu-Imer and Karagunduz, 2018).*

Baumann, & Bourcier, 2012) and, consequently, the ions in the solution migrate toward the poles having opposite charges. Thus the cations migrate to the cathode (electrode with a negative charge), while anions migrate to the anode (electrode with a positive charge) (Mitko & Turek, 2015). Upon reaching the surface of the electrodes, ions are adsorbed resulting in a stream of demineralized water (Agartan, Akuzum, Caglan Kumbur, & Agar, 2020). In the second step, the electrodes are regenerated, when occurs the ions desorption. Thus by interrupting the electric current (electric potential = 0) or by reversing the polarity (Fig. 14.5B), the ions migrate from the electrodes back to the feed solution, generating a brine stream that is discarded. Therefore this possibility of working alternating adsorption and regeneration cycles ideally allows the electrodes to have a low maintenance cost and a long service life. To this end, the cell potential should not exceed the point that the chemical bonds between oxygen and hydrogen atoms in the water molecule are broken; that is, E_{cell} = 1.23 V must not be exceeded (Porada et al., 2013). Otherwise, chemical reactions between ions and electrodes can occur, thereby reducing the adsorption capacity of the electrodes. This results that, in practical applications, CDI is usually operating between 0.8 and 1.2 V (Strathmann, 2010).

The integration of IEMs with the CDI resulted in the technique currently known as MCDI (Bazinet & Geoffroy, 2020). In MCDI cells, CEMs and AEMs are accommodated in front of the cathode and anode, respectively (Fig. 14.6B). Thus after polarization of the electrodes, the cations in the solution migrate toward the cathode permeating the CEM,

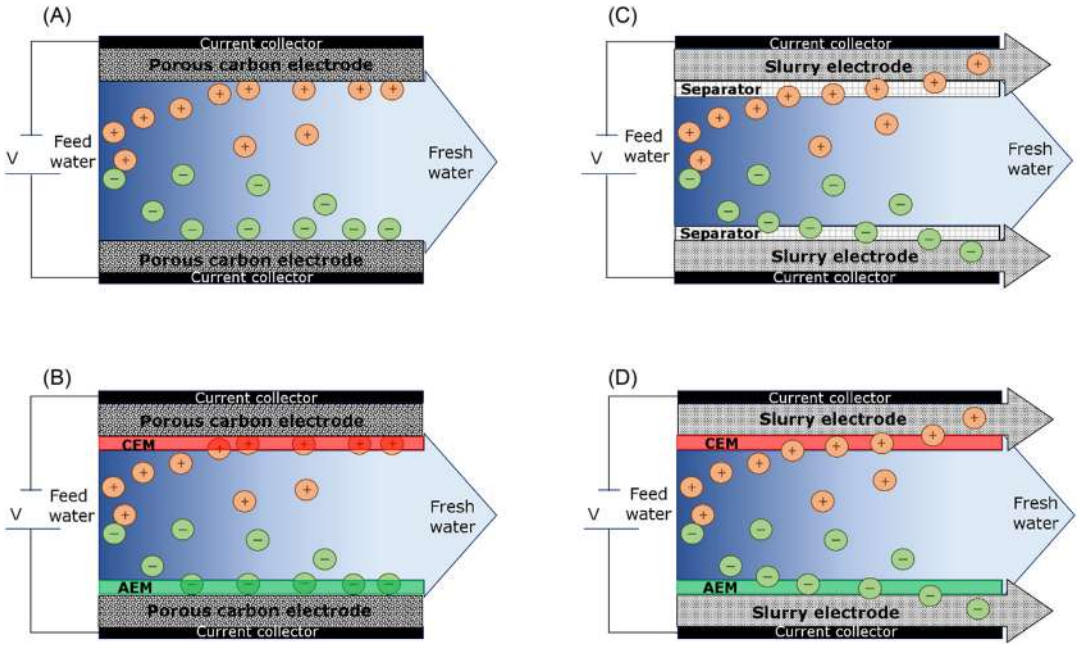

FIGURE 14.6 Schematic representation of the main capacitive deionization based technologies applied to water remediation. (A) CDI, (B) MCDI, (C) FCDI and (D) MFCDI. *Source: Adapted from Koseoglu-Imer D.Y., Karagunduz A. Recent developments of electromembrane desalination processes.* Environmental Technology Reviews. *2018;7(1):199–219. doi:10.1080/21622515.2018.1483974.*

while the anions migrate toward the anode permeating the AEM. In the electrodes regeneration step, similarly to the CDI (Fig. 14.6A), when reversing the polarity, the ions desorb from the electrodes and migrate toward the feed water, producing a stream of brine (Van Limpt & van der Wal, 2014). In fact, IEMs do not seem to affect the performance of the process during the sorption step. On the other hand, they play a fundamental role in the desorption step (electrodes regeneration), which is to prevent the ions from migrating to the electrodes positioned on the opposite side and being again adsorbed, thus making the ions remain in the brine solution (Lee & Choi, 2012).

The most recent and promising CDI-based technology uses flow electrodes instead of static ones and is called FCDI (Bazinet & Geoffroy, 2020). Indeed, the term FCDI has been used for processes that use flow electrodes associated with IEMs (Bazinet & Geoffroy, 2020; Ma et al., 2020; Rommerskirchen et al., 2020) and also without IEMs (Koseoglu-Imer & Karagunduz, 2018). However, in this chapter, a distinction will be made between FCDI with (Fig. 14.6D) and without IEMs (Fig. 14.6C).

The flow electrodes consist of suspensions of activated carbon circulated by the system in an electrode compartment separate from the feed stream. When IEMs are used for this separation, the technology is named membrane flow-electrode capacitive deionization (MFCDI); but when just porous separators are used, it is denominated FCDI. As a result of the circulation of the flow electrodes, they can be regenerated in another place, such as in the electrode compartment with the opposite charge of a single (M)FCDI module or even in another module (Rommerskirchen et al., 2020). Besides that, it is also possible mixing the discharged flow electrodes from both the cathodic and anodic compartments (Shin, Lim, Boo, & Hong, 2021). Thus the flow electrodes can continuously be regenerated and recirculated back to the module, enabling the continuous production of desalinated water; unlike the CDI and MCDI that are operated in cycles, producing alternately desalinated water or brine (Strathmann, 2010). Furthermore, the flow electrodes improve the effective removal of ions, the lifespan of the electrodes, and the energy consumption of the process, as well as enabling the treatment of feed streams with higher salt amounts than those treated in CDI and MCDI, which use static porous carbon electrodes (Bazinet & Geoffroy, 2020). Fig. 14.6 display a schematic illustration of the main CDI-based technologies employed as water remediation methods, namely CDI, MCDI, FCDI, and MFCDI.

14.4.2 Evaluation of the efficiency and performance of the capacitive deionization-based technologies

The desalination performance of CDI-based technologies is intrinsically associated with operating conditions such as operation mode (current or voltage constant mode) and flow rate and composition of the feed stream, as well as the cell characteristics (Shin et al., 2021). Therefore the performance of these technologies has been expressed in different ways, such as removal efficiency and rate and salt adsorption capacity, as well as charge efficiency and energy consumption [Eqs. (14.12)–(14.17)] (Ha, Lee, & Yoon, 2021; Kim, Lee, & Kim, 2020; Rommerskirchen et al., 2020). The salt removal efficiency (*SRE*) is given as:

$$SRE(\%) = \frac{(C_0 - C_F)}{C_0} 100 \tag{14.12}$$

where C_0 and C_F are the initial and final salt concentrations in the feed water in mg L^{-1}, respectively. Salt adsorption capacity (*SAC*) expresses the total mass of ions removed by the total mass of electrodes (m) during the sorption step, while the salt adsorption rate (*SAR*), represents the ratio of *SAC* by the operation time t (Datar, Mohanapriya, Ahirrao, & Jha, 2021).

$$SAC\left(\text{mg g}^{-1}\right) = \frac{(C_0 - C_F)V}{m} \tag{14.13}$$

$$SAR\left(\text{mg g}^{-1}\,\text{s}^{-1}\right) = \frac{SAC}{t} = \frac{(C_0 - C_F)V}{mt} \tag{14.14}$$

in which V is the volume of feed water treated. The salt adsorption rate has also been reported in terms of the effective area of electrodes (A_E) and is defined as the average salt adsorption rate (*ASAR*) (Shin et al., 2021):

$$ASAR\left(\text{mg cm}^{-2}\,\text{s}^{-1}\right) = \frac{(C_0 - C_F)V}{A_E t} \tag{14.15}$$

The charge efficiency (*CE*) expresses the amount of ions removed in relation to the electric charge applied, being an important parameter to determine both energy consumption and the occurrence of parasitic reactions, since it shows the degree of electric charge used for ion removal. Thus

$$CE(\%) = \frac{(C_0 - C_F)VF}{M\int_0^t Idt}100, \tag{14.16}$$

where I is the electric current (A), F is the Faraday constant (96,485 C mol^{-1}), and M is the molar mass (Fang et al., 2018), which usually refers to the NaCl salt (58.44 g mol^{-1}) (Agartan et al., 2020). Nevertheless, the electric energy consumption (*EEC*) for the constant voltage operating mode is described as Fang et al. (2018):

$$EEC\left(\text{J mg}^{-1}\right) = \frac{E\int_0^t tdt}{(C_0 - C_F)V} \quad , \tag{14.17}$$

in which E is the applied voltage (V) through the cell.

14.4.3 Achievements in use of capacitive deionization-based technologies as water remediation methods

Six decades have passed since the first studies on CDI and despite the advances achieved and the variety of application possibilities, its use on an industrial scale is still incipient and has been restricted to water desalination with low to moderate levels of salts (Agartan et al., 2020; Koseoglu-Imer & Karagunduz, 2018).

In one of the first pilot-scale studies, operating at a flow rate of 3785 $m^3\,d^{-1}$, Welgemoed and Schutte (2005) demonstrated that CDI using carbon aerogel electrodes is more advantageous than reverse osmosis (RO) and EDR for desalting brackish water (TDS $\sim$2000 mg L^{-1}) (Welgemoed & Schutte, 2005). The authors determined a treatment cost of 0.11$ m^{-3} for CDI

and 0.35$ m^{-3} for RO, achieving a 70% water recovery rate, based on experimental results. Also, CDI showed a 70% energy saving compared to EDR, which consume 0.59 and 2.03 kWh m^{-3}, respectively. Importantly, the authors also displayed that carbon aerogel electrodes may be cost-effectively produced on a large scale. Also using a CDI unit equipped with carbon aerogel electrodes, but treating brackish water of 5000 mg L^{-1} TDS, Xu, Drewes, Heil, and Wang (2008) were able to accomplish the required water quality standards of 500 mg L^{-1} TDS; however, this resulted in higher energy consumption: 0.95 kWh m^{-3}. The authors observed that using a higher electric current shortens the electrode regeneration time (Xu et al., 2008). Nonetheless, this implies excessively high specific energy consumption per gram of removed salt, as it represents about half of the energy spent in the process, making the CDI energetically nonefficient in treating high-salinity water. On the other hand, it is possible to reduce energy consumption by recovering energy during the electrode regeneration stage.

An important aspect in the development of the CDI was the incorporation of IEMs into the process, resulting in the MCDI. This technological advance has made it possible to block and repel co-ions, thus improving charge efficiency and desalination capacity, in addition to increasing the stability of the system due to the reduction of parallel reactions such as carbon oxidation and oxygen reduction (Kim et al., 2020). Moreover, IEMs act as protective shields of electrodes against foulants (Pawlowski, Huertas, Galinha, Crespo, & Velizarov, 2020); so, fouling ends up occurring in IEMs similarly to other electromembrane processes, as in ED, for example (Hassanvand, Chen, Webley, & Kentish, 2019; Wang, Bai, & Zhang, 2020).

Studies performed by Van Limpt and van der Wal (2014) assessed the performance of two full-scale MCDI systems treating municipal water to be used as makeup water in cooling systems. In that work, feed water with conductivities of 650 and 350 μS cm^{-1} were treated in the MCDI systems 1 and 2, respectively, aiming at a 70% conductivity reduction in both systems and an 80%–84% water recovery, being the systems monitored for up to one year. The authors (Van Limpt & van der Wal, 2014) observed low energy consumption for both systems in relation to RO treatment, 0.234 kWh m^{-3} and 0.105 kWh m^{-3} for systems 1 and 2, respectively. They highlighted the possibility of reducing, even more, energy consumption by implementing an energy recovery system in the electrodes regeneration stage and also by applying a lower electrical current during regeneration. They also observed that MCDI preferentially removed calcium and chloride, reducing the concentration of these ions in the recirculation water, thereby decreasing the risk of corrosion and scaling in the cooling system. Consequently, fewer chemicals (anticorrosion and antiscalant products) were used to control these undesirable phenomena, saving up to 85% of chemicals. The authors also claimed that additional increases in chemicals and water savings are possible using IEMs with greater selectivity for calcium and chloride (Van Limpt & van der Wal, 2014). Subsequently, monovalent cation permselective exchange membrane integrated with MCDI was investigated for the selective removal of monovalent and divalent cations (Choi, Lee, & Hong, 2016). Under optimal operating conditions, it was found that MCDI required less energy and was more effective for the selective removal of monovalent cations than nanofiltration. The authors also reported a worsening in MCDI selectivity and a drop in pH as the TDS concentration in the feed water increased. In another study, it was also demonstrated the feasibility of producing ultrapure water stably with resistivity below 10 MΩ cm using a feed water conductivity below 20 μS cm^{-1} and applying an electric potential of 1.5 V (Lee and Choi, 2012).

In fact, the association of IEMs with CDI increased the potential for using the technique, mainly because MCDI presents a lower energy consumption than RO in the treatment of water with a salt concentration below 25 mM; with values around 0.25 and 0.80 kWh m^3, respectively (Pawlowski et al., 2020; Porada, Zhang, & Dykstra, 2020). Recently, assuming that 100% of the energy stored in the EDLs can be recovered, Porada et al. (2020) demonstrated that the total energy consumption in an MCDI cycle for the treatment of a 40 mM salinity feedwater is 0.40 kWh m^{-3}; this was achieved under optimal operating conditions, with 80% salt rejection, 93.5% water recovery, and 11.9 L h^{-1} m^{-2} feed flow rate (Porada et al., 2020). The authors also partitioned the total energy consumption according to each component of the MCDI system, in such a way that 1% was attributed to the ionic resistances in the electrodes, 6% to the ionic resistances in the membranes, 14% to the ionic resistances in the spacer channel, 17% to electronic resistances in current collectors and cables, and 62% corresponded to Donnan's potentials at the membrane interfaces (Porada et al., 2020).

Nevertheless, the introduction of flow electrodes further increased the range of possibilities of the CDI-based technologies as they allow continuous production of desalinated water, due to the flow electrodes can be regenerated (ion desorption) in an external system (Liu, Lee, Ong, & Ng, 2020). Then, the flow electrodes discharged from the anodic and cathodic compartments can be mixed and regenerated together, in just one system (Ma et al., 2020); or they can be regenerated separately, with a regeneration system for the electrodes discharged from the anodic compartment and another for the cathodic one (Shin et al., 2021). In addition, there are also studies showing that (M)FCDI can effectively treat water and wastewater with higher salt contents, with concentrations in the range of seawater (up to 4% NaCl) (Park, Choi, & Yang, 2016; Yang et al., 2016) and even saline brines (6%−12% NaCl) (Rommerskirchen, Linnartz, Egidi, Kendir, & Wessling, 2020). Therefore these advantages give prominence for (M)FCDI to be applied in desalination plants on an industrial scale.

As reported in an extensive review paper (Xing, Liang, & Tang, 2020), it is evident that the CDI-based technologies are in growing development and much of this is intrinsically connected to the improvement of the performance of the electrodes. It is estimated that 60% of the efforts employed in the CDI field were directed toward the development of superior electrode materials. As a result, various type of several single carbon capacitive materials like activated carbon, activated carbon cloth, carbon aerogels, carbon nanofibers, carbon nanotubes, mesoporous carbon, carbide-derived carbons, graphene, and metal-organic framework-derived carbons have been investigated; however, the electrodes made of these materials displayed relatively low SAC, usually below 15 mg g^{-1}. Nevertheless, the next generation of electrodes, Faradic or Battery electrodes, are being manufactured using carbon-based composite materials, such as carbon−polymer composites, carbon−metal oxide composites, carbon−carbon composites, and carbon−polymer−metal oxide composites. Thus the additional components in the carbon-based composite electrodes may potentially improve the desalination performance of single carbon materials by adjusting the intrinsic pore structure, increasing the wettability, inhibiting the tendency of aggregation, improving surface chemistry, changing the zeta potential, or adding pseudocapacitance. Thus the recent use of Faradic electrodes in the CDI-based technologies has increased the adsorption capacity, reaching SAC above 30 mg g^{-1}. Besides that, the latest

advances have shown that it is possible to further enhance the charge efficiency and overall cell conductivity by working under overlimiting regimes and thus increasing electroconvection (Bazinet & Geoffroy, 2020).

As indicated for CDI technologies, also ED, EDR and selective ED (Section 14.3) may present limitations in treatment efficiency. Not rare, membranes (Section 14.2) are responsible for these problems, which are presented in the next section.

14.5 Limitations and key mitigation strategies

Throughout this chapter, it has been discussed how electromembrane processes became mature and well-established technologies, able to be applied in a multitude of processes. Insofar as such processes present promising results for a specific application, naturally they will start being assessed for several other processes. Looking back in time, one may find the first uses of ED systems in the desalination of brackish water for industrial purposes (Aly, Darwish, & Fathalah, 1989). Since then, many other applications have been evaluated and an incredible evolution in the development of novel IEMs has arisen.

If, on the one hand, ED, EDR, BPED, and MCDI have proven to be feasible and cleaner technologies, on the other hand, some limitations should be considered and overcome. In this section, the most important limitations of the electromembrane technologies will be introduced and the most widespread mitigation strategies will be discussed.

14.5.1 Process cost

When scaling up an electromembrane process, operating costs may determine the feasibility of the chosen technique. The costs may be divided into two major categories as given below.

14.5.1.1 Plant investment costs

Refer to the costs for installations, building site, stack, and control devices (Strathmann, 2010). Such costs are dependent on the size and capacity of the plant. Nevertheless, several studies have shown the ease adaptation of ED and EDR to small-scale equipment, able to supply water for small villages, which could drastically reduce plant investment costs and, at the same time, supply water for needy populations (Bian, Watson, & Wright, 2019; Xu et al., 2020).

Herein, it is essential to mention the costs of membrane acquisition, which are strongly related to the required effective area and the lifespan of the membranes. It is not possible to discuss such costs without considering the specific application for which the membrane process is being considered. Thus the composition of the feed stream will play a major role in the membrane-related costs. In a hypothetical desalination process, the concentration of salts in the feedwater (brackish or salt water) will affect the required membrane area according to Eq. (14.18) (Strathmann, 1995).

$$A = \frac{zFQ\Delta Cn}{i\varepsilon} \tag{14.18}$$

In Eq. (14.18), z is the charge of the ion, F is the Faraday constant (C mol^{-1}), Q is the volumetric flow rate of produced water (m^3 s^{-1}), ΔC is the concentration difference

between the feed stream and the produced water (mol L^{-1}), n is the number of cell pairs, i is the current density (A m^{-2}), and ε is the current utilization. Eq. (14.18) states that the higher the concentration of the feed, the higher is the membrane area required to produce desalted water. If the calculated area is too high or if it does not meet the design requirements of the stack, multiple desalination stages may be evaluated.

For applications in the food industry or wastewater treatment, the lifespan of the membranes may be strongly decreased due to fouling, poisoning, aging, or oxidation. Shortened lifespans may result in increased costs for the acquisition of membranes. In some cases, the application of EDR has a positive influence to enhance the lifespan of the membranes. Cleaning procedures and in-site monitoring may also be helpful, as discussed in item 14.5.2.

14.5.1.2 Operating costs

Operating costs involve mainly personal, energy consumption, and maintenance (Strathmann, 2010). While personal costs are strongly related to the capacity of the plant, energy consumption and maintenance may depend on several factors and even on each other.

The energy consumption may be divided into the amount of energy used to pump the solutions and the energy to transfer ions from one stream to another. One promising alternative for reducing the energy consumption employed in electrical devices is the use of photovoltaic-powered systems (Bian et al., 2019; Xu et al., 2020). Although such costs cannot be fully eliminated, they may be reduced or optimized. For classical desalination applications, the relation between the concentration of the feed and the diluate will determine the feasibility of the technique. Such a relationship was established in the study of McGovern, Zubair, and Lienhard (2014) for optimizing costs in classical ED systems (McGovern et al., 2014). In terms of energy consumption, Patel, Qin, Walker, and Elimelech (2020) reported that the desalination of brackish water using ED is more advantageous than capacitive deionization (Patel et al., 2020). The utilization of hybrid systems may also reduce costs and enhance the performance of desalination units (La Cerva et al., 2019; Maheshwari & Agrawal, 2020).

For other applications, the estimative of energy costs related to the transfer of ions may be quite complex since low-mobility ions, organic acids, and metal ions may be present in the streams. Hence, a reliable estimative may be achieved by using Eqs. (14.16) and (14.17), presented previously in Section 14.4.2, to calculate the current efficiency and the energy consumption for each ionic species.

Recently, it has been reported that a novel trend to reduce the costs related to the transfer of ions in electromembrane systems is the application of overlimiting regimes, considering that when using current densities higher than the "limiting current density," lower membrane areas are required (Nikonenko et al., 2014). From such perspective, some authors have shown that efficient operation may be achieved in overlimiting current densities (Barros et al., 2020; Beaulieu, Perreault, Mikhaylin, & Bazinet, 2020). However, to ensure a higher transport efficiency, water dissociation must be avoided, since the energy is wasted in the transport of protons and hydroxyls instead of the ions of interest, and electroconvection must be favored (Nikonenko et al., 2014).

Finally, the costs related to the maintenance and cleaning or substitution of the membranes must be considered. During long-term operation applications, insite monitoring combined with periodic cleaning is the cheapest and feasible way to achieve cost optimization (Virtanen, Reinikainen, Lahti, Mänttäri, & Kallioinen, 2018). However, it is worth mentioning that the maintenance costs are related to energy expenditure costs insofar as they are both dependent on the composition of the feed. The low-mobility species which cause high-energy consumption may clog the membranes and cause the need for more frequent cleaning procedures, which would increase the maintenance costs. Also, the constant use of high current densities may injure the physical structure of the membranes and increase their periodicity of substitution. The occurrence of clogging of membranes may injure the efficiency of the process, affecting energy consumption and the need for maintenance.

14.5.2 Membrane clogging

Membrane clogging is one of the most important limitations of a membrane process. When formed by inorganic salts which precipitate on the interface or in the bulk of the membranes, it is usually called scaling. Scaling often occurs due to a high concentration of salts, surpassing the solubility limit of the feed, or due to a drastic pH change, as a consequence of intense water dissociation. Another form of clogging is fouling, which occurs by the action of organic substances, and it usually takes place on AEMs since organic species often present negative charges. Fouling may also emerge because of the growth of microorganisms on the membrane surface and, in this case, is named biofouling (Fig. 14.7)

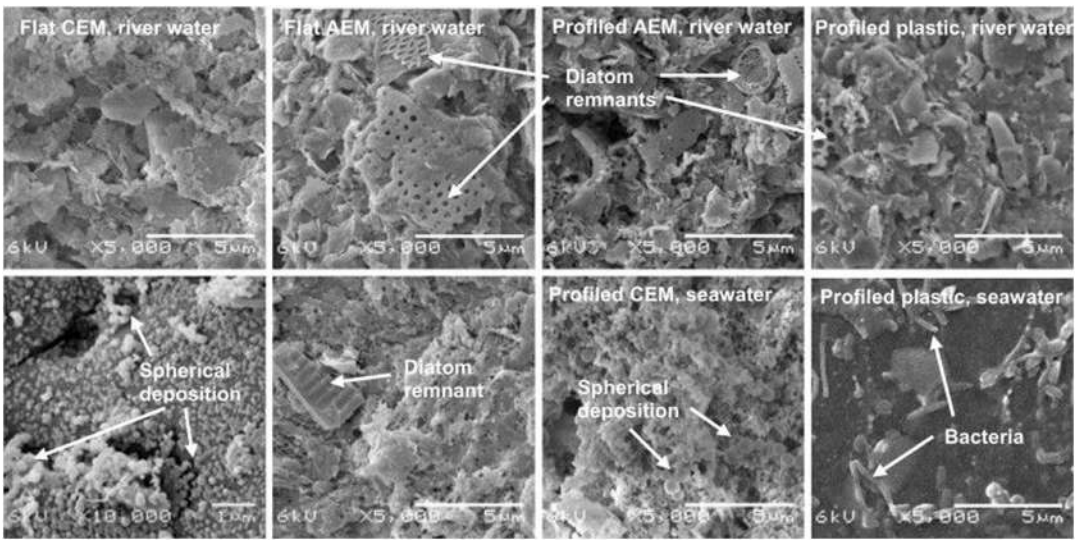

FIGURE 14.7 Biofouling in anion-exchange membranes caused by different microorganisms during natural waters desalination. *Source: From Vermaas, D., Kunteng, D., Saakes, M., & Nijmeijer, K. (2013). Fouling in reverse electrodialysis under natural conditions.* Water Research, 47*(3), 1289–1298. doi:10.1016/j.watres.2012.11.053 1293*

(Vermaas, Kunteng, Saakes, & Nijmeijer, 2013). Electromembrane processes cannot remove such microorganisms without suitable prior treatment and they may attach to the membrane, causing an increase in energy consumption, or even complete degradation of the membranes (Warsinger, Chakraborty, & Tow, 2018).

The mitigation strategies against fouling are divided into four main categories: modification of IEMs; periodic cleaning procedures (chemical or mechanical); pretreatment to remove microorganisms, and operational modifications (Mikhaylin & Bazinet, 2016). The surface modification of IEMs has been studied throughout the years. Long-chain surfactants were amongst the very first coating agents with antifouling properties (Grebenyuk, Chebotareva, Peters, & Linkov, 1998). The objective is to promote modification of the membrane surface by using chemicals that decrease hydrophobicity and increase the negative surface charge density (Mikhaylin & Bazinet, 2016). In the case of biofouling, two main measures can be purposed: to avoid the attachment of microorganisms on the membrane surface or to eliminate them (Vaselbehagh, Karkhanechi, Takagi, & Matsuyama, 2016). Improved antifouling and antibiofouling properties through surface modification were most recently reported in the studies of Park et al. (2021), Zhao, Li, Jin, Van, and der Bruggen (2021) and Li, Shi, Cao, and Cao (2021) (Li et al., 2021; Park et al., 2021; Zhao et al., 2021). An illustrative scheme of the mechanisms to prevent fouling and biofouling by the modification of IEM is shown in Fig. 14.8

Chemical cleaning procedures are widely used in electromembrane applications. They are based on the use of acidic and basic solutions to remove organic and inorganic remnants from the membranes and restore partially or totally their properties. The main advantage of periodical cleaning procedures is the use of common chemical reactants, such as NaOH and HCl (Guo, You, Yu, Li, & Zhao, 2015). On the other hand, depending on the type of application (for instance, in the food industry), care must be taken to avoid

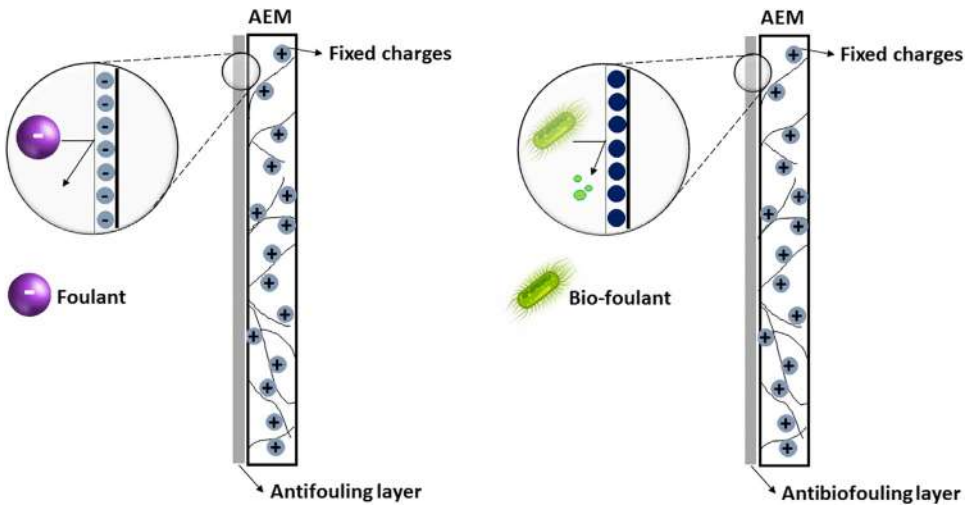

FIGURE 14.8 Illustrative scheme of the mechanisms of membrane surface modification to enhance their antifouling and antibiofouling properties.

contamination of the streams with cleaning solutions (Mikhaylin & Bazinet, 2016). As alternatives, some mechanical cleaning has been proposed in the literature, such as the use of ultrasound (Aghapour Aktij, Taghipour, Rahimpour, Mollahosseini, & Tiraferri, 2020). However, the industrial-scale use of mechanical cleaning is not effective until the present moment (Aghapour Aktij et al., 2020).

The most widely used operational modification methods are the EDR (Hansima et al., 2021) and the application of pulsed electric field (Gonzalez-Vogel, Moltedo, Reyes, Schwarz, & Rojas, 2021). The first one proposes a periodical reversion of the polarization of the electromembrane system, causing the detachment of the organic and inorganic substances from the surface of the membrane and their resolubilization in the solution. The latter is based on the periodical application of an electro-field during a short time, followed by a short break, which would decrease fouling and scaling due to electrophoretic effects. EDR and PEF may be applied individually or in combination, as the so-called pulsed electrodialysis reversal (PER) (Merkel & Ashrafi, 2019).

Finally, pretreatments of the working solutions may include a wide range of procedures, which aim at removing microorganisms before the electromembrane step. The best option will depend on the composition of the stream, the type of microorganisms to be removed, and the availability of each industrial site. In this sense, ultrafiltration, nanofiltration, ultraviolet radiation, and adsorption are some of the most common alternatives (Mikhaylin & Bazinet, 2016).

14.5.3 Membrane selectivity

One of the main drawbacks of electromembrane processes, when compared to other separation processes, is the lack of selectivity for ions having the same valence. The structure of the IEMs will favor the transport of some ions (Luo, Abdu, & Wessling, 2018), so as reported in the work of Luo et al. (2018). Nevertheless, in long-run electromembrane processes, all ions with the same charge eventually will be transferred from the diluted stream to the concentrate stream, although at different transfer rates. However, as aforementioned, electromembrane processes have been used for multiple applications and, currently, they have been assessed for situations that require the transport of a specific ion against other, so as the case of the recovery of lithium from brines which contain other cations, mainly Mg^{2+}, Ca^{2+}, and Na^{+} (An et al., 2012; Ji, Ji, & Chen, 2018).

Thus monovalent-selective membranes are being constantly developed and characterized (Besha, Tsehaye, Aili, Zhang, & Tufa, 2020; Ge, Wu, & Yu, 2017). Their structural modification is based on Coulomb's law that states that the repulsion between ions of the same charge is greater when multivalent ions are involved in the interaction. Hence, monovalent ions are easily transported across modified monoselective membranes, while multivalent ions are retained (Besha et al., 2020).

Another way of increasing the selective transport of specific ions through IEMs is the use of overlimiting regimes. This trend was studied by Rotta et al. (2019) to perform preferential recovery of sulfate over phosphate anions. However, the authors reported intense alkalinization of the concentrate stream which caused significant damage to the AEM, which requires the use of alkali-resistant membranes (Rotta et al., 2019).

14.6 Summary and future directions

Ion-exchange membranes are undoubtedly an important advancement in technologies for water remediation. Mechanical and thermal stability, selectivity, and chemical stability in alkaline conditions are crucial properties that must appear in the new IEMs produced. To identify the most suitable modification procedure, in addition to knowledge about the properties of membranes, understanding and knowing the physicochemical properties of modifying agents (including their cost-benefit, toxicity, durability, and stability) is essential to develop highly efficient membranes.

Electrodialysis has shown to be a promising technique in several water remediation applications; its use has shown special relevance in the treatment of industrial and municipal wastewater, allowing water reuse and the recovery of valuable metals, nutrients, and pharmaceuticals. Several adaptations in the ED cell design and operating conditions have been frequently tested in recent years to improve its performance. One of them is the ED operation in overlimiting current regimes, since authors have noticed greater mass transfer rates and shorter operating times. However, the effects of overlimiting current densities on fouling/scaling occurrence and the integrity of membrane structure must be further studied because controversial results have been reported.

Electrodialysis reversal is another alternative operating mode often tested, since it tends to mitigate fouling/scaling and requires almost no adaptation in the conventional ED design. Electrodialysis reversal has been mostly used to treat brackish water; and in future studies, authors tend to test this technique more intensively in wastewater treatment. The use of selective membranes in ED has also been frequently considered in wastewater treatment because it allows the selective separation of ions in function of their charges; in the coming years, authors tend to evaluate the manufacture of new selective monovalent membranes using new materials and techniques of membrane development. The combination of ED with other separation techniques also tends to be evaluated intensively in the coming years, since it may reduce the limitations of each technique when they are operated separately.

Since the 1960s, when capacitive deionization was introduced, it has progressed and gained attention. However, efforts have been mostly directed toward the development and improvement of the electrodes. An essential advent in the development of the CDI was the incorporation of IEMs in the technique, resulting in the MCDI. This important and crucial enhancement, in addition to improving performance, also played a fundamental role in the development of the technique and enabled the introduction of flow electrodes, which, in turn, further increased the possibilities of use. Thus with the possibility of treating water and wastewater with higher content of salts associated with the use of faradic electrodes and the regeneration of the flow electrodes in a separate module, they allow the (M)FCDI to also be used for energy recovery. Besides, the use of cells with multichannels is a good alternative to overcome the main limitations of conventional CDI with single-cell architecture.

Nevertheless, there is further room for improvement in CDI-based technologies, such as increasing the adsorption capacity of the electrodes and reducing the electrical resistance of the cell and the flow electrodes, as well as optimizing the cell design and operating conditions. Also, there is still a need to increase the implementation of CDI-based technologies on large scale and with long operating times, so that, finally, these promising techniques

can expand their quota in the water and wastewater treatment field and, thus, be effectively consolidated as water remediation methods.

Development of new membranes to improve their transport properties, technologies association for water remediation, and optimization of operational parameters may increase the energy efficiency and the water/materials recovery rate. Additionally, it may extend the lifespan of the membranes and reduce global costs for water remediation. The continuous advances in IEMs and electromembrane processes allow the expansion of water remediation capacity to minimize water crisis effects for human consumption and industrial uses.

Acknowledgments

CAPES, FAPESB, and CNPq (grant numbers 408282/2018-5 and 160320/2019-4).

References

Abbas, A., Abichandani, J. P., Hu, A., Al-Awady, M., Stevens, A. M., Townsend, F. Mark., & Reid (George, G. W. Wayne). (1968). Field operation of a 20 gallons per day pilot plant unit for electrochemical desalination of brackish. In *water*, Washington, D.C: University of Oklahoma Research Institute., United States. Office of Saline WaterU.S. Dept. of the Interior, [Office of Saline Water]. Available from https://babel.hathitrust.org/cgi/pt?id = mdp.39015078507913&view = 1up&seq = 3

Agartan, L., Akuzum, B., Caglan Kumbur, E., & Agar, E. (2020). Impact of flow configuration on electrosorption performance and energy consumption of CDI systems. *Journal of Water Supply: Research and Technology - AQUA*, *69*(2), 134–144. Available from https://doi.org/10.2166/aqua.2020.012.

Aghapour Aktij, S., Taghipour, A., Rahimpour, A., Mollahosseini, A., & Tiraferri, A. (2020). A critical review on ultrasonic-assisted fouling control and cleaning of fouled membranes. *Ultrasonics*, *108*, 106228. Available from https://doi.org/10.1016/j.ultras.2020.106228.

Ahangar, I., & Mir, F. Q. (2020). Development of polyvinyl alcohol (PVA) supported zirconium tungstate (ZrW/PVA) composite ion-exchange membrane. *International Journal of Hydrogen Energy*, *45*(56), 32433–32441. Available from https://doi.org/10.1016/j.ijhydene.2020.08.216.

Albornoz, L. L., Marder, L., Benvenuti, T., & Bernardes, A. M. (2019). Electrodialysis applied to the treatment of an university sewage for water recovery. *Journal of Environmental Chemical Engineering*, *7*(2), 102982. Available from https://doi.org/10.1016/j.jece.2019.102982.

AlMarzooqi, F. A., Al Ghaferi, A. A., Saadat, I., & Hilal, N. (2014). Application of capacitive deionisation in water desalination: A review. *Desalination*, *342*, 3–15. Available from https://doi.org/10.1016/j.desal.2014.02.031.

Aly, S., Darwish, M., & Fathalah, K. (1989). Potential drop & ionic flux in desalting electrodialysis units. *Journal of King Abdulaziz University-Engineering Sciences*, 31–48. Available from https://doi.org/10.4197/Eng.1-1.4.

An, J. W., Kang, D. J., Tran, K. T., Kim, M. J., Lim, T., & Tran, T. (2012). Recovery of lithium from Uyuni salar brine. *Hydrometallurgy*, *117–118*, 64–70. Available from https://doi.org/10.1016/j.hydromet.2012.02.008.

Arnold, B. B., & Murphy, G. W. (1961). Studies on the electrochemistry of carbon and chemically-modified carbon surfaces. *Journal of Physical Chemistry*, *65*(1), 135–138. Available from https://doi.org/10.1021/j100819a038.

Bacher, L. E., de Oliveira, C., Giacobbo, A., et al. (2017). Coupling coagulation using tannin-based product with electrodialysis reversal to water treatment: A case study. *Journal of Environmental Chemical Engineering*, *5*(6), 6008–6015. Available from https://doi.org/10.1016/j.jece.2017.11.002.

Bak, C., Yun, Y. M., Kim, J. H., & Kang, S. (2019). Electrodialytic separation of volatile fatty acids from hydrogen fermented food wastes. *International Journal of Hydrogen Energy*, 3356–3362. Available from https://doi.org/10.1016/j.ijhydene.2018.07.134.

Barros, K. S., & Espinosa, D. C. R. (2018). Chronopotentiometry of an anion-exchange membrane for treating a synthesized free-cyanide effluent from brass electrodeposition with EDTA as chelating agent. *Separation and Purification Technology*, *201*, 244–255. Available from https://doi.org/10.1016/j.seppur.2018.03.013.

Barros, K. S., Martí-Calatayud, M. C., Ortega, E. M., Pérez-Herranz, V., & Espinosa, D. C. R. (2020). Chronopotentiometric study on the simultaneous transport of EDTA ionic species and hydroxyl ions through an anion-exchange membrane for electrodialysis applications. *Journal of Electroanalytical Chemistry*, *879*, 114782. Available from https://doi.org/10.1016/j.jelechem.2020.114782.

Barros, K. S., Martí-Calatayud, M. C., Pérez-Herranz, V., & Espinosa, D. C. R. (2020). A three-stage chemical cleaning of ion-exchange membranes used in the treatment by electrodialysis of wastewaters generated in brass electroplating industries. *Desalination*, *492*, 114628. Available from https://doi.org/10.1016/j.desal.2020.114628.

Barros, K. S., Ortega, E. M., Pérez-Herranz, V., & Espinosa, D. C. R. (2020). Evaluation of brass electrodeposition at RDE from cyanide-free bath using EDTA as a complexing agent. *Journal of Electroanalytical Chemistry*, 865. Available from https://doi.org/10.1016/j.jelechem.2020.114129.

Barros, K. S., Scarazzato, T., & Espinosa, D. C. R. (2018). Evaluation of the effect of the solution concentration and membrane morphology on the transport properties of Cu(II) through two monopolar cation-exchange membranes. *Separation and Purification Technology*, *193*, 184–192. Available from https://doi.org/10.1016/j.seppur.2017.10.067.

Barros, K. S., Scarazzato, T., Pérez-Herranz, V., & Espinosa, D. C. R. (2020). Treatment of cyanide-free wastewater from brass electrodeposition with EDTA by electrodialysis: Evaluation of underlimiting and overlimiting operations. *Membranes*, *10*(4), 69. Available from https://doi.org/10.3390/membranes10040069.

Bazinet, L., & Geoffroy, T. R. (2020). Electrodialytic processes: Market overview, membrane phenomena, recent developments and sustainable strategies. *Membranes*, *10*(9), 1–72. Available from https://doi.org/10.3390/membranes10090221.

Bazrgar Bajestani, M., Moheb, A., & Dinari, M. (2020). Preparation of lithium ion-selective cation exchange membrane for lithium recovery from sodium contaminated lithium bromide solution by electrodialysis process. *Desalination*, *486*, 114476. Available from https://doi.org/10.1016/j.desal.2020.114476.

Beaulieu, M., Perreault, V., Mikhaylin, S., & Bazinet, L. (2020). How overlimiting current condition influences lactic acid recovery and demineralization by electrodialysis with nanofiltration membrane: Comparison with conventional electrodialysis. *Membranes*, *10*(6), 113. Available from https://doi.org/10.3390/membranes10060113.

Benvenuti, T., Siqueira Rodrigues, M. A., Bernardes, A. M., & Zoppas-Ferreira, J. (2017). Closing the loop in the electroplating industry by electrodialysis. *Journal of Cleaner Production*, *155*, 130–138. Available from https://doi.org/10.1016/j.jclepro.2016.05.139.

Bernardes, A. M., Rodrigues, M. A. S., Zoppas., & Ferreira, J. (2014). General aspects of electrodialysis. In A. M. Bernardes, M. A. S. Rodrigues, & J. Z. Ferreira (Eds.), *Electrodialysis and water reuse: Novel approaches* (pp. 11–24). Elsevier.

Besha, A. T., Tsehaye, M. T., Aili, D., Zhang, W., & Tufa, R. A. (2020). Design of monovalent ion selective membranes for reducing the impacts of multivalent ions in reverse electrodialysis. *Membranes*, *10*(1), 7. Available from https://doi.org/10.3390/membranes10010007.

Bian, D. W., Watson, S. M., Wright, N. C., et al. (2019). Optimization and design of a low-cost, village-scale, photovoltaic-powered, electrodialysis reversal desalination system for rural India. *Desalination*, *452*, 265–278. Available from https://doi.org/10.1016/j.desal.2018.09.004.

Blair, J. W., & Murphy, G. W. (1960). Electrochemical demineralization of water with porous electrodes of large surface area. *Saline water conversion* (pp. 206–223). American Chemical Society. Available from http://doi.org/10.1021/ba-1960-0027.ch020.

Bukhovets, A., Eliseeva, T., Dalthrope, N., & Oren, Y. (2011). The influence of current density on the electrochemical properties of anion-exchange membranes in electrodialysis of phenylalanine solution. *Electrochimica Acta*, *56*(27), 10283–10287. Available from https://doi.org/10.1016/j.electacta.2011.09.025.

Campione, A., Gurreri, L., Ciofalo, M., Micale, G., Tamburini, A., & Cipollina, A. (2018). Electrodialysis for water desalination: A critical assessment of recent developments on process fundamentals, models and applications. *Desalination*, *434*, 121–160. Available from https://doi.org/10.1016/j.desal.2017.12.044.

Campione, A., Cipollina, A., Bogle, I. D. L., Gurreri, L., Tamburini, A., Tedesco, M., & Micale, G. (2019). A hierarchical model for novel schemes of electrodialysis desalination. *Desalination* (465), 79–93. Available from https://doi.org/10.1016/j.desal.2019.04.020.

Chao, Y. M., & Liang, T. M. (2008). A feasibility study of industrial wastewater recovery using electrodialysis reversal. *Desalination*, *221*(1–3), 433–439. Available from https://doi.org/10.1016/j.desal.2007.04.065.

Chen, S. S., Li, C. W., Hsu, H. D., Lee, P. C., Chang, Y. M., & Yang, C. H. (2009). Concentration and purification of chromate from electroplating wastewater by two-stage electrodialysis processes. *Journal of Hazardous Materials*, *161*(2–3), 1075–1080. Available from https://doi.org/10.1016/j.jhazmat.2008.04.106.

Chen, Y., Zhang, S., Liu, Q., & Jian, X. (2021). The effect of counter-ion substitution on poly(phthalazinone ether ketone) amphoteric ion exchange membranes for vanadium redox flow battery. *Journal of Membrane Science*, *620*, 118816. Available from https://doi.org/10.1016/j.memsci.2020.118816.

Choi, J., Lee, H., & Hong, S. (2016). Capacitive deionization (CDI) integrated with monovalent cation selective membrane for producing divalent cation-rich solution. *Desalination*, *400*, 38–46. Available from https://doi.org/10.1016/j.desal.2016.09.016.

Datar, S. D., Mohanapriya, K., Ahirrao, D. J., & Jha, N. (2021). Comparative study of electrosorption performance of solar reduced graphene oxide in flow-between and flow-through capacitive deionization architectures. *Separation and Purification Technology*, *257*, 117972. Available from https://doi.org/10.1016/j.seppur.2020.117972.

da Trindade, C. d M., Giacobbo, A., Ferreira, V. G., Rodrigues, M. A. S., & Bernardes, A. M. (2015). Membrane separation processes applied to the treatment of effluents from nanoceramic coating operations. *Desalination and Water Treatment*, *55*(1), 28–38. Available from https://doi.org/10.1080/19443994.2014.911703.

De Schepper, W., Moraru, M. D., Jacobs, B., Oudshoorn, M., & Helsen, J. (2019). Electrodialysis of aqueous NaCl-glycerol solutions: A phenomenological comparison of various ion exchange membranes. *Separation and Purification Technology*, *217*, 274–283. Available from https://doi.org/10.1016/j.seppur.2019.02.030.

Díaz, J. C., & Kamcev, J. (2021). Ionic conductivity of ion-exchange membranes: Measurement techniques and salt concentration dependence. *Journal of Membrane Science*, *618*, 118718. Available from https://doi.org/10.1016/j.memsci.2020.118718.

Fan, H., Huang, Y., & Yip, N. Y. (2020). Advancing the conductivity-permselectivity tradeoff of electrodialysis ion-exchange membranes with sulfonated CNT nanocomposites. *Journal of Membrane Science*, *610*, 118259. Available from https://doi.org/10.1016/j.memsci.2020.118259.

Fang, K., Gong, H., He, W., Peng, F., He, C., & Wang, K. (2018). Recovering ammonia from municipal wastewater by flow-electrode capacitive deionization. *Chemical Engineering Journal*, *348*, 301–309. Available from https://doi.org/10.1016/j.cej.2018.04.128.

Farmer, J. C., Fix, D. V., Mack, G. V., Pekala, R. W., & Poco, J. F. (1996). Capacitive deionization of NaCI and $NaNO_3$ solutions with carbon aerogel electrodes. *Journal of the Electrochemical Society*, *143*(1), 159–169. Available from https://doi.org/10.1149/1.1836402.

Ferreira, C. A., Müller, F., & Amado, F. D. R. (2014). Ionic membranes. *Electrodialysis and water reuse: Novel approaches* (pp. 41–61). Berlin, Heidelberg: Springer. Available from http://doi.org/10.1007/978-3-642-40249-4_5.

Ge, L., Wu, B., Yu, D., et al. (2017). Monovalent cation perm-selective membranes (MCPMs): New developments and perspectives. *Chinese Journal of Chemical Engineering*, *25*(11), 1606–1615. Available from https://doi.org/10.1016/j.cjche.2017.06.002.

Gonzalez-Vogel, A., Moltedo, J. J., Reyes, R. Q., Schwarz, A., & Rojas, O. J. (2021). High frequency pulsed electrodialysis of acidic filtrate in kraft pulping. *Journal of Environmental Management*, *282*, 111891. Available from https://doi.org/10.1016/j.jenvman.2020.111891.

Goodman, N. B., Taylor, R. J., Xie, Z., Gozukara, Y., & Clements, A. (2013). A feasibility study of municipal wastewater desalination using electrodialysis reversal to provide recycled water for horticultural irrigation. *Desalination*, *317*, 77–83. Available from https://doi.org/10.1016/j.desal.2013.02.010.

Grebenyuk, V. D., Chebotareva, R. D., Peters, S., & Linkov, V. (1998). Surface modification of anion-exchange electrodialysis membranes to enhance anti-fouling characteristics. *Desalination*, *115*(3), 313–329. Available from https://doi.org/10.1016/S0011-9164(98)00051-4.

Guo, H., You, F., Yu, S., Li, L., & Zhao, D. (2015). Mechanisms of chemical cleaning of ion exchange membranes: A case study of plant-scale electrodialysis for oily wastewater treatment. *Journal of Membrane Science*, *496*, 310–317. Available from https://doi.org/10.1016/j.memsci.2015.09.005.

Ha, Y., Lee, H., Yoon, H., et al. (2021). Enhanced salt removal performance of flow electrode capacitive deionization with high cell operational potential. *Separation and Purification Technology*, *254*, 117500. Available from https://doi.org/10.1016/j.seppur.2020.117500.

Han, J. H., Jeong, N., Kim, C. S., et al. (2019). Reverse electrodialysis (RED) using a bipolar membrane to suppress inorganic fouling around the cathode. *Water Research*, *166*, 115078. Available from https://doi.org/10.1016/j.watres.2019.115078.

Handojo, L., Wardani, A. K., Regina, D., Bella, C., Kresnowati, M. T. A. P., & Wenten, I. G. (2019). Electromembrane processes for organic acid recovery. *RSC Advances*, *9*(14), 7854–7869. Available from https://doi.org/10.1039/C8RA09227C.

Hansima, M. A. C. K., Makehelwala, M., Jinadasa, K. B. S. N., et al. (2021). Fouling of ion exchange membranes used in the electrodialysis reversal advanced water treatment: A review. *Chemosphere*, *263*, 127951. Available from https://doi.org/10.1016/j.chemosphere.2020.127951.

Hassanvand, A., Chen, G. Q., Webley, P. A., & Kentish, S. E. (2019). An investigation of the impact of fouling agents in capacitive and membrane capacitive deionisation. *Desalination*, *457*, 96–102. Available from https://doi.org/10.1016/j.desal.2019.01.031.

Hosseini, S. M., Jeddi, F., Nemati, M., Madaeni, S. S., & Moghadassi, A. R. (2014). Electrodialysis heterogeneous anion exchange membrane modified by PANI/MWCNT composite nanoparticles: Preparation, characterization and ionic transport property in desalination. *Desalination*, *341*(1), 107–114. Available from https://doi.org/10.1016/j.desal.2014.03.001.

İpekçi, D., Kabay, N., Bunani, S., et al. (2020). Application of heterogeneous ion exchange membranes for simultaneous separation and recovery of lithium and boron from aqueous solution with bipolar membrane electrodialysis (EDBM). *Desalination*, *479*, 114313. Available from https://doi.org/10.1016/j.desal.2020.114313.

Irfan, M., Xu, T., Ge, L., Wang, Y., & Xu, T. (2019). Zwitterion structure membrane provides high monovalent/divalent cation electrodialysis selectivity: Investigating the effect of functional groups and operating parameters. *Journal of Membrane Science*, *588*, 117211. Available from https://doi.org/10.1016/j.memsci.2019.117211.

Ji, P. Y., Ji, Z. Y., Chen, Q. B., et al. (2018). Effect of coexisting ions on recovering lithium from high Mg^{2+}/Li^{+} ratio brines by selective-electrodialysis. *Separation and Purification Technology*, *207*, 1–11. Available from https://doi.org/10.1016/j.seppur.2018.06.012.

Kim, D. H., Seo, S. J., Lee, M. J., et al. (2014). Pore-filled anion-exchange membranes for non-aqueous redox flow batteries with dual-metal-complex redox shuttles. *Journal of Membrane Science*, *454*, 44–50. Available from https://doi.org/10.1016/j.memsci.2013.11.051.

Kim, J., Kim, S., & Kwak, R. (2021). Controlling ion transport with pattern structures on ion exchange membranes in electrodialysis. *Desalination*, *499*, 114801. Available from https://doi.org/10.1016/j.desal.2020.114801.

Kim, N., Lee, J., Kim, S., et al. (2020). Short review of multichannel membrane capacitive deionization: Principle, current status, and future prospect. *Applied Sciences (Switzerland)*, *10*(2), 683. Available from https://doi.org/10.3390/app10020683.

Koseoglu-Imer, D. Y., & Karagunduz, A. (2018). Recent developments of electromembrane desalination processes. *Environmental Technology Reviews*, *7*(1), 199–219. Available from https://doi.org/10.1080/21622515.2018.1483974.

Kotoka, F., Merino-Garcia, I., & Velizarov, S. (2020). Surface modifications of anion exchange membranes for an improved reverse electrodialysis process performance: A review. *Membranes*, *10*(8), 1–22. Available from https://doi.org/10.3390/membranes10080160.

La Cerva, M., Gurreri, L., Cipollina, A., Tamburini, A., Ciofalo, M., & Micale, G. (2019). Modelling and cost analysis of hybrid systems for seawater desalination: Electromembrane pre-treatments for reverse osmosis. *Desalination*, *467*, 175–195. Available from https://doi.org/10.1016/j.desal.2019.06.010.

Larchet, C., Nouri, S., Auclair, B., Dammak, L., & Nikonenko, V. (2008). Application of chronopotentiometry to determine the thickness of diffusion layer adjacent to an ion-exchange membrane under natural convection. *Advances in Colloid and Interface Science*, *139*(1–2), 45–61. Available from https://doi.org/10.1016/j.cis.2008.01.007.

Lee, H. J., Sarfert, F., Strathmann, H., & Moon, S. H. (2002). Designing of an electrodialysis desalination plant. *Desalination*, *142*(3), 267–286. Available from https://doi.org/10.1016/S0011-9164(02)00208-4.

Lee, J. H., & Choi, J. H. (2012). The production of ultrapure water by membrane capacitive deionization (MCDI) technology. *Journal of Membrane Science*, *409–410*, 251–256. Available from https://doi.org/10.1016/j.memsci.2012.03.064.

Lee, S., Meng, W., Wang, Y., et al. (2021). Comparison of the property of homogeneous and heterogeneous ion exchange membranes during electrodialysis process. *Ain Shams Engineering Journal*, *12*(1), 159–166. Available from https://doi.org/10.1016/j.asej.2020.07.018.

Li, Y., Shi, S., Cao, H., & Cao, R. (2021). Robust antifouling anion exchange membranes modified by graphene oxide (GO)-enhanced Co-deposition of tannic acid and polyethyleneimine. *Journal of Membrane Science*, *625*, 119111. Available from https://doi.org/10.1016/j.memsci.2021.119111.

Liao, J., Chen, Q., Pan, N., et al. (2020). Amphoteric blend ion-exchange membranes for separating monovalent and bivalent anions in electrodialysis. *Separation and Purification Technology*, *242*, 116793. Available from https://doi.org/10.1016/j.seppur.2020.116793.

Liao, J., Yu, X., Pan, N., Li, J., Shen, J., & Gao, C. (2019). Amphoteric ion-exchange membranes with superior mono-/bi-valent anion separation performance for electrodialysis applications. *Journal of Membrane Science*, *577*, 153–164. Available from https://doi.org/10.1016/j.memsci.2019.01.052.

Liu, E., Lee, L. Y., Ong, S. L., & Ng, H. Y. (2020). Treatment of industrial brine using capacitive deionization (CDI) towards zero liquid discharge – challenges and optimization. *Water Research*, *183*, 116059. Available from https://doi.org/10.1016/j.watres.2020.116059.

Liu, R., Wang, Y., Wu, G., Luo, J., & Wang, S. (2017). Development of a selective electrodialysis for nutrient recovery and desalination during secondary effluent treatment. *Chemical Engineering Journal*, *322*, 224–233. Available from https://doi.org/10.1016/j.cej.2017.03.149.

Liu, Y., & Wang, J. (2020). Performance enhancement of catalytic bipolar membrane based on polysulfone single base membrane for electrodialysis. *Journal of Membrane Science*, *606*, 118151. Available from https://doi.org/10.1016/j.memsci.2020.118151.

Luo, T., Abdu, S., & Wessling, M. (2018). Selectivity of ion exchange membranes: A review. *Journal of Membrane Science*, *555*, 429–454. Available from https://doi.org/10.1016/j.memsci.2018.03.051.

Ma, J., Ma, J., Zhang, C., Song, J., Dong, W., & Waite, T. D. (2020). Flow-electrode capacitive deionization (FCDI) scale-up using a membrane stack configuration. *Water Research*, *168*, 115186. Available from https://doi.org/10.1016/j.watres.2019.115186.

Maheshwari, K., & Agrawal, M. (2020). Advances in capacitive deionization as an effective technique for reverse osmosis reject stream treatment. *Journal of Environmental Chemical Engineering*, *8*(6), 104413. Available from https://doi.org/10.1016/j.jece.2020.104413.

Mareev, S. A., Evdochenko, E., Wessling, M., et al. (2020). A comprehensive mathematical model of water splitting in bipolar membranes: Impact of the spatial distribution of fixed charges and catalyst at bipolar junction. *Journal of Membrane Science* (603), 118010. Available from https://doi.org/10.1016/j.memsci.2020.118010.

Martí-Calatayud, M. C., Buzzi, D. C., García-Gabaldón, M., et al. (2014). Sulfuric acid recovery from acid mine drainage by means of electrodialysis. *Desalination*, *343*, 120–127. Available from https://doi.org/10.1016/j.desal.2013.11.031.

McGovern, R. K., Zubair, S. M., & Lienhard, V. J. H. (2014). The cost effectiveness of electrodialysis for diverse salinity applications. *Desalination*, *348*, 57–65. Available from https://doi.org/10.1016/j.desal.2014.06.010.

Merkel, A., & Ashrafi, A. M. (2019). An investigation on the application of pulsed electrodialysis reversal in whey desalination. *International Journal of Molecular Sciences*, *20*(8), 1918. Available from https://doi.org/10.3390/ijms20081918.

Mikhaylin, S., & Bazinet, L. (2016). Fouling on ion-exchange membranes: Classification, characterization and strategies of prevention and control. *Advances in Colloid and Interface Science*, *229*, 34–56. Available from https://doi.org/10.1016/j.cis.2015.12.006.

Mitko, K., & Turek, M. (2015). Innovations in electromembrane processes. *Copernican Letters*, *6*, 34–40. Available from https://doi.org/10.12775/cl.2015.005.

Nikonenko, V. V., Kovalenko, A. V., Urtenov, M. K., et al. (2014). Desalination at overlimiting currents: State-of-the-art and perspectives. *Desalination*, *342*, 85–106. Available from https://doi.org/10.1016/j.desal.2014.01.008.

Nikonenko, V. V., Pismenskaya, N. D., Belova, E. I., et al. (2010). Intensive current transfer in membrane systems: Modelling, mechanisms and application in electrodialysis. *Advances in Colloid and Interface Science*, *160*(1–2), 101–123. Available from https://doi.org/10.1016/j.cis.2010.08.001.

Park, H. R., Choi, J., Yang, S., et al. (2016). Surface-modified spherical activated carbon for high carbon loading and its desalting performance in flow-electrode capacitive deionization. *RSC Advances*, *6*(74), 69720–69727. Available from https://doi.org/10.1039/c6ra02480g.

Park, S. G., Rajesh, P. P., Hwang, M. H., Chu, K. H., Cho, S., & Chae, K. J. (2021). Long-term effects of anti-biofouling proton exchange membrane using silver nanoparticles and polydopamine on the performance of microbial electrolysis cells. *International Journal of Hydrogen Energy*, *46*(20), 11345–11356. Available from https://doi.org/10.1016/j.ijhydene.2020.04.059.

Patel, S. K., Qin, M., Walker, W. S., & Elimelech, M. (2020). Energy efficiency of electro-driven brackish water desalination: Electrodialysis significantly outperforms membrane capacitive deionization. *Environmental Science and Technology*, *54*(6), 3663–3677. Available from https://doi.org/10.1021/acs.est.9b07482.

Pawlowski, S., Huertas, R. M., Galinha, C. F., Crespo, J. G., & Velizarov, S. (2020). On operation of reverse electrodialysis (RED) and membrane capacitive deionisation (MCDI) with natural saline streams: A critical review. *Desalination*, *476*, 114183. Available from https://doi.org/10.1016/j.desal.2019.114183.

Porada, S., Zhang, L., & Dykstra, J. E. (2020). Energy consumption in membrane capacitive deionization and comparison with reverse osmosis. *Desalination*, *488*, 114383. Available from https://doi.org/10.1016/j.desal.2020.114383.

Porada, S., Zhao, R., Van Der Wal, A., Presser, V., & Biesheuvel, P. M. (2013). Review on the science and technology of water desalination by capacitive deionization. *Progress in Materials Science*, *58*(8), 1388–1442. Available from https://doi.org/10.1016/j.pmatsci.2013.03.005.

Pärnamäe, R., Mareev, S., Nikonenko, V., et al. (2021). Bipolar membranes: A review on principles, latest developments, and applications. *Journal o Membrane Science* (617):118538). Available from https://doi.org/10.1016/j.memsci.2020.118538.

Ran, J., Wu, L., He, Y., et al. (2017). Ion exchange membranes: New developments and applications. *Journal of Membrane Science*, *522*, 267–291. Available from https://doi.org/10.1016/j.memsci.2016.09.033.

Ravikumar, Y. V. L., Sridhar, S., & Satyanarayana, S. V. (2013). Development of an electrodialysis-distillation integrated process for separation of hazardous sodium azide to recover valuable DMSO solvent from pharmaceutical effluent. *Separation and Purification Technology* (110), 20–230. Available from https://doi.org/10.1016/j.seppur.2013.02.031.

Reig, M., Vecino, X., Valderrama, C., Gibert, O., & Cortina, J. L. (2018). Application of selectrodialysis for the removal of As from metallurgical process waters: Recovery of Cu and Zn. *Separation and Purification Technology*, *195*, 404–412. Available from https://doi.org/10.1016/j.seppur.2017.12.040.

Rommerskirchen, A., Alders, M., Wiesner, F., Linnartz, C. J., Kalde, A., & Wessling, M. (2020). Process model for high salinity flow-electrode capacitive deionization processes with ion-exchange membranes. *Journal of Membrane Science*, *616*, 118614. Available from https://doi.org/10.1016/j.memsci.2020.118614.

Rommerskirchen, A., Linnartz, C. J., Egidi, F., Kendir, S., & Wessling, M. (2020). Flow-electrode capacitive deionization enables continuous and energy-efficient brine concentration. *Desalination*, *490*, 114453. Available from https://doi.org/10.1016/j.desal.2020.114453.

Rotta, E. H., Bitencourt, C. S., Marder, L., & Bernardes, A. M. (2019). Phosphorus recovery from low phosphate-containing solution by electrodialysis. *Journal of Membrane Science*, *573*, 293–300. Available from https://doi.org/10.1016/j.memsci.2018.12.020.

Scarazzato, T., Barros, K. S., Benvenuti, T., Rodrigues, M. A. S., Espinosa, D. C. R., Bernardes, A. M., … Pérez-Herranz, V. (2020). *Achievements in electrodialysis processes for wastewater and water treatment*. *Current Trends and Future Developments on (Bio-) Membranes: Recent Achievements in Wastewater and Water Treatments* (pp. 127–160). Elsevier BV. Available from http://doi.org/10.1016/b978-0-12-817378-7.00005-7.

Shen, B., Sana, B., & Pu, H. (2020). Multi-block poly(ether sulfone) for anion exchange membranes with long side chains densely terminated by piperidinium. *Journal of Membrane Science*, *615*, 118537. Available from https://doi.org/10.1016/j.memsci.2020.118537.

Shi, L., Hu, Z., Simplicio, W. S., et al. (2020). Antibiotics in nutrient recovery from pig manure via electrodialysis reversal: Sorption and migration associated with membrane fouling. *Journal of Membrane Science*, *597*, 117633. Available from https://doi.org/10.1016/j.memsci.2019.117633.

Shin, Y. U., Lim, J., Boo, C., & Hong, S. (2021). Improving the feasibility and applicability of flow-electrode capacitive deionization (FCDI): Review of process optimization and energy efficiency. *Desalination*, *502*, 114930. Available from https://doi.org/10.1016/j.desal.2021.114930.

Shukla, G., & Shahi, V. K. (2019). Sulfonated poly(ether ether ketone)/imidized graphene oxide composite cation exchange membrane with improved conductivity and stability for electrodialytic water desalination. *Desalination*, *451*, 200–208. Available from https://doi.org/10.1016/j.desal.2018.03.018.

Souza, L. A. d, Benvenuti, T., Buzzi, D. C., Rodrigues, M. A. S., & Amado, F. D. R. (2020). Electrodialysis reversal applied to tertiary treatment of Kraft pulp mill effluent. *Chemical Engineering Communications*, *208*(151), 1–14. Available from https://doi.org/10.1080/00986445.2020.1789603.

Strathmann, H. (1995). In D. Editor(s)RichardNoble, & AlexanderS. Stern (Eds.), *Membrane science and technology* (2, pp. 213–281). Elsevier. Available from https://doi.org/10.1016/S0927-5193(06)80008-2.

Strathmann, H. (2004). Ion-exchange Membrane Separation Processes. *Membrane Science Technology*, *9*, 1–348.

Strathmann, H. (2010). Electrodialysis, a mature technology with a multitude of new applications. *Desalination*, *264*(3), 268–288. Available from https://doi.org/10.1016/j.desal.2010.04.069.

Strathmann, H. (2011). *Introduction to membrane science and technology*. Wiley.
Suss, M. E., Baumann, T. F., Bourcier, W. L., et al. (2012). Capacitive desalination with flow-through electrodes. *Energy and Environmental Science*, *5*(11), 9511–9519. Available from https://doi.org/10.1039/c2ee21498a.
Tran, A. T. K., Zhang, Y., De Corte, D., et al. (2014). P-recovery as calcium phosphate from wastewater using an integrated selectrodialysis/crystallization process. *Journal of Cleaner Production*, *77*, 140–151. Available from https://doi.org/10.1016/j.jclepro.2014.01.069.
Van Limpt, B., & van der Wal, A. (2014). Water and chemical savings in cooling towers by using membrane capacitive deionization. *Desalination*, *342*, 148–155. Available from https://doi.org/10.1016/j.desal.2013.12.022.
Van der Bruggen, B. (2018). Ion-exchange membrane systems—Electrodialysis and other electromembrane processes. *Fundamental modeling of membrane systems: Membrane and process performance* (pp. 251–300). Elsevier. Available from http://doi.org/10.1016/B978-0-12-813483-2.00007-1.
Vaselbehagh, M., Karkhanechi, H., Takagi, R., & Matsuyama, H. (2016). Effect of polydopamine coating and direct electric current application on anti-biofouling properties of anion exchange membranes in electrodialysis. *Journal of Membrane Science*, *515*, 98–108. Available from https://doi.org/10.1016/j.memsci.2016.05.049.
Venzke, C. D., Giacobbo, A., Ferreira, J. Z., Bernardes, A. M., & Rodrigues, M. A. S. (2018). Increasing water recovery rate of membrane hybrid process on the petrochemical wastewater treatment. *Process Safety and Environmental Protection*, *117*, 152–158. Available from https://doi.org/10.1016/j.psep.2018.04.023.
Vermaas, D. A., Kunteng, D., Saakes, M., & Nijmeijer, K. (2013). Fouling in reverse electrodialysis under natural conditions. *Water Research*, *47*(3), 1289–1298. Available from https://doi.org/10.1016/j.watres.2012.11.053.
Virtanen, T., Reinikainen, S. P., Lahti, J., Mänttäri, M., & Kallioinen, M. (2018). Visual tool for real-time monitoring of membrane fouling via Raman spectroscopy and process model based on principal component analysis. *Scientific Reports*, *8*(1). Available from https://doi.org/10.1038/s41598-018-29268-y.
Vogel, C., & Meier-Haack, J. (2014). Preparation of ion-exchange materials and membranes. *Desalination*, *342*, 156–174. Available from https://doi.org/10.1016/j.desal.2013.12.039.
Wang, T., Bai, L., Zhang, C., et al. (2020). Formation mechanism of iron scale in membrane capacitive deionization (MCDI) system. *Desalination*, *495*, 114636. Available from https://doi.org/10.1016/j.desal.2020.114636.
Warsinger, D. M., Chakraborty, S., Tow, E. W., et al. (2018). A review of polymeric membranes and processes for potable water reuse. *Progress in Polymer Science*, *81*, 209–237. Available from https://doi.org/10.1016/j.progpolymsci.2018.01.004.
Welgemoed, T. J., & Schutte, C. F. (2005). Capacitive Deionization Technology™: An alternative desalination solution. *Desalination*, *183*(1–3), 327–340. Available from https://doi.org/10.1016/j.desal.2005.02.054.
Xing, W., Liang, J., Tang, W., et al. (2020). Versatile applications of capacitive deionization (CDI)-based technologies. *Desalination*, *482*, 114390. Available from https://doi.org/10.1016/j.desal.2020.114390.
Xu, H., Ji, X., Wang, L., Huang, J., Han, J., & Wang, Y. (2020). Performance study on a small-scale photovoltaic electrodialysis system for desalination. *Renewable Energy*, *154*, 1008–1013. Available from https://doi.org/10.1016/j.renene.2020.03.066.
Xu, P., Drewes, J. E., Heil, D., & Wang, G. (2008). Treatment of brackish produced water using carbon aerogel-based capacitive deionization technology. *Water Research*, *42*(10–11), 2605–2617. Available from https://doi.org/10.1016/j.watres.2008.01.011.
Xu, T. (2005). Ion exchange membranes: State of their development and perspective. *Journal of Membrane Science*, *263*(1–2), 1–29. Available from https://doi.org/10.1016/j.memsci.2005.05.002.
Yang, S., Choi, J., Yeo, J. G., Jeon, S. I., Park, H. R., & Kim, D. K. (2016). Flow-electrode capacitive deionization using an aqueous electrolyte with a high salt concentration. *Environmental Science and Technology*, *50*(11), 5892–5899. Available from https://doi.org/10.1021/acs.est.5b04640.
Yu, Y., Yan, N., Freeman, B. D., & Chen, C. C. (2021). Mobile ion partitioning in ion exchange membranes immersed in saline solutions. *Journal of Membrane Science*, *620*, 118760. Available from https://doi.org/10.1016/j.memsci.2020.118760.
Zabolotskii, V., Sheldeshov, N., & Melnikov, S. (2014). Heterogeneous bipolar membranes and their application in electrodialysis. *Desalination*, *342*, 183–203. Available from https://doi.org/10.1016/j.desal.2013.11.043.
Zabolotsky, V. I., Novak, L., Kovalenko, A. V., et al. (2017). Electroconvection in systems with heterogeneous ion-exchange membranes. *Petroleum Chemistry*, *57*(9), 779–789. Available from https://doi.org/10.1134/S0965544117090109.

Zhao, J., Ren, L., Chen, Qb, Li, P., & Wang, J. (2020). Fabrication of cation exchange membrane with excellent stabilities for electrodialysis: A study of effective sulfonation degree in ion transport mechanism. *Journal of Membrane Science*, *615*, 118539. Available from https://doi.org/10.1016/j.memsci.2020.118539.

Zhao, Z., Li, Y., Jin, D., Van., & der Bruggen, B. (2021). Modification of an anion exchange membrane based on rapid mussel-inspired deposition for improved antifouling performance. *Colloids and Surfaces A: Physicochemical and Engineering Aspects*, *615*, 126267. Available from https://doi.org/10.1016/j.colsurfa.2021.126267.

Zhu, L., Pan, J., Wang, Y., Han, J., Zhuang, L., & Hickner, M. A. (2016). Multication side chain anion exchange membranes. *Macromolecules*, *49*(3), 815−824. Available from https://doi.org/10.1021/acs.macromol.5b02671.

CHAPTER

15

Polymeric membranes in electrodialysis, electrodialysis reversal, and capacitive deionization technologies

K. Khoiruddin[1,2], *Anita K. Wardani*[1], *Putu T.P. Aryanti*[3] *and I.G. Wenten*[1,2]

[1]Department of Chemical Engineering, Institut Teknologi Bandung, Bandung, Indonesia [2]Research Center for Nanosciences and Nanotechnology, Institut Teknologi Bandung, Bandung, Indonesia [3]Department of Chemical Engineering, Universitas Jenderal Achmad Yani, Cimahi, Indonesia

15.1 Introduction

Ion-exchange membrane (IEM) is a charged membrane that can separate cations and anions from an electrolyte according to a well-known phenomenon Donnan exclusion mechanism (Szczepański & Szczepańska, 2017). The IEM plays an important role in ionic separation by electro-membrane processes such as electrodialysis (ED), electrodialysis reversal (EDR), and membrane capacitive deionization (MCDI). The electro-membrane processes have various applications, especially in water and wastewater treatment (Khoiruddin, Hakim, & Wenten, 2014; Scarazzato, Panossian, Tenório, Pérez-Herranz, & Espinosa, 2017). For example, ED has been applied in brackish water desalination with lower energy than reverse osmosis (RO) (Banasiak, Kruttschnitt, & Schäfer, 2007). In addition, ED can achieve higher water recovery than RO because it is not limited by osmotic pressure (Al-Amshawee et al., 2020). The higher water recovery allows ED to produce a concentrate at a very high concentration. The concentrate can be further used as a feed of the evaporation process in the production of table salt

Advancement in Polymer-Based Membranes for Water Remediation
DOI: https://doi.org/10.1016/B978-0-323-88514-0.00009-7

© 2022 Elsevier Inc. All rights reserved.

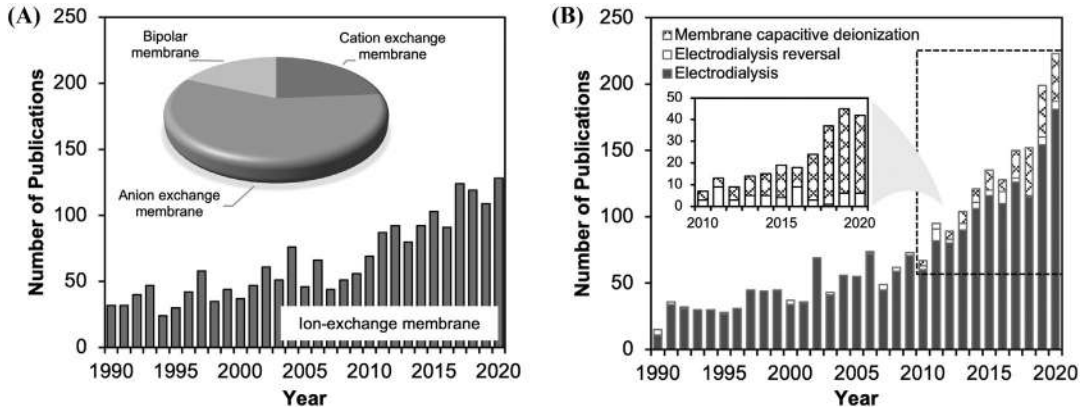

FIGURE 15.1 Number of publications related to ion-exchange membrane (IEM) and electro-membrane processes. (A) Type of IEM. (B) IEM-based processes. Source: *Based on Scopus database; queries: TITLE(terms); attained on January 28, 2021.*

(Ariono, Purwasasmita, & Wenten, 2016; Strathmann, 2010). When compared with conventional deionization processes, such as the conventional ion-exchange process, ED and related processes require no chemicals for regeneration, eliminating spent regenerant treatment and its associated processes (Alvarado & Chen, 2014; Hakim, Khoiruddin, Ariono, & Wenten, 2020; Jin, Du, Zheng, & Zhang, 2016; Wardani, Hakim, Khoiruddin, & Wenten, 2017; Wenten, Khoiruddin, Aryanti, & Hakim, 2016). These advantages drive numerous research as shown in the last 30 years (Fig. 15.1A and B).

One of the strategies to obtain an efficient and low-cost ion separation process is to use an IEM, which is conductive, selective, durable, and at the same, requires low production cost (Stenina, Golubenko, Nikonenko, & Yaroslavtsev, 2020). To obtain such characteristics, the IEM must be prepared from the appropriate material. Polymers are generally easy to process into membranes and are low cost. Therefore, almost all types of IEM are polymeric. Although there are many commercial IEMs, developments are continuously being made to obtain membranes that have better electrochemical characteristics, are resistant to fouling (especially organic fouling), have special characteristics, and are durable (Hansima et al., 2021; Mikhaylin & Bazinet, 2016). Several attempts have been made to achieve these goals, especially with material strategies, such as types of polymers, modifying membrane surfaces, or using materials as additives (Khoiruddin, Ariono, Subagjo, & Wenten, 2017; Lee, Hwang, Jung, & Choi, 2016). Some of these approaches have succeeded in improving the characteristics of IEM so that the ion separation process becomes more efficient.

This chapter reviews the classification and general preparation of polymeric IEMs. It is followed by the discussion of the latest developments of IEMs. The application of IEMs in various electro-membrane processes, particularly ED, EDR, and MCDI will also be discussed in more detail in the next sections.

15.2 Ion-exchange membranes and their fabrication processes

15.2.1 Ion-exchange membranes' classification

There are several categories for IEMs classification. IEMs can be classified based on their charge, namely anion-exchange membrane (AEM), cation-exchange membrane (CEM), and bipolar membrane (BM). AEM has a positive fixed charge in its membrane matrix, which is usually provided by amine-based functional groups, such as quaternary ammonium. The functional groups allow anions to pass through the membrane while excluding cations. CEM has a negative fixed charge provided by functional groups such as sulfonic, phosphoric, or carboxylic (Xu, Wu, & Wu, 2008), thus allowing the permeation of cations and excluding anions. BM is fabricated by laminating CEM and AEM layers together to form a membrane having two charged sides. The join of CEM and AEM creates a bipolar interface that is capable of catalyzing the water dissociation reaction (Neděla, Křivčík, Válek, Stránská, & Marek, 2015). In contrast to CEM and AEM, BM is used to produce H^+ and OH^- ions, such as in the preparation of acid and bases. Acid and bases can be synthesized from their corresponding salt by ED with a bipolar membrane (Hoffmann, Ye, & Hahn, 2016).

IEMs can be classified according to the structure, namely homogeneous and heterogeneous membranes (Ariono, Khoiruddin, & Wenten, 2017; Wenten & Khoiruddin, 2016) (Fig. 15.2). A homogeneous membrane usually consists of one type of polymer serving as a membrane matrix or structure and as the holder of functional groups or charge. On the other hand, a heterogeneous membrane comprises at least two polymers. The first one acts as a membrane structure and usually does not have functional sites. Meanwhile, the second is the carrier of the functional group. The second polymer is usually ion-exchange resin powder. Since heterogeneous membranes contain nonconductive or noncharged phases, they tend to be less conductive and less selective than homogeneous membranes. However, heterogeneous IEMs still become an attractive alternative because of their excellent mechanical strength and low production cost (Garcia-Vasquez et al., 2014). Several types of commercial IEMs and their characteristics are shown in Table 15.1.

15.2.2 Preparation of ion-exchange membranes

Fluorinated ionomer, styrene–divinylbenzene copolymer, polysulfone, sulfonated poly(ether ether ketone), polybenzimidazole, polyimide, and styrene/ethylene-butadiene/styrene triblock copolymers are the type of materials used for IEM preparation (Nagarale, Gohil, & Shahi, 2006). In addition, many other membrane materials are used as polymer binders for fabricating heterogeneous IEMs, such as polyvinyl chloride (Nemati, Hosseini, & Shabanian, 2017), polyethylene (Weinertová, Křivčík, Neděla, Stránská, & Václavíková, 2018), and acrylonitrile–butadiene–styrene (Zendehnam, Robatmili, Hosseini, Arabzadegan, & Madaeni, 2014).

IEMs can be fabricated through a variety of procedures, depending on the type of membrane. The synthesize of homogeneous IEMs generally uses the following approaches: (1) preparation of charged polymers by polymerization or polycondensation of monomers, one of

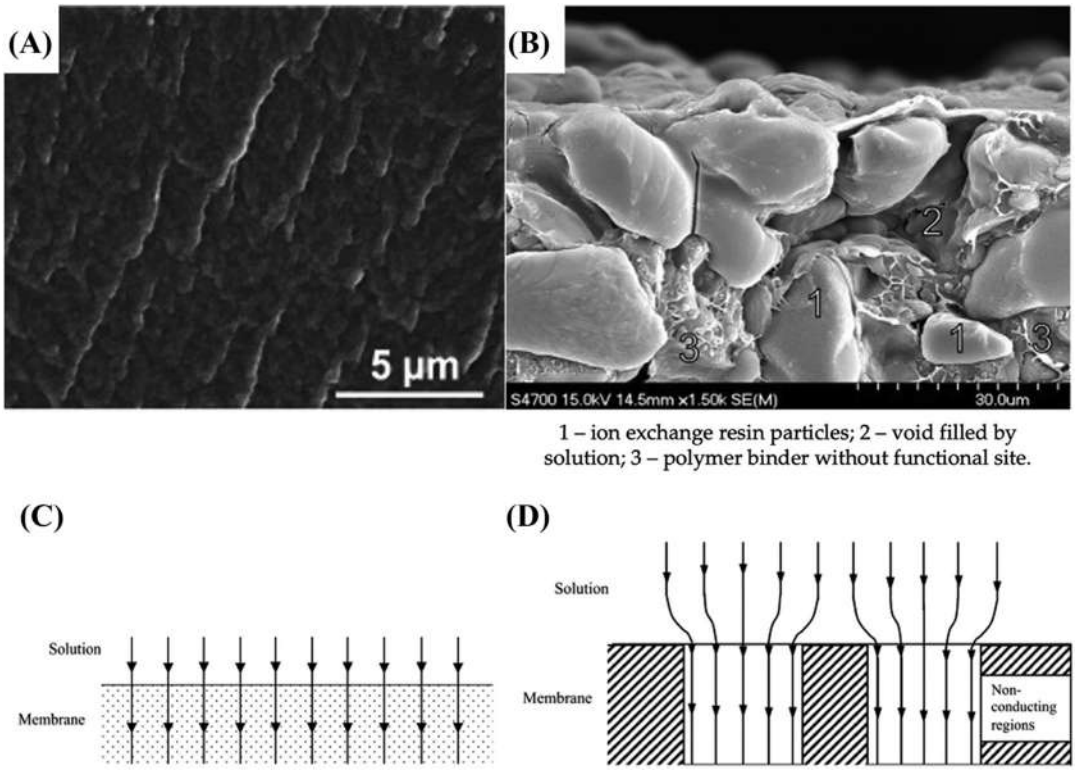

FIGURE 15.2 Homogeneous versus heterogeneous ion-exchange membranes (IEMs). Scanning electron microscope (SEM) image of (A) homogeneous Nafion membrane (Wei et al., 2019) and (B) heterogeneous membrane (Paidar, Fateev, & Bouzek, 2016). Current lines through (C) homogeneous and (D) heterogeneous membrane (Pismenskaia, Sistat, Huguet, Nikonenko, & Pourcelly, 2004). Source: *(A) Reproduced from Wei, Y., Qian, T., Liu, J., Guo, X., Gong, Q., Liu, Z., ..., Qiao, J. (2019). Novel composite Nafion membranes modified with copper phthalocyanine tetrasulfonic acid tetrasodium salt for fuel cell application.* Journal of Materials, 5, *252–257. https://doi.org/10.1016/j.jmat.2019.01.006, with permission, ©2019 Elsevier. (B) Reproduced from Paidar, M., Fateev, V., & Bouzek, K. (2016). Membrane electrolysis—History, current status and perspective.* Electrochimica Acta, 209, *737–756. https://doi.org/10.1016/j.electacta.2016.05.209, with permission, ©2016 Elsevier. (C and D) Reproduced from Pismenskaia, N., Sistat, P., Huguet, P., Nikonenko, V., & Pourcelly, G. (2004). Chronopotentiometry applied to the study of ion transfer through anion exchange membranes.* Journal of Membrane Science, 228, *65–76. https://doi.org/10.1016/j.memsci.2003.09.012, with permission, ©2003 Elsevier.*

which contains functional groups, (2) introduction of functional groups to the polymer, or (3) the introduction of functional groups to the polymer film (Nagarale, Gohil, & Shahi, 2006). For the first two approaches, the functional polymer is then molded into a film or membrane sheet. Examples of homogeneous IEMs prepared by the first process are fluorocarbon-based membranes, such as Nafion (Savadogo, 2004) and styrene–divinylbenzene-based membranes (Shahi, Thampy, & Rangarajan, 2000). Examples of the second approach are preparing sulfonated polysulfone-based (Nagarale, Gohil, Shahi, & Rangarajan, 2005) and the sulfonated polyether ether ketone membrane (Cha, Ul Haq, Choi, & Lee, 2018).

TABLE 15.1 Properties of commercial ion-exchange membranes (IEMs).

Membrane	Polymer matrix	Type	Structure	IEC (meq g^{-1})	Wu (wt.%)	Rm ($\times 10^{-4}$ Ω m^{-2})	Ps (–)	Thickness (μm)	References
Fujifilm, CEM RP1 80050–04	Polyolefin	CEM	Homogenous	1.45	–	2.96	0.90	120	Sarapulova et al. (2019); Tedesco et al. (2016)
Fujifilm, AEM RP1 80045–01	Polyolefin	AEM	Homogenous	1.28	–	1.55	0.65	120	Tedesco et al. (2016)
Dupont, Nafion 117	Perfluorinated ionomer	CEM	Homogenous	0.90	16	1.5	0.97	200	Nagarale, Gohil, & Shahi (2006)
Neosepta, CMX	Styrene–divinylbenzene copolymer	CEM	Homogenous	1.62	18	2.91	0.99	164	Długołęcki, Nymeijer, Metz, and Wessling (2008)
Neosepta, AMX	Styrene–divinylbenzene copolymer	AEM	Homogenous	1.25	16	2.35	0.91	134	Długołęcki et al. (2008)
Ralex, CM	Polyethylene/polyester	CEM	Heterogeneous	2.15	60	9.36	0.84	–	Hosseini, Madaeni, and Khodabakhshi (2011)
Ralex, AMH-PES	Polyethylene/polyester	AEM	Heterogeneous	1.97	56	7.66	0.89	714	Długołęcki et al. (2008)

IEC, ion-exchange capacity; *Ps*, permselectivity; *Rm*, membrane resistance; *Wu*, water uptake.

Heterogeneous IEMs can be fabricated by solution casting techniques (Hosseini et al., 2019; Hosseini, Rafiei, Salabat, & Ahmadi, 2020; Khoiruddin, Ariono, Subagjo, & Wenten, 2018, 2020). First, the polymer binder is dissolved into the solvent. Then, the polymer containing functional groups, usually ion-exchange resin powder with a 300−400 mesh size, is dispersed into the polymer solution. Afterward, the solution is cast, followed by solvent separation, either by evaporation or by the solvent−nonsolvent exchange process. The second method is hot pressing (Křivčík, Vladařová, Hadrava, Černín, & Brožová, 2010). The polymer and ion-exchange resin powder are mixed and then molded at a temperature that is sufficient to melt the polymer binder. Unlike solution casting, this method does not require solvents.

15.2.3 Recent developments in polymeric ion-exchange membranes

Currently, there are also many other types of IEMs being developed, such as amphoteric membranes. In contrast to BM, which has positive and negative charges in different layers, amphoteric IEMs have both charges in the membrane matrix (Liu et al., 2021). Amphoteric IEMs can be prepared by blending (Chen, Zhang, Liu, & Jian, 2020), grafting (Hu et al., 2012; Yuan et al., 2013), polymerization (Fei et al., 2016; Wang et al., 2014), cross-linking (Liao et al., 2019; Ling et al., 2019), and pore-filling (Lee, Kang, Jeon, Choi, & Yoon, 2016) methods. One of the purposes of developing amphoteric membrane is to improve membrane permselectivity towards monovalent ions.

Another interesting IEMs development is the preparation of profiled/patterned membranes (Fig. 15.3A−E). Profiled IEMs have unique nonflat or curvature surfaces. Profiled IEMs can be prepared by the solution casting method with a specially designed mold (Fig. 15.3A) (Güler, Elizen, Saakes, & Nijmeijer, 2014). Profiled membranes are also fabricated by hot pressing (Sheldeshov, Zabolotskii, & Loza, 2014). In this method, a membrane is pressed on a mold with a special design at a high temperature. 3D printing is a more advanced membrane preparation, that has been used to produce profiled IEMs (Xie, Luo, & Gray, 2017). In this method, the membrane solution is printed with a special printer to create a three-dimensional shape. With its unique curvature surface, profiled IEMs offer better fluid mixing in the diffusive boundary layer than the flat membrane (Pawlowski et al., 2017) so that for an ED module, spacers are no longer needed. Profiled membranes can also prevent fouling formation on the membrane (Won et al., 2016). Foulant deposition on the membrane surface can be prevented, especially at high crossflow velocity due to vortex formation on the membrane surface's valley region (Won et al., 2016). The profiled surface may trigger electroconvection formation, thereby increasing ion transport through the membrane (De Valença et al., 2018).

15.3 Application and performance of ion-exchange membranes in electrodialysis

15.3.1 Desalination with electrodialysis

ED is referred as a membrane separation process that uses an electric potential difference as a driving force to promote ionic transport from different solutions with the aid of

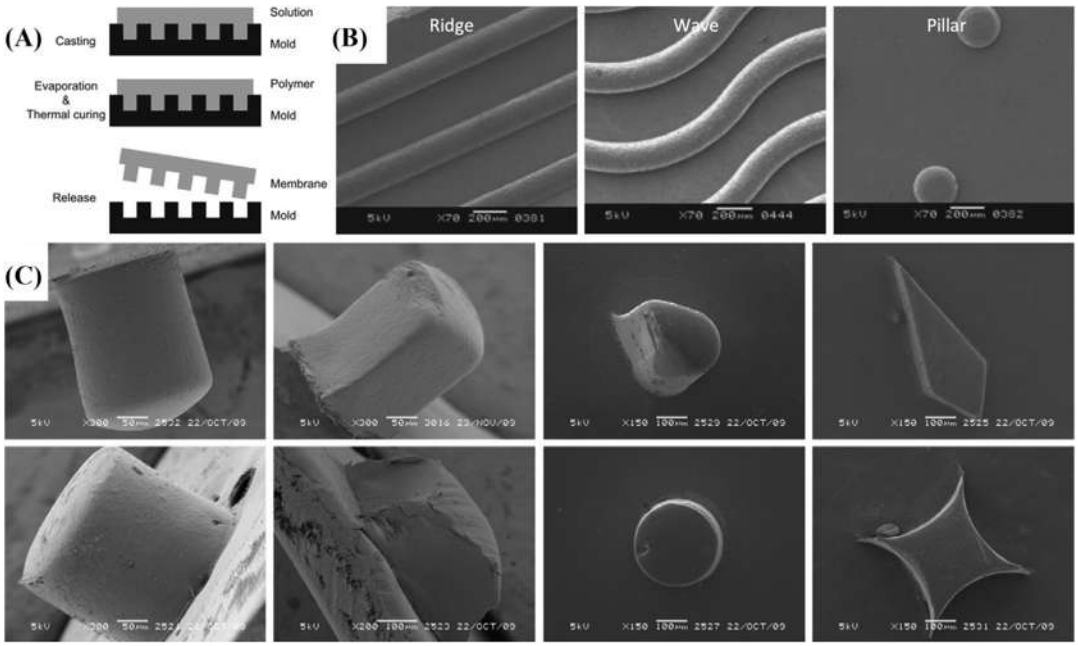

FIGURE 15.3 Profiled or patterned ion-exchange membranes (IEMs). (A) Preparation of profiled membrane by solution casting method. (B) Profiled membrane developed by Güler et al. (2014). (C) Profiled membrane developed by Ngene, Lammertink, Wessling, & Van der Meer, 2010. Source: *(A and B) Reproduced from Güler, E., Elizen, R., Saakes, M., & Nijmeijer, K. (2014). Micro-structured membranes for electricity generation by reverse electrodialysis*. Journal of Membrane Science, 458, *136–148. https://doi.org/10.1016/j.memsci.2014.01.060, with permission, ©2019 Elsevier. (C) Reproduced from Ngene, I. S., Lammertink, R. G. H., Wessling, M., & Van der Meer, W. G. J. (2010). Particle deposition and biofilm formation on microstructured membranes*. Journal of Membrane Science, 364, *43–51. https://doi.org/10.1016/j.memsci.2010.07.048, with permission, ©2010 Elsevier.*

semipermeable membranes (Scarazzato et al., 2017; Wenten, Khoiruddin, Wardani, & Widiasa, 2020). An ED unit consists of AEMs and CEMs that are placed between cathode and anode electrodes. AEMs and CEMs play an essential role as a barrier to prevent and allow ions from passing based on their electric charge and create alternating concentrate and diluate solution compartments (Mohammadi, Tang, & Sillanpää, 2021).

ED has been used for various applications as summarized in Table 15.2. Asahi Chemical Industries from Japan used ED for the concentration of seawater for salt production (Strathmann, 1991), and the first salt production was successfully realized in the 1960s (Karidurаganavar, Kittur, & Kulkarni, 2012). This system was then adopted by Dow Chemical in the United States to produce potable water from brackish water in 1976 (Strathmann, 1991). Meanwhile, the first ED system for brackish water desalination was installed by the Saudi oil company Aramco in 1954 (Aly, Darwish, & Fathalah, 1989), and brackish water desalination plants with ED systems have been installed in India since 1985 (Harkare et al., 1982; Karidurаganavar et al., 2012) where ED units powered by photovoltaic cell were also developed (Adiga et al., 1987). Over the last decade, ED has become the main process for the treatment of brackish or groundwater in some regions of the United

TABLE 15.2 Performance of electrodialysis (ED) in various applications.

Application	Membrane	Membrane material	Operating condition	Main result	References
BWRO brine	Asahi glass membranes (Selemion CMT and AMT)	Styrene–divinylbenzene copolymer	• Cell pairs: 5–20 • *A*: 225 • *Q*: 400–500 • *V*: 0.5–1 • *I*: 10–27	• Water recovery: 97%–98% • Salt concentration in diluate: 18–20 mN • Energy requirement: 7.0–8.0 kWh m^{-3}	Korngold, Aronov, and Daltrophe (2009)
SWRO brine	Neosepta cation-exchange membranes (CEMs) and anion-exchange membranes (ACS)		• Cell pairs: 50 • *A*: 1000 • *I*: 30–60	• NaCl recovery: 92% • Energy consumption: 0.12–0.38 kWh kg^{-1} NaCl	Reig et al. (2014)
Zn^{2+} Cu^{2+} Cr^{2+} SO_4^{2-} Cl^-	Polystyrene-based IEM ion-exchange membrane (SCEF, Shanghai, China)	Polystyrene	• Cell pairs: *15* • *A*: 200 • *Q*: 200–300	• Zn^{2+}, Cu^{2+}, Cr^{2+} removal: 90% • SO_4^{2-}, Cl^- removal: 97%	Zuo et al. (2008)
CrO_4^{2-}	Asahi Selemion AST/CMV membrane	Styrene–divinylbenzene copolymer	• *A*: 400 and 800 • *Q*: 5 and 10 • *I*: 10 and 30	• CrO_4^{2-} removal: 45%	Chen et al. (2009)
NO_3^- HPO_4^{2-}	Neosepta CMX, AMX, and ACS	Styrene–divinylbenzene copolymer/polyvinyl chloride	• *A*: 25 • *C*: NaCl: 355 • *C*: $NaNO_3$: 30 • *C*: Na_2HPO_4: 10 • *V*: 3, 5, 7	• NO_3^- concentration: 40.64 mg-N L^{-1} • HPO_4^{2-} concentration: 1.2 mg-P L^{-1} • Energy consumption: 1.10–04.42 kWh m^{-3}	Liu et al. (2017)
Clarified passion fruit juice	Selemion CMV (Asahi Glass), Selemion AMV (Asahi Glass), Neosepta AXE01 (Tokuyama), IonClad R4030 (Pall), Neosepta BP-1 (Tokuyama)	• Selemion: Styrene–divinylbenzene copolymer • Neosepta: Styrene–divinylbenzene copolymer/polyvinyl chloride	• *A*: 20 • *Q*: 10.2 • *I*: 200 and 400	• Organic anions removal: 60% • Inorganic anions removal: 85% • Titrable acidity: 1.14%	Vera et al. (2003)
Acid whey	Neosepta CMB and AHA		• Cell pairs: 2 • *A*: 36 • *V*: 0–60	• Demineralization: 90% • Energy consumption: 0.014 kWh kg^{-1}	Chen et al. (2016)

A, active membrane surface area per cell (cm^2); *Q*, flowrate (L h^{-1}); *V*, voltage (V); *I*, current density (mA cm^{-2}); *C*, ion concentration (mg L^{-1}); *n/a*, not available.

States such as Oklahoma, Arizona, Virginia, Texas, and San Diego, as well as in Europe, including Barcelona and the Canary Islands, Spain, and Donnington in the UK (Bernardes, Rodrigues, Marco, & Ferreira, 2014).

ED has been widely investigated to recover water and salts from the brine of brackish water reverse osmosis (BWRO) and seawater reverse osmosis (SWRO). The use of ED can boost water recovery as well as facilitate the salts separation. A pilot test was conducted by Xu et al. (2018) using a commercial size ED unit and BWRO brine with 10 g L^{-1} total dissolved solids (TDSs) as ED feed water. The results indicated the ED was able to recover up to 55% of its feed. A pilot test was also conducted for SWRO brine (70 g L^{-1} TDS) by Reig et al. (2014). The brine was concentrated through an ED unit with a single-pass diluate and tested for 24 months. Cl^- ions were recovered from this study to 92% with a higher concentration at 245 g L^{-1}.

Generally, ED has the advantage of better resistance to the membrane fouling and scaling than RO; thus higher recovery rates could be obtained. Also, ED has good chemical and mechanical stability at high and low pH and elevated temperatures above 50°C (Bernardes, Rodrigues, Marco, & Ferreira, 2014). However, the utilization of ED for desalination has several limitations too. ED is not able to remove neutral toxic components such as viruses and bacteria. Another issue is the corrosion problem at the anode due to the generation of chlorine gas. Therefore pretreatments of ED feed water are required to minimize the operational failures.

15.3.2 Wastewater treatment

ED has also been applied to reclaim water from a wide range of industrial wastewater (Chen et al., 2009). Rao et al. (1989) used ED to recover chromium from other neutral salts of residual tanning baths. The results showed that around 90% for chloride and 50% for sulfates could be removed while the chromium content remained unchanged. Meanwhile, Rodrigues et al. (2008) investigated the application of ED for tannery effluents treatment using the photo-electrooxidation (PEO) technique as pretreatment. The integrated PEO/ED system could remove more than 98% of sodium, magnesium, chloride, sulfate, and ammonium nitrogen.

Another prospective application of ED is metal industry wastewater treatment. In metal production, substrate coating is one of the vital processes to prevent metal corrosion. The coating process includes several rinsing processes; thus ions including PO_4^{3-}, Fe^{2+}, Ni^{2+}, and Zn^{2+} are generally found in its wastewater with concentrations above the environmental limits (Bernardes, Rodrigues, Marco, & Ferreira, 2014). Zuo, Zhang, Meng, and Zhang (2008) reported that ED could remove 97% of heavy metals including Zn^{2+}, Cu^{2+}, and Cr^{2+} and 95% of anions with final heavy metal concentrations below 0.01 mg L^{-1}. Chen et al. (2009) proposed a two-stage monovalent selective ED for chromate concentrating and purifying from electroplating wastewater. This proposed system was able to remove monovalent impurities, such as chlorides. Meanwhile, Vallejo, Persin, Innocent, Sistat, and Pourcelly (2000) utilized an ED with three compartments to concentrate Cr^{6+}. The Cr^{6+} was transported through the AEMs and impurities are transported through the CEMs. In the utilization of ED for recovery of hexavalent chromium, the AEM's poor stability still becomes the main drawback; thus further studies to develop resistant, highly conductive, and selective membranes are required.

15.3.3 Preferential ion separation

Selective removal of specific ions can be achieved through utilizing selective IEMs. ED with selective IEMs can reduce the unwanted ions concentration. Several reports showed excellent performance of ED against iron compounds, cationic surfactants, and divalent cations (Ghyselbrecht et al., 2013; Reverberi, Maga, Cerrato, & Fabiano, 2014). ED has also been applied to recover nutrients from various wastewater effluents, such as the recovery of ammonia and ammonium nitrate from swine manure (Ippersiel et al., 2012), phosphate from excess anaerobic sludge (Wang et al., 2015), and effluent of equalization tank (Hikmawati, Bagastyo, & Warmadewanthi, 2019).

Ward, Arola, Thompson Brewster, Mehta, and Batstone (2018) and Liu, Wang, Wu, Luo, and Wang (2017) applied monovalent selective AEMs to separate monovalent anions from the solution containing multivalent anions. After a period of operation, one concentrate compartment was filled with nitrate while another concentrate compartment contained phosphate. With the same approach, Zhang et al. (2013) used selective ED and a hybrid system (ED + struvite) to enhance the phosphate recovery effluent of an upflow anaerobic sludge blanket reactor. The primary current efficiency attained a level of 72%, with a sufficient phosphate concentration of 9 mmol L^{-1}.

Nowadays, lithium extraction has become the most attractive application of selective ED. Obtaining lithium from aqueous resources such as the waste of lithium-ion batteries and electronic industries requires lower cost and more available reserves than extracting it from hard rock (Li et al., 2019). Nie, Sun, Sun, Song, and Yu (2017) studied selective ED performance to recover Li + from synthetic brine with a Mg^{2+}/Li^{+} mass ratio of 150. The results showed high Li^{+} recovery of 95.3% could be achieved while the Mg^{2+}/Li^{+} mass ratio decreased to 8 after treatment. Chen et al. (2018) and Ji et al. (2018) investigated the effect of the coexisting monovalent cations (K^{+} and Na^{+}) and anions (SO_4^{2-} and HCO_3^{-}) on the transport of lithium. K^{+} had a more significant influence on the lithium migration than Na^{+}. Meanwhile, the coexisting anions have a negligible effect on the migration of lithium. Unfortunately, some technical and economic barriers still become the drawbacks of selective ED, especially its relatively low production efficiency and the high investment capital required during industrial-scale applications (Li et al., 2019). Therefore developing a cost-effective CEM remains a challenge for future studies to obtain high lithium-ion selectivity.

15.3.4 Other ionic separations

ED is a comparatively new process in terms of its use in food and biotechnology industries. Utilization of ED system involving electrolyte reduction from an organic solution has been applied for fruit juice deacidification and demineralization (Julian, Khoiruddin, Julies, Edwina, & Wenten, 2021; Rai & De, 2011), tartrate stabilization of wine (De Pinho, 2010; Lasanta & Gómez, 2012), dairy whey demineralization (Bazinet, 2005), immunoglobulin removal from blood plasma (Nifong & Gerhard, 2002), or organic acid separation (Handojo et al., 2019; Kresnowati, Regina, Bella, Wardani, & Wenten, 2019).

The main application of ED in the food industry is fruit juice deacidification. A high sugars/acid ratio is desirable in juices, and it can be effectively done by minimizing the

juice's acid content using ED (Bhattacharjee, Saxena, & Dutta, 2017). ED has been recommended for deacidifying several fruit juices such as orange, pineapple, grape (Adhikary, Harkare, Govindan, & Nanjundaswamy, 1983), mandarin orange (Kang & Rhee, 2002), clarified passion fruit (Vera et al., 2003), and cranberry juices (Serre, Rozoy, Pedneault, Lacour, & Bazinet, 2016).

Whey demineralization is another promising application of ED. The high lactic acid in acid whey concentration leads to operational problems in downstream spray drying operations due to increased powder stickiness. Therefore ED is needed to remove the lactate ions from acid whey. Dufton, Mikhaylin, Gaaloul, and Bazinet (2018) reported the utilization of ED for demineralization and deacidification of whey. The results showed that ED allowed reaching interesting demineralization (67%) and deacidification (44%) rates. Chen, Eschbach, Weeks, Gras, and Kentish (2016) also investigated the ED performance for the removal of lactate anions at relatively low concentrations from a whey solution. When 80% of the lactate ions were removed to achieve a similar ratio of lactic acid to lactose as found in sweet whey, 90% of the minerals were simultaneously removed.

15.4 Application and performance of ion-exchange membranes in electrodialysis reversal

15.4.1 Principle of electrodialysis reversal

EDR was first developed in 1970s by Ionics Inc. to overcome fouling problems in the conventional ED process during the desalination process (Katz, 1979). Fouling and scaling have become major problems due to the precipitation of suspended solids, colloidal matters, polyelectrolytes, and insoluble salts on the membrane surface (Kunrath, Patrocínio, Siqueira Rodrigues, Benvenuti, & Amado, 2020). The addition of antiscaling (such as acids and polyphosphates) and pH adjustment are periodically used during the ED process to eliminate fouling or scaling formation. However, local blocking by the chemicals on the membrane surface becomes a problem because it reduces the membrane array's flow distribution (Katz, 1979). Therefore the EDR concept was developed to improve the conventional ED process.

The configuration of the EDR system is similar to the ED system. However, in the EDR system, the polarity of electrodes is periodically reversed by changing the direction of the direct current field every two to four times per hour for a few seconds (Goodman, Taylor, Xie, Gozukara, & Clements, 2013). When the reverse electricity is applied, the deposited particles are returned to the bulk solution. During the reverse electricity time, the dilute stream becomes the concentrate stream, and vice versa, the concentrate becomes the dilute stream. The use of periodic reversal provides a continuous self-cleaning before the charged particles become permanently attached electrostatically on the membrane surface. The solid accumulation on the membrane surface becomes a challenge during the long-term operation of ED system, which is mainly governed by supersaturation of the inorganic ions in the solution, for examples, iron (Fe), manganese (Mg^{2+}), calcium (Ca^{2+}), and sulfate (SO_4^{2-}) ions (Dydo, Turek, Ciba, Wandachowicz, & Misztal, 2004). A pretreatment process is generally required to remove soluble inorganic compounds and minimize the

scaling formation on the ion-exchange membrane surface. The iron and manganese ion concentration is commonly kept below 0.3 and 0.05 mg L^{-1}, respectively, before entering the EDR stacks (Strathmann, 2010).

15.4.2 Desalination of high-concentration solution

EDR is generally operated continuously to treat RO brine (Tanaka, 2007). It has been reported that the EDR system can be more economical in a salinity concentration above 8000 ppm TDS (Bernardes & Rodrigues, 2014). At the mentioned concentration, the RO-EDR system produced water recovery between 92% and 98%, depending on the feed salt concentration (Medina, Johnson, Waisner, Wade, & Mattei-Sosa, 2015).

Several EDR plants have been installed in different scales for the desalination process (Table 15.3). In 1995, a large EDR plant was installed in Sarasota County, Florida, United States with a production capacity of 12 mg day^{-1} (45.425 m^3 day^{-1}) (Missimer, 2018). The largest desalination plant that includes the EDR stage is The Llobregat-Abrera plant near Barcelona with a capacity of 200,000 m^3 day^{-1} (Valero, Barceló, Medina, & Arbós, 2013). The EDR system was operated in 2008 with a recovery of over 90%. The EDR system consisted of a cartridge filter and two hydraulic EDR stages, including 576 EDR stacks. In the same year, 6 mg day^{-1} (or 27,727 m^3 day^{-1}) of EDR system was built in Utah, United States, to remove dissolved solid, harmful arsenic, and perchlorate from the community's well.

In treating RO concentrate with high TDS level, scaling formation becomes more susceptible in the EDR system. Zhao et al. (2019) found that resistance of IEM was increased in the 8 h of operation due to supersaturating conditions of the brine solution. However, the EDR system achieved 85% water recovery with a brine volume reduction by six times. The concentration of silica and $CaSO_4$ in the brine of RO unit was close to saturation. In some cases, integration with a precipitator unit is required to eliminate the foulants prior to the EDR system. Korngold et al. (2009) prevented the $CaSO_4$ by removing gypsum continuously from the brine RO using a separate precipitator. The ED process combined with a separate precipitator successfully concentrated brine from 1.5% to 10% with an energy consumption between 7.0 and 8.9 kWh m^{-3} and a recovery of 97%–98%. Turek, Dydo, and Waś (2006) investigated the relationship between EDR concentrate chamber residence time and calcium sulfate nucleation time. They found that the EDR system can be operated at high $CasSO_4$ saturation levels (326%–364%) using single-pass mode, and a polarity cycle time prolonged from 17 to 30 min. For recycling mode, the stable long-term operation of EDR system can be achieved at $CaSO_4$ supersaturation degree close to 175% (Turek et al., 2006). The EDR process can be operated without the addition of antiscaling agent when the LSI (Langelier Saturation Index) is approximately 1.8. Meanwhile, the scale precipitation begins to form when the LSI near 2.2 (Tanaka, 2007). If the antiscaling agent or other chemical is added into the concentrate solution, a higher supersaturation condition can be achieved. This condition leads to the scaling formation when the concentrate is recycled. Unlike $CaSO_4$ or other inorganic compounds that generate scaling, silica in water does not limit the EDR recovery. Therefore a high water recovery can be achieved, although the feed water contains a high concentration of silica.

TABLE 15.3 Some electrodialysis reversal (EDR) plants.

EDR plant (location, year)	Feed	Capacity	Feed water conditions	Water recovery	Product quality	Power consumption and cost production	References
Abrera, Barcelona (United States)	Brackish surface water (full scale)	200,000 m^3 day^{-1}	Conductivity: 500–2500 μS cm^{-1} Chloride: 150–1300 mg L^{-1} Sulfate: 140–210 mg L^{-1} TOC: 3.5–7 mg L^{-1}	90%	Conductivity reduction >65% Chloride removal >60% Sulfate removal >70% TOC removal: >30%	0.5 kWh m^{-3}	Valero and Arbós (2010); Valero et al. (2013)
Magna, Utah (United States)	Groundwater (full scale)	22,728 m^3 day^{-1}	TDS: 1300–1620 mg L^{-1}	70%	TDS: 500 mg L^{-1} Arsenic: 2.2 mg L^{-1} (82% removal)	Not reported	Fidaleo et al. (2016)
Barranco Seco, Canary Is. (Spain, 2002)	Wastewater treatment plant effluent	26,000 m^3 day^{-1}	Turbidity: 5–30 NTU BOD: 10 mg L^{-1} COD: 25 mg L^{-1} pH: 7–8	90%	Turbidity: 0.2 NTU BOD: 5 mg L^{-1} COD: 20 mg L^{-1} pH: 7–8	Power: 0.5 kWh m^{-3} Cost: 0.114 € m^{-3}	Broens, Liebrand, Futselaar, and De Armas Torrent (2004)

(*Continued*)

TABLE 15.3 (Continued)

EDR plant (location, year)	Feed	Capacity	Feed water conditions	Water recovery	Product quality	Power consumption and cost production	References
Kleylehof (Austria, 1997)	Groundwater	3500 m^3 day^{-1}	Conductivity: 850 μS cm^{-1} Alkalinity: 4.21 mEq L^{-1} Calcium: 115 mg Ca L^{-1} Sodium: 11 mg L^{-1} Sulfate: 113 mg L^{-1}	Not reported	Conductivity: 640 μS cm^{-1} Alkalinity: 3.97 mEq L^{-1} Calcium: 85 mg L^{-1} Sodium: 11 mg L^{-1} Sulfate: 110 mg L^{-1}	Not reported	Hell & Lahnsteiner (2002)
Washington, Iowa	Groundwater	4164 m^3 day^{-1}	TDS: 1200 mg L^{-1} Silica: 9.5 mg L^{-1} Hardness ($CaCO_3$): 480 mg L^{-1}	85%	TDS: 527–628 mg L^{-1} Silica: 10 mg L^{-1}Hardness ($CaCO_3$): 183 mg L^{-1}	Power: 0.715–1.43 kWh m^{-3} Cost: 0.287–0.314 US$ m^{-3}	Hays (2000); Sajtar and Bagley (2009)
Sant Boi de Llobregat, Barcelona	WTTP	57,000 m^3 day^{-1}	Conductivity: 3040 μS cm^{-1}	85%	Conductivity reduction: 60%–80%	Not reported	Sanz and Miguel (2013)

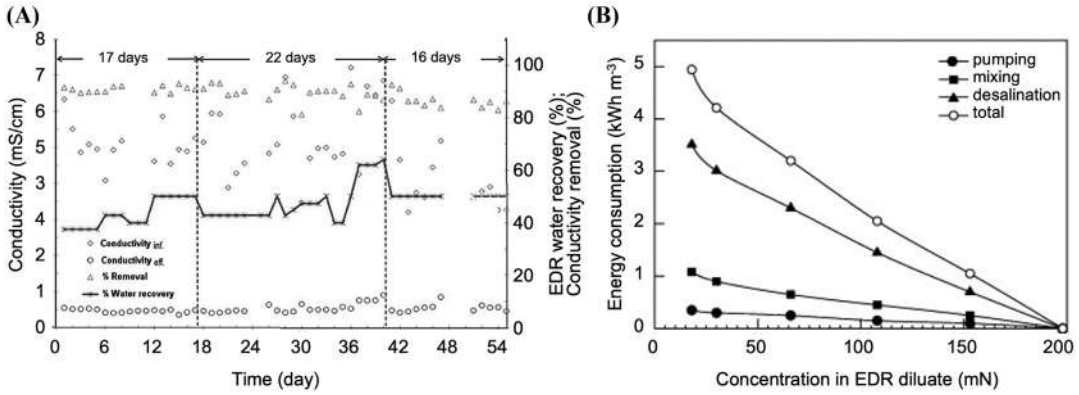

FIGURE 15.4 (A) Desalination efficiency and flux profile of electrodialysis reversal (EDR) system during wastewater treatment in Taiwan (without sand filtration (SF) within days 1–40 and with SF within days 41–56). (B) Cumulative energy requirement for brackish water reverse osmosis (BWRO) concentrate desalination by EDR (Oren et al., 2010). Source: *(A) Reproduced from Yen, F.-C., You, S.-J., & Chang, T.-C. (2017). Performance of electrodialysis reversal and reverse osmosis for reclaiming wastewater from high-tech industrial parks in Taiwan: A pilot-scale study.* Journal of Environmental Management, 187, *393–400. https://doi.org/10.1016/j.jenvman.2016.11.001, with permission, ©2016 Elsevier Ltd. (B) Reprinted from Oren, Y., Korngold, E., Daltrophe, N., Messalem, R., Volkman, Y., Aronov, L., …, Gilron, J. (2010). Pilot studies on high recovery BWRO-EDR for near zero liquid discharge approach.* Desalination, 261, *321–330. https://doi.org/10.1016/j.desal.2010.06.010, with permission, ©2010 Elsevier B.V.*

A pilot study of integrated sand-filter (SS) and EDR for treating industrial high-conductivity effluent from Xianxi wastewater treatment in Taiwan has been reported (Yen, You, & Chang, 2017). The performance of the EDR system during the wastewater treatment is shown in Fig. 15.4A. The EDR performance is observed using three types of feed water, that is, from secondary clarifier (day 1–7), the discharge station (day 18–40), and SS effluent (day 41–56). The conductivity level of the feed water is varied from 4.0 to 7.5 mS cm^{-1}. The EDR system reduced the feed water's conductivity by 89.7%, with a 40%–50% water recovery rate. The application of SS as pretreatment could be sufficient to diminish the particles from the water and prevent fouling on the EDR membrane. Another performance of EDR systems is shown in Fig. 15.4B.

15.4.3 Other ion separation processes

Nutrient recoveries from animal manure using EDR have attracted attention due to its high resistance to membrane fouling compared to other technologies, such as RO and nanofiltration. In the EDR system, the antibiotics can be removed from the feed solution and then transported to the product solution. The nitrogen and phosphorus recovery from animal manure has been studied using the EDR process (Shi et al., 2020). The EDR system can extract NH_4^+ and PO_4^{3-} with efficiencies of 100% and 84%, respectively. A significant change in membrane mass, conductivity, and ion-exchange capacity is observed in anion membrane compared to the cation membrane. The result shows that the anion membrane is more susceptible to fouling by organic substance than cation membrane. Shi et al. (2020)

examined the behaviors of two widely used antibiotics for the animal livestock, namely sulfadiazine (SD) and tetracycline (TC), during the EDR process. Both antibiotics showed two different transport mechanisms. The transport of SD through the membrane was attributed to electro-migration and migrated to the product side. Meanwhile, the TC compounds were diffused due to membrane sorption. The TC compounds were easily associated with organic foulants, and thus most of TC remained on the membrane surface (Shi et al., 2020). Chao and Liang (2008) used a mini-plant EDR system to treat raw wastewater at the site of China Steel Corporation (CSC) with a capacity of 350 CMD. The EDR process removed chlorine ions by 98%, sulfate ions by 80%, calcium ions by 99%, and chemical oxygen demand (COD) by 51% at 75% of water reclamation rate and 92% of desalination rate. The operating cost was estimated at 0.146 US$ m^{-3} with a power consumption of 0.85 kWh m^{-3}.

15.5 Application and performance of ion-exchange membranes in membrane capacitive deionization

15.5.1 Role of ion-exchange membrane in membrane capacitive deionization

Capacitive deionization (CDI) relies on adsorption process in porous electrode assisted by electrical potential to separate ions from the feed solution. In MCDI, two main components are involved: the IEM and porous electrodes (Fig. 15.5A and B). The process begins with flowing electrolytes into the compartments of the MCDI module. When an electric potential difference is applied to the electrode, the ions move towards the electrode having opposite charge and are stored in it. After a desalination process, the electrode will be saturated by ions; thus the electrode must be regenerated by reversing its polarity. In this regeneration process, the ions will be desorbed from the electrode and carried away by the rinse solution. In the CDI, desorbed ions will be readsorbed at the opposite electrode, making the electrode regeneration process less efficient. With the introduction of IEMs, MCDI can achieve a higher regeneration efficiency than CDI because the membrane can prevent ion readsorption during the desorption process (Folaranmi, Bechelany, Sistat, Cretin, & Zaviska, 2020).

The use of IEMs provides several positive effects in MCDI (Fig. 15.5C). One of the critical effects is the reduction of Faradaic reaction (Yu, Jo, Kim, Lee, & Yoon, 2018). The IEM prevents oxygen gas contact with the cathode so that oxygen reduction and hydrogen peroxide generation are minimized and vice versa. The less Faradaic reaction makes the pH of product water from MCDI more stable than those from CDI (Yu et al., 2018). The presence of a membrane helps maintain the electrode's salt adsorption capacity as it facilitates near-complete regeneration. Therefore after some adsorption–desorption cycles in a long-term operation, the normalized salt adsorption capacity of MCDI tends to be more stable than CDI (Yu et al., 2018), as shown in Fig. 15.5D and E. The use of IEM also enables MCDI to separate specific ions. MCDI can be used to remove monovalent ions from the feed solution if the membrane is monovalent permselective (Sahin, Dykstra, Zuilhof, Zornitta, & De Smet, 2020). Moreover, IEMs may act as the guard that restricts the foulant to contact with the electrodes. Therefore for solutions with organic foulants, MCDI shows a better resistance to fouling than CDI (Hassanvand, Chen, Webley, & Kentish, 2019).

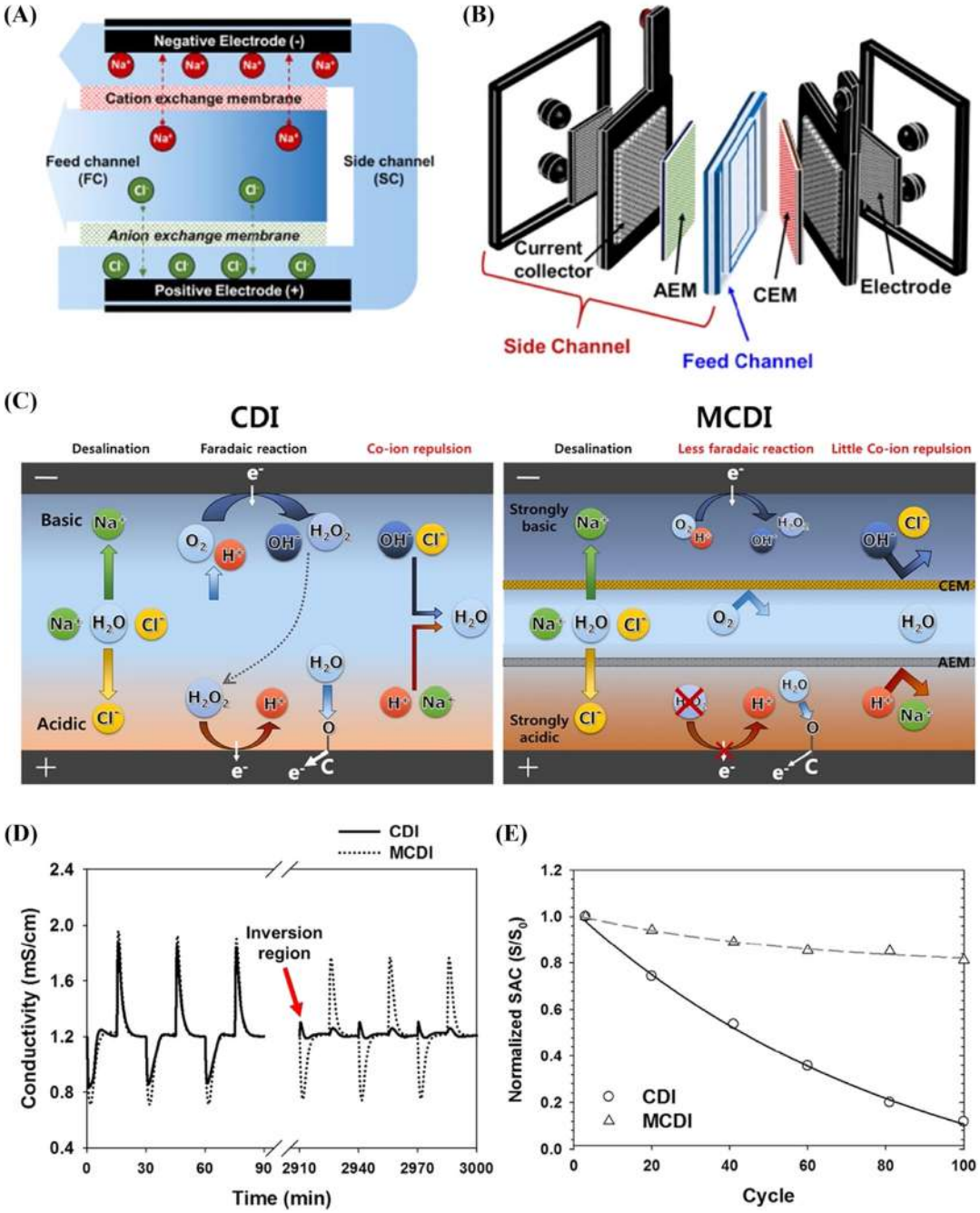

FIGURE 15.5 Effect of ion-exchange membranes (IEMs) usage in membrane capacitive deionization (MCDI). (A) Schematic MCDI process. (B) Illustration of simple MCDI module (Kim, Lee, Su, & Kim, 2021). (C) Comparison of capacitive deionization (CDI) versus MCDI. (D) Adsorption–desorption cycle of CDI versus MCDI. (E) Normalized salt adsorption capacity of CDI and MCDI. Source: *(A and B) Reproduced from Kim, N., Lee, E.-A., Su, X., & Kim, C. (2021). Parametric investigation of the desalination performance in multichannel membrane capacitive deionization (MC-MCDI).* Desalination, 503. https://doi.org/10.1016/j.desal.2021.114950, *with permission,* ©*2021 Elsevier. (C–E) Reproduced from Yu, J., Jo, K., Kim, T., Lee, J., & Yoon, J. (2018). Temporal and spatial distribution of pH in flow-mode capacitive deionization and membrane capacitive deionization.* Desalination, 439, *188–195.* https://doi.org/10.1016/j.desal.2018.04.011, *with permission,* ©*2018 Elsevier.*

15.5.2 Desalination processes

Desalination is one of the main applications of MCDI. For instance, MCDI with mesoporous carbon electrodes has been used to desalinate NaCl solution with a 0.5 M concentration. It could achieve a salt adsorption capacity of 64.7 mg g^{-1}, which is almost eight times that that can be achieved by CDI with the same electrode (Tang et al., 2019). In addition to its high salt removal capacity, the MCDI could also reduce the feed solution conductivity up to 99.9% (Tang et al., 2019). A comparison of energy consumption shows that MCDI requires two to three times higher energy than RO (Porada, Zhang, & Dykstra, 2020). The MCDI would be competitive if the feed solution had a salt concentration of less than 2 g L^{-1} (Zhao, Porada, Biesheuvel, & Van der Wal, 2013). At this feed condition, MCDI needs less than 1 kWh for producing 1 m^3 of freshwater. MCDI can also be applied as the second stage in the SWRO system (Zhao et al., 2013). As the second stage, MCDI can remove bromide from the first-stage SWRO product efficiently (Dorji, Kim, Hong, Phuntsho, & Shon, 2020).

The potential application of MCDI for desalination of low-concentration solution has been demonstrated, such as for the production of ultrapure water (Lee & Choi, 2012). MCDI can produce 2–9 MΩ cm ultrapure water from feed water with a conductivity of 20 μS cm^{-1} (Lee & Choi, 2012). Besides, MCDI has been demonstrated in the treatment of process water, such as cooling water, by integrating MCDI with a cooling tower. Here, MCDI acts as partial desalination which can improve the quality of cooling water. A pilot-scale study shows that the integration of MCDI can reduce water consumption by up to 80% (De Schepper, Vanschepdael, Huynh, & Helsen, 2020).

15.5.3 Membrane capacitive deionization applications in other deionization processes

The prospect of MCDI for the separation of monovalent/bivalent ions is also examined by several studies (Mao et al., 2019). It was reported that the selectivity of Ca^{2+} removal could be adjusted by controlling the operating conditions of the MCDI, such as current density and residence time of the solution (Wang & Lin, 2019). The adsorption selectivity of Ca^{2+} to Na^{+} increases with an increase in the concentration ratio of Ca^{2+} to Na^{+} in the feed solution but decreases with current density and hydraulic retention time (Wang & Lin, 2019). Calcium is easier to remove because it has a higher charge and higher electrostatic interaction with the electrode than sodium. As previously mentioned, the use of IEM in MCDI can also assist the selective separation of monovalent/bivalent ions (Choi, Lee, & Hong, 2016; Sahin et al., 2020). MCDI equipped with monovalent cation-selective IEM can remove up to 40% sodium with selective removal of up to 1.75 (Na^{+}/Ca^{2+}) (Choi et al., 2016). Unlike in the previous case, monovalent permselective IEM promotes the adsorption of monovalent ions while leaving behind bivalent ions.

Selective ion removal has also been performed on a pilot scale to separate arsenic (up to 0.3 mg L^{-1}), ammonium (up to 25 mg L^{-1}), and manganese (up to 6 mg L^{-1}) from brackish water at concentrations up to 2 g L^{-1} (Kurz, Hellriegel, Luong, Bundschuh, & Hoinkis, 2020). From the pilot test results, the specific energy requirements at optimum conditions are below 1 kWh m^{-3}. MCDI also shows promising performance for specific ion removal, such as removing nitrates from drinking water sources (Çetinkaya, 2020). MCDI is able to

remove ~83% nitrate from a 250 mg L^{-1} nitrate solution with a relatively low cell potential of 0.8 V. Another essential application of MCDI is the recovery of metals, for example, chromium, lead, cadmium, copper, and lithium, from waste water (Ali et al., 2020; Wang, Chen, & Liu, 2019; Yang et al., 2020). This selective separation is also used for metal recovery from wastewater, such as removing Pb^{2+} from Ca^{2+} and Mg^{2+} (Dong et al., 2019). At optimum conditions, MCDI can achieve Pb^{2+}/Ca^{2+} selectivity of 7.5. With this application, valuable components contained in wastewater or that can pollute the environment can be separated.

15.6 Concluding remarks

Ionic separation is one of the important processes used in water treatment and other solution processing. ED, EDR, and MCDI are membrane-based technologies that can be used to remove or separate ions from a feed solution without requiring the addition of chemicals. These technologies are also interesting alternatives for desalination as they transport the solute, which is a small electrolyte component. This feature brings significant all of the advantages of these technologies. They tend to require relatively low energy, especially for solutions with low ion concentration, such as brackish water or dilute solution. In addition, these technologies are not limited by the osmotic pressure to attain higher water recovery than RO. Even though these technologies have been commercialized, many developments are being made to improve their performances, expand their applications, and lower their costs.

IEMs are the key to the ionic separation process of electro-membrane technologies. Apart from determining the separation capability, IEMs also determine the process costs associated with energy requirements and the module cost. Although commercial IEMs are already available, much research has been done to develop IEMs with better properties. Numerous efforts have been devoted to obtaining IEMs with good separation characteristics (such as high ion conductivity and high counter-ion permselectivity), high durability, as well as low production costs. Besides, IEMs with specific properties, for example, permselective to specific ions, are also developed for special applications. Another development, such as profiled membranes, can improve electro-membrane technologies' performance by providing excellent fluid mixing inside the cells to suppress concentration polarization and surpass the diffusion-limited transport. With these developments, electro-membrane technologies can become more economically competitive in the future.

References

Adhikary, S. K., Harkare, W. P., Govindan, K. P., & Nanjundaswamy, A. M. (1983). Deacidification of fruit juices by electrodialysis. *Indian Journal of Technology*, *21*, 120–123.

Adiga, M. R., Adhikary, S. K., Narayanan, P. K., Harkare, W. P., Gomkale, S. D., & Govindan, K. P. (1987). Performance analysis of photovoltaic electrodialysis desalination plant at Tanote in Thar desert. *Desalination*, *67*, 59–66. Available from https://doi.org/10.1016/0011-9164(87)90232-3.

Al-Amshawee, S., Yunus, M. Y. B. M., Azoddein, A. A. M., Hassell, D. G., Dakhil, I. H., & Hasan, H. A. (2020). Electrodialysis desalination for water and wastewater: A review. *Chemical Engineering Journal*, *380*, 122231. Available from https://doi.org/10.1016/j.cej.2019.122231.

Ali, A., Quist-Jensen, C. A., Jørgensen, M. K., Siekierka, A., Christensen, M. L., Bryjak, M., ... Drioli, E. (2020). A review of membrane crystallization, forward osmosis and membrane capacitive deionization for liquid mining. *Resources, Conservation & Recycling*., 105273. Available from https://doi.org/10.1016/j.resconrec.2020.105273.

Alvarado, L., & Chen, A. (2014). Electrodeionization: Principles, strategies and applications. *Electrochimica Acta*, *132*, 583–597. Available from https://doi.org/10.1016/j.electacta.2014.03.165.

Aly, S. E., Darwish, M., & Fathalah, K. (1989). Potential drop and ionic flux in desalting electrodialysis units. *Journal of King Saud University: Engineering and Science*, *1*, 31–48.

Ariono, D., Khoiruddin, S., & Wenten, I. G. (2017). Heterogeneous structure and its effect on properties and electrochemical behavior of ion-exchange membrane. *Materials Research Express*, *4*, 24006. Available from https://doi.org/10.1088/2053-1591/aa5cd4.

Ariono, D., Purwasasmita, M., & Wenten, I. G. (2016). Brine effluents: Characteristics, environmental impacts, and their handling. *Journal of Engineering and Technological Sciences*, *48*, 367–387. Available from https://doi.org/10.5614/j.eng.technol.sci.2016.48.4.1.

Banasiak, L. J., Kruttschnitt, T. W., & Schäfer, A. I. (2007). Desalination using electrodialysis as a function of voltage and salt concentration. *Desalination*, *205*, 38–46. Available from https://doi.org/10.1016/j.desal.2006.04.038.

Bazinet, L. (2005). Electrodialytic phenomena and their applications in the dairy industry: A review. *Critical Reviews in Food Science and Nutrition*, *45*, 307–326. Available from https://doi.org/10.1080/10408690490489279.

Bernardes, A. M., & Rodrigues, M. A. S. (2014). Electrodialysis in water treatment. In A. M. Bernardes, M. A. S. Rodrigues, & J. Z. Ferreira (Eds.), *Electrodialysis and water reuse: Novel approaches* (pp. 63–75). Berlin, Heidelberg: Springer Berlin Heidelberg. Available from https://doi.org/10.1007/978-3-642-40249-4_6.

Bernardes, A. M., Rodrigues, Marco, A. S., & Ferreira, J. Z. (2014). General aspects of electrodialysis. In A. M. Bernardes, M. A. S. Rodrigues, & J. Z. Ferreira (Eds.), *Electrodialysis and water reuse* (pp. 11–23). Springer. Available from https://doi.org/10.1007/978-3-642-40249-4_3.

Bhattacharjee, C., Saxena, V. K., & Dutta, S. (2017). Fruit juice processing using membrane technology: A review. *Innovative Food Science and Emerging Technologies*, *43*, 136–153. Available from https://doi.org/10.1016/j.ifset.2017.08.002.

Broens, L., Liebrand, N., Futselaar, H., & De Armas Torrent, J. C. (2004). Effluent reuse at Barranco Seco (Spain): A 1,000 m^3/h case study. *Desalination*, *167*, 13–16. Available from https://doi.org/10.1016/j.desal.2004.06.106.

Çetinkaya, A. Y. (2020). Life cycle assessment of environmental effects and nitrate removal for membrane capacitive deionization technology. *Environmental Monitoring and Assessment*, *192*, 543. Available from https://doi.org/10.1007/s10661-020-08501-0.

Cha, J.-H., Ul Haq, O., Choi, J.-H., & Lee, Y.-S. (2018). Sulfonated poly(ether ether ketone) ion-exchange membrane for membrane capacitive deionization applications. *Macromolecular Research*, *26*, 1273–1275. Available from https://doi.org/10.1007/s13233-019-7043-2.

Chao, Y.-M., & Liang, T. M. (2008). A feasibility study of industrial wastewater recovery using electrodialysis reversal. *Desalination*, *221*, 433–439. Available from https://doi.org/10.1016/j.desal.2007.04.065.

Chen, G. Q., Eschbach, F. I. I., Weeks, M., Gras, S. L., & Kentish, S. E. (2016). Removal of lactic acid from acid whey using electrodialysis. *Separation and Purification Technology*, *158*, 230–237. Available from https://doi.org/10.1016/j.seppur.2015.12.016.

Chen, Q.-B., Ji, Z.-Y., Liu, J., Zhao, Y.-Y., Wang, S.-Z., & Yuan, J.-S. (2018). Development of recovering lithium from brines by selective-electrodialysis: Effect of coexisting cations on the migration of lithium. *Journal of Membrane Science*, *548*, 408–420. Available from https://doi.org/10.1016/j.memsci.2017.11.040.

Chen, S.-S., Li, C.-W., Hsu, H.-D., Lee, P.-C., Chang, Y.-M., & Yang, C.-H. (2009). Concentration and purification of chromate from electroplating wastewater by two-stage electrodialysis processes. *Journal of Hazardous Materials*, *161*, 1075–1080. Available from https://doi.org/10.1016/j.jhazmat.2008.04.106.

Chen, Y., Zhang, S., Liu, Q., & Jian, X. (2020). Investigation of poly(phthalazinone ether ketone) amphoteric ion exchange membranes in vanadium redox flow batteries. *Journal of Materials Science*, *55*, 13964–13979. Available from https://doi.org/10.1007/s10853-020-04968-x.

Choi, J., Lee, H., & Hong, S. (2016). Capacitive deionization (CDI) integrated with monovalent cation selective membrane for producing divalent cation-rich solution. *Desalination*, *400*, 38–46. Available from https://doi.org/10.1016/j.desal.2016.09.016.

De Pinho, M. N. (2010). Membrane processes in must and wine industries. In K. Peinemann, S. P. Nunes, & L. Giorno (Eds.), *Membrane technology: Volume 3: Membranes for food applications* (pp. 105–118). John Wiley & Sons Inc., Wiley Online Books. Available from https://doi.org/10.1002/9783527631384.ch5.

De Schepper, W., Vanschepdael, C., Huynh, H., & Helsen, J. (2020). Membrane capacitive deionization for cooling water intake reduction in thermal power plants: Lab to pilot scale evaluation. *Energies*, *13*. Available from https://doi.org/10.3390/en13061305.

De Valença, J., Jõgi, M., Wagterveld, R. M., Karatay, E., Wood, J. A., & Lammertink, R. G. H. (2018). Confined electroconvective vortices at structured ion exchange membranes. *Langmuir: The ACS Journal of Surfaces and Colloids*, *34*, 2455–2463. Available from https://doi.org/10.1021/acs.langmuir.7b04135.

Długołęcki, P., Nymeijer, K., Metz, S., & Wessling, M. (2008). Current status of ion exchange membranes for power generation from salinity gradients. *Journal of Membrane Science*, *319*, 214–222. Available from https://doi.org/10.1016/j.memsci.2008.03.037.

Dong, Q., Guo, X., Huang, X., Liu, L., Tallon, R., Taylor, B., & Chen, J. (2019). Selective removal of lead ions through capacitive deionization: Role of ion-exchange membrane. *Chemical Engineering Journal*, *361*, 1535–1542. Available from https://doi.org/10.1016/j.cej.2018.10.208.

Dorji, P., Kim, D. I., Hong, S., Phuntsho, S., & Shon, H. K. (2020). Pilot-scale membrane capacitive deionisation for effective bromide removal and high water recovery in seawater desalination. *Desalination*, 479. Available from https://doi.org/10.1016/j.desal.2020.114309.

Dufton, G., Mikhaylin, S., Gaaloul, S., & Bazinet, L. (2018). How electrodialysis configuration influences acid whey deacidification and membrane scaling. *Journal of Dairy Science*, *101*, 7833–7850. Available from https://doi.org/10.3168/jds.2018-14639.

Dydo, P., Turek, M., Ciba, J., Wandachowicz, K., & Misztal, J. (2004). The nucleation kinetic aspects of gypsum nanofiltration membrane scaling. *Desalination*, *164*, 41–52. Available from https://doi.org/10.1016/S0011-9164(04)00154-7.

Fei, Z.-J., Wang, S.-B., Li, C.-P., Zhang, X.-F., Zhao, Y.-B., Xie, X.-F., & Huang, H.-Y. (2016). Preparation of amphoteric ion exchange membranes via an one-step method and their properties. *Gao Xiao Hua Xue Gong Cheng Xue Bao/Journal of Chemical Engineering of Chinese Universities*, *30*, 926–932. Available from https://doi.org/10.3969/j.issn.1003-9015.2016.04.027.

Fidaleo, M., Stazi, S. R., Vinciguerra, V., Cellucci, P., Marabottini, R., & Moresi, M. (2016). Assessment of the energy needs for the arsenic remediation of drinking water by electrodialysis. *Desalination and Water Treatment*, *57*, 19475–19487. Available from https://doi.org/10.1080/19443994.2015.1100557.

Folaranmi, G., Bechelany, M., Sistat, P., Cretin, M., & Zaviska, F. (2020). Towards electrochemical water desalination techniques: A review on capacitive deionization, membrane capacitive deionization and flow capacitive deionization. *Membranes*, *10*, 96. Available from https://doi.org/10.3390/membranes10050096.

Garcia-Vasquez, W., Ghalloussi, R., Dammak, L., Larchet, C., Nikonenko, V., & Grande, D. (2014). Structure and properties of heterogeneous and homogeneous ion-exchange membranes subjected to ageing in sodium hypochlorite. *Journal of Membrane Science*, *452*, 104–116. Available from https://doi.org/10.1016/j.memsci.2013.10.035.

Ghyselbrecht, K., Huygebaert, M., Van der Bruggen, B., Ballet, R., Meesschaert, B., & Pinoy, L. (2013). Desalination of an industrial saline water with conventional and bipolar membrane electrodialysis. *Desalination*, *318*, 9–18. Available from https://doi.org/10.1016/j.desal.2013.03.020.

Goodman, N. B., Taylor, R. J., Xie, Z., Gozukara, Y., & Clements, A. (2013). A feasibility study of municipal wastewater desalination using electrodialysis reversal to provide recycled water for horticultural irrigation. *Desalination*, *317*, 77–83. Available from https://doi.org/10.1016/j.desal.2013.02.010.

Güler, E., Elizen, R., Saakes, M., & Nijmeijer, K. (2014). Micro-structured membranes for electricity generation by reverse electrodialysis. *Journal of Membrane Science*, *458*, 136–148. Available from https://doi.org/10.1016/j.memsci.2014.01.060.

Hakim, A. N., Khoiruddin, K., Ariono, D., & Wenten, I. G. (2020). Ionic separation in electrodeionization system: Mass transfer mechanism and factor affecting separation performance. *Separation & Purification Reviews*, *49*, 294–316. Available from https://doi.org/10.1080/15422119.2019.1608562.

Handojo, L., Wardani, A. K., Regina, D., Bella, C., Kresnowati, M. T. A. P., & Wenten, I. G. (2019). Electromembrane processes for organic acid recovery. *RSC Advances*, *9*, 7854–7869. Available from https://doi.org/10.1039/C8RA09227C.

Hansima, M. A. C. K., Makehelwala, M., Jinadasa, K. B. S. N., Wei, Y., Nanayakkara, K. G. N., Herath, A. C., & Weerasooriya, R. (2021). Fouling of ion exchange membranes used in the electrodialysis reversal advanced water treatment: A review. *Chemosphere*, *263*, 127951. Available from https://doi.org/10.1016/j.chemosphere.2020.127951.

Harkare, W. P., Adhikary, S. K., Narayanan, P. K., Bhayani, V. B., Dave, N. J., & Govindan, K. P. (1982). Desalination of brackish water by electrodialysis. *Desalination*, *42*, 97–105. Available from https://doi.org/10.1016/S0011-9164(00)88745-7.

Hassanvand, A., Chen, G. Q., Webley, P. A., & Kentish, S. E. (2019). An investigation of the impact of fouling agents in capacitive and membrane capacitive deionisation. *Desalination*, *457*, 96–102. Available from https://doi.org/10.1016/j.desal.2019.01.031.

Hays, J. (2000). Iowa's first electrodialysis reversal water treatment plant. *Desalination*, *132*, 161–165. Available from https://doi.org/10.1016/S0011-9164(00)00144-2.

Hell, F., & Lahnsteiner, J. (2002). The application of electrodialysis for drinking water treatment. In Rubin, H., Shamir, U., Nachtnebel, P., & Fürst, J. (Eds.), Water resources quality (pp. 315–327). Springer. Available from https://doi.org/10.1007/978-3-642-56013-2_18.

Hikmawati, D. N., Bagastyo, A. Y., & Warmadewanthi, I. (2019). Electrodialytic recovery of ammonium and phosphate ions in fertilizer industry wastewater by using a continuous-flow reactor. *Journal of Ecological Engineering*, *20*, 255–263. Available from https://doi.org/10.12911/22998993/109461.

Hoffmann, E., Ye, J., & Hahn, H. H. (2016). Recent advances in application of electrodialysis with bipolar membranes for organic acid recovery from fermentation broth. *Current Organic Chemistry*, *20*, 2753–2761. Available from https://doi.org/10.2174/1385272820666160513151103.

Hosseini, S. M., Madaeni, S. S., & Khodabakhshi, A. R. (2011). Preparation and characterization of heterogeneous cation exchange membranes based on S-poly vinyl chloride and polycarbonate. *Separation Science and Technology*, *46*, 794–808. Available from https://doi.org/10.1080/01496395.2010.534122.

Hosseini, S. M., Rafiei, N., Salabat, A., & Ahmadi, A. (2020). Fabrication of new type of barium ferrite/copper oxide composite nanoparticles blended polyvinylchloride based heterogeneous ion exchange membrane. *Arabian Journal of Chemistry*, *13*, 2470–2482. Available from https://doi.org/10.1016/j.arabjc.2018.06.001.

Hosseini, S. M., Usefi, M. M. B., Habibi, M., Parvizian, F., Van der Bruggen, B., Ahmadi, A., & Nemati, M. (2019). Fabrication of mixed matrix anion exchange membrane decorated with polyaniline nanoparticles to chloride and sulfate ions removal from water. *Ionics*, *25*, 6135–6145. Available from https://doi.org/10.1007/s11581-019-03151-w.

Hu, G., Wang, Y., Ma, J., Qiu, J., Peng, J., Li, J., & Zhai, M. (2012). A novel amphoteric ion exchange membrane synthesized by radiation-induced grafting α-methylstyrene and N,N-dimethylaminoethyl methacrylate for vanadium redox flow battery application. *Journal of Membrane Science*, *407–408*, 184–192. Available from https://doi.org/10.1016/j.memsci.2012.03.042.

Ippersiel, D., Mondor, M., Lamarche, F., Tremblay, F., Dubreuil, J., & Masse, L. (2012). Nitrogen potential recovery and concentration of ammonia from swine manure using electrodialysis coupled with air stripping. *Journal of Environmental Management*, *95*, S165–S169. Available from https://doi.org/10.1016/j.jenvman.2011.05.026.

Ji, P.-Y, Ji, Z.-Y., Chen, Q.-B., Liu, J., Zhao, Y.-Y., Wang, S.-Z., . . ., & Yuan, J.-S. (2018). Effect of coexisting ions on recovering lithium from high Mg2 + /Li + ratio brines by selective-electrodialysis. *Separation and Purification Technology*, *207*, 111. Available from https://doi.org/10.1016/j.seppur.2018.06.012

Jin, W., Du, H., Zheng, S., & Zhang, Y. (2016). Electrochemical processes for the environmental remediation of toxic Cr(VI): A review. *Electrochimica Acta*. Available from https://doi.org/10.1016/j.electacta.2016.01.130.

Julian, H., Khoiruddin, K., Julies, N., Edwina, V., & Wenten, I. G. (2021). Pineapple juice acidity removal using electrodeionization (EDI). *Journal of Food Engineering*, *110595*. Available from https://doi.org/10.1016/j.jfoodeng.2021.110595.

Kang, Y.-J., & Rhee, K.-C. (2002). Deacidification of mandarin orange juice by electrodialysis combined with ultrafiltration. *Preventive Nutrition and Food Science*, *7*, 411–416.

Kariduraganavar, M. Y., Kittur, A. A., & Kulkarni, S. S. (2012). Ion exchange membranes: Preparation, properties, and applications. In M. Inamuddin, Luqman (Ed.), *Ion exchange technology I* (pp. 233–276). Dordrecht: Springer. Available from https://doi.org/10.1007/978-94-007-1700-8_7.

Katz, W. E. (1979). The electrodialysis reversal (EDR) process. *Desalination*, *28*, 31–40. Available from https://doi.org/10.1016/S0011-9164(00)88124-2.

Khoiruddin, K., Ariono, D., Subagjo, S., & Wenten, I. G. (2017). Surface modification of ion-exchange membranes: Methods, characteristics, and performance. *Journal of Applied Polymer Science*, *134*, 45540. Available from https://doi.org/10.1002/app.45540.

Khoiruddin, K., Ariono, D., Subagjo, S., & Wenten, I. G. (2018). Effect of hydrophilic additive and PVC polymerization degree on morphology and electrochemical properties of PVC-based heterogeneous cation-exchange membrane. *Journal of Applied Polymer Science*, *135*, 46690. Available from https://doi.org/10.1002/app.46690.

Khoiruddin, K., Ariono, D., Subagjo, S., & Wenten, I. G. (2020). Structure and transport properties of polyvinyl chloride-based heterogeneous cation-exchange membrane modified by additive blending and sulfonation. *Journal of Electroanalytical Chemistry*, *873*, 114304. Available from https://doi.org/10.1016/j.jelechem.2020.114304.

Khoiruddin, K., Hakim, A. N., & Wenten, I. G. (2014). Advances in electrodeionization technology for ionic separation—A review. *Membrane and Water Treatment*, *5*, 87–108. Available from https://doi.org/10.12989/mwt.2014.5.2.087.

Kim, N., Lee, E.-A., Su, X., & Kim, C. (2021). Parametric investigation of the desalination performance in multi-channel membrane capacitive deionization (MC-MCDI). *Desalination*, *503*, 114950. Available from https://doi.org/10.1016/j.desal.2021.114950.

Korngold, E., Aronov, L., & Daltrophe, N. (2009). Electrodialysis of brine solutions discharged from an RO plant. *Desalination*, *242*, 215–227. Available from https://doi.org/10.1016/j.desal.2008.04.008.

Kresnowati, M. T. A. P., Regina, D., Bella, C., Wardani, A. K., & Wenten, I. G. (2019). Combined ultrafiltration and electrodeionization techniques for microbial xylitol purification. *Food and Bioproducts Processing*, *114*, 245–252. Available from https://doi.org/10.1016/j.fbp.2019.01.005.

Křivčík, J., Vladařová, J., Hadrava, J., Černín, A., & Brožová, L. (2010). The effect of an organic ion-exchange resin on properties of heterogeneous ion-exchange membrane. *Desalination and Water Treatment*, *14*, 179–184. Available from https://doi.org/10.5004/dwt.2010.1025.

Kunrath, C. C. N., Patrocínio, D. C., Siqueira Rodrigues, M. A., Benvenuti, T., & Amado, F. D. R. (2020). Electrodialysis reversal as an alternative treatment for producing drinking water from brackish river water: A case study in the dry season, northeastern Brazil. *Journal of Environmental Chemical Engineering*, *8*, 103719. Available from https://doi.org/10.1016/j.jece.2020.103719.

Kurz, E. E. C., Hellriegel, U., Luong, V. T., Bundschuh, J., & Hoinkis, J. (2020). Selective ion adsorption with pilot-scale membrane capacitive deionization (MCDI): Arsenic, ammonium, and manganese removal. *Desalination and Water Treatment.*, *198*, 163–169. Available from https://doi.org/10.5004/dwt.2020.26036.

Lasanta, C., & Gómez, J. (2012). Tartrate stabilization of wines. *Trends in Food Science and Technology*, *28*, 52–59. Available from https://doi.org/10.1016/j.tifs.2012.06.005.

Lee, J.-H., & Choi, J.-H. (2012). The production of ultrapure water by membrane capacitive deionization (MCDI) technology. *Journal of Membrane Science*, *409–410*, 251–256. Available from https://doi.org/10.1016/j.memsci.2012.03.064.

Lee, J.-S., Hwang, I.-T., Jung, C.-H., & Choi, J.-H. (2016). Surface modification of Nafion membranes by ion implantation to reduce methanol crossover in direct methanol fuel cells. *RSC Advances*, *6*, 62467–62470. Available from https://doi.org/10.1039/C6RA12756H.

Lee, M. S., Kang, H. G., Jeon, J. D., Choi, Y. W., & Yoon, Y. G. (2016). A novel amphoteric ion-exchange membrane prepared by the pore-filling technique for vanadium redox flow batteries. *RSC Advances*, *6*, 63023–63029. Available from https://doi.org/10.1039/c6ra07790k.

Li, X., Mo, Y., Qing, W., Shao, S., Tang, C. Y., & Li, J. (2019). Membrane-based technologies for lithium recovery from water lithium resources: A review. *Journal of Membrane Science*, *591*, 117317. Available from https://doi.org/10.1016/j.memsci.2019.117317.

Liao, J., Yu, X., Pan, N., Li, J., Shen, J., & Gao, C. (2019). Amphoteric ion-exchange membranes with superior mono-/bi-valent anion separation performance for electrodialysis applications. *Journal of Membrane Science*, *577*, 153–164. Available from https://doi.org/10.1016/j.memsci.2019.01.052.

Ling, J., Li, Y., Zhou, B., Zhu, B., Zhang, X., Wang, Y., ..., & Feng, W. (2019). The amphoteric ion exchange membrane based on CS/CMC for tobacco-protein adsorption and separation from tobacco extract. *International Journal of Polymer Science*, 2019, 3261798. Available from https://doi.org/10.1155/2019/3261798.

Liu, L., Wang, C., He, Z., Das, R., Dong, B., Xie, X., & Guo, Z. (2021). An overview of amphoteric ion exchange membranes for vanadium redox flow batteries. *Journal of Materials Science & Technology*, *69*, 212–227. Available from https://doi.org/10.1016/j.jmst.2020.08.032.

Liu, R., Wang, Y., Wu, G., Luo, J., & Wang, S. (2017). Development of a selective electrodialysis for nutrient recovery and desalination during secondary effluent treatment. *Chemical Engineering Journal*, *322*, 224–233. Available from https://doi.org/10.1016/j.cej.2017.03.149.

Mao, S., Chen, L., Zhang, Y., Li, Z., Ni, Z., Sun, Z., & Zhao, R. (2019). Fractionation of mono- and divalent ions by capacitive deionization with nanofiltration membrane. *Journal of Colloid and Interface Science*, *544*, 321–328. Available from https://doi.org/10.1016/j.jcis.2019.02.093.

Medina, V. F., Johnson, J. L., Waisner, S. A., Wade, R., & Mattei-Sosa, J. (2015). Development of a treatment process for electrodialysis reversal concentrate with intermediate softening and secondary reverse osmosis to approach 98-percent water recovery. *Journal of Environmental Engineering*, *141*, 04015002. Available from https://doi.org/10.1061/(ASCE)EE.1943-7870.0000929.

Mikhaylin, S., & Bazinet, L. (2016). Fouling on ion-exchange membranes: Classification, characterization and strategies of prevention and control. *Advances in Colloid and Interface Science*, *229*, 34–56. Available from https://doi.org/10.1016/j.cis.2015.12.006.

Missimer, T. M. (2018). *Water supply development for membrane water treatment facilities*. CRC Press.

Mohammadi, R., Tang, W., & Sillanpää, M. (2021). A systematic review and statistical analysis of nutrient recovery from municipal wastewater by electrodialysis. *Desalination*, *498*, 114626. Available from https://doi.org/10.1016/j.desal.2020.114626.

Nagarale, R. K., Gohil, G. S., & Shahi, V. K. (2006). Recent developments on ion-exchange membranes and electromembrane processes. *Advances in Colloid and Interface Science*, *119*, 97–130. Available from https://doi.org/10.1016/j.cis.2005.09.005.

Nagarale, R. K., Gohil, G. S., Shahi, V. K., & Rangarajan, R. (2005). Preparation and electrochemical characterization of sulfonated polysulfone cation-exchange membranes: Effects of the solvents on the degree of sulfonation. *Journal of Applied Polymer Science*, *96*, 2344–2351. Available from https://doi.org/10.1002/app.21630.

Neděla, D., Křivčík, J., Válek, R., Stránská, E., & Marek, J. (2015). Influence of water content on properties of a heterogeneous bipolar membrane. *Desalination and Water Treatment*, *56*, 3269–3272. Available from https://doi.org/10.1080/19443994.2014.981412.

Nemati, M., Hosseini, S. M., & Shabanian, M. (2017). Developing thin film heterogeneous ion exchange membrane modified by 2-acrylamido-2-methylpropanesulfonic acid hydrogel-co-super activated carbon nanoparticles coating layer. *Korean Journal of Chemical Engineering*, *34*, 1813–1821. Available from https://doi.org/10.1007/s11814-017-0049-6.

Ngene, I. S., Lammertink, R. G. H., Wessling, M., & Van der Meer, W. G. J. (2010). Particle deposition and biofilm formation on microstructured membranes. *Journal of Membrane Science*, *364*, 43–51. Available from https://doi.org/10.1016/j.memsci.2010.07.048.

Nie, X.-Y., Sun, S.-Y., Sun, Z., Song, X., & Yu, J.-G. (2017). Ion-fractionation of lithium ions from magnesium ions by electrodialysis using monovalent selective ion-exchange membranes. *Desalination*, *403*, 128–135. Available from https://doi.org/10.1016/j.desal.2016.05.010.

Nifong, T. P., & Gerhard, G. S. (2002). Separation of IgG and IgM from albumin in citrated human plasma using electrodialysis and metal ion affinity precipitation. *ASAIO Journal*, *48*.

Oren, Y., Korngold, E., Daltrophe, N., Messalem, R., Volkman, Y., Aronov, L., ..., & Gilron, J. (2010). Pilot studies on high recovery BWRO-EDR for near zero liquid discharge approach, *Desalination*, *261*, 321–330, Available from https://doi.org/10.1016/j.desal.2010.06.010.

Paidar, M., Fateev, V., & Bouzek, K. (2016). Membrane electrolysis—History, current status and perspective. *Electrochimica Acta*, *209*, 737–756. Available from https://doi.org/10.1016/j.electacta.2016.05.209.

Pawlowski, S., Rijnaarts, T., Saakes, M., Nijmeijer, K., Crespo, J. G., & Velizarov, S. (2017). Improved fluid mixing and power density in reverse electrodialysis stacks with chevron-profiled membranes. *Journal of Membrane Science*, *531*, 111–121. Available from https://doi.org/10.1016/j.memsci.2017.03.003.

Pismenskaia, N., Sistat, P., Huguet, P., Nikonenko, V., & Pourcelly, G. (2004). Chronopotentiometry applied to the study of ion transfer through anion exchange membranes. *Journal of Membrane Science*, *228*, 65–76. Available from https://doi.org/10.1016/j.memsci.2003.09.012.

Porada, S., Zhang, L., & Dykstra, J. E. (2020). Energy consumption in membrane capacitive deionization and comparison with reverse osmosis. *Desalination*, *488*, 114383. Available from https://doi.org/10.1016/j.desal.2020.114383.

Rai, P., & De, S. (2011). Membrane-based separation process for juice processing. In K. Mohanty, & M. K. Purkait (Eds.), *Membrane technologies and applications* (pp. 213–230). CRC Press LLC. Available from https://doi.org/10.1201/b11416-18.

Rao, J. R., Prasad, B. G. S., Narasimhan, V., Ramasami, T., Shah, P. R., & Khan, A. A. (1989). Electrodialysis in the recovery and reuse of chromium from industrial effluents. *Journal of Membrane Science*, *46*, 215–224. Available from https://doi.org/10.1016/S0376-7388(00)80336-1.

Reig, M., Casas, S., Aladjem, C., Valderrama, C., Gibert, O., Valero, F., ... Cortina, J. L. (2014). Concentration of NaCl from seawater reverse osmosis brines for the chlor-alkali industry by electrodialysis. *Desalination*, *342*, 107–117. Available from https://doi.org/10.1016/j.desal.2013.12.021.

Reverberi, A. P., Maga, L., Cerrato, C., & Fabiano, B. (2014). Membrane processes for water recovery and decontamination. *Current Opinion in Chemical Engineering*, *6*, 75–82. Available from https://doi.org/10.1016/j.coche.2014.10.004.

Rodrigues, M. A. S., Amado, F. D. R., Xavier, J. L. N., Streit, K. F., Bernardes, A. M., & Ferreira, J. Z. (2008). Application of photoelectrochemical–electrodialysis treatment for the recovery and reuse of water from tannery effluents. *Journal of Cleaner Production*, *16*, 605–611. Available from https://doi.org/10.1016/j.jclepro.2007.02.002.

Sahin, S., Dykstra, J. E., Zuilhof, H., Zornitta, R. L., & De Smet, L. C. P. M. (2020). Modification of cation-exchange membranes with polyelectrolyte multilayers to tune ion selectivity in capacitive deionization. *ACS Applied Materials & Interfaces*, *12*, 34746–34754. Available from https://doi.org/10.1021/acsami.0c05664.

Sajtar, E. T., & Bagley, D. M. (2009). Electrodialysis reversal: Process and cost approximations for treating coal-bed methane waters. *Desalination and Water Treatment*, *2*, 284–294. Available from https://doi.org/10.5004/dwt.2009.259.

Sanz, M. A., & Miguel, C. (2013). The role of SWRO Barcelona-Llobregat plant in the water supply system of Barcelona area. *Desalination and Water Treatment*, *51*, 111–123. Available from https://doi.org/10.1080/19443994.2012.699250.

Sarapulova, V., Shkorkina, I., Mareev, S., Pismenskaya, N., Kononenko, N., Larchet, C., ..., & Nikonenko, V. (2019). Transport characteristics of fujifilm ion-exchange membranes as compared to homogeneous membranes and and to heterogeneous membranes MK-40 and MA-41. *Membranes*, *9*, 84. Available from https://doi.org/10.3390/membranes9070084.

Savadogo, O. (2004). Emerging membranes for electrochemical systems: Part II. High temperature composite membranes for polymer electrolyte fuel cell (PEFC) applications. *Journal of Power Sources*, *127*, 135–161. Available from https://doi.org/10.1016/j.jpowsour.2003.09.043.

Scarazzato, T., Panossian, Z., Tenório, J. A. S., Pérez-Herranz, V., & Espinosa, D. C. R. (2017). A review of cleaner production in electroplating industries using electrodialysis. *Journal of Cleaner Production*, *168*, 1590–1602. Available from https://doi.org/10.1016/j.jclepro.2017.03.152.

Serre, E., Rozoy, E., Pedneault, K., Lacour, S., & Bazinet, L. (2016). Deacidification of cranberry juice by electrodialysis: Impact of membrane types and configurations on acid migration and juice physicochemical characteristics. *Separation and Purification Technology*, *163*, 228–237. Available from https://doi.org/10.1016/j.seppur.2016.02.044.

Shahi, V. K., Thampy, S. K., & Rangarajan, R. (2000). Preparation and electrochemical characterization of sulfonated interpolymer of polyethylene and styrene–divinylbenzene copolymer membranes. *Reactive & Functional Polymers*, *46*, 39–47. Available from https://doi.org/10.1016/S1381-5148(00)00031-6.

Sheldeshov, N. V., Zabolotskii, V. I., & Loza, S. A. (2014). Electric conductivity of profiled ion-exchange membranes. *Petroleum Chemistry*, *54*, 664–668. Available from https://doi.org/10.1134/s0965544114080143.

Shi, L., Hu, Z., Simplicio, W. S., Qiu, S., Xiao, L., Harhen, B., & Zhan, X. (2020). Antibiotics in nutrient recovery from pig manure via electrodialysis reversal: Sorption and migration associated with membrane fouling. *Journal of Membrane Science*, *597*, 117633. Available from https://doi.org/10.1016/j.memsci.2019.117633.

Stenina, I., Golubenko, D., Nikonenko, V., & Yaroslavtsev, A. (2020). Selectivity of transport processes in ion-exchange membranes: Relationship with the structure and methods for its improvement. *International Journal of Molecular Sciences*, *21*, 1–33. Available from https://doi.org/10.3390/ijms21155517.

Strathmann, H. (1991). *Electrodialysis state of the art. Membranes—Proceedings of India-EC workshop* (pp. 25–69). New Delhi: Oxford & IBH.

Strathmann, H. (2010). Electrodialysis, a mature technology with a multitude of new applications. *Desalination*, *264*, 268–288. Available from https://doi.org/10.1016/j.desal.2010.04.069.

Szczepański, P., & Szczepańska, G. (2017). Donnan dialysis – A new predictive model for non – steady state transport. *Journal of Membrane Science*, *525*, 277–289. Available from https://doi.org/10.1016/j.memsci.2016.11.017.

Tanaka, Y. (2007). *Ion exchange membrane fundamentals and applications. Membrane science and technology series*. Amsterdam: Elsevier.

Tang, K., Kim, Y.-H., Chang, J., Mayes, R. T., Gabitto, J., Yiacoumi, S., & Tsouris, C. (2019). Seawater desalination by over-potential membrane capacitive deionization: Opportunities and hurdles. *Chemical Engineering Journal*, *357*, 103–111. Available from https://doi.org/10.1016/j.cej.2018.09.121.

Tedesco, M., Scalici, C., Vaccari, D., Cipollina, A., Tamburini, A., & Micale, G. (2016). Performance of the first reverse electrodialysis pilot plant for power production from saline waters and concentrated brines. *Journal of Membrane Science*, *500*, 33–45. Available from https://doi.org/10.1016/j.memsci.2015.10.057.

Turek, M., Dydo, P., & Waś, J. (2006). Electrodialysis reversal in high $CaSO_4$ supersaturation mode. *Desalination*, *198*, 288–294. Available from https://doi.org/10.1016/j.desal.2006.01.029.

Valero, F., & Arbós, R. (2010). Desalination of brackish river water using electrodialysis reversal (EDR): Control of the THMs formation in the Barcelona (NE Spain) area. *Desalination*, *253*, 170–174. Available from https://doi.org/10.1016/j.desal.2009.11.011.

Valero, F., Barceló, A., Medina, M. E., & Arbós, R. (2013). Barcelona, three years of experience in brackish water desalination using EDR to improve quality. New O&M procedures to reduce low-value work and increase productivity. *Desalination and Water Treatment*, *51*, 1137–1142. Available from https://doi.org/10.1080/19443994.2012.714583.

Vallejo, M. E., Persin, F., Innocent, C., Sistat, P., & Pourcelly, G. (2000). Electrotransport of Cr(VI) through an anion exchange membrane. *Separation and Purification Technology.*, *21*, 61–69. Available from https://doi.org/10.1016/S1383-5866(00)00189-1.

Vera, E., Ruales, J., Dornier, M., Sandeaux, J., Sandeaux, R., & Pourcelly, G. (2003). Deacidification of clarified passion fruit juice using different configurations of electrodialysis. *Journal of Chemical Technology and Biotechnology*, *78*, 918–925. Available from https://doi.org/10.1002/jctb.827.

Wang, C., Chen, L., & Liu, S. (2019). Activated carbon fiber for adsorption/electrodeposition of Cu (II) and the recovery of Cu (0) by controlling the applied voltage during membrane capacitive deionization. *Journal of Colloid and Interface Science*, *548*, 160–169. Available from https://doi.org/10.1016/j.jcis.2019.04.030.

Wang, L., & Lin, S. (2019). Mechanism of selective ion removal in membrane capacitive deionization for water softening. *Environmental Science & Technology*, *53*, 5797–5804. Available from https://doi.org/10.1021/acs.est.9b00655.

Wang, X., Zhang, X., Wang, Y., Du, Y., Feng, H., & Xu, T. (2015). Simultaneous recovery of ammonium and phosphorus via the integration of electrodialysis with struvite reactor. *Journal of Membrane Science*, *490*, 65–71. Available from https://doi.org/10.1016/j.memsci.2015.04.034.

Wang, Y., Wang, S., Xiao, M., Song, S., Han, D., Hickner, M. A., & Meng, Y. (2014). Amphoteric ion exchange membrane synthesized by direct polymerization for vanadium redox flow battery application. *International Journal of Hydrogen Energy*, *39*, 16123–16131. Available from https://doi.org/10.1016/j.ijhydene.2014.04.049.

Ward, A. J., Arola, K., Thompson Brewster, E., Mehta, C. M., & Batstone, D. J. (2018). Nutrient recovery from wastewater through pilot scale electrodialysis. *Water Research*, *135*, 57–65. Available from https://doi.org/10.1016/j.watres.2018.02.021.

Wardani, A. K., Hakim, A. N., Khoiruddin, K., & Wenten, I. G. (2017). Combined ultrafiltration-electrodeionization technique for production of high purity water. *Water Science and Technology*, *75*, 2891–2899. Available from https://doi.org/10.2166/wst.2017.173.

Wei, Y., Qian, T., Liu, J., Guo, X., Gong, Q., Liu, Z., ..., & Qiao, J. (2019). Novel composite Nafion membranes modified with copper phthalocyanine tetrasulfonic acid tetrasodium salt for fuel cell application. *Journal of Materiomics*, *5*, 252–257. Available from https://doi.org/10.1016/j.jmat.2019.01.006.

Weinertová, K., Křivčík, J., Neděla, D., Stránská, E., & Václavíková, N. (2018). Optimization of polyethylene binder for heterogeneous ion exchange membrane manufacture to improve its mechanical stability. *Journal of Applied Polymer Science*, *135*, 46415. Available from https://doi.org/10.1002/app.46415.

Wenten, I. G., & Khoiruddin, K. (2016). Recent developments in heterogeneous ion-exchange membrane: Preparation, modification, characterization and performance evaluation. *Journal of Engineering Science and Technology*, *11*, 916–934.

Wenten, I. G., Khoiruddin, K., Aryanti, P. T. P., & Hakim, A. N. (2016). Scale-up strategies for membrane-based desalination processes: A review. *Journal of Membrane Science and Research*, *2*, 42–58. Available from https://doi.org/10.22079/JMSR.2016.19152.

Wenten, I. G., Khoiruddin, K., Wardani, A. K., & Widiasa, I. N. (2020). Synthetic polymer-based membranes for heavy metal removal. In A. F. Ismail, W. N. W. Salleh, & N. Yusof (Eds.), *Synthetic polymeric membranes for advanced water treatment, gas separation, and energy sustainability* (pp. 71–101). Elsevier. Available from https://doi.org/10.1016/B978-0-12-818485-1.00005-8.

Won, Y. J., Jung, S. Y., Jang, J. H., Lee, J. W., Chae, H. R., Choi, D. C., Ahn, K. H., Lee, C. H., & Park, P.K. (2016). Correlation of membrane fouling with topography of patterned membranes for water treatment. *Journal of Membrane Science*, Volume 498, 14–19. Available from https://doi.org/10.1016/j.memsci.2015.09.058.

Xie, M., Luo, W., & Gray, S. R. (2017). Surface pattern by nanoimprint for membrane fouling mitigation: Design, performance and mechanisms. *Water Research*, *124*, 238–243. Available from https://doi.org/10.1016/j.watres.2017.07.057.

Xu, T., Wu, D., & Wu, L. (2008). Poly(2,6-dimethyl-1,4-phenylene oxide) (PPO)—A versatile starting polymer for proton conductive membranes (PCMs). *Progress in Polymer Science*, *33*, 894–915. Available from https://doi.org/10.1016/j.progpolymsci.2008.07.002.

Xu, X., Lin, L., Ma, G., Wang, H., Jiang, W., He, Q., ..., & Xu, P. (2018). Study of polyethyleneimine coating on membrane permselectivity and desalination performance during pilot-scale electrodialysis of reverse osmosis concentrate. *Separation and Purification Technology*, *207*, 396–405. https://doi.org/10.1016/j.seppur.2018.06.070.

Yang, J., Bu, Y., Liu, F., Zhang, W., Cai, D., Sun, A., . . . Zhang, C. (2020). Potential application of membrane capacitive deionization for heavy metal removal from water: A mini-review. *International Journal of Electrochemical Science*, *15*, 7848–7859. Available from https://doi.org/10.2096/4/2020.08.98.

Yen, F.-C., You, S.-J., & Chang, T.-C. (2017). Performance of electrodialysis reversal and reverse osmosis for reclaiming wastewater from high-tech industrial parks in Taiwan: A pilot-scale study. *Journal of Environmental Management*, *187*, 393–400. Available from https://doi.org/10.1016/j.jenvman.2016.11.001.

Yu, J., Jo, K., Kim, T., Lee, J., & Yoon, J. (2018). Temporal and spatial distribution of pH in flow-mode capacitive deionization and membrane capacitive deionization. *Desalination*, *439*, 188–195. Available from https://doi.org/10.1016/j.desal.2018.04.011.

Yuan, J., Yu, C., Peng, J., Wang, Y., Ma, J., Qiu, J., ..., & Zhai, M. (2013). Facile synthesis of amphoteric ion exchange membrane by radiation grafting of sodium styrene sulfonate and N,N-dimethylaminoethyl methacrylate for vanadium redox flow battery. *Journal of Polymer Science Part A: Polymer Chemistry*, *51*, 5194–5202. https://doi.org/10.1002/pola.26949.

Zendehnam, A., Robatmili, N., Hosseini, S. M., Arabzadegan, M., & Madaeni, S. S. (2014). Fabrication and modification of acrylonitrile–butadiene–styrene-based heterogeneous ion-exchange membranes by plasma treatment: Investigation of the nanolayer deposition rate and temperature effects. *Journal of Applied Polymer Science*, *131*, 1–9. Available from https://doi.org/10.1002/app.40025.

Zhang, Y., Desmidt, E., Van Looveren, A., Pinoy, L., Meesschaert, B., & Van der Bruggen, B. (2013). Phosphate separation and recovery from wastewater by novel electrodialysis. *Environmental Science & Technology*, *47*, 5888–5895. Available from https://doi.org/10.1021/es4004476.

Zhao, D., Lee, L. Y., Ong, S. L., Chowdhury, P., Siah, K. B., & Ng, H. Y. (2019). Electrodialysis reversal for industrial reverse osmosis brine treatment. *Separation and Purification Technology.*, *213*, 339–347. Available from https://doi.org/10.1016/j.seppur.2018.12.056.

Zhao, R., Porada, S., Biesheuvel, P. M., & Van Der Wal, A. (2013). Energy consumption in membrane capacitive deionization for different water recoveries and flow rates, and comparison with reverse osmosis. *Desalination*, *330*, 35–41. Available from https://doi.org/10.1016/j.desal.2013.08.017.

Zuo, W., Zhang, G., Meng, Q., & Zhang, H. (2008). Characteristics and application of multiple membrane process in plating wastewater reutilization. *Desalination*, *222*, 187–196. Available from https://doi.org/10.1016/j.desal.2007.01.149.

CHAPTER

16

Polymeric nano-enhanced membranes in electrodialysis, electrodialysis reversal and capacitive deionization technologies

Elham Jashni and Sayed Mohsen Hosseini

Department of Chemical Engineering, Faculty of Engineering, Arak University, Arak, Iran

16.1 Introduction

The provision of freshwater is one of the most pervasive challenges of the current era. Although water is the greatest widespread substance in the environment, only 2.5% of the water on earth is freshwater. The global freshwater shortage is expected to become worse in the coming decades, which will affect economic and social development. An expanding list of stressors such as climate change, population growth, urbanization, water pollution, as well as enhancing living standards have led to the increasing demand for treatment of different water sources (Ahmed, Hashaikeh, & Hilal, 2020; Jashni & Hosseini, 2020a; Pan et al., 2019). Among the many strategies adopted to provide adequate water resources of desirable quality, membrane-based separations for desalination and wastewater treatment are playing an increasingly substantial role in reducing water stress and in avoiding the complete depletion of water supplies. The low operational cost, high separation efficiency, extreme flexibility, low-energy consumption, and easy scale-up's are the major benefits that favor membrane processes over their conventional counterpart technologies (Goh, Matsuura, Ismail, & Hilal, 2016; Li, Sotto, Li, & Van der Bruggen, 2017; Yin & Deng, 2015). Ion-exchange membranes (IEMs), the main component in the industrial water desalination and electrochemical processes, play a significant role in the further development of membrane technologies in unexplored areas, thanks to their potential practical applications (Alabi et al., 2018; Pismenskaya, Pokhidnia, Pourcelly, & Nikonenko, 2018; Ran et al., 2017). The timeline of the scientific development of IEMs and their related processes is shown in Fig. 16.1.

Advancement in Polymer-Based Membranes for Water Remediation
DOI: https://doi.org/10.1016/B978-0-323-88514-0.00013-9

© 2022 Elsevier Inc. All rights reserved.

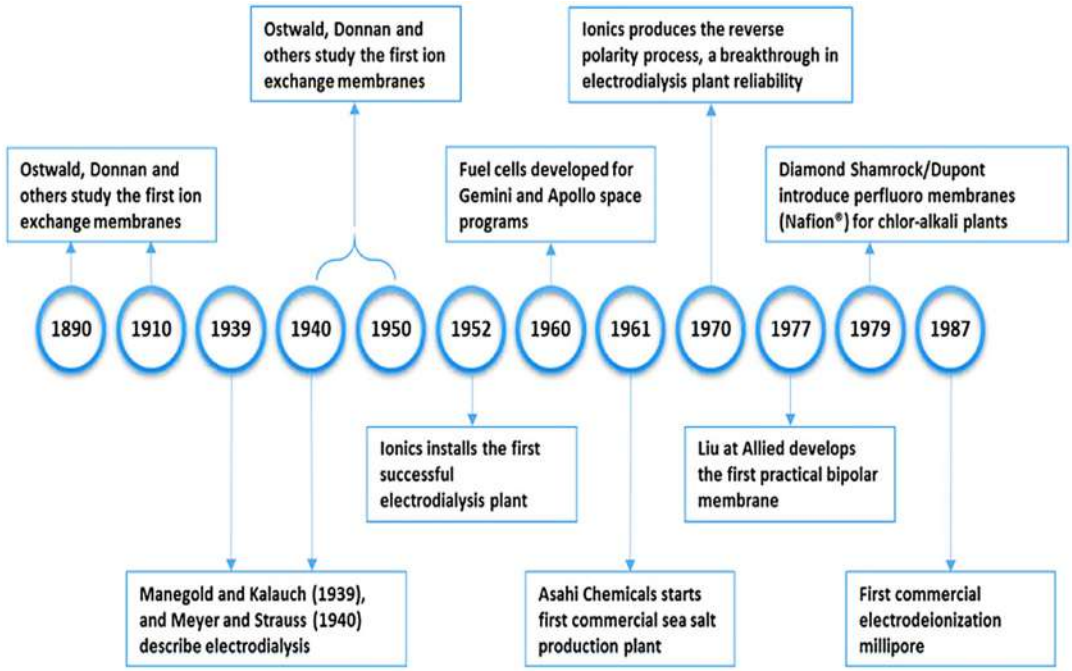

FIGURE 16.1 Milestones in the development of ion-exchange membranes (IEMs) and their related processes (Alabi et al., 2018).

Based on the charge of ionic groups affixed to the membrane matrix, IEMs can be categorized into anion-exchange membranes (AEMs) and cation-exchange membranes (CEMs) (see Fig. 16.2). Membranes containing positively fixed ionic groups (such as ammonium and phosphonium), termed AEMs, allow the passage of anions but reject cations. While, membranes containing negatively fixed ionic groups (such as sulfonic acid, carboxylic acid, phosphonic acid, and phenolic hydroxide), termed CEMs, permit the passage of cationsbut preclude the anions to pass through (Ran et al., 2017; Scarazzato, Panossian, Tenorio, Perez-Herranz, & Espinosa, 2017). Different structures of repeating patterns of cation-exchange and anion-exchange groups present in polymer architectures are illustrated in Fig. 16.3A and B, respectively.

According to their microstructure, IEMs can also be divided into two types: heterogeneous (composite) and homogeneous (ionomer) membranes (see Fig. 16.4). In general, homogeneous IEMs have good electrochemical properties but do not have any required mechanical strength. Heterogeneous IEMs, on the other hand, have good mechanical strength but show poor electrochemical performance. The other difference between these two types of IEMs is related to their dimensional stability that the heterogeneous IEMs have better dimensional stability than homogeneous ones (Ariono, Khoiruddin, Subagjo, & Wenten, 2017; Pismenskaya et al., 2018; Radmanesh, Rijnaarts, Moheb, Sadeghi, & De Vos, 2019; Vogel & M-Haack, 2014).

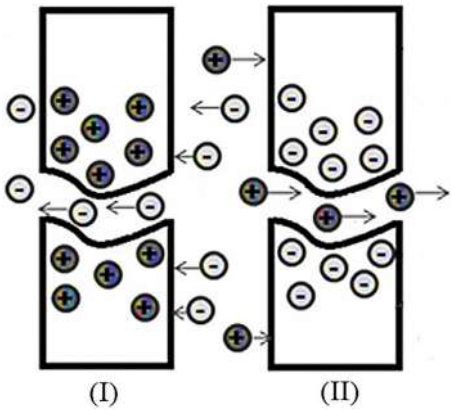

FIGURE 16.2 Schematic illustration of (A) the anion-exchange membrane (AEM) and (B) the cation-exchange membrane (CEM) (Scarazzato et al., 2017).

Ionizable functional groups of IEMs allow the transfer of counter-ions across the membrane; while effectively inhibiting the passage of co-ions. This is one kind of permselectivity stemming from Donnan exclusion and essential property that makes the operation of electro-membrane processes possible. Additionally, for the success of a wide spectrum of technical processes, ion selectivity between different counter-ions (with the same or different valences) is essential. Generally, in an IEM, ion interactions with the host medium (water and pore walls) bring about the most significant mechanisms to induce ion selectivity. Fig. 16.5 shows the schematic diagram of the energy barriers for the counter- and co-ions (blue and red spheres, respectively) and also the various molecular-level mechanisms that govern the selectivity of an IEM. It is worth noting that in the case of selectivity between two counter-ions, blue and red spheres refer to two different counter-ions with the same or different valences. As shown in Fig. 16.5A, ideally, the IEM is only permeable for the counter-ion, showing a lower energy barrier (E_a) compared to the co-one (also, in the case of selectivity between two counter-ions, the IEM is permeable only for counter-ion with the lower energy barrier). Principally, entering the pore mouth and crossing through the pore channel of an IEM can be considered as two stages that can impose the transport resistance or the energy barrier to an ion. When entering the pore mouth, an ion may face the energy barrier due to: (1) steric hindrance (imposed by their size and shape); (2) electrostatic repulsion (on account of Donnan exclusion effect); and (3) dielectric effects (that is, variation in ion interaction with its closest vicinity, such as partial dehydration). Also, an ion may experience additional energy barriers while crossing through the membrane pore because of (4) frictional effects (due to physical collisions with rough inner pore walls, resulting in momentum exchange); and (5) viscous effects (owing to the different interactions with the pore wall). Thus, the observed selectivity in an IEM relies on the relative contribution of ion entering the pore mouth and its crossing through the pore to the overall energy barrier (Epsztein, Duchanois, Ritt, Noy, & Elimelech, 2020; Luo, Roghmans, & Wessling, 2020).

However, for particular applications of IEMs, priorities are given to certain properties of theirs; generally speaking, it is expected that these membranes show high permselectivity, low electrical resistance, high permeability, good chemical, mechanical, and thermal stabilities

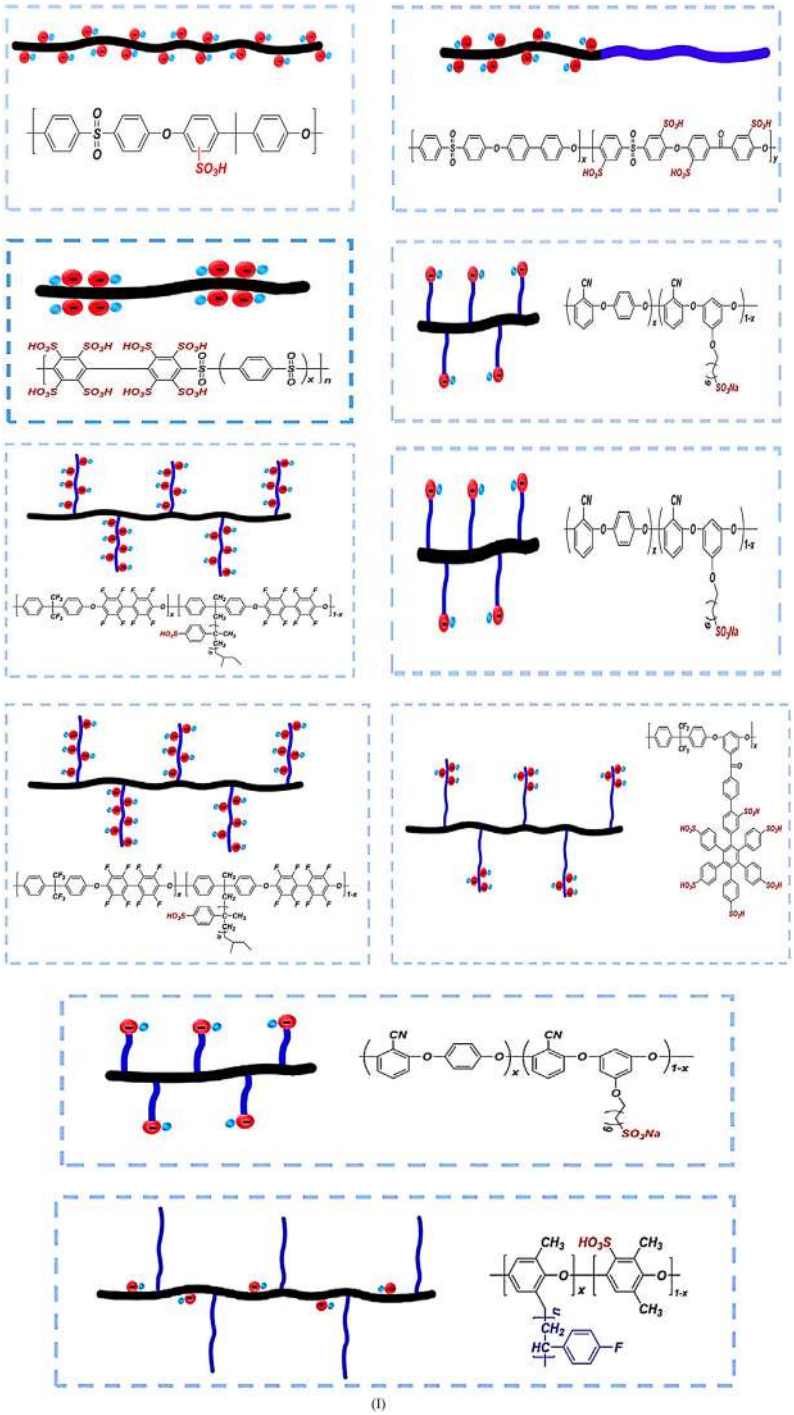

FIGURE 16.3 Different structures of repeating patterns of (A) cation-exchange and (B) anion-exchange groups present in polymer architectures (Ran et al., 2017).

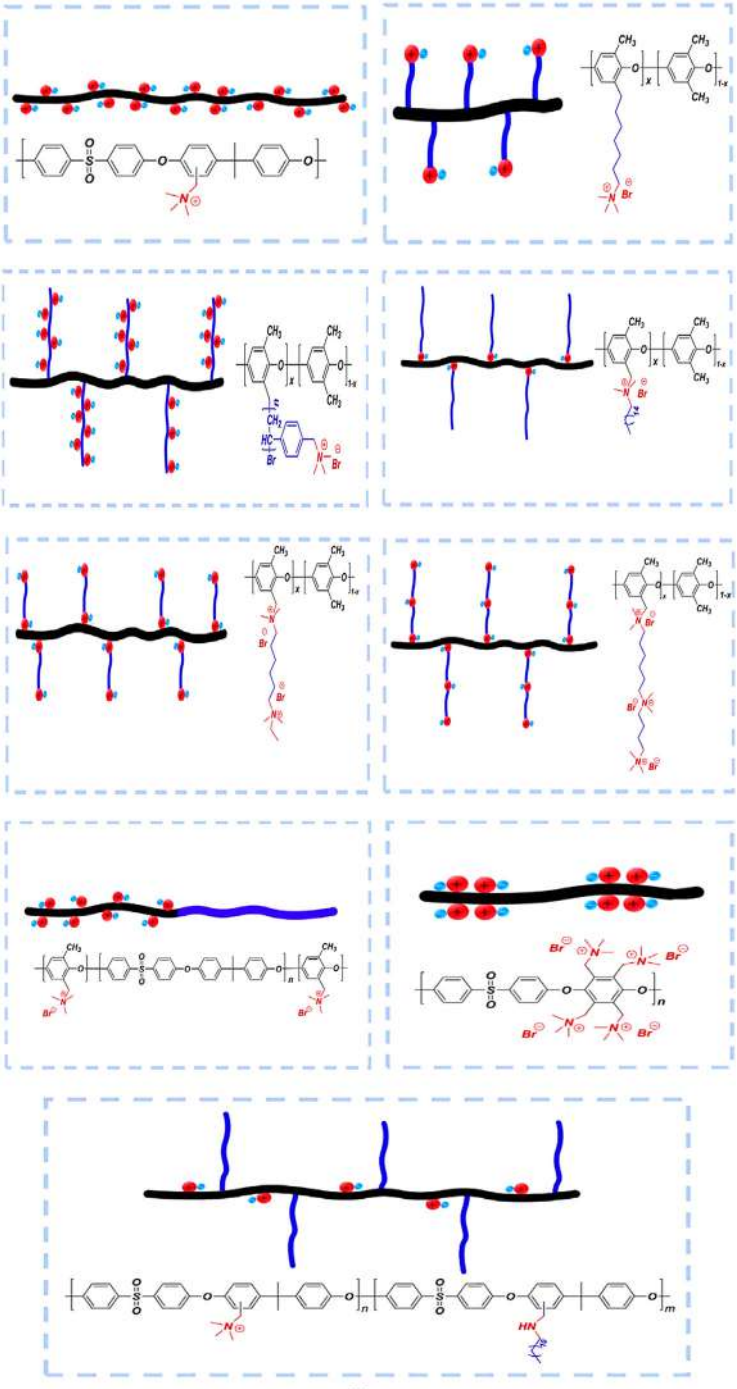

FIGURE 16.3 (Continued)

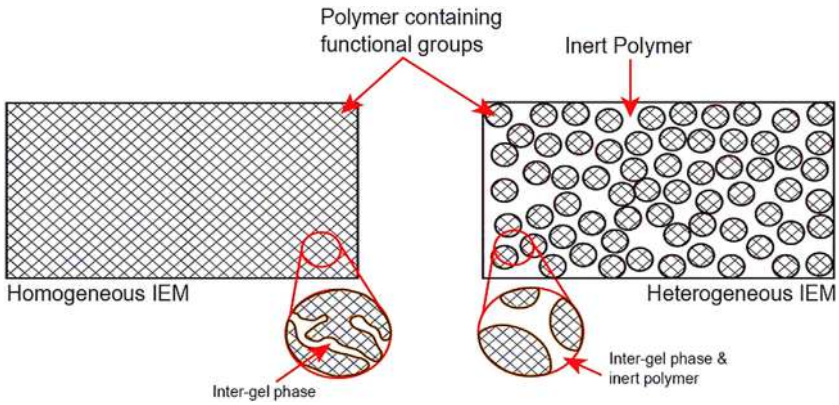

FIGURE 16.4 Schematic description of homogeneous and heterogeneous ion exchange membranes (Ariono et al., 2017).

(Radmanesh et al., 2019; Vogel & M-Haack, 2014). Fabrication of membranes with both high selectivity and high ionic permeability has been a long-standing challenge in membrane science. The inherent permeability-selectivity trade-off is a substantial barrier restricting the broad application of IEMs. The size of the transfer channels has a direct influence on the selectivity and permeability of these membranes. IEMs containing smaller pore sizes than the hydration size of ions often represent high selectivity, but low permeability of ions since dehydration becomes dominant [Fig. 16.6A(I)]. On the other hand, membranes containing larger pore size than Debye screening length of the electric double layer often demonstrate high permeability of ions, but nearly no selectivity [Fig. 16.6A(III)] since the electric potential of their charged sidewalls cannot cover the whole channel (see Fig. 16.6B). Finally, when the pore size of IEMs is between the two cases, the IEM shows a balance between permeability and selectivity together [Fig. 16.6A(II)] (Jashni, Hosseini, Shen, & Van der Bruggen, 2019).

For the description of the IEM structure, their transport processes, and quantitative treatment of their properties, three types of membrane microstructure models have been suggested. The first type that considers the membrane as a homogeneous solution is based on models from which the classical Donnan effect was first derived. The second one that considers the presence of cluster-channels in the membrane matrix takes into account the structure in homogeneity on the submicroscopic scale. Finally, the third type, micro heterogeneous model, assumes an IEM as a two-phase system [(gel phase that involves polymer chains with fixed ions, an inert binder, and charged internal solution) and (intergel phase, where the electro neutral bulk-like solution that occupies the central parts of the meso- and macro-pores)]. Schematic illustrations of the IEM structure in accordance with the second and third models are shown in Figs. 16.7 and 16.8, respectively (Bdiri et al., 2019; Jashni & Hosseini, 2020b; Luo, Abdu, & Wessling, 2018).

It is generally hard to identify the exact ion transportation mechanisms in an IEM because they are complicated and occur next to each other. The possible mechanisms for the transportation of common ions in the IEM matrix can be divided into four categories, including (1) diffusion (owing to the concentration gradient); (2) convection [imposed by the electroosmotic solvent (water) transfer]; (3) electro-migration (due to the electric potential gradient); and (4)

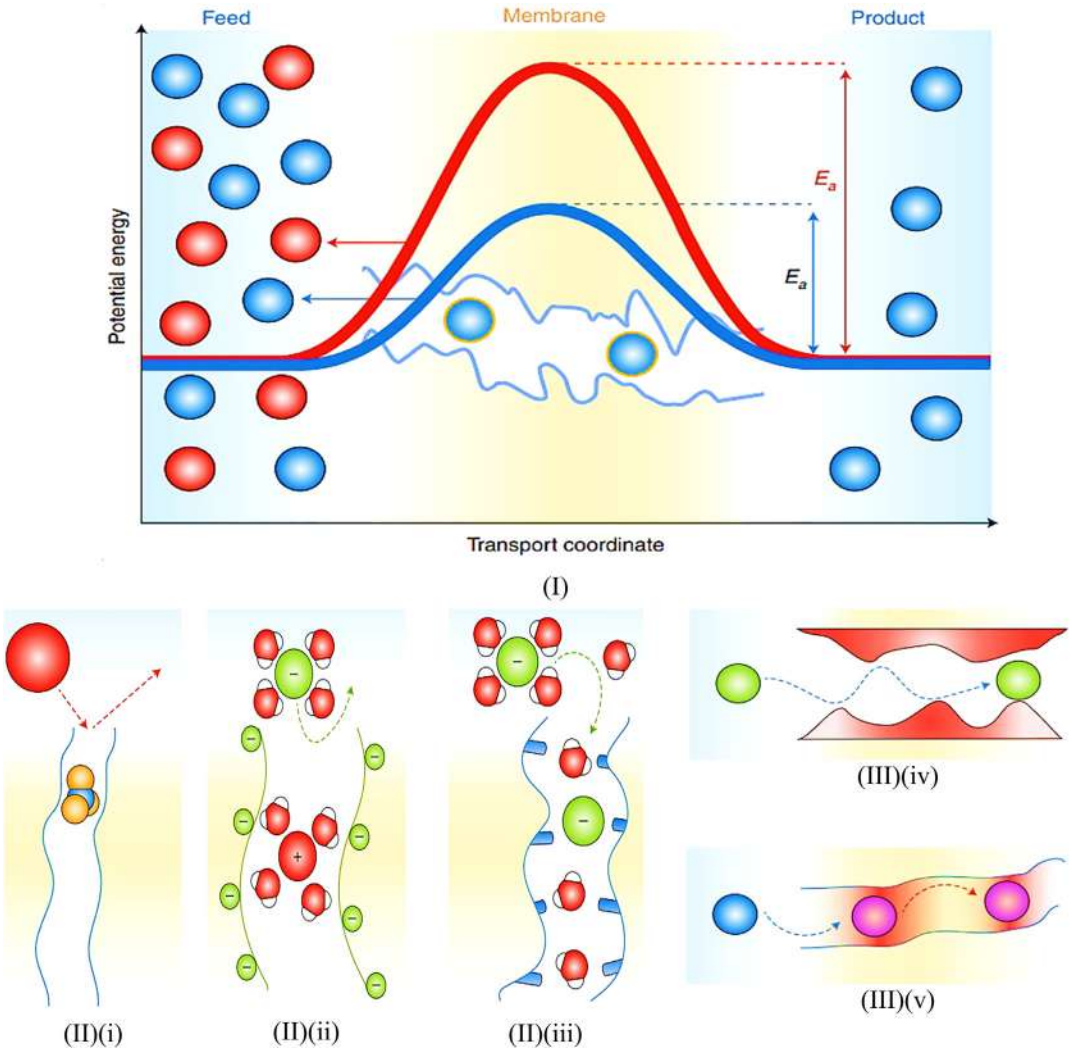

FIGURE 16.5 (A) Energy barrier profile for two different ions [blue sphere: counter-ion, red sphere: co-ion (in the case of selectivity between two counter-ions these spheres refer to two different counter-ions with the same or different valences)] transported through an ion-exchange membrane (IEM), molecular-level mechanisms affecting energy barrier of an ion during (B) the entering to the confined environment of the IEM and (C) crossing through it. (B) (i) steric hindrance, (B) (ii) electrostatic repulsion, (B) (iii) dielectric effects, (C) (iv) frictional, and (C) (v) viscous effects (Epsztein et al., 2020).

surface site hopping. The first three mechanisms occur predominantly in the interstitial phase of free water, while the last one is proposed to account for the transportation of counter-ions along with the fixed ionic groups at the interface. Although the exact transportation mechanisms of ions in the IEM are ambiguous, the contribution of mass diffusion and convection are small in the electro-driven membrane processes. Also, researchers still doubt the degree of

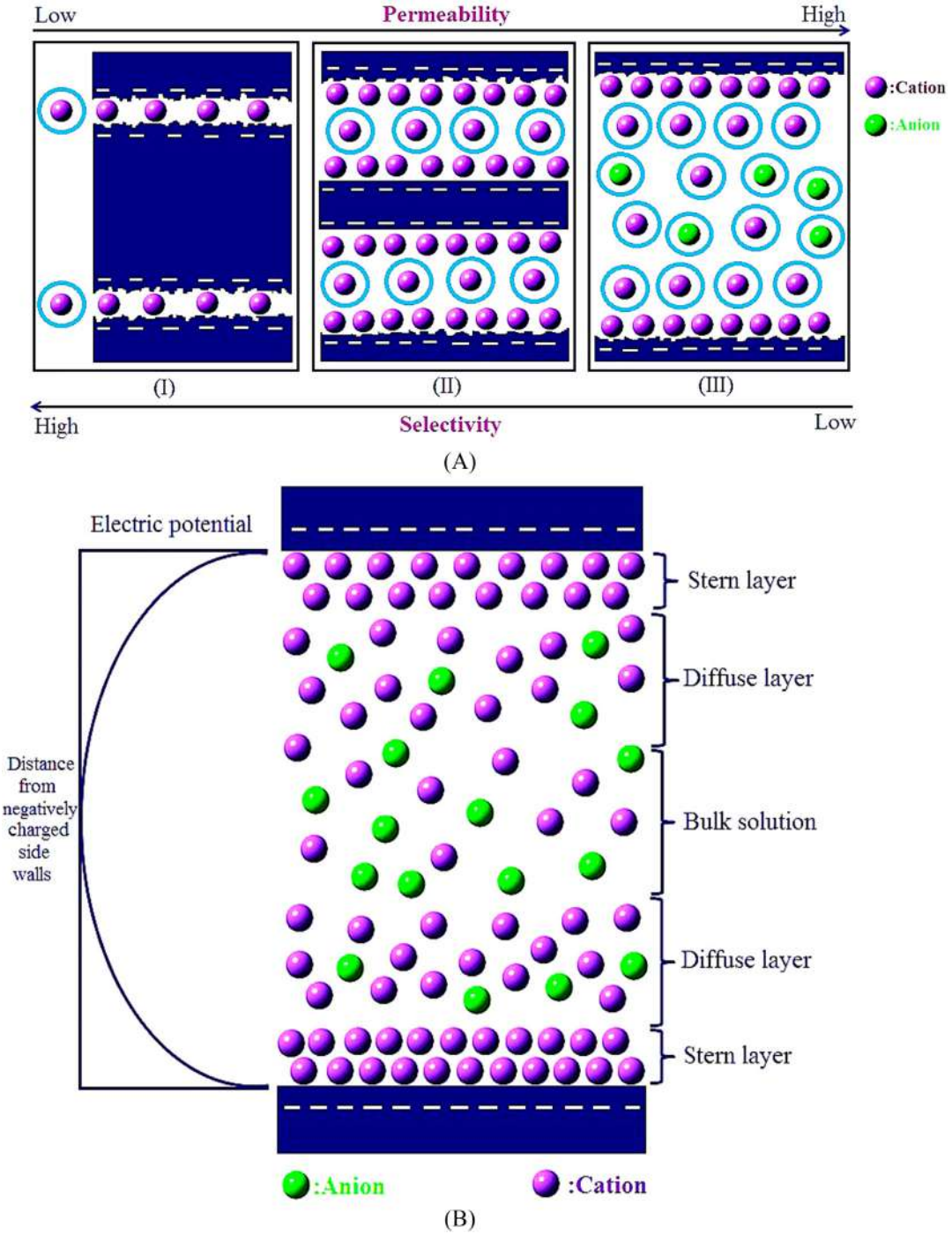

FIGURE 16.6 (A) Schematic representation of three ionic transport mechanisms as the pore size increases in cation-exchange membranes (CEMs) and (B) electric potential gradient relative to the distance from negatively charged sidewalls (Jashni et al., 2019).

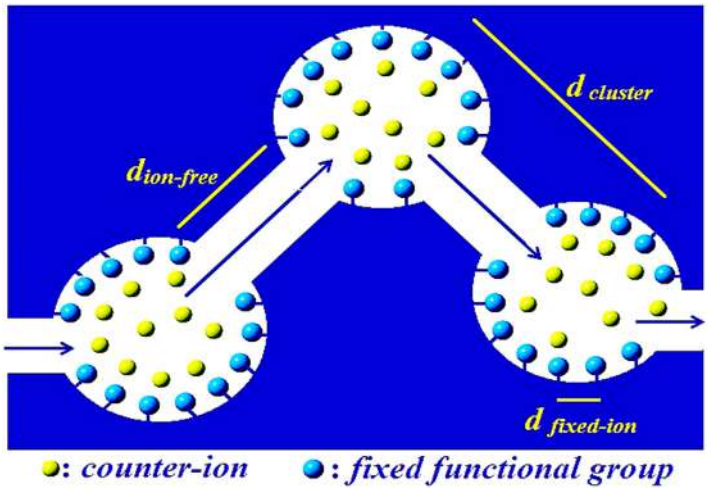

FIGURE 16.7 Schematic cluster-network morphology of ion-exchange membrane (IEM) ($d_{cluster}$: average space between ionic clusters, $d_{ion\text{-}free}$: average space between regions without ions, and $d_{fixed\text{-}ion}$: average space between fixed ionic groups) (Jashni & Hosseini, 2020b).

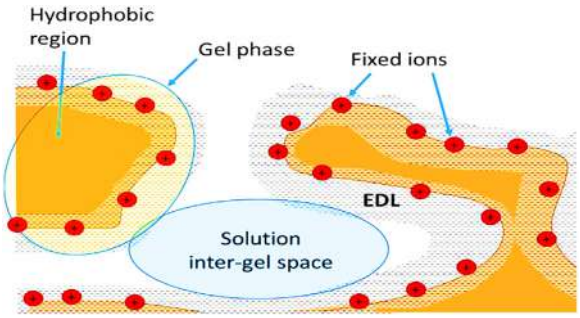

FIGURE 16.8 Schematic representation of ion-exchange membrane (IEM) structure in accordance with micro heterogeneous model (Bdiri et al., 2019).

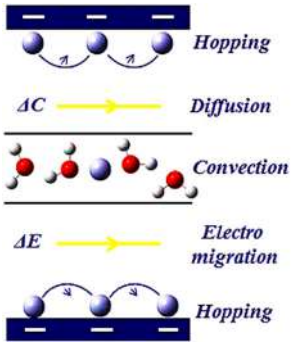

FIGURE 16.9 Possible mechanisms for ion transportation in an ion-exchange membrane (IEM) with negatively fixed ionic groups (Jashni et al., 2020c).

contribution of the surface site hopping mechanism. A schematic representation of ion transport mechanisms in an IEM is illustrated in Fig. 16.9 (Jashni, Hosseini, & Shen, 2020c; Luo et al., 2018).

Today, IEMs are playing more and more substantial roles in diverse applications, especially electro-membrane processes where selective transport of charged particles is required. Electro-membrane processes have recently gained significant attention and several studies have led to remarkable advances. These processes have a wide range of applications such as the treatment of water, production of bioactive compounds having health benefits, preservation of food products, recovery of energy from natural and wastewaters with minimal environmental impact, extraction of organic acids, and so on (Bazinet & Geoffroy, 2020; Gurreri, Tamburini, Cipollina, & Micale, 2020; Luo et al., 2018; Patel, Qin, Walker, & Elimelech, 2020; Vogel & M-Haack, 2014).

The mother technology of electro-driven membrane processes is electrodialysis (ED), which utilizes an electric field to transport ions through IEMs. In ED processes, CEMs and AEMs are alternatively arranged in series and upon application of an electric potential across the electrodes, ions selectively migrate from one side of the membrane (dilute compartment) to the other side (concentrated compartment) (see Fig. 16.10). The concept of multicompartment ED was demonstrated successfully in 1950, when W. Juda and W. A. McRay manufactured the first synthetic IEMs from ion exchange resins. In 1952 Ionics used IEMs to install the first successful ED desalination plant in Saudi Arabia. Since that year, with the development of IEMs, ED has become a practical process. However, the desalination of brackish water is still currently the most important industrial application of ED processes; this technology has also been utilized in several commercial applications, such as the production of ultra-pure water, acid/base, and sea salt, highlighting the technology's flexibility and practicality (Bazinet & Geoffroy, 2020; Campione et al., 2018, 2020; Vaselbehagh, Karkhanechi, Takagi, & Matsuyama, 2015).

ED has historically stood as the flagship electrodialytic process and many electro-driven membrane technologies are derived from the principle of this system. Electrodialysis reversal (EDR) and membrane capacitive deionization (MCDI) are two ED-derived technologies commercially available at the industrial scale (Bazinet & Geoffroy, 2020; Patel et al., 2020).

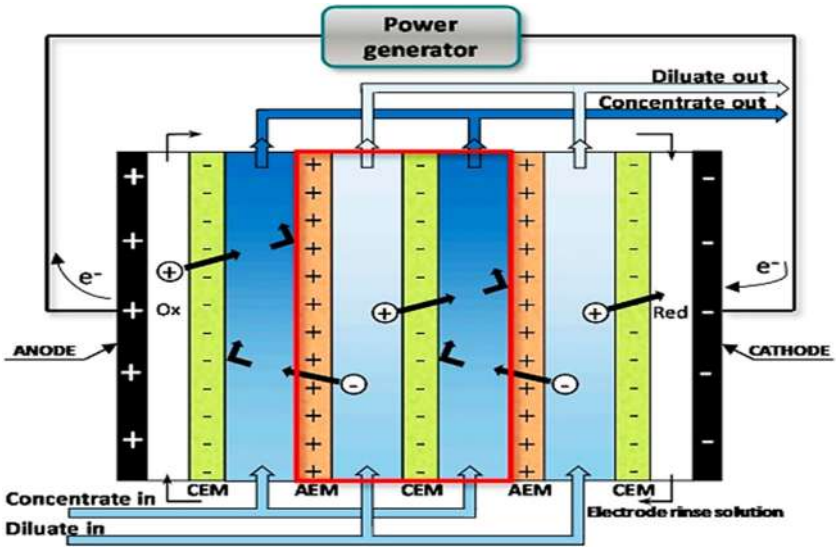

FIGURE 16.10 Scheme of the electrodialysis/electrodialysis reversal (ED/EDR) systems (Gurreri et al., 2020).

The EDR is a promising technology for reducing the effects caused by concentration polarization, fouling, and scaling phenomena in ED processes. These three phenomena that are the Achilles heel of membrane processes adversely affect the separation performance of IEMs during ED. Reversing the polarity of the electrodes at regular time intervals causes the removal of electrically charged foulants deposited on the membrane surface. This novel operational strategy surely extends the lifespan of the membrane and maintains constant system performance. EDR systems have been commercially deployed for brackish water desalination since the late 1970s, with variants designed for city-scale desalination, village-scale desalination, and even in-home water treatment (Campione et al., 2018; Gurreri et al., 2020; Nayar & Lienhard, 2020).

In the mid-2000s, capacitive deionization (CDI) faced a significant breakthrough with the development of the MCDI. This new strategy has the crucial role of improving charge efficiency by restricting co-ions from accessing the electrodes. Differing from the conventional CDI (a nonmembrane technique), in MCDI technology, a CEM is placed in front of the porous electrode that is defined as the cathode, while an AEM is placed in front of the other electrode that is defined as the anode. Incorporating IEMs in MCDI, owing to the inhibition of co-ions access to the electrodes, significantly boosts the salt adsorption capacity of the process when compared to CDI. The schematic diagrams of CDI and MCDI systems are depicted in Fig. 16.11 (Bazinet & Geoffroy, 2020; Porada, Zhao, Van der Wal, Presser, & Biesheuvel, 2013; Yu, Jo, Kim, Lee, & Yoon, 2018).

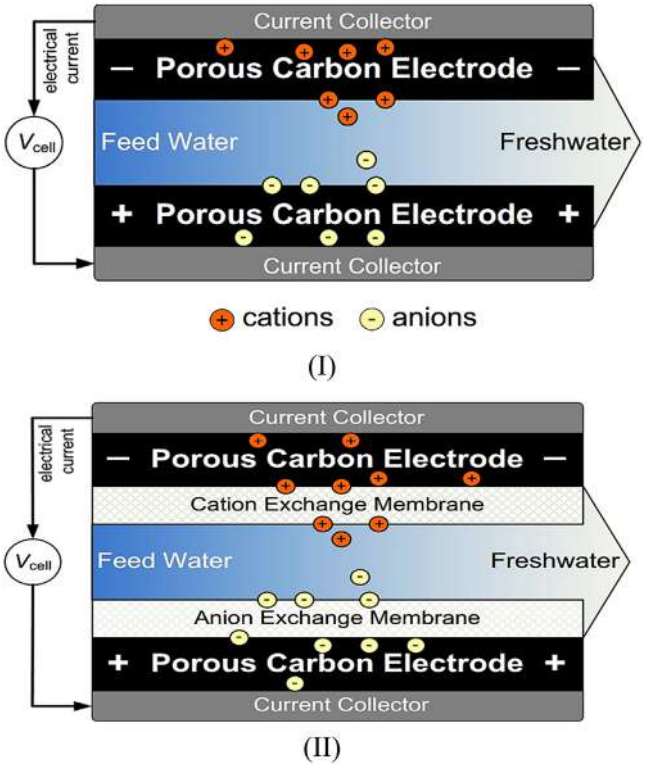

FIGURE 16.11 Schematic design of (A) capacitive deionization (CDI) and (B) membrane capacitive deionization (MCDI) systems (Porada et al., 2013).

This chapter is an overview of the IEMs utilized in electro-driven membrane technologies, including ED, EDR, and MCDI for water treatment. We first introduce different preparation methods of nano-enhanced IEMs and then demonstrate the application of these membranes in water treatment. Finally, the commercialization status and commercial viability are also discussed.

16.2 Preparation of polymer-based nano-enhanced ion-exchange membranes

Polymeric membranes are the most used separation media at the industrial level because they are economically and practically beneficial. Though these membranes are still restricted by several challenges, such as low resistance to fouling and the trade-off relationship between permeability and selectivity, they are the core part of many membrane-based technologies. The quest for developing polymeric membranes with excellent properties is ongoing and many approaches have been conducted to develop new materials and methods for fabricating and modifying polymeric membranes suitable for different applications (Figoli et al., 2017; Jose, Kappen, & Alagar, 2018; Madaeni, Ghaemi, & Rajabi, 2015; Yin & Deng, 2015). As mentioned in the above section, the key components in the ED and their derived technologies are IEMs (as a kind of polymeric membrane) so that their properties considerably determine the efficiency of these processes in a certain application. Although commercially available IEMs have been utilized in industrial applications, their separation performance and price remain unsatisfactory. Therefore, it is crucial to develop low-cost IEMs with high performance. The properties of the polymeric IEMs are tied to several factors, including the density of the polymer network, the hydrophobic or hydrophilic character of the polymer matrix, the morphology of the membrane, and the type and concentration of the fixed charges in the polymer. The most desired properties of the IEMs are high selectivity, low electrical resistance, high mechanical, chemical, and thermal stability, and low production cost (Golubenko & Yaroslavtsev, 2020; Li et al., 2018; Strathman, 2010). To meet these requirements, enormous research activity has been carried out in the last decades. Although the progress in exploring IEMs is prominent, there are still a few challenges that need to be addressed. The extending application of IEMs also stimulates researchers to look for new solutions in order to improve the IEM performances taking into account that a specific application can demand specific properties. Several studies were performed to improve the physicochemical properties of IEMs, which resulted in various methods to modify IEMs. Variations of functional groups, alteration of the cross-linking density, the selection of optimized polymeric matrices, polymer blending, surface modification, and the use of various additives, including nanomaterials, are important strategies to obtain superior IEMs. Among these strategies, the development of advanced membrane materials is a promising solution to achieve the above-mentioned criteria (Hosseini, Madaeni, & Khodabakhshi, 2010b, 2010c; Hosseini, Madaeni, Khodabakhshi, & Zendehnam, 2010d; Khoiruddin, Ariono, Subagjo, & Wenten, 2017; Mofrad, Moheb, Masigol, Sadeghi, & Radmanesh, 2018). Today, nanotechnology has opened the way for producing polymer-based IEMs with excellent physicochemical properties. Nanotechnology refers to the study, analyzation and application of the materials at nanoscale where molecules and atoms behave corresponding to their unique characterization in comparison with the same larger

counterparts. During recent decades, nanotechnology has become one of the most interesting subjects of scientific research due to its great potential in advanced technologies. The significance of nanoscale materials was figured out when researchers found that size affects the physicochemical properties of a material, including its electrical, chemical, optical, and mechanical properties. Thus, nano-particulate substances have attracted tremendous interest thanks to their unparalleled properties. There is a general agreement that the term nanomaterial defines the materials with sizes less than 100 nm in at least one dimension. Generally, these nanoscale materials are classified into different categories depending on their morphology, dimensionality, state, and chemical composition. This classification also depends on their size, ranging from 1−100 nm in at least one dimension (Peters et al., 2016; Saleh, 2020; Singh, Yadav, & Mishra, 2020; Taghipour, Hosseini, & Ashtiani, 2019).

Though the idea of introducing nanomaterials in polymeric membranes is not new, the potential for the development of completely novel and exceptional IEMs by integrating nanomaterials into their structure inspires the imagination of researchers worldwide and has raised high expectations. These nanoscale substances, thanks to their high surface area, high chemical reactivity, excellent mechanical strength, adsorption capability, and cost-effectiveness (Mohapi et al., 2020), have a huge potential to develop IEMs effectively.

Despite the different membrane processes, all nano-enhanced membranes can be categorized as (1) nanomembranes; and (2) nanocomposite membranes (NCMs). The nanomembranes can be further classified into two subcategories, including membranes that contain a bare layer of nanomaterials supported onto a porous substrate and ones that are prepared as a freestanding ordered nanomaterial film. NCMs, in which nanomaterials are incorporated along with a polymer binder, are also subclassified into two categories: (1) thin-film nanocomposite membranes (TFNCMs); and (2) mixed matrix membranes (MMMs). In TFNCMs, engineered nanomaterials are immobilized/entrapped within the top layer of the membrane (in the forms of surface coated TFNCMs or substrate coated TFNCMs, which in the first nanomaterials are coated onto the top active surface of the membrane and in the latter nanomaterials are located on the substrate of the membrane) or in the matrix of the substrate. According to this classification, MMMs are also defined as NCMs comprised of nanosized additives dispersed within the membrane matrix (see Fig. 16.12) (Gohil & Choudhury, 2019).

In MMMs, the nanomaterials are commonly embedded and randomly distributed within the polymer matrix before the formation of the NCM via the phase inversion technique. Certainly, the properties of MMMs are tied to the mixed components, nature of the interactions between organic and inorganic phase, and distribution of the dispersed phase. In preparation of ion-exchange MMMs, various polymers have been elected as a continuous phase because of their flexibility, processing ability, and adjustable IEC (Ion Exchange Capacity); however, inorganic particles are dispersed into the polymer matrices to raise mechanical and thermal stability and also to incorporate desired electrochemical properties. Nanomaterials can be dispersed in polymer matrices of IEMs through mechanical doping of the particles (MM-I) or linking them on polymer backbone through a chemical bond (MM-II) (see Fig. 16.13). On the other side, in the formation of TFNCMs, the nanomaterials can be selectively introduced in/on the polymeric supportive substrate or/and within the selective layer. Hence, TFNCMs generally allow a higher degree of freedom in terms of the NCM design. The properties of NCMs completely differ from their original

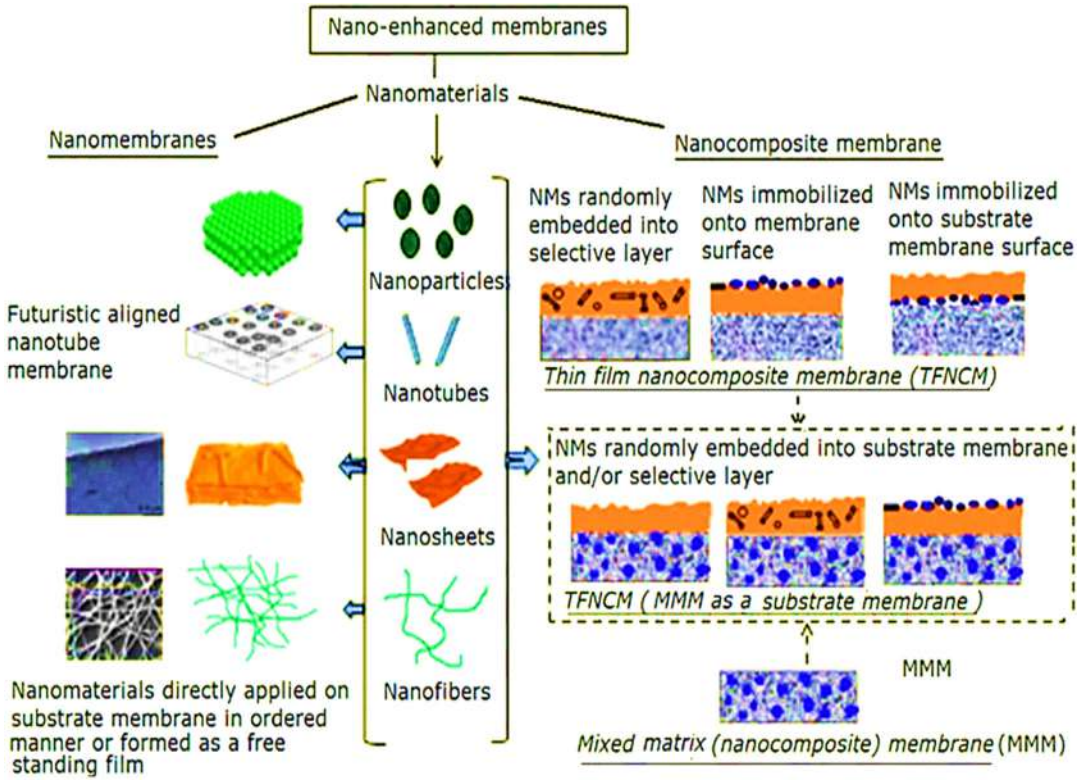

FIGURE 16.12 Schematic illustration of different nano-enhanced membranes (Gohil & Choudhury, 2019).

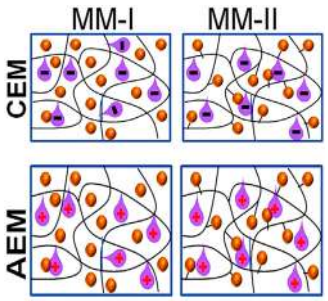

FIGURE 16.13 Ion-exchange mixed matrix membranes (MMMs) with particle doped in the polymer matrix (MM-I) and particles dispersed in polymer matrix via chemical bonding (MM-II) (Ran et al., 2017).

polymeric forms, and a remarkable improvement in separation properties is expected for the resultant membranes. Generally, these nanomaterials own favorable properties such as surface charge, hydrophilicity, and mechanical strength to heighten the performance of the resultant NCMs. These properties are crucial for resolving some intrinsic membrane drawbacks, such as concentration polarization and fouling (Goh, Ong, Ng, & Ismail, 2019; Ran et al., 2017; Yin & Deng, 2015).

In developing an advanced polymer-based nano-enhanced membrane, improving the compatibility of nanomaterials with polymer, restraining the agglomeration of nanomaterials, and suppressing the leaching of nanomaterials from the polymeric matrix are arguably the most important aspects. The weak compatibility of nanomaterials with the polymer backbone that leads to their aggregation in the polymer matrix is the dominant drawback hindering the successful application of these additives. These phenomena bring about the formation of nonselective voids at the interface of the polymer and nanomaterials, which is the Achilles heel of IEMs. The inhomogeneous distribution of nanomaterials also enhances the hardness in fundamentally understanding the structure-property relationship of a nanocomposite IEM. Besides utilizing novel materials having promising properties for IEMs, appropriate preparation techniques are of equal significance to guarantee the quality of resulting IEMs. Consequently, there is an essential need for designing innovative preparation methods for nano-enhanced IEMs to fully exploit the potential of nanomaterials in enhancing the membrane characteristics. Also, due to the trade-off relationship between different properties of IEMs, it is generally hard to fabricate these membranes with an all-around performance. To beat this obstacle and balance different parameters of IEMs, we need novel membrane materials and strategies to fine-tune their properties for providing the following functional aspects (Jashni & Hosseini, 2020a; Li et al., 2017; Ran et al., 2017; Yin & Deng, 2015):

- Increasing selectivity for selective separation of different ions
- Enhancing ionic permeability
- Improving antifouling and antimicrobial properties
- Decreasing electrical resistance
- Increasing chemical, thermal, and mechanical stability
- Extending application of membranes for diverse separation processes

Till now, a wide range of methods such as melt mixing, blending, and in-situ techniques have been employed for the preparation of nano-enhanced IEMs (Alabi et al., 2018). Note that, although the incorporation of particles inside the membrane structure can improve its performance, the inaccessibility of ion-exchange resin particles may also occur. Therefore, in all techniques, an optimal content of nanomaterials should be determined.

Due to the large extent of the preparation methods, in this chapter, the main emphasis is put on: (1) the blending manner as the most frequently used technique for preparation of nano-enhanced IEMs and (2) the in situ method as the established technique for the next generating nano-enhanced membranes with molecular-level design.

16.2.1 Blending

Solution blending is a highly recognized method in fabricating polymeric nanocomposites and is thus commonly used in synthesizing nano-enhanced IEMs. The blending manner that is based on the solubility of the polymer and a suitable solvent comprises the dispersion of nanomaterials in polymer solutions and subsequent casting of the film. The main advantages of this technique are its simplicity and easy reproducibility. It is considered the most frequently employed method due to the availability of solvents that readily

dissolve any polymer type. In this manner, a good solubility of the polymer in the selected solvent and excellent dispersion of the nanomaterials in the polymer solution are needed for obtaining a well-dispersed composite film (Alabi et al., 2018).

In our group, nano-enhanced IEMs prepared by the blending manner have been widely studied. These nanosized additives that were used for the preparation of MMMs include (1) carbon-based nanomaterials such as multiwalled carbon nanotubes (MWCNTs) (Hosseini et al., 2013), activated carbon (AC) (Hosseini, Madaeni, & Khodabakhshi, 2010a), graphene oxide (GO) (Hosseini, Jashni, Habibi, Nemati, & Van der Bruggen, 2017b), carbon nanofibers (CNFs) (Jashni et al., 2019), and graphite (Hosseini, Chehreh, Jashni, & Shen, 2020b); (2) nanosized metal oxides such as iron-nickel oxide (Fe_2NiO_4) (Hosseini, Madaeni, Heidari, & Amirimehr, 2012), iron oxide (Fe_3O_4) (Hosseini, Askari, Koranian, Madaeni, & Moghadassi, 2014a), aluminum oxide (Al_2O_3) (Hosseini et al., 2014b), zinc oxide (ZnO) (Parvizian, Hosseini, Hamidi, Madaeni, & Moghadassi, 2014), titanium dioxide (TiO_2) (Hosseini et al., 2015), barium ferrite/copper oxide ($BaFe_{12}O_{19}$/CuO) (Hosseini, Rafiei, Salabat, & Ahmadi, 2020c), and cobalt ferrite ($CoFe_2O_4$) (Hosseini et al., 2019b); (3) silicate-based nanomaterials such as zeolite (Hosseini, Rafiei, Hamidi, Moghadassi, & Madaeni, 2014d), nanosized metal-organic complex such as bis(8-hydroxyquinoline)zinc(II) (ZnQ_2) (Hosseini, Jashni, Jafari, Van der Bruggen, & Shahedi, 2018b), and tris(8-hydroxyquinoline)aluminum (AlQ_3) (Hosseini et al., 2019a); (4) composite nanomaterials such as polyaniline-co-multiwalled carbon nanotubes (PANI/MWCNTs) (Hosseini, Jeddi, Nemati, Madaeni, & Moghadassi, 2014c), polyacrylic acid-co-iron oxide (PAA/Fe_3O_4) (Nemati & Hosseini, 2015), polyaniline-co-graphene oxide (PANI/GO) (Hosseini, Jashni, Habibi, & Van der Bruggen, 2018a), poly(N-vinylpyrrolidone)-co-iron oxide (PVP/Fe_3O_4) (Jashni et al., 2020c); and (5) a hybrid system such as the simultaneous utilizing GO and TiO_2 in different weight ratios (Hosseini, Jashni, Amani, & Van der Bruggen, 2017a). In all cases, an improvement in the electrochemical properties of fabricated MMMs was observed.

16.2.2 In situ technique

In situ technique has been broadly utilized in the last decades for the preparation of NCMs with excellent dispersion and distribution of nanomaterials. In view of molecular-level design, in situ technique, permitting the in situ generations of nanomaterials into/onto the polymeric matrix, undoubtedly offers a route for the development of the next generation of nano-enhanced membranes. Under this in situ design platform, researchers discovered that the fabrication and functions of nano-enhanced membranes could be deliberately designed to aim at a distinctly defined problem. The rationale of the in situ technique for ameliorating the membrane efficiency is based on improved additive dispersion and polymer-additive interaction through the molecular-level mixing of monomers, nanomaterial/nanomaterial precursors, and solvent in a particular system. Interpenetrating networks between the nanomaterials and polymeric matrix formed in the in situ preparation process raises the compatibility between constituent components and constructs strong interfacial interactions between phases (Grothe, Kaskel, & Leuteritz, 2012; Li et al., 2017, 2013, 2014). The interactions between the nanomaterials/nanomaterial precursors and the monomers are of prime significance as they adjust the

particle size distribution, stabilize the interaction strength, and prevent nanomaterials release. The desired solubility of nanomaterials/nanomaterial precursors in the monomer solution brings about adequate interaction with the polymer chain, thereby ameliorating the nanomaterials or their precursors' dispersion in the reaction medium. Thus, in this system, a proper selection of constituent components plays a substantial role in regulating the quality of these interactions. In general, in the in situ preparation technique, the formation step of nanomaterials can be subject to the creative combination of their synthesis mechanism with multiple fabrication processes for the membrane. It is worth mentioning that the concept in situ implies the synergetic integration of fabrication manners for nanomaterials and the membrane preparation process and not only to the simultaneous or local formation of nanomaterials in a composite membrane system. Generally, in situ formations of nanomaterials can happen in one of three steps: (1) within the casting solution; (2) during the solidification of the casting solution; and (3) after the solidification of the casting solution (Grothe et al., 2012; Li et al., 2017). In situ preparation of nanomaterials in polymeric membrane systems can be carried out with different strategies such as in situ reduction, in situ sol-gel, in situ polymerization, and so forth. The fabrication strategy of in situ reduction is based on the in situ reduction of metal salts from solutions or suspensions in the presence of a polymer or of mononuclear metal complexes bonded to the polymer. This method may be attractive, particularly for manufacturing membranes with Ag, Fe, Cu, and Au nanoparticles. The sol-gel process can be considered a two-step network forming process, the first step consisting of the hydrolysis of precursor and the second being a polycondensation reaction. The most common precursors applied are either inorganic metal salts or metal-organic species like a metal alkoxide or acetylacetonate (Alabi et al., 2018; Grothe et al., 2012; Li et al., 2017; Ramesh, Sivasamy, Rhee, Park, & Hui, 2015; Vona et al., 2007). In a typical in situ polymerization process, the nanomaterials/nanomaterial precursors are also dispersed in a monomer or monomer solution, and subsequent polymerization of the monomer through standard polymerization manners causes NCMs. The polymerization step that is typically induced by the diffusion of a suitable initiator or by applying heat or UV irradiation is the distinction between in situ polymerization and solution blending. In the traditional preparation of IEMs, a large amount of organic solvent used during both the reaction and membrane formation processes will bring toxicity risks to the environment. In situ polymerization is a solvent-free strategy that can overcome the obstacles encountered in solvent-aided polymerization. This technique can also be applied for the fabrication of ion-exchange NCMs, with polymers being appropriate neither for melt processing due to low thermal stability nor for solution blending owing to insolubility in any solvent (Grothe et al., 2012; Li et al., 2017, 2014, 2013; Ran et al., 2017). Various approaches have been implemented to fabricate nano-enhanced IEMs with superior performance via in situ preparation method. In our group, in situ polymerization of PAA and MWCNTs was employed for surface modification of a polyvinyl chloride-based heterogeneous CEM by mixing MWCNTs with hydrophilic acrylic acid monomer. Results showed that utilizing this strategy resulted in an improvement in the separation performance of the fabricated membranes (Moghadassi, Koranian, Hosseini, Askari, & Madaeni, 2014). Also, Hao and co-workers modified a commercial AEM with a sandwich-like architecture composed of upper/bottom bi-layers of polydopamine (PDA) and alternating bi-layers of poly (sodium 4-styrene sulfonate) (PSS)/hydroxypropyl-trimethyl ammonium chloride chitosan-nanosilver particles (HACC-AgNP). By this strategy, the chloride/sulfate selectivity of the resultant membranes reached 5.1, which

was more than that of the unmodified commercial one (Hao et al., 2018). Besides, Zhang et al. (2019) coated a PDA layer on the surface of pristine AEMs, followed by in situ reduction of Ag without adding any extra reductant. Finally, two 5-diaminobenzene sulfonic acid (DSA) was grafted onto the PDA layer. The resultant samples showed an improved permselectivity and remarkable inhibition effect on *Escherichia coli*. Zhu et al. (2019) also fabricated three-dimensional stable CEM by in situ synthesis of silver nanoparticles. Results exhibited that this strategy led to an enhanced mechanical, electrochemical, and antibacterial performance.

Generally, by utilizing the above-mentioned modification methods, the electrochemical characteristics of IEMs can be improved. Furthermore, the methods provide the possibility to produce nano-enhanced IEMs with specific characteristics such as high monovalent selectivity, antifouling property, antibacterial property, and so on.

16.3 Analysis of different ion-exchange membranes for water treatment

As stated in the introduction, water scarcity and the problems associated with the lack of clean water have become the most significant environmental concerns facing today's world. Since seawater holds above ~97% of water resources on the globe, the potential of desalination for solving these challenges is staggering (Jashni & Hosseini, 2020a, 2020b). Over the years, different desalination methods have been studied and developed and among them, ED and MCDI, as electrochemical water treatment processes, are particularly attractive due to their inherent advantages. These two systems also have great potentials for dangerous pollutant removal from water, especially heavy metals (Bales, Lian, Fletcher, Wang, & Waite, 2021; Chen, Wang, Liu, & Zhu, 2019; Dong et al., 2019; Jashni et al., 2020c, 2019; Lee et al., 2019; Yang et al., 2020). It is a well-established fact that toxic heavy metals are major contaminants present in water which possesses a serious menace to human health and the aquatic ecosystem. These ions are toxic even at very low concentrations and can cause serious biological dangers (Jashni et al., 2020c).

The environmental legislation on heavy metals is increasingly strict, whereas the global demands for heavy metals continue to increase owing to the rapid development of modern industrial activities. These pollutants may come from various industrial sources such as the manufacture of pesticides, alloys, batteries, electroplating, textile, mining, and dyes (Jashni & Hosseini, 2020b). Since the IEMs are the key elements in these systems, the need for the development of high-performance IEMs is crucial. To obtain superior IEMs for heavy metal ions removal, various strategies have been employed. In this regard, our group reported that incorporation of PANI/GO composite nanoplates in polyvinylchloride-based heterogeneous CEMs caused an increment in the capacity of prepared cation-exchange MMMs for Pb^{2+} ions removal (Hosseini et al., 2018a).

Similarly, L-Cyst as an amino acid containing three functional groups was utilized as an additive in the preparation of cation-exchange MMMs. These prepared IEMs showed good ability in Pb^{2+} ions removal from water solution. Fig. 16.14 demonstrates the molecular electrostatic potential (MEP) of L-Cyst, and also EDX spectrum and elemental mapping analysis of the membrane surface after Pb^{2+} ion removal study (Jashni & Hosseini, 2020a). Introducing $CoFe_2O_4$ as superior magnetic nanoparticles (Hosseini et al., 2019b) and 8-hydroxyquinoline (8-HQ) as a chelating agent (Jashni & Hosseini, 2020b) in polyvinyl chloride-based heterogeneous CEM also led to the

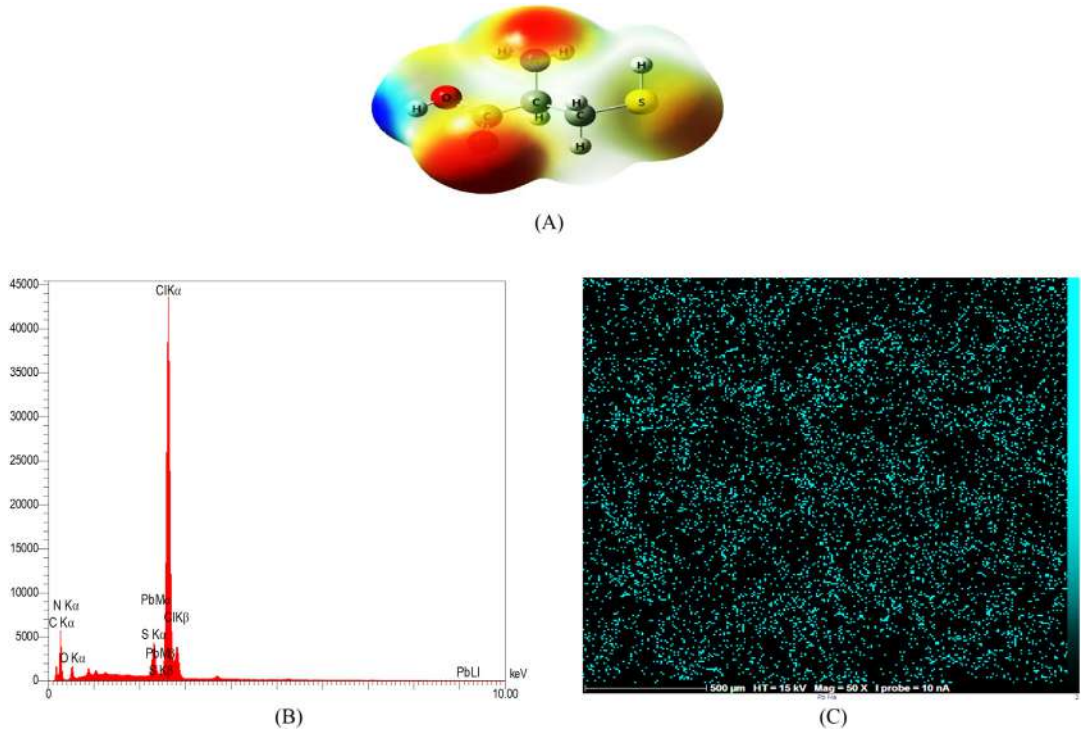

FIGURE 16.14 (A) Molecular electrostatic potential of L-Cyst, (B) energy dispersive using X-ray (EDX) spectrum, and (C) elemental mapping analysis of the membrane surface containing L-Cyst after Pb^{2+} ion removal study (Jashni & Hosseini, 2020a).

enhancement in dialytic rate for chromium ions removal. MEP of 8-HQ, the elemental mapping, EDX spectrum analysis of the membrane surface after chromium ions removal study, and the most possible binding mechanism of chromium ion onto 8-HQ molecule are illustrated in Fig. 16.15. Layer-by-layer (LbL) CEMs were also fabricated by our group and were employed in the separation of heavy metal ions from water solution. ED experiment showed good ability in heavy metal ions removal for LbL membrane that follows ($Cu^{2+} > Ni^{2+} > Pb^{2+}$) sequence. EDX analysis also showed competitive adsorption for heavy metal ions on the LbL membrane ($Pb^{2+} > Cu^{2+} \geq Ni^{2+}$). EDX analysis, digital photo, and FESEM image of used LbL membrane are shown in Fig. 16.16 (Hosseini et al., 2020a).

16.4 Commercialization status and commercial viability

The fundamental studies of IEMs and electro-membrane processes began over sixty years ago, and continuous research and ongoing progress have steadily broadened IEMs' characteristics and application range (Parnamae et al., 2021). These

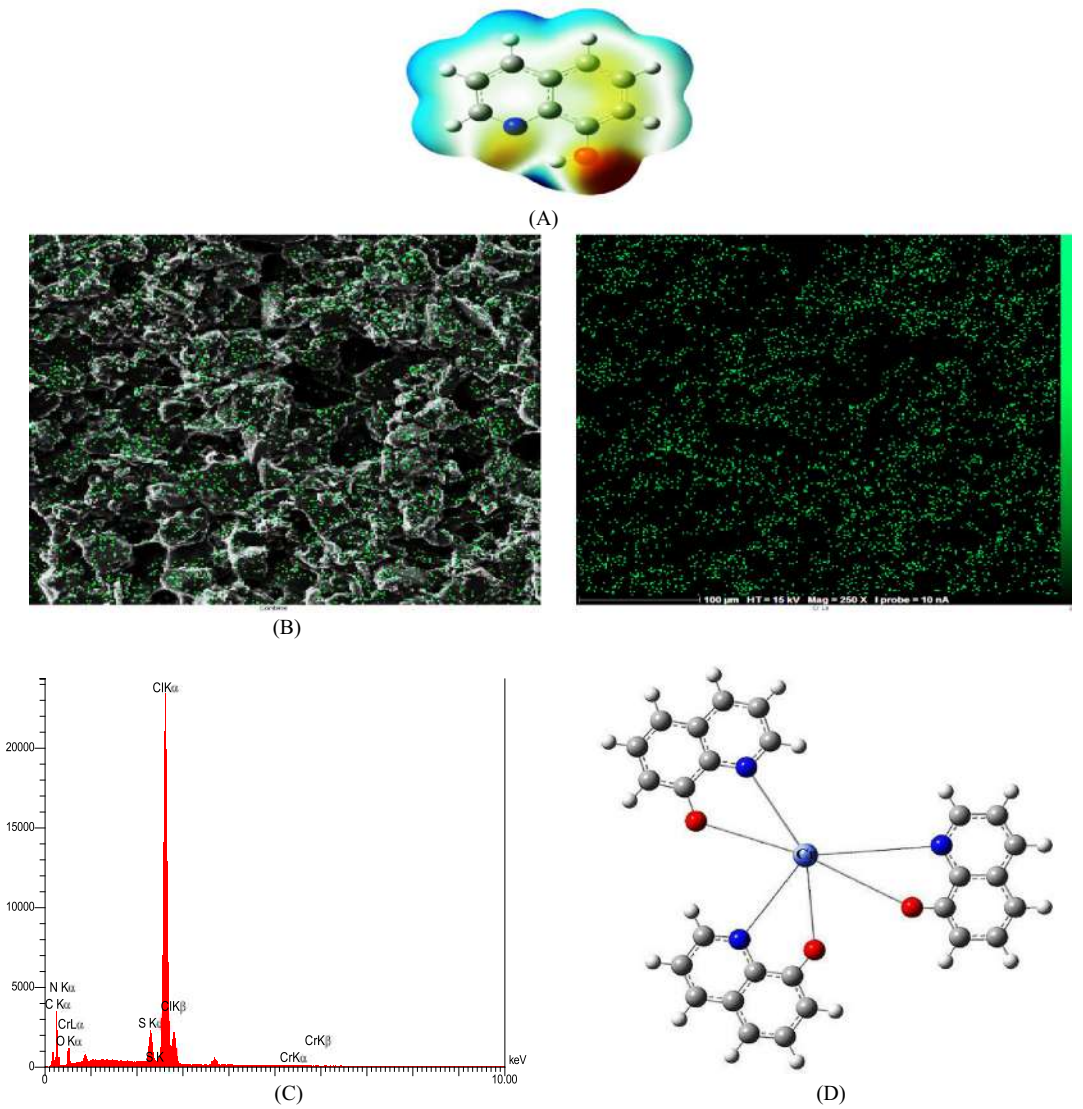

FIGURE 16.15 (A) Molecular electrostatic potential of 8-HQ, (B) the elemental mapping, (C) EDX spectrum analysis of the membrane surface containing 8-HQ after chromium ions removal study, and (D) the most possible binding mechanism of chromium ion onto 8-HQ molecule (Jashni & Hosseini, 2020b).

advancements have paved the way for the commercialization of IEMs. At present, ASTOM Co., Asahi Glass Co., Ltd. in Japan, FuMa-Tech GmbH in Germany, and DuPont Co. in America account for abundant market shares of IEMs. Fumasep IEMs yielded by FuMa-Tech GmbH, Selemion IEMs yielded by Asahi Glass Co., Ltd., and

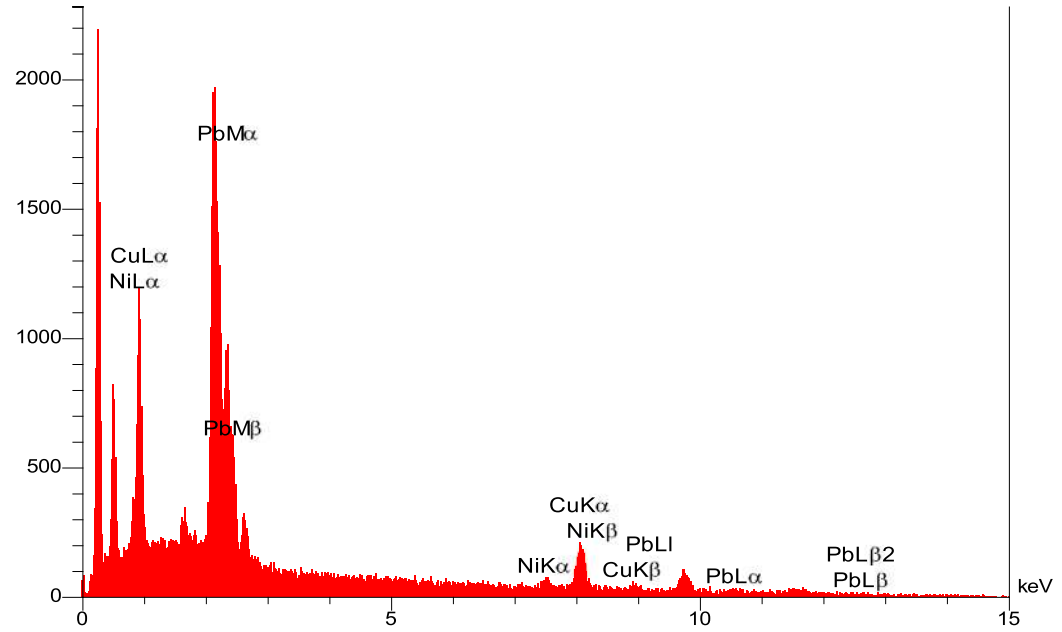

(A)

(B)

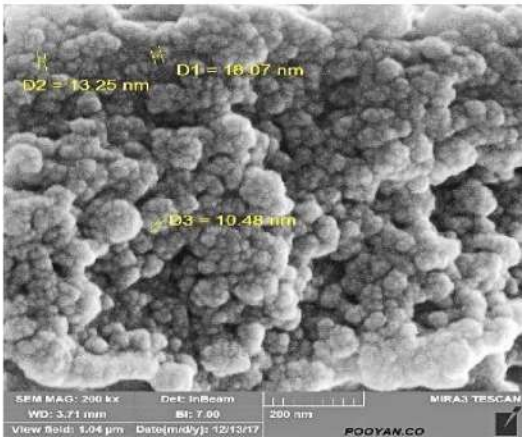

(C)

FIGURE 16.16 (A) EDX analysis, (B) digital photo, and (C) field emission scanning electron microscopy (FESEM) image of used layer-by-layer (LbL) membrane: adsorption/interaction of heavy metal ions with LbL (Hosseini et al., 2020a).

NEOSEPTA IEMs yielded by ASTOM Co., that represent low electrical resistance, high ion selectivity, and sufficient chemical stability, have been broadly employed in electrochemical-related technologies. Particularly, Nafion perfluorinated CEMs produced by DuPont Co. belong to highly efficient fuel cell membranes, promoting the commercialization process of fuel cells (Ran et al., 2017). The focus of the membrane research community is put on designing and creating reliable membranes that are entirely appropriate in commercial environments. The convergence between nanotechnology and membrane science offers leapfrogging opportunities to develop a new generation of IEMs endowed with suitable characteristics, which is an attractive proposition to the industry. To date, significant attempts have been made in establishing innovative nanomaterials and designing novel fabrication methods to improve the large-scale utilization of nanocomposite IEMs. However, key issues such as the nanomaterials' cost-effectiveness, potential environmental and human risks, nanomaterials efficiency, the stability and production scalability of these membranes should be considered for their future development and commercialization. Therefore, extra efforts should be carried out to resolve these limitations and close the gaps between fundamental research and practical application (Alabi et al., 2018; Goh et al., 2016; Li et al., 2017; Ran et al., 2017).

16.5 Summary and future directions

The global research on IEMs at a fundamental and applied level is intensifying because of their great potential in advanced technologies. Though the progress in exploring IEMs is prominent, further research is still needed to develop novel membranes that could boost new applications. Advancement in nanotechnology plays a vital role in developing membrane materials with novel functionalities and superior characteristics that can effectively be employed for the design and fabrication of nano-enhanced IEMs. These NCMs have become increasingly important due to their extraordinary properties, which arise from the synergism between the properties of both organic and inorganic components. Though nano-enhanced IEMs enable water/wastewater treatment processes with great promise in laboratory studies, substantial research is still required before they can be moved from the laboratory to the industry. Besides appropriate preparation techniques and utilizing novel materials having promising properties for IEMs, understanding well the underlying transportation mechanisms and performance details of these membranes are of equal significance to finding the right solution in order to solve their challenges. To date, most studies dealing with IEMs have been focused on expanding various fabrication methods, exploring promising materials, and developing a wide variety of applications. Nevertheless, research on the IEMs' performance details is not fully mature, and there are several stages in which improvements are still necessary. A more comprehensive and coherent understanding of the complex phenomena occurring in the IEMs not only provides fundamental knowledge for the progress of IEMs but also opens up the opportunity to address IEMs' challenges. Therefore, much endeavor is needed to combine theoretical, experimental, and simulation data for a comprehensive understanding of the IEM phenomena.

References

Ahmed, F. E., Hashaikeh, R., & Hilal, N. (2020). Hybrid technologies: The future of energy efficient desalination—A review. *Desalination*, *495*, 114659. Available from https://doi.org/10.1016/j.desal.2020.114659.

Alabi, A., Alhajaj, A., Cseri, L., Szekely, G., Budd, P., & Zou, L. (2018). Review of nanomaterials-assisted ion exchange membranes for electromembrane desalination. *NPJ Clean Water*, *1*, 10. Available from https://doi.org/10.1038/s41545-018-0009-7.

Ariono, D., Khoiruddin., Subagjo., & Wenten, I. G. (2017). Heterogeneous structure and its effect on properties and electrochemical behavior of ion-exchange membrane. *Materials Research Express*, *4*, 024006. Available from https://doi.org/10.1088/2053-1591/aa5cd4.

Bales, C., Lian, B., Fletcher, J., Wang, Y., & Waite, T. D. (2021). Site specific assessment of the viability of membrane capacitive deionization (mCDI) in desalination of brackish groundwaters for selected crop watering. *Desalination*, *502*, 114913. Available from https://doi.org/10.1016/j.desal.2020.114913.

Bazinet, L., & Geoffroy, T. R. (2020). Electrodialytic processes: Market overview, membrane phenomena, recent developments and sustainable strategies. *Membranes*, *10*, 221. Available from https://doi.org/10.3390/membranes10090221.

Bdiri, M., Dammak, L., Larchet, C., Hellal, F., Porozhnyy, M., Nevakshenova, E., ... Nikonenko, V. (2019). Characterization and cleaning of anion-exchange membranes used in electrodialysis of polyphenol-containing food industry solutions; comparison with cation-exchange membranes. *Separation and Purification Technology*, *210*, 636–650. Available from https://doi.org/10.1016/j.seppur.2018.08.044.

Campione, A., Cipollina, A., Toet, E., Gurreri, L., David, I., Bogle, L., & Micale, G. (2020). Water desalination by capacitive electrodialysis: Experiments and modelling. *Desalination*, *473*, 114150. Available from https://doi.org/10.1016/j.desal.2019.114150.

Campione, A., Gurreri, L., Ciofalo, M., Micale, G., Tamburini, A., & Cipollina, A. (2018). Electrodialysis for water desalination: A critical assessment of recent developments on process fundamentals, models and applications. *Desalination*, *434*, 121–160. Available from https://doi.org/10.1016/j.desal.2017.12.044.

Chen, L., Wang, Ch, Liu, Sh, & Zhu, L. (2019). Investigation of adsorption/desorption behavior of Cr(VI) at the presence of inorganic and organic substance in membrane capacitive deionization (MCDI). *Journal of Environmental Science*, *78*, 303–314. Available from https://doi.org/10.1016/j.jes.2018.11.005.

Dong, Q., Guo, X., Huang, X., Liu, L., Tallon, R., Taylor, B., & Chen, J. (2019). Selective removal of lead ions through capacitive deionization: Role of ion-exchange membrane. *Chemical Engineering Journal*, *361*, 1535–1542. Available from https://doi.org/10.1016/j.cej.2018.10.208.

Epsztein, R., Duchanois, R. M., Ritt, C. L., Noy, A., & Elimelech, M. (2020). Towards single-species selectivity of membranes with subnanometre pores. *Nature Nanotechnology*, *15*, 426–436. Available from https://doi.org/10.1038/s41565-020-0713-6.

Figoli, A., Marino, T., Galiano, F., Dorraji, S. S., Di Nicolo, E., & He, T. (2017). Sustainable route in preparation of polymeric membranes. In A. Figoli, & A. Criscuoli (Eds.), *Sustainable membrane technology for water and wastewater treatment* (pp. 97–120). Singapore: Green Chemistry and Sustainable Technology, Springer.

Goh, P. S., Matsuura, T., Ismail, A. F., & Hilal, N. (2016). Recent trends in membranes and membrane processes for desalination. *Desalination*, *391*, 43–60. Available from https://doi.org/10.1016/j.desal.2015.12.016.

Goh, P. S., Ong, C. S., Ng, B. C., & Ismail, A. F. (2019). Application of emerging nanomaterials for oily wastewater treatment. In A. Ahsan, & A. F. Ismail (Eds.), *Nanotechnology in water and wastewater treatment* (pp. 101–113). Elsevier.

Gohil, J. M., & Choudhury, R. R. (2019). Introduction to nanostructured and nano-enhanced polymeric membranes: Preparation, function, and application for water purification. In S. Thomas, D. Pasquini, Sh. Y. Leo, & D. A. Gopakumar (Eds.), *Nanoscale materials in water purification* (pp. 22–57). Elsevier.

Golubenko, D., & Yaroslavtsev, A. (2020). Development of surface-sulfonated graft anion-exchange membranes with monovalent ion selectivity and antifouling properties for electromembrane processes. *Journal of Membrane Science*, *612*, 118408. Available from https://doi.org/10.1016/j.memsci.2020.118408.

Grothe, J., Kaskel, S., & Leuteritz, A. (2012). Nanocomposites and Hybrid Materials. *Polymer Science: A Comprehensive Reference*, *8*, 177–209. Available from https://doi.org/10.1016/B978-0-444-53349-4.00206-5.

Gurreri, L., Tamburini, A., Cipollina, A., & Micale, G. (2020). Electrodialysis applications in wastewater treatment for environmental protection and resources recovery: A systematic review on progress and perspectives. *Membranes*, *10*, 146. Available from https://doi.org/10.3390/membranes10070146.

Hao, L., Liao, J., Jiang, Y., Zhu, J., Li, J., Zhao, Y., ... Shen, J. (2018). Sandwich-like structure modified anion exchange membrane with enhanced monovalent selectivity and fouling resistance. *Journal of Membrane Science*, *556*, 98–106. Available from https://doi.org/10.1016/j.memsci.2018.03.082.

Hosseini, S. M., Ahmadi, A., Van der Bruggen, B., Jafari, M. R., Shahedi, Z., & Nemati, M. (2019a). New approach to adapting electrochemical properties of cation-exchange membrane by incorporating tris(8-hydroxyquinoline) aluminum nanoparticles. *Ionics*, *25*, 1147–1156. Available from https://doi.org/10.1007/s11581-018-2770-5.

Hosseini, S. M., Alibakhshi, H., Jashni, E., Parvizian, F., Shen, J. N., Taheri, M., ... Rafiei, N. (2020a). A novel layer-by-layer heterogeneous cation exchange membrane for heavy metal ions removal from water. *Journal of Hazardous Materials*, *381*, 120884. Available from https://doi.org/10.1016/j.jhazmat.2019.120884.

Hosseini, S. M., Askari, M., Koranian, P., Madaeni, S. S., & Moghadassi, A. R. (2014a). Fabrication and electrochemical characterization of PVC based electrodialysis heterogeneous ion exchange membranes filled with Fe_3O_4 nanoparticles. *Journal of Industrial and Engineering Chemistry*, *20*, 2510–2520. Available from https://doi.org/10.1016/j.jiec.2013.10.034.

Hosseini, S. M., Chehreh, M., Jashni, E., & Shen, J. N. (2020b). Electrochemical characterization of electrodialysis cation exchange membrane incorporated with graphite nanoparticles for deionization. *Ionics*, *26*, 1525–1535. Available from https://doi.org/10.1007/s11581-019-03334-5.

Hosseini, S. M., Gholami, A., Koranian, P., Nemati, M., Madaeni, S. S., & Moghadassi, A. R. (2014b). Electrochemical characterization of mixed matrix heterogeneous cation exchange membrane modified by aluminum oxide nanoparticles: Mono/bivalent ionic transportation. *Journal of the Taiwan Institute of Chemical Engineers*, *45*, 1241–1248. Available from https://doi.org/10.1016/j.jtice.2014.01.011.

Hosseini, S. M., Jashni, E., Amani, S., & Van der Bruggen, B. (2017a). Tailoring the electrochemical properties of ED ion exchange membranes based on the synergism of TiO_2 nanoparticles-co-GO nanoplates. *Journal of Colloid and Interface Science*, *505*, 763–775. Available from https://doi.org/10.1016/j.jcis.2017.06.045.

Hosseini, S. M., Jashni, E., Habibi, M., Nemati, M., & Van der Bruggen, B. (2017b). Evaluating the ion transport characteristics of novel graphene oxide nanoplates entrapped mixed matrix cation exchange membranes in water deionization. *Journal of Membrane Science*, *541*, 641–652. Available from https://doi.org/10.1016/j.memsci.2017.07.022.

Hosseini, S. M., Jashni, E., Habibi, M., & Van der Bruggen, B. (2018a). Fabrication of novel electrodialysis heterogeneous ion exchange membrane by incorporating PANI/GO functionalized composite nanoplates. *Ionics*, *24*, 1789–1801. Available from https://doi.org/10.1007/s11581-017-2319-z.

Hosseini, S. M., Jashni, E., Jafari, M. R., Van der Bruggen, B., & Shahedi, Z. (2018b). Nanocomposite polyvinyl chloride-based heterogeneous cation exchange membrane prepared by synthesized ZnQ_2 nanoparticles: Ionic behavior and morphological characterization. *Journal of Membrane Science*, *560*, 1–10. Available from https://doi.org/10.1016/j.memsci.2018.05.007.

Hosseini, S. M., Jeddi, F., Nemati, M., Madaeni, S. S., & Moghadassi, A. R. (2014c). Electrodialysis heterogeneous anion exchange membrane modified by PANI/MWCNT composite nanoparticles: Preparation, characterization and ionic transport property in desalination. *Desalination*, *341*, 107–114. Available from https://doi.org/10.1016/j.desal.2014.03.001.

Hosseini, S. M., Koranian, P., Gholami, A., Madaeni, S. S., Moghadassi, A. R., Sakinejad, P., & Khodabakhshi, A. R. (2013). Fabrication of mixed matrix heterogeneous ion exchange membrane by multiwalled carbon nanotubes: Electrochemical characterization and transport properties of mon and bivalent cations. *Desalination*, *329*, 62–67. Available from https://doi.org/10.1016/j.desal.2013.09.007.

Hosseini, S. M., Madaeni, S. S., Heidari, A. R., & Amirimehr, A. (2012). Preparation and characterization of ion-selective polyvinyl chloride based heterogeneous cation exchange membrane modified by magnetic iron-nickel oxide nanoplates. *Desalination*, *284*, 191–199. Available from https://doi.org/10.1016/j.desal.2011.08.057.

Hosseini, S. M., Madaeni, S. S., & Khodabakhshi, A. R. (2010a). Preparation and characterization of ABS/HIPS heterogeneous anion exchange membrane filled with activated carbon. *Applied Polymer Science*, *118*, 3371–3383. Available from https://doi.org/10.1002/app.32369.

Hosseini, S. M., Madaeni, S. S., & Khodabakhshi, A. R. (2010b). Preparation and characterization of ABS/HIPS heterogeneous cation exchange membranes with various blend ratios of polymer binder. *Journal of Membrane Science*, *351*, 178–188. Available from https://doi.org/10.1016/j.memsci.2010.01.045.

Hosseini, S. M., Madaeni, S. S., & Khodabakhshi, A. R. (2010c). Preparation and characterization of PC/SBR heterogeneous cation exchange membrane filled with carbon nano-tubes. *Journal of Membrane Science*, *362*, 550–559. Available from https://doi.org/10.1016/j.memsci.2010.07.015.

Hosseini, S. M., Madaeni, S. S., Khodabakhshi, A. R., & Zendehnam, A. (2010d). Preparation and surface modification of PVC/SBR heterogeneous cation exchange membrane with silver nanoparticles by plasma treatment. *Journal of Membrane Science*, *365*, 438–446. Available from https://doi.org/10.1016/j.memsci.2010.09.043.

Hosseini, S. M., Nemati, M., Jeddi, F., Salehi, E., Khodabakhshi, A. R., & Madaeni, S. S. (2015). Fabrication of mixed matrix heterogeneous cation exchange membrane modified by titanium dioxide nanoparticles: Mono/bivalent ionic transport property in desalination. *Desalination*, *359*, 167–175. Available from https://doi.org/10.1016/j.desal.2014.12.043.

Hosseini, S. M., Rafiei, N., Salabat, A., & Ahmadi, A. (2020c). Fabrication of new type of barium ferrite/copper oxide composite nanoparticles blended polyvinyl chloride based heterogeneous ion exchange membrane. *Arabian Journal of Chemistry*, *13*, 2470–2482. Available from https://doi.org/10.1016/j.arabjc.2018.06.001.

Hosseini, S. M., Rafiei, S., Hamidi, A. R., Moghadassi, A. R., & Madaeni, S. S. (2014d). Preparation and electrochemical characterization of mixed matrix heterogeneous cation exchange membranes filled with zeolite nanoparticles: Ionic transport property in desalination. *Desalination*, *351*, 138–144. Available from https://doi.org/10.1016/j.desal.2014.07.036.

Hosseini, S. M., Sohrabnejad, S., Nabiyouni, G., Jashni, E., Van der Bruggen, B., & Ahmadi, A. (2019b). Magnetic cation exchange membrane incorporated with cobalt ferrite nanoparticles for chromium ions removal via electrodialysis. *Journal of Membrane Science*, *583*, 292–300. Available from https://doi.org/10.1016/j.memsci.2019.04.069.

Jashni, E., & Hosseini, S. M. (2020a). High selective heterogeneous cation exchange membrane modified by L-cysteine with enhanced electrochemical performance. *Ionics*, *26*, 875–894. Available from https://doi.org/10.1007/s11581-019-03253-5.

Jashni, E., & Hosseini, S. M. (2020b). Promoting the electrochemical and separation properties of heterogeneous cation exchange membrane by embedding 8-hydroxyquinoline ligand: Chromium ions removal. *Separation and Purification Technology*, *234*, 116118. Available from https://doi.org/10.1016/j.seppur.2019.116118.

Jashni, E., Hosseini, S. M., & Shen, J. (2020c). A new approach to providing heterogeneous cation-exchange membrane with enhanced electrochemical and desalination performance by incorporation of Fe_3O_4/PVP composite nanoparticles. *Ionics*, *26*, 861–874. Available from https://doi.org/10.1007/s11581-019-03218-8.

Jashni, E., Hosseini, S. M., Shen, J. N., & Van der Bruggen, B. (2019). Electrochemical characterization of mixed matrix electrodialysis cation exchange membrane incorporated with carbon nanofibers for desalination. *Ionics*, *25*, 5595–5610. Available from https://doi.org/10.1007/s11581-019-03068-4.

Jose, A. J., Kappen, J., & Alagar, M. (2018). Polymeric membranes: Classification, preparation, structure physicochemical, and transport mechanisms. In S. Thomas, P. Balakrishnan, & M. S. Sreekala (Eds.), *Fundamental biomaterials: Polymers* (pp. 21–35). Woodhead Publishing Series in Biomaterials.

Khoiruddin., Ariono, D., Subagjo., & Wenten, I. G. (2017). Surface modification of ion-exchange membranes: methods, characteristics, and performance. *Journal of Applied Polymer Science*, *134*, 45540. Available from https://doi.org/10.1002/app.45540.

Lee, M., Fan, Ch, Sh., Chen, Y. W., Chang, K. Ch, Chiueh, P. T., & Hou, Ch. H. (2019). Membrane capacitive deionization for low-salinity desalination in the reclamation of domestic wastewater effluents. *Chemosphere*, *235*, 413–422. Available from https://doi.org/10.1016/j.chemosphere.2019.06.190.

Li, J., Yuan, Sh, Wang, J., Zhu, J., Shen, J., & Van der Bruggen, B. (2018). Mussel-inspired modification of ion exchange membrane for monovalent separation. *Journal of Membrane Science*, *553*, 139–150. Available from https://doi.org/10.1016/j.memsci.2018.02.046.

Li, X., Fang, X., Pang, R., Li, J., Sun, X., Shen, J., ... Wang, L. (2014). Self-assembly of TiO_2 nanoparticles around the pores of PES ultrafiltration membrane for mitigating organic fouling. *Journal of Membrane Science*, *467*, 226–235. Available from https://doi.org/10.1016/j.memsci.2014.05.036.

Li, X., Pang, R., Li, J., Sun, X., Shen, J., Han, W., & Wang, L. (2013). In situ formation of nanoparticles in PVDF ultrafiltration membrane to mitigate organic and bacterial fouling. *Desalination*, *324*, 48–56. Available from https://doi.org/10.1016/j.desal.2013.05.021.

Li, X., Sotto, A., Li, J., & Van der Bruggen, B. (2017). Progress and perspectives for synthesis of sustainable antifouling composite membranes containing in situ generated nanoparticles. *Journal of Membrane Science*, *524*, 502–528. Available from https://doi.org/10.1016/j.memsci.2016.11.040.

Luo, T., Abdu, S., & Wessling, M. (2018). Selectivity of ion exchange membranes: A review. *Journal of Membrane Science*, *555*, 429–454. Available from https://doi.org/10.1016/j.memsci.2018.03.051.

Luo, T., Roghmans, F., & Wessling, M. (2020). Ion mobility and partition determine the counter-ion selectivity of ion exchange membranes. *Journal of Membrane Science*, *597*, 117645. Available from https://doi.org/10.1016/j.memsci.2019.117645.

Madaeni, S. S., Ghaemi, N., & Rajabi, H. (2015). Advances in polymeric membranes for water treatment. In A. Basile, A. Cassano, & N. K. Rastogi (Eds.), *Advances in membrane technologies for water treatment* (pp. 3–41). Woodhead Publishing Series in Energy.

Mofrad, A. E., Moheb, A., Masigol, M., Sadeghi, M., & Radmanesh, F. (2018). An investigation into electrochemical properties of poly (ether sulfone)/ poly (vinyl pyrrolidone) heterogeneous cation-exchange membranes by using design of experiment method. *Journal of Colloid and Interface Science*, *532*, 546–556. Available from https://doi.org/10.1016/j.jcis.2018.08.026.

Moghadassi, A. R., Koranian, P., Hosseini, S. M., Askari, M., & Madaeni, S. S. (2014). Surface modification of heterogeneous cation exchange membrane through simultaneous using polymerization of PAA and multiwalled carbon nanotubes. *Journal of Industrial and Engineering Chemistry*, *20*, 2710–2718. Available from https://doi.org/10.1016/j.jiec.2013.10.059.

Mohapi, M., J. Sefadi, Sh, M. Mochane, J., Magagula, S. I., & Lebelo, K. (2020). Composite in adsorptive removal of contaminants: A review. *Crystals*, *10*, 957. Available from https://doi.org/10.3390/cryst10110957.

Nayar, K. G., & Lienhard, V. J. H. (2020). Brackish water desalination for greenhouse agriculture: Comparing the costs of RO, CCRO, EDR, and monovalent-selective EDR. *Desalination*, *475*, 114188. Available from https://doi.org/10.1016/j.desal.2019.114188.

Nemati, M., & Hosseini, S. M. (2015). Fabrication and electrochemical property modification of mixed matrix heterogeneous cation exchange membranes filled with Fe_3O_4/PAA core-shell nanoparticles. *Ionics*, *22*, 899–909. Available from https://doi.org/10.1007/s11581-015-1603-z.

Pan, Z., Song., Ch, Li. L., Wang, H., Pan, Y., Wang., ... Feng, X. (2019). Membrane technology coupled with electrochemical advanced oxidation processes for organic wastewater treatment: Recent advances and future prospects. *Chemical Engineering Journal*, *376*, 120909. Available from https://doi.org/10.1016/j.cej.2019.01.188.

Parnamae, R., Mareev, S., Nikonenko, V., Melnikov, S., Sheldeshov, N., Zabolotskii, V., ... Tedesco, M. (2021). Bipolar membranes: A review on principles, latest developments, and applications. *Journal of Membrane Science*, *617*, 118538. Available from https://doi.org/10.1016/j.memsci.2020.118538.

Parvizian, F., Hosseini, S. M., Hamidi, A. R., Madaeni, S. S., & Moghadassi, A. R. (2014). Electrochemical characterization of mixed matrix nanocomposite ion exchange membrane modified by ZnO nanoparticles at different electrolyte condition pH/concentration. *Journal of the Taiwan Institute of Chemical Engineering*, *45*, 2878–2887. Available from https://doi.org/10.1016/j.jtice.2014.08.017.

Patel, S. K., Qin, M., Walker, W. Sh, & Elimelech, M. (2020). Energy efficiency of electro-driven brackish water desalination: electrodialysis significantly outperforms membrane capacitive deionization. *Environmental Science and Technology*, *54*, 3663–3677. Available from https://doi.org/10.1021/acs.est.9b07482.

Peters, R. J., Bouwmeester, H., Gottardo, S., Amenta, V., Arena, M., Brandhoff, P., ... Aschberger, K. (2016). Nanomaterials for products and application in agriculture, feed and food. *Trends in Food Science and Technology*, *54*, 155–164. Available from https://doi.org/10.1016/j.tifs.2016.06.008.

Pismenskaya, N. D., Pokhidnia, E. V., Pourcelly, G., & Nikonenko, V. V. (2018). Can the electrochemical performance of heterogeneous ion-exchange membranes be better than that of homogeneous membranes? *Journal of Membrane Science*, *566*, 54–68. Available from https://doi.org/10.1016/j.memsci.2018.08.055.

Porada, S., Zhao, R., Van der Wal, A., Presser, V., & Biesheuvel, P. M. (2013). Review on the science and technology of water desalination by capacitive deionization. *Progress in Materials Science*, *58*, 1388–1442. Available from https://doi.org/10.1016/j.pmatsci.2013.03.005.

Radmanesh, F., Rijnaarts, T., Moheb, A., Sadeghi, M., & De Vos, W. M. (2019). Enhanced selectivity and performance heterogeneous cation exchange membranes through addition of sulfonated and protonated Montmorillonite. *Journal of Colloid and Interface Science*, *533*, 658–670. Available from https://doi.org/10.1016/j.jcis.2018.08.100.

Ramesh, S., Sivasamy, A., Rhee, K. Y., Park, S. J., & Hui, D. (2015). Preparation and characterization of maleimide-polystyrene/SiO_2-Al_2O_3 hybrid nanocomposites by an in situ sol-gel process and its antimicrobial activity. *Composites Part B*, *75*, 167–175. Available from https://doi.org/10.1016/j.compositesb.2015.01.040.

Ran, J., Wu, L., He, Y., Yang, Zh, Wang, Y., Jiang, Ch, ... Xu, T. (2017). Ion exchange membranes: New developments and applications. *Journal of Membrane Science*, *522*, 267–291. Available from https://doi.org/10.1016/j.memsci.2016.09.033.

Saleh, T. A. (2020). Nanomaterials: Classification, preparation, and environmental toxicities. *Environmental Technology and Innovation*, *20*, 101067. Available from https://doi.org/10.1016/j.eti.2020.101067.

Scarazzato, T., Panossian, Z., Tenorio, J. A. S., Perez-Herranz, V., & Espinosa, D. C. R. (2017). A review of cleaner production in electroplating industries using electrodialysis. *Journal of Cleaner Production*, *168*, 1590–1602. Available from https://doi.org/10.1016/j.jclepro.2017.03.152.

Singh, V., Yadav, P., & Mishra, V. (2020). Recent advances on classification, properties, synthesis, and characterization of nanomaterials. In N. Srivastava, M. Srivastava, P. K. Mishra, & V. K. Gupta (Eds.), *Green synthesis of nanomaterials for bioenergy applications* (pp. 83–97). John Wiley & Sons Ltd.

Strathman, H. (2010). Electrodialysis, a mature technology with a multitude of new applications. *Desalination*, *264*, 268–288. Available from https://doi.org/10.1016/j.desal.2010.04.069.

Taghipour, Sh, Hosseini, S. M., & Ashtiani, B. A. (2019). Engineering nanomaterials for water and wastewater treatment: Review of classifications, properties and applications. *New Journal of Chemistry*, *43*, 7902–7927. Available from https://doi.org/10.1039/C9NJ00157C.

Vaselbehagh, M., Karkhanechi, H., Takagi, R., & Matsuyama, H. (2015). Surface modification of an anion exchange membrane to improve the selectivity for monovalent anions in electrodialysis—Experimental verification of theoretical predictions. *Journal of Membrane Science*, *490*, 301–310. Available from https://doi.org/10.1016/j.memsci.2015.04.014.

Vogel, C., & M-Haack, J. (2014). Preparation of ion-exchange materials and membranes. *Desalination*, *342*, 156–174. Available from https://doi.org/10.1016/j.desal.2013.12.039.

Vona, M. L. D., Ahmed, Z., Bellitto, S., Lenci, A., Traversa, E., & Licoccia, S. (2007). SPEEK-TiO_2 nanocomposite hybrid proton conductive membranes via in situ mixed sol-gel process. *Journal of Membrane Science*, *296*, 156–161. Available from https://doi.org/10.1016/j.memsci.2007.03.037.

Yang, J., Bu, Y., Liu, F., Zhang, W., Cai, D., Sun, A., ... Zhang, Ch (2020). Potential application of membrane capacitive deionization for heavy metal removal from water: A mini-review. *International Journal of Electrochemical Science*, *15*, 7848–7859. Available from https://doi.org/10.20964/2020.08.98.

Yin, J., & Deng, B. (2015). Polymer-matrix nanocomposite membranes for water treatment. *Journal of Membrane Science*, *479*, 256–275. Available from https://doi.org/10.1016/j.memsci.2014.11.019.

Yu, J., Jo, K., Kim, T., Lee, J., & Yoon, J. (2018). Temporal and spatial distribution of pH in flow-mode capacitive deionization and membrane capacitive deionization. *Desalination*, *439*, 188–195. Available from https://doi.org/10.1016/j.desal.2018.04.011.

Zhang, Z., Xiao, P., Ruan, H., Liao, J., Gao, C., Van der Bruggen, B., & Shen, J. (2019). Mussel-inspired surface functionalization of AEM for simultaneous improved monovalent anion selectivity and antibacterial property. *Membranes*, *9*, 36. Available from https://doi.org/10.3390/membranes9030036.

Zhu, J., Luo, B., Qian, Y., Sotto, A., Gao, C., & Shen, J. (2019). Three-dimensional stable cation-exchange membrane with enhanced mechanical, electrochemical, and antibacterial performance by in situ synthesis of silver nanoparticles. *ACS Omega*, *4*, 16619–16628. Available from https://doi.org/10.1021/acsomega.9b02537.

CHAPTER

17

Polymer-based membranes for membrane distillation

Arun Saravanan, Kanupriya Nayak and Bijay P. Tripathi

Department of Materials Science and Engineering, Indian Institute of Technology Delhi, New Delhi, India

Abbreviations

AGMD	air gap membrane distillation
CA	contact angle
CNT	carbon nanotubes
CP	concentration polarization
DCMD	direct contact membrane distillation
ENM	electrospun nanofibrous membrane
GO	graphene oxide
LEP	liquid entry pressure
MD	membrane distillation
MED	multiple-effect distillation
MF	microfiltration
MMM	mixed matrix membrane
MOFs	metal-organic frameworks
MSF	multistage flash
MWCNT	multiwalled carbon nanotubes
NF	nanofiltration
NOM	natural organic materials
PE	polyethylene
PES	polyethersulfone
PET	polyethylene terephthalate
PP	polypropylene
PS	polystyrene
PTFE	polytetrafluoroethylene
PVA	polyvinyl alcohol
PVDF	polyvinylidene fluoride
RO	reverse osmosis
SGMD	sweep gas membrane distillation

Advancement in Polymer-Based Membranes for Water Remediation
DOI: https://doi.org/10.1016/B978-0-323-88514-0.00020-6

© 2022 Elsevier Inc. All rights reserved.

SMM	surface-modifying macromolecules
SiO_2	silicon dioxide
TiO_2	titanium dioxide
TP	temperature polarization
UF	ultrafiltration
VMD	vacuum membrane distillation
VOCs	volatile organic compounds
ZnO	zinc oxide

Nomenclature

L	liter
m	meter
h	hour
kg	kilogram
kPa	kilopascal
W	watt
cm	centimeter
mm	millimeter
mM	millimolar
$\mu S\ cm^{-1}$	MicroSiemens per centimeter
ΔT	temperature difference (Kelvin)
Å	angstrom
μm	micrometer
°C	degree Celsius
kV	kilovolt
γ_L	surface tension (N m^{-1})
θ	contact angle between liquid and membrane [° (degrees)]
r_{max}	largest pore size
ε	porosity (%)
τ	tortuosity
ρ_m	membrane density (kg m^{-3})
ρ_{Pol}	polymer density (kg m^{-3})
K_m	thermal conductivity of membrane (W m^{-1} K^{-1})
K_p	thermal conductivity of polymer (W m^{-1} K^{-1})
K_g	thermal conductivity of gas (W m^{-1} K^{-1})

17.1 Introduction

17.1.1 Dearth of water

Water and energy play a pivotal role in economic development. Abundant water and energy are being exploited due to the increasing population and evolution of various industries, leading to water scarcity worldwide. Reuse and recycling are the two keys used to subdue this problem. Mainly, the world is surrounded by 97% of seawater, and the possibility of desalination is higher than wastewater treatment from anthropogenic and industrial activities. Surprisingly, membrane-based technologies have gained much recognition for their high separation efficiency, relatively low cost, small footprint, and operation ease. A membrane performs like a barrier amidst two phases and allows the substances (that exist in water) very selectively to move from one side to another.

Membrane technologies such as ultrafiltration (UF), microfiltration (MF), nanofiltration (NF), and reverse osmosis (RO) have been applied in several separation processes like wastewater treatment and desalination. RO is increasingly used in desalination processes due to its high efficiency with high rejection rates; however, it requires high hydraulic pressure to work (Ahmed, Lalia, & Hashaikeh, 2015). As compared to RO and other thermal desalination processes (e.g., multistage flash (MSF), multiple effect distillation (MED)), membrane distillation (MD) does not require any external high pressure or high temperature. MD has been developed as an alternative process for seawater desalination and wastewater treatment. Furthermore, it can also be used in juice concentration, heavy metal removal, and solvent recovery (Gupta, Chakraborty, Roy, Farinas, & Mitra, 2021). MD is a thermally driven separation process due to the vapor pressure gradient formed by the temperature difference between hot feed (60°C−90°C) and cold permeate (20°C) across the hydrophobic porous membrane (Roy, Bhadra, & Mitra, 2014). Since the operating temperature is remarkably lower than typical distillation processes, even waste heat from industries, geothermal and solar energy can be utilized for heating the feed solution (Dow et al., 2016; Ma, Irfan, Wang, Feng, & Xu, 2018; Sarbatly & Chiam, 2013). Despite these advantages, MD suffers from various limitations such as lower flux due to temperature polarization (TP), lower energy efficiency, membrane surface wetting, and fouling (Chen et al., 2021).

17.1.2 History of membrane distillation

In 1963, Bodell filed the first patent of MD. After four years, Findley published the first research paper in the journal "Industrial & Engineering Chemistry Process Design Development," describing the fundamental theory and results (Findley, 1967). Later that same year, Weyl argued about hot feed and cold permeate in direct contact using PTFE having 3.2 mm, 9 μm, and 42% of the thickness, pore size, and porosity, respectively (Weyl, 1967). Moreover, Van Haute and Henderyckx (1967) provided further insight regarding the permeability of water vapor in relation to the temperature. Besides, Bodell filed a second patent in 1968, in which a tubular membrane made of silicone was used to treat the aqueous solution. In 1969, Findley reported the relations between heat and mass transfer in evaporation applying porous membranes (Findley, Tanna, Rao, & Yeh, 1969). Nevertheless, MD had not been recognized till the 1980s. In 1982, an expanded PTFE spiral membrane named Gore-Tex membrane (supplied by Gore & Associated Co.) modules, with superior characteristics, became accessible in the market (Esato & Eiseman, 1975), and commercial membranes evolved (Amjad, 1988; Schneider & van Gassel, 1984). After some years, research studies on MD were published and hydrophobic membranes such as PP and PTFE were developed. The effect of temperature and concentration polarization (TP, CP) on MD was explained comprehensibly (Schofield, Fane, & Fell, 1987, 1990). The solidarity between conventional distillation and MD is the operation procedure because both processes depend on liquid−vapor equilibrium. The feed stream of both processes needs to be heated to achieve vaporization (Khayet, 2011). Although there is significant increasing interest within the academic circle, low flux and constant degradation of membrane performance prevent MD from being commercially viable.

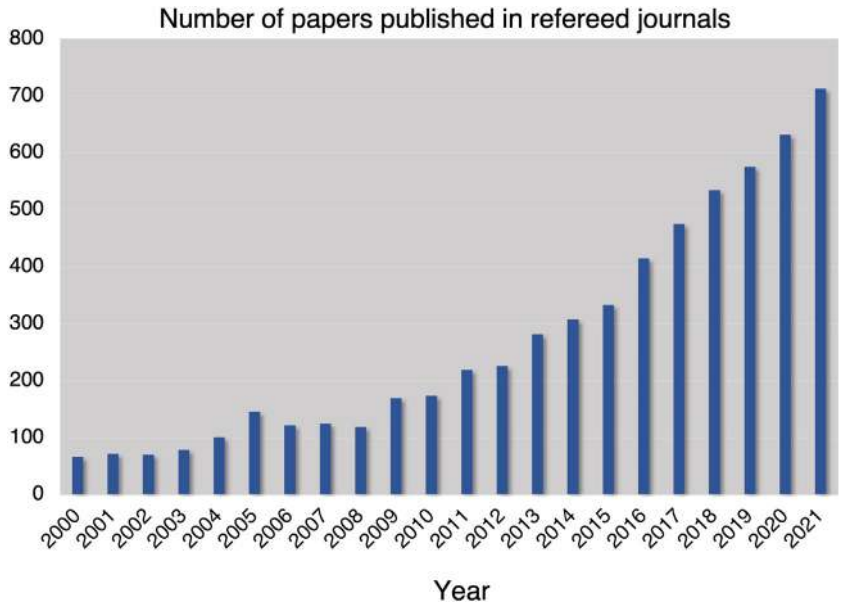

FIGURE 17.1 The progress of research activity on membrane distillation in the last 20 years (up to December 2021) using the keyword "membrane distillation" in the search field of Scopus.

17.1.3 Recent trends in polymer-based membranes in membrane distillation

Although the large-scale operation of MD has not yet multiplied worldwide, the research has aided in exploring the characteristics of an ideal membrane that fuels the development of this technology. Membranes with high liquid entry pressure (LEP), low fouling and wetting rate, high permeability, and good mechanical strength are expected to be the ideal membranes. Specifically, ceramic membranes with their high tolerance against harsh conditions have been valued; however, they are less favorable due to their high cost. Contrastingly, polymeric membranes are identified as a credible inexpensive alternative and have occupied research done on MD so far. Polymers such as PTFE, PVDF, PE, PP are more suitable for MD applications because of their excellent mechanical and thermal properties and long-term performance. Many novel attempts described different methods to fabricate polymeric membranes in simple, economical, and environmentally friendly ways. The latest reported researches using polymeric membranes in MD is discussed elaborately in the membrane materials section. Fig. 17.1 shows the number of research papers published in the last two decades.

17.2 Principle and different configurations of membrane distillation

17.2.1 Membrane distillation principle

In MD, the temperature difference (ΔT) on both sides of the membrane induces partial vapor pressure difference across the hydrophobic porous membrane, allowing the water

molecules to move from the hot side to the cold side through the membrane. The hot feed solution (saline water) is in direct contact with the membrane, while the cold solution (pure water) directly or indirectly proceeds to contact another side of the membrane, based on different MD configurations (Lee et al., 2020). In detail, initially, evaporation at the feed side due to heating at a specific temperature initiates the mass transport. Later, vapor molecules diffusion through the porous membrane leads to condensation at the cold permeate side (Eykens, De Sitter, Dotremont, Pinoy, & Van der Bruggen, 2017). Diffusion of vapor molecules happen through Knudsen and molecular diffusion, or Poiseuille flow, relying on the membrane's pore size, the mean free path of the vapor molecules, and the trapped air in the pores (Eykens et al., 2017). Generally, MD can be classified into four major types such as (1) direct contact MD, (2) air gap MD, (3) sweeping gas MD, and (4) vacuum MD.

17.2.2 Direct contact membrane distillation

In general, direct contact membrane distillation (DCMD) comprises feed and permeate sides divided by the hydrophobic porous membrane, as shown in Fig. 17.2A. An aqueous stream (generally distilled water) is kept in direct contact with the membrane's downstream side, which is colder than the feed stream (Nguyen & Lee, 2015). Hence, the feed flows through the membrane and gets vaporized, which is later condensed in the permeate cold section. DCMD is the most applied MD configuration owing to its simplest operational design that requires no external fittings like condenser and vacuum. So, the condensation will take place within the MD module (Khayet, 2011). Nevertheless, conductive heat loss in DCMD is higher than in other configurations because the conduction provokes heat transfer via the membrane (Prince et al., 2014a). Since the liquids from both sides are in direct contact with the membrane, the author suggested that the membrane should possess hydrophobic behavior (Shirazi, Kargari, & Tabatabaei, 2014). The surface patterned hydrophobic microporous membrane with a uniform structure and pore size on both sides and a multilayered (i.e., double or triple layered) composite membrane could raise significant interest in the future (Deka, Guo, & An, 2021; Li et al., 2020).

17.2.3 Air gap membrane distillation

In this configuration (Fig. 17.2B), the condensation occurs at the permeate side after the evaporated vapor molecules pass through the hydrophobic membrane pores and the interposed stagnant air gap inside the system (Alkhudhiri, Darwish, & Hilal, 2013b). The imposed air gap existence minimizes heat loss conduction and TP due to the higher thermal resistance, making air gap membrane distillation (AGMD) more capable of energy efficiency (Summers, Arafat, & Lienhard, 2012). In the case of applications, AGMD and DCMD are similarly used in desalination and food, particularly AGMD. Moreover, heat-sensitive products such as fruit juices and milk products could also be treated due to their low operating temperatures (around 60°C) (Moejes, van Wonderen, Bitter, & van Boxtel, 2020). The separation of alcohols could also be possible because it is less prone to membrane fouling and wetting during the test (Kujawska, Kujawski, Bryjak, Cichosz, &

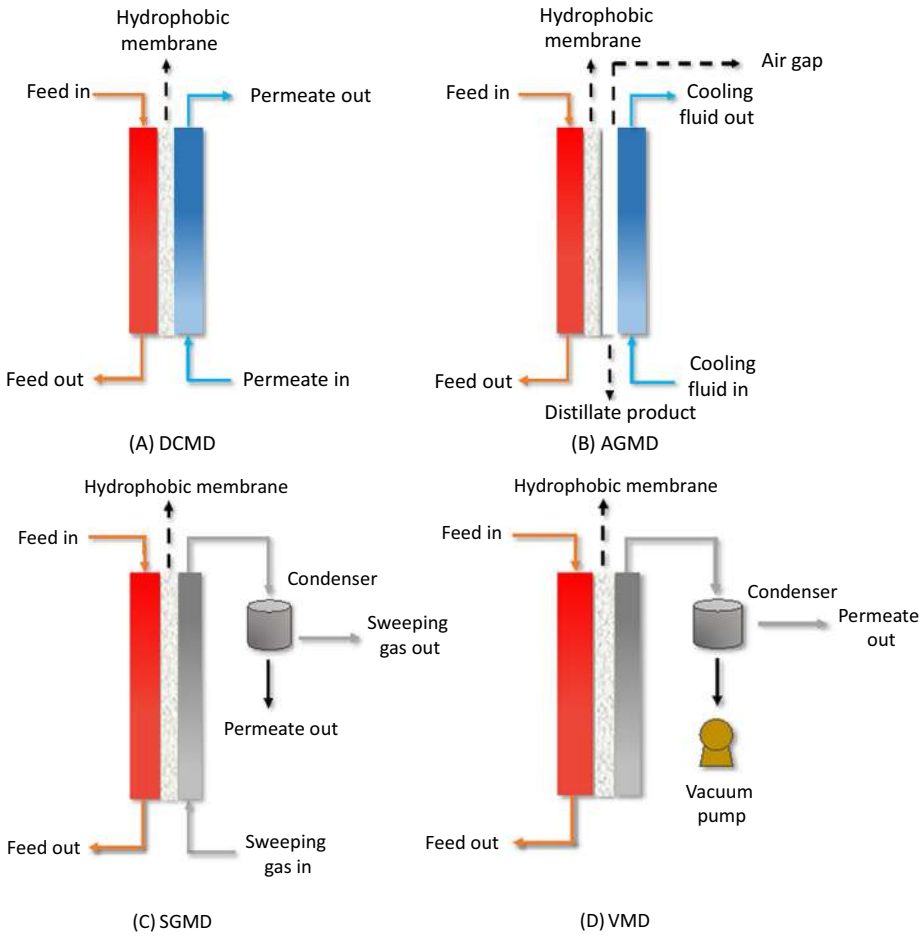

FIGURE 17.2 Different configurations of MD: (A) DCMD, (B) AGMD, (C) SGMD, and (D) VMD.

Kujawski, 2016; Meindersma, Guijt, & de Haan, 2006). More focus on surface properties during condensation, film condensation resistance, and heat-conductivity propagation could be more effective in the future (Warsinger, Swaminathan, Maswadeh, & Lienhard V, 2015). Even though the system exhibits a significant decrement in heat loss conduction, the mass transfer resistance is inevitable, leading to flux reduction (Shirsath, Muralidhar, & Pala, 2020). Furthermore, intricacy in designing the module and large footprint are critical areas to be investigated more for future issues.

17.2.4 Sweep gas membrane distillation

Sweep gas membrane distillation (SGMD) is similar to the AGMD process, but a cold, inert gas is applied instead of a stagnant air gap to collect the distilled water vapor, as

shown in Fig. 17.2C. In brief, an inert gas (usually cold) is employed to sweep permeated vapor molecules, followed by removing them at the distillate side (Khayet & Matsuura, 2011). The assistance of sweep gas flow at the downstream-permeates side leads to a decrement in conductive heat transfer and mass transfer resistance. In contrast, heat recovery during SGMD operation is complicated (Said, Chomiak, Floyd, & Li, 2020). The temperature of the feed solution and the flow rate of sweeping gas are the most prominent operating parameters in this system (Shirazi, Kargari, Bastani, & Fatehi, 2014). SGMD is a more attractive research area due to its lower membrane pore wetting phenomena. However, the complexity and expenditure in conjoining condenser with the configuration and energy recovery system implementation prohibit SGMD from reaching new heights. Despite these drawbacks, SGMD yields promising results in preliminary studies (Said et al., 2020). It is worth suggesting that selecting shorter length modules over longer length for choosing as an alternative would not lower the heat transfer driving force in the system. The sweeping flow gas temperature will increase on the cold permeate side (Alkhudhiri, Darwish, & Hilal, 2012).

17.2.5 Vacuum membrane distillation

In vacuum membrane distillation (VMD), a vacuum pump is assisted with the system for creating suction at the distillate side. Generally, the condensation occurs externally from the membrane module. The saturation pressure of volatile molecules containing hot feed solution should be higher than applying vacuum pressure to supply the driving force. Therefore, the potential for vapor condensation within or outside the membrane segment is considered (Al-Asheh, Banat, Qtaishat, & Al-Khateeb, 2006; Cheng, Li, & Zhang, 2018; Li & Sirkar, 2005). Nevertheless, VMD could achieve high flux due to a high-level partial pressure gradient (Abu-Zeid et al., 2015). Furthermore, the minimum conductive heat loss with high transmembrane flux makes VMD the best-equipped MD system (Chiam & Sarbatly, 2013; Drioli, Ali, & Macedonio, 2015). The condensation happens outside by applying an extra vacuum pump, which will lead to wetting and difficulty in systems heat recovery (Drioli et al., 2015; Khayet, 2013). Hence, it is emphasized that the LEP should be maximum when compared to hydrostatic pressure to deter wetting on the membrane as the feed solution moving through the pores of the hydrophobic membrane (Khayet & Matsuura, 2011). In addition, mass transfer resistance due to air trapping inside the pores of the membrane shall be removed using deaeration or applying a continuous vacuum on the permeate side (Abu-Zeid et al., 2015). Fig. 17.2D depicts the VMD configuration.

17.3 Fabrication techniques and module designs of MD membrane

As stated before, hydrophobicity and porosity are crucial characteristics of the membrane used for MD. Hence, it can be fabricated in the pattern of single-layer, dual-layer, and triple-layer composite. In terms of a single-layer, dual-layer and triple-layer membrane could be hydrophobic (Wang, Zheng, Wu, Zhang, & Zhang, 2016), hydrophobic/hydrophilic (Teoh, Chung, & Yeo, 2011; Zuo, Chung, O'Brien, & Kosar, 2017), and hydrophobic/hydrophilic/hydrophobic

(Li et al., 2020; Prince, Anbharasi, Shanmugasundaram, & Singh, 2013), respectively. The MD membrane pore size is between 100 Å and 1 μm. The fabrication of MD membranes can be done using stretching, sintering, phase inversion, and electrospinning (Liao, Loh, Tian, Wang, & Fane, 2018). The most used method is phase inversion and the combination of the above-mentioned methods can yield several kinds of membranes. For instance, Zhu et al. (2013) combined extrusion, sintering, and stretching to fabricate hollow fiber (HF) membranes.

17.3.1 Phase inversion

Phase inversion is a demixing process and is one of the most used techniques for MD membrane fabrication, in which the homogenous polymeric solution gets solidified during phase transformation in a controlled manner. Nonsolvent induced phase separation (NIPS), thermally induced phase separation (TIPS), evaporation-induced phase separation (EIPS), and vapor-induced phase separation (VIPS) are the various types of phase inversion methods (Lalia, Kochkodan, Hashaikeh, & Hilal, 2013). Also, the above techniques can be combined for membrane fabrication (Dehban, Kargari, & Ashtiani, 2020; Jung et al., 2016).

In the NIPS process, the dissolved polymer solution can be cast onto either a glass plate or nonwoven support. Later, the cast membrane is immersed in a nonsolvent (water or solvent mixed water) coagulation bath. The film of liquid solution gradually transformed to a solid state and get detached from the glass support. The two rich phases, such as polymer-rich and solvent-rich, are formed. This exchange extends until the entire polymer solution becomes solid (Abdel-Karim et al., 2019; Munirasu, Banat, Durrani, & Haija, 2017; Sabzekar et al., 2021). It is worth mentioning that the solvent (from homogeneous polymer solution) and nonsolvent (from coagulation bath) must be miscible for phase inversion.

TIPS is one of the prolific and useful techniques for fabricating porous polymeric membranes. In this process, a polymer/diluent homogeneous solution formed at an elevated temperature (above 200°C) is used to cast at favorable conditions followed by precipitation via simple cooling and the pores are formed by diluent extraction. Here, the polymer-rich phase forms the membrane matrix while the polymer lean-phase forms pores (Fang et al., 2021). The decrease in temperature results in a decrement of solvent quality, and so evaporation, diluent extraction, and freeze-drying can be used to remove the solvent after the demixing is instigated.

The VIPS is indubitably a phase separation technique that helps achieve unprecedented control over membrane structure compared with other phase inversion techniques because of the gas/liquid interface system. The nonsolvent flow and solvent outflow (mass transfers) are slowed down, which generally permits a better structure control of the membrane. In the VIPS chamber, the process parameters like exposure time of nonsolvent vapors, including relative humidity, influence the polymeric membrane structure (Chang & Venault, 2019). Moreover, nonsolvent absorption causes demixing/precipitation. The four essential morphologies can be achieved through the VIPS technique, such as symmetric and asymmetric cellular, symmetric modular, and symmetric bi-continuous structures (Ismail et al., 2020). Fan and Peng fabricated flat-sheet PVDF membranes via VIPS for desalination application using the DCMD system. As prepared, thin membranes displayed a higher flux of 18.9 kg m^{-2} h^{-1} and salt rejection of 99.7% over 6 h test with hardly occurring wetting (Fan & Peng, 2012).

EIPS is a facile method to fabricate membranes for several purposes and is called the dry casting method. This process is relatively less explored for using liquid monomers instead of polymers (Tan & Rodrigue, 2019) compared with other phase inversion techniques even though ease in case of a process, cost, time, and control over final morphology. The controlled evaporation like temperature and relative humidity of the solvent and nonsolvent assists in attaining the liquid−liquid phase separation from the homogeneous polymeric solution (Pervin, Ghosh, & Basavaraj, 2019). The prepared polymer solution is used for membrane fabrication through the doctor blade technique (Silva, De Francesco, & Pozio, 2004), in which the polymer solution can be prepared from solvent (binary/ternary mixture) and nonsolvent. For example, different membranes (PVDF, PVC, PS, and PVA) were developed using various organic solvents, and the effect of various solvents on the pore size and structure was explored by the authors (Nguyen, Alaoui, Yang, & Mbareck, 2010).

17.3.2 Stretching

The stretching technique was applied for the polymer membrane fabrication in various separation processes, including MF, UF, and MD (Sarada, Sawyer, & Ostler, 1983). This solvent-free and economical technique (Esfahani et al., 2019) can be used for semicrystalline polymers like PTFE and PE. The amorphous part lends the porous structure while crystals provide strength. Two types of stretching, such as cold stretching (to nucleate the microporosity) and hot stretching (controlling the porous structure), are generally used in membrane construction, resulting in uniform pores and 90% porosity (Souhaimi & Matsuura, 2011). The desired morphology is attained via heating (higher than a melting point) followed by extrusion. Therefore, stretching perpendicularly towards extrusion confers the membrane porosity. PTFE is highly hydrophobic as compared to the PE but fabrication of PE membrane is much easier than PTFE. Apart from thin performant layers, thicker layers (after laminating multiple layers) affect the performances of the PTFE membrane due to ballooning (condensation happens within the dense layers). Some of the commercially available stretched membranes are followed by (1) for PTFE-Memsys, Memstill, Solarspring, and Scarab; and (2) for PE-Aquastill (Eykens et al., 2017).

17.3.3 Sintering

In this process, the powdered polymer particles are converted to a plate or a film after pressing and later sintered below the melting temperature of the particular polymer. However, the prepared membrane has irregular pore size distribution (PSD) and microporous structure with 10%−40% of porosity. Moreover, the polymer particle size (ranging between 0.2 and 20 mm) decides the pore size (Curcio & Drioli, 2005; Souhaimi & Matsuura, 2011).

17.3.4 Electrospinning

Electrospinning is comparatively a different technique that is employed for the fabrication of ultrathin nanofibrous membranes. These membranes can be directly used in desalination and wastewater treatment (Prince et al., 2012; Ray, Chen, Li, Nguyen, & Nguyen,

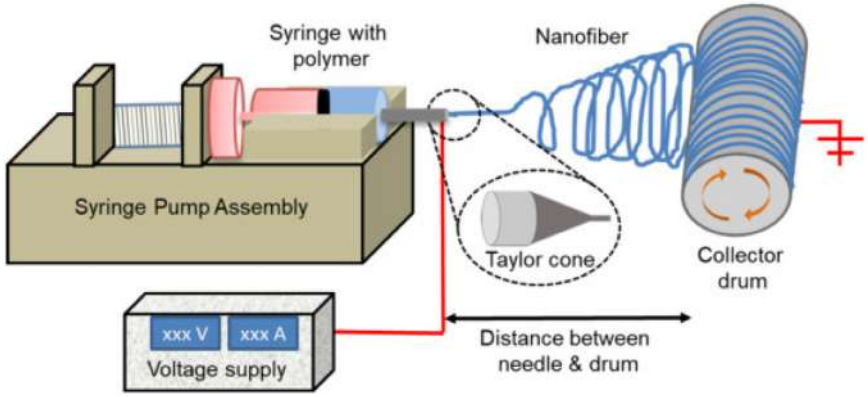

FIGURE 17.3 Schematic representation of the basic electrospinning process. Source: *Reprinted with permission from Deka, B. J., Guo, J., & An, A. K. (2021). Robust dual-layered omniphobic electrospun membrane with anti-wetting and anti-scaling functionalised for membrane distillation application.* Journal of Membrane Science, *119089. Copyright 2021, Elsevier.*

2016). Generally, nanofiber membranes can be produced from the viscous homogeneous polymeric solution by supplying a high voltage. The overall electrospinning assembly is depicted in Fig. 17.3. The nanofibers from electro-spinneret contain a metallic syringe, power supply (high voltage), and a collector drum. As compared to previously discussed techniques, electrospinning is simple to operate and has the flexibility to produce controllable nanofibers structure with a wide range of architectures using different types of polymer solutions. The different morphologies can be achieved through varying the parameters of electrospinning and polymer solution (Ahmed et al., 2015). Besides, electrospun membranes used for MD possess several advantages over conventional membranes, involving enhanced hydrophobicity, high porosity, pore size, interconnected pore structures, high gas permeability, and a high surface-to-volume ratio (Gopal et al., 2006; Ray et al., 2016). These benefits enable them to be implemented in various sectors like energy, pharmaceutical, biotechnology, and environmental engineering (Deka et al., 2021).

PVDF membrane is extensively fabricated by electrospinning technique for MD application. Prince et al. fabricated a nanocomposite membrane using PVDF/clay using electrospinning. The prepared membrane displayed a higher contact angle and flux when higher concentration amounts of clay were introduced. In addition, improved performance without pore wetting was observed during 8 h continuous DCMD test (Prince et al., 2012). Membranes with multiple layers (dual or triple) can also be fabricated via an electrospinning process followed by electrospraying (forming microspheres through grafting). For instance, Deka et al. prepared a robust dual-layered omniphobic membrane using electrospinning. The voltage of 16 kV with a flow rate of 0.8 mL h^{-1} was applied, and a 15 cm distance was maintained between the syringe (10 mL) and metallic drum (rotating at 150 rpm) throughout the experiment. To form another layer, the electrospraying method was conducted with 18 kV applied voltage and 1.5 mL h^{-1} of flow rate. The electrospun/electrosprayed membrane (Fig. 17.4) showed superior flux against brine feed having low surface tension. Moreover, high surface roughness (3.26 μm) and a low sliding angle of 3.9° were observed (Deka et al., 2021).

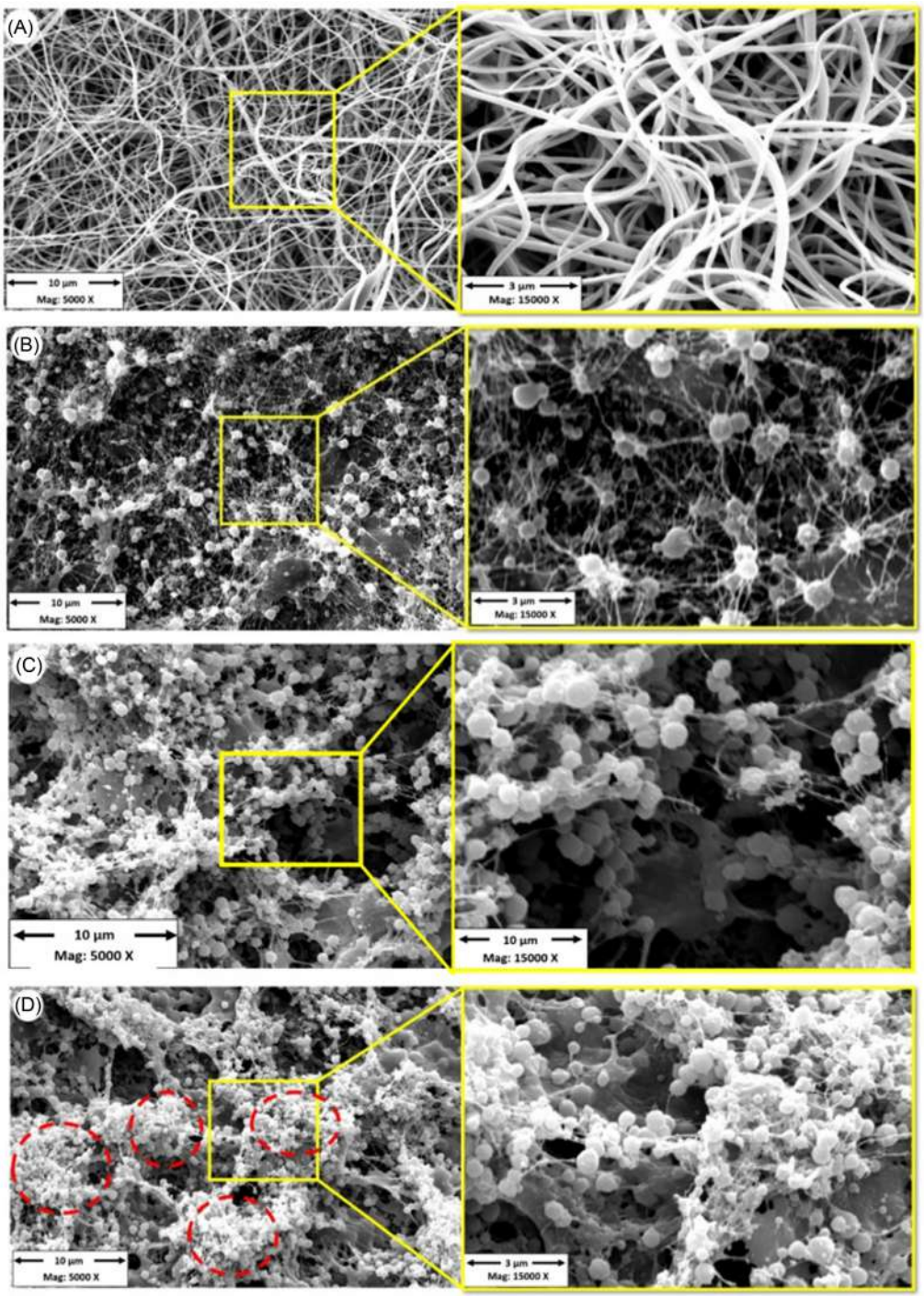
(A)
10 µm
Mag: 5000 X
3 µm
Mag: 15000 X
(B)
10 µm
Mag: 5000 X
3 µm
Mag: 15000 X
(C)
10 µm
Mag: 5000 X
10 µm
Mag: 15000 X
(D)
10 µm
Mag: 5000 X
3 µm
Mag: 15000 X

The fabrication of nanofibers with <100 nm diameter is still indurate because of the electrodynamic instability, which forms beads instead of linear fiber leading to poor filtration. Hence, preparing nanofiber membranes without incorporating additional ingredients is highly advisable because it will affect the membrane application (Cao, Gu, Rao, Fu, & Zhao, 2019). More focus on surface modification, including nanoparticles incorporation, will be useful to avoid agglomeration with homogeneity and stability. Furthermore, large pore size in electrospun causes wetting, so extra attention to this area would solve future issues.

17.3.5 MD membrane modules and designs

Membrane modules play a crucial role in the MD process, which limits the operation parameters. Moreover, designing a proper module for MD could result in better MD performance. Accordingly, it should possess better chemical and thermal stability, high packing density (ratio between membrane area and given packing volume) and mechanical strength, low-pressure drop and heat loss, and user friendly in terms of membrane cleaning or replacement. MD modules are classified into three major types: plate-frame module, spiral wound module, and capillary module (Pangarkar, Sane, Parjane, & Guddad, 2014). Typically, a spiral wound module comprises wrapped flat sheet membranes around the central tube, which is in spiral form as depicted in Fig. 17.5 (Winter, Koschikowski, & Wieghaus, 2011). This module could produce tangential flow and display a high surface-to-volume ratio, which shapes it to become a favorable MD operation choice. The flow channel area is crucial in MD operation and they are applied in the membrane module, especially for flat sheet membranes.

The plate-frame module is the easiest one as compared with all MD modules. This module contains flat sheet membrane series, spacers, and supports inside them, which are concatenated in the axial direction as shown in Fig. 17.6 (Cipollina, Di Sparti, Tamburini, & Micale, 2012). The liquid solution is directly in contact with the membrane surface so that the plate-frame module has good potential to become commercialized because of its tangential flow. In MD modules, the small nature of flow channels could lead to partial wetting across the hydrophobic membrane. Furthermore, pressure drop could decrease the LEP (at the feed or permeate side) when hydrostatic pressure exceeds and would cause a full wetting. The reduction of flow channel area may be resulting in high TP (Pangarkar et al., 2014). Flat sheet membranes are mostly applied in crossflow and dead-end stirred cells where the removal and replacement are easy. Therefore, these flat sheet membranes are highly preferred for plat-frame and spiral wound modules.

Capillary modules are separated into three main patterns: (1) capillary, (2) tubular, and (3) HF. The inner and outer diameter differentiate the capillary, tubular, and HF membranes,

FIGURE 17.4 FE-SEM images of electrospun/electrosprayed membrane. (A) Nanofibrous mat-like structure of the E-PVDF-HFP membrane. (B) 20% ZnO NPs embedded PVDF/HFP membrane (i.e., ePFP-20Z). (C) 25% ZnO NPs embedded PVDF/HFP membrane (i.e., ePFP-25Z). (D) 30% ZnO NPs embedded PVDF/HFP membrane (i.e., ePFP-30Z). Source: *Reprinted with permission from Deka, B. J., Guo, J., & An, A. K. (2021). Robust dual-layered omniphobic electrospun membrane with anti-wetting and anti-scaling functionalised for membrane distillation application.* Journal of Membrane Science, *119089. Copyright 2021, Elsevier.*

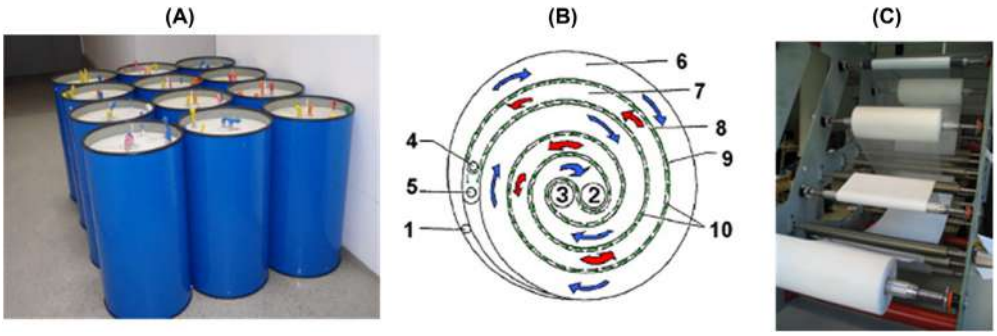

FIGURE 17.5 (A) Spiral wound modules for desalination (ready to use condition). (B) Schematic depiction of spiral wound concept: (1) condenser inlet; (2) condenser outlet; (3) evaporator outlet; (4) evaporator outlet; (5) distillate outlet; (6) condenser channel; (7) evaporator channel; (8) condenser foil; (9) distillate channel; and (10) hydrophobic membrane. (C) Winding machine for spiral wound modules fabrication. Source: *Reprinted with permission from Winter, D., Koschikowski, J., & Wieghaus, M. (2011). Desalination using membrane distillation: experimental studies on full scale spiral wound modules.* Journal of Membrane Science, 375(1), 104–112. *Copyright 2011, Elsevier.*

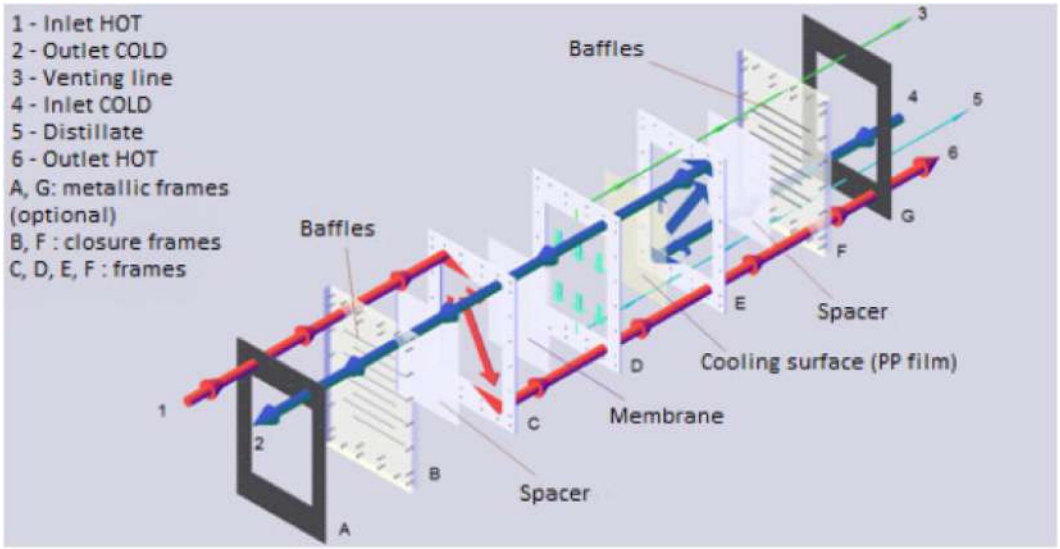

FIGURE 17.6 Schematic depiction of the plate-frame module. Source: *Reprinted with permission Cipollina, A., Di Sparti, M. G., Tamburini, A., & Micale, G. (2012). Development of a Membrane Distillation module for solar energy seawater desalination.* Chemical Engineering Research and Design, 90(12), 2101–2121. *Copyright 2012, Elsevier.*

affecting packing density. The diameter and packing density of tubular, capillary, and HF membranes range from 5–25 mm, 1–3 mm, 1 mm, and 300 $m^2\,m^{-3}$, 1200 $m^2\,m^{-3}$, 9000 $m^2\,m^{-3}$, respectively (Chiam & Sarbatly, 2013). These kinds of membrane are assembled and bundled in shell-and-tube modules. The HF membrane (diameter <0.5 mm) possesses a high surface-to-volume ratio, which renders greater flux density. Additionally, fewer difficulties in cleaning and

scaling treatments facilitate the HF module to treat higher concentration feeds. It does not require spacers and offers a densely packed, higher effective surface of the membrane (Wan, Yang, Lipscomb, Stookey, & Chung, 2017). Nevertheless, internal heat recovery has not been manifested yet clearly, so it must depend on exterior equipment (in terms of large scale). It generally demands more expenditure and electrical consumption for feed circulation due to lower hydraulic diameters than spiral wound (Zaragoza, Andrés-Mañas, & Ruiz-Aguirre, 2018).

Unlike flat sheets, the replacement of damaged membranes in the shell-and-tube module is very complicated. In addition, owing to the lack of membrane design and modules, more efforts should be paid to fabricate suitable MD membrane modules and configurations. To promote turbulence across the membrane surface for reduced fouling, several modifications have been performed in the standard version of shell-and-tube configuration (Pangarkar et al., 2014).

17.4 Membrane materials for MD

MD membranes should generally possess specific properties, including high hydrophobicity, excellent thermal stability, chemical resistance, and mechanical strength since it works against extreme temperatures, severely contaminated wastewater, and oily seawater, under high flow rates and long-time operation. In detail, the membrane with (1) high hydrophobicity to prevent pore wetting (LEP should be between 48 and 368 KPa); (2) thin layer for high permeability (thickness between 30 and 60 μm, 5 μm of the top layer for composite membranes); (3) reasonable pore size (ranging between 0.1 and 0.6 μm) to deter water penetration as well as to mitigate mass transfer resistance; (4) high porosity (60%−80%), and low tortuosity (assumed value is 2 but 3.9 was also mentioned); (5) low thermal conductivity (0.11−0.27 $W\,m^{-1}\,K^{-1}$ at 23°C) to achieve high heat transfer resistance (Le & Nunes, 2016). Therefore, polymeric materials like PTFE, PVDF, PP, and PE are the most favorable materials for different MD configurations and applications because of covering the demands mentioned above. However, they cannot meet all the requirements to become an excellent membrane, still commercially available and cheap. According to the application, membranes can be laminated with felts, woven and nonwoven fabric substrates from different materials such as polyolefins, polyolefins, and fluoropolymers requirements (Wikol et al., 2008).

PTFE has the highest hydrophobicity superior thermal and chemical stability, but the conductivity value is high and the manufacturing process is complicated. PVDF exhibits good hydrophobic behavior, thermal and chemical resistance, and mechanical strength. PP displays better thermal and chemical resistance (Huang, Xiao, Hu, & Li, 2011). PE possesses good chemical resistance and a low value of thermal conductivity. The researchers have started to focus on improving the membrane properties for sustainable MD performance. Feng, Shi, Li, and Wu (2004) compared two hydrophobic microporous membranes (PVDF and PVDF-co-tetrafluoroethylene), and the modified membrane showed better hydrophobicity and mechanical property with 100% salt rejection. Xu, Liu, Song, and Xiao (2017) prepared a superhydrophobic PP HF membrane using silica NPs. The modified membrane exhibited higher flux and rejection with a high retention rate. Su et al. (2019) fabricated a PTFE HF membrane and it demonstrated increased permeate flux with nearly complete NaCl rejection during long-term operation. Li et al. (2003) reported that PE membranes delivered more flux than PP

membranes and melt extrusion/cold-stretching methods were used to fabricate PP and PE HF membranes. However, the applications of PE membrane are limited. In another research, Zuo, Bonyadi, and Chung (2016) observed that the TIPS-made commercial PE membranes showed impressive flux (123.0 L m^{-2} h^{-1}) and stable performance over 100 h at 80°C. Except for the pristine MD membranes, the surface-modified membranes using NPs such as CNTs, graphene, SiO_2, and TiO_2 have also been applied in MD. The NPs embedment will improve fouling resistance and tackle wettability (Nthunya et al., 2019). The surface modification has been performed through surface segregation, cross-linking, incorporation, coextrusion, coating, grafting, and plasma polymerization (Le & Nunes, 2016).

17.5 Characteristics of MD membrane

17.5.1 Liquid entry pressure

The membrane pores should not be inundated by the liquid from both feed and permeate sides during the MD process. So, LEP is one of the most vital parameters, which measures the liability for liquid intrusion into the membrane pores. If the LEP is high during operation, the membrane is compromised due to the exposure to operating conditions such as salt concentration in the feed or pressure or temperature; once the membrane starts wetting (by liquid penetration through the membrane pores), the liquid can directly move from the hot feed to cold permeate section without purification and can lead to loss of selectivity (Guo, Servi, Liu, Gleason, & Rutledge, 2015). In brief, the minimum transmembrane pressure is required for the liquid to penetrate inside the membrane pores. To avoid pore wetting in MD, LEP should be greater than the hydrostatic pressure. The value of LEP mainly relies on the membrane hydrophobicity and pore size, so it should be maintained as maximum as possible during the operation (Chen, Soroush, & Rahaman, 2018). Various methods have been reported to measure LEP, and the widely used model is suggested by Franken, as expressed by the Cantor−Laplace equation (Franken, Nolten, Mulder, Bargeman, & Smolders, 1987),

$$\mathrm{LEP} = -\frac{2B\gamma_{\mathrm{L}}\cos\theta}{r_{\max}} \tag{17.1}$$

where B, θ, γ_{L}, and $r_{\max}$ are geometric factor (for cylindrical pores, $B = 1$; noncylindrical pores, $0 < B < 1$), contact angle between the membrane and liquid feed, surface tension, and the largest pore size, respectively. Here, pore radius can be determined by different analytical techniques such as gas permeation test, capillary flow porometer (Chang et al., 2020). The increase in temperature generally decreases LEP because of the decrement in contact angle and surface tension. Since the VMD process is driven by a pressure gradient, it requires a narrow PSD to evade wetting. Jacob et al. reported that the LEP relies on the surface tension of the liquid and the membrane contact angle (Jacob, Laborie, & Cabassud, 2018). The suggested optimum pore size to deter wetting is between 0.1 and 0.6 μm (Alkhudhiri et al., 2012). It is worth mentioning that even partial wetting may occur when the pressure becomes lower than LEP because wetting can take place slowly. Hence, specific operating conditions must be assessed for long-term stability before applying to large-scale applications.

17.5.2 Membrane thickness

In general, the membrane thickness is indirectly proportional to the MD permeate flux because a thicker membrane can reduce the permeate flux. The increased thickness could resist the mass transfer rate, which diminishes heat loss as well (Lawson & Lloyd, 1997). The thickness can significantly govern the permeate flux together with heat and mass transfer coefficients. The MD performance starts to degrade when the membrane thickness decreases, which will result in heat transfer increment. To address these defects, it is advantageous to possess thicker or multilayered structures; still, this is destructive to mass transport (Adnan, Hoang, Wang, & Xie, 2012; Bonyadi & Chung, 2009; Khayet, Cojocaru, & García-Payo, 2010). In the case of a single-layer membrane, the layer thickness should be referred to as an optimum thickness, resulting in flux enhancement and reduction of mass transfer resistance. However, the top layer of the multilayer membrane (triple-layer − hydrophobic/hydrophilic/hydrophobic; double-layer−hydrophobic/hydrophilic) should be a thin layer to minimize the mass transfer resistance. Additionally, the entire thickness of dual-layer membranes should be thicker to restrain heat loss (Khayet, 2011). Intelligibly, poising these parameters is a predominant feature of membrane design. Some simulation studies and experimental reports have emphasized that the optimized thickness range is between 20 and 60 μm (Eykens, De Sitter, Dotremont, Pinoy, & Van der Bruggen, 2016; Laganà, Barbieri, & Drioli, 2000; Martínez & Rodríguez-Maroto, 2008; Mohammad et al., 2015). Khalifa et al. discussed that the thickness of 154 μm and pore size of 379 nm offer less mass transfer resistance. So membrane with a small thickness and large pore size resulted in a higher flux by generating a high driving force over the membrane (Khalifa, Ahmad, Antar, Laoui, & Khayet, 2017). In another research, Li et al. prepared an electrospun nanofiber membrane (ENM) with two different thicknesses (i.e., 60 and 120 μm). The thicker membrane displayed higher LEP, porosity, and pore size over a thinner membrane, but the vapor flux was relatively lower (Fig. 17.7). This indicated that thickness is one of the dominant factors among other membrane parameters (Li et al., 2014). Nevertheless, further studies are required to optimize the thickness for making MD an energy-efficient process in both pilot and large-scale applications.

17.5.3 Pore size and pore size distribution

The pore size and PSD are vital characteristics of MD membranes. The permeate flux is directly related to pore size, so increasing pore size results in higher flux. The largest pore size is more desirable to refer to as mean pore size, including narrow PSD. Usually, in MD systems, the membrane pore size is between 100 nm and 1 μm (El-Bourawi, Ding, Ma, & Khayet, 2006; Lawson & Lloyd, 1997). The pore size in ENMs is extremely connected to the fiber diameter (Zhang et al., 2017). The mass transfer occurs simultaneously since there is no uniform pore size in the membrane. The PSD imparts quantitative data of pore size ranges exist in a membrane material. Usually, it demonstrates a more definite rendition of the size of particles likely to be eliminated or retained back by the membrane (Ray et al., 2018). The mean pore size and PSD can be measured through a capillary flow porometer, and the working principle is based on the bubble-point and gas permeation test (Zhang et al., 2017). Winter et al. reported that the small pore size influences flux reduction (Winter, Koschikowski, Düver, Hertel, & Beuscher, 2013). Khayet et al. discussed that to evaluate the heat transfer coefficient, mean pore size must be

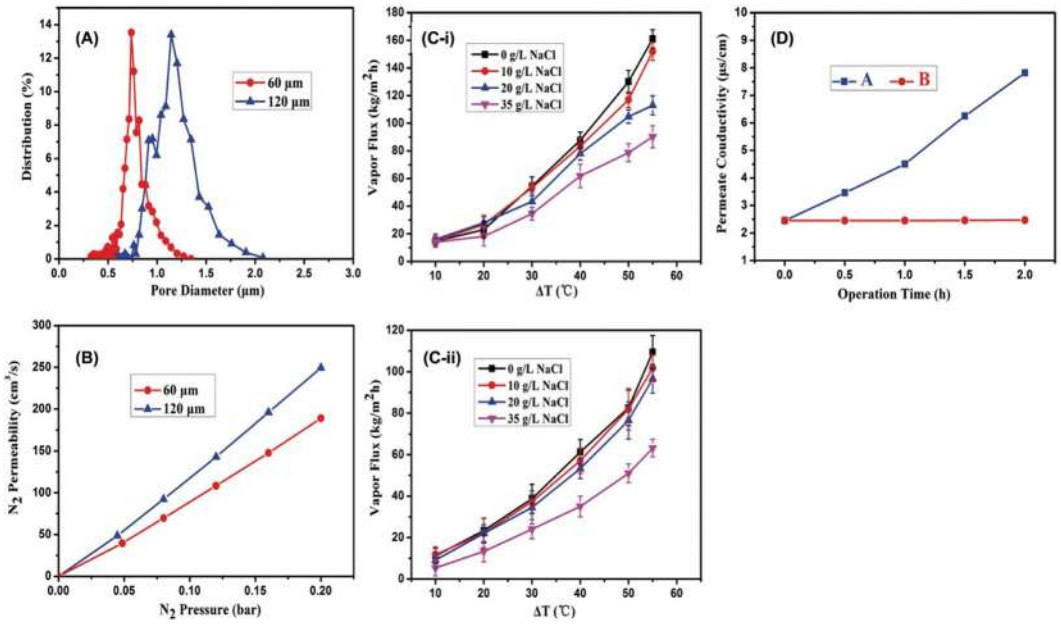

FIGURE 17.7 The influence of membrane thickness on (A) pore size distribution, (B) LEP, (C-i and C-ii) flux, (D) conductivity at permeate side. *Source: Reprinted with permission from X. Li et al. (2014). Copyright 2014, American Chemical Society.*

used rather than PSD (Khayet, Velázquez, & Mengual, 2004). In contrast, Martinez et al. assumed PSD and pore size to calculate heat transfer coefficient (Martínez, Florido-Díaz, Hernández, & Prádanos, 2003). Therefore, optimizing the pore size for better MD performance is mandatory because a large pore size will result in high flux and high liquid penetration. It could affect the salt rejection rate, so optimum pore size must be determined for better operating condition.

17.5.4 Porosity and tortuosity of membrane

Porosity and tortuosity are the determinant characteristics of the membrane, which precisely characterize the membrane structures and play a significant role in MD performance (Eykens, De Sitter, et al., 2016; Eykens, Hitsov, et al., 2016). The ratio of membrane pores volume to the total membrane volume (i.e., the volume fraction of membrane pores) is defined as the membrane porosity (Khayet & Matsuura, 2001). Generally, the porosity range is between 30 and 85% (El-Bourawi et al., 2006). The calculation of membrane porosity can be done by using the Smolder–Franken equation (Khayet & Matsuura, 2001),

$$\varepsilon = 1 - \left(\frac{\rho_m}{\rho_{Pol}}\right) \tag{17.2}$$

where ε, ρ_m, and ρ_{Pol} are membrane porosity, membrane density, and polymer density, respectively. IPA (isopropyl alcohol: can pass through the pores) and water (cannot penetrate through the pores) are the two different liquids used for calculating the porosity. The distillate flux increases when porosity rises, and also conductive heat loss is reduced by raising membrane-free volume (Pagliero, Bottino, Comite, & Costa, 2020).

Tortuosity is the pore structure deviation from the cylindrical position, which is inverse to the distillate flux owing to its membrane geometric dependency (Khayet, 2011). Although various methodologies like X-ray computed tomography (XCT) have been referred to measure tortuosity (Manickam, Gelb, & McCutcheon, 2014; Paluri, Maleky, & Heldman, 2017), measurements are susceptible to artifacts. Most of the studies have been used a rough evaluation for tortuosity. The correlation used in the present models is expressed below (Kim, Campanella, & Heldman, 2021).

$$\tau = \frac{1}{\varepsilon}(\text{in loose} - \text{packed domains}) \tag{17.3}$$

$$\tau = \frac{(2-\varepsilon)^2}{\varepsilon}(\text{in distances between closed domains}) \tag{17.4}$$

Since the calculation of membrane tortuosity is complicated, some studies assumed it is 2 in the estimation of flux and modeling (Kim et al., 2021). High porosity and low pore tortuosity are quadrated with high permeate flux and thermal efficiency, despite MD system conditions (Leitch, Li, Ikkala, Mauter, & Lowry, 2016). So, it is worth mentioning that both porosity and tortuosity are useful characteristics of mass transfer mechanisms.

17.5.5 Mechanical properties

Although the MD process requires relatively low pressures, the membrane may start rupturing in industrial applications during the operation due to hydraulic effects and flow disruption. Hence, MD membrane should possess better mechanical properties (Zhang et al., 2017).

17.5.6 Thermal conductivity

For the MD membrane, thermal conductivity should be lower because it will affect the membrane by transferring the heat across the membrane. The reported thermal conductivity is from 0.04 to 0.06 $W\,m^{-1}\,K^{-1}$ (Khayet, 2011). It can be evaluated by the following equation (Ibrahim & Alsalhy, 2013; Lawson & Lloyd, 1997),

$$K_m = (1-\varepsilon)K_p + K_g \tag{17.5}$$

where K_m, K_p, and K_g are the thermal conductivity of membrane, polymer, and gas (i.e., air), respectively.

17.6 Operational parameters in membrane distillation

17.6.1 Feed temperature

Feed temperature is one of the vital factors that affect and decides the permeate flux. An exponential increase in MD flux and TP (temperature polarization) effect can be found due to the rise in aqueous feed temperature (Pangarkar et al., 2014). For example, Li et al. applied a mathematical simulation to investigate the impact of feed temperature on thermal efficiency and the permeate flux. In which the differed feed temperature ranges from 40°C to 90°C caused a nearly 3.7 times increment in vapor flux (Li et al., 2014). Bogler and Bar-Zeev (2018) studied the influence of raising feed temperatures (47°C, 55°C, 65°C) on the growth of biofilm, and the biofilm growth is inhibited at maximum temperature (65°C) as compared to lower temperatures. The thermal efficiency generally increased linearly at high feed temperatures due to an exponential relationship (from Antoine equation) between vapor flux and temperature (Alklaibi & Lior, 2005). Moreover, it was determined that the computed thermal efficiency was increased when increasing the feed temperatures in both DCMD and VMD methods. In coolant temperature, a significant difference in the permeate flux occurs with the decrease in cold side temperature. Also, it can be possible to achieve considerably more permeate flux at identical temperature difference. The author discussed the cold side temperature effect on the vapor permeate flux ignored at stabled hot side temperature due to less vapor pressure variation at low temperatures (Matheswaran, Kwon, Kim, & Moon, 2007). The diffusivity and temperature have a direct relationship, so the mass transfer coefficient also increases across the membrane when it works at a high temperature. Besides that, the TP decreases when feed temperature increases (Srisurichan, Jiraratananon, & Fane, 2006).

17.6.2 Flow rate

In MD, the flow rate (or stirring rate) enhances the distillate flux when it increases. At this high flow rate, the formation of shear forces reduces the hydrodynamic boundary layer thickness, resulting in a reduction of both polarization effects and increment of heat transfer coefficient. Whence the temperature and concentration at the liquid–vapor membrane interface become nearer to the identical values in the bulk aqueous feed (Pangarkar et al., 2014). The impact of flow rate becomes more discernible at higher temperatures on MD flux, specifically related to a higher drop in temperature across the membrane. Accordingly, high flux production can be attained by performing under a turbulent flow condition. Altogether, the LEP must be monitored to prevent the membrane from pore wetting while optimizing the flow rate of bulk feed (Ullah et al., 2018). The author implied that the increase in the flow rate of feed could enhance the thermal efficiency with transmembrane flux, especially by developing the hydrodynamic conditions, which are appropriate to the Reynolds number, coefficients of heat, and mass transfer. The flux product increased by 24% (experimental) and 38% (simulation), but the thermal efficiency increased by only 2% and 5% at 40°C and 60°C (feed temperatures), respectively. It was obtained when the increment of feed flow velocity from 0.2 to 1.0 m s^{-1}, and the permeate side flow velocity was 0.28 m s^{-1} at 15°C of permeate temperature (Al-Obaidani et al., 2008). In AGMD, the inlet velocities (both hot and cold) had fewer effects. In which the impact

of hot solution inlet velocity was larger than the velocity of a cold solution. Both the solution's velocities had "local" consequences; they affected mass transfer resistance on their domains. The hot solution mass transfer resistance in the AGMD method developed the total mass transfer resistance with a smaller fraction than in DCMD. The positive approach to improve the DCMD performance with enhanced permeate flux and increased thermal efficiency is by increasing the hot solution velocity (Alklaibi & Lior, 2006). It should be noted that high flow velocity will induce wetting at a particular stage, therefore, detailed studies must be done to optimize the suitable flow rate combination for achieving sustainable MD performance.

17.6.3 Feed concentration

Feed concentration is a crucial parameter for investigating the permeate flux rate in MD systems. A well-known fact is that MD can treat the feed with high concentrations by not affecting the permeability, which differs from other membrane processes driven by pressure. This phenomenon makes them employed whenever high recovery or retentate concentrations are required (i.e., fresh juices concentration) (Bhattacharjee, Saxena, & Dutta, 2017). The permeate flux reduces when the feed concentration increases, which can be ascribed to the driving force decrement because of vapor pressure reduction in the feed solution. The viscosity of the aqueous feed solution increases exponentially with increasing the feed concentration. As compared with the effects of TP, the contribution is significantly less from the CP effects (Pangarkar et al., 2014). Several studies have reported that the permeate flux is decreased due to vapor pressure reduction. For instance, the reduction in flux has been found with increased acid concentration (Couto, Amaral, Lange, & Santos, 2019; Feng, Jiang, & Song, 2016), bovine plasma protein concentration (Sakai, Koyano, Muroi, & Tamura, 1988), and NaCl concentration (12% reduction from 0 to 2 M) (Qtaishat, Matsuura, Kruczek, & Khayet, 2008). So, it is necessary to optimize the feedwater concentration and temperature to deter overcome TP and CP in the MD process for better MD performance.

17.6.4 Air gap and long operation

In general, the flux decreases linearly with $1/l$ (Lawson & Lloyd, 1997). Correspondingly, the author observed a linear relationship between the flux product and the number of gaskets removed. They received a minute reduction in flux product due to opening the gap at the upper side to the atmosphere compared with closing the gap. In another study, the author argued that the flux would be double when minimizing the air gap (less than 1 mm) with a special effect (Izquierdo-Gil, García-Payo, & Fernández-Pineda, 1999). In AGMD configuration, air gap thickness is a crucial parameter that can affect the permeate flux. The width of the air gap associated with membrane thickness normally paves the way for transporting the diffusive species in AGMD. The larger distance in the air gap could reduce the vapor permeate flux by decreasing the mass transfer rate. So, the air gap thickness and AGMD permeate flux are inversely proportional to each other. The air gap thickness should be optimized for controlling both the heat and mass transfer resistance because the heat transfer resistance decreases with the increment in thickness while mass transfer resistance increases (Banat & Simandl, 1994). To overcome this defect, different gaskets can be applied for maintaining the

different thicknesses. Noteworthy to mention, the heat loss through conduction costs decreases in thermal efficiency because of minimizing the air gap thickness. Many researchers have studied the impact of airgap, mostly the width of the air gap employed in the range of 2–10 mm (Kalla, Upadhyaya, & Singh, 2019).

In long operation, the flux will not be lasting with high or constant flux. It will start to reduce gradually from their performance due to membrane wetting and fouling (Pangarkar et al., 2014). The author did not receive any change in product flux by performing them for a month (Izquierdo-Gil et al., 1999). Aforementioned, the membrane wetting and fouling caused the vapor to permeate flux decline (Lawson & Lloyd, 1997). In another study, the test was done for 10 days to treat the seawater, and the flux declined before it attained a steady state (Banat & Simandl, 1998). A similar result was found when treating the 1 M NaCl for 288 h (Drioli & Wu, 1985).

17.6.5 Membrane type

The membrane-type (flat, HF, and spiral) is essential to maintain the desired flux rate. Generally, the MD membranes are hydrophobic and microporous, and the water flux can be decided through some of the structure parameters like membrane thickness, membrane pore size, and porosity (Pangarkar et al., 2014). The different types of modules are already discussed in the previous section. The permeation flux of membrane and porosity are proportional to each other, while thickness and tortuosity are inversely related. Accordingly, Izquierdo-Gil et al. mentioned that the obtained permeate flux is higher because the membrane pore size is larger (Izquierdo-Gil et al., 1999). Moreover, the flux varies on the membrane with and without the support, significantly higher flux obtained in a membrane without support than the membrane (same pore size) with support (García-Payo, Izquierdo-Gil, & Fernández-Pineda, 2000). Similarly, the authors recommended applying the material (unsupported membrane) with lower thermal conductivity for attaining an efficient MD process. Several studies have reported that the impact of the applied operating parameters (Alklaibi & Lior, 2005; Izquierdo-Gil et al., 1999).

17.7 Fouling and wetting phenomena

The hydrophobic membrane is a vital part of the MD process, acting as a barrier against direct liquid penetration and a channel for vapor transfer. However, these membranes can face two major problems that may lead to operational failures in MD when treating hypersaline water and wastewater with complex compositions (Wang & Lin, 2017). The first possible problem is due to the attachment of fouling agents as summarized in Fig. 17.8. The deposition of foulants such as organic macromolecules, microorganisms, sparingly soluble inorganic salts, and suspended particles onto the porous membrane surface causes severe fouling and leads to significant vapor flux decline by blocking the membrane pores. This particular concern occurs in treating feed waters containing oil or organic contaminants due to the intense hydrophobic-hydrophobic interaction (Wang, Hou, & Lin, 2016;

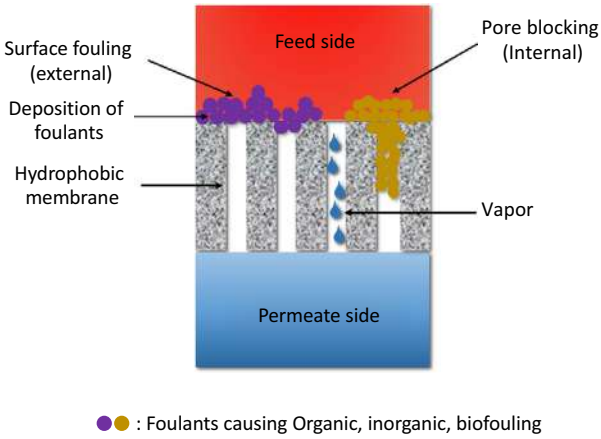

FIGURE 17.8 Schematic depiction of different types of fouling generally occurs in the membrane distillation process.

Warsinger, Swaminathan, Guillen-Burrieza, Arafat, & Lienhard V, 2015a). The three broad groups of fouling are: (1) inorganic fouling or scaling; (2) organic fouling; and (3) biological fouling (Khayet, 2016). Generally, Inorganic fouling is formed by one of three patterns: (1) alkaline scaling by $CaCO_3$ salts; (2) nonalkaline scaling by $CaSO_4$ salts; and (3) uncharged molecule scaling by silica. Although MD operation occurs at high temperatures and hypersaline conditions, it is still prone to biofouling due to bacteria and microorganisms in wastewater and ocean water. Organic fouling due to natural organic matters such as proteins, amino sugars, and humic substances (Tijing et al., 2015; Warsinger et al., 2015a). Moreover, temperature, feed concentration, and type and dissolve gases can be the factors of scaling.

The second potential problem is wetting by organic liquids (such as oils and alcohols) that may cause the whole operation failure in the MD system (Lee, Boo, Ryu, Taylor, & Elimelech, 2016). In brief, when the saline water with amphiphilic molecules like surfactants and various amphiphilic organics is applied for treatment, the hydrophobic-hydrophobic interaction (i.e., the amphiphilic molecules hydrophobic tails onto the hydrophobic membrane surface) makes the hydrophilic head exposed. Ultimately, the membrane pores become hydrophilic, and the consequences in membrane pore wetting (partial or fully) because of direct feed water penetration into the distillate side and a significantly compromised salt rejection rate (Huang, Wang, Jin, & Lin, 2017; Wang & Lin, 2017).

The different extents of membrane wetting (Fig. 17.9) are nonwetted, surface wetted, partial-wetted, and fully wetted membrane (Gryta, 2007b). Surface wetting occurs during long-term operation due to the surface phenomena, and it will not favorably affect the vaporization-distillation process by maintaining a gap for passing the vapor. Some portions are opened in partial wetting, and others have reduced the gap between the hot feed and cold permeate, which allows water vapor to transfer and leads to poor quality permeate, respectively (Tijing et al., 2015). As mentioned earlier, maintaining LEP higher than hydrostatic pressure would prevent the ME membrane from wetting. Also, surface tension, contact angle, the surface charge can influence the wetting in the system.

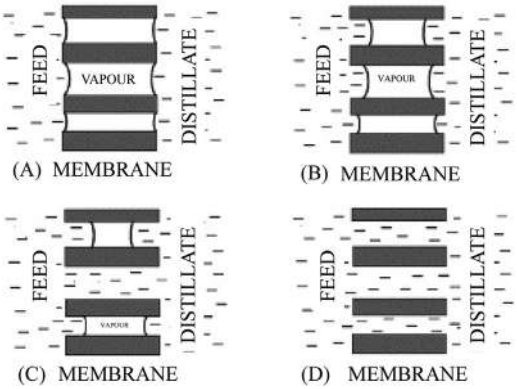

FIGURE 17.9 Different forms in membrane wetting: (A) nonwetted, (B) surface wetted, (C) partial-wetted, (D) fully wetted. Source*: Reprinted with permission from Gryta, M. (2007b). Influence of polypropylene membrane surface porosity on the performance of membrane distillation process*. Journal of Membrane Science, 287*(1), 67–78. Copyright 2006, Elsevier*.

In MD, fouling and wetting are shown to be correlated: fouling induces increased wetting while wetting induces increased fouling. This cycle can result in deterioration of MD performance and raising the number of membranes replacement (Warsinger et al., 2017). Inorganic fouling is the leading cause of partial wetting in membranes. Moreover, the membrane wetting can control the potential of treating fouling-susceptible solutions during the process (Warsinger et al., 2017). Feed pretreatment, cleaning (chemical or physical), applying antiscalants, membrane surface modifications, and rectification in operation conditions are the methods to control fouling, scaling, and wetting.

17.8 Prevention methods of fouling and wetting

MD is a beneficial technology but the limitations and technical challenges, such as wetting, fouling, and scaling, restrict the practical implementation for treating an extensive spectrum of hypersaline feedwater. The current methods to control the fouling are pretreatment of feed and cleaning the membrane (Tijing et al., 2015; Warsinger, Swaminathan, Guillen-Burrieza, Arafat, & Lienhard V, 2015b).

Feed pretreatment is the typical procedure in most desalination processes, along with various technology and quality of feed. Pretreatment can modify the feedwater properties, including physicochemical or biological, which will result in lower fouling and improvement in MD performance. General pretreatment methods involve filtration, flocculation, chlorination, coagulation, and precipitation. Some reports suggest that MD may not demand this pretreatment range since it does not allow the liquid to pass via membrane until no cake formation occurs (Mistry, Mitsos, & Lienhard, 2011; Tijing et al., 2015). Other filtration processes like MF, UF, and NF have been used before the MD process for removing large molecules and particulate materials in the feed (Tijing et al., 2015). For example, El-Abbassi et al. examined the impact of pretreatments such as coagulation/flocculation and MF in the olive mill wastewater treatment using DCMD. In which MF exhibited superior results over coagulation/flocculation when coupled with DCMD. Thus, it became an effective technique by enhancing the flux by 25% and 30% reduction of total solids during the pretreatment (El-Abbassi, Hafidi, Khayet, & García-Payo, 2013). Regular membrane

flushing is also one of the approaches to mitigate the scaling. Nghiem and Cath (2011) reported the membrane flushing in the DCMD test where PTFE membranes were used for scaling tests using foulants like $CaSO_4$, $CaCO_3$, and silicate at various feed temperatures (40°C−60°C). The $CaSO_4$ (severe formation as compared to other scaling) induction period was minimized with increased temperature. To remove bicarbonates from feedwater, thermal pretreatment (boiling of water) can be applied to lessen the MD membrane scaling. Usually, groundwater contains high hardness, so it would be more advantageous to break down the bicarbonates at higher temperatures (Gryta, 2010). Moreover, it was used to mitigate the protein fouling formation (Gryta, 2008b).

In chemical cleaning, the standard method to reclaim the fouled membrane is acid cleaning. Both strong and weak acids have been used in various studies to eliminate the scale components deposited on the membrane surface. Generally, the removal of $CaCO_3$ scaling can be done by using HCl due to its effectiveness (Gryta, 2005, 2008a). Gryta (2007a) observed that HCl could be transported (since it is volatile) to the permeate section and vapor during DCMD operation using HF membranes. So, the permeate must be discarded while the process is executed as a batch process being replaced with an acidic solution. Apart from acids, Dow et al. (2017) conducted three different approaches for cleaning the membrane: (1) warm caustic cleaning with NaOH; (2) ambient chlorine cleaning with NaClO; and (3) DI water. Among them, caustic cleaning displayed better in-membrane flux recovery (4 L m^{-2} h^{-1}) and mass transfer coefficient (61%). In the case of biofouling, biocides can be used to deter the growth of biofilms. Moreover, the bioactive agents, including enzymes, a mixture of enzymes, or signal molecules, can be used for foulant removals (Ezugbe & Rathilal, 2020). It should be noted that the drying process is mandatory after cleaning to retain the membrane hydrophobicity (Guillen-Burrieza, Ruiz-Aguirre, Zaragoza, & Arafat, 2014). In general, physical cleaning contains mechanical treatment for dislodging and removing the membrane foulants. This cleaning comprises various treatments such as periodic back flushing, pneumatic cleaning, ultra-sonic cleaning, and sponge ball cleaning (Ezugbe & Rathilal, 2020). Magnetic water treatment (MWT) is another technology in which the magnetic field relaxes the nucleation while raising the growth rate of crystals. It is applied in water treatment as well as power plant heat exchangers to reduce the scaling formation. Gryta used a commercial MWT device (Magnetizer RWE-S), and it could run with 0.1 T magnetic field. The created magnetic field resulted in 10%−25% reduction of $CaCO_3$ layer thickness and mitigated flux decrement (Gryta, 2011).

Antiscalants are a general appliance to deter inorganic scaling on the membrane through interfering in scales precipitation reaction and weakening the scale adherence on the surface. Although it is applied commonly due to its low costs and less dosing concentration (10 ppm), still which molecules can induce membrane wetting by reducing the water surface tension (Warsinger et al., 2015b). For instance, polyphosphate-based antiscalants were applied to control calcite scaling in MD. In which, $CaCO_3$ crystallite formation was observed to be almost removed, but the permeate flux was compromised because of the thin layer created by amorphous organics (Gryta, 2012). In contrast, Qu et al. (2020) used three different commercial antiscalants, namely, SHMP (polymeric metaphosphates mixture), MDC220 [phosphonic acid and (1-hydroxyethylidene) bissodium salt], and PTP-0100, to examine gypsum scaling. In which the antiscalants retarded permeate flux reduction and distillate conductivity increment. Both SHMP and MDC220 showed better results than PTP-0100 in constraining gypsum scaling.

Several approaches to restrict MD membrane wetting have been recommended by many researchers. The paramount goal of superiority in the fabrication of membrane is to attain a superior nonwettable surface. The focus is almost on membrane fabrication and surface modification to corroborate a less affinity between the feed solution and the polymeric substrate. The investigation revealed that the operating conditions, integration of other filtration processes, and novel flow techniques applied for wetting control. As mentioned above, pretreatments like MF, UF, NF can effectually eliminate amphiphilic proteins that ultimately cause wetting on the hydrophobic membrane. Nevertheless, it is difficult to mitigate the low surface tension water-miscible liquids or surfactants instigated pore wetting. All the pretreatment methods are not tested by far; still, surfactants in the solution can be removed through ion exchange, coagulation, floatation/foam fractionation, or biodegradation (Horseman et al., 2021). The membranes that can resist wetting caused by low surface tension liquids like oils are known as oleophobic membranes. Moreover, they are referred to as amphiphobic (surface shows wetting resistance against water or oil) or omniphobic membranes (surface exhibits wetting resistance against all liquids) predominantly, since oleophobic membranes are mostly hydrophobic or superhydrophobic (surface resistance to water) (Horseman et al., 2021). Surface energy and surface tension are the factors of membrane wetting that can affect membrane efficiency. So, membrane fabrication and modification mostly pivoted on reducing surface energy and increasing surface roughness to achieve superhydrophobic, omniphobic surfaces (Rezaei et al., 2018). Rinsing and drying is not an effective process for the wetted membrane regeneration due to salt crystals deposition inside the pores and hydrophilic groups on the surface of the membrane, respectively (Rezaei et al., 2018). Alternatively, Warsinger et al. (2017) studied air backwashing and removed the wetting liquid from the pores (also maintaining the solutes from the precipitation) because the applied air pressure was higher than LEP. Membrane modification can be done in two ways: (1) physical modification that contains plasma treatment, layer-by-layer assembly, template replication, phase separation, electrospinning, thermal treatment, and double re-entrant cavities; and (2) chemical modification through the incorporation of SMM (surface-modifying molecules) or functional groups having low surface tension (Rezaei et al., 2018).

Superhydrophobic membranes ($CA > 150^{\circ}$) have been fabricated to achieve high MD system performance by enhancing wetting resistance to water. It is developed by roughening, followed by coating (energy materials with a low surface) on the hydrophobic surfaces. MD membranes with high roughness have been prepared by inorganic nanoparticles such as SiO_2 (silica) and TiO_2 (titanium oxide). In addition to that, these superhydrophobic MD membranes have several benefits over conventional membranes applied in MD, including with low fouling tendency and long durable wetting resistance. Despite that, superhydrophobic membranes are prone to wetting due to low surface tension (Rezaei et al., 2018; Yao et al., 2020). Omniphobic MD membranes can repel oil and water, which results in enriched robustness of MD separation. Though both the omniphobic and superhydrophobic membrane require ultralow surface tension on the surfaces, achieving the omniphobicity is complicated by minimizing the surface-free energy. Because wetting due to the liquids with low surface tension becomes thermodynamically more favorable on lower energy surfaces. Especially, omniphobic surfaces demand a re-entrant structure for developing a local kinetic barrier to transit, wholly wetting the Wenzel state from the metastable Cassie Baxter state for low surface energy liquids. The electrospinning method has been indicated to be an effective strategy to construct omniphobic MD membranes. Cylindrical electrospun fibers and spherical nanoparticles incorporated fibers to bestow an ideal

platform to develop omniphobic membrane substrates and enhance wetting resistance against the substances with low surface tension, respectively. Also, both the fibers have an increase in the level of re-entrant structure (Lu, Chen, & Chung, 2019; Yao et al., 2020). The authors (Lee et al., 2016; Lin et al., 2014) have developed omniphobic membranes using silica NPs followed by fluorination and achieved excellent wetting resistance against different feed solutions like mineral oil and ethanol.

Excluding superhydrophobic and omniphobic, Prince et al. (2014b) fabricated a triple-layer membrane (nanofiber/hydrophobic/hydrophilic) is shown in Fig. 17.10, which exhibited enhanced CA and LEP and high resistance to pore wetting. The narrowed pore size on the intermediate hydrophobic surface increases LEP, and the hydrophilic SMM carries water vapor from the intermediate hydrophobic layer via adsorption.

As mentioned previously, surfactants can also significantly lower the surface energy of saline (feed) solution by their accretion at the air-liquid interface, which results in the wetting of superhydrophobic membranes in MD. Moreover, the accumulation of nonpolar contaminants blocks pores on the membrane surface and diminishes the permeability of omniphobic

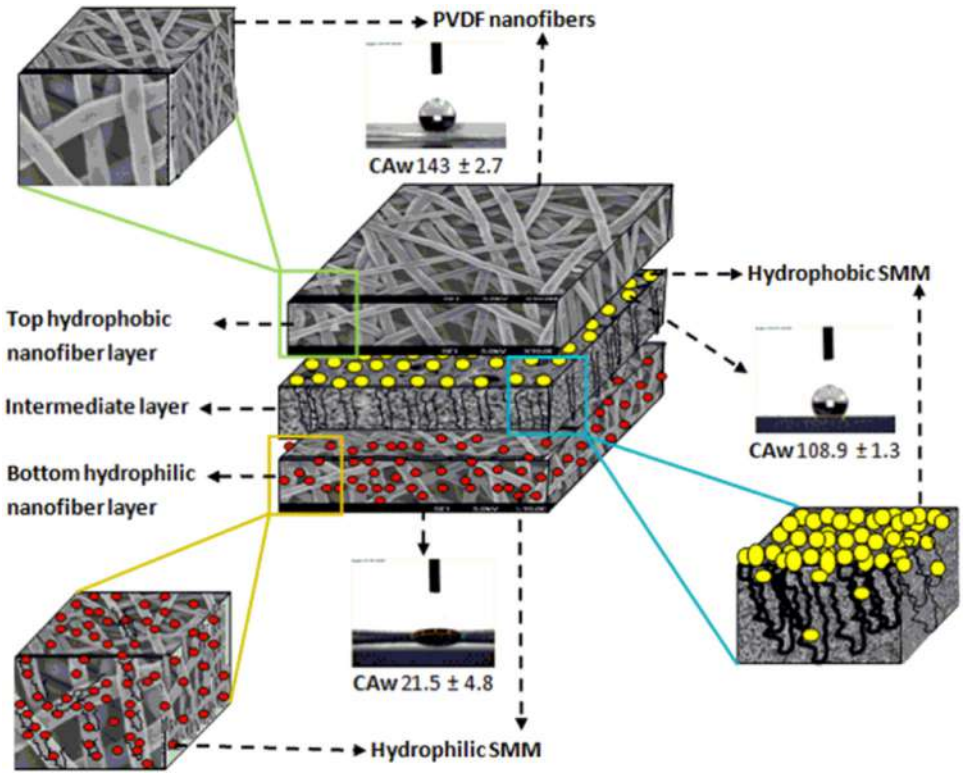

FIGURE 17.10 The construction of a triple-layer membrane. Source: *Reprinted with permission from Prince, J. A., Rana, D., Matsuura, T., Ayyanar, N., Shanmugasundaram, T. S., & Singh, G. (2014b). Nanofiber based triple layer hydro-phili/-phobic membrane—A solution for pore wetting in membrane distillation.* Scientific Reports, 4. *Copyright 2014, Nature.*

membranes. So nowadays, more researchers started to focus on fabricating Janus membrane (hydrophilic on superhydrophobic) to achieve higher flux with superior antifouling and anti-wetting properties without affecting bulk membrane properties (Yao et al., 2020).

17.9 Temperature and concentration polarization

The decrement in feed temperature and increment in solute concentration due to the vaporization phenomenon at the hot feed liquid−vapor interface is called TP and CP, respectively (Abu-Zeid et al., 2015). Since MD is a thermally driven process, the thermal boundary layers can be developed on two sides (i.e., hot feed and cold permeate) of the membranes. Those layers restrict the heat transfer and affect the driving force, causing 50% to 80% deterioration. They also turn down the temperature lower at the feed side liquid−vapor interfaces compared with the bulk stream. This temperature difference phenomenon is known as TP. The temperature polarization coefficient (TPC) is usually defined as the ratio of temperature difference at feed side (T_{fm}) and permeate side (T_{pm}) membrane surface to the difference in temperature of bulk feed stream (T_{bf}) and bulk permeate stream (T_{bp}).

$$\mathrm{TPC} = \frac{T_{fm} - T_{pm}}{T_{bf} - T_{bp}} \tag{17.6}$$

Since VMD comprises vacuum at the permeate, the above equation cannot be applicable, and the TP occurs at the feed side. So, the TPC in VMD is only the ratio of temperature at the feed side membrane surface to the temperature at the feed side bulk stream.

$$\mathrm{TPC} = \frac{T_{fm}}{T_{bf}} \tag{17.7}$$

When the TPC numerical value approaches 1, the difference in the liquid−vapor membrane interface temperature is closed to the bulk stream temperature. Alongside, zero means the system is limited by vast boundary layer resistance. Commonly, the TPC value for DCMD situates between 0.4 and 0.7 (Alkhudhiri et al., 2012; Anvari, Azimi Yancheshme, Kekre, & Ronen, 2020; Luo & Lior, 2016).

CP is nothing but a concentration boundary layer that develops near the membrane surface (feed side) in the MD module by the accumulation of salt particles eluded with vapor molecules. So, the concentration at the membrane interface is higher than the bulk stream, resulting in resistance to the mass transfer of vapor molecules and reduction in transmembrane flux. Nevertheless, the CP can be minimized by the operation conditions of MD. Because the flow rates are low to moderate, and the heat transfer coefficient is high in the MD process. The CP effect can be explained via the concentration polarization coefficient (CPC). CPC is the ratio of solute concentration in the feed side membrane interface (C_{mf}) and the solute concentration in the bulk feed solution (C_{bf}) (Alkhudhiri et al., 2012; Luo & Lior, 2016).

$$\mathrm{CPC} = \left(\frac{C_{mf}}{C_{bf}}\right) \tag{17.8}$$

CP usually causes scaling on the membranes by blocking the pores, also resists the diffusion of water vapor molecule and deteriorate the permeate flux. The similarity between heat and mass transfer processes indicates that it could reduce the CP by increasing the heat transfer rate in fluid flow, fluid flow velocity, flow inserts, and species transmission. Besides, CPC evaluates the transport phenomena in MD, which is associated with the product quality, production rate of the product, and energy efficiency (Ezugbe & Rathilal, 2020; Luo & Lior, 2016).

17.10 Applications of membrane distillation

MD is an attractive and a key technology for separation methods owing to its distinctive properties. The predominant application is seawater desalination through chemical and physical processes with high separation factors. MD is applied in many industries these days, including food, pharmaceutical, environmental, and nanotechnology. It can also be used as a standalone process or integrated process with other separation processes as a final stage process to achieve zero-liquid discharge (Abu-Zeid et al., 2015; Ashoor, Mansour, Giwa, Dufour, & Hasan, 2016; Said et al., 2020). The different applications of MD are stated in Table 17.1.

17.11 Economics and energy consumption of membrane distillation

The essential cost criteria for MD are thermal energy for heating the feed, the electrical energy for pumping the feed and permeate, and the fabrication of membranes using different materials. Even though DCMD demands two pumps for the process, the required pressures are still lesser than those applied for RO operation. As previously discussed, the advantages such as (1) separation without pressure; (2) 100% theoretical rejection of VOCs; (3) low-grade heat used for operation, particularly VMD; (4) fewer corrosion problems because of polymeric materials applied in plant construction (components like pipes, pumps, etc.) and membrane module fabrication; (5) ability to treat high feed concentration; and (6) possibility of applying renewable energy or waste heat sources like solar, geothermal, or industrial waste heat, make MD more economically viable. However, fouling and wetting, complexity in larger-sized membrane fabrication, high energy consumption, and water production cost restrict the implementation of MD on a larger scale rather than a small pilot or lab scale. As mentioned throughout this chapter, an energy source to heat the feed to a specific temperature is required. It can be achieved by integrating MD with other separation processes like FO (Zeweldi et al., 2021) and RO (Drioli, Laganà, Criscuoli, & Barbieri, 1999).

Topaloglu et al. (2018) reported that the FO and MD process integration could be sustainable economically and environmentally to produce potable water. Moreover, the zero-liquid discharge target becomes more feasible when the low-grade waste is available for operation. Drioli et al. (1999) integrated MD with RO for desalination and achieved higher recovery (87%) than standalone MD (77%) and RO (40%). It is worth reporting, for MD hybrid systems, solar-based thermal energy could be advantageous because of a low-cost renewable source (Ricci et al., 2019). The energy consumption cost can be substantially

TABLE 17.1 Summary of the different applications using membrane distillation technology.

Membrane distillation configuration	Membrane material	Feed solution	Application	References
DCMD	PVDF-HFP (HF)	3 wt.% NaCl	Desalination	García-Fernández, García-Payo, and Khayet (2017)
DCMD	SAN (nanofibrous)	0, 35, 70 g L^{-1} NaCl in DI water	Desalination	Niknejad, Bazgir, Sadeghzadeh, and Shirazi (2020)
DCMD	PTFE (FS)	Simulated water	Chromium removal	Bhattacharya, Dutta, Sikder, and Mandal (2014)
Submerged DCMD	PP (HF)	Commercial apple juice	Apple juice concentration	Gunko, Verbych, Bryk, and Hilal (2006)
DCMD	PTFE (FS)	Produced water	Desalination	Singh and Sirkar (2012)
DCMD	PVDF (FS)	Seawater	Boron removal	Hou et al. (2013)
DCMD	PVDF (HF)	Simulated radioactive wastewater	Radioactive treatment	Liu and Wang (2013)
AGMD	PTFE (FS)	Produced water	Desalination	Alkhudhiri, Darwish, and Hilal (2013a)
AGMD	PTFE (FS)	Synthetic textile wastewater	Wastewater treatment	Leaper, Abdel-Karim, Gad-Allah, and Gorgojo (2019)
AGMD	PTFE (FS)	HCl/H_2O	Breaking of azeotropic mixtures	Kalla, Upadhyaya, Singh, and Baghel (2019)
VMD	PVDF (FS)	200 g L^{-1} NaCl	Desalination	Wang et al. (2018)
VMD	PU coated PTFE (DL)	Synthetic wastewater	VOC removal	Zhang et al. (2019)
VMD	PP (FS)	Date juices	Date juice concentration	Criscuoli and Drioli (2020)
VMD	PTFE (FS)	Human Urine	Water regeneration	Zhao, Xu, Shang, and Chen (2013)
VMD	PP and PVDF (FS)	Wastewater containing arsenic	Arsenic removal	Criscuoli, Bafaro, and Drioli (2013)
SGMD	PP (shell-and-tube)	Distilled water, NaCl	Desalination	Khayet, Godino, and Mengual (2003)
SGMD	PTFE (FS)	NaCl and seawater	Desalination	Khayet, Cojocaru, and Baroudi (2012)
SGMD	PTFE (FS)	Ammonia containing wastewater	Ammonia removal	Xie, Duong, Hoang, Nguyen, and Bolto (2009)
SGMD	PTFE (FS)	Distilled water and absolute ethanol	Ethanol-water separation	Shirazi, Kargari, and Tabatabaei (2015)
SGMD	PP (shell-and-tube)	DMI aqueous solution	Concentration of DMI	Abejón, Saidani, Deratani, Richard, and Sánchez-Marcano (2019)

HF, hollow fiber; *SAN*, styrene-acrylonitrile; *FS*, flat sheet; *DL*, dual-layer.

reduced if the availability of a waste heat source increases the feed temperature up to MD operation level (Subramani & Jacangelo, 2015; Woldemariam et al., 2016). Furthermore, the water production cost will be decreased automatically when the energy source cost decreases. Generally, the MD's production cost range is from 0.26 to 130 \$ m^{-3} and total energy consumption could differ between 1 and 9000 kWh m^{-3}. These are based on MD configurations type and size, operation parameters, energy sources, recovery strategies, and cost estimation approaches (Xing, Anthony, & Rong, 2014). To evaluate the costs of water production in MD, the author (Khayet, 2013) emphasized that the standard techniques should be implemented to overcome the vague in specific energy consumption since a smaller number of research papers have been published in this area.

17.12 Conclusion and future directions in membrane distillation

Although MD has been used in several applications like desalination and wastewater treatment, many barriers still restrict them from industrialization. After many decades of tenacious evaluation for comprehending MD's concept and difficulties, the obstacles such as high energy consumption, module fabrication, fouling, and wetting in long-time operation need to be overcome. However, MD is gradually reaching commercialization in desalination; fewer studies only represented wastewater treatment on the demonstrative scale, mainly when volatile compounds exist. Therefore, more research on untended fields, including MD membrane modules or scale-up parameters in both experimental and modeling areas, will be extremely advantageous. Novel configurations, development in process design, and improvement of high-performance MD membrane materials have carried to a remarkable reduction in energy consumption cost throughout the decades.

Nevertheless, a further decrease in energy can be attained through MD hybridization with different separation techniques to surpass each limitation and profit from their strength. It is vital to sight for definite and controlled MD membrane morphology and properties (for instance, multilayer membranes fabricated with nano-additives) to improve the performance of several feeds accordingly. Membranes with different surface behaviors such as superhydrophobic, omniphobic, Janus have been developed to combat fouling and wetting when dealing with high salinity water containing oil, industrial wastewater, etc. Even though they showed better antifouling and antiwetting resistance, still lacking in achieving desirable flux. More studies on fabricating multilayer membranes without disturbing their bulk properties would be more attractive in the future. Precaution should be taken care of on the membrane not to damage while cleaning (both chemical and physical). Pretreatment of feed using other filtration methods without raising their energy consumption could be an ideal one. Due to some excellent characteristics of ceramic membranes, the combination of polymeric-ceramic membranes could be prepared as a hybrid and differentiated with polymeric membranes. Researchers can inspect the replacement of typical polymers with biodegradable polymers and nontoxic solvents in tests by considering the environment. New membranes with optimized properties could contribute to MD performance improvement and introduce them to the commercial and industrial levels.

Acknowledgments

BPT acknowledges seed funding from IIT Delhi and the Early Career Research Award (ECR/2017/001638) from the Science and Engineering Research Board (SERB, Government of India). AS and KN acknowledge the PhD scholarship from the Ministry of Education, Government of India.

References

Abdel-Karim, A., Luque-Alled, J. M., Leaper, S., Alberto, M., Fan, X., Vijayaraghavan, A., et al. (2019). PVDF membranes containing reduced graphene oxide: Effect of degree of reduction on membrane distillation performance. *Desalination*, *452*, 196–207.

Abejón, R., Saidani, H., Deratani, A., Richard, C., & Sánchez-Marcano, J. (2019). Concentration of 1,3-dimethyl-2-imidazolidinone in aqueous solutions by sweeping gas membrane distillation: From bench to industrial scale. *Membranes*, *9*(12).

Abu-Zeid, M. A. E.-R., Zhang, Y., Dong, H., Zhang, L., Chen, H.-L., & Hou, L. (2015). A comprehensive review of vacuum membrane distillation technique. *Desalination*, *356*, 1–14.

Adnan, S., Hoang, M., Wang, H., & Xie, Z. (2012). Commercial PTFE membranes for membrane distillation application: Effect of microstructure and support material. *Desalination*, *284*, 297–308.

Ahmed, F. E., Lalia, B. S., & Hashaikeh, R. (2015). A review on electrospinning for membrane fabrication: Challenges and applications. *Desalination*, *356*, 15–30.

Al-Asheh, S., Banat, F., Qtaishat, M., & Al-Khateeb, M. (2006). Concentration of sucrose solutions via vacuum membrane distillation. *Desalination*, *195*(1), 60–68.

Alkhudhiri, A., Darwish, N., & Hilal, N. (2012). Membrane distillation: A comprehensive review. *Desalination*, *287*, 2–18.

Alkhudhiri, A., Darwish, N., & Hilal, N. (2013a). Produced water treatment: Application of Air Gap Membrane Distillation. *Desalination*, *309*, 46–51.

Alkhudhiri, A., Darwish, N., & Hilal, N. (2013b). Treatment of saline solutions using air gap membrane distillation: Experimental study. *Desalination*, *323*, 2–7.

Alklaibi, A. M., & Lior, N. (2005). Membrane-distillation desalination: Status and potential. *Desalination*, *171*(2), 111–131.

Alklaibi, A. M., & Lior, N. (2006). Heat and mass transfer resistance analysis of membrane distillation. *Journal of Membrane Science*, *282*(1), 362–369.

Al-Obaidani, S., Curcio, E., Macedonio, F., Di Profio, G., Al-Hinai, H., & Drioli, E. (2008). Potential of membrane distillation in seawater desalination: Thermal efficiency, sensitivity study and cost estimation. *Journal of Membrane Science*, *323*(1), 85–98.

Amjad, Z. (1988). Calcium sulfate dihydrate (gypsum) scale formation on heat exchanger surfaces: The influence of scale inhibitors. *Journal of Colloid and Interface Science*, *123*(2), 523–536.

Anvari, A., Azimi Yancheshme, A., Kekre, K. M., & Ronen, A. (2020). State-of-the-art methods for overcoming temperature polarization in membrane distillation process: A review. *Journal of Membrane Science*, *616*, 118413.

Ashoor, B. B., Mansour, S., Giwa, A., Dufour, V., & Hasan, S. W. (2016). Principles and applications of direct contact membrane distillation (DCMD): A comprehensive review. *Desalination*, *398*, 222–246.

Banat, F. A., & Simandl, J. (1994). Theoretical and experimental study in membrane distillation. *Desalination*, *95*(1), 39–52.

Banat, F. A., & Simandl, J. (1998). Desalination by membrane distillation: A parametric study.

Bhattacharjee, C., Saxena, V. K., & Dutta, S. (2017). Fruit juice processing using membrane technology: A review. *Innovative Food Science & Emerging Technologies*, *43*, 136–153.

Bhattacharya, M., Dutta, S. K., Sikder, J., & Mandal, M. K. (2014). Computational and experimental study of chromium (VI) removal in direct contact membrane distillation. *Journal of Membrane Science*, *450*, 447–456.

Bogler, A., & Bar-Zeev, E. (2018). Membrane distillation biofouling: Impact of feedwater temperature on biofilm characteristics and membrane performance. *Environmental Science & Technology*, *52*(17), 10019–10029.

Bonyadi, S., & Chung, T.-S. (2009). Highly porous and macrovoid-free PVDF hollow fiber membranes for membrane distillation by a solvent-dope solution co-extrusion approach. *Journal of Membrane Science*, *331*(1), 66–74.
Cao, M., Gu, F., Rao, C., Fu, J., & Zhao, P. (2019). Improving the electrospinning process of fabricating nanofibrous membranes to filter PM2.5. *Science of The Total Environment*, *666*, 1011–1021.
Chang, H., Liu, B., Zhang, Z., Pawar, R., Yan, Z., Crittenden, J. C., & Vidic, R. D. (2020). A critical review of membrane wettability in membrane distillation from the perspective of interfacial interactions. *Environmental Science & Technology*, *55*(3), 1395–1418.
Chang, H.-Y., & Venault, A. (2019). Adjusting the morphology of poly(vinylidene fluoride-co-hexafluoropropylene) membranes by the VIPS process for efficient oil-rich emulsion separation. *Journal of Membrane Science*, *581*, 178–194.
Chen, T., Soroush, A., & Rahaman, M. S. (2018). Highly hydrophobic electrospun reduced graphene oxide/poly (vinylidene fluoride-co-hexafluoropropylene) membranes for use in membrane distillation. *Industrial & Engineering Chemistry Research*, *57*(43), 14535–14543.
Chen, Y.-R., Xin, R., Huang, X., Zuo, K., Tung, K.-L., & Li, Q. (2021). Wetting-resistant photothermal nanocomposite membranes for direct solar membrane distillation. *Journal of Membrane Science*, *620*, 118913.
Cheng, D., Li, N., & Zhang, J. (2018). Modeling and multi-objective optimization of vacuum membrane distillation for enhancement of water productivity and thermal efficiency in desalination. *Chemical Engineering Research and Design*, *132*, 697–713.
Chiam, C.-K., & Sarbatly, R. (2013). Vacuum membrane distillation processes for aqueous solution treatment—A review. *Chemical Engineering and Processing: Process Intensification*, *74*, 27–54.
Cipollina, A., Di Sparti, M. G., Tamburini, A., & Micale, G. (2012). Development of a membrane distillation module for solar energy seawater desalination. *Chemical Engineering Research and Design*, *90*(12), 2101–2121.
Couto, C. F., Amaral, M. C. S., Lange, L. C., & Santos, L. V. D. S. (2019). Effect of humic acid concentration on pharmaceutically active compounds (PhACs) rejection by direct contact membrane distillation (DCMD). *Separation and Purification Technology*, *212*, 920–928.
Criscuoli, A., Bafaro, P., & Drioli, E. (2013). Vacuum membrane distillation for purifying waters containing arsenic. *Desalination*, *323*, 17–21.
Criscuoli, A., & Drioli, E. (2020). Date juice concentration by vacuum membrane distillation. *Separation and Purification Technology*, *251*, 117301.
Curcio, E., & Drioli, E. (2005). Membrane Distillation and Related Operations—A review. *Separation & Purification Reviews*, *34*(1), 35–86.
Dehban, A., Kargari, A., & Ashtiani, F. Z. (2020). Preparation and optimization of antifouling PPSU/PES/SiO_2 nanocomposite ultrafiltration membranes by VIPS-NIPS technique. *Journal of Industrial and Engineering Chemistry*, *88*, 292–311.
Deka, B. J., Guo, J., & An, A. K. (2021). Robust dual-layered omniphobic electrospun membrane with anti-wetting and anti-scaling functionalised for membrane distillation application. *Journal of Membrane Science*, *624*, 119089.
Dow, N., Gray, S., Li, J.-D., Zhang, J., Ostarcevic, E., Liubinas, A., & Duke, M. (2016). Pilot trial of membrane distillation driven by low grade waste heat: Membrane fouling and energy assessment. *Desalination*, *391*, 30–42.
Dow, N., Villalobos García, J., Niadoo, L., Milne, N., Zhang, J., Gray, S., & Duke, M. (2017). Demonstration of membrane distillation on textile waste water: Assessment of long term performance, membrane cleaning and waste heat integration. *Environmental Science: Water Research & Technology*, *3*(3), 433–449.
Drioli, E., Ali, A., & Macedonio, F. (2015). Membrane distillation: Recent developments and perspectives. *Desalination*, *356*, 56–84.
Drioli, E., Laganà, F., Criscuoli, A., & Barbieri, G. (1999). Integrated membrane operations in desalination processes. *Desalination*, *122*(2), 141–145.
Drioli, E., & Wu, Y. (1985). Membrane distillation: An experimental study. *Desalination*, *53*(1), 339–346.
El-Abbassi, A., Hafidi, A., Khayet, M., & García-Payo, M. C. (2013). Integrated direct contact membrane distillation for olive mill wastewater treatment. *Desalination*, *323*, 31–38.
El-Bourawi, M. S., Ding, Z., Ma, R., & Khayet, M. (2006). A framework for better understanding membrane distillation separation process. *Journal of Membrane Science*, *285*(1), 4–29.
Esato, K., & Eiseman, B. (1975). Experimental evaluation of Gore-Tex membrane oxygenator. *The Journal of Thoracic and Cardiovascular Surgery*, *69*(5), 690–697.

Esfahani, M. R., Aktij, S. A., Dabaghian, Z., Firouzjaei, M. D., Rahimpour, A., Eke, J., ... Koutahzadeh, N. (2019). Nanocomposite membranes for water separation and purification: Fabrication, modification, and applications. *Separation and Purification Technology*, *213*, 465–499.
Eykens, L., De Sitter, K., Dotremont, C., Pinoy, L., & Van der Bruggen, B. (2016). How to optimize the membrane properties for membrane distillation: A review. *Industrial & Engineering Chemistry Research*, *55*(35), 9333–9343.
Eykens, L., De Sitter, K., Dotremont, C., Pinoy, L., & Van der Bruggen, B. (2017). Membrane synthesis for membrane distillation: A review. *Separation and Purification Technology*, *182*, 36–51.
Eykens, L., Hitsov, I., De Sitter, K., Dotremont, C., Pinoy, L., Nopens, I., & Van der Bruggen, B. (2016). Influence of membrane thickness and process conditions on direct contact membrane distillation at different salinities. *Journal of Membrane Science*, *498*, 353–364.
Ezugbe, E. O., & Rathilal, S. (2020). Membrane technologies in wastewater treatment: A review. *Membranes*.
Fan, H., & Peng, Y. (2012). Application of PVDF membranes in desalination and comparison of the VMD and DCMD processes. *Chemical Engineering Science*, *79*, 94–102.
Fang, C., Liu, W., Zhang, P., Yao, M., Rajabzadeh, S., Kato, N., ... Matsuyama, H. (2021). Controlling the inner surface pore and spherulite structures of PVDF hollow fiber membranes in thermally induced phase separation using triple-orifice spinneret for membrane distillation. *Separation and Purification Technology*, *258*, 117988.
Feng, C., Shi, B., Li, G., & Wu, Y. (2004). Preparation and properties of microporous membrane from poly(vinylidene fluoride-co-tetrafluoroethylene) (F2.4) for membrane distillation. *Journal of Membrane Science*, *237*(1), 15–24.
Feng, X., Jiang, L. Y., & Song, Y. (2016). Titanium white sulfuric acid concentration by direct contact membrane distillation. *Chemical Engineering Journal*, *285*, 101–111.
Findley, M. E. (1967). Vaporization through porous membranes. *Industrial & Engineering Chemistry Process Design and Development*, *6*(2), 226–230.
Findley, M. E., Tanna, V. V., Rao, Y. B., & Yeh, C. L. (1969). Mass and heat transfer relations in evaporation through porous membranes. *AIChE Journal*, *15*(4), 483–489.
Franken, A. C. M., Nolten, J. A. M., Mulder, M. H. V., Bargeman, D., & Smolders, C. A. (1987). Wetting criteria for the applicability of membrane distillation. *Journal of Membrane Science*, *33*(3), 315–328.
García-Fernández, L., García-Payo, C., & Khayet, M. (2017). Hollow fiber membranes with different external corrugated surfaces for desalination by membrane distillation. *Applied Surface Science*, *416*, 932–946.
García-Payo, M. C., Izquierdo-Gil, M. A., & Fernández-Pineda, C. (2000). Air gap membrane distillation of aqueous alcohol solutions. *Journal of Membrane Science*, *169*(1), 61–80.
Gopal, R., Kaur, S., Ma, Z., Chan, C., Ramakrishna, S., & Matsuura, T. (2006). Electrospun nanofibrous filtration membrane. *Journal of Membrane Science*, *281*(1), 581–586.
Gryta, M. (2005). Long-term performance of membrane distillation process. *Journal of Membrane Science*, *265*(1), 153–159.
Gryta, M. (2007a). Effect of iron oxides scaling on the MD process performance. *Desalination*, *216*(1), 88–102.
Gryta, M. (2007b). Influence of polypropylene membrane surface porosity on the performance of membrane distillation process. *Journal of Membrane Science*, *287*(1), 67–78.
Gryta, M. (2008a). Alkaline scaling in the membrane distillation process. *Desalination*, *228*(1), 128–134.
Gryta, M. (2008b). Fouling in direct contact membrane distillation process. *Journal of Membrane Science*, *325*(1), 383–394.
Gryta, M. (2010). Desalination of thermally softened water by membrane distillation process. *Desalination*, *257*(1), 30–35.
Gryta, M. (2011). The influence of magnetic water treatment on $CaCO_3$ scale formation in membrane distillation process. *Separation and Purification Technology*, *80*(2), 293–299.
Gryta, M. (2012). Polyphosphates used for membrane scaling inhibition during water desalination by membrane distillation. *Desalination*, *285*, 170–176.
Guillen-Burrieza, E., Ruiz-Aguirre, A., Zaragoza, G., & Arafat, H. A. (2014). Membrane fouling and cleaning in long term plant-scale membrane distillation operations. *Journal of Membrane Science*, *468*, 360–372.
Gunko, S., Verbych, S., Bryk, M., & Hilal, N. (2006). Concentration of apple juice using direct contact membrane distillation. *Desalination*, *190*(1), 117–124.
Guo, F., Servi, A., Liu, A., Gleason, K. K., & Rutledge, G. C. (2015). Desalination by membrane distillation using electrospun polyamide fiber membranes with surface fluorination by chemical vapor deposition. *ACS Applied Materials & Interfaces*, *7*(15), 8225–8232.
Gupta, I., Chakraborty, J., Roy, S., Farinas, E. T., & Mitra, S. (2021). Nanocarbon immobilized membranes for generating bacteria and endotoxin free water via membrane distillation. *Separation and Purification Technology*, *259*, 118133.

Henderyckx, Y. (1967). Diffusion doublet research. *Desalination*, *3*(2), 237–242.
Horseman, T., Yin, Y., Christie, K. S. S., Wang, Z., Tong, T., & Lin, S. (2021). Wetting, scaling, and fouling in membrane distillation: State-of-the-art insights on fundamental mechanisms and mitigation strategies. *ACS ES&T Engineering*, *1*(1), 117–140.
Hou, D., Dai, G., Wang, J., Fan, H., Luan, Z., & Fu, C. (2013). Boron removal and desalination from seawater by PVDF flat-sheet membrane through direct contact membrane distillation. *Desalination*, *326*, 115–124.
Huang, Q.-L., Xiao, C.-F., Hu, X.-Y., & Li, X.-F. (2011). Study on the effects and properties of hydrophobic poly (tetrafluoroethylene) membrane. *Desalination*, *277*(1), 187–192.
Huang, Y.-X., Wang, Z., Jin, J., & Lin, S. (2017). Novel janus membrane for membrane distillation with simultaneous fouling and wetting resistance. *Environmental Science & Technology*, *51*(22), 13304–13310.
Ibrahim, S. S., & Alsalhy, Q. F. (2013). Modeling and simulation for direct contact membrane distillation in hollow fiber modules. *AIChE Journal*, *59*(2), 589–603.
Ismail, N., Venault, A., Mikkola, J.-P., Bouyer, D., Drioli, E., & Tavajohi Hassan Kiadeh, N. (2020). Investigating the potential of membranes formed by the vapor induced phase separation process. *Journal of Membrane Science*, *597*, 117601.
Izquierdo-Gil, M. A., García-Payo, M. C., & Fernández-Pineda, C. (1999). Air gap membrane distillation of sucrose aqueous solutions. *Journal of Membrane Science*, *155*(2), 291–307.
Jacob, P., Laborie, S., & Cabassud, C. (2018). Visualizing and evaluating wetting in membrane distillation: New methodology and indicators based on detection of dissolved tracer intrusion (DDTI). *Desalination*, *443*, 307–322.
Jung, J. T., Kim, J. F., Wang, H. H., di Nicolo, E., Drioli, E., & Lee, Y. M. (2016). Understanding the non-solvent induced phase separation (NIPS) effect during the fabrication of microporous PVDF membranes via thermally induced phase separation (TIPS). *Journal of Membrane Science*, *514*, 250–263.
Kalla, S., Upadhyaya, S., & Singh, K. (2019). Principles and advancements of air gap membrane distillation. *Reviews in Chemical Engineering*, *35*(7), 817–859.
Kalla, S., Upadhyaya, S., Singh, K., & Baghel, R. (2019). Experimental and mathematical study of air gap membrane distillation for aqueous HCl azeotropic separation. *Journal of Chemical Technology & Biotechnology*, *94*(1), 63–78.
Khalifa, A., Ahmad, H., Antar, M., Laoui, T., & Khayet, M. (2017). Experimental and theoretical investigations on water desalination using direct contact membrane distillation. *Desalination*, *404*, 22–34.
Khayet, M. (2011). Membranes and theoretical modeling of membrane distillation: A review. *Advances in Colloid and Interface Science*, *164*(1), 56–88.
Khayet, M. (2013). Solar desalination by membrane distillation: Dispersion in energy consumption analysis and water production costs (a review). *Desalination*, *308*, 89–101.
Khayet, M. (2016). Fouling and scaling in desalination. *Desalination*, *393*, 1.
Khayet, M., & Matsuura, T. (2001). Preparation and characterization of polyvinylidene fluoride membranes for membrane distillation. *Industrial & Engineering Chemistry Research*, *40*(24), 5710–5718.
Khayet, M., & Matsuura, T. (2011). *Membrane distillation: Principles and applications*. Elsevier.
Khayet, M., Cojocaru, C., & Baroudi, A. (2012). Modeling and optimization of sweeping gas membrane distillation. *Desalination*, *287*, 159–166.
Khayet, M., Cojocaru, C., & García-Payo, M. C. (2010). Experimental design and optimization of asymmetric flat-sheet membranes prepared for direct contact membrane distillation. *Journal of Membrane Science*, *351*(1), 234–245.
Khayet, M., Godino, M. P., & Mengual, J. I. (2003). Theoretical and experimental studies on desalination using the sweeping gas membrane distillation method. *Desalination*, *157*(1), 297–305.
Khayet, M., Velázquez, A., & Mengual, J. I. (2004). Modelling mass transport through a porous partition: Effect of pore size distribution. *Journal of Non-Equilibrium Thermodynamics*, *29*(3), 279–299.
Kim, W.-J., Campanella, O., & Heldman, D. R. (2021). Predicting the performance of direct contact membrane distillation (DCMD): Mathematical determination of appropriate tortuosity based on porosity. *Journal of Food Engineering*, *294*, 110400.
Kujawska, A., Kujawski, J. K., Bryjak, M., Cichosz, M., & Kujawski, W. (2016). Removal of volatile organic compounds from aqueous solutions applying thermally driven membrane processes. 2. Air gap membrane distillation. *Journal of Membrane Science*, *499*, 245–256.
Laganà, F., Barbieri, G., & Drioli, E. (2000). Direct contact membrane distillation: Modelling and concentration experiments. *Journal of Membrane Science*, *166*(1), 1–11.

Lalia, B. S., Kochkodan, V., Hashaikeh, R., & Hilal, N. (2013). A review on membrane fabrication: Structure, properties and performance relationship. *Desalination*, *326*, 77–95.
Lawson, K. W., & Lloyd, D. R. (1997). Membrane distillation. *Journal of Membrane Science*, *124*(1), 1–25.
Le, N. L., & Nunes, S. P. (2016). Materials and membrane technologies for water and energy sustainability. *Sustainable Materials and Technologies*, *7*, 1–28.
Leaper, S., Abdel-Karim, A., Gad-Allah, T. A., & Gorgojo, P. (2019). Air-gap membrane distillation as a one-step process for textile wastewater treatment. *Chemical Engineering Journal*, *360*, 1330–1340.
Lee, J., Boo, C., Ryu, W.-H., Taylor, A. D., & Elimelech, M. (2016). Development of omniphobic desalination membranes using a charged electrospun nanofiber scaffold. *ACS Applied Materials & Interfaces*, *8*(17), 11154–11161.
Lee, W. J., Ng, Z. C., Hubadillah, S. K., Goh, P. S., Lau, W. J., Othman, M. H. D., … Hilal, N. (2020). Fouling mitigation in forward osmosis and membrane distillation for desalination. *Desalination*, *480*, 114338.
Leitch, M. E., Li, C., Ikkala, O., Mauter, M. S., & Lowry, G. V. (2016). Bacterial Nanocellulose aerogel membranes: Novel high-porosity materials for membrane distillation. *Environmental Science & Technology Letters*, *3*(3), 85–91.
Li, B., & Sirkar, K. K. (2005). Novel membrane and device for vacuum membrane distillation-based desalination process. *Journal of Membrane Science*, *257*(1), 60–75.
Li, J., Ren, L.-F., Shao, J., Tu, Y., Ma, Z., Lin, Y., & He, Y. (2020). Fabrication of triple layer composite membrane and its application in membrane distillation (MD): Effect of hydrophobic-hydrophilic membrane structure on MD performance. *Separation and Purification Technology*, *234*, 116087.
Li, J.-M., Xu, Z.-K., Liu, Z.-M., Yuan, W.-F., Xiang, H., Wang, S.-Y., & Xu, Y.-Y. (2003). Microporous polypropylene and polyethylene hollow fiber membranes. Part 3. Experimental studies on membrane distillation for desalination. *Desalination*, *155*(2), 153–156.
Li, X., Wang, C., Yang, Y., Wang, X., Zhu, M., & Hsiao, B. S. (2014). Dual-biomimetic superhydrophobic electrospun polystyrene nanofibrous membranes for membrane distillation. *ACS Applied Materials and Interface*, *6*(4), 2423–2440.
Li, Z., Peng, Y., Dong, Y., Fan, H., Chen, P., Qiu, L., et al. (2014). Effects of thermal efficiency in DCMD and the preparation of membranes with low thermal conductivity. *Applied Surface Science*, *317*, 338–349.
Liao, Y., Loh, C.-H., Tian, M., Wang, R., & Fane, A. G. (2018). Progress in electrospun polymeric nanofibrous membranes for water treatment: Fabrication, modification and applications. *Progress in Polymer Science*, *77*, 69–94.
Lin, S., Nejati, S., Boo, C., Hu, Y., Osuji, C. O., & Elimelech, M. (2014). Omniphobic membrane for robust membrane distillation. *Environmental Science & Technology Letters*, *1*(11), 443–447.
Liu, H., & Wang, J. (2013). Treatment of radioactive wastewater using direct contact membrane distillation. *Journal of Hazardous Materials*, *261*, 307–315.
Lu, K. J., Chen, Y., & Chung, T.-S. (2019). Design of omniphobic interfaces for membrane distillation – A review. *Water Research*, *162*, 64–77.
Luo, A., & Lior, N. (2016). Critical review of membrane distillation performance criteria. *Desalination and Water Treatment*, *57*(43), 20093–20140.
Ma, J., Irfan, H. M., Wang, Y., Feng, X., & Xu, D. (2018). Recovering wastewater in a cooling water system with thermal membrane distillation. *Industrial & Engineering Chemistry Research*, *57*(31), 10491–10499.
Manickam, S. S., Gelb, J., & McCutcheon, J. R. (2014). Pore structure characterization of asymmetric membranes: Non-destructive characterization of porosity and tortuosity. *Journal of Membrane Science*, *454*, 549–554.
Martínez, L., Florido-Díaz, F. J., Hernández, A., & Prádanos, P. (2003). Estimation of vapor transfer coefficient of hydrophobic porous membranes for applications in membrane distillation. *Separation and Purification Technology*, *33*(1), 45–55.
Martínez, L., & Rodríguez-Maroto, J. M. (2008). Membrane thickness reduction effects on direct contact membrane distillation performance. *Journal of Membrane Science*, *312*(1), 143–156.
Matheswaran, M., Kwon, T. O., Kim, J. W., & Moon, I. S. (2007). Factors affecting flux and water separation performance in air gap membrane distillation. *Journal of Industrial and Engineering Chemistry*, *13*(6), 965–970.
Meindersma, G. W., Guijt, C. M., & de Haan, A. B. (2006). Desalination and water recycling by air gap membrane distillation. *Desalination*, *187*(1), 291–301.
Mistry, K. H., Mitsos, A., & Lienhard, J. H. (2011). Optimal operating conditions and configurations for humidification–dehumidification desalination cycles. *International Journal of Thermal Sciences*, *50*(5), 779–789.
Moejes, S. N., van Wonderen, G. J., Bitter, J. H., & van Boxtel, A. J. B. (2020). Assessment of air gap membrane distillation for milk concentration. *Journal of Membrane Science*, *594*, 117403.

Mohammad, A. W., Teow, Y. H., Ang, W. L., Chung, Y. T., Oatley-Radcliffe, D. L., & Hilal, N. (2015). Nanofiltration membranes review: Recent advances and future prospects. *Desalination*, *356*, 226–254.
Munirasu, S., Banat, F., Durrani, A. A., & Haija, M. A. (2017). Intrinsically superhydrophobic PVDF membrane by phase inversion for membrane distillation. *Desalination*, *417*, 77–86.
Nghiem, L. D., & Cath, T. (2011). A scaling mitigation approach during direct contact membrane distillation. *Separation and Purification Technology*, *80*(2), 315–322.
Nguyen, Q.-M., & Lee, S. (2015). Fouling analysis and control in a DCMD process for SWRO brine. *Desalination*, *367*, 21–27.
Nguyen, Q. T., Alaoui, O. T., Yang, H., & Mbareck, C. (2010). Dry-cast process for synthetic microporous membranes: Physico-chemical analyses through morphological studies. *Journal of Membrane Science*, *358*(1), 13–25.
Niknejad, A. S., Bazgir, S., Sadeghzadeh, A., & Shirazi, M. M. A. (2020). Styrene-acrylonitrile (SAN) nanofibrous membranes with unique properties for desalination by direct contact membrane distillation (DCMD) process. *Desalination*, *488*, 114502.
Nthunya, L. N., Gutierrez, L., Derese, S., Nxumalo, E. N., Verliefde, A. R., Mamba, B. B., & Mhlanga, S. D. (2019). A review of nanoparticle-enhanced membrane distillation membranes: Membrane synthesis and applications in water treatment. *Journal of Chemical Technology & Biotechnology*, *94*(9), 2757–2771.
Pagliero, M., Bottino, A., Comite, A., & Costa, C. (2020). Novel hydrophobic PVDF membranes prepared by nonsolvent induced phase separation for membrane distillation. *Journal of Membrane Science*, *596*, 117575.
Paluri, S., Maleky, F., & Heldman, D. R. (2017). Development of a structure-based model for moisture diffusion in multiphase lipid networks. *Journal of Food Engineering*, *214*, 60–68.
Pangarkar, B. L., Sane, M. G., Parjane, S. B., & Guddad, M. (2014). Status of membrane distillation for water and wastewater treatment—A review. *Desalination and Water Treatment*, *52*(28–30), 5199–5218.
Pervin, R., Ghosh, P., & Basavaraj, M. G. (2019). Tailoring pore distribution in polymer films via evaporation induced phase separation. *RSC Advances*, *9*(27), 15593–15605.
Prince, J. A., Anbharasi, V., Shanmugasundaram, T. S., & Singh, G. (2013). Preparation and characterization of novel triple layer hydrophilic–hydrophobic composite membrane for desalination using air gap membrane distillation. *Separation and Purification Technology*, *118*, 598–603.
Prince, J. A., Rana, D., Matsuura, T., Ayyanar, N., Shanmugasundaram, T. S., & Singh, G. (2014a). Nanofiber based triple layer hydro-philic/-phobic membrane – A solution for pore wetting in membrane distillation. *Scientific Reports*, *4*(1), 6949.
Prince, J. A., Rana, D., Matsuura, T., Ayyanar, N., Shanmugasundaram, T. S., & Singh, G. (2014b). Nanofiber based triple layer hydro-philic/-phobic membrane—A solution for pore wetting in membrane distillation. *Scientific Reports*, *4*.
Prince, J. A., Singh, G., Rana, D., Matsuura, T., Anbharasi, V., & Shanmugasundaram, T. S. (2012). Preparation and characterization of highly hydrophobic poly(vinylidene fluoride) – Clay nanocomposite nanofiber membranes (PVDF–clay NNMs) for desalination using direct contact membrane distillation. *Journal of Membrane Science*, *397–398*, 80–86.
Qtaishat, M., Matsuura, T., Kruczek, B., & Khayet, M. (2008). Heat and mass transfer analysis in direct contact membrane distillation. *Desalination*, *219*(1), 272–292.
Qu, F., Yan, Z., Yu, H., Fan, G., Pang, H., Rong, H., & He, J. (2020). Effect of residual commercial antiscalants on gypsum scaling and membrane wetting during direct contact membrane distillation. *Desalination*, *486*, 114493.
Ray, S. S., Chen, S.-S., Chang, H.-M., Dan Thanh, C. N., Quang Le, H., & Nguyen, N. C. (2018). Enhanced desalination using a three-layer OTMS based superhydrophobic membrane for a membrane distillation process. *RSC Advances*, *8*(18), 9640–9650.
Ray, S. S., Chen, S.-S., Li, C.-W., Nguyen, N. C., & Nguyen, H. T. (2016). A comprehensive review: Electrospinning technique for fabrication and surface modification of membranes for water treatment application. *RSC Advances*, *6*(88), 85495–85514.
Rezaei, M., Warsinger, D. M., Lienhard V, J. H., Duke, M. C., Matsuura, T., & Samhaber, W. M. (2018). Wetting phenomena in membrane distillation: Mechanisms, reversal, and prevention. *Water Research*, *139*, 329–352.
Ricci, B. C., Skibinski, B., Koch, K., Mancel, C., Celestino, C. Q., Cunha, I. L. C., & Amaral, M. C. S. (2019). Critical performance assessment of a submerged hybrid forward osmosis – Membrane distillation system. *Desalination*, *468*, 114082.

Roy, S., Bhadra, M., & Mitra, S. (2014). Enhanced desalination via functionalized carbon nanotube immobilized membrane in direct contact membrane distillation. *Separation and Purification Technology*, *136*, 58–65.
Sabzekar, M., Pourafshari Chenar, M., Maghsoud, Z., Mostaghisi, O., García-Payo, M. C., & Khayet, M. (2021). Cyclic olefin polymer as a novel membrane material for membrane distillation applications. *Journal of Membrane Science*, *621*, 118845.
Said, I. A., Chomiak, T., Floyd, J., & Li, Q. (2020). Sweeping gas membrane distillation (SGMD) for wastewater treatment, concentration, and desalination: A comprehensive review. *Chemical Engineering and Processing - Process Intensification*, *153*, 107960.
Sakai, K., Koyano, T., Muroi, T., & Tamura, M. (1988). Effects of temperature and concentration polarization on water vapour permeability for blood in membrane distillation. *The Chemical Engineering Journal*, *38*(3), B33–B39.
Sarada, T., Sawyer, L. C., & Ostler, M. I. (1983). Three dimensional structure of celgard® microporous membranes. *Journal of Membrane Science*, *15*(1), 97–113.
Sarbatly, R., & Chiam, C.-K. (2013). Evaluation of geothermal energy in desalination by vacuum membrane distillation. *Applied Energy*, *112*, 737–746.
Schneider, K., & van Gassel, T. J. (1984). Membrandestillation. *Chemie Ingenieur Technik*, *56*(7), 514–521.
Schofield, R. W., Fane, A. G., & Fell, C. J. D. (1987). Heat and mass transfer in membrane distillation. *Journal of Membrane Science*, *33*(3), 299–313.
Schofield, R. W., Fane, A. G., & Fell, C. J. D. (1990). Gas and vapour transport through microporous membranes. I. Knudsen-Poiseuille transition. *Journal of Membrane Science*, *53*(1), 159–171.
Shirazi, M. M. A., Kargari, A., Bastani, D., & Fatehi, L. (2014). Production of drinking water from seawater using membrane distillation (MD) alternative: Direct contact MD and sweeping gas MD approaches. *Desalination and Water Treatment*, *52*(13–15), 2372–2381.
Shirazi, M. M. A., Kargari, A., & Tabatabaei, M. (2014). Evaluation of commercial PTFE membranes in desalination by direct contact membrane distillation. *Chemical Engineering and Processing: Process Intensification*, *76*, 16–25.
Shirazi, M. M. A., Kargari, A., & Tabatabaei, M. (2015). Sweeping gas membrane distillation (SGMD) as an alternative for integration of bioethanol processing: Study on a commercial membrane and operating parameters. *Chemical Engineering Communications*, *202*(4), 457–466.
Shirsath, G. B., Muralidhar, K., & Pala, R. G. S. (2020). Variable air gap membrane distillation for hybrid solar desalination. *Journal of Environmental Chemical Engineering*, *8*(3), 103751.
Silva, R. F., De Francesco, M., & Pozio, A. (2004). Solution-cast Nafion® ionomer membranes: Preparation and characterization. *Electrochimica Acta*, *49*(19), 3211–3219.
Singh, D., & Sirkar, K. K. (2012). Desalination of brine and produced water by direct contact membrane distillation at high temperatures and pressures. *Journal of Membrane Science*, *389*, 380–388.
Souhaimi, M. K., & Matsuura, T. (2011). Membrane distillation: Principles and applications.
Srisurichan, S., Jiraratananon, R., & Fane, A. G. (2006). Mass transfer mechanisms and transport resistances in direct contact membrane distillation process. *Journal of Membrane Science*, *277*(1), 186–194.
Su, C., Li, Y., Cao, H., Lu, C., Li, Y., Chang, J., & Duan, F. (2019). Novel PTFE hollow fiber membrane fabricated by emulsion electrospinning and sintering for membrane distillation. *Journal of Membrane Science*, *583*, 200–208.
Subramani, A., & Jacangelo, J. G. (2015). Emerging desalination technologies for water treatment: A critical review. *Water Research*, *75*, 164–187.
Summers, E. K., Arafat, H. A., & Lienhard, J. H. (2012). Energy efficiency comparison of single-stage membrane distillation (MD) desalination cycles in different configurations. *Desalination*, *290*, 54–66.
Tan, X., & Rodrigue, D. (2019). A review on porous polymeric membrane preparation. part I: Production techniques with polysulfone and poly (vinylidene fluoride). *Polymers*, *11*(7), 1160.
Teoh, M. M., Chung, T.-S., & Yeo, Y. S. (2011). Dual-layer PVDF/PTFE composite hollow fibers with a thin macrovoid-free selective layer for water production via membrane distillation. *Chemical Engineering Journal*, *171*(2), 684–691.
Tijing, L. D., Woo, Y. C., Choi, J.-S., Lee, S., Kim, S.-H., & Shon, H. K. (2015). Fouling and its control in membrane distillation—A review. *Journal of Membrane Science*, *475*, 215–244.

Topaloglu, D., Tilki, Y. M., Aksu, S., Yilmaz, T. N., Celebi, E. E., Oncel, S., & Aydiner, C. (2018). Novel technological solutions for eco-protective water supply by economical and sustainable seawater desalination. *Chemical Engineering Research and Design*, *136*, 177–198.
Ullah, R., Khraisheh, M., Esteves, R. J., McLeskey, J. T., AlGhouti, M., Gad-el-Hak, M., et al. (2018). Energy efficiency of direct contact membrane distillation. *Desalination*, *433*, 56–67.
Van Haute, A., & Henderyckx, Y. (1967). The permeability of membranes to water vapor. *Desalination*, *3*(2), 169–173.
Wan, C. F., Yang, T., Lipscomb, G. G., Stookey, D. J., & Chung, T.-S. (2017). Design and fabrication of hollow fiber membrane modules. *Journal of Membrane Science*, *538*, 96–107.
Wang, J., Zheng, L., Wu, Z., Zhang, Y., & Zhang, X. (2016). Fabrication of hydrophobic flat sheet and hollow fiber membranes from PVDF and PVDF-CTFE for membrane distillation. *Journal of Membrane Science*, *497*, 183–193.
Wang, M., Liu, G., Yu, H., Lee, S.-H., Wang, L., Zheng, J., … Lee, J. K. (2018). ZnO nanorod array modified PVDF membrane with superhydrophobic surface for vacuum membrane distillation application. *ACS Applied Materials & Interfaces*, *10*(16), 13452–13461.
Wang, Z., Hou, D., & Lin, S. (2016). Composite membrane with underwater-oleophobic surface for anti-oil-fouling membrane distillation. *Environmental Science & Technology*, *50*(7), 3866–3874.
Wang, Z., & Lin, S. (2017). Membrane fouling and wetting in membrane distillation and their mitigation by novel membranes with special wettability. *Water Research*, *112*, 38–47.
Warsinger, D. E. M., Swaminathan, J., Maswadeh, L. A., & Lienhard V, J. H. (2015). Superhydrophobic condenser surfaces for air gap membrane distillation. *Journal of Membrane Science*, *492*, 578–587.
Warsinger, D. M., Servi, A., Connors, G. B., Mavukkandy, M. O., Arafat, H. A., Gleason, K. K., & Lienhard, V. J. H. (2017). Reversing membrane wetting in membrane distillation: Comparing dryout to backwashing with pressurized air. *Environmental Science: Water Research & Technology*, *3*(5), 930–939.
Warsinger, D. M., Swaminathan, J., Guillen-Burrieza, E., Arafat, H. A., & Lienhard, V. J. H. (2015a). Scaling and fouling in membrane distillation for desalination applications: A review. *Desalination*, *356*, 294–313.
Warsinger, D. M., Swaminathan, J., Guillen-Burrieza, E., Arafat, H. A., & Lienhard V, J. H. (2015b). *Scaling and fouling in membrane distillation for desalination applications: A review* (Vol. 356, pp. 294–313). Elsevier.
Weyl, P. K. (1967). Recovery of demineralized water from saline waters: Google Patents.
Wikol, M., Hartmann, B., Brendle, J., Crane, M., Beuscher, U., Brake, J., & Shickel, T. (2008). Expanded polytetrafluoroethylene membranes and their applications. *Drugs and the Pharmaceutical Sciences*, *174*, 619.
Winter, D., Koschikowski, J., Düver, D., Hertel, P., & Beuscher, U. (2013). Evaluation of MD process performance: Effect of backing structures and membrane properties under different operating conditions. *Desalination*, *323*, 120–133.
Winter, D., Koschikowski, J., & Wieghaus, M. (2011). Desalination using membrane distillation: Experimental studies on full scale spiral wound modules. *Journal of Membrane Science*, *375*(1), 104–112.
Woldemariam, D., Kullab, A., Fortkamp, U., Magner, J., Royen, H., & Martin, A. (2016). Membrane distillation pilot plant trials with pharmaceutical residues and energy demand analysis. *Chemical Engineering Journal*, *306*, 471–483.
Xie, Z., Duong, T., Hoang, M., Nguyen, C., & Bolto, B. (2009). Ammonia removal by sweep gas membrane distillation. *Water Research*, *43*(6), 1693–1699.
Xing, Y., Anthony, G. F., & Rong, W. (2014). *Membrane distillation: Now and future* (pp. 373–424). New Jersey: John Wiley & Sons Inc.
Xu, Z., Liu, Z., Song, P., & Xiao, C. (2017). Fabrication of super-hydrophobic polypropylene hollow fiber membrane and its application in membrane distillation. *Desalination*, *414*, 10–17.
Yao, M., Tijing, L. D., Naidu, G., Kim, S.-H., Matsuyama, H., Fane, A. G., & Shon, H. K. (2020). A review of membrane wettability for the treatment of saline water deploying membrane distillation. *Desalination*, *479*, 114312.
Zaragoza, G., Andrés-Mañas, J. A., & Ruiz-Aguirre, A. (2018). Commercial scale membrane distillation for solar desalination. *NPJ Clean Water*, *1*(1), 20.
Zeweldi, H. G., Bendoy, A. P., Park, M. J., Shon, H. K., Johnson, E. M., Kim, H.-S., … Nisola, G. M. (2021). Forward osmosis with direct contact membrane distillation using tetrabutylphosphonium p-toluenesulfonate as an effective and safe thermo-recyclable osmotic agent for seawater desalination. *Chemosphere*, *263*, 128070.
Zhang, J., Li, N., Ng, D., Ike, I. A., Xie, Z., & Gray, S. (2019). Depletion of VOC in wastewater by vacuum membrane distillation using a dual-layer membrane: Mechanism of mass transfer and selectivity. *Environmental Science: Water Research & Technology*, *5*(1), 119–130.

Zhang, Y., Yang, B., Li, K., Hou, D., Zhao, C., & Wang, J. (2017). Electrospun porous poly(tetrafluoroethylene-co-hexafluoropropylene-co-vinylidene fluoride) membranes for membrane distillation. *RSC Advances*, *7*(89), 56183–56193.

Zhao, Z.-P., Xu, L., Shang, X., & Chen, K. (2013). Water regeneration from human urine by vacuum membrane distillation and analysis of membrane fouling characteristics. *Separation and Purification Technology*, *118*, 369–376.

Zhu, H., Wang, H., Wang, F., Guo, Y., Zhang, H., & Chen, J. (2013). Preparation and properties of PTFE hollow fiber membranes for desalination through vacuum membrane distillation. *Journal of Membrane Science*, *446*, 145–153.

Zuo, J., Bonyadi, S., & Chung, T.-S. (2016). Exploring the potential of commercial polyethylene membranes for desalination by membrane distillation. *Journal of Membrane Science*, *497*, 239–247.

Zuo, J., Chung, T.-S., O'Brien, G. S., & Kosar, W. (2017). Hydrophobic/hydrophilic PVDF/Ultem® dual-layer hollow fiber membranes with enhanced mechanical properties for vacuum membrane distillation. *Journal of Membrane Science*, *523*, 103–110.

Index

Note: Page numbers followed by "*f*" and "*t*" refer to figures and tables, respectively.

A

Aquaporins, 292
Asymmetric polymer-based reverse osmosis membranes
  CA membrane, 313
  cellulose acetate, 315–316
  finger-like structure, 314*f*
  phase inversion method, 315*f*
  polymer, solvent, and nonsolvent, 315*t*
  skin layer and porous support, 312–313
  sponge-like structure, 313, 314*f*
  ternary diagram, 313–314

B

Bioinspired membranes applications
  amino acid ionic liquid-modified, 249*f*
  3D interwoven silicon sponge formation, 250*f*
  dopamine-based, 238–246
  dopamine/trimesoyl chloride composite, 239–240
  layer-by-layer electrostatic assembly, 241–242
  mussel polydopamine-based, 241*f*
  nanofiltration, 240*f*, 245*f*
  PDA-a-LBL nanofiltration fabrication, 242*f*
  PDA and polyetheylenimine, 242–243
  PDA formation, 243
  polyethylene glycol-based nanofiltration, 244*f*
  tannic acid-based, 246–249
    hollow fiber configuration, 249
  toxic pollutants, 244–246
Biomimetic, and stimuli-responsive nanofiltration membranes
  bioinspired and their applications, 238–251
  commercial status and future directions, 264–265
  membranes, 251–257
  stimuli-responsive/smart, 257–264
Biomimetic membranes, 456–457, 457*t*
  aquaporin, 251–254, 252*f*, 253*t*
  CA NF hollow fiber, 451
  double-skinned forward osmosis (FO), 448*f*
  hollow fiber configuration, 256–257
  Langmuir–Blodgett method, 252
  lipid and microporous support layer, 448–449
  lipid- and polymer-based vesicle, 254*t*
  low flux and fouling problems, 252*f*
  performance, 450*t*
  pore size distribution, 451
  schematic of, 255*f*
  single-layer hollow fiber forward osmosis, 452*t*
Biomineralization, 250

C

Capacitive deionization-based technology
  cell configuration and operation, 520*f*
  efficiency and performance, 522–523
  general description of, 520–522
  IEMs integration, 521–522
  water remediation, 521*f*, 523–526
    application possibility, 523
    CDI-based technologies, 525–526
    flow electrodes, 525
    full-scale MCDI systems, 524
    IEMs, 524
    salt concentration, 525
    TDS concentration, 524
Carbon nanotubes and graphene oxide
  fouling, 92–93
    CNT/GO complex, 93
    cross-flow permeation tests, 92
    layer of, 92–93
  n-TFN membrane, 90
  permeability and selectivity, 93–94
    natural organic materials, 93
    PES nanocomposite membrane, 94
    trade-off relationship, 93–94
  physical properties, 94–95
  physico-chemical properties of membranes, 89–90
  polar functional groups, 90
  wastewater treatment, 90–91
Cell pair, 513
Chemical composition of the membrane surface
  attenuated total reflectance Fourier transform infrared spectroscopy, 19
  energy dispersive X-ray spectroscopy, 20
  X-ray photoelectron spectroscopy, 19
Christmas tree design, 28
Commercial fabrication techniques

Commercial fabrication techniques (*Continued*)
flat-sheet membranes, 30, 31*f*
hollow-fiber membranes, 30–32, 33*t*
nonsolvent-induced phase separation (NIPS), 32*f*
Commercialization status, nanoenhanced nanofiltration membranes
desalination and OSN, 183*t*
industrial and scientific advancement, 182–185
organic solvent nanofiltration (OSN), 185*f*
physicochemical characteristics, 182
polymer-based NF membrane, 182
research papers on, 185
Commercialization status of forward osmosis membranes, 495–496
Commercially available membranes, 142*t*
Dow Filmtec, 141–145
drug recovery and zinc, 141
Commercial status of membrane fabrication techniques
conventional polymeric fabrication methods, 54*t*
flat-sheet membrane, 58
hollow-fiber membrane, 58*t*, 59, 59*t*
MF and UF, 56*t*
Concentration polarization in osmotic-driven membrane
external, 281–282
internal, 282–283
water flux transport, 282*f*
Conductive polymers, 508–509
Counter-ions, 513
Critical miscibility temperature (T_c), 313

D

Diffusion boundary layer (DBL), 514
Donnan exclusion mechanism, 541–542
Double-skinned membranes, 454–456
Drag reduction effect, 94
Draw solutions, 420
Dry casting method, 605
Dual-layer membranes
active layer
additive, 437–438
monomers, 435–436
performance of, 439*t*
post-modification, 436–437
reaction conditions, 438
solvent, 436
hollow fiber forward osmosis (FO), 455*t*
hollow fiber thin-film composite, 453
pharmaceutical dilute solutions, 453
support layer, 430–435
cellulosic, 432–433
field emission scanning electron microscopy (FESEM), 434*f*
polyacrylonitrile (PAN)-based, 432
polyazole-based, 435
poly(vinylidene difluoride) (PVDF)-based, 433–434
polyethersulfone-based, 431–432
polysulfone-based, 430–431
polyvinyl chloride, 433
TFC FO hollow fiber membrane, 453–454
Duracid, 141–145

E

Electrodialysis reversal and capacitive deionization technology
anion-exchange groups, 573*f*
anion-exchange membrane, 571*f*
application and performance of, 546–551
applications of, 571–574
capacitive deionization (CDI), 579, 579*f*
cation exchange, 573*f*
CDI-based technologies, 519–526
classification and general preparation, 542
commercialization status, 587–590
commercial viability, 587–590
efficient and low-cost ion separation process, 542
electrodialysis reversal, 578*f*
electro-driven membrane processes, 578
electro-membrane process, 542*f*
energy barrier, 575*f*
evaporation process, 541–542
future directions, 531–532, 590
global freshwater shortage, 569
homogeneous and heterogeneous ion, 574*f*
IEM structure, 574
ion-exchange membrane (IEM), 542*f*, 551–556, 569, 570*f*, 577*f*
ion-exchange membranes and their fabrication processes, 543–546
ion-exchange mixed matrix membranes (MMMs), 582*f*
ionizable functional groups, 571
ion transportation in IEM, 574–577, 577*f*
limitations and key mitigation strategy, 526–530
membrane capacitive deionization (MCDI), 579*f*
membrane processes, 581
microstructure, 570
nano-enhanced membranes, 582*f*
network morphology of ion exchange, 577*f*
polymer-based nano-enhanced ion-exchange, 580–586
promising technology, 579
selective, 513–519
structure of ion-exchange, 507–512
three ionic transport mechanisms, 576*f*
for water treatment, 586–587

Electrodialysis reversal and selective
achievements, 517–519
ED processes development, 517
electrochemical demineralization of water, 519
mathematical models, 519
metallurgical processes, 519
municipal wastewater treatment, 518
reversal, 518
water remediation method, 518
configuration and operating principles, 513–515
anion-exchange membranes (AEMs), 514*f*
cation-exchange membranes (CEMs), 514*f*
conventional ED operations, 514
Donnan exclusion effect, 513
electromembrane technique, 515
fouling/scaling in ED systems, 515
membrane property, 513
transport equations and driving forces, 515–517
binary electrolytes, 516
membrane/solution interface, 516
Nernstian form, 516–517
Electrospun nanofibrous polymers for nanofiltration applications
cellulose acetate (CA), 223
cross-linked network, 221
electrospinning, 217–218
environmental parameters on the electrospinning process, 219*t*
free radical formation procedure, 220–221
functional monomer, 220
nanofibrous layer, 220*f*
PDA interlayer, 221–222
reverse proportionality, 218
surface tension, 218
TFC membrane, 221
End-of-life reverse osmosis membrane modules
cleaning strategy, 395–398
chemical, 395–396
enzymatic, 396
recycling, 396
reverse osmosis fouled, 397*t*
ultrasonic techniques, 395
irreversible fouling and chemical damage, 396
oxidizing agent dose, 400*f*
recycling, 399–402
discarded RO, 400, 402
exposure time, 399–400
pilot plant, 400–401
pilot scale, 403*f*
polyamide (PA) thin-film composite (TFC) reverse osmosis (RO), 402*f*
reflectance-Fourier transform infrared (ATR-FTIR), 400
total reflectance-Fourier transform infrared (ATR-FTIR) spectra, 401*f*
UF separation process, 401–402
waste management hierarchy, 399*f*
End-of-life reverse osmosis membranes recycling
fouling, 386–394
modules, 384–386
technology, 382–384
Energy consumption of membrane distillation
advantages, 624
energy consumption cost, 624–626
fouling and wetting, 624
External concentration polarization (ECP), 421

F

Fabrication techniques and module designs of MD membrane
electrospinning, 605–608, 606*f*
electrospun/electrosprayed, 608*f*
modules and designs, 608–610
phase inversion, 604–605
plate-frame module, 609*f*
sintering, 605
spiral wound modules, 609*f*
stretching, 605
Fixed-charged models, 121–122
FO polymeric membranes
advantages and disadvantages, 460
challenge in FO membranes, 461
developmental research, 460
structural parameter, 460
water desalination, 461
Forward osmosis and reverse osmosis membranes' structures and property
desalination technology, 284
development, 284–292
interfacial polymerization process, 285*f*
Forward osmosis membrane development
backing fabric custom design, 300–301
phase inversion, 285–292
biomimetic, 292
categories and classifications, 287*f*
cellulose acetate, 285–288
composite, 288–290
layer-by-layer composite, 292
polyamide-imide, 288
polybenzimidazole, 288
thin-film composite, 290–291
thin-film composite reverse osmosis, 286*t*
thin-film nanocomposite, 291
recent development, 296*t*
selective rejection layer, 296
support backing fabric, 298–301, 301*t*

Forward osmosis membrane development (*Continued*)
support polymeric layer, 297–298
in support polymeric layer, 299*t*
Fouling, 514
Fouling and wetting methods
air-liquid interface, 622–623
inorganic scaling, 620
limitations and technical challenges, 619
pretreatment methods, 619–620
strong and weak acids, 620
surface energy and surface tension, 621
triple-layer membrane, 622*f*
Fouling and wetting phenomena
MD process, 617–618
membrane, 619*f*
organic liquids, 618
types, 618*f*
Fouling in reverse osmosis separation process
biofouling
chemical treatments, 390
induction phase, 390–391
types of, 391
bulk and surface crystallization processes, 388*f*
colloidal, 388–389
crystals growth, 388*f*
inorganic, 387–388
membrane fouling, 387*f*
organic, 389
adsorption-desorption mechanism, 389, 390*f*
foulant, 389
prevention and mitigation, 391–394
coagulants and flocculants, 391–392
pretreatment of feed water, 392
pretreatment processes, 393
research study, 394
ultrathin PA layer, 393
Frictional coefficient, 7
Functionalization methods for membrane surface
enzyme immobilization, 65–66
chemical binding, 65
entrapment, 66
other methods, 66
physical absorption, 65
polymeric by molecular imprinting, 64–65
emulsion polymerization, 65
photo-grafting, 64–65
surface deposition, 65
surface modification, 61–64
chemical treatment, 62–63
coating, 61–62
graft polymerization, 63–64
MF/UF membranes, 62*t*
plasma treatment, 63
self-assembly, 61

H

Historical development of nanofiltration membranes, 124*f*
Hollow fiber nano-enhanced, 84–87

I

Immersion casting, 49–50
Impregnated membranes, 446–448
Internal concentration polarization (ICP), 421
Invasive methods, 19
Ion-exchange membranes and their fabrication processes
classification, 543
commercial, 545*t*
homogeneous *versus* heterogeneous ion-exchange, 544*f*
ion-exchange, 543–546
polymeric, 546
profiled or patterned, 547*f*
Ion-exchange membranes for water treatment
digital photo, 589*f*
EDX spectrum, 587*f*, 588*f*, 589*f*
electrostatic potential of 8-HQ, 588*f*
elemental mapping, 587*f*, 588*f*
FESEM image of used layer-by-layer, 589*f*
functional groups, 586–587
industrial sources, 586
water scarcity, 586
Ion-exchange membranes in electrodialysis performance
desalination with, 546–549
ionic separations, 550–551
preferential ion separation, 550
in various applications, 548*t*
wastewater treatment, 549
Ion-exchange membranes in electrodialysis reversal
desalination of high-concentration solution, 552–555
flux profile system, 555*f*
integrated sand-filter (SS), 555
ion separation processes, 555–556
plants, 553*t*
principle of, 551–552
Ion-exchange membranes in membrane capacitive deionization
desalination processes, 558
processes, 558–559
role of, 556–557
schematic MCDI process, 557*f*
simple module, 557*f*
Ion-exchange membranes structure
anion, 507, 511
bipolar, 512
electrochemical property, 512
electromembrane processes, 512

interfaces types, 512
junction, 512
BPMs, 507
cation-exchange membrane (CEM), 507, 509*f*, 511
conductive polymers and, 508
electrochemical technology, 510–511
functional groups, 507–508
groups distribution and homogeneous, 507*f*
homogeneous and/heterogeneous, 508
hydrophobic substrates, 510
isotropic and anisotropic, 510*f*
matrix, 507
selective synthesis, 509
structural characteristic, 509

L

Layer assembled polyelectrolyte membrane, 325
Layer-by-layer membranes, 454
double-skinned, 446
impregnated, 446–448, 448*t*
performance of, 447*t*
Limitations and key mitigation strategy
antifouling and antibiofouling property, 529*f*
biofouling in anion-exchange membranes, 528*f*
chemical cleaning procedures, 529–530
fouling and antifouling, 145–147
fouling and its mechanism, 147*f*
membrane clogging, 528–530
membrane fouling, 146–147
membrane retentate generation, 147–148
mitigation strategy, 529
operational modification methods, 530
physical cleaning hydraulic and pneumatic, 146–147
process cost, 526–528
operating, 527–528
plant investment, 526–527
selectivity
lack for ions, 530
monovalent-selective, 530
transport of specific ions, 530
Limiting current density, 514

M

MD membrane characteristics
liquid entry pressure, 611
mechanical property, 614
pore size distribution, 612–613
porosity and tortuosity of, 613–614
thermal conductivity, 614
thickness, 612, 613*f*
Melt casting, 50
Membrane characterization methods
invasive methods, 19–22
atomic force microscopy (AFM), 22*f*
chemical composition of the surface, 19–20
surface morphologies, 20–22
noninvasive methods, 22–24
at-line method, 23–24, 24*f*
inline, 22–23, 23*f*
offline method, 24
Membrane distillation applications, 624
Membrane distillation configurations, 602*f*
air gap, 601–602
direct contact, 601
principle, 600–601
sweep gas, 602–603
vacuum, 603
Membrane distillation technology, 625*t*
Membrane materials for MD, 610–611
Membrane performances
fouling, 88, 88*f*
hydrophobic membrane surface, 88*f*
permeability and selectivity, 89
physical properties, 89
Membrane process basics
industrial scale, 4
porous MF, 5
schematic representation of, 4*f*
separation efficiency of, 3
Membrane science and theory
concentration polarization, 9–10
bulk feed concentration, 10
mass balance equation, 10
mass transport model, 10
cross-flow filtration, 13*f*
dead-end filtration, 12*f*
fouling in, 14–18
back-flushing, 16*f*
chemical cleaning, 17–18
effect of back-flushing, 17*f*
regeneration by physical cleaning, 15–17
standard mode of filtration, 16*f*
hybrid-flow filtration, 14*f*
material and geometry, 11
CA powder, 11
flat sheet membrane, 11
models of, 15*t*
mode of operation in, 12–13
molecules size, 8*f*
pore geometry in porous membranes, 7*f*
solute and solvent transport, 6–9
cross-sectional structure, 6
Hagen–Poiseuille equation, 6–7
Kozeny–Carman equation, 7
pore geometry, 6–7

Metallic nanoparticles
aminated-polyethersulfone (APES) membranes, 98*f*
antifouling mechanisms, 103*f*
bare PVDF, 96*f*
biofouling properties of Cu containing polyethersulfone (PES), 102*f*
copper, 100–101
antifouling property, 101
PAN membrane, 100–101
fouling, 102–104
grafted by mixture of PAA and TiO_2, 96*f*
location of AgNP, 97*f*
PAA and self-assembling of TiO_2, 96*f*
permeability and selectivity, 104
physical properties, 104
silver, 96–100
Ag-based materials, 96–97
antibiofouling performance, 98
direct biological effects, 97–98
immobilization mechanism, 98–99
PDA coating, 99–100
vermiculite nanoparticles, 100
titanium dioxide, 95–96
antifouling agents, 95
PVDF membranes, 95–96
zinc oxide, 101–102
physical and chemical property, 101–102
PSF membranes, 101–102
ZnONPs in membranes, 102
Microfiltration and ultrafiltration membrane technology
characterization methods, 18–24
conventional filtration processes, 3
driving force, 4
membrane selectivity, 3–4
module design and process configuration, 25–32
polymeric application, 33–39
porous MF, 5
pressure-driven membrane processes, 4
science and theory, 6–18
semipermeable barrier, 3
water purification, 4–5
Microfiltration/ultrafiltration membranes
classification, 44
fabrication, 44–53, 45*t*
chemical techniques, 47–53
electrospinning, 51–52, 51*f*
liquid-induced phase separation, 49–50
mechanical techniques, 47
nanoimprint lithography, 52–53
phase inversion techniques, 48–50
sintering process, 47*f*
template leaching, 48
thermally induced phase separation, 50, 50*f*
3D-printing, 52
track etching, 47–48, 48*f*
vapor-induced phase separation, 49, 49*f*
Microfiltration/ultrafiltration membranes for water remediation application
nanocomposite membranes, 69–70
fabrication via phase inversion, 69–70
using nanoparticle, 69
Microfiltration membranes, 5
Microplastics and polymeric membranes
chemical/structural characteristics, 73
filtration characteristics, 73
mechanical and thermochemical characteristics, 74
morphological characteristics, 74
surface characteristics, 73
Mixed matrix membranes (MMMs), 203–204, 471–472
Mixed matrix polymer-based nanoenhanced nanofiltration membranes
asymmetric mixed matrix, 204–208
fabrication of TFN-GO, 209*f*
phase inversion method, 207*f*
salt retention order, 204–208
thin-film nanocomposite, 209*f*, 210–217
carbon nanotube-incorporated, 211–212
fabrication illustration, 216*f*
FESEM images, 213*f*
graphene oxide-based, 210–211
graphene oxide, 211*f*
IP method, 216–217
metal-organic framework-integrated, 213–214
MOF materials' embedment, 214
nanohybrid structure-based, 214–217
thin-film polymer nanocomposite nanofiltration membranes, 208–217
via phase inversion technique, 205*t*
Module design
hollow fiber/shell and tube, 26–27
plate-and-frame membrane, 25
spiral-wound module, 25–26, 26*f*
tubular, 25, 25*f*
Molecular species, 278
Morphologies of the membrane surface
atomic force microscopy, 21–22
environmental scanning electron microscopy, 21
scanning electron microscope, 20–21
Multipass system, 27

N

Nanocomposite membranes. *See also* Nano-enhanced membranes
blended, 83–84
polymer, 84*f*

pressure-driven technology, 83*f*
thin-film, 83–84
Nanocomposite membranes stability chemical, 106
Nano-enhanced forward osmosis membranes
commercialization status, 495–496
flat sheet, 475–486
future directions, 496–497
hollow fiber, 486–490
mixed matrix, 472–475
nanofibrous-based, 490–491
stimuli-responsive, 491–495
surface modification, 491
Nanoenhanced hollow-fiber nanofiltration membranes
HF, 224–225
polysulfone hollow fiber, 224*f*
pretreatment costs, 224–225
Nano-enhanced ion-exchange membranes
blending, 583–584
IEMs, 584
suitable solvent, 583–584
nano-enhanced IEMs, 583
NCM formation, 581–582
polymer-based, 583
polymeric IEMs, 580–581
research activity, 580–581
in situ technique, 584–586
IEMs electrochemical characteristics, 586
nanomaterials/ nanomaterial precursors, 584–586
solvent-free strategy, 584–586
Nano-enhanced membranes, 69–70
Nano-enhanced microfiltration/ultrafiltration membranes
carbon nanotubes and graphene oxide, 89–95
challenges and future perspectives, 107–108
future research, 106–107
hollow fiber, 84–87
metallic nanoparticles, 95–104
nanocomposite membranes, 83–84
stability, 105–106
performances, 88–89
Nanoenhanced nanofiltration membranes
chemical reactions and multiple preparation, 202–203
fabricating process of GA-g-CS/PS membrane, 203*f*
fabrication, 200*t*
graphene oxide (GO), 198*f*
graphene oxide (GO) embedded thin-film nanocomposite (TFN), 202*f*
PAA-g-MWCNT/PES mixed matrix, 199*f*
porous, 201–202
preparation of, 200–203
rejection performance, 202–203
thin-film nanocomposite (TFN), 197–198
tight NF, 201
wastewater treatment applications, 197–198
Nanofibrous-based forward osmosis membranes
hydrophilic/hydrophobic interpenetrating network, 490
scaffold-like, 490
thin and fine nanofiber upper layer, 490
Nanofiltration membrane operating range, 122*t*
Nanofiltration membrane technology
aqueous environment, 121
commercially available membranes, 141–145
historical development, 123–124
limitations and key mitigation strategy, 145–148
market expansion, 122
operation principle and transport mechanism, 124–127
polymeric and application domain, 127–134
polymeric structure and configurations, 134–136
pore size distribution, 122–123
preparation, 136–141
three-dimensional network, 121–122
transport phenomena, 121–122
Nanostructured membranes, 82*f*
NF membrane preparation technology
hollow fiber, 140–141
interfacial polymerization, 136–137
layer-by-layer assembly, 139–140
phase inversion, 137–138
post-treatment of porous support, 138–139
techniques for, 138*f*
Noninvasive methods, 19

O

Oleophobic membranes, 621
Operating principle and transport mechanism
diffusion and filtration mechanism, 125–126
diffusion cell, 126*f*
nanofiltration pore model development and progress, 124–125
pore model of membrane milestone, 125*f*
role of membrane charge on NF performance, 126–127
Operational parameters in membrane distillation
air gap and long operation, 616–617
feed concentration, 616
feed temperature, 615
flow rate, 615–616
type, 617
Organic solvent nanofiltration (OSN), 187*f*
Osmotic processes concept
hydraulic pressure, 276
relationship, 277*f*
retarded osmosis (PRO), 276*f*

Osmotic processes concept (*Continued*)
reverse osmosis (RO), 276*f*
transport membrane mechanism, 277–280
extended solution-diffusion model, 279–280
homogeneous models, 278–279
irreversible thermodynamics models, 277–278
pore models, 280
solution-diffusion-imperfection model, 279

P

Permeate, 3
Phase inversion, 285
Photo nanoimprint lithography, 53
Physiochemical properties
hydrophobic/amphiphilic materials, 68
fluoropolymers, 68
polymers, 68
using hydrophilic materials, 67–68
PEG-based coatings, 67
polydopamine, 67–68
zwitterionic materials, 68
Polymer-based flat sheet forward osmosis membranes
dual-layer, 429–438
single-layer, 422–428
CA morphology, 425
casting substrates and coagulant baths, 424
cellular, spinodal and beads-like morphology, 426*f*
cellulosic, 422–425
chemical structure of polyamide-imide (PAI), 426*f*
flat sheet forward osmosis (FO) membranes, 428*t*
hybrid system, 423
NaCl concentrations, 424
polyamide-imide-based, 426–427
polybenzimidazole (PBI), 427, 427*f*
polymeric materials, 427–428
woven and nonwoven fabrics microscopically, 425
typical thin-film composite (TFC) membranes, 429*f*
Polymer-based forward osmosis membranes
commercialization status and commercial viability, 458–459
concentration polarization, 420–422
different orientations, 421*f*
dual-layer membranes, 429–438
flat sheet, 422–449
FO process, 420, 422
future directions, 460–461
hollow fiber, 449–457
ICP effect, 422
important notes, 419–420
water transfer, 420
Polymer-based hollow fiber forward osmosis membranes
high-flux and high-rejection, 451
osmotic pressure efficiency, 451
single-layer, 449–452
Polymer-based membranes for membrane distillation
applications of, 624
characteristics of, 611–614
dearth of water, 598–599
economics and energy consumption, 624–626
fabrication techniques and module designs, 603–610
fouling and wetting phenomena, 617–619
fouling and wetting prevention methods, 619–623
future directions in, 626
history of, 599
materials for, 610–611
operational parameters in, 615–617
principle and different configurations, 600–603
recent trends in, 600
research activity on, 600*f*
temperature and concentration polarization, 623–624
Polymer-based microfiltration/ultrafiltration membranes
microplastics and polymeric membranes, 73–74
polymer-enhanced effect, 59–68
raw material to synthesize, 44–59
water remediation application, 68–72
Polymer-based mixed matrix forward osmosis membranes
dispersed phase, 472–473
nanomaterials category, 475*f*
nanomaterials classification
organic, inorganic, and bionanomaterials, 474–475
overview, 472–473
preparation and modification approaches, 473–474
chemical methods, 473
LbL method, 474
physical methods, 473
in situ IP method, 473–474
surface grafting method, 474
pure inorganic, 472*f*
pure polymer, 472*f*
Polymer-based nanocomposite flat sheet forward osmosis membranes
active layer modifications
Aquaporin Inside hollow fiber membrane module, 489*f*
biomimetic forward osmosis, 489–490
carbon-based nanomaterials, 487–488
hollow-fiber thin-film, 488*f*
metal-based nanomaterials, 488–489
desalination and water treatment, 475–479
different nanomaterials, 476*t*
hollow fiber, 486–490
nanocomposite forward preparation, 479
process of, 480*f*

selective/active layer
carbon-based nanomaterials, 483
control and graphene oxide (GO), 485*f*
flat-sheet membrane, 484*t*
metal-based nanomaterials, 483–486
titanate nanotubes, 485*f*
support/substrate and selective/active layers, 486
support/substrate layer, 479–482
carbon-based nanomaterials, 480–482
metal-based nanomaterials, 482
nanomaterials-embedded, 481*t*
thin-film composite membrane, 479*f*
Polymer-based nanoenhanced nanofiltration membranes
commercialization status and commercial viability, 225–226
electrospun nanofibrous, 217–223
mixed matrix, 203–217
nanoenhanced hollow-fiber, 224–225
Polymer-based nano-enhanced reverse osmosis membranes
category, 337
chemical bonding mechanism, 341
chemical grafting of silver nanoparticles, 341*f*
commercialization status and viability, 369
conventional nanocomposite or mixed matrix, 338
fabrication process, 339*f*
layer-by-layer assemble of graphene oxide (GO), 341*f*
nanocomposite located at surface, 339–341, 340*t*
nanocomposite types, 337*f*
thin-film composite, 338
thin-film nanocomposite, 338
for water desalination, 363–368
in water treatment, 368
way forward, 369–370
Polymer-based nanofiltration membranes
AQP-based, 164–165
bioinspiration for molecularly precise, 165*f*
block-copolymer, 166
commercialization status and commercial viability, 181–185
effect of, 175–178
Elimelech's group, 161
energy-efficient liquid separation, 161
finger-like structure, 169–170
industrial scale, 161–162
instantaneous demixing, 169–170
interfacial polymerization, 170–171
intrinsic microporous, 167–168
intrinsic properties and separation mechanism, 162–163
layer-by-layer assembly, 171–172, 171*f*
mass transfer region, 163*f*
membrane technology, 159
mixed-matrix, 165–166
nanofiltration (NF) membrane technology, 160
natural and bioinspired, 164–165
NF membranes, 160–162
nonsolvent-induced phase separation method, 169*f*
phase inversion, 168–170
pore wall chemistries, 167*f*
posttreatment, 172–174
preparation of, 168–174
semiaromatic thin-film composite membrane, 173*f*
separation mechanisms of, 162*f*
solvent-polymer solution, 168–169
solvent-resistant, 180–181
surface hydrophilicity, 163
thermodynamic and kinetic property, 169–170
thermodynamic equilibrium, 169–170
thin-film polymer composite, 174–175
water channeling, 162–163
for water desalination, 178–180
Polymer-based reverse osmosis membranes
asymmetric, 312–316
brackish water desalination, 323
commercialization status and commercial viability, 328
thin-film composite membrane, 316–323
Polymer-composite nanofiltration membranes for water desalination, 178–180
Polymer-enhanced microfiltration/ultrafiltration membranes
functionalization methods, 61–66
physiochemical properties, 66–68
structural property, 59–61
Polymeric membranes and application domain
application, 132–134
food processing industry, 133
heavy metals removal from industrial waste, 133–134
wastewater treatment in textile industry, 132–133
synthesis, 128–129
types, 129–131
carbon nanomaterials-based NF, 129–130
metal-organic framework (MOF), 131*f*
metal-organic framework-based NF, 130–131
permeability and antifouling, 130*f*
zeta potential, 128*t*
Polymeric membrane structure and configurations
commercial polyamide nanofiltration, 134*f*
IP process, 135
monomer, 136
NF membrane performance, 136
nonwoven support, 135
porous support layer, 135

Polymeric support effect
MF porous support, 175–177
patterned membranes preparation, 178*f*
physicochemical property, 175
polyamide thin-film composite membrane, 177*f*
single-wall carbon tube (SWCNT), 176*f*
support-free IP (SIPF) technique, 178
TFC NF membrane, 175–177
ultrathin separation layers, 175–177
Polymeric ultrafiltration and microfiltration membranes
dairy processing industry, 36–37
heavy metal from industry effluent, 37–39, 38*t*
oily wastewater, 37
potable water reuse, 33–36
recovery of dye and pigments, 36
water and wastewater treatment, 34*t*
Polymer nanocomposite reverse osmosis membranes
Ag nanoparticles-induced nanochannels, 354*f*
carbon based, 342–350
foulants attachment over, 345*f*
graphene oxide, 346–348
graphene oxide quantum dots (GOQD), 351*f*
interfacial polymerization, 349*f*
nanotubes, 342–346
PA TFN RO, 345
quantum dots, 348–350
TFN RO, 350
thin-film nanocomposite (TFN) reverse osmosis (RO), 343*t*
GO-embedded TFC, 348
interfacial polymerization (IP) process, 361*t*
metal and metal oxides based, 350–360
alumina, 358
copper, 355
organic frameworks, 358–360
silver, 351–354
titanium dioxide, 355–357
zinc oxide, 357–358
other nanoparticles, 360–363
cellulose nanocrystals, 363
halloysite (aluminosilicate), 360–362
silica, 360
zeolite, 363
profile of water flux, 356*f*
salt rejection of thin-film composite, 356*f*
in situ polymerization reaction, 362*f*
specific energy consumption (SEC), 347*f*
thin-film nanocomposite (TFN) reverse osmosis (RO), 352*t*
titanate nanotubes, 357*f*
ZIF-8 deposition on polysulfone (PSF) substrate, 359*f*
Polymer nanocomposite reverse osmosis membranes in water treatment, 368
Pressure casting, 50
Pressure-induced phase separation. *See* Pressure casting
Process configuration
batch filtration, 28
batch-type, 28*f*
continuous filtration, 27
feed-and-bleed/fed-batch filtration, 28
feed-and-bleed/fed-batch type, 29*f*
membrane module designs, 27*t*
single and multipass, 29, 30*f*
single and multistage, 28
single-pass membrane, 28*f*
Pulsed electrodialysis reversal (PER), 530

R

Rapid prototyping, 52
Reverse and forward osmosis membrane technology
driven membrane, 281–283
fabrication methods, 283–284
flat sheet, 292–301
osmosis and, 280–281
osmotic processes and basic concept, 276–280
structures and property, 284–292
Reverse osmosis and forward osmosis membranes
fabrication methods, 283–284, 284*f*
modification, 281
research on FO process, 280–281
Reverse osmosis membranes and modules
common thin-film composite polyamide (TFC PA), 385*f*
concentration polarization layer, 385–386
control technology, 385
phase inversion (PI) method, 384–385
salt rejection factor, 384
spiral wound modules, 386*f*
Reverse osmosis membranes for brackish water desalination
commercial, 324*t*
crucial performance parameters, 323
PA-TFC, 323
unit energy costs, 323
Reverse osmosis membranes for seawater desalination
aquaporin biomimetic, 326, 326*f*
commercial, 327*t*
polyelectrolyte, 325, 325*f*
supramolecular polymers and water-soluble polymers, 327–328
Reverse osmosis membranes for water desalination, 363–368

Reverse osmosis membrane technology
costs and environmental impacts, 384
desalination plant, 383*f*
permeable and selective, 382
process, 383*f*
separation process, 382
Reverse osmosis recycled membranes
biofilms reactors, and electrodialysis separation processes, distillation, 407–408
economic and environmental costs, 408
microcystins-degrading, 407
recycling methodology, 408
PA active layer, 403
research study, 407
separation processes, 404*t*
ultrafiltration and microfiltration, 406–407
waste treatment, 406–407

S
Scaling, 528–529
Selectrodialysis, 515
Softening membrane, 141–145
Solute, 6
Solvent, 6
Solvent-resistant nanofiltration (SRNF), 180–181
Max–Dewax process, 180–181
molecular dynamics simulations, 181
Szekely's group, 181
Space-charged models, 121–122
Stability of nanocomposite membranes
polymer matrix degradation, 105*f*
UV degradation, 105–106
Stimuli-responsive forward osmosis membranes
advancements in the forward osmosis (FO), 494*t*
drug delivery, 491–492
electric field, 494–495
membranes, 492
pH-responsive groups and materials, 493*t*
responsive polymer, 492
salt-responsive and temperature-responsive, 495
Stimuli-responsive/smart membranes
CO_2-responsive nanofiltration, 263
hollow fiber configuration, 263–264
magnetically responsive, 258–260
multicharged nanofilms, 258*f*
NF membranes' fouling, 259–260
photo-responsive, 261–263
pH-responsive, 257–258
temperature, 260–261
TFC method, 259
thin-film composite nanofiltration, 262*f*
Structural property
polymer crystallinity, 59–60
pore, 60
surface, 60–61
charge, 60–61
hydrophilic and hydrophobic property, 60
Surface modification of forward osmosis membranes, 491
Synthetic metals, 508–509

T
Taylor cone, 52
Temperature and concentration polarization
heat and mass transfer processes, 624
MD module, 623–624
numerical value, 623
TFN membrane, 298
Thermal nanoimprint lithography, 53
Thin-film composite (TFC) membrane, 239, 316–317
active layer of, 320*t*
antifouling/chlorine tolerant, 321–322
asymmetric, 316
hollow fiber reverse, 322–323
interfacial polymerization, 319*f*
nonwoven fabric, 317
polyamide and cellulose acetate, 318, 319*t*
polymer materials structure, 318*t*
reverse osmosis (RO), 316*f*
reverse osmosis membranes for boron removal, 321, 322*t*
ultrathin barrier layer, 319–321
Thin-film polymer composite nanofiltration membranes, 174–175
3D-printing. *See* Rapid prototyping
TiO_2 and SiO_2 nanocomposite membranes, 70*t*

U
Ultrafiltration membrane, 5–6

W
Wet casting, 49–50

Y
Young's modulus, 95